NASA Contractor Report 178272

# Time-Temperature-Stress Capabilities of Composite Materials for Advanced Supersonic Technology Application

J.R. Kerr and J.F. Haskins

General Dynamics Corporation
Convair Division
San Diego, CA 92138

Contract NAS1-12308
May 1987

National Aeronautics and
Space Administration

Langley Research Center
Hampton, Virginia 23665-5225

# FOREWORD

The work presented in this report was performed at General Dynamics Convair Division, San Diego, California, under Contract NAS1-12308 for the National Aeronautics and Space Administration, Langley Research Center, Hampton, Virginia. Mr. Bland A. Stein and Dr. Donald R. Rummler served as project monitors.

Mr. James F. Haskins and Dr. James R. Kerr served as General Dynamics program managers. Dr. Dick J. Wilkins formerly with the General Dynamics Fort Worth Division provided the random load spectrum and assisted in the wearout theory analysis. Other key contributors to the program were:

| | |
|---|---|
| Composite Fabrication | J.E. Hilzinger<br>Chuck May<br>Dr. Michael Miller<br>Mike Varlas |
| Specimen Preparation | Charlie Maikish<br>N.R. Martin |
| Quality Assurance | Gerald O'Barr<br>Jack Christian |
| Testing and Fixture Design | Dr. Ray Adsit<br>E.S. Harrison<br>Curt Tanner<br>Ron Torgerson<br>Dr. John Waszczak<br>Bill Witzell |
| Thermal Aging | Roscoe Anderson<br>Mal Campbell |
| Flight Simulation Exposure and Fixture Design | Don Bowers<br>Charlie Dunkel<br>Dick Gilbert<br>A.A. McClain |
| SEM and Metallographic Evaluation | Dr. Mike Featherby<br>Bob Pettyjohn<br>Dr. K.L. Agarwal |

PRECEDING PAGE BLANK NOT FILMED

# TABLE OF CONTENTS


| Section | | Page |
|---|---|---|
| 1 | INTRODUCTION | 1-1 |
| 2 | DESCRIPTION OF PROGRAM | 2-1 |
| 3 | MATERIAL SELECTION AND ACQUISITION | 3-1 |
| 3.1 | MATERIAL SELECTION | 3-1 |
| 3.1.1 | Metal Matrix Composite Material | 3-1 |
| 3.1.2 | Resin Matrix Composite Material | 3-2 |
| 3.2 | MATERIAL ACQUISITION | 3-7 |
| 3.2.1 | Metal Matrix Composite Material | 3-7 |
| 3.2.2 | Resin Matrix Composite Material | 3-8 |
| 4 | PREPREG QUALITY ASSURANCE TESTING | 4-1 |
| 4.1 | BORON EPOXY | 4-1 |
| 4.2 | GRAPHITE EPOXY | 4-2 |
| 4.3 | BORON POLYIMIDE | 4-3 |
| 4.4 | GRAPHITE POLYIMIDE | 4-4 |
| 4.4.1 | HT-S/710 | 4-4 |
| 4.4.2 | Celion 6000/LARC-160 | 4-5 |
| 5 | LAMINATE PROCESSING AND SPECIMEN FABRICATION | 5-1 |
| 5.1 | LAMINATE PROCESSING | 5-1 |
| 5.1.1 | Boron/Epoxy | 5-1 |
| 5.1.2 | Graphite/Epoxy | 5-1 |
| 5.1.3 | Boron/Polyimide | 5-3 |
| 5.1.4 | Graphite/Polyimide | 5-5 |
| 5.2 | BORON/ALUMINUM TUBE FABRICATION | 5-6 |
| 5.3 | SPECIMEN FABRICATION | 5-8 |
| 5.3.1 | Panel Layouts and Specimen Identification | 5-8 |
| 5.3.2 | Machining Operations | 5-8 |
| 5.3.3 | Doubler Bonding | 5-14 |
| 6 | LAMINATE QUALITY ASSURANCE TESTING | 6-1 |
| 6.1 | METAL MATRIX COMPOSITE MATERIAL | 6-1 |
| 6.2 | RESIN MATRIX COMPOSITE MATERIALS | 6-7 |
| 6.2.1 | Boron/Epoxy | 6-7 |
| 6.2.2 | Graphite/Epoxy | 6-9 |
| 6.2.3 | Boron/Polyimide | 6-17 |
| 6.2.4 | Graphite/Polyimide | 6-17 |


PRECEDING PAGE BLANK NOT FILMED

# TABLE OF CONTENTS, Contd


| Section | | Page |
|---|---|---|
| 7 | BASELINE TESTING | 7-1 |
| 7.1 | TENSILE TESTING | 7-2 |
| 7.1.1 | Specimen Design and Test Procedure | 7-2 |
| 7.1.2 | Test Results and Discussion | 7-9 |
| 7.2 | SHEAR TESTING | 7-46 |
| 7.2.1 | Specimen Design and Test Procedure | 7-48 |
| 7.2.2 | Test Results and Discussion | 7-54 |
| 7.3 | FRACTURE TESTING | 7-61 |
| 7.3.1 | Specimen Design | 7-63 |
| 7.3.2 | Test Procedure, Results and Discussion | 7-63 |
| 7.4 | COMPRESSIVE TESTING | 7-81 |
| 7.4.1 | Specimen Design and Test Procedure | 7-86 |
| 7.4.2 | Test Results and Discussion | 7-88 |
| 8 | THERMAL AGING | 8-1 |
| 8.1 | TEST EQUIPMENT AND TEST PROCEDURE | 8-2 |
| 8.2 | THERMAL AGING/TENSION — TEST RESULTS AND DISCUSSION | 8-4 |
| 8.2.1 | Boron/Epoxy and Graphite/Epoxy | 8-4 |
| 8.2.2 | Graphite/Polyimide | 8-39 |
| 8.2.3 | Boron/Aluminum | 8-67 |
| 8.3 | THERMAL AGING/COMPRESSION — TEST RESULTS AND DISCUSSION | 8-93 |
| 8.3.1 | Graphite/Epoxy | 8-93 |
| 8.3.2 | Celion 6000/LARC-160 Graphite/Polyimide | 8-99 |
| 9 | ENVIRONMENTAL AGING | 9-1 |
| 9.1 | RESIN MATRIX COMPOSITE SYSTEMS | 9-1 |
| 9.1.1 | Specimen Design and Test Procedures | 9-1 |
| 9.1.2 | Test Results and Discussion | 9-3 |
| 9.2 | METAL MATRIX COMPOSITE SYSTEM | 9-11 |
| 9.2.1 | Specimen Design and Test Procedure | 9-11 |
| 9.2.2 | Test Results and Discussion | 9-13 |
| 10 | CREEP TESTING | 10-1 |
| 10.1 | Specimen Design | 10-1 |
| 10.2 | Test Equipment and Test Procedure | 10-2 |
| 10.3 | Test Results and Discussion | 10-4 |
| 10.3.1 | Boron/Epoxy | 10-7 |
| 10.3.2 | Graphite/Epoxy | 10-12 |
| 10.3.3 | Graphite/Polyimide | 10-14 |

# TABLE OF CONTENTS, Contd


| Section | | Page |
|---|---|---|
| | 10.3.4 Boron/Aluminum | 10-19 |
| 11 | BASELINE FATIGUE TESTING | 11-1 |
| | 11.1 SPECIMEN DESIGN | 11-1 |
| | 11.2 TEST EQUIPMENT AND TEST PROCEDURE | 11-2 |
| | 11.3 TEST RESULTS AND DISCUSSION | 11-5 |
| | 11.3.1 Boron/Epoxy and Graphite/Epoxy | 11-5 |
| | 11.3.2 Graphite/Polyimide | 11-12 |
| | 11.3.3 Boron/Aluminum | 11-16 |
| | 11.3.4 Stacking Sequence Evaluation | 11-19 |
| | 11.3.5 Poisson's Ratio Evaluation | 11-37 |
| | 11.3.6 Baseline Fatigue Data for the Thermal Aging/ Compression Study | 11-38 |
| 12 | FLIGHT SIMULATION TESTING | 12-1 |
| | 12.1 INTRODUCTION | 12-1 |
| | 12.2 DESCRIPTION OF SIMULATOR | 12-3 |
| | 12.2.1 Test Fixtures | 12-4 |
| | 12.2.2 Load Programmer and Controllers | 12-4 |
| | 12.2.3 Programmer Safety Features | 12-4 |
| | 12.2.4 Hydraulic System | 12-6 |
| | 12.2.5 Heating System | 12-6 |
| | 12.2.6 Cooling System | 12-8 |
| | 12.2.7 Control Console | 12-8 |
| | 12.2.8 Data Recording System | 12-10 |
| | 12.2.9 Monitor/Safety System | 12-10 |
| | 12.2.10 Checkout | 12-11 |
| | 12.2.11 Automatic Operation | 12-11 |
| | 12.3 SPECIMEN CONFIGURATION | 12-12 |
| | 12.4 RANDOM LOAD SPECTRUM | 12-15 |
| | 12.4.1 Spectrum Generation for the Long-Term Tests | 12-17 |
| | 12.4.2 Spectrum for the Short-Term Tests | 12-18 |
| | 12.5 WEAROUT MODEL | 12-20 |
| | 12.6 SHORT-TERM FLIGHT SIMULATION | 12-27 |
| | 12.6.1 Test Plan and Procedures | 12-28 |
| | 12.6.2 Short-Term Test Results | 12-36 |
| | 12.6.3 Short-Term Analysis | 12-57 |
| | 12.7 LONG-TERM FLIGHT SIMULATION | 12-67 |
| | 12.7.1 Test Plan and Procedures | 12-67 |
| | 12.7.2 Phase I Long-Term Test Results | 12-70 |
| | 12.7.3 Phase II Long-Term Test Results | 12-128 |
| 13 | THERMAL EXPOSURE TEST PROGRAM SUMMARY | 13-1 |

# TABLE OF CONTENTS, Contd


| Section | | Page |
|---|---|---|
| 14 | CONCLUSIONS | 14-1 |
| 15 | REFERENCES | 15-1 |

APPENDIX

| | | |
|---|---|---|
| A | AN ANALYSIS OF THE B/P105AC BORON POLYIMIDE SYSTEM | |
| B | QUALITY ASSURANCE TEST PROCEDURES | |

# TIME-TEMPERATURE-STRESS CAPABILITIES OF COMPOSITE MATERIALS FOR ADVANCED SUPERSONIC TECHNOLOGY APPLICATION

**J.R. Kerr and J.F. Haskins**
**Convair Division of General Dynamics**

## SUMMARY

High temperature composite materials have the potential of significantly reducing the weight of future supersonic aircraft structures. However, implementation of the material into vehicle usage is contingent upon demonstrating its airworthiness when exposed to the long-time supersonic flight service environment. The primary objective of this research was to establish the time-temperature-stress characteristics and capabilities of five classes of high temperature composite materials to determine their suitability for advanced supersonic technology consideration. The systems studied were B/E, G/E, B/PI, G/PI, and B/Al. The tests that were conducted on the composite systems were baseline tensile, notched tensile, compressive, shear, and fracture; environmental and thermal aging; constant amplitude fatigue, creep and creep rupture; and both accelerated and real-time flight simulation testing using totally random fatigue loading. Phase I of the two-phase program included the baseline, fatigue, and creep determinations and all the aging and flight simulation studies up through 10,000 hours of cumulative exposure. Phase II continued this effort up to 50,000 cumulative hours of simulated flight service. The baseline, constant amplitude fatigue, and creep tests characterized the composite materials and formed a basis for comparison with the post-exposure test results. The baseline tests were also used to set the test conditions for the short-term exposures (100 and 200 hours, random fatigue at temperature). The short-term service history tests were performed to generate wearout analysis model data, and to set the stress levels for the long-term service history tests. Finally, the long-term tests were to provide data on the effect of 10,000-, 25,000-, and 50,000-hour simulated supersonic flight service on residual properties of the composites. The thermal aging and the environmental aging exposures were concurrent with the service history tests. The considerable quantity of data that have been obtained from the baseline tests, the 50,000 hour thermal and environmental aging studies, and the flight simulation exposures of almost 40,000 cumulative hours are presented in this report.

# SECTION 1

# INTRODUCTION

Approximately one year after the cancellation of the United States Supersonic Transport Program, the National Aeronautics and Space Administration initiated the Advanced Supersonic Technology (AST) Program. The name of the AST Program, which started in 1972, was subsequently changed to Supersonic Cruise Aircraft Research (SCAR), and then shortened to Supersonic Cruise Research (SCR). The overall objectives of this program were:

a. To provide an expanded technology base for future civil and military supersonic aircraft.

b. To provide the data needed to assess the environmental and economic impacts on the United States of present, and in particular, future foreign supersonic transport aircraft.

c. To provide a good technical basis for any future consideration that may be given by the Unites States to the development of an environmentally acceptable and economically viable commercial supersonic transport.

A block diagram showing the structure of the program is given in Figure 1-1. An extensive review of the activities associated with the SCR Program from 1972 to 1983 is presented in the bibliographies found in NASA Reference Publications 1003, 1063, and 1117 (ref. 1 to 3). The scope of the program included the development base, system studies, and the following disciplines:

SCR PROPULSION

SCR STRATOSPHERID EMISSIONS IMPACT

SCR STRUCTURES AND MATERIALS

SCR AERODYNAMIC PERFORMANCE

SCR STABILITY AND CONTROL

The work being reported on here was done under the Structures and Materials discipline of the SCR program. One of the primary goals in the Structures and Materials area was to advance the technology and establish a data base for advanced composites so that sound technical decisions may be made in the future regarding the use of these materials in supersonic cruise aircraft structures. Primary emphasis was placed on composites because of their high potential for reducing both weight and cost of future supersonic cruise aircraft structures. Information on the effects of long-time cyclic exposure to the environments and loads representative of long-time supersonic cruise aircraft service for composite materials of interest was not available in 1972, and, as a result, this program to generate such information was initiated in 1973. A range of baseline properties was determined for representatives of five composite materials classes: boron/epoxy, graphite/epoxy, boron/polyimide, graphite/polyimide, and boron/aluminum. Long term exposures out to 10,000; 25,000; and 50,000 hours were attempted in static thermal environments (thermal aging) and in ones that simultaneously combined programmed thermal histories and mechanical load histories (flight simulation). Material behavior during these exposures and the post-exposure residual property tests provided exposure effects and assisted in understanding material degradation mechanisms.

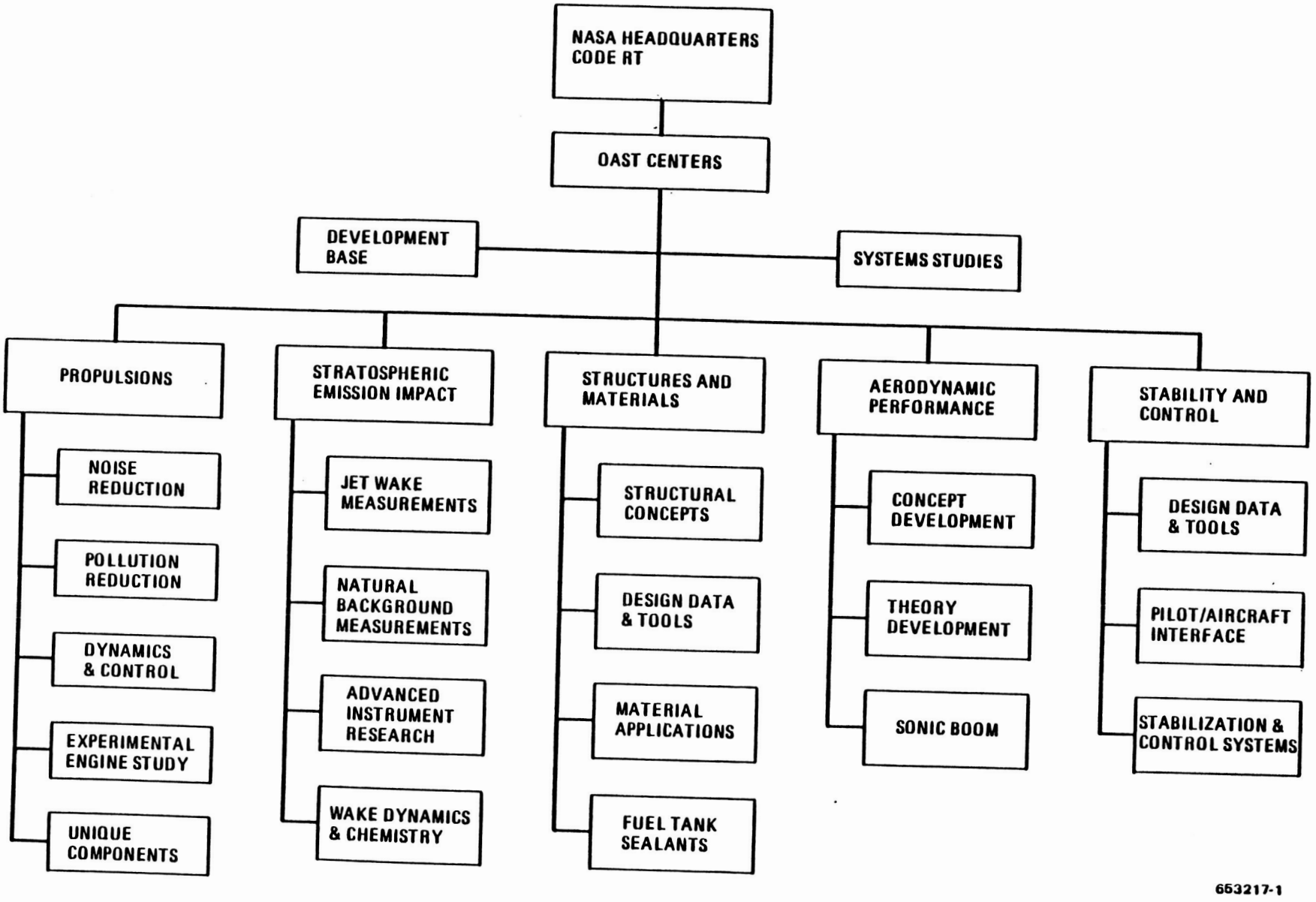



**Figure 1-1 SCR Program Elements**

Because of the goal of 50,000 hours of real-time exposure for both the thermal aging and the flight simulation tests the program was, of necessity, a very long one. The commercially produced composite materials selected at the beginning of the contract were thought to be ones that would be readily available for many years. In fact, one of the criteria for selecting the composites was that each material shall be reasonably well established, i.e., currently available and with a firm manufacturing maturity. As the program progressed it became apparent that, in general, the composites did not possess these requirements. Material problems that were encountered included: low tensile properties and lack of elevated temperature stability for one of the systems, significant changes in mechanical properties for a second material when repurchased several years after the initial purchase, change in designation with some mechanical property changes for a third material, and unavailability of a fourth material several years into the program. This made it very difficult, when adding tests later in the study, to correlate results from two batches of supposedly identical material.

Another problem, experienced at the beginning of the program, was overly optimistic estimates of the maximum use temperatures (for extended service) of each of the composite systems. For graphite/polyimide and boron/aluminum preliminary thermal aging data assisted in the selection of realistic flight simulation temperature profiles, which were considerably lower than those currently being proposed by the composite community. For the two epoxy classes, however, selection of excessive temperatures for the flight simulation tests resulted in numerous specimen failures and considerable overall property degradation prior to the first 10,000 hours of exposure. As discussed later, these tests were restarted with replacement specimens using a considerably modified thermal profile.

In spite of these problems, thermal aging exposures of up to 50,000 hours and flight simulation exposures of almost 40,000 hours were accomplished.

# SECTION 2

# DESCRIPTION OF PROGRAM

The general objective of this study was to assess the suitability of advanced filamentary reinforced composite materials for future supersonic cruise aircraft structures. The study had two phases. The first included all material property determinations and aging simulation exposures up through 10,000 hours. The second continued these tests toward a goal of 50,000 hours.

Representative materials from each of the five composite classes listed in Figure 2-1 were selected for evaluation in Phase I. These were:

a. Rigidite 5505/4 boron/epoxy.

b. A-S/3501 graphite/epoxy.

c. 5.6-mil boron/6061 boron/aluminum.

d. HT-S/710 graphite/polyimide.

e. 4.0-mil B/P105AC boron/polyimide.

Early in Phase I the boron/polyimide was removed from test because of low tensile properties and extensive thermal degradation during elevated temperature exposure. During Phase II a second graphite/polyimide, Celion 6000/LARC-160, was added to the program for evaluation up through 10,000 hours.

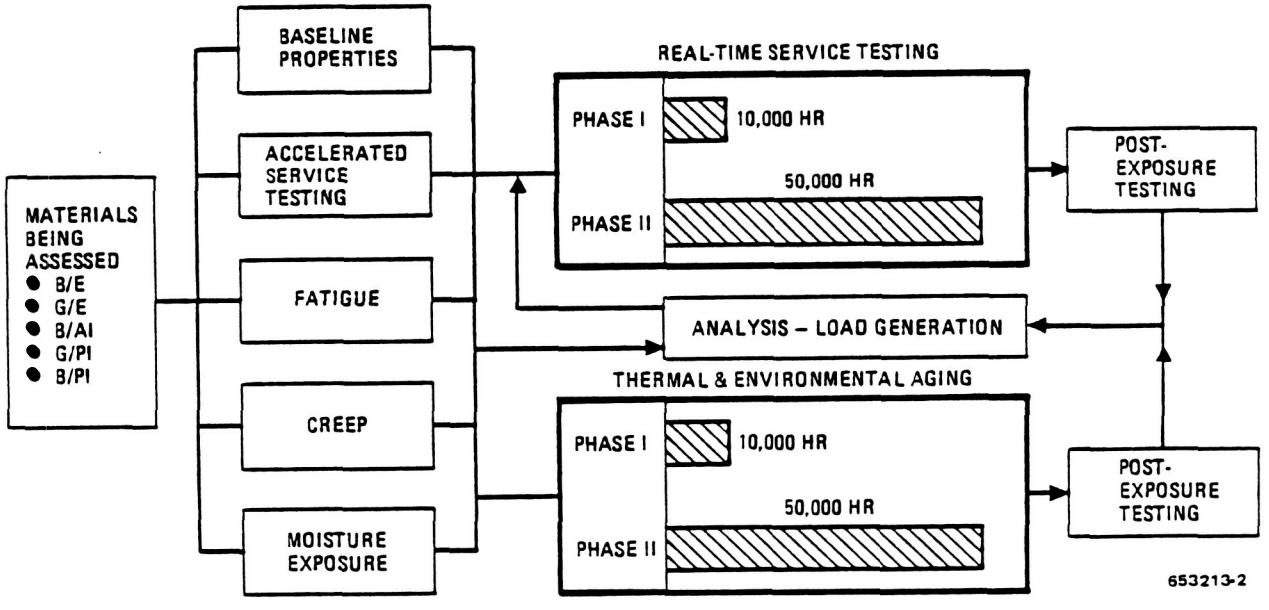



**Figure 2-1 Time-Temperature-Stress Capabilities of Composite Materials — Program Outline**

Figure 2-1 is a schematic diagram that shows the principal elements of this work. The baseline properties are typical mechanical properties for each of the composites, and these properties were generated in sufficient detail so that any changes in them due to repeated loading and thermal or environmental aging could be measured and reported. Fatigue life was measured before and after various load and temperature histories. The materials' creep behavior was measured early in the program in order to fully evaluate filamentary composites of this type. The aging characteristics of the materials were measured at various temperatures and pressures. A limited study of moisture exposure effects was included for the resin matrix materials. However, with this exception, moisture effects have been deliberately avoided by use of standard bakeout procedures prior to the various tests conducted during the program. Inclusion of moisture effects to each of the test areas was beyond the scope of the overall program.

The changes in baseline tensile and fatigue, notched tensile and fatigue, compressive, and shear properties that occurred during times out to 50,000 hours were measured for environmental and thermal aging conditions, as well as, random cyclic loading with cyclic temperature variations.

These latter tests were intended to simulate conditions experienced in a lower wing surface during supersonic flight and, hence, consisted almost entirely of tensile loads. For the same reason the majority of the residual property specimens were intended to be tested in tension. As will be discussed later, the failure modes and degradation mechanisms for the various exposure tests were found to be primarily matrix dominated. Because of these observations, residual compressive and shear tests were included with the tensile and fatigue tests already scheduled to increase the usefulness of the data.

One other change to the original program occurred as a result of the matrix dominated failure modes observed during Phase I. A study to determine the effects of thermal aging on the compressive properties of graphite/epoxy and graphite/polyimide was added during Phase II to supplement the thermal aging/tensile program conducted on all of the composites in Phase I.

In order to provide a device capable of simulating supersonic flight conditions of load and temperature, a machine was built that was capable of not only random loading and temperature variation but could test a large number of specimens at the same time. It was desirable that the apparatus be able to accommodate a large number of test specimens because of the expected data scatter associated with advanced composites. The machine was also capable of operating for long periods of time with little maintenance and monitoring and was designed in such a manner as to possess adequate safeguards against either overloading or overheating the specimens.

Several assumptions were made to define the loading spectrum. The mission profile and loads were obtained from reference 4. These data were also used for the study described in reference 5. The life of a supersonic airplane was assumed to consist of 25,000 flights of 2 hours duration each. For this work, each flight was assumed to be an "operational flight" as defined in reference 4. Each flight consisted of a 10-minute climb, a 90-minute cruise, a 20-minute descent, and a single landing load. The number of loads per flight and the number of loads in each of the segments were modeled after the reference 1 load sequence. However, the loads were randomized such that all the loads expected to occur in 25,000 flights were included. Since the 90-minute cruise was scheduled to include only about eight loads per flight, the mean load was held for 44 minutes before and after the imposition of a 2-minute cruise loading period. The climb and descent loads were distributed over the entire climb and descent time.

The job of setting load levels for each of the composites materials for the random load spectrum so that some but not all specimens would fail during the 50,000-hour program was indeed a difficult task. This had to be done by running accelerated tests in which many loads could be applied at elevated temperature in a fairly short time. We chose to apply a one-half lifetime of loads in 200 hours, which worked out to be about one load a second. The real-time flight spectrum is more like 20 loads per hour. The accelerated tests were run for both 100 and 200 hours at load levels such that we would have 80% survival if the tests were run to 400 hours.

The residual strength was measured after specimens had been subjected to one-fourth and one-half lifetime of loads at elevated temperature. These strengths were then used to calculate, using the Halpin wearout model (ref. 6), the load levels for real-time testing, again using 80% survival at the end of 50,000 hours.

The calculated mean and peak load levels set by the 80% survival for the 50,000 hours or one lifetime were used to set the real-time load levels for the flight simulator. These differed for each composite system and also differed for the notched and unnotched specimens of the same composite. Thus each composite system was to be subjected to 50,000 hours of real-time flight simulation testing using random loading and temperature described by the climb, cruise, and descent portions of the flight.

Following completion of the 10,000-hour Phase I portion of flight simulation exposure, half of the specimens were removed from test. An extensive examination of the specimens was conducted to determine the extent of damage and, for those specimens that had failed, to identify the degradation mechanisms responsible for these early failures. The specimens that survived the 10,000 hours of flight simulation exposure were used to determine residual tensile and fatigue, notched tensile and fatigue, compressive, and shear properties. At the end of Phase I, two modifications were made to the test plan. Because of the high failure rate and extensive visual degradation of the epoxy specimens, all the remaining epoxy specimens were removed and new specimens were fabricated to replace them. A significantly reduced cruise temperature (calculated from thermal aging data) was used for subsequent flight simulation testing of these replacement specimens.

The second modification was the addition of three more flight simulation specimens of each material to be exposed for 25,000 hours. The specimens remaining in the simulator after Phase I were intended to complete 25,000 or 50,000 hours of exposure in Phase II and provide residual strength data similar to that obtained in Phase I. As will be shown, this goal of 50,000 hours was not realized. However, considerable residual strength data was obtained from specimens that survived exposures up to 36,000 hours, as well as, from the undamaged portions of specimens that failed after times up through 40,000 hours. The results of these long-term flight simulation tests, both Phase I and Phase II, were then compared with the wearout model predictions based on accelerated flight simulation exposure.

# SECTION 3

# MATERIAL SELECTION AND ACQUISITION

The "Structural Design Guide for Advanced Composites Applications" (ref. 7) has limited the term "advanced composites" to those systems characterized by high-strength, high-modulus fibers. For this study, advanced composites are those systems whose reinforcements have a filament tensile strength greater than 2100 $MN/m^2$ (300 ksi) and a filament modulus greater than 210 $GN/m^2$ (30 million psi).

At the time this contract was initiated, a multitude of advanced composite material systems had been developed and evaluated to various degrees. In general, five classes of material systems had been used by numerous workers in this field: boron/epoxy (B/E), graphite/epoxy (G/E), boron/polyimide (B/PI), graphite/polyimide (G/PI), and boron/aluminum (B/Al). Within each of these five classes there were several types of matrix materials and different types of fibers. The following sections discuss each of the five classes of materials and Convair's choices as to the specific advanced composite systems that were evaluated. It should be pointed out that this program was started in the early 1970s, and selection of all but one of the composite materials was based on the best available systems at that time. The exception was the second G/PI, Celion 6000/LARC-160, that was added after the completion of Phase I in 1980.

## 3.1 MATERIAL SELECTION

**3.1.1 METAL MATRIX COMPOSITE MATERIAL.** Table 3-1 shows the large variety of filaments and matrix materials that were available when the program was initiated. Table 3-2 lists a number of the most promising and widely used processing methods for the primary fabrication of sheet, plate, and structural shapes of metal-matrix composite materials.

**Table 3-1. Metal-Matrix Composite Raw Materials**

| Fibers | Matrix |
|---|---|
| Boron (4 mil) | Aluminum |
| Boron (5.6 mil) | 1100 |
| Borsic (4.2 mil) | 2024 |
| Borsic (5.7 mil) | 2219 |
| Nitride-coated Boron | 6061 |
| Silicon Carbide | 7002 |
| Stainless Steel | 7075 |
| Graphite | 7178 |
| | 713 |
| | 718 |
| | K01 |
| | Magnesium |
| | Titanium |
| | Nickel |

Table 3-2. Primary Processing Methods

| Processing Method | Typical Forms Produced |
|---|---|
| Diffusion Bonding | Mono- or multilayer tape, sheet, plate, structural shapes |
| Braze Bonding | Mono- or multilayer tape, sheet, plate, shapes |
| Eutectic Bonding | Sheet, plate, structural shapes |
| Plasma Spraying | Monolayer tape |
| Molten-metal Infiltration (Casting) | Mono- or multilayer tape, sheet, plate, structural shapes |

It has been found that no one metal-matrix composite material is superior for all possible applications. However, data based on filament-matrix compatibility, comprehensive physical and mechanical property tests, primary and secondary fabrication studies, raw material and processing costs, and extensive experience in working with composite materials indicated that diffusion-bonded B/Al, in particular the large diameter (5.6-mil) boron with 6061 aluminum matrix, offered the most promise for widespread structural applications in various aircraft systems. B/Al composite material had also been found to be highly resistant to various environmental exposures, with excellent retention of properties at cryogenic and elevated temperatures, and with little or no effect of space exposures on mechanical or physical properties. Another attribute of B/Al, and metal-matrix composite material in general, was its very high transverse modulus, about 140 $GN/m^2$ (20 million psi) for B/Al. This enables the use of unidirectional layups in a number of structural applications that would not be possible with organic-matrix materials with their low transverse modulii. Because of these considerations (ref. 8 to 14) diffusion bonded, 5.6 mil boron/6061 aluminum was chosen for evaluation on this program.

Single-step hot pressing was the technique selected for fabricating the B/Al sheet material because of the ability to produce large panel sizes in a single pressing operation, and because of lower processing costs. In this method, boron filaments are wound over a mandrel onto thin-gage sheet material. These layers are then cut and stacked to the desired thickness and the material consolidated in a hot press. Because of more economical production of large sheet material in pressing operations, this method was chosen over the isostatic pressing technique that required consolidation of prefabricated laminates (tape material). At the beginning of the program two qualified suppliers were available. They had been using the single-step hot pressing technique to supply high-quality metal-matrix composites on a production basis for numerous hardware programs at Convair and other laboratories.

### 3.1.2 RESIN MATRIX COMPOSITE MATERIAL

**3.1.2.1 Boron/Epoxy.** At the time that this program started B/E was the most highly characterized of the advanced composite materials. As a result of approximately 7 years of evaluation, the industry had generally settled on two resin systems (Avco 5505 and 3M

SP-272). 3M also provided the same resin on uncoated boron (SP-292) and maintained the same basic properties. Other 3M systems such as SP-290 had some better high-temperature properties than the SP-292 but were not as thoroughly characterized. General Dynamics had generated extensive design-allowable data on the Avco 5505 under Contracts F33615-68-C-1474 and AF33(615)-5257 (ref. 15 and 16). Convair preferred the Avco 5505 system because of its somewhat higher temperature resistance and its wide application at that time.

Most early work, conducted by Convair and elsewhere, used the 4.0-mil boron filaments. Some work had been conducted using 5.6- and 6.0-mil-diameter boron filaments, but selection of the 4.0-mil filament was made to avoid an extensive program necessary to characterize the larger diameter material. Considerable engineering data already existed on the coated 4.0-mil diameter boron including static and fatigue characteristics for many configurations with and without imperfections. IITRI (ref. 17) generated extensive data on the effects of environmental exposure on the mechanical and physical properties of the 4.0-mil Avco 5505. Since the purpose of this program was to evaluate long-term effects, selection of a fully characterized system was desirable. In addition, the long-term effects were thought to be primarily matrix dependent and independent of filament diameter.

**3.1.2.2 Graphite/Epoxy.** Convair had worked on high-strength, high-modulus graphite fibers as a reinforcement for epoxy and polyimide resins since 1965. In this period there had been a proliferation of graphite fibers. Early fibers based on visose rayon, such as Thornel 25, Thornel 40, and HITCO HMG-30, had been surpassed and were no longer seriously considered for structural aircraft applications. Newer fibers, primarily based on polyarcrylonitrile precursors, had become the serious contenders for present and future aircraft applications. These fibers could be generally divided into four categories:

a. Low modulus/ultra-high strength.

b. Medium modulus/high strength.

c. High modulus/medium strength.

d. Ultra-high modulus/medium strength.

The first category of low modulus, 207 to 221 $GN/m^2$ (30 to 32 million psi), coupled with ultra-high strength, greater than 2760 $MN/m^2$ (400 ksi), was finding most usage in current aircraft applications because of its high strength and very low cost. Fibers that fell in this category were Hercules Type A-S and Stackpole Panex 30/A. Others having the same modulus but somewhat lower strength were Thornel 300, Fortafil 30-T, and Morganite III. Type A-S had had the most usage at that time. General Dynamics has used this type of fiber extensively in the F-111 pivot fitting fairing program and the F-5 fuselage program.

The second category of fibers, those having medium modulus, 262 to 276 $GN/m^2$ (38 to 40 million psi), and high strength, greater than 2410 $MN/m^2$ (350 ksi), included such products as HT-S, Modmor Type II, and Fortafil 4-T and had been used extensively in the preceding years. They were inherently costlier than the 207 $GN/m^2$ (30 million psi) fibers and were expected to have lower utilization in the future than they had in the past.

The third category of fibers, those having high modulus, 345 to 414 $GN/m^2$ (50 to 60 million psi), and medium strength, 2070 to 2760 $MN/m^2$ (300 to 400 ksi), included such products as

HM-S, Modmor Type I, and Fortafil 6-T. These fibers had not been used as extensively as the first two categories because of higher cost, lower strength, and poorer resin compatibility (lower shear strength in composites).

The fourth category of fibers, those having ultra-high modulus, greater than 483 $GN/m^2$ (70 million psi), and medium strength, 1520 to 2240 $MN/m^2$ (220 to 325 ksi), included GY-70 and Thornel 75 materials. They had the same general problems as the third category described above.

Based on the above review of available graphite fibers, Convair selected the epoxy resin-impregnated Type A-S fiber.

In the area of high-temperature 450 K (350 ° F) epoxy resins, there had also been a profileration of candidate systems. Up to 1971, the prime resins evaluated and used for structural aerospace applications were Fiberite X-904, Hercules 3002, Whittaker 5205 and 5206. The 3002 was extensively evaluated for design properties by IITRI (ref. 17) and North American Rockwell (ref. 18). However, the 3002 was adversely affected by moisture, was costly, and was difficult to process into prepreg; the availability of this resin for future programs was in doubt at this time period.

In 1972 and 1973 a number of new high-temperature epoxy resins had been introduced, such as Ferro E-350 and E-450; Fiberite X-911, X-915, and X-934; Whittaker 5208; and Hercules 3501. Of these, the E-350, X-934, 5208, and 3501 were seeing the most use in evaluations and in production of aircraft parts.

Convair conducted an extensive screening of in-house data, vendor information, and outside literature relating to the newer high-temperature epoxy resins. The leading candidates were Ferro E-350 and Hercules 3501 with the E-350 appearing to be slightly better. However, at that time Ferro Corporation had recently moved its plant, lost some key personnel, and was leaving the graphite prepreg business. In addition to the favorable rating in the screening evaluation, the A-S/3501 system was currently being used in large commercial applications, was being evaluated extensively for missile applications, and was believed to be the system that would be the standard G/E composite for aircraft applications. Based on these considerations and an excellent cost picture, the A-S/3501 system was selected for the program.

**3.1.2.3 Boron/Polyimide.** Early studies of B/PI composites were conducted with the P13N, P10P, and 703 polyimide resin systems (ref. 19 to 23). Initially, attention was paid strictly to the fabrication of low-void laminates. As such, the prepegs were tack-free, highly imidized materials that were acceptable for making flat laminates but unacceptable for large parts. Later work led to modifications in the P13N and P10P resin systems to produce P105A, which was the first step toward developing a tacky prepreg that would yield low-void polyimide laminates. At about this time Convair under contracts NAS 8-26198 "Development of Boron and Graphite Polyimide Design Data," and NAS 8-28201, "Polyimide Compression Panel," was investigating the development and use of B/PI advanced composites. Some of the candidate resin systems evaluated were: 700, 703, 709, 710, P13N, P10P, P105A, Gemon L, 4707, and BPI-373. Two of these, P105A and 703, were selected for additional processing studies, and some preliminary test data were developed for each system using both the 5.6- and 4.0-mil diameter boron fiber. Test results showed that 1) the data for the B/P105A composite system was significantly better than the B/703 composite system, and 2) the 4.0-mil boron fiber was

superior to the 5.6-mil boron fiber in that resin contents and laminate shear properties were higher (ref. 24). For these reasons the 4.0-mil boron fiber and the P105A polyimide resin system were selected for the program. At about the time that the B/PI composite was being selected, Ciba-Geigy, the manufacturer of the resin, replaced the P105A with a newer version designated P105AC. It was this polyimide that was evaluated on the test program.

**3.1.2.4 Graphite/Polyimide.** Unlike the B/PI composite systems, a fully developed and characterized G/PI system was available at the time that the program was initiated. The G/PI system (HT-S/710) was developed by Convair under Contract NAS 8-26198 (ref. 24). Substantial quantities of mechanical property, thermal aging (short time), moisture resistance, and creep data were available on this system (ref. 25). At the same time, under Contract NAS 8-28201 (ref. 26), Convair was determining baseline design properties for A-S/710 G/PI composite systems. These data were used to design, fabricate, and analyze a large compression panel for short-term applications at 589 K (600° F). Based on the results of these two contracts, Convair selected the HT-S/710 system.

The HT-S graphite fiber was selected because of its high strength and lower weight loss at 589 K (600° F) than the Type A-S graphite fiber. Data developed and reported by Morgan Hanson of the NASA Lewis Research Center at the National SAMPE Conference in Huntsville, Alabama in 1971 indicated that the Type A-S fiber oxidized severely at 589 K (600° F). After 1000 hours, the uncoated A-S fiber had weight losses approaching 100 % (ash). What happens in a composite was unknown. However, for this program Convair believed the extra $5 to $10 per pound for the HT-S fiber was justified since it had higher oxidative stability than the Type A-S fiber. The A-S fiber appeared to be fully acceptable for use at 450 K (350° F) with epoxy resin systems but not for use at 589 K (600° F) with polyimide systems.

The 710 resin system was selected because it was believed to be fully characterized, compatible with graphite fibers, commercially available as prepreg from three material suppliers, and showed higher temperature stability than any of the other then available polyimide resins.

One of the goals of the overall program was to follow the progress of advanced composite systems development and to add new materials if sufficiently promising ones appeared. Prior to the completion of Phase I, but several years into the program, several high temperature graphite fiber reinforced polyimide systems were beginning to become commercially available, and a decision was made to add one of the these to the program. To select the best of these emerging systems a screening test was planned. The selection criteria were:

a. Availability and cost of prepreg material.

b. Ability to fabricate both full-size 12-ply panels and a simple structural shape.

c. Moisture resistance.

d. High temperature thermal stability and oxidation resistance.

Three resin systems with the HT-S graphite fiber were to be evaluated. The HT-S fiber was chosen because it was the reinforcement used in the system already in the program (HT-S/710).

The potential candidates at that time are listed in Table 3-3. Of those only the NR-150B2, PMR-15, and HR-600 were considered likely candidates, and only the first two were available from a commercial prepregger. The remaining resins were eliminated because of insufficient

Table 3-3. Candidates for a Screening Evaluation to Select an Additional Graphite Polyimide System

| Material System | Potential Vendors |
|---|---|
| HT-S/NR-150B2 | Narmco, Fiberite, U.S. Polymeric |
| HT-S/PMR-15 | U.S. Polymeric, Ferro |
| HT-S/HR-600 | Fiberite |
| HT-S/5230 | Narmco |
| HT-S/F-178 | Hexcel |
| HT-S/4397 | Hercules |

high temperature thermal stability and oxidation resistance. A screening test was conducted on HT-S/NR-150B2 and HT-S/PMR-15 with the current system, HT-S/710, included as a baseline comparison. A major portion of the screening evaluation was devoted to thermal aging exposures.

Drastic decreases in weight and flexural strength were observed for all three systems. The poor results were traced to a lack of elevated temperature stability, with very high weight loss, of the HT-S graphite fiber (ref. 27). Modifications in the fiber processing conditions at the producer during this time period (several years after the purchase of the initial HT-S/710) appeared to have been responsible for the changes. Because of the unacceptable thermal aging results, testing of the three systems was discontinued. Since General Dynamics did not believe that HT-S fiber with good elevated temperature stability could be obtained at that time, it was necessary to select another graphite fiber. The most promising choices were Modmor II, Celion, and HT-S-2, a low-sodium modification of HT-S. At about this time Morganite Ltd. discontinued the manufacture of Modmor II graphite fiber. For the two remaining fibers, good results during high temperature aging studies (on both bare fibers and panels) had been reported for both. Availability, current and future, as well as a somewhat larger data base favored Celion fiber at that time, and it was selected.

For the renewed screening test program, batches of Celion 6000/710, Celion 6000/NR-150B2, and Celion 6000/PMR-15 were obtained. They were ordered with an epoxy sizing on the Celion 6000 graphite fiber. The sizing was necessary to facilitate handling of the graphite during the prepregging operation. An epoxy rather than a polyimide sizing was selected because at the time of placing the order it was the only material available. In addition, previous studies at Convair had shown that Celion/NR-150B2 G/PI panels fabricated from both epoxy sized and polyimide sized fiber were essentially identical with regard to fabricability and short time mechanical properties. The small amount of sizing (approximately 0.2 to 0.4%) is uncured and dissolves into the matrix during fabrication. Even though this small amount of epoxy resin is probably not detectable after cure and post cure of a panel, the question arose as to its effect after long time thermal exposure (i.e., 50,000 hours at 450 °F). Because no data were available on long-time effects, the decision was made that for the SCR program only polyimide sized graphite would be used. Consequently, revised purchase orders were prepared for prepreg with polyimide sized graphite.

The screening evaluation was becoming a much longer program than originally planned. Several important events occurred during this time period (1980-1981). First, the 710 resin that

had been removed from production by Monsanto somewhat earlier was now no longer available as all the stock had been depleted. Second, the NR-150B2 resin producer, DuPont, terminated sales because current and projected profitability did not justify continued production. Third, a very promising polyimide resin, LARC-160, developed at NASA Langely Research Center was becoming commercially available.

Because of the lengthy delays that had occurred it became evident that if a new material was to be added to the program it must be done very soon. Further delays could prevent completion of the thermal aging and flight simulation exposures of this material by the time that the Phase II tests on the original materials were finished.

Consequently, the planned screening tests were canceled, and selection of the new material was made based on current data and prepreg availability. Because of availability, the choice was limited to Celion 6000/PMR-15 and Celion 6000/LARC-160. The LARC-160 system was selected because of superior fabricability. At that time the PMR-15 system required a press cure for panel fabrication. In addition, the Celion 6000/PMR-15 prepreg tended to be quite boardy, and fabricated panels had shown a greater tendency to microcrack.

### 3.2 MATERIAL ACQUISITION

Because of changes in the scope of the Phase II test program, the addition of a new material, and the added thermal aging/compression study, it was necessary to purchase material at three times during the performance of the contract. The initial order was made in 1973 for the five composite systems selected at the beginning of Phase I. The second order was made in 1976 for B/E, G/E, HT-S/710 G/PI, and B/Al systems to be used in the new material screening evaluation. The final order was placed in 1980 for Celion 6000/LARC-160 G/PI and G/E to satisfy the requirements of the new material addition and the thermal aging/compression evaluation.

The following sections describe the procedures involved in purchasing the advanced composite systems selected for evaluation on this program. For three of the materials, B/E, B/Al, and Celion 6000/LARC-160 G/PI, little or no difficulties were encountered in procurement or during quality assurance testing. For three of the materials, however, considerable problems occurred either in acquiring the prepregs or during acceptance testing.

**3.2.1 METAL-MATRIX COMPOSITE MATERIAL.** The 5.6-mil boron/6061 aluminum composite, referred to as B/Al, was obtained from AVCO Corporation, Systems Division, Lowell, Massachusetts. The material, ordered to General Dynamics Specification 0-00854, was received in the form of finished sheets, 0.3 m by 0.6 m (12 in. by 24 in.) in dimensions. The requirements for the program were:

Phase I

- 6 ply, $[0° \pm 45°]_s$ layup — 11 sheets
- 12 ply, $[0° \pm 45°]_{s2}$ layup — 1 sheet
- 6 ply, $[0°]_6$ layup — 14 sheets
- 12 ply, $[0°]_{12}$ layup — 1 sheet

Phase II

- 6 ply, $[0° \pm 45°]_s$ layup — 1 sheet
- 6 ply, $[0°]_6$ layup — 2 sheets

Delivery of the B/Al was on schedule, and, with the exception of one 6-ply unidirectional panel, all were of acceptable quality. The one panel showed indications of poor bonding during ultrasonic C-scan testing and was returned to AVCO for replacement.

### 3.2.2 RESIN MATRIX COMPOSITE MATERIAL

**3.2.2.1 Boron/Epoxy.** The Rigidite 5505/4 boron/epoxy composite, referred to as B/E, was also obtained from AVCO Corporation, Systems Division, Lowell, Massachusetts. The material was ordered to meet the requirements of General Dynamics Specification FMS-2001B. A total of 12.7 kg (28 lb) in the form of 0.08 m (3 in.) wide prepreg tape was required for Phase I. An additional 1.8 kg (4 lb) was required for Phase II of the program. The material was delivered on schedule and successfully passed all the quality assurance requirements for both the prepreg and fabricated laminates.

**3.2.2.2 Graphite/Epoxy.** The A-S/3501-5 graphite/epoxy, referred to as G/E, was obtained from Hercules Incorporated, Bacchus Works, Magna, Utah. Three batches were required to meet the needs of the program. At the beginning of Phase I 17 kg (37 lb) of 0.08 m (3 in.) wide prepreg tape was purchased to the following Hercules Specifications: fiber properties per HD-SG-2-6001; prepreg properties per HD-SG-2-6006A except flow to be run at 436 K (325 ° F), 100 psi, 15 minutes; composite properties per HD-SG-6002A. This batch of material was received on schedule and checked out perfectly in the prepreg quality assurance tests. The flexural and short beam shear properties determined from the quality assurance panels were also satisfactory. Based on these quality assurance results, 12 full size panels were fabricated for the test program. The baseline tensile data, however, were widely scattered and significantly lower than normal. The transverse tensile strengths were particularly bad, with an average value of 22.8 $MN/m^2$ (3.3 ksi) at room temperature. To check that the panels were unacceptable, resin and fiber content determinations and three tensile tests were made on each of the 6-ply unidirectional and crossply panels. The results are given in Table 3-4. The wide scatter and generally low values are clearly evident. Expected values of $F_{tu}$ are about 1400 $MN/m^2$ (200 ksi) and 55 $MN/m^2$ (8 ksi) for the longitudinal and transverse directions of the unidirectional layups and about 550 $MN/m^2$ (80 ksi) for the crossply layups. The resin and fiber contents shown in Table 3-4 are all acceptable, although Panel No. 10 has a somewhat low fiber content. A check with the vendor (Hercules) revealed that the material was among the first to come off the line from a new prepregging process. Although the resin content was acceptable (determined during quality assurance testing), the resin distribution through the material was poor because of a lack of penetration into the graphite tows. Similar results were reported by others from material obtained during the same time period. Hercules corrected the production problem and replaced the material at no charge, but a considerable time delay was incurred because of the rejected material.

Visual examination of the replacement batch of G/E prepreg revealed none of the resin poor areas that were typical of the previously rejected batch. The material successfully passed all of the quality assurance requirements for both the prepreg and fabricated laminates. As an added check on the acceptability of the panels, tensile coupons were prepared from unused portions of the unidirectional quality assurance panel and the first full size crossply panel. The values obtained, 1655 $MN/m^2$ (240 ksi) and 579 $MN/m^2$ (84 ksi), were typical of good G/E material. Transverse tensile tests on the unidirectional panel gave an average ultimate strength of 59 $MN/m^2$ (8.6 ksi). This value is again typical of good G/E material.

Table 3-4. Quality Assurance Data for G/E Panels from Rejected Batch of A-S/3501-5 Prepreg

| Panel No. | Orientation | Plies | Resin Content (wt %) | Fiber Content (vol. %) | Tensile Strength $MN/m^2$ | Tensile Strength (ksi) |
|---|---|---|---|---|---|---|
| 10 | $[0°]_6$ | 6 | 36.2 | 55.5 | 1310 | 190 |
| | | | | | 752 | 109 |
| | | | | | 696 | 101 |
| 11 | $[0°]_6$ | 6 | 32.6 | 59.4 | 1080 | 157 |
| | | | | | 1350 | 196 |
| | | | | | 1380 | 200 |
| 13 | $[0°]_6$ | 6 | 32.2 | 59.8 | 1903 | 276 |
| | | | | | 1510 | 219 |
| | | | | | 1030 | 150 |
| 16 | $[0°]_{12}$ | 12 | 27.8 | 64.6 | [a]1640 | [a]238 |
| | | | | | [a]1730 | [a]251 |
| | | | | | [a]1780 | [a]258 |
| 17 | $[0° \pm 45°]_{s2}$ | 12 | 28.5 | 63.8 | [a] 786 | [a]114 |
| | | | | | [a]793 | [a]115 |
| | | | | | [a]848 | [a]123 |
| 22 | $[0° \pm 45°]_s$ | 6 | 32.3 | 59.7 | 331 | 48 |
| | | | | | 379 | 55 |
| | | | | | 352 | 51 |
| 23 | $[0° \pm 45°]_s$ | 6 | 31.7 | 60.4 | 337 | 49 |
| | | | | | 317 | 46 |
| | | | | | 483 | 70 |
| 24 | $[0° \pm 45°]_s$ | 6 | 30.9 | 61.2 | 414 | 60 |
| | | | | | 434 | 63 |
| | | | | | 538 | 78 |
| 25 | $[0° \pm 45°]_s$ | 6 | 29.2 | 63.2 | 414 | 60 |
| | | | | | 414 | 60 |
| | | | | | 455 | 66 |
| 26 | $[0° \pm 45°]_s$ | 6 | 30.6 | 61.6 | 345 | 50 |
| | | | | | 538 | 78 |
| | | | | | 379 | 55 |

[a]Flexural strength.

The second batch, 2.3 kg (5 lb) of a 0.08 m (3 in.) wide prepreg tape, was purchased at the completion of the Phase I 10,000 hour flight simulation tests. The third batch, 5.4 kg (12 lb) of 0.3 m (12 in.) wide prepreg tape, was ordered midway through Phase II to provide test specimens for the add-on effort to study the effect of thermal aging on compression properties. Both of these orders were delivered on schedule and passed all the quality assurance requirements for both the prepreg and fabricated laminates. At the time of the last purchase the designation had changed from A-S/3501-5 to A-S/3501-5A. Data sheets from Hercules Incorporated for the two designations showed them to be very similar with only a few slight differences in properties.

**3.2.2.3 Boron/Polyimide.** The 4.0-mil B/P105AC boron/polyimide, referred to as B/PI, was obtained from AVCO Corporation, Systems Division, Lowell, Massachusetts. As no General Dynamics procurement specification existed, the material was ordered to the following requirements:

a. Fiber Strength: 500,000 psi minimum

b. Resin Content: 38 to 48%

c. Volatiles: 10 to 20%

d. Flow: 450 K (350° F) 30 to 42%

A total of 28 kg (62 lb) of prepreg in 0.3 m by 1.8 m (12 in. by 72 in.) sheets was required for the program. Delivery of the prepreg was delayed approximately 3 months because of difficulties encountered by AVCO in obtaining the polyimide resin from the manufacturer, Ciba-Geigy. Upon receipt of the prepreg, quality assurance testing was performed. The material was found to be acceptable and two quality assurance panels were fabricated. Quality assurance testing of the laminates was completed with the material being found acceptable. While the B/PI material passed the prepreg and laminate quality assurance requirements, it was later removed from the test program because of low tensile properties and extensive thermal degradation observed during thermal aging and short-term flight simulation testing. Complete details of the problems encountered with this material system and the reasons for the poor results are found in Appendix A.

**3.2.2.4 Graphite/Polyimide.** The graphite/polyimide (G/PI) system selected at the beginning of the contract was HT-S/710. In like manner to the G/E material, three batches were required: one for Phases I and II, one for the Phase II 25,000 hour flight simulation tests and the G/PI new material screening evaluation, and the third for the add-on effort to study the effects of thermal aging on compression properties. A second G/PI system, Celion 6000/LARC-160, was added midway in the contract for testing to the Phase I requirements including 10,000 hours of thermal aging and flight simulation exposure and for evaluation in the add-on thermal aging/compression study.

**HT-S/710 G/PI.** This composite system was the most difficult material to procure. More than a year passed from the time of placing the initial order until completion of quality assurance testing and acceptance of the test material. One of the reasons for selecting HT-S/710 was the belief that the prepreg was readily available from at least three material suppliers. As it turned out one source was not interested in the small volume required for the program while the other two sources experienced considerable problems in fabricating acceptable prepreg. Because no General Dynamics procurement specification existed the material was ordered to the following requirements:

a. Fiber Strength: 350,000 psi minimum

b. Resin Content: 35-45%

c. Volatiles: 10-20%

d. Flow: 15-25%

e. Acid Equivalent No.: 520 to 540

The following is a chronological account of how the initial material was obtained.

Jul 1973 — An order for 17 kg (37 lb) of prepreg tape was placed with E.I. DuPont De Nemours and Company, Fabrics and Finishes Department, Saugus, California.

Aug 1973 — The prepreg was delivered on schedule but was rejected because of low fiber volume and low acid equivalent number.

Sep 1973 — A second batch was delivered. The prepreg properties were within specification requirements; however, a panel fabricated from the prepreg showed precipitation and waviness. At this time a second source of the prepreg was being checked. Hercules Incorporated quoted a 50% higher price and an 8 to 10 week delivery schedule. DuPont reported that they discovered that the resin used to fabricate the first two batches of prepreg was bad and that a third batch, made with new resin, would be prepared.

Oct 1973 — The third batch of prepreg delivered by DuPont failed to produce acceptable panels and was also rejected. A new order was placed with Hercules for the 17 kg (37 lb). While the price was about 50% higher, Hercules had had considerable experience with the prepreg, and no further difficulties were anticipated. Delivery, however, was not expected until December 1973.

Dec 1973 — Delivery was delayed to allow the acid equivalent number of the polyimide resin to reach an acceptable value prior to manufacturing the prepreg.

Jan 1974 — Delivery was further delayed when it was determined that the HT-S graphite fibers were not within specifications. A new batch of fibers was obtained and manufacture of the prepreg material was scheduled for February 1974.

Feb 1974 — The first batch of prepreg manufactured by Hercules failed to meet specifications. A second batch was prepared from the remaining fiber and resin. This material was found to be acceptable, but the quantity was less than that ordered, 11 kg (24 lb) of an order of 17 kg (37 lb). Because of the high costs incurred and the small size of the order Hercules was not willing to complete the order.

Mar 1974 — DuPont agreed to prepare a demonstration sample of prepreg. If the material was found to be satisfactory an order for the 17 kg (37 lb) was to be given to them.

Apr 1974 — DuPont reported a delay in preparation of the demonstration sample because of out of date resin that was unacceptable for manufacturing prepreg. A new batch of resin was ordered from Monsanto.

May 1974 — The small demonstration sample of prepreg was received from DuPont. The first panel fabricated from this batch was acceptable, but later panels tended to precipitate and blister. Because of these inconsistencies no order was placed with DuPont. As a result of the numerous delays encountered in obtaining the material it was decided that the 11 kg (24 lb) batch produced by Hercules would be purchased for the test program if satisfactory test panels could be fabricated. It was thought that sufficient panels could be made from the 11 kg (24 lb) to satisfy the program requirements. A small test sample was, therefore, ordered from Hercules.

| | |
|---|---|
| Jun 1974 | The sample submitted by Hercules was evaluated and found to produce an excellent laminate. To check the consistency of the prepreg a second panel was fabricated, and, again, an acceptable laminate was obtained. Based on these results the remaining 10 kg (22 lb) of prepreg were purchased from Hercules. |
| Jul/ Aug 1974 | The material was delivered and successfully passed all of the quality assurance requirements for both the prepreg and fabricated laminates. |

The second batch of HT-S/710, 4.1 kg (9 lb) of 0.08 m (3 in.) wide prepreg tape, was purchased from E.I. DuPont De Nemours and Company. The material was delivered on schedule and passed the prepreg requirements. Quality assurance results from a fabricated laminate were comparable to those obtained from the Phase I batch and the material was accepted.

The third batch of HT-S/710 G/PI, required for the thermal aging/compression study, could not be obtained. As discussed in Section 3.1.2.4, problems existed with both the fiber and the resin system.

**Celion 6000/LARC-160.** The Celion 6000/LARC-160 graphite/polyimide composite was obtained from Fiberite Corporation, Winona, Minnesota. Twenty-three kg (50.7 lb) of 0.3 m (12 in.) prepreg tape were purchased to a Fiberite specification for hy-E1678E. The material was received on schedule and passed all the quality assurance requirements for both the prepreg and fabricated laminates.

# SECTION 4

# PREPREG QUALITY ASSURANCE TESTING

The organic matrix composite materials were purchased to specific requirements on the purchase orders or, when available, to existing General Dynamics or industry specifications. To ensure that these requirements were satisfied the following properties were determined upon receipt of the prepreg:

a. Fiber content (percentage by weight).

b. Resin solids (percentage by weight).

c. Volatiles (percentage by weight).

d. Resin flow (percentage by weight).

e. Process gel.

A description of the test methods that were used is given in Appendix B.

## 4.1 BORON EPOXY

B/E was purchased from AVCO Corporation to General Dynamics Specification FMS-2001B. Two batches of material were obtained during the program.

The FMS-2001B specification requirements, the values from the AVCO Certified Test Reports received with the shipments, and the results of the Convair quality assurance tests are given in Tables 4-1 and 4-2. Both the AVCO and Convair results for batch one satisfied the procurement specification requirements and the material was considered to be acceptable. For batch two, the Convair results for resin solids and resin flow were slightly above the procurement specification requirements but the material was considered acceptable contingent on satisfying the laminate quality assurance tests.

**Table 4-1. Prepreg Requirements and Properties for Rigidite 5505 B/E — Batch One**

| Property | Requirements of Specification FMS-2001B, % | AVCO Certified Test Report Data, % | Convair Quality Assurance Test Results, % |
|---|---|---|---|
| Fiber Content (wt %) | — | — | 68.1 |
| Resin Solids Content (wt %) | 29-34 | 31.7 | 31.0 |
| Volatile Content (wt %) | 2% max. | 1.08 | 0.9 |
| Resin Flow (wt %) | 10-20 | 13.5 | 15.7 |

Table 4-2. Prepreg Requirements and Properties for Rigidite 5505 B/E — Batch Two

| Property | Requirements of Specification FMS-2001B, % | AVCO Certified Test Report Data, % | Convair Quality Assurance Test Results, % |
|---|---|---|---|
| Fiber Content (wt %) | — | — | 64.5 |
| Resin Solids Content (wt %) | 29-34 | 32.7 | 34.8 |
| Volatile Content (wt %) | 2% max. | 0.6 | 0.7 |
| Resin Flow (wt %) | 10-20 | 17.0 | 24.9 |

## 4.2 GRAPHITE EPOXY

The G/E prepreg was purchased from Hercules Incorporated to Hercules Specification HD-SG-26006A. Three batches of material were obtained during the program.

The HD-SG-2-6006A specification requirements, the values from the Hercules Quality Assurance tests received with the shipments, and the results of the Convair Quality Assurance tests are given in Tables 4-3 through 4-5. Both the Hercules and Convair results satisfied the procurement specification requirements and the materials were considered to be acceptable.

Table 4-3. Prepreg Requirements and Properties for A-S/3501-5 G/E — Batch One

| Property | Requirements of Specification HD-SG-2-6006A, % | Hercules Quality Assurance Test Results, % | Convair Quality Assurance Test Results, % |
|---|---|---|---|
| Fiber Content (wt %) | — | 58.3 | 57.2 |
| Resin Solids Content (wt %) | 39-45 | 40.5 | 41.6 |
| Volatile Content (wt %) | 2% max. | 1.2 | 1.2 |
| Resin Flow (wt %) | 15-35 | 18 | 21.7 |

Table 4-4. Prepreg Requirements and Properties for A-S/3501-5 G/E — Batch Two

| Property | Requirements of Specification HD-SG-2-6006A, % | Hercules Quality Assurance Test Results, % | Convair Quality Assurance Test Results, % |
|---|---|---|---|
| Fiber Content (wt %) | — | — | 58.8 |
| Resin Solids Content (wt %) | 39-45 | 41 | 40.7 |
| Volatile Content (wt %) | 2% max. | 0.61 | 0.49 |
| Resin Flow (wt %) | 15-35 | — | 21.1 |

Table 4-5. Prepreg Requirements and Properties for A-S/3501-5A G/E — Batch Three

| Property | Requirements of Specification HD-SG-2-6006A, % | Hercules Quality Assurance Test Results, % | Convair Quality Assurance Test Results, % |
|---|---|---|---|
| Fiber Content (wt %) | — | — | 56.1 |
| Resin Solids Content (wt %) | 39-45 | 43.6 | 43.2 |
| Volatile Content (wt %) | 2% max. | — | 0.7 |
| Resin Flow (wt %) | 15-35 | — | 24.5 |
| Fiber Areal Weight ($gm/m^2$) | — | 146 | 151 |

## 4.3 BORON POLYIMIDE

The B/PI prepreg was purchased from AVCO Corporation with a list of Convair requirements. No procurement specification or industry specification was available. Table 4-6 lists these Convair requirements, the values from the AVCO Certificate of Conformance received with the shipment, and the results of the Convair quality assurance tests. All of the AVCO and Convair results except for the slightly high Convair value for volatile content satisfied the Purchase Order requirements. The small difference, 0.7% high, was not considered to be sufficient cause for rejection of the shipment.

Table 4-6. Prepreg Requirements and Properties for B/P105AC B/PI — Resin Batch Number 5-73, Sheet Numbers AX-P105A-38 to AX-P105A-105

| Property | Requirements of Convair Purchase Order, % | AVCO Certificate of Conformance Data, % | Convair Quality Assurance Test Results, % |
|---|---|---|---|
| Fiber Content (wt %) | — | — | 35.7 |
| Resin Solids Content (wt %) | 38-48 | 38-46 | 43.6 |
| Volatile Content (wt %) | 10-20 | 14-20 | 20.7 |
| Resin Flow (wt %) | 30-42 | — | 38.3 |

## 4.4 GRAPHITE POLYIMIDE

**4.4.1 HT-S/710.** The HT-S/710 G/PI prepreg was purchased from Hercules Incorporated with a list of Convair specified requirements. No procurement specification or industry specification was available. For the two batches of material required on the program, Tables 4-7 and 4-8 list these Convair requirements and the results of the Convair quality assurance tests. No quality assurance test results from Hercules were received with the shipments. As shown in the tables, the Convair results satisfied the Purchase Order requirements and the material was considered to be acceptable.

Table 4-7. Prepreg Requirements and Properties for HT-S/710 G/PI — Batch One

| Property | Requirements of Convair Purchase Order, % | Convair Quality Assurance Test Results, % |
|---|---|---|
| Fiber Content (wt %) | — | 44.4 |
| Resin Solids Content (wt %) | 35-40 | 40.0 |
| Volatile Content (wt %) | 10-20 | 15.6 |
| Resin Flow (wt %) | 15-25 | 17.2 |

Table 4-8. Prepreg Requirements and Properties for HT-S/710 G/PI — Batch Two

| Property | Requirements of Convair Purchase Order, % | Convair Quality Assurance Test Results, % |
|---|---|---|
| Fiber Content (wt %) | — | 48.5 |
| Resin Solids Content (wt %) | 35-40 | 35.5 |
| Volatile Content (wt %) | 10-20 | 16.0 |
| Resin Flow (wt %) | 15-25 | 18.2 |

**4.4.2 CELION 6000/LARC-160.** The Celion 6000/LARC-160 prepreg was purchased from Fiberite Corporation to the Fiberite Specification for hy-E 1678E. The results of the Convair quality assurance tests and the values from the Fiberite Certification received with the shipment of prepreg are given in Table 4-9.

Table 4-9. Prepreg Properties for Celion 6000/LARC-160

| Property | Fiberite Certified Test Report Data, % | Convair Quality Assurance Test Results, % |
|---|---|---|
| Fiber Content (wt %) | 47.0 | 54.6 |
| Resin Solids Content (wt %) | 40.4 | 37.5 |
| Volatile Content (wt %) | 12.6 | 7.9 |
| Resin Flow (wt %) | — | 27.6 |
| Fiber Areal Weight ($gm/m^2$) | 140.9 | 145 |

# SECTION 5

# LAMINATE PROCESSING AND SPECIMEN FABRICATION

## 5.1 LAMINATE PROCESSING

All of the composite fabrications on this program were processed using autoclave curing methods. This included flat panels that ranged in size up to 0.93 $m^2$ (10 $ft^2$), and 0.025 m (1 in.) diameter by 0.3 m (12 in.) long tubes. Two of the materials, G/E and B/PI, were fabricated into both flat panels and the torsion tube configuration. In addition, precompaction and/or "B" staging operations were included in several of the overall processes and are described in detail.

The G/E tubes and the B/PI tubes both included the precompaction operations prior to final cure. HT-S/710 G/PI panels also required a precompaction and "B" staging of the condensation type polyimide system in order to achieve satisfactory densification during cure. The B/E, G/E, and Celion 6000/LARC-160 G/PI systems, however, were processed using simple rapid curing schedules.

**5.1.1 BORON/EPOXY.** The fabrication of the B/E panels from prepreg consisting of 4-mil diameter boron and AVCO 5505 resin was accomplished using the relatively straight-forward vacuum bag and autoclave cure cycle shown below.

1. With full vacuum in the bag, heat at 1.7 to 2.8 K (3 to 5 ° F) per minute to 450 K (350 ° F).
2. Apply 0.59 $MN/m^2$ (85 psi), venting vacuum bag to atmosphere when autoclave pressure reaches 0.34 $MN/m^2$ (50 psi).
3. Hold 2 hours at 450 K (350 ° F) and 0.34 $MN/m^2$ (50 psi).
4. Cool under pressure to 353 K (175 ° F).

Laminates produced by this process exhibited good densification with measured specific gravities exceeding 2 and having resin contents of 26 to 32 weight percent. The layup procedure used for the 6 and 12 ply laminates (Figure 5-1) was identical except for the number of bleeder plies used. In all cases the prepreg was laid up with the scrim side down and with 0.001 m (0.04 in.) holes on 0.025 m (1 in.) centers perforating the Teflon film applied above the 120 glass bleeder.

**5.1.2 GRAPHITE/EPOXY.** A-S/3501-5 prepreg produced by Hercules Incorporated was the G/E system used to fabricate the flat panels and the 0.025 m (1 in.) diameter by 0.3 m (12 in.) long tubes required for Phases I and II. Both the 6 and 12 ply laminate fabrications used identical cure schedules and layup procedures with one exception: the thinner panels used two 120 glass bleeders while the thicker panels used four plies of the same glass fabric for bleeders. The cure cycle used a constant heatup rate of 1.1 to 1.7 K (2 to 3 ° F) per minute to 380 K (225 ° F) with full vacuum starting at room temperature. After applying 0.69 $MN/m^2$ (100 psi) the temperature was held 1 hour at 380 K (225 ° F) before heating to 450 K (350 ° F). A hold of 1 hour at 450 K (350 ° F) was followed by cooldown to below 350 K (150 ° F) under pressure. Details of the layup material stacking sequence are shown in Figure 5-2.

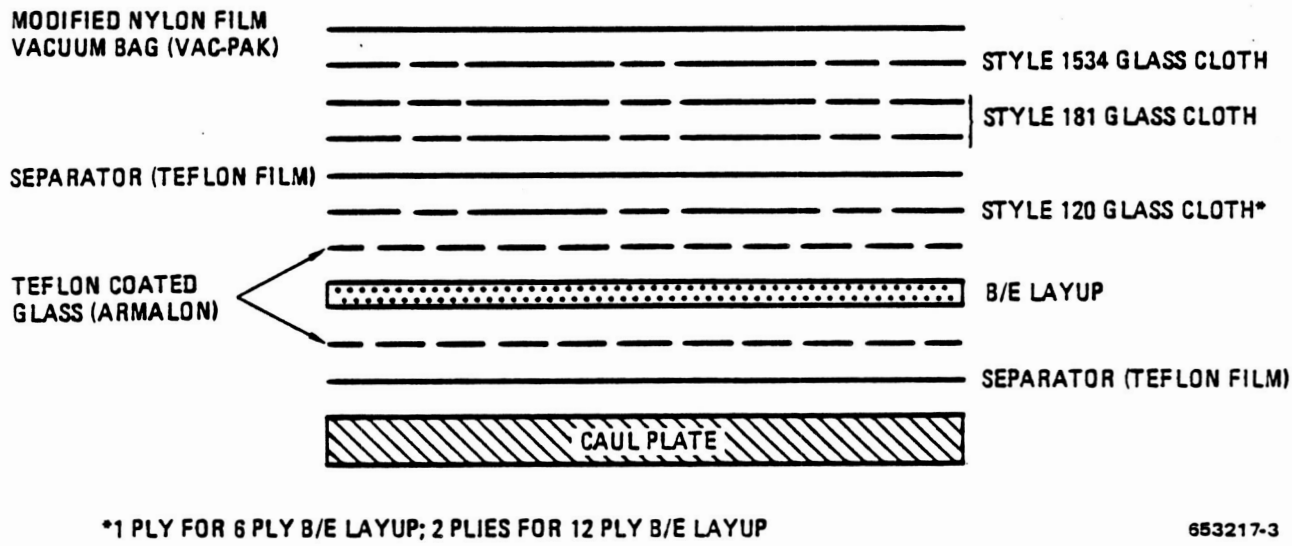



**Figure 5-1 Schematic of B/E Cure Layup**

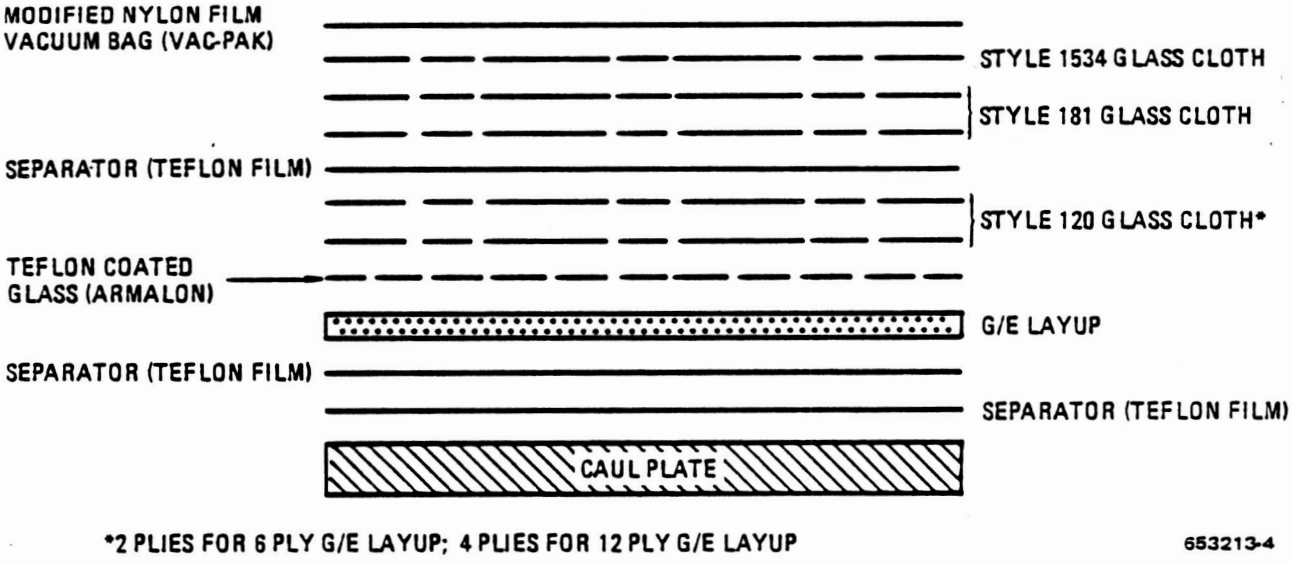



**Figure 5-2 Schematic of G/E Cure Layup**

Fabrication of the G/E tubes was accomplished with an aluminum mandrel covered with a silicone rubber bladder. Two plies of G/E prepreg, 0.31 m (12.25 in.) by 0.30 m (12 in.) were cut and laid up with a 0.013 m (0.5 in.) offset. These plies were precompacted (Figure 5-3) in an oven at 338 K (150° F) to 344 K (160° K) for 20 minutes with full vacuum in the bag and 0.10 $MN/m^2$ (15 psi) external pressure before wrapping on the mandrel. A spiral wrap of paper bleeder 0.038 m (1.5 in.) wide was then applied over the separator covering the prepreg. Vent material addition and bagging were followed by the following short cure cycle.

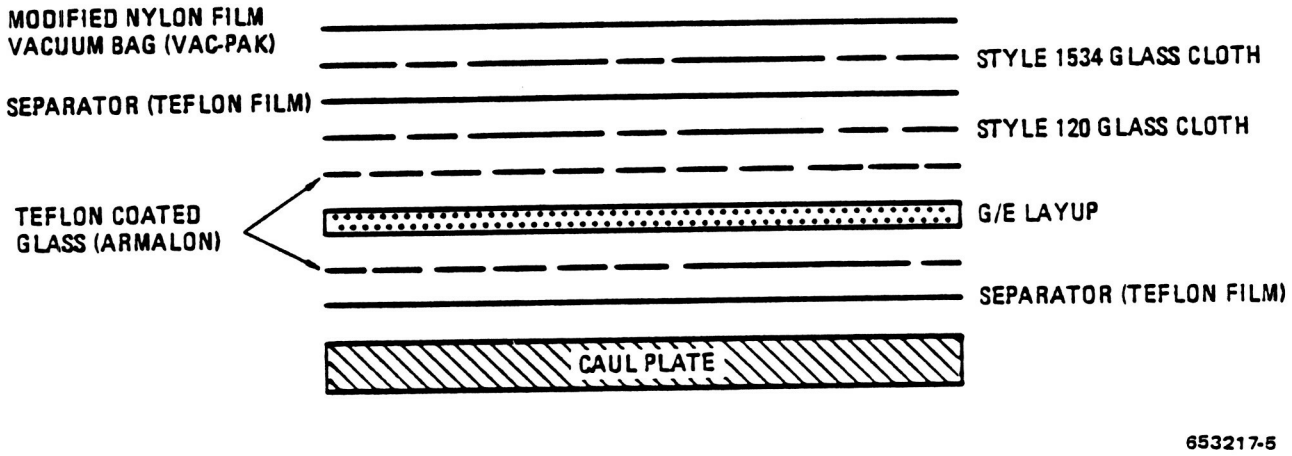



**Figure 5-3 Schematic of G/E Tube Precompaction Layup**

1. With full vacuum in the bag and 0.10 $MN/m^2$ (15 psi) in the autoclave, heat to 450 K (350° F) at 1.7 to 2.8 K (3 to 5° F) per minute.
2. Hold 1 hour and cool to 338 K (150° F) with vacuum in the bag and 0.10 $MN/m^2$ (15 psi) pressure in the autoclave.

This procedure produced composite tubes having a specific gravity of 1.56, resin contents of 31 to 33 weight percent, and uniform wall thicknesses ranging from 0.00097 to 0.00102 m (0.038 to 0.040 in.).

The A-S/3501-5A prepreg purchased for the thermal aging/compression study was processed using the same cure schedules and layup procedures as the A-S/3501-5 prepreg except that for the 24 ply laminate, eight plies (or equivalent) of 120 glass bleeder were used.

**5.1.3 BORON/POLYIMIDE.** AVCO Corporation's 4.0-mil B/P105AC prepreg was the system used to fabricate the B/PI panels and tubes. The flat laminates used a top caul plate and bleeding from both sides, as shown in Figure 5-4. A single layer of 104 scrim cloth was added to the prepreg stack to balance the layup. Full vacuum in the bag was applied at room temperature and the layup was heated in the autoclave to 464 K (375° F) at 2.2 K (4° F) per minute and held there 2 hours. Pressure of 0.69 $MN/m^2$ (100 psi) was applied and the temperature was raised to 561 K (550° F), again at 2.2 K (4° F) per minute. After a 2-hour hold, the layup was cooled to 353 K (175° F) at 1.1 K (2° F) per minute under autoclave pressure. Post cure consisted of a free standing heating cycle of 4 hours at 589 K (600° F).

Torsional tubes were fabricated using the 4.0-mil B/P105AC prepreg in a manner similar to the technique used for the G/E tubes. Aluminum mandrels covered with silicone shrink tubing were rolled with a two-ply 0.311 m (12.25 in.) by 0.308 m (12.125 in.) staggered prepreg that had been precompacted for 15-20 minutes at 383 K (230° F) with full vacuum in a bag using the layup shown in Figure 5-5. As before, bleeder paper 0.038 m (1.5 in.) wide was spirally wrapped, but two layers of bleeder were used for the more volatile polyimide resin system. One ply of a polyimide film was applied over the bleeder, followed by a venting system consisting of one layer of 1534 glass cloth, a layer of mat, and a final layer of 1534 glass fabric. The following cure and post cure cycles were used.

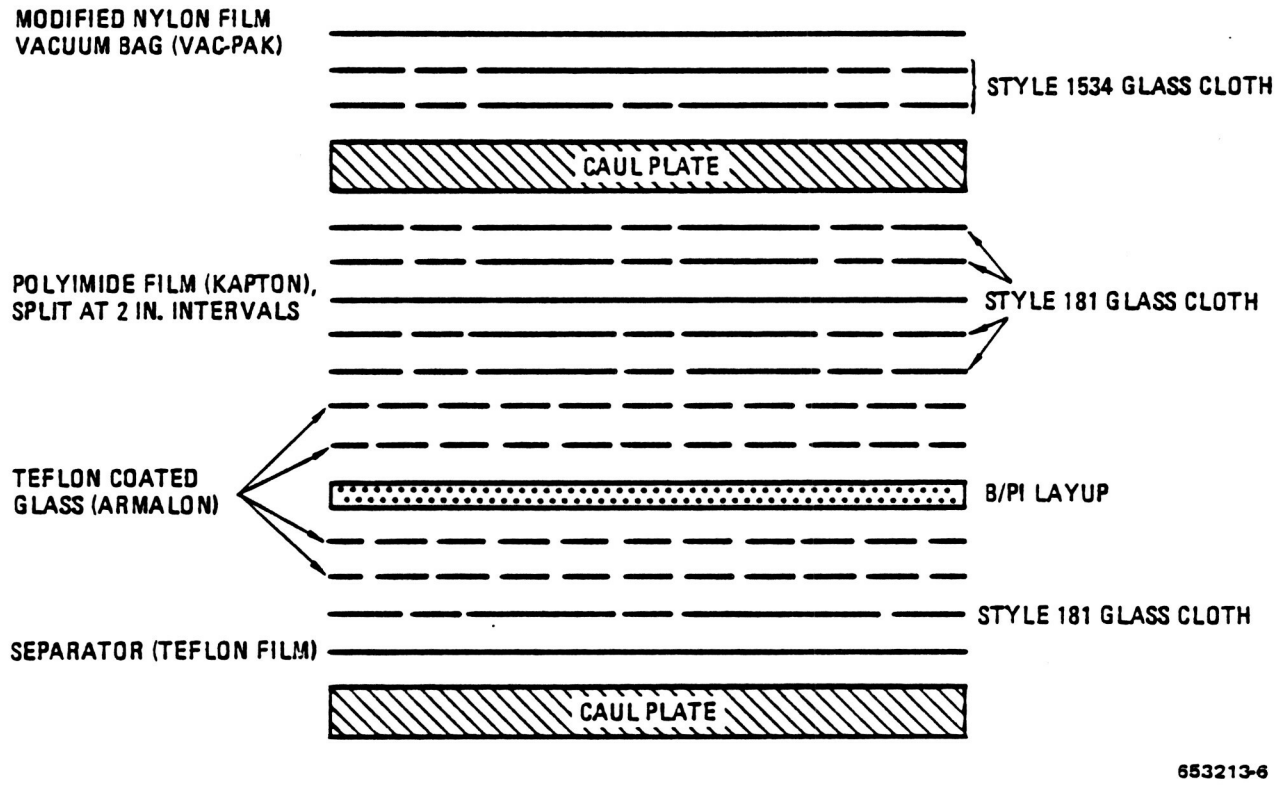



**Figure 5-4 Schematic of B/PI Cure Layup**

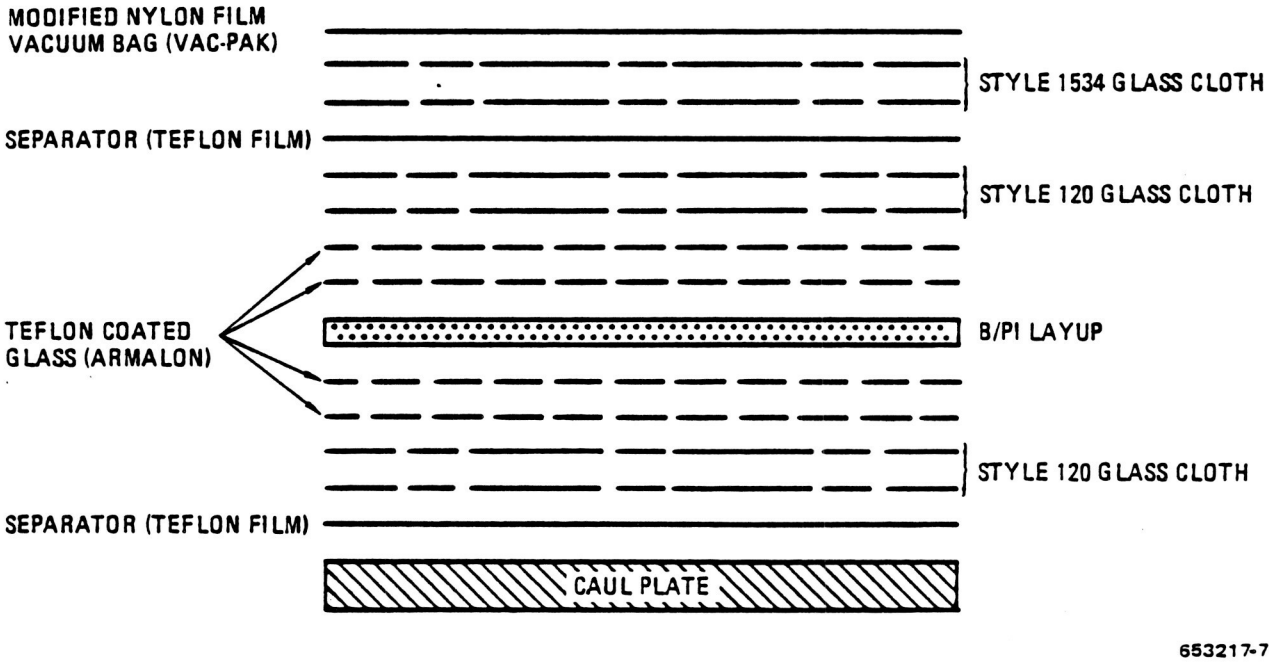



**Figure 5-5 Schematic of B/PI Tube Precompaction Layup**

a. Cure

1. With full vacuum in the bag and 0.17 $MN/m^2$ (25 psi) autoclave pressure, heat to 464 K (375° F) ± 6 K (10° F) at 2.2 K (4° F) per minute.
2. Hold 2 hours and apply 0.69 $MN/m^2$ (100 psi).
3. Heat at 2.2 K (4° F) per minute to 561 K (550° F) and hold 2 hours.
4. Cool to 353 K (175° F) or below at 1.1 K (2° F) per minute under autoclave pressure.

b. Postcure

1. Heat to 589 K (600° F) at 2.2 K (4° F) per minute and hold 4 hours.
2. Cool below 366 K (200° F) at 1.7 K (3° F) per minute maximum.

Several of the tubes fabricated in this manner used lightweight glass sleeving as bleeder in lieu of the paper.

### 5.1.4 GRAPHITE/POLYIMIDE

**5.1.4.1 HT-S/710.** Processing of the HT-S/710 G/PI system required a precompaction cycle for "B" staging and volatile removal before cure. This procedure consisted of sandwiching the prepreg layup using six plies of 120 glass cloth bleeder covered by separator applied to both sides. The layup was vacuum bagged and heated to 353 K (175° F) at 2.8 K (5° F) per minute. An external pressure of 0.17 $MN/m^2$ (25 psi) was then applied and held 15 minutes before cooling to 325 K (125° F). The layup was then bagged and fresh bleeder applied (Figure 5-6) before applying the following cycle.

1. With full vacuum in the bag, heat to 353 K (175° F) at 1.7 K (3° F) to 2.8 K (5° F) per minute.
2. Hold 30 minutes at 353 K (175° F), heat to 400 K (260° F).
3. Hold 25 minutes at 400 K (260° F), apply 0.69 $MN/m^2$ (100 psi) autoclave pressure.
4. Heat to 450 K (350° F) and hold 2 hours.
5. Cool at 1.1 K (2° F) per minute under autoclave pressure to 353 K (175° F).

A slow 1.1 K (2° F) per minute, postcure in air to 644 K (700° F) completed the processing cycle.

**5.1.4.2 Celion 6000/LARC-160.** The procedure used for fabrication of the Celion 6000/LARC-160 laminates was the following:

A partial vacuum of 0.010 $MN/m^2$ (1.5 psi) was applied to a laminate, and the temperature was increased to 366 K (200°F). The laminate was held at this temperature for 15 minutes to allow most of the solvent to be removed. The temperature was then increased to 435 K (325°F) and held for 1 hour to allow the laminate to imidize and to remove the imidization by-products. The laminate was then heated to 603 K (625°F) and held for 2 hours. During the heat-up to 603 K

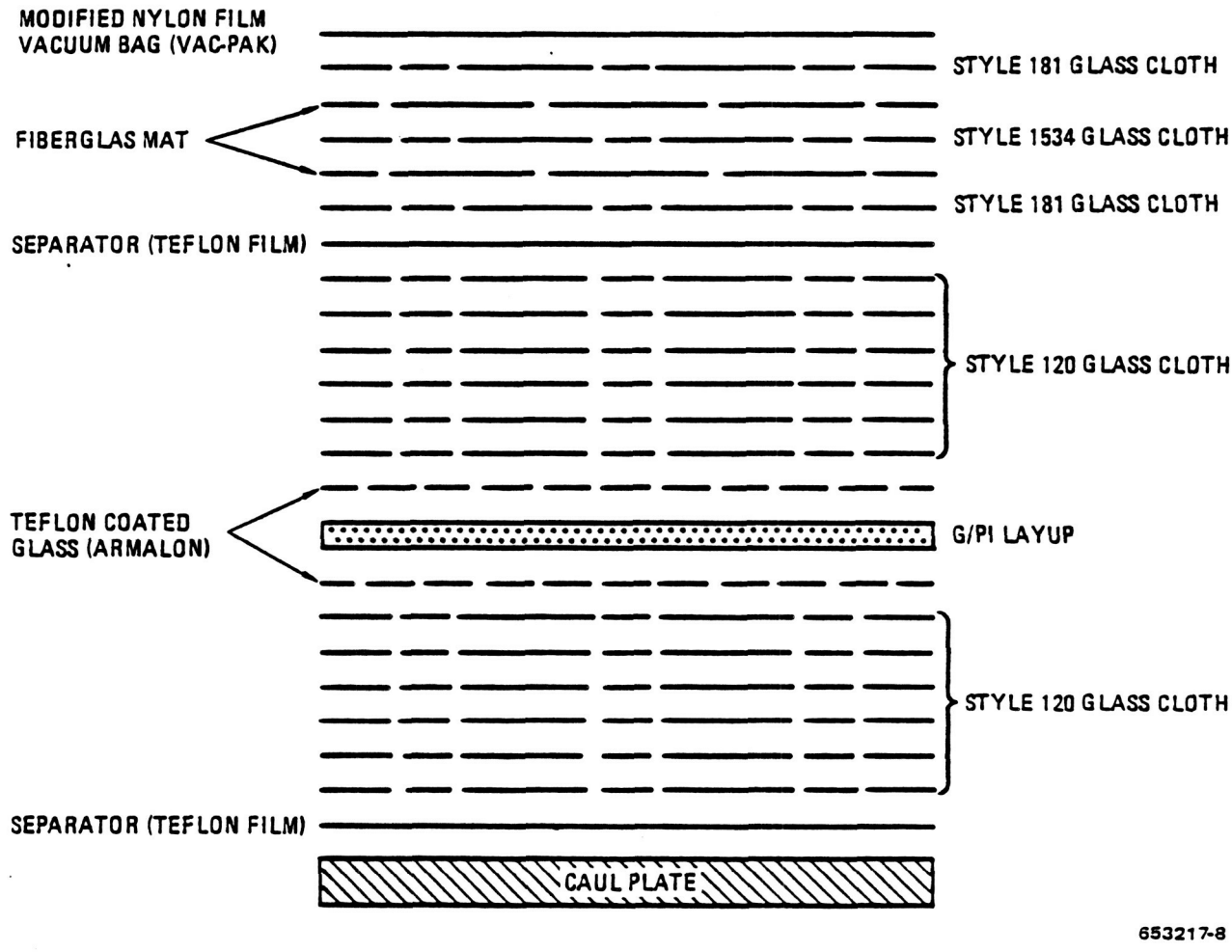



**Figure 5-6 Schematic of HT-S/710 G/PI Cure Layup**

(625 °F), a full vacuum and 1.4 $MN/m^2$ (200 psi) were applied to the laminate when the laminate temperature reached 546 K (525 °F). After the 2-hour hold at 603 K (625 °F) the temperature was decreased to 338 K (150 °F), the pressure and vacuum were released, and the laminate was removed from the autoclave. Details of the layup material stacking sequence are shown in Figure 5-7.

## 5.2 BORON/ALUMINUM TUBE FABRICATION

The unidirectional B/Al tubes were specially designed and fabricated for the torsion tests (baseline shear) using a variation in the General Dynamics Convair B/Al tube making process. The tubular specimen was 0.15 m (6 in.) long, 0.025 m (1 in.) in diameter, and 0.001 m (0.004 in.) (6 ply) in thickness. The boron filaments were 5.6 mils in diameter and oriented in the long-axis direction of the tube. The composite was 48 volume percent boron in a 6061 aluminum matrix. A sketch of the tube is shown in Figure 5-8.

The B/Al tube with steel reinforced ends was made by winding unidirectional, single-layer tape on a thin-wall, annealed, mild steel tube (inner mandrel). The assembly was then inserted into a thick-wall steel tool (outer mandrel). The assembly was next sealed by welding rings to the

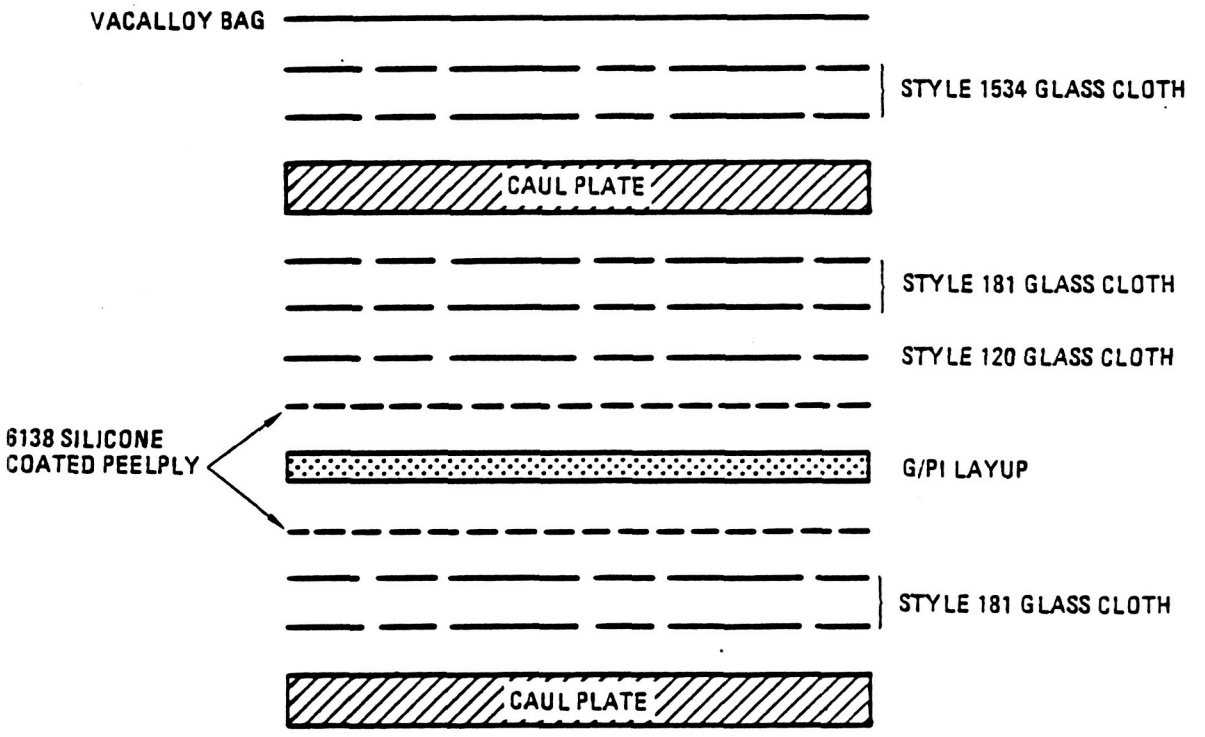
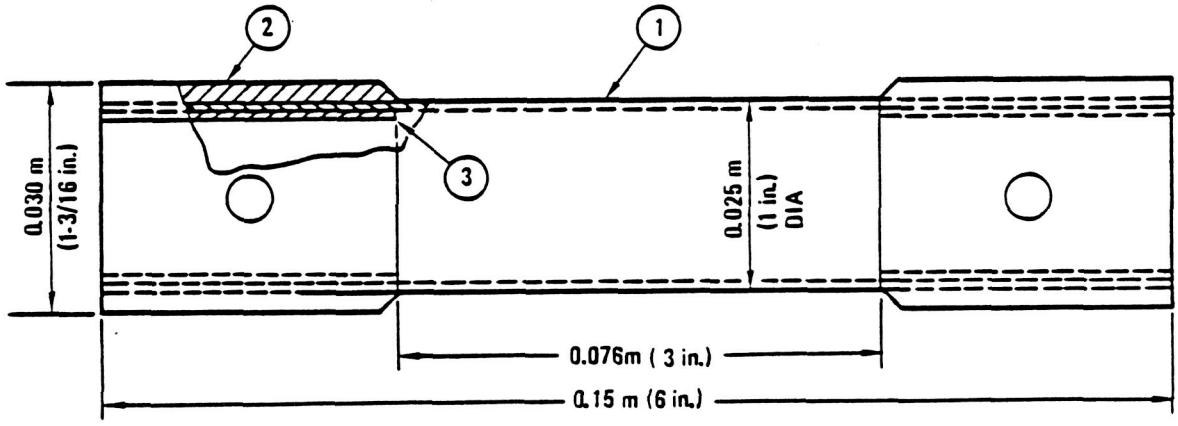



**Figure 5-7 Schematic of Celion 6000/LARC-160 G/PI Cure Layup**




DETAIL:
1. 0.001 m (0.040 in.) THICKNESS (6 PLY) B/Al TUBE
2. 0.0024 m (0.094 in.) THICKNESS STEEL REINFORCEMENT
3. 0.00071 m (0.028 in.) THICKNESS STEEL REINFORCEMENT

653217-9

**Figure 5-8 Unidirectional B/Al Tube**

ends of the inner and outer mandrels. An air evacuation tube was installed through the outer mandrel. The assembly was then helium leak tested, evacuated, heated to outgas any contaminants, and sealed (at the evacuation tube) while still under vacuum.

High temperature, high pressure autoclave bonding followed. The ductile, thin-walled inner mandrel yields during the cycle, transferring the applied pressure to the composite and its near-molten aluminum matrix. The result is complete bonding of the B/Al layers together and the bonding of the inner and outer steel tubes to the composite.

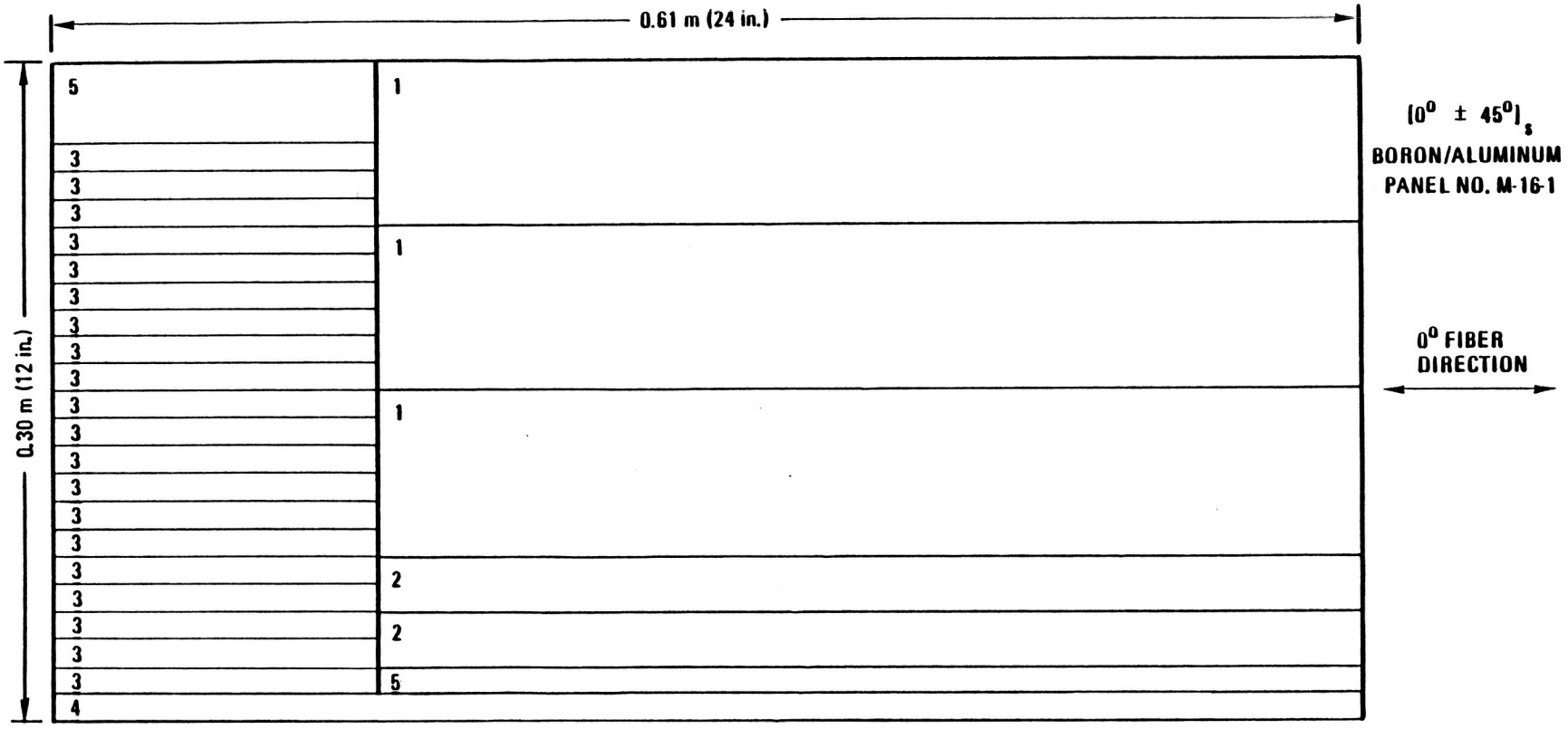
The bonded assembly was masked prior to etching by dipping each end in a molten plastic maskant to a depth of 0.038 m (1.5 in.), thus leaving the center portion free. The assembly was then submerged in a nitric acid bath that selectively dissolved both the inner and out steel jackets, leaving a B/Al tube with steel reinforced ends.

## 5.3 SPECIMEN FABRICATION

**5.3.1 PANEL LAYOUTS AND SPECIMEN IDENTIFICATION.** Cutting plans were prepared for each composite laminate showing the location and identification number of each specimen. These plans accompanied each laminate through the cutting and machining operations and then were retained to keep a permanent record as to which panel and the specific location from which each specimen was obtained. A typical cutting plan for a B/Al laminate is shown in Figure 5-9 and for a G/E laminate in Figure 5-10. The B/Al panels had good edges and could be used without trimming. For the resin matrix composites, a 0.013 m (0.5 in.) strip was cut from the perimeter of each panel because of edge thinning. A cutting allowance of 0.0032 m (0.125 in.) was used in preparing the cutting plans. Specific gravity and resin content samples were cut from scrap pieces (not from the perimeter) for each resin matrix laminate. For the B/Al panels a 0.013 m (0.5 in.) strip in the longitudinal direction was cut from one edge of each panel for quality assurance testing (fiber content, tensile properties, and metallographic examination).

The numerous test specimens used during this program were identified according to the system described in Table 5-1. The ID numbers were placed on the resin matrix specimens with either a white pencil on the composite itself or with permanent black ink on the end doublers. For the B/Al specimens either permanent black ink on the B/Al or vibra-tool marking of the metal end doublers was used. No difficulties with unreadable ID numbers were experienced during any of the moisture or thermal exposures. Data books with a record of each specimen were prepared for the six material systems. All test results were filed in these logs, thus ensuring ready access to any of the data developed during the lengthy program.

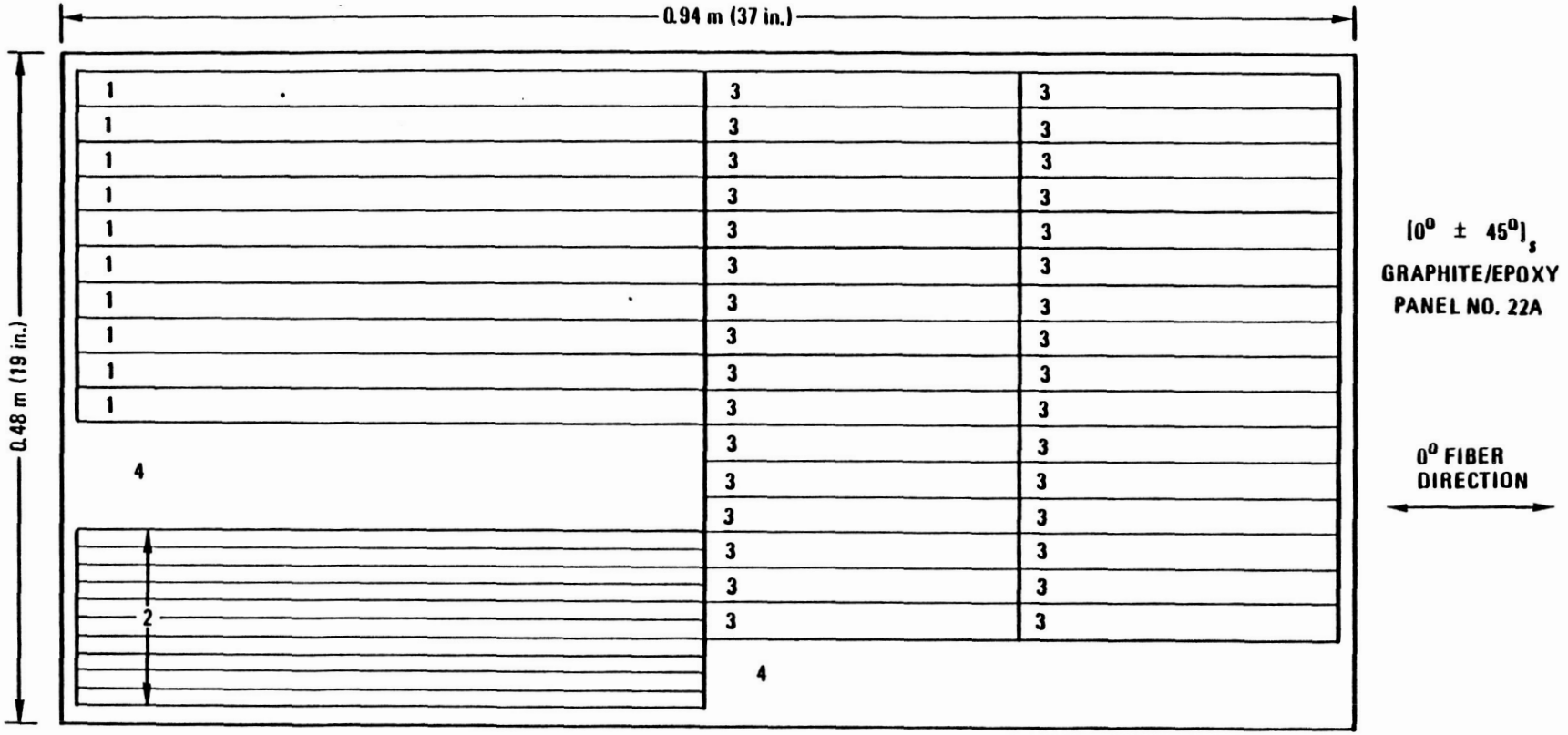
**5.3.2 MACHINING OPERATIONS.** The machining operations required for the fabrication of the composite specimens included sawing, hole drilling, and slotting. Cutting of the flat laminates and torsion tubes into specimen blanks was accomplished with the large gantry-type diamond radial saw pictured in Figures 5-11 and 5-12. The resin matrix materials were cut using a 0.25 m (10 in.) diameter diamond plated blade. The diamond size was grit number 60 (270 micron). Sawing was done without coolant at a cutting rate of 5600 sfm with powered feed rates of 6 to 10 ipm. The specimens were cut to final size with no edge finishing required. For B/Al a 0.25 m (10 in.) diameter diamond impregnated (grit number 46 (350 micron) metal bond) saw blade was used. Cutting rates were the same as those used for the resin matrix composites. The B/Al specimens were cut wet using a 24 to 1 ratio water soluble oil with flood application. Again, good edges were obtained without additional finishing operations.




KEY:
1. LONG TERM FLIGHT SIMULATION – 0.076 m (3 in.) BY 0.46 m (18 in.)
2. SHORT TERM FLIGHT SIMULATION – 0.025 m (1 in.) BY 0.46 m (18 in.)
3. BASELINE TENSILE – 0.013 m (0.5 in.) BY 0.15 m (6 in.)
4. QUALITY ASSURANCE – 0.013 m (0.5 in.) BY 0.61 m (24 in.)
5. CUTTING ALLOWANCE AND SCRAP

663217-10

**Figure 5-9 Cutting Plan for 6 Ply B/Al Panel**




KEY:
1. NOTCHED FATIGUE (ELEVATED TEMPERATURE) – 0.025 m (1 in.) BY 0.46 m (18 in.)
2. FATIGUE (ELEVATED TEMPERATURE)– 0.013 m (0.5 in.) BY 0.46 m (18 in.)
3. NOTCHED TENSILE – 0.025 m (1 in.) BY 0.23 m ( 9 in.)
4. QUALITY ASSURANCE, CUTTING ALLOWANCE, AND SCRAP

653217-11

**Figure 5-10 Cutting Plan for 6 Ply G/E Panel**

## Table 5-1. Specimen Identification Code

| Material | Laminate Orientation | Task | Test | Specimen No. |
|---|---|---|---|---|
| A B/E<br>B G/E<br>C B/PI<br>D G/PI (HT-S/710)<br>E B/Al<br>F G/PI (Celion 6000/LARC-160) | U Unidirectional<br>C Crossply<br>[a]F Notched Crossply | 0 Baseline | 1. Tensile<br>2. Notched Tensile<br>5. Fracture<br>6. Shear | |
| | | 1 Thermal Aging | 1. Tensile<br>2. Shear | |
| | | 2 Ambient Aging | 1. Control<br>2. 20 Weeks<br>3. 52 Weeks | |
| | | 3 Moisture Exposure | 1. 24 hr $H_2O$ Boil<br>2. 6 Week Humidity | |
| | | 4 Atmospheric Exposure | 1. Resin Matrix<br>2. Metal Matrix | |
| | | 5 Creep | | |
| | | 6 Stacking Sequence | 1. $[45°, -45°, 0°]_s$<br>2. $[0°, 45°, -45°]_s$<br>3. $[45°, 0° -45°]_s$ | |
| | | 7 Fatigue | 1. Notched<br>2. Unnotched | |
| | | 8 Short-Term Flight Simulation | | |
| | | 9 Long-Term Flight Simulation | | |
| | | 10 Thermal Aging/ Compression | 1. Compression<br>2. Sheer<br>3. Fatigue<br>4. Weight Change | |

Transverse specimens are marked with "T" before the regular ID No.

For example: E-C-7-1-24 is B/Al, Crossply, Notched Fatigue Specimen No. 24

[a]Used on notched flight simulation specimens only.

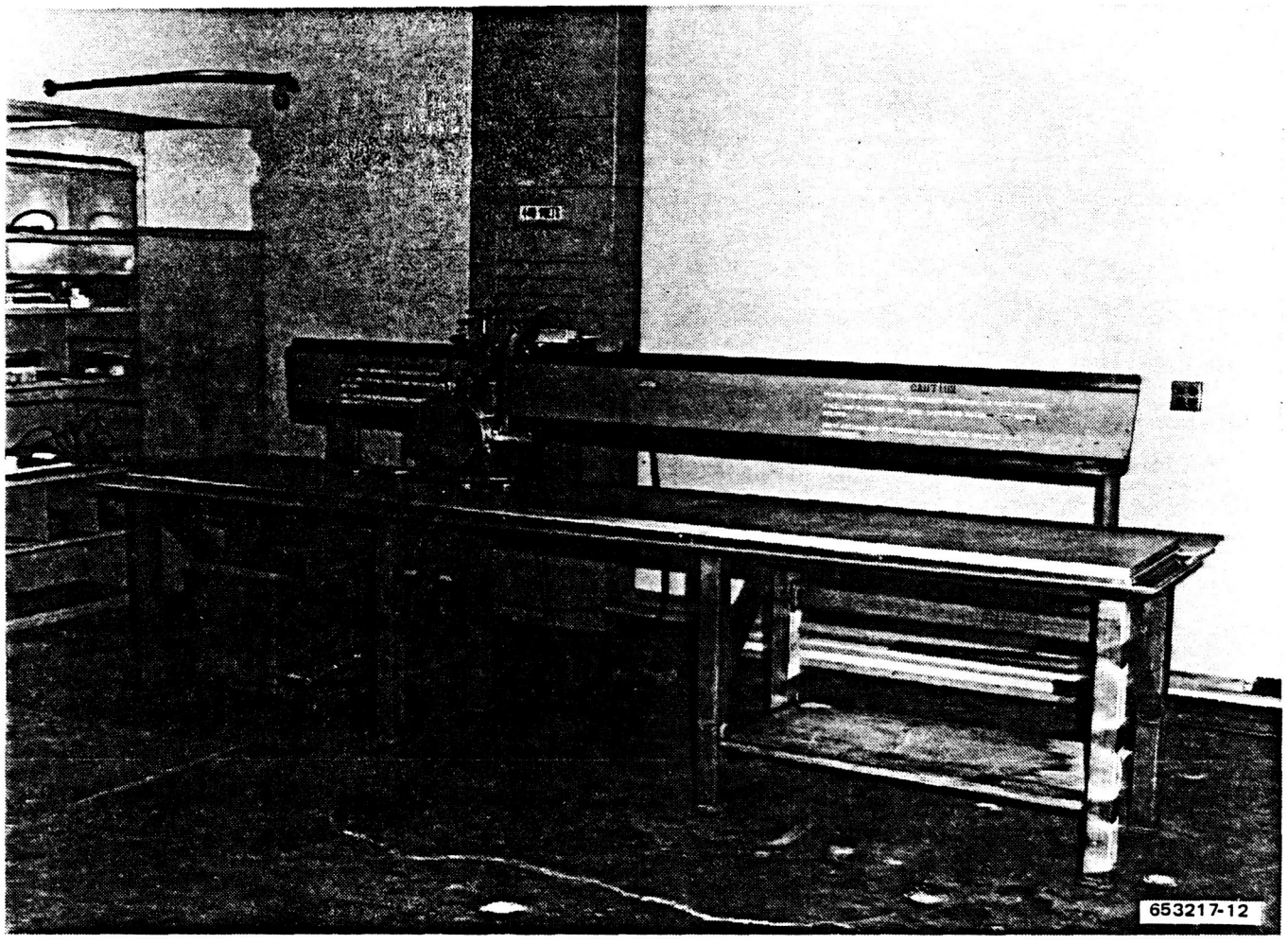



**Figure 5-11 Gantry-Type Diamond Radial Saw**

Holes were required in the notched tensile, fatigue, and flight simulation (both short- and long-term) specimens of the resin matrix materials and in the notched tensile and fatigue specimens of B/Al. Carbide and diamond coated core drills were used in a No. 2 Moore jig bore machine for fabricating the 0.0064 m (0.250 in.) holes in the resin matrix composites. No coolant was used. Electro-discharge machining (EDM) was used to produce the 0.0032 m (0.125 in.) holes in the B/Al specimens. The equipment used was an Elox HRP 104 EDM machine with a graphite electrode.

The other machining operations were cutting the center and edge slots in the B/Al laminate interfiber shear specimens and the center notches in the fracture specimens of all the composite materials. The B/Al shear specimens were slotted with the EDM method in a manner similar to that used for producing the holes in the notched tensile and fatigue specimens. For the fracture specimens, a rather narrow trapezoidal center notch with tip radii of approximately 0.00005 m (0.002 in.) was desired. Cutting of these notches was accomplished with a Sheffield ultrasonic impact grinding machine. The machine was operated at 20 kHz using 600 grit (17 micron) boron carbide abrasive. Optical comparator measurements of the notch radii gave values of 0.000038 m (0.0015 in.) to 0.000064 m (0.0025 in.) for both the resin matrix and the metal matrix specimens.



ORIGINAL PAGE IS
OF POOR QUALITY

ORIGINAL PAGE IS
OF POOR QUALITY

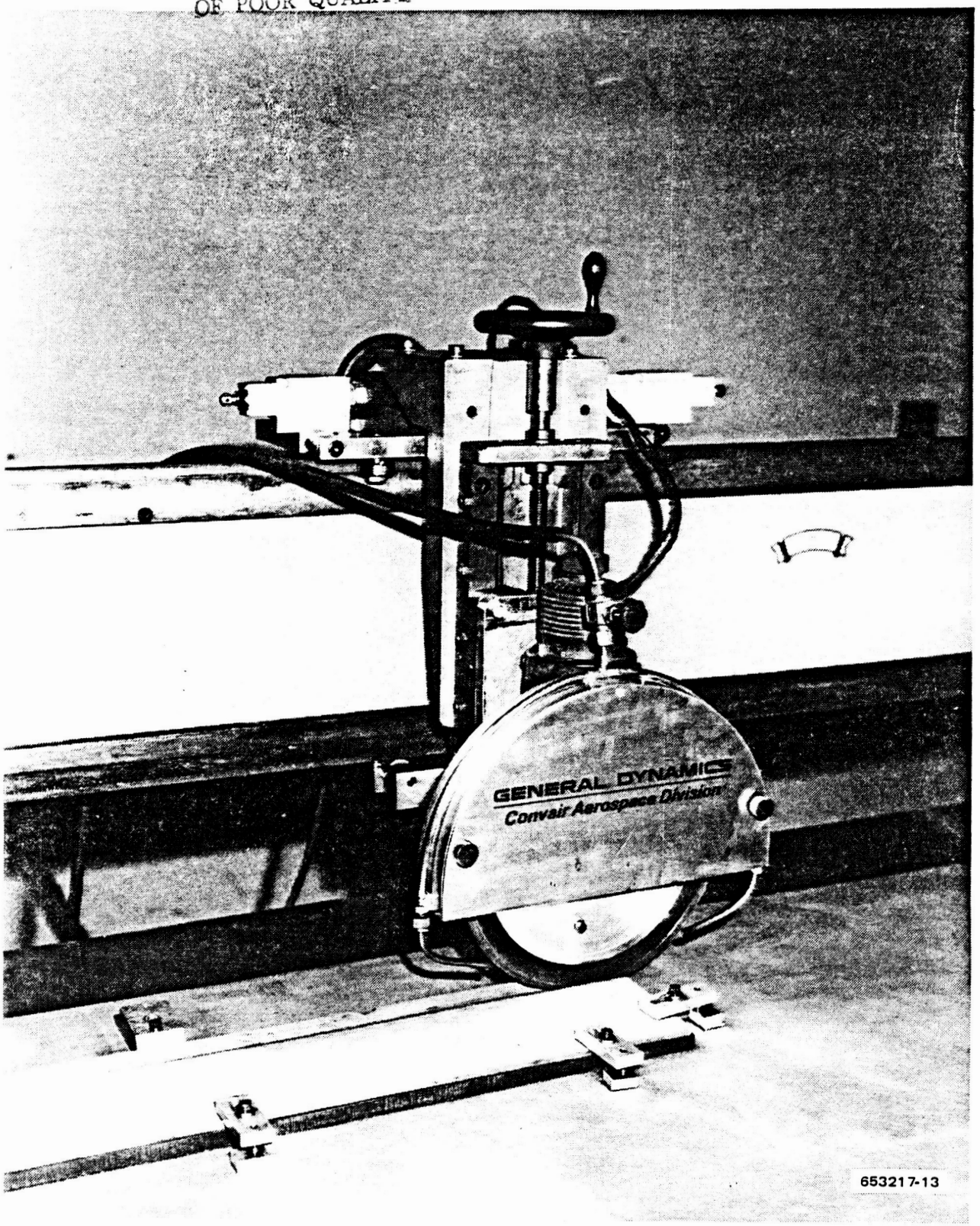



**Figure 5-12 Closeup View of Diamond Radial Saw**

In addition to the machining operations required on the composite materials, it was necessary to drill loading fixture attachment pinholes in the titanium end doublers of the creep and flight simulation specimens. These holes were produced using standard drilling practices with the aid of a drill fixture that was fabricated for this purpose. The holes were drilled on the centerline of the test specimens to within ± 0.000064 m (0.0025 in.).

**5.3.3 DOUBLER BONDING.** With the exception of 1) short beam shear, 2) flexural, 3) fracture, and 4) laminate shear, all specimens required tapered doublers bonded to the ends to prevent failures in the gripping fixtures during testing. The major criteria considered in the selection of the doubler materials were:

a. Temperature capability.

b. Thermal expansion matching of doubler and specimen.

c. Strength.

d. Cost.

Most of the resin matrix specimens were fabricated with either epoxy-glass laminate or polyimide-quartz laminate doublers depending on the test temperature. Early in the program, two epoxy-glass laminate types were used. One, Scotchply Type 1002, was used at and below room temperature and the second, Scotchply Type 1007, a high temperature epoxy, was used for elevated temperature tests up to 450 K (350° F). To avoid the possibility of mistakenly using the Type 1002 material at elevated temperature, where its strength is quite low, a change was made midway in the program, and the Type 1007 epoxy was used for both the low and high temperature test specimens. For testing of resin matrix specimens at temperatures above 450 K (350° F) a polyimide-quartz (Skybond 703/Astroquartz) doubler material was used. Both the epoxy and the polyimide doublers were 0.0015 m (0.060 in.) in thickness. Doublers for the majority of B/Al specimens were made from 6061-T4, aluminum alloy of the same nominal thickness as the composite being tested.

The exceptions to the above described specimens were the creep and flight simulation specimens of both the resin and metal matrix systems. These specimens were pin loaded in contrast to the others, which were either clamped or loaded through a wedge action type of gripping fixture. The creep and flight simulation specimens also had the requirement of being able to sustain a long-time elevated temperature test environment. For a pin loaded application, particularly at elevated temperature, a metal doubler is far superior to either the epoxy or polyimide types discussed above. Titanium was chosen as having the best combination of elevated temperature strength and thermal expansion match with the composite systems. For the $[0° \pm 45°]_s$ crossplied specimens, annealed A-70 titanium alloy (MIL-T-9046F, Type I, Composition B) was used. Because of the requirement of much higher test loads, solution treated and aged Ti-6Al-4V titanium alloy (MIL-T-9046F, Type III, Composition C) was selected for the unidirectional B/Al specimens. The thickness of the titanium alloy doublers was 0.0018 m (0.070 in.).

Of equal importance to selection of doubler material was the choice of adhesives used in bonding them to the specimen ends. The major considerations were strength at temperature and, for the creep and flight simulation specimens, long-time thermal stability. At room temperature and below, EA-9309[1] was selected for the resin matrix specimens and EC-2216 for the

B/Al specimens. EA-9309 is a two-part epoxy paste adhesive manufactured by the Hysol Division of the Dexter Corporation. EC-2216 is a modified amine-cured filled epoxy manufactured by the 3M Company. Both were cured at room temperature for at least 72 hours prior to use. The adhesive that was considered to have had the best combination of elevated temperature strength and stability and the one selected for all elevated test specimens was HT-424. This is a modified epoxy-phenolic film adhesive with an aluminum filler on a glass carrier manufactured by the Bloomingdale Department of American Cyanamid Company. The cure cycle used for HT-424 was 1 hour at 450 K (350° F). The specimens were vacuum bagged and cured in an autoclave at 0.14 $MN/m^2$ (20 psi). Prior to application of the adhesive the specimens and doublers are prepared as follows:

a. Resin-matrix specimens and doublers: lightly polished with A-1 very fine Scotch-Brite and solvent wiped.

b. B/Al specimens and 6061-T4 Al doublers: degreased, lightly polished with A-1 very fine Scotch-Brite, solvent wiped, acid etched with Pasa-Jell 105, and rinsed with deionized water.

c. Titanium alloy doublers: degreased, acid etched in nitric plus hydrofluoric solution, and rinsed with deionized water.

[1]Midway through the program EA-9309 was replaced by EA934, also a room temperature curing two-part epoxy paste adhesive manufactured by Hysol Division.

# SECTION 6

# LAMINATE QUALITY ASSURANCE TESTING

Quality assurance testing was performed on all purchased (B/Al) or Convair fabricated (B/E, G/E, B/PI, and G/PI) laminates to ensure good quality and, where applicable, concurrence with all specification requirements. Unacceptable material was rejected and replaced. In general, quality assurance testing consisted of visual examination, ultrasonic C-scan, volume or weight percent determinations, mechanical property testing, thickness measurement, and, for the B/Al panels, metallographic examination. Metallographic examinations were also made on all laminates fabricated for the thermal aging/compression study. The following sections describe the tests and present the results for the materials included in the program.

## 6.1 METAL MATRIX COMPOSITE MATERIAL

The B/Al quality assurance test program consisted of nondestructive testing, volume percent determinations, thickness measurements, tensile tests, and metallographic examinations. All the composite panels were nondestructively evaluated by ultrasonic testing. The ultrasonic technique was pulse-reflection through-transmission with a single short-focused, 5 MHz lithium sulfate transducer. The results are recorded on a C-scan recording wherein shades of gray lighter than some maximum are relatable to acoustic transmission losses within the test panel. The overall integrity of a test panel is described by an arbitrary rating system with numerical values from 0 to 5 assigned on the basis of Convair's experience in ultrasonic testing of hundreds of composite panels. The rating reflects variations from normal conditions. Normal does not necessarily mean perfect. For example, a few widely scattered stray boron filament fragments have no measurable effect on the structural performance of a given component. Although undesired from a workmanship standpoint, if small isolated defects cause no structural effects, they are judged to be normal. Degrees of variation from normalcy are subjectively determined by engineers with wide experience in the evaluation of composite materials. Ratings of 3, 4, and 5 represent severe or widespread defects judged to have detrimental effects upon the structural performance of the component. Ratings of 1 or 2 relate to scattered or isolated defects caused by faulty workmanship or minor loss of process control. These ratings apply to defects that should not adversely affect the structural performance of the component. Table 6-1 summarizes the ultrasonic test results of both the unidirectional and crossply panels. Overall panel integrity was excellent.

Table 6-1. Results of Nondestructive Evaluation of B/Al Panels

| Panel No. | Orientation | No. of Plies | Intended Use (a) | Thickness mm | Thickness (in.) | Ultrasonic Rating (b) |
|---|---|---|---|---|---|---|
| 9-1 | $[0°]_6$ | 6 | 0, 8, 9 | 0.91-0.97 | 0.037-0.038 | 0 |
| 9-2 | | 6 | 0, 5, 8, 9 | .91- .97 | .036- .038 | 0 |
| 12-1 | | 6 | 2, 5, 7, 8 | .94- .97 | .037- .038 | 0 |
| 12-2 | | 6 | 1, 5, 7, 8 | .94- .99 | .037- .039 | 0 |
| 13-2 | | 6 | 0, 1, 5, 8, 9 | .91- .97 | .036- .038 | 1 |
| 13-3 | | 6 | 1, 2, 8, 9 | .94- .99 | .037- .039 | 0 |
| 14-3 | | 6 | 7 | .91- .97 | .036- .038 | 0 |
| 14-4 | | 6 | 0, 7 | .91- .94 | .036- .037 | 0 |
| 15-1 | | 6 | 0, 2, 8, 9 | .94- .97 | .037- .038 | 0 |
| 15-3 | | 6 | 0, 1, 2, 5, 8 | .84- .99 | .033- .039 | 0 |
| 21-4 | | 6 | 2, 5, 7, 8 | .97-1.02 | .038- .040 | 0 |
| 304 | | 6 | 8, 9 | 1.09-1.17 | .043- .046 | 0 |
| 305 | | 6 | 8, 9 | 1.07-1.19 | .042- .047 | 0 |
| 306 | $[0°]_6$ | 6 | 8 | 1.09-1.17 | .043- .046 | 0 |
| 54-1 | $[0°]_{12}$ | 12 | 7 | 2.06-2.11 | .081- .083 | 0 |
| 15-2 | $[0° \pm 45°]_s$ | 6 | 0, 8 | .97- .99 | .038- .039 | 0 |
| 16-1 | | 6 | 0, 8, 9 | .97- .99 | .038- .039 | 1 |
| 17-1 | | 6 | 0, 8, 9 | .97-1.02 | .038- .040 | 1 |
| 19-1 | | 6 | 0, 1, 5, 8, 9 | .99-1.04 | .039- .041 | 1 |
| 19-2 | | 6 | 1, 5, 7, 8, 9 | .97- .99 | .038- .039 | 0 |
| 19-3 | | 6 | 0, 5, 7, 8 | .99-1.02 | .039- .040 | 1 |

Table 6-1. Results of Nondestructive Evaluation of B/Al Panels — Concluded

| Panel No. | Orientation | No. of Plies | Intended Use (a) | Thickness mm | Thickness (in.) | Ultrasonic Rating (b) |
|---|---|---|---|---|---|---|
| 20-1 | | 6 | 7 | .99-1.02 | .039- .040 | 0 |
| 20-2 | | 6 | 0, 7 | .99-1.04 | .039- .041 | 0 |
| 20-4 | | 6 | 0, 5, 8 | 1.02-1.07 | .040- .042 | 0 |
| 21-2 | | 6 | 5, 7, 8 | .97-1.02 | .038- .040 | 0 |
| 21-3 | $[0° \pm 45°]_s$ | 6 | 5, 7, 8 | .99-1.04 | .039- .041 | 0 |
| 54-2 | $[0° \pm 45°]_{s2}$ | 12 | 7 | 2.06-2.11 | .081- .083 | 0 |
| 749-1 | $[0°]_6$ | 6 | 1 | 1.12-1.14 | .044- .045 | 0 |
| 749-2 | $[0°]_6$ | 6 | 9 | 1.12-1.14 | .044- .045 | 0 |
| 748 | $[0° \pm 45]_s$ | 6 | 1,9 | 1.12-1.14 | .044- .045 | 0 |

a 0 Baseline
1 Thermal Aging
2 Ambient Aging
5 Creep
7 Fatigue
8 Short-Term Exposure
9 Long-Term Exposure

b Rating: 0 is completely uniform, 1 to 5 is deviation from normal in increasing severity

Volume percent (v/o) determinations were performed on each B/Al panel to determine the amount of filaments and matrix present in the composite test materials. Broken tensile specimens were used as test samples. Each specimen was washed, dried, and weighed. The filaments were leached from the samples in a 50% solution of sodium hydroxide at approximately 339 K (150° F). The filaments were collected, washed, dried, and weighed. Assuming the density of aluminum is 2700 kg/m$^3$ and the density of the filaments is 2510 kg/m$^3$ for 5.6 mil boron, the volume percentages of filaments were calculated using the following formula:

$$\text{Filament Volume Percent (v/o)} = \frac{\dfrac{W_F}{\varrho_F}}{\dfrac{W_A}{\varrho_A} + \dfrac{W_F}{\varrho_F}} \times 100$$

$W_F$ = Weight of filaments

$\varrho_F$ = Density of filaments

$W_A$ = Weight of Aluminum

$\varrho_A$ = Density of Aluminum

The results of the v/o determinations are given in Table 6-2. For the 6 ply laminates the variation ranged from a low of 46.1 to a high of 51.4 v/o of boron with an overall average of 48.8 v/o boron. These results are typical of a nominal 50 v/o B/Al composite material. The 12 ply laminates were somewhat lower with values of 43.3 and 42.5 v/o boron.

Thickness measurements were made on the B/Al panels using micrometers. The results (Table 6-1) show relatively small differences in thickness within each panel or between the unidirectional and $[0° \pm 45°]_s$ crossplied B/Al panels.

Tensile tests were performed on each of the B/Al panels. The configuration of the tensile specimen used was a simple, straight-sided specimen 0.15 m (6 in.) long and 0.013 m (0.5 in.) wide cut in the longitudinal direction. Bonded doublers were utilized to minimize stress concentrations in the gripping areas. The doublers were made from 6061 T-4 bare aluminum and were of the same nominal thickness as the composite being tested. The doublers were bonded to the composite specimens with EC-2216 epoxy, a modified amine-cured filled epoxy that cures at room temperature. Tensile specimens were tested in an Instron testing machine using a head rate of 0.00025 m per minute (0.01 in. per minute). Stress-strain curves and strain measurements were made with Baldwin microformers. Modulus values were calculated from the stress-strain curves. Results of the tensile tests on the 6 ply laminates, shown in Table 6-2, indicate an average tensile strength of 1450 MN/m$^2$ (211 ksi) for the unidirectional B/Al material and 581 MN/m$^2$ (84.2 ksi) for the $[0° \pm 45°]_s$ crossplied layup. This is in good agreement with early work at Convair on 5.6-mil B/Al composite material. The elastic modulus values of 200 GN/m$^2$ (29.0 million psi) for the unidirectional and 127 GN/m$^2$ (18.4 million psi) for the crossplied layup, however, are about 6% less than typical of previous results. No reason could be found for the lower modulus properties. Because of the lower fiber contents, the tensile strengths of the 12 ply panels were somewhat lower than those obtained from the 6 ply panels.

Table 6-2. Results of B/Al Quality Assurance Test Program

| Panel No. | Orientation | Fiber Content (Vol. %) | Tensile Strength MN/m$^2$ | Tensile Strength (ksi) | Tensile Modulus GN/m$^2$ | Tensile Modulus (psi × 10$^6$) | Comments on Metallographic Examination |
|---|---|---|---|---|---|---|---|
| 9-1 | $[0°]_6$ | 50.2 | 1480 | 214 | 193 | 28.0 | OK |
| 9-2 | | 49.8 | 1480 | 214 | 205 | 29.8 | OK |
| 12-1 | | 48.7 | 1300 | 188 | 213 | 30.9 | OK |
| 12-2 | | 48.3 | 1340 | 194 | 220 | 31.9 | OK |
| 13-2 | | 46.7 | 1540 | 224 | — | — | Partial disbond on 2 surfaces |
| 13-3 | | 48.2 | 1540 | 223 | 207 | 30.0 | OK |
| 14-3 | | 46.5 | 1530 | 222 | 209 | 30.3 | OK |
| 14-4 | | 48.2 | 1430 | 208 | 170 | 24.7 | Partial disbond on 1 surface |
| 15-1 | | 48.6 | 1330 | 193 | 181 | 26.3 | OK |
| 15-3 | | 48.0 | 1570 | 228 | 170 | 24.7 | Small amount of scattered disbond |
| 21-4 | | 48.7 | 1280 | 185 | 173 | 25.1 | Scattered disbonds |
| 304 | | 46.1 | 1440 | 209 | 211 | 30.6 | OK |
| 305 | | 47.7 | 1510 | 219 | 183 | 26.6 | OK |
| 306 | $[0°]_6$ | 46.4 | 1530 | 222 | 234 | 34.0 | OK |
| 54-1 | $[0°]_{12}$ | 43.3 | 1190 | 173 | 215 | 31.2 | OK |
| 15-2 | $[0° \pm 45°]_s$ | 48.4 | 594 | 86.1 | 103 | 14.9 | OK |
| 16-1 | | 49.0 | 629 | 91.2 | 150 | 21.7 | OK |
| 17-1 | | 48.2 | 576 | 83.5 | 152 | 22.0 | Scattered disbonds |
| 19-1 | | 50.0 | 550 | 79.8 | 103 | 14.9 | Scattered disbonds |

Table 6-2. Results of B/Al Quality Assurance Test Program — Concluded

| Panel No. | Orientation | Fiber Content (Vol. %) | Tensile Strength MN/2² | (ksi) | Tensile Modulus GN/m² (psi × 10⁶) | | Comments on Metallographic Examination |
|---|---|---|---|---|---|---|---|
| 19-2 | | 51.4 | 525 | 76.1 | 103 | 15.0 | OK |
| 19-3 | | 50.1 | 544 | 78.9 | 134 | 19.4 | OK |
| 20-1 | | 50.4 | 641 | 92.9 | 125 | 18.2 | OK |
| 20-2 | | 51.2 | 548 | 79.5 | 149 | 21.6 | Small amount of scattered disbonds |
| 20-4 | | 49.8 | 576 | 83.6 | 109 | 15.8 | Scattered disbonds |
| 21-2 | | 49.1 | 581 | 84.2 | 123 | 17.8 | OK |
| 21-3 | $[0° \pm 45°]_s$ | 50.1 | 579 | 84.0 | 110 | 15.9 | Scattered disbonds |
| 54-2 | $[0° \pm 45°]_{s2}$ | 42.5 | 495 | 71.8 | — | — | OK |
| 749-1 | $[0°]_6$ | 47.1 | 1540 | 224 | 221 | 32.0 | OK |
| 749-2 | $[0°]_6$ | 46.7 | 1460 | 212 | 212 | 30.7 | OK |
| 748 | $[0° \pm 45°]_s$ | 44.5 | 625 | 90.6 | 160 | 23.2 | OK |

Metallographic examinations were also made of each panel to substantiate the nondestructive evaluation (NDE) tests and to observe the microstructure, layup, and filament array. Samples cut from the broken tensile specimens were metallographically mounted and polished. Several of the samples showed some disbonding, which probably occurred during tensile testing or specimen preparation. Additional samples taken from the center of the B/Al panels instead of the edge where the quality assurance (QA) test specimens were taken showed none of the disbonding present in the broken tensile specimens. Photomicrographs of typical microstructures for the unidirectional and $[0° \pm 45°]_s$ crossplied material are shown in Figures 6-1 and 6-2.

## 6.2 RESIN MATRIX COMPOSITE MATERIALS

The quality assurance test program for the resin-matrix fabricated laminates consisted of ultrasonic C-scan, resin and fiber content, and specific gravity, and for the 12 and 24 ply panels, flexural and short beam shear strength. For the Phase II laminates and the new material addition, Celion 6000/LARC-160, room and elevated temperature tensile tests and metallographic examinations were also performed. Metallographic examinations and glass transition temperature (Tg) determinations were also included for the laminates fabricated for the thermal aging/compression study. The following sections present the results for the four resin-matrix composite systems.

**6.2.1 BORON/EPOXY.** Ultrasonic C-scan testing was performed on all fabricated panels to detect possible delamination or voids in the laminates. Among the most useful nondestructive test methods for locating defects aligned parallel to principal surfaces is the ultrasonic through-transmission method. A variation of this method, and the one employed for this program, is the single-transducer reflector plate method shown in Figure 6-3.

Ultrasonic energy transmitted through the specimen is returned to the transducer from a smooth reflector. If disbonds (or voids) are present, reflection of the sound at the interfaces results in less transmitted energy. The resultant energy drop is readily detected as a decrease in the strength (amplitude) of the return signal. The gated signal, input to a recorder amplifier, provides an output voltage to the recorder that is proportional to the signal amplitude.

The C-scan recorder is mechanically linked to scan and index motions of the transducer and is electrically connected to the recorder amplifier. With a signal in the gate, the recorder receives the amplified signal and "writes" during that time. A series of the line scans synchronized with the movement of the test transducer (or test specimen) produces a full scale plan of the test object and shows defects in either black and white or variable shades.

No rating system similar to that used for the B/Al C-scan evaluation was available for the resin-matrix materials. The C-scan recordings were studied by an experienced NDE engineer who rated the panels as being either acceptable or unacceptable. Areas of suspected delaminations or voids that were not sufficiently large enough to reject a laminate were marked on the panel, and these areas were avoided during specimen machining. For the B/E system all fabricated laminates were judged to be acceptable based on the ultrasonic C-scan tests.

Resin and fiber content and specific gravity determinations were made on all of the B/E panels using the test methods described in Appendix B. The results are listed in Table 6-3 along with the dimensions and intended use for each panel.

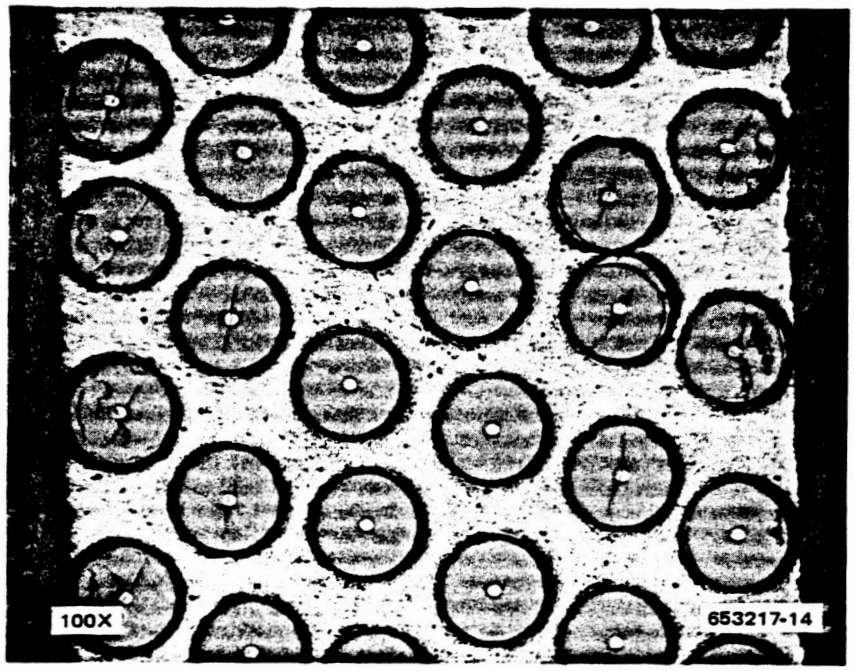



**Figure 6-1 Photomicrograph Showing Typical Microstructure of Unidirectional B/Al**

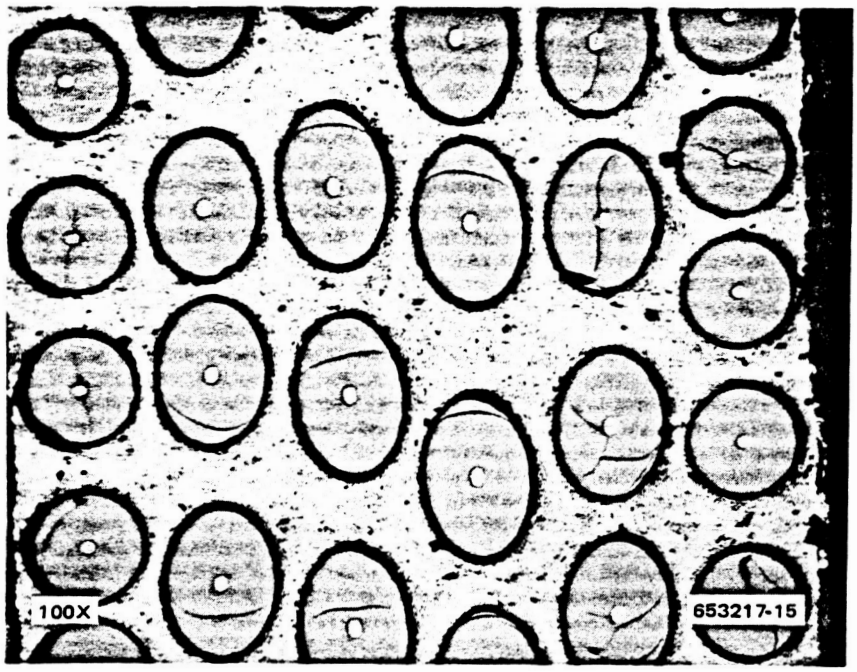



**Figure 6-2 Photomicrograph Showing Typical Microstructure of $[0° \pm 45°]_s$ Crossplied B/Al**

ORIGINAL PAGE IS
OF POOR QUALITY

ORIGINAL PAGE IS
OF POOR QUALITY

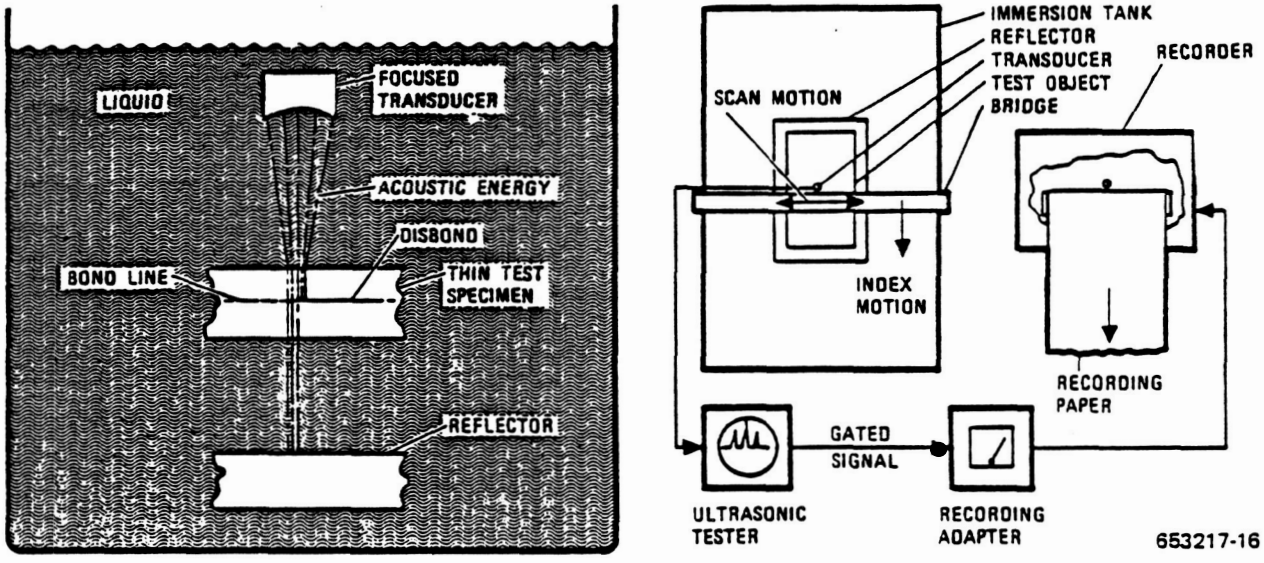



**Figure 6-3 Single-Transducer Ultrasonic Technique**

In addition to the nondestructive examination and the weight percent determinations conducted on each panel, a series of mechanical property tests was performed. Flexural strengths at 297 K (75 °F) and 450 K (350 °F) and short beam shear strength at 297 K (75 °F) were obtained for the two 12 ply QA panels. Details of the test procedures are described in Appendix B. Table 6-4 lists the results. Tensile tests at 297 K (75 °F) and 450 K (350 °F) were performed on material from the 6 ply Phase II panel, LRC77-1. Test procedures are described in Section 7, Baseline Testing. Table 6-5 lists the results. Based on the results of the QA tests, all of the B/E fabricated laminates were considered to be satisfactory.

**6.2.2 GRAPHITE/EPOXY.** Using the same technique described for the B/E material, all G/E fabricated laminates were ultrasonic C-scan tested for delaminations and voids. All panels were judged to be acceptable based on this evaluation.

The results of the remaining quality assurance tests on the Phase I and II G/E laminates are presented in Table 6-6 for resin and fiber contents and specific gravity values, Table 6-7 for room and elevated temperature flexural and room temperature short beam shear strengths (Phase I material only), and Table 6-5 for room and elevated temperature tensile strengths (Phase II material only).

Specific gravity and fiber and resin contents for the three panels fabricated for the thermal aging/compression study are listed in Table 6-8. Also included is the glass transition temperature (Tg) for the 6 ply panel. The Tg measurements were made using a Perkin Elmer 3600 Thermal Analysis System utilizing a TMS-2 Thermomechanical Analyzer Module. Short beam shear and flexural strength data are presented in Table 6-9 for the 12 and 24 ply panels. The metallographic examinations of the full size panels are discussed in the thermal aging section of the report.

In addition to the G/E panels, four G/E 8 ply unidirectional tubes were fabricated for the baseline shear tests. From each 0.30 m (12 in.) long tube, three specimens and one QA sample were obtained. Resin and fiber contents and specific gravity determinations were made on each quality assurance sample. The results are listed in Table 6-10.



ORIGINAL PAGE IS
OF POOR QUALITY

Table 6-3. Quality Assurance Data for B/E Laminates (Phases I and II)

| Panel No. | Orientation | No. of Plies | Size m | Size (in.) | Intended Use (a) | Fiber Content (wt %) (b) | Resin Content (wt %) | Specific Gravity |
|---|---|---|---|---|---|---|---|---|
| LRC-1 | $[\pm 45°/0°]_s$ | 6 | 0.23 × 0.25 | 9 × 10 | 6 | 71.7 | 28.3 | 2.04 |
| LRC-2 | $[0° \pm 45°]_s$ | 6 | .23 × .25 | 9 × 10 | 6 | 71.4 | 28.6 | 2.05 |
| LRC-3 | $[45°/0°/-45°]_s$ | 6 | .23 × .25 | 9 × 10 | 6 | 70.0 | 30.0 | 2.04 |
| LRC-4 | $[0°]_6$ | 6 | .94 × 1.02 | 37 × 40 | 1, 5, 8 | 73.5 | 26.5 | 2.04 |
| LRC-5 | $[0°]_6$ | 6 | .51 × 1.14 | 20 × 45 | 9 | 72.4 | 27.6 | 2.05 |
| LRC-6 | $[0°]_6$ | 6 | .38 × .51 | 15 × 20 | 1, 5 | 72.7 | 27.3 | 2.03 |
| LRC-14 | $[0°]_{12}$ | 12 | .23 × .30 | 9 × 12 | QA, 2 | 73.9 | 26.1 | 2.05 |
| LRC-15 | $[0° \pm 45°]_{s2}$ | 12 | .23 × .30 | 9 × 12 | QA, 2 | 73.3 | 26.7 | 2.05 |
| LRC-18 | $[0° \pm 45°]_s$ | 6 | .86 × .91 | 34 × 36 | 1, 5, 8 | 71.5 | 28.5 | 2.01 |
| LRC-19 | $[0° \pm 45°]_s$ | 6 | .33 × .41 | 13 × 16 | 0 | 67.5 | 32.5 | 2.04 |
| LRC-20 | $[0° \pm 45°]_s$ | 6 | .86 × .91 | 34 × 36 | 8 | 71.6 | 28.4 | 2.04 |
| LRC-21 | $[0° \pm 45°]_s$ | 6 | .91 × 1.02 | 36 × 40 | 9 | 72.0 | 28.0 | 2.04 |
| LRC 77-1 | $[0° \pm 45°]_s$ | 6 | .76 × .97 | 30 × 38 | 9 | 64.8 | 35.2 | 1.96 |

a QA Quality Assurance
0 Baseline
1 Thermal Aging
2 Ambient Aging
5 Creep
6 Stacking Sequence Evaluation
8 Short-Term Exposure
9 Long-Term Exposure

b Includes approximately 9% glass fiber from scrim cloth.

Table 6-4. Quality Assurance Mechanical Property Data for B/E Laminates (Phase I)

| Panel No. | Orientation | Temperature K | Temperature (°F) | Flexural Strength MN/m² | Flexural Strength (ksi) | Shear Strength MN/m² | Shear Strength (ksi) |
|---|---|---|---|---|---|---|---|
| LRC-14 | $[0°]_{12}$ | 297 | 75 | 2100 | 304 | 104 | 15.1 |
| | | | | 2060 | 298 | 99.9 | 14.4 |
| | | | | 2060 | 299 | 95.8 | 13.9 |
| Average | | | | 2070 | 300 | 99.9 | 14.5 |
| LRC-14 | $[0°]_{12}$ | 450 | 350 | 1680 | 244 | | |
| | | | | 1740 | 252 | | |
| | | | | 1770 | 257 | | |
| Average | | | | 1730 | 251 | | |
| LRC-15 | $[0° \pm 45°]_{s2}$ | 297 | 75 | 924 | 134 | 62.7 | 9.1 |
| | | | | 958 | 139 | 64.8 | 9.4 |
| | | | | 931 | 135 | 69.6 | 10.1 |
| Average | | | | 938 | 136 | 65.7 | 9.5 |
| LRC-15 | $[0° \pm 45°]_{s2}$ | 450 | 350 | 889 | 129 | | |
| | | | | 820 | 119 | | |
| | | | | 882 | 128 | | |
| Average | | | | 864 | 125 | | |

Table 6-5. Quality Assurance Tensile Data for 6 Ply $[0° \pm 45°]_s$ Phase II Laminates

| Material System and Panel No. | Orientation | Temperature K | Temperature (°F) | Tensile Strength $MN/m^2$ | Tensile Strength (ksi) | Tensile Modulus $GN/m^2$ | Tensile Modulus (Msi) |
|---|---|---|---|---|---|---|---|
| 5505/4 B/E | $[0°\pm45°]_s$ | 297 | 75 | 539 | 78.2 | 79 | 11.4 |
| | | | | 529 | 76.7 | 52 | 7.6 |
| LRC 77-1 | | | | 524 | 76.0 | 81 | 11.7 |
| Average | | | | 531 | 77.0 | 71 | 10.2 |
| 5505/4 B/E | $[0°\pm45°]_s$ | 450 | 350 | 408 | 59.2 | 65 | 9.4 |
| | | | | 459 | 66.5 | 62 | 9.0 |
| LRC 77-1 | | | | 450 | 65.3 | 67 | 9.7 |
| Average | | | | 439 | 63.7 | 65 | 9.4 |
| A-S/3501 G/E | $[0°\pm45°]_s$ | 297 | 75 | 456 | 66.1 | 50 | 7.2 |
| | | | | 459 | 66.5 | 51 | 7.4 |
| LRC 77-2 | | | | 556 | 80.6 | 53 | 7.7 |
| Average | | | | 490 | 71.1 | 51 | 7.4 |
| A-S/3501 G/E | $[0°\pm45°]_s$ | 450 | 350 | 557 | 80.8 | 47 | 6.8 |
| | | | | 584 | 84.7 | 47 | 6.8 |
| LRC 77-2 | | | | 623 | 90.4 | 50 | 7.3 |
| Average | | | | 588 | 85.3 | 48 | 7.0 |
| HT-S/710 G/PI | $[0°\pm45°]_s$ | 297 | 75 | 385 | 55.8 | 57 | 8.2 |
| | | | | 388 | 56.3 | 70 | 10.1 |
| KN-9 | | | | 405 | 58.8 | 51 | 7.4 |
| Average | | | | 393 | 57.0 | 59 | 8.6 |
| HT-S/710 G/PI | $[0°\pm45°]_s$ | 505 | 450 | 492 | 71.4 | 56 | 8.1 |
| | | | | 372 | 53.9 | — | — |
| KN-9 | | | | 437 | 63.4 | — | — |
| Average | | | | 434 | 62.9 | 56 | 8.1 |

Table 6-6. Quality Assurance Data for G/E Laminates (Phases I and II)

| Panel No. | Orientation | No. of Plies | Size m | Size (In.) | Intended Use (a) | Fiber Content (wt %) | Resin Content (wt %) | Specific Gravity |
|---|---|---|---|---|---|---|---|---|
| LRC 7 | $[\pm 45°/0°]_s$ | 6 | 0.23 × 0.25 | 9 × 10 | 6 | 67.5 | 32.5 | — |
| LRC 8 | $[0° \pm 45°]_s$ | 6 | .23 × .25 | 9 × 10 | 6 | 67.2 | 32.8 | — |
| LRC 9 | $[45°/0°/45°]_s$ | 6 | .23 × .25 | 9 × 10 | 6 | 68.0 | 32.0 | — |
| LRC 10A | $[0°]_6$ | 6 | .69 × .91 | 27 × 36 | 0, 5, 7 | 67.1 | 32.9 | 1.56 |
| LRC11A | $[0°]_6$ | 6 | .76 × .91 | 30 × 36 | 0, 1, 7 | 66.8 | 33.2 | 1.56 |
| LRC12A | $[0° \pm 45°]_s$ | 6 | .91 × 1.02 | 36 × 40 | 9 | 66.8 | 33.2 | 1.57 |
| LRC16A | $[0°]_{12}$ | 12 | .61 × .61 | 24 × 24 | QA, 0, 2, 7 | 67.4 | 32.6 | 1.55 |
| LRC17A | $[0° \pm 45°]_{s2}$ | 12 | .30 × .71 | 12 × 28 | QA, 0, 2, 7 | 65.6 | 34.4 | 1.56 |
| LRC22A | $[0° \pm 45°]_s$ | 6 | .48 × .91 | 19 × 36 | 0, 7 | 65.5 | 34.5 | 1.58 |
| LRC23A | $[0° \pm 45°]_s$ | 6 | .69 × .76 | 27 × 30 | 0, 7 | 68.2 | 31.8 | 1.56 |
| LRC24A | $[0° \pm 45°]_s$ | 6 | .86 × .91 | 34 × 36 | 1, 5, 8 | 68.0 | 32.0 | 1.57 |
| LRC25A | $[0° \pm 45°]_s$ | 6 | .91 × .91 | 36 × 36 | 8 | 68.7 | 31.3 | 1.56 |
| LRC77-2 | $[0° \pm 45°]_s$ | 6 | .76 × .97 | 30 × 38 | 9 | 67.3 | 32.7 | 1.60 |

a QA Quality Assurance
0 Baseline
1 Thermal Aging
2 Ambient Aging
5 Creep
6 Stacking Sequence Evaluation
7 Fatigue
8 Short-Term Exposure
9 Long-Term Exposure

Table 6-7. Quality Assurance Mechanical Property Data for G/E Laminates (Phase I)

| Panel No. | Orientation | Temperature K | Temperature (°F) | Flexural Strength MN/m² | Flexural Strength (ksi) | Shear Strength MN/m² | Shear Strength (ksi) |
|---|---|---|---|---|---|---|---|
| LRC-16A | $[0°]_{12}$ | 297 | 75 | 1720 | 249 | 95.2 | 13.8 |
| | | | | 1716 | 248 | 99.3 | 14.4 |
| | | | | 1620 | 235 | 101.0 | 14.6 |
| Average | | | | 1680 | 244 | 98.5 | 14.3 |
| LRC-16A | $[0°]_{12}$ | 450 | 350 | 1220 | 177 | | |
| | | | | 1450 | 211 | | |
| | | | | 1210 | 176 | | |
| Average | | | | 1300 | 188 | | |
| LRC-17A | $[0° \pm 45°]_{s2}$ | 297 | 75 | 882 | 128 | 69.6 | 10.1 |
| | | | | 779 | 113 | 81.4 | 11.8 |
| | | | | 910 | 132 | 70.3 | 10.2 |
| Average | | | | 857 | 124 | 73.8 | 10.7 |
| LRC-17A | $[0° \pm 45°]_{s2}$ | 450 | 350 | 658 | 95.4 | | |
| | | | | 710 | 103 | | |
| | | | | 676 | 98.1 | | |
| Average | | | | 681 | 98.8 | | |

Table 6-8. Quality Assurance Data for G/E Laminates (Thermal Aging/Compression Study)

| Panel No. | Orientation | No. of Plies | Size m | Size (in.) | Intended Use (a) | Fiber Content (wt %) | Resin Content (wt %) | Specific Gravity | Tg K | Tg (°F) |
|---|---|---|---|---|---|---|---|---|---|---|
| IV-0 | $[0°]_{12}$ | 12 | 0.15 × 0.15 | 6 × 6 | QA | 75.4 | 24.6 | 1.58 | — | — |
| IV-1 | $[0° \pm 45°]_s$ | 6 | 0.66 × 0.66 | 26 × 26 | 0,1 | 72.5 | 27.5 | 1.58 | 446 | 342 |
| IV-2 | $[0° \pm 45°]_{s4}$ | 24 | 0.53 × 0.53 | 21 × 21 | 0,1 | 75.0 | 25.0 | 1.59 | — | — |

a QA Quality Assurance
0 Baseline
1 Thermal Aging

Table 6-9. Quality Assurance Mechanical Property Data for G/E Laminates (Thermal Aging/Compression Study)

| Panel No. | Orientation | Temperature K | Temperature (°F) | Flexural Strength MN/m² | Flexural Strength (ksi) | Shear Strength MN/m² | Shear Strength (ksi) |
|---|---|---|---|---|---|---|---|
| IV-0 | $[0°]_{12}$ | 297 | 75 | 1770 | 257 | 87 | 12.7 |
| | | | | 1660 | 241 | 84 | 12.2 |
| | | | | 1710 | 248 | 72 | 10.4 |
| Average | | | | 1710 | 249 | 81 | 11.8 |
| IV-0 | $[0°]_{12}$ | 450 | 350 | 1220 | 177 | 52 | 7.6 |
| | | | | 1190 | 172 | 53 | 7.7 |
| | | | | 1260 | 183 | 56 | 8.1 |
| Average | | | | 1220 | 177 | 54 | 7.8 |
| IV-2 | $[0° \pm 45°]_{S4}$ | 297 | 75 | 696 | 101 | 61 | 8.8 |
| | | | | 703 | 102 | 57 | 8.3 |
| | | | | 779 | 113 | 50 | 7.2 |
| Average | | | | 726 | 105 | 56 | 8.1 |
| IV-2 | $[0° \pm 45°]_{S4}$ | 450 | 350 | 571 | 82.8 | 51 | 7.4 |
| | | | | 561 | 81.4 | 50 | 7.2 |
| | | | | 594 | 86.1 | 50 | 7.2 |
| Average | | | | 575 | 83.4 | 50 | 7.3 |

Table 6-10. Quality Assurance Data for G/E Tubes

| Tube No. | Fiber Content (wt %) | Resin Content (wt %) | Specific Gravity |
|---|---|---|---|
| 1 | 66.6 | 33.4 | 1.56 |
| 2 | 68.6 | 31.4 | 1.55 |
| 3 | 67.5 | 32.5 | 1.56 |
| 4 | 68.2 | 31.8 | 1.56 |

Based on the results of the QA tests, all of the G/E fabricated laminates and tubes were considered to be satisfactory.

**6.2.3 BORON/POLYIMIDE.** Using the same technique described for the B/E material, all B/PI fabricated laminates were ultrasonic C-scan tested for delaminations and voids. All panels were judged to be acceptable based on this evaluation.

The results of the remaining QA tests on the B/PI laminates are presented in Table 6-11 for resin and fiber contents and specific gravity values and Table 6-12 for room and elevated temperature flexural and room temperature short beam shear strengths.

In addition to the B/PI panels, five B/PI 8 ply unidirectional tubes were fabricated for the baseline shear tests. Resin and fiber contents and specific gravity determinations were made on two of the tubes. The other three tubes were not tested as a result of the decision to drop the B/PI system from the program because of the very low tensile properties and the extensive thermal degradation observed during thermal aging and short-term flight simulation testing. Data for the two tubes that were tested are listed in Table 6-13.

Based on the results of the quality assurance tests, all of the B/PI fabricated laminates and tubes were considered to be satisfactory.

**6.2.4 GRAPHITE/POLYIMIDE**

**6.2.4.1 HT-S/710.** Using the same technique described for the B/E material, all HT-S/710 G/PI fabricated laminates were ultrasonic C-scan tested for delaminations and voids. All panels were judged to be acceptable based on this evaluation.

The results of the remaining QA tests on the HT-S/710 G/PI laminates are presented in Table 6-14 for resin and fiber contents and specific gravity values, Table 6-15 for room and elevated temperature flexural and room temperature short beam shear strengths (Phase I material only), and Table 6-5 for room and elevated temperatures tensile strengths (Phase II material only).

Based on the results of the QA tests all of the HT-S/710 G/PI fabricated laminates were considered to be satisfactory.

Table 6-11. Quality Assurance Data for B/Pl Laminates

| Panel No. | Orientation | No. of Plies | Size m | Size (in.) | Intended Use (a) | Fiber Content (wt %) (b) | Resin Content (wt %) | Specific Gravity |
|---|---|---|---|---|---|---|---|---|
| LRC-28R | $[0°]_{12}$ | 12 | 0.33 × 0.56 | 13 × 22 | QA, 0, 2 | 76.8 | 23.2 | 2.01 |
| LRC-29 | $[0° \pm 45°]_{s2}$ | 12 | .23 × .30 | 9 × 12 | QA, 2 | 69.2 | 30.8 | 1.85 |
| LRC-32 | $[0°]_6$ | 6 | .46 × .69 | 18 × 27 | 0, 7 | 71.6 | 28.4 | 1.98 |
| LRC-33 | $[0° \pm 45°]_s$ | 6 | .46 × .69 | 18 × 27 | 0 | 67.5 | 32.5 | 1.97 |
| LRC-34 | $[0°]_6$ | 6 | .48 × .91 | 19 × 36 | 0, 7 | 73.1 | 26.9 | 1.93 |
| LRC-35 | $[0° \pm 45°]_s$ | 6 | .48 × .91 | 19 × 36 | 0, 7 | 69.4 | 30.6 | 1.94 |
| LRC-36 | $[0° \pm 45°]_s$ | 6 | .46 × .86 | 18 × 34 | 8 | | | |
| LRC-37 | $[0° \pm 45°]_s$ | 6 | .46 × .86 | 18 × 34 | 8 | 66.5 | 33.5 | 1.91 |
| LRC-38 | $[0° \pm 45°]_s$ | 6 | .46 × .86 | 18 × 34 | 8 | 73.7 | 26.3 | 1.98 |
| LRC-39 | $[0°]_6$ | 6 | .58 × .69 | 23 × 27 | 1, 5 | 73.0 | 27.0 | 1.98 |
| LRC-40 | $[0° \pm 45°]_s$ | 6 | .51 × .61 | 20 × 24 | 0, 5 | 62.8 | 37.2 | 1.90 |
| LRC-41 | $[0° \pm 45°]_s$ | 6 | .25 × .46 | 10 × 18 | 1 | 69.0 | 31.0 | 1.91 |
| LRC-42 | $[0° \pm 45°]_s$ | 6 | .46 × 1.02 | 18 × 40 | 9 | | | |
| LRC-43 | $[0° \pm 45°]_s$ | 6 | .46 × 1.02 | 18 × 40 | 9 | | | |

a QA Quality Assurance
0 Baseline
1 Thermal Aging
2 Ambient Aging
5 Creep
7 Fatigue
8 Short-Term Exposure
9 Long-Term Exposure

b Includes approximately 9% glass fiber from scrim cloth

Table 6-12. Quality Assurance Mechanical Property Data for B/PI Laminates

| Panel No. | Orientation | Temperature K | Temperature (°F) | Flexural Strength MN/m² | Flexural Strength (ksi) | Shear Strength MN/m² | Shear Strength (ksi) |
|---|---|---|---|---|---|---|---|
| LRC-28R | $[0°]_{12}$ | 297 | 75 | 1770 | 257 | 55.8 | 8.1 |
| | | | | 1860 | 269 | 53.1 | 7.7 |
| | | | | 1340 | 195 | 49.0 | 7.1 |
| Average | | | | 1660 | 240 | 52.6 | 7.6 |
| LRC-28R | $[0°]_{12}$ | 450 | 350 | 1400 | 203 | | |
| | | | | 1390 | 202 | | |
| | | | | 1550 | 225 | | |
| Average | | | | 1450 | 210 | | |
| LRC-29 | $[0° \pm 45°]_{s2}$ | 297 | 75 | 972 | 141 | 35.2 | 5.1 |
| | | | | 896 | 130 | 36.5 | 5.3 |
| | | | | 993 | 144 | 36.5 | 5.3 |
| Average | | | | 954 | 138 | 36.1 | 5.2 |
| LRC-29 | $[0° \pm 45°]_{s2}$ | 450 | 350 | 745 | 108 | | |
| | | | | 841 | 122 | | |
| | | | | 820 | 119 | | |
| Average | | | | 803 | 116 | | |

Table 6-13. Quality Assurance Data for B/PI Tubes

| Tube No. | Fiber Content (wt %) | Resin Content (wt %) | Specific Gravity |
|---|---|---|---|
| 2 | 64.6 | 26 | 1.98 |
| 3 | 66.6 | 24 | 2.02 |

**6.2.4.2 Celion 6000/LARC-160.** Using the same technique described for the B/E material, all Celion 6000/LARC-160 G/PI fabricated laminates were ultrasonic C-scan tested for delaminations and voids. All panels were judged to be acceptable based on this evaluation.

The results of the remaining quality assurance tests on the Celion 6000/LARC-160 G/PI laminates fabricated for the Phase I series of tests are presented in Table 6-16 for resin and fiber contents and specific gravity values, Table 6-17 for room and elevated temperature flexural and short beam shear strengths, and Table 6-18 for room and elevated temperature tensile strengths of the 6 ply panels.

Specific gravity and fiber and resin contents for the two panels fabricated for the thermal aging/compression study are listed in Table 6-19. Also included is the Tg value for the 6 ply panel. Short beam shear and flexural strength data for the 24 ply panel have been included in Table 6-17. Again, the metallographic examinations of the two panels are discussed in the thermal aging section of the report.

Based on the results of the QA tests all of the Celion 6000/LARC-160 G/PI fabricated laminates were considered to be satisfactory.

Table 6-14. Quality Assurance Data for HT-S/710 G/PI Laminates (Phases I and II)

| Panel No. | Orientation | No. of Plies | Size m | Size (in.) | Intended Use (a) | Fiber Content (wt %) | Resin Content (wt %) | Specific Gravity |
|---|---|---|---|---|---|---|---|---|
| LRC-50 | $[0°]_{12}$ | 12 | 0.46 × 0.58 | 18 × 23 | QA, 0, 2, 7 | 68.8 | 31.2 | 1.41 |
| LRC-51 | $[0° \pm 45°]_{s2}$ | 12 | .46 × .46 | 18 × 18 | QA, 2, 7 | 67.7 | 32.3 | 1.40 |
| LRC-52 | $[0°]_6$ | 6 | .38 × .69 | 15 × 27 | 0, 7 | 67.6 | 32.4 | 1.49 |
| LRC-53 | $[0°]_6$ | 6 | .48 × .91 | 19 × 36 | 0, 7 | 67.3 | 32.7 | 1.51 |
| LRC-54 | $[0° \pm 45°]_s$ | 6 | .48 × .91 | 19 × 36 | 0, 7 | 68.4 | 31.6 | 1.42 |
| LRC-55 | $[0° \pm 45°]_s$ | 6 | .46 × .69 | 18 × 27 | 0, 7 | 68.6 | 31.4 | 1.40 |
| LRC-56 | $[0° \pm 45°]_s$ | 6 | .51 × .61 | 20 × 24 | 0, 5 | 68.4 | 31.6 | 1.55 |
| LRC-57 | $[0° \pm 45°]_s$ | 6 | .25 × .46 | 10 × 18 | 1 | 67.8 | 32.2 | 1.48 |
| LRC-58 | $[0°]_6$ | 6 | .58 × .69 | 23 × 27 | 1, 5 | 71.6 | 28.4 | 1.48 |
| LRC-59 | $[0° \pm 45°]_s$ | 6 | .46 × .69 | 18 × 27 | 8 | 68.3 | 31.7 | 1.43 |
| LRC-60 | $[0° \pm 45°]_s$ | 6 | .46 × .69 | 18 × 27 | 8 | 64.7 | 35.3 | 1.46 |
| LRC-61 | $[0° \pm 45°]_s$ | 6 | .46 × 1.02 | 18 × 40 | 9 | | | |
| LRC-62 | $[0° \pm 45°]_s$ | 6 | .46 × 1.02 | 18 × 40 | 9 | | | |
| KN-9 | $[0° \pm 45°]_s$ | 6 | .51 × .66 | 20 × 26 | 9 | 71.8 | 28.2 | 1.44 |

a QA Quality Assurance
0 Baseline
1 Thermal Aging
2 Ambient Aging
5 Creep
7 Fatigue
8 Short-Term Exposure
9 Long-Term Exposure

Table 6-15. Quality Assurance Mechanical Property Data for HT-S/710 G/PI Laminates (Phase I)

| Panel No. | Orientation | Temperature K | Temperature (°F) | Flexural Strength MN/m² | Flexural Strength (ksi) | Shear Strength MN/m² | Shear Strength (ksi) |
|---|---|---|---|---|---|---|---|
| LRC-50 | $[0°]_{12}$ | 297 | 75 | 1330 | 193 | 46.9 | 6.8 |
| | | | | 993 | 144 | 48.3 | 7.0 |
| | | | | 1220 | 177 | 49.6 | 7.2 |
| Average | | | | 1180 | 171 | 48.3 | 7.0 |
| LRC-50 | $[0°]_{12}$ | 450 | 350 | 869 | 126 | | |
| | | | | 952 | 138 | | |
| | | | | 807 | 117 | | |
| Average | | | | 876 | 127 | | |
| LRC-51 | $[0° \pm 45°]_{s2}$ | 297 | 75 | 664 | 96.4 | 40.7 | 5.9 |
| | | | | 567 | 82.2 | 37.9 | 5.5 |
| | | | | 703 | 102 | 33.8 | 4.9 |
| Average | | | | 645 | 93.5 | 37.5 | 5.4 |
| LRC-51 | $[0° \pm 45°]_{s2}$ | 450 | 350 | 538 | 78.0 | | |
| | | | | 661 | 95.8 | | |
| | | | | 439 | 63.7 | | |
| Average | | | | 546 | 79.2 | | |

Table 6-16. Quality Assurance Data for Celion 6000/LARC-160 G/PI Laminates

| Panel No. | Orientation | No. of Plies | Size m | Size in. | Intended Use (a) | Fiber Content (wt. %) | Resin Content (wt. %) | Specific Gravity |
|---|---|---|---|---|---|---|---|---|
| III-0 | $[0°]_{12}$ | 12 | 0.15 × 0.15 | 6 × 6 | QA | 71.6 | 28.4 | 1.54 |
| III-1 | $[0° \pm 45°]_{s4}$ | 24 | .38 × .48 | 15 × 19 | 7 | 71.7 | 28.3 | 1.56 |
| III-2 | $[0° \pm 45°]_{s2}$ | 12 | .38 × .48 | 15 × 19 | 0, 7 | 73.4 | 26.6 | 1.58 |
| III-3 | $[0° \pm 45°]_{s2}$ | 12 | .38 × .48 | 15 × 19 | 0, 2, 7 | 70.8 | 29.2 | 1.56 |
| III-4 | $[0° \pm 45°]_{s}$ | 6 | .41 × .64 | 16 × 25 | 5 | 72.4 | 27.6 | 1.58 |
| III-5 | $[0° \pm 45°]_{s}$ | 6 | .64 × .74 | 25 × 29 | 0, 1 | 72.5 | 27.5 | 1.58 |
| III-7 | $[0° \pm 45°]_{s}$ | 6 | .53 × .74 | 21 × 29 | 0, 1 | 70.7 | 29.3 | 1.56 |
| III-8 | $[0° \pm 45°]_{s}$ | 6 | .53 × .74 | 21 × 29 | 9 | 69.3 | 30.7 | 1.58 |
| III-9 | $[0° \pm 45°]_{s}$ | 6 | .53 × .74 | 21 × 29 | 9 | 71.3 | 28.7 | 1.60 |
| III-10 | $[0° \pm 45°]_{s}$ | 6 | .53 × .74 | 21 × 29 | 9 | 70.7 | 29.3 | 1.56 |
| III-11 | $[0° \pm 45°]_{s}$ | 6 | .51 × .79 | 20 × 31 | 7 | 72.1 | 27.9 | 1.59 |

(a) QA Quality Assurance
0 Baseline
1 Thermal Aging
2 Ambient Aging
5 Creep
7 Fatigue
9 Long-Term Exposure

Table 6-17. Quality Assurance Mechanical Property Data for Celion 6000/LARC-160 G/PI

| Panel No. | Orientation | Temperature K | Temperature (°F) | Flexural Strength MN/m² | Flexural Strength (ksi) | Shear Strength MN/m² | Shear Strength (ksi) |
|---|---|---|---|---|---|---|---|
| III-0 | $[0°]_{12}$ | 297 | 75 | 1380 | 200 | 61 | 8.8 |
| | | | | 1410 | 205 | 61 | 8.8 |
| | | | | 1270 | 184 | 66 | 9.5 |
| Average | | | | 1350 | 196 | 63 | 9.0 |
| III-0 | $[0°]_{12}$ | 450 | 350 | 1090 | 158 | 55 | 8.0 |
| | | | | 945 | 137 | 65 | 9.4 |
| | | | | 958 | 139 | 61 | 8.9 |
| Average | | | | 998 | 145 | 60 | 8.8 |
| III-1 | $[0° \pm 45°]_{s4}$ | 297 | 75 | 738 | 107 | 48 | 7.0 |
| | | | | 717 | 104 | 57 | 8.3 |
| | | | | 636 | 92.2 | 56 | 8.1 |
| Average | | | | 697 | 101 | 54 | 7.8 |
| III-1 | $[0° \pm 45°]_{s4}$ | 450 | 350 | 627 | 91.0 | 57 | 8.2 |
| | | | | 594 | 86.1 | 52 | 7.5 |
| | | | | 681 | 98.8 | 49 | 7.1 |
| Average | | | | 634 | 92.0 | 53 | 7.6 |
| III-2 | $[0° \pm 45°]_{s2}$ | 297 | 75 | 876 | 127 | 52 | 7.5 |
| | | | | 924 | 134 | 41 | 6.0 |
| | | | | 820 | 119 | 54 | 7.8 |
| Average | | | | 873 | 127 | 49 | 7.1 |
| III-2 | $[0° \pm 45°]_{s2}$ | 450 | 350 | 972 | 141 | 54 | 7.9 |
| | | | | 882 | 128 | 56 | 8.1 |
| | | | | 869 | 126 | 54 | 7.8 |
| Average | | | | 908 | 132 | 55 | 7.9 |

Table 6-17. Quality Assurance Mechanical Property Data for Celion 6000/LARC-160 G/PI, — Concluded

| Panel No. | Orientation | Temperature K | Temperature (°F) | Flexural Strength MN/m² | Flexural Strength (ksi) | Shear Strength MN/m² | Shear Strength (ksi) |
|---|---|---|---|---|---|---|---|
| III-3 | $[0° \pm 45°]_{s2}$ | 297 | 75 | 1070 | 155 | 73 | 10.6 |
| | | | | 972 | 141 | 74 | 10.7 |
| | | | | 1000 | 145 | 70 | 10.1 |
| Average | | | | 1010 | 147 | 72 | 10.5 |
| III-3 | $[0° \pm 45°]_{s2}$ | 450 | 350 | 765 | 111 | 47 | 6.8 |
| | | | | 793 | 115 | 54 | 7.8 |
| | | | | 827 | 120 | 47 | 6.8 |
| Average | | | | 795 | 115 | 49 | 7.1 |
| IV-4 | $[0° \pm 45°]_{s4}$ | 297 | 75 | 592 | 85.8 | 54 | 7.8 |
| | | | | 731 | 106 | 49 | 7.1 |
| | | | | 710 | 103 | 48 | 7.0 |
| Average | | | | 678 | 98.3 | 50 | 7.3 |
| IV-4 | $[0° \pm 45°]_{s4}$ | 450 | 350 | 627 | 91.0 | 50 | 7.3 |
| | | | | 631 | 91.5 | 50 | 7.2 |
| | | | | 724 | 105 | 54 | 7.9 |
| Average | | | | 661 | 95.8 | 51 | 7.5 |

Table 6-18. Quality Assurance Tensile Data for 6 Ply $[0° \pm 45°]_s$ Celion 6000/LARC-160 G/PI

| Panel No. | Temperature K | Temperature (°F) | Tensile Strength MN/m² | Tensile Strength (ksi) | Tensile Modulus GN/m² | Tensile Modulus (Msi) |
|---|---|---|---|---|---|---|
| III-4 | 297 | 75 | 643 | 93.3 | 57 | 8.3 |
| | | | 669 | 97.1 | 52 | 7.6 |
| | | | 506 | 73.4 | 49 | 7.1 |
| Average | | | 606 | 87.9 | 53 | 7.7 |
| III-4 | 450 | 350 | 680 | 98.6 | 62 | 9.0 |
| | | | 717 | 104 | 74 | 10.8 |
| | | | 745 | 108 | 52 | 7.5 |
| Average | | | 714 | 104 | 63 | 9.1 |
| III-5 | 297 | 75 | 758 | 110 | 57 | 8.3 |
| | | | 752 | 109 | 52 | 7.6 |
| | | | 703 | 102 | 54 | 7.9 |
| Average | | | 738 | 107 | 54 | 7.9 |
| III-5 | 450 | 350 | 738 | 107 | — | — |
| | | | 731 | 106 | 73 | 10.6 |
| | | | 665 | 96.5 | 49 | 7.1 |
| Average | | | 711 | 103 | 61 | 8.8 |
| III-7 | 297 | 75 | 474 | 68.8 | 50 | 7.2 |
| | | | 527 | 76.5 | 62 | 9.0 |
| | | | 554 | 80.4 | 57 | 8.3 |
| Average | | | 518 | 75.2 | 56 | 8.2 |
| III-7 | 450 | 350 | 629 | 91.3 | 56 | 8.1 |
| | | | 540 | 78.3 | 60 | 8.7 |
| | | | 518 | 75.2 | 59 | 8.6 |
| Average | | | 562 | 81.6 | 58 | 8.5 |
| III-8 | 297 | 75 | 745 | 108 | 60 | 8.7 |
| | | | 710 | 103 | 57 | 8.3 |
| | | | 643 | 93.2 | 53 | 7.7 |
| Average | | | 699 | 101 | 57 | 8.2 |
| III-8 | 450 | 350 | 724 | 105 | 52 | 7.6 |
| | | | 625 | 90.6 | 54 | 7.8 |
| | | | 595 | 86.3 | — | — |
| Average | | | 648 | 94.0 | 53 | 7.7 |
| III-9 | 297 | 75 | 703 | 102 | 63 | 9.1 |
| | | | 745 | 108 | 62 | 9.0 |
| | | | 667 | 96.7 | 66 | 9.5 |
| Average | | | 705 | 102 | 64 | 9.2 |

Table 6-18. Quality Assurance Tensile Data for 6 Ply $[0° \pm 45°]_s$ Celion 6000/LARC-160 G/PI — Concluded

| Panel No. | Temperature K | Temperature (°F) | Tensile Strength MN/m² | Tensile Strength (ksi) | Tensile Modulus GN/m² | Tensile Modulus (Msi) |
|---|---|---|---|---|---|---|
| III-9 | 450 | 350 | 678 | 98.4 | 67 | 9.7 |
| | | | 786 | 114 | 59 | 8.6 |
| | | | 738 | 107 | 49 | 7.1 |
| Average | | | 734 | 106 | 58 | 8.5 |
| III-10 | 297 | 75 | 745 | 108 | 65 | 9.4 |
| | | | 745 | 108 | 59 | 8.6 |
| | | | 752 | 109 | 63 | 9.2 |
| Average | | | 747 | 108 | 62 | 9.1 |
| III-10 | 450 | 350 | 848 | 123 | 61 | 8.8 |
| | | | 703 | 102 | 52 | 7.6 |
| | | | 710 | 103 | 51 | 7.4 |
| Average | | | 757 | 109 | 55 | 7.9 |
| III-11 | 297 | 75 | 643 | 93.3 | 55 | 7.9 |
| | | | 546 | 79.2 | 60 | 8.7 |
| | | | 629 | 91.2 | 59 | 8.5 |
| Average | | | 606 | 87.9 | 58 | 8.4 |
| III-11 | 450 | 350 | 731 | 106 | 55 | 8.0 |
| | | | 731 | 106 | 54 | 7.9 |
| | | | 690 | 100 | 57 | 8.3 |
| Average | | | 717 | 104 | 55 | 8.1 |

Table 6-19. Quality Assurance Data for Celion 6000/LARC-160 G/PI Laminates (Thermal Aging/Compression Study)

| Panel No. | Orientation | No. of Plies | Size m | Size (in.) | Intended Use (a) | Fiber Content (wt %) | Resin Content (wt %) | Specific Gravity | Tg K | Tg (°F) |
|---|---|---|---|---|---|---|---|---|---|---|
| IV-3 | $[0° \pm 45°]_s$ | 6 | 0.66 × 0.66 | 26 × 26 | 0,1 | 70.7 | 29.3 | 1.57 | 581 | 585 |
| IV-4 | $[0° \pm 45°]_{s4}$ | 24 | .53 × .53 | 21 × 21 | 0,1 | 63.1 | 36.9 | 1.52 | — | — |

a QA Quality Assurance
0 Baseline
1 Thermal Aging

# SECTION 7

# BASELINE TESTING

The purpose of the baseline tests was threefold. First, these data served to characterize the composite materials and add to any existing data bases. Second, the baseline tests provided the scale and shape parameters necessary to define the statistical distribution of the ultimate tensile strengths for each of the material systems. These, in turn, were used to set the loads for the short-term tests, and with the short-term results, were used in a wearout analysis model to relate static and fatigue strengths. Finally, the baseline tests provided a rational starting point against which the various environmental effects may be measured.

Tests that were conducted included ultimate tensile, tensile modulus, Poisson's ratio, notched tensile ($K_t = 2.43$), transverse tensile (unidirectional laminates only), ultimate shear strength, shear modulus, and fracture. In addition to those tests that were originally planned, a limited number of compressive tests were also performed. These were added late in Phase I of the program because of indications during thermal aging and flight simulation testing that matrix-dominated failure modes were operating. Testing was performed over the temperature range from 218 K (−67 ° F) to 450 K (350 ° F) for the epoxy specimens, to 533 K (500 ° F) for the Celion 6000/LARC-160 polyimide specimens, to 616 K (650 °F) for the HT-S/710 polyimide specimens, and to 700 K (800 ° F) for the B/Al specimens. Because of the large amount of data already available for the B/E system, only limited testing was conducted on this material. Baseline testing of the B/PI system had not been completed when the material was removed from the test program because of low tensile properties and extensive thermal degradation during thermal aging and short-term flight simulation testing. The HT-S/710 G/PI torsion tube tests were not run because of a lack of material with which to fabricate the test specimens. Some shear data were available at General Dynamics Convair, however, from a then current program evaluating the same HT-S/710 system. For the Celion 6000/LARC-160 G/PI that was added after completion of Phase I, several changes were made to the baseline test program. As stated earlier, no unidirectional panels were fabricated for this material, and, consequently, all the unidirectional baseline tests were eliminated. Also eliminated were the fracture tests on the $[0° \pm 45°]_s$ crossplied material. Based on the Phase I results it was thought that the limited amount of fracture data obtained would not be worth the rather high cost of specimen fabrication and testing. Two tests were added to the baseline evaluation of Celion 6000/LARC-160 G/PI. These were compressive and interlaminar shear strength tests on specimens made by bonding together several pieces of the 6 ply $[0° \pm 45°]_s$ laminates. Again, these tests were included because of the matrix-dominated failure modes observed during Phase I.

The testing procedures used for this study were those that had been adopted by General Dynamics Convair and the composites industry at the time this contract was initiated. In general, there were no standards other than those called out in the Structural Design Guide for Advanced Composite Applications (ref. 7).

All tests were conducted on calibrated test equipment. Temperature measurements were also made with calibrated thermocouples and recording devices. The General Dynamics Standards Laboratory utilizes a fully documented system that meets all the requirements of NASA and DOD. The system has reports to establish traceability to the National Bureau of Standards or equivalent.

The baseline tests, which are discussed below, have been grouped into four categories: 1) tensile, 2) shear, 3) fracture, and 4) compressive.

## 7.1 TENSILE TESTING

Included in this section are the unnotched and notched tensile tests, elastic modulus determinations, and the Poisson's ratio measurements.

**7.1.1 SPECIMEN DESIGN AND TEST PROCEDURE.** The tensile specimen configuration was rectangular with adhesively bonded end tabs to reduce stress concentrations at the gripping fixtures. Unidirectional and crossplied longitudinal specimens, both notched and unnotched, were prepared from 6 ply laminates while the unidirectional transverse specimens were 6 ply for B/Al and 12 ply for the epoxy and polyimide systems. The widths and lengths were dependent on the type of composite, the test direction, and the configuration, i.e., notched or unnotched. Details of the specimen geometry for the various materials and configurations are listed in Table 7-1. Based on results from numerous test programs conducted previously at General Dynamics, a width of 0.013 m (0.5 in.) was selected for the longitudinal tensile specimens of both the resin and metal matrix composites. The same width was suitable for the transverse B/Al specimens but was increased to 0.025 m (1.0 in.) for the transverse epoxy and polyimide specimens because of their low strength. The wider specimen reduced the likelihood of accidental failures during handling in the machining, doubler bonding, or testing operations. The notched configuration for the resin matrix specimens was the same as that used for the short-term flight simulation specimens. It consisted of a 0.025 m (1.0 in.) wide specimen with a 0.0064 m (0.25 in.) hole in the center. The theoretical stress concentration ($K_t$) for this configuration is 2.43 (ref. 28). The original plan for the B/Al system called for a side notched specimen, 0.013 m (0.5 in.) in width, with a theoretical notch acuity ($K_t$) of 6.3. After cutting the blanks but before machining the side notches, a decision was made to use a configuration similar to that chosen for the resin matrix specimens. To keep the hole-to-specimen width ratio the same, a 0.00318 m (0.125 in.) diameter hole was machined in the center of the B/Al specimens.

The tensile specimens used on the program are shown in Figure 7-1 for the longitudinal resin matrix and metal matrix specimens and in Figure 7-2 for the transverse resin matrix specimens. The transverse B/Al specimen is identical in dimensions to the longitudinal specimen of Figure 7-1. The notched tensile configurations are shown in Figure 7-3 for the resin and metal matrix composites.

Tensile testing was conducted in both Instron and Tinius-Olsen testing machines using Instron capstan grips with ball or universal joints to ensure axial loading of the specimens. A crosshead rate of 0.0025 m (0.01 in.) per minute was used for all tests. Strain was measured in two ways. For the specimens where Poisson's ratio was required, four strain gages were bonded to the test section. Elastic modulus values could also be determined from these specimens. A few of the G/PI and B/Al specimens were also strain gaged (two gages only) to determine modulus values at the higher temperatures where conventional extensometer measurements were not always reliable. The second method of strain measurement was with a clamp-on strain gage extensometer. The extensometer was used from 218 K (−67° F) to 561 K (550° F) with reasonably good results. At the higher temperatures, however, the bonded strain gage method was superior. An elevated temperature tensile specimen mounted in the capstan grips with a strain gage extensometer and thermocouple attached ready for test is shown in Figure 7-4.

Table 7-1. Details of Tensile Specimen Geometry

| Material System | Specimen Configuration | Test Direction | Length | | Width | | Hole Diameter | | Test Section | |
|---|---|---|---|---|---|---|---|---|---|---|
| | | | m | in. | m | in. | m | in. | m | in. |
| Resin Matrix | Unnotched | Longitudinal | 0.23 | 9 | 0.013 | 0.5 | — | — | 0.10 | 4 |
| | Unnotched | Transverse | .23 | 9 | .025 | 1 | — | — | .10 | 4 |
| | Notched | Longitudinal | .23 | 9 | .025 | 1 | .0064 | .25 | .10 | 4 |
| Metal Matrix | Unnotched | Longitudinal | .15 | 6 | .013 | 0.5 | — | — | .051 | 2 |
| | Unnotched | Transverse | .15 | 6 | .013 | .5 | — | — | .051 | 2 |
| | Notched | Longitudinal | .15 | 6 | .013 | .5 | .00318 | .125 | .051 | 2 |

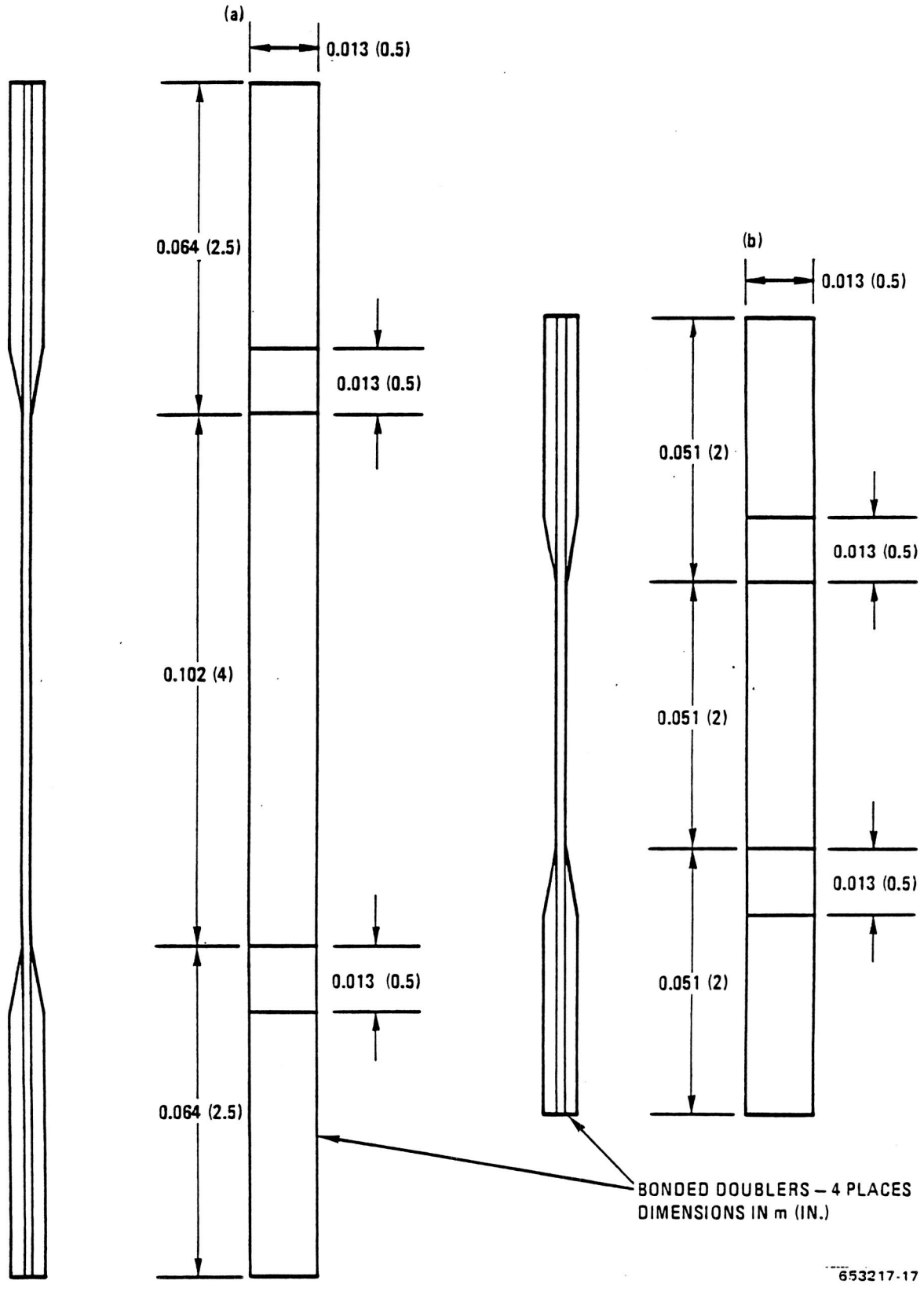



**Figure 7-1 Tensile Test Specimen for (a) Resin Matrix Composites and (b) Metal Matrix Composites**

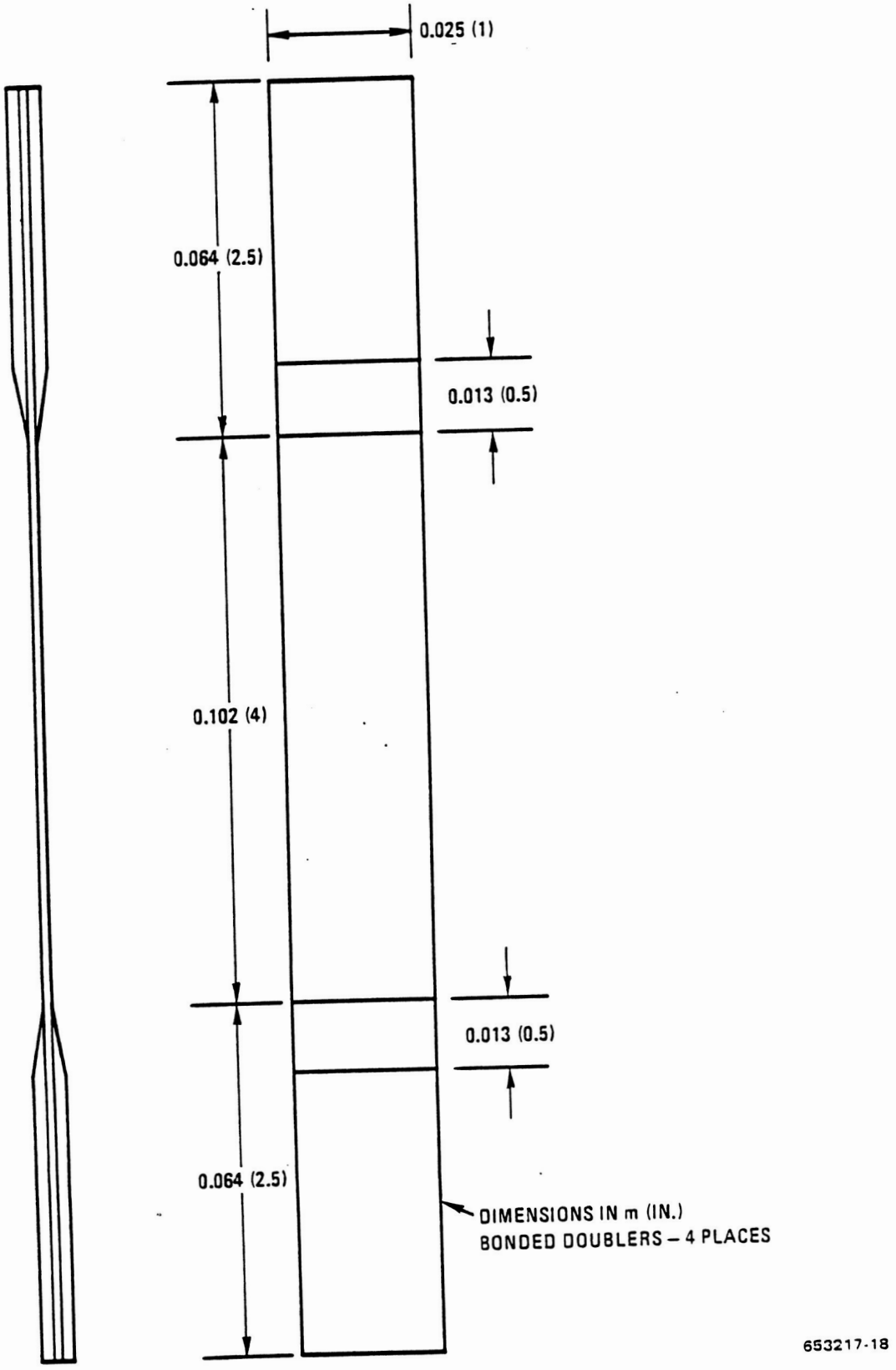



**Figure 7-2 Transverse Tensile Test Specimen for Resin Matrix Composites**

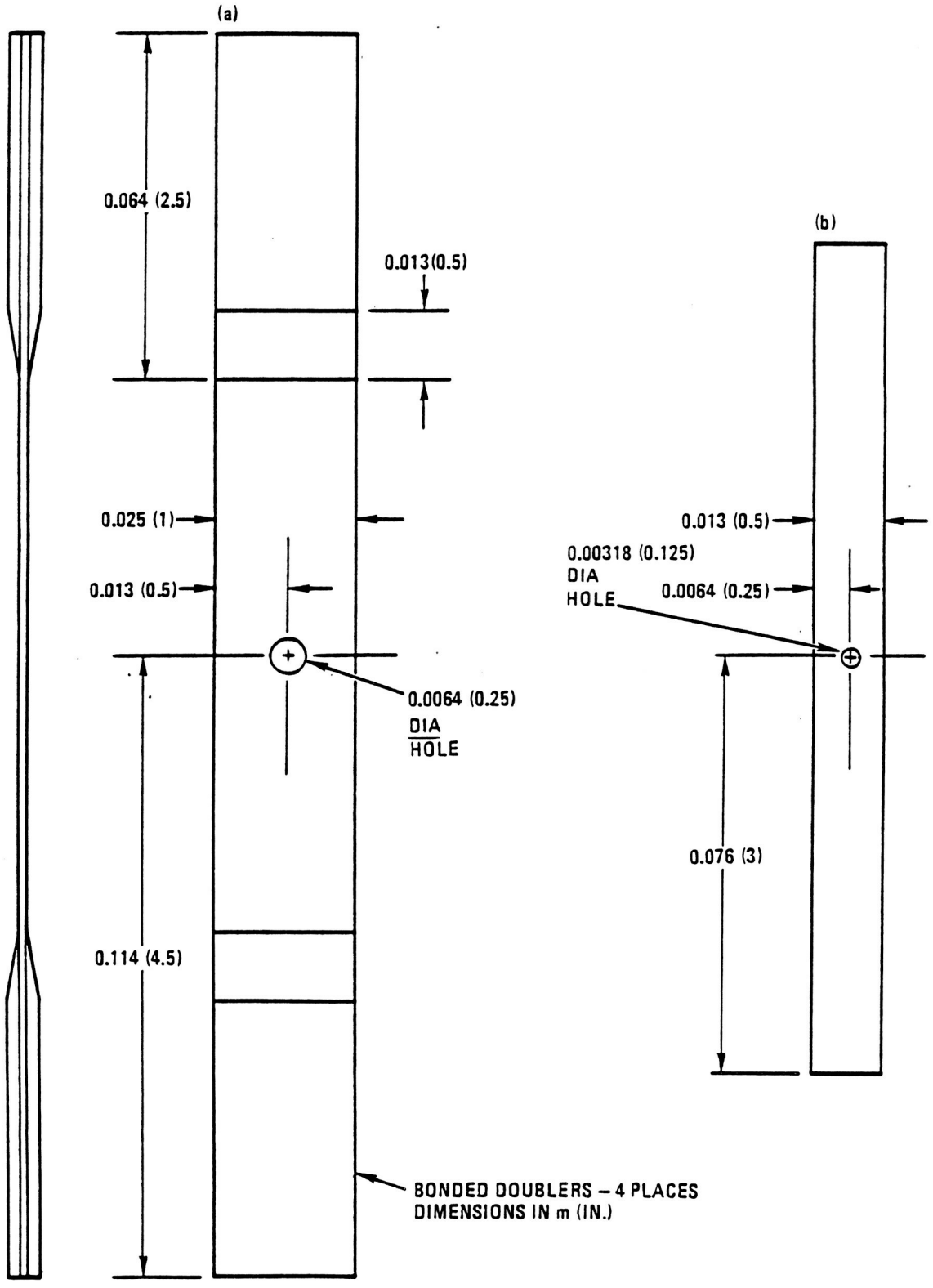



**Figure 7-3 Notched Tensile Test Specimen for (a) Resin Matrix Composites and (b) Metal Matrix Composites**

ORIGINAL PAGE IS
OF POOR QUALITY

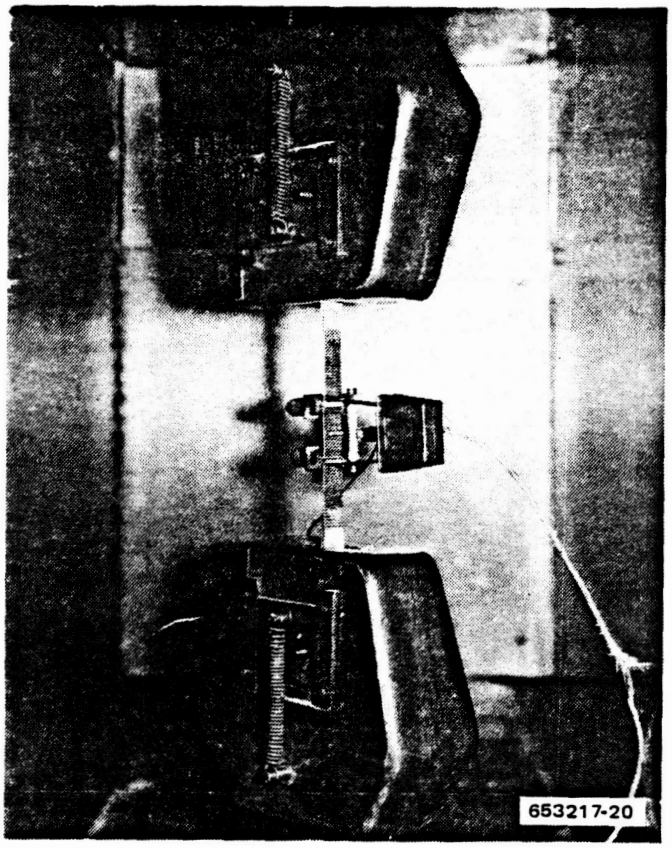



**Figure 7-4 Elevated Temperature Tensile Test Setup**

Elevated temperature tests were conducted with either a Conrad-Missimer chamber or a small ring furnace. The advantage of the ring furnace was that the grips were not directly heated and doubler bond failures were reduced. The ring furnace was particularly beneficial at temperatures above about 561 K (550° F). All the tests at 218 K (−67° F) were performed in the Conrad-Missimer chamber. Temperature was measured with a thermocouple clipped to the specimen such that the bead was in contact with the surface. Specimens were held at temperature for a minimum of 10 minutes prior to loading.

For the specimens that were to be strain gaged the following procedure was used. Prior to application of the gages, the specimens were lightly sanded in the gage section and precoated with M-bond 900 adhesive (manufactured by Micro-Measurement) to fill any void areas in the surface. The precoat was cured at 366 K (200° F) for two hours, and the specimens were again lightly sanded. The strain gages were then installed on the clean surfaces. Poisson's ratio specimens were instrumented with four strain gages, one longitudinal and one transverse gage on each side. For determination of elastic modulus only two gages were required, one longitudinal gage on each side.

Table 7-2 lists the type of gages (manufactured by BLH Electronics, Inc.), adhesives, and cure cycles selected for the different test specimens.

**Table 7-2. Strain Gage Data for Poisson's Ratio and Elastic Modulus Testing**

| Material System | Orientation | Test Temperature K | Test Temperature (°F) | Type of Gage Longitudinal | Type of Gage Transverse | Adhesive | Cure Cycle Temperature K | Cure Cycle Temperature (°F) | Cure Cycle Time hr |
|---|---|---|---|---|---|---|---|---|---|
| 5505/4 B/E | $[0° \pm 45°]_s$ | 297 | 75 | FAE-25-12-SO | FAE-12-12-SO | M-bond 200 | — | — | — |
| A-S/3501 G/E | $[0°]_6$ | 297 | 75 | FAE-25-12-SO | FAE-12-12-S15 | M-bond 200 | — | — | — |
| | $[0°]_6$ | 394 | 250 | FAE-25-12-SO | FAE-12-12-S15 | M-bond 610 | 436 | 325 | 2 |
| | $[0°]_6$ | 450 | 350 | FAE-25-12-SO | FAE-12-12-S15 | M-bond 610 | 450 | 350 | 1.5 |
| | $[0° \pm 45°]_s$ | 297 | 75 | FAE-25-12-SO | FAE-12-12-SO | M-bond 200 | — | — | — |
| HT-S/710 G/PI | $[0°]_6$ | 505 | 450 | FAE-25-12-SO | FAE-12-12-S15 | M-bond 610 | 505 | 450 | 1 |
| | $[0°]_6$ | 561 | 550 | FSM-25-35-SO | FSM-12-35-S13 | PLD-700 | 561 | 550 | 1 |
| | $[0° \pm 45°]_s$ | 297 | 75 | FAE-25-12-SO | FAE-12-12-SO | M-bond 200 | — | — | — |
| | $[0° \pm 45°]_s$ | 505 | 450 | FAE-25-12-SO | (a) | M-bond 610 | 505 | 450 | 1 |
| | $[0° \pm 45°]_s$ | 561 | 550 | FSM-25-35-SO | (a) | PLD-700 | 561 | 550 | 1 |
| Celion 6000/ LARC-160 G/PI | $[0° \pm 45°]_s$ | 297 | 75 | FAE-25-12-SO | (a) | M-bond 200 | — | — | — |
| | $[0° \pm 45°]_s$ | 450 | 350 | FAE-25-12-SO | (a) | M-bond 610 | 450 | 350 | 1.5 |
| B/Al | $[0°]_6$ | 561 | 550 | FSM-25-35-SO | FSM-12-35-S13 | PLD-700 | 561 | 550 | 1 |
| | $[0°]_6$ | 700 | 800 | FSM-25-35-SO | FSM-12-35-S13 | PLD-700 | 700 | 800 | 1 |
| | $[0° \pm 45°]_s$ | 505 | 450 | FAE-25-12-S3 | (a) | M-bond 610 | 505 | 450 | 1 |
| | $[0° \pm 45°]_s$ | 561 | 550 | FSM-25-35-SO | (a) | PLD-700 | 561 | 550 | 1 |
| | $[0° \pm 45°]_s$ | 616 | 650 | FSM-25-35-SO | (a) | PLD-700 | 616 | 650 | 1 |
| | $[0° \pm 45°]_s$ | 700 | 800 | FSM-25-35-SO | (a) | PLD-700 | 700 | 800 | 1 |

[a] Modulus only — no transverse gage required

Testing of the strain gaged specimens was conducted in a manner similar to that used for the specimens tested with a clamp-on extensometer except for the method of loading. These specimens were loaded incrementally to failure with strain measurements recorded automatically with a B & F Instruments, Inc. Multichannel Digital Strain Indicator, 161 Mini-System, at each load level. The output was both a typewritten recording of load versus strain and a punched paper tape that could be processed by a computer, programmed to produce a stress-strain plot. A typical computer generated plot is shown in Figure 7-5. Poisson's ratio and elastic modulus values were determined from these curves. Figure 7-6 shows the Mini-System in operation during a room temperature tensile test.

Prior to tensile testing of the resin matrix material, all elevated temperature specimens and those room temperature specimens that were not strain gaged were heated at 394 K (250 ° F) for at least 24 hours to remove any absorbed moisture. The strain-gaged room temperature specimens were baked out prior to application of the gages and then stored in a desiccator until test.

### 7.1.2 TEST RESULTS AND DISCUSSION

**7.1.2.1 Boron/Epoxy.** Because a large data base was already available for the B/E system, no baseline tensile testing was needed. However, for later comparisons with the residual strength data from the flight simulation exposure specimens it was desirable to have baseline unnotched and notched tensile data from the same batch of material. Therefore, room temperature unnotched and notched tensile tests were conducted on $[0° \pm 45°]_s$ crossply material using the same test conditions and specimen configurations as were used later in evaluating the B/E flight simulation specimens after 10,000 hours of exposure. The unnotched specimens were strain gaged so that Poisson's ratio values could also be determined. The results are listed in Table 7-3. A tensile load-strain diagram is shown in Figure 7-7 for one of the strain gaged specimens. The points plotted are the average of the two longtitudinal or transverse gages. Based on the few tests that were run, there was an approximately 30% decrease in the net tensile strength in $[0° \pm 45°]_s$ crossply B/E for the notched specimen configuration chosen. The Poisson's ratio values appear to be quite large (values for metals are generally about one-third) but are close to what is calculated from lamination theory for a crossplied layup.

Also included in Table 7-3 are tensile data from the quality assurance evaluation of the Phase II batch of B/E. The tensile strength of the Phase I material is approximately 15% higher than that of the Phase II material. The Phase I specimens were cut from an area of panel that was somewhat thin. A comparison of failure loads for the two sets of data shows less than a 5% difference. Additional data indicating that the Phase I baseline tensile strengths are not representative are the tensile data obtained from the stacking sequence fatigue study (Section 11.3.4) and tensile data from short time thermal aging exposures (Section 8.2.1). Both sets of results show good agreement with the Phase II quality assurance tensile data.

**7.1.2.2 Graphite/Epoxy.** The initial plan for the Phase I G/E baseline tensile tests was to test at four temperatures. This was later changed to seven temperatures with three specimens each (total of 21 specimens). From the tensile strength versus temperature curve obtained, two of the temperatures would then be selected for an additional seven tests each (total of 14 specimens). It was planned to select these two temperatures in the region just below that where a distinct change in the slope of the strength versus temperature curve occurred and then to use these data to set the loads for the flight simulation exposures. For G/E, however, no fall-off in strength was observed out to the maximum test temperature of 450 K (350 ° F). Because of the

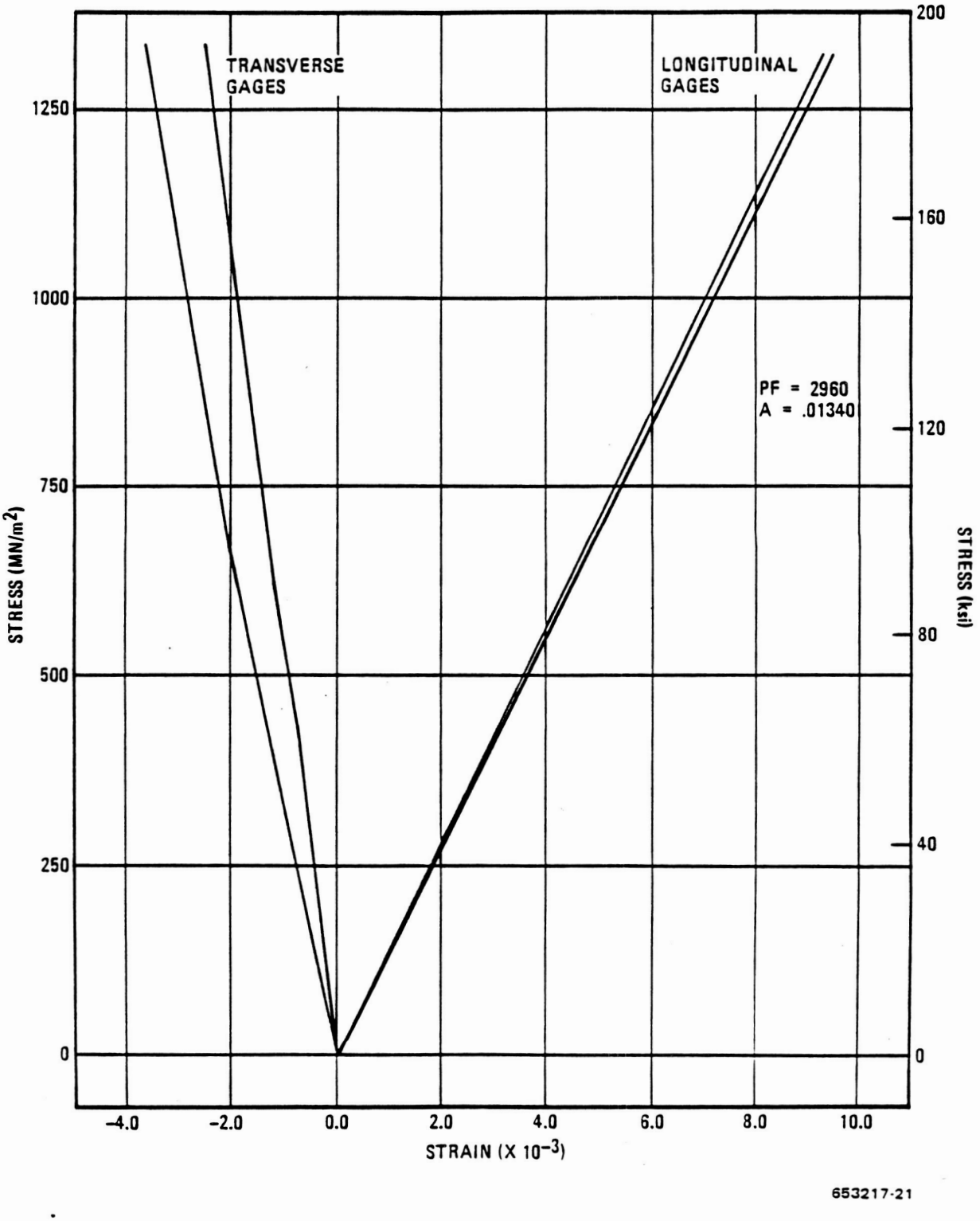



**Figure 7-5 Typical Stress-Strain Curve for Tensile Test of $[0°]_6$ G/E**

ORIGINAL PAGE IS
OF POOR QUALITY

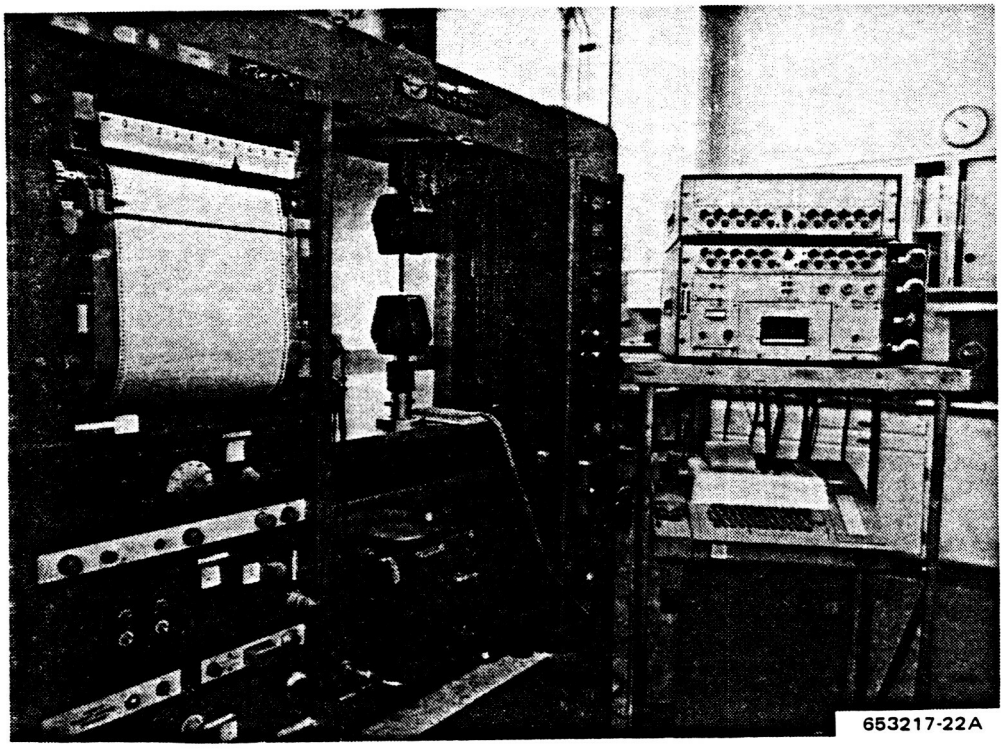



**Figure 7-6 Automatic Strain Recording Instrumentation for Strain Gaged Tensile Specimen**

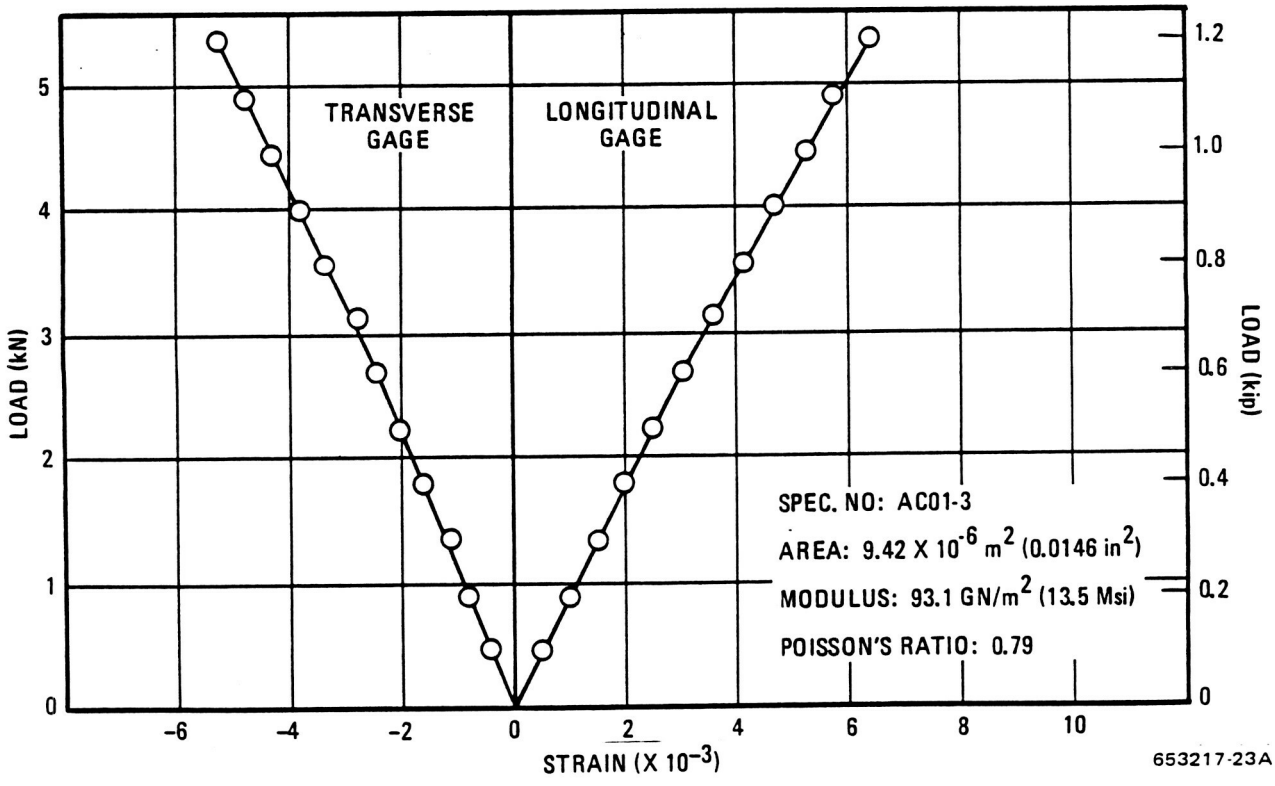



**Figure 7-7 Tensile Load-Strain Diagram for $[0° \pm 45°]_s$ B/E at 297 K (75° F)**

Table 7-3. Baseline Tensile Properties of $[0° \pm 45°]_s$ B/E at Room Temperature

| Specimen Number | Configuration | Tensile Strength MN/m² | (ksi) | Tensile Modulus GN/m² | (psi × 10⁶) | Poisson's Ratio |
|---|---|---|---|---|---|---|
| Phase I Material | | | | | | |
| AC01-1 | Unnotched | 596 | 86.4 | [a]96.5 | [a]14.0 | [a]0.76 |
| -2 | | 617 | 89.5 | [a]93.1 | [a]13.5 | [a] .80 |
| -3 | | 643 | 93.2 | [a]93.1 | [a]13.5 | [a] .79 |
| Average | | 619 | 89.7 | 94.2 | 13.7 | .78 |
| AC02-1 | Notched | 399 | 57.9 | — | — | — |
| -2 | | 476 | 69.0 | — | — | — |
| -3 | | 454 | 65.8 | — | — | — |
| Average | | 443 | 64.2 | | | |
| Phase II Material | | | | | | |
| A-1 | Unnotched | 539 | 78.2 | 79 | 11.4 | — |
| -2 | | 529 | 76.7 | 52 | 7.6 | — |
| -3 | | 524 | 76.0 | 81 | 11.7 | — |
| Average | | 531 | 77.0 | 71 | 10.2 | |

[a] Strain gage measurement

uncertainty in the maximum use temperature of G/E for very long times, the two additional tensile test temperatures were selected such as to cover a wide range of temperature. They were 394 K (250 ° F) and 450 K (350 ° F). As it later was found during the long-term flight simulation tests, both temperatures were above the maximum use temperature of the epoxy systems for 10,000 hour service.

Baseline tensile tests, both unnotched and notched, were performed on unidirectional and $[0° \pm 45°]_s$ crossplied specimens in the longitudinal direction. Some unnotched tensile tests were also performed in the transverse direction on unidirectional material, and a limited amount of Poisson's ratio testing was conducted. Results are listed in Tables 7-4 through 7-9. Figure 7-8 shows a typical example of a load-strain diagram obtained from one of the strain gaged Poisson's ratio specimens. The longitudinal unnotched and notched data are plotted as a function of temperature in Figures 7-9 and 7-10. A summary of all the G/E tensile properties is presented in Table 7-10.

Modulus values are given for the majority of unnotched specimens. For some specimens, however, modulus values were not determined because of the change in the test plan discussed above. Specimens that had originally been scheduled for testing at room temperature had been prepared with doublers bonded on with low temperature adhesive. To test these samples at an elevated temperature, a small ring furnace that heated only the center section of the specimen was required. With this type of heater, the clamp-on extensometer could not be accommodated. In addition to these specimens, a few others are shown without modulus values because of extensometer malfunctions. Several of the specimens were strain gaged in order to measure

Table 7-4. Baseline Tensile Properties of $[0°]_6$ G/E

| Specimen Number | Temperature K | Temperature (°F) | Tensile Strength $MN/m^2$ | Tensile Strength (ksi) | Tensile Modulus $GN/m^2$ | Tensile Modulus (Msi) |
|---|---|---|---|---|---|---|
| BU01-1 | 218 | −67 | 917 | 133 | — | — |
| -2 | | | 1050 | 153 | — | — |
| -3 | | | 683 | 99 | — | — |
| | | | avg 883 | 128 | | |
| BU01-4 | 297 | 75 | 1460 | 211 | [a]143 | [a]20.8 |
| -5 | | | 1660 | 240 | [a]134 | [a]19.4 |
| -6 | | | 1540 | 223 | [a]145 | [a]21.0 |
| | | | avg 1550 | 225 | 141 | 20.4 |
| BU01-7 | 394 | 250 | 1650 | 239 | [a]141 | [a]20.4 |
| -8 | | | 1440 | 209 | [a]136 | [a]19.8 |
| -9 | | | 1490 | 216 | [a]136 | [a]19.8 |
| -22 | | | 1460 | 212 | — | — |
| -23 | | | 1560 | 227 | 161 | 23.3 |
| -24 | | | 1520 | 221 | 152 | 22.1 |
| -25 | | | 1350 | 196 | 141 | 20.4 |
| -26 | | | 1630 | 236 | 150 | 21.8 |
| -27 | | | 1450 | 210 | 144 | 20.9 |
| -28 | | | 1570 | 228 | 152 | 22.1 |
| | | | avg 1510 | 219 | 146 | 21.2 |
| BU01-10 | 408 | 275 | 1660 | 241 | — | — |
| -11 | | | 1740 | 252 | 165 | 23.9 |
| -12 | | | 1610 | 233 | 166 | 24.1 |
| | | | avg 1670 | 242 | 166 | 24.0 |
| BU01-13 | 422 | 300 | 1540 | 224 | [a]141 | [a]20.5 |
| -14 | | | 1520 | 221 | [a]140 | [a]20.3 |
| -15 | | | 1450 | 210 | [a]136 | [a]19.9 |
| | | | avg 1500 | 218 | 139 | 20.2 |
| BU01-16 | 436 | 325 | 1600 | 232 | 143 | 20.7 |
| -17 | | | 1660 | 240 | 141 | 20.5 |
| -18 | | | 1600 | 232 | 131 | 19.0 |
| | | | avg 1620 | 235 | 138 | 20.1 |
| BU01-19 | 450 | 350 | 1630 | 237 | 150 | 21.7 |
| -20 | | | 1630 | 237 | 150 | 21.8 |
| -21 | | | 1550 | 225 | 131 | 19.0 |
| -29 | | | 1580 | 229 | 154 | 22.3 |
| -30 | | | 1630 | 237 | 148 | 21.5 |
| -31 | | | 1630 | 236 | 154 | 22.4 |
| -32 | | | 1590 | 231 | 160 | 23.2 |
| -33 | | | 1310 | 190 | 144 | 20.9 |
| -34 | | | 1630 | 236 | 156 | 22.6 |
| -35 | | | 1680 | 243 | 155 | 22.5 |
| | | | avg 1590 | 230 | 150 | 21.8 |

[a] Strain gage measurement

Table 7-5. Baseline Tensile Properties of $[0° \pm 45°]_s$ G/E

| Specimen Number | Temperature K | Temperature (°F) | Tensile Strength MN/m² | Tensile Strength (ksi) | Tensile Modulus GN/m² | Tensile Modulus (Msi) |
|---|---|---|---|---|---|---|
| BC01-1 | 218 | −67 | 416 | 60.4 | 49 | 7.1 |
| -2 | | | 439 | 63.6 | 43 | 6.2 |
| -3 | | | 493 | 71.5 | 50 | 7.3 |
| | | avg | 449 | 65.2 | 47 | 6.9 |
| BC01-6 | 297 | 75 | 578 | 83.8 | [a]61 | [a] 8.8 |
| -7 | | | 447 | 64.8 | [a]54 | [a] 7.9 |
| -8 | | | 463 | 67.2 | [a]56 | [a] 8.1 |
| | | avg | 496 | 71.9 | 57 | 8.3 |
| BC01-4 | 394 | 250 | 478 | 69.4 | — | — |
| -5 | | | 505 | 73.2 | — | — |
| -16 | | | 443 | 64.2 | 55 | 8.0 |
| -22 | | | 524 | 76.0 | 46 | 6.6 |
| -23 | | | 518 | 75.2 | — | — |
| -24 | | | 623 | 90.3 | 43 | 6.2 |
| -25 | | | 596 | 86.4 | 48 | 7.0 |
| -26 | | | 541 | 78.4 | 65 | 9.4 |
| -27 | | | 521 | 75.5 | 74 | 10.8 |
| -28 | | | 509 | 73.8 | 62 | 9.0 |
| | | avg | 526 | 76.2 | 56 | 8.1 |
| BC01-9 | 408 | 275 | 494 | 71.6 | — | — |
| -10 | | | 407 | 59.0 | — | — |
| -17 | | | 552 | 80.1 | 54 | 7.8 |
| | | avg | 484 | 70.2 | 54 | 7.8 |
| BC01-11 | 422 | 300 | 569 | 82.5 | — | — |
| -18 | | | 460 | 66.7 | 48 | 6.9 |
| -19 | | | 497 | 72.1 | 54 | 7.8 |
| | | avg | 509 | 73.8 | 51 | 7.4 |
| BC01-12 | 436 | 325 | 508 | 73.7 | — | — |
| -13 | | | 520 | 75.4 | — | — |
| -20 | | | 477 | 69.2 | 53 | 7.7 |
| | | avg | 502 | 72.8 | 53 | 7.7 |
| BC01-14 | 450 | 350 | 457 | 66.3 | — | — |
| -15 | | | 522 | 75.7 | — | — |
| -21 | | | 499 | 72.4 | 46 | 6.6 |
| -29 | | | 514 | 74.6 | 78 | 11.3 |
| -30 | | | 499 | 72.4 | 70 | 10.1 |
| -31 | | | 430 | 62.4 | 52 | 7.5 |
| -32 | | | 470 | 68.1 | 47 | 6.8 |
| -33 | | | 558 | 81.0 | 63 | 9.2 |
| -34 | | | 506 | 73.4 | 53 | 7.7 |
| -35 | | | 544 | 78.9 | 57 | 8.2 |
| | | avg | 500 | 72.5 | 58 | 8.4 |

[a] Strain gage measurement

Table 7-6. Baseline Notched Tensile Properties of $[0°]_6$ G/E

| Specimen Number | Temperature K | Temperature (°F) | | Notched Tensile Strength $MN/m^2$ (a) | Notched Tensile Strength (ksi) |
|---|---|---|---|---|---|
| BU02-1 | 218 | −67 | | 1100 | 159 |
| -2 | | | | 938 | 136 |
| -3 | | | | 1060 | 154 |
| | | | avg | 1030 | 150 |
| BU02-4 | 297 | 75 | | 1340 | 194 |
| -5 | | | | 1310 | 190 |
| -6 | | | | 1490 | 216 |
| | | | avg | 1380 | 200 |
| BU02-7 | 394 | 250 | | 1390 | 202 |
| -8 | | | | 1210 | 176 |
| -9 | | | | 1200 | 174 |
| -22 | | | | 1380 | 200 |
| -23 | | | | 1210 | 176 |
| -24 | | | | 1560 | 226 |
| -25 | | | | 1250 | 181 |
| -26 | | | | 1570 | 228 |
| -27 | | | | 1630 | 236 |
| -28 | | | | 1510 | 219 |
| | | | avg | 1390 | 202 |
| BU02-10 | 408 | 275 | | 1640 | 238 |
| -11 | | | | 1630 | 237 |
| -12 | | | | 1590 | 230 |
| | | | avg | 1620 | 235 |
| BU02-13 | 422 | 300 | | 1610 | 234 |
| -14 | | | | 1480 | 214 |
| -15 | | | | 1270 | 184 |
| | | | avg | 1450 | 211 |
| BU02-16 | 436 | 325 | | 1400 | 203 |
| -17 | | | | 1320 | 192 |
| -18 | | | | 1510 | 219 |
| | | | avg | 1410 | 205 |
| BU02-19 | 450 | 350 | | [b]1170 | [b]170 |
| -20 | | | | 1240 | 180 |
| -21 | | | | 1260 | 182 |
| -29 | | | | [b]1160 | [b]168 |
| -30 | | | | 1340 | 195 |
| -31 | | | | [b]1180 | [b]171 |
| -32 | | | | [b]1260 | [b]183 |
| -33 | | | | 1590 | 230 |
| -34 | | | | 1340 | 194 |
| -35 | | | | [b] 910 | [b]132 |
| | | | avg | 1350 | 196 |

[a] Net section strength, i.e., based on total width less hole diameter.
[b] Doubler failure, values not included in average.

Table 7-7. Baseline Notched Tensile Properties of $[0° \pm 45°]_s$ G/E

| Specimen Number | Temperature K | Temperature (°F) | | Notched Tensile Strength MN/m² (a) | Notched Tensile Strength (ksi) |
|---|---|---|---|---|---|
| BC02-1 | 218 | −67 | | 317 | 46.0 |
| -2 | | | | 309 | 44.8 |
| -3 | | | | 311 | 45.1 |
| | | | avg | 312 | 45.3 |
| BC02-4 | 297 | 75 | | 367 | 53.2 |
| -5 | | | | 477 | 69.2 |
| -6 | | | | 391 | 56.7 |
| | | | avg | 412 | 59.7 |
| BC02-7 | 394 | 250 | | 461 | 66.9 |
| -8 | | | | 398 | 57.7 |
| -9 | | | | 536 | 77.8 |
| -22 | | | | 324 | 47.0 |
| -23 | | | | 360 | 52.2 |
| -24 | | | | 429 | 62.2 |
| -25 | | | | 443 | 64.3 |
| -26 | | | | 385 | 55.8 |
| -27 | | | | 319 | 46.2 |
| -28 | | | | 358 | 51.9 |
| | | | avg | 401 | 58.2 |
| BC02-10 | 408 | 275 | | 448 | 65.0 |
| -11 | | | | 367 | 53.3 |
| -12 | | | | 377 | 54.7 |
| | | | avg | 397 | 57.7 |
| BC02-13 | 422 | 300 | | 456 | 66.2 |
| -14 | | | | 372 | 54.0 |
| -15 | | | | 353 | 51.2 |
| | | | avg | 394 | 57.1 |
| BC02-16 | 436 | 325 | | 429 | 62.2 |
| -17 | | | | 425 | 61.6 |
| -18 | | | | 436 | 63.2 |
| | | | avg | 430 | 62.3 |
| BC02-19 | 450 | 350 | | 445 | 64.6 |
| -20 | | | | 396 | 57.5 |
| -21 | | | | 553 | 80.2 |
| -29 | | | | 419 | 60.8 |
| -30 | | | | 334 | 48.4 |
| -31 | | | | 403 | 58.4 |
| -32 | | | | 396 | 57.4 |
| -33 | | | | 445 | 64.5 |
| -34 | | | | 398 | 57.7 |
| -35 | | | | 369 | 53.5 |
| | | | avg | 416 | 60.3 |

[a] Net section strength, i.e., based on total width less hole diameter.

**Table 7-8. Baseline Tensile Properties of $[0°]_{12}$ G/E Tested in the Transverse Direction**

| Specimen Number | Temperature K | Temperature (°F) | Edge Condition | Specimen Width m | Specimen Width (in.) | | Tensile Strength $MN/m^2$ | Tensile Strength (ksi) |
|---|---|---|---|---|---|---|---|---|
| TBU01-1 | 297 | 75 | Poor | 0.0025 | 1.00 | | 29 | 4.2 |
| -2 | | | | .0025 | 1.00 | | 40 | 5.8 |
| -3 | | | | .0025 | .99 | | 27 | 3.9 |
| -4 | | | | .0025 | 1.00 | | 38 | 5.5 |
| -5 | | | | .0025 | 1.00 | | 38 | 5.5 |
| -6 | | | | .0025 | 1.00 | | 32 | 4.6 |
| | | | | | | avg | 34 | 4.9 |
| TBU01-A | 297 | 75 | Good | .0013 | .50 | | 54 | 7.8 |
| -B | | | | .0019 | .75 | | 59 | 8.6 |
| -C | | | | .0019 | .75 | | 64 | 9.3 |
| -11 | | | | .0020 | .80 | | 57 | 8.2 |
| -12 | | | | .0019 | .75 | | 62 | 9.0 |
| | | | | | | avg | 59 | 8.6 |
| TBU01-7 | 450 | 350 | Good | .0016 | .62 | | 39 | 5.6 |
| -8 | | | | .0019 | .75 | | 37 | 5.4 |
| -9 | | | | .0019 | .75 | | 32 | 4.7 |
| -10 | | | | .0020 | .80 | | 41 | 6.0 |
| | | | | | | avg | 37 | 5.4 |

**Table 7-9. Baseline Poisson's Ratio Data in Tension of G/E**

| Specimen Number | Laminate Orientation | Test Direction | Test Temperature K | Test Temperature (°F) | | Poisson's Ratio |
|---|---|---|---|---|---|---|
| BU01-4 | $[0°]_6$ | Longitudinal | 297 | 75 | | 0.35 |
| -5 | | | | | | .33 |
| -6 | | | | | | .32 |
| | | | | | avg | .33 |
| BU01-7 | $[0°]_6$ | Longitudinal | 394 | 250 | | .30 |
| -8 | | | | | | .30 |
| -9 | | | | | | .37 |
| | | | | | avg | .34 |
| BU01-13 | $[0°]_6$ | Longitudinal | 422 | 300 | | .39 |
| -14 | | | | | | .32 |
| -15 | | | | | | .35 |
| | | | | | avg | .35 |
| BC01-6 | $[0° \pm 45°]_s$ | Longitudinal | 297 | 75 | | .71 |
| -7 | | | | | | .70 |
| -8 | | | | | | .70 |
| | | | | | avg | .70 |

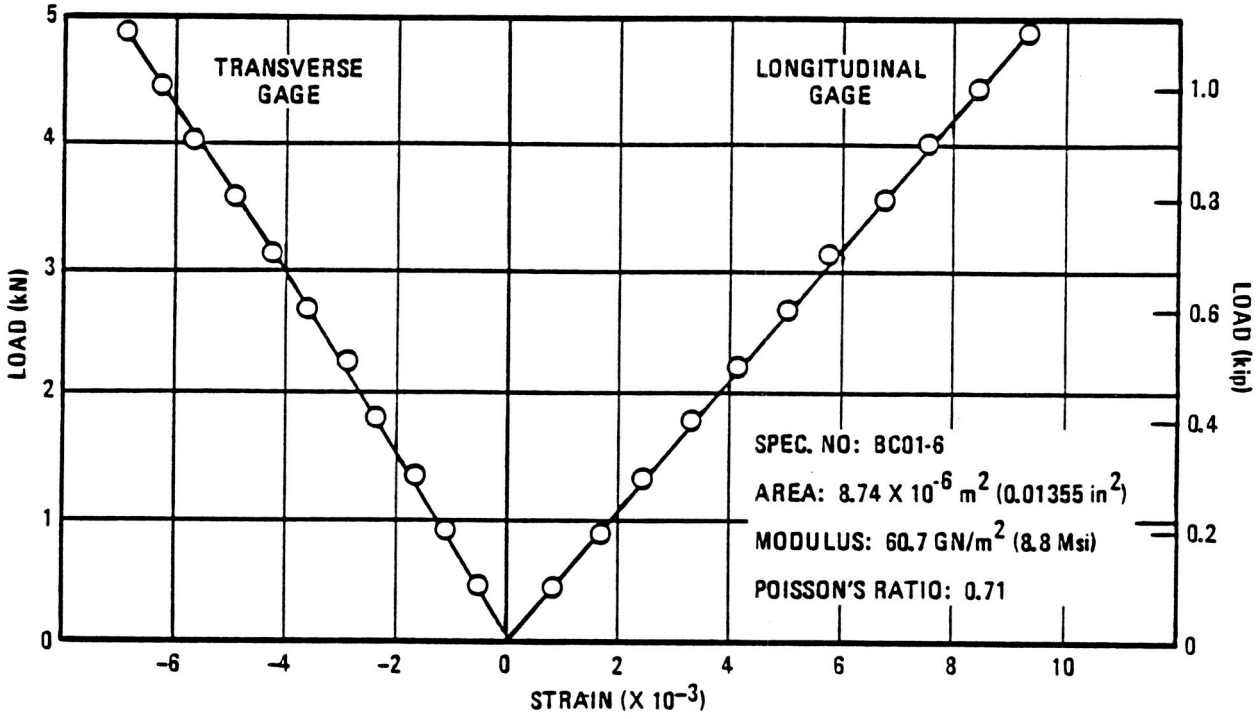



**Figure 7-8 Tensile Load-Strain Diagram for $[0° \pm 45°]_s$, G/E at 297 K (75° F)**

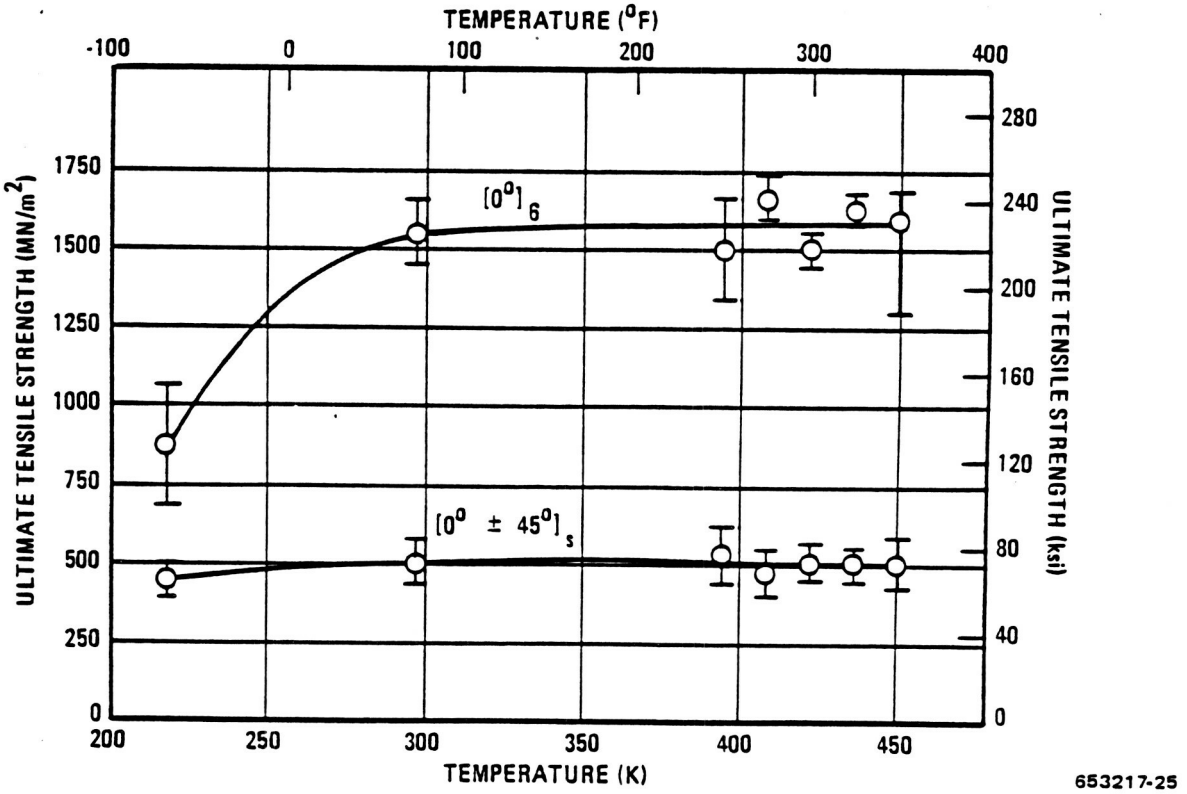



**Figure 7-9 Baseline Tensile Properties of G/E**

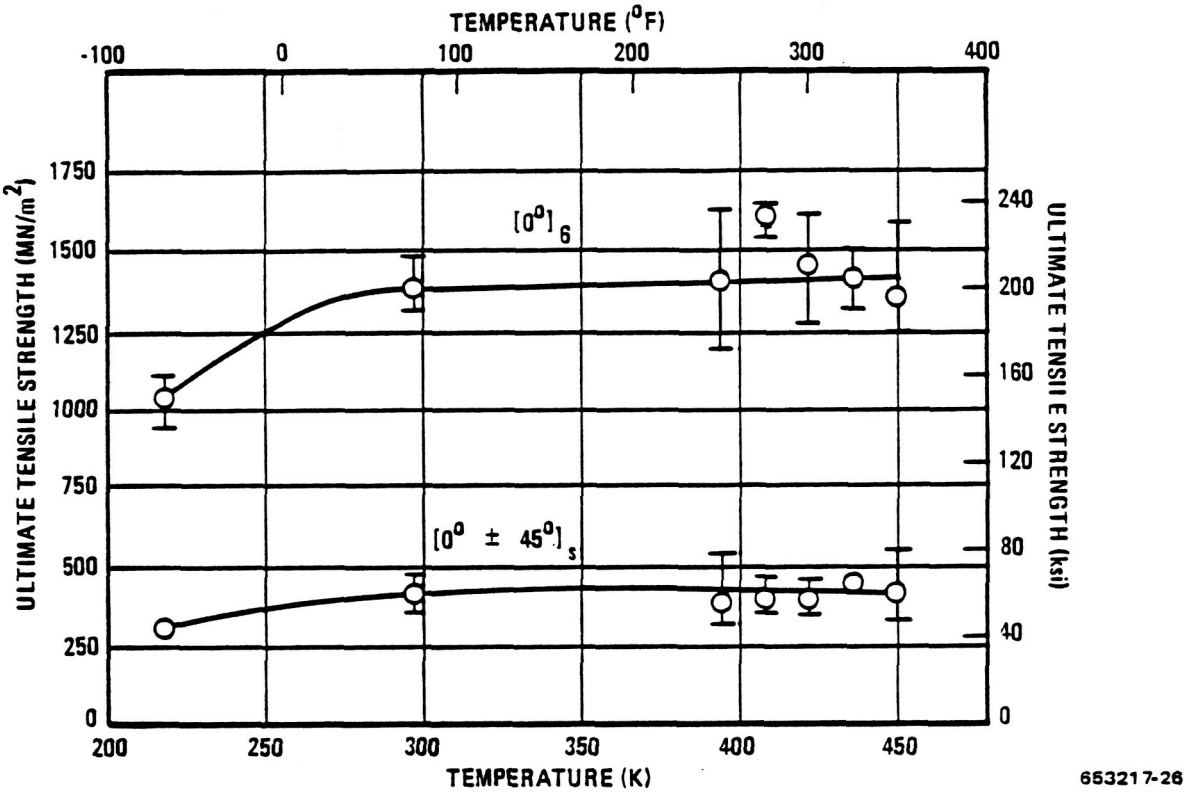



**Figure 7-10 Baseline Notched Tensile Properties of G/E**

Poisson's ratio. The modulus values measured on these specimens are noted in the tables. In general, these values are more reliable than those determined with the mechanical extensometer.

The effect of temperature on the tensile strength of G/E is shown on Figures 7-9 and 7-10. With the exception of the 218 K (−67° F) results, the tensile strength exhibited almost no change with increasing temperature out to the maximum test temperature of 450 K (350° F). At 218 K (−67° F) the strength showed a moderate decrease for the crossplied material and a rather large one for the unidirectional material (almost 50%) for the unnotched specimens. This strength decrease at low temperatures is not uncommon for resin matrix composites. The effect is believed to be related to residual stresses in the material, which increase as the difference between the cure temperature and the test temperature is increased. Also shown on Figure 7-9 and 7-10 are the scatter bands for the various tests. For both unnotched and notched specimens the data scatter was numerically greater for the unidirectional material, but, percentagewise, the crossplied material showed a significantly greater degree of scatter. Because of the larger number of specimens tested at 394 K (250° F) and 450 K (350° F), the scatter bands at these temperature tended to be somewhat wider.

In like manner to the tensile strength data, the tensile modulus was also not significantly affected by increasing temperature out to the maximum test temperatures of 450 K (350° F). At 218 K (−67° F) the average value for the crossplied material was slightly lower than those obtained at higher temperatures, but all of the 218K (−67° F) data fell within the scatter band of the tests conducted at 394 K (250° F). No modulus values were obtained from the 218 K (−67° F) tests on the unidirectional specimens because of extensometer malfunctioning.

**Table 7-10. Summary of Baseline Tensile Properties of G/E**

| | Temperature, K (°F) | | | | | | |
|---|---|---|---|---|---|---|---|
| | 218 (−67) | 297 (75) | 394 (250) | 408 (275) | 422 (300) | 436 (325) | 450 (350) |
| Tensile Strength, $MN/m^2$ (ksi) | | | | | | | |
| $[0°]_6$ | 882 (128) | 1540 (224) | 1510 (219) | 1670 (242) | 1500 (218) | 1610 (234) | 1590 (230) |
| $[0° \pm 45°]_s$ | 449 (65.2) | 496 (71.9) | 525 (76.2) | 484 (70.2) | 509 (73.8) | 502 (72.8) | 500 (72.5) |
| $[90]_{12}$ | — | 59 (8.6) | — | — | — | — | 37 (5.4) |
| Tensile Modulus, $GN/m^2$ (Msi) | | | | | | | |
| $[0°]_6$ | — | 141 (20.4) | 146 (21.2) | 166 (24.0) | 139 (20.2) | 139 (20.1) | 150 (21.8) |
| $[0° \pm 45°]_s$ | 48 (6.9) | 57 (8.3) | 56 (8.1) | 54 (7.8) | 51 (7.4) | 53 (7.7) | 58 (8.4) |
| Poisson's Ratio | | | | | | | |
| $[0°]_6$ | — | 0.33 | 0.34 | — | 0.35 | — | — |
| $[0° \pm 45°]_s$ | — | .70 | — | — | — | — | — |
| Notched Tensile Strength, $MN/m^2$ (ksi) | | | | | | | |
| $[0°]_6$ | 1030 (150) | 1380 (200) | 1390 (202) | 1620 (235) | 1450 (210) | 1410 (204) | 1350 (196) |
| $[0° \pm 45°]_s$ | 312 (45.3) | 412 (59.7) | 401 (58.2) | 398 (57.7) | 394 (57.1) | 429 (62.3) | 416 (60.3) |

A comparison of the ratio of the notched to the unnotched tensile strength of G/E at each of the test temperatures has been made in Table 7-11. For the unidirectional material the effect of a notch on the net section strength is quite small. The effect of the notch was frequently seen during testing, particularly fatigue testing, in that longitudinal cracks propagated tangent to the edges of the notch (center hole) along the entire length of the test section. Examples of the failure mode of the unidirectional notched specimens can be seen in Figure 7-11. Figure 7-12 is a closeup view of the bottom specimen showing the longitudinal splitting that has occurred tangent to the 0.0064 m (0.25 in.) hole. The net effect is to divide the specimen into two smaller parallel specimens. In a tensile test the two strips act as one and very little reduction in the net tensile strength was observed. During fatigue testing, however, as will be shown in Section 11, the notch was observed to either increase or decrease the fatigue life compared to unnotched specimens depending on the test conditions. For crossplied material the notched specimens gave a tensile strength that was 10 to 30% lower than the unnotched specimens. Similar effects of a center hole notch were observed for the HT-S/710 G/PI system in both unidirectional and crossplied specimens. No unidirectional specimens of the Celion 6000/LARC-160 G/PI system were tested, but the notched crossplied specimens were also significantly lower in tensile strength than the unnotched specimens.

Tensile data for the unidirectional material tested in the transverse direction are listed in Table 7-8. The plan called for six specimens each to be tested at room and one elevated temperature. The specimens, which were taken from the first G/E laminate that was fabricated, were intended to be used as a quality assurance check on the material as well as for baseline tensile property determinations. The wrong blade was used on the table saw when cutting the specimens. Six of these specimens were tested at room temperature, giving the low values shown in Table 7-8. An examination of the saw cut edges of the failed specimens revealed a very poor edge condition and one at which premature failure could readily be initiated. The remaining six untested specimens and three spares that were available were salvaged by trimming the chipped edges with the correct blade. The two types of edge conditions are shown in Figure 7-13 and 7-14. The room temperature tensile strength of the somewhat narrow specimens with good edges was nearly double that of those with the badly damaged edges. Unlike longitudinal tensile properties, the transverse strength showed a considerable decrease at 450 K (350 ° F). The transverse strength is a matrix dominated property and would be expected to be more temperature dependent that the fiber dominated longitudinal strength.

The remaining baseline tensile data for the Phase I G/E, Poisson's ratio values, are listed in Table 7-9. For the unidirectional material values of approximately one-third (similar to that obtained for most metals) were obtained at all three temperatures. Room temperature measurements on crossplied specimens gave values that were similar to those determined for the B/E system.

Tensile data at room and 450 K (350 °F) were obtained for the Phase II batch of G/E during quality assurance testing (Table 6-5). The data, however, did not show good agreement with the residual strength data (Phase II material) obtained after long term flight simulation exposure. For this reason and because extra material was available, ten additional tensile tests were conducted at each temperature. The results (including the QA data) are listed in Table 7-12. The Phase II batch of G/E shows significantly higher tensile strength values than the original material purchased in Phase I. However, as will be seen in Section 12, the room temperature residual strength of the Phase II material after flight simulation exposure was considerably higher than the baseline data of Table 7-12.

Table 7-11. Ratio of Notched to Unnotched Tensile Strength of G/E at Various Temperatures

| Temperature K | Temperature (°F) | Ratio of Notched to Unnotched Strength $[0°]_6$ | Ratio of Notched to Unnotched Strength $[0° \pm 45°]_s$ |
|---|---|---|---|
| 218 | −67 | 1.2 | 0.7 |
| 297 | 75 | .9 | .8 |
| 394 | 250 | .9 | .8 |
| 408 | 275 | 1.0 | .8 |
| 422 | 300 | 1.0 | .8 |
| 436 | 325 | .9 | .9 |
| 450 | 350 | .9 | .8 |

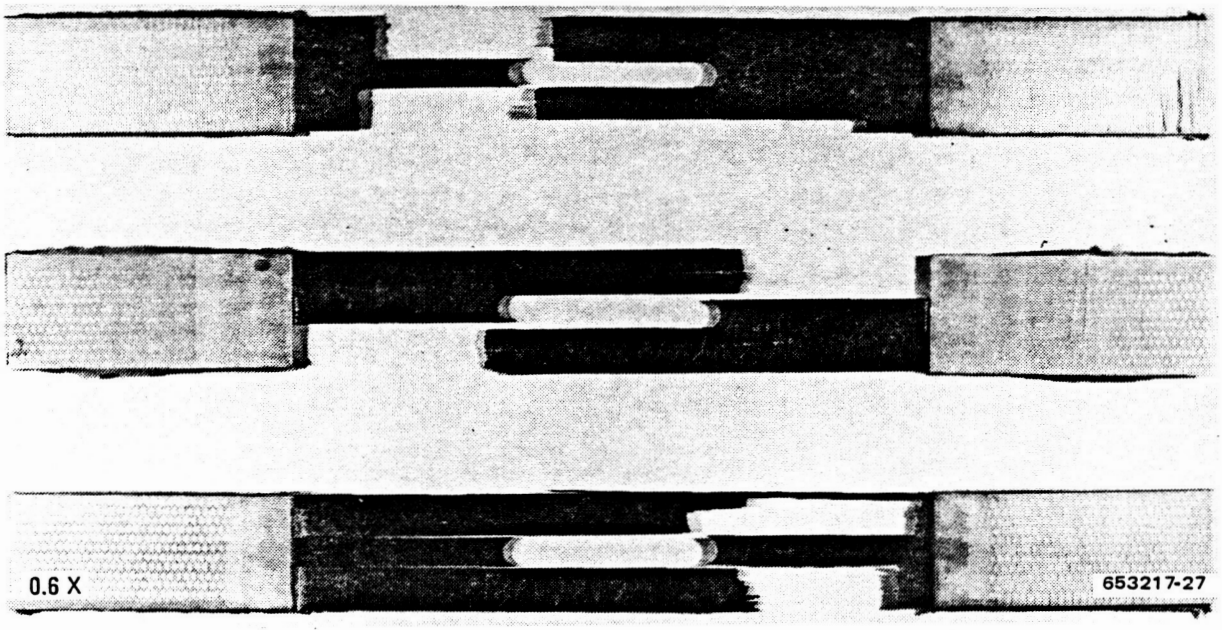



Figure 7-11 Unidirectional G/E Notched Tensile Specimens

### 7.1.2.3 Graphite/Polyimide

**HT-S/710 G/PI.** The test plan for the HT-S/710 G/PI baseline tensile specimens was similar to that used for the G/E specimens in that three tests were performed at each of seven temperatures. It differed slightly, however, in that all remaining specimens were then tested at one of the seven original temperatures rather than at two. This temperature was the one that had been selected for the flight simulation exposure tests, 505 K (450 ° F). Testing at one temperature was done to increase the tensile strength data base that was required for selection of the short-term flight simulation load levels. At the time these tests were performed very little data was available for the HT-S/710 system. Selection of the temperatures for the flight simulation tests is discussed in Section 12.



ORIGINAL PAGE IS
OF POOR QUALITY

ORIGINAL PAGE IS
OF POOR QUALITY

ORIGINAL PAGE IS

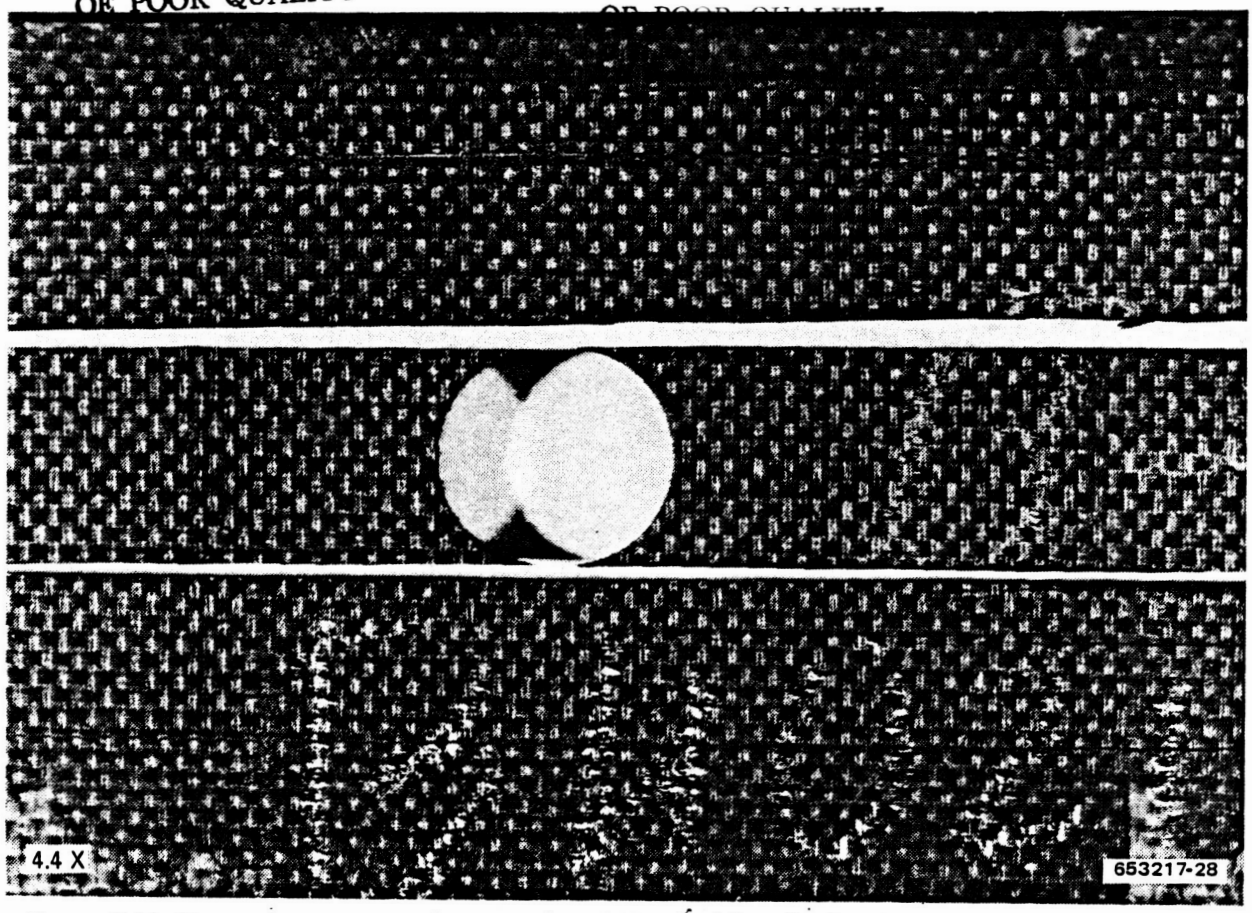



**Figure 7-12 Closeup View of Unidirectional G/E Notched Tensile Specimens Showing Longitudinal Splitting Tangent to the Center Hole**

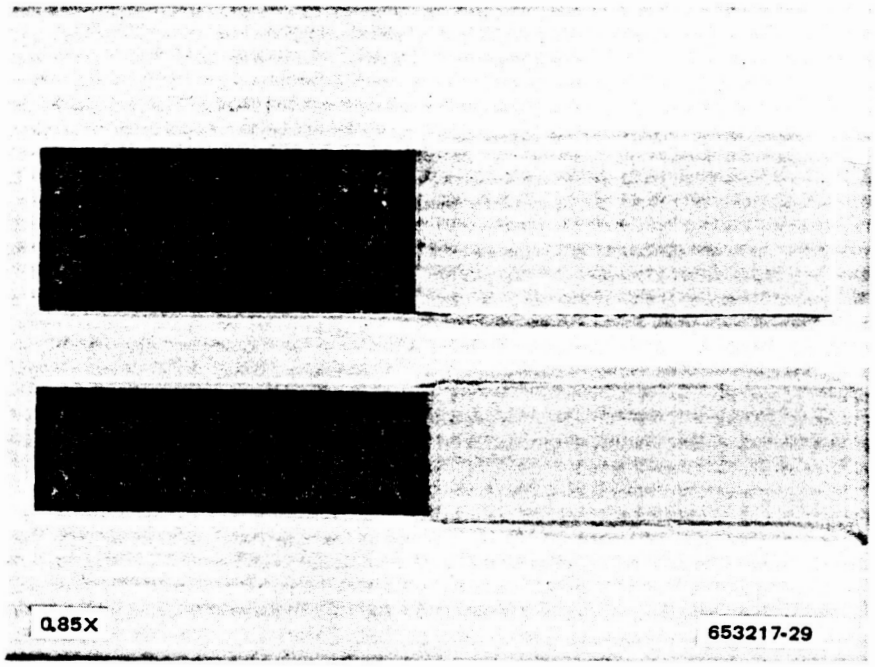



**Figure 7-13 Transverse Tensile Specimens of G/E Showing Poor Edge Condition of Improperly Machined Specimen (upper) and Good Edge Condition of Properly Machined Specimen (lower)**

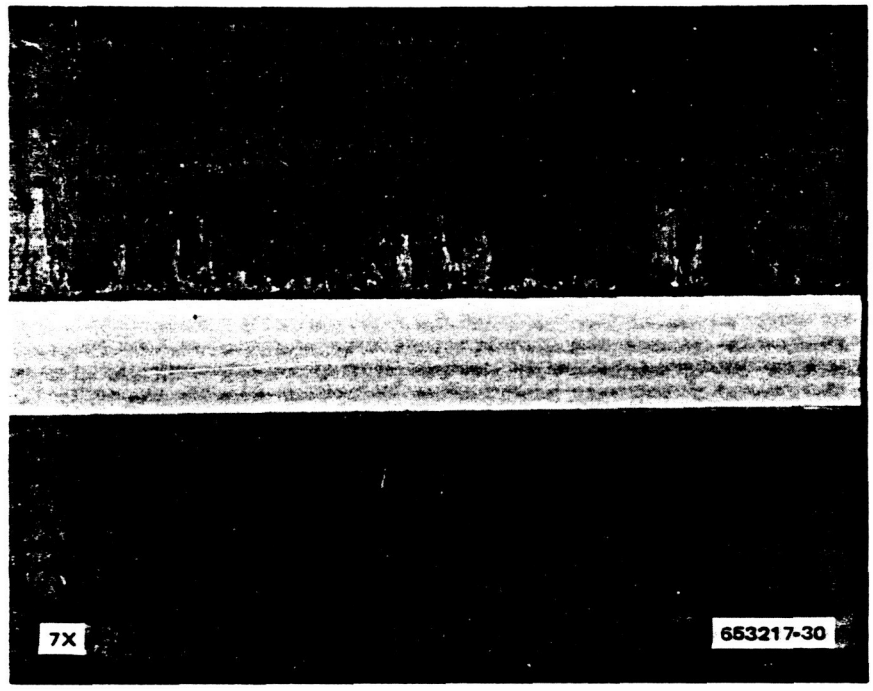



**Figure 7-14 Transverse Tensile Specimens of G/E Showing Poor Edge Condition of Improperly Machined Specimen (upper) and Good Edge Condition of Properly Machined Specimen (lower)**

Baseline tensile tests, both unnotched and notched, were performed on unidirectional and $[0° \pm 45°]_s$ crossplied specimens in the longitudinal direction. Some unnotched tensile tests were also performed in the transverse direction on unidirectional material, and a limited amount of Poisson's ratio testing was conducted. Results are listed in Tables 7-13 through 7-18. A typical load-strain diagram from one of the strain gaged Poisson's ratio specimens is shown in Figure 7-15. The longitudinal unnotched and notched data are plotted as a function of temperature in Figure 7-16 and 7-17. A summary of all the HT-S/710 G/PI tensile properties is presented in Table 7-19.

Modulus values were determined at four temperatures for the specimens tested in the longitudinal direction. A mechanical extensometer was used for the 218 K (−67 ° F) tests while strain gages were used at room temperature and the two elevated temperatures. Poisson's ratio values were also determined for some of these specimens. For the material tested in the transverse direction, modulus values were obtained at room temperature only. A mechanical extensometer was used for these tests.

The temperature dependence of the HT-S/710 G/PI tensile strength is shown in Figures 7-16 and 7-17. At the maximum test temperature, 616 K (650 ° F), the unidirectional unnotched and notched specimens had lost approximately 10% of the room temperature strength. The loss for the crossplied specimens was somewhat higher, 37% for the unnotched and 30% for the notched specimens. Because of the limited amount of tests and the scatter in the data, the temperature at which the tensile strength begins to decrease is difficult to determine precisely. The curves indicate this decrease to occur between 561 K (550 ° F) and 616 K (650 ° F). Some decrease in strength was also observed at 218 K (−67 ° F) but the effect was generally less than that found for the G/E system. The spread in the HT-S/710 G/PI tensile data as shown by the scatter bands in Figures 7-16 and 7-17 was similar to that observed for G/E. The tensile modulus for



C-2

ORIGINAL PAGE IS
OF POOR QUALITY

Table 7-12. Baseline Tensile Properties of $[0° \pm 45°]_s$ G/E (Phase II Material)

| Specimen Number | Temperature K | Temperature (°F) | Tensile Strength $MN/m^2$ | Tensile Strength (ksi) | Tensile Modulus $GN/m^2$ | Tensile Modulus (Msi) |
|---|---|---|---|---|---|---|
| B-1 | 297 | 75 | 456 | 66.1 | 50 | 7.2 |
| -2 | | | 459 | 66.5 | 51 | 7.4 |
| -3 | | | 556 | 80.6 | 53 | 7.7 |
| -17 | | | 487 | 70.7 | 48 | 6.9 |
| -18 | | | 590 | 85.5 | 53 | 7.7 |
| -19 | | | 572 | 82.9 | 55 | 8.0 |
| -20 | | | 509 | 73.8 | 50 | 7.3 |
| -21 | | | 604 | 87.6 | 56 | 8.1 |
| -22 | | | 570 | 82.7 | 54 | 7.9 |
| -23 | | | 554 | 80.4 | 48 | 7.0 |
| -24 | | | 570 | 82.6 | 59 | 8.5 |
| -25 | | | 538 | 78.1 | 57 | 8.2 |
| -26 | | | 681 | 98.7 | 57 | 8.2 |
| | | | 550 | 79.7 | 53 | 7.7 |
| B-4 | 450 | 350 | 557 | 80.8 | 47 | 6.8 |
| -5 | | | 584 | 84.7 | 47 | 6.8 |
| -6 | | | 623 | 90.4 | 50 | 7.3 |
| -27 | | | 578 | 83.8 | 56 | 8.1 |
| -28 | | | 626 | 90.8 | 52 | 7.6 |
| -29 | | | 632 | 91.6 | 54 | 7.8 |
| -30 | | | 568 | 82.4 | 48 | 6.9 |
| -31 | | | 664 | 96.3 | 56 | 8.1 |
| -32 | | | 614 | 89.1 | 50 | 7.2 |
| -33 | | | 629 | 91.3 | 53 | 7.7 |
| -34 | | | 647 | 93.8 | 52 | 7.6 |
| -35 | | | 666 | 96.6 | 56 | 8.1 |
| -36 | | | 689 | 100 | 57 | 8.3 |
| | | | 621 | 90.1 | 52 | 7.5 |

Table 7-13. Baseline Tensile Properties of $[0°]_6$ HT-S/710 G/PI

| Specimen Number | Temperature K | Temperature (°F) | | Tensile Strength $MN/m^2$ | Tensile Strength (ksi) | Tensile Modulus $GN/m^2$ | Tensile Modulus (Msi) |
|---|---|---|---|---|---|---|---|
| DU01-1 | 218 | −67 | | 1300 | 188 | 144 | 20.9 |
| -2 | | | | 1180 | 171 | 97 | 14.1 |
| -3 | | | | 1100 | 160 | 134 | 19.4 |
| | | | avg | 1190 | 173 | 125 | 18.1 |
| DU01-4 | 297 | 75 | | 1260 | 182 | [a]127 | [a]18.4 |
| -5 | | | | 1190 | 172 | [a]126 | [a]18.2 |
| 66 | | | | 1120 | 163 | [a]126 | [a]18.3 |
| | | | avg | 1190 | 172 | 126 | 18.3 |
| DU01-7 | 505 | 450 | | 1090 | 158 | [a]121 | [a]17.6 |
| -8 | | | | 1260 | 182 | [a]128 | [a]18.6 |
| -9 | | | | 1270 | 184 | [a]126 | [a]18.3 |
| -22 | | | | 1360 | 197 | — | — |
| -23 | | | | 1260 | 182 | — | — |
| -24 | | | | 1130 | 164 | — | — |
| -25 | | | | 1160 | 168 | — | — |
| | | | avg | 1220 | 176 | 125 | 18.2 |
| DU01-10 | 533 | 500 | | 1270 | 184 | — | — |
| -11 | | | | 1260 | 182 | — | — |
| -12 | | | | 1210 | 176 | — | — |
| | | | avg | 1250 | 181 | | |
| DU01-13 | 561 | 550 | | 1370 | 199 | [a]141 | [a]20.5 |
| -14 | | | | 1400 | 203 | [a]133 | [a]19.3 |
| -15 | | | | 1190 | 173 | [a]128 | [a]18.5 |
| | | | avg | 1320 | 192 | 134 | 19.4 |
| DU01-16 | 589 | 600 | | 1150 | 167 | — | — |
| -17 | | | | 1200 | 174 | — | — |
| -18 | | | | 1240 | 180 | — | — |
| | | | avg | 1200 | 174 | | |
| DU01-19 | 616 | 650 | | 1080 | 156 | — | — |
| -20 | | | | 1120 | 162 | — | — |
| -21 | | | | 1060 | 154 | — | — |
| | | | avg | 1090 | 157 | | |

[a] Strain gage measurement

Table 7-14. Baseline Tensile Properties of $[0° \pm 45°]_s$ HT-S/710 G/PI

| Specimen Number | Temperature K | Temperature (°F) | Tensile Strength $MN/m^2$ | Tensile Strength (ksi) | Tensile Modulus $GN/m^2$ | Tensile Modulus (Msi) |
|---|---|---|---|---|---|---|
| DC01-1 | 218 | −67 | 387 | 56.1 | 41 | 5.9 |
| -2 | | | 417 | 60.5 | 37 | 5.4 |
| -3 | | | 411 | 59.6 | 36 | 5.2 |
| | | avg | 405 | 58.7 | 38 | 5.5 |
| DC01-4 | 297 | 75 | 510 | 74.0 | [a]50 | [a]7.3 |
| -5 | | | 505 | 73.2 | [a]56 | [a]8.1 |
| -6 | | | 543 | 78.7 | [a]53 | [a]7.7 |
| | | avg | 519 | 75.3 | 53 | 7.7 |
| DC01-7 | 505 | 450 | 423 | 61.3 | [a]47 | [a]6.8 |
| -8 | | | 299 | 43.4 | [a]39 | [a]5.7 |
| -9 | | | 441 | 63.9 | [a]54 | [a]7.9 |
| -22 | | | 478 | 69.3 | — | — |
| -23 | | | 525 | 76.2 | — | — |
| -24 | | | 478 | 69.4 | — | — |
| -25 | | | 437 | 63.4 | — | — |
| -26 | | | 463 | 67.1 | — | — |
| -27 | | | 496 | 71.9 | — | — |
| -28 | | | 496 | 71.9 | — | — |
| -29 | | | 485 | 70.3 | — | — |
| -30 | | | 478 | 69.3 | — | — |
| -31 | | | 560 | 81.2 | — | — |
| -32 | | | 432 | 62.7 | — | — |
| -33 | | | 512 | 74.3 | — | — |
| -34 | | | 543 | 78.8 | — | — |
| -35 | | | 449 | 65.1 | — | — |
| | | avg | 470 | 68.2 | 57 | 6.8 |
| DC01-10 | 533 | 500 | 398 | 57.7 | — | — |
| -11 | | | 410 | 59.5 | — | — |
| -12 | | | 385 | 55.9 | — | — |
| | | avg | 398 | 57.7 | | |
| DC01-13 | 561 | 550 | 257 | 37.5 | [a]41 | [a]6.0 |
| -14 | | | 301 | 43.7 | [a]44 | [a]6.4 |
| -15 | | | 463 | 67.2 | [a]46 | [a]6.7 |
| | | avg | 340 | 49.4 | 44 | 6.4 |
| DC01-16 | 589 | 600 | 352 | 51.1 | — | — |
| -17 | | | 432 | 62.6 | — | — |
| -18 | | | 409 | 59.3 | — | — |
| | | avg | 398 | 57.7 | | |
| DC01-19 | 616 | 650 | 305 | 44.3 | — | — |
| -20 | | | 330 | 47.9 | | |
| -21 | | | 345 | 50.0 | | |
| | | avg | 327 | 47.4 | | |

[a] Strain gage measurement

Table 7-15. Baseline Notched Tensile Properties of $[0°]_6$ HT-S/710 G/PI

| Specimen Number | Temperature K | Temperature (°F) | Notched Tensile Strength $MN/m^2$ (a) | Notched Tensile Strength (ksi) |
|---|---|---|---|---|
| DU02-1 | 218 | −67 | 1180 | 171 |
| -2 | | | 820 | 119 |
| -3 | | | 972 | 141 |
| | | | avg 991 | 144 |
| DU02-4 | 297 | 75 | 1310 | 190 |
| -5 | | | 1140 | 166 |
| -6 | | | 1320 | 192 |
| | | | avg 1260 | 183 |
| DU02-7 | 505 | 450 | 1230 | 178 |
| -8 | | | 1160 | 169 |
| -9 | | | 1340 | 195 |
| -22 | | | 986 | 143 |
| -23 | | | 1250 | 181 |
| -24 | | | 1040 | 151 |
| -25 | | | 1110 | 161 |
| -26 | | | 1130 | 164 |
| -27 | | | 1060 | 154 |
| -28 | | | 1080 | 157 |
| -29 | | | 1120 | 163 |
| -30 | | | 1210 | 175 |
| -31 | | | 1240 | 180 |
| -32 | | | 1190 | 173 |
| -33 | | | 1140 | 166 |
| -34 | | | 1070 | 155 |
| -35 | | | 1050 | 152 |
| | | | avg 1140 | 166 |
| DU02-10 | 533 | 500 | 1240 | 180 |
| -11 | | | 1240 | 180 |
| -12 | | | 1140 | 166 |
| | | | avg 1210 | 175 |
| DU02-13 | 561 | 550 | 1040 | 151 |
| -14 | | | 1120 | 162 |
| -15 | | | 1280 | 186 |
| | | | avg 1150 | 166 |
| DU02-16 | 589 | 600 | 979 | 142 |
| -17 | | | 1060 | 154 |
| -18 | | | 1030 | 150 |
| | | | avg 1020 | 149 |
| DU02-19 | 616 | 650 | 1130 | 164 |
| -20 | | | 1140 | 166 |
| -21 | | | 1050 | 153 |
| | | | avg 1110 | 161 |

[a] Net section strength, i.e., based on total width less hole diameter.

Table 7-16. Baseline Notched Tensile Properties of $[0^\circ \pm 45^\circ]_s$ HT-S/710 G/PI

| Specimen Number | Temperature K | Temperature (°F) | Notched Tensile Strength $MN/m^2$ (a) | Notched Tensile Strength (ksi) |
|---|---|---|---|---|
| DC02-1 | 218 | −67 | 328 | 47.5 |
| -2 | | | 288 | 41.8 |
| -3 | | | 339 | 49.1 |
| | | | avg 318 | 46.1 |
| DC02-4 | 297 | 75 | 367 | 53.3 |
| -5 | | | 332 | 48.2 |
| -6 | | | 372 | 54.0 |
| | | | avg 357 | 51.8 |
| DC02-7 | 505 | 450 | 343 | 49.7 |
| -8 | | | 352 | 51.0 |
| -9 | | | 330 | 47.8 |
| -22 | | | 334 | 48.4 |
| -23 | | | 350 | 50.8 |
| -24 | | | 350 | 50.7 |
| -25 | | | 301 | 43.7 |
| -26 | | | 332 | 48.2 |
| -27 | | | 386 | 56.0 |
| -28 | | | 354 | 51.4 |
| -29 | | | 305 | 44.2 |
| -30 | | | 373 | 54.1 |
| -31 | | | 333 | 48.3 |
| -32 | | | 363 | 52.7 |
| -33 | | | 303 | 43.9 |
| -34 | | | 292 | 42.4 |
| -35 | | | 314 | 45.5 |
| | | | avg 336 | 48.8 |
| DC02-10 | 533 | 500 | 361 | 52.3 |
| -11 | | | 386 | 56.0 |
| -12 | | | 308 | 44.7 |
| | | | avg 352 | 51.0 |
| DC02-13 | 561 | 550 | 250 | 36.3 |
| -14 | | | 355 | 51.5 |
| -15 | | | 339 | 49.2 |
| | | | avg 315 | 45.7 |
| DC02-16 | 589 | 600 | 242 | 35.1 |
| -17 | | | 232 | 33.6 |
| -18 | | | 272 | 39.4 |
| | | | avg 249 | 36.1 |
| DC02-19 | 616 | 650 | 221 | 32.0 |
| -20 | | | 262 | 38.0 |
| -21 | | | 270 | 39.2 |
| | | | avg 251 | 36.4 |

[a] Net section strength, i.e., based on total width less hole diameter.

Table 7-17. Baseline Tensile Properties of $[0°]_{12}$ HT-S/710 G/PI Tested in the Transverse Direction

| Specimen Number | Temperature K | (°F) | Tensile Strength MN/m² | (ksi) | Tensile Modulus GN/m² | (Msi) |
|---|---|---|---|---|---|---|
| TDU01-1 | 297 | 75 | 21 | 3.0 | 5.2 | 0.75 |
| -2 | | | 31 | 4.5 | 6.3 | .91 |
| -3 | | | 21 | 3.1 | 4.8 | .69 |
| -4 | | | 23 | 3.4 | 5.2 | .76 |
| -5 | | | 20 | 2.9 | 4.8 | .69 |
| -6 | | | 25 | 3.6 | 4.8 | .69 |
| | | avg | 24 | 3.4 | 5.2 | .75 |
| TDU01-7 | 505 | 450 | (a) | (a) | — | — |
| -8 | | | 22 | 3.2 | — | — |
| -9 | | | (a) | (a) | — | — |
| -10 | | | 21 | 3.1 | — | — |
| -11 | | | 28 | 4.0 | — | — |
| -12 | | | 19 | 2.8 | — | — |
| | | avg | 22 | 3.3 | | |

[a] Failed in handling

Table 7-18. Baseline Poisson's Ratio Data in Tension of HT-S/710 G/PI

| Specimen Number | Laminate Orientation | Test Direction | Test Temperature K | (°F) | Poisson's Ratio |
|---|---|---|---|---|---|
| DU01-7 | $[0°]_6$ | Longitudinal | 505 | 450 | 0.38 |
| -8 | | | | | .35 |
| -9 | | | | | .45 |
| | | | | avg | .39 |
| DU01-13 | $[0°]_6$ | Longitudinal | 561 | 550 | .50 |
| -14 | | | | | .45 |
| -15 | | | | | .44 |
| | | | | avg | .46 |
| DC01-4 | $[0° \pm 45°]_s$ | Longitudinal | 297 | 75 | .71 |
| -5 | | | | | .65 |
| -6 | | | | | .64 |
| | | | | avg | .67 |

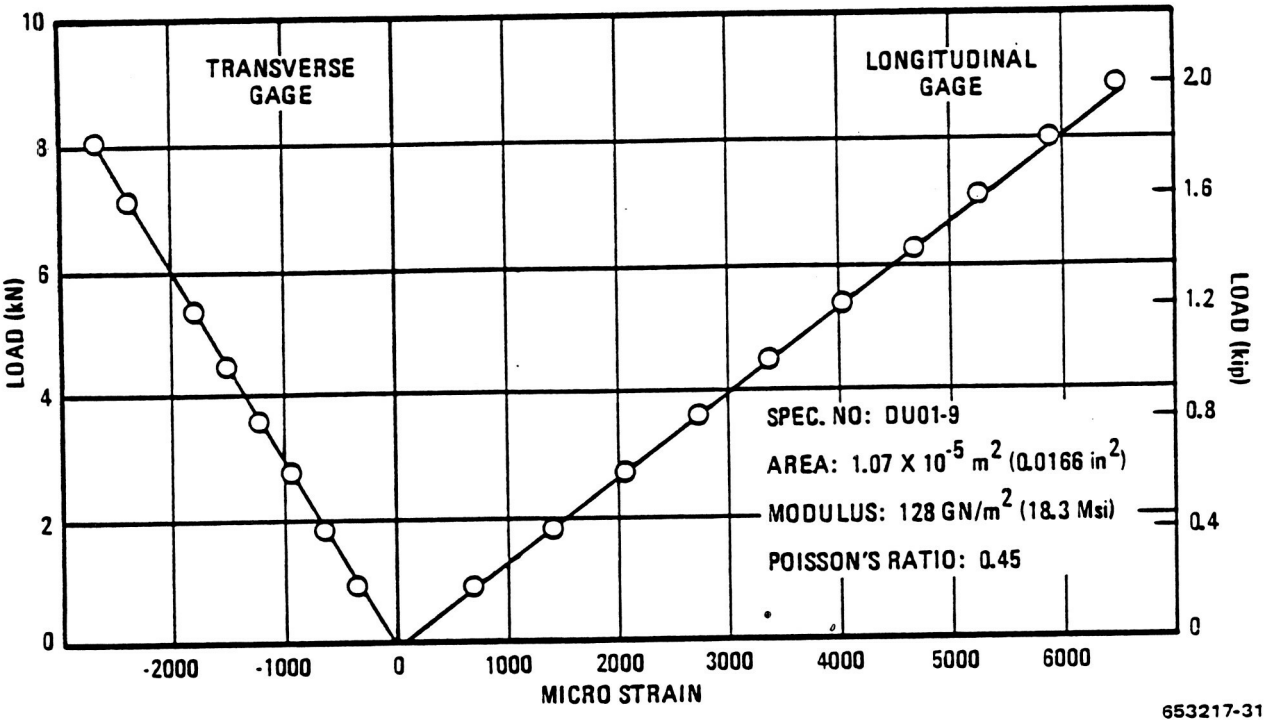



**Figure 7-15 Tensile Load-Strain Diagram for $[0^o]_6$ HT-S/710 G/PI at 500 K (450° F)**

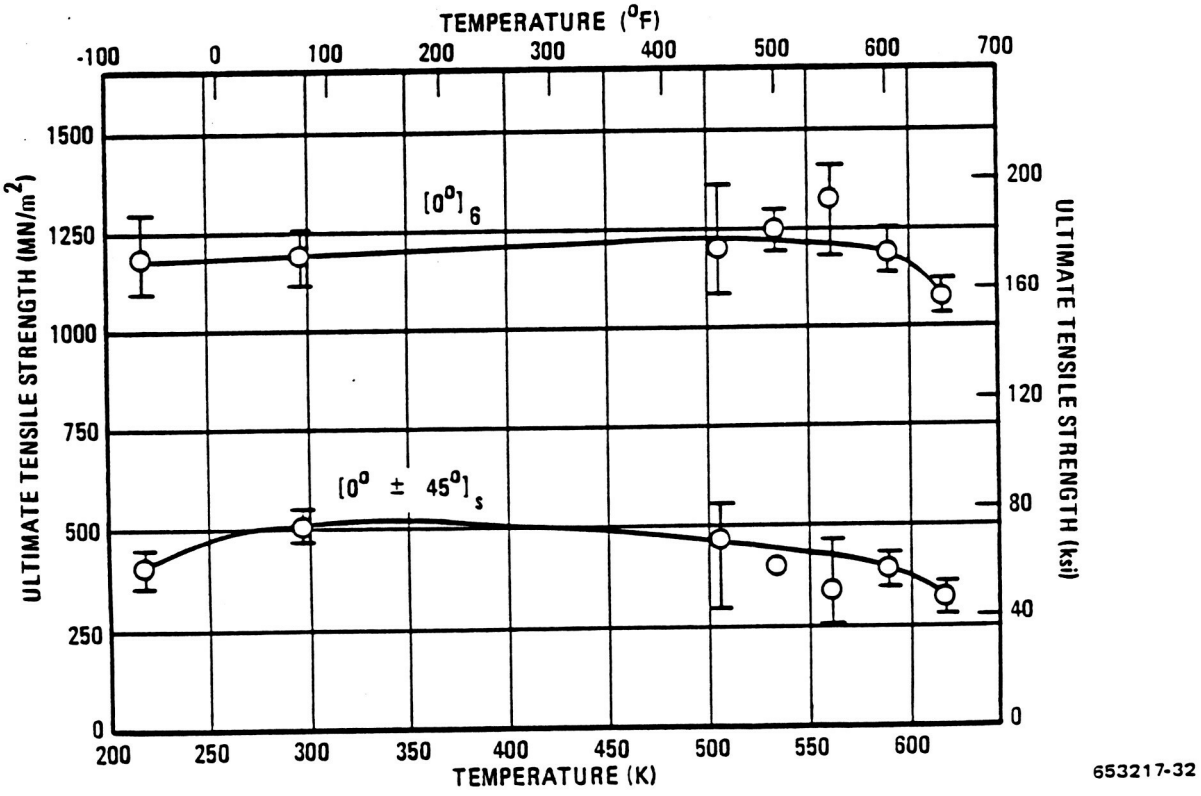



**Figure 7-16 Baseline Tensile Properties of HT-S/710 G/PI**

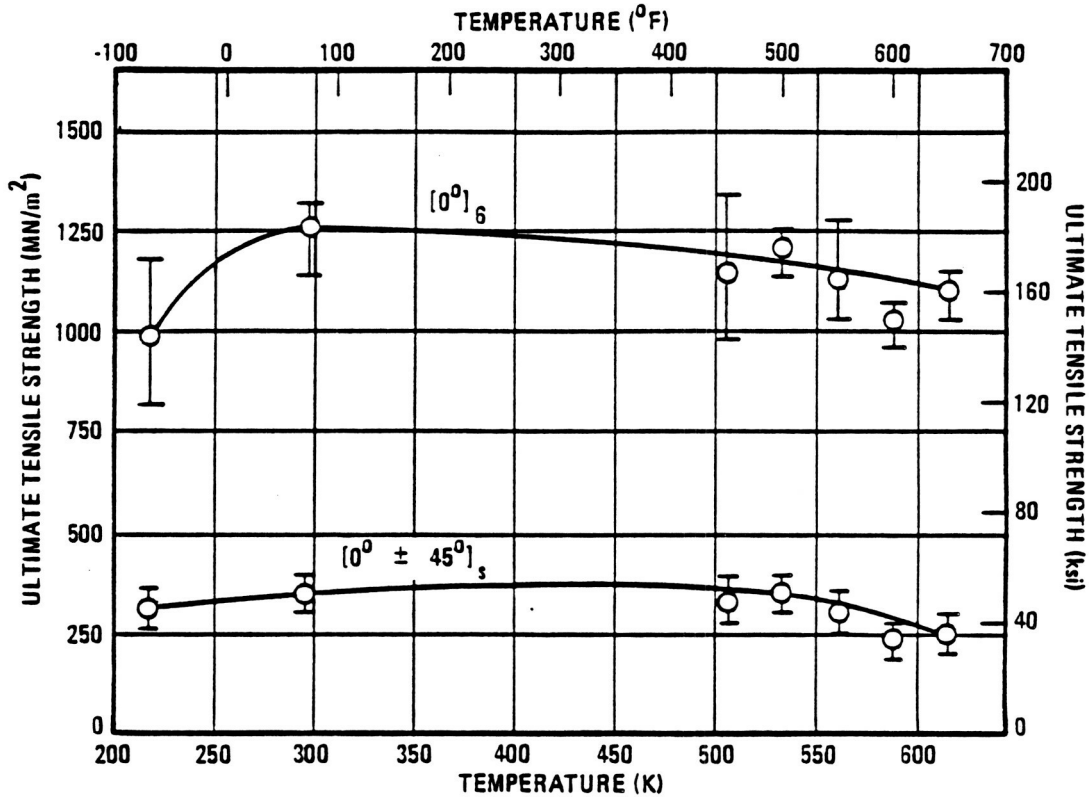



**Figure 7-17 Baseline Notched Tensile Properties of HT-S/710 G/PI**

the unidirectional material was not lowered by increasing temperatures out to the maximum test temperature of 561 K (550° F). The crossplied material did show a decrease in modulus, however, of about 15% at 561 K (550° F) and nearly 30% at 218 K (−67° F).

A comparison of the ratio of the notched to unnotched tensile strength of HT-S/710 G/PI at each of the test temperatures has been made in Table 7-20. The results are very similar to those found for the G/E system. For the unidirectional material the effect of a center hole notch was quite small except at 218 K (−67° F). The crossplied material, on the other hand, experienced decreases in tensile strength of 10 to 40% when tested in the notched configuration.

Transverse tensile data are presented in Table 7-17 for room and elevated temperatures. Strength values were considerably lower than those presented earlier for the G/E system but were about 50% higher than values reported by others (ref. 24). The modulus values, however, were considerably lower than those reported in reference 24. No significant effect of temperature on the transverse strength was observed out to 505 K (450° F). Evidence of the low transverse strength of this material is shown by the two accidental specimen failures that occurred when installing the specimens in the tensile machine grips. Only slight flexing of the specimens will result in fracture.

Poisson's ratio values, Table 7-18, for unidirectional HT-S/710 G/PI were somewhat larger than those obtained for G/E. An increase in value with increase in temperature was also observed. In like manner to the B/E and G/E data, the room temperature Poisson's ratio for crossplied material was also quite large.

## Table 7-19. Summary of Baseline Tensile Properties of HT-S/710 G/PI

| | Temperature, K (°F) | | | | | | |
|---|---|---|---|---|---|---|---|
| | 218 (−67) | 297 (75) | 505 (450) | 533 (500) | 561 (550) | 589 (600) | 616 (650) |
| **Tensile Strength, $MN/m^2$ (ksi)** | | | | | | | |
| $[0°]_6$ | 1190 (173) | 1190 (172) | 1210 (176) | 1240 (180) | 1320 (191) | 1200 (174) | 1080 (157) |
| $[0° \pm 45°]_s$ | 405 (58.7) | 519 (75.3) | 470 (68.2) | 398 (57.7) | 341 (49.4) | 398 (57.7) | 327 (47.4) |
| $[90]_{12}$ | — | 23 (3.4) | 23 (3.3) | — | — | — | — |
| **Tensile Modulus, $GN/m^2$ (Msi)** | | | | | | | |
| $[0°]_6$ | 125 (18.1) | 126 (18.3) | 126 (18.2) | — | 134 (19.4) | — | — |
| $[0° \pm 45°]_s$ | 38 (5.5) | 53 (7.7) | 47 (6.8) | — | 44 (6.4) | — | — |
| **Poisson's Ratio** | | | | | | | |
| $[0°]_6$ | — | — | 0.39 | — | 0.46 | — | — |
| $[0° \pm 45°]_s$ | — | .67 | — | — | — | — | — |
| **Notched Tensile Strength, $MN/m^2$ (ksi)** | | | | | | | |
| $[0°]_6$ | 993 (144) | 1260 (183) | 1140 (166) | 1210 (176) | 1140 (166) | 1030 (149) | 1110 (161) |
| $[0° \pm 45°]_s$ | 318 (46.1) | 357 (51.8) | 336 (48.8) | 352 (51.0) | 315 (45.7) | 249 (36.1) | 251 (36.4) |

Table 7-20. Ratio of Notched to Unnotched Tensile Strength of HT-S/710 G/PI at Various Temperatures

| Temperature K | Temperature (°F) | Ratio of Notched to Unnotched Strength $[0°]_6$ | Ratio of Notched to Unnotched Strength $[°0 \pm 45°]_s$ |
|---|---|---|---|
| 218 | −67 | 0.8 | 0.8 |
| 297 | 75 | 1.1 | .7 |
| 505 | 450 | .9 | .7 |
| 533 | 500 | 1.0 | .9 |
| 561 | 550 | .9 | .9 |
| 589 | 600 | .9 | .6 |
| 616 | 650 | 1.0 | .8 |

**Celion 6000/LARC-160 G/PI.** The plan for baseline tensile testing of the second G/PI system was to test three specimens at each of seven temperatures with the remaining 14 specimens equally divided between two of these temperatures. The temperatures selected for additional testing were room temperature and that used later for the flight simulation exposures, 450 K (350 °F). Selection of the temperatures for the flight simulation tests is discussed in Section 12. These two temperatures were the ones used for residual strength testing after both thermal aging and flight simulation exposures.

Only $[0° \pm 45°]_s$ crossplied tensile data were obtained for the Celion 6000/LARC-160 G/PI as no unidirectional panels were fabricated. Testing was performed on both unnotched and notched specimens in the longitudinal direction. Results are listed in Tables 7-21 and 7-22. A typical load-strain diagram from one of the strain gaged specimens is shown in Figure 7-18. The unnotched and notched tensile data are plotted as a function of temperature in Figures 7-19 and 7-20. A summary of the Celion 6000/LARC-160 G/PI tensile properties is presented in Table 7-23.

Modulus values were determined on the unnotched specimens at four temperatures using a mechanical extensometer. In addition, three each of the room temperature and 450 K (350 °F) specimens were also strain gaged for modulus measurements. As shown in Table 7-21, considerable scatter was observed in the modulus data obtained with the mechanical extensometer. The data from the strain gaged specimens, however, were much more consistent. They showed no effect of temperature on the modulus between room temperature and 450 K (350 °F).

The effect of temperature on unnotched and notched tensile strength of $[0° \pm 45°]_s$ Celion 6000/LARC-160 G/PI is presented in Figures 7-19 and 7-20. For both unnotched and notched specimens very little change in strength was observed over the entire range of temperatures studied. This is in contrast to the other organic matrix composite systems evaluated where decreases in strength at 218 K (−67 °F) were generally found. The data scatter, as shown by the scatter bands in Figures 7-19 and 7-20, was somewhat less for this G/PI than for the HT-S/710 system. A comparison of the notched and unnotched tensile strengths of the two G/PI systems shows the Celion 6000/LARC-160 material to be significantly higher at all temperatures.

Table 7-21. Baseline Tensile Properties of $[0° \pm 45°]_s$ Celion 6000/LARC-160 G/PI

| Specimen Number | Temperature K | Temperature (°F) | Tensile Strength MN/m² | Tensile Strength (ksi) | Tensile Modulus GN/m² | Tensile Modulus (Msi) |
|---|---|---|---|---|---|---|
| FC01-1 | 218 | −67 | 745 | 108 | 59 | 8.5 |
| -2 | | | 738 | 107 | 60 | 8.7 |
| -3 | | | 752 | 109 | 53 | 7.7 |
| | | | avg 745 | 108 | 57 | 8.3 |
| FC01-4 | 297 | 75 | 758 | 110 | 61 | a 8.8 |
| -5 | | | 752 | 109 | 62 | a 9.0 |
| -6 | | | 703 | 102 | 62 | a 9.0 |
| -7 | | | 745 | 108 | 52 | 7.6 |
| -8 | | | 703 | 102 | 52 | 7.5 |
| -9 | | | 710 | 103 | 44 | 6.4 |
| -10 | | | 674 | 97.7 | 71 | 10.3 |
| -11 | | | 676 | 98.1 | 74 | 10.7 |
| -12 | | | 681 | 98.7 | 54 | 7.9 |
| -13 | | | 652 | 94.5 | 81 | 11.7 |
| | | | avg 705 | 102 | 61 | 8.9 |
| FC01-14 | 394 | 250 | 745 | 108 | 66 | 9.5 |
| -15 | | | 668 | 96.9 | 64 | 9.3 |
| -16 | | | 800 | 116 | 66 | 9.6 |
| | | | avg 738 | 107 | 65 | 9.5 |
| FC01-17 | 450 | 350 | 738 | 107 | 62 | a 9.0 |
| -18 | | | 731 | 106 | 63 | a 9.2 |
| -19 | | | 665 | 96.5 | 59 | a 8.6 |
| -20 | | | 703 | 102 | 55 | 8.0 |
| -21 | | | 627 | 90.9 | 46 | 6.7 |
| -22 | | | 638 | 92.5 | 54 | 7.8 |
| -23 | | | 724 | 105 | 63 | 9.2 |
| -24 | | | 738 | 107 | 63 | 9.2 |
| -25 | | | 703 | 102 | 51 | 7.4 |
| -26 | | | 690 | 100 | 63 | 9.2 |
| | | | avg 696 | 101 | 57 | 8.4 |
| FC01-27 | 478 | 400 | 690 | 100 | | |
| -28 | | | 696 | 101 | | |
| -29 | | | 683 | 99.1 | | |
| | | | avg 690 | 100 | | |
| FC01-30 | 505 | 450 | 703 | 102 | | |
| -31 | | | 663 | 96.1 | | |
| -32 | | | 703 | 102 | | |
| | | | avg 690 | 100 | | |
| FC01-33 | 533 | 500 | 683 | 99.0 | | |
| -34 | | | 717 | 104 | | |
| -35 | | | 681 | 96.8 | | |
| | | | avg 694 | 101 | | |

[a] Strain gage measurement

Table 7-22. Baseline Notched Tensile Properties of $[0° \pm 45°]_s$ Celion 6000/LARC-160 G/PI

| Specimen Number | Temperature K | (°F) | | Notched Tensile Strength[a] NM/m$^2$ | (ksi) |
|---|---|---|---|---|---|
| FC02-1 | 218 | −67 | | 442 | 64.1 |
| -2 | | | | 401 | 58.1 |
| -3 | | | | 404 | 58.6 |
| | | | avg | 416 | 60.3 |
| FC02-4 | 297 | 75 | | 381 | 55.2 |
| -5 | | | | 345 | 50.1 |
| -6 | | | | 396 | 57.4 |
| -7 | | | | 452 | 65.6 |
| -8 | | | | 487 | 70.7 |
| -9 | | | | 432 | 62.6 |
| -10 | | | | 500 | 72.5 |
| -11 | | | | 390 | 56.5 |
| -12 | | | | 419 | 60.8 |
| -13 | | | | 474 | 68.7 |
| | | | avg | 428 | 62.0 |
| FC02-14 | 394 | 250 | | 458 | 66.4 |
| -15 | | | | 469 | 68.0 |
| -16 | | | | 395 | 57.3 |
| | | | avg | 441 | 63.9 |
| FC02-17 | 450 | 350 | | 441 | 63.9 |
| -18 | | | | 481 | 69.8 |
| -19 | | | | 445 | 64.6 |
| -20 | | | | 468 | 67.9 |
| -21 | | | | 430 | 62.4 |
| -22 | | | | 483 | 70.0 |
| -23 | | | | 439 | 63.7 |
| -24 | | | | 517 | 75.0 |
| -25 | | | | 492 | 71.4 |
| -26 | | | | 554 | 80.3 |
| | | | avg | 475 | 68.9 |
| FC02-27 | 478 | 400 | | 534 | 77.5 |
| -28 | | | | 414 | 60.0 |
| -29 | | | | 472 | 68.5 |
| | | | avg | 473 | 68.7 |
| FC02-30 | 505 | 450 | | 555 | 80.5 |
| -31 | | | | 544 | 78.9 |
| -32 | | | | 500 | 72.5 |
| | | | avg | 533 | 77.3 |
| FC02-33 | 533 | 500 | | 514 | 74.5 |
| -34 | | | | 564 | 81.8 |
| -35 | | | | 456 | 66.1 |
| | | | avg | 511 | 74.1 |

[a] Net section strength, i.e., based on total width less hole diameter.

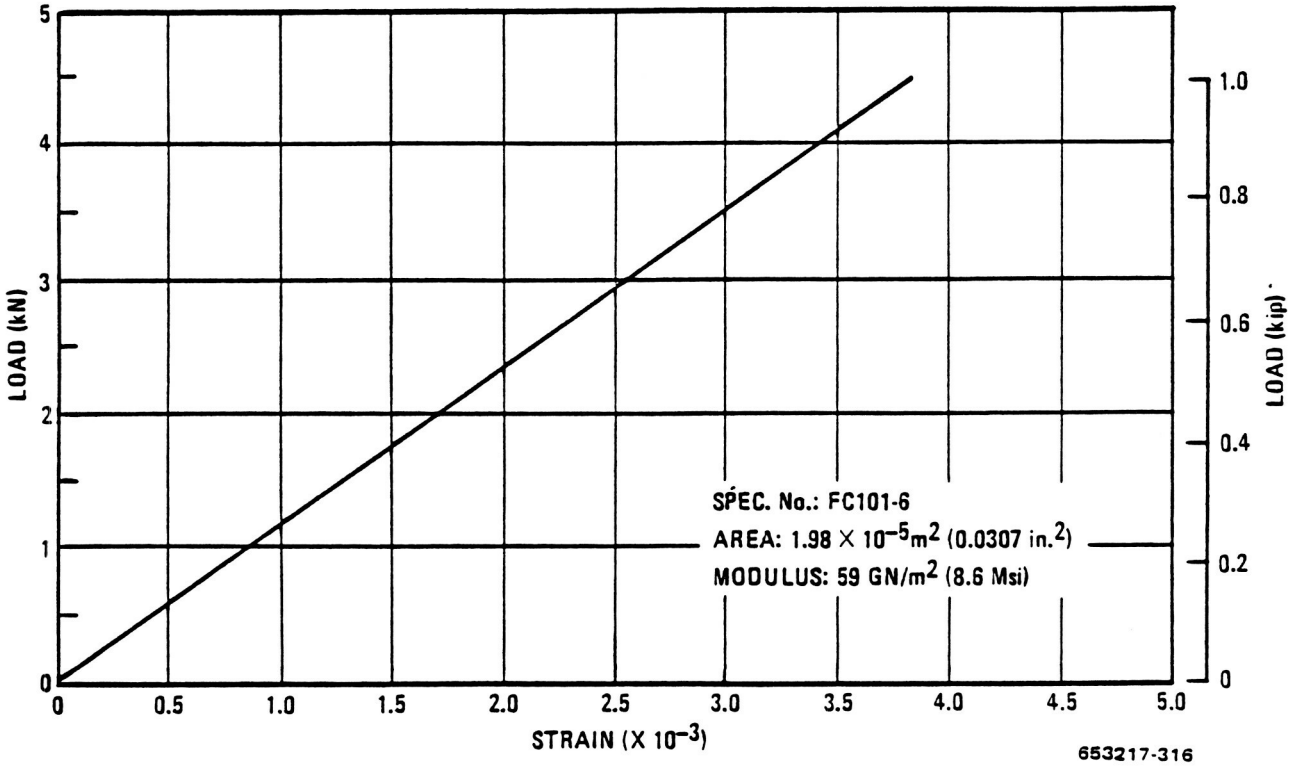



**Figure 7-18 Tensile Load-Strain Diagram for $[0° \pm 45°]_s$ Celion 6000/LARC-160 G/PI at 297 K (75°F)**

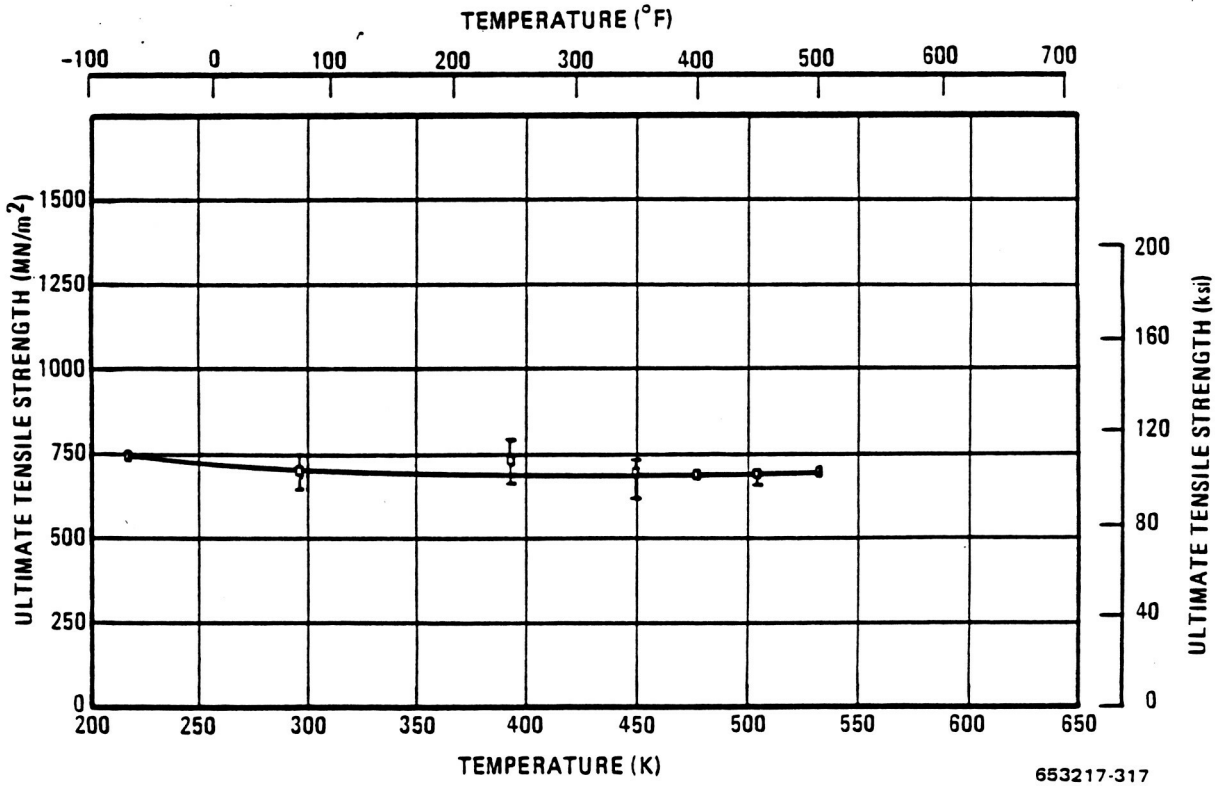
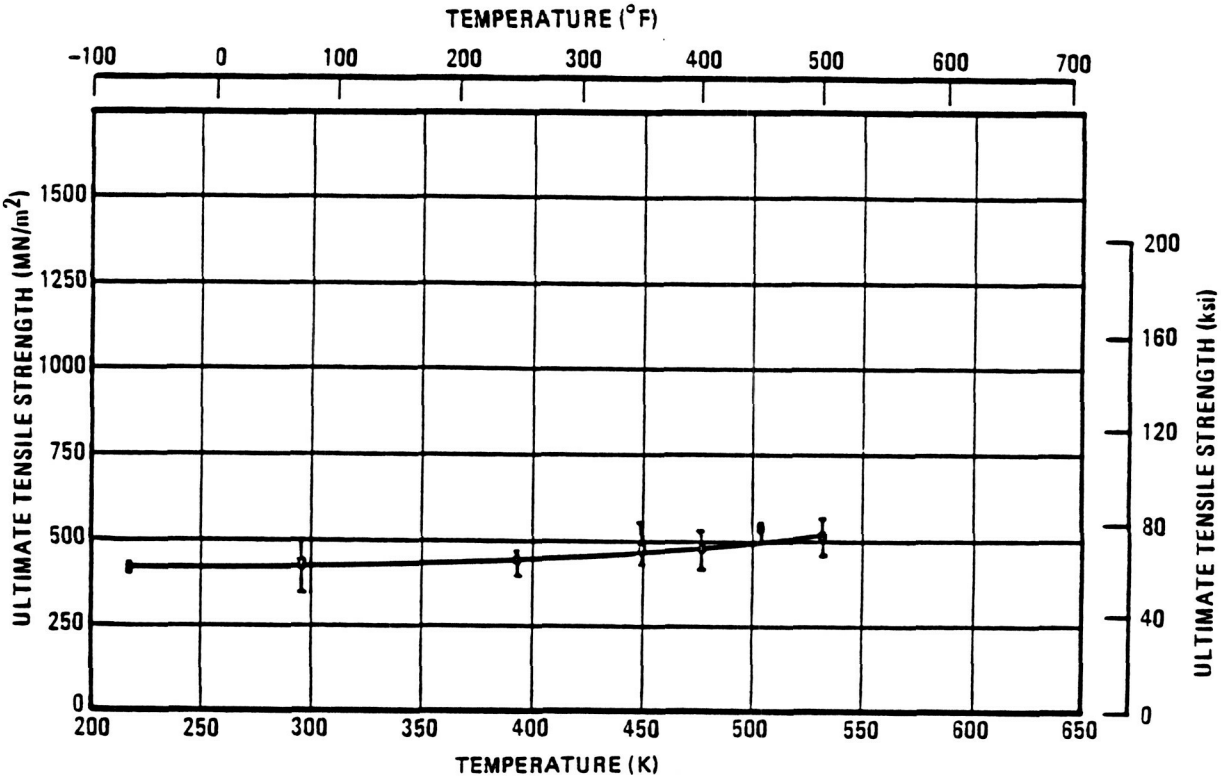



**Figure 7-19 Baseline Tensile Properties of $[0° \pm 45°]_s$ Celion 6000/LARC-160 G/PI**




653217-318

**Figure 7-20 Baseline Notched Tensile Properties of $[0° \pm 45°]_s$ Celion 6000/LARC-160 G/PI**

The notched to unnotched tensile strength ratios of the $[0° \pm 45°]_s$ Celion 6000/LARC-160 G/PI specimens at each of the test temperatures are listed in Table 7-24. The effect of the notch was a reduction in the net section strength of 20 to 40%. Similar results were observed for the other G/PI system and both the epoxy systems with the $[0° \pm 45°]_s$ layups.

**7.1.2.4 Boron/Aluminum.** The baseline tensile test plan for the B/Al system as originally proposed included tests at 218 K (−67° F) and 297 K (75° F) as used for the resin matrix systems and at 561 K (550° F) and 700 K (800° F). The 700 K (800° F) temperature was considered to be the maximum short-time use temperature and 561 K (550° F) the maximum use temperature for very long time applications. However, fatigue tests conducted on this program (see Section 11), revealed the existence of a severe surface degradation effect during fatigue cycling of B/Al at 561 K (550° F) in an air environment. The effect was not observed at 505 K (450° F). Because of this severe surface degradation the flight simulation temperature initially selected for B/Al, 561 K (550° F), was lowered to 505 K (450° F). At the time of this decision all baseline testing was completed except for the unnotched $[0° \pm 45°]_s$ crossplied material. A change was made to include several tensile tests at 505 K (450° F) to assist in selection of the short-term flight simulation load levels. Three specimens were also tested at 616 K (650° F) to fill in the tensile strength versus temperature curve for unnotched $[0° \pm 45°]_s$ crossplied B/Al.

Baseline tensile tests, both unnotched and notched, were performed on unidirectional and $[0° \pm 45°]_s$ crossplied specimens in the longitudinal direction. Some unnotched tensile tests were also performed in the transverse direction on unidirectional material, and a limited amount of Poisson's ratio testing was conducted. Results are listed in Table 7-25 through 7-30. A typical load-strain diagram is plotted in Figure 7-21. The longitudinal unnotched and notched data are

**Table 7-23. Summary of Baseline Tensile Properties of Celion 6000/LARC-160 G/PI**

| | Temperature, K (°F) | | | | | | |
|---|---|---|---|---|---|---|---|
| | 218 (−67) | 297 (75) | 394 (250) | 450 (350) | 478 (400) | 505 (450) | 533 (500) |
| Tensile Strength, $MN/m^2$ (ksi) | | | | | | | |
| $[0° \pm 45°]_s$ | 745 (108) | 705 (102) | 738 (107) | 696 (101) | 690 (100) | 690 (100) | 694 (101) |
| Tensile Modulus, $GN/m^2$ (Msi) | | | | | | | |
| $[0° \pm 45°]_s$ | 57 (8.3) | 59 (8.9) | 65 (9.5) | 57 (8.4) | — | — | — |
| Notched Tensile Strength, $MN/m^2$ (ksi) | | | | | | | |
| $[0° \pm 45°]_s$ | 416 (60.3) | 428 (62.0) | 441 (63.9) | 475 (68.9) | 473 (68.7) | 533 (77.3) | 511 (74.1) |

Table 7-24. Ratio of Notched to Unnotched Tensile Strength of $[0° \pm 45°]_s$ Celion 6000/LARC-160 G/PI at Various Temperatures

| Temperature K | Temperature (°F) | Ratio of Notched to Unnotched Strength |
|---|---|---|
| 218 | −67 | 0.6 |
| 297 | 75 | 0.6 |
| 394 | 250 | 0.6 |
| 450 | 350 | 0.7 |
| 478 | 400 | 0.7 |
| 505 | 450 | 0.8 |
| 533 | 500 | 0.7 |

Table 7-25. Baseline Tensile Properties of $[0°]_6$ B/Al

| Specimen Number | Temperature K | Temperature (°F) | Tensile Strength MN/m² | Tensile Strength (ksi) | Tensile Modulus GN/m² | Tensile Modulus (Msi) |
|---|---|---|---|---|---|---|
| EU01-1 | 218 | −67 | 1640 | 238 | 178 | 25.8 |
| -2 | | | 1620 | 235 | 197 | 28.6 |
| -3 | | | 1580 | 229 | 172 | 25.0 |
| -4 | | | 1540 | 223 | 166 | 24.1 |
| -5 | | | 1610 | 234 | 157 | 22.8 |
| | | | avg 1600 | 232 | 174 | 25.3 |
| EU01-6 | 561 | 550 | 1200 | 174 | [a]199 | [a]28.9 |
| -7 | | | 1360 | 197 | [a]212 | [a]30.7 |
| -8 | | | 1200 | 174 | [a]207 | [a]30.0 |
| -9 | | | 1430 | 207 | — | — |
| | | | avg 1300 | 188 | 206 | 29.9 |
| EU01-10 | 700 | 800 | 1360 | 198 | [a]192 | [a]27.8 |
| -11 | | | 1150 | 167 | [a]194 | [a]28.2 |
| -12 | | | 1380 | 200 | [a]214 | [a]31.0 |
| -13 | | | 1320 | 192 | — | — |
| | | | avg 1300 | 189 | 200 | 29.0 |

[a] Strain gage measurement

Table 7-26. Baseline Tensile Properties of $[0° \pm 45°]_s$ B/Al

| Specimen Number | Temperature K | Temperature (°F) | Tensile Strength MN/m² | Tensile Strength (ksi) | Tensile Modulus GN/m² | Tensile Modulus (Msi) |
|---|---|---|---|---|---|---|
| EC01-1 | 218 | −67 | 499 | 72.4 | — | — |
| -2 | | | 550 | 79.8 | — | — |
| -3 | | | 525 | 76.1 | — | — |
| -4 | | | 554 | 80.4 | — | — |
| -5 | | | 511 | 74.1 | — | — |
| | | | avg 528 | 76.6 | | |
| EC01-6 | 297 | 75 | 487 | 70.7 | 155 | 22.5 |
| -7 | | | 545 | 79.1 | 158 | 22.9 |
| -8 | | | 482 | 69.9 | 160 | 23.2 |
| -9 | | | 458 | 66.4 | 140 | 20.3 |
| -10 | | | 552 | 80.0 | 167 | 24.2 |
| -11 | | | 565 | 82.0 | 163 | 23.7 |
| -12 | | | 549 | 79.6 | 169 | 24.5 |
| -13 | | | 459 | 66.5 | 154 | 22.4 |
| -14 | | | 545 | 79.1 | 141 | 20.4 |
| -15 | | | 514 | 74.5 | 139 | 20.1 |
| | | | avg 516 | 74.8 | 155 | 22.4 |
| EC01-16 | 505 | 450 | 459 | 66.6 | [a]104 | [a]15.1 |
| -17 | | | 447 | 64.9 | 142 | 20.6 |
| -18 | | | 468 | 67.9 | 100 | 14.5 |
| -28 | | | 454 | 65.9 | 136 | 19.8 |
| -29 | | | 457 | 66.3 | 126 | 18.3 |
| -30 | | | 471 | 68.3 | 116 | 16.9 |
| -31 | | | 410 | 59.5 | 124 | 18.0 |
| | | | avg 452 | 65.6 | 121 | 17.6 |
| EC01-19 | 561 | 550 | 450 | 65.2 | [a]103 | [a]15.0 |
| -20 | | | 365 | 53.0 | 123 | 17.9 |
| -21 | | | 416 | 60.3 | 102 | 14.8 |
| -32 | | | 450 | 65.3 | 120 | 17.4 |
| -33 | | | 474 | 68.8 | 128 | 18.5 |
| -34 | | | 455 | 66.0 | 103 | 15.0 |
| -35 | | | 464 | 67.3 | 108 | 15.6 |
| | | | avg 439 | 63.7 | 112 | 16.3 |
| EC01-22 | 616 | 650 | 423 | 61.3 | [a]108 | [a]15.6 |
| -23 | | | 397 | 57.6 | — | — |
| -24 | | | 499 | 72.4 | — | — |
| | | | avg 440 | 63.8 | 108 | 15.6 |
| EC01-25 | 700 | 800 | 467 | 67.7 | [a]93.1 | [a]13.5 |
| -26 | | | 338 | 49.0 | — | — |
| -27 | | | 335 | 48.6 | — | — |
| | | | avg 380 | 55.1 | 93.1 | 13.5 |

[a] Strain gage measurement

Table 7-27. Baseline Notched Tensile Properties of $[0°]_6$ B/Al

| Specimen Number | Temperature K | Temperature (°F) | Notched Tensile Strength $MN/m^2$ (a) | Notched Tensile Strength (ksi) |
|---|---|---|---|---|
| EU02-1 | 218 | −67 | 1200 | 174 |
| -2 | | | 1210 | 175 |
| -3 | | | 1240 | 180 |
| -4 | | | 1230 | 178 |
| -5 | | | 1210 | 176 |
| | | | avg 1220 | 177 |
| EU02-6 | 561 | 550 | 1190 | 173 |
| -7 | | | 1130 | 164 |
| -8 | | | 1140 | 165 |
| -9 | | | 1130 | 164 |
| | | | avg 1150 | 166 |
| EU02-10 | 700 | 800 | 986 | 143 |
| -11 | | | 1100 | 159 |
| -12 | | | 1080 | 157 |
| -13 | | | 1030 | 150 |
| | | | avg 1050 | 152 |

[a] Net section strength, i.e., based on total width less hole diameter.

plotted as a function of temperature in Figures 7-22 and 7-23. A summary of all the B/Al tensile properties is presented in Table 7-31.

Modulus measurements were made using both a mechanical extensometer and strain gages at temperatures to 561 K (550° F). Above 561 K (550° F) a small number of tests was made using only strain gaged specimens. Modulus values were obtained at 218 K (−67° F) for the unidirectional specimens, but extensometer malfunctions during tests on the crossplied specimens gave poorly defined stress strain curves that did not allow determination of modulus. For the material tested in the transverse direction, modulus was determined only at room temperature using a mechanical extensometer.

The effect of temperature on the tensile strength of B/Al is shown in Figures 7-22 and 7-23. No tests were conducted on the unnotched unidirectional material at room temperature, but data were available from the QA panels, and these data are plotted at room temperature in Figure 7-22. The curves show a gradual decrease in strength with increasing temperature for both orientations and configurations. The B/Al data are similar to those for HT-S/710 G/PI in that the decrease is somewhat greater for the crossplied material, both unnotched and notched, than for the unidirectional material. The tensile strength was slightly higher at 218 K (−67° F) for the unnotched specimens but essentially unchanged for the notched specimens. In like manner to both the G/E and HT-S/710 G/PI systems, the data scatter for B/Al was numerically greater for the unidirectional material, but, percentagewise, was greater for the crossplied

Table 7-28. Baseline Notched Tensile Properties of $[0° \pm 45°]_s$ B/Al

| Specimen Number | Temperature K | Temperature (°F) | | Notched Tensile Strength $MN/m^2$ (a) | Notched Tensile Strength (ksi) |
|---|---|---|---|---|---|
| EC02-1 | 218 | −67 | | 486 | 70.5 |
| -2 | | | | 492 | 71.3 |
| -3 | | | | 460 | 66.7 |
| -4 | | | | 442 | 64.1 |
| -5 | | | | 495 | 71.8 |
| | | | avg | 475 | 68.9 |
| EC02-6 | 297 | 75 | | 470 | 68.1 |
| -7 | | | | 465 | 67.4 |
| -8 | | | | 470 | 68.1 |
| -9 | | | | 467 | 67.7 |
| -10 | | | | 455 | 66.0 |
| -11 | | | | 496 | 72.0 |
| -12 | | | | 485 | 70.4 |
| -13 | | | | 490 | 71.0 |
| -14 | | | | 495 | 71.8 |
| -15 | | | | 501 | 72.7 |
| | | | avg | 479 | 69.5 |
| EC02-16 | 561 | 550 | | 434 | 62.9 |
| -17 | | | | 433 | 62.8 |
| -18 | | | | 423 | 61.4 |
| -19 | | | | 461 | 66.9 |
| -20 | | | | 454 | 65.9 |
| -21 | | | | 439 | 63.7 |
| -22 | | | | 421 | 61.1 |
| -23 | | | | 451 | 65.4 |
| -24 | | | | 455 | 66.0 |
| -25 | | | | 462 | 67.0 |
| | | | avg | 443 | 64.3 |
| EC02-26 | 700 | 800 | | 361 | 52.3 |
| -27 | | | | 361 | 52.4 |
| -28 | | | | 363 | 52.6 |
| -29 | | | | 377 | 54.7 |
| -30 | | | | 341 | 49.5 |
| -31 | | | | 361 | 52.3 |
| -32 | | | | 378 | 54.8 |
| -33 | | | | 371 | 53.8 |
| -34 | | | | 363 | 52.7 |
| -35 | | | | 351 | 50.9 |
| | | | avg | 363 | 52.6 |

[a] Net section strength, i.e., based on total width less hole diameter.

Table 7-29. Baseline Tensile Properties of $[0°]_6$ B/Al Tested in the Transverse Direction

| Specimen Number | Temperature K | Temperature (°F) | Tensile Strength MN/m² | Tensile Strength (ksi) | Tensile Modulus GN/m² | Tensile Modulus (Msi) |
|---|---|---|---|---|---|---|
| TEU01-1 | 297 | 75 | 94.5 | 13.7 | 48.3 | 7.0 |
| -2 | | | 122 | 17.7 | 67.6 | 9.8 |
| -3 | | | 51.0 | 7.4 | 133 | 19.3 |
| -4 | | | 74.5 | 10.8 | 121 | 17.6 |
| -5 | | | 57.9 | 8.4 | 105 | 15.2 |
| -6 | | | 76.5 | 11.1 | 140 | 20.3 |
| | | avg | 79.4 | 11.5 | 102 | 14.9 |
| TEU01-7 | 700 | 800 | 44.1 | 6.4 | — | — |
| -8 | | | 31.7 | 4.6 | — | — |
| -9 | | | 38.6 | 5.6 | — | — |
| -10 | | | 29.0 | 4.2 | — | — |
| -11 | | | 35.8 | 5.2 | — | — |
| -12 | | | 33.1 | 4.8 | — | — |
| | | avg | 35.4 | 5.1 | | |

Table 7-30. Baseline Poisson's Ratio Data in Tension of B/Al

| Specimen Number | Laminate Orientation | Test Direction | Test Temperature K | Test Temperature (°F) | | Poisson's 0.31 |
|---|---|---|---|---|---|---|
| EU01-6 | $[0°]_6$ | Longitudinal | 561 | 550 | | 0.31 |
| -7 | | | | | | .34 |
| -8 | | | | | | .34 |
| | | | | | avg | .33 |
| EU01-10 | $[0°]_6$ | Longitudinal | 700 | 800 | | .32 |
| -11 | | | | | | .30 |
| -12 | | | | | | .39 |
| | | | | | avg | .34 |

material. The scatter bands for the notched tests, Figure 7-23, were considerably smaller than those obtained for the unnotched specimen tests, Figure 7-22. This effect was not observed for the resin matrix systems.

No decrease in tensile modulus was found for the unidirectional B/Al out to 700 K (800° F). There was a decrease of about 15% however, for tests at 218 K (−67° F). The $[0° \pm 45°]_s$ cross-plied material exhibited a continuous decrease in modulus out to 700 K (800° F). The total change between room temperature and 700 K (800° F) was approximately 40%.

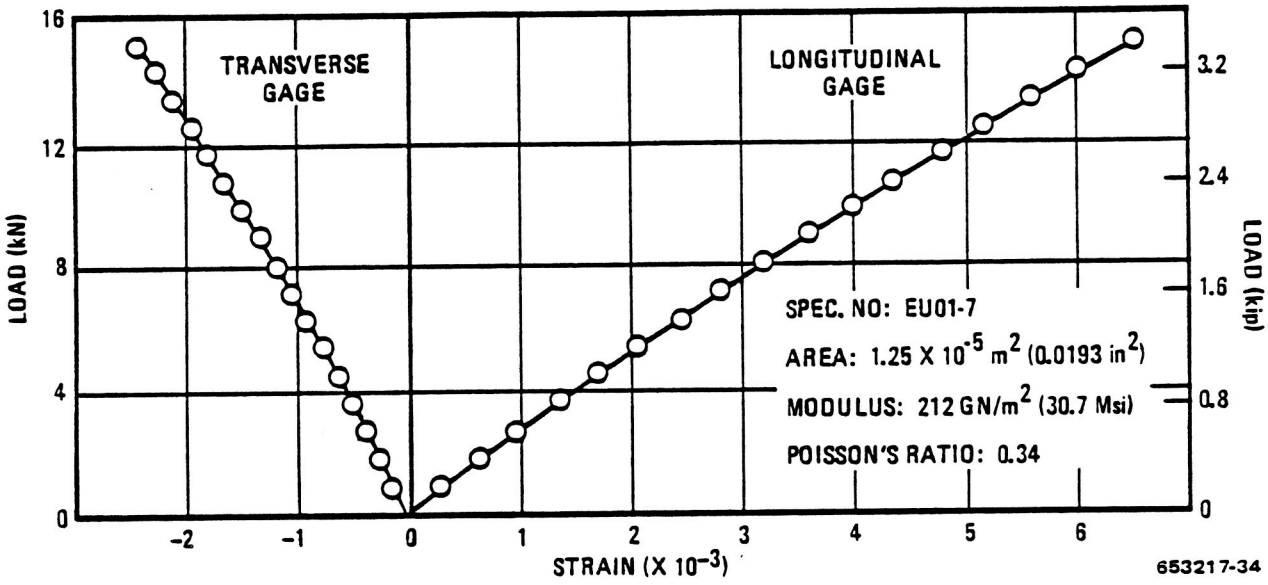



**Figure 7-21 Tensile Load-Strain Diagram for $[0°]_6$ B/Al at 561 K (550° F)**

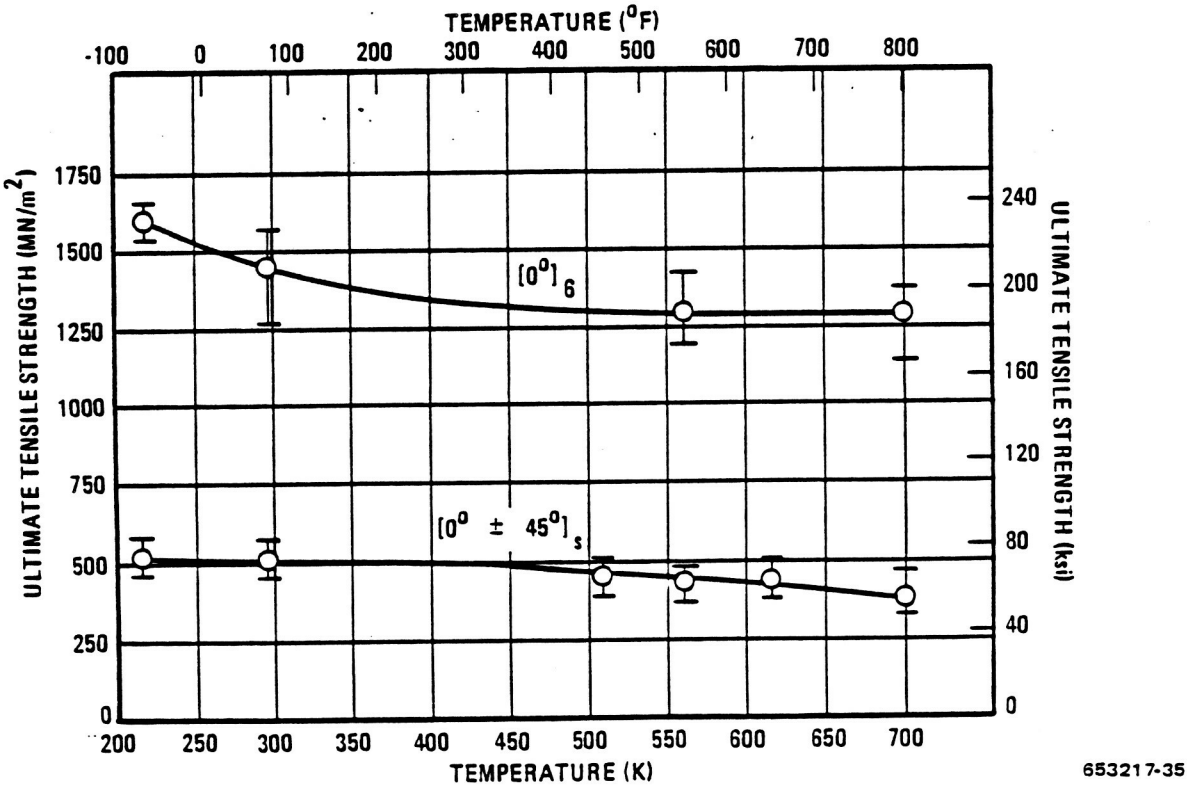



**Figure 7-22 Baseline Tensile Properties of B/Al**

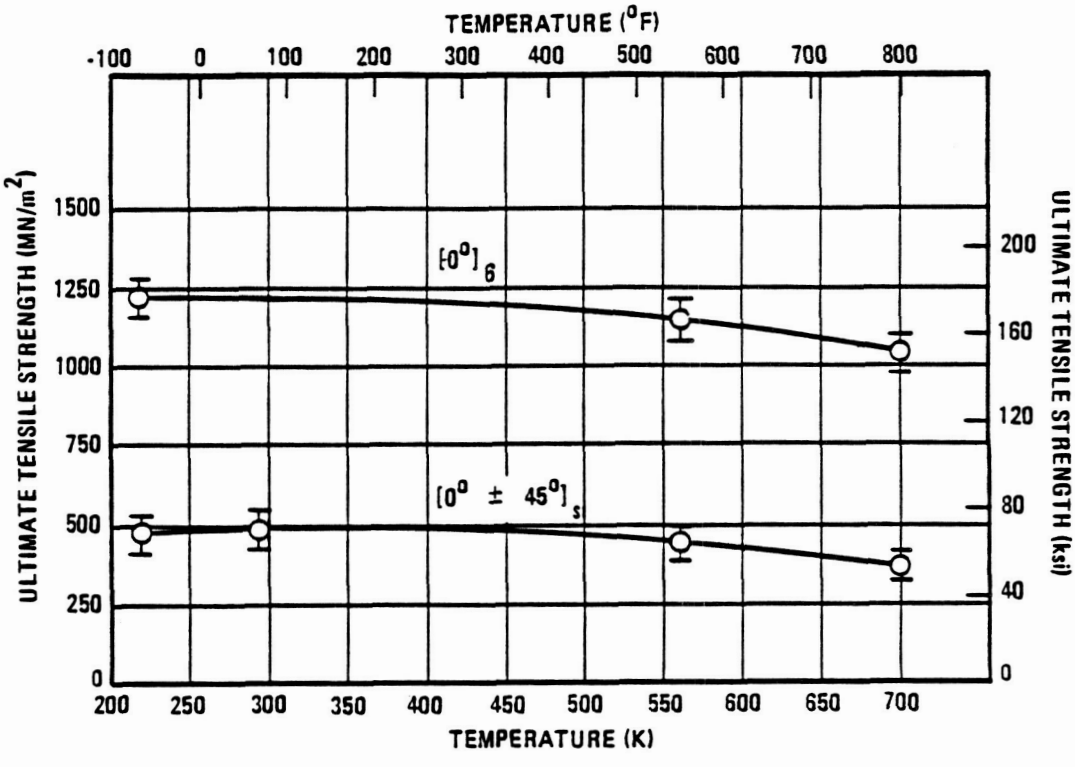



**Figure 7-23 Baseline Notched Tensile Properties of B/Al**

The ratios of the notched to the unnotched tensile strengths of B/Al have been calculated for several temperatures and are shown in Table 7-32. The data differ from those presented earlier for the resin matrix systems in that the crossplied specimens were not greatly affected by the notch; whereas, the unidirectional specimens experienced decreases in tensile strength of approximately 20% when tested in the notched configuration.

Tensile data for unidirectional material tested in the transverse direction are given in Table 7-29. The effect of temperature on the transverse tensile strength was much more pronounced than that for longitudinal strength with values at 700 K (800 ° F) approximately half of those measured at room temperature.

Results of the Poisson's ratio tests are listed in Table 7-30. Values at both test temperatures were approximately one-third, similar to those found for most unreinforced metals.

## 7.2 SHEAR TESTING

Two methods of shear testing were utilized for both the resin matrix and the metal matrix systems. For the resin matrix materials, a torsion tube specimen configuration that measures in-plane shear and a short beam configuration that measures interlaminar shear were tested. Short beam shear testing, which requires a specimen thickness between 0.0015 m (0.060 in.) and 0.064 m (0.25 in.), was performed on all 12 and 24 ply resin matrix laminates. These data

**Table 7-31. Summary of Baseline Tensile Properties of B/Al**

| | Temperature, K (°F) | | | | | |
|---|---|---|---|---|---|---|
| | 218 (−67) | 297 (75) | 505 (450) | 561 (550) | 616 (650) | 700 (800) |
| Tensile Strength, $MN/m^2$ (ksi) | | | | | | |
| $[0°]_6$ | 1600 (232) | 1430 (208) | — | 1300 (188) | — | 1300 (189) |
| $[0° \pm 45°]_s$ | 528 (76.6) | 516 (74.8) | 452 (65.6) | 439 (63.7) | 440 (63.8) | 380 (55.1) |
| Tensile Modulus, $GN/m^2$ (Msi) | | | | | | |
| $[0°]_6$ | 174 (25.3) | 194 (28.2) | — | 206 (29.9) | — | 200 (29.0) |
| $[0° \pm 45°]_s$ | — | 154 (22.4) | 121 (17.6) | 112 (16.3) | 108 (15.6) | 93 (13.5) |
| Poisson's Ratio | | | | | | |
| $[0°]_6$ | — | 0.23 | — | 0.33 | — | 0.34 |
| Notched Tensile Strength, $MN/m^2$ (ksi) | | | | | | |
| $[0°]_6$ | 1220 (177) | 1210 (176) | — | 1140 (166) | — | 1050 (152) |
| $[0° \pm 45°]_s$ | 475 (68.9) | 479 (69.5) | — | 443 (64.3) | — | 363 (52.6) |

Table 7-32. Ratio of Notched to Unnotched Tensile Strength of B/Al at Various Temperatures

| Temperature K | Temperature (°F) | Ratio of Notched to Unnotched Strength $[0°]_6$ | Ratio of Notched to Unnotched Strength $[0° \pm 45°]_s$ |
|---|---|---|---|
| 218 | −67 | 0.8 | 0.9 |
| 297 | 75 | [a] .8 | .9 |
| 561 | 550 | .9 | 1.0 |
| 700 | 800 | .8 | 1.0 |

[a]Estimated from curves of tensile strength versus temperature

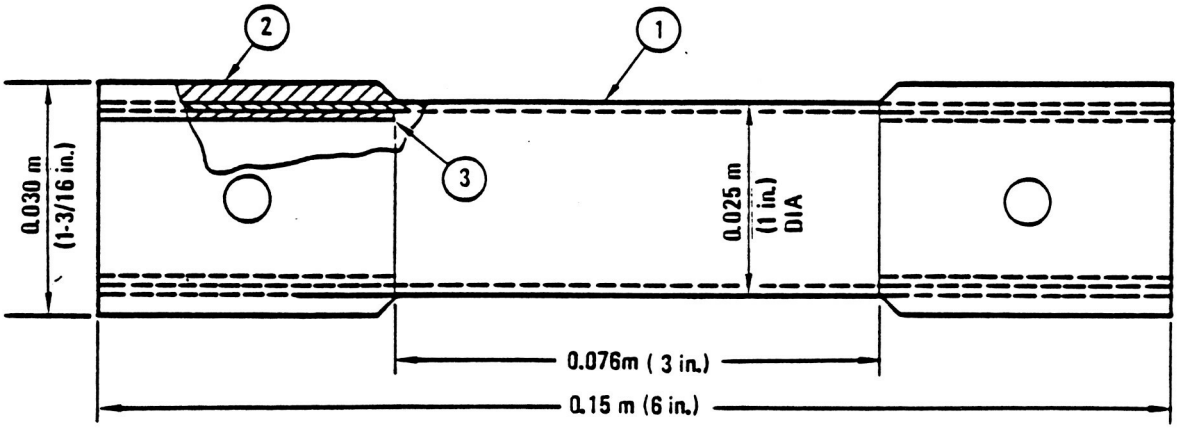
have been reported in the Laminate Quality Assurance Testing section. Shear strength properties of the 6 ply $[0° \pm 45°]_s$ material also became of interest, however, because of the matrix-dominated failure modes observed in the 6 ply Phase I flight simulation specimens. A specimen made by bonding three or four pieces to obtain a sufficiently thick laminate was devised, and short beam shear strength was included in the baseline property testing for the thermal aging/compression study materials. For B/Al the torsion tube specimen and a slotted rectangular interfiber shear specimen were used. Specimens, test procedures, and results are presented in the following sections for the methods that used the tube and rectangular interfiber shear specimens. Only the test results are given for the short beam shear tests of the bonded 18 or 24 ply specimens as the specimen dimensions and test procedure are discussed in Appendix B, Quality Assurance Test Procedures.

**7.2.1 SPECIMEN DESIGN AND TEST PROCEDURE.** The B/Al torsion tube specimen was 0.15 m (6 in.) long by 0.024 m (1 in.) outside diameter with a nominal 0.001 m (0.040 in.) wall thickness. The specimens were fabricated from 6 plies of B/Al tape oriented with the boron filaments in the long-axis direction of the tube. Steel end fittings were diffusion bonded to the tube in the manufacturing process. Loading was accomplished by cylindrical male fixtures that were pin-attached to the steel reinforced tube ends with 0.0064 m (0.25 in.) steel bolts. A sketch of the B/Al tube is shown in Figure 7-24.

The G/E torsion tube specimen, also shown in Figure 7-24, was similar to the B/Al tube except for the length and end fittings. These specimens were 0.089 m (3.5 in.) in length and had steel fittings adhesively bonded to the ends after fabrication and cutting to the correct lengths. To obtain a wall thickness of 0.001 m (0.040 in.) (to prevent buckling during test) it was necessary to use an 8 ply tube for the G/E specimens rather than the 6 plies used for the B/Al specimens.

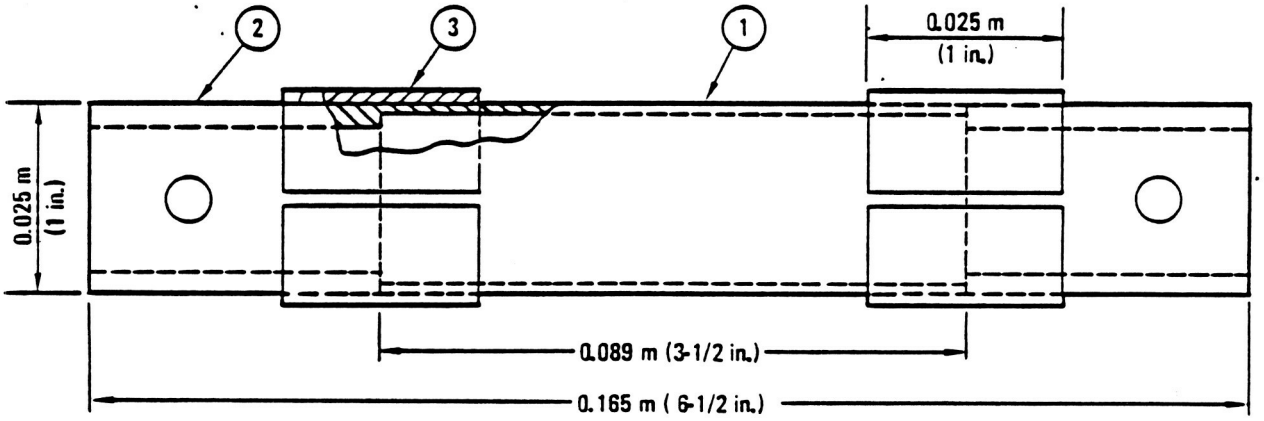
To determine the shear modulus, all of the torsion tube specimens were strain gaged prior to test. A half bridge, shear-torque rosette strain gage was bonded to each tube with M-bond 610 adhesive. The gages and adhesive cure cycles that were used are:

a. Gages:
   B/Al — FAED-12C-12-S3
   G/E — FAED-12C-12-SO




DETAIL:
1. 0.001 m (0.040 in.) THICKNESS (6 PLY) B/Al TUBE
2. 0.0024 m (0.094 in.) THICKNESS STEEL REINFORCEMENT
3. 0.00071 m (0.028 in.) THICKNESS STEEL REINFORCEMENT

(a)




DETAIL:
1. 0.001 m (0.040 in.) THICKNESS (8 PLY) A-S/3501 G/E TUBE
2. 0.0032 m (1/8 in.) WALL STEEL TUBE
3. 0.0016 m (1/16 in.) WALL SPLIT STEEL COLLAR

(b)

653217-37

**Figure 7-24 Torsion Tube Configurations (a) B/Al Specimen and (b) G/E Specimen**

b. Cure Cycles:

| Test Temperature | Cure Cycles |
|---|---|
| 297 K (75° F) | 2 hours at 394 K (250° F) |
| 394 K (250° F) | 2 hours at 394 K (250° F) |
| 450 K (350° F) | 1.5 hours at 450 K (350° F) |
| 505 K (450° F) | 1 hour at 505 K (450° F) |

Application techniques were the same as those described earlier for the Poisson's ratio and tensile modulus specimens.

Testing of the strain gaged tube specimens was conducted in an MTS Closed-Loop Tension-Torsion machine. The specimens were loaded (in torsion) incrementally to failure with strain readings recorded automatically at each load step with a B & F Instruments, Inc. Multichannel Digital Strain Indicator, 161 Mini-System. The output was both a typewritten recording of torque versus strain and a punched paper tape that could be processed by a computer, programmed to produce a shear stress versus strain plot. In addition, a torque-twist curve was also recorded for each test. Typical torque-twist and stress-strain curves are shown in Figures 7-25 and 7-26. An overall view of the torsion testing machine and the Mini-System strain recorder is presented in Figure 7-27. For elevated temperature tests the specimens were heated in the mid-section with a small ring furnace and held 10 minutes prior to twisting. A closeup view of a B/Al tube installed in the test machine is shown in Figure 7-28 prior to testing at room temperature and in Figure 7-29 before testing at elevated temperature. The white material packed around the tube above and below the ring furnace in Figure 7-29 is Fiberfrax insulation batting for maintaining good temperature uniformity. Temperature was monitored with a chromel-alumel thermocouple attached to the center of the tube and controlled manually to ± 3 K (± 5 °F) during the short time period required for the test.

Shear strengths were calculated from the torsion test data and tube dimensions by using the following thin walled tube approximation of the torsion formula for circular shafts:

$$\tau = \frac{2\,T\,Do}{\pi\,t\,(Do - t)^3}$$

$\tau$ = ultimate shear strength, $N/m^2$ ($lb/in^2$)

T = Maximum torque, Nm (in-lb)

Do = Outside diameter of tube, m (in.)

t = Wall thickness of tube, m (in.)

The shear modulus, G, was determined from the stress-strain curves as follows:

$$G = \frac{\tau}{\gamma} = \frac{\tau}{\epsilon_1 - \epsilon_2}$$

where $\gamma$ (equal to $\epsilon_1 - \epsilon_2$) is the angle of twist and $\epsilon_1$ and $\epsilon_2$ are strain readings taken at a value of shear stress, $\tau$, in the linear portions of the stress-strain curves (see Figure 7-26).

The second type of shear specimen, which was used only for the B/Al system, is shown in Figure 7-30. The slots were cut in the specimens by the EDM method. All specimens were prepared from 6 ply unidirectional material with the boron filaments oriented in the long direction

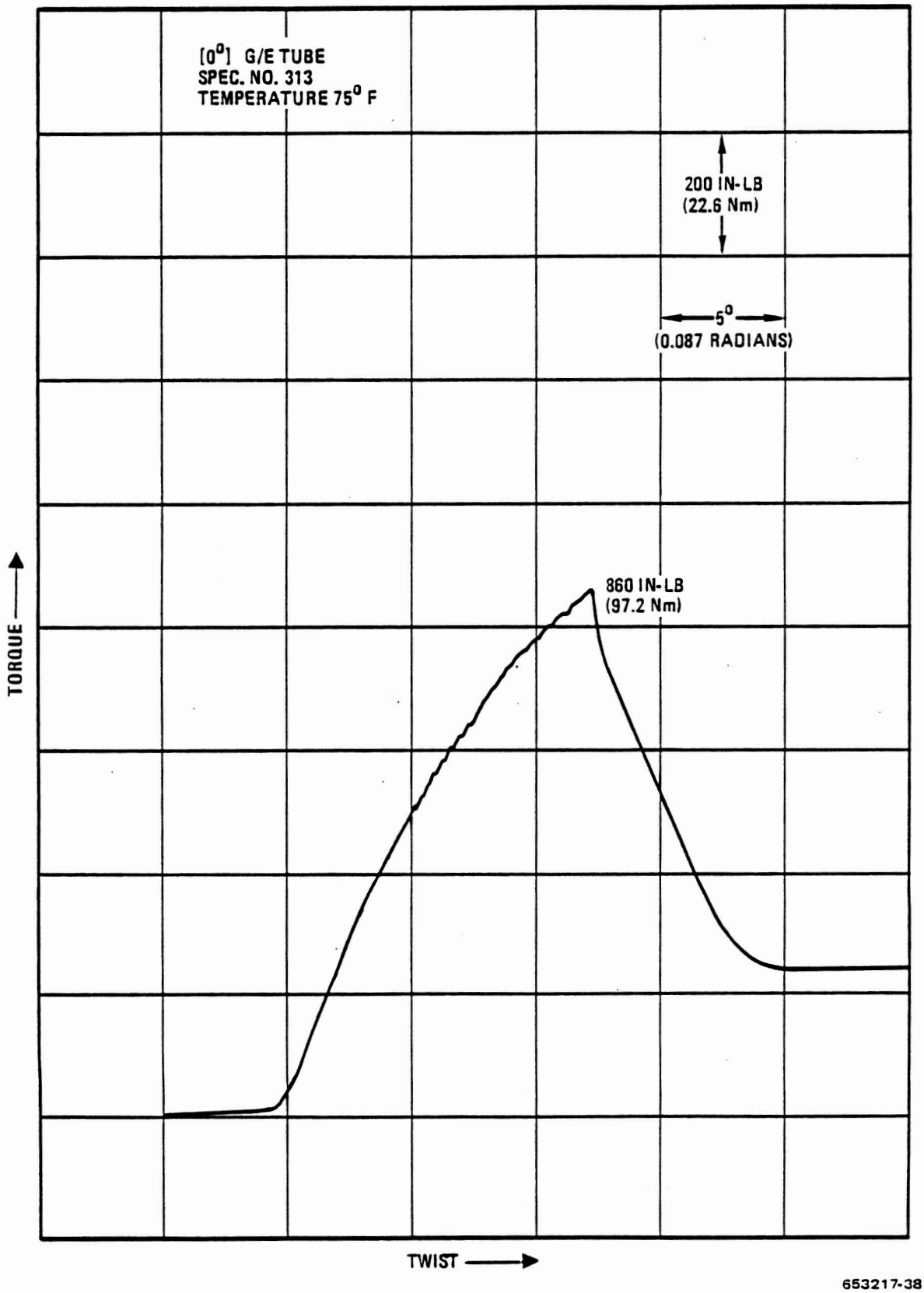



Figure 7-25 Typical Torque-Twist Curve for Torsion Test of Unidirectional G/E Tube Specimen BU06-13

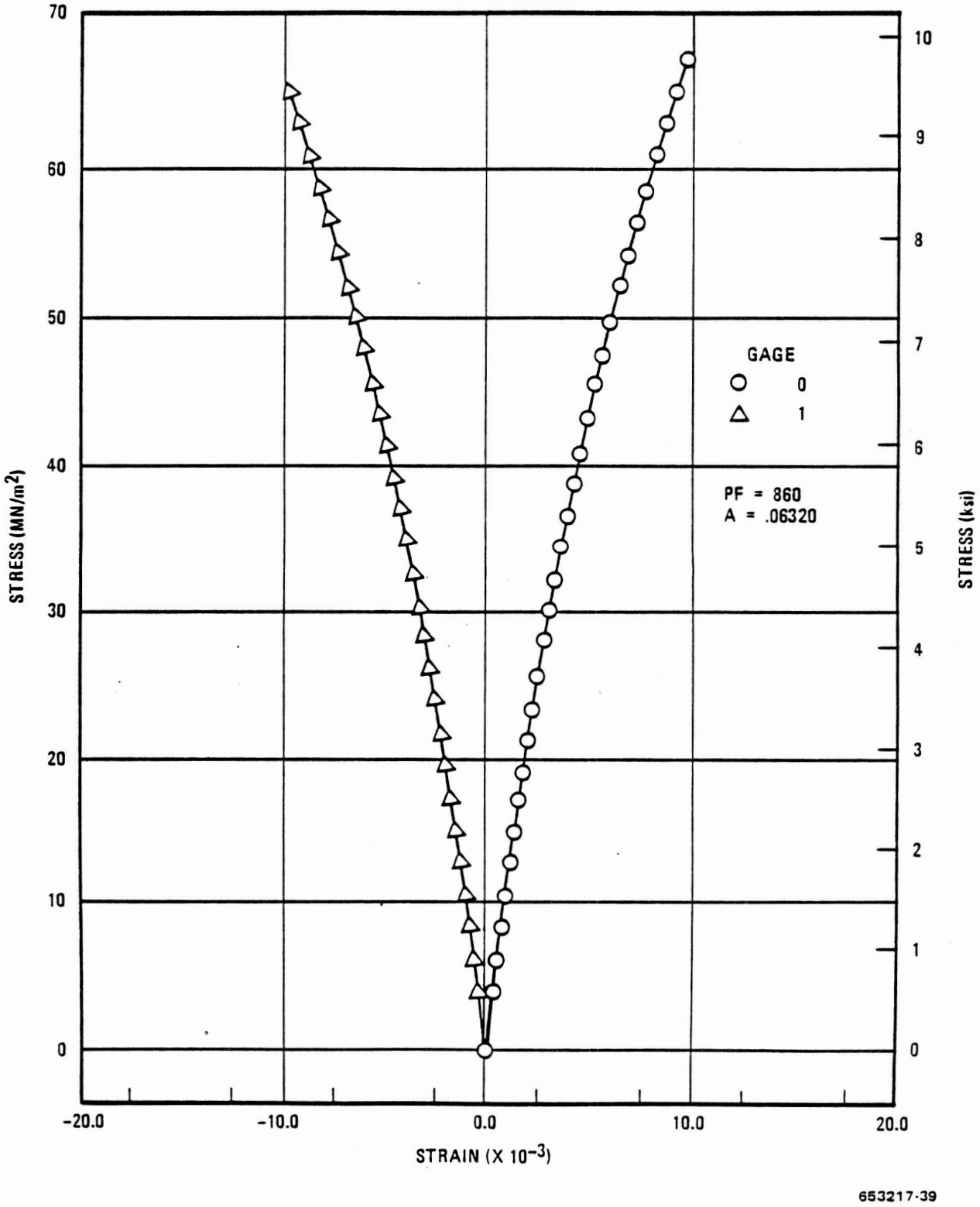



**Figure 7-26 Typical Stress-Strain Curve for Torsion Test of Unidirectional G/E Tube, Specimen BU06-13**

ORIGINAL PAGE IS
OF POOR QUALITY

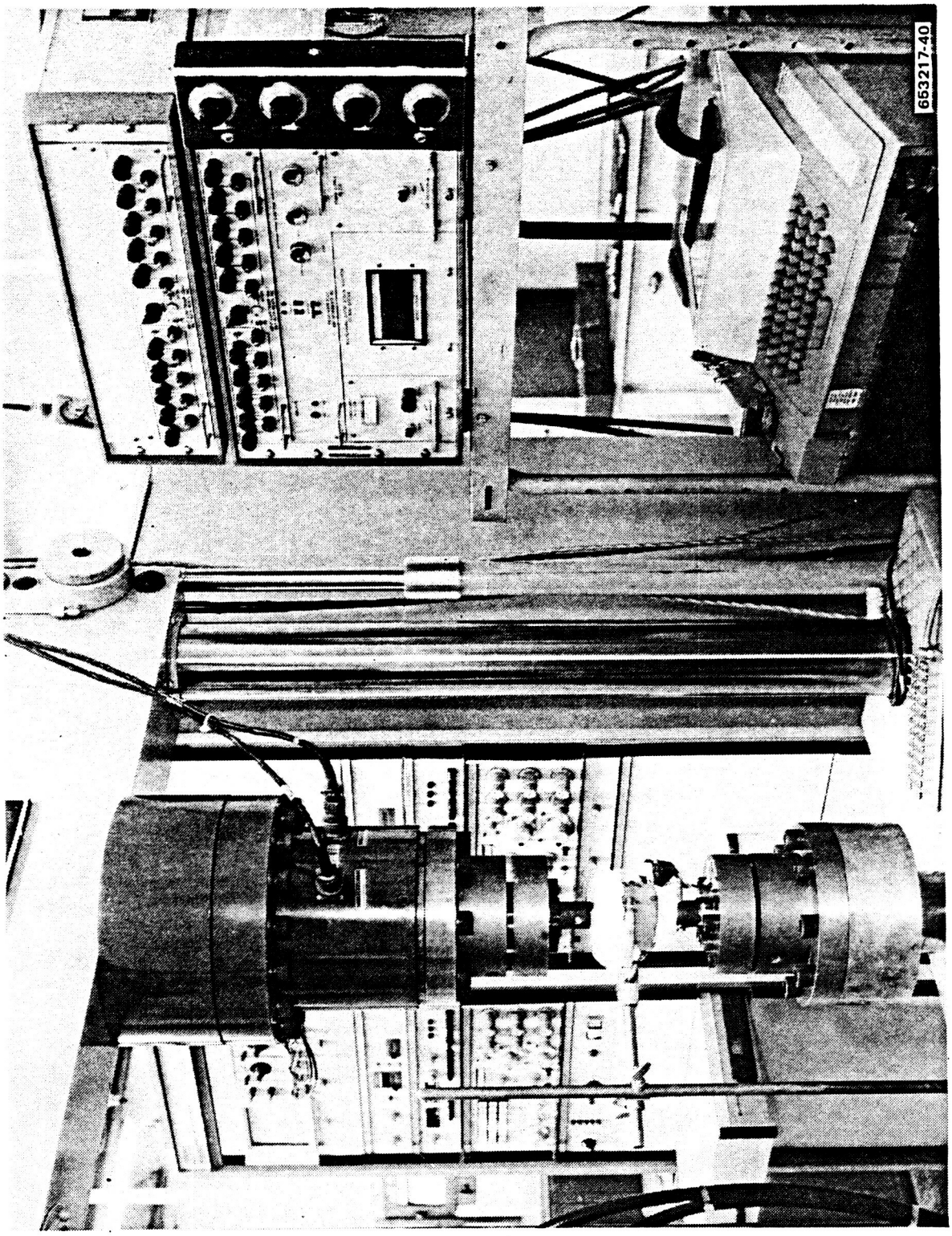



Figure 7-27 Test Apparatus for Torsion Testing of Unidirectional Tubes

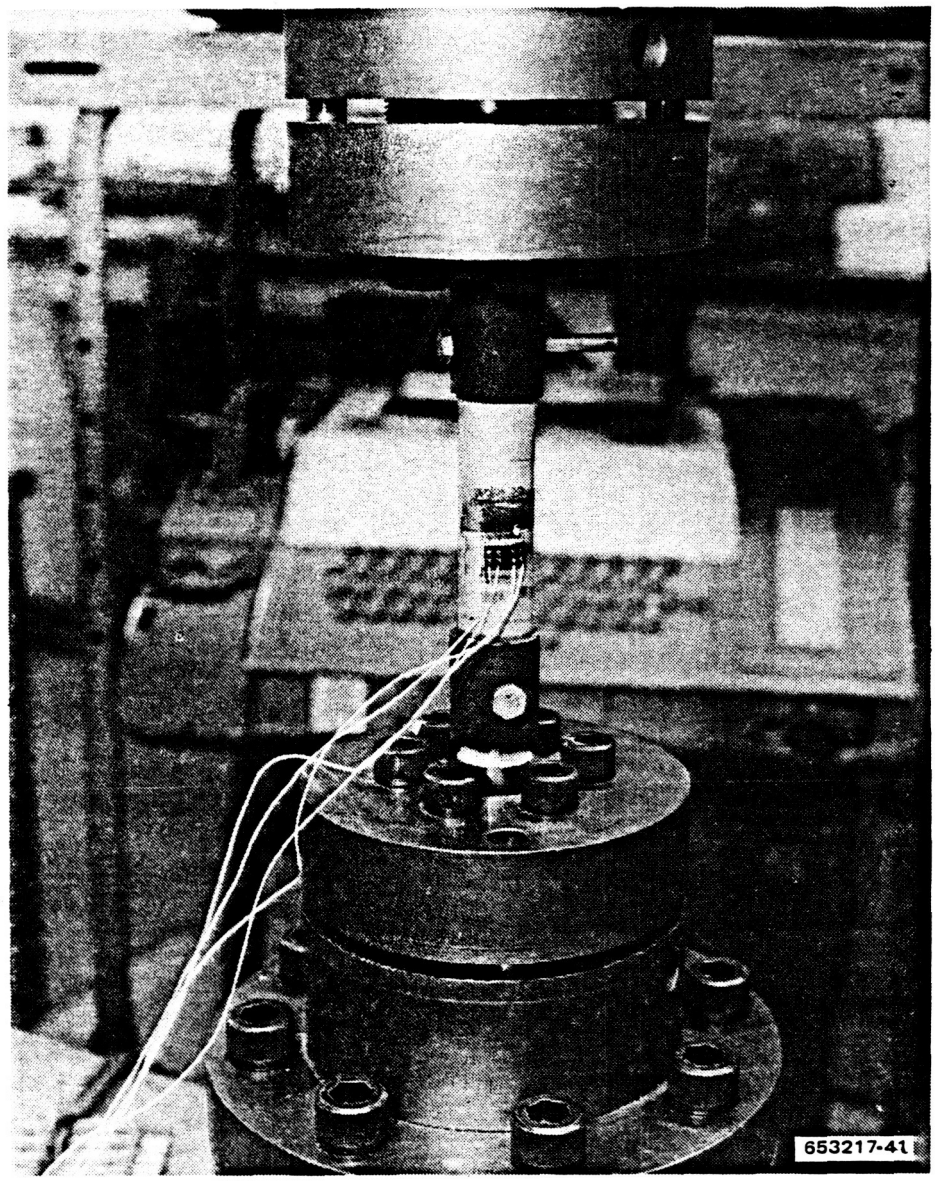



**Figure 7-28 Strain Gaged B/Al Tube Specimen Installed in Torsion Test Machine**

of the specimen. No end doublers were required because of the low failure loads. These low loads ensured failure in the test sections rather than the grips. The specimens were tested in Instron or Tinius-Olsen testing machines using Instron capstan grips with ball or universal joints to ensure axial loading. A head rate of 0.0025 m (0.01 in.) per minute was used. No strain measurements were made during testing of these B/Al interfiber shear specimens. Tests at 218 K (−67° F) and 561 K (550° F) were conducted in a Conrad-Missimer Chamber. The 700 K (800° F) tests were performed with a small ring furnace. As in the tensile tests, temperature was measured with a thermocouple clipped to the surface of the specimen. Temperature was maintained at the desired level for 10 minutes prior to loading.

### 7.2.2 TEST RESULTS AND DISCUSSION

**7.2.2.1 Graphite/Epoxy System.** The initial plan for the G/E system was to test six tubes each at room temperature and 450 K (350° F). This was later changed such that at elevated temperature three were tested at 394 K (250° F) and three at 450 K (350° F). The revision was made to



ORIGINAL PAGE IS
OF POOR QUALITY

ORIGINAL PAGE IS
OE POOR QUALITY

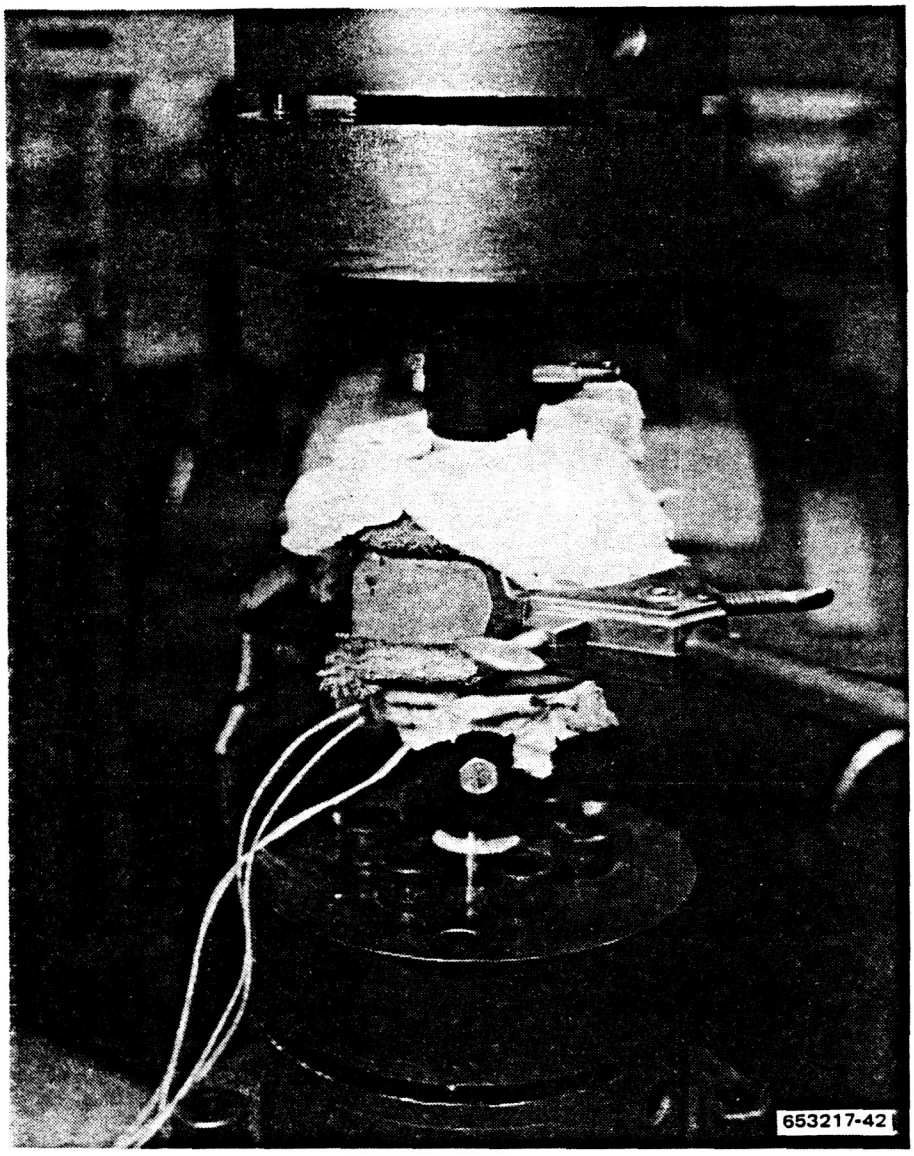



**Figure 7-29 Test Setup for Elevated Temperatures Torsion Testing of B/Al Tube**

better define the shear strength versus temperature relationship. Shear strength and shear modulus data for G/E are presented in Table 7-33. Shear modulus values were obtained from torque-strain diagrams such as the one shown in Figure 7-31. The effect of temperature was to reduce the strength by approximately 30% at both 394 K (250° F) and 450 K (350° F). While the strength leveled off at 394 K (250° F) and 450 K (350° F), the shear modulus exhibited a continuous decrease out to 450 K (350° F). The percentage change in modulus was, however, significantly less than that for the shear strength. Data from one of the tests (tube no. BU06-37) was not usable because of overheating of the tube. The overheated tube failed at a torque level that was less than one-tenth that of the other tubes tested at 450 K (350° F).

Short beam shear strength of the 6 ply material used in the thermal aging/compression study is given in Table 7-34. These G/E specimens were made by bonding together three pieces of the 6 ply panels to obtain 18 ply laminates.

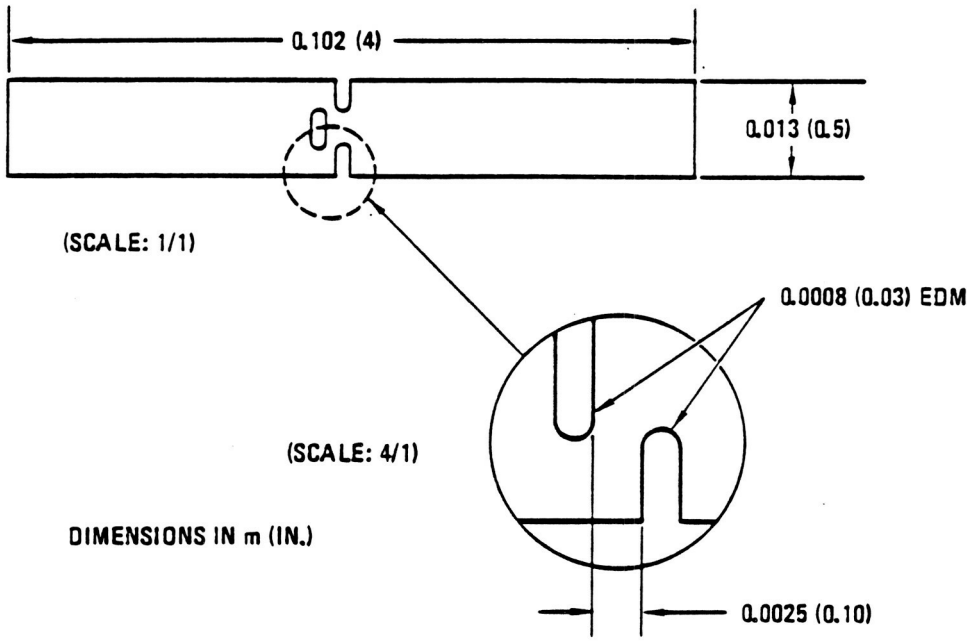



**Figure 7-30 B/Al In-plane Shear Specimen**

**7.2.2.2 Boron/Aluminum System.** Data for the two types of shear specimen used in testing of B/Al are listed in Tables 7-35 and 7-36. Strain measurements for determination of shear modulus were made only on the tube tests. A typical torque-strain diagram is shown in Figure 7-32. The initial test plan was to conduct laminate shear tests at the four temperatures shown in Table 7-36 and to conduct the tube tests at 297 K (75° F) and 561 K (550° F). As discusssed in the baseline tensile section, 561 K (550° F) was considered to be the maximum use temperature of B/Al for very long time applications. Because of a surface degradation of the B/Al observed during fatigue testing on this program at 561 K (550° F), the maximum use temperature was lowered to 505 K (450° F). At the time of this decision all shear testing was completed except for the elevated temperature tube tests. A change was made to conduct these tests at the lower temperature, 505 K (450° F).

The shear strength of B/Al as determined from the tube tests, Table 7-35, was not lowered by increasing the temperature from room temperature to 505 K (450° F). There was a decrease in shear modulus, however, of approximately 15%. For the laminate specimen tests, Table 7-36, a decrease in shear strength of 30 to 40% was observed at elevated temperatures. At room temperature higher shear strengths were obtained with the laminate specimen configuration than with the tubular configuration although, presumably, the two measure the same property. The two groups of specimens were from different batches of material, which could account for some of the difference. Another possible reason for the lower values obtained from the tube tests was the presence of some small longitudinal cracks on the outside surface of half of the tubes. These cracks, shown in Figure 7-33, were shallow and did not extend beyond the first ply. Whether or not other cracks were present in any of the inner plies of the 6 ply tubes could not be determined. There was no correlation between the individual values of shear strength and the presence or absence of the surface cracks, however. While the longitudinal cracks in the tubes may well have been responsible for low values of ultimate shear strength, it is not believed that the cracks had much effect during the early portions of the tests where the shear modulus was determined. In the past, agreement of shear strength values determined by different test methods has generally been poor for composite systems.

**Table 7-33. Baseline Interfiber Shear Properties of G/E Unidirectional Tubes**

| Specimen Number | Temperature K | Temperature (°F) | Shear Strength MN/m² | Shear Strength (ksi) | Shear Modulus GN/m² | Shear Modulus (Msi) |
|---|---|---|---|---|---|---|
| BU06-11 | 297 | 75 | 94 | 13.7 | 5.1 | 0.74 |
| -12 | | | 94 | 13.6 | 6.1 | .88 |
| -13 | | | 106 | 15.4 | 5.4 | .78 |
| -24 | | | 89 | 12.9 | 5.5 | .80 |
| -25 | | | 92 | 13.4 | 5.5 | .80 |
| -26 | | | 86 | 12.5 | 5.9 | .85 |
| | | | avg 94 | 13.6 | 5.6 | .81 |
| BU06-38 | 394 | 250 | 52 | 7.6 | 4.7 | .68 |
| -40 | | | 72 | 10.5 | 4.8 | .70 |
| -42 | | | 70 | 10.1 | 5.4 | .78 |
| | | | avg 65 | 9.4 | 5.0 | .72 |
| BU06-37 | 450 | 350 | (a) | (a) | (a) | (a) |
| -39 | | | 67 | 9.7 | 4.4 | .64 |
| -41 | | | 70 | 10.2 | 4.5 | .65 |
| | | | avg 68 | 9.9 | 4.4 | .64 |

[a]Specimen overheated

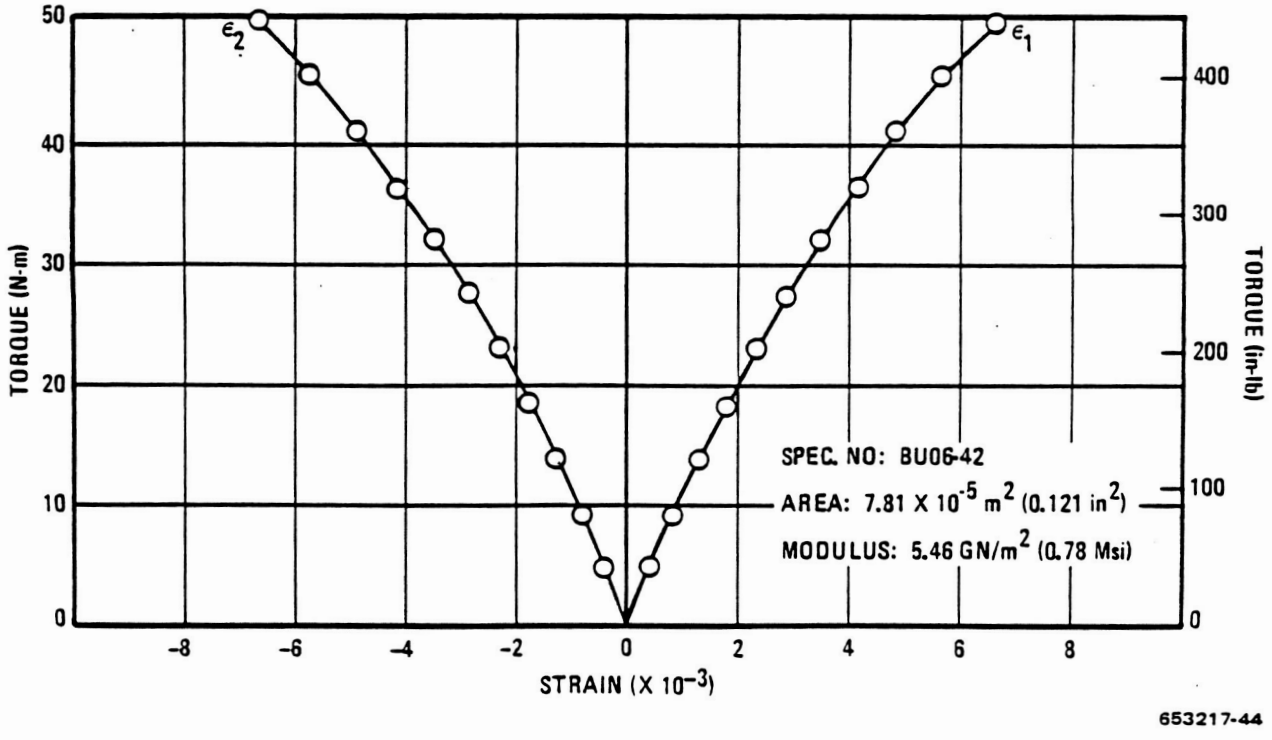



**Figure 7-31 Shear Load-Strain Diagram for $[0°]_8$ G/E at 394 K (250° F)**

Table 7-34. Baseline Short Beam Shear Strength of $[0° \pm 45°]_s$ G/E at 297 K (75°F) (Thermal Aging/Compression Study — 18 Ply Laminates)

| Specimen Number | | Shear Strength $MN/m^2$ | (ksi) |
|---|---|---|---|
| BC102-1 | | 72 | 10.4 |
| -2 | | 68 | 9.9 |
| -3 | | 75 | 10.9 |
| | avg | 72 | 10.4 |

Table 7-35. Baseline Interfiber Shear Properties of B/Al Unidirectional Tubes

| Specimen Number | Temperature K | (°F) | Shear Strength $MN/m^2$ | (ksi) | Shear Modulus $GN/m^2$ | (Msi) |
|---|---|---|---|---|---|---|
| EU06-1 | 297 | 75 | 61 | 8.8 | 5.0 | 7.3 |
| -2 | | | 90 | 13.0 | (a) | (a) |
| -3 | | | 66 | 9.5 | 4.3 | 6.2 |
| -4 | | | 61 | 8.8 | 4.5 | 6.5 |
| -5 | | | 63 | 9.1 | 4.6 | 6.7 |
| -6 | | | 61 | 8.8 | 4.2 | 6.1 |
| | | avg | 67 | 9.7 | 4.5 | 6.6 |
| EU06-7 | 505 | 450 | 82 | 11.9 | 4.1 | 5.9 |
| -8 | | | 64 | 9.3 | 3.2 | 4.6 |
| -9 | | | 70 | 10.1 | 3.6 | 5.2 |
| -10 | | | 65 | 9.4 | 2.8 | 4.1 |
| -11 | | | 77 | 11.1 | 5.2 | 7.5 |
| -12 | | | [b]74 | [b]10.8 | 4.5 | 6.4 |
| | | avg | 72 | 10.4 | 3.9 | 5.6 |

[a]Strain gage malfunction

[b]Torque still rising — machine at maximum twist

One of the tube specimens, EU06-12, did not fail before the test machine had reached its limit of twist, 100 degrees. At this point the torque was still increasing slightly. Consequently, the value of ultimate shear strength reported in Table 7-35 is slightly low. The unfailed, but twisted, specimen in shown in Figure 7-34 with a similar specimen that has failed in shear in the longitudinal direction of the tube.

Data from one of the laminate specimens, EU06-32, was not reported because of improper machining. The slot on one side of the specimen was not sufficiently deep and several continuous boron filaments remained across the test section. With this configuration a shear failure was not possible thus invalidating the test.

Table 7-36. Baseline Interfiber Shear Strength of $[0°]_6$ B/Al Laminates

| Specimen Number | Temperature K | Temperature (°F) | Shear Strength MN/m² | Shear Strength (ksi) |
|---|---|---|---|---|
| EU06-13 | 218 | −67 | 90 | 13.1 |
| -14 | | | 100 | 14.5 |
| -15 | | | 91 | 13.2 |
| -16 | | | 100 | 14.5 |
| -17 | | | 93 | 13.5 |
| | | | avg 95 | 13.8 |
| EU06-18 | 297 | 75 | 97 | 14.0 |
| -19 | | | 100 | 14.5 |
| -20 | | | 94 | 13.6 |
| -21 | | | 94 | 13.7 |
| -22 | | | 81 | 11.8 |
| | | | avg 93 | 13.5 |
| EU06-23 | 561 | 550 | 61 | 8.9 |
| -24 | | | 52 | 7.5 |
| -25 | | | 54 | 7.8 |
| -26 | | | 62 | 9.0 |
| -27 | | | 50 | 7.2 |
| | | | avg 56 | 8.1 |
| EU06-28 | 700 | 800 | 66 | 9.5 |
| -29 | | | 64 | 9.5 |
| -30 | | | 66 | 9.6 |
| -31 | | | 63 | 9.1 |
| -32 | | | (a) | (a) |
| | | | 65 | 9.4 |

[a]Specimen improperly machined

One interesting point in comparing the B/Al data with that for the resin matrix materials is the striking difference in values of shear modulus. Values for the metal matrix material are almost an order of magnitude higher than those obtained for the resin matrix systems. Shear strength values (at room temperature), on the other hand, differ by no more than 30%. Similar results are obtained when comparing transverse tensile data (modulus and strength) of metal and resin matrix systems.

#### 7.2.2.3 Graphite/Polyimide

**HT-S/710 G/PI.** Because sufficient HT-S/710 prepreg was unavailable, it was not possible to fabricate the tube specimens necessary to conduct the G/PI shear tests. However, some shear data, for the same HT-S/710 system, had been obtained in a study performed at General Dynamics Convair during 1973. These dates are listed in Table 7-37 (unpublished data from

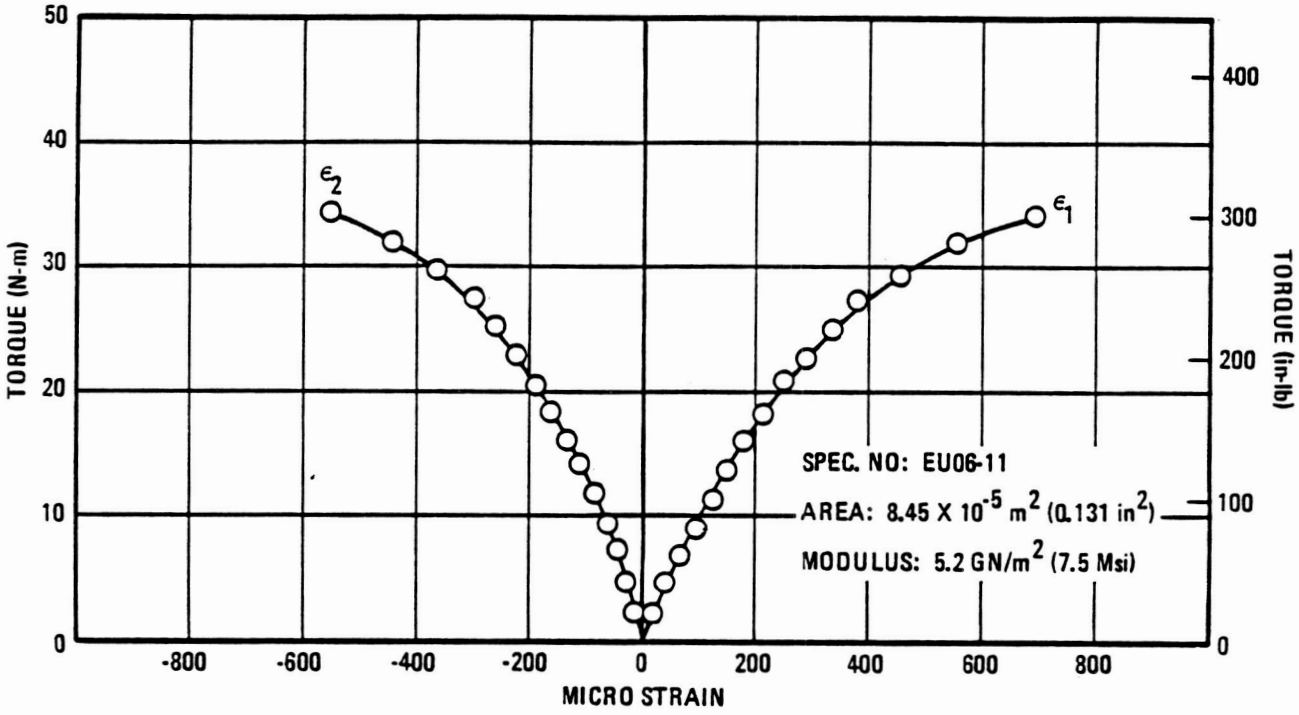



**Figure 7-32 Shear Load-Strain Diagram for $[0°]_6$ B/Al at 505 K (450° F)**

ORIGINAL PAGE IS
OF POOR QUALITY

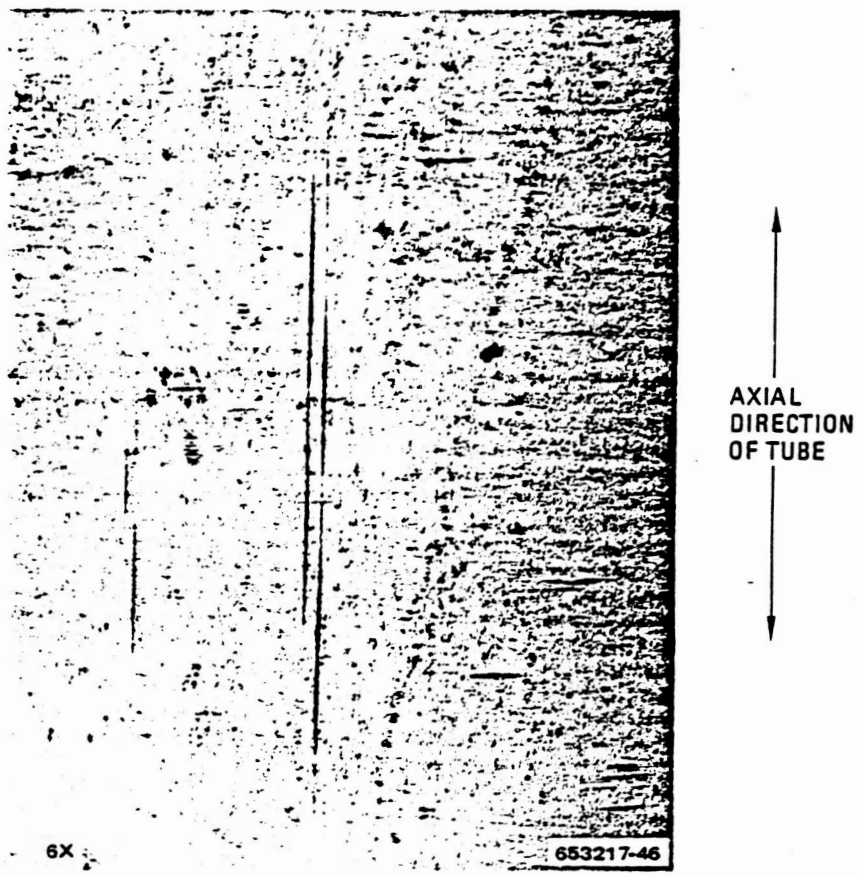



**Figure 7-33 B/Al Tube Specimen, EU06-12, Showing Longitudinal Surface Cracks**

ORIGINAL PAGE IS
OF POOR QUALITY

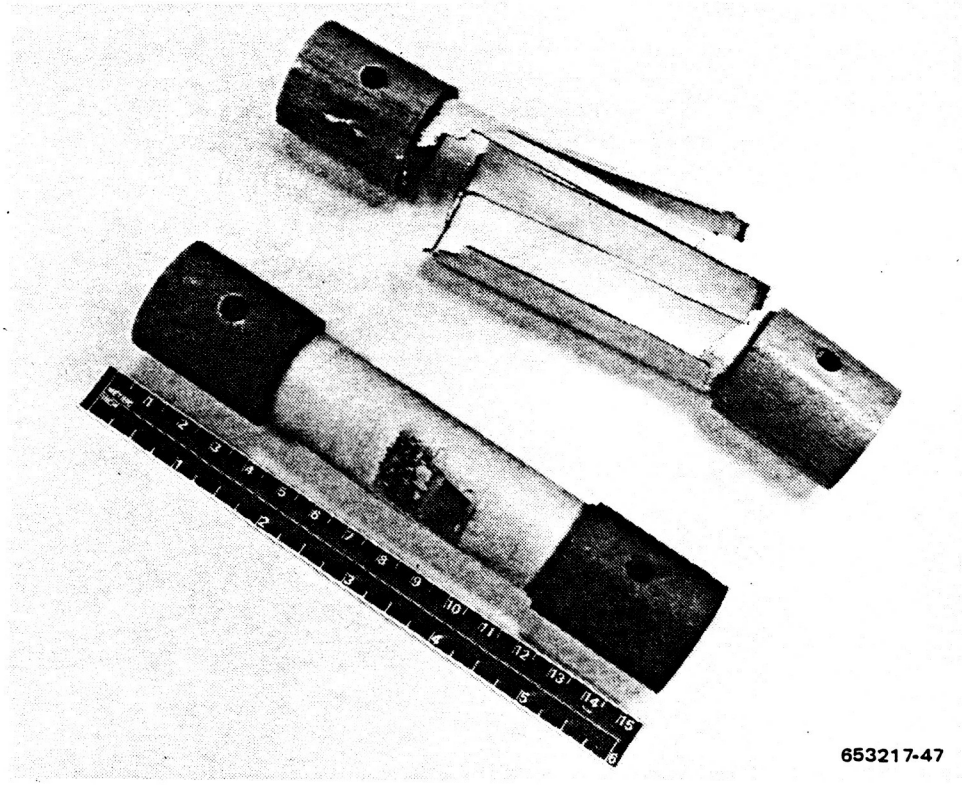



**Figure 7-34 B/Al Tube Specimens After Shear Testing: Upper, Specimen EU06-1, Twisted to Failure in Shear; Lower, Specimen EU06-12, Twisted to Maximum Capability of Test Machine**

W.G. Scheck). The G/PI tubular specimens were processed using the same fabrication techniques described in Section 5 for G/E and B/PI tubes and the autoclave cure cycle given in Section 5 for the HT-S/710 G/PI laminates. The tubes were 0.15 m (6 in.) long by 0.025 m (1 in.) outside diameter with a nominal wall thickness of 0.001 m (0.040 in.). Test techniques were similar to those described above for the B/Al and G/E tubes (Section 7.2.1).

The data of Table 7-37 show a decrease in shear strength of G/PI of approximately 30% of the room temperature value for specimens tested at both 77 K (−320 °F) and 589 K (600 °F). The modulus, on the other hand, decreases slightly as the test temperature is raised from 77 K (−320 °F) to 589 K (600 °F).

**Celion 6000/LARC-160 G/PI.** As no unidirectional layups were evaluated for the Celion 6000/LARC-160 system, the only shear tests performed were those using the short beam configuration. Test results for the crossplied 12 and 24 ply panels have been reported in the Laminate Quality Assurance Testing section. The tests on the crossplied 6 ply panels were made on specimens fabricated by bonding together three pieces to make an 18 ply laminate. These data, which were used as the baseline shear data for the thermal aging/compression study, are given in Table 7-38.

## 7.3 FRACTURE TESTING

The effects of stress risers (cutouts, cracks, damage zones, material discontinuities, etc.) in composite materials has been the subject of a number of recent investigations. Methods are

Table 7-37. Interfiber Shear Properties of HT-S/710 G/PI Unidirectional Tubes

| Specimen Number | Temperature K | (°F) | Shear Strength MN/m² | (ksi) | Shear Modulus GN/m² | (Msi) |
|---|---|---|---|---|---|---|
| TU-1 | 77 | −320 | 52 | 7.6 | 6.8 | 0.98 |
| A-3 | | | 44 | 6.4 | 7.2 | 1.04 |
| A-4 | | | 50 | 7.3 | 7.2 | 1.05 |
| | | avg | 49 | 7.1 | 7.1 | 1.02 |
| TU-4 | 297 | 75 | 87 | 12.6 | 5.8 | .84 |
| TU-5 | | | 68 | 9.9 | 6.6 | .96 |
| TU-6 | | | 57 | 8.2 | 6.1 | .89 |
| | | avg | 71 | 10.2 | 6.2 | .90 |
| TU-7 | 589 | 600 | 49 | 7.1 | 7.2 | 1.04 |
| A-5 | | | 49 | 7.1 | 4.8 | .69 |
| | | avg | 49 | 7.1 | 6.0 | .86 |

Table 7-38. Baseline Short Beam Shear Strength of $[0° \pm 45°]_s$ Celion 6000/LARC-160 G/PI at 297 K (75°F) (Thermal Aging/Compression Study — 18 Ply Laminates)

| Specimen Number | | Shear Strength MN/m² | (ksi) |
|---|---|---|---|
| FC102-1 | | 50 | 7.2 |
| -2 | | 51 | 7.4 |
| -3 | | 52 | 7.6 |
| | avg | 51 | 7.4 |

being sought to predict both the static and fatigue behavior of composite materials that contain such stress risers. Waddoups, Eisenman, and Kaminski (ref. 29) have developed a fracture mechanics based model, the Wearout Model, which has been moderately successful in predicting the degradation of coupon strength as a function of loading. Whereas in metals, crack growth rate (i.e., da/dn) is normally measured and used as an indication of strength degradation such is not the case for composites. Flaw growth is usually not observed in composites, even though such crack growth has been observed for both B/Al and B/E (ref. 30 and 31).

The objective of this study was to attempt to observe damage accumulation in flawed composite tension coupons and to reduce the data to a da/dn format. Since crack growth is not readily observed in composites, changes in material compliance (load, P, divided by crack opening displacement, COD) were to be related to changes in effective crack length. Given da/dn data for a composite material, conventional fracture mechanics theories can then be applied to predict effective crack length as a function of loading history, and failure characteristics.

**7.3.1 SPECIMEN DESIGN.** The study included six specimens each of four different materials to determine fracture behavior. The four materials investigated are described in Table 7-39. For each material, six $(0° \pm 45°]_s$ specimens measuring 0.064 m (2.5 in.) by 0.30 m (12 in.) were fabricated and identified by dash numbers as shown in Table 7-40. Specimen configuration is shown in Figure 7-35.

Initial flaws were applied by drilling a No. 13 hole, 0.0047 m (0.185 in.) diameter, in the center of the specimen and then extending symmetrical narrow slits, 0.00066 m (0.026 in.), from each side of the hole by ultrasonic impact grinding. The end of a flaw made in this manner in B/E is shown in Figure 7-36. Dash three specimens required that the slots be progressively increased during testing without losing the clip gage instrumentation. This was done by hand with a 0.00013 m (0.005 in.) diameter diamond coated wire. All flaw lengths at the beginning of each test sequence are shown in Table 7-41.

**7.3.2 TEST PROCEDURE, RESULTS AND DISCUSSION.** The test plan is summarized in Table 7-42. The procedure for -1 and -2 tests was to try to initiate crack growth, either visual or effective delta length, by progressively increasing static loads and then applying cyclic fatigue loads to extend the effective crack length. Clip gages were used to monitor COD, and any change in compliance, P/COD, was considered to represent an increase in effective crack length. These specimens would then be static pulled to determine their residual strengths.

Table 7-43 shows results of compliance testing of -1 and -2 specimens. The expected systematic damage growth and corresponding change in slope of the compliance curve did not occur. Only isolated damage growth was observed, and this was mostly in the form of cracks parallel to surface fibers. More recent experiments suggest that synergistic effects of moisture and cyclic rate play a large role in damage growth in composites. The failed specimens are shown in Figures 7-37 and 7-38.

The purpose of the -3 specimens was to determine load versus COD for progressively increased crack lengths. Clip gages were used to measure COD and flaws (slits) were lengthened in small increments by hand sawing with a diamond coated wire. For each flaw length the specimen was slowly cycled, three times, up to a maximum load of 1000 pounds. Test results for the four specimens are shown in Figures 7-39 through 7-42. Load divided by COD versus flaw length was then plotted for each material as shown in Figure 7-43. All four specimens yielded an exponential decaying type of curve with the data points of the G/E and G/PI specimens lying on the same curve. The consistent shape of these curves warrants further investigation of a Load/COD $= Ae^{-\text{flaw size}}$ fatigue model. The failed specimens are shown in Figure 7-44.

The -4 specimens were fatigue tested with the 0.0047 m (0.185 in.) diameter hole only. No slits were applied. COD was measured after cycle numbers 1, 2, 19, 100, 1000, 10,000 and 2,500,000. Specimens were then static pulled to determine residual strengths.

Fatigue test results are shown in Table 7-44. There was no fatigue crack growth observed in any of the four specimens. When these specimens were static pulled for residual strength, only one, AC05-4, failed at the 0.0047 m (0.185 in.) diameter hole. The other three failed in or near the grips. The failed specimens are shown in Figure 7-45.

The objective of -5 and -6 specimen tests was to determine static strengths at two different flaw lengths. The -5's had 0.0286 m (1.125 in.) flaws and the -6's had 0.00349 m (1.375 in.) flaws. All were simply pulled to static failure.

**Table 7-39. Composite Materials Studied**

| Material | Layup | Panel Thickness m | Panel Thickness in. | Material ID |
|---|---|---|---|---|
| 5505/4 B/E | $[0° \pm 45°]_s$ | 0.00076 | 0.030 | AC05 |
| A-S/3501-5 G/E | $[0° \pm 45°]_s$ | .00076 | .030 | BC05 |
| HT-S/710 G/PI | $[0° \pm 45°]_s$ | .00076 | .030 | DC05 |
| B/Al | $[0° \pm 45°]_s$ | .00107 | .042 | EC05 |

**Table 7-40. Specimen Identification**

| Material | Specimens |
|---|---|
| 5505/4 B/E | AC05-1, AC05-2, AC05-3, AC05-4, AC05-5, AC05-6 |
| A-S/3501-5 G/E | BC05-1, BC05-2, BC05-3, BC05-4, BC05-5, BC05-6 |
| HT-S/710 G/PI | DC05-1, DC05-2, DC05-3, DC05-4, DC05-5, DC05-6 |
| B/Al | EC05-1, EC05-2, EC05-3, EC05-4, EC05-5, EC05-6 |

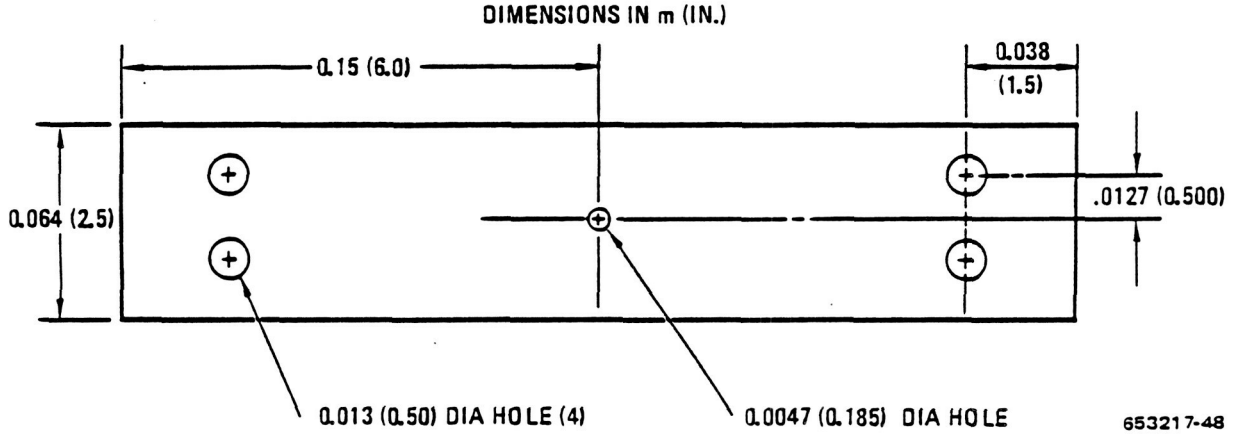



**Figure 7-35 Test Specimen Configuration**

Results of static strength tests are shown in Table 7-45, and the failed specimens are shown in Figures 7-46 and 7-47. Results of all residual strength tests are shown in Table 7-46. The effect of flaw length on gross area static failure stress is plotted in Figure 7-48.

ORIGINAL PAGE IS
OF POOR QUALITY

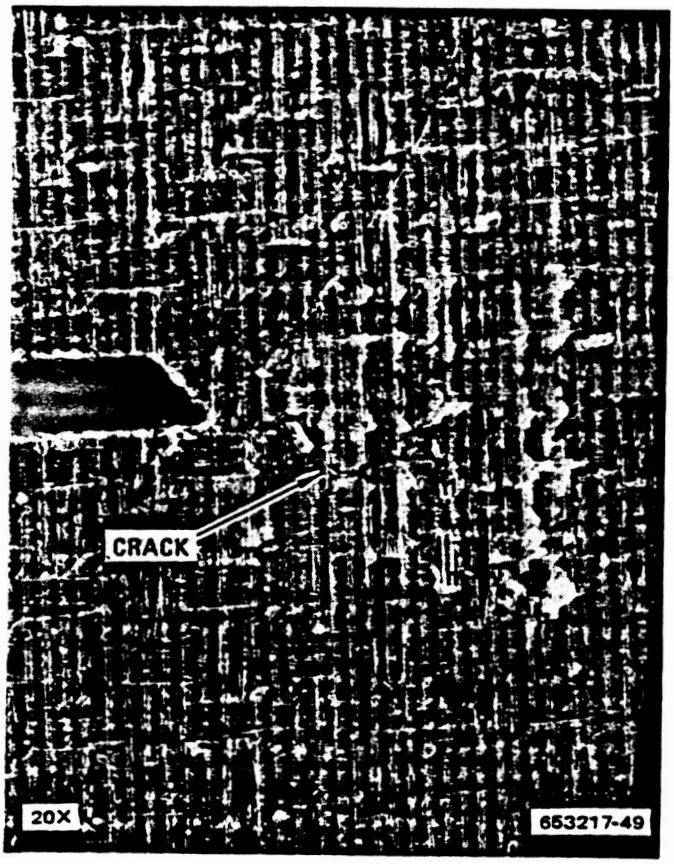



**Figure 7-36 End of Slot in Specimen AC05-1 Showing Crack**

Values for the apparent stress intensity factor, $K_Q$, were calculated for each notched specimen that was pulled to failure. The following equation from reference 32 was used.

$$K_Q = \Sigma \sqrt{\pi a} \left( \frac{2b}{\pi a} \tan \frac{\pi a}{2b} \right)^{1/2}$$

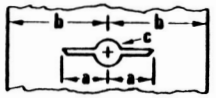
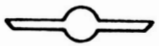
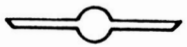
where $K_Q$ = apparent stress intensity factor, $MN/m^2 \sqrt{m}$ (ksi $\sqrt{in.}$)
$\Sigma$ = gross stress, $MN/m^2$ (ksi)
2a = crack length, m (in.)
2b = specimen width, m (in.)

Figure 7-49 shows the variation of $K_Q$ with crack length for both fatigued and nonfatigued specimens.

Four composite laminates were studied to determine their flaw growth and fracture behavior. All tests were run at room temperature and moisture was not controlled. All fatigue cycling was at R = 0.1 and 30 Hz. Based on the test program and data reduction presented above, the following conclusions are drawn:

1. Under these test conditions, cracks (or effective cracks) in crossplied composite laminates grow only when applied cyclic loads are very near the breaking strength.

## Table 7-41. Initial Flaw Configuration and Length

| SPECIMEN IDENTIFICATION | INITIAL FLAW CONFIGURATION | INITIAL FLAW LENGTH, 2a, m (in.) | | | | | | | | | |
|---|---|---|---|---|---|---|---|---|---|---|---|
| | | SEQ. 1 | 2 | 3 | 4 | 5 | 6 | 7 | 8 | 9 | 10 |
| AC05-1 |  | | | | | | | | | | |
| B | | 0.0222(.875) | 0.0222(.875) | 0.0222(.875) | 0.0239(.94) | 0.0239(.94) | | | | | |
| D | | .0222(.875) | .0236(.93) | .0236(.93) | .0236(.93) | .0236(.93) | 0.0236(.93) | | | | |
| E | | .0222(.875) | .0222(.875) | .0222(.875) | .0222(.875) | .0222(.875) | .0222(.875) | 0.0222(.875) | 0.0381(1.50) | | |
| | | .0222(.875) | .0222(.875) | .0222(.875) | .0222(.875) | .0222(.875) | .0222(.875) | | | | |
| AC05-2 |  | | | | | | | | | | |
| B | | .0222(.875) | .0222(.875) | .0222(.875) | .0222 (.875) | .0222(.875) | .0222(.875) | .0222(.875) | | | |
| D | | .0222(.875) | .0249(.98) | .0249(.98) | .0249(.98) | .0249(.98) | .0249(.98) | .0249(.98) | | | |
| E | | .0222(.875) | .0222(.875) | .0222(.875) | .0222(.875) | .0292(1.15) | | | | | |
| | | .0222(.875) | .0222(.875) | .0222(.875) | .0222(.875) | .0222(.875) | .0222(.875) | .0222(.875) | .0222(.875) | | |
| AC05-3 |  | | | | | | | | | | |
| B | | .0047(.185) | .00724(.285) | .00978(.385) | .0123(.485) | .0149(.585) | .0174(.685) | .0225(.885) | .0276(1.085) | 0.0326(1.285) | 0.033(1.30) |
| D | | .0047(.185) | .00724(.285) | .00978(.385) | .0123(.485) | .0149(.585) | .0174(.685) | .0225(.885) | .0276(1.085) | .0326(1.285) | .033(1.30) |
| E | | .0047(.185) | .00724(.285) | .00978(.385) | .0123(.485) | .0149 (.585) | .0174(.685) | .0225(.885) | .0276(1.085) | .0326(1.285) | .033(1.30) |
| | | .0047(.185) | .00724(.285) | .00978(.385) | .0123(.485) | .0149 (.585) | .0174(.685) | .0225(.885) | .0276(1.085) | .0326(1.285) | .033(1.30) |
| AC05-4 |  | | | | | | | | | | |
| B | | .0047(.185) | .0047(.185) | .0047(.185) | .0047(.185) | .0047(.185) | .0047(.185) | .0047(.185) | .0047(.185) | .0047(.185) | |
| D | | .0047(.185) | .0047(.185) | .0047(.185) | .0047(.185) | .0047(.185) | .0047(.185) | .0047(.185) | .0047(.185) | .0047(.185) | |
| E | | .0047(.185) | .0047(.185) | .0047(.185) | .0047(.185) | .0047(.185) | .0047(.185) | .0047(.185) | .0047(.185) | .0047(.185) | |
| | | .0047(.185) | .0047(.185) | .0047(.185) | .0047(.185) | .0047(.185) | .0047(.185) | .0047(.185) | .0047(.185) | .0047(.185) | |
| AC05-5 |  | | | | | | | | | | |
| B | | .0286(1.125) | | | | | | | | | |
| D | | .0286(1.125) | | | | | | | | | |
| E | | .0286(1.125) | | | | | | | | | |
| | | .0286(1.125) | | | | | | | | | |
| AC05-6 |  | | | | | | | | | | |
| B | | .0349(1.375) | | | | | | | | | |
| D | | .0349(1.375) | | | | | | | | | |
| E | | .0349(1.375) | | | | | | | | | |
| | | .0349(1.375) | | | | | | | | | |

a: Flaw length – see table.
b: Specimen width – 2b = 0.064m (2.5 in.)
c: Hole diameter – c = 0.0047m (.185 in.)

653217-60



ORIGINAL PAGE IS
OF POOR QUALITY

Table 7-42. Matrix of Tests Performed

| Material | Identification | No. of Sizes | Number of Tests/Sequences: Static Strength | Compliance Sequences | Fatigue Sequences | Residual Strength | Objectives |
|---|---|---|---|---|---|---|---|
| B/E | AC05-1 | 2 | | 3 | 1 | 1 | $\Delta \frac{P}{(COD)}$, R.S. |
| | -2 | 1 | | 4 | 3 | 1 | $\Delta \frac{P}{(COD)}$, R.S. |
| | -3 | 10 | | 9 | | 1 | P vs COD |
| | -4 | 1 | | | 8 | 1 | Fat., R.S. |
| | -5 | 1 | 1 | | | | UTS |
| | -6 | 1 | 1 | | | | UTS |
| G/E | BC05-1 | 2 | | 3 | 3 | 1 | $\Delta \frac{P}{(COD)}$, R.S. |
| | -2 | 2 | | 4 | 4 | 1 | $\Delta \frac{P}{(COD)}$, R.S. |
| | -3 | 10 | | 9 | | 1 | P vs COD |
| | -4 | 1 | | | 8 | 1 | Fat., R.S. |
| | -5 | 1 | 1 | | | | UTS |
| | -6 | 1 | 1 | | | | UTS |

Table 7-42. Matrix of Tests Performed — Concluded

| Material | Identification | No. of Sizes | Number of Tests/Sequences: Static Strength | Compliance Sequences | Fatigue Sequences | Residual Strength | Objectives |
|---|---|---|---|---|---|---|---|
| G/PI | DC05-1 | 2 | 1 | 5 | 3 | 1 | $\Delta \frac{P}{(COD)}$, R.S. |
| | -2 | 2 | | 4 | 1 | | $\Delta \frac{P}{(COD)}$, R.S. |
| | -3 | 10 | | 9 | | 1 | P vs COD |
| | -4 | 1 | | | 8 | 1 | Fat., R.S. |
| | -5 | 1 | 1 | | | | UTS |
| | -6 | 1 | 1 | | | | UTS |
| B/Al | EC05-1 | 1 | | 4 | 1 | 1 | $\Delta \frac{P}{(COD)}$, R.S. |
| | -2 | 1 | | 5 | 4 | 1 | $\Delta \frac{P}{(COD)}$, R.S. |
| | -3 | 10 | | 9 | | 1 | P vs COD |
| | -4 | 1 | | | 8 | 1 | Fat., R.S. |
| | -5 | 1 | 1 | | | | UTS |
| | -6 | 1 | 1 | | | | UTS |

## Table 7-43. Results of Compliance Tests

| SPECIMEN IDENTIFICATION | LOAD MN (Kip) | FATIGUE R = +0.1 CYCLES | FATIGUE R = +0.1 PMAX MN (Kip) | COMPLIANCE, $\Delta\frac{P}{(COD)}$, MN/m (KIP/in.) N = 1 | 2 | 3 | 4 | 5 | 6 | 7 | 8 | 9 | 10 |
|---|---|---|---|---|---|---|---|---|---|---|---|---|---|
| AC05-1 B/E | 0.0062(1.4)<br>.0080(1.8)<br>.0098(2.2) | 0<br>0<br>0<br>56 000 | 0<br>0<br>0<br>0.0098(2.2) | 74(420)<br>72(410)<br>70(400) | 74(420)<br>72(410)<br>67(380) | 74(420)<br>72(410)<br>(a) | 74(420)<br>72(410) | 74(420)<br>72(410) | 74(420)<br>72(410) | 74(420)<br>72(410) | 75(430)<br>72(410) | 74(420)<br>72(410) | 74(420)<br>72(410) |
| AC05-2 B/E | .0062(1.4)<br>.0080(1.8)<br>.0080(1.8)<br>.0080(1.8) | 0<br>0<br>10 000<br>100 000<br>2 565 000 | 0<br>0<br>.0080(1.8)<br>.0080(1.8)<br>.0080(1.8) | 74(420)<br>74(420)<br>70(400)<br>67(380) | 74(420)<br>74(420)<br>74(420)<br>67(380) | 74(420)<br>74(420)<br>74(420)<br>67(380) | 74(420)<br>74(420)<br>(b) | 74(420)<br>74(420) | 74(420)<br>74(420) | 74(420)<br>74(420) | 74(420)<br>74(420) | 74(420)<br>74(420) | 72(410)<br>74(420) |
| BC05-1 G/E | .0051(1.15)<br>.0051(1.15)<br>.0051(1.15) | 0<br>10 000<br>100 000<br>2 515 000 | 0<br>.0051(1.15)<br>.0051(1.15)<br>.0051(1.15) | 44(250)<br>42(240)<br>40(230) | 44(250)<br>42(240)<br>40(230) | 44(250)<br>42(240)<br>40(230) | 44(250)<br>(c) | 44(250) | 44(250) | 44(250) | 44(250) | 44(250) | 44(250) |
| BC05-2 G/E | .0051(1.15)<br>.0062(1.39)<br>.0062(1.39)<br>.0062(1.39) | 0<br>0<br>10 000<br>100 000<br>105 000<br>2 515 000 | 0<br>0<br>.0062(1.39)<br>.0062(1.39)<br>.0062(1.39)<br>.0062(1.39) | 44(250)<br>40(226)<br>37(210)<br>37(210)<br>(e) | 44(250)<br>(d)<br>34(195)<br>37(210) | 44(250)<br>39(220)<br>37(210) | 44(250) | 44(250) | 44(250) | 44(250) | 44(250) | 44(250) | 44(250) |
| DC05-1 G/PI | .0042(.95)<br>.0056(1.25)<br>.0069(1.55)<br>.0069(1.55)<br>.0069(1.55) | 0<br>0<br>0<br>10 000<br>100 000<br>2 611 000 | 0<br>0<br>0<br>.0024(.55)<br>.0069(1.55)<br>.0069(1.55) | 40(230)<br>40(230)<br>38(169)<br>43(248)<br>35(202)<br>40(226)<br>29(167)<br>38(216) | 42(240)<br>40(230)<br>39(225)<br>44(250)<br>39(224)<br>36(206) | 42(240)<br>39(220)<br>42(240)<br>39(224)<br>36(206) | 42(240)<br>40(230)<br>42(240)<br>36(208) | 42(240)<br>40(230)<br>42(240) | 42(240)<br>40(230)<br>42(240) | 42(240)<br>40(230)<br>42(240) | 44(250)<br>40(230)<br>42(240) | 42(240)<br>40(230)<br>42(240) | 44(250)<br>40(230)<br>42(240) |
| DC05-2 G/PI | .0039(.875)<br>.0056(1.25)<br>.0069(1.55)<br>.0080(1.79) | 0<br>0<br>0<br>0<br>~1 000 | 0<br>0<br>0<br>0<br>.0080(1.79) | 38(216)<br>35(200)<br>39(220)<br>47(269)<br>NG<br>FAILURE | 40(228)<br>37(211)<br>46(262)<br>DATA IN QUESTION - DATA PLOTS AS CURVE, LOAD AND UNLOAD | 40(230)<br>37(212)<br>46(261) | 40(230)<br>37(211)<br>46(260) | 40(230)<br>37(211)<br>46(261) | 40(231)<br>37(211)<br>46(265) | 40(231)<br>37(213)<br>46(265) | 40(231)<br>37(213)<br>46(261) | 40(231)<br>37(212)<br>45(259) | 40(230)<br>37(211)<br>46(260) |
| EC05-1 B/Al | .0044(1.0)<br>.0067(1.5)<br>.0089(2.0)<br>.0111(2.5) | 0<br>0<br>0<br>0<br>2 500 000 | 0<br>0<br>0<br>0<br>.0111(2.5) | 154(880)<br>147(840)<br>154(880)<br>149(850) | 175(1000)<br>145(830)<br>165(940)<br>154(880)<br>CRACK INITIATION, ONE BROKEN FIBER, CRACK ON ONE SIDE OF NOTCH, BOTH FACES | 176 (1000)<br>149(850)<br>165(940)<br>154(880) | 228(1300)<br>151(860)<br>170(970)<br>154(880) | 228(1300)<br>149(850)<br>166(950)<br>156(890) | 176(1000)<br>149(850)<br>168(960)<br>156(890) | 180(1030)<br>149(850)<br>165(940)<br>154(880) | 184(1050)<br>149(850)<br>165(940)<br>152(870) | 184(1050)<br>151(860)<br>165(940)<br>152(870) | 184(1050)<br>149(850)<br>163(930)<br>154(880) |
| EC05-2 B/Al | .0044(1.0)<br>.0067(1.5)<br>.0089(2.0)<br>.0089(2.0)<br>.0089(2.0) | 0<br>0<br>0<br>10 000<br>100 000<br>600 000<br>2 515 000 | 0<br>0<br>0<br>.0089(2.0)<br>.0089(2.0)<br>.0089(2.0)<br>.0089(2.0) | 203(1160)<br>165(940)<br>156(890)<br>173(990)<br>172(980) | 191(1090)<br>179(1020)<br>170(970)<br>175(1000)<br>173(990)<br>LONG CRACK AT END OF SLOT | 191(1090)<br>179(1020)<br>166(950) | 187(1070)<br>177(1010)<br>166(950) | 191(1090)<br>179(1020)<br>168(960) | 187(1070)<br>175(1000)<br>166(950) | 187(1070)<br>175(1000)<br>172(980) | 191(1090)<br>175(1000)<br>170(970) | 187(1070)<br>179(1020)<br>172(980) | 187(1070)<br>177(1010)<br>168(960) |

[a] Longitudinal cracks at end of slot.
[b] No cracks.
[c] Crack at end of slot, CL = 0.000177m (0.0697 in.).
[d] Cracks at end of slot, CL = 0.000200m (0.0787 in.)
[e] CL = 0.000198m (0.078 in.) and 0.0000790m (0.0311 in.)
[f] Crack at end of slot, CL = 0.0000549m (0.0216 in.)

663217 61



ORIGINAL PAGE IS
OF POOR QUALITY

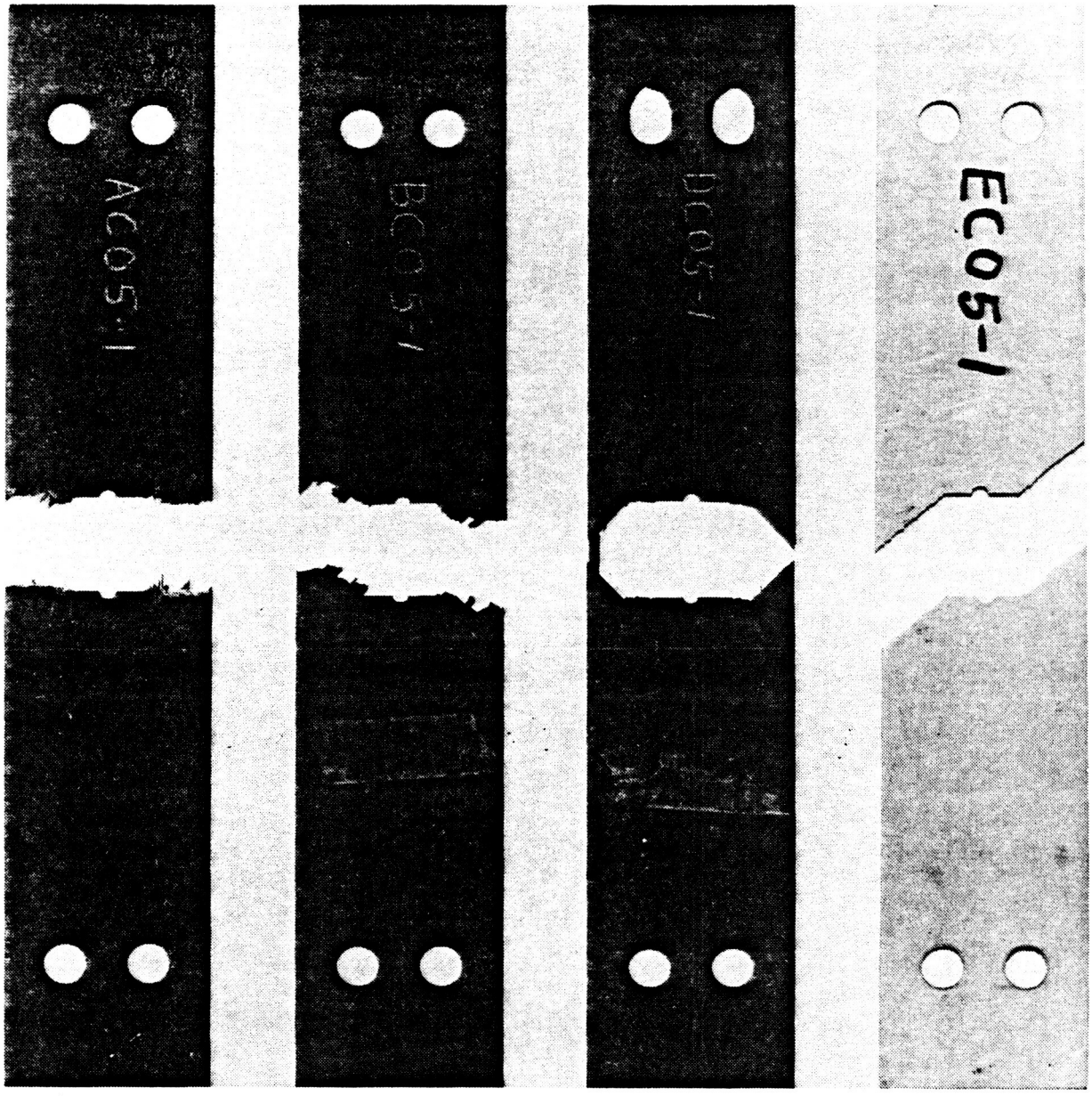



**Figure 7-37 Compliance Specimens (-1's) After Failure in Residual Strength Tests**

ORIGINAL PAGE IS
OF POOR QUALITY

ORIGINAL PAGE IS
OF POOR QUALITY

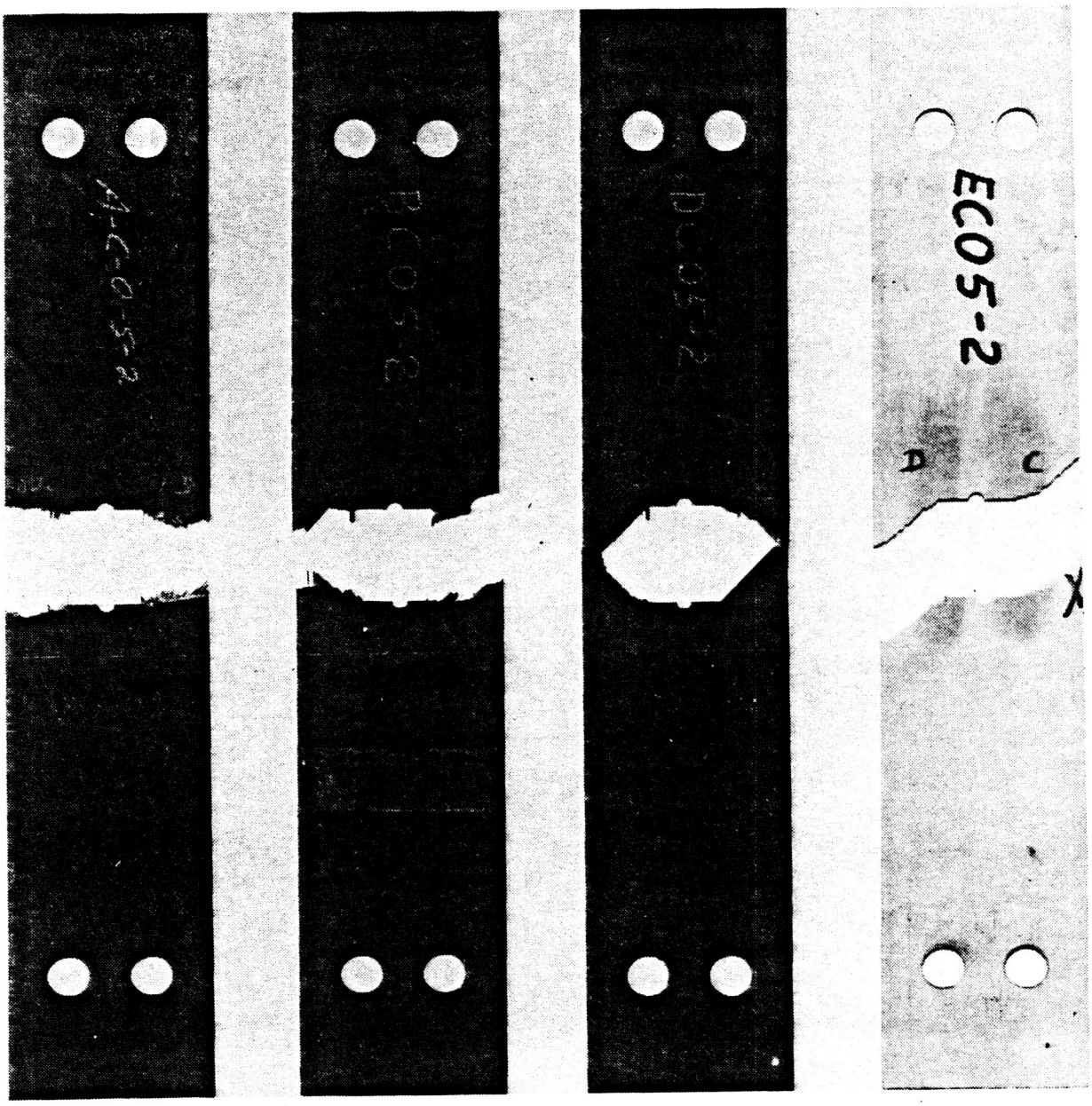



**Figure 7-38 Compliance Specimens (-2's) After Failure in Residual Strength Tests**

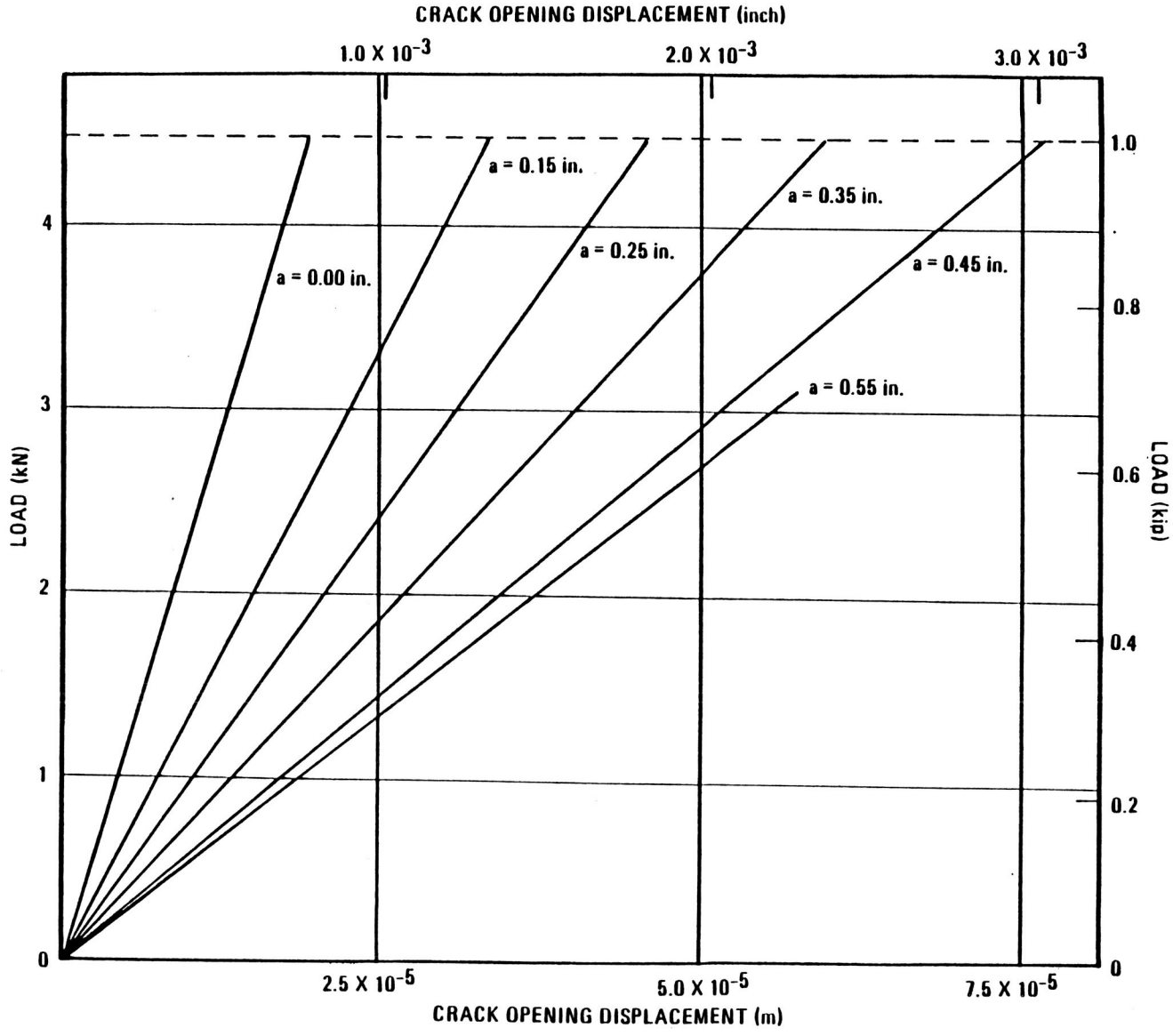



Figure 7-39 Load Versus Crack Opening Displacement for Specimen AC05-3

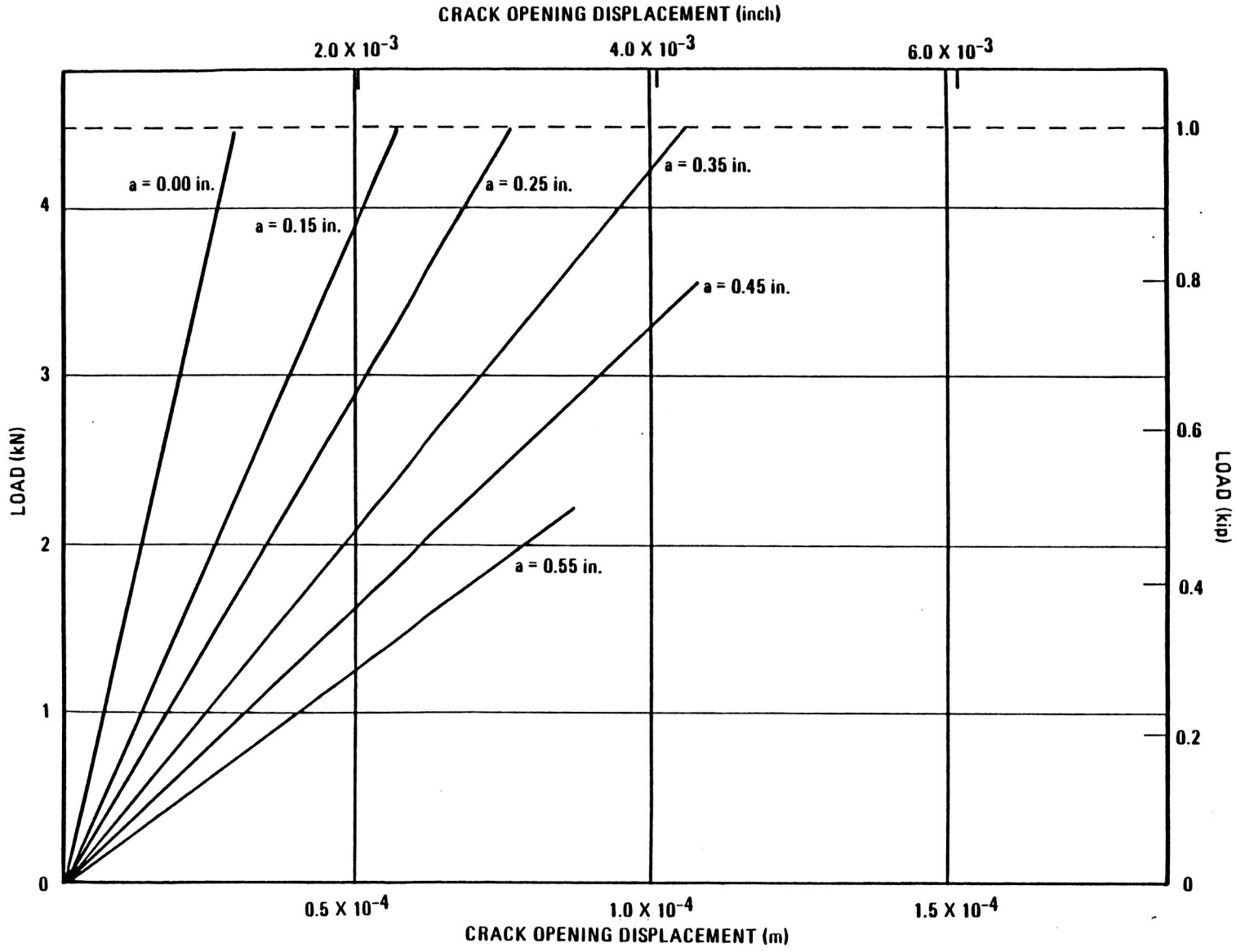



Figure 7-40 Load Versus Crack Opening Displacement for Specimen BC05-3

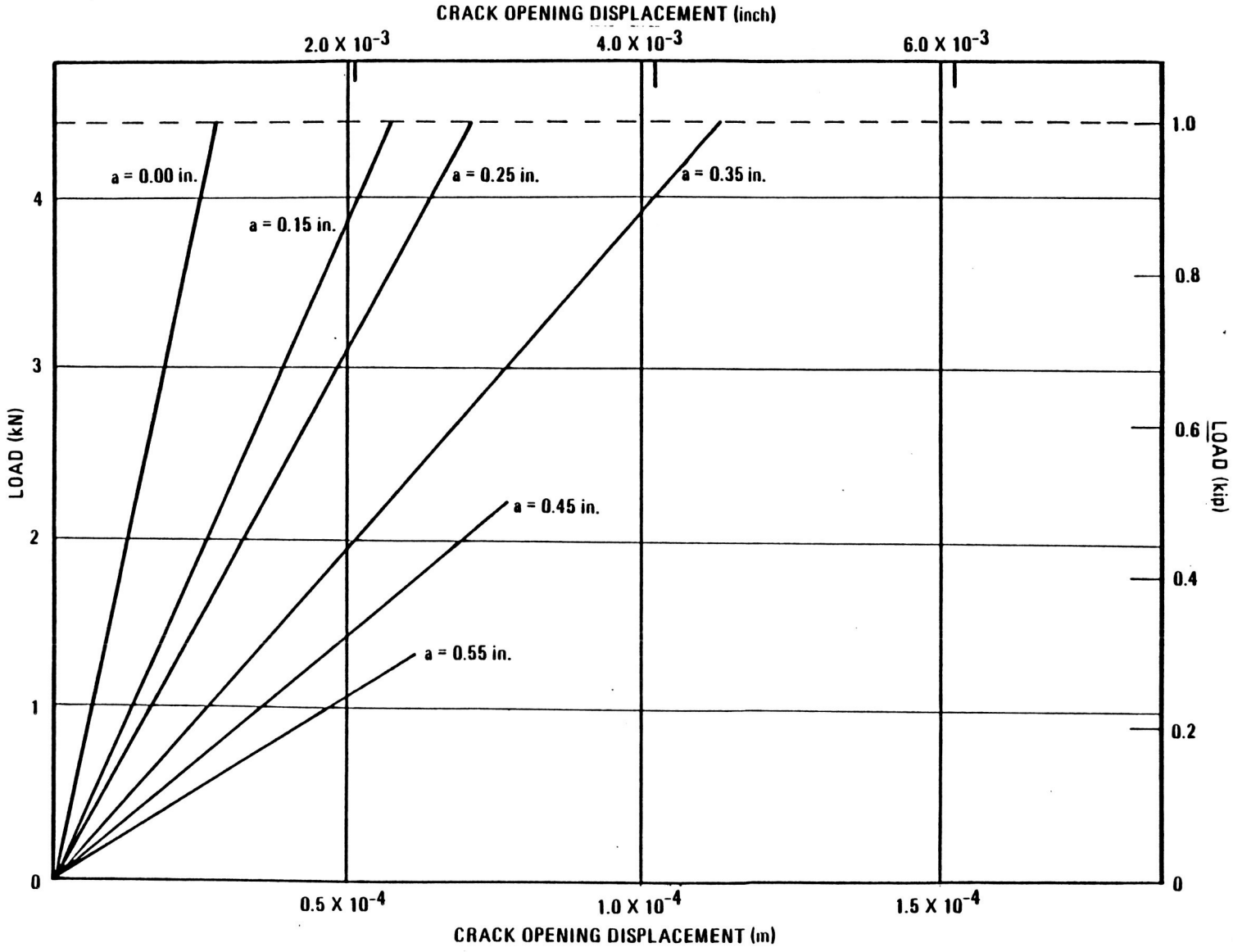



Figure 7-41 Load Versus Crack Opening Displacement for Specimen DC05-3

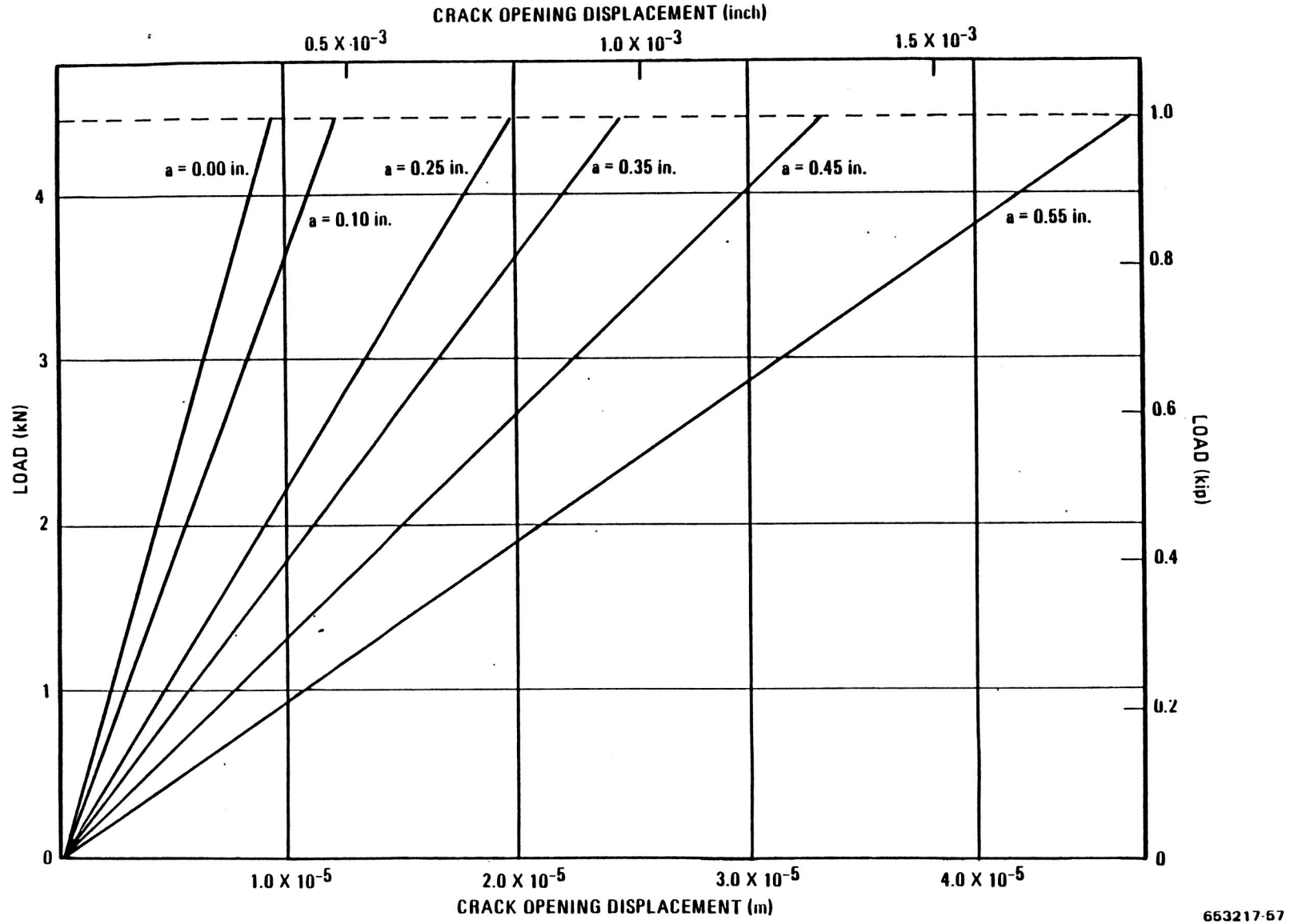



Figure 7-42 Load Versus Crack Opening Displacement for Specimen EC05-3

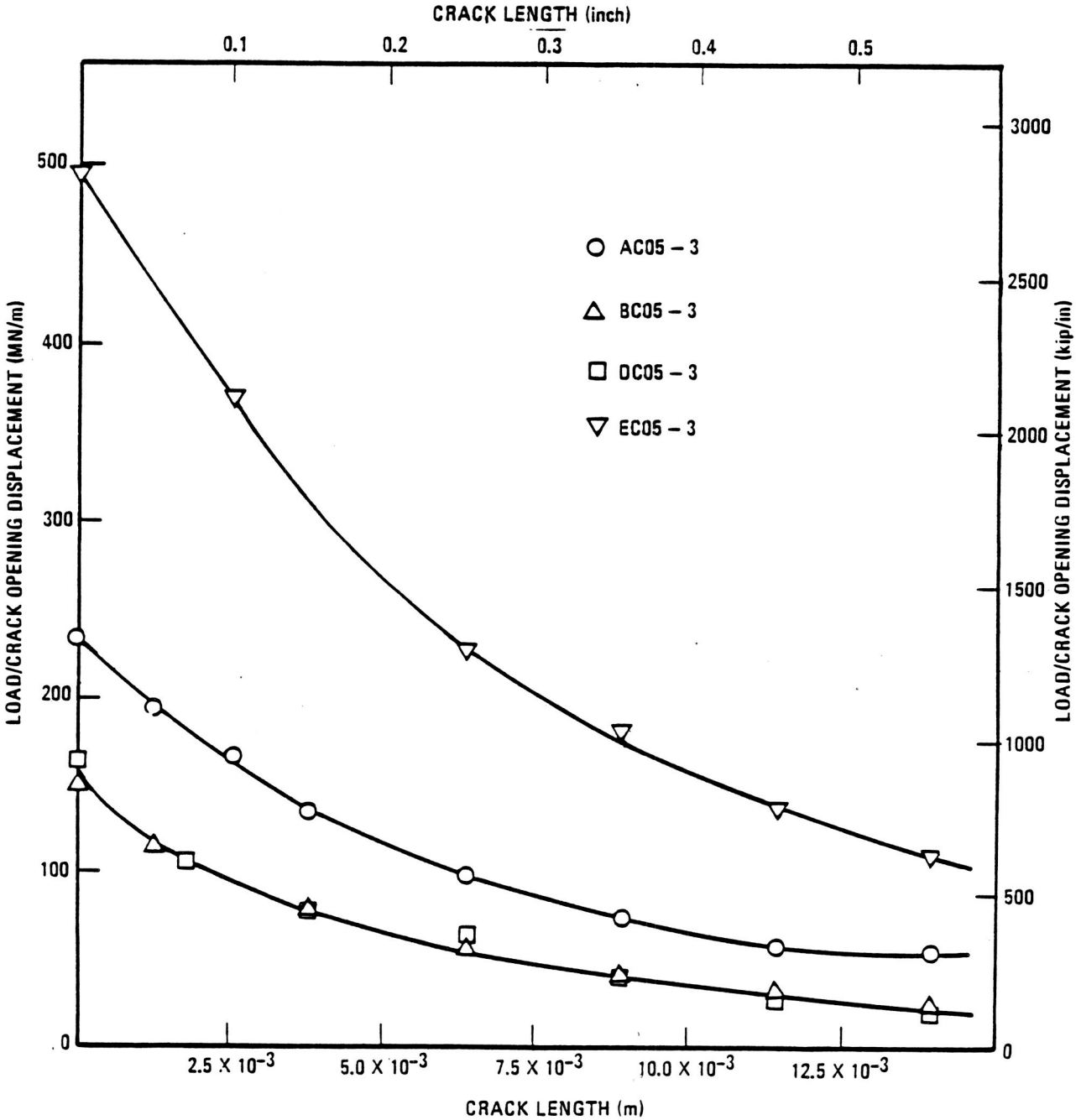



**Figure 7-43 Load/Crack Opening Displacement Versus Crack Length**

ORIGINAL PAGE IS
OF POOR QUALITY

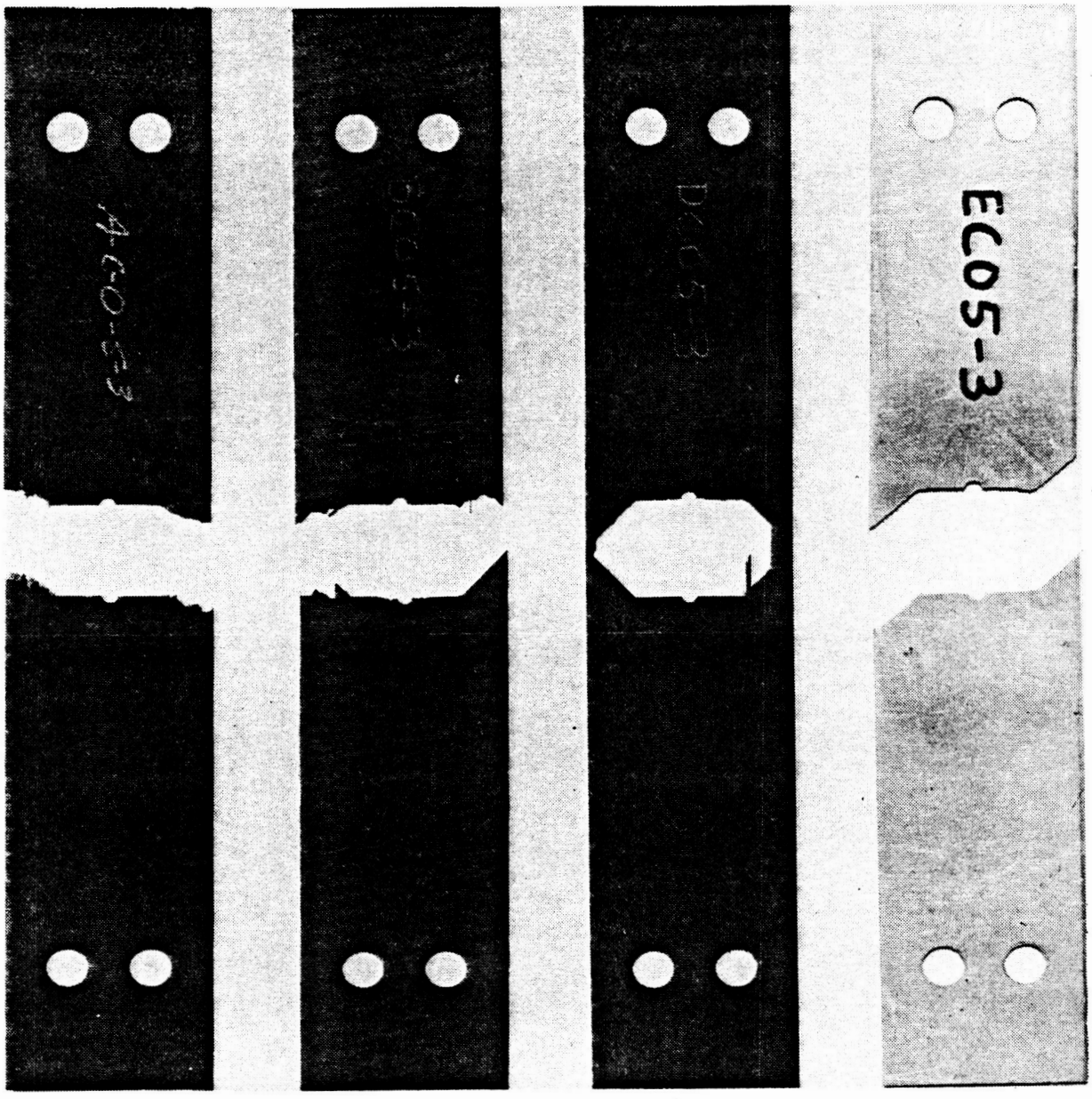



**Figure 7-44 Compliance Specimens (-3's) After Failure in Residual Strength Tests**

## Table 7-44. Results of Fatigue Tests[a]

| MATERIAL | SPECIMEN IDENTIFICATION | SEQUENCE NO. 1 | | | SEQUENCE NO. 2 | | | SEQUENCE NO. 3 | | | RESIDUAL STRENGTH MN (Kip) |
|---|---|---|---|---|---|---|---|---|---|---|---|
| | | INITIAL FLAW $2a_i$ m (in.) | MAX. LOAD, P MN (Kip) | CYCLES N | INITIAL FLAW $2a_i$ m (in.) | MAX. LOAD, P MN (Kip) | CYCLES N | INITIAL FLAW $2a_i$ m (in.) | MAX. LOAD, P MN (Kip) | CYCLES N | |
| B/E | AC05-1 | 0.0239(.94) | 0.00979(2.2) | 56 000 | | | | | | | 0.0110(2.475) |
| | -2 | .0222(.875) | .00801(1.8) | 10 000 | 0.0222(.875) | 0.00801(1.8) | 100 000 | | | | .0107(2.4) |
| | -4 | .00470(1.85) | .0125(2.8) | 2 611 121 | | | | | | | .0209(4.7) |
| G/E | BC05-1 | .0236(.93) | .00512(1.15) | 10 000 | .0236(.93) | .00512(1.15) | 100 000 | | | | .00773(1.737) |
| | -2 | .0249(.98) | .00618(1.39) | 10 000 | .0249(.98) | .00618(1.39) | 100 000 | | | | .00775(1.742) |
| | -4 | .00470(.185) | .0111(2.5) | 2 611 121 | | | | | | | [b].00992(2.23) |
| G/PI | DC05-1 | .0222(.875) | .00689(1.55) | 10 000 | .0222(.875) | .00689(1.55) | 100 000 | | | | [c].00420(.945) |
| | -2 | .0292(1.15) | .00796(1.79) | [d]<1 000 | | | | | | | |
| | -4 | .00470(.185) | .0111(2.5) | 2 611 121 | | | | | | | [e].0147(3.3) |
| B/Al | EC05-1 | .0222(.875) | .0111(2.5) | 2500000 | | | | | | | .0175(3.94) |
| | -2 | .0222(.875) | .00890(2.0) | 10 000 | .0222(.875) | .00890(2.0) | 100 000 | 0.0222(.875) | 0.00890(2.0) | [f]600 000 | .0162(3.635) |
| | -4 | .00470(.185) | .0171(3.84) | 2 611 125 | | | | | | | [b].0265(5.95) |

[a] R = +.1 for all fatigue tests.
[b] Failed in grips.
[c] Flaw extended to 2a = 0.0381m (1.50 in) before residual strength test.
[d] Failed during this sequence.
[e] Failed near grips. Damage was evident around hole.
[f] Crack growing parallel to fibers, L = 0.0025m (0.10 in).



653217-60

ORIGINAL PAGE IS
OF POOR QUALITY

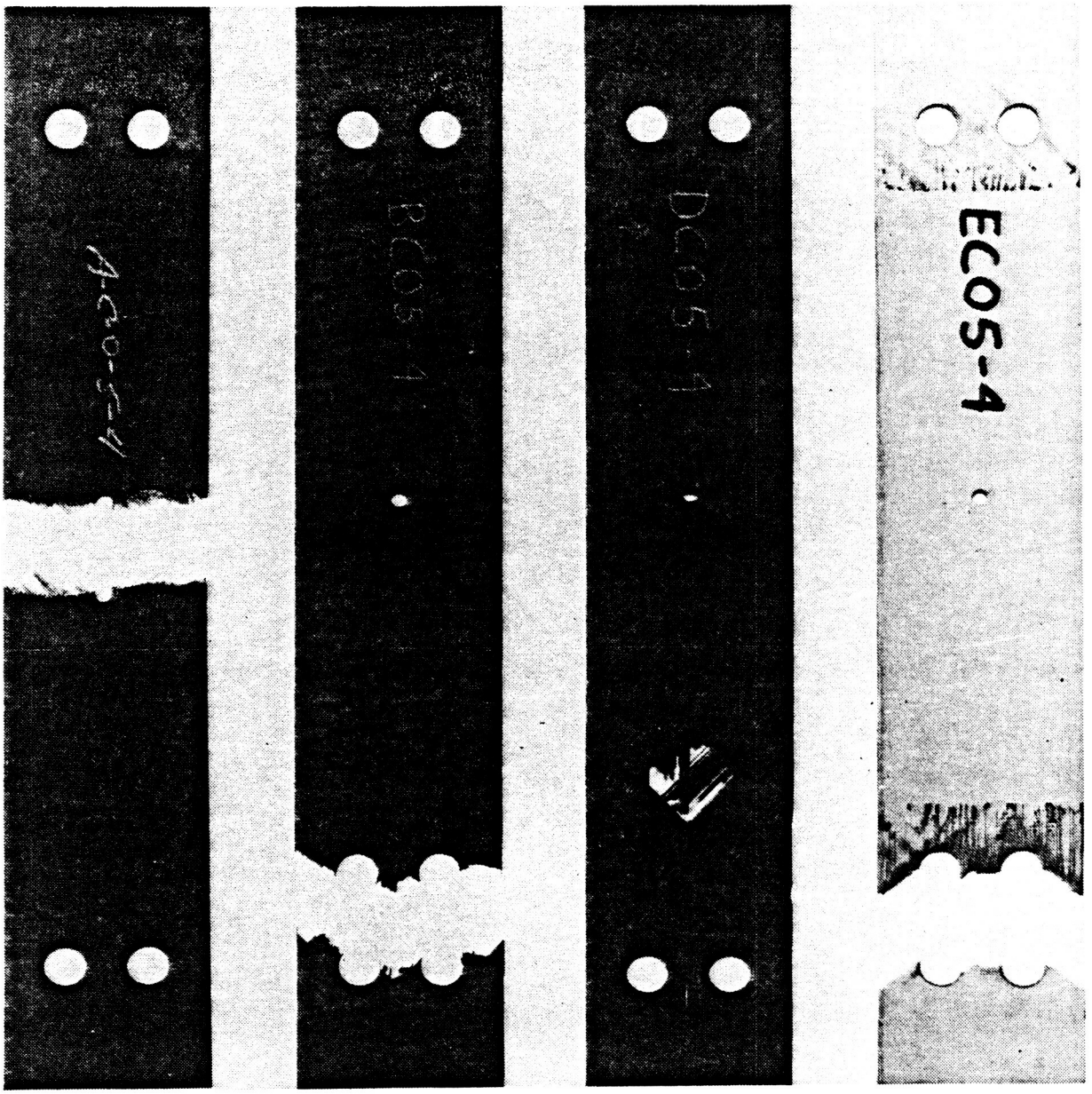



**Figure 7-45 Fatigue Specimens (-4's) After Failure in Residual Strength Tests**

## Table 7-45. Results of Static Tests

| Material | Specimen Identification | Flaw Length 2a m | (in.) | Failure Load MN | (kip) | Gross Area Stress $MN/m^2$ | (ksi) | Net Area Stress $MN/m^2$ | (ksi) | $K_Q$ $MN/m^2\sqrt{m}$ | (ksi $\sqrt{in.}$) |
|---|---|---|---|---|---|---|---|---|---|---|---|
| B/E | AC05-5 | 0.0286 | 1.125 | 0.00910 | 2.045 | 188 | 27.3 | 342 | 49.6 | 43.8 | 39.9 |
| | -6 | .0349 | 1.375 | .00694 | 1.56 | 143 | 20.8 | 319 | 46.2 | 39.0 | 35.5 |
| G/E | BC05-5 | 0.0286 | 1.125 | 0.00656 | 1.475 | 136 | 19.7 | 247 | 35.8 | 31.6 | 28.8 |
| | -6 | .0349 | 1.375 | .00411 | .925 | 84.8 | 12.3 | 189 | 27.4 | 23.1 | 21.0 |
| G/PI | [a]DC05-1 | 0.0381 | 1.500 | 0.00420 | .945 | 86.9 | 12.6 | 217 | 31.5 | 25.6 | 23.3 |
| | -5 | .0286 | 1.125 | .00605 | 1.36 | 125 | 18.1 | 228 | 33.0 | 29.0 | 26.4 |
| | -6 | .0349 | 1.375 | .00489 | 1.10 | 101 | 14.7 | 225 | 32.6 | 27.6 | 25.1 |
| B/Al | EC05-5 | 0.0286 | 1.125 | 0.0148 | 3.325 | 219 | 31.7 | 397 | 57.6 | 50.9 | 46.3 |
| | -6 | .0349 | 1.375 | .0117 | 2.625 | 172 | 25.0 | 383 | 55.6 | 46.9 | 42.7 |

[a] This specimen was fatigue cycled with a smaller flaw, 2a = 0.0222m (0.875 in.).

**Table 7-46. Results of Residual Strength Tests**

| MATERIAL | SPECIMEN IDENTIFICATION | INITIAL FLAW SIZE $2a_i$ m (in.) | NO. OF FATIGUE & COMPLIANCE CYCLES | FINAL FLAW SIZE 2a m (in.) | FAILURE LOAD MN (Kip) | GROSS AREA STRESS $MN/m^2$ (ksi) | NET AREA STRESS $MN/m^2$ (ksi) | $K_Q$ $MN/m^2\sqrt{m}$ (ksi$\sqrt{in}$) |
|---|---|---|---|---|---|---|---|---|
| B/E | AC05-1 | 0.0222(.875) | 56 022 | 0.0239(.94) | 0.0110(2.475) | 228(33.0) | 365(52.9) | 46.9(42.7) |
| | -2 | .0222(.875) | 110 000 | .0222(.875) | .0107(2.40) | 221(32.0) | 339(49.2) | 43.5(39.6) |
| | -3 | .0047(.185) | 27 | [a].0330(1.30) | .00667(1.50) | 138(20.0) | 288(41.7) | 35.8(32.6) |
| | -4 | .0047(.185) | 2 611 121 | .0047(.185) | .0209(4.70) | 432(62.7) | 467(67.7) | - - |
| G/E | BC05-1 | .0222(.875) | 110 016 | .0236(.93) | .00773(1.737) | 159(23.0) | 254(36.9) | 32.5(29.6) |
| | -2 | .0222(.875) | 110 017 | .0249(.98) | .00775(1.742) | 160(23.2) | 263(38.2) | 33.8(30.8) |
| | -3 | .0047(.185) | 27 | [a].0330(1.30) | .00540(1.215) | 112(16.2) | 233(33.8) | 29.0(26.4) |
| | -4 | .0047(.185) | 2 611 121 | .0047(.185) | [b].00992(2.23) | 205(29.7) | 221(32.1) | - - |
| G/PI | DC05-1 | .0222(.875) | 110 056 | [a].0381(1.50) | .00420(0.945) | 88.9(12.6) | 217(31.5) | 25.6 23.3 |
| | -2 | .0222(.875) | < 1 030 | .0292(1.15) | [c].00796(1.79) | 165(23.9) | 305(44.2) | 38.9 35.4 |
| | -3 | .0047(.185) | 27 | [a].0330(1.30) | .00533(1.198) | 110(16.0) | 230(33.3) | 28.7 26.1 |
| | -4 | .0047(.185) | 2 611 121 | .0047(.185) | [d].0147(3.30) | 303(44.0) | 328(47.5) | - - |
| B/Al | EC05-1 | .0222(.875) | 2 500 040 | .0222(.875) | .0175(3.94) | 258(37.5) | 398(57.7) | 51.0 46.4 |
| | -2 | .0222(.875) | 710 036 | [e].0222(.875) | .0162(3.635) | 239(34.6) | 248(35.9) | 47.0 42.8 |
| | -3 | .0047(.185) | 27 | [a].0330(1.30) | .0129(2.90) | 190(27.6) | 396(57.5) | - - |
| | -4 | .0047(.185) | 2 611 125 | .0047(.185) | [b].0265(5.95) | 391(56.7) | 423(61.3) | - - |

[a] Flaw extended to this length by hand with diamond coated wire.
[b] Failure in grips.
[c] Failed during fatigue cycling.
[d] Failure not at flaw but damage at flaw was noted.
[e] Crack parallel to fiber, 0.0025m (0.1 in.) in length.

653217-64

2. The apparent stress intensity factor, $K_Q$, calculated from fracture tests does not lie on a straight horizontal line when plotted versus *visual* crack length. The testing showed only very limited evidence of growth of *effective* crack length. This leads to the conclusion that the fracture mechanics approach is not appropriate for characterizing crack growth in composite materials. Delaminations were not investigated, hence, no conclusions can be made regarding that type of flaw.

3. Fatigue cycling showed no trend effects on stress intensity factors calculated from residual strength tests when compared to results from uncycled static tests.

4. Results from the "-3" specimens, Figure 7-43, indicate that the B/Al is more resistive to crack opening displacement than the B/E. The G/E and G/PI possess the same resistance to crack opening displacement and are less resistant than the B/E. As the two graphite reinforced systems were the same, this would indicate that the fibers dominate the fatigue mechanism, i.e., whether the matrix is epoxy or polyimide is of less importance. The large difference between the B/Al and B/E materials, on the other hand, indicates that for boron reinforced systems the matrix, either a ductile metal or a brittle resin, plays a major role in the fatigue mechanism.

## 7.4 COMPRESSIVE TESTING

Results of the Phase I thermal aging and flight simulation tests indicated that matrix properties such as compressive and shear strength were affected to a greater degree than tensile strength, a fiber dominated property. For this reason it was decided to include a limited number of residual compressive tests in the 10,000 hour flight simulation test program. To check out the feasibility of determining compressive strength of a 6 ply laminate such as that

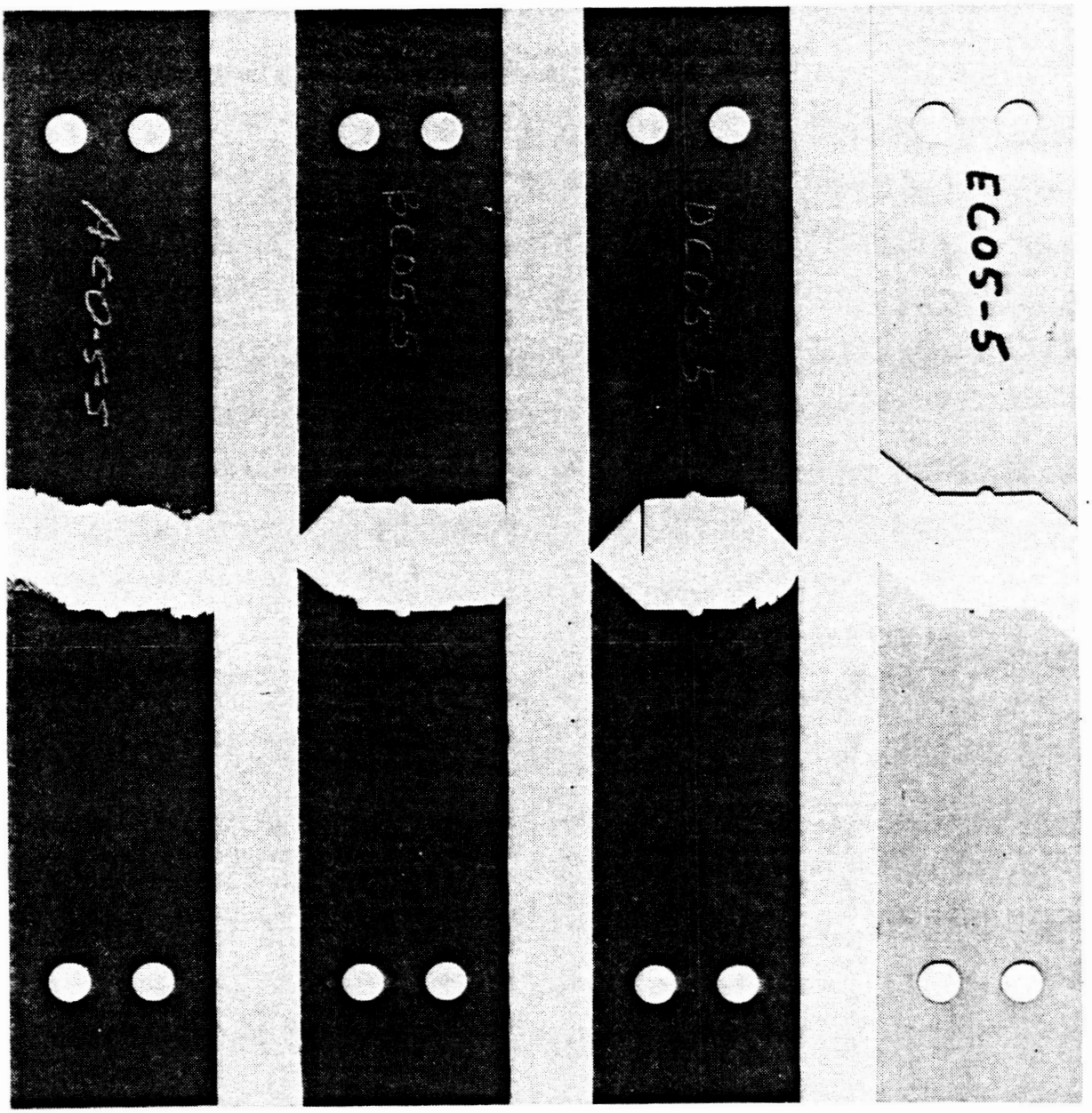



**Figure 7-46 Static Strength Specimens (-5's) After Failure**

ORIGINAL PAGE IS
OF POOR QUALITY

ORIGINAL PAGE IS
OF POOR QUALITY

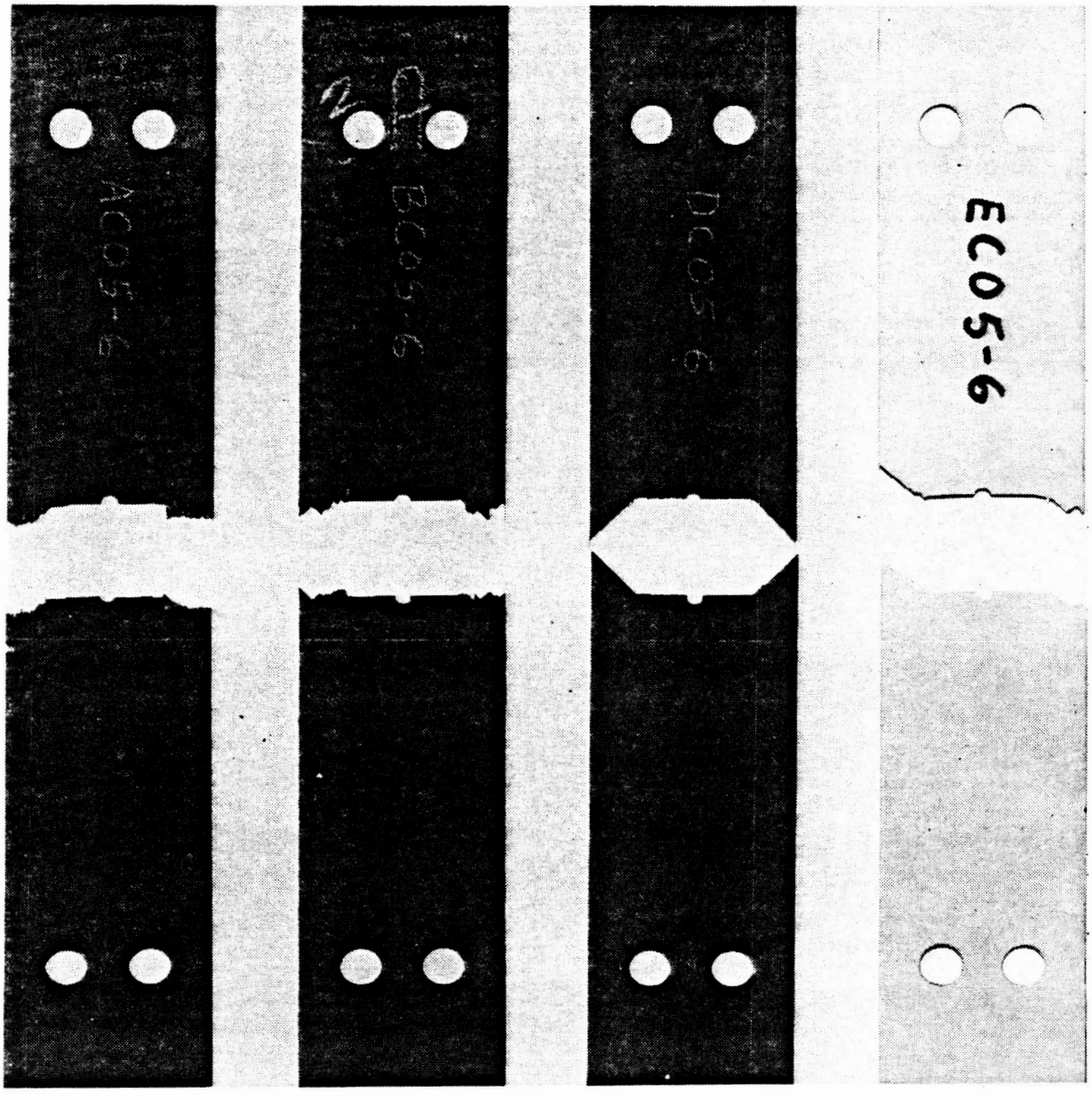



**Figure 7-47 Static Strength Specimens (-6's) After Failure**

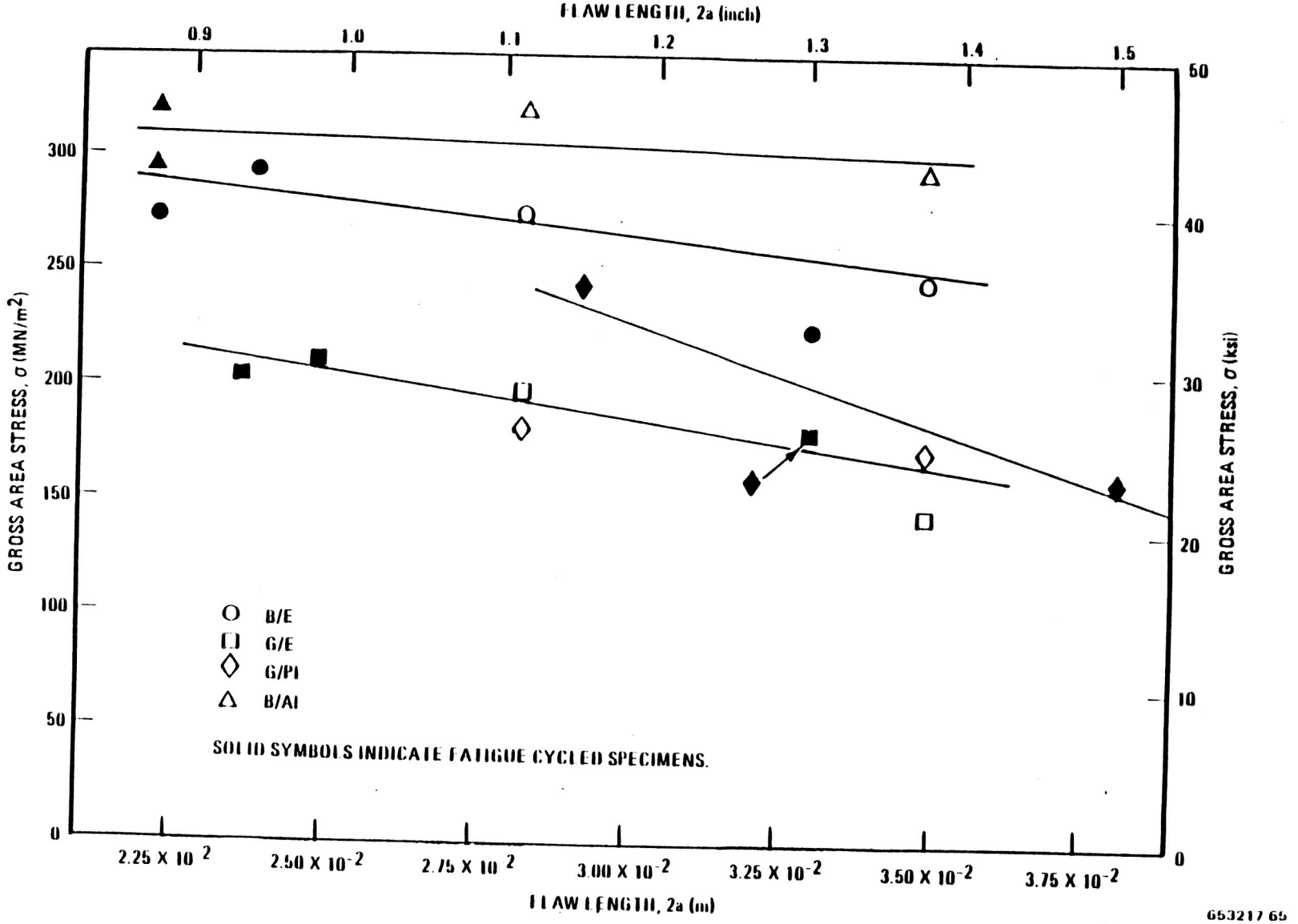



Figure 7-48 Effect of Flaw Length on Gross Area Static Failure Stress

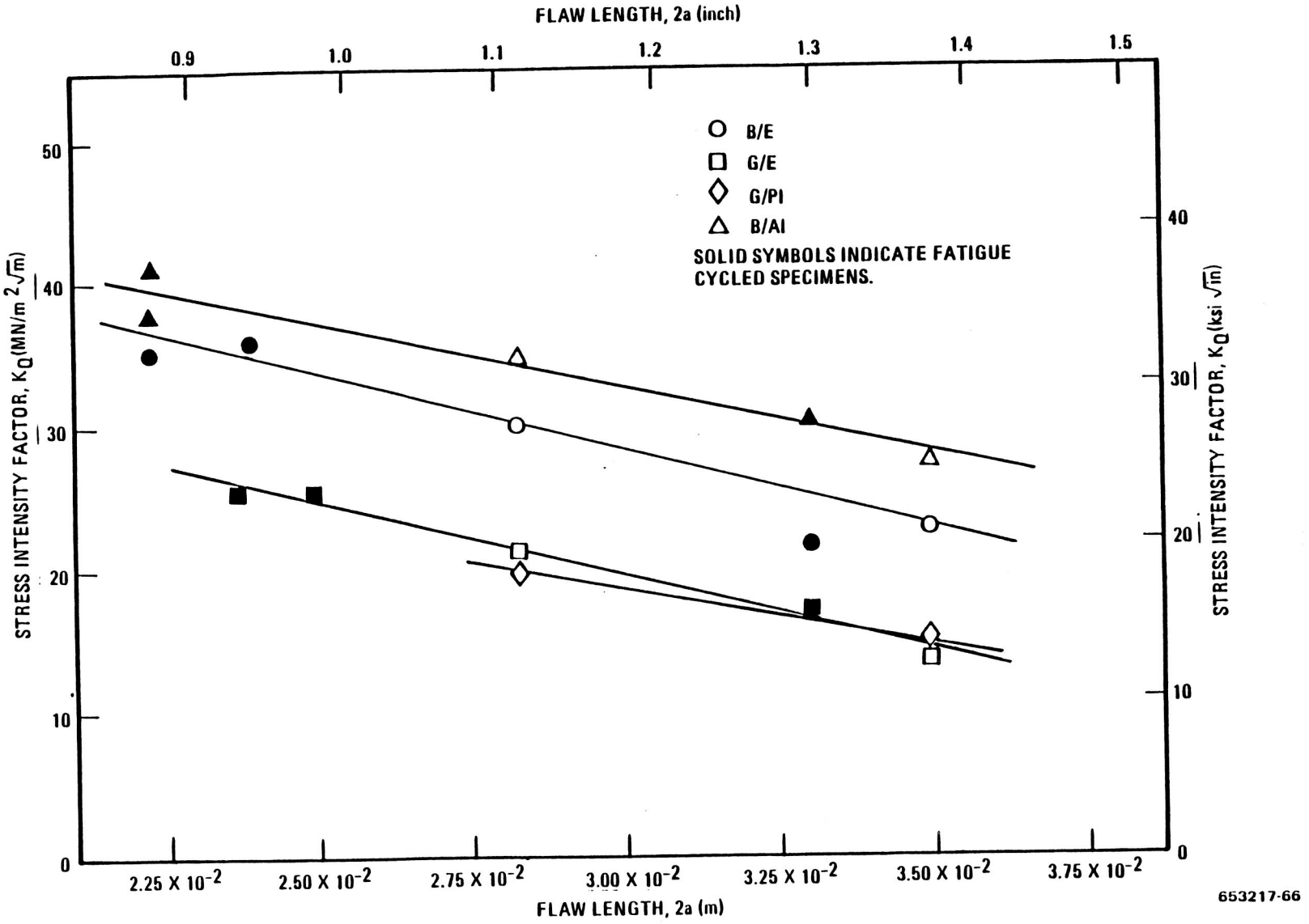
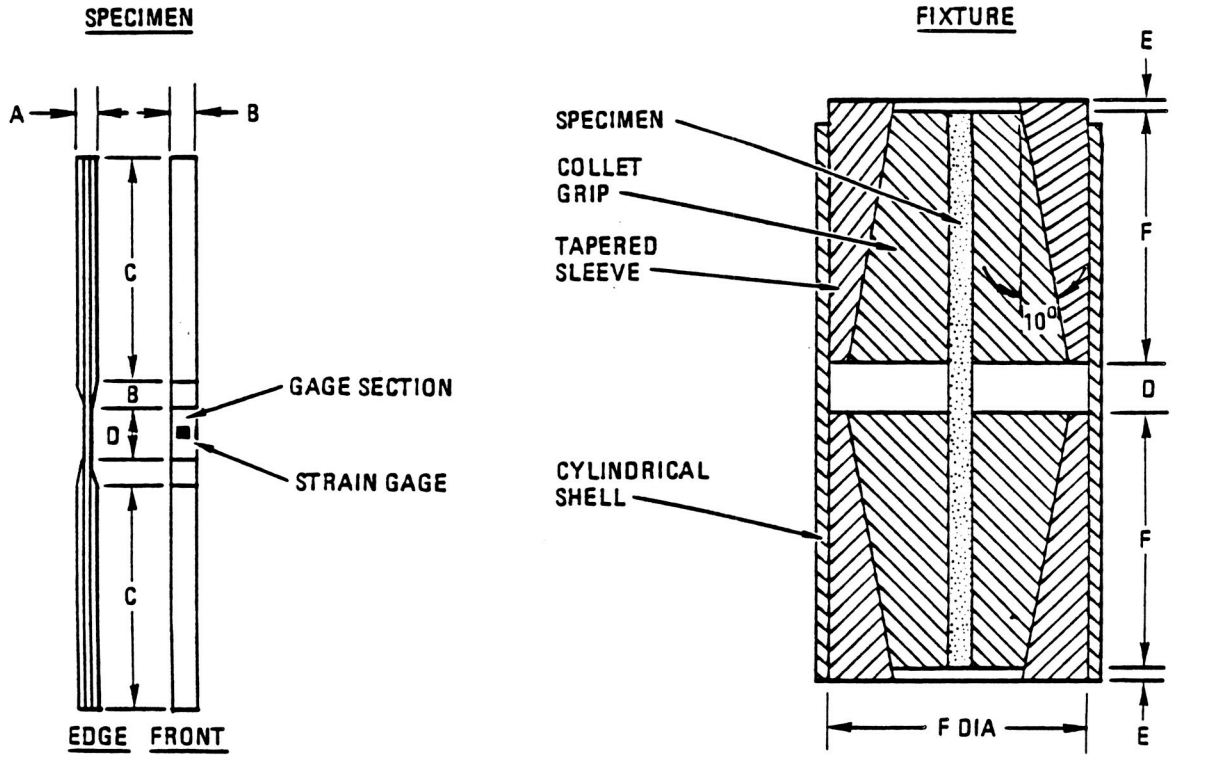



**Figure 7-49 Effect of Flaw Length on Stress Intensity Factor**

used in the flight simulation exposures, a series of baseline compressive tests was conducted on laminated B/E, G/E, and G/PI specimens. The results obtained from the laminated specimen design were satisfactory, and similar compressive tests were performed on the 6 ply thermal aging/compression study materials, Celion 6000/LARC-160 G/PI and A-S/3501-5A G/E. Compressive tests were also conducted on the 24 ply thermal aging/compression study materials.

**7.4.1 SPECIMEN DESIGN AND TEST PROCEDURE.** At the time that the compressive tests were performed, an ASTM standard test method, D3410-75, had been prepared for determination of compressive properties of oriented fiber composites. The specimen configuration, test fixture, and procedure used in the baseline tests were those called out in this ASTM Specification. Figure 7-50 shows the test specimen and test fixture. To obtain the required specimen thickness of 0.0015 m (0.060 in.) to 0.003 m (0.120 in.) for the 6 ply material it was necessary to bond together several pieces. For the Phase I B/E and G/E systems, four layers were used, while for the somewhat thicker Phase I HT-S/710 G/PI and the thermal aging/compression study




| DIMENSIONS | m | in. |
|---|---|---|
| A | 0.00399 | 0.157 |
| B | 0.00635 | 0.250 |
| C | 0.05715 | 2.250 |

| DIMENSIONS | m | in. |
|---|---|---|
| D | 0.01270 | 0.500 |
| E | 0.00318 | 0.125 |
| F | 0.06350 | 2.500 |

653217-67

**Figure 7-50 Compression Test Specimen and Fixture**

ORIGINAL PAGE IS
OF POOR QUALITY

materials, Celion 6000/LARC-160 G/PI and A-S/3501-5A G/E only three layers were required. The procedure for fabrication of the laminated specimens was:

1. Cut three or four pieces of $[0° \pm 45°]_s$ composite approximately 0.038 m (1.5 in.) by 0.140 m (5.5 in.) with 0° plies in long direction.
2. Heat at 394 K (250 °F) for 24 hours to remove any absorbed moisture.
3. Bond pieces together with fiberglass doublers at each end using EA 934 adhesive.
4. Cut 0.0064 m (0.25 in.) wide specimens from the 18 or 24 ply laminates.
5. Apply two strain gages to each specimen using the procedures described in Section 7.1.1. Gages used were B/E, FAE-12-12-S3; G/E and G/PI, FAE-12-12-S0.
6. Store in desiccator until tested.

A similar procedure was used to prepare the compression specimens from the 24 ply thermal aging/compression study materials except that no laminating was required.

The compressive tests were conducted in an Instron testing machine using a fixture of the type described in Figure 7-50. The test setup is shown in Figure 7-51. After the specimen is loaded into the fixture, a slight preload is applied to exercise the gages and ensure that the specimen is properly positioned. The specimen is then loaded incrementally to failure with

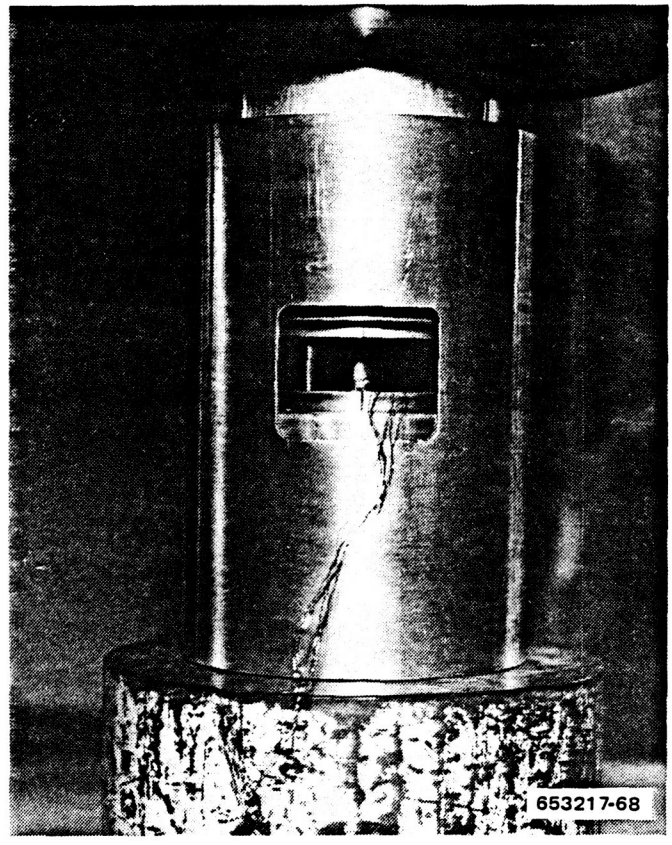



**Figure 7-51 Test Setup for Compressive Tests**

strain measurements recorded automatically with the same equipment that was used for the tensile tests. The output was both a typewritten recording of load versus strain and a punched paper tape that could be processed by a computer, programmed to produce a stress-strain plot. Compressive modulus values were determined from the stress-strain curves.

**7.4.2 TEST RESULTS AND DISCUSSION.** Compressive strength and modulus data for the three Phase I resin matrix systems are given in Table 7-47, and typical load-strain curves for each system are shown in Figures 7-52 to 7-54. In agreement with results of others, the strength and modulus values of the boron reinforced system are considerably larger than either of the graphite reinforced systems. The higher compressive properties of the B/E over the G/E and G/PI would be anticipated from a comparison of the reinforcing fibers. The boron fibers in the 0° plies are aligned along their entire length in the loading direction, whereas the much smaller diameter graphite fibers that are twisted into multi-filament tows are, on a micro scale, generally aligned slightly off axis to the compressive load. Both the strength and modulus values of the graphite systems are less than half of the values for the boron system.

Data for the two thermal aging/compression study materials are given in Tables 7-48 and 7-49. Examples of typical load-strain curves for each material are shown in Figures 7-55 and 7-56. In like manner to the tensile properties, the compressive properties of the Celion 6000/LARC-160 G/PI are significantly higher than those of the HT-S/710 system. The laminated G/E data are in relatively good agreement for the two batches of material (Tables 7-47 and 7-48). The compressive strength of the 24 ply material, however, was considerably lower than the values obtained for the laminated 6 ply materials. The low values for the 24 ply material can be partially accounted for by a somewhat larger cured ply thickness, 0.00015 m (0.0060 in.) compared to 0.00013 m (0.0051 in.) and 0.00014 m (0.0055 in.) for the 6 ply materials.

Table 7-47. Baseline Compressive Properties of Laminated $[0° \pm 45°]_s$ Crossplied Composite Systems at Room Temperature

| Material System | Specimen Number | Compressive Strength $MN/m^2$ | (ksi) | Compressive Modulus $GN/m^2$ (a) | (Msi) (a) |
|---|---|---|---|---|---|
| 5505/4 B/E | AC04-1 | 1459 | 211.6 | 103 | 14.9 |
| | -2 | 1665 | 241.5 | 101 | 14.7 |
| | -3 | 1497 | 217.1 | 101 | 14.7 |
| | avg | 1540 | 223.4 | 102 | 14.8 |
| A-S/3501-5 G/E | BC04-1 | 571 | 82.8 | 47 | 6.8 |
| | -2 | 570 | 82.6 | 43 | 6.3 |
| | avg | 570 | 82.7 | 45 | 6.6 |
| HT-S/710 G/PI | DC04-1 | 382 | 55.4 | 46 | 6.6 |
| | -2 | 363 | 52.6 | 48 | 7.0 |
| | -3 | 386 | 56.0 | 44 | 6.4 |
| | avg | 377 | 54.7 | 46 | 6.7 |

[a]Strain gage measurements

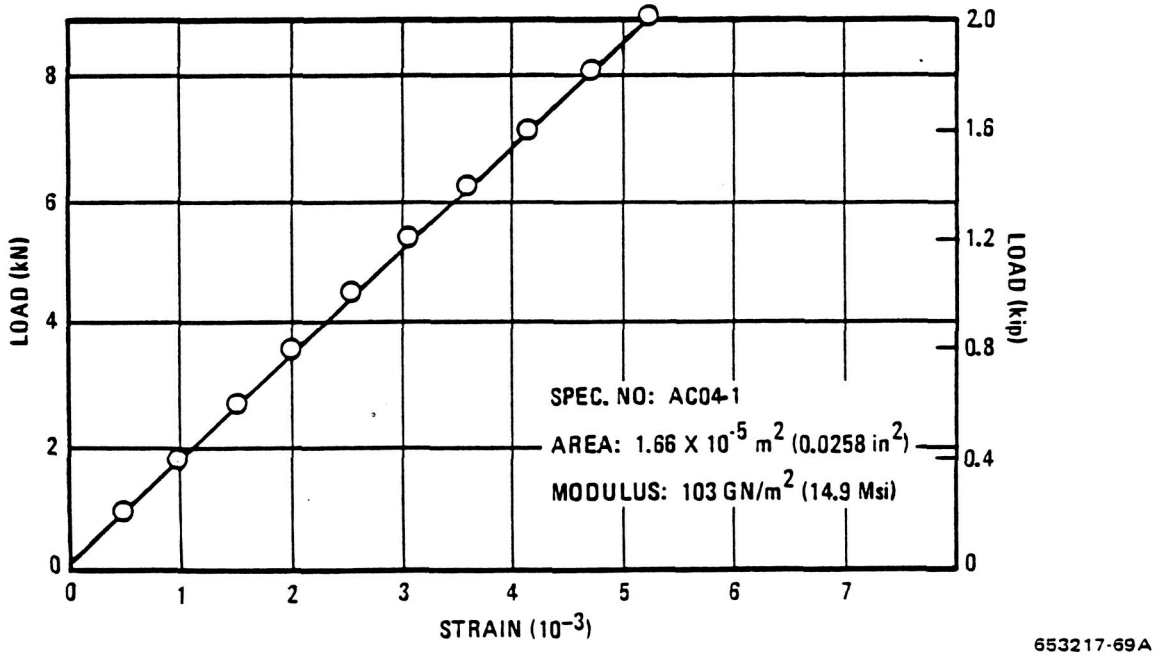



Figure 7-52 Compressive Load-Strain Diagram for $[0° \pm 45°]_{s2s}$ B/E at 297 K (75° F)

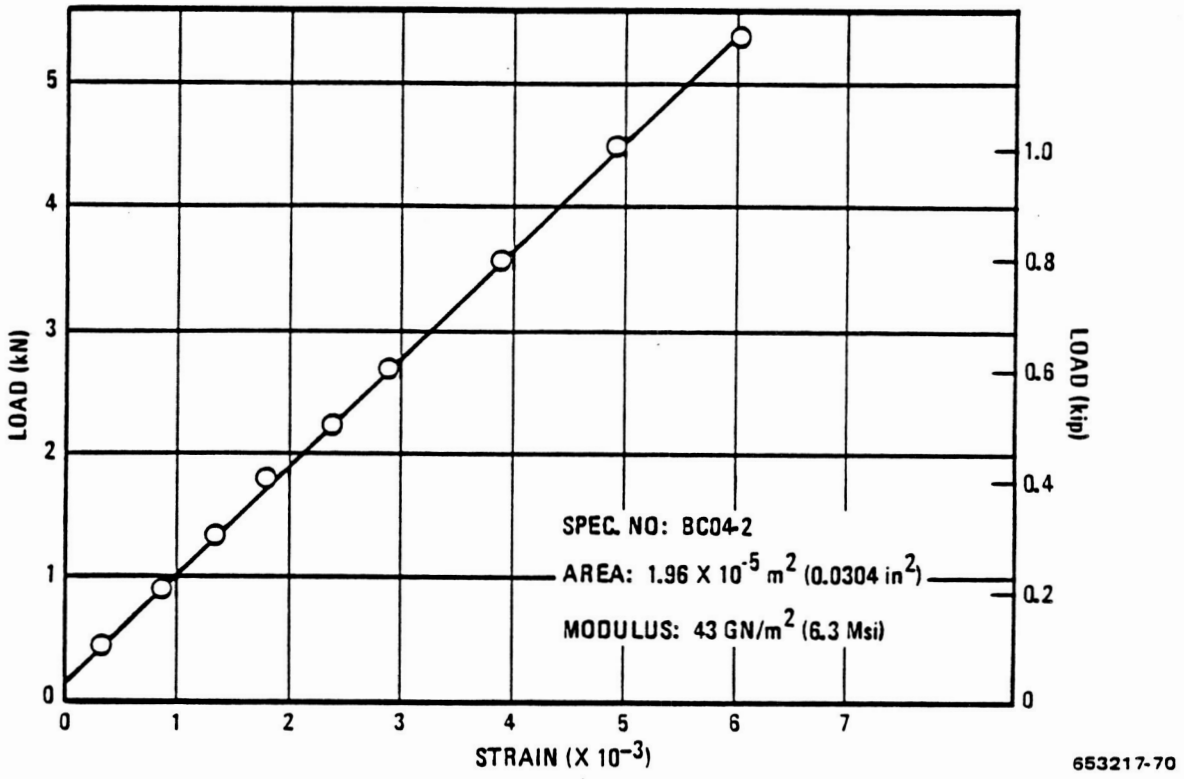



**Figure 7-53 Compressive Load-Strain Diagram for $[0° \pm 45°]_{s2s}$ G/E at 297 K (75° F)**

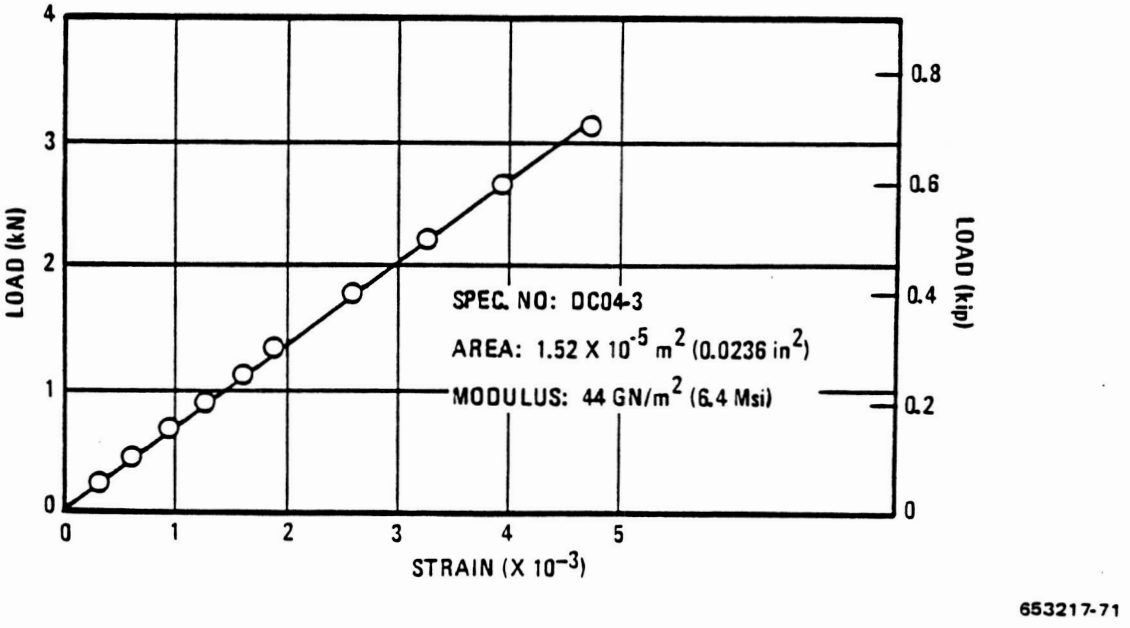



**Figure 7-54 Compressive Load-Strain Diagram for $[0° \pm 45°]_{s3}$ HT-S/710 G/PI at 297 K (75° F)**

**Table 7-48. Baseline Compressive Properties of Laminated $[0° \pm 45°]_s$ Crossplied Composite Systems at Room Temperature — Thermal Aging/Compression Study**

| Material System | Specimen Number | | Compressive Strength MN/m² | (ksi) | Compressive Modulus GN/m² (a) | (Msi) (a) |
|---|---|---|---|---|---|---|
| A-S/3501-5A G/E | BC101-1 | | 536 | 77.8 | 55 | 8.0 |
| | -2 | | 514 | 74.6 | 53 | 7.7 |
| | -3 | | 576 | 83.5 | 52 | 7.5 |
| | | avg | 542 | 78.6 | 53 | 7.7 |
| Celion 6000/LARC-160 G/PI | FC101-1 | | 622 | 90.2 | 50 | 7.3 |
| | -2 | | 532 | 77.2 | 52 | 7.5 |
| | -3 | | 598 | 86.8 | 54 | 7.8 |
| | | avg | 584 | 84.7 | 52 | 7.5 |

[a]Strain gage measurements

**Table 7-49. Baseline Compressive Properties of 24 Ply $[0° \pm 45°]_{4s}$ Crossplied Composite Systems at Room Temperature — Thermal Aging/Compression Study**

| Material System | Specimen Number | | Compressive Strength MN/m² | (ksi) | Compressive Modulus GN/m² (a) | (Msi) (a) |
|---|---|---|---|---|---|---|
| A-S/3501-5A G/E | BC101-4 | | 447 | 64.8 | 39 | 5.7 |
| | -5 | | 467 | 67.8 | 44 | 6.4 |
| | -6 | | 402 | 58.3 | — | — |
| | | avg | 439 | 63.6 | 41 | 6.0 |
| Celion 6000/LARC-160 G/PI | FC101-4 | | 565 | 82.0 | 57 | 8.2 |
| | -5 | | 556 | 80.6 | 57 | 8.3 |
| | -6 | | 652 | 94.5 | 59 | 8.6 |
| | | avg | 591 | 85.7 | 58 | 8.4 |

[a]Strain gage measurements

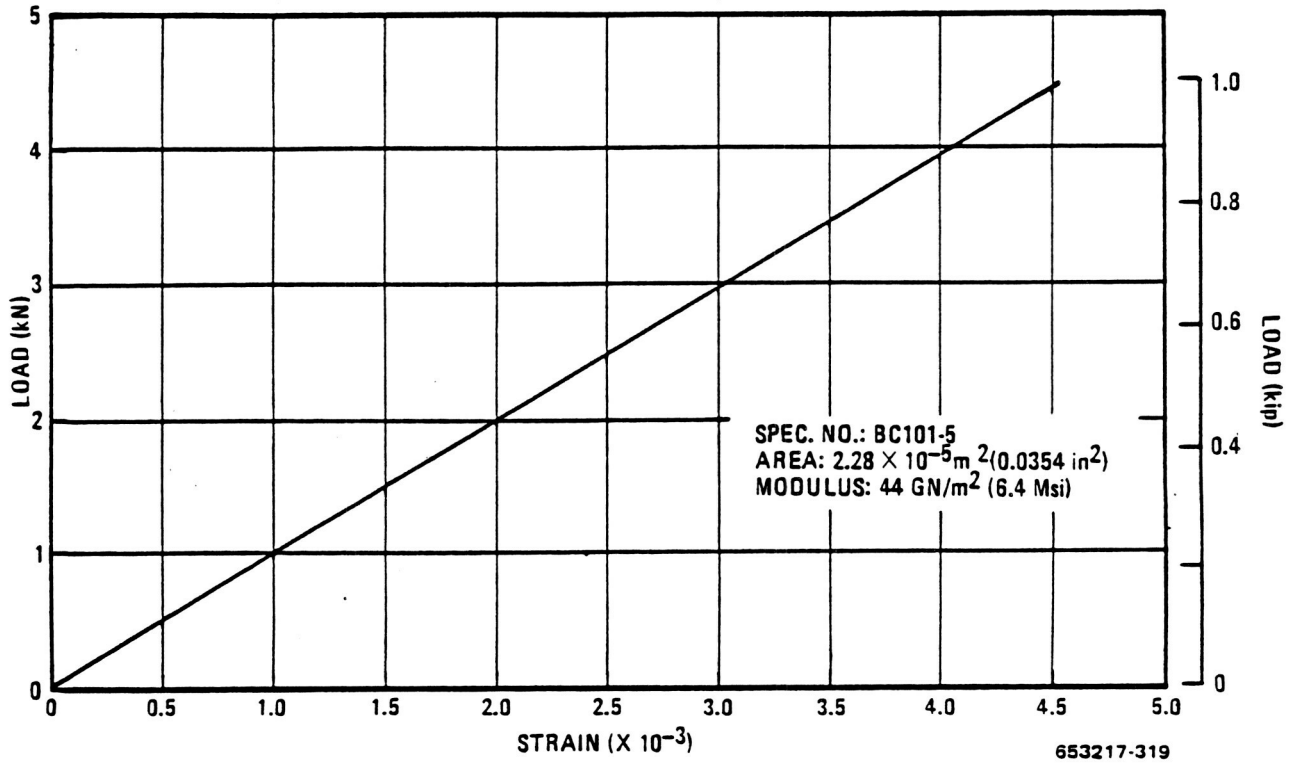



**Figure 7-55 Compressive Load-Strain Diagram for $[0° \pm 45°]_{s3}$ G/E at 297 K (75°F)**

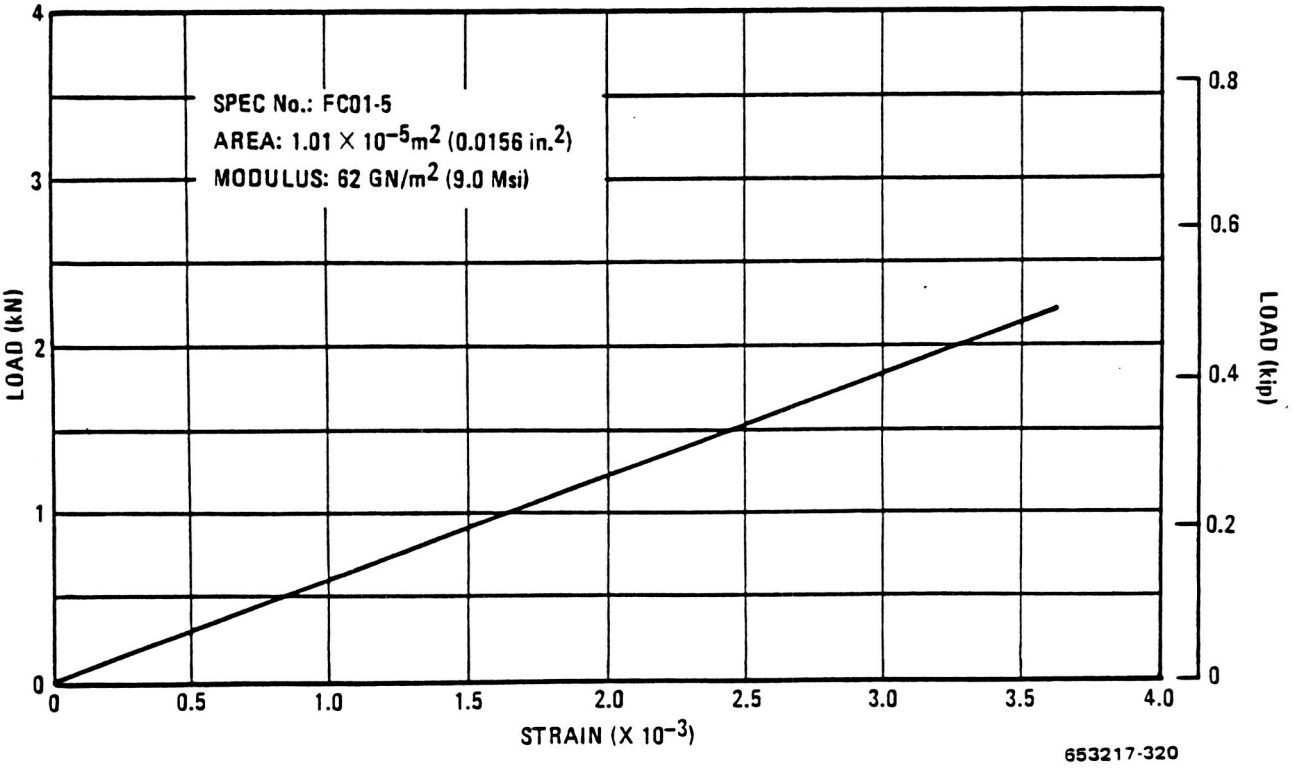



**Figure 7-56 Compressive Load-Strain Diagram for $[0° \pm 45°]_{s3}$ Celion 6000/LARC-160 G/PI at 297 K (75°F)**

# SECTION 8

# THERMAL AGING

To determine the effects of elevated temperature exposure on the stability of advanced composites an extensive thermal aging study was conducted. It was thought that these data, together with the fatigue data also generated during the program, would be very valuable in understanding the results of the flight simulation exposures.

Initially, the thermal aging program was structured so that tensile strength changes were the primary means of following the effects of thermal exposure on the Phase I composite systems. Tensile properties were selected because the intent of the contract was to investigate material requirements and capabilities for the lower wing surfaces of a supersonic aircraft where the major loading is in tension. Early results from the flight simulation tests, however, indicated that a more useful measure of the changes occurring during thermal aging of composites might be obtained from residual compressive or shear strength testing. These are properties that were thought to be more likely to signal the early changes in a material's strength as a result of matrix degradation. For this reason a limited study of thermal aging/compression effects was added during Phase II.

The thermal aging section has been divided into three parts. The first is a description of the test equipment and the procedures used. The second presents and discusses the thermal aging/tension experimental results. The third part covers the thermal aging/compression study.

In the thermal aging/tension study all composite materials were aged for 10,000 hours in Phase I. Additional exposures, out to 40,000 hours for B/Al and 50,000 hours for the B/E, G/E, and HT-S/710 G/PI systems were carried out during Phase II. At various times during aging, specimens were removed for examination and determination of residual tensile strength and, for B/Al, also residual interfiber shear strength. Test specimens were taken from both unidirectional and $[0° \pm 45°]_s$ crossplied laminates except for Celion 6000/LARC-160 G/PI for which only $[0° \pm 45°]_s$ material was evaluated. All were 6 ply in thickness. The aging temperatures were: epoxy 394K (250°F) and 450K (350°F); HT-S/710 G/PI 505K (450°F) and 561K (550°F); Celion 6000/LARC-160 G/PI 450K (350°F); and B/Al 450K (350°F), 505K (450°F), 561K (550°F), and 700K (800°F). The resin matrix composites were aged at ambient pressure and at a reduced pressure of 0.014 $MN/m^2$ (2 psi) to simulate high altitude flight conditions. The B/Al system was aged at ambient pressure only. A second oxygen pressure was selected for the thermal aging of the organic composites because, in general, the organics are oxidation prone. Previous work had shown a direct correlation of thermal aging and oxygen pressure on residual strength of resin matrix composites (ref. 33). In actual use, a SCR vehicle would be at very high altitude during much of the time at which the structure has reached its maximum temperature. Thus, if oxygen pressure is taken into account, the organic materials can likely be used at higher temperatures and for longer times than would be predicted from ambient pressure data.

For the thermal aging/compression program two composites, G/E and Celion 6000/LARC-160 G/PI, were selected for evaluation. The other polyimide, HT-S/710, would have been included in the study but was no longer commercially available at that time. Aging was conducted at 373K (212°F) and 394K (250°F) for G/E and 450K (350°F) and 505K (450°F) for G/PI for time periods

out to 10,000 hours. All exposures were done at 1 atmosphere pressure. For both systems 6 ply $[0° \pm 45°]_s$ and 24 ply $[0° \pm 45°]_{s4}$ laminates were tested. The post aging evaluation consisted of weight change measurements, room temperature compressive, interlaminar shear, and fatigue tests, and $T_g$ tests. As a part of the thermal aging/compression study a small number of Celion 6000/LARC-160 G/PI samples coated with a solution of a polyphenylquinoxaline (PPQ) were also exposed. Preliminary work at NASA-Langely Research Center had shown a significant improvement in the long term thermooxidative stability of LARC-160/G/PI laminates that were coated with PPQ. Sets of three specimens each were fabricated, coated, and aged for 10,000 hours at 450K (350°F) and 505K (450°F) followed by residual interlaminar shear and compressive strength determinations. A set of coated weight change specimens was also prepared for each temperature and weighed after 1000; 5000; and 10,000 hours. The PPQ coated specimens were exposed in the same thermal aging containers as the uncoated specimens.

The following sections describe the test procedures and equipment for the thermal aging studies and present and discuss the experimental results.

### 8.1 TEST EQUIPMENT AND TEST PROCEDURE

The 700K (800°F) thermal age of B/Al was carried out in a small, commercial, electrical resistance oven. The built-in "on/off" temperature controller was replaced by a more accurate controller. After modifying the control system, the entire oven was enclosed with ceramic bricks to improve the temperature stability over the lengthy aging period. With this arrangement the temperature was held to 700 ±6K (800° ±10°F).

All other exposures were conducted in specially constructed aging furnaces similar to the sketch in Figure 8-1. The heater plates consist of insulated wire sandwiched between two thin aluminum plates. The reduced pressure specimens are enclosed in containers consisting of an aluminum picture frame with vacuum fittings and thin aluminum covers. The top cover is sealed with a weld after the specimens are in place. The top is cut off and rewelded periodically during the 50,000 hours to remove specimens for testing. This is less expensive and more reliable than a gasket sealed container. The reduced pressure is obtained by a vacuum pump simultaneously pumping on one side of each container. Bleed air is valved into the other side of each to maintain 0.014 $MN/m^2$ (2 psi). This assures a constant fresh supply of air to each container. All furnace temperatures were initially equilibrium controlled, i.e., a constant amount of power was supplied to the heaters. The power equals that lost through the insulation at equilibrium temperature. This method does not require the use of expensive controllers, and temperature fluctuations are generally smaller than those achieved with active controls. There is also essentially zero probability of a malfunction allowing the specimens to overheat. However, there was a problem that developed on very warm days when the temperature could rise slightly above the desired limits. To prevent this from happening while still retaining the assurance that a failure in a power supply, thermocouple, or some control element would not cause overheating, a small modification was made. This was to add a controller to the system on about 10% of the available power. The furnace would operate as before, except when the outside temperature rose too high the controller would override the system and maintain the desired temperature range. The temperatures were generally maintained to ±3K (±5°F) with infrequent excursions to a maximum of ±6K (± 10°F).

The procedure followed for the thermal aging/tension exposures was to cut the specimen blanks to final size including machining of the B/Al interfiber shear specimens (Figure 7-30), drying the

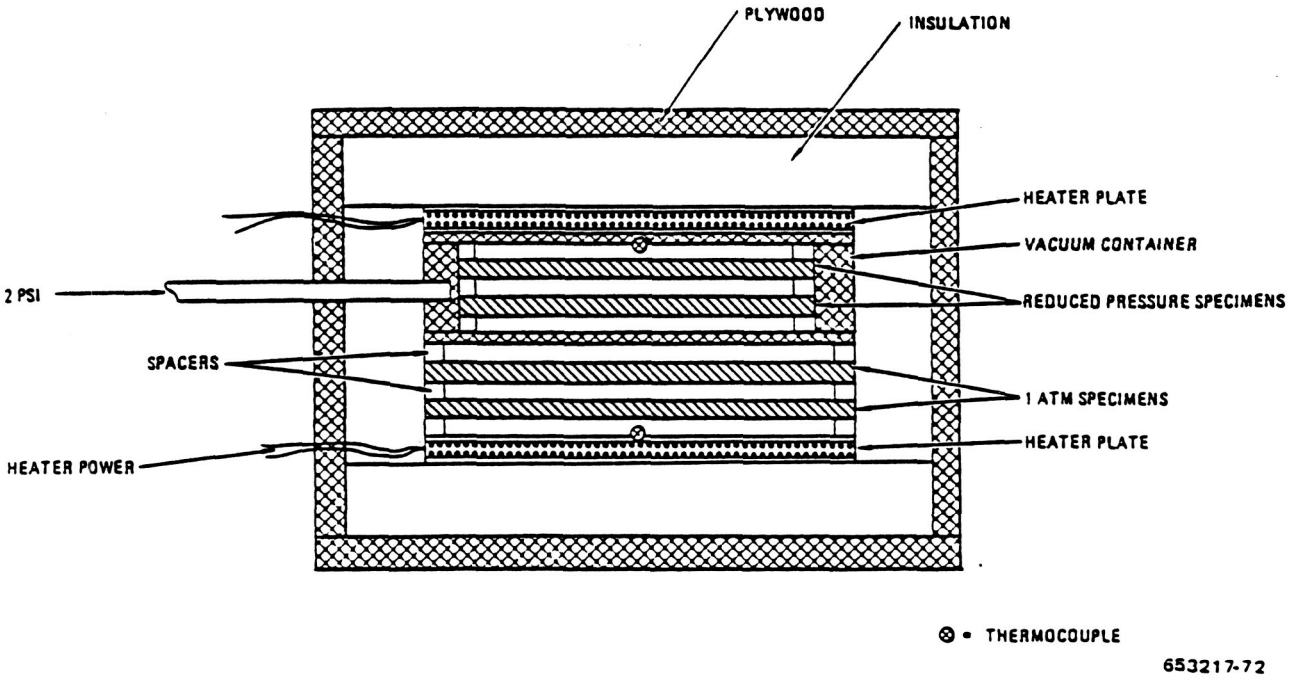



**Figure 8-1 Thermal Aging Furnace Configuration**

resin matrix composites at 394K (250°F) for 24 hours, and loading into the aging furnaces. The specimens were supported at their ends by narrow strips of stainless steel so that almost the entire surface was exposed to the air atmosphere within the furnaces. At the required time intervals the ovens were shut down, opened, and the specimens were removed and stored in a desiccator until doubler bonding and tensile testing. Only the resin matrix specimens were placed in the desiccator, as moisture absorption was not a problem with the B/Al. Residual strength testing was performed at 297K (75°F) for the B/Al, 450K (350K°F) for the epoxies, 505K (450°F) and 561K (550°F) for HT-S/710 G/PI, and 450K (350°F) for Celion 6000/LARC-160 G/PI. The tensile and shear specimen configurations and test procedures were the same as those described in Section 7.

The procedure for the thermal aging/compression exposures differed slightly from that for the thermal aging/tensile exposures. Because of the requirement of performing shear and compressive testing on 6 ply material it was necessary to use the technique described earlier of bonding three pieces together to obtain specimens of sufficient thickness. For this reason oversize sample blocks were aged rather than pre-cut specimens. The dimensions of these aging samples were: compression, 0.038 m by 0.14 m (1.5 in. by 5.5 in.) and shear, 0.038 m by 0.038 m (1.5 in. by 1.5 in.). The same sizes were used for the 24 ply material with test specimens again being machined after aging. This method may have eliminated edge effects of oxidation that would have been present for the thermal aging/tension specimens. The tension-compression (R = -1) fatigue specimens were also prepared after aging. These were cut from 0.10 m by 0.28 m (4 in. by 11 in.) aging blanks of 24 ply material. Fatigue strengths of the 6 ply materials were not evaluated. The specimen configurations and test procedures were the same as those described in Section 7 for compression and shear and Section 11 for fatigue. In addition to mechanical property determinations,

periodic weight change measurements were performed during the course of aging using 0.038 m by 0.038 m (1.5 in. by 1.5 in.) samples of both the 6 ply and 24 ply materials. Finally, 0.038 m by 0.038 m (1.5 in. by 1.5 in.) pieces of 6 ply laminates were exposed for determining $T_g$ changes and to use for metallographic examination after aging.

In addition to the Celion 6000/LARC-160 specimens described above, a number of 6 ply specimens were coated with PPQ to evaluate its ability to improve the long term thermooxidative stability of the G/PI laminates. The PPQ was applied at a solution concentration of 12% in a mixed solvent of meta-cresol, mixed xylenes, and chloroform. The following procedure was used for applying the solution to the specimens and for subsequent solvent removal.

1. Thoroughly wipe the surface of the laminate with acetone using a lint-free cloth and, thereafter, handle with lint-free gloves.
2. Dry in a forced air oven at 473K (392°F) for 2 hours.
3. Apply the PPQ solution to the cooled laminate within a few hours after drying by brush coating a light coat using natural bristle brush in a well-ventilated hood. It was necessary to coat one side, dry, and then coat the other side.
4. Remove the solvent mixture by stage-drying in a forced air oven from room temperature to 333K (140°F) in 1/2 hour, hold at 333K (140°F) 1 hour, increase the temperature to 363K (194°F) and hold for 1/2 hour, increase the temperature to 393K (248°F) and hold for 1/2 hour, increase the temperature to 433K (320°F) and hold for 1/2 hour, and increase the temperature to 473K (392°F) and hold for 2 hours. After drying at 473K (392°F), cool to room temperature in the forced air oven relatively fast.

## 8.2 THERMAL AGING/TENSION — TEST RESULTS AND DISCUSSION

**8.2.1 BORON/EPOXY AND GRAPHITE/EPOXY.** Residual tensile strength data for the epoxy systems are presented in Tables 8-1 through 8-4 for B/E aged at ambient pressure, Table 8-5 for B/E aged at reduced pressure, Tables 8-6 through 8-9 for G/E aged at ambient pressure, and Table 8-10 for G/E aged at reduced pressure. Aging was carried out at 394K (250°F) and 450K (350°F) for both unidirectional and $[0° \pm 45°]_s$ crossplied specimens. The tensile strength data have also been plotted as a function of aging time for the two epoxy systems. These curves are found in Figures 8-2 through 8-7. A summary of the effects of 10,000 hours and 50,000 hours of thermal aging on the tensile strength retention of B/E and G/E is shown in Table 8-11. In Table 8-11 and in others throughout the report that list percentage strength retention, whenever residual strength is greater than baseline strength a value of 100% retention has been used.

**394K, 0.10 MN/m² (250°F, 14.7 psi) EXPOSURE.** After 25,000 hours of aging the appearance of the B/E and G/E specimens had not changed appreciably. Compared with unexposed material, the only observable differences were slight color changes that were first noted after 10,000 hours. No surface damage was found. After 50,000 hours the specimen condition still appeared to be excellent. Some shallow cracking at the edges of the crossply specimens was visible but did not appear to be of much consequence. During the cure of the doubler adhesive at 450K (350°F), however, delamination of the 50,000 hour crossplied G/E specimens occurred. Similar effects were observed for the G/E specimens aged at 450K (350°F) in one atmosphere air for 10,000 hours (see Figure 8-12). In neither case was the damage sufficient to preclude tensile testing.

**Table 8-1 Thermal Aging Data for $[0°]_6$ B/E in 0.10 MN/m² (14.7 psi) Air**

| Aging Temperature K | Aging Temperature (°F) | Test Temperature K | Test Temperature (°F) | Aging Time (hr) | Tensile Strength MN/m2 | Tensile Strength (ksi) |
|---|---|---|---|---|---|---|
| 394 | 250 | 450 | 350 | Baseline avg | 1380 | 200 |
| | | | | 100 | 1390 | 202 |
| | | | | | 1350 | 196 |
| | | | | | 1370 | 198 |
| | | | | | avg 1370 | 199 |
| | | | | 500 | 1460 | 212 |
| | | | | | 1360 | 197 |
| | | | | | 1340 | 194 |
| | | | | | avg 1390 | 201 |
| | | | | 1,000 | 1330 | 193 |
| | | | | | 1390 | 201 |
| | | | | | 1380 | 200 |
| | | | | | avg 1370 | 198 |
| | | | | 5,000 | 1480 | 214 |
| | | | | | 1450 | 210 |
| | | | | | 1520 | 220 |
| | | | | | avg 1480 | 215 |
| | | | | 10,000 | 1410 | 204 |
| | | | | | 1430 | 208 |
| | | | | | 1450 | 211 |
| | | | | | avg 1430 | 208 |
| | | | | 25,000 | 1240 | 180 |
| | | | | | 1400 | 203 |
| | | | | | 1390 | 202 |
| | | | | | avg 1340 | 195 |
| | | | | 50,000 | 1280 | 186 |
| | | | | | 1320 | 192 |
| | | | | | 1300 | 188 |
| | | | | | avg 1300 | 189 |

**Table 8-2 Thermal Aging Data for $[0° \pm 45°]_s$ Crossply B/E in 0.10 MN/m2 (14.7 psi) Air**

| Aging Temperature K | Aging Temperature (°F) | Test Temperature K | Test Temperature (°F) | Aging Time (hr) | Tensile Strength MN/m2 | Tensile Strength (ksi) |
|---|---|---|---|---|---|---|
| 394 | 250 | 450 | 350 | Baseline avg | 550 | 79.8 |
| | | | | 100 | 510 | 73.9 |
| | | | | | 496 | 71.9 |
| | | | | | 493 | 71.5 |
| | | | | | avg 500 | 72.4 |
| | | | | 500 | 478 | 69.4 |
| | | | | | 428 | 62.1 |
| | | | | | 474 | 68.7 |
| | | | | | avg 460 | 66.7 |
| | | | | 1,000 | 512 | 74.2 |
| | | | | | 504 | 73.1 |
| | | | | | 539 | 78.2 |
| | | | | | avg 518 | 75.2 |
| | | | | 5,000 | 535 | 77.6 |
| | | | | | 527 | 76.4 |
| | | | | | 533 | 77.3 |
| | | | | | avg 532 | 77.1 |
| | | | | 10,000 | 538 | 78.1 |
| | | | | | 534 | 77.4 |
| | | | | | 522 | 75.7 |
| | | | | | avg 531 | 77.1 |
| | | | | 25,000 | 443 | 64.2 |
| | | | | | 462 | 67.0 |
| | | | | | 404 | 58.6 |
| | | | | | avg 436 | 63.3 |
| | | | | 50,000 | 428 | 62.1 |
| | | | | | 388 | 56.3 |
| | | | | | 448 | 65.0 |
| | | | | | avg 421 | 61.1 |

Table 8-3 Thermal Aging Data for $[0°]_6$ B/E in 0.10 MN/m² (14.7 psi) Air

| Aging Temperature K | Aging Temperature (°F) | Test Temperature K | Test Temperature (°F) | Aging Time (hr) | Tensile Strength MN/m2 | Tensile Strength (ksi) |
|---|---|---|---|---|---|---|
| 450 | 350 | 450 | 350 | Baseline avg | 1380 | 200 |
| | | | | 5,000 | 1230 | 179 |
| | | | | | 1240 | 180 |
| | | | | | 1250 | 182 |
| | | | | | avg 1240 | 180 |
| | | | | 10,000 | 1010 | 146 |
| | | | | | 1010 | 147 |
| | | | | | 1080 | 156 |
| | | | | | avg 1030 | 150 |
| | | | | 25,000 | 1130 | 164 |
| | | | | | 1160 | 168 |
| | | | | | 1030 | 150 |
| | | | | | avg 1110 | 161 |
| | | | | 50,000 | 986 | 143 |
| | | | | | 1010 | 147 |
| | | | | | 1000 | 145 |
| | | | | | avg 1000 | 145 |

Table 8-4 Thermal Aging Data for $[0° \pm 45°]_s$ Crossply B/E in 0.10 MN/m² (14.7 psi) Air

| Aging Temperature K | Aging Temperature (°F) | Test Temperature K | Test Temperature (°F) | Aging Time (hr) | Tensile Strength MN/m2 | Tensile Strength (ksi) |
|---|---|---|---|---|---|---|
| 450 | 350 | 450 | 350 | Baseline avg | 550 | 79.8 |
| | | | | 500 | 544 | 78.9 |
| | | | | | 461 | 66.9 |
| | | | | | 517 | 75.0 |
| | | | | | avg 507 | 73.6 |
| | | | | 1,000 | 581 | 84.2 |
| | | | | | 508 | 73.7 |
| | | | | | 493 | 71.5 |
| | | | | | avg 527 | 76.5 |
| | | | | 5,000 | 310 | 44.9 |
| | | | | | 319 | 46.3 |
| | | | | | 309 | 44.8 |
| | | | | | avg 313 | 45.3 |
| | | | | 10,000 | 339 | 49.2 |
| | | | | | 342 | 49.6 |
| | | | | | 314 | 45.6 |
| | | | | | avg 332 | 48.1 |
| | | | | 25,000 | 310 | 45.0 |
| | | | | | 293 | 42.5 |
| | | | | | 301 | 43.7 |
| | | | | | avg 301 | 43.7 |
| | | | | 50,000 | 325 | 47.2 |
| | | | | | 297 | 43.1 |
| | | | | | 268 | 38.8 |
| | | | | | avg 296 | 43.0 |

**Table 8-5 Thermal Aging Data for B/E Aged in 0.014 MN/m² (2 psi) Air**

| Aging Temperature K | Aging Temperature (°F) | Orientation | Test Temperature K | Test Temperature (°F) | Aging Time (hr) | Tensile Strength MN/m2 | Tensile Strength (ksi) |
|---|---|---|---|---|---|---|---|
| 450 | 350 | $[0°]_6$ | 450 | 350 | Baseline avg | 1380 | 200 |
| | | | | | 5,000 | 1520 | 220 |
| | | | | | | 1290 | 187 |
| | | | | | | 1400 | 203 |
| | | | | | | avg 1400 | 203 |
| | | | | | 10,000 | 1390 | 201 |
| | | | | | | 1340 | 195 |
| | | | | | | 1400 | 203 |
| | | | | | | avg 1380 | 200 |
| | | | | | 25,000 | 979 | 142 |
| | | | | | | 1010 | 146 |
| | | | | | | 1090 | 158 |
| | | | | | | avg 1030 | 149 |
| | | | | | 50,000 | 958 | 139 |
| | | | | | | 1090 | 158 |
| | | | | | | 1210 | 176 |
| | | | | | | avg 1090 | 158 |
| 450 | 350 | $[0 \pm 45°]_s$ | 450 | 350 | Baseline avg | 550 | 79.8 |
| | | | | | 5,000 | 519 | 75.3 |
| | | | | | | 529 | 76.7 |
| | | | | | | 590 | 85.6 |
| | | | | | | avg 546 | 79.2 |
| | | | | | 10,000 | 379 | 54.9 |
| | | | | | | 367 | 53.2 |
| | | | | | | 381 | 55.3 |
| | | | | | | avg 376 | 54.5 |
| | | | | | 25,000 | 290 | 42.0 |
| | | | | | | 297 | 43.1 |
| | | | | | | 355 | 51.5 |
| | | | | | | avg 314 | 45.5 |
| | | | | | 50,000 | 332 | 48.1 |
| | | | | | | 327 | 47.4 |
| | | | | | | 350 | 50.8 |
| | | | | | | avg 336 | 48.8 |

Table 8-6 Thermal Aging Data for $[0°]_6$ G/E in 0.10 MN/m² (14.7 psi) Air

| Aging Temperature K | Aging Temperature (°F) | Test Temperature K | Test Temperature (°F) | Aging Time (hr) | Tensile Strength MN/m2 | Tensile Strength (ksi) |
|---|---|---|---|---|---|---|
| 394 | 250 | 450 | 350 | Baseline avg | 1590 | 230 |
| | | | | 100 | 1520 | 220 |
| | | | | | 1590 | 230 |
| | | | | | 1540 | 224 |
| | | | | | avg 1550 | 225 |
| | | | | 500 | 1410 | 205 |
| | | | | | 1270 | 184 |
| | | | | | 1470 | 213 |
| | | | | | avg 1390 | 201 |
| | | | | 1,000 | 1480 | 214 |
| | | | | | 1560 | 227 |
| | | | | | 1450 | 210 |
| | | | | | avg 1500 | 217 |
| | | | | 5,000 | 1630 | 236 |
| | | | | | 1600 | 232 |
| | | | | | 1440 | 209 |
| | | | | | avg 1560 | 226 |
| | | | | 10,000 | 1650 | 240 |
| | | | | | 1650 | 239 |
| | | | | | 1850 | 268 |
| | | | | | avg 1720 | 249 |
| | | | | 25,000 | 1670 | 242 |
| | | | | | 1650 | 239 |
| | | | | | 1520 | 220 |
| | | | | | avg 1610 | 234 |
| | | | | 50,000 | 1560 | 226 |
| | | | | | 1500 | 217 |
| | | | | | 1510 | 219 |
| | | | | | avg 1520 | 221 |

Table 8-7 Thermal Aging Data for $[0° \pm 45°]_s$ Crossply G/E in 0.10 MN/m² (14.7 psi) Air

| Aging Temperature K | Aging Temperature (°F) | Test Temperature K | Test Temperature (°F) | Aging Time (hr) | Tensile Strength MN/m2 | Tensile Strength (ksi) |
|---|---|---|---|---|---|---|
| 394 | 250 | 450 | 350 | Baseline avg | 500 | 72.5 |
| | | | | 100 | 496 | 72.0 |
| | | | | | 542 | 78.6 |
| | | | | | 483 | 70.0 |
| | | | | | avg 507 | 73.5 |
| | | | | 500 | 475 | 68.9 |
| | | | | | 492 | 71.4 |
| | | | | | 494 | 71.7 |
| | | | | | avg 487 | 70.7 |
| | | | | 1,000 | 494 | 71.6 |
| | | | | | 552 | 80.0 |
| | | | | | 626 | 90.8 |
| | | | | | avg 557 | 80.8 |
| | | | | 5,000 | 589 | 85.4 |
| | | | | | 559 | 81.8 |
| | | | | | 536 | 77.7 |
| | | | | | avg 561 | 81.4 |
| | | | | 10,000 | 559 | 81.1 |
| | | | | | 593 | 86.0 |
| | | | | | 585 | 84.9 |
| | | | | | avg 579 | 84.0 |
| | | | | 25,000 | 405 | 58.8 |
| | | | | | 492 | 71.3 |
| | | | | | 441 | 63.9 |
| | | | | | avg 446 | 64.7 |
| | | | | 50,000 | 245 | 35.5 |
| | | | | | 258 | 37.4 |
| | | | | | 287 | 41.6 |
| | | | | | avg 263 | 38.2 |

Table 8-8 Thermal Aging Data for $[0°]_6$ G/E in 0.10 MN/m2 (14.7 psi) Air

| Aging Temperature K | Aging Temperature (°F) | Test Temperature K | Test Temperature (°F) | Aging Time (hr) | Tensile Strength MN/m2 | Tensile Strength (ksi) |
|---|---|---|---|---|---|---|
| 450 | 350 | 450 | 350 | Baseline avg | 1590 | 230 |
| | | | | 100 | 1500 | 218 |
| | | | | | 1650 | 239 |
| | | | | | 1460 | 212 |
| | | | | | avg 1540 | 223 |
| | | | | 500 | 1630 | 236 |
| | | | | | 1620 | 235 |
| | | | | | 1550 | 225 |
| | | | | | avg 1600 | 232 |
| | | | | 1,000 | 1260 | 182 |
| | | | | | 1500 | 218 |
| | | | | | 1540 | 223 |
| | | | | | avg 1430 | 208 |
| | | | | 5,000 | 1210 | 175 |
| | | | | | 1370 | 199 |
| | | | | | 1300 | 188 |
| | | | | | avg 1290 | 188 |
| | | | | 10,000 | 1360 | 198 |
| | | | | | 1270 | 184 |
| | | | | | 1210 | 176 |
| | | | | | avg 1280 | 186 |
| | | | | 25,000 | 958 | 139 |
| | | | | | 1010 | 147 |
| | | | | | 1070 | 155 |
| | | | | | avg 1010 | 147 |
| | | | | 50,000 | 986 | 143 |
| | | | | | 952 | 138 |
| | | | | | 945 | 137 |
| | | | | | avg 958 | 139 |

Table 8-9 Thermal Aging Data for $[0° \pm 45°]_s$ Crossply G/E in 0.10 MN/m² (14.7 psi) Air

| Aging Temperature K | Aging Temperature (°F) | Test Temperature K | Test Temperature (°F) | Aging Time (hr) | Tensile Strength MN/m2 | Tensile Strength (ksi) |
|---|---|---|---|---|---|---|
| 450 | 350 | 450 | 350 | Baseline avg | 500 | 72.5 |
| | | | | 500 | 494 | 71.6 |
| | | | | | 608 | 88.2 |
| | | | | | 559 | 81.1 |
| | | | | | avg 554 | 80.3 |
| | | | | 1,000 | 552 | 80.0 |
| | | | | | 501 | 72.6 |
| | | | | | 563 | 81.6 |
| | | | | | avg 539 | 78.1 |
| | | | | 5,000 | 485 | 70.3 |
| | | | | | 440 | 63.8 |
| | | | | | 474 | 68.7 |
| | | | | | avg 466 | 67.6 |
| | | | | 10,000 | 265 | 38.5 |
| | | | | | 60 | 8.7 |
| | | | | | 238 | 34.5 |
| | | | | | avg 188 | 27.2 |
| | | | | 25,000 | 253 | 36.7 |
| | | | | | 316 | 45.9 |
| | | | | | 321 | 46.5 |
| | | | | | avg 296 | 43.0 |
| | | | | 50,000 | 251 | 36.4 |
| | | | | | 194 | 28.2 |
| | | | | | 272 | 39.5 |
| | | | | | avg 239 | 34.7 |

**Table 8-10 Thermal Aging Data for G/E Aged in 0.014 MN/m² (2 psi) Air**

| Aging Temperature K | Aging Temperature (°F) | Orientation | Test Temperature K | Test Temperature (°F) | Aging Time (hr) | | Tensile Strength MN/m2 | Tensile Strength (ksi) |
|---|---|---|---|---|---|---|---|---|
| 450 | 350 | $[0°]_6$ | 450 | 350 | Baseline avg | | 1590 | 230 |
| | | | | | 5,000 | | 1730 | 251 |
| | | | | | | | 1740 | 252 |
| | | | | | | | 1560 | 227 |
| | | | | | | avg | 1680 | 243 |
| | | | | | 10,000 | | 1770 | 257 |
| | | | | | | | 1870 | 271 |
| | | | | | | | 1760 | 255 |
| | | | | | | avg | 1800 | 261 |
| | | | | | 25,000 | | 1630 | 236 |
| | | | | | | | 1620 | 235 |
| | | | | | | | 1440 | 209 |
| | | | | | | avg | 1560 | 227 |
| | | | | | 50,000 | | 1400 | 203 |
| | | | | | | | 1020 | 148 |
| | | | | | | | 1170 | 170 |
| | | | | | | avg | 1200 | 174 |
| 450 | 350 | $[0 \pm 45°]_s$ | 450 | 350 | Baseline avg | | 500 | 72.5 |
| | | | | | 5,000 | | 584 | 84.7 |
| | | | | | | | 596 | 86.4 |
| | | | | | | | 571 | 82.8 |
| | | | | | | avg | 584 | 84.6 |
| | | | | | 10,000 | | 535 | 77.6 |
| | | | | | | | 498 | 72.3 |
| | | | | | | | 548 | 79.5 |
| | | | | | | avg | 527 | 76.5 |
| | | | | | 25,000 | | 432 | 62.7 |
| | | | | | | | 476 | 69.1 |
| | | | | | | | 485 | 70.3 |
| | | | | | | avg | 465 | 67.4 |
| | | | | | 50,000 | | 358 | 51.9 |
| | | | | | | | 340 | 49.3 |
| | | | | | | | 309 | 44.8 |
| | | | | | | avg | 336 | 48.7 |

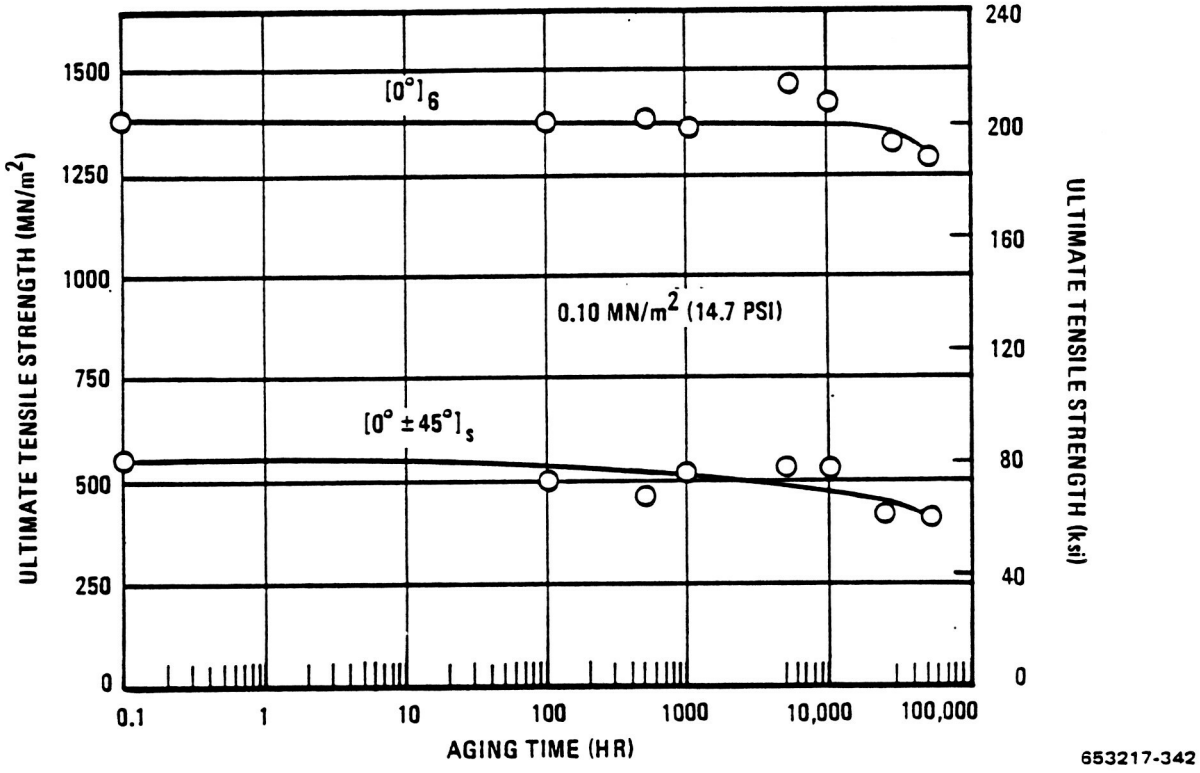



**Figure 8-2 Tensile Strength of B/E at 450K (350°F) After Thermal Aging at 394K (250°F)**

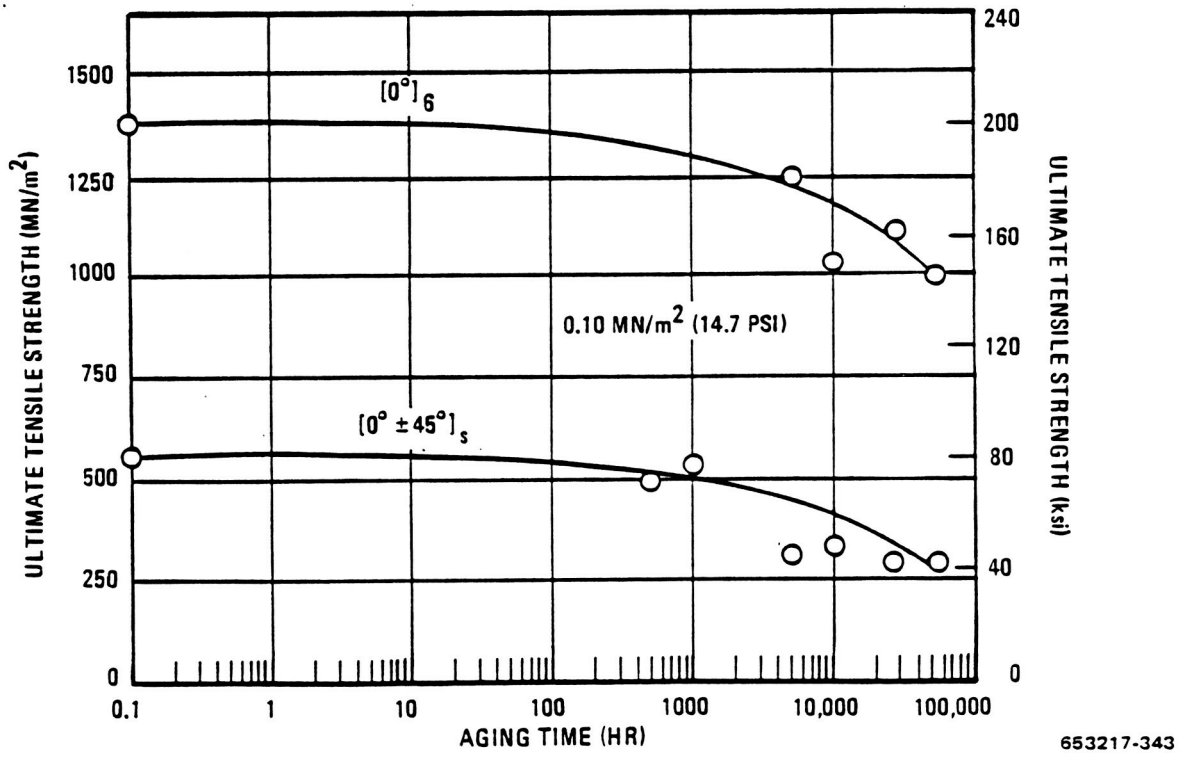



**Figure 8-3 Tensile Strength of B/E at 450K (350°F) After Thermal Aging at the Same Temperature**

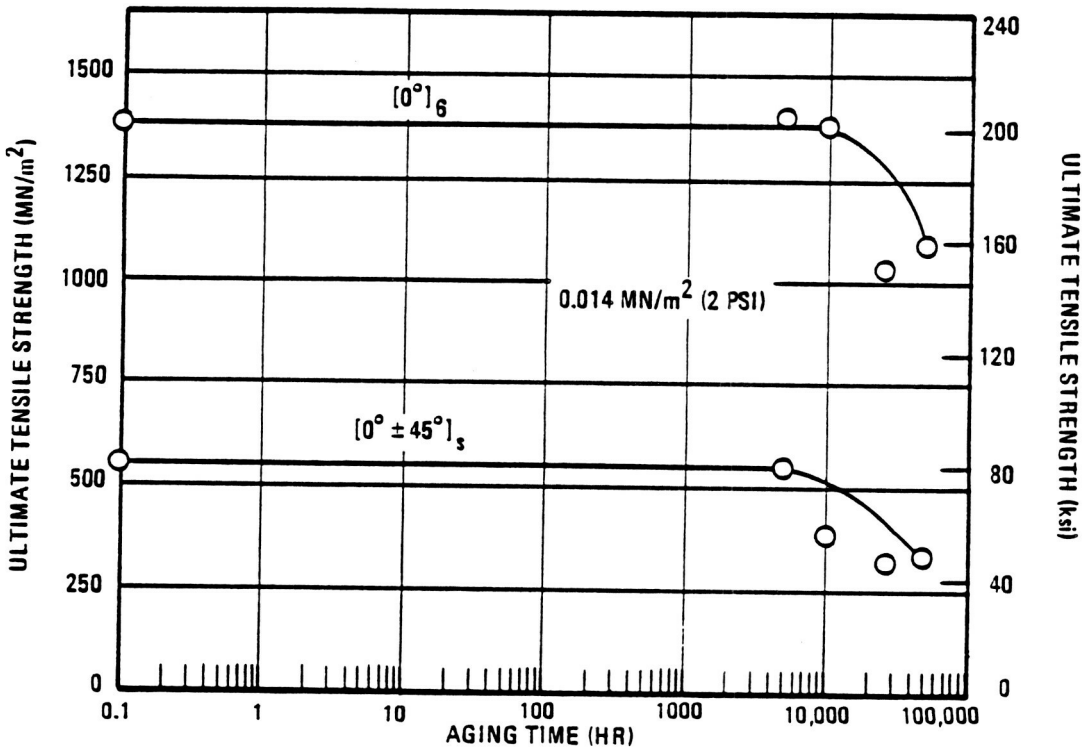



**Figure 8-4 Tensile Strength of B/E at 450K (350°F) After Thermal Aging at the Same Temperature**

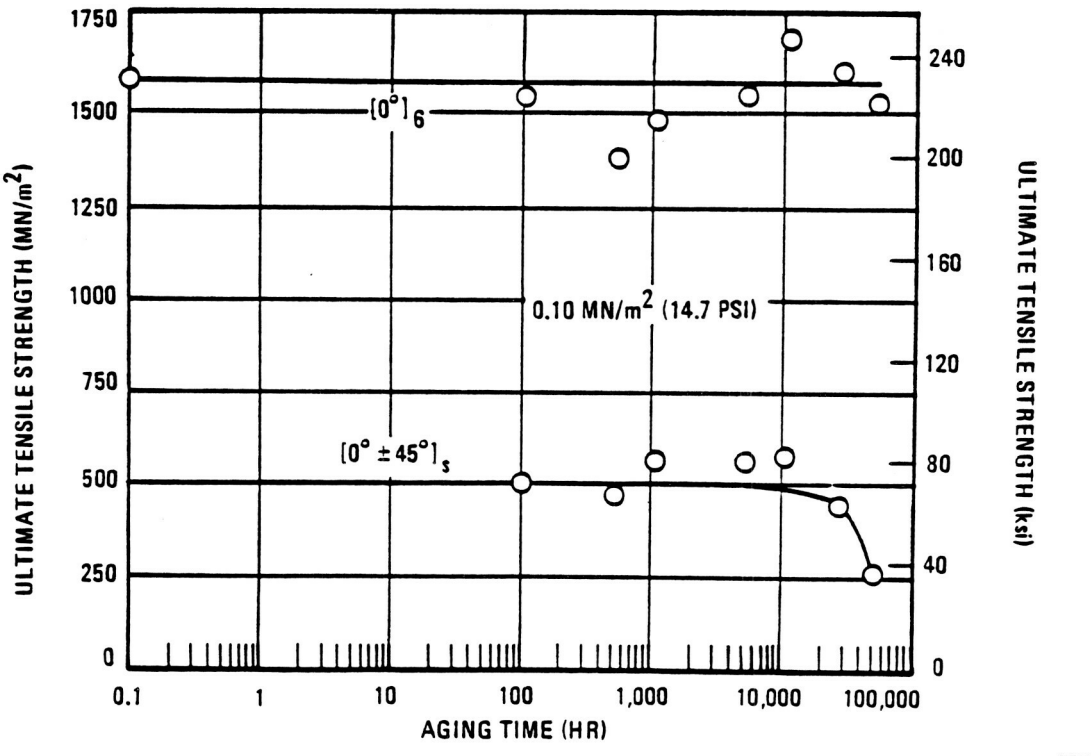



**Figure 8-5 Tensile Strength of G/E at 450K (350°F) After Thermal Aging at 394K (250°F)**

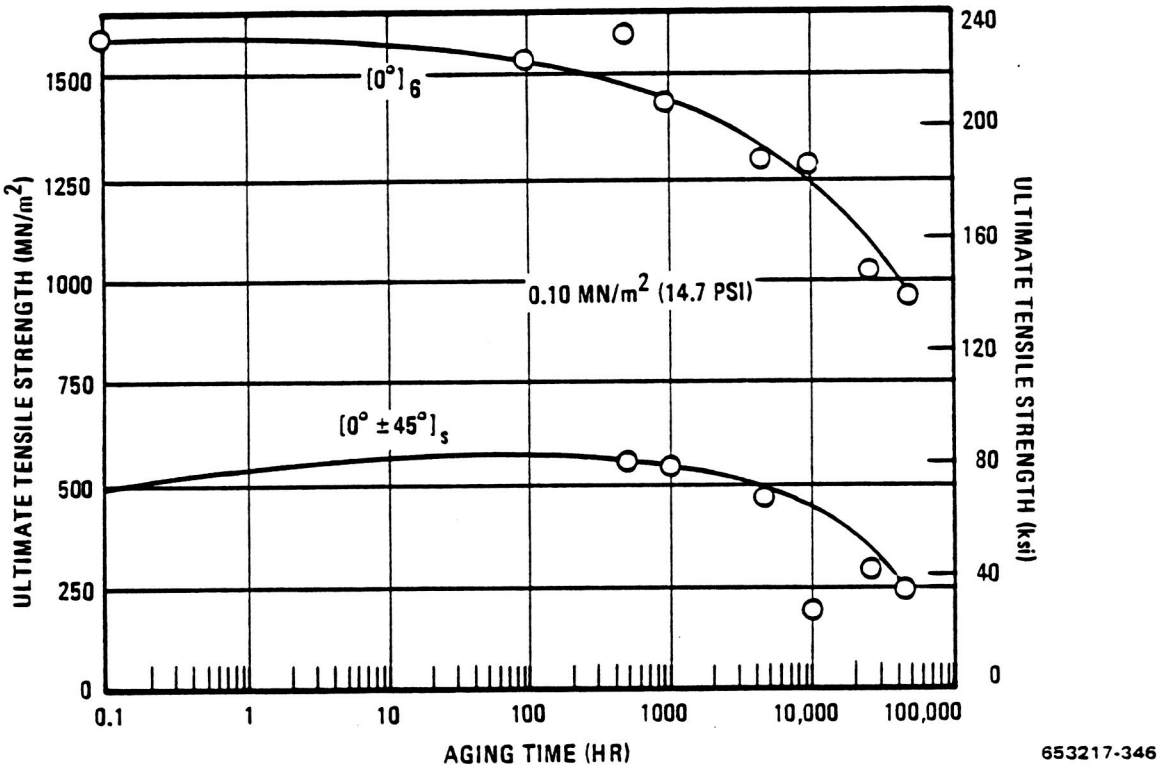



**Figure 8-6 Tensile Strength of G/E at 450K (350°F) After Thermal Aging at the Same Temperature**

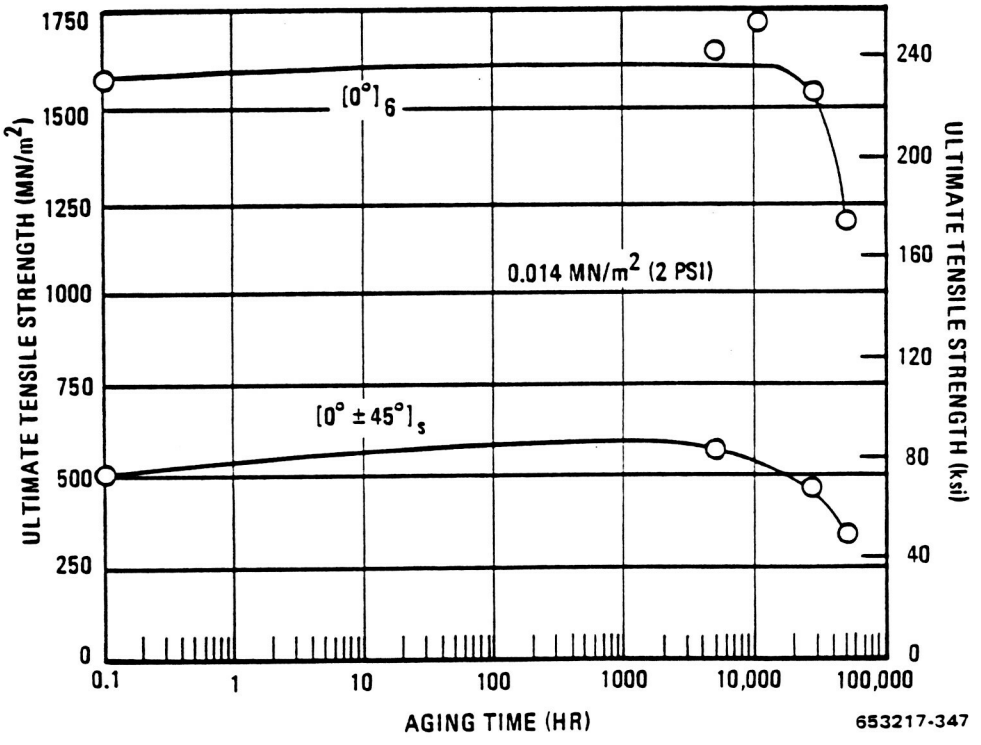



**Figure 8-7 Tensile Strength of G/E at 450K (350°F) After Thermal Aging at the Same Temperature**

**Table 8-11 Summary of Tensile Strength Retention After Thermal Aging of B/E and G/E**

| Material System | Orientation | Aging Temp K | Aging Temp (°F) | Aging Pressure MN/m2 | Aging Pressure (psi) | Test Temp K | Test Temp (°F) | Retention of Tensile Strength (%) 10,000 hrs | Retention of Tensile Strength (%) 50,000 hrs |
|---|---|---|---|---|---|---|---|---|---|
| B/E | $[0°]_6$ | 394 | 250 | 0.10 | 14.7 | 450 | 350 | 100 | 94 |
| | $[0° \pm 45°]_s$ | 394 | 250 | 0.10 | 14.7 | 450 | 350 | 97 | 77 |
| | $[0°]_6$ | 450 | 350 | 0.10 | 14.7 | 450 | 350 | 75 | 72 |
| | $[0° \pm 45°]_s$ | 450 | 350 | 0.10 | 14.7 | 450 | 350 | 60 | 54 |
| | $[0°]_6$ | 450 | 350 | 0.014 | 2 | 450 | 350 | 100 | 79 |
| | $[0° \pm 45°]_s$ | 450 | 350 | 0.014 | 2 | 450 | 350 | 68 | 61 |
| G/E | $[0°]_6$ | 394 | 250 | 0.10 | 14.7 | 450 | 350 | 100 | 96 |
| | $[0° \pm 45°]_s$ | 394 | 250 | 0.10 | 14.7 | 450 | 350 | 100 | 53 |
| | $[0°]_6$ | 450 | 350 | 0.10 | 14.7 | 450 | 350 | 81 | 60 |
| | $[0° \pm 45°]_s$ | 450 | 350 | 0.10 | 14.7 | 450 | 350 | 38 | 48 |
| | $[0°]_6$ | 450 | 350 | 0.014 | 2 | 450 | 350 | 100 | 76 |
| | $[0° \pm 45°]_s$ | 450 | 350 | 0.014 | 2 | 450 | 350 | 100 | 67 |

The residual tensile strengths after aging at 394K (250°F) are shown in Figures 8-2 and 8-5. For the first 10,000 hours of aging, no degradation of the 350°F tensile properties was observed for either system. After 25,000 hours, however, a decrease in tensile strength of the crossply material, both B/E and G/E, had occurred. The effect was not large but appeared to be a real one. Some slight drop in the unidirectional tensile strength of the B/E was also found. Additional decreases in strength were observed for the 50,000 hour specimens, particularly the crossplied G/E.

While no changes in appearance, other than slight color differences, were noticed following aging for 25,000 hours, there were significant changes after tensile testing. The failed tensile coupons, particularly the G/E, were markedly different than those from material that had been aged for times up through 10,000 hours. The epoxy matrix at the surface of the 25,000 hour G/E specimens had broken up during test and crumbled off, revealing the the graphite fibers in the outer plies. At failure, the graphite tows opened up, giving a very fuzzy appearance to the test section of the specimens. The specimens aged at 450K (350°F) in one atmosphere air showed this effect to some degree after 5000 hours. Specimens aged 10,000 hours at 450K (350°F) were almost identical to the ones described above that were aged 25,000 hours at 394K (250°F). The appearance of the failed specimens is supporting evidence that the slight fall-off in tensile properties after 25,000 hours marks the beginning of significant degradation to the epoxy matrix specimens when aged at 394K (250°F) in one atmosphere air. After 50,000 hours of exposure the failed G/E tensile specimens had lost not only the resin at the surface but much of the matrix throughout the thickness. Some changes in appearance from those after 10,000 hours were also observed in the as-tested B/E specimens aged 25,000 hours at 394K (250°F). There was very little damage to the 10,000 hour specimens after tensile testing except near the fracture location. For the 25,000 hour specimens, however, the matrix at the surface was beginning to show evidence of breaking up during testing, revealing some of the boron fibers. The effect was not as pronounced as that seen in the G/E specimens after 25,000 hours. The breaking up and loss of the epoxy matrix during tensile testing increased considerably for the 50,000 hour B/E specimens. Numerous boron fibers were visible in these specimens. In comparison with other exposures, the specimen condition was intermediate between the 10,000 hour, 450K (350°F), 0.014 MN/m$^2$ (2 psi) and the 5000 hour, 450K (350°F), 0.10 MN/m$^2$ (14.7 psi) B/E specimens.

Portions of failed test specimens before and after aging at 394K (250°F) are shown in Figure 8-8 for B/E and Figure 8-9 for G/E. Evidence of the excellent condition of the B/E after 25,000 hours and the G/E after 10,000 hours can be seen by comparing the failed tensile specimens before and after aging. No significant differences are visible. On the other hand, the change in appearance of the failed specimens between 25,000 hours and 50,000 hours of exposure for B/E and between 10,000 hours and 25,000 hours of exposure for G/E is quite distinct.

**450K, 0.10 MN/m$^2$ (350°F, 14.7 psi) EXPOSURE.** Thermal aging of the epoxy systems at 450K (350°F) produced significant degradation when exposure was carried out at ambient pressure. Degradation in tensile properties combined with a significant change in appearance of the specimens, particularly after tensile testing, occurred after 5000 hours. For these specimens the epoxy resin matrix, in many areas, crumbled away during tensile testing — exposing the boron or graphite filaments. Portions of failed test specimens of each material before and after aging at 450 K (350°F) are shown in Figures 8-10 and 8-11. The change in appearance of the failed specimens between 1000 hours and 5000 hours of exposure is quite distinct. While not apparent from Figure 8-10 and 8-11, the loss of resin after 5000 hours was somewhat greater for the B/E than for the G/E material. One other observation was made during bonding of doublers to the 5000 hour tensile specimens. Prior to applying the adhesive, the ends were lightly polished with Scotch-

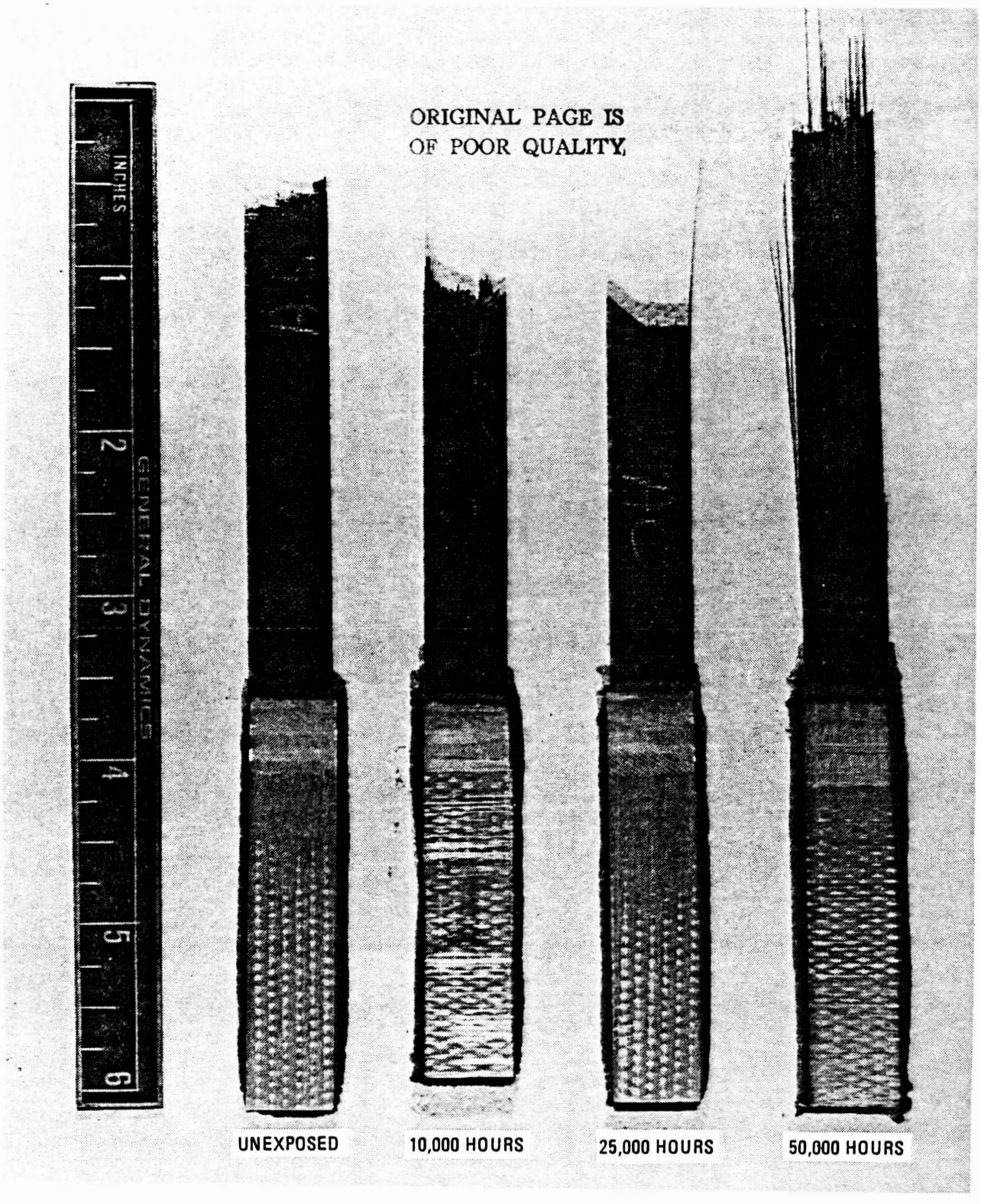



**Figure 8-8 B/E Before and After Thermal Aging at 394K (250°F) in One Atmosphere Air and Tensile Testing at 450K (350°F)**

ORIGINAL PAGE IS
OE POOR QUALITY

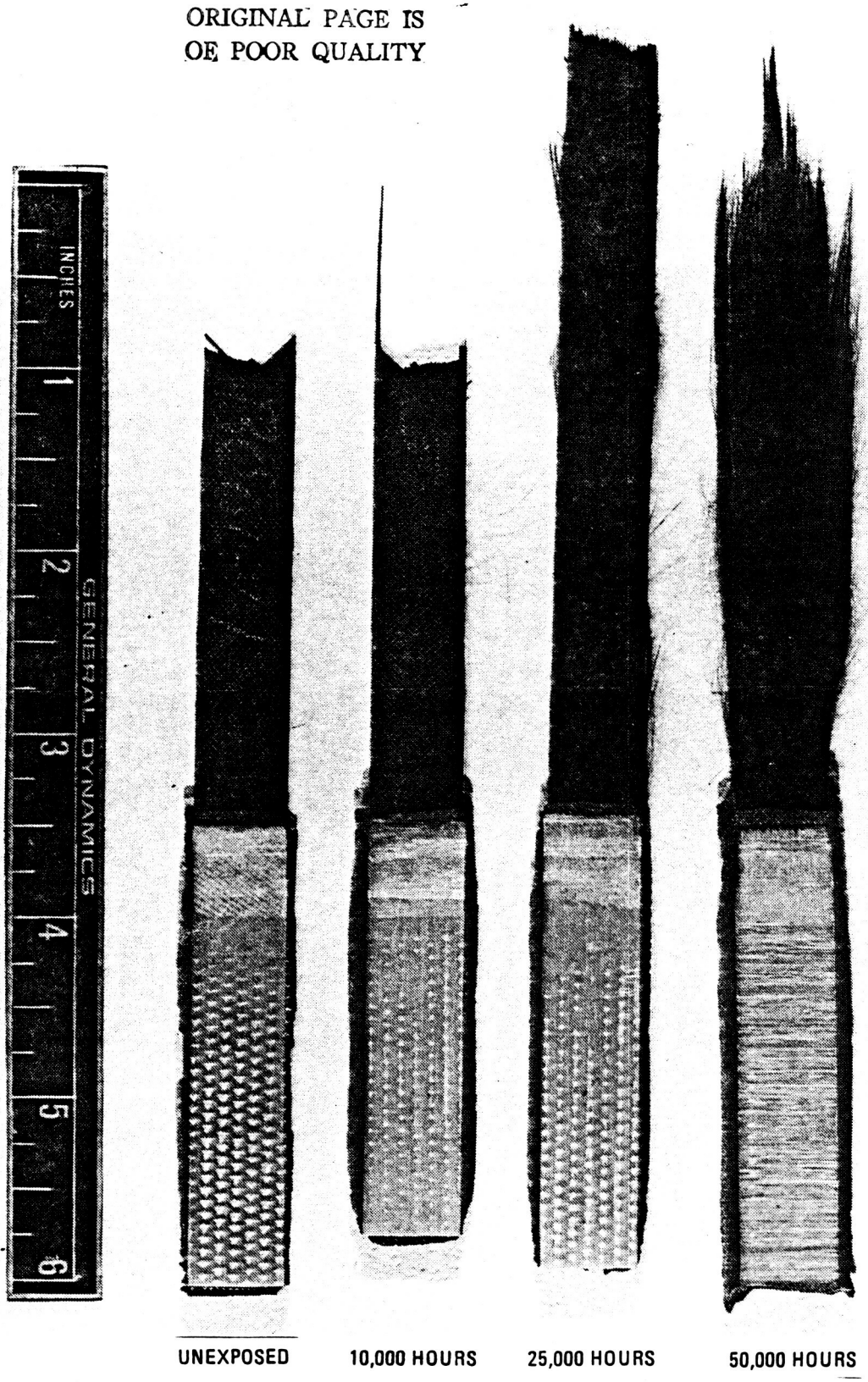



**Figure 8-9 G/E Before and After Thermal Aging at 394K (250°F) in One Atmosphere Air and Tensile Testing at 450K (350°F)**

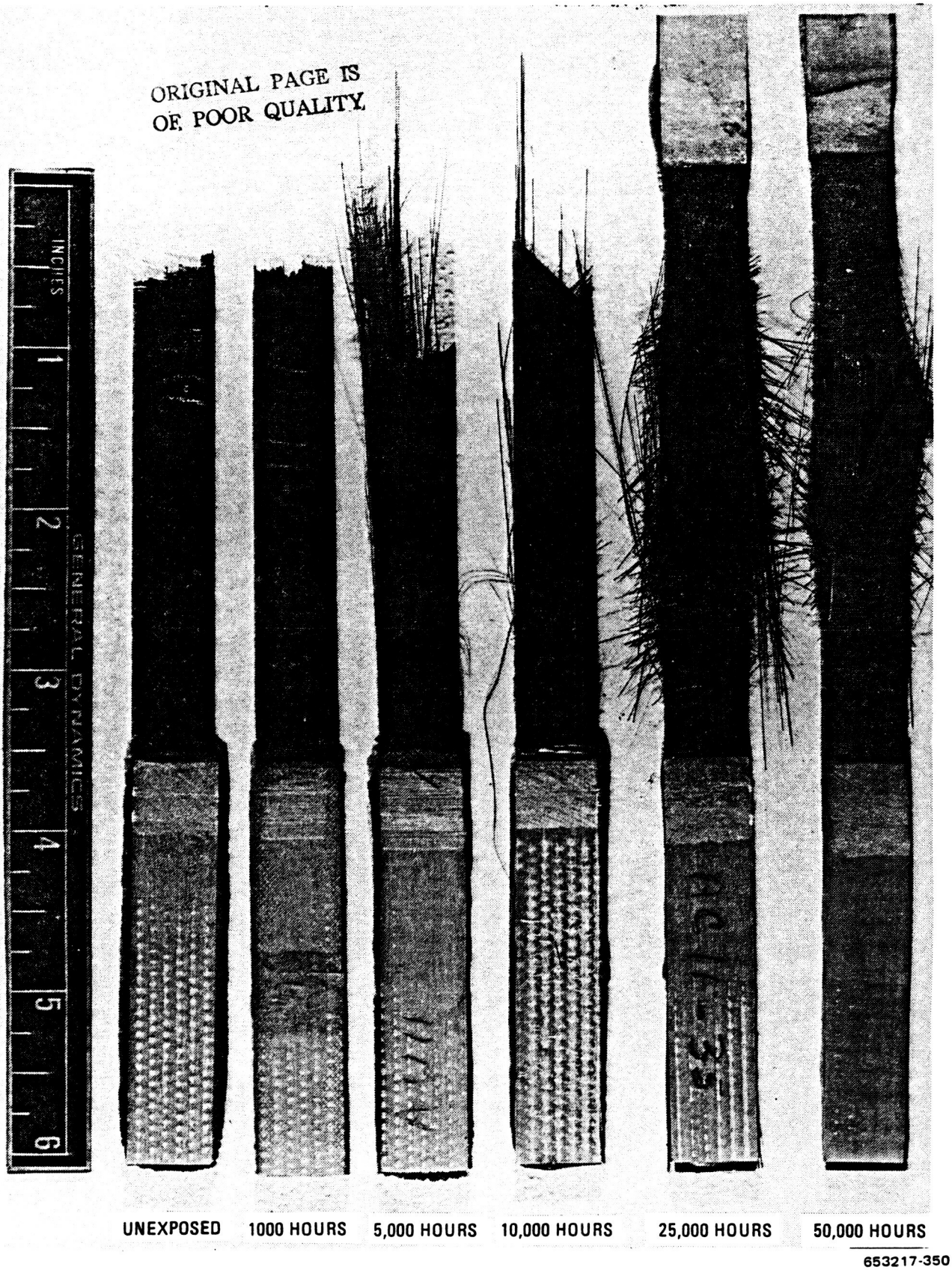



**Figure 8-10 B/E Before and After Thermal Aging at 450K (350°F) in One Atmosphere Air and Tensile Testing at the Same Temperature**

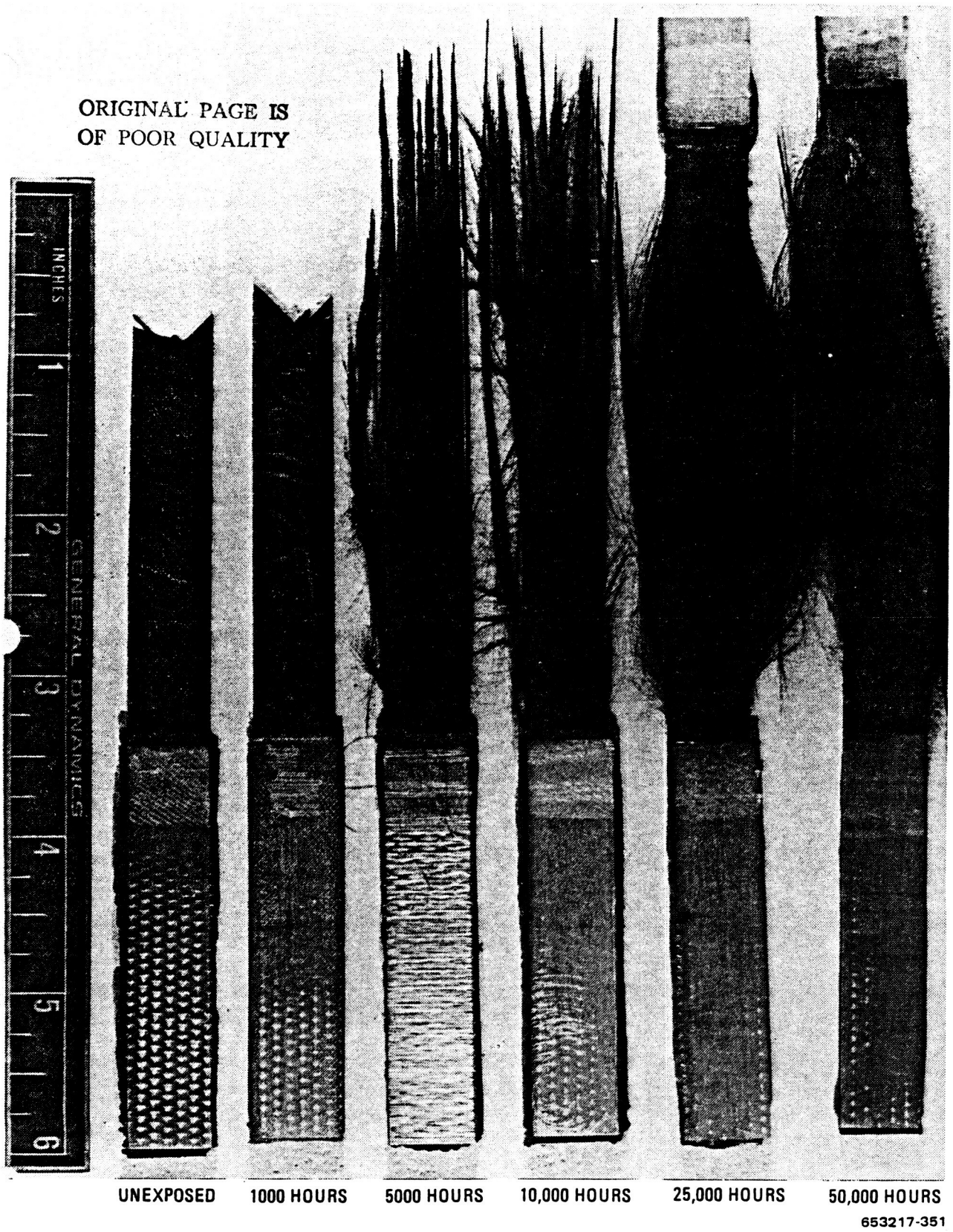



**Figure 8-11 G/E Before and After Thermal Aging at 450K (350°F) in One Atmosphere Air and Tensile Testing at the Same Temperature**

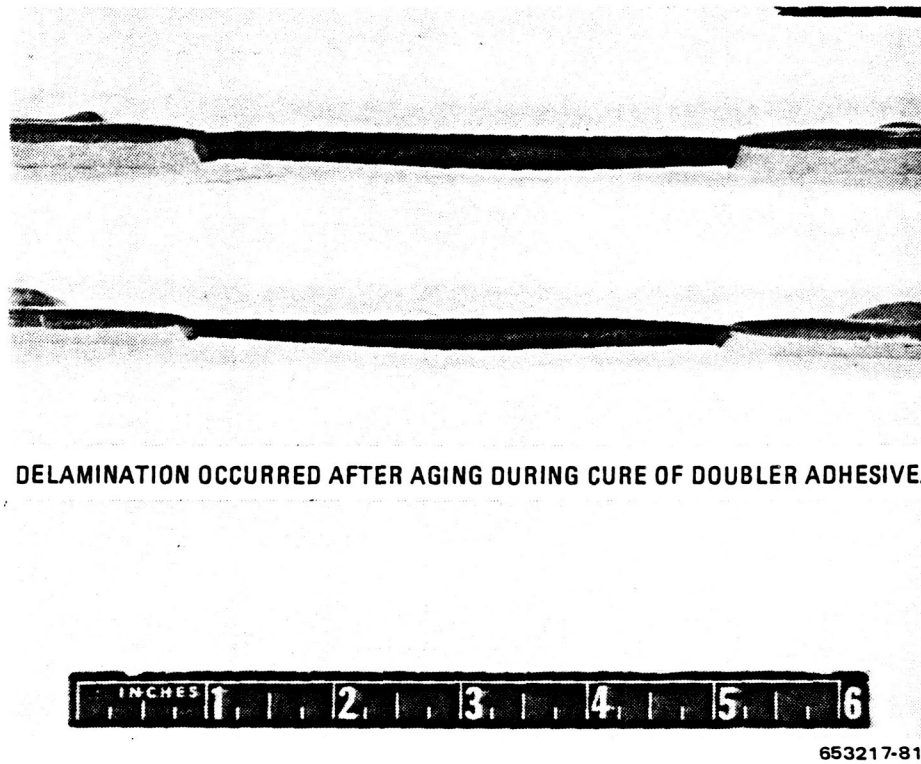



**Figure 8-12 G/E Tensile Specimens After 10,000 Hours of Thermal Aging at 450K (350°F) in One Atmosphere Air**

Brite. For the B/E samples exposed at ambient pressure, just a slight amount of rubbing removed the outer powdery layer of resin and revealed the boron fibers of the outer plies. Such an effect was not observed for the G/E specimens or the reduced pressure B/E specimens.

After 10,000 hours of thermal aging at 456K (350°F), further degradation of the epoxy materials was observed. The G/E specimens showed a slight color change (to a darker brown) but, otherwise, were visually unchanged by the 10,000 hour exposure. However, during doubler bonding the $[0° \pm 45°]_s$ specimens aged at ambient pressure all delaminated. Figure 8-12 shows the poor condition of these specimens. The tensile strength of these crossplied specimens was very low, while the unidirectional specimens showed a decrease of about 25%. The appearance of the specimens after test was similar to those aged for 5000 hours at 450K (350°F), see Figure 8-11.

The epoxy matrix crumbled away during tensile testing leaving the bare graphite tows looking like a bundle of yarn. The relatively high tensile strength of the unidirectional specimens, 1680 $MN/m^2$ (186 ksi), after 10,000 hours exposure is somewhat misleading as to the actual quality of the material. A transverse tensile or shear test that measures the matrix strength would undoubtedly give extremely poor results.

The B/E specimens aged in ambient air were in very poor condition after the 10,000 hour exposure at 450K (350°F). Two of the crossplied specimens were delaminated when removed from the aging furnace, and slight flexing of the third specimen during handling also resulted in delamination. Figure 8-13 shows the two delaminated crossplied specimens prior to doubler bonding. For the unidirectional specimens much of the resin was gone from the surface, exposing many of the outer boron filaments. Some of these outer filaments were lost during the doubler bonding opera-



ORIGINAL PAGE IS
OF POOR QUALITY

ORIGINAL PAGE IS
OF POOR QUALITY

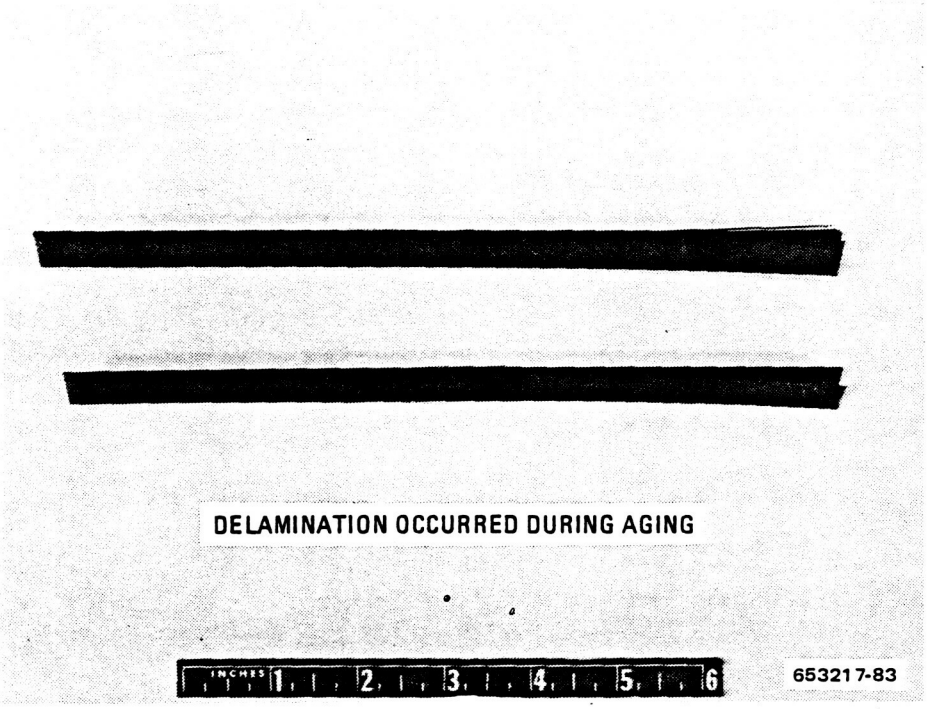



**Figure 8-13 Crossplied B/E After 10,000 Hours of Thermal Aging at 450K (350°F) in One Atmosphere Air**

tion. The unidirectional specimens had very little transverse stiffness and could easily be bent by hand. Again, the crossplied specimens showed a greater decrease in tensile properties than the unidirectional specimens. In like manner to the G/E material, the tensile results don't indicate how badly the B/E had been degraded by the 10,000 hours in ambient air at 450K (350°F). The resin matrix has retained almost no strength after the aging exposure. Figure 8-10 shows failed tensile specimens after various exposure times at 450K (350°F) in ambient air. The 10,000 hour specimens consist primarily of broken boron fibers and scrim cloth with much of the epoxy matrix having crumbled and fallen away from the test section between the doublers.

In addition to the slight color changes, first observed after 10,000 hours, the G/E showed a few small edge cracks after 25,000 hours at 450K (350°F). Otherwise, the appearance was visually unchanged by the exposure. After 50,000 hours the surface of the specimens had a burned appearance with some loose graphite fibers at the edges. There was some slight edge cracking and indications that delamination might be starting. The specimens gave off a dead sound when dropped on a hard surface rather than the typical ringing sound associated with unaged material. The specimens offered little resistance to bending.

In contrast to the G/E material the B/E specimens were in very poor condition after the 25,000 hour exposure at 450K (350°F). The matrix, because of severe oxidation, was very brittle and crumbled away at the touch. All specimens showed edge cracks, exposed and loosened surface fibers, and color changes. One of the specimens delaminated into three separate layers as a result of the handling required to perform the visual examination. After 50,000 hours, edge cracking,

loss of resin from the surface, and loose fibers had all increased. Several of the specimens were delaminated, and all offered little resistance to bending. In like manner to the G/E system the specimens gave off a dead sound when dropped on a hard surface.

Because of the poor condition of the specimens after 25,000 hours and 50,000 hours of exposure, a room temperature curing adhesive was selected for doubler bonding, and the tensile tests at 450K (350°F) were conducted using a short ring furnace. With this furnace, only the center portion of the specimens was heated to 450K (350°F), while the grips remained very close to the ambient temperature. Even so, all of the B/E specimens delaminated in the central section between the doublers during the doubler bonding operation. Two of the 25,000 hour and all three of the 50,000 hour crossply G/E specimens also delaminated during doubler bonding. Crossply specimens have typically shown more tendency toward delamination after thermal aging. In spite of the extensive delamination all of these epoxy specimens could be tensile tested. These tensile results, Figures 8-3 and 8-6, are similar to those after 10,000 hours of aging and give no indication of how severely the B/E and G/E composites had been degraded by the 25,000 and 50,000 hours of exposure. The resin matrix in each system had retained almost no strength as a result of the aging. A test that measures matrix strength, e.g., shear, compressive, or transverse tensile would have produced results very close to zero. After test, the failed B/E specimens, Figure 8-10, consisted primarily of broken boron fibers and scrim cloth with most of the epoxy matrix having crumbled and fallen away from the test section between the doublers. For the G/E specimens, Figure 8-11, the resin matrix also crumbled away during tensile testing, leaving the bare graphite tows looking like a bundle of yarn.

**450K, 0.014 MN/m² (350°F, 2 psi) EXPOSURE.** Thermal aging of the epoxy systems at 450K (350°F) for 5000 hours produced significant degradation when exposure was carried out at ambient pressure but almost no effects when aging was done at a reduced pressure of 0.014 MN/m² (2 psi). Specimens of both B/E and G/E exposed at the reduced pressure showed essentially no reduction in 450K (350°F) tensile strength and failed in a manner typical of unexposed material.

After 10,000 hours of aging the G/E specimens still retained 100% of the 450K (350°F) tensile strength and had a failure appearance after tensile testing similar to that of unexposed material. In contrast to the G/E material, the B/E specimens aged for 10,000 hours at 450K (350°F) and 0.014 MN/m² (2 psi) showed both a reduction in strength and a change in failure appearance. The unidirectional specimens retained 100% of the 450K (350°F) tensile strength, but the crossplied specimens only approximately 70% (Figure 8-4). Many bare filaments were visible in the failed specimens of both layups where the resin matrix had broken up. The effect was not as pronounced as that observed for the 450K (350°F) and 0.10 MN/m² (14.7 psi) tests, but, compared to unexposed specimens where almost no bare filaments occur, the indications are clear that the matrix is starting to degrade even at reduced pressure. The difference between the 5000 hour and 10,000 hour failure appearance can be seen in Figure 8-14.

The first change in appearance after aging at reduced pressure but before tensile testing was observed for the 25,000 hour specimens. Both the B/E and G/E showed slight color changes and a few small edge cracks. After 50,000 hours the B/E specimens showed considerable degradation in the form of loss of resin, loosened boron fibers, delamination, and a dead sound when dropped. The condition was similar to the specimens exposed at one atmosphere for the same time and temperature. The G/E specimens, on the other hand, were not much different from the 25,000 hour group other than a somewhat burned looking surface and slightly less ring when dropped.

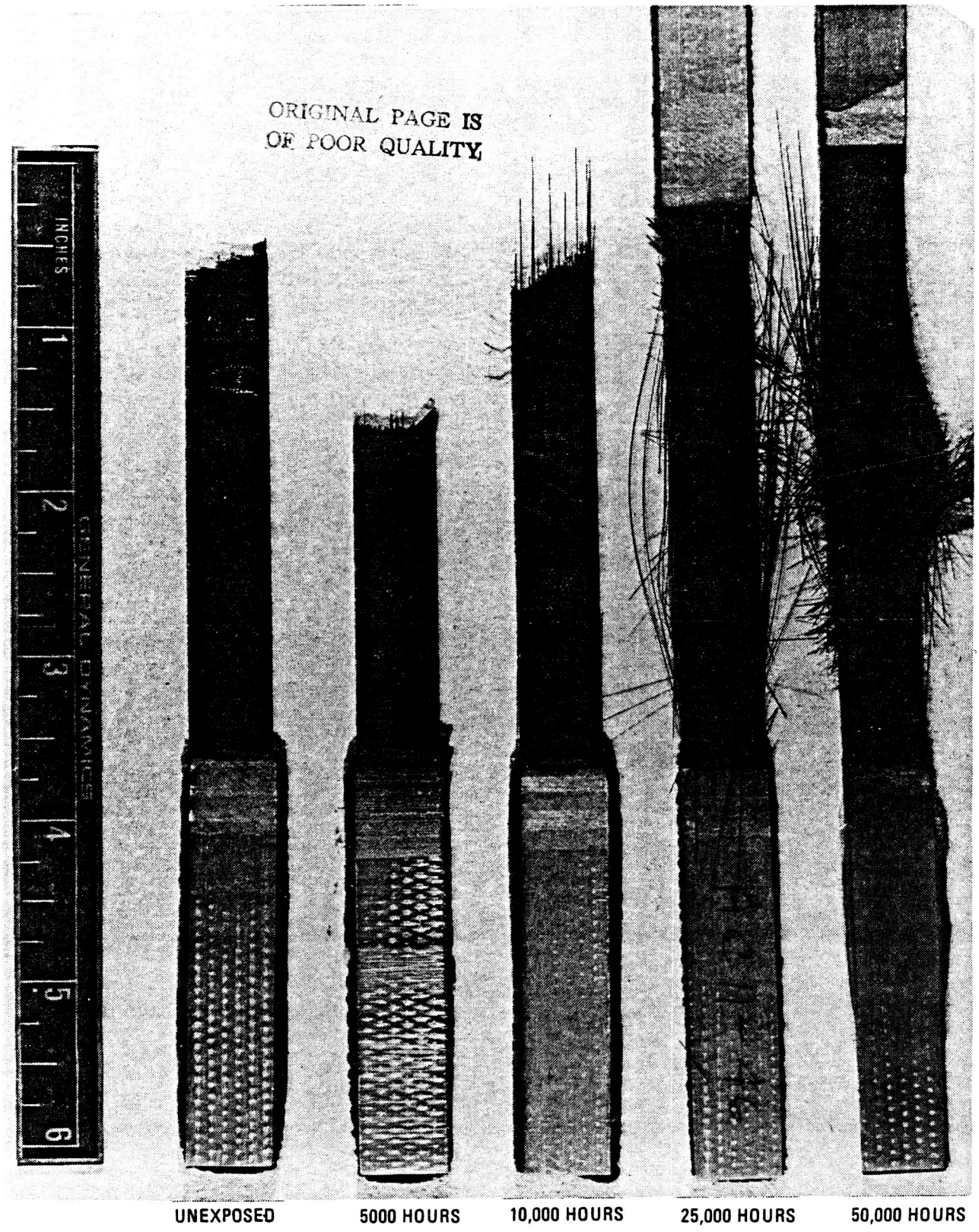



**Figure 8-14 B/E Before and After Thermal Aging at 450K (350°F) in 0.014 MN/m² (2 psi) Air and Tensile Testing at the Same Temperature**

Tensile results for the specimens aged at reduced pressure are plotted in Figures 8-4 and 8-7. The degradation in 450K (350°F) tensile strength and the appearance of the failed B/E specimens after both 25,000 and 50,000 hours were very nearly the same as those for the one atmosphere specimens. At a reduced pressure of 0.014 MN/m² (2 psi) air, B/E begins to experience some matrix degradation between 5000 and 10,000 hours. By 25,000 hours, the degradation, as shown in Figure 8-14, is very severe. For the G/E specimens aged in 0.014 MN/m² (2 psi) air, a slight decrease in tensile strength after 25,000 hours accompanied by a change in appearance of the failed test specimens indicates the beginning of matrix degradation. After 50,000 hours the tensile strength had decreased considerably, and the appearance of the failed specimens was much worse than the 25,000 hour group. Failed tensile specimens before and after thermal aging are shown in Figure 8-15. The resin loss and amount of graphite fibers exposed after 50,000 hours of aging at reduced pressure were about the same as observed for the 5000 hour, 450K (350°F), 0.10 MN/m² (14.7 psi) specimens after tensile testing (see Figure 8-11).

In summary, at 394K (250°F) and 0.10 MN/m² (14.7 psi) matrix embrittlement of the B/E and G/E systems began between 10,000 and 25,000 hours, and slight decreases in tensile strength occurred. The effects were worse for the G/E. After 50,000 hours of exposure matrix embrittlement was severe for both systems. At 450K (350°F) and 0.10 MN/m² (14.7 psi) matrix embrittlement of the B/E and G/E systems began between 1000 and 5000 hours, and at the same time tensile strength losses were observed. Severe matrix embrittlement was found for all exposures from 5000 to 50,000 hours. For thermal aging at 450K (350°F) and 0.014 MN/m² (2 psi), matrix embrittlement of the B/E system began between 5000 and 10,000 hours and was severe by 25,000 hours. The G/E system was somewhat better with the beginning of embrittlement starting between 10,000 and 25,000 hours. By 50,000 hours the effect was severe.

**8.2.1.1 Microscopic Examination of the Thermal Aging Specimens.** After tensile testing, many of the thermal aging specimens were sectioned and mounted for study using both an optical microscope (metallograph) and scanning electron microscope (SEM). These studies were intended to detect changes that occurred in the composites during exposure in order to assist in identifying degradation mechanisms. Additional examinations were conducted of the fractured surfaces (primarily with the SEM) to determine failure modes and to further study the degradation processes. The most conclusive results were obtained from examination of the G/E specimens, and, for this reason, the majority of this section discusses the G/E system.

Figure 8-16 shows photomicrographs of G/E aging specimens using a metallograph and a SEM at 100X and 500X magnifications. These pictures are for 10,000 hours at 450K (350°F) and 0.014 MN/m² (2 psi) pressure. Close examination of these photomicrographs shows only surface changes in the resin and some cracking, which probably occurred during post exposure tensile testing. Some of the cracks are located at boundaries between lamina and others within a particular lamina, as shown in the upper two photomicrographs. The lighter cast at the specimen edges in the SEM pictures will be shown later to be oxidation. Here it has occurred only at the surfaces exposed to oxygen.

The pictures in Figure 8-17 taken at 100X with the metallograph show good examples of how oxidation of the epoxy resin can proceed inward as a function of time and temperature. The upper pictures show that there is little difference between the as-received material and that aged for 10,000 hours 394K (250°F) in one atmosphere air. The lower pictures, on the other hand, show extensive degradation in the outside plies after 5000 hours at 450K (350°F), and considerable degradation in both the inner and outer layers after 10,000 hours. The SEM pictures in

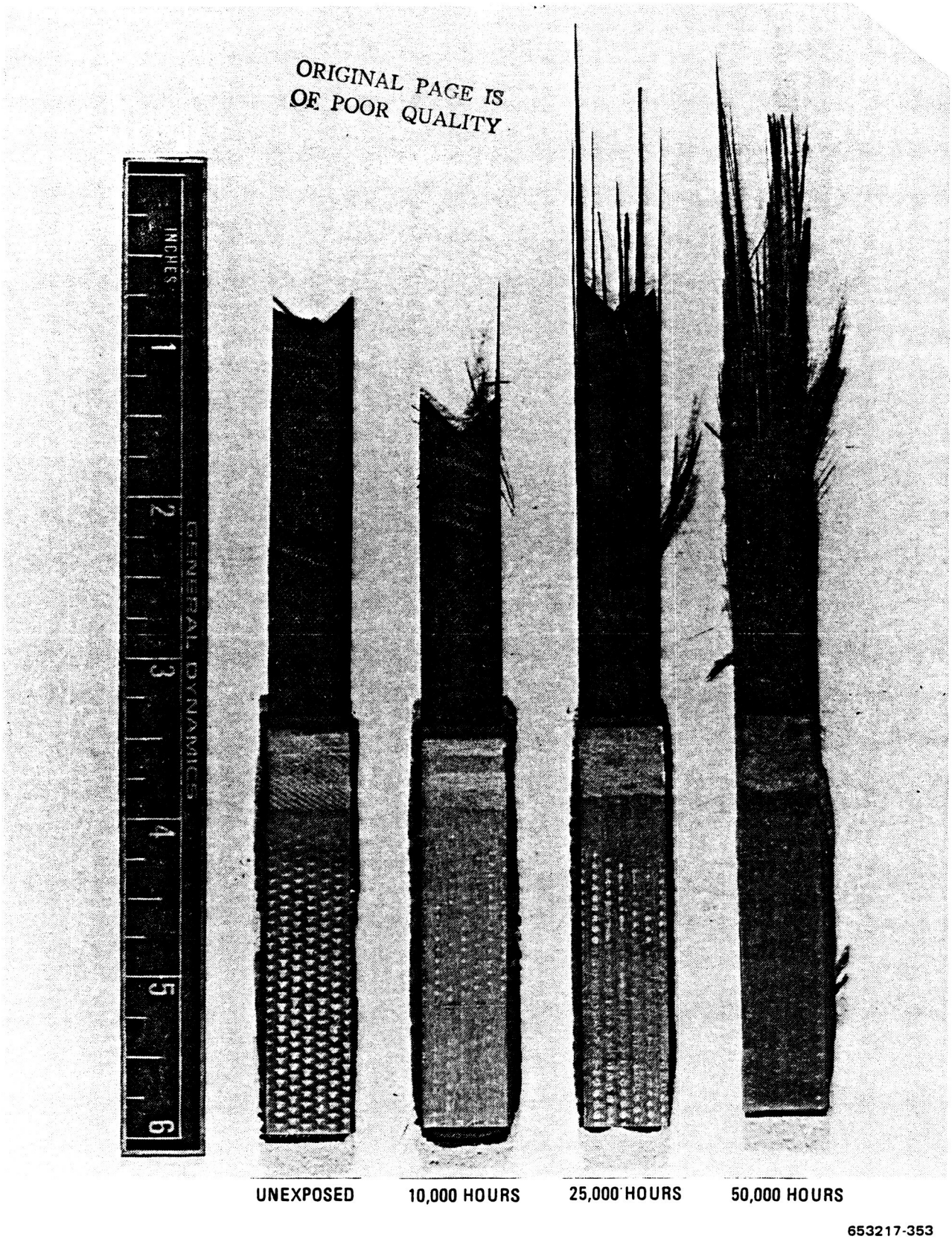



**Figure 8-15 G/E Before and After Thermal Aging at 450K (350°F) in 0.014 MN/m² (2 psi) Air and Tensile Testing at the Same Temperature**

Figure 8-16 Photomicrographs of G/E After Thermal Aging at 450K (350°F) in 0.014 MN/m² (2 psi) Air for 10,000 Hours

ORIGINAL PAGE IS
OF POOR QUALITY

Figure 8-17 Photomicrographs (Metallograph) of G/E After Thermal Aging In One Atmosphere Air at Indicated Temperature, 100X



ORIGINAL PAGE IS
OF POOR QUALITY

Figure 8-18 taken from the same specimens show the identical effects, but even more clearly than the metallographic pictures. For example, the slight amount of surface oxidation after 10,000 hours at 394K (250°F) is easily distinguished in the SEM photograph in Figure 8-18, while scarcely visible in Figure 8-17.

The changes from light to dark for pictures taken using the metallograph and dark to light using the SEM are explained by the amount of relief polishing around the individual fibers that increases with the degree of oxidation. When the epoxy resin oxidizes, it is more prone to crumble, and differences in the amount of oxidation in the polished mounts can easily be detected using the SEM at higher magnifications.

Figure 8-19 shows typically how this occurs. The as-received specimen has little and uniform relief for all plies as shown at 2500X using the SEM to examine a typical polished surface. The inner plies of a specimen aged for 10,000 hours at 394K (250°F) look much the same except for the filaments being oriented at 45 degrees to the surface. If one moves to the outer ply, the relief has increased as shown at the lower right of Figure 8-19. This effect becomes more pronounced for specimens aged at 450K (350°F) and 10,000 hours as shown in the lower left picture. The magnification was lowered to a 1000X for clarity.

The initial examinations were conducted after 10,000 hours of exposure. Additional studies were also made later in the program after time periods out to 50,000 hours. Figures 8-20 through 8-22 show the results of these examinations for crossplied specimens of G/E exposed to the three different aging conditions for 10,000, 25,000, and 50,000 hours. The lighter cast, beginning at the specimen edges and spreading inward with exposure time is again caused by the amount of relief polishing around the individual fibers and is related to the degree of oxidization of the epoxy resin. The degree of oxidation, as shown in Figures 8-20 and 8-21, is quite similar for the first two conditions, i.e., 394K (250°F) and one atmosphere air, and 450K (350°F) and reduced pressure. Slight oxidation at the outer edges is visible after 10,000 hours. At 25,000 hours, considerable oxidation has occurred in the outer plies, and is beginning to extend into the second plies. The effect is somewhat more pronounced for the 450K (350°F), 0.014 $MN/m^2$ (2 psi) exposure. After 50,000 hours of aging, evidence of oxidation is visible in all the plies, with the effect again more pronounced for the 0.014 $MN/m^2$ (2 psi) specimen. The metallographic results show slight effects after 10,000 hours, with major changes after 25,000 and 50,000 hours. These results agree well with both the residual tensile data and the condition of the specimens after tensile testing discussed earlier. Photomicrographs of specimens exposed to the third and most severe aging condition, 450K (350°F) and one atmosphere air, are presented in Figure 8-22. At 10,000 hours, the effects of oxidation are visible throughout the thickness of the laminate. After 25,000 and 50,000 hours, extensive matrix embrittlement has occurred. These effects are particularly pronounced in the two middle plies, where resin loss is quite severe.

Samples of B/E were also examined after thermal aging using both a metallograph and a SEM. No evidence of time dependent oxidation similar to that for the G/E specimens was observed. Overall, very little information was gained from examination of the aged B/E samples. This can be seen in Figure 8-23, which shows the 4.0 mil boron fibers and the epoxy matrix of specimens aged for 10,000, 25,000, and 50,000 hours. No significant changes in the structure were found as the aging proceeded to 50,000 hours. As discussed later in Section 12, some evidence of increased matrix cracking was found for flight simulation specimens that had been exposed for the longer time periods (36,000 hours). These specimens, however, were subjected to fatigue cycling and thermal cycling as opposed to only constant thermal exposure for the thermal aging specimens.

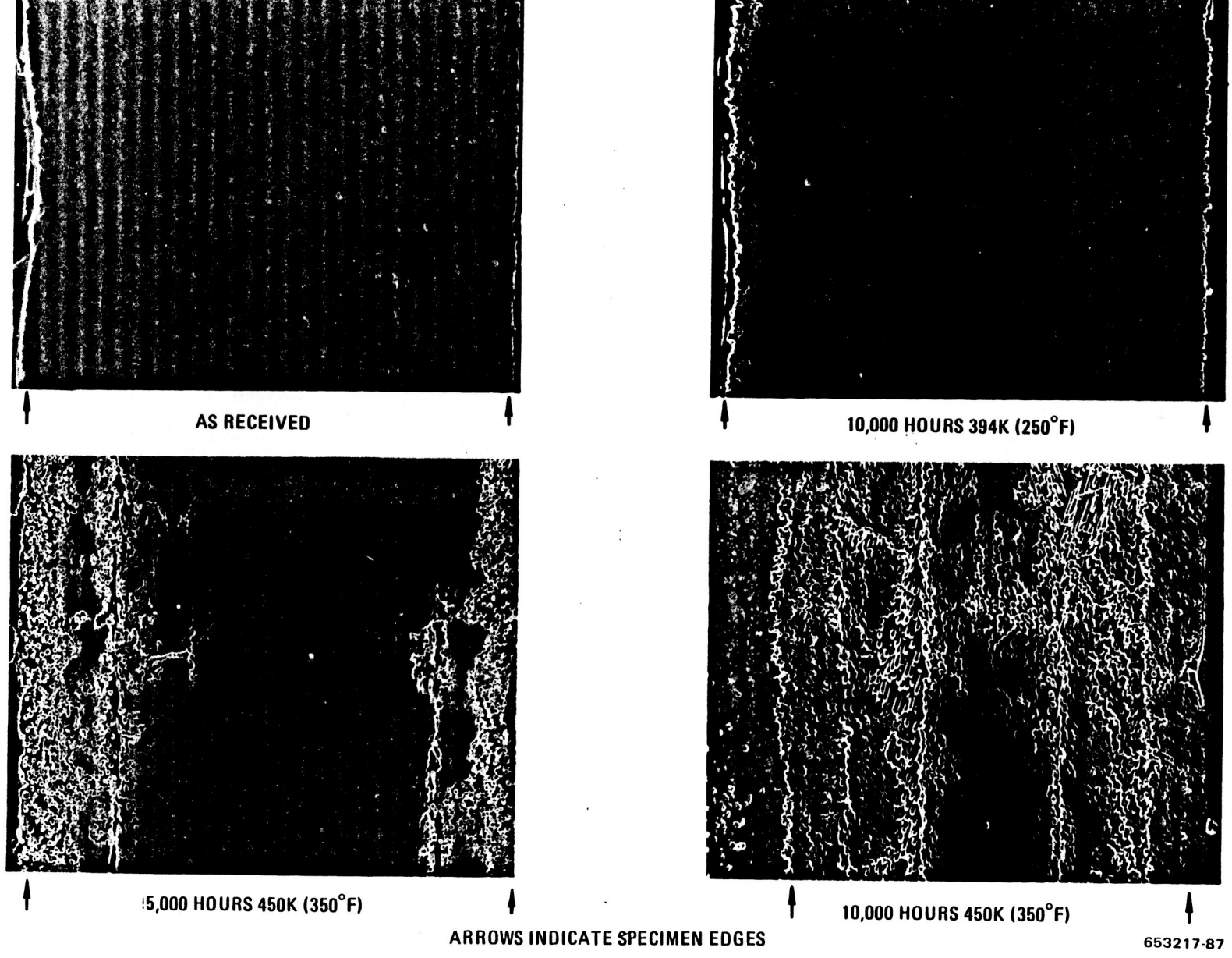



**Figure 8-18 Photomicrographs (SEM) of G/E After Thermal Aging in One Atmosphere Air at Indicated Temperature, 100X**

ORIGINAL PAGE IS
OF POOR QUALITY

Figure 8-19 Photomicrographs (SEM) of G/E After Thermal Aging in One Atmosphere Air at Indicated Temperature



ORIGINAL PAGE IS
OF POOR QUALITY

ORIGINAL PAGE IS
OF POOR QUALITY

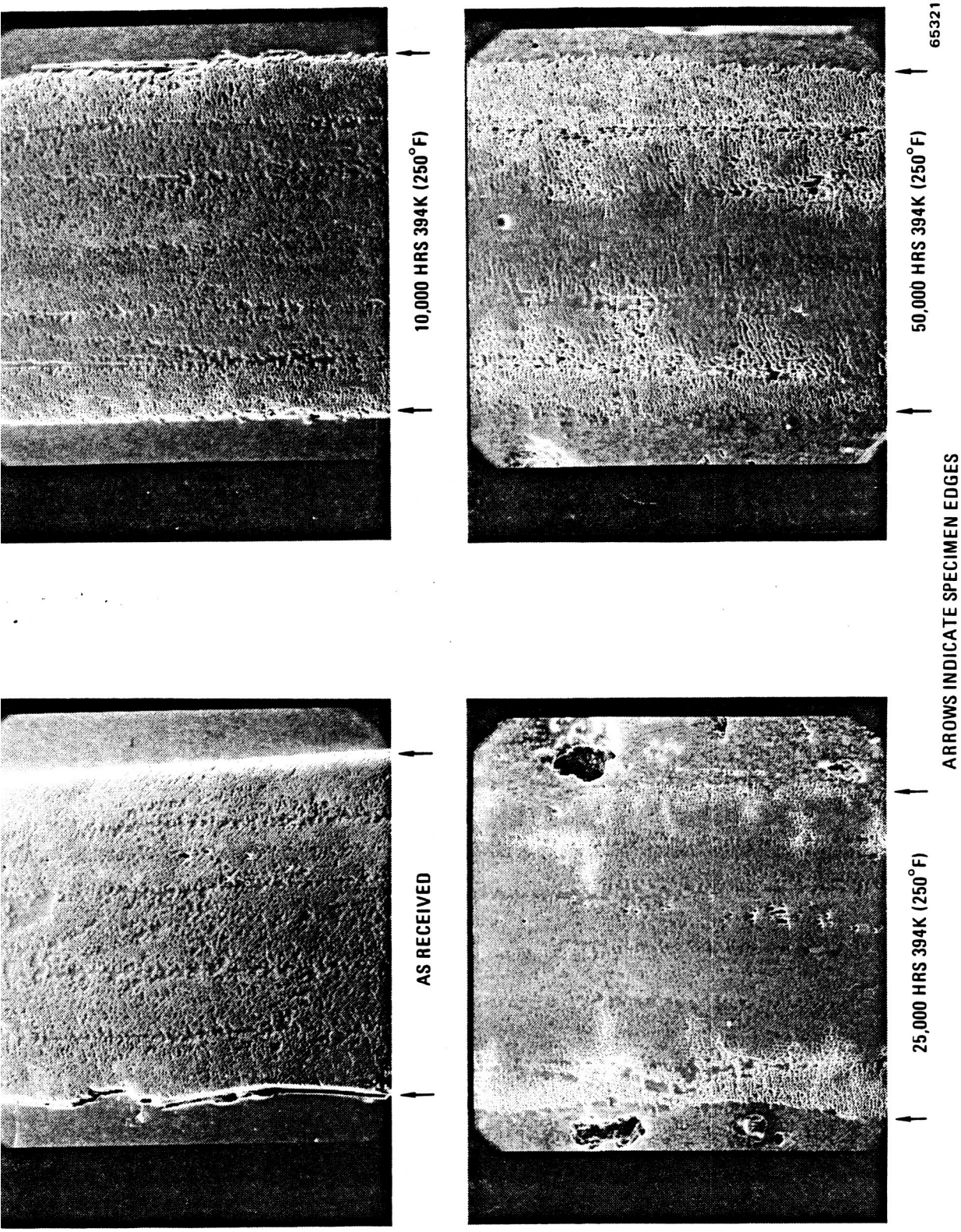



Figure 8-20 Photomicrographs (SEM) of G/E After Thermal Aging in One Atmosphere Air at Indicated Temperature, 100X

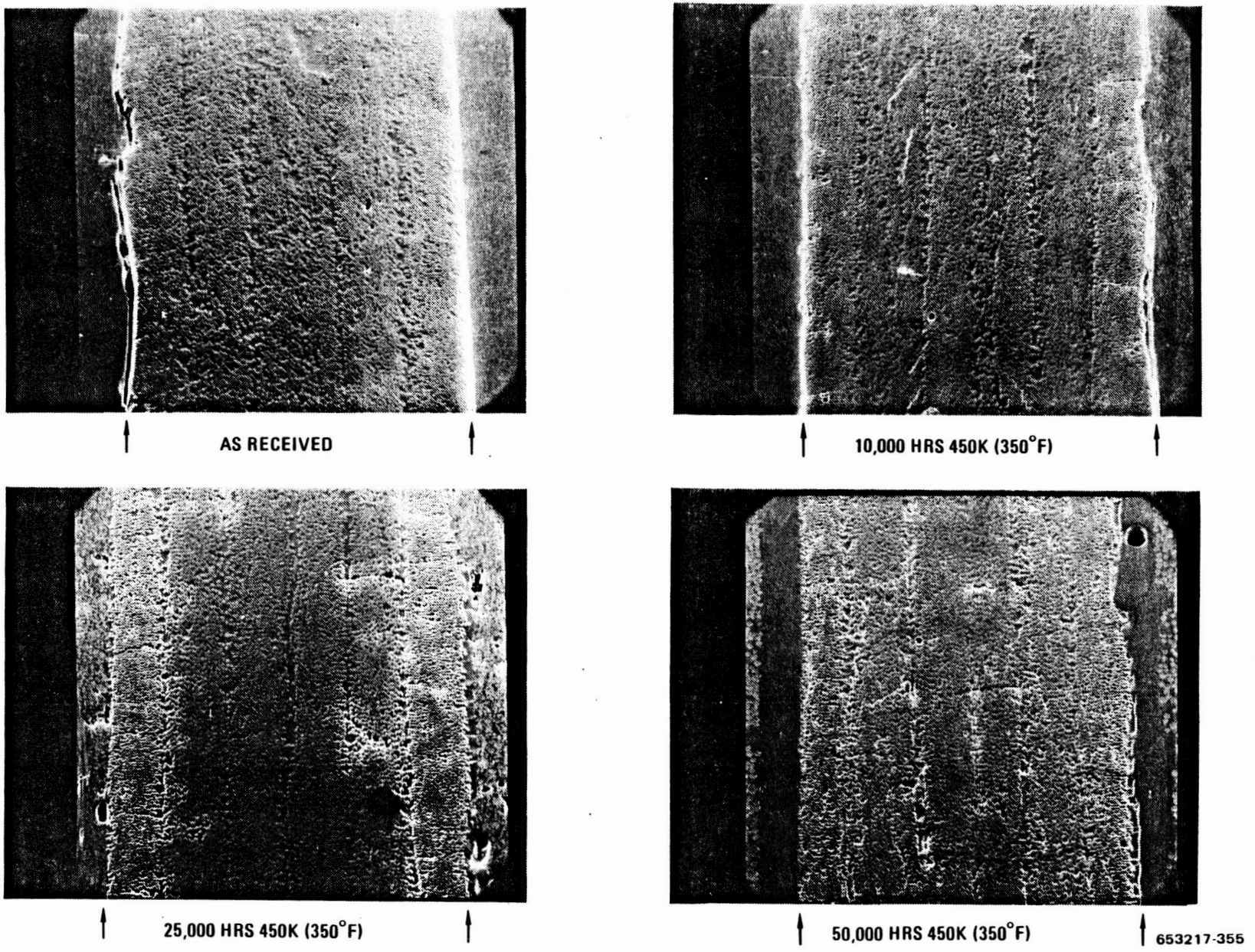



**Figure 8-21 Photomicrographs (SEM) of G/E After Thermal Aging in 0.014 MN/m$^2$ (2 psi) Air at Indicated Temperature, 100X**

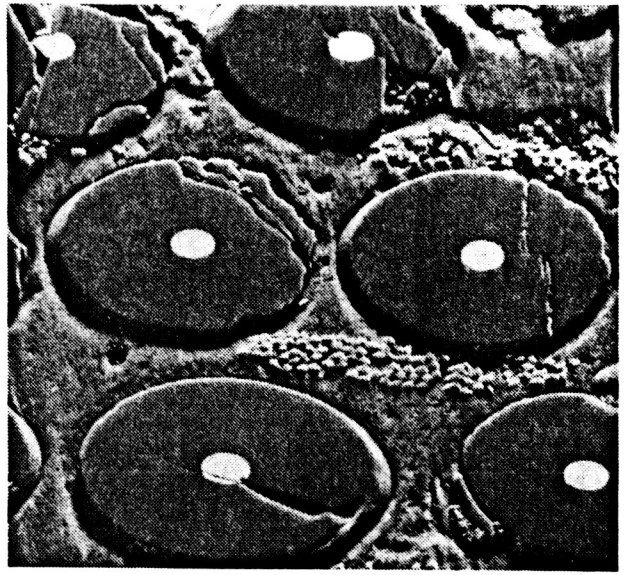


ORIGINAL PAGE IS
OF POOR QUALITY

ORIGINAL PAGE IS
OE POOR QUALITY



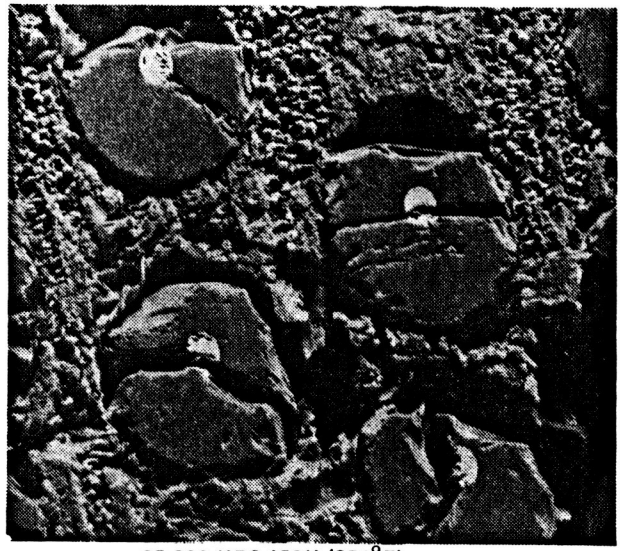

Figure 8-22 Photomicrographs (SEM) of G/E After Thermal Aging in One Atmosphere Air at Indicated Temperature, 100X



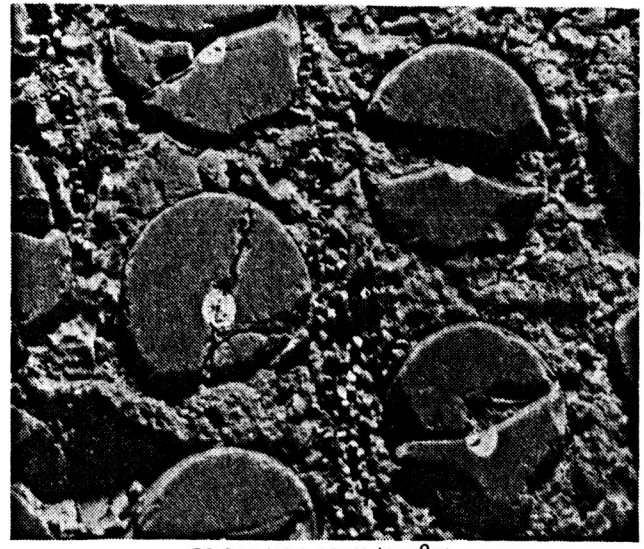
AS RECEIVED



10,000 HRS 450K (350°F)



25,000 HRS 450K (350°F)



50,000 HRS 450K (350°F)

653217-357

**Figure 8-23 Photomicrographs (SEM) of B/E After Thermal Aging in One Atmosphere Air at Indicated Temperature, 300X**



ORIGINAL PAGE IS
OF POOR QUALITY

**8.2.1.2 Fractographs.** In addition to the metallographic cross sectional examinations, a study was also made of the fracture surfaces of several of the specimens. Examples are presented in Figures 8-24 and 8-25. Typical fractographs of G/E unaged and aged at 394K (250°F) and ambient pressure for 10,000 hours are shown in the upper portion of Figure 8-24. As might be predicted from the tensile results, the appearance of the fracture surfaces is very similar for the two specimens. The matrix is relatively intact and there is little fiber pullout. For specimens aged at 450K (350°F) and ambient pressure for 5000 hours or longer, it was not possible to get a good SEM picture of the fracture. The very brittle resin had crumbled away from the filaments in the area of the fracture so that only a few filament ends would have appeared in the field of view.

The pictures in the lower portion of Figure 8-24 show some of the filaments near the fracture locations in specimens aged at 450K (350°F). The filaments are quite different in appearance than those in the upper two photographs in the amount of resin adhering to the surface. The presence of this much resin on the graphite filaments indicates a severe degradation of the epoxy matrix, which accounts for the failure within the matrix rather than at the fiber/resin interface.

An interesting example of the gradient of oxidation into the specimens is illustrated in the fractographs of Figure 8-25. These pictures were taken from areas near the surface of specimens aged at 394K (250°F) and reduced pressure. As shown in Figure 8-16 and 8-18 only a slight amount of oxidation (only at the outer surfaces) had occurred in these specimens in 10,000 hours. In Figure 8-25 the depth to which the oxidation had progressed is readily visible. The resin near the outer surface has been embrittled by oxidation and has broken away from the filaments during tensile testing. Deeper into the specimen the fracture more closely resembles that of an unaged specimen.

**8.2.1.3 Glass Transition Temperature Studies.** Further studies of the changes in the epoxy resin were made by measuring the glass transition temperature ($T_g$) of small samples cut from the G/E thermal aging specimens. These tests were performed using a DuPont 942 Thermomechanical Analyzer module in conjunction with a DuPont 990 Thermal Analyzer. The results are tabulated in Table 8-12. For aging at 394K (250°F) no change was observed for aging times out to 10,000 hours, in agreement with the tensile results. For the reduced pressure, 0.014 NM/m$^2$ (2 psi), exposures at 450K (350°F), however, significant increases in $T_g$ were found. These changes in the resin were not detected by either the mechanical property tests or microscopic examinations. No measurements could be made on the 5000 hour and 10,000 hour specimens aged at ambient pressure and 450K (350°F) or the 25,000 hour and 50,000 hour specimens aged at any of the three conditions because of the damage that occurred during tensile testing.

The full significance of the changes in the $T_g$ values and their relationship to the changes in the resin system during aging are not clearly understood at this time. Additional $T_g$ measurements made on thermal aging/compression specimens (see Section 8.3.1) and flight simulation specimens (see Section 12) were also of little value in understanding the resin system changes that occur during the thermal exposures of this program.

### 8.2.2 GRAPHITE/POLYIMIDE

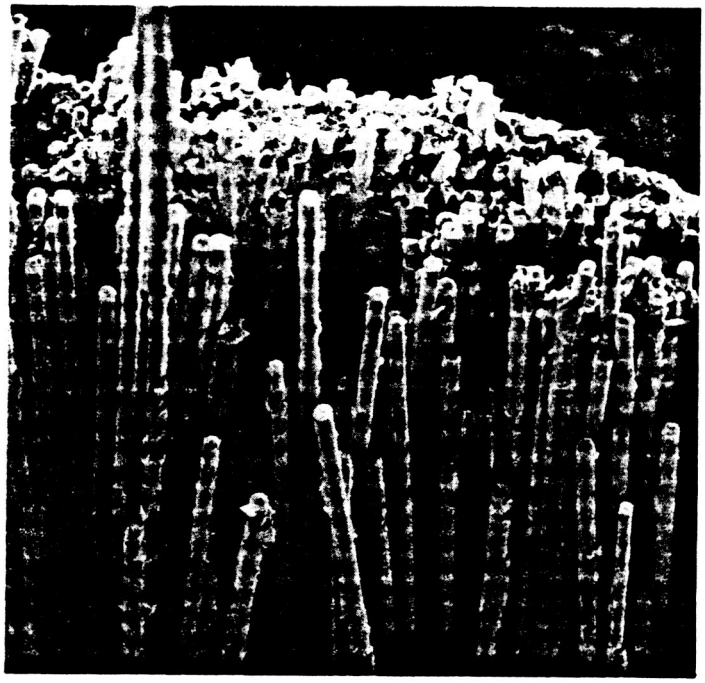
**8.2.2.1 HT-S/710 G/PI.** Residual tensile strength data for the HT-S/710 G/PI system are presented in Tables 8-13 through 8-16 for aging at ambient pressure and Table 8-17 for aging at reduced pressure. Aging was carried out at 505K (450°F) and 561K (550°F) for both unidirectional and $[0° \pm 45°]_s$ crossplied specimens. Residual tensile strength testing was performed at

Figure 8-24 SEM Fractographs of G/E After Thermal Aging in One Atmosphere Air at Indicated Temperature

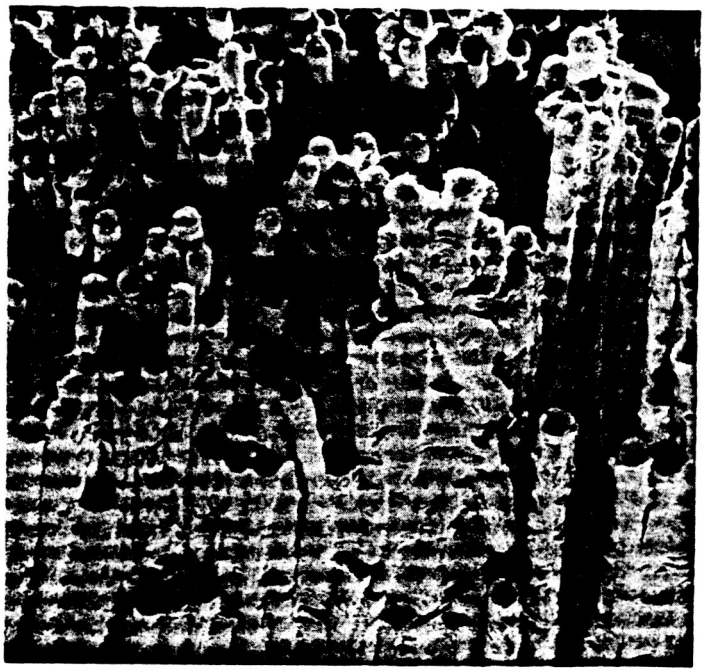


ORIGINAL PAGE IS
OF POOR QUALITY

ORIGINAL PAGE IS
OF POOR QUALITY



10,000 HOURS 394K (250°F), 101 kN/m$^2$ (14.7 psi)
(250X)



10,000 HOURS 450K (350°F), 13.8 kN/m$^2$ (2 psi)
(400X)

653217-90

**Figure 8-25 SEM Fractographs of G/E (Surface of Specimen Toward Viewer)**

Table 8-12 Glass Transition, $T_g$, Data for $[0° \pm 45°]_s$ G/E

| Condition | Aging Temperature K | Aging Temperature (°F) | Aging Pressure MN/m2 | Aging Pressure (psi) | Aging Time (hr) | $T_g$ K | $T_g$ (°F) |
|---|---|---|---|---|---|---|---|
| As-Received | | | | | | 463 | 374 |
| Aged | 394 | 250 | 0.10 | 14.7 | 5,000 | 463 | 374 |
| Aged | 394 | 250 | 0.10 | 14.7 | 10,000 | 464 | 375 |
| Aged | 450 | 350 | 0.014 | 2 | 5,000 | 490 | 422 |
| Aged | 450 | 350 | 0.014 | 2 | 10,000 | 505 | 449 |

the same temperatures that were used for the thermal aging exposures. The tensile data have been plotted as a function of aging time and are presented in Figures 8-26 through 8-28. A summary of the effects of 10,000 hours and 50,000 hours of thermal aging on the tensile strength retention of G/PI is shown in Table 8-18.

**505K, 0.10 MN/m² and 0.014 MN/m² (450°F, 14.7 psi and 2 psi) EXPOSURE.** Exposures of up to 25,000 hours at both one atmosphere and reduced pressure had essentially no effect on the 505K (450°F) tensile strength (see Figure 8-26 and 8-28). Compared with unexposed material there was no apparent difference in appearance for the one atmosphere specimens. The reduced pressure specimens did show some small spots, but these did not appear to be either serious or significant. After tensile testing the specimens again resembled unexposed specimens with no bare graphite fibers visible as a result of breaking up of an embrittled matrix.

After 50,000 hours significant decreases in tensile strength were found in specimens aged at both ambient and reduced pressure. Specimen condition, however, was still quite good. Before tensile testing, a small amount of edge cracking and a slightly burned appearance were observed. After tensile testing a very slight loss of resin with a few bare graphite fibers could be seen, perhaps an indication of the start of matrix degradation. As shown in Figures 8-29 and 8-30, however, the effects were minor.

There was one group of three specimens that gave unusually poor results. These were the unidirectional specimens aged for 500 hours at 595K (450°F). Residual strength values were obtained that were lower than all others of this group including those aged for 50,000 hours. Examination of the broken specimens and the test data, as well as careful review of the specimen preparation and test procedures failed to reveal the cause of this anomally. Because the 500 hour data appeared to be in error, they were not included on the aging plot in Figure 8-26.

**561K, 0.10 MN/m² and 0.014 MN/m² (550°F, 14.7 psi and 2 psi) EXPOSURE.** In contrast to the lower temperature exposures, those at 561K (550°F) produced significant decreases in tensile strength in times as early as 200 hours for ambient pressure (Figure 8-27). Although the strength decreases were quite large, very little change in the appearance of the specimens was observed after the first 10,000 hours of aging. The color and surface texture remained almost unchanged. Only slight edge cracks and some small spots on the surface with a charred appearance were

**Table 8-13 Thermal Aging Data for $[0°]_6$ HT-S/710 G/PI in 0.10 MN/m² (14.7 psi) Air**

| Aging Temperature K | Aging Temperature (°F) | Test Temperature K | Test Temperature (°F) | Aging Time (hr) | | Tensile Strength MN/m² | Tensile Strength (ksi) |
|---|---|---|---|---|---|---|---|
| 505 | 450 | 505 | 450 | Baseline avg | | 1210 | 176 |
| | | | | 500 | | 827 | 120 |
| | | | | | | 752 | 120 |
| | | | | | | 758 | 110 |
| | | | | | avg | 779* | 113* |
| | | | | 1,000 | | 1210 | 175 |
| | | | | | | 990 | 144 |
| | | | | | | 1370 | 198 |
| | | | | | avg | 1190 | 172 |
| | | | | 5,000 | | 1190 | 173 |
| | | | | | | 1420 | 206 |
| | | | | | | 1240 | 180 |
| | | | | | avg | 1280 | 186 |
| | | | | 10,000 | | 1280 | 185 |
| | | | | | | 1390 | 201 |
| | | | | | | 1350 | 196 |
| | | | | | avg | 1340 | 194 |
| | | | | 25,000 | | 1210 | 176 |
| | | | | | | 1350 | 196 |
| | | | | | | 1210 | 176 |
| | | | | | avg | 1260 | 183 |
| | | | | 50,000 | | 848 | 123 |
| | | | | | | 882 | 128 |
| | | | | | | 965 | 140 |
| | | | | | avg | 898 | 130 |

*Not included in Figure 8-26

Table 8-14 Thermal Aging Data for $[0° \pm 45°]_s$ Crossply HT-S/710 G/PI in 0.10 MN/m² (14.7 psi) Air

| Aging Temperature K | Aging Temperature (°F) | Test Temperature K | Test Temperature (°F) | Aging Time (hr) | Tensile Strength MN/m2 | Tensile Strength (ksi) |
|---|---|---|---|---|---|---|
| 505 | 450 | 505 | 450 | Baseline avg | 470 | 68.2 |
| | | | | 1,000 | 521 | 75.5 |
| | | | | | 443 | 64.3 |
| | | | | | 328 | 47.5 |
| | | | | | avg 431 | 62.4 |
| | | | | 5,000 | 435 | 63.1 |
| | | | | | 501 | 72.6 |
| | | | | | 576 | 83.5 |
| | | | | | avg 504 | 73.1 |
| | | | | 10,000 | 335 | 48.6 |
| | | | | | 525 | 76.2 |
| | | | | | 454 | 65.9 |
| | | | | | avg 438 | 63.6 |
| | | | | 25,000 | 502 | 72.8 |
| | | | | | 463 | 67.2 |
| | | | | | 434 | 63.0 |
| | | | | | avg 467 | 67.7 |
| | | | | 50,000 | 410 | 59.5 |
| | | | | | 338 | 49.0 |
| | | | | | 341 | 49.4 |
| | | | | | avg 363 | 52.6 |

Table 8-16 Thermal Aging Data for $[0° \pm 45°]_s$ Crossply HT-S/710 G/PI in 0.10 MN/m² (14.7 psi) Air

| Aging Temperature K | Aging Temperature (°F) | Test Temperature K | Test Temperature (°F) | Aging Time (hr) | Tensile Strength MN/m2 | Tensile Strength (ksi) |
|---|---|---|---|---|---|---|
| 561 | 550 | 561 | 550 | Baseline avg | 434 | 63.0 |
| | | | | 1,000 | 443 | 64.2 |
| | | | | | 474 | 68.7 |
| | | | | | 394 | 57.1 |
| | | | | | avg 437 | 63.3 |
| | | | | 5,000 | 276 | 40.0 |
| | | | | | 276 | 40.0 |
| | | | | | 258 | 37.4 |
| | | | | | avg 270 | 39.1 |
| | | | | 10,000 | 192 | 27.8 |
| | | | | | 211 | 30.6 |
| | | | | | 274 | 39.7 |
| | | | | | avg 226 | 32.7 |
| | | | | 25,000 | 34 | 5.0 |
| | | | | | 48 | 6.9 |
| | | | | | 43 | 6.2 |
| | | | | | avg 42 | 6.0 |
| | | | | 50,000 | * | * |
| | | | | | * | * |
| | | | | | * | * |

*Specimens not suitable for tensile testing

Table 8-15 Thermal Aging Data for $[0°]_6$ HT-S/710 G/PI in 0.10 MN/m² (14.7 psi) Air

| Aging Temperature K | Aging Temperature (°F) | Test Temperature K | Test Temperature (°F) | Aging Time (hr) | Tensile Strength MN/m2 | Tensile Strength (ksi) |
|---|---|---|---|---|---|---|
| 561 | 550 | 561 | 550 | Baseline avg | 1320 | 191 |
| | | | | 200 | 1290 | 187 |
| | | | | | 1280 | 185 |
| | | | | | 1350 | 196 |
| | | | | | avg 1310 | 189 |
| | | | | 500 | 1170 | 170 |
| | | | | | 1300 | 189 |
| | | | | | 1200 | 174 |
| | | | | | avg 1220 | 178 |
| | | | | 1,000 | 1100 | 159 |
| | | | | | 1170 | 169 |
| | | | | | 1190 | 173 |
| | | | | | avg 1150 | 167 |
| | | | | 5,000 | 1170 | 169 |
| | | | | | 1070 | 155 |
| | | | | | 1010 | 147 |
| | | | | | avg 1080 | 157 |
| | | | | 10,000 | 1117 | 162 |
| | | | | | 876 | 127 |
| | | | | | 807 | 117 |
| | | | | | avg 933 | 135 |
| | | | | 25,000 | 254 | 36.9 |
| | | | | | 260 | 37.7 |
| | | | | | 277 | 40.2 |
| | | | | | avg 264 | 38.3 |
| | | | | 50,000 | * | * |
| | | | | | * | * |
| | | | | | * | * |

*Specimens not suitable for tensile testing

**Table 8-17 Thermal Aging Data for HT-S/710 G/PI Aged in 0.014 MN/m² (2 psi) Air**

| Aging Temperature K | Aging Temperature (°F) | Orientation | Test Temperature K | Test Temperature (°F) | Aging Time (hr) | | Tensile Strength MN/m2 | Tensile Strength (ksi) |
|---|---|---|---|---|---|---|---|---|
| 505 | 450 | $[0°]_6$ | 505 | 450 | Baseline avg | | 1210 | 176 |
| | | | | | 5,000 | | 1370 | 198 |
| | | | | | | | 1210 | 175 |
| | | | | | | | 1480 | 215 |
| | | | | | | avg | 1350 | 196 |
| | | | | | 10,000 | | 1280 | 185 |
| | | | | | | | 1140 | 166 |
| | | | | | | | 1180 | 171 |
| | | | | | | avg | 1200 | 174 |
| | | | | | 25,000 | | 1210 | 176 |
| | | | | | | | 1330 | 193 |
| | | | | | | | 1190 | 172 |
| | | | | | | avg | 1240 | 180 |
| | | | | | 50,000 | | 1082 | 157 |
| | | | | | | | 882 | 128 |
| | | | | | | | 896 | 130 |
| | | | | | | avg | 953 | 138 |
| 561 | 550 | $[0°]_6$ | 561 | 550 | Baseline avg | | 1320 | 191 |
| | | | | | 5,000 | | 1300 | 188 |
| | | | | | | | 980 | 142 |
| | | | | | | | 1300 | 188 |
| | | | | | | avg | 1190 | 173 |
| | | | | | 10,000 | | 1060 | 154 |
| | | | | | | | 1010 | 146 |
| | | | | | | | 970 | 140 |
| | | | | | | avg | 1010 | 147 |
| | | | | | 25,000 | | 1010 | 147 |
| | | | | | | | 1060 | 154 |
| | | | | | | | 979 | 142 |
| | | | | | | avg | 1020 | 148 |
| | | | | | 50,000 | | 696 | 101 |
| | | | | | | | 841 | 122 |
| | | | | | | | 752 | 109 |
| | | | | | | avg | 763 | 111 |

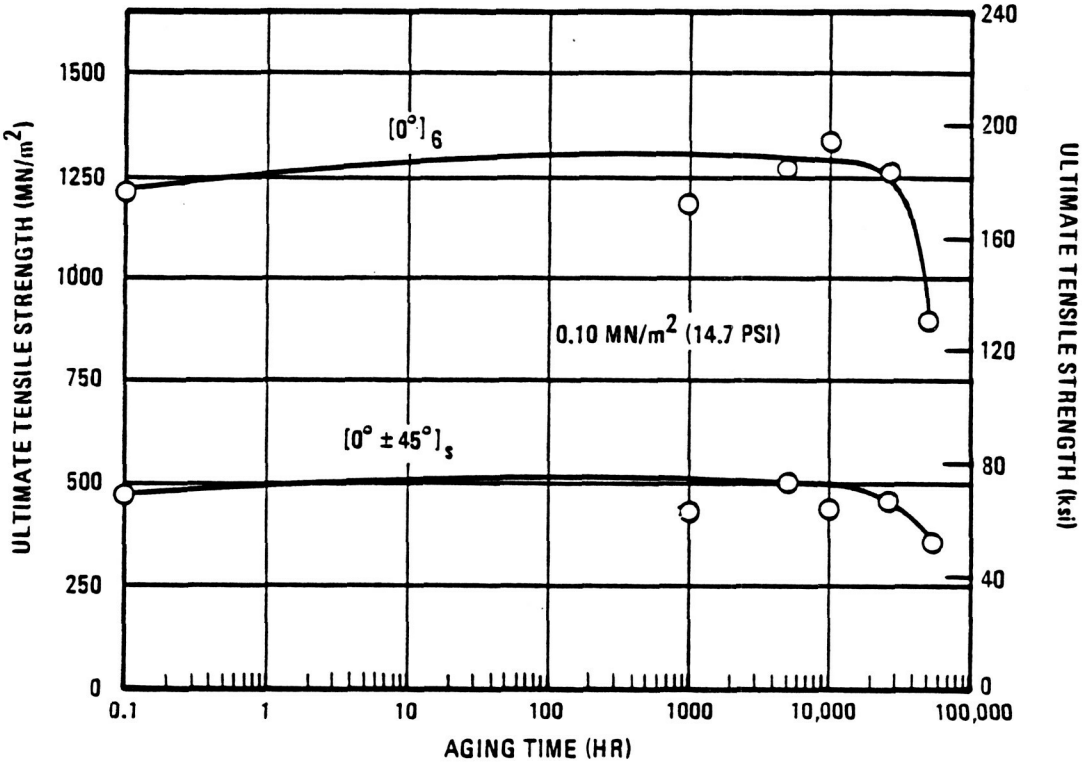



**Figure 8-26 Tensile Strength of HT-S/710 G/PI at 505K (450°F) After Thermal Aging at the Same Temperature**

found. After tensile testing, the specimens aged for 10,000 hours or less were almost identical to unexposed tensile specimens (Figures 8-31 and 8-32) indicating no change in the failure mode as a result of the exposure.

A major change in specimen condition occurred after 25,000 hours in one atmosphere air. These specimens experienced considerable weight loss and, in the case of the crossplied material, severe edge delamination as shown in Figure 8-33. Both orientations were warped and curved, badly discolored with a burned appearance, and were covered with orange and white spots. Compared to the one atmosphere specimens the reduced pressure specimens looked very good. They did, however, show some loss of resin with some exposed fibers and were somewhat faded as compared to unexposed material. For the specimens aged in one atmosphere air, 25,000 hours of exposure severely degraded the tensile strength with losses in both the crossplied and unidirectional material of 80% or more (Figure 8-27). The specimens aged at reduced pressure showed approximately the same tensile strength (Figure 8-28) as those aged for 10,000 hours (75 to 80% of that for unaged material). After tensile testing, the one atmosphere specimens were markedly different from those from material that had been aged for times up through 10,000 hours. The polyimide matrix had broken up during test and crumbled off revealing the graphite fibers. At failure the graphite tows opened up and resembled pieces of yarn. Figure 8-31 shows the change in appearance in failed tensile specimens after 25,000 hours of exposure at 561K (550°F). The 25,000 hour reduced pressure specimens were discolored after tensile testing but showed very little resin loss or exposed fibers as shown in Figure 8-32.

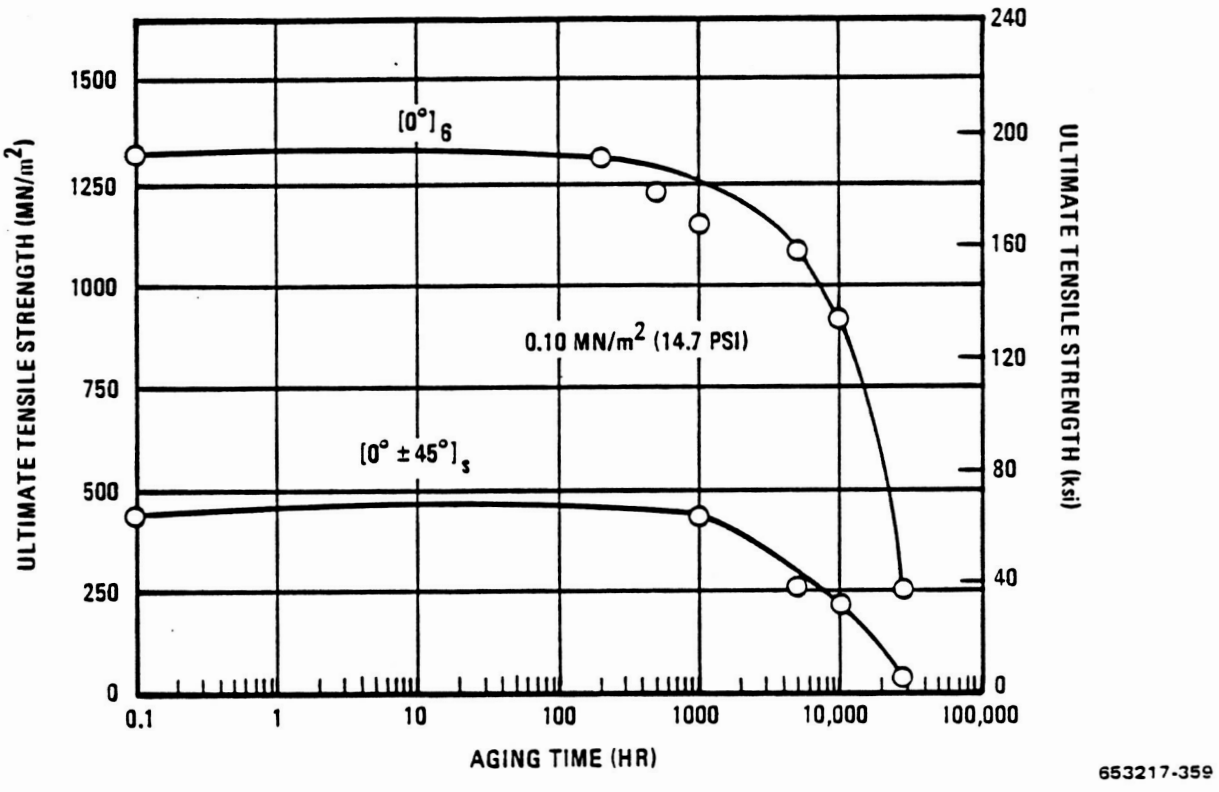



**Figure 8-27 Tensile Strength of HT-S/710 G/PI at 561K (550°F) After Thermal Aging at the Same Temperature.**

After 50,000 hours of aging in one atmosphere air almost no resin was left in the specimen, only graphite fibers. The specimens were badly warped and delaminated and were no longer suitable for tensile testing. Figure 8-34 shows these specimens and the reduced pressure specimens that were in considerably better condition. The reduced pressure specimens were discolored and showed some loss of resin and exposed surface fibers but could be tested. The residual tensile strength, as shown in Figure 8-28, was slightly less than 60% of the unexposed value. The failed specimens showed evidence of the beginning of matrix embrittlement with loss of the matrix material and numerous exposed graphite fibers (see Figure 8-32).

In summary, the HT-S/710 G/PI system survived 25,000 hours of thermal aging at 505K (450°F) with no effects. Some decrease in tensile strength was measured after 50,000 hours, but matrix degradation was not observed. Raising the aging temperature to 561K (550°F) reduced the time at which tensile strength decreases were observed to 1000 hours. In like manner to the 505K (450°F) exposures, this initial fall-off in tensile strength was not accompanied by matrix embrittlement. After 25,000 hours the material was partially delaminated and showed high weight loss. The tensile strength was greatly reduced and severe matrix embrittlement had occurred. Degradation after 50,000 hours was such that the specimens could not be tested. Again, aging effects were less severe for exposures conducted in a reduced pressure environment.

The results of the metallographic examinations of the thermal aging specimens of HT-S/710 G/PI are shown in Figures 8-35 through 8-37. The changes in appearance as a result of the thermal exposures were far less obvious for the G/PI system than for the G/E system. For specimens aged at 505K (450°F), the only indication of matrix embrittlement was observed in specimens

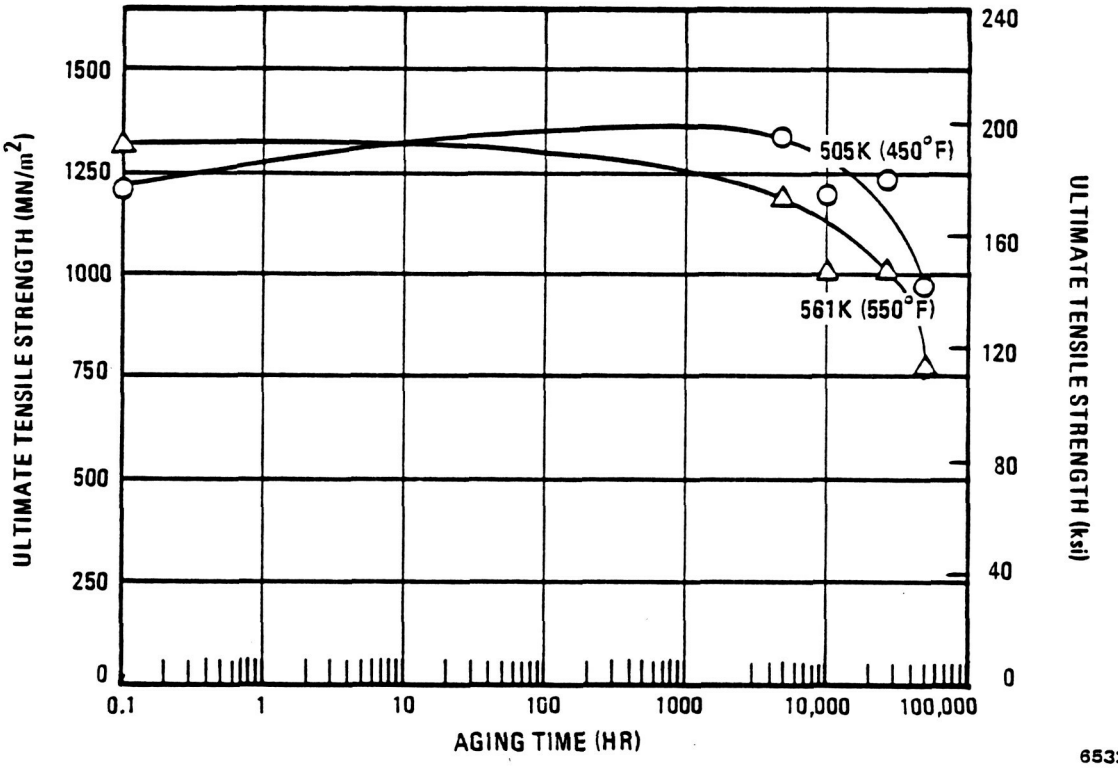



**Figure 8-28 Tensile Strength of Unidirectional HT-S/710 G/PI at the Indicated Temperature After Thermal Aging in 0.014 MN/m² (2 psi) Air at the Same Temperature**

**Table 8-18 Summary of Tensile Strength Retention After Thermal Aging of HT-S/710 G/PI**

| Orientation | Aging Temperature K | Aging Temperature (°F) | Aging Pressure MN/m2 | Aging Pressure (psi) | Test Temperature K | Test Temperature (°F) | Retention of Tensile Strength (%) 10,000 hrs | Retention of Tensile Strength (%) 50,000 hrs |
|---|---|---|---|---|---|---|---|---|
| $[0°]_6$ | 505 | 450 | 0.10 | 14.7 | 505 | 450 | 100 | 74 |
| $[0° \pm 45°]_s$ | 505 | 450 | 0.10 | 14.7 | 505 | 450 | 93 | 77 |
| $[0°]_6$ | 505 | 450 | 0.014 | 2 | 505 | 450 | 99 | 78 |
| $[0°]_6$ | 561 | 550 | 0.10 | 14.7 | 561 | 550 | 71 | 0 |
| $[0° \pm 45°]_s$ | 561 | 550 | 0.10 | 14.7 | 561 | 550 | 52 | 0 |
| $[0°]_6$ | 561 | 550 | 0.014 | 2 | 561 | 550 | 77 | 58 |

ORIGINAL PAGE IS
OF POOR QUALITY



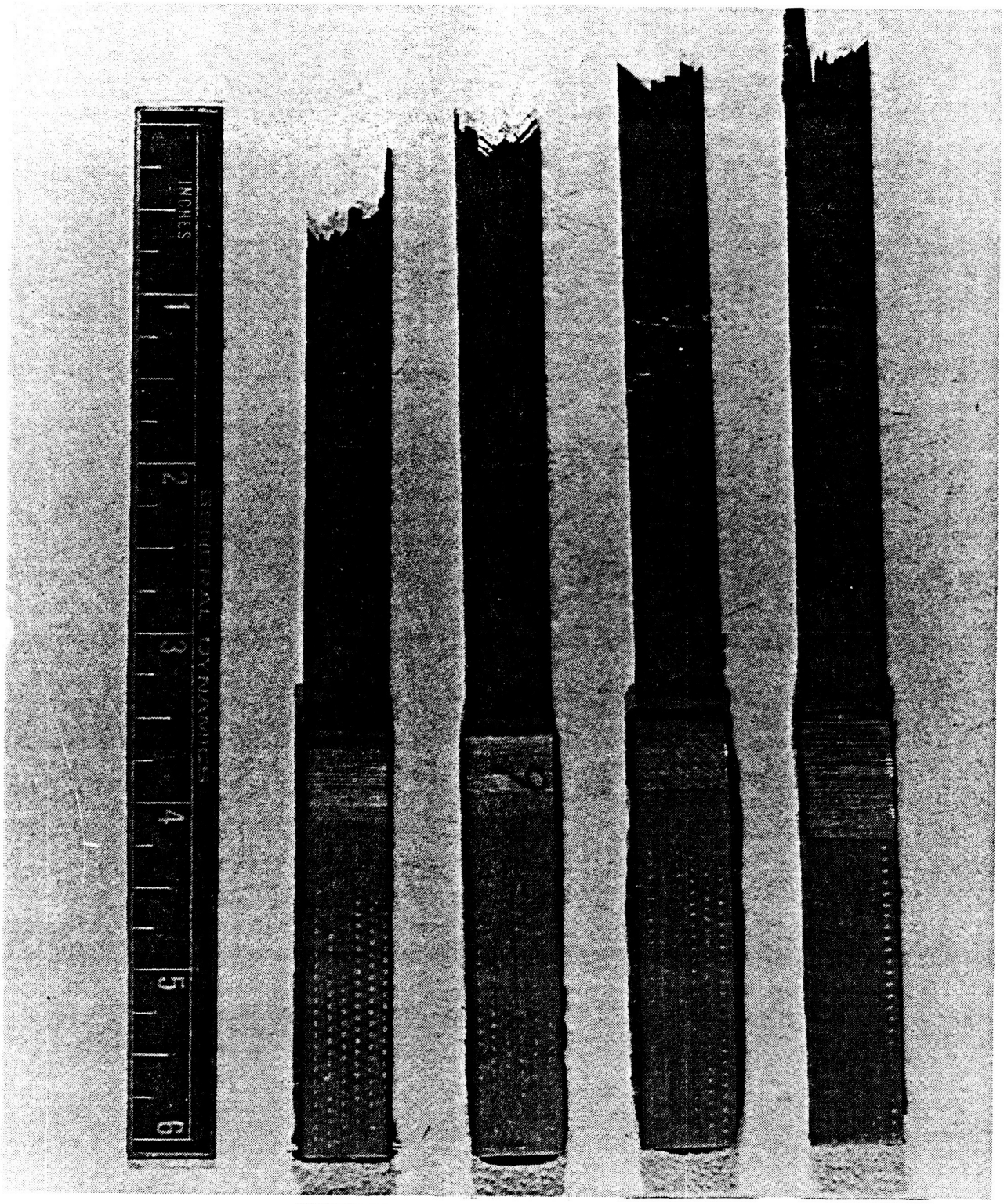



**Figure 8-29 HT-S/710 G/PI Before and After Thermal Aging at 505K (450°F) in One Atmosphere Air and *Tensile Testing at the Same Temperature***

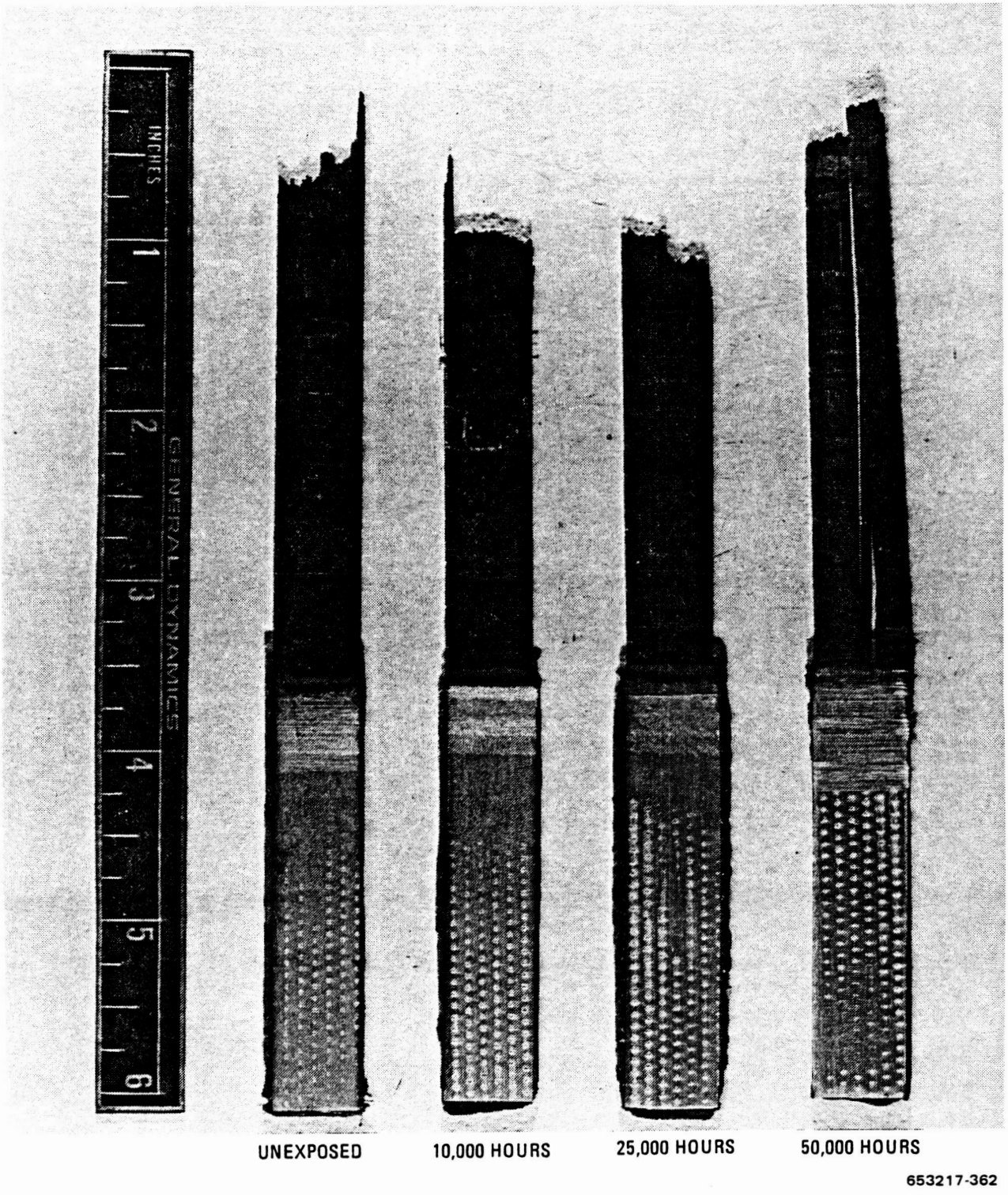



**Figure 8-30 HT-S/710 G/PI Before and After Thermal Aging at 505K (450°F) in 0.014 MN/m² (2 psi) Air and Tensile Testing at the Same Temperature**



ORIGINAL PAGE IS
OF POOR QUALITY

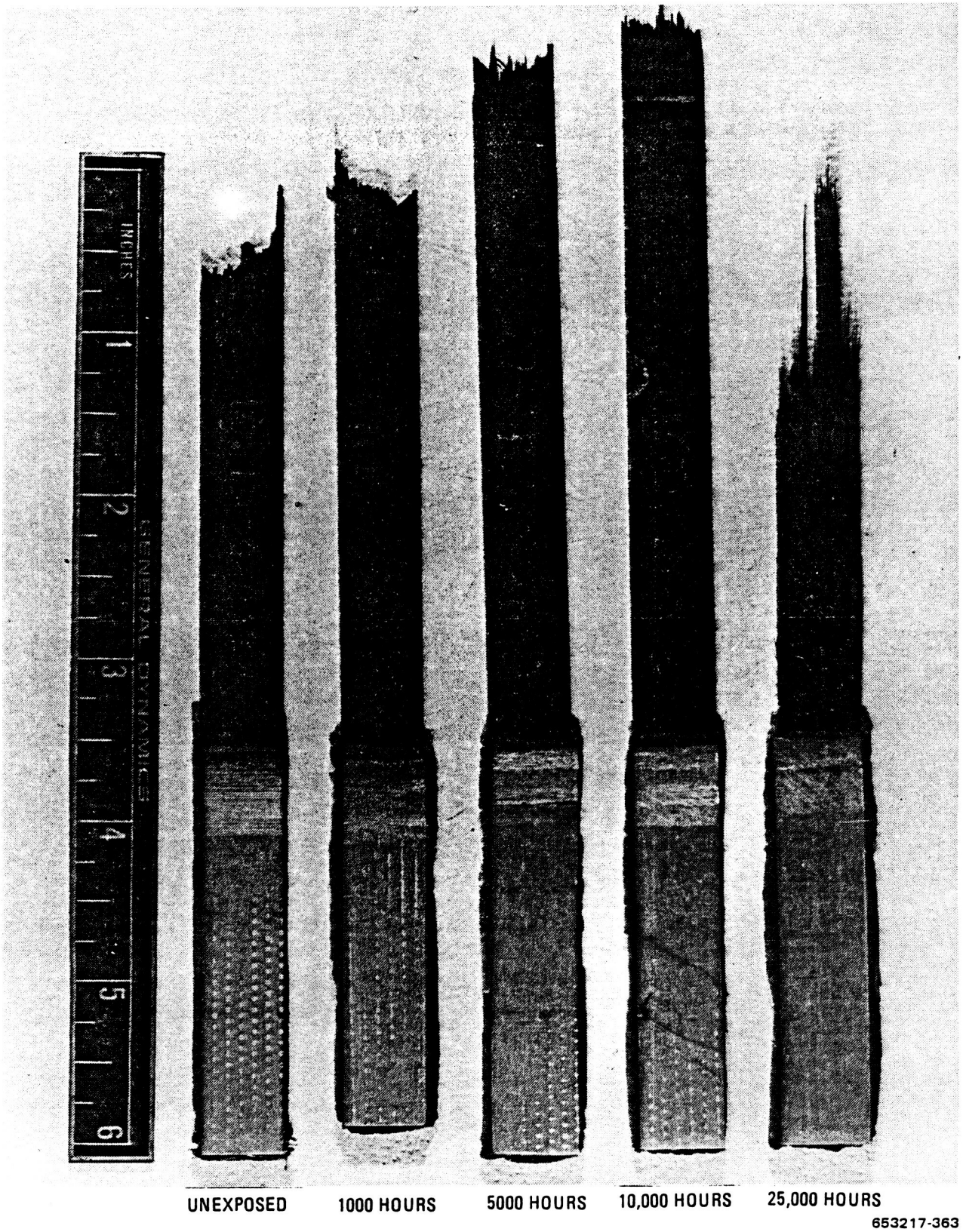



**Figure 8-31 HT-S/710 G/PI Before and After Thermal Aging at 561K (550°F) in One Atmosphere Air and Tensile Testing at the Same Temperature**

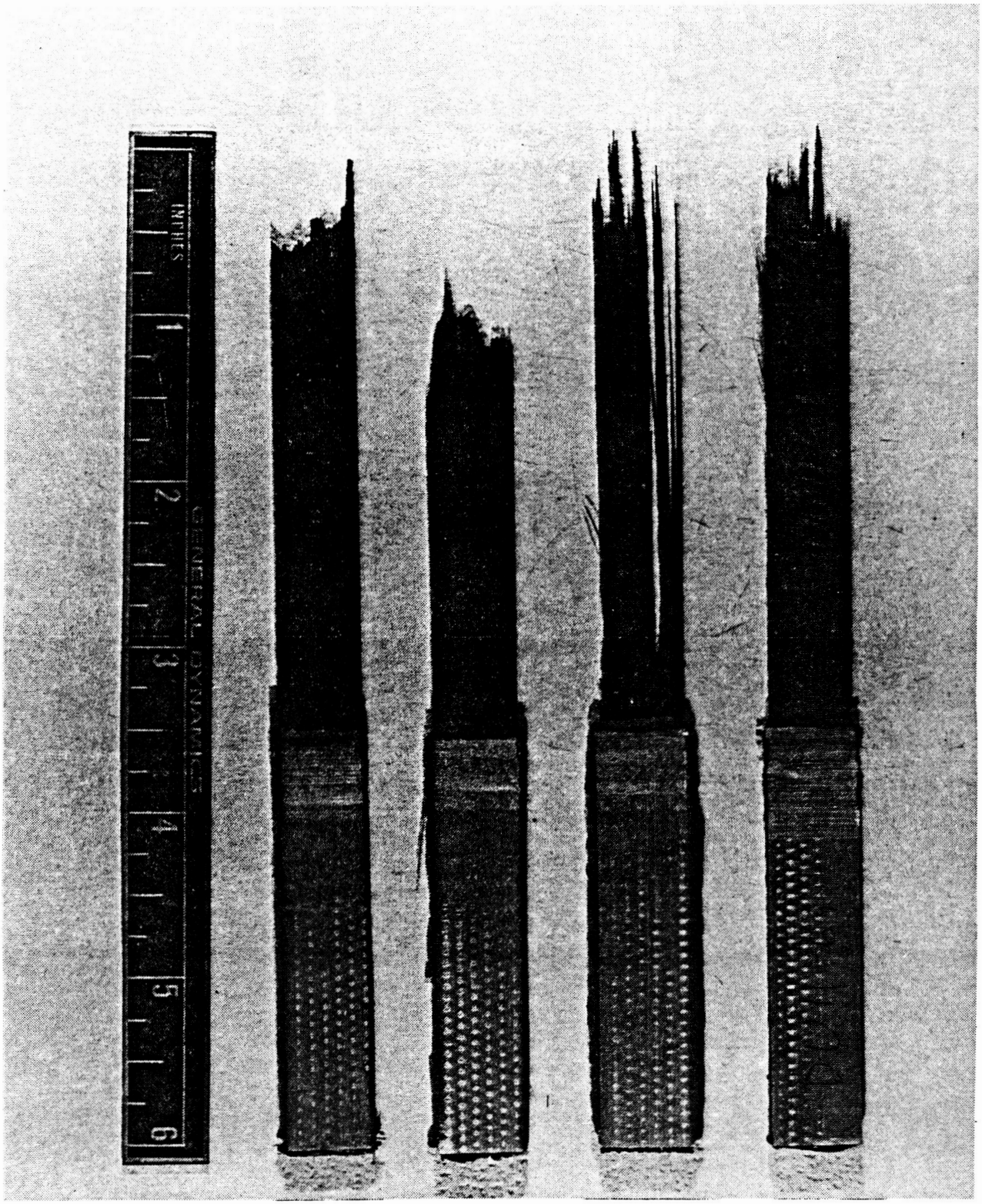
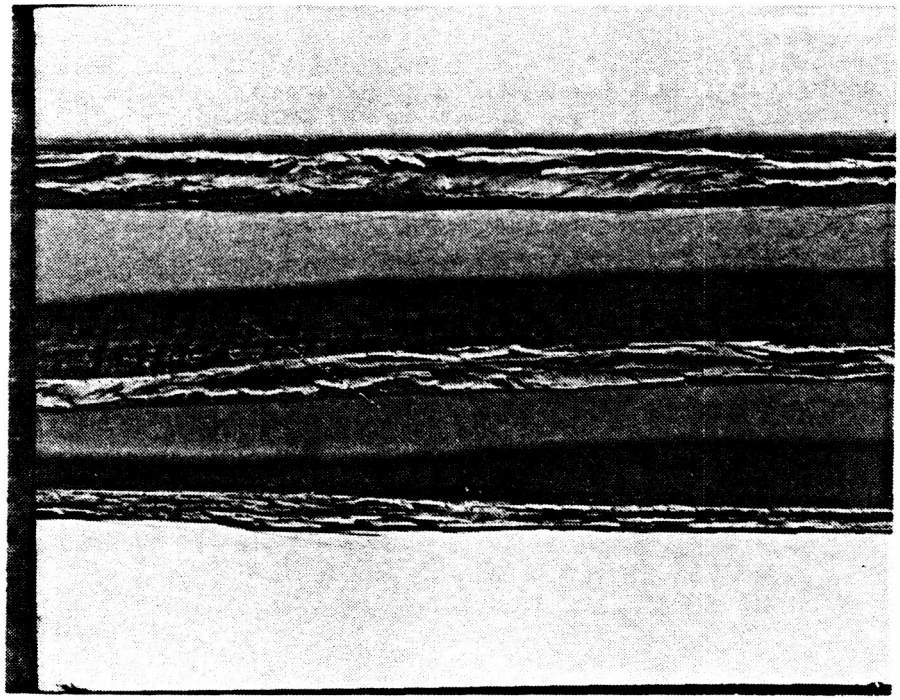



**Figure 8-32 HT-S/710 G/PI Before and After Thermal Aging at 561K (550°F) in 0.014 MN/m² (2 psi) Air and Tensile Testing at the Same Temperature**



ORIGINAL PAGE IS
OF POOR QUALITY

ORIGINAL PAGE IS
OF POOR QUALITY



653217-365

**Figure 8-33 Crossplied HT-S/710 G/PI After 25,000 Hours of Thermal Aging at 561K (550°F) in One Atmosphere Air Showing Severe Edge Cracking and Delamination, 5X***

exposed for 50,000 hours in one atmosphere air. This specimen, Figure 8-35, shows more relief polishing around the graphite fibers, more porosity, and more fiber-matrix separation than the specimens aged for shorter times or at reduced pressure. The effects, particularly the relief polishing, are more pronounced in the center than at the edges. Visual effects starting at the edges and moving inward, as seen in the G/E system, were not observed for the G/PI system. The effect of oxygen pressure can readily be seen, however, as evidenced by the two 50,000 hour specimens in Figure 8-35. The start of matrix degradation, as determined by the condition of the 50,000 hour, one atmosphere specimens after tensile testing, appears to be confirmed by the metallographic results.

Raising the aging temperature to 561K (550°F) greatly increased the degree of matrix degradation of the HT-S/710 G/PI system. Comparison of Figures 8-35 and 8-36 shows that in one atmosphere air, 10,000 hours at 561K (5550°F) has a slightly greater effect on the microstructure than 50,000 hours at 505K (450°F). The amount of relief polishing around the graphite fibers is more pronounced, while the porosity and fiber-matrix separation are about the same. After 25,000 hours at 561K (550°F) in air, the matrix is severely embrittled with considerable loss of resin from the center plies. The final photomicrograph in Figure 8-36, 50,000 hours at reduced pressure, shows little effect to the matrix. At higher magnification, however, (Figure 8-37) considerable relief polishing has occurred. This metallographic evidence of the onset of matrix embrittlement agrees well with the tensile data and the appearance of the failed tensile specimens. The remaining photomicrographs in Figure 8-37 clearly show the effect of matrix condition on the degree of relief polishing around the graphite fibers.

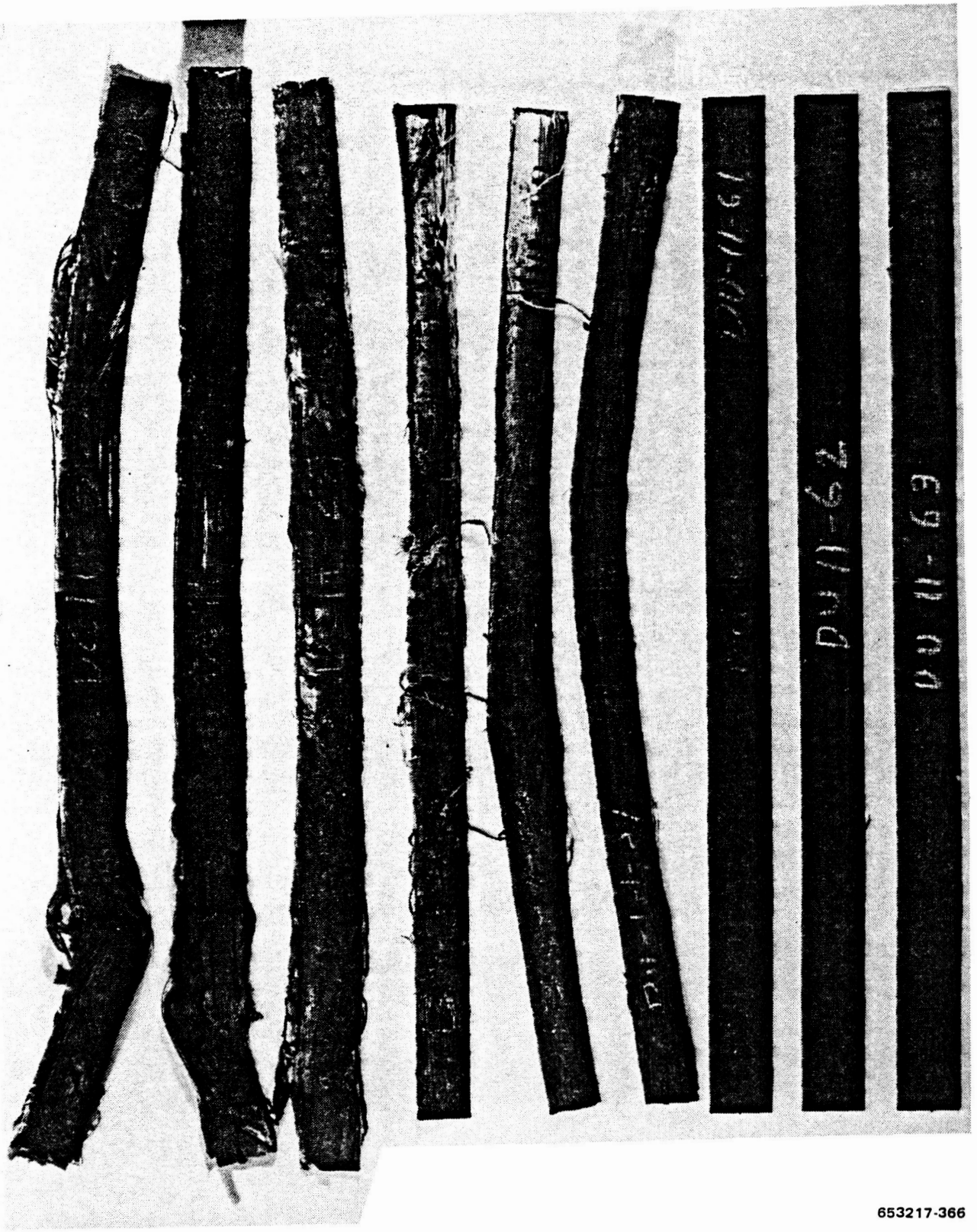



Figure 8-34 HT-S/710 G/PI After 50,000 Hours of Thermal Aging at 561K (550°F) — Left and Center Specimens, One Atmosphere Air; Right Specimens, Reduced Pressure



ORIGINAL PAGE IS
OF POOR QUALITY

ORIGINAL PAGE IS
OF POOR QUALITY

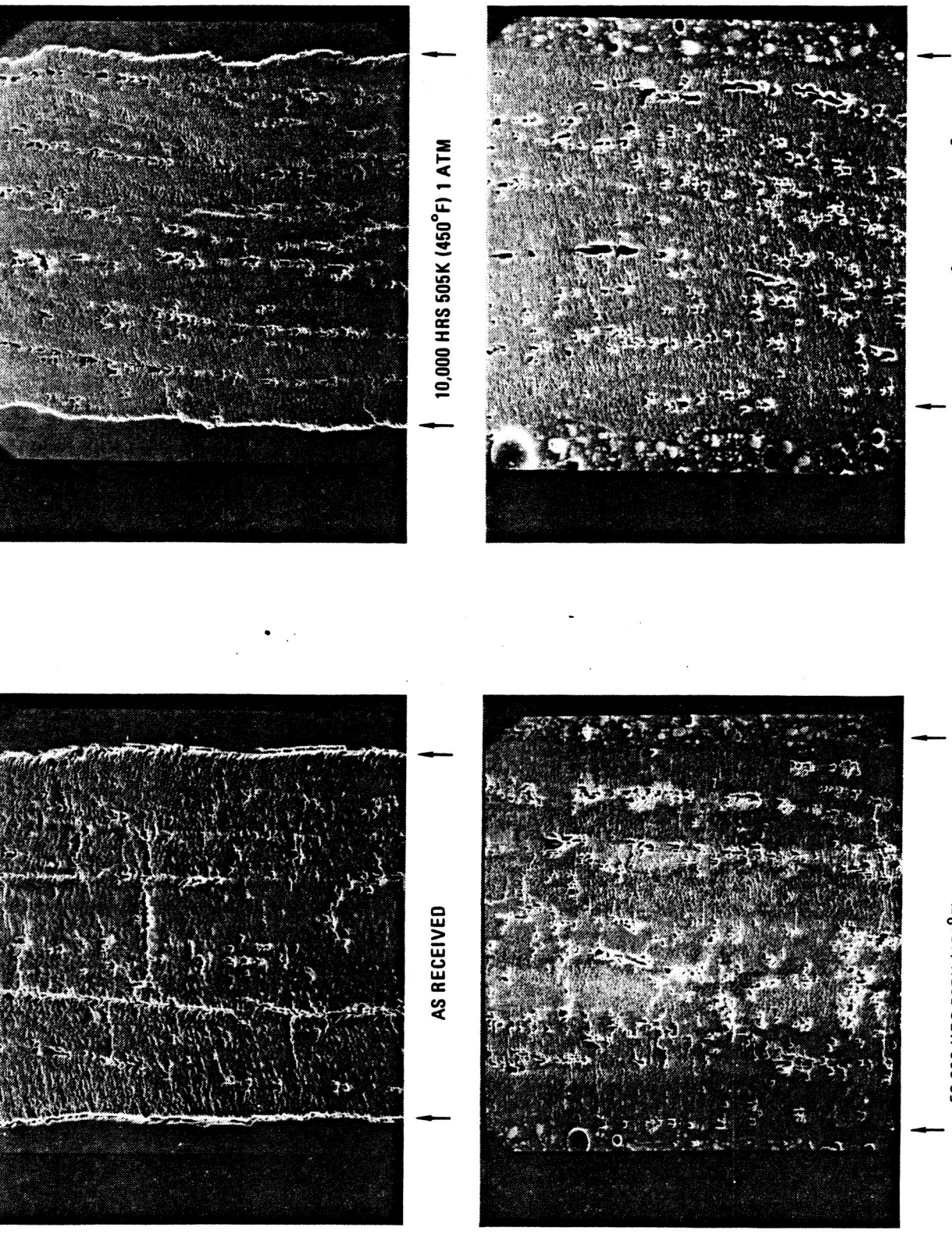



Figure 8-35 Photomicrographs (SEM) of HT-S/710 G/PI After Thermal Aging at Indicated Conditions, 100K

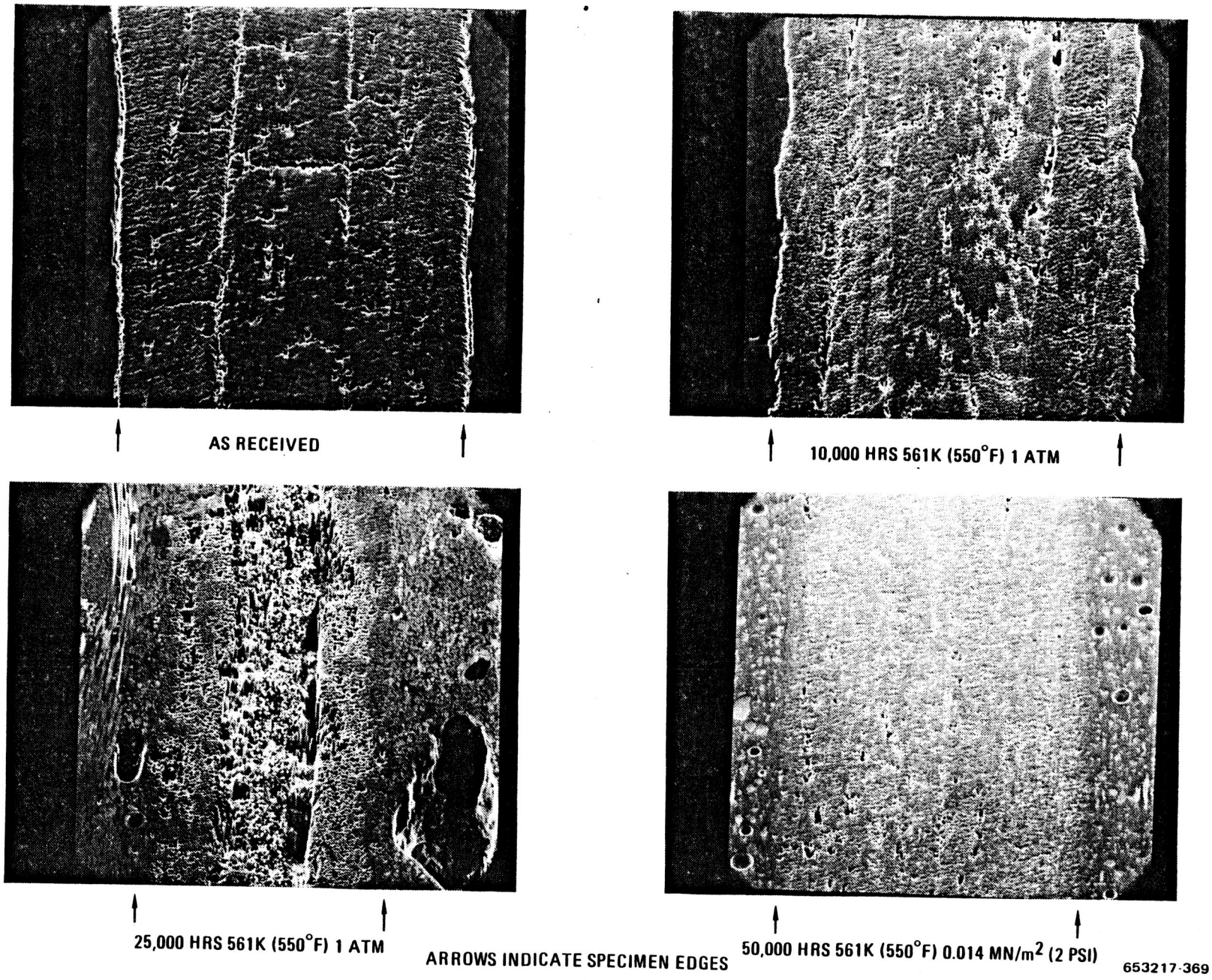



**Figure 8-36 Photomicrographs (SEM) of HT-S/710 G/PI After Thermal Aging at Indicated Conditions, 100X**



ORIGINAL PAGE IS
OF POOR QUALITY

ORIGINAL PAGE IS
OF POOR QUALITY




Figure 8-37 Photomicrographs (SEM) of HT-S/710 G/PI After Thermal Aging at Indicated Conditions, 1000X

**8.2.2.2 Celion 6000/LARC-160 G/PI.** The thermal aging study of Celion 6000/LARC-160 G/PI was performed using only $[0° \pm 45°]_s$ crossplied specimens. Exposures were conducted at 450K (350°F) and 505K (450°F) for time periods out to 10,000 hours. Both one atmosphere and 0.014 $MN/m^2$ (2 psi) environments were included. Post aging evaluation consisted of weight change measurements (one atmosphere specimens only), 450K (350°F) tensile tests, and metallographic and SEM examinations. Results of the weight change measurements are presented in Tables 8-19 and 8-20. Residual tensile strength data are tabulated in Tables 8-21 and 8-22 for aging at ambient pressure and Tables 8-23 and Table 8-24 for aging at reduced pressure. The tensile data are also plotted as a function of aging time in Figures 8-38 and 8-39. A summary of the effects of 10,000 hours of thermal aging on the tensile strength retention of this G/PI is shown in Table 8-25. Six extra specimens were available after 10,000 hours of exposure for each of the aging conditions. These were tensile tested and are included in the data of Tables 8-21 through 8-24.

The appearance of the specimens was relatively unchanged by the 10,000 hours of exposure. Some slight color changes and slight changes in the ring when the specimens were dropped were observed. After 5000 hours some edge cracking had occurred in the specimens aged at 505K (450°F). Similar edge cracking was found in the specimens aged at 450K (350°F) after 10,000 hours. The degree of edge cracking in these 6 ply laminates was not severe.

During cure of the adhesive for bonding the doublers seven of the nine 10,000 hour, 450K (350°F), one atmosphere specimens delaminated. None of the other specimens experience this problem. The delamination did not prevent tensile testing.

After tensile testing, the specimens that had been aged at reduced pressure were similar in appearance to the unexposed baseline tensile specimens. Specimens aged at one atmosphere were somewhat more broken up following tensile testing after 5000 hours of exposure. There was no visible difference between specimens aged at the two temperatures, however. After 10,000 hours of aging in ambient air, the specimens (for both temperatures) showed an increased amount of breaking up and splintering. Some exposed fibers were visible where the matrix had crumbled away. The amount of bare fibers was not large.

At 450K (350°F) weight changes, as shown in Table 8-19, were small with the maximum being a loss of 1.5% after 10,000 hours. At 505K (450°F), however, significant weight loss occurred after 5000 hours (6%) and increased to about 9% after 10,000 hours. No weight change measurements were made on the reduced pressure specimens.

As shown in Figure 8-38 thermal aging at 450K (350°F) had little effect for specimens exposed at reduced pressure with a decrease in tensile strength of only 8%. Ambient exposure at this temperature, on the other hand, reduced the tensile strength by 35% after 10,000 hours. By way of comparison, the crossplied G/E material lost 40% of the strength for the same exposure. Reduced pressure exposure at 505K (450°F) had about the same effect on residual tensile strength as did the 450K (350°F) exposure. Aging at 505K (450°F) in one atmosphere air was not detrimental to tensile strength retention as that at 450K (350°F). A decrease of approximately 20% was measured after 10,000 hours. This is in contrast to thermal aging effects measured on several other composite systems where higher aging temperatures have resulted in increased loss in strength. Compared to the HT-S/710 G/PI system where crossplied specimens survived 25,000 hours at 505K (450°F) and one atmosphere with almost no loss in tensile strength, the Celion 6000/LARC-160 system possessed considerably less thermal stability.

**Table 8-19 Thermal Aging Data (Weight Changes) for Celion 6000/LARC-160 G/PI in 0.10 MN/m² (14.7 psi) Air**

| Aging Temperature K | Aging Temperature (°F) | Aging Time (hr) | Weight Change gm | Weight Change % |
|---|---|---|---|---|
| 450 | 350 | 500 | +0.006 | +0.2 |
| | | | +0.008 | +0.2 |
| | | | +0.006 | +0.2 |
| | | | | avg +0.2 |
| | | 1,000 | +0.004 | +0.1 |
| | | | +0.005 | +0.1 |
| | | | +0.006 | +0.2 |
| | | | | avg +0.1 |
| | | 5,000 | 0.000 | 0.0 |
| | | | −0.001 | 0.0 |
| | | | −0.001 | 0.0 |
| | | | | avg 0.0 |
| | | 10,000 | −0.056 | −1.6 |
| | | | −0.045 | −1.3 |
| | | | −0.063 | −1.7 |
| | | | | avg −1.5 |

**Table 8-20 Thermal Aging Data (Weight Changes) for Celion 6000/LARC-160 G/PI in 0.10 MN/m² (14.7 psi) Air**

| Aging Temperature | | Aging Time | Weight Change | |
|---|---|---|---|---|
| K | (°F) | (hr) | gm | % |
| 505 | 450 | 500 | −0.02 | −0.6 |
| | | | −0.02 | −0.6 |
| | | | −0.02 | −0.5 |
| | | | | avg −0.6 |
| | | 1,000 | −0.03 | −0.7 |
| | | | −0.03 | −0.8 |
| | | | −0.03 | −0.8 |
| | | | | avg −0.8 |
| | | 5,000 | −0.21 | −5.9 |
| | | | −0.21 | −5.8 |
| | | | −0.19 | −5.5 |
| | | | | avg −5.7 |
| | | 10,000 | −0.31 | −8.7 |
| | | | −0.32 | −8.9 |
| | | | −0.31 | −8.7 |
| | | | | avg −8.8 |

Table 8-21 Thermal Aging Data for $[0° \pm 45°]_s$ Celion 6000/LARC-160 G/PI in 0.10 MN/m² (14.7 psi) Air

| Aging Temperature K | Aging Temperature (°F) | Test Temperature K | Test Temperature (°F) | Aging Time (hr) | Tensile Strength MN/m2 | Tensile Strength (ksi) |
|---|---|---|---|---|---|---|
| 450 | 350 | 450 | 350 | Baseline avg | 696 | 101 |
| | | | | 500 | 597 | 86.6 |
| | | | | | 596 | 86.5 |
| | | | | | 628 | 91.1 |
| | | | | | avg 607 | 88.1 |
| | | | | 1,000 | 518 | 75.2 |
| | | | | | 564 | 81.8 |
| | | | | | 578 | 83.8 |
| | | | | | avg 553 | 80.3 |
| | | | | 5,000 | 506 | 73.4 |
| | | | | | * | * |
| | | | | | 550 | 79.8 |
| | | | | | avg 528 | 76.6 |
| | | | | 10,000 | 482 | 69.9 |
| | | | | | 423 | 61.4 |
| | | | | | 496 | 72.0 |
| | | | | | 432 | 62.7 |
| | | | | | 479 | 69.5 |
| | | | | | 433 | 62.8 |
| | | | | | 465 | 67.5 |
| | | | | | 419 | 60.7 |
| | | | | | 428 | 62.1 |
| | | | | | avg 451 | 65.4 |

*Doubler bond failure

Table 8-22 Thermal Aging Data for $[0° \pm 45°]_s$ Celion 6000/LARC-160 G/PI in 0.10 MN/m² (14.7 psi) Air

| Aging Temperature K | Aging Temperature (°F) | Test Temperature K | Test Temperature (°F) | Aging Time (hr) | Tensile Strength MN/m2 | Tensile Strength (ksi) |
|---|---|---|---|---|---|---|
| 505 | 450 | 450 | 350 | Baseline avg | 696 | 101 |
| | | | | 500 | 609 | 88.3 |
| | | | | | 663 | 96.2 |
| | | | | | 685 | 99.4 |
| | | | | | avg 652 | 94.6 |
| | | | | 1,000 | 667 | 96.8 |
| | | | | | 579 | 84.0 |
| | | | | | 607 | 88.1 |
| | | | | | avg 618 | 89.6 |
| | | | | 5,000 | 571 | 82.8 |
| | | | | | 562 | 81.5 |
| | | | | | 566 | 82.1 |
| | | | | | avg 566 | 82.1 |
| | | | | 10,000 | 514 | 74.6 |
| | | | | | 516 | 74.8 |
| | | | | | 510 | 74.0 |
| | | | | | 549 | 79.6 |
| | | | | | 581 | 84.2 |
| | | | | | 521 | 75.6 |
| | | | | | 536 | 77.7 |
| | | | | | 585 | 84.8 |
| | | | | | 618 | 89.7 |
| | | | | | avg 547 | 79.4 |

**Table 8-23 Thermal Aging Data for $[0° \pm 45°]_s$ Celion 6000/LARC-160 G/PI in 0.014 MN/m² (2 psi) Air**

| Aging Temperature K | Aging Temperature (°F) | Test Temperature K | Test Temperature (°F) | Aging Time (hr) | Tensile Strength MN/m2 | Tensile Strength (ksi) |
|---|---|---|---|---|---|---|
| 450 | 350 | 450 | 350 | Baseline avg | 696 | 101 |
| | | | | 5,000 | 565 | 81.9 |
| | | | | | 613 | 88.9 |
| | | | | | 614 | 89.0 |
| | | | | | avg 597 | 86.6 |
| | | | | 10,000 | 687 | 99.7 |
| | | | | | 685 | 99.4 |
| | | | | | 685 | 99.3 |
| | | | | | 623 | 90.4 |
| | | | | | 596 | 86.4 |
| | | | | | 629 | 91.3 |
| | | | | | 630 | 91.4 |
| | | | | | 632 | 91.7 |
| | | | | | 584 | 84.7 |
| | | | | | avg 639 | 92.7 |

**Table 8-24 Thermal Aging Data for $[0° \pm 45°]_s$ Celion 6000/LARC-160 G/PI in 0.014 MN/m² (2 psi) Air**

| Aging Temperature K | Aging Temperature (°F) | Test Temperature K | Test Temperature (°F) | Aging Time (hr) | Tensile Strength MN/m2 | Tensile Strength (ksi) |
|---|---|---|---|---|---|---|
| 505 | 450 | 450 | 350 | Baseline avg | 696 | 101 |
| | | | | 5,000 | 562 | 81.5 |
| | | | | | 555 | 80.5 |
| | | | | | 570 | 82.6 |
| | | | | | avg 563 | 81.5 |
| | | | | 10,000 | 621 | 90.1 |
| | | | | | 588 | 85.3 |
| | | | | | 593 | 86.0 |
| | | | | | 635 | 92.1 |
| | | | | | 624 | 90.5 |
| | | | | | 591 | 85.7 |
| | | | | | 658 | 95.4 |
| | | | | | 573 | 83.1 |
| | | | | | 607 | 88.0 |
| | | | | | avg 610 | 88.5 |

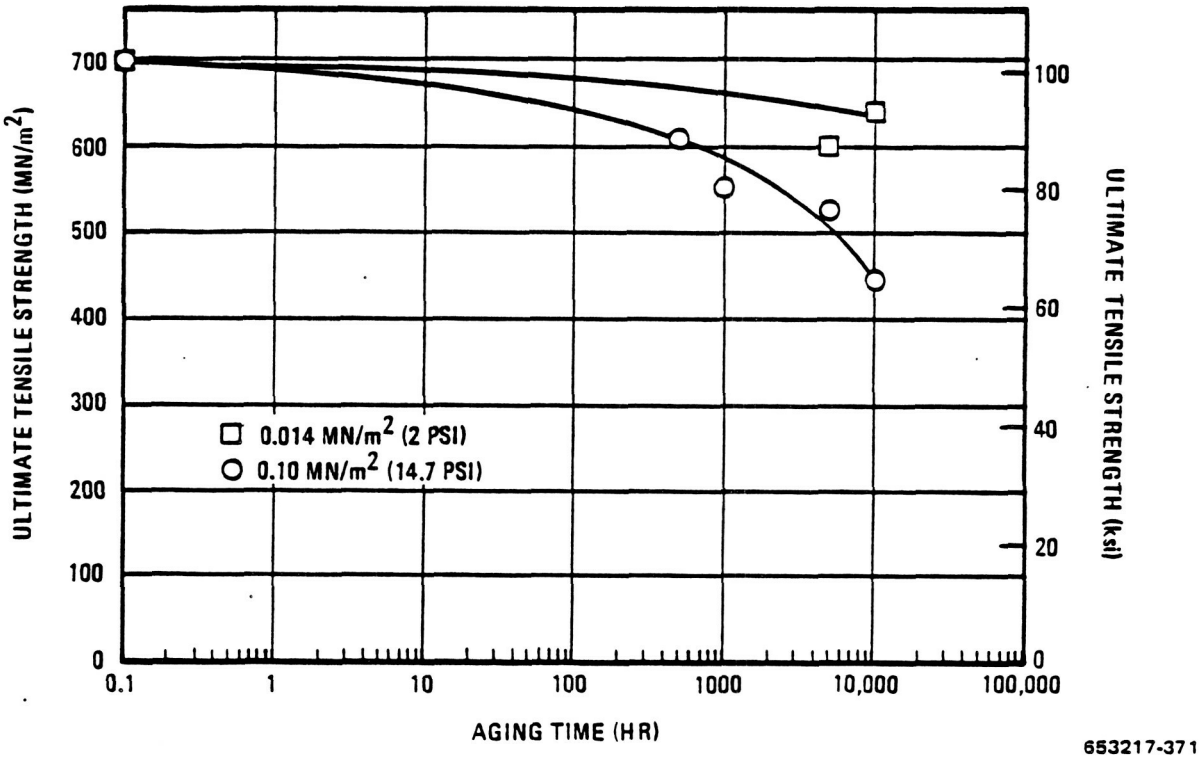



**Figure 8-38 Tensile Strength of Celion 6000/LARC-160 G/PI at 450K (350°F) After Thermal Aging at 450K (350°F) and the Indicated Pressure**

In summary, the effects of 10,000 hours of thermal aging in one atmosphere on Celion 6000/LARC-160 G/PI were significant losses in tensile strength, beginning as early as 500 hours, and some matrix degradation. Tensile strength losses were higher for the 450K (350°F) exposures, 35%, than for those at 505K (450°F), about 20%, and were accompanied by greater matrix degradation. Weight loss during aging, however, was higher at the higher temperature. For the reduced pressure exposures no matrix degradation was observed, and strength losses were only of the order of 10% after 10,000 hours.

Samples of Celion 6000/LARC-160 G/PI in the unexposed condition and after 5000 and 10,000 hours of exposure were mounted, polished, and examined using optical and scanning electron microscopes. At lower magnifications the degree of microcracking and relief polishing at the graphite fibers was found to be related to both the temperature and length of time of aging (increasing with both increasing temperature and time). At higher magnification, evidence of oxidation, similar in nature to that observed in the G/E system, was found. Figure 8-40 shows the results of the higher magnification examinations. When the polyimide resin matrix oxidized, it was more prone to crumble and resulted in an increased amount of relief polishing around the individual fibers. After 10,000 hours of aging at both temperatures, considerable oxidation had occurred in the outer plies but almost none in the center plies. This would be expected for an oxidation mechanism where attack begins at the outer surfaces and proceeds inward. Careful examination of Figure 8-40 also reveals an effect of temperature on oxidation where the degree of relief polishing around the graphite fibers is slightly greater at 505K (450°F) than at 450K (350°F). This oxidation effect was not observed for the HT-S/710 G/PI system.

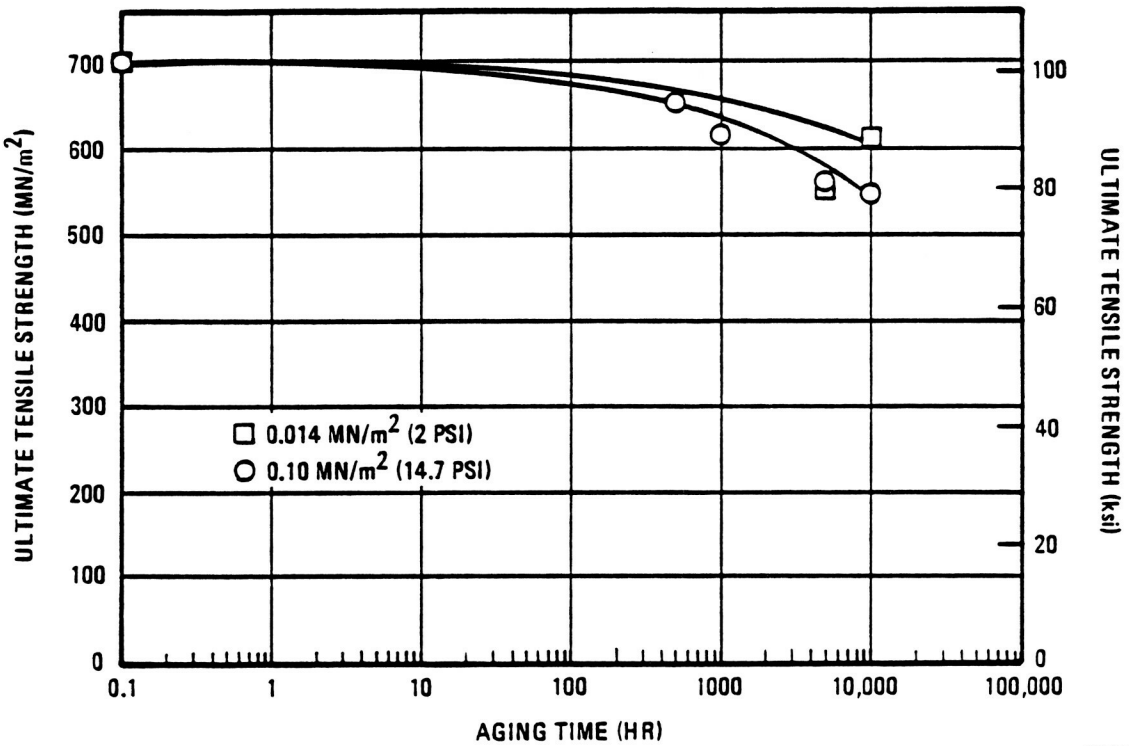



**Figure 8-39 Tensile Strength of Celion 6000/LARC-160 G/PI at 450K (350°F) After Thermal Aging at 505K (450°F) and the Indicated Pressure**

**8.2.3 BORON/ALUMINUM.** In Phase I of the thermal aging test program exposures were conducted on B/E, G/E, HT-S/710 G/PI, and B/Al for time periods up to and including 10,000 hours. For the B/E, G/E, and G/PI systems additional specimens had been prepared and placed in the thermal aging furnaces at the beginning of Phase I for removal during Phase II at 25,000 and 50,000 hours. No such provision was made for the B/Al system. However, at the beginning of Phase II some excess material purchased for fabrication of the 25,000 hour flight simulation specimens was available, and B/Al specimens were prepared and placed in the aging furnaces for

**Table 8-25 Summary of Tensile Strength Retention After 10,000 Hours of Thermal Aging for $[0° \pm 45°]_s$ Crossplied Celion 6000/LARC-160 G/PI**

| Aging Temperature | | Aging Pressure | | Test Temperature | | Retention of Tensile |
|---|---|---|---|---|---|---|
| K | (°F) | MN/m2 | (psi) | K | (°F) | Strength (%) |
| 450 | 350 | 0.10 | 14.7 | 450 | 350 | 65 |
| 450 | 350 | 0.014 | 2 | 450 | 350 | 92 |
| 505 | 450 | 0.10 | 14.7 | 450 | 350 | 79 |
| 505 | 450 | 0.014 | 2 | 450 | 350 | 88 |

**Figure 8-40 Photomicrographs (SEM) of Celion 6000/LARC-160 G/PI After Thermal Aging at Indicated Conditions, 1000X**

ORIGINAL PAGE IS
OF POOR QUALITY

exposures of 25,000 and 40,000 hours. The 40,000 hour figure was chosen so that all the material systems would complete the thermal aging exposures at about the same time. As will be shown the two batches of B/Al, obtained 3 years apart, exhibited considerably different behavior during thermal exposure. For this reason the Phase I and Phase II results are discussed separately.

**8.2.3.1 Phase I.** The Phase I B/Al thermal aging study was conducted on unidirectional and $[0° \pm 45°]_s$ crossplied laminates for time periods of 5000 and 10,000 hours. Exposures were carried out in one atmosphere air at temperatures of 450K (350°F), 561K (550°F), and 700K (800°F). Following aging, residual tensile and interfiber shear tests were performed at room temperature. Longitudinal tensile strengths of the unidirectional and crossplied materials were determined to evaluate fiber degradation while transverse tensile and longitudinal shear properties of the unidirectional material were obtained to study matrix effects. The data from the various exposures are presented in Tables 8-26 to 8-29. A summary of the effects of 10,000 hours of thermal aging on the strength retention of B/Al is given in Table 8-30. The tensile and shear strength data have also been plotted as a function of aging time. These curves are shown in Figures 8-41 to 8-43.

At 561K (550°F) and 700K (800°F) extensive degradation was observed in the tensile strength of material tested in the 0 degree direction of both layups. These decreases were as high as 80% at 700K (800°F) and 60% at 561K (550°F). Decreases were also observed (particularly in the unidirectional material) at 450K (350°F), although not as large. The physical appearance of the specimens was unchanged after 10,000 hours of aging at the two lowest temperatures. At the highest temperature, 700K (800°F), some surface discoloration was observed. Of more importance, however, was oxidation and loss of the exposed ends of the boron fibers in the transverse tensile and interfiber shear specimens. Figure 8-44 is a SEM photomicrograph of the edge of a transverse tensile specimen that was aged for 5000 hours at 700K (800°F). The boron fibers are oxidized to a depth of approximately 0.00064m (0.025 in.). After 10,000 hours of aging, loss of the boron fibers extends to a depth of approximately 0.0015m (0.06 in.). No oxidation of the boron was found in specimens aged at the other temperatures.

Because of the notches in the interfiber shear specimens were fabricated prior to aging, oxidation of the boron filaments had a significant effect on the residual shear strength. At 450K (350°F) and 561K (550°F), where no oxidation was found, no decrease in shear strength was observed. However, at 700K (800°F) decreases of 30 and 60% were measured after 5000 and 10,000 hours respectively. The machined edges at each end of the shearing regions were exposed to the air environment during aging and extensive oxidation of the boron occurred. This can be seen in the fracture surfaces of shear specimens shown in Figures 8-45 and 8-46. These figures show samples of B/Al after aging periods of 5000 and 10,000 hours and, for comparison, one that had not been exposed prior to shear testing. The length of the shear region is approximately 0.0025m (0.10 in.) as shown in Figure 7-30. For the unexposed specimen, Figure 8-45, where no oxidation of the boron has occurred, the fracture surface is uniform along its length. The primary failure mode was matrix failure with some failure at the filament-matrix interface. In the specimen aged for 5000 hours at 700K (800°F), Figure 8-45, loss of boron by oxidation is readily visible at either end of the sheared region. This attack extends for approximately 0.00064m (0.025 in.) from each end and has consumed about half of the fiber length. With the loss of the filaments, the area over which fracture occurred was considerably reduced and the specimen had lower strength. The residual shear stress was calculated using the original shearing area. It is this effect that accounts for the apparent 30% decrease in shear strength after 5000 hours at 700K (800°F). Had the notches been machined in the specimens after aging, the residual shear strengths would probably have shown little change from the unexposed value. The failure mode in the center por-

**Table 8-26 Thermal Aging Data for $[0°]_6$ B/Al Aged in One Atmosphere Air and Tested at 297K (75°F) — Longitudinal Test Direction**

| Aging Temperature K | Aging Temperature (°F) | Aging Time (hr) | | Tensile Strength MN/m2 | Tensile Strength (ksi) |
|---|---|---|---|---|---|
| 450 | 350 | Baseline avg | | 1450 | 210 |
| | | 5,000 | | 1320 | 191 |
| | | | | 1230 | 179 |
| | | | | 1070 | 155 |
| | | | avg | 1210 | 175 |
| | | 10,000 | | 1010 | 146 |
| | | | | 986 | 143 |
| | | | | 869 | 126 |
| | | | avg | 955 | 138 |
| 561 | 550 | 5,000 | | 841 | 122 |
| | | | | 855 | 124 |
| | | | | 889 | 129 |
| | | | avg | 862 | 125 |
| | | 10,000 | | 855 | 124 |
| | | | | 703 | 102 |
| | | | | 786 | 114 |
| | | | avg | 781 | 113 |
| 700 | 800 | 5,000 | | 327 | 47.4 |
| | | | | 631 | 91.5 |
| | | | | 315 | 45.7 |
| | | | avg | 424 | 61.5 |
| | | 10,000 | | 263 | 38.1 |
| | | | | 320 | 46.4 |
| | | | | 318 | 46.1 |
| | | | avg | 300 | 43.5 |

Table 8-27 Thermal Aging Data for $[0°]_6$ B/Al Aged in One Atmosphere Air and Tested at 297K (75°F) — Transverse Test Direction

| Aging Temperature K | Aging Temperature (°F) | Aging Time (hr) | | Tensile Strength MN/m2 | Tensile Strength (ksi) |
|---|---|---|---|---|---|
| 450 | 350 | Baseline avg | | 79.3 | 11.5 |
| | | 5,000 | | 159 | 23.1 |
| | | | | 143 | 20.7 |
| | | | | 116 | 16.8 |
| | | | avg | 139 | 20.2 |
| | | 10,000 | | 104 | 15.1 |
| | | | | 93.8 | 13.6 |
| | | | | 121 | 17.5 |
| | | | avg | 106 | 15.4 |
| 561 | 550 | 5,000 | | 98.6 | 14.3 |
| | | | | 102 | 14.8 |
| | | | | 104 | 15.1 |
| | | | avg | 102 | 14.7 |
| | | 10,000 | | 108 | 15.7 |
| | | | | 74.5 | 10.8 |
| | | | | 75.2 | 10.9 |
| | | | avg | 85.9 | 12.5 |
| 700 | 800 | 5,000 | | 104 | 15.1 |
| | | | | 101 | 14.7 |
| | | | | 94.5 | 13.7 |
| | | | avg | 100 | 14.5 |
| | | 10,000 | | 80.0 | 11.6 |
| | | | | 76.5 | 11.1 |
| | | | | 100 | 14.5 |
| | | | avg | 85.5 | 12.4 |

**Table 8-28 Thermal Aging Data for $[0°]_6$ B/Al Aged in One Atmosphere Air and Tested at 297K (75°F) — Interfiber Shear in Longitudinal Direction**

| Aging Temperature K | Aging Temperature (°F) | Aging Time (hr) | | Tensile Strength MN/m2 | Tensile Strength (ksi) |
|---|---|---|---|---|---|
| 450 | 350 | Baseline avg | | 93.1 | 13.5 |
| | | 5,000 | | 82.0 | 11.9 |
| | | | | 93.1 | 13.5 |
| | | | | 109 | 15.8 |
| | | | avg | 94.7 | 13.7 |
| | | 10,000 | | 109 | 15.8 |
| | | | | 100 | 14.5 |
| | | | | 108 | 15.7 |
| | | | avg | 106 | 15.3 |
| 561 | 550 | 5,000 | | 85.5 | 12.4 |
| | | | | 93.8 | 13.6 |
| | | | | 91.7 | 13.3 |
| | | | avg | 90.3 | 13.1 |
| | | 10,000 | | 97.2 | 14.1 |
| | | | | 91.7 | 13.3 |
| | | | | 91.0 | 13.2 |
| | | | avg | 93.3 | 13.5 |
| 700 | 800 | 5,000 | | 42.1 | 6.1 |
| | | | | 77.2 | 11.2 |
| | | | | 79.3 | 11.5 |
| | | | avg | 66.2 | 9.6 |
| | | 10,000 | | 71.7 | 10.4 |
| | | | | 18.6 | 2.7 |
| | | | | 24.8 | 3.6 |
| | | | avg | 38.4 | 5.6 |

**Table 8-29 Thermal Aging Data for $[0° \pm 45°]_s$ Crossplied B/Al Aged in One Atmosphere Air and Tested at 297K (75°F) — Longitudinal Test Direction**

| Aging Temperature K | Aging Temperature (°F) | Aging Time (hr) | | Tensile Strength MN/m2 | Tensile Strength (ksi) |
|---|---|---|---|---|---|
| 450 | 350 | Baseline avg | | 516 | 74.8 |
| | | 5,000 | | 430 | 62.3 |
| | | | | 467 | 67.7 |
| | | | | 535 | 77.6 |
| | | | avg | 477 | 69.2 |
| | | 10,000 | | 459 | 66.6 |
| | | | | 444 | 64.4 |
| | | | | 428 | 62.1 |
| | | | avg | 444 | 64.4 |
| 561 | 550 | 5,000 | | 276 | 40.4 |
| | | | | 251 | 36.4 |
| | | | | 257 | 37.3 |
| | | | avg | 261 | 37.9 |
| | | 10,000 | | 184 | 26.7 |
| | | | | 214 | 31.1 |
| | | | | 210 | 30.4 |
| | | | avg | 203 | 29.4 |
| 700 | 800 | 5,000 | | 168 | 24.4 |
| | | | | 185 | 26.8 |
| | | | | 198 | 28.7 |
| | | | avg | 184 | 26.6 |
| | | 10,000 | | 142 | 20.6 |
| | | | | 143 | 20.7 |
| | | | | 154 | 22.3 |
| | | | avg | 146 | 21.2 |

**Table 8-30 Summary of Room Temperature Strength Retention After 10,000 Hours of Thermal Aging in One Atmosphere Air for B/Al**

| Laminate Orientation | Test Direction | Property | Strength Retention (%) After 10,000 Hours | | |
|---|---|---|---|---|---|
| | | | 450K (350°F) | 561K (550°F) | 700K (800°F) |
| $[0°]_6$ | [0°] | Tensile | 66 | 54 | 21 |
| $[0°]_6$ | [90°] | Tensile | 100 | 100 | 100 |
| $[0°]_6$ | [0°] | Shear | 100 | 100 | 41 |
| $[0° \pm 45°]_s$ | [0°] | Tensile | 86 | 39 | 28 |

tion of the aged specimen is similar to that of the unexposed specimen in Figure 8-45 with the addition of a small amount of filament splitting. In the two end portions, failure has occurred in the narrow aluminum regions between the hollow areas previously occupied by the oxidized boron filaments. Figure 8-46 shows the two fracture surfaces (specimens are tested in double shear — Figure 7-30) of a specimen aged for 10,000 hours at 700K (800°F). For this specimen oxidation of the boron was more extensive on one side than on the other. As can be seen in Figure 8-46, oxidation has consumed almost all the boron on the surface on the left. The opposite sheared surface, on the right in Figure 8-46, shows somewhat less filament oxidation. The failure

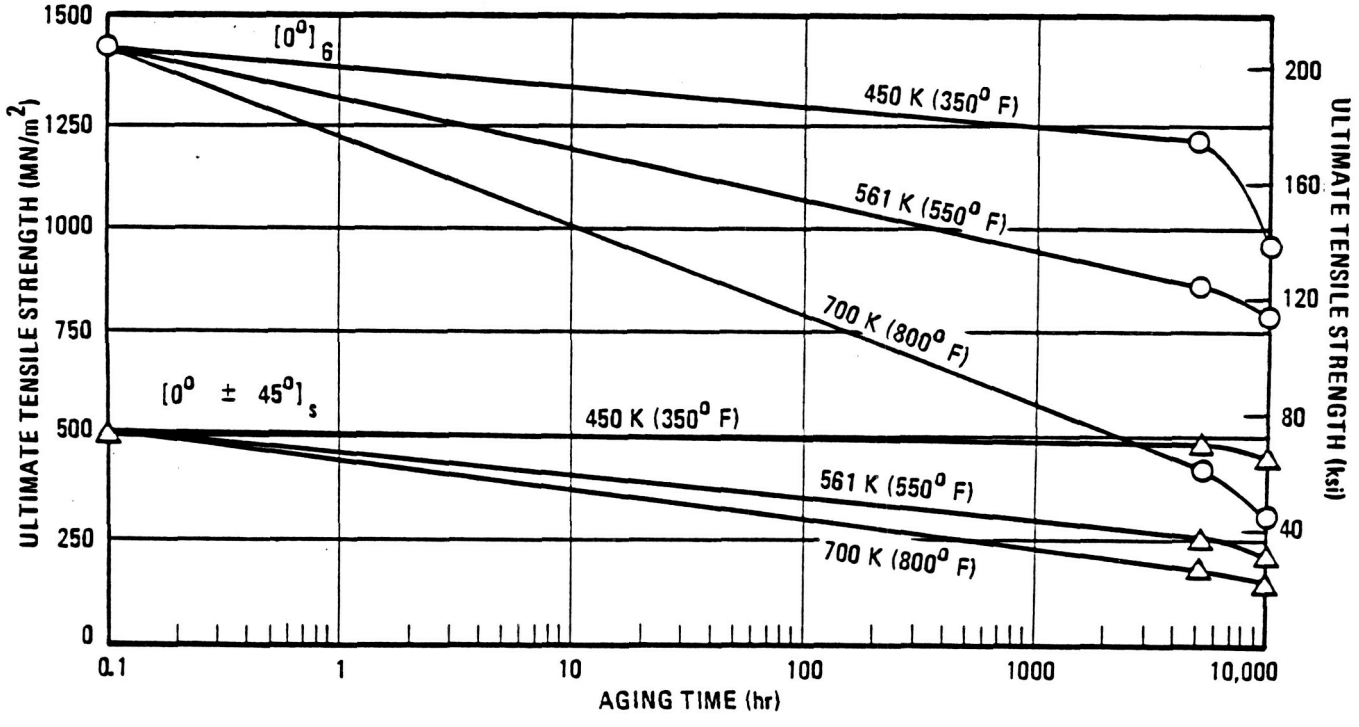



**Figure 8-41 Tensile Strength of B/Al at 297K (75°F) After Thermal Aging at Indicated Temperature**

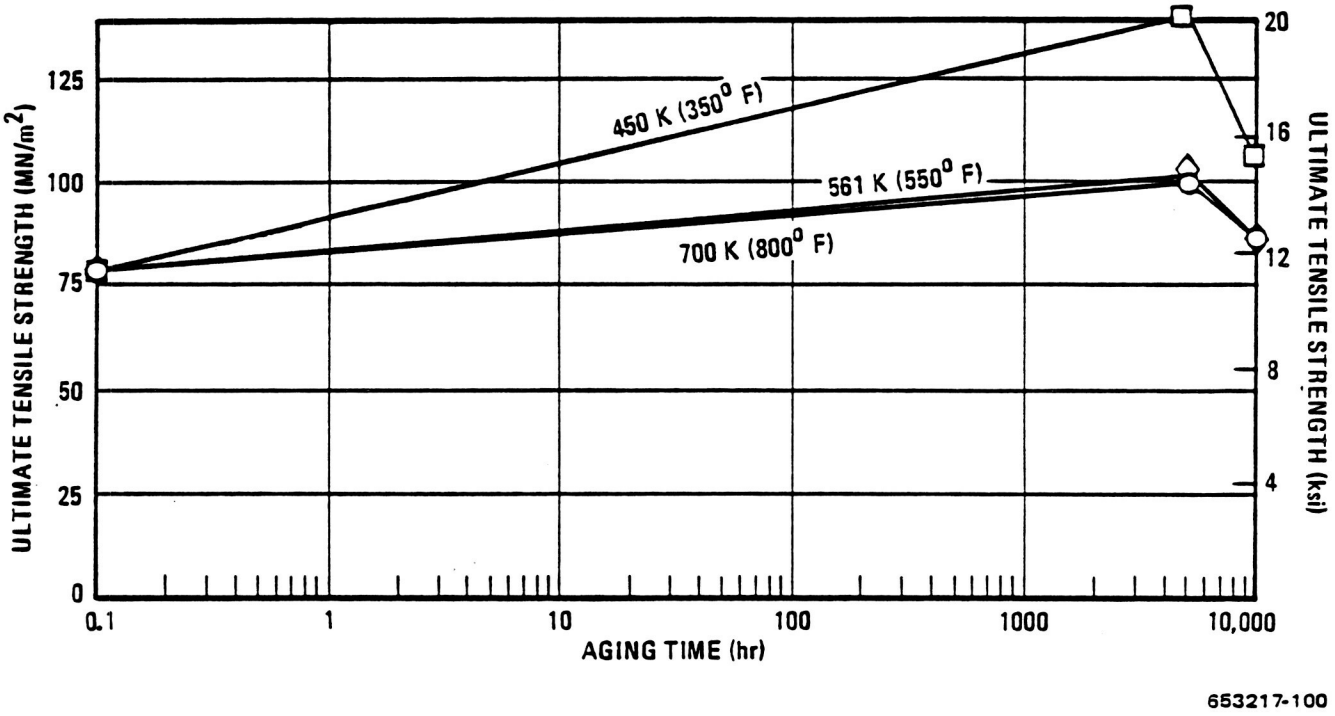



**Figure 8-42 Transverse Tensile Strength of B/Al at 297K (75°F) After Thermal Aging at Indicated Temperature**

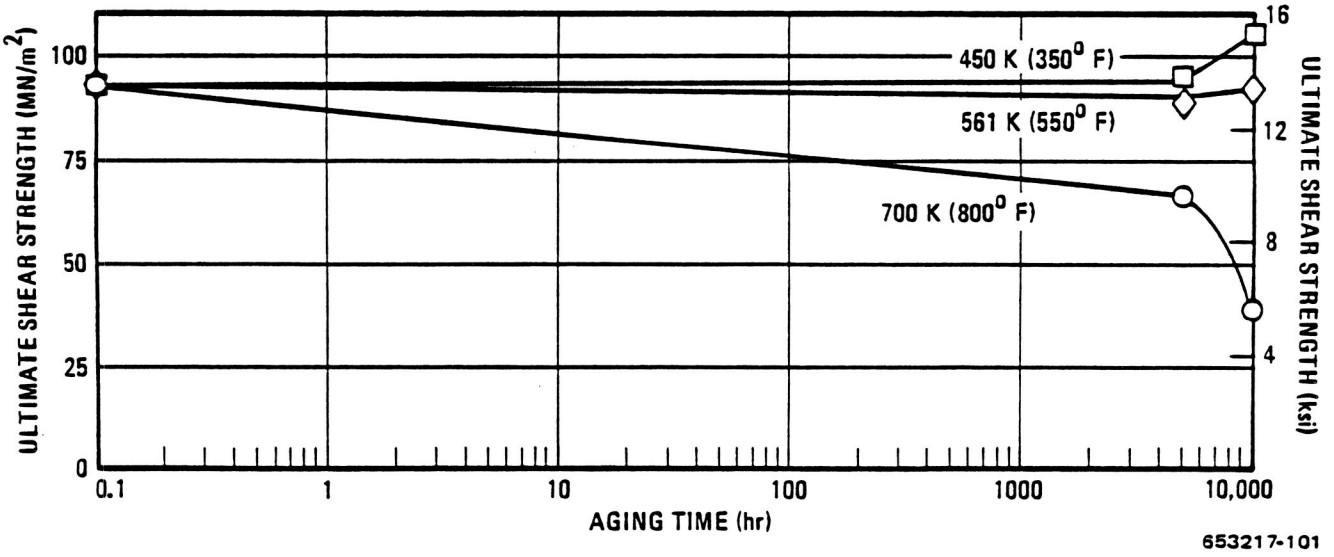



**Figure 8-43 Shear Stength of Unidirectional B/Al at 297K (75°F) After Thermal Aging at Indicated Temperature**

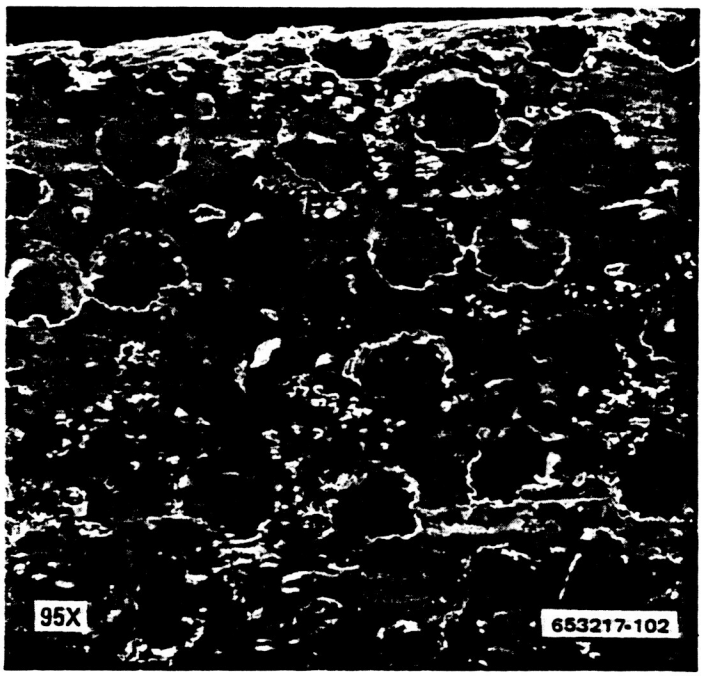



**Figure 8-44 Edge View of B/Al After 5000 Hours of Thermal Aging at 700K (800°F) in One Atmosphere Air Showing Loss of Boron Through Oxidation**

mode of the specimens aged for 10,000 hours was again matrix dominated but showed an increase in the amount of filament splitting over that observed after 5000 hours.

Table 8-30 shows 100% retention of the transverse tensile strength for all the thermal aging exposures. These results, however, are somewhat misleading because of the low values obtained from the baseline tests. The baseline specimens were taken from a different panel than was used for the thermal aging tests and showed considerable scatter when tensile tested. The transverse tensile data from aged material, Table 8-27, indicate some decrease in strength has occurred for the 10,000-hour exposures, at 56K (550°F) and 700K (800°F). These decreases are thought to be the result of changes in the boron and boron aluminum interface rather than degradation of the aluminum matrix. Figures 8-47 through 8-49 show the fracture surfaces of transverse tensile specimens that were tested after the following thermal treatments:

a. Figure 8-47, unexposed.

b. Figure 8-48, 5000 hours at 450K (350°F).

c. Figure 8-49, 10,000 hours at 561K (550°F).

In the unexposed specimen, Figure 8-47, the primary failure mode is matrix failure with some failure near, but not quite at, the filament-matrix interface. As thermal aging temperatures and times increase the failure mode changes from primarily matrix dominated to one in which, first, increased fracture at the filament-matrix interface occurs and, second, for more severe exposures, considerable filament splitting is observed. Figure 8-48 shows the increased interface fracture. A good example of filament splitting is illustrated by Figure 8-49. Two boron fibers have fractured lengthwise through their centers revealing the fine tungsten cores used in fabricating



ORIGINAL PAGE IS
OF POOR QUALITY

ORIGINAL PAGE IS
OF POOR QUALITY




Figure 8-45 Fracture Surface of Interfiber Shear Specimens of B/Al Before and After Thermal Aging at 700K (800°F) in One Atmosphere Air

Figure 8-46 Fracture Surfaces of Interfiber Shear Specimen of B/Al After 10,000 Hours of Thermal Aging at 700K (800°F) in One Atmosphere Air (Specimen was Tested in Double Shear)



ORIGINAL PAGE IS
OE POOR QUALITY

ORIGINAL PAGE IS
OF POOR QUALITY

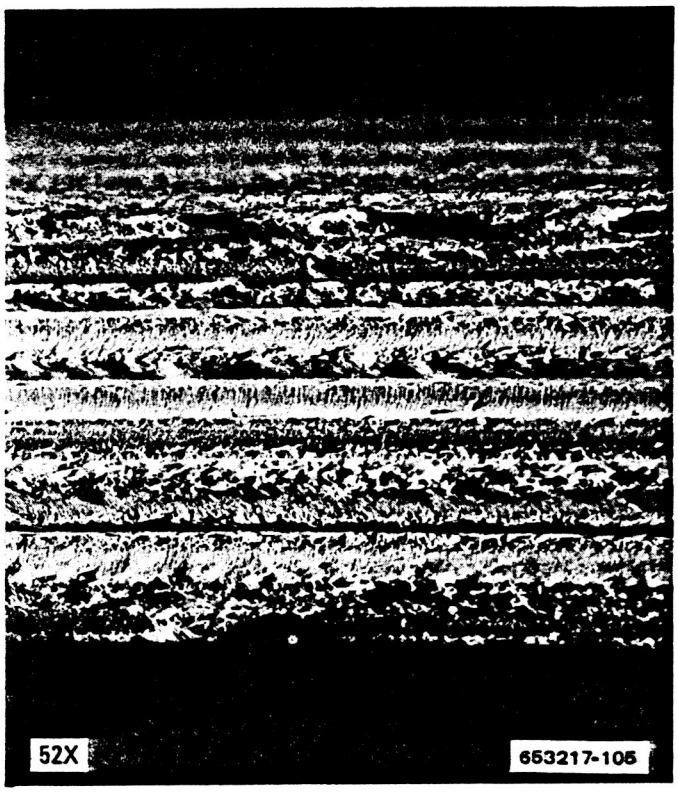



**Figure 8-47 Fracture Surface of Transverse Tensile Specimen of Unexposed B/Al Showing Predominantly Matrix Failure**

the filaments. An element scan taken with the SEM is also shown in Figure 8-49. With this technique the higher the atomic number of the constituent of the specimen the lighter the trace that is shown on the screen of the SEM. The two very light lines indicate the tungsten cores, the darkest areas are the low atomic number boron fibers, and the remaining grey area is the aluminum matrix. The change in the failure mode and the accompanying decrease in transverse tensile strength apparently occurs because the boron filaments become weakened as a result of interdiffusion between the boron and the 6061 aluminum alloy at the fiber-matrix interface during thermal exposure. Electron microprobe studies (reference 34) have shown that degradation of boron fibers can occur at elevated temperatures as a result of the diffusion of various elements from the aluminum alloy to the filaments. An excellent review of interfacial effects on the strength of B/Al after thermal exposure can be found in reference 35.

The effect of boron fiber oxidation during aging at 700K (800°F) was shown to have contributed considerably to the decrease in shear strength. For the transverse tensile specimens aged at 700K (800°F) the contribution was considerably less because of the lower percentage of test section affected, e.g., after 5000 hours at 700K (800°F) oxidation has consumed approximately 0.00064m (0.025 in.) from each end of the test section or 50% of the 0.0025m (0.10 in.) long shear region but only 10% of the 0.0127m (0.50 in.) wide tensile specimen. Figure 8-50 shows the extent of oxidation inward from the surface of transverse tensile specimens aged for 5000 and 10,000 hours. The appearance of split tubes is similar to that of Figure 8-45 and 8-46 for the shear specimens. The fracture surface away from the ends again reveals filament splitting and interfacial fracture in addition to the matrix failure.

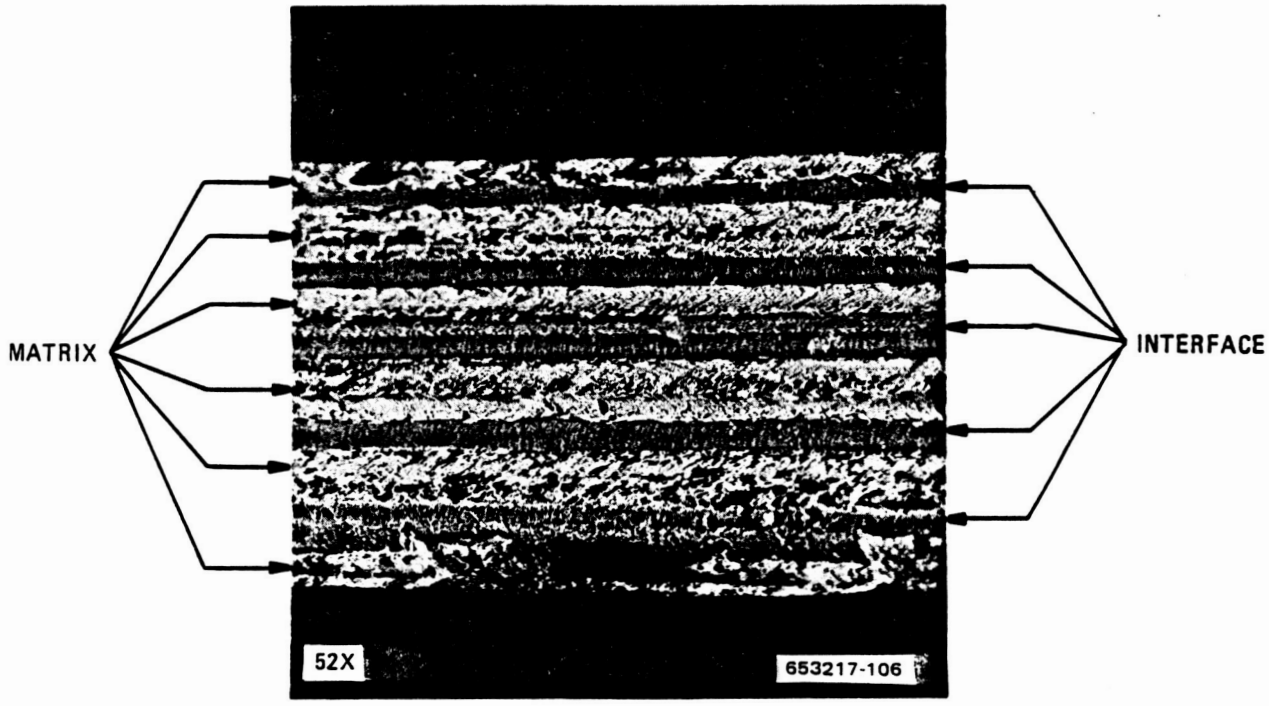



**Figure 8-48 Fracture Surface of Transverse Tensile Specimen of B/Al After 5000 Hours of Thermal Aging at 450K (350°F) in One Atmosphere Air Showing Both Matrix and Interface Failure Modes**

Further evidence that the decrease in tensile and shear strength of B/Al during thermal aging was the result of degradation of the boron filaments rather than the aluminum matrix was found during examination of the failed $[0° \pm 45°]_s$ crossplied specimens aged for 5000 hours at 561K (550°F). The outer 0 degree ply (on both sides) showed a series of closely spaced, 0.0013m (0.05 in.) to 0.0025m (0.10 in.), cracks across the width of the specimens. An overall view of these specimens showing the surface cracks as well as the necking that occurred during tensile testing is presented in Figure 8-51. Magnified views of the surface cracks are shown in Figure 8-52. Examination of the cracks with a stereographic microscope revealed that the cracks extended only through the outer 0 degree plies and that the boron filaments in these outside plies were broken at each one of the surface cracks. This can be seen on the right in Figure 8-52. It is believed that the boron filaments became weakened as a result of diffusion to the filament-matrix interface during thermal exposure. Following the multiple failures along the brittle filaments in the outside 0 degree layers, the load was picked up by the 45° plies. With the 0 degree plies no longer active, the specimens necked down considerably prior to final failure. This necking, which is not typical of $[0° \pm 45°]_s$ material that has not been exposed, is clearly visible in Figure 8-51. In the specimens aged for 10,000 hours at 561K (550°F), surface cracks were not as prevalent as those observed in the 5000 hour specimens but were similar in appearance. A very small number of surface cracks were also found after tensile testing the specimens aged at 450K (350°F) while none were observed in the specimens aged at 700K (800°F). Apparently the fracturing of the 0 degree outer boron filaments with the attendant surface cracks is highly dependent on the degree of filament embrittlement and is optimum after 5000 hours of exposure at 561K (550°F).

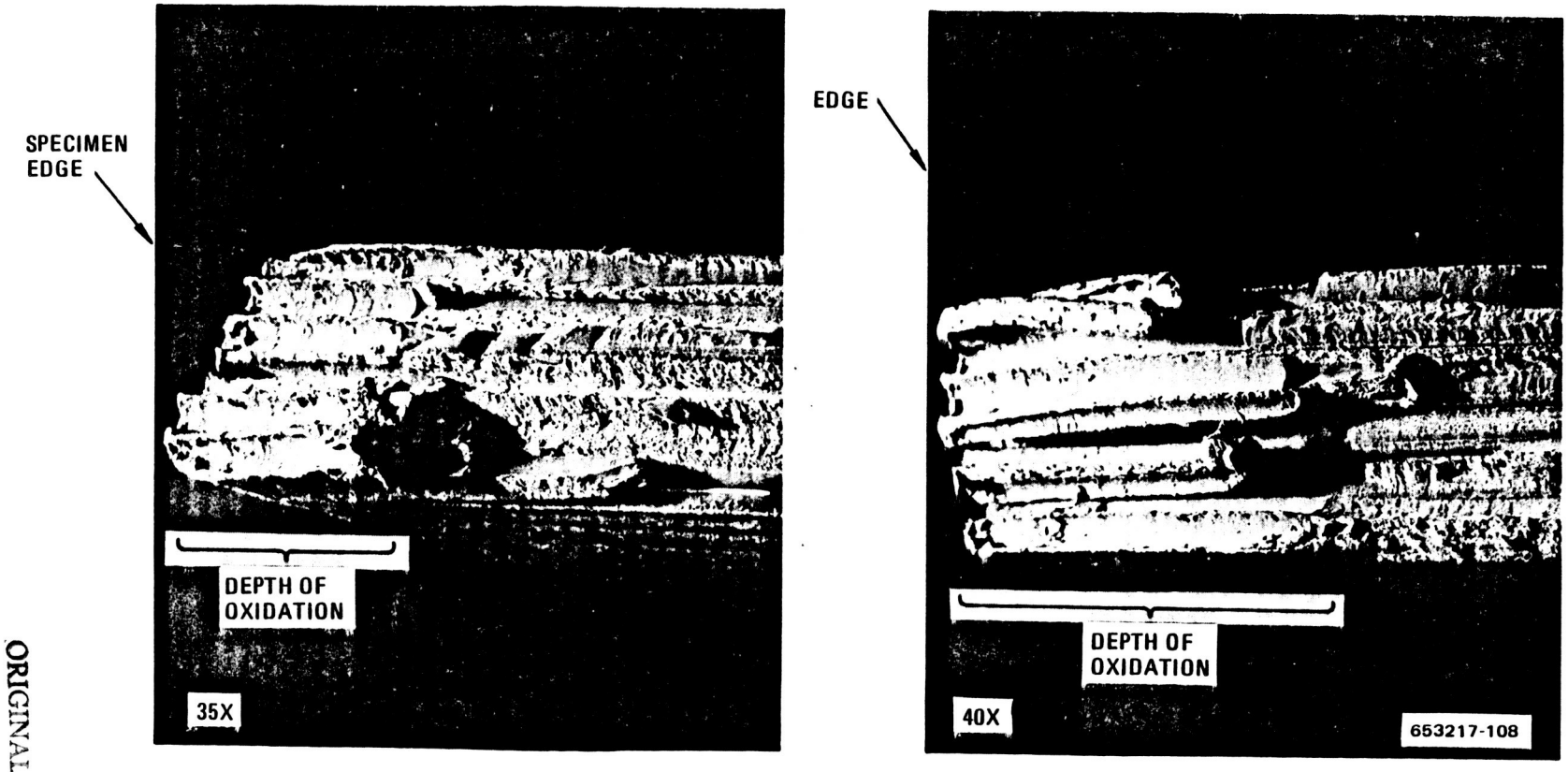


ORIGINAL PAGE IS
OF POOR QUALITY

ORIGINAL PAGE IS
OF POOR QUALITY




Figure 8-49 Fracture Surface of Transverse Tensile Specimen of B/Al After 10,000 Hours of Thermal Aging at 561K (550°F) in One Atmosphere Air Showing Matrix, Interface, and Filament Failure Modes




5000 HOURS 35X MAGNIFICATION

10,000 HOURS 40X MAGNIFICATION

**Figure 8-50 Portion of Fracture Surface of Transverse Tensile Specimens of B/Al After Thermal Aging at 700K (800°F) in One Atmosphere Air Showing Extent of Loss of Boron Through Oxidation**



ORIGINAL PAGE IS
OF POOR QUALITY

ORIGINAL PAGE IS
OF POOR QUALITY

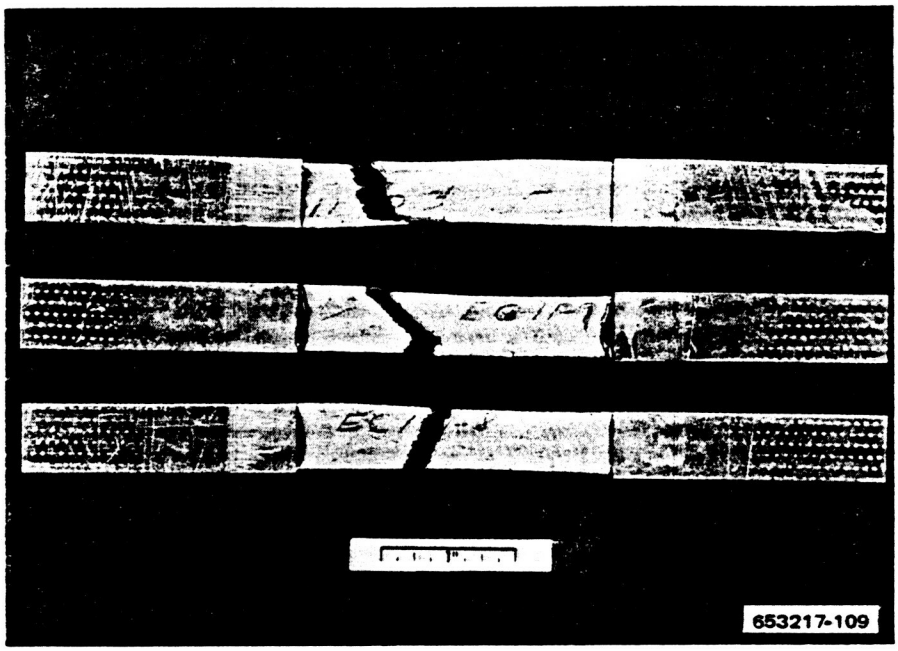



**Figure 8-51 B/Al After 5000 Hours of Thermal Aging at 561K (550°F) in One Atmosphere Air and Tensile Testing at Room Temperature Showing Transverse Surface Cracks and Necking in the Test Section**

**8.2.3.2 Phase II.** The Phase II B/Al thermal aging evaluation was similar to that conducted in Phase I in that both unidirectional and $[0° \pm 45°]_s$ crossplied laminates were thermally exposed in one atmosphere air. Also, post-exposure tensile and shear tests and metallographic and SEM examinations were performed. The 561K (550°F) aging temperature was retained, but the 700K (800°F) age was discontinued because of the severe degradation after 10,000 hours in Phase I, and the 450K (350°F) age was changed to 505K (450°F) to match the flight simulation exposure temperature. The exposure times were 25,000 hours and 40,000 hours. Data from the various exposures are presented in Tables 8-31 to 8-34. A summary of the effects of 25,000 and 40,000 hours of thermal aging on the strength retention of B/Al is given in Table 8-35.

Visual examination of the B/Al specimens after 25,000 hours and 40,000 hours of aging revealed no changes in the aluminum surface for either exposure temperatures. There was, however, oxidation and loss of the exposed ends of the boron fibers. At 505K (450°F) oxidation of the fine tungsten core in the center of the boron fibers was visible after 25,000 hours. After 40,000 hours some oxidation of the boron had occurred. The effect was considerably more pronounced for the specimens aged at 561K (550°F). Figure 8-53 shows the holes formerly occupied by the boron fibers in the edges of specimens aged at 561K (550°F) for 25,000 hours and 40,000 hours.

After 25,000 hours the fine tungsten core has been oxidized, leaving a yellow-green residue. This can be seen in some of the holes in Figure 8-53. Oxidation of the boron has also occurred, although the amount is not very great for 25,000 hours. After 40,000 hours no traces of the tungsten oxida-

Figure 8-52 B/Al After 5000 Hours of Thermal Aging at 561K (550°F) in One Atmosphere and Tensile Testing at Room Temperature Showing Transverse Surface Cracks



ORIGINAL PAGE IS
OF POOR QUALITY

**Table 8-31 Thermal Aging Data for $[0°]_6$ B/Al Aged in One Atmosphere Air and Tested at 297K (75°F) — Longitudinal Test Direction**

| Aging Temperature K | Aging Temperature (°F) | Aging Time (hr) | Tensile Strength MN/m2 | Tensile Strength (ksi) |
|---|---|---|---|---|
| 505 | 450 | Baseline avg | 1500 | 218 |
| | | 25,000 | 862 | 125 |
| | | | 896 | 130 |
| | | | 1430 | 208 |
| | | | avg 1060 | 154 |
| | | 40,000 | 1450 | 210 |
| | | | 1340 | 195 |
| | | | 1230 | 179 |
| | | | avg 1340 | 195 |
| 561 | 550 | 25,000 | 1360 | 198 |
| | | | 1510 | 219 |
| | | | 1180 | 171 |
| | | | avg 1350 | 196 |
| | | 40,000 | 917 | 133 |
| | | | 1230 | 179 |
| | | | 820 | 119 |
| | | | avg 990 | 144 |

**Table 8-32 Thermal Aging Data for $[0°]_6$ B/Al Aged in One Atmosphere Air and Tested at 297K (75°F) — Transverse Test Direction**

| Aging Temperature K | Aging Temperature (°F) | Aging Time (hr) | | Tensile Strength MN/m2 | Tensile Strength (ksi) |
|---|---|---|---|---|---|
| 505 | 450 | Baseline avg | | 79.3 | 11.5 |
| | | 25,000 | | 109 | 15.8 |
| | | | | 109 | 15.8 |
| | | | | 103 | 15.0 |
| | | | avg | 110 | 16.0 |
| | | 40,000 | | 105 | 15.2 |
| | | | | 103 | 14.9 |
| | | | | 101 | 14.7 |
| | | | avg | 103 | 14.9 |
| 561 | 550 | 25,000 | | 91.7 | 13.3 |
| | | | | 93.1 | 13.5 |
| | | | | 91.0 | 13.2 |
| | | | avg | 91.7 | 13.3 |
| | | 40,000 | | 91.0 | 13.2 |
| | | | | 86.2 | 12.5 |
| | | | | 99.3 | 14.4 |
| | | | avg | 92.2 | 13.4 |

**Table 8-33 Thermal Aging Data for $[0°]_6$ B/Al Aged in One Atmosphere Air and Tested at 297K (75°F) — Interfiber Shear in Longitudinal Direction**

| Aging Temperature K | Aging Temperature (°F) | Aging Time (hr) | | Tensile Strength MN/m2 | Tensile Strength (ksi) |
|---|---|---|---|---|---|
| 505 | 450 | Baseline avg | | 93.1 | 13.5 |
| | | 25,000 | | 88.2 | 12.8 |
| | | | | 87.6 | 12.7 |
| | | | | 89.6 | 13.0 |
| | | | avg | 88.2 | 12.8 |
| | | 40,000 | | 91.0 | 13.2 |
| | | | | 86.9 | 12.6 |
| | | | | 78.6 | 11.4 |
| | | | avg | 85.5 | 12.4 |
| 561 | 550 | 25,000 | | 51 | 7.4 |
| | | | | 50 | 7.2 |
| | | | | 51 | 7.4 |
| | | | avg | 50 | 7.3 |
| | | 40,000 | | 47 | 6.8 |
| | | | | 52 | 7.6 |
| | | | | 46 | 6.6 |
| | | | avg | 48 | 7.0 |

**Table 8-34 Thermal Aging Data for $[0° \pm 45°]_s$ Crossplied B/Al Aged in One Atmosphere Air and Tested at 297K (75°F) — Longitudinal Test Direction**

| Aging Temperature K | Aging Temperature (°F) | Aging Time (hr) | Tensile Strength MN/m2 | Tensile Strength (ksi) |
|---|---|---|---|---|
| 505 | 450 | Baseline avg | 625 | 90.6 |
| | | 25,000 | 573 | 83.1 |
| | | | 585 | 84.9 |
| | | | 584 | 84.7 |
| | | | avg 581 | 84.2 |
| | | 40,000 | 584 | 84.7 |
| | | | 593 | 86.0 |
| | | | 574 | 83.3 |
| | | | avg 584 | 84.7 |
| 561 | 550 | 25,000 | 576 | 83.6 |
| | | | 574 | 83.2 |
| | | | 552 | 80.0 |
| | | | avg 567 | 82.3 |
| | | 40,000 | 525 | 76.1 |
| | | | 518 | 75.1 |
| | | | 558 | 80.9 |
| | | | avg 534 | 77.4 |

**Table 8-35 Summary of Room Temperature Strength Retention After Thermal Aging in One Atmosphere Air for B/Al**

| Laminate Orientation | Test Direction | Property | Aging Time (hr) | Strength Retention (%) 505K (450°F) | 561K (550°F) |
|---|---|---|---|---|---|
| $[0°]_6$ | [0°] | Tensile | 25,000 | 95* | 90 |
| | | | 40,000 | 89 | 66 |
| $[0°]_6$ | [90°] | Tensile | 25,000 | 100 | 100 |
| | | | 40,000 | 100 | 100 |
| $[0°]_6$ | [0°] | Shear | 25,000 | 95 | 54 |
| | | | 40,000 | 92 | 52 |
| $[0° \pm 45°]_s$ | [0°] | Tensile | 25,000 | 93 | 91 |
| | | | 40,000 | 93 | 85 |

*See text for method of calculation of this value.

Figure 8-53 Edge View of Phase II B/Al After Thermal Aging at 561K (550°F) in One Atmosphere Air Showing Loss of Boron Through Oxidation



ORIGINAL PAGE IS
OF POOR QUALITY

tion products are visible, but oxidation of the boron is quite pronounced. Similar oxidation of the boron was observed during Phase I (Figure 8-44) but only in specimens aged at 700K (800°F).

The longitudinal residual tensile results, Tables 8-31 and 8-34, indicate that the B/Al material used in the Phase II work behaved quite differently than did the Phase I material. For example, at 561K (550°F) the loss in strength for both the unidirectional and crossplied specimens was considerably less for the 40,000 hour specimens (Phase II material) than for the 5000 hour or 10,000 hour specimens (Phase I material). The 505K (450°F) data also show the Phase II material to be superior when compared to the Phase I results for 450K (350°F) aging.

There was an unexplained inconsistency in the 505K (450°F) Phase II data for the 25,000 hour exposure. Two of the unidirectional specimens gave residual strength values considerably lower than the third and also lower than the three 40,000 hour specimens. Metallographic examination failed to resolve the differences. It is presumed that the two low values are not representative of this material and, consequently, the percent retention value for 25,000 hours at 505K (450°F) in Table 8-35 has been calculated using only the one tensile value.

A comparison of the quality assurance data obtained for the Phase I material and the Phase II material shows that the greatest difference between the two batches of material is the thickness. The Phase II B/Al sheets were approximately 12% thicker. The photomicrographs obtained during QA testing show that one consequence of the thickness difference is that the outside layers of boron fibers in the Phase I material are much closer to the surface than those of the Phase II material. Whether this could be responsible for the loss of strength found during Phase I (perhaps as a result of oxygen penetration, for example) could not be determined. Additional studies with metallographic sectioning and optical and SEM examinations failed to reveal the reason for the significant difference in thermal aging behavior of the Phase I and Phase II batches of B/Al.

While the longitudinal tensile results varied considerably for the two batches of material, the transverse tensile data and interfiber shear data appeared to fit reasonably well with the Phase I results. This would indicate that the problem lies with the boron fiber and/or fiber-matrix interface rather than with the aluminum alloy matrix. In like manner to the Phase I results, the decrease in strength at 561K (550°F) was caused by oxidation of the boron fibers beginning at the exposed ends. For the transverse specimens, the percentage of test section affected was small, and the decrease in strength with time was also small. For the interfiber shear specimens aged at 561K (550°F), the oxidation effect occurred over the entire length of the shearing area and the decrease in shear strength was almost 50% for both 25,000 hours and 40,000 hours.

Figure 8-54 shows the extent of oxidation on the fracture surface of a transverse tensile specimen after 40,000 hours at 561K (550°F). The tungsten core has oxidized to a much greater extent than the boron. The effect of the tungsten oxidation appears to be to embrittle the boron fiber as shown in Figure 8-54. The depth to which the tungsten core has oxidized appears to affect the nature of the failure. Splitting of the boron fibers occurred at the specimen edges where the tungsten has oxidized; otherwise failure was in the aluminum matrix and at the fiber-matrix interface. For specimens aged at 505K (450°F) for either time period the depth of oxidation was no more than 0.00025m (0.01 in.). At 561K (550°F), oxidation was considerably increased with depths of 0.0013m (0.05 in.) after 25,000 hours and 0.0020m (0.08 in.) after 40,000 hours. Figure 8-55 shows the fracture surface of the same specimen shown in Figure 8-54 but at a location away from the edges where oxidation of the fibers had occurred. Of interest in this photomicrograph is the

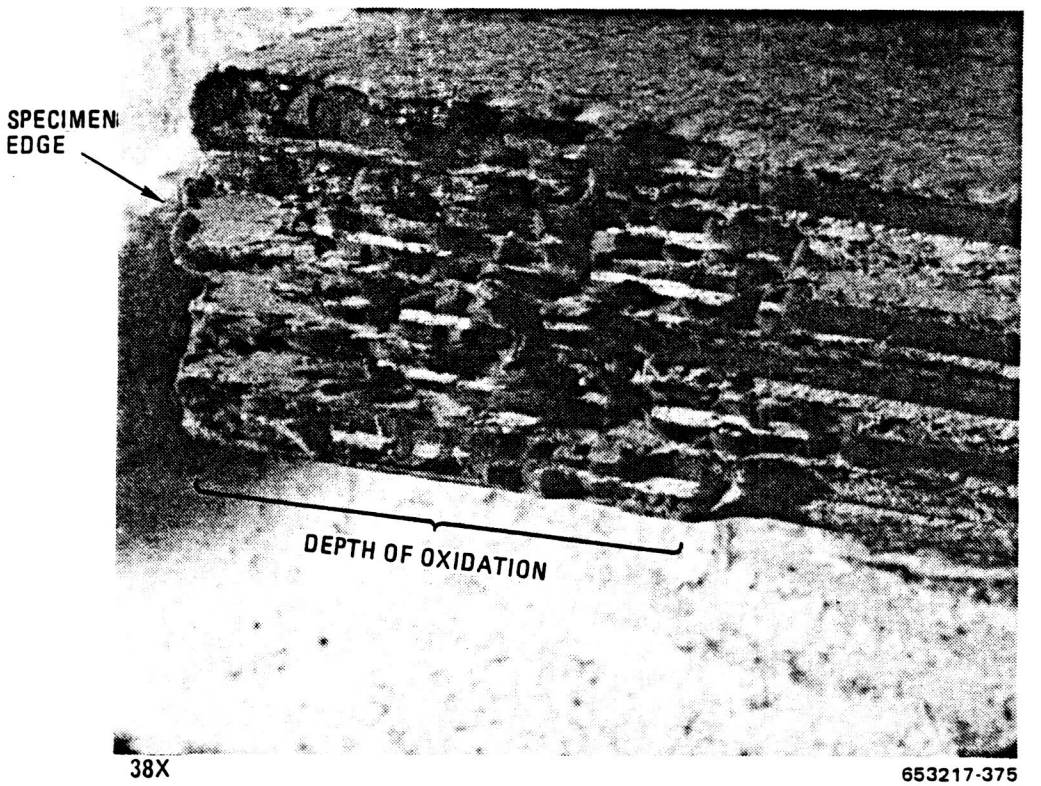



**Figure 8-54 Portion of Fracture Surface of Transverse Tensile Specimen of Phase II B/Al After 40,000 Hours of Thermal Aging at 561K (550°F) in One Atmosphere Air Showing Extent of Embrittlement of Boron Through Oxidation of the Tungsten Core**

absence of filament splitting. For the Phase I material, splitting was observed after only 10,000 hours at 561K (550°F). This observation would appear to indicate that the boron fibers in the Phase II B/Al had a considerably improved thermal stability over that of the Phase I fibers.

The results of the metallographic examination of the interfiber shear specimens showed a considerable difference in the fracture appearance of specimens aged at the two temperatures. At the lower temperature almost no oxidation of the fibers was found, and failure was in shear, primarily in the aluminum matrix. For the 40,000 hour specimens, some interface failure was observed as shown in Figure 8-56, but, as with the transverse specimens, no filament splitting was present. At 561K (550°F), oxidation of the filaments (primarily the tungsten cores) had occurred over the entire shearing length of the specimens. As shown in Figure 8-56, the boron filaments were broken into many small fragments with the oxidized remnants of the tungsten cores readily visible. Failure did not take place in one shear plane as was seen for the 505K (450°F) specimens but occurred in more or less a tearing manner across several planes in a direction 45 degrees to the direction of loading. The weakened boron filaments appear to have been responsible for the lowered shear strength values of these specimens.

Transverse surface cracks of the type found on Phase I $[0° \pm 45°]_s$ crossplied specimens after tensile testing (see Figure 8-52) were observed on several of the Phase II specimens. They were few in number, however, as shown on a typical specimen in Figure 8-57. This may be further evidence of the improved thermal stability of the boron filaments in the Phase II B/Al material.



ORIGINAL PAGE IS
OF POOR QUALITY

ORIGINAL PAGE IS
OF POOR QUALITY

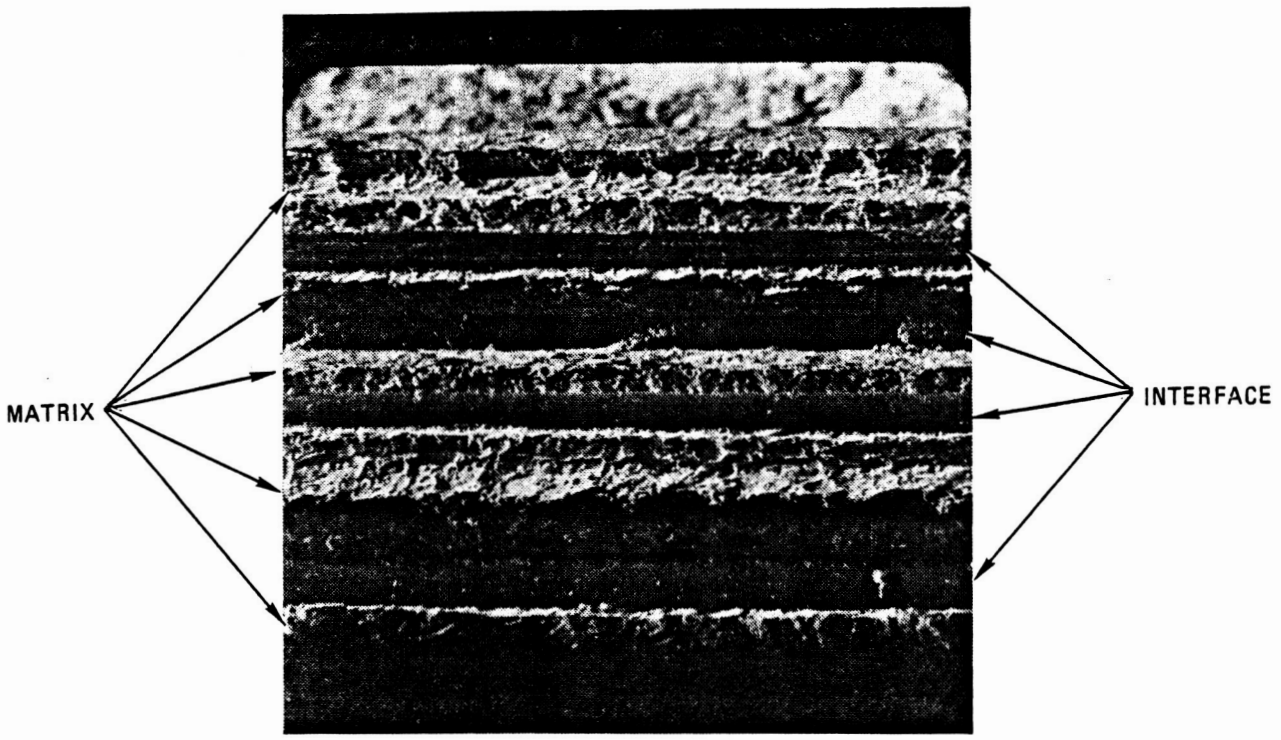


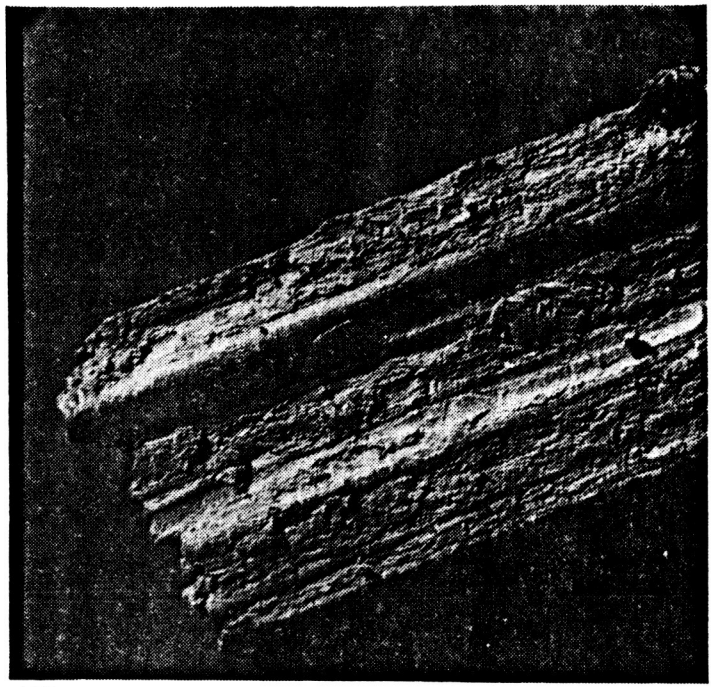

**Figure 8-55 Fracture Surface of Transverse Tensile Specimen of Phase II B/Al After 40,000 Hours of Thermal Aging at 561K (550°F) in One Atmosphere Air Showing Both Matrix and Interface Failure Modes (Note Absence of Filament Splitting)**

In summary of these data, the B/6061 boron/aluminum used in the Phase II portion of the program was much superior to that used during Phase I. The Phase I data indicated a maximum use temperature of only 450K (350°F) for exposures longer than 10,000 hours. The Phase II data, on the other hand, indicate that a maximum use temperature of 505K (450°F) for 40,000 hours of exposure is possible. Some precautions may be required, however, to protect the material edges to prevent oxidation of the boron fibers.

## 8.3 THERMAL AGING/COMPRESSION — TEST RESULTS AND DISCUSSION

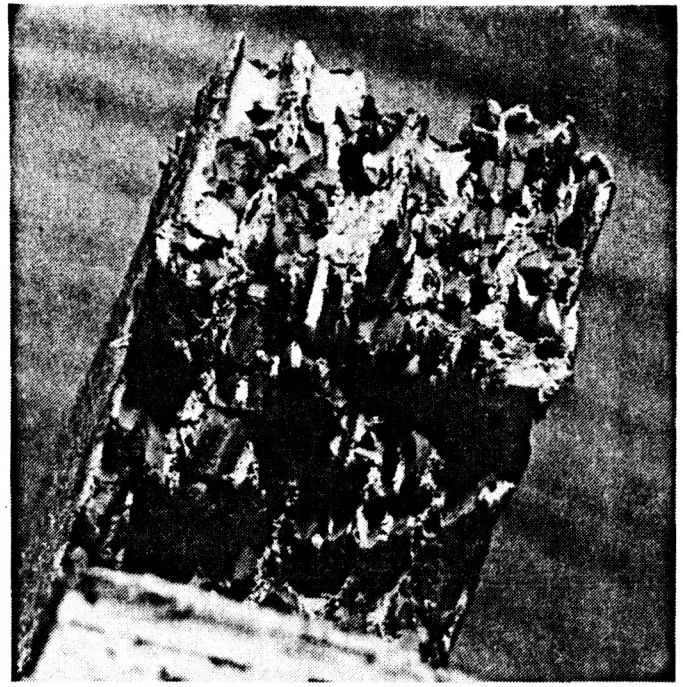
**8.3.1 GRAPHITE/EPOXY.** The results of the weight change measurements, the compressive strength and modulus tests, and the shear strength tests are given in Tables 8-36 and 8-37. The data have also been plotted as a function of aging time for the two laminate thicknesses and the two aging temperatures in Figures 8-58 through 8-60. The effect of aging on the fully reversed tension-compression fatigue strength of the 24 ply laminate was also determined. These data are listed in Table 8-38, and S-N curves are plotted in Figure 8-61.

All specimens were examined visually with a stereo microscope after aging (1000, 5000, or 10,000 hours). For the G/E specimens aged at 373K (212°F), no changes in appearance were observed for any of the time periods. The only difference noted was a slight change in the ring of the 24 ply specimens when dropped after the 10,000 hour exposure. At 394K (250°F), slight edge cracking was seen after 5000 hours in the 24 ply specimens and after 10,000 hours also in the 6 ply speci-



43X

505K (450°F)



50X

561K (550°F)

653217-377

**Figure 8-56 Fracture Surface of Interfiber Shear Specimens of Phase II B/Al After 40,000 Hours of Thermal Aging in One Atmosphere Air at the Indicated Temperature**



ORIGINAL PAGE IS
OF POOR QUALITY

ORIGINAL PAGE IS
OF POOR QUALITY

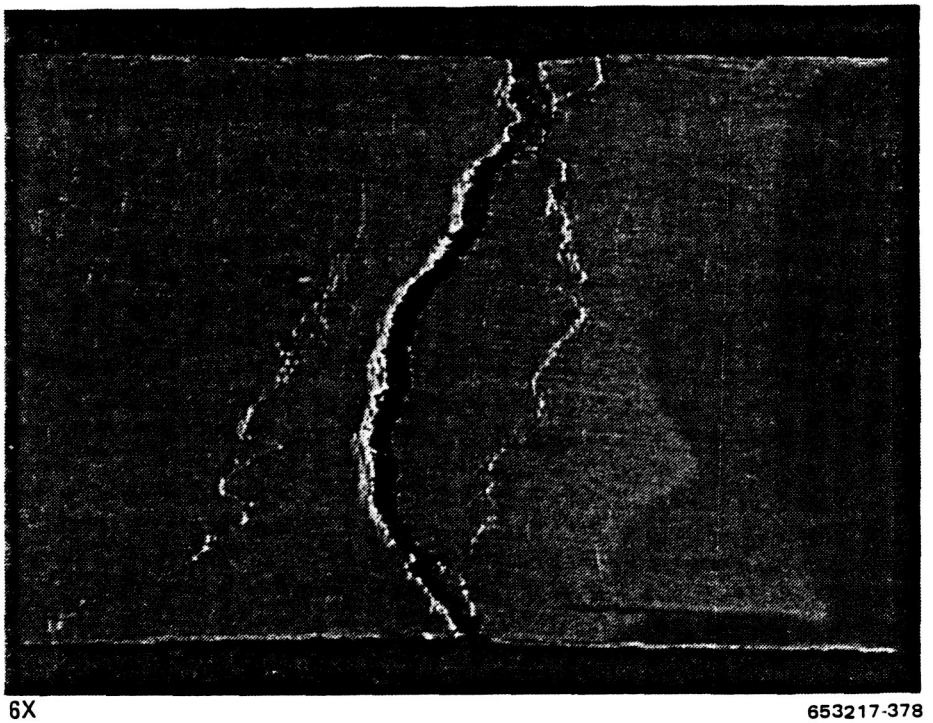



**Figure 8-57 Phase II B/Al After 40,000 Hours of Thermal Aging at 505K (450°F) in One Atmosphere Air and Tensile Testing at Room Temperature Showing Slight Transverse Surface Cracking Near Fracture**

mens. Both layups showed a slight loss in ring after 10,000 hours. In general, all the specimens were in excellent condition except for the slight edge cracking. Examples of these cracks are shown in Figure 8-62 for 6 ply and 24 ply specimens aged 10,000 hours at 394K (250°F).

Weight change for the G/E system was small during thermal aging as shown in Figure 8-58. The respective weight losses were as expected for the four combinations of aging temperature and specimen thickness. The greatest effect, which was only 1%, was for the 6 ply material at 394K (250°F).

Figure 8-59 shows that the 10,000 hours of aging at both temperatures did not lower the compressive strength. In fact, values were increased after aging, particularly for the 24 ply specimens. Similar results were obtained for the compressive modulus measurements. These apparent increases in compressive properties may be the result of faulty baseline property tests. However, this is not believed to be the explanation, as the specimen preparation, test procedures, and appearance of the failed specimens were the same for all the tests. The superior properties after exposure may be the result of a postcure effect at the aging temperatures.

For G/E, the only detrimental effects of thermal aging were the shear strength losses of the 6 ply material. As shown in Figure 8-60, these decreases were found as early as 1000 hours and became quite large by 10,000 hours. Since the effect was observed only in the 6 ply material, the possibility exists that the method of specimen preparation (bonding of three 6 ply laminates to get an 18 ply specimen) may have influenced the data. However, based on results from both the Phase I

**Table 8-36 Thermal Aging Data for 6 Ply $[0° \pm 45°]_s$ A-S/3501 G/E Aged in 0.10 MN/m² (14.7 psi) Air and Tested at Room Temperature**

| Aging Temperature K | Aging Temperature (°F) | Aging Time (hr) | | Weight Change (%) | Compressive Strength MN/m2 | Compressive Strength (ksi) | Compressive Modulus GN/m2 | Compressive Modulus (Msi) | Shear Strength MN/m2 | Shear Strength (ksi) |
|---|---|---|---|---|---|---|---|---|---|---|
| 373 | 212 | Baseline avg | | | 542 | 78.6 | 53 | 7.7 | 72 | 10.4 |
| | | 1,000 | | −0.1 | 616 | 89.3 | 52 | 7.5 | 67 | 9.7 |
| | | | | −0.1 | 623 | 90.3 | 52 | 7.6 | 55 | 8.0 |
| | | | | −0.1 | 620 | 90.0 | 56 | 8.1 | 70 | 10.2 |
| | | | avg | −0.1 | 620 | 89.9 | 53 | 7.7 | 64 | 9.3 |
| | | 5,000 | | 0.0 | 510 | 74.0 | 57 | 8.2 | 63 | 9.9 |
| | | | | 0.0 | 490 | 71.1 | 56 | 8.1 | 65 | 9.4 |
| | | | | −0.1 | 512 | 74.2 | 57 | 8.3 | 61 | 8.8 |
| | | | avg | 0.0 | 504 | 73.1 | 57 | 8.2 | 63 | 9.1 |
| | | 10,000 | | −0.1 | 546 | 79.2 | 53 | 7.7 | 23 | 3.4 |
| | | | | −0.1 | 580 | 84.1 | 57 | 8.3 | 23 | 3.3 |
| | | | | −0.1 | 586 | 85.0 | 55 | 8.0 | 23 | 3.3 |
| | | | avg | −0.1 | 571 | 82.8 | 55 | 8.0 | 23 | 3.3 |
| 394 | 250 | 1,000 | | −0.3 | 565 | 82.0 | 52 | 7.5 | 63 | 9.2 |
| | | | | −0.3 | 643 | 93.3 | 69 | 10.0 | 60 | 8.7 |
| | | | | −0.3 | 572 | 83.0 | 56 | 8.1 | 64 | 9.3 |
| | | | avg | −0.3 | 594 | 86.1 | 59 | 8.5 | 63 | 9.1 |
| | | 5,000 | | −0.5 | 558 | 81.0 | 51 | 7.4 | 52 | 7.6 |
| | | | | −0.5 | 597 | 86.6 | 53 | 7.7 | 48 | 7.0 |
| | | | | −0.5 | 561 | 81.3 | 52 | 7.6 | 50 | 7.2 |
| | | | avg | −0.5 | 572 | 83.0 | 52 | 7.6 | 50 | 7.3 |
| | | 10,000 | | −1.0 | 562 | 81.5 | 54 | 7.8 | 41 | 6.0 |
| | | | | −1.1 | 549 | 79.6 | 54 | 7.9 | 45 | 6.5 |
| | | | | −1.1 | 573 | 83.1 | 55 | 8.0 | 43 | 6.2 |
| | | | avg | −1.1 | 561 | 81.4 | 54 | 7.9 | 43 | 6.2 |

**Table 8-37 Thermal Aging Data for 24 Ply $[0° \pm 45°]_{s4}$ A-S/3501 G/E Aged in 0.10 MN/m² (14.7 psi) Air and Tested at Room Temperature**

| Aging Temperature K | Aging Temperature (°F) | Aging Time (hr) | Weight Change (%) | Compressive Strength MN/m2 | Compressive Strength (ksi) | Compressive Modulus GN/m2 | Compressive Modulus (Msi) | Shear Strength MN/m2 | Shear Strength (ksi) |
|---|---|---|---|---|---|---|---|---|---|
| 373 | 212 | Baseline avg | | 439 | 63.6 | 41 | 6.0 | 56 | 8.1 |
| | | 1,000 | 0.0 | 623 | 90.3 | 58 | 8.4 | 76 | 11.0 |
| | | | 0.0 | 661 | 95.8 | 59 | 8.5 | 76 | 11.0 |
| | | | 0.0 | 676 | 98.1 | 57 | 8.3 | 79 | 11.5 |
| | | | avg 0.0 | 653 | 94.7 | 58 | 8.4 | 77 | 11.2 |
| | | 5,000 | 0.0 | 644 | 93.4 | 63 | 9.1 | 68 | 9.8 |
| | | | 0.0 | 636 | 92.2 | 62 | 9.0 | 68 | 9.9 |
| | | | 0.0 | 583 | 84.5 | 58 | 8.4 | 55 | 8.0 |
| | | | avg 0.0 | 620 | 90.0 | 61 | 8.8 | 63 | 9.2 |
| | | 10,000 | 0.0 | 684 | 99.1 | 61 | 8.9 | 70 | 10.2 |
| | | | 0.0 | 649 | 94.1 | 65 | 9.4 | 73 | 10.6 |
| | | | 0.0 | 662 | 96.0 | 59 | 8.5 | 77 | 11.2 |
| | | | avg 0.0 | 665 | 96.4 | 61 | 8.9 | 74 | 10.7 |
| 394 | 250 | 1,000 | −0.1 | 578 | 83.8 | 53 | 7.7 | 83 | 12.1 |
| | | | −0.1 | 583 | 84.5 | 48 | 7.0 | 75 | 10.9 |
| | | | −0.1 | 618 | 89.6 | 51 | 7.4 | 70 | 10.1 |
| | | | avg −0.1 | 593 | 86.0 | 51 | 7.4 | 76 | 11.0 |
| | | 5,000 | −0.2 | 607 | 88.1 | 52 | 7.5 | 61 | 8.8 |
| | | | −0.2 | 598 | 86.8 | 53 | 7.7 | 54 | 7.9 |
| | | | −0.2 | 631 | 91.5 | 55 | 8.0 | 54 | 7.9 |
| | | | avg −0.2 | 612 | 88.8 | 53 | 7.7 | 57 | 8.2 |
| | | 10,000 | −0.5 | 606 | 87.9 | 54 | 7.8 | 60 | 8.7 |
| | | | −0.5 | 603 | 87.5 | 56 | 8.1 | 59 | 8.5 |
| | | | −0.5 | 576 | 83.6 | 54 | 7.8 | 50 | 7.2 |
| | | | avg −0.5 | 595 | 86.3 | 54 | 7.9 | 56 | 8.1 |

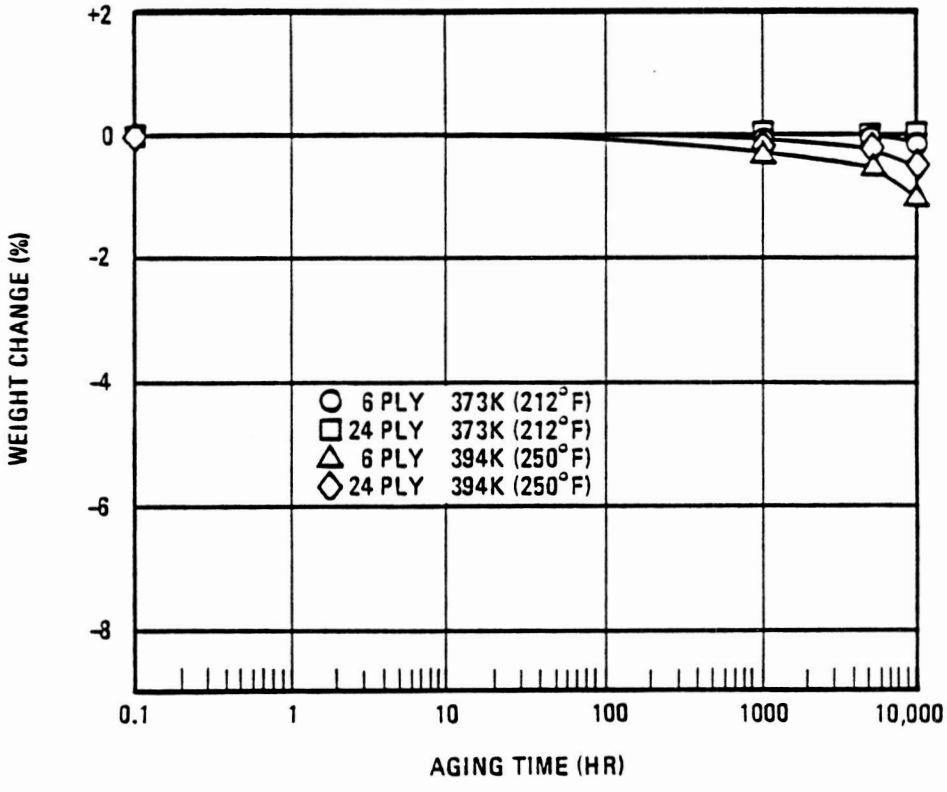



**Figure 8-58 Weight Change of G/E After Thermal Aging at the Indicated Temperature**

and Phase II flight simulation tests of this specimen configuration the method is believed to be a satisfactory one. Careful visual examination of the failed specimens, both baseline and aged, with a stereo microscope failed to reveal any information on the degradation process involved in the loss in shear strength.

In agreement with the residual compressive and shear strength values for 24 ply material, the residual fatigue strength showed no decrease as a result of the 10,000 hour thermal age at either 373K (212°F) or 394K (250°F). The data, plotted in Figure 8-61, show that the scatter bands for each temperature overlap those of the baseline data. Individual curves for the three data sets were not drawn because of their close proximity to each other. The net effect is that the thermal aging has not changed the fatigue properties of the 24 ply G/E material.

Metallographic samples were prepared from 6 ply specimens before aging and after 5000 hours and 10,000 hours of exposure at both 373K (212°F) and 394K (250°F). The results were the same as found in the Phase I thermal aging/tension study of G/E. Slight oxidation effects could be seen to be just starting in the outside plies after 10,000 hours of aging. The specimens resembled those in Figures 8-17 and 8-18. No explanations were uncovered to explain the high losses in shear strength of the 6 ply material after aging. It was thought that the slight edge cracking might have contributed, but the polished samples of material aged for 10,000 hours at each temperature showed no evidence of internal matrix cracking. Figure 8-63 shows samples after 10,000 hours of aging at each of the temperatures. The condition of both specimens with regard to matrix cracking is the same as unexposed material (see Figure 8-17).

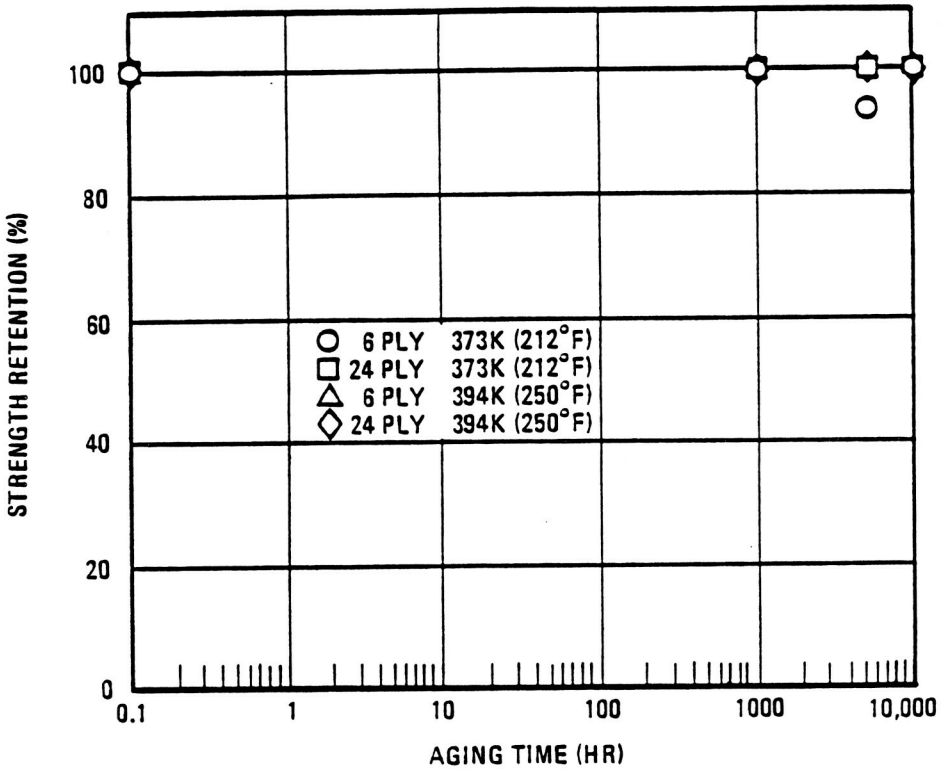



**Figure 8-59 Retention of Compressive Strength of G/E at 297K (75°F) After Thermal Aging at the Indicated Temperature**

Glass transition temperatures ($T_g$) were also measured on samples cut from the same specimens that provided the metallographic samples. The results are given in Table 8-39. The $T_g$ values appear to offer no assistance to understanding the changes that occur in the epoxy resin during long term thermal exposure in air.

In summary, 10,000 hours of thermal aging in one atmosphere air at 373K (212°F) and 394K (250°F) produced no significant reduction in compressive strength or compressive fatigue strength of G/E. A slight weight loss, about 1%, was found after 10,000 hours at 394K (250°F) for 6 ply material. The major effect of the thermal exposure was a considerable decrease in shear strength of 6 ply material. These reductions were observed as early as 1000 hours and increased to 40% or more by 10,000 hours. A mechanism to account for the poor shear strength retention of G/E during thermal aging was not found.

By way of comparison with the thermal aging/compression data, the thermal aging/tension results showed no decrease in tensile strength after 10,000 hours of exposure in air at 394K (250°F).

**8.3.2 CELION 6000/LARC-160 GRAPHITE/POLYIMIDE.** The results of the weight change measurements, the compressive strength and modulus tests, and the shear strength tests are given in Tables 8-40 through 8-42. These data have also been plotted as a function of aging time for the two laminate thicknesses and the two aging temperatures in Figures 8-64 through 8-66. Table 8-42 and Figure 8-64 give the data for the PPQ coated material. The results of aging on the

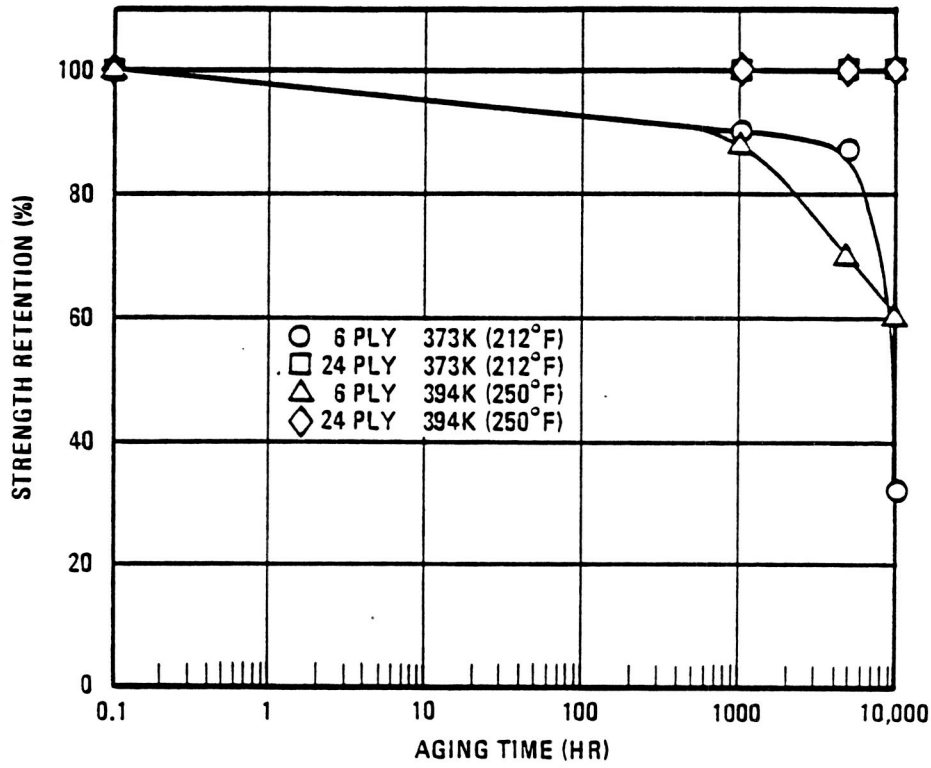



**Figure 8-60 Retention of Short Beam Shear Strength of G/E at 297K (75°F) After Thermal Aging at the Indicated Temperature**

R = -1 fatigue strength of the 24 ply laminate are presented in Table 8-43 and Figure 8-67. Table 8-44 compares the results of the uncoated and PPQ coated samples of 6 ply material.

Visual examinations were performed on the specimens at intervals of 1000 hours, 5000 hours, and 10,000 hours during aging. For the exposures at 450K (350°F) the major changes noted were for the 24 ply samples. After 5000 hours, slight edge cracking had occurred and by 10,000 hours the cracking was quite extensive. These cracks are readably visible in Figure 8-68. For the 6 ply specimens aged at 450K (350°F) very slight edge cracking appeared to be starting in the specimens that had been exposed for 10,000 hours. Overall, the appearance of the G/PI material after 10,000 hours was excellent with no surface degradation, color changes, or decreases in the ring of the specimens when dropped on a hard surface.

Aging at 505K (450°F) also had little visual effect on the specimens except for edge cracking. For the 24 ply samples extensive cracking was observed after 1000 hours. The number of cracks was about the same after 5000 hours, but they were considerably wider. The 10,000 hour samples were similar in appearance to the 5000 hours samples. Figure 8-69 shows the degree of edge cracking in the 24 ply laminates after 1000 hours and 10,000 hours. For the 6 ply material no edge cracks were observed until after 10,000 hours of exposure. Figure 8-70 shows an example of edge cracks and what appears to be delamination. The degree of cracking is less than that found in the 24 ply material.

After the observation of these edge cracks the question arose as to the depth to which they extended. Some spare specimens of the 24 ply material had been included in the 10,000 hour

Table 8-38 Axial Fatigue Data for $[0° \pm 45°]_{2s}$ G/E After 10,000 Hours of Thermal Aging, 297K (75°F), R = —1, Unnotched

| Aging Temperature K | (°F) | Specimen Number | Maximum Stress MN/m2 | (ksi) | Cycles | Comments |
|---|---|---|---|---|---|---|
| 373 | 212 | B-10-3-10 | 241 | 35 | 7,000 | |
| | | -11 | 276 | 40 | 9,000 | |
| | | -12 | 224 | 32.5 | 894,000 | |
| | | -13 | 258 | 37.5 | 14,000 | |
| | | -14 | 241 | 35 | 11,000 | |
| | | -15 | 224 | 32.5 | 48,000 | |
| | | -16 | 276 | 40 | 6,000 | |
| | | -17 | 207 | 30 | 3,460,000 | |
| | | -18 | 190 | 27.5 | 11,450,000 | Did not fail |
| 394 | 250 | B-10-3-28 | 224 | 32.5 | 25,000 | Fixture misaligned |
| | | -29 | 207 | 30 | 12,210,000 | |
| | | -30 | 224 | 32.5 | 4,341,000 | |
| | | -32 | 241 | 35 | 705,000 | |
| | | -31 | 224 | 32.5 | 1,190,000 | |
| | | -33 | 241 | 35 | 1,415,000 | |
| | | -34 | 258 | 37.4 | 13,000 | |
| | | -35 | 258 | 37.5 | 14,000 | |
| | | -36 | 280 | 40.6 | 10,000 | |

exposures and were available for examination. Two samples, one with 10,000 hours at 450K (350°F) and one with 10,000 hours at 505K (450°F), were sectioned in the plane of the laminate near the mid-plane. Using a stereo microscope one could follow the extent of the edge cracks into the specimens. As shown in Figure 8-71 these edge cracks extended all the way through the plane of the 0.038m by 0.038m (1.5 in. by 1.5 in.) samples. The pieces shown in Figure 8-71 are one-quarter of the original samples so that the lower right corner of each is approximately the center of the specimen.

The PPQ coated 6 ply samples were also examined after 1000 hours, 5000 hours, and 10,000 hours. For the 450K (350°F) exposures no changes in appearance were detected. Two of these specimens after 10,000 hours are shown in Figure 8-72. At 505K (450°F) peeling of the coating was visible after 1000 hours and increased slightly after 5000 hours. For the three specimens examined one showed extensive peeling after 1000 hours while the other two showed only slight peeling after 5000 hours. There was very little change in appearance from 5000 hours to 10,000 hours. Figure 8-73 shows two of these specimens after 10,000 hours of exposure, one with extensive peeling of the coating and one with slight peeling. Because the peeling and cracking occurred early in the aging exposure and did not change much with time, it would appear to be an application problem with the coating not adhering properly.

Using chloroform as a solvent, the PPQ coating was removed after 10,000 hours of aging prior to preparation of the compression and shear specimens. Examination of the samples after coating removal showed them to be in excellent condition and, unlike the uncoated 6 ply material, to be free of edge cracking. Figure 8-74 shows a typical edge from one of these samples after removal of the PPQ coating.

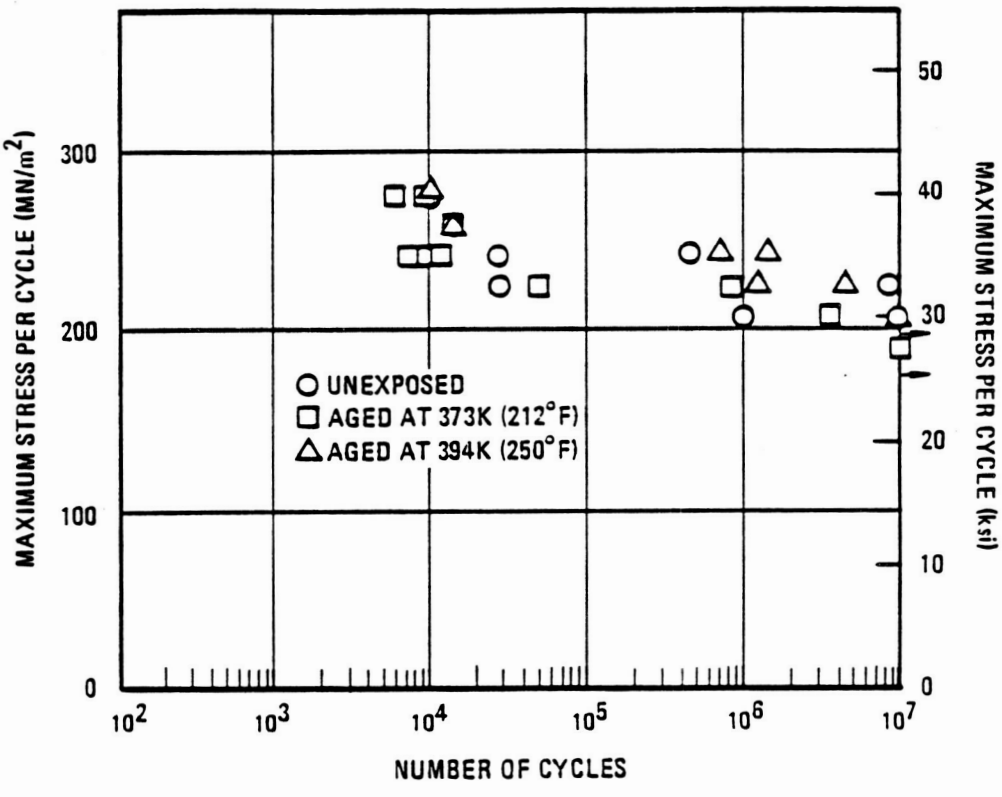


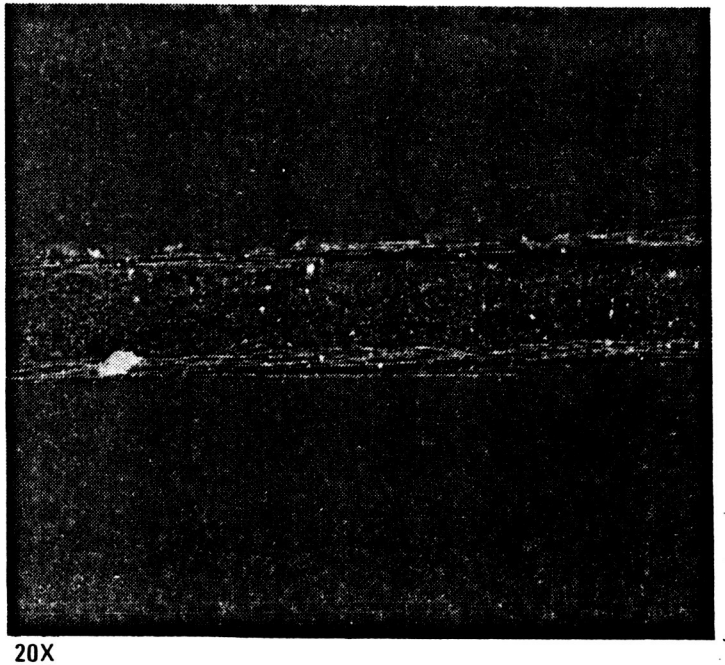

**Figure 8-61 Axial Fatigue Properties of $[0° \pm 45°]_{s4}$ G/E Before and After 10,000 Hours of Thermal Aging, 297K (75°K), R = —1, Unnotched**

Weight change for the Celion 6000/LARC-160 G/PI during thermal aging is plotted in Figure 8-64. Significant weight losses occurred at both aging temperatures during the 10,000 hours of exposure. As expected, greater losses were found at the higher aging temperature, and the 6 ply laminates lost more weight, percentagewise, than the 24 ply laminates. The effect of the PPQ coating on the 6 ply material was a slightly lower weight loss at all of the time-temperature conditions. Comparison of the weight loss of the 6 ply compressive specimens with the 6 ply tensile specimens (Table 8-20) after aging at 505K (450°F) gives very good agreement. At 450K (350°F), however, the tensile specimens (Table 8-19) showed weight losses somewhat lower than those of the compressive specimens. The aging conditions and weighing procedures were identical for the two groups of specimens. The weight change differences would appear to be related to the two different panels from which the specimens were obtained.

In contrast to the weight change data, but in agreement with the thermal aging tensile data, the compressive strength in most cases showed a greater decrease with aging time at 450K (350°F) than at 505K (450°F). As shown in Figure 8-65 this is particularly evident for the 24 ply material and the 6 ply specimens after 5000 hours. For two of the data sets (6 ply at 450K and 24 ply at 505K) the results showed greater decreases in compressive strength after 5000 hours than after 10,000 hours. Similar inconsistencies were found in the compressive modulus values for these two data sets. No explanation was found for these results, but data scatter cannot be ruled out. For 6 ply Celion 6000/LARC-160 G/PI the loss of compressive strength and tensile strength (Section 8.2.2.2) after 10,000 hours of thermal aging in air at both 450K (350°F) and 505K (450°F) was significant with decreases in excess of 20%.

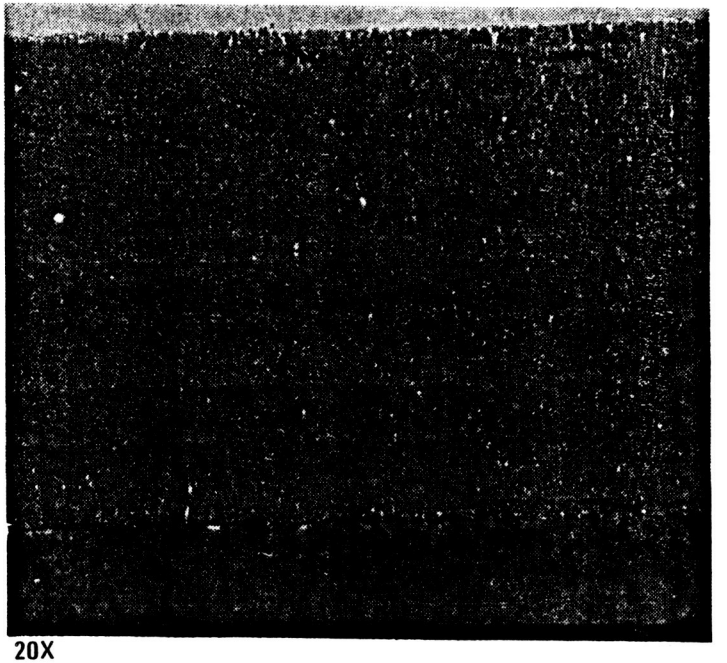
663217-384

Figure 8-62 Edge View of G/E Specimens After 10,000 Hours of Thermal Aging at 394K (250°F) in One Atmosphere Air Showing Slight Edge Cracking



20X

6 PLY SPECIMEN



20X

24 PLY SPECIMEN

653217-383

**Figure 8-63 Photomicrographs (metallograph) of G/E After 10,000 Hours of Thermal Aging in One Atmosphere Air at Indicated Temperature (Note Absence of Matrix Cracking)**



ORIGINAL PAGE IS
OF POOR QUALITY

Table 8-39 Glass Transition Temperature, $T_g$, Data for $[0° \pm 45°]_s$ G/E

| Condition | Aging Temperature K | Aging Temperature (°F) | Aging Time (hr) | $T_g$ K | $T_g$ (°F) |
|---|---|---|---|---|---|
| As-Received | | | | 441 | 333 |
| Aged | 373 | 212 | 1,000 | 434 | 322 |
| Aged | 373 | 212 | 5,000 | 419 | 295 |
| Aged | 373 | 212 | 10,000 | 440 | 332 |
| Aged | 394 | 250 | 1,000 | 428 | 311 |
| Aged | 394 | 250 | 5,000 | 449 | 348 |
| Aged | 394 | 250 | 10,000 | 420 | 296 |

For both the G/E and the G/PI systems the most damaging effects of the thermal aging were found in the shear strength measurements. The 6 ply G/PI material aged for 10,000 hours at 450K (350°F) retained only 35% of its room temperature shear strength. Aging at 505K (450°F) was only slightly better with a retention of about 50%. Again, the unexpected result of greater property loss in the 6 ply material when aged at the lower temperature was observed. For the 24 ply material, shear strength losses after 10,000 hours at 505K (450°F) were also quite large. However, the 24 ply material showed good resistance to aging at the lower temperature with over 90% retention of shear strength after 10,000 hours. The effects of thermal aging on shear strength are plotted in Figure 8-66.

The thermal aging tension-compression fatigue data for the 24 ply Celion 6000/LARC-160 G/PI are plotted as S-N curves in Figure 8-67. Unlike the G/E material, which showed no effects of aging on fatigue strength, the G/PI fatigue strength was lowered significantly after 10,000 hours of aging at both temperatures. Room temperature fatigue strength was about 15% lower after aging at 450K (350°F) and 30% lower for the 505K (450°F) aging exposure.

As discussed earlier the PPQ coating was applied to a batch of specimens in an attempt to improve the long term thermooxidative stability during aging. Table 8-44 summarizes the results of this study. The coated samples showed slightly better results in almost every case. These included less edge cracking, lower weight loss, and better shear strength retention. For compressive strength and modulus, the coated samples gave better results than uncoated when aged at 505K (450°F) but poorer results for the 450K (350°F) age. These preliminary results indicate that the PPQ coating has potential for providing increased thermooxidative stability to G/PI laminates.

Metallographic examinations were made on 6 ply samples aged for 5000 and 10,000 hours at each temperature. The same matrix oxidation effects described earlier for the thermal aging/tension samples of Celion 6000/LARC-160 (Figure 8-40) were also found for the thermal aging/compression samples. Extensive internal matrix cracking was also observed. Figure 8-75 shows the extent of cracking after 5000 hours at the lower aging temperature and after 5000

**Table 8-40 Thermal Aging Data for 6 Ply $[0° \pm 45°]_s$ Celion 6000/LARC-160 G/PI Aged in 0.10 MN/m² (14.7 psi) Air and Tested at Room Temperature**

| Aging Temperature K | Aging Temperature (°F) | Aging Time (hr) | Weight Change (%) | Compressive Strength MN/m2 | Compressive Strength (ksi) | Compressive Modulus GN/m2 | Compressive Modulus (Msi) | Shear Strength MN/m2 | Shear Strength (ksi) |
|---|---|---|---|---|---|---|---|---|---|
| 450 | 350 | Baseline avg | | 584 | 84.7 | 52 | 7.5 | 51 | 7.4 |
| | | 1,000 | +0.1 | 592 | 85.8 | 54 | 7.8 | 50 | 7.3 |
| | | | +0.1 | 634 | 92.0 | 52 | 7.6 | 44 | 6.4 |
| | | | +0.1 | 609 | 88.3 | 52 | 7.5 | 46 | 6.6 |
| | | | avg +0.1 | 612 | 88.7 | 52 | 7.6 | 47 | 6.8 |
| | | 5,000 | −0.4 | 397 | 57.6 | 50 | 7.2 | 47 | 6.8 |
| | | | −0.4 | 390 | 56.5 | 50 | 7.2 | 44 | 6.4 |
| | | | −0.4 | 404 | 58.6 | 50 | 7.2 | 42 | 6.1 |
| | | | avg −0.4 | 397 | 57.6 | 50 | 7.2 | 44 | 6.4 |
| | | 10,000 | −2.3 | 461 | 66.8 | 54 | 7.9 | 19 | 2.8 |
| | | | −2.3 | 408 | 59.2 | 54 | 7.8 | 18 | 2.6 |
| | | | −2.3 | 398 | 57.7 | 56 | 8.1 | 16 | 2.3 |
| | | | avg −2.3 | 422 | 61.2 | 54 | 7.9 | 18 | 2.6 |
| 505 | 450 | 1,000 | −1.2 | 588 | 85.3 | 51 | 7.4 | 52 | 7.5 |
| | | | −1.0 | 587 | 85.2 | 51 | 7.4 | 52 | 7.6 |
| | | | −0.9 | 629 | 91.3 | 52 | 7.5 | 43 | 6.2 |
| | | | avg −1.0 | 602 | 87.3 | 51 | 7.4 | 49 | 7.1 |
| | | 5,000 | −5.6 | 477 | 69.2 | 52 | 7.5 | 43 | 6.3 |
| | | | −5.5 | 407 | 59.1 | — | — | 46 | 6.6 |
| | | | −5.6 | 472 | 68.5 | 54 | 7.8 | 45 | 6.5 |
| | | | avg −5.6 | 452 | 65.6 | 52 | 7.6 | 45 | 6.5 |
| | | 10,000 | −8.2 | 423 | 61.4 | 47 | 6.8 | 27 | 3.9 |
| | | | −8.1 | 436 | 63.3 | 45 | 6.5 | 24 | 3.5 |
| | | | −8.2 | 401 | 58.2 | 46 | 6.7 | 30 | 4.4 |
| | | | avg −8.2 | 421 | 61.0 | 46 | 6.7 | 27 | 3.9 |

**Table 8-41 Thermal Aging Data for 24 Ply $[0° \pm 45°]_{2s}$ Celion 6000/LARC-160 G/PI Aged in 0.10 MN/m² (14.7 psi) Air and Tested at Room Temperature**

| Aging Temperature | | Aging Time | Weight Change | Compressive Strength | | Compressive Modulus | | Shear Strength | |
|---|---|---|---|---|---|---|---|---|---|
| K | (°F) | (hr) | (%) | MN/m2 | (ksi) | GN/m2 | (Msi) | MN/m2 | (ksi) |
| 450 | 350 | Baseline avg | | 591 | 85.7 | 58 | 8.4 | 50 | 7.3 |
| | | 1,000 | 0.0 | 490 | 71.0 | 49 | 7.1 | 54 | 7.9 |
| | | | 0.0 | 481 | 69.7 | 48 | 7.0 | 57 | 8.3 |
| | | | 0.0 | 521 | 75.5 | 48 | 7.0 | 63 | 9.2 |
| | | | avg 0.0 | 497 | 72.1 | 48 | 7.0 | 59 | 8.5 |
| | | 5,000 | 0.0 | 449 | 65.1 | 45 | 6.5 | 53 | 7.7 |
| | | | 0.0 | 470 | 68.2 | 48 | 7.0 | 50 | 7.2 |
| | | | 0.0 | 492 | 71.4 | 49 | 7.1 | 57 | 8.2 |
| | | | avg 0.0 | 470 | 68.2 | 48 | 6.9 | 53 | 7.7 |
| | | 10,000 | −0.6 | 373 | 54.1 | 47 | 6.8 | 48 | 7.0 |
| | | | −0.5 | 451 | 65.4 | 46 | 6.7 | 40 | 5.8 |
| | | | −0.5 | 428 | 62.0 | 47 | 6.8 | 50 | 7.2 |
| | | | avg −0.5 | 417 | 60.5 | 47 | 6.8 | 46 | 6.7 |
| 505 | 450 | 1,000 | −0.2 | 559 | 81.1 | 46 | 6.7 | 63 | 9.2 |
| | | | −0.2 | 531 | 77.0 | 46 | 6.6 | 67 | 9.7 |
| | | | −0.2 | 519 | 75.3 | 43 | 6.3 | 58 | 8.4 |
| | | | avg −0.2 | 536 | 77.8 | 45 | 6.5 | 63 | 9.1 |
| | | 5,000 | −2.3 | 401 | 58.1 | 47 | 6.8 | 44 | 6.4 |
| | | | −2.6 | 483 | 70.0 | — | — | 55 | 8.0 |
| | | | −2.7 | 415 | 60.2 | 47 | 6.8 | 41 | 5.9 |
| | | | avg −2.5 | 433 | 62.8 | 47 | 6.8 | 47 | 6.8 |
| | | 10,000 | −3.7 | 467 | 67.7 | 51 | 7.4 | 29 | 4.2 |
| | | | −4.8 | 454 | 65.8 | 50 | 7.2 | 32 | 4.6 |
| | | | −5.4 | 520 | 75.4 | 51 | 7.4 | 33 | 4.8 |
| | | | avg −4.6 | 480 | 69.6 | 50 | 7.3 | 31 | 4.5 |

**Table 8-42 Thermal Aging Data for PPQ Coated 6 Ply $[0° \pm 45°]_s$ Celion 6000/LARC-160 G/PI Aged in 0.10 MN/m² (14.7 psi) Air and Tested at Room Temperature**

| Aging Temperature K | Aging Temperature (°F) | Aging Time (hr) | Weight Change (%) | Compressive Strength MN/m2 | Compressive Strength (ksi) | Compressive Modulus GN/m2 | Compressive Modulus (Msi) | Shear Strength MN/m2 | Shear Strength (ksi) |
|---|---|---|---|---|---|---|---|---|---|
| | | Baseline avg | | 584 | 84.7 | 52 | 7.5 | 51 | 7.4 |
| 450 | 350 | 1,000 | 0.1 | | | | | | |
| | | | 0.0 | | | | | | |
| | | | 0.0 | | | | | | |
| | | | avg 0.0 | | | | | | |
| | | 5,000 | −1.0 | | | | | | |
| | | | 0.0 | | | | | | |
| | | | 0.0 | | | | | | |
| | | | avg 0.0 | | | | | | |
| | | 10,000 | −1.6 | 397 | 57.6 | 51 | 7.4 | 22 | 3.2 |
| | | | −1.9 | 259 | 37.6 | 44 | 6.4 | 21 | 3.0 |
| | | | −1.7 | 249 | 36.1 | 50 | 7.2 | 21 | 3.1 |
| | | | | | | | | 19 | 2.8 |
| | | | | | | | | 15 | 2.2 |
| | | | | | | | | 19 | 2.7 |
| | | | avg −1.7 | 302 | 43.8 | 48 | 7.0 | 19 | 2.8 |
| 505 | 450 | 1,000 | −1.0 | | | | | | |
| | | | −0.8 | | | | | | |
| | | | −1.0 | | | | | | |
| | | | avg −0.9 | | | | | | |
| | | 5,000 | −5.3 | | | | | | |
| | | | −4.9 | | | | | | |
| | | | −5.1 | | | | | | |
| | | | avg −5.1 | | | | | | |
| | | 10,000 | −8.0 | 422 | 61.2 | 52 | 7.6 | 34 | 4.9 |
| | | | −7.6 | 446 | 64.7 | 52 | 7.5 | 30 | 4.3 |
| | | | −8.0 | 434 | 63.0 | 49 | 7.1 | 24 | 3.5 |
| | | | | | | | | 26 | 3.8 |
| | | | | | | | | 30 | 4.3 |
| | | | | | | | | 30 | 4.4 |
| | | | avg −7.9 | 434 | 63.0 | 51 | 7.4 | 29 | 4.2 |

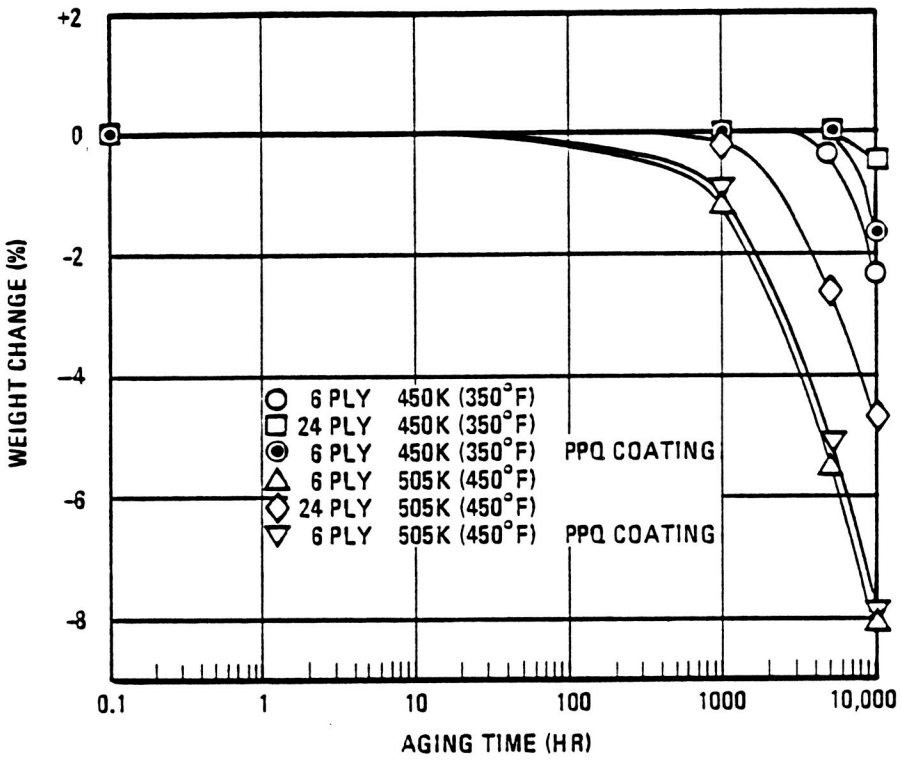



**Figure 8-64 Weight Change of Celion 6000/LARC-160 G/PI After Thermal Aging at the Indicated Temperature**

hours at the higher temperature. Neither of these specimens had been tested prior to polishing so that the cracks are the result of thermal aging and not mechanical testing. It was thought that these internal cracks might be responsible for the decrease in mechanical properties, i.e., compressive, shear, and fatigue strengths after aging. However, cracks of this type were not seen in the 6 ply G/E material for any of the aging conditions up to 10,000 hours of exposure, although large decreases in shear strength were found. It is possible that the compressive and fatigue strength losses in the G/PI are related to the internal cracking, but a mechanism to explain the large shear strength decreases was not found. Certainly, fatigue strength would be affected by the presence of matrix cracks.

Glass transition temperatures ($T_g$) were determined from samples cut from the same specimens that were used for the metallographic examinations. These results are listed in Table 8-45 for the two aging temperatures. Unlike the data from the G/E material, the $T_g$ values show a trend to lower values as aging proceeds. The effect is somewhat greater for the higher aging temperature.

In summary, thermal aging of Celion 6000/LARC-160 G/PI at 450K (350°F) and 505K (450°F) produced significant reductions in compressive, shear, and fatigue strengths after 10,000 hours of exposure. In like manner to the thermal aging/tension results for this material, the compressive and 6 ply shear strength losses were higher for the 450K (350°F) exposures. The other properties, however, showed greater decreases at the higher aging temperature. Weight loss was also greater at the higher temperature. For the 6 ply specimens these losses were quite large, greater than 8%. Again, as with the G/E system, the property most affected was the shear strength of

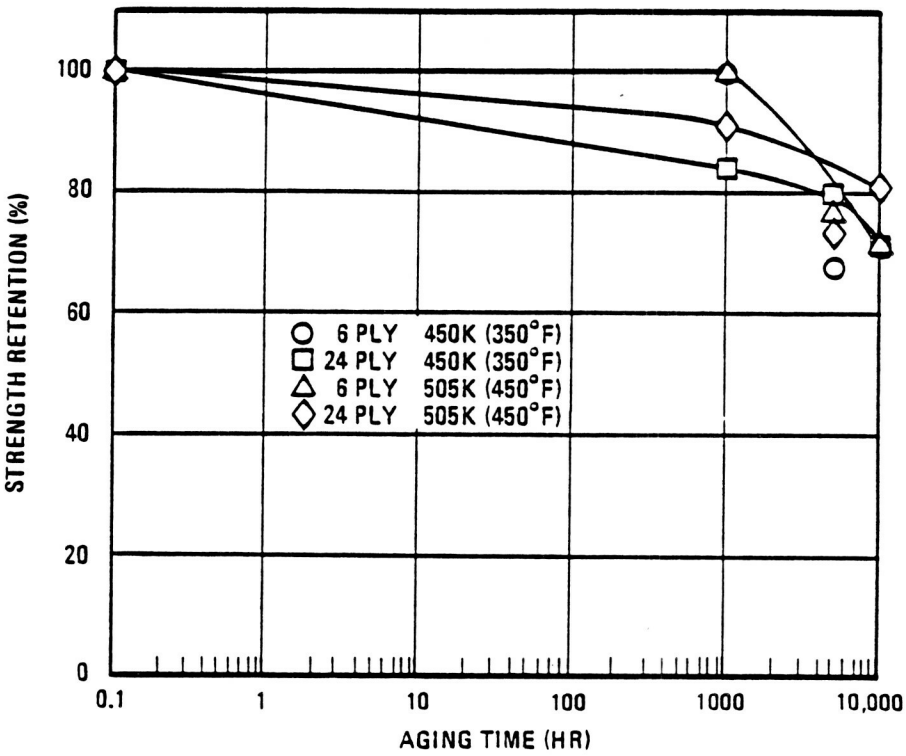



**Figure 8-65 Retention of Compressive Strength of Celion 6000/LARC-160 G/PI at 297K (75°F) After Thermal Aging at the Indicated Temperature**

the 6 ply material. Losses of 65% were found after 10,000 hours at 450K (350°F). Extensive edge cracking, particularly in the 24 ply specimens, was found as early as 1000 hours into the exposure. After 10,000 hours these cracks extended throughout the matrix. One set of 6 ply specimens was coated with PPQ in an effort to improve the thermooxidative stability of the G/PI material. Preliminary results were promising, with slight improvements over the uncoated specimens in almost every case.

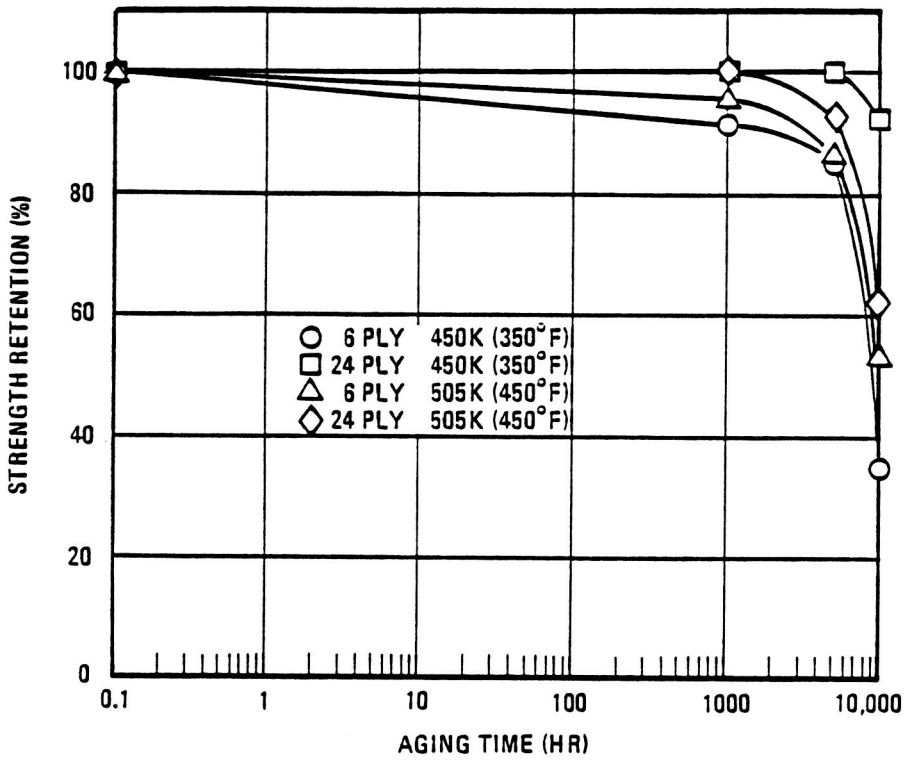



**Figure 8-66 Retention of Short Beam Shear Strength of Celion 6000/LARC-160 G/PI at 297K (75°F) After Thermal Aging at the Indicated Temperature**

**Table 8-43 Axial Fatigue Data for $[0° \pm 45°]_{s4}$ Celion 6000/LARC-160 G/PI After 10,000 Hours of Thermal Aging, 297K (75°F), R = —1, Unnotched**

| Aging Temperature K | (°F) | Specimen Number | Maximum Stress MN/m2 | (ksi) | Cycles | Comments |
|---|---|---|---|---|---|---|
| 450 | 350 | F-10-3-10 | 258 | 37.5 | 1,840 | |
| | | -11 | 293 | 42.5 | 400 | |
| | | -12 | 207 | 30 | 350,000 | |
| | | -13 | 224 | 32.5 | 122,000 | |
| | | -14 | 241 | 35 | — | Machine malfunction |
| | | -15 | 241 | 35 | 94,000 | |
| | | -16 | 276 | 40 | — | Machine malfunction |
| | | -17 | 190 | 27.5 | 12,810 | Bond failure |
| | | -18 | 172 | 25 | 38,320 | Failed under doubler |
| 505 | 450 | F-10-3-28 | 207 | 30 | 1,280 | |
| | | -29 | 172 | 25 | 35,760 | |
| | | -30 | 138 | 20 | 22,760 | Bond failure |
| | | -31 | 138 | 20 | 21,810 | Bond failure |
| | | -32 | 138 | 20 | 6,531,000 | Failed under doubler |
| | | -33 | 155 | 22.5 | 8,277,000 | |
| | | -34 | 190 | 27.5 | 440 | |
| | | -35 | 190 | 27.5 | 592,000 | |
| | | -36 | 172 | 25 | 7,569,000 | Failed under doubler |

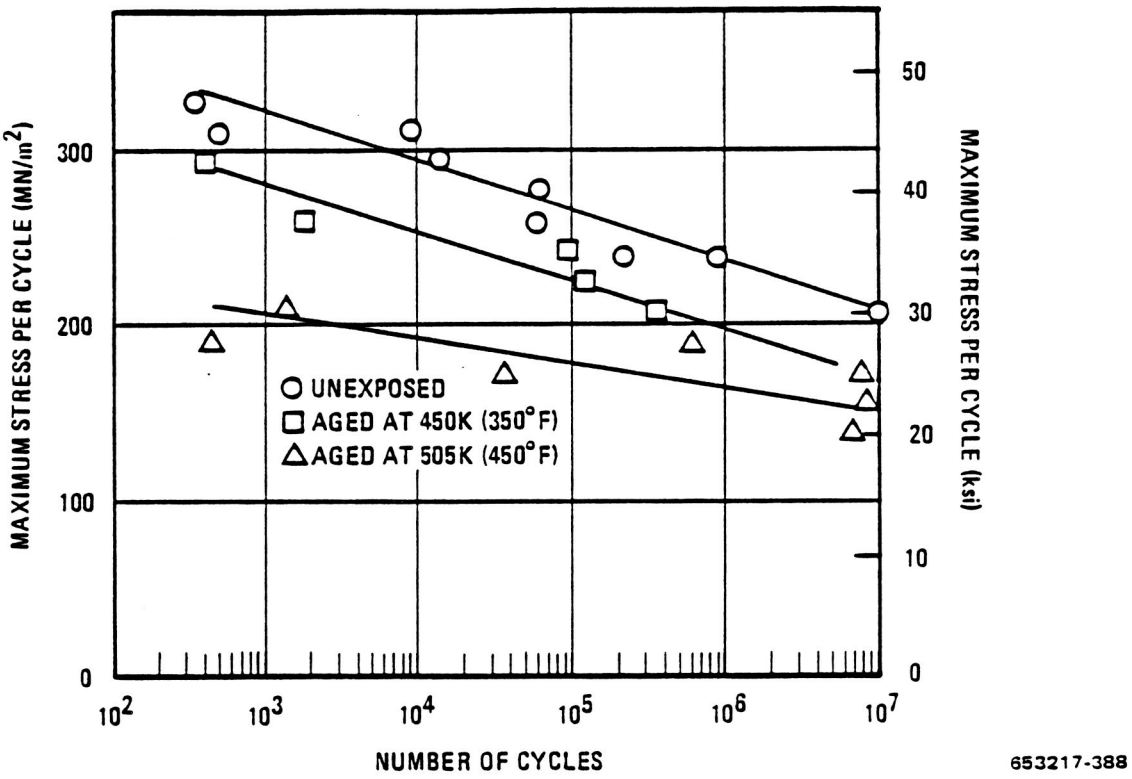



**Figure 8-67 Axial Fatique Properties of $[0° \pm 45°]_{S4}$ Celion 6000/LARC-160 G/PI Before and After 10,000 Hours of Thermal Aging, 297K (75°F), R = —1, Unnotched**

**Table 8-44 Effect of PPQ Coating on Weight Change and Compressive and Shear properties of 6 Ply $[0° \pm 45°]_s$ Celion 6000/LARC-160 G/PI After 10,000 Hours of Thermal Aging in Air**

| Item | Aging Temperature K | Aging Temperature (°F) | Uncoated | PPQ Coated |
|---|---|---|---|---|
| Weight Change (%) | 450 | 350 | —2.3 | —1.7 |
| | 505 | 450 | —8.2 | —7.9 |
| Compressive Strength (% Retention) | 450 | 350 | 72 | 52 |
| | 505 | 450 | 72 | 74 |
| Compressive Modulus (% Retention) | 450 | 350 | 100 | 93 |
| | 505 | 450 | 89 | 99 |
| Shear Strength (% Retention) | 450 | 350 | 35 | 38 |
| | 505 | 450 | 53 | 57 |

Figure 8-68 Edge Cracking in 24 Ply Celion 6000/LARC-160 G/PI After Thermal Aging at 450K (350°F) in Air



ORIGINAL PAGE IS
OF POOR QUALITY

Figure 8-69 Edge Cracking in 24 Ply Celion 6000/LARC-160 G/PI After Thermal Aging at 505K (450°F) in Air

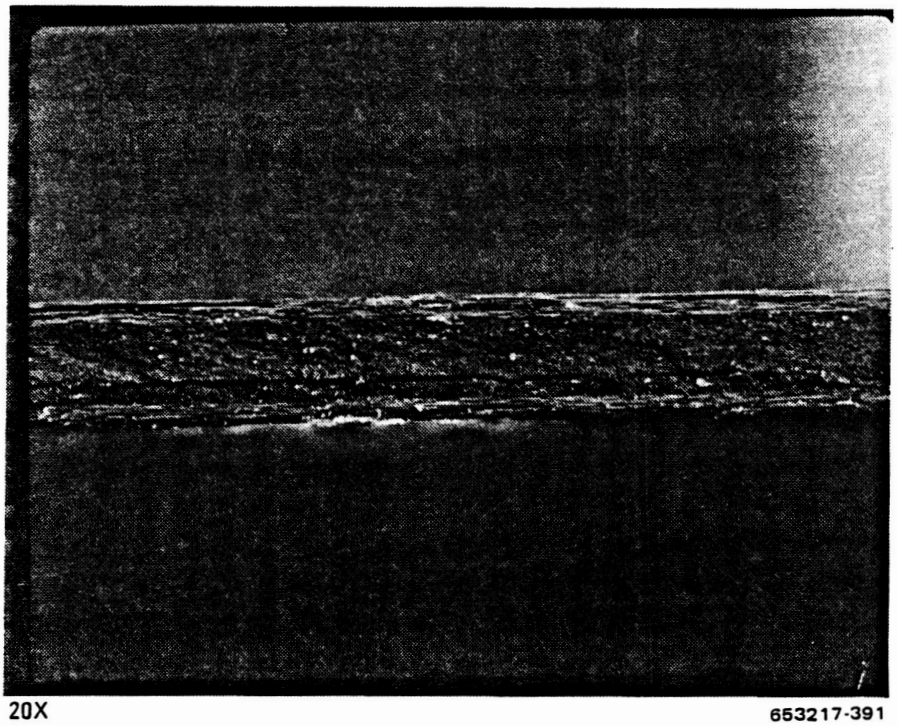


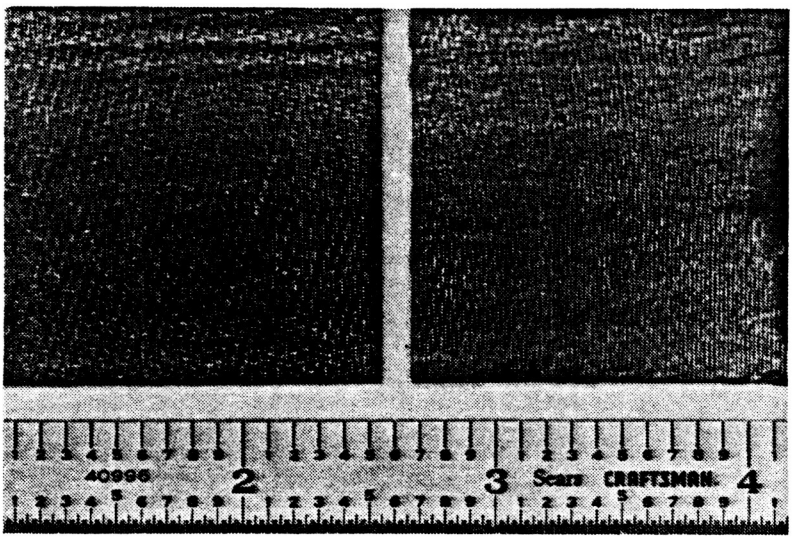

**Figure 8-70 Edge Cracking in 6 Ply Celion 6000/LARC-160 G/PI After 10,000 Hours of Aging at 505K (450°F) in Air**

ORIGINAL PAGE IS
OF POOR QUALITY

ORIGINAL PAGE IS
OF POOR QUALITY




Figure 8-71 Plan View of Section Through 24 Ply Celion 6000/LARC-160 G/PI After 10,000 Hours of Thermal Aging in One Atmosphere Air at Indicated Temperature

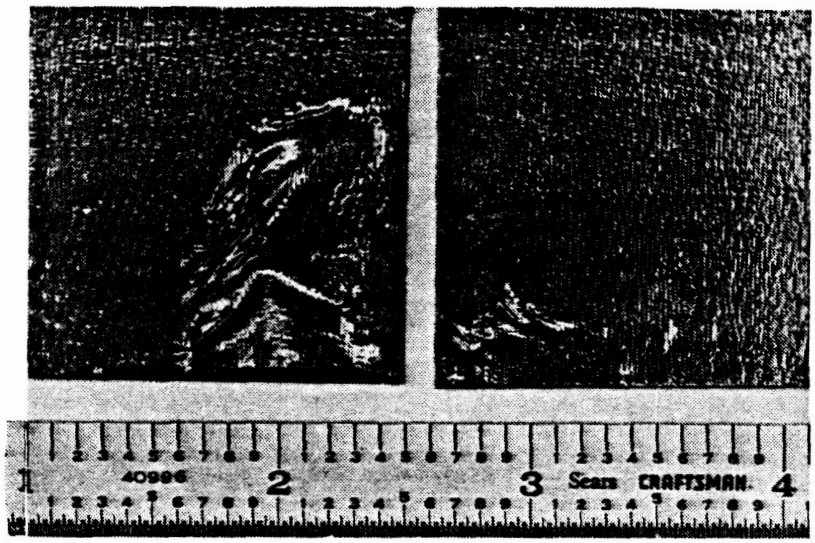



653217-393

**Figure 8-72 PPQ Coating on 6 Ply Celion 6000/LARC-160 G/PI Showing Good Adherence After 10,000 Hours of Thermal Aging at 450K (350°F) in Air**

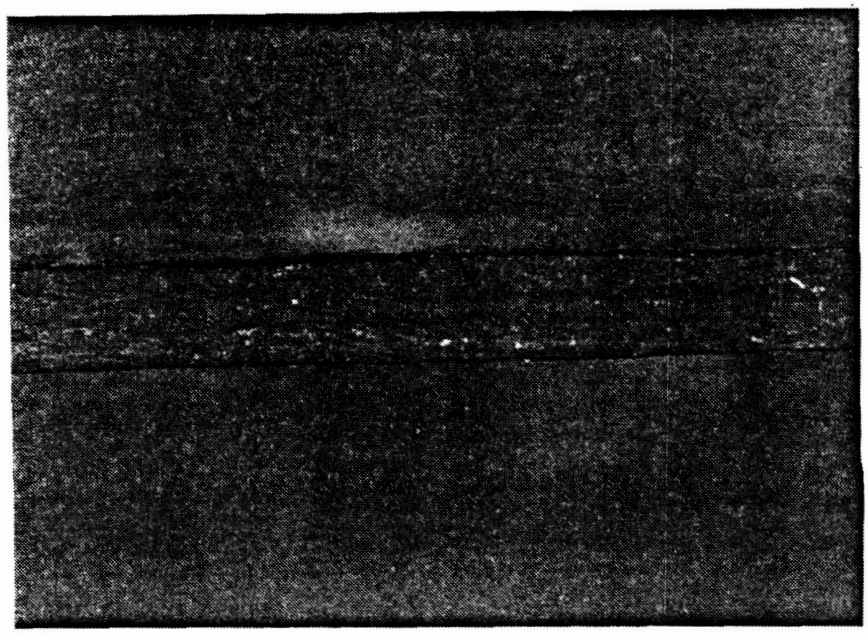
ORIGINAL PAGE IS
OF POOR QUALITY

ORIGINAL PAGE IS
OF POOR QUALITY




653217-394

**Figure 8-73 PPQ Coating on 6 Ply Celion 6000/LARC-160 G/PI Showing Varying Degrees of Peeling After 10,000 Hours of Thermal Aging at 505K (450°F) in Air**

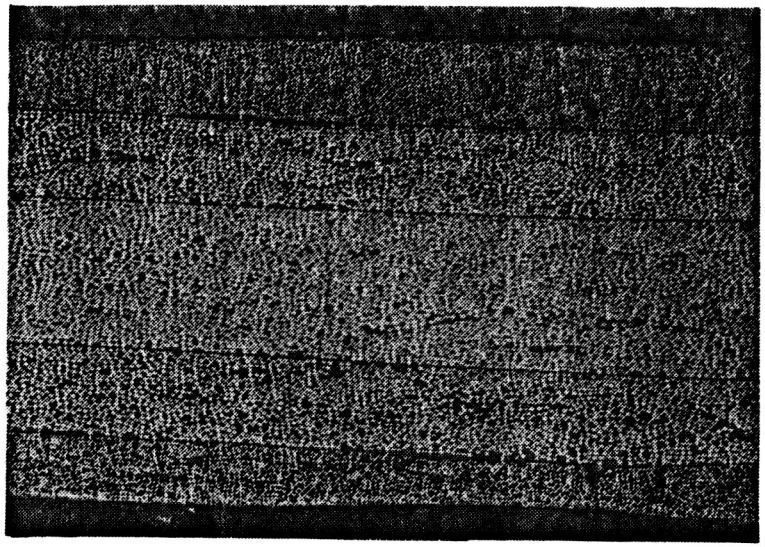


PPQ COATING REMOVED. NOTE ABSENCE OF EDGE CRACKS

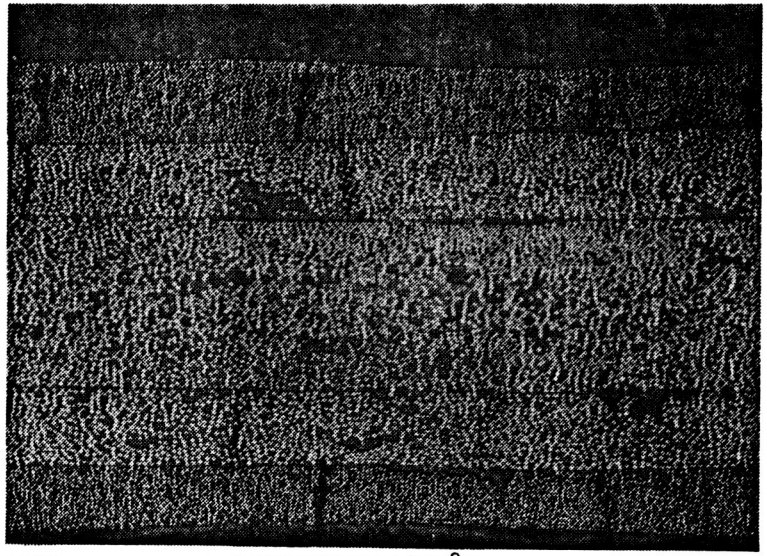
653217-395

**Figure 8-74 Edge View of 6 Ply Celion 6000/LARC-160 G/PI After 10,000 Hours of Thermal Aging at 505K (450°F) in Air**

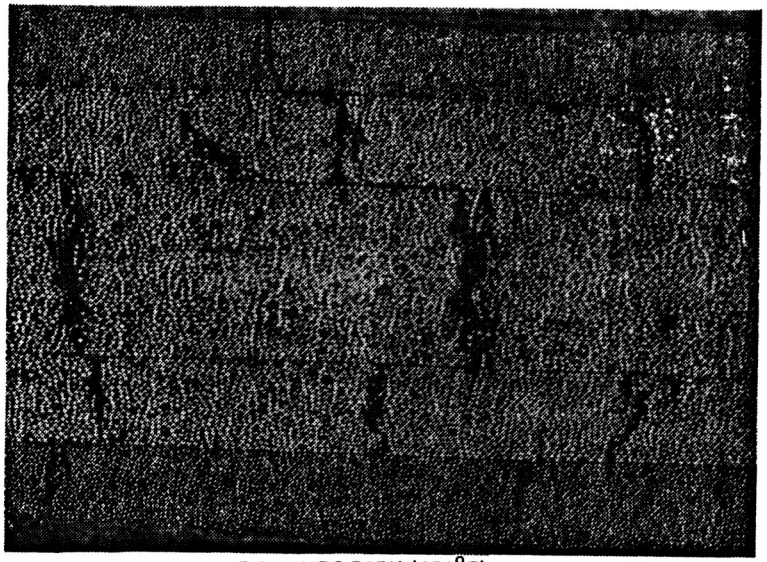
ORIGINAL PAGE IS
OF POOR QUALITY



100X AS RECEIVED



100X 5,000 HRS 450K (350°F)



100X 5,000 HRS 505K (450°F)

653217-396

**Figure 8-75 Photomicrographs (Metallograph) of Celion 6000/LARC-160 G/PI After Thermal Aging in One Atmosphere Air at Indicated Temperature**

Table 8-45 Glass Transition Temperature, $T_g$, Data for $[0° \pm 45°]_s$ Celion 6000/LARC-160 G/PI

| Condition | Aging Temperature K | Aging Temperature (°F) | Aging Time (hr) | $T_g$ K | $T_g$ (°F) |
|---|---|---|---|---|---|
| As-Received | | | | 643 | 698 |
| Aged | 450 | 350 | 1,000 | 646 | 702 |
| Aged | 450 | 350 | 5,000 | 622 | 660 |
| Aged | 450 | 350 | 10,000 | 603 | 626 |
| Aged | 505 | 450 | 1,000 | 646 | 702 |
| Aged | 505 | 450 | 5,000 | 598 | 616 |
| Aged | 505 | 450 | 10,000 | 592 | 606 |

# SECTION 9

# ENVIRONMENTAL AGING

At the time that this study was initiated, most of the data generated on advanced composite materials had been initial strength data without regard to environmental conditions. The small amount that was available was generally for only relatively short periods of exposure compared to the lifetime of a commercial airliner. This portion of the program was intended to evaluate the composite systems as a function of exposure to moisture, ambient aging, and atmospheric contaminants over relatively long periods of time.

In Phase I, 24-hour water boil, 6-week humidity, and 20-week and 52-week ambient aging tests were conducted on the resin matrix composites as accelerated means of simulating long-term ambient exposures. Residual strength testing (flexure) of unidirectional and $[0° \pm 45°]_{s2}$ crossplied specimens at room and elevated temperatures was performed after exposure and compared to tests on control (unexposed) specimens. For the B/Al system the Phase I environmental study was a determination of the effects of corrosion and atmospheric contaminants. Tensile and shear specimens of both coated and bare B/Al were placed in an outdoor industrial seacoast atmosphere corrosion test facility maintained by General Dynamics Convair Division in San Diego, California. Residual strength was determined on specimens after 10,000 hours of exposure.

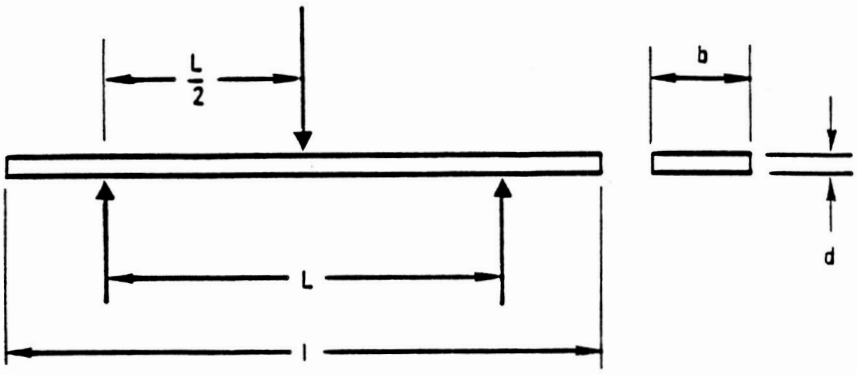
For the Celion 6000/LARC-160 G/PI that was added after completion of Phase I, 24-hour water boil, 6-week humidity, and 20-week and 52-week ambient aging exposures were carried out on $[0° \pm 45°]_{s2}$ crossplied material. No unidirectional Celion 6000/LARC-160 laminates were evaluated in the environmental aging study. After exposure, residual flexural strength tests were conducted at room and three elevated temperatures.

The Phase II task in the Environmental Aging portion of the program was a 50,000-hour outdoor exposure to determine the effects of weather and atmospheric contaminants on flexural properties of uncoated B/E, G/E, and HT-S/710 G/PI and tensile and shear properties of uncoated and coated B/Al. These exposures were initiated early in Phase I. One batch of B/Al specimens was removed during Phase I after 10,000 hours for examination and residual property testing. No interim evaluations were made on the resin matrix materials.

The following sections describe the test procedures for the environmental aging studies and present and discuss the experimental results.

## 9.1 RESIN MATRIX COMPOSITE SYSTEMS

**9.1.1 SPECIMEN DESIGN AND TEST PROCEDURES.** The longitudinal flexure specimen was used for all the environmental aging studies of the resin matrix composites. The flexure specimen does not provide data that can be used directly for design but is an effective and relatively inexpensive method for making comparisons between materials or evaluating effects of various exposures. The specimen configuration is shown in Figure 9-1. As no universally accepted specification for flexural testing of composites was available, the test methods that were used were generally in accordance with ANSI/ASTM D 790-71 and Federal Test Method Standard No. 406, Method 1031. Details of the test procedure are given in Appendix B.




SPECIMEN DIMENSIONS

LENGTH (l) = 0.076 m (3.0 in.)

WIDTH (b) = 0.01270 m (0.500 in.)

THICKNESS (d) = APPROXIMATELY 0.0015 m (0.060 in.)

SPAN/THICKNESS RATIO ($\frac{L}{d}$) = 32 TO 1

LOADING HEAD AND REACTION SUPPORTS ARE 0.00635 m (0.250 in.) DIAMETER STEEL ROD

OVERHANG MUST BE THE SAME OVER EACH END

653217-111

**Figure 9-1 Longitudinal Flexural Specimen**

Prior to conducting the moisture environmental exposures, the flexure specimens were heated at 394 K (250 °F) for 24 hours to ensure that all were in a dry condition at the start of exposure. The control specimens were also dried for 24 hours at 394 K (250 °F) before testing. All testing after exposure was accomplished within four hours after the exposure cycle had been completed.

The 24-hour water boil exposures were carried out in a reflux condenser using deionized water. An American Instrument Co., Inc. Climate-Lab, Complete Humidity-Temperature Apparatus was used to conduct the 6-week humidity exposures. The chamber was maintained at 322 K (120 °F) with a controlled environment of 95 to 100% relative humidity. The ambient aging test specimens were kept in a desiccator at 294 ± 3 K (70 ± 5 °F) and 52% relative humidity. The humidity level was maintained by a saturated aqueous solution of $Na_2Cr_2O_7 \cdot 7H_2O$. Specimens were removed from the desiccator and tested after 20 weeks and a second batch after 52 weeks. Painted redwood racks were made to hold the 50,000-hour outdoor exposure specimens. The racks were placed in an outdoor industrial-seacoast atmosphere, corrosion test facility (Figure 9-2) maintained by General Dynamics Convair on the rooftop of a building in San Diego, California approximately 800 meters (0.5 mile) from San Diego Bay.

The Phase I material environmental aging exposures were conducted with specimens cut from both unidirectional and $[0° \pm 45°]_{s2}$ crossplied panels. Residual strength testing was done at 297 K (75 °F) and 450 K (350 °F) on the unidirectional specimens for all exposure conditions.

ORIGINAL PAGE IS
OF POOR QUALITY

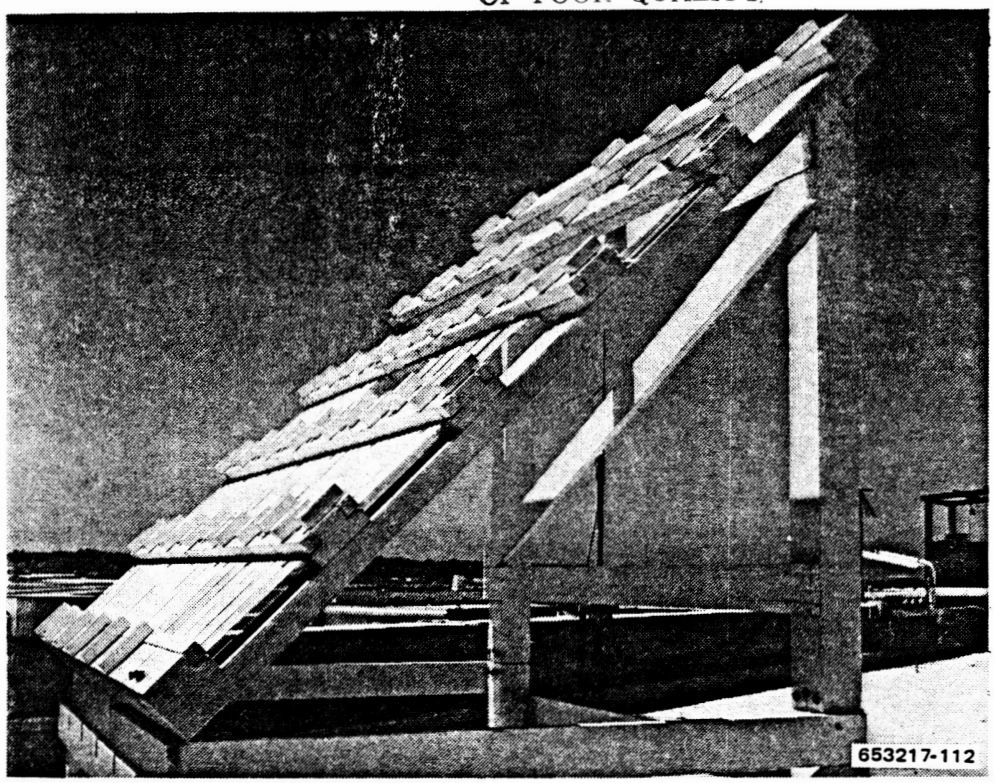



**Figure 9-2 Outdoor Corrosion Test Facility**

For the crossplied specimens, only 450 K (350 °F) tests were performed for the humidity, ambient aging, and weather exposures. The 24-hour water boil crossplied specimens were tested at both 297 K (75 °F) and 450 K (350 °F). For the new material addition, Celion 6000/LARC-160 G/PI, only $[0° \pm 45°]_{s2}$ crossplied specimens were used with residual strength testing conducted at 297 K (75 °F), 394 K (250 °F), 450 K (350 °F), and 505 K (450 °F). Testing at elevated temperatures was accomplished by heating the specimens to the test temperature in a Conrad-Missimer chamber (held in a standard test machine—Instron, Tinius-Olsen or Baldwin), holding at temperature for 10 minutes before test, and then loading to failure. It has been found that the 10-minute hold is a good compromise for getting good temperature stabilization without driving off all the moisture.

**9.1.2 TEST RESULTS AND DISCUSSION.** Residual flexural strength data after 24-hour water boil, 6-week humidity, and 20-week and 52-week ambient aging exposures are presented in Table 9-1 for B/E, Table 9-2 for G/E, Table 9-3 for HT-S/710 G/PI, and Table 9-4 for Celion 6000/LARC-160 for G/PI. Listed in the tables are the control and exposed values and the percent retention of flexural strength after the different environmental ages. In order of increasing effect on mechanical properties, the various exposures are generally ranked as one might predict, i.e., 20-week ambient, 52-week ambient, and either 6-week humidity or 24-hour water boil. The results are typical of those obtained by others (ref. 24 and 36).

For epoxy systems, crossplied laminates traditionally have shown better 450 K (350 °F) strength retention after exposure than unidirectional laminates. No definite theory has been

**Table 9-1. Effects of Moisture and Ambient Aging on B/E Laminates**

| Exposure | Orientation | Flexural Strength/Temperature 297 K (75° F) MN/m² | (ksi) | Retention % | 450 K (350° F) MN/m² | (ksi) | Retention % |
|---|---|---|---|---|---|---|---|
| Control | $[0°]_{12}$ | 2100 | 304 | | 1680 | 244 | |
| | | 2060 | 298 | | 1740 | 252 | |
| | | 2060 | 299 | | 1770 | 257 | |
| | | 2070 | 300 | | 1730 | 251 | |
| | $[0° \pm 45°]_{s2}$ | 924 | 134 | | 889 | 129 | |
| | | 958 | 139 | | 820 | 119 | |
| | | 931 | 135 | | 882 | 128 | |
| | | 938 | 136 | | 864 | 125 | |
| 24-Hour Water Boil | $[0°]_{12}$ | 1900 | 276 | | 415 | 60.2 | |
| | | 1990 | 288 | | 341 | 49.4 | |
| | | 1960 | 284 | | 428 | 62.1 | |
| | | 1950 | 283 | 94 | 395 | 57.2 | 23 |
| | $[0° \pm 45°]_{s2}$ | 924 | 134 | | 431 | 62.5 | |
| | | 896 | 130 | | 437 | 63.4 | |
| | | 820 | 119 | | 758 | 110 | |
| | | 880 | 128 | 94 | 542 | 78.6 | 63 |
| 6-Week Humidity | $[0°]_{12}$ | 2060 | 298 | | 724 | 105 | |
| | | 2190 | 318 | | 738 | 107 | |
| | | 2130 | 309 | | 586 | 85.0 | |
| | | 2130 | 308 | 100 | 683 | 99.0 | 39 |
| | $[0° \pm 45°]_{s2}$ | | — | | 690 | 100 | |
| | | | — | | 648 | 94.0 | |
| | | | — | | 586 | 85.0 | |
| | | | | | 641 | 93.0 | 74 |
| 20-Week Ambient Age | $[0°]_{12}$ | 2190 | 317 | | 1060 | 154 | |
| | | 2120 | 308 | | 1000 | 145 | |
| | | 2220 | 322 | | 1030 | 149 | |
| | | 2180 | 316 | 100 | 1030 | 149 | 59 |
| | $[0° \pm 45°]_{s2}$ | | — | | 869 | 126 | |
| | | | — | | 834 | 121 | |
| | | | — | | 952 | 138 | |
| | | | | | 885 | 128 | 100 |
| 52-Week Ambient Age | $[0°]_{12}$ | 2210 | 320 | | 965 | 140 | |
| | | 2300 | 334 | | 862 | 125 | |
| | | 2320 | 337 | | 896 | 130 | |
| | | 2280 | 330 | 100 | 908 | 132 | 53 |
| | $[0° \pm 45°]_{s2}$ | | — | | 882 | 128 | |
| | | | — | | 772 | 112 | |
| | | | — | | 772 | 112 | |
| | | | | | 809 | 117 | 94 |

**Table 9-2. Effects of Moisture and Ambient Aging on G/E Laminates**

| Exposure | Orientation | Flexural Strength/Temperature 297 K (75° F) MN/m² | (ksi) | Retention % | 450 K (350° F) MN/m² | (ksi) | Retention % |
|---|---|---|---|---|---|---|---|
| Control | $[0°]_{12}$ | 1720 | 294 | | 1220 | 177 | |
| | | 1710 | 248 | | 1460 | 211 | |
| | | 1620 | 235 | | 1210 | 176 | |
| | | 1680 | 244 | | 1230 | 188 | |
| | $[0° \pm 45°]_{s2}$ | 882 | 128 | | 658 | 95.4 | |
| | | 779 | 113 | | 710 | 103 | |
| | | 910 | 132 | | 676 | 98.1 | |
| | | 857 | 124 | | 681 | 98.8 | |
| 24-Hour Water Boil | $[0°]_{12}$ | 1850 | 268 | | 424 | 61.5 | |
| | | 1620 | 235 | | 405 | 58.7 | |
| | | 1580 | 229 | | 464 | 67.3 | |
| | | 1680 | 244 | 100 | 431 | 62.5 | 33 |
| | $[0° \pm 45°]_{s2}$ | 855 | 124 | | 345 | 50.1 | |
| | | 834 | 121 | | 415 | 60.2 | |
| | | 820 | 119 | | 334 | 48.4 | |
| | | 836 | 121 | 98 | 365 | 52.9 | 54 |
| 6-Week Humidity | $[0°]_{12}$ | 1720 | 250 | | 405 | 58.7 | |
| | | 1640 | 238 | | 372 | 54.0 | |
| | | 1680 | 244 | | 388 | 56.3 | |
| | | 1680 | 244 | 100 | 388 | 56.3 | 30 |
| | $[0° \pm 45°]_{s2}$ | | — | | 268 | 38.9 | |
| | | | — | | 289 | 41.9 | |
| | | | — | | 272 | 39.4 | |
| | | | | | 276 | 40.1 | 41 |
| 20-Week Ambient Age | $[0°]_{12}$ | 1960 | 284 | | 634 | 91.9 | |
| | | 1690 | 245 | | 690 | 100 | |
| | | 1900 | 275 | | 793 | 115 | |
| | | 1850 | 268 | 100 | 706 | 102 | 54 |
| | $[0° \pm 45°]_{s2}$ | | — | | 609 | 88.3 | |
| | | | — | | 479 | 69.5 | |
| | | | — | | 535 | 77.6 | |
| | | | | | 541 | 78.5 | 79 |
| 52-Week Ambient Age | $[0°]_{12}$ | 1670 | 242 | | 605 | 87.8 | |
| | | 1660 | 240 | | 564 | 81.8 | |
| | | 1540 | 223 | | 598 | 86.7 | |
| | | 1620 | 235 | 96 | 589 | 85.4 | 45 |
| | $[0° \pm 45°]_{s2}$ | | — | | 394 | 57.1 | |
| | | | — | | 392 | 56.8 | |
| | | | — | | 376 | 54.5 | |
| | | | | | 387 | 56.1 | 57 |

C-4

**Table 9-3. Effects of Moisture and Ambient Aging on HT-S/710 G/PI Laminates**

| Exposure | Orientation | Flexural Strength/Temperature 297 K (75° F) MN/m² | (ksi) | Retention % | 450 K (350° F) MN/m² | (ksi) | Retention % |
|---|---|---|---|---|---|---|---|
| Control | $[0°]_{12}$ | 1330 | 193 | | 869 | 126 | |
| | | 993 | 144 | | 952 | 138 | |
| | | 1220 | 177 | | 807 | 117 | |
| | | 1180 | 171 | | 876 | 127 | |
| | $[0° \pm 45°]_{s2}$ | 665 | 96.4 | | 538 | 78.0 | |
| | | 567 | 82.2 | | 661 | 95.8 | |
| | | 701 | 101.7 | | 439 | 63.7 | |
| | | 644 | 93.4 | | 546 | 79.2 | |
| 24-Hour Water Boil | $[0°]_{12}$ | 1140 | 166 | | 848 | 123 | |
| | | 1020 | 148 | | 986 | 143 | |
| | | 841 | 122 | | 938 | 136 | |
| | | 1000 | 145 | 85 | 924 | 134 | 100 |
| | $[0° \pm 45°]_{s2}$ | 578 | 83.9 | | 476 | 69.0 | |
| | | 567 | 82.3 | | 374 | 54.3 | |
| | | 351 | 50.9 | | 385 | 55.9 | |
| | | 499 | 72.4 | 78 | 412 | 59.7 | 75 |
| 6-Week Humidity | $[0°]_{12}$ | 938 | 136 | | 1080 | 156 | |
| | | 889 | 129 | | 848 | 123 | |
| | | 1190 | 172 | | 848 | 123 | |
| | | 1010 | 146 | 85 | 925 | 134 | 100 |
| | $[0° \pm 45°]_{s2}$ | | — | | 348 | 50.6 | |
| | | | — | | 501 | 72.6 | |
| | | | — | | 486 | 70.5 | |
| | | | | | 445 | 64.5 | 81 |
| 20-Week Ambient Age | $[0°]_{12}$ | 1150 | 167 | | 703 | 102 | |
| | | 1210 | 176 | | 690 | 100 | |
| | | 1280 | 186 | | 827 | 120 | |
| | | 1210 | 176 | 100 | 740 | 107 | 84 |
| | $[0° \pm 45°]_{s2}$ | | — | | 523 | 75.9 | |
| | | | — | | 703 | 102 | |
| | | | — | | 590 | 85.5 | |
| | | | | | 605 | 87.8 | 100 |
| 52-Week Ambient Age | $[0°]_{12}$ | 1290 | 187 | | 869 | 126 | |
| | | 1180 | 171 | | 931 | 135 | |
| | | 1100 | 159 | | 1020 | 148 | |
| | | 1190 | 172 | 100 | 940 | 136 | 100 |
| | $[0° \pm 45°]_{s2}$ | | — | | 537 | 77.9 | |
| | | | — | | 523 | 75.9 | |
| | | | — | | 458 | 66.4 | |
| | | | | | 506 | 73.4 | 93 |

Table 9-4. Effects of Moisture and Ambient Aging on Celion 6000/LARC-160 G/PI Laminates

| Exposure | Flexural Strength/Temperature 297 K (75°F) MN/m² | (ksi) | Retention % | 394 K (250°F) MN/m² | (ksi) | Retention % | 450° K (350°F) MN/m² | (ksi) | Retention % | 505 K (450°F) MN/m² | (ksi) | Retention % |
|---|---|---|---|---|---|---|---|---|---|---|---|---|
| Control | 1070 | 155 | | 800 | 116 | | 765 | 111 | | 724 | 105 | |
| | 972 | 141 | | 793 | 115 | | 793 | 115 | | 758 | 110 | |
| | 1000 | 145 | | 800 | 116 | | 827 | 120 | | 731 | 106 | |
| | 1010 | 147 | | 798 | 116 | | 795 | 115 | | 738 | 107 | |
| 24-Hour Water Boil | 889 | 129 | | 807 | 117 | | 827 | 120 | | 772 | 112 | |
| | 952 | 138 | | 896 | 130 | | 827 | 120 | | 690 | 110 | |
| | 896 | 130 | | 896 | 130 | | 834 | 121 | | 724 | 105 | |
| | 912 | 132 | 90 | 866 | 126 | 100 | 829 | 120 | 100 | 729 | 106 | 99 |
| 6-Week Humidity | 952 | 138 | | 814 | 118 | | 752 | 109 | | 710 | 103 | |
| | 882 | 128 | | 795 | 115 | | 779 | 113 | | 710 | 103 | |
| | 952 | 138 | | 834 | 121 | | 800 | 116 | | 717 | 104 | |
| | 929 | 135 | 92 | 814 | 118 | 100 | 777 | 113 | 98 | 712 | 103 | 96 |
| 20-Week Ambient Age | 862 | 125 | | 855 | 124 | | 807 | 117 | | 779 | 113 | |
| | 855 | 124 | | 862 | 125 | | 795 | 115 | | 786 | 114 | |
| | 903 | 131 | | 862 | 125 | | 841 | 122 | | 796 | 115 | |
| | 873 | 127 | 86 | 860 | 125 | 100 | 814 | 118 | 100 | 787 | 114 | 100 |
| 52-Week Ambient Age | 972 | 141 | | 827 | 120 | | 841 | 122 | | 807 | 117 | |
| | 910 | 132 | | 814 | 118 | | 827 | 120 | | 827 | 120 | |
| | 986 | 143 | | 834 | 121 | | 834 | 121 | | 779 | 113 | |
| | 956 | 139 | 95 | 825 | 120 | 100 | 834 | 121 | 100 | 804 | 117 | 100 |

advanced to explain this, but contributing factors might include specimen configuration, built-in thermal stresses from curing, compressive mode of failure after exposure, etc. An examination of the epoxy flexural strength data (Tables 9-1 and 9-2) shows that after long term aging, the failure strengths for both unidirectional and crossplied laminates are nearly the same. This would be anticipated for a matrix dominated failure mode. The room temperature flexural strengths were nearly unaffected by any of these exposures, while those at 450 K (350 °F) were, in general, severely degraded; the only exceptions were the crossplied B/E material after the 20- and 52-week ambient age. The unidirectional specimens were particularly affected with losses in the 450 K (350 °F) flexural strength of from 77 to 41% depending on the type of exposure.

The effects of the moisture exposures on the polyimide specimens were generally less damaging than for the epoxy systems. For the HT-S/710 some decreases in flexural strength of the crossplied material were observed at 450 K (350 °F) after the 24-hour water boil and 6-week humidity tests, but no significant effects were observed as a result of the 20- and 52-week ambient ages. The Celion 6000/LARC-160 behaved even better with almost no loss in flexural strength at elevated temperatures and only minor losses at room temperature.

The Phase II task in the environmental aging portion of the program was a 50,000-hour outdoor exposure to determine the effects of weather and atmospheric contaminants on flexural properties of uncoated B/E, G/E, and HT-S/710 G/PI. At the completion of 50,000 hours of exposure it was discovered that six of the nine G/E specimens and four of the nine G/PI specimens were missing. Whether the missing specimens were the result of vandalism or unusual weather conditions could not be determined. After exposure the recovered specimens were photographed and examined by eye and with a low power stereo microscope. Before and after photographs of the three systems are shown in Figures 9-3 through 9-6. The following is a description of the condition of the different batches of material:

B/E — The outer glass scrim cloth layer on the upper surface had been loosened and was no longer present on seven of the specimens and was quite loose on the other two. There were no loose boron fibers, but some shallow grooves were visible between the fibers, perhaps an indication of the loss of resin from the surface. The lower sides of the specimens did not show much change. The specimens were held in the racks only at the ends so that both upper and lower surfaces were exposed to the atmosphere. The lower surfaces were, however, shielded from direct sunlight, rain, and any falling particulate matter.

G/E — The three G/E specimens had a considerable number of graphite fibers exposed on the upper surfaces as a result of the loss of resin. The undersides showed only a very few exposed fibers.

G/PI — On the upper surfaces of the specimens the outer portion of the polyimide resin had also been lost so that considerable graphite fibers were exposed. On the surfaces facing the rack no loose fibers were visible.

Residual flexural strength data after the 50,000 hours of exposure are presented in Table 9-5 for the three materials. Also listed are the percent retention values based on the control data shown in Tables 9-1 through 9-3. For B/E the effect of the 50,000 hours of exposure was more severe than that for the 20-and 52-week ambient exposures but less than those observed after the 24-hour water boil or the 6-week humidity tests. The room temperature strength was nearly

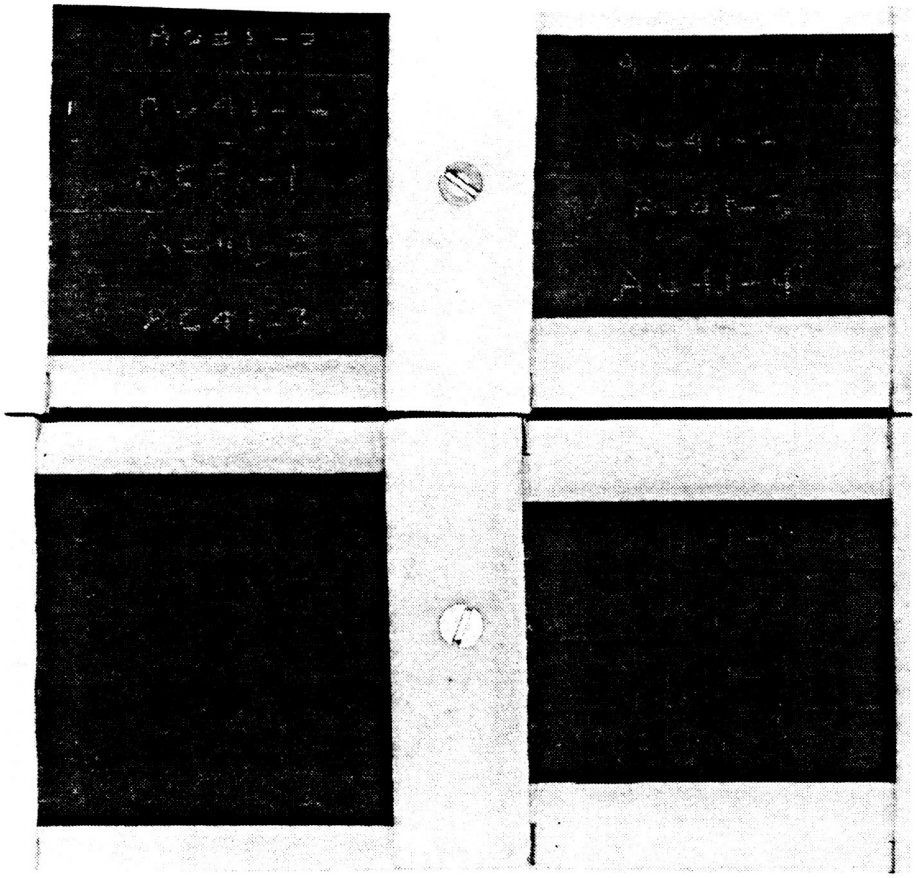



**Figure 9-3 Corrosion Racks Containing B/E and G/E Specimens — Before Exposure**

unchanged while the 450K (350 °F) properties were degraded approximately 50 and 25 percent respectively for the unidirectional and the [0 ° ± 45 °] crossplied layups. The loss in elevated temperature strength is believed to have been primarily the result of absorbed moisture in like manner to the results obtained during the Phase I studies. The limited results obtained from the three unidirectional G/E specimens indicate that the 50,000 hours of exposure produced effects at 450K (350 °F) that were no worse than those obtained after any of the exposures conducted during Phase I with the possible exception of the 20-week ambient age of the crossplied layup. While the HT-S/710 G/PI data are also limited, it appears that the 50,000 hour weather exposure has been more damaging to the flexural properties of this system than any of the Phase I exposure conditions.

Fiber reinforced resin matrix composites (particularly epoxies) absorb moisture from the atmosphere. This absorption causes two basic problems, i.e., 1) losses in matrix dominated mechanical properties, and 2) changes in physical dimensions. The effects are mostly reversible in that heat or vacuum will drive off the moisture and will return the composites to their dry control properties and dimensions. The absorption of moisture primarily occurs in the resin matrix, and the resulting changes in composite mechanical and physical properties are a result of this absorption by the resin. Therefore, the type of reinforcement does not greatly influence the moisture effects. This was seen in the results presented earlier in that both the boron and graphite reinforced epoxies exhibited considerable property degradation from the absorbed moisture.



ORIGINAL PAGE IS
OF POOR QUALITY

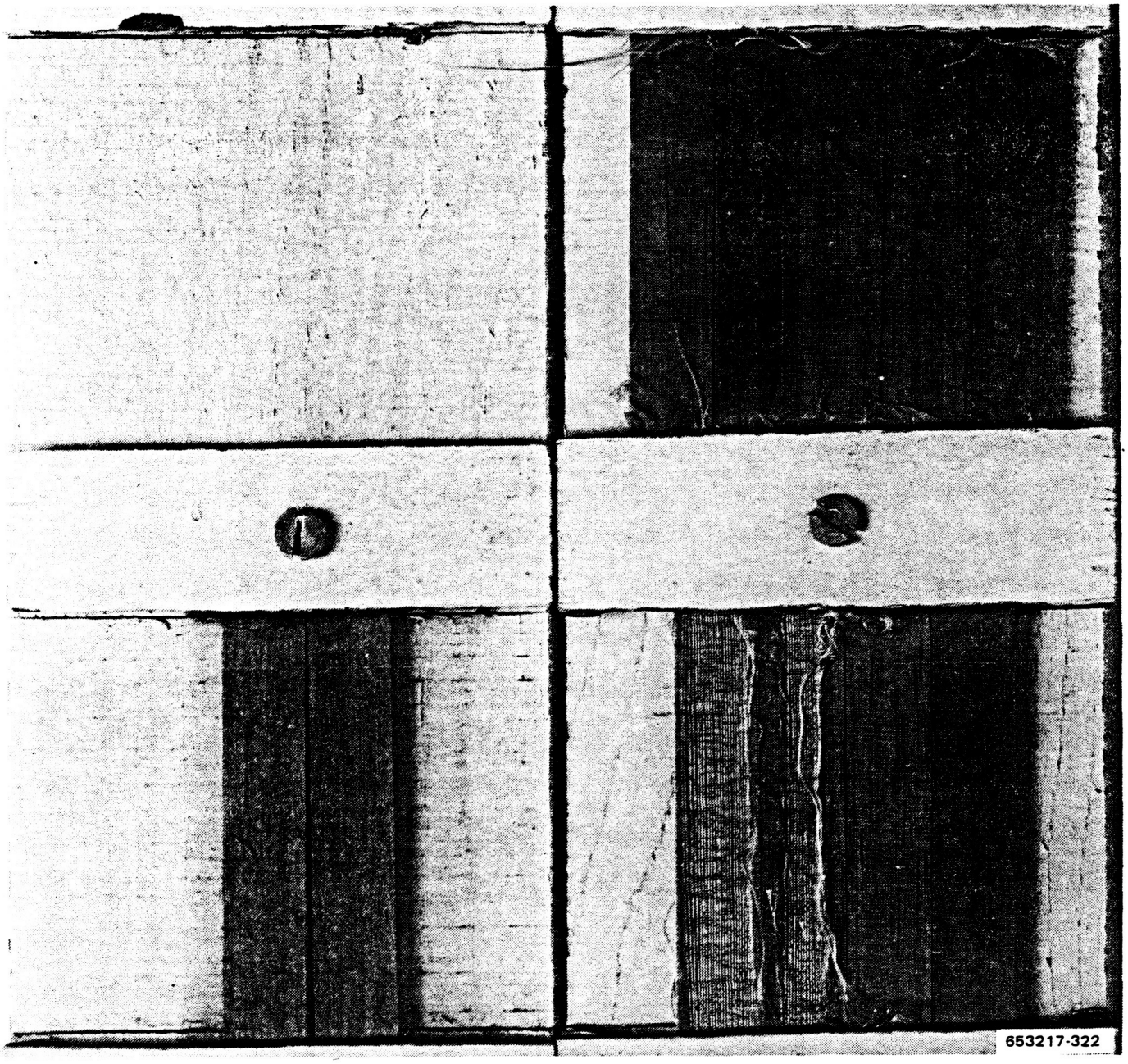



**Figure 9-4 Corrosion Racks Containing B/E and G/E Specimens — Exposed for 50,000 hours in an Industrial-Seacoast Atmosphere**

The general moisture problem was discovered by General Dynamics Convair Division in 1970 (ref. 8 and 24). The problem manifested itself initially by unusually low longitudinal flexure strength at 450 K (350 °F) in G/E after short terms of aging at ambient temperature and humidity in air conditioned laboratories. Extensive work on this problem (ref. 36) led to the conclusion that the cause of the problem was plasticization of the epoxy resin by moisture, which subsequently lowers the glass transition temperature of the resin. The high temperature composite properties generally affected by moisture absorption are shear strength and modulus, edge compressive strength, bolt bearing and flat-wise tensile strengths. Since the initial work at General Dynamics Convair significant efforts have been made and are still in progress at several laboratories in this country to determine moisture effects on mechanical



ORIGINAL PAGE IS
OF POOR QUALITY

ORIGINAL PAGE IS
OF POOR QUALITY

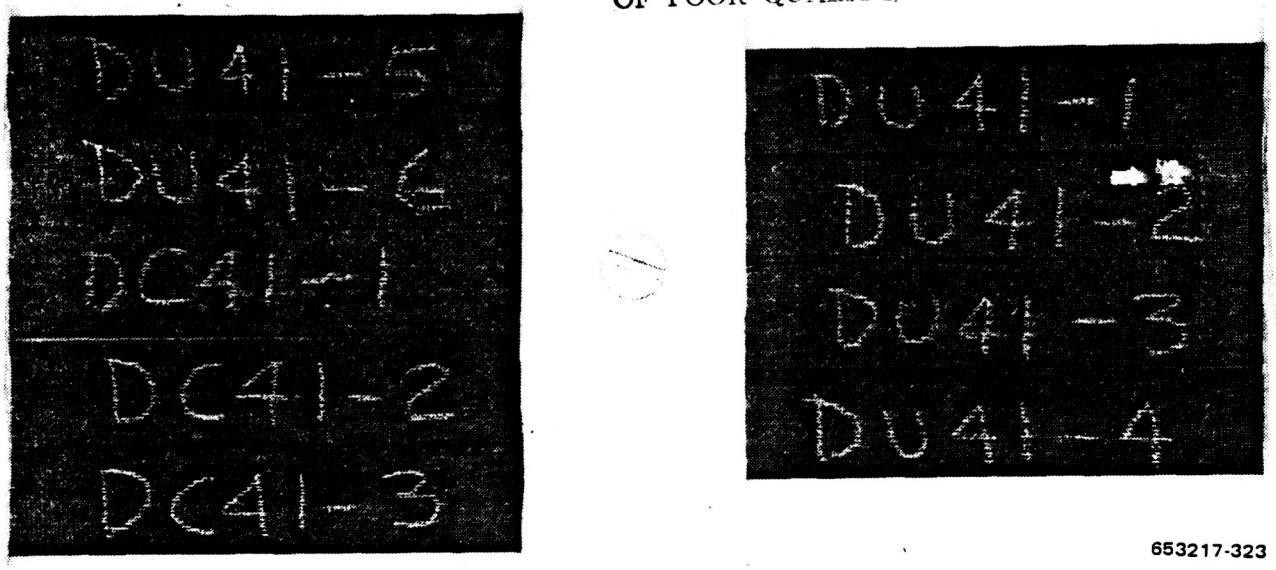



**Figure 9-5 Corrosion Rack Containing HT-S/710 G/PI Specimens — Before Exposure**

properties of polymer matrix composites. Many of these early results were presented in 1975 at a U.S. Air Force Materials Laboratory and Society of Aerospace Materials and Process Engineers Workshop, which examined the environmental durability of resin matrix composites. A summary of the data presented along with the conclusions and recommendations of the participants can be found in reference 37.

## 9.2 METAL MATRIX COMPOSITE SYSTEM

**9.2.1 SPECIMEN DESIGN AND TEST PROCEDURE.** The tensile and interfiber shear specimen configurations used for the B/Al environmental study were identical to those described previously in Section 7, Baseline Testing. All specimens were machined from 6 ply unidirectional B/Al. Tensile specimens were cut from both the longitudinal and transverse directions while the interfiber shear specimens were cut from only the longitudinal direction.

In addition to determining the susceptibility of B/Al composite material to corrosion and atmospheric contaminants, an objective of the study was to evaluate an elevated temperature corrosion protection system for B/Al. In previous work at General Dynamics Convair (ref. 38) it was found that B/Al composite materials are somewhat more susceptible to corrosion than aluminum structures, especially at the edges, where both boron and aluminum are exposed to the corrosive environment. In these same studies, effective corrosion resistance was achieved by a paint finish system applied over a chemical film treatment. These systems, however, were effective to only approximately 422 K (300 °F), somewhat below the range desired for the SCR application. Later work on a corrosion protection system for B/Al composites serviceable up to 589K (600 °F) was also accomplished at Convair (ref. 39). While not completely effective in preventing corrosion of the aluminum, the polyimide, silicone, and fluorocarbon coating systems studied showed promise. Using these results as a starting point, a limited test program was conducted to develop a coating for use on these environmental exposures. The finish system that was selected consisted of a chemical conversion coating followed by an epoxy primer and a polyimide topcoat. Before the chemical conversion coating, the specimens were degreased, alkaline cleaned, and deoxidized. The epoxy primer was applied over the chemical

Figure 9-6 Corrosion Rack Containing HT-S/710 G/PI Specimens — Exposed for 50,000 hours in an Industrial-Seacoast Atmosphere



ORIGINAL PAGE IS
OF POOR QUALITY

**Table 9-5. Effects of 50,000-hour Weather Exposure on Flexural Strength of B/E, G/E, and HT-S/710 G/PI Laminates**

| Material | Orientation | Flexural Strength/Temperature 297 K (75° F) MN/m² | (ksi) | Retention % | 450 K (350° F) MN/m² | (ksi) | Retention % |
|---|---|---|---|---|---|---|---|
| B/E | $[0°]_{12}$ | 2020 | 293 | | 869 | 126 | |
| | | 1860 | 270 | | 800 | 116 | |
| | | 1830 | 266 | | 779 | 113 | |
| | | 1900 | 276 | 92 | 816 | 118 | 47 |
| | $[0° \pm 45°]_{s2}$ | | — | | 568 | 82.4 | |
| | | | — | | 550 | 79.7 | |
| | | | — | | 820 | 119 | |
| | | | | | 646 | 93.7 | 75 |
| G/E | $[0°]_{12}$ | | — | | 786 | 114 | |
| | | | — | | 685 | 99.3 | |
| | | | | | 736 | 107 | 57 |
| | $[0° \pm 45°]_{s2}$ | | — | | 341 | 49.4 | 50 |
| HT-S/710 G/PI | $[0°]_{12}$ | 972 | 141 | | 632 | 91.6 | |
| | | 945 | 137 | | 724 | 105 | |
| | | 958 | 139 | 81 | 678 | 98.3 | 77 |
| | $[0° \pm 45°]_{s2}$ | | — | | 425 | 61.7 | 78 |

conversion coating and allowed to dry. Aluminum powder pigment (5% by weight) was added to the polyimide coating material before application over the primer. After application of the aluminized polyimide coating, the specimens were cured at 436 K (325 °F) for 14 hours. This coating has a maximum use temperature of about 589 K (600 °F). Half of the B/Al specimens used for the environmental exposure tests were coated and the other were bare.

The same type of painted redwood racks that were used for the resin matrix specimens were made to hold the B/Al specimens during exposure. The racks were placed in the outdoor industrial-seacoast atmosphere, corrosion test facility shown in Figure 9-2. Half of the coated and half of the bare specimens were removed after 10,000 hours for examination and residual strength testing. The remaining half of the specimens were removed after 50,000 hours of exposure. Tensile and interfiber shear tests were conducted at room temperature using the procedures described in Section 7.

**9.2.2 TEST RESULTS AND DISCUSSION.** After 10,000 hours of outdoor exposure no change in appearance was observed in the coated B/Al specimens, but the bare specimens all showed evidence of extensive surface corrosion with some concentrated attack at localized areas (pitting). This attack was much heavier on the side of the specimen facing away from the rack. The samples were held in the racks only on the ends so that both front and back surfaces were exposed to the environment. Photographs of the specimens mounted in the wooden racks before exposure are shown in Figure 9-7, and after 10,000 hours in Figure 9-8. The corrosion of the uncoated specimens is clearly visible in Figure 9-8.

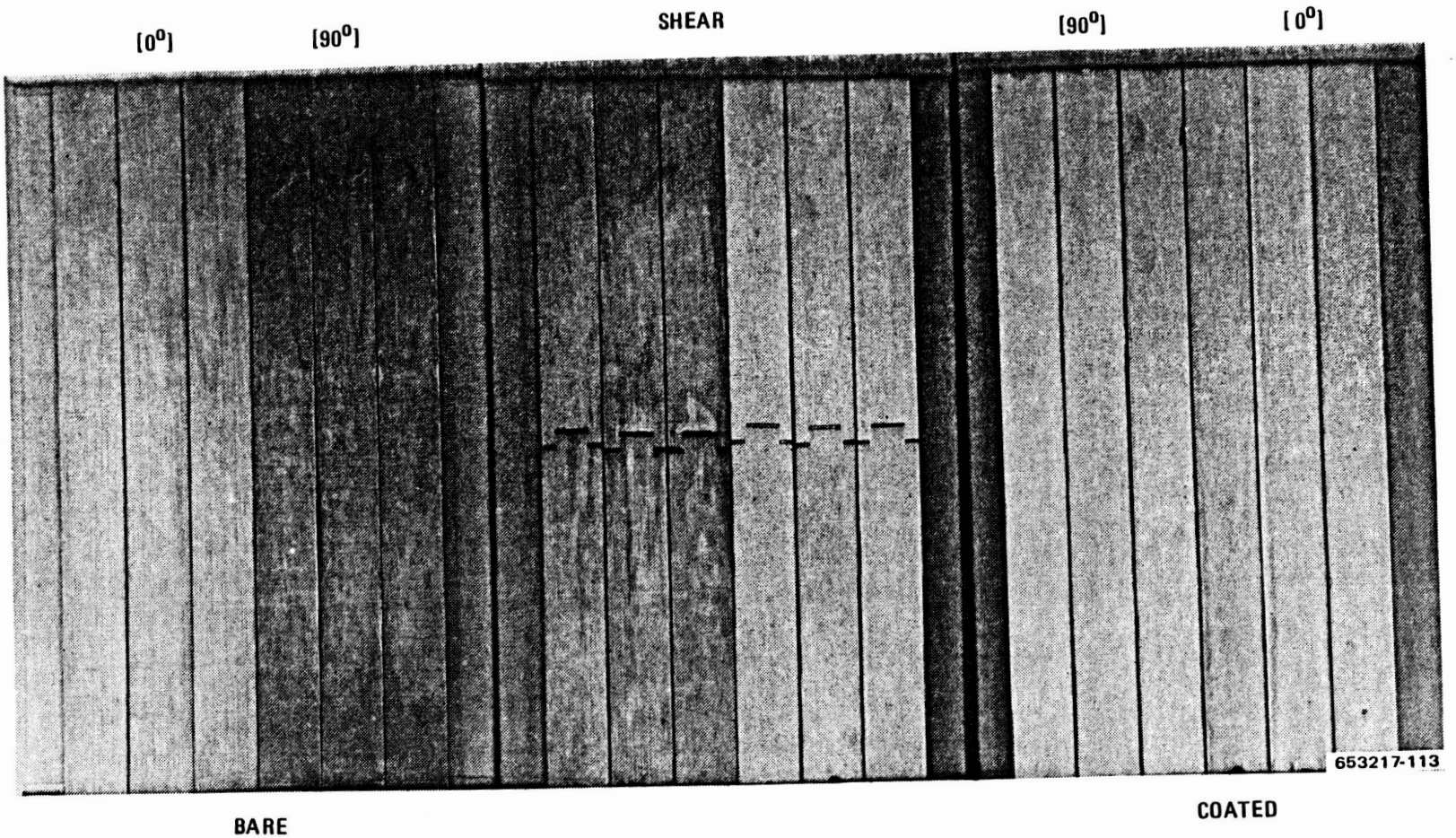



Figure 9-7 Corrosion Racks Containing Unidirectional B/Al Specimens — Before Exposure



ORIGINAL PAGE IS
OF POOR QUALITY

ORIGINAL PAGE IS
OF POOR QUALITY

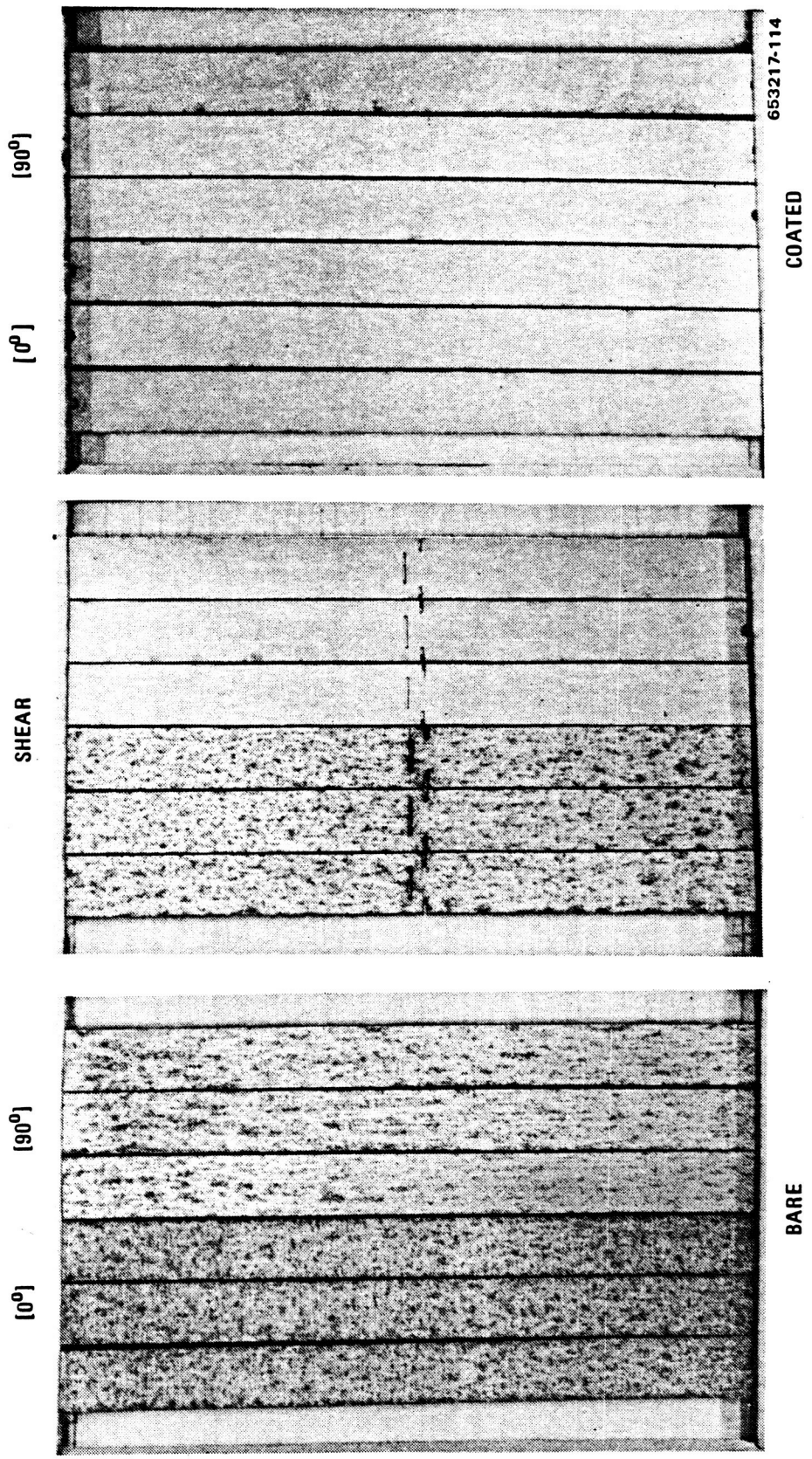



Figure 9-8 Corrosion Racks Containing Unidirectional B/Al Specimens — Exposed for 10,000 hr in an Industrial-Seacoast Atmosphere

The results of post exposure tensile and shear testing are presented in Tables 9-6 and 9-7. Only typical values of the unexposed strengths are given because the environmental aging specimens were cut from different panels than those used for the baseline tests. No effects to either tensile or shear properties were observed for the coated samples. For the uncoated specimens, significant decreases were found in the transverse tensile strength and the shear strength, while the longitudinal tensile strength was unaffected by the 10,000-hour exposure. A surface effect such as corrosion of the bare aluminum would be expected to decrease the matrix controlled properties, i.e., transverse tensile and shear, but have little effect on longitudinal tensile, a fiber controlled property.

To check the extent and nature of the surface corrosion, a metallographic examination of bare and coated specimens was performed. No change in appearance was found for the coated specimen after the 10,000-hour exposure as the coating had provided complete protection. Examination of the uncoated specimen, on the other hand, revealed extensive intergranular attack at the surface, which extended to a depth of approximately 0.00007 m (0.003 in.). An example of these corrosion crack regions is shown in Figure 9-9. Some surface disruption has also occurred near one of the boron filaments.

The uncoated interfiber shear specimens, see Figure 7-30, had been prepared prior to placing in the test facility so that the machined edges as well as the surfaces were exposed to the atmosphere. These specimens showed a decrease in shear strength of approximately one-third. Later, a second set of shear specimens was prepared by re-machining half of each of the three failed specimens. For these specimens, only the surface of the test area had been exposed and subjected to corrosive attack. The shear strength of these specimens, Table 9-7, was only slightly lower than the coated material. The configuration of the shear specimen used for these tests is one in which stress concentrations build up at the machined surfaces at either end of the shearing regions. If these surfaces are exposed to a corrosive environment, the subsequent corrosion cracks can initiate failures at loads substantially lower than those obtained from undamaged specimens. It is this phenomenon that is believed to have been responsible for the significant effect on shear strength of machining the notch before or after exposure.

Photographs of the 50,000 hour B/Al specimens before and after exposure are shown in Figures 9-10 and 9-11. Again, the coating provided excellent protection with no visible failures. The upper surfaces of the specimens contained a small amount of debris but no evidence of corrosion. The bottom surfaces were quite clean. The uncoated specimens, on the other hand, showed considerable evidence of surface corrosion with extensive pitting. The attack was much more severe on the side of the specimen facing away from the rack. This upper surface also contained a great deal of debris, much of which had the crystalline appearance of salt. These uncoated 50,000 hour specimens showed much greater surface degradation than did those (Figure 9-8) that had been removed after 10,000 hours. At the completion of the 50,000 hours of exposure it was found that two of the notched shear specimens had been broken in the shearing regions. These are the first and last of the set of shear specimens shown in Figure 9-11. No reason could be found for these unexpected failures.

The results of post-exposure tensile and shear testing are presented in Tables 9-6 and 9-7 along with the data from the 10,000 hour specimens. The tensile properties of the coated specimens in both the longitudinal and transverse directions were still relatively unaffected even after 50,000 hours of exposure. For the bare specimens, however, both orientations showed lower strengths after exposure. The longitudinal specimens that showed no effects after 10,000 hours were down in tensile strength from 4 to 12% after 50,000 hours.

Table 9-6. Tensile Data for Bare and Coated $[0°]_6$ B/Al After Atmospheric Contaminants Exposure in an Industrial-Seacoast Environment

| Condition | Orientation | Typical Strength Unexposed | | Strength After 10,000 Hours | | Strength After 50,000 Hours | |
|---|---|---|---|---|---|---|---|
| | | MN/m² | (ksi) | MN/m² | (ksi) | MN/m² | (ksi) |
| Bare | [90°] | | | 121 | 17.6 | 139 | 20.2 |
| | | | | 127 | 18.4 | 90.3 | 13.1 |
| | | | | 134 | 19.5 | 90.3 | 13.1 |
| | | 152 | 22 | 127 | 18.5 | 106.5 | 15.5 |
| Coated | [90°] | | | 176 | 25.6 | 152 | 22.1 |
| | | | | 156 | 22.7 | 190 | 27.5 |
| | | | | 167 | 24.2 | 162 | 23.5 |
| | | 152 | 22 | 166 | 24.2 | 168 | 24.4 |
| Bare | [0°] | | | 1410 | 205 | 1280 | 185 |
| | | | | 1400 | 203 | 1340 | 194 |
| | | | | 1560 | 226 | 1390 | 202 |
| | | 1450 | 210 | 1460 | 211 | 1340 | 194 |
| Coated | [0°] | | | 1500 | 217 | 1320 | 192 |
| | | | | 1500 | 218 | 1560 | 227 |
| | | | | 1390 | 202 | 1340 | 195 |
| | | 1450 | 210 | 1460 | 212 | 1410 | 205 |

The average tensile strength of the bare transverse specimens had decreased nearly 30% after 50,000 hours of exposure. The 10,000 hour decrease had been about one-half this value. Again, corrosion of the aluminum matrix would be expected to affect the matrix controlled transverse strength to a greater degree than the fiber controlled longitudinal strength, and such was the case. The other matrix controlled property, interfiber shear strength, was also significantly decreased by the 50,000 hours of exposure (approximately 30%). However, in this case, both the bare and the coated specimens were affected. Remachining the shear configuration in one-half of each of the failed specimens and retesting did not appreciably affect the shear strength values as was found after the 10,000 hour exposures. The decrease in shear strength of the uncoated material after both the 10,000 hour and 50,000 hour exposures is thought to have been caused by the surface corrosion of the aluminum at either end of the shearing regions. No explanation has been found, however, for the shear strength drop in the coated specimens that did not experience any surface corrosion. To verify the absence of corrosion on the coated specimens and to determine the extent and nature of the corrosion on the bare specimens, additional metallograhpic examinations were conducted. As shown in Figure 9-12, no change in appearance was found in a coated specimen after the 50,000 hour exposure as the coating had provided complete protection. Examination of an uncoated specimen, on the other hand, revealed extensive intergranular attack near the surface, which extended to a depth of approximately 0.00018 m (0.007 in.). The attack, shown in Figure 9-13, was considerably deeper and more widespread than that observed for a specimen that had been exposed for 10,000 hours (Figure 9-9).

Table 9-7. Shear Data for Bare and Coated $[0°]_6$ B/Al After Atmospheric Contaminants Exposure in an Industrial-Seacoast Environment

| Condition | Orientation | Typical Strength Unexposed MN/m² | Typical Strength Unexposed (ksi) | Strength After 10,000 Hours MN/m² | Strength After 10,000 Hours (ksi) | Strength After 50,000 Hours MN/m² | Strength After 50,000 Hours (ksi) |
|---|---|---|---|---|---|---|---|
| Bare, Machined Before Exposure | [0°] | | | 82.0 | 11.9 | * | * |
| | | | | 75.2 | 10.9 | 83.4 | 12.1 |
| | | | | 77.2 | 11.2 | 64.8 | 9.4 |
| | | 110 | 16 | 78.1 | 11.3 | 74.1 | 10.8 |
| Bare, Machined After Exposure | [0°] | | | 109 | 15.8 | 76.5 | 11.1 |
| | | | | 102 | 14.8 | 82.0 | 11.9 |
| | | | | 106 | 15.4 | 77.2 | 11.2 |
| | | 110 | 16 | 106 | 15.3 | 78.6 | 11.4 |
| Coated, Machined Before Exposure | [0°] | | | 119 | 17.3 | * | * |
| | | | | 108 | 15.7 | 75.8 | 11.0 |
| | | | | 97.2 | 14.1 | 82.0 | 11.9 |
| | | 110 | 16 | 108 | 15.7 | 78.9 | 11.4 |
| Coated, Machined After Exposure | [0°] | | | | — | 86.9 | 12.6 |
| | | | | | — | 68.3 | 9.9 |
| | | | | | — | ** | ** |
| | | 110 | 16 | | | 77.6 | 11.2 |

*Failed during exposure

**Specimen damaged during machining

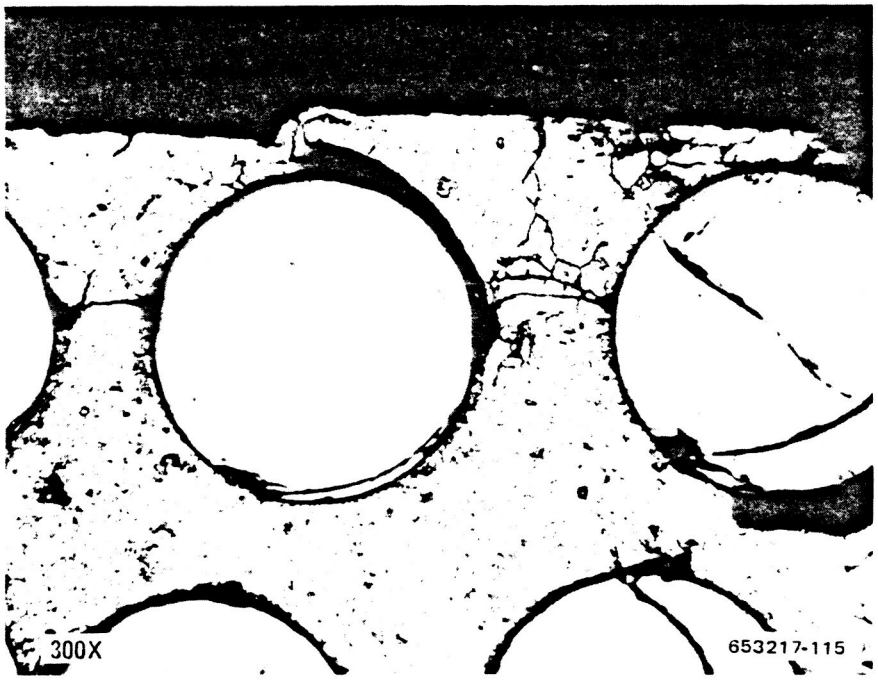



**Figure 9-9 Intergranular Corrosion Cracks in Unidirectional B/Al After 10,000 hr of Atmospheric Contaminants Exposure in an Industrial-Seacoast Environment**

ORIGINAL PAGE IS
OF POOR QUALITY

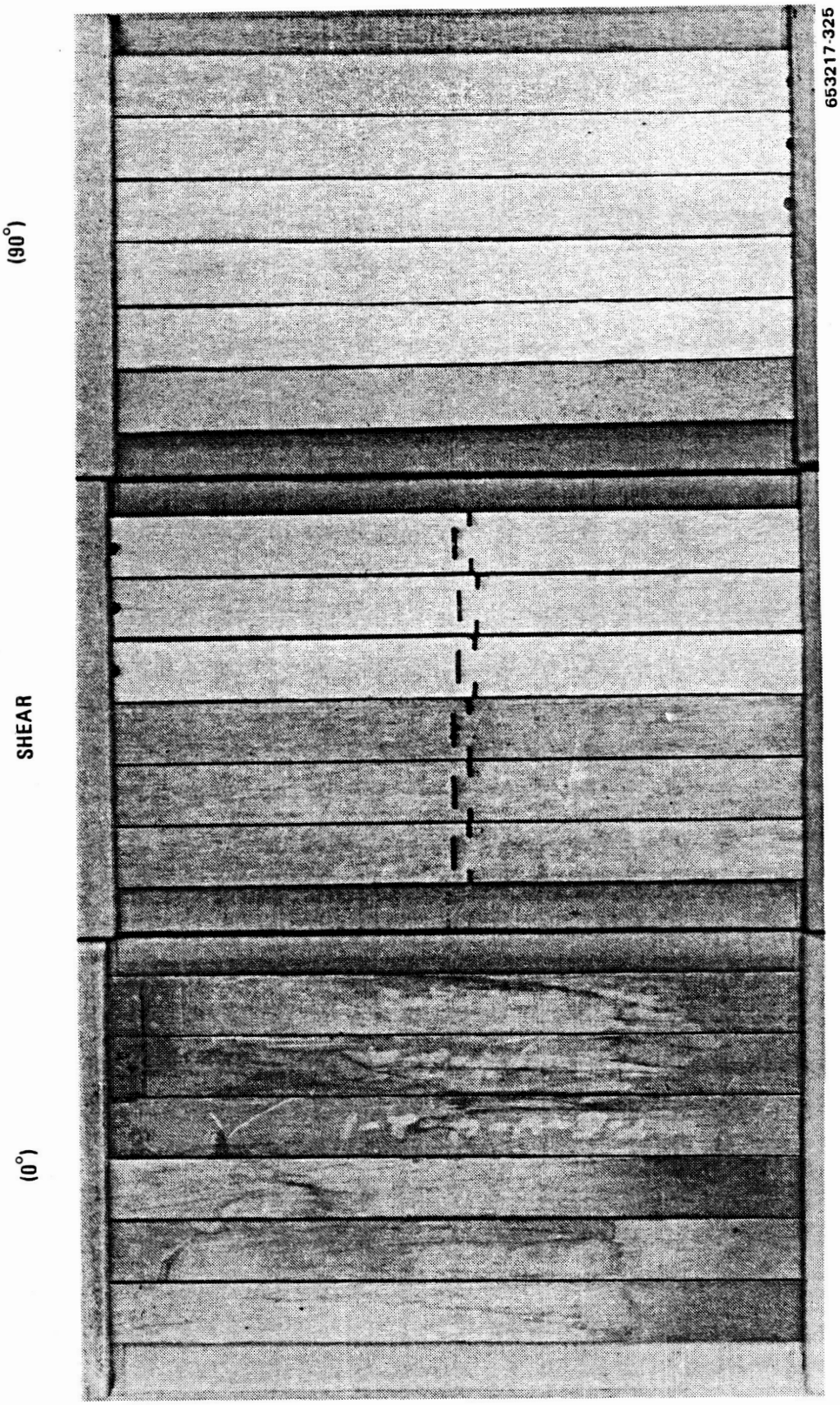



Figure 9-10 Corrosion Racks Containing Unidirectional B/Al Specimens — Before Exposure



ORIGINAL PAGE IS
OF POOR QUALITY

ORIGINAL PAGE IS
OF POOR QUALITY



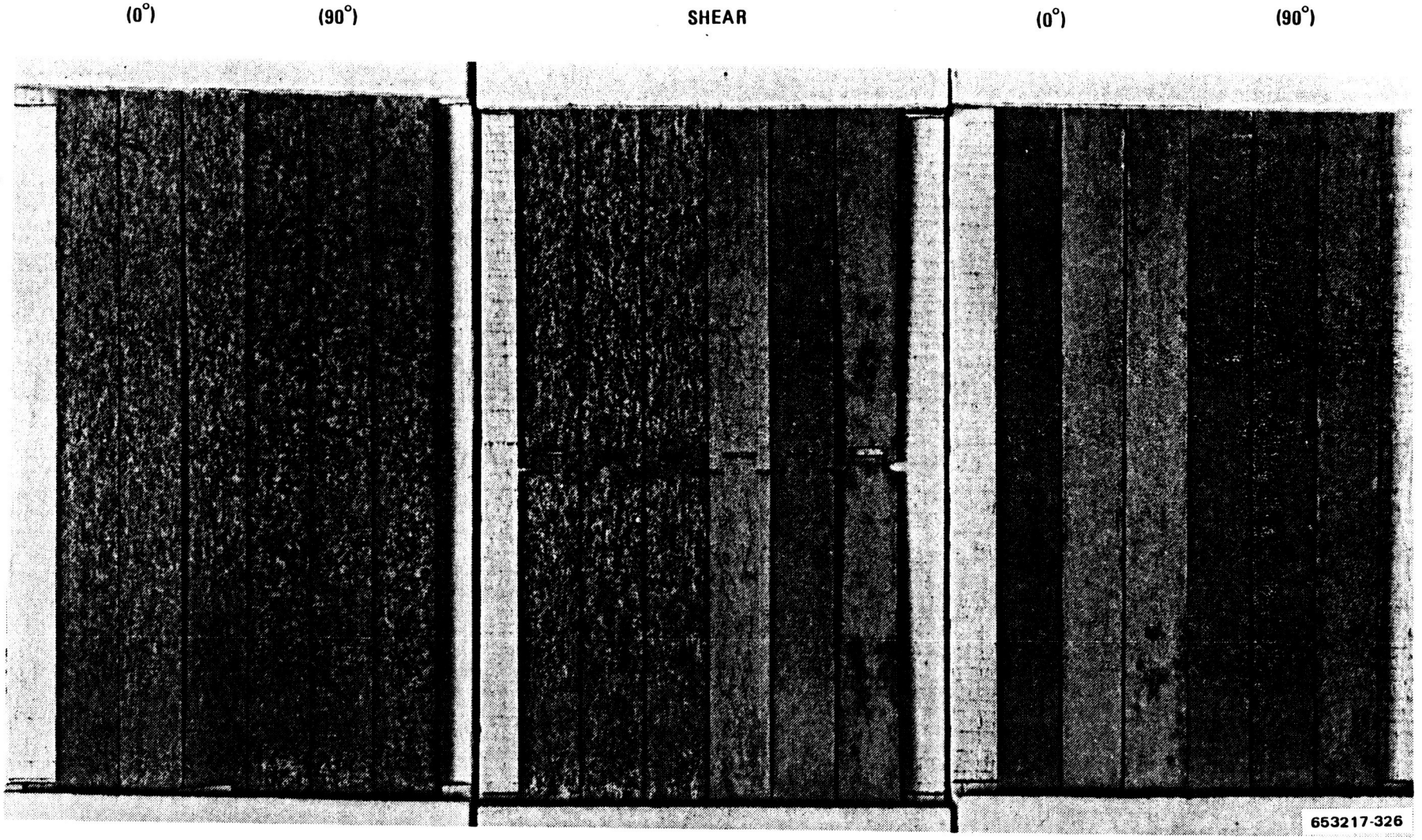



**Figure 9-11 Corrosion Racks Containing Unidirectional B/Al Specimens — Exposed for 50,000 hr in an Industrial-Seacoast Atmosphere**

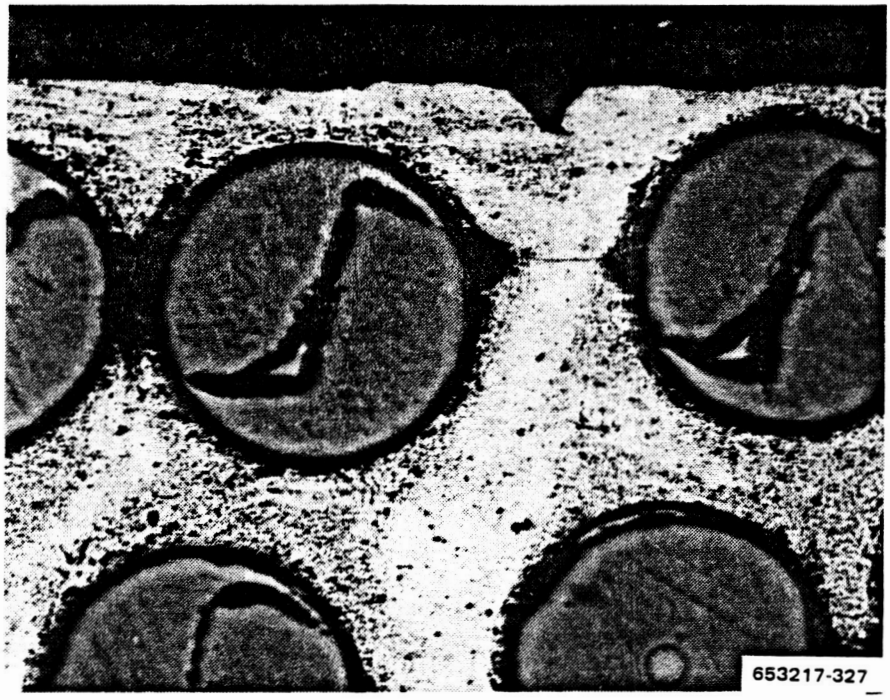



**Figure 9-12 Coated, Unidirectional B/Al After 50,000 hr of Atmospheric Contaminants Exposure in an Industrial-Seacoast Environment. No Corrosion has Occurred**

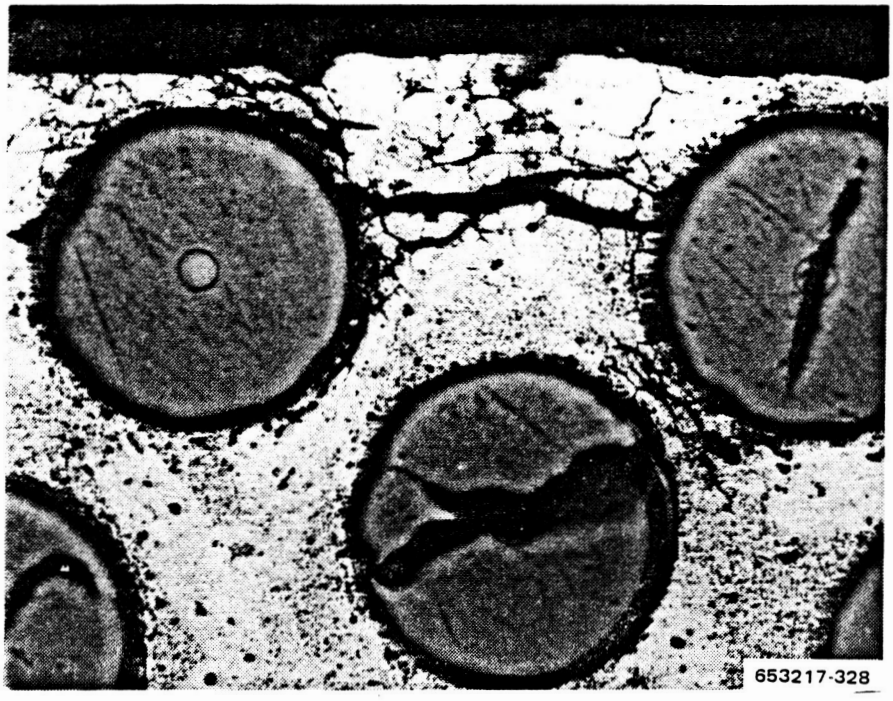



**Figure 9-13 Intergranular Corrosion Cracks in Unidirectional B/Al After 50,000 hr of Atmospheric Contaminants Exposure in an Industrial-Seacoast Environment**



ORIGINAL PAGE IS
OF POOR QUALITY

# SECTION 10

# CREEP TESTING

The objective of this task was to determine experimentally the creep and creep rupture behavior of the four advanced composite materials selected for evaluation in Phase I of the SCR program. Axial creep tests were performed at two temperatures for exposure times of 100 and 1000 hours for each system. The two test temperatures were the proposed maximum use temperature for each material and one selected lower temperature in the potential application range. Results obtained during Phase I of this contract study have since proven these proposed maximum use temperatures to have been overly optimistic for all four composites. The lower temperatures were, however, well chosen, and agree quite closely with those used for the flight simulation tests. Creep properties were determined for two layups, unidirectional and $[0° \pm 45°]_s$ crossply, of each material. All specimens were taken from 6 ply laminates. The creep/creep rupture test program is summarized in Table 10-1.

For the Celion 6000/LARC-160 G/PI that was added after completion of the Phase I creep testing, a decision was made to eliminate the creep testing portion from the baseline material characterization. This was done because of the results obtained in this section on the four Phase I composites. Composite materials with 0° plies aligned in the direction of loading were observed to undergo very little creep deformation prior to failure. These small amounts of strain and the scatter in the measurements combined to make creep testing a questionable parameter for material characterization of filamentary reinforced composites.

## 10.1 SPECIMEN DESIGN

No standard specimen for creep testing of composites had been established at the time the creep testing task was initiated. Previous work at General Dynamics Convair (ref. 24 and 38) with a straight sided specimen similar to that used for tensile testing had given good results for material with no fibers aligned in the loading direction. For specimens with fibers in the loading direction the high loads required resulted in frequent bond failures in the end doublers. A slightly modified specimen was used for this program. To reduce misalignment and ensure axial loading the grips were changed from wedge to pin loaded. Tapered titanium doublers were bonded to the grip areas to minimize stress concentrations. The length of the specimens was such that it would help prevent premature grip failures by permitting the grip ends to extend outside the furnace. A length of 0.56 m (22 in.) was selected, and the B/E and B/Al specimens were prepared. No problems were encountered with bond failures in the B/E specimens, but four of the B/Al specimens failed prematurely in the doubler bonds. As heating of the adhesive during testing was thought to have contributed to the problem, the length of the G/E and G/PI specimens was increased to 0.71 m (28 in.) to further extend the grip ends outside the furnace. While the longer specimen undoubtedly helped, the combination of high loads and temperatures also resulted in several bond failures in both the G/E and G/PI systems. The configuration of the creep specimen is shown in Figure 10-1.

Table 10-1. Summary of Creep/Creep Rupture Test Program

| Material | Laminate Orientation | Temperature K | Temperature (°F) | Time (hr) | Number of Specimens |
|---|---|---|---|---|---|
| 5505/4 B/E | $[0° \pm 45°]_s$ | 394 | 250 | 100 | 2 |
| | | | | 1000 | 3 |
| | | 450 | 350 | 100 | 6 |
| | | | | 1000 | 1 |
| | $[0°]_6$ | 450 | 350 | 100 | 4 |
| | | | | 1000 | 2 |
| A-S/3501-5 G/E | $[0° \pm 45°]_s$ | 394 | 250 | 100 | 5 |
| | | | | 1000 | 2 |
| | | 450 | 350 | 100 | 4 |
| | | | | 1000 | 1 |
| | $[0°]_6$ | 394 | 250 | 100 | 5 |
| | | | | 1000 | 1 |
| | | 450 | 350 | 100 | 4 |
| | | | | 1000 | 2 |
| HT-2/710 G/PI | $[0° \pm 45°]_s$ | 505 | 450 | 1000 | 6 |
| | | 561 | 550 | 100 | 6 |
| | $[0°]_6$ | 505 | 450 | 100 | 6 |
| | | 561 | 550 | 100 | 6 |
| B/Al | $[0° \pm 45°]_s$ | 505 | 450 | 100 | 3 |
| | | | | 1000 | 3 |
| | | 561 | 550 | 100 | 3 |
| | | | | 1000 | 3 |
| | $[0°]_6$ | 505 | 450 | 100 | 6 |
| | | 561 | 550 | 100 | 6 |

## 10.2 TEST EQUIPMENT AND TEST PROCEDURE

All creep tests were performed in air using Arcweld Creep Testing Machines, Model JE, 5440 kg (12,000 lb) or Model EE, 9070 kg (20,000 lb), and Arcweld Power Positioning Furnaces, Model F8. The furnaces are 0.43 m (17 in.) in length with 0.064 m (2.5 in.) diameter ceramic muffle tubes in which the specimens are radiant heated. The resistance heated furnaces have three zones that can be manually adjusted to minimize temperature gradients along the central test section of the specimens. A centrally located viewing port is available for optical measurements. Temperature control for the furnaces is provided by Wheelco controllers using chromel-alumel thermocouples inserted through the wire heating elements and in contact with the outside of the muffle tube. The test temperature was measured with three chromel-alumel thermocouples attached at 0.0444 m (1.75 in.) intervals to the gage section of the test specimen with high temperature fiberglass tape. Temperature variations at any one location were generally less than $\pm$ 1.75 K (3° F) while temperature uniformity along the 0.0889 m (3.50 in.) section was generally maintained to $\pm$ 2.8 K (5° F). Strain measurements were made with an optical

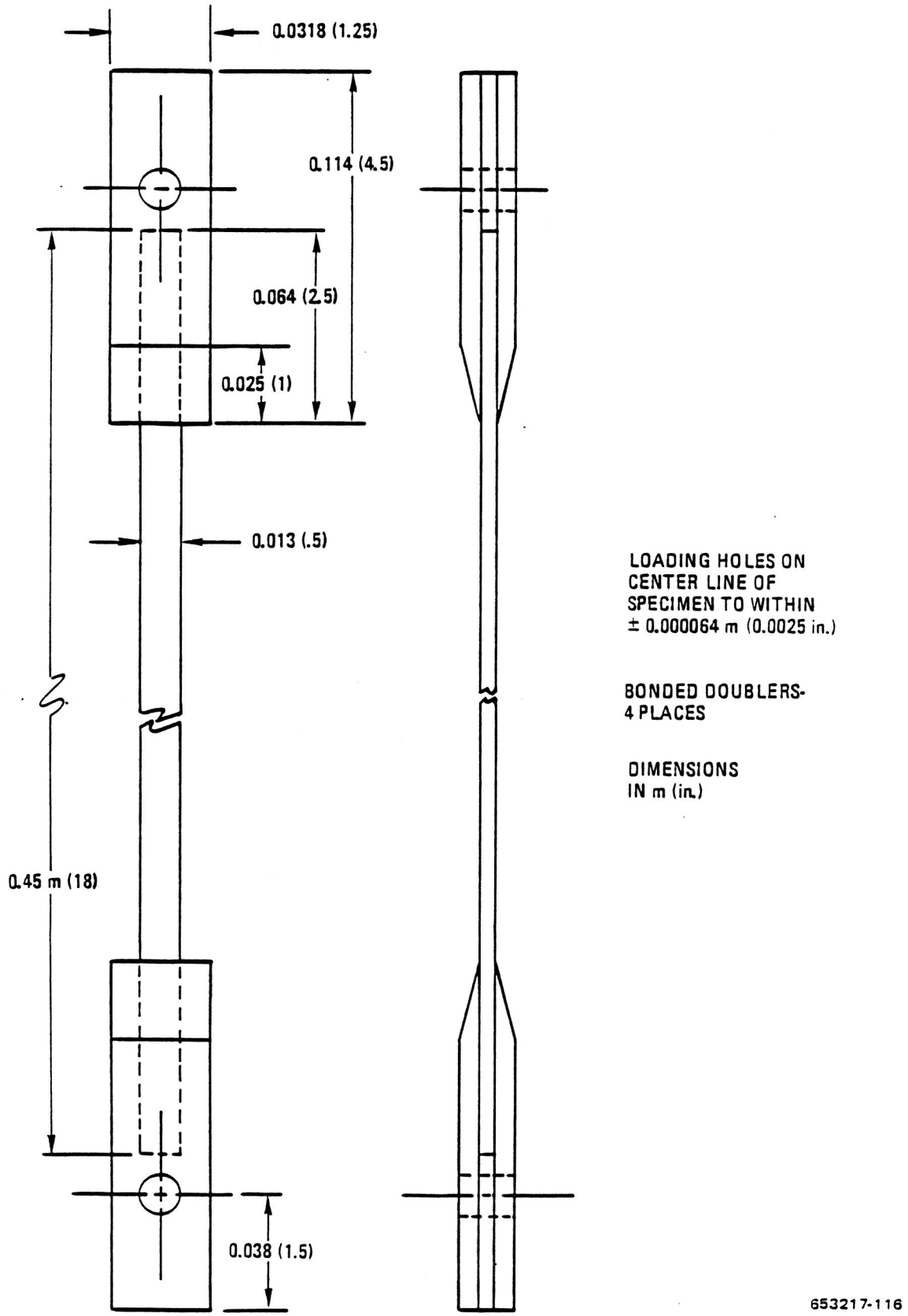



**Figure 10-1 Creep Test Specimen**

method employing a platinum sliding-strip extensometer mechanically attached to the specimen. The optical equipment consisted of a Gaertner filar micrometer 50X magnification microscope mounted on the furnace and sighted through the central viewing port. Illumination of the platinum extensometer was provided by a lamp system within the microscope.

A creep machine and furnace with a specimen in test is shown in Figure 10-2. A closeup view of the Gaertner microscope in place on the furnace can be seen in Figure 10-3. Figure 10-4 shows the platinum sliding-strip extensometer attached to a composite specimen prior to loading into the creep testing apparatus. Also visible are the chromel-alumel thermocouples.

Prior to testing, the resin matrix composite specimens were dried at 394 K (250° F) for 24 hours. The specimen dimensions were measured, and the creep machine loads were calculated for the particular stress level desired. Fiducial marks were lightly penciled at 0.0508 m (2 in.) intervals in the region where the platinum extensometer was to be attached in order to determine the total strain by before and after measurements with a cathotometer. These measurements were later discontinued when the scatter in the readings was found to be of the same magnitude as the total strains obtained during creep testing. The platinum extensometer was attached, and the three thermocouples were taped to the specimen, above, below, and opposite the extensometer. The specimen, which was connected to the upper and lower pullrods, was then carefully loaded through the preheated furnace and attached to the loading arms of the creep machine. A small load, 0.45 kg (1 lb), was applied while the temperature was stabilized, and the microscope was focused and positioned on the platinum extensometer. The full load was then gradually applied, and strain measurements were begun immediately. The elapsed time between the initial small load application and the full load application was approximately 0.25 hour. The difference in measurements between zero and full load is due to elastic strain. These values are shown on the individual creep curves but are not reported in the total strain values presented in the tables. Optical measurements were continued for either 100 hours or for 1000 hours or until specimen failure. At the conclusion of the tests for those specimens that did not fail, the load, except for 0.45 kg (1 lb), was removed, and a final strain measurement was recorded. The final measurement was generally not made at exactly 100 or 1000 hours because of a one shift operation in the testing laboratory. Consequently, the creep curves are plotted out to the times of the last measurement. The values listed in the data tables for total creep strain, however, have been, when possible, taken from the creep versus time curves at either 100 or 1000 hours.

## 10.3 TEST RESULTS AND DISCUSSION

The creep testing program, which is summarized in Table 10-1, consisted of 100- and 1000-hour tests at two temperatures and two layups for each of the four material systems. The data are presented in tabular form and as creep strain versus time curves. The elastic strain values obtained during loading are shown on the individual creep curves but are not reported in the total creep strain values presented in the tables. Also shown on the creep curves are the strain values after unloading at the conclusion of a test in which failure did not occur. The difference between the initial full load strain and the final unloaded strain should be equal to the permanent plastic creep strain. However, as a result of the very small creep strains obtained in these tests the agreement was generally poor. Only for the $[0° \pm 45°]_s$ crossplied B/Al and B/E was the agreement reasonably close. Again, these values were not reported in the tabular data but can be obtained from the creep curves.

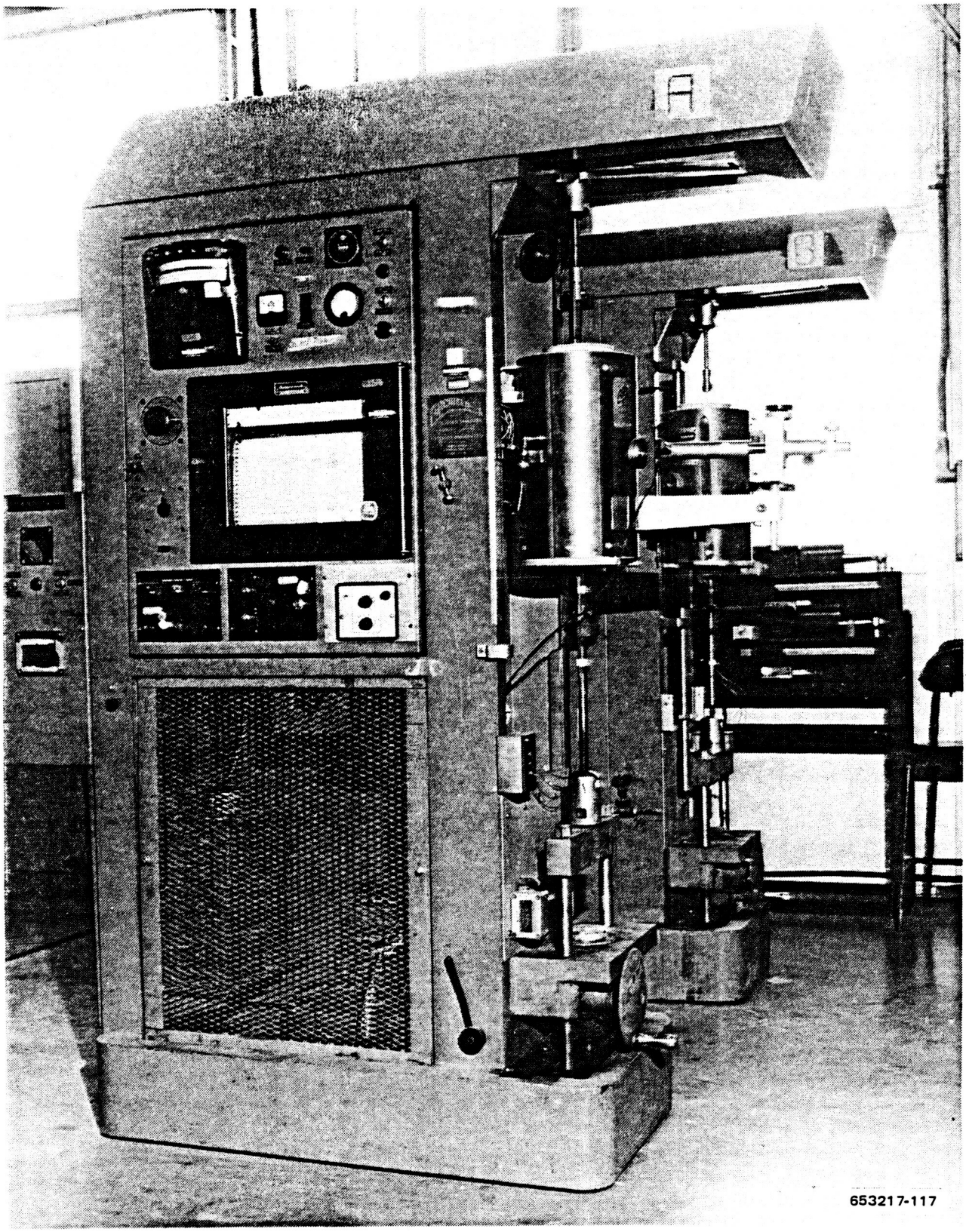



**Figure 10-2 Creep Testing Apparatus**



ORIGINAL PAGE IS
OF POOR QUALITY

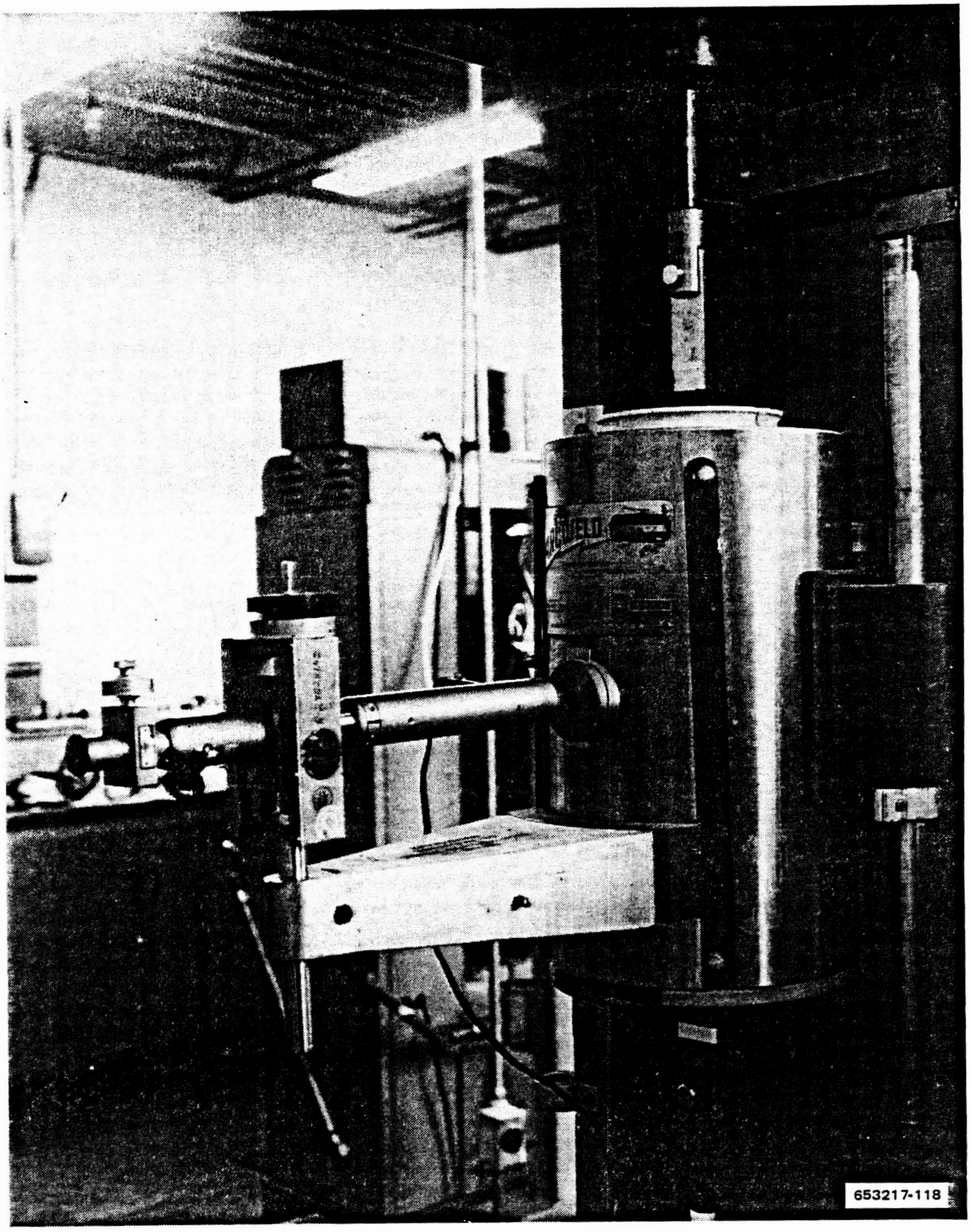



**Figure 10-3 Furnace Mounted Filar Micrometer Microscope for Creep Measurements**



ORIGINAL PAGE IS
OF POOR QUALITY

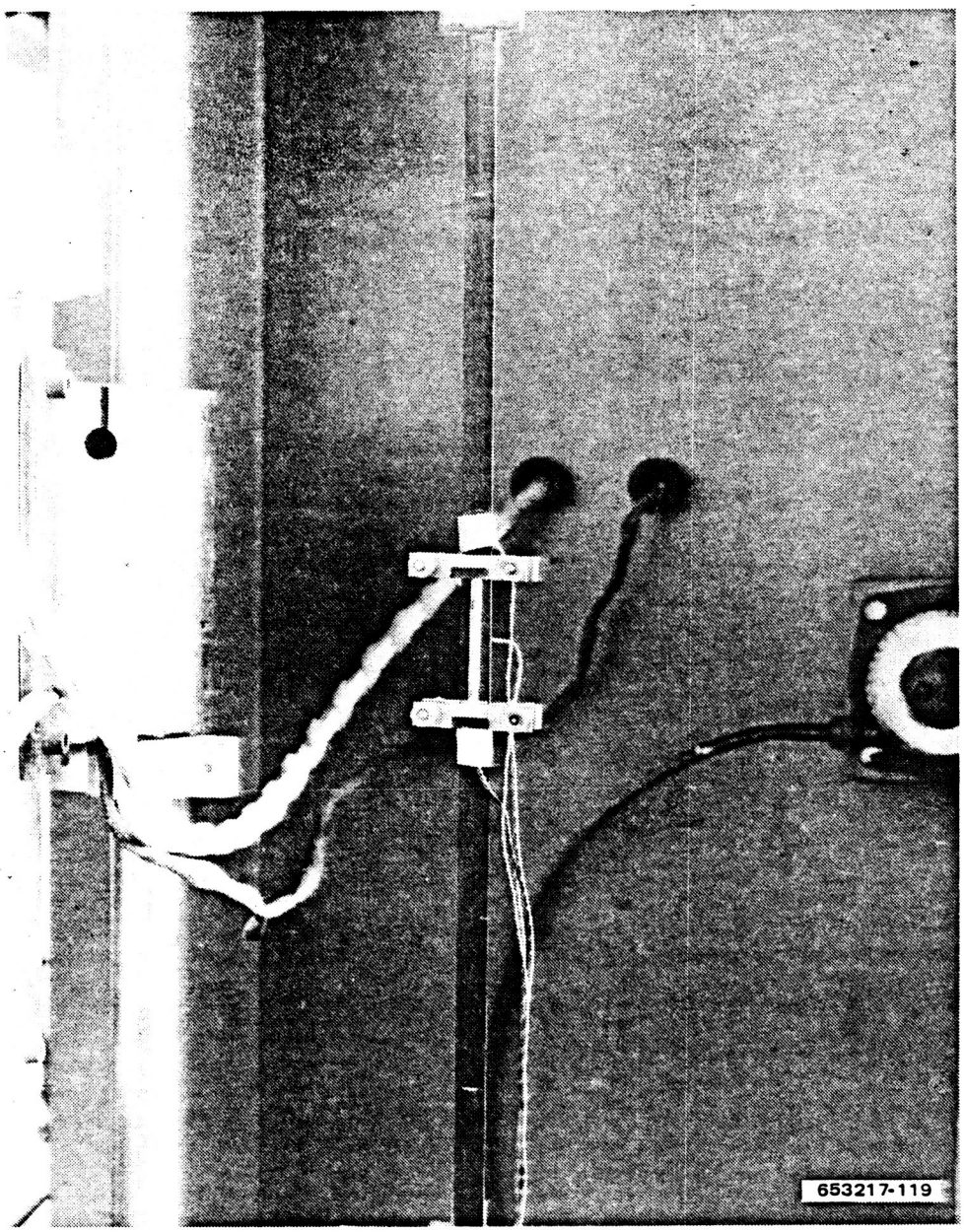



**Figure 10-4 Creep Specimen with Platinum Sliding-Strip Extensometer and Thermocouples Attached**

The specimens that failed during load application and for which no curves could be drawn are identified in the tables. Also noted in both the tables and on the curves are the specimens that failed during testing or that experienced doubler bond failures during testing.

**10.3.1 BORON/EPOXY.** Results of creep testing of B/E at 394 K (250° F) and 450 K (350° F) are listed in Table 10-2. Data are presented for 18 specimens.

Creep strain versus time curves are presented in Figures 10-5 and 10-6 for crossplied material at 394 K (250° F), in Figures 10-7 through 10-9 for unidirectional material at 450 K (350° F), and in Figures 10-10 and 10-11 for crossplied material at 450 K (350° F).



ORIGINAL PAGE IS
OF POOR QUALITY

Table 10-2. Summary of Creep Test Results for B/E

| Specimen Number | Orientation | Test Temperature K | (°F) | Stress MN/m$^2$ | (ksi) | Total Creep Time (hr) | Creep Strain (%) | Comments |
|---|---|---|---|---|---|---|---|---|
| AC5-11 | $[0° \pm 45°]_s$ | 394 | 250 | 310 | 45 | 1000 | 0.08 | |
| -9 | | | | 345 | 50 | 100 | .08 | |
| -7 | | | | 379 | 55 | 1000 | .22 | |
| -8 | | | | 414 | 60 | 1000 | .13 | |
| -10 | | | | 448 | 65 | [a]8 | [a].03 | Failed in 9 hours |
| AU5-1 | $[0°]_6$ | 450 | 350 | 896 | 130 | 100 | .07 | |
| -4 | | | | 931 | 135 | 552 | .17 | |
| -2 | | | | 965 | 140 | 100 | .11 | |
| -5 | | | | 1000 | 145 | 1000 | .27 | |
| -6 | | | | 1020 | 147.5 | [a]93 | [a].23 | Failed in 97 hours |
| -3 | | | | 1030 | 150 | [a]1.8 | [a].15 | Failed in 2.2 hours |
| AC5-13 | $[0° \pm 45°]_s$ | 450 | 350 | 345 | 50 | 1000 | .18 | |
| -6 | | | | 379 | 55 | [a]4.5 | [a].08 | Failed in 14 hours |
| -5 | | | | 396 | 57.5 | [a]5 | [a].08 | Failed in 18 hours |
| -1 | | | | 414 | 60 | 100 | .19 | |
| -3 | | | | 431 | 62.5 | — | — | Failed in 0.03 hour |
| -4 | | | | 431 | 62.5 | — | — | Failed on loading |
| -2 | | | | 448 | 65 | — | — | Failed in 0.17 hour |

[a]Last measurement prior to failure

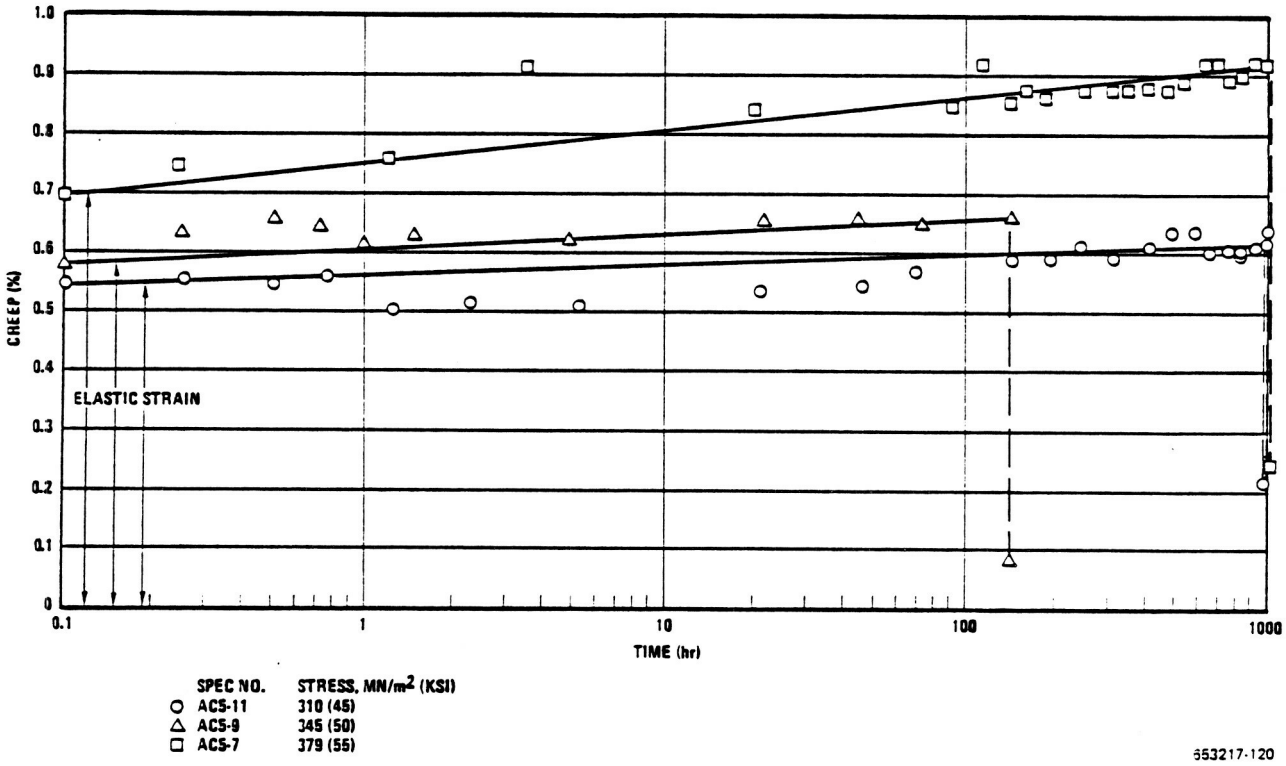



**Figure 10-5 Creep Strain for $[0° \pm 45°]_s$ B/E at 394 K (250° F)**

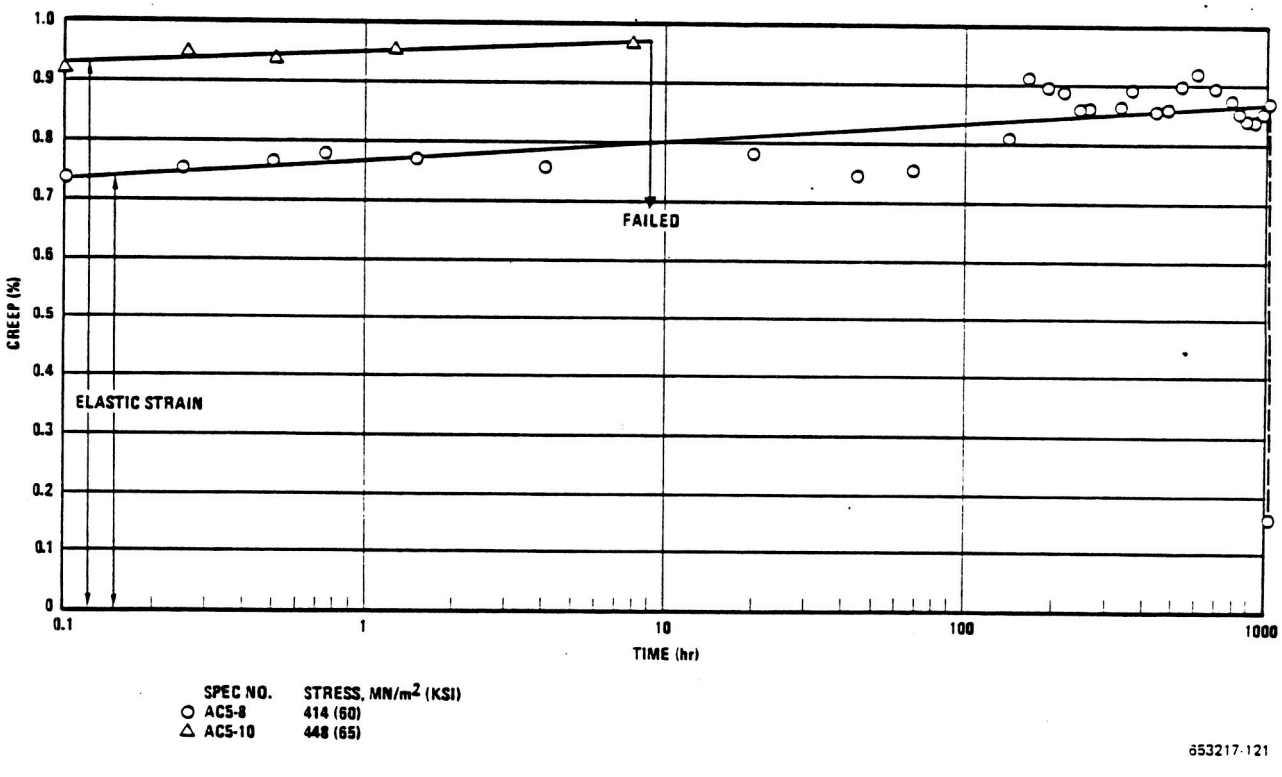



**Figure 10-6 Creep Strain for $[0° \pm 45°]_s$ B/E at 394 K (250° F)**

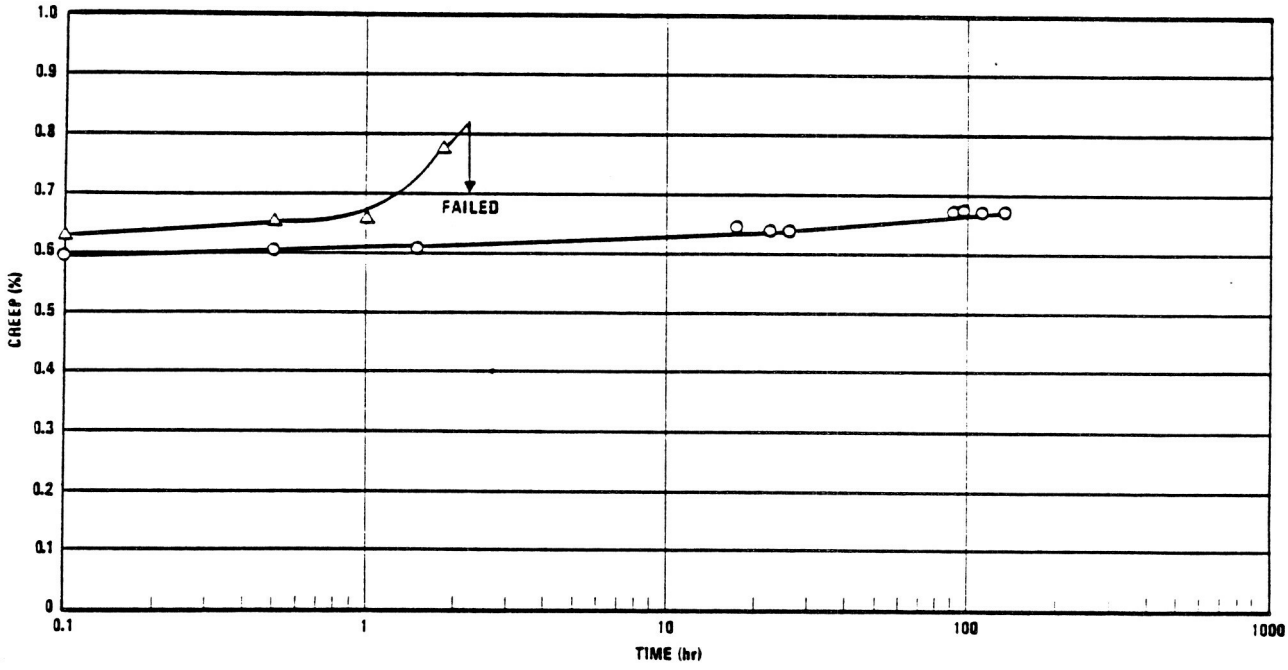



**Figure 10-7 Creep Strain for $[0°]_6$ B/E at 450 K (350° F)**

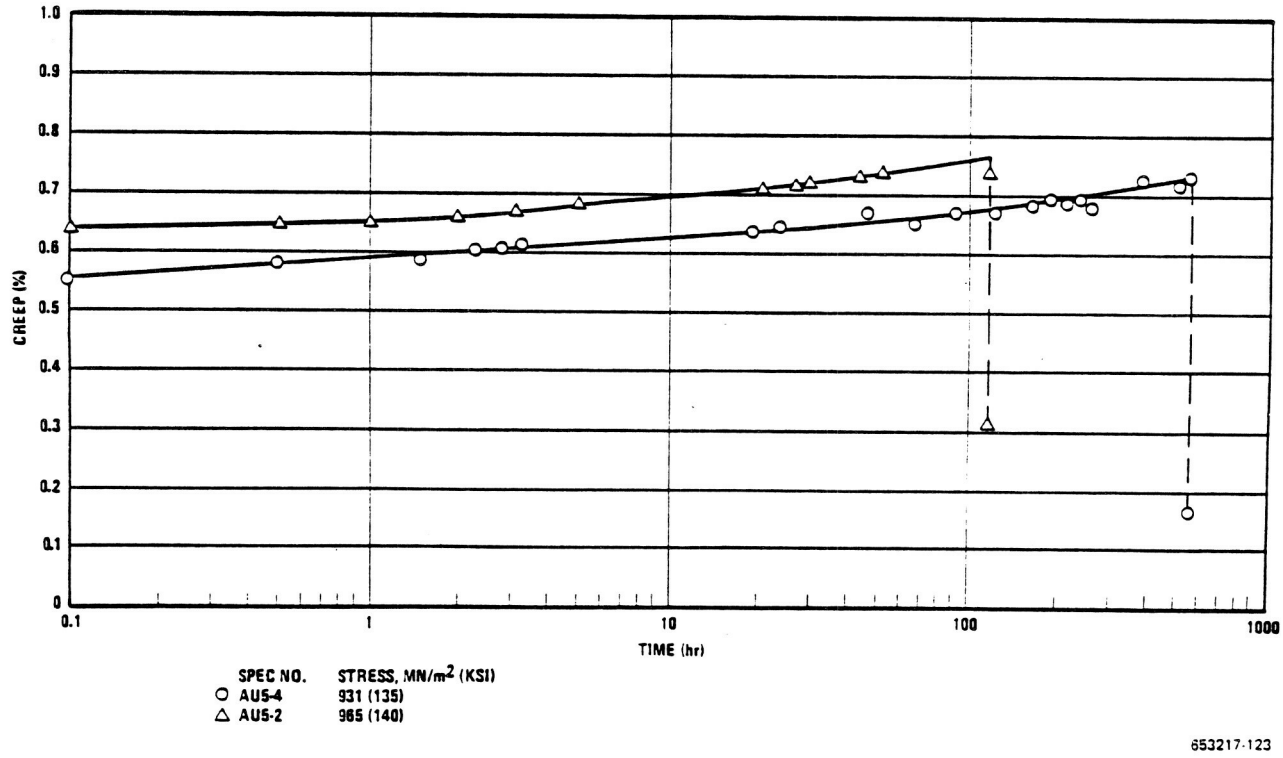



**Figure 10-8 Creep Strain for $[0°]_6$ B/E at 450 K (350° F)**

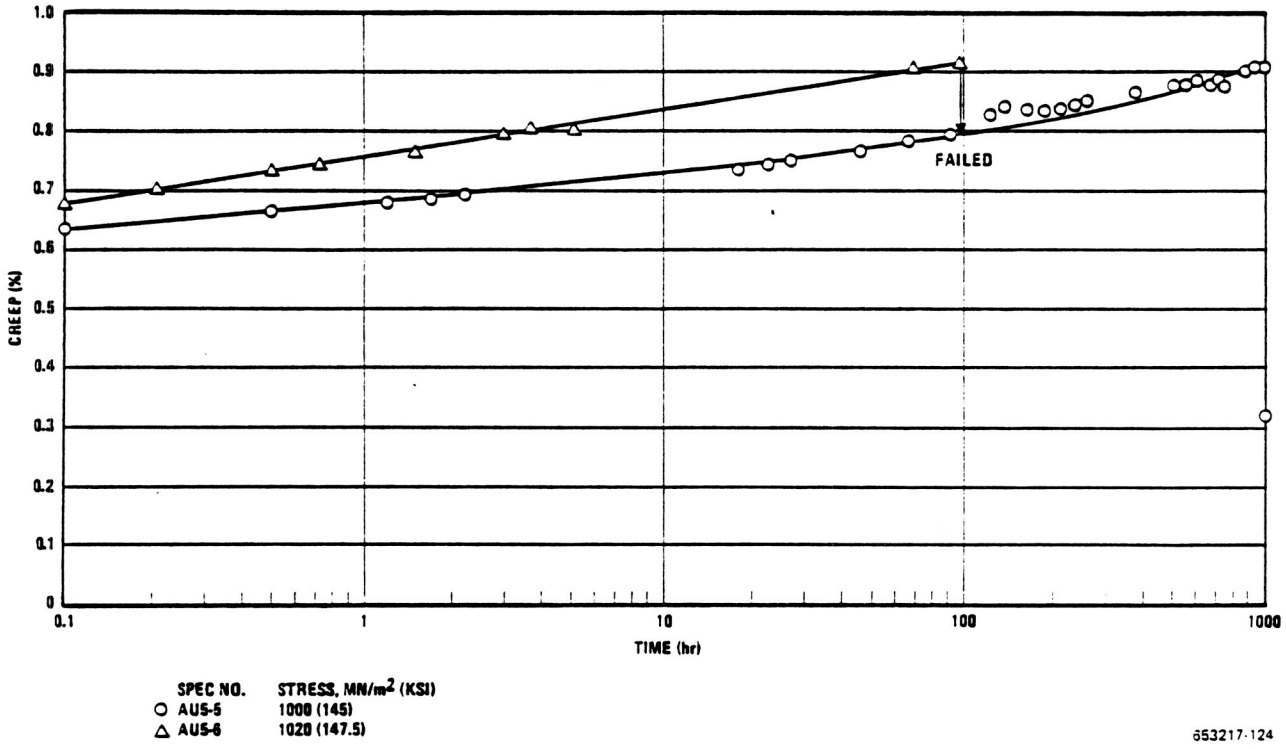



**Figure 10-9 Creep Strain for $[0°]_6$ B/E at 450 K (350° F)**

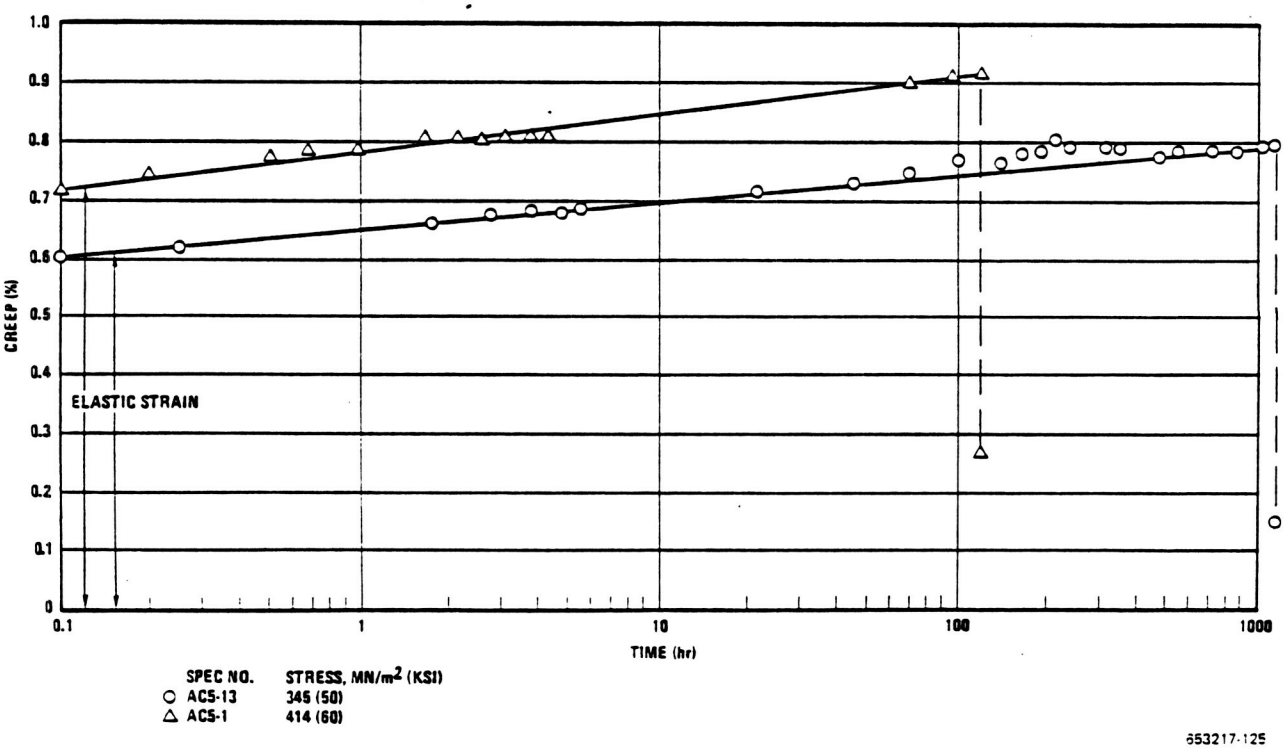



**Figure 10-10 Creep Strain for $[0° \pm 45°]_s$ B/E at 450 K (350° F)**

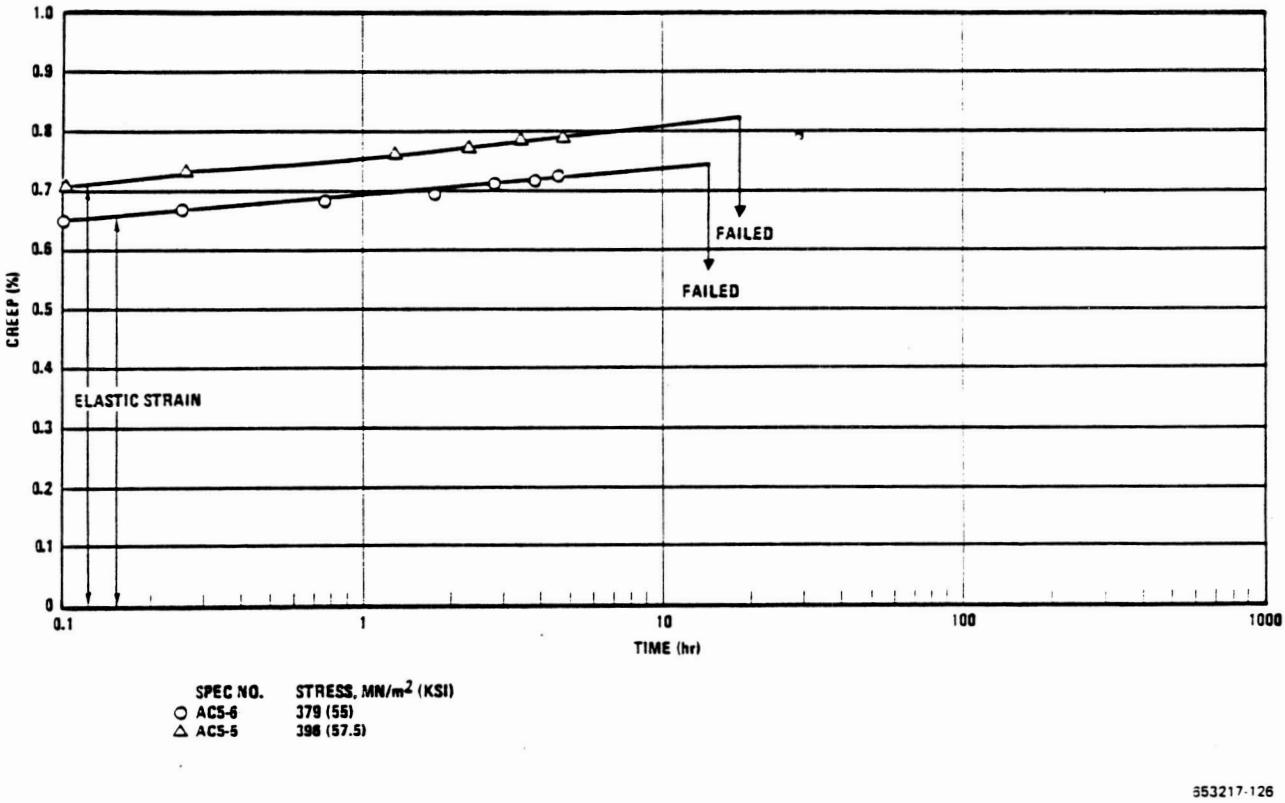



**Figure 10-11 Creep Strain for $[0° \pm 45°]_s$ B/E at 450 K (350° F)**

The data show that the amount of creep obtained in B/E material with boron filaments aligned in the loading direction is very small. No specimen gave values of more than a few tenths of a percent of permanent creep strain. For example, specimen AC5-8 (crossplied) exhibited only 0.13% creep in 1000 hours at 394 K (250 ° F) when loaded at 79% of the average ultimate tensile strength, and specimen AU5-5 (unidirectional) exhibited only 0.27% creep in 1000 hours at 450 K (350 ° F) when loaded at 88% of the average ultimate tensile strength. Specimens that failed prior to completing 100 hours of exposure also underwent very little creep as indicated by measurements just before fracture. See, for example, Figures 10-6 and 10-9. One specimen, AU5-3, Figure 10-7, did show a sharp rise in the creep curve before failure, but the total creep strain was still less than 0.2%. Before-after measurements were not successful in determining the total creep strain of failed specimens. For specimens that fractured in the gage section the combination of low creep strain and the difficulty of accurate fit-back of the failed specimen halves made the measurements unreliable.

In analyzing the creep data an effort was made to prepare composite creep curves for 0.05, 0.10, 0.15, 0.20, and 0.25% creep by determining the time periods required for varying amounts of creep strain as a function of stress level. The limited amount of creep data available, the small amount of creep strain measured, and the scatter in the data combined to give results that were unsuitable for the plotting of this type of creep curve. This was found to apply to all the other composite systems as well as the B/E.

**10.3.2 GRAPHITE/EPOXY.** Results of creep testing of G/E at 394 K (250 ° F) and 450 K (350 ° F) are listed in Table 10-3. Data are presented for 24 specimens.

Table 10-3. Summary of Creep Test Results for G/E

| Specimen Number | Orientation | Test Temperature K | (°F) | Stress MN/m² | (ksi) | Total Creep Time (hr) | Creep Strain (%) | Comments |
|---|---|---|---|---|---|---|---|---|
| BU5-4 | $[0°]_6$ | 394 | 250 | 896 | 130 | 100 | 0.01 | |
| -14 | | | | 931 | 135 | 1000 | .01 | |
| -3 | | | | 965 | 140 | 100 | .02 | |
| -6 | | | | 1000 | 145 | 100 | .01 | |
| -2 | | | | 1030 | 150 | — | — | Failed on loading |
| -1 | | | | 1100 | 160 | — | — | Failed on loading |
| BC5-7 | $[0° \pm 45°]_s$ | 394 | 250 | 414 | 60 | 100 | .04 | |
| -13 | | | | 448 | 65 | 1000 | .02 | |
| -8 | | | | 448 | 65 | 100 | .07 | |
| -11 | | | | 465 | 67.5 | 100 | .03 | |
| -9 | | | | 483 | 70 | 100 | .08 | |
| -10 | | | | 500 | 72.5 | 570 | .17 | |
| -12 | | | | 517 | 75 | — | — | Failed on loading |
| BU5-12 | $[0°]_6$ | 450 | 350 | 896 | 130 | 1000 | .01 | |
| -7 | | | | 965 | 140 | 100 | .01 | |
| -10 | | | | 1000 | 145 | [a]1.6 | [a].02 | Bond failure in 3 hours |
| -11 | | | | 1000 | 145 | — | — | Failed on loading |
| -9 | | | | 1030 | 150 | 1000 | .02 | |
| -13 | | | | 1070 | 155 | 100 | .06 | |
| BC5-5 | $[0° \pm 45°]_s$ | 450 | 350 | 396 | 57.5 | — | — | Bond failure on loading |
| -1 | | | | 414 | 60 | 100 | .05 | Bond failure in 170 hours |
| -4 | | | | 431 | 62.5 | 1000 | .15 | |
| -3 | | | | 448 | 65 | — | — | Failed on loading |
| -2 | | | | 448 | 65 | — | — | Bond failure on loading |

[a]Last measurement prior to failure

Creep strain versus time curves are presented in Figures 10-12 through 10-14 for unidirectional material at 394 K (250° F), in Figures 10-15 through 10-18 for crossplied material at 394 K (250° F), in Figures 10-19 and 10-20 for unidirectional material at 450 K (350° F), and in Figure 10-21 for crossplied material at 450 K (350° F).

The G/E data are very similar to those for B/E in that the amount of permanent creep strain was very small for all test conditions. For only two specimens was the creep greater than 0.1% and for these specimens the values were below 0.2%. An example of the small amount of creep observed in the G/E material can be seen for specimen BC5-10 (crossplied). This specimen showed only 0.17% creep in 570 hours when loaded to 500 MN/m$^2$ (72.5 ksi) or 95% of the average ultimate tensile strength. A similar specimen, when tested at 517 MN/m$^2$ (75 ksi), failed during application of the load in the test machine. Two of the crossplied specimens failed in this manner (during loading) but at stresses that were within the scatter band found during baseline testing at the same temperatures. Three of the unidirectional specimens also failed during loading. These failures, however, occurred at stresses well below the scatter band obtained in the baseline test program. Differences in material strengths were not the cause of the premature failures because both the baseline and the creep specimens were all cut from the same panel, LRC-10A. Of the three specimens that failed on loading, one failed at the center, the second failed in two locations — at the center and approximately 0.04 m (1.5 in.) from the top doubler, and the third, also failing at two locations, at the edge of each doubler. It may have been the rapid application of load that led to the early failure of these specimens. The loads were added in incremental steps of 181 kg (400 lb) to reach a value of slightly more than 907 kg (2000 lb).

**10.3.3 GRAPHITE/POLYIMIDE.** Results of creep testing HT-S/710 G/PI at 505 K (450° F) and 561 K (550° F) are listed in Table 10-4. Data are presented for 24 specimens.

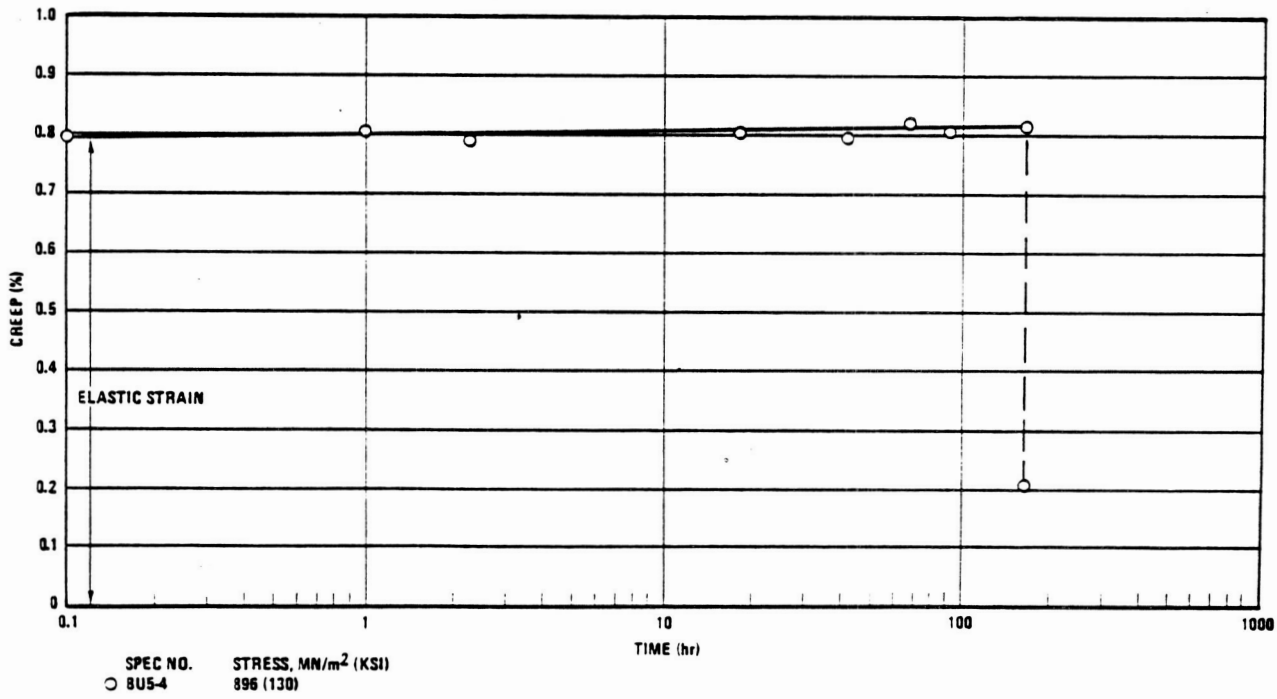



**Figure 10-12 Creep Strain for $[0°]_6$ G/E at 394 K (250° F)**

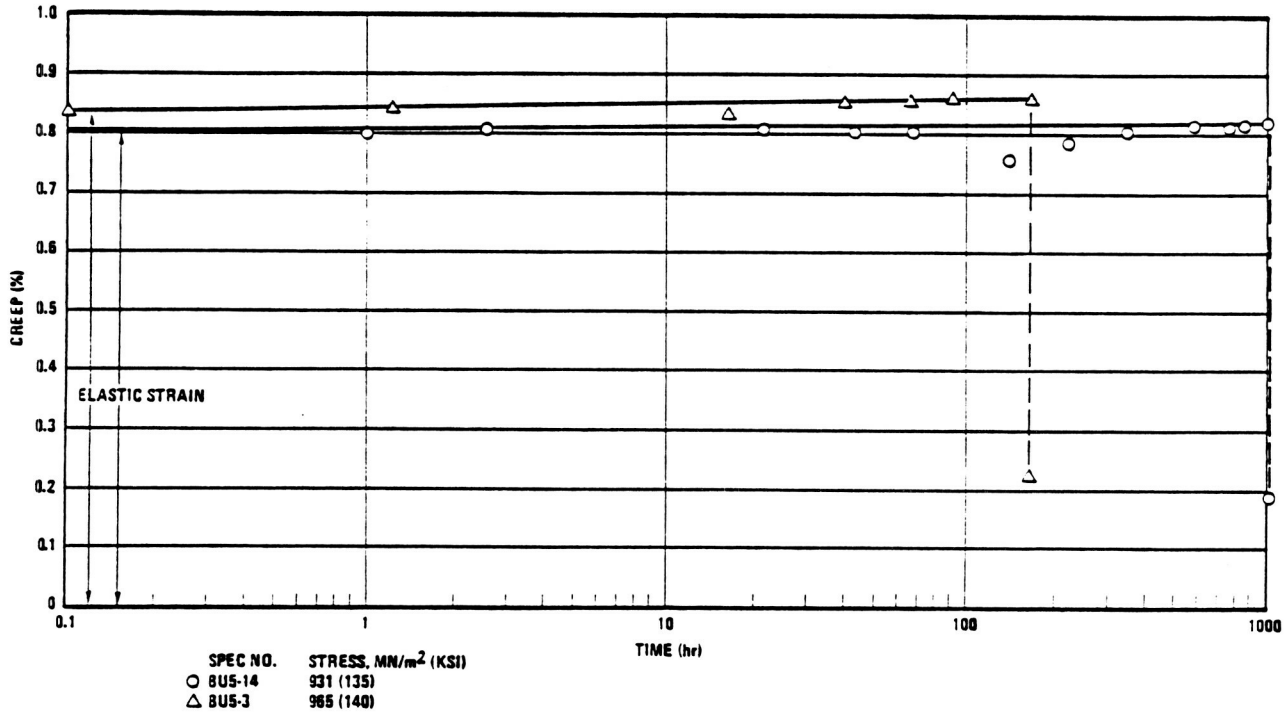
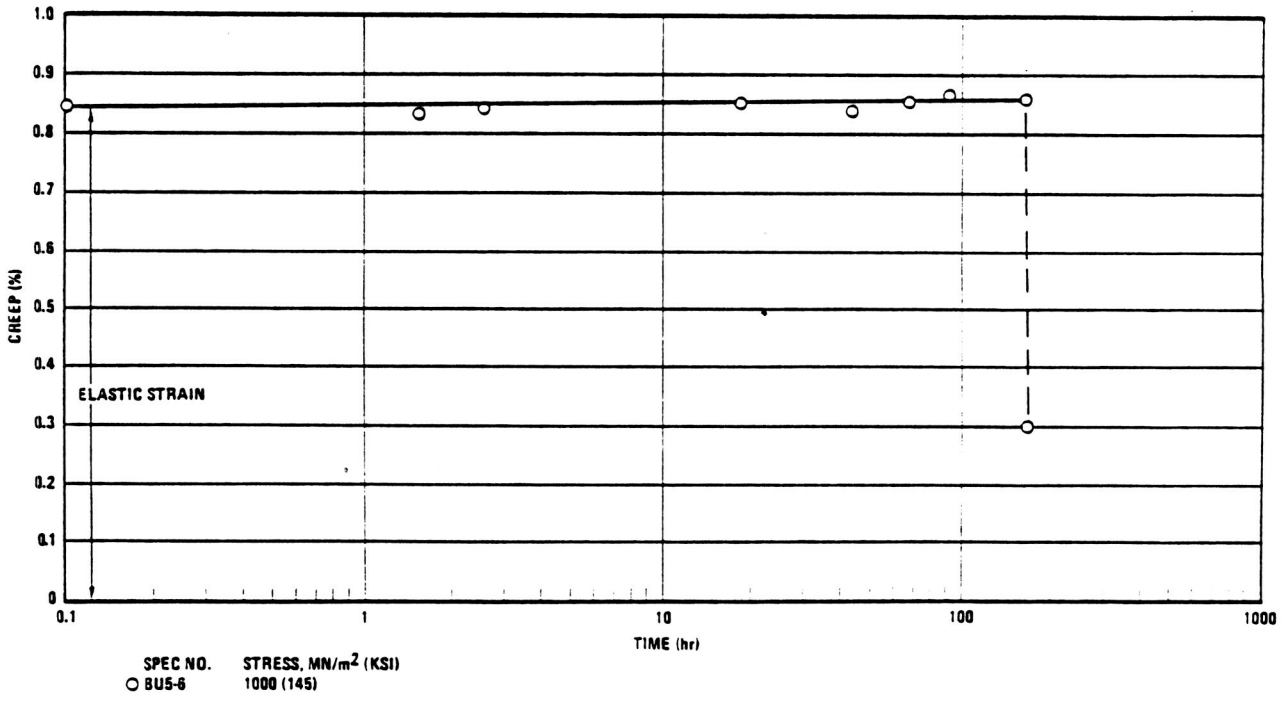



**Figure 10-13 Creep Strain for $[0°]_6$ G/E at 394 K (250° F)**




653217 129

**Figure 10-14 Creep Strain for $[0°]_6$ G/E at 394 K (250° F)**

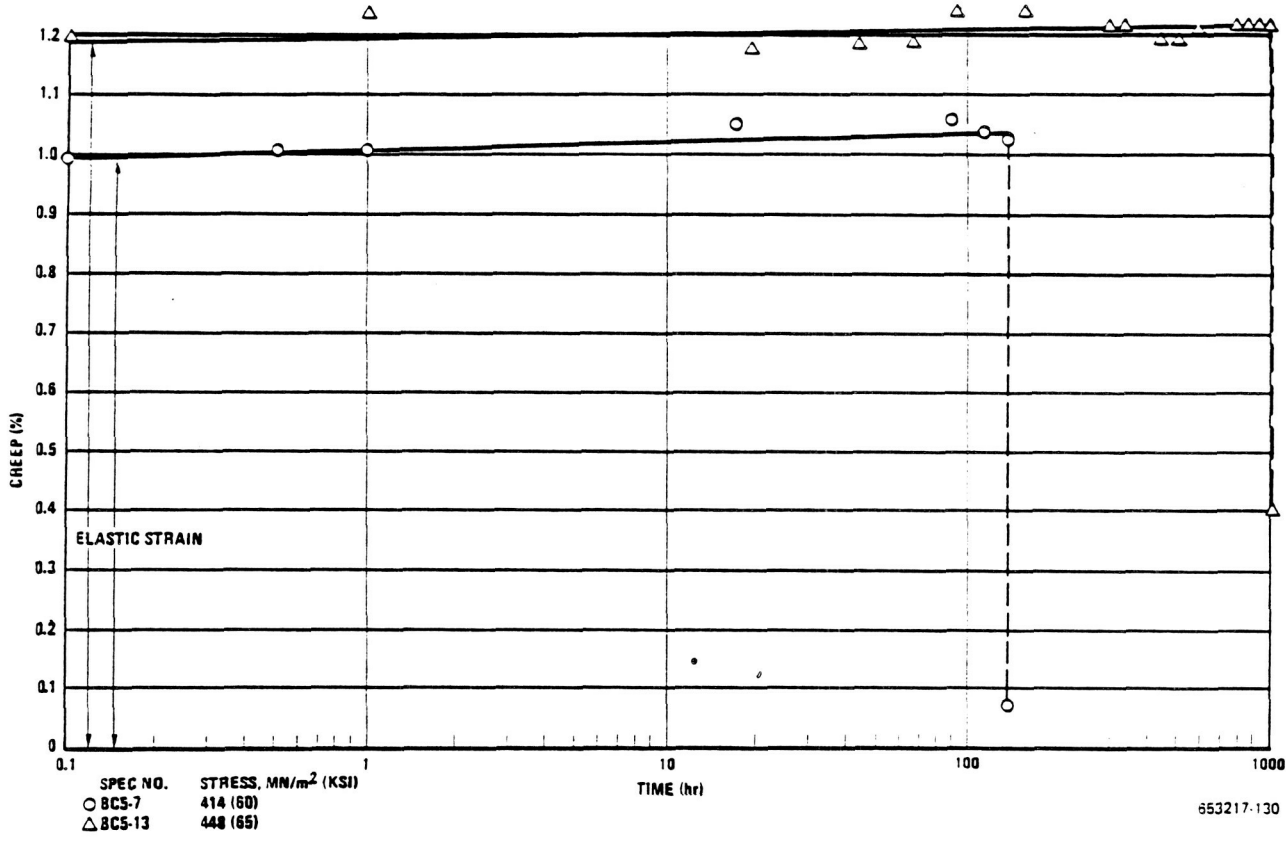



Figure 10-15 Creep Strain for $[0° \pm 45°]_s$ G/E at 394 K (250° F)

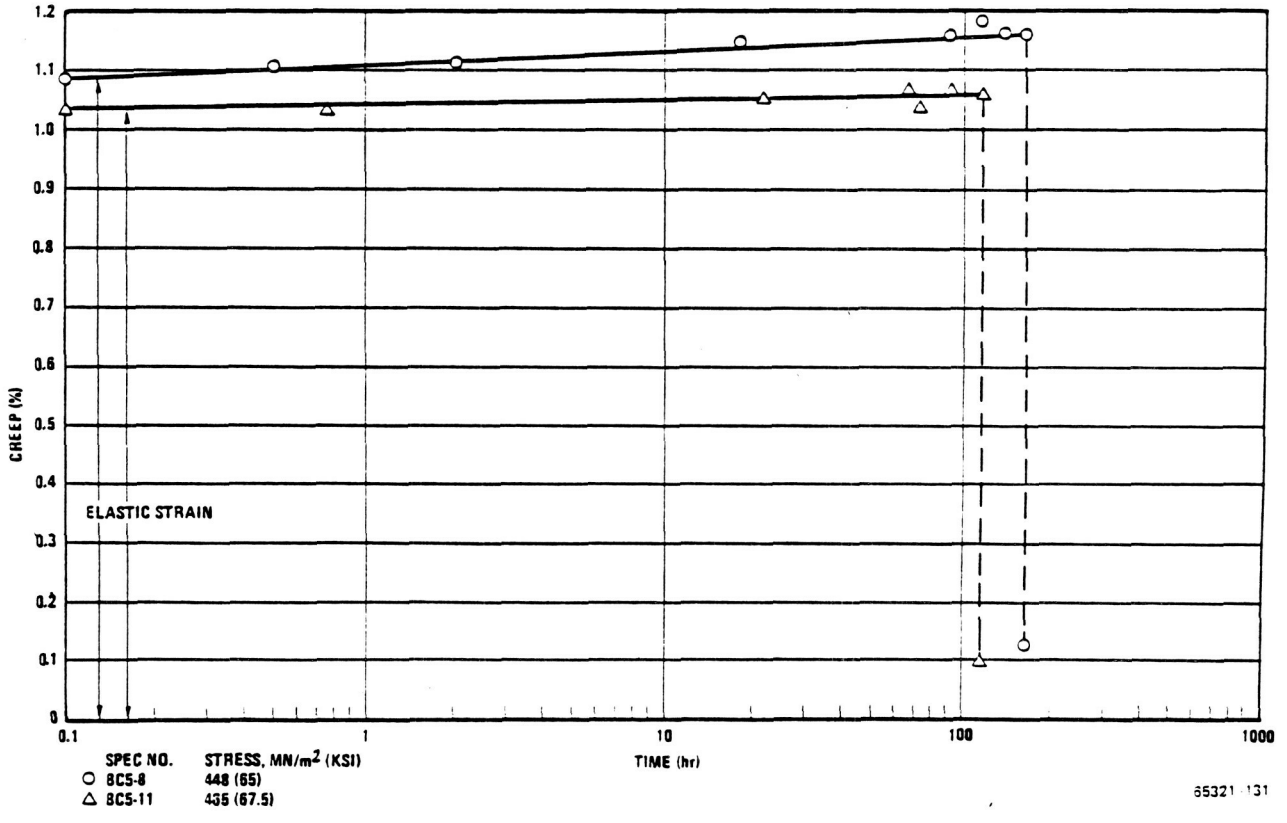



Figure 10-16 Creep Strain for $[0° \pm 45°]_s$ G/E at 394 K (250° F)

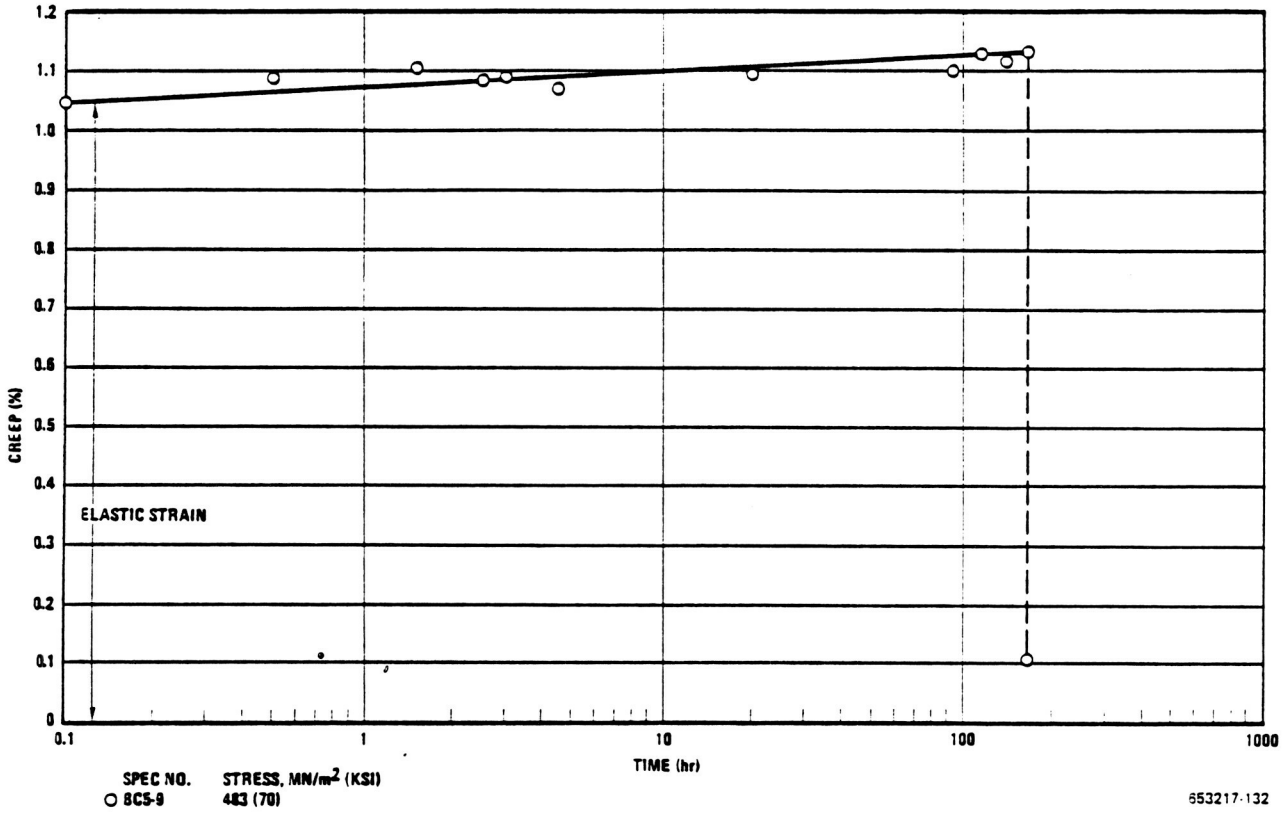



**Figure 10-17 Creep Strain for $[0° \pm 45°]_s$ G/E at 394 K (250° F)**

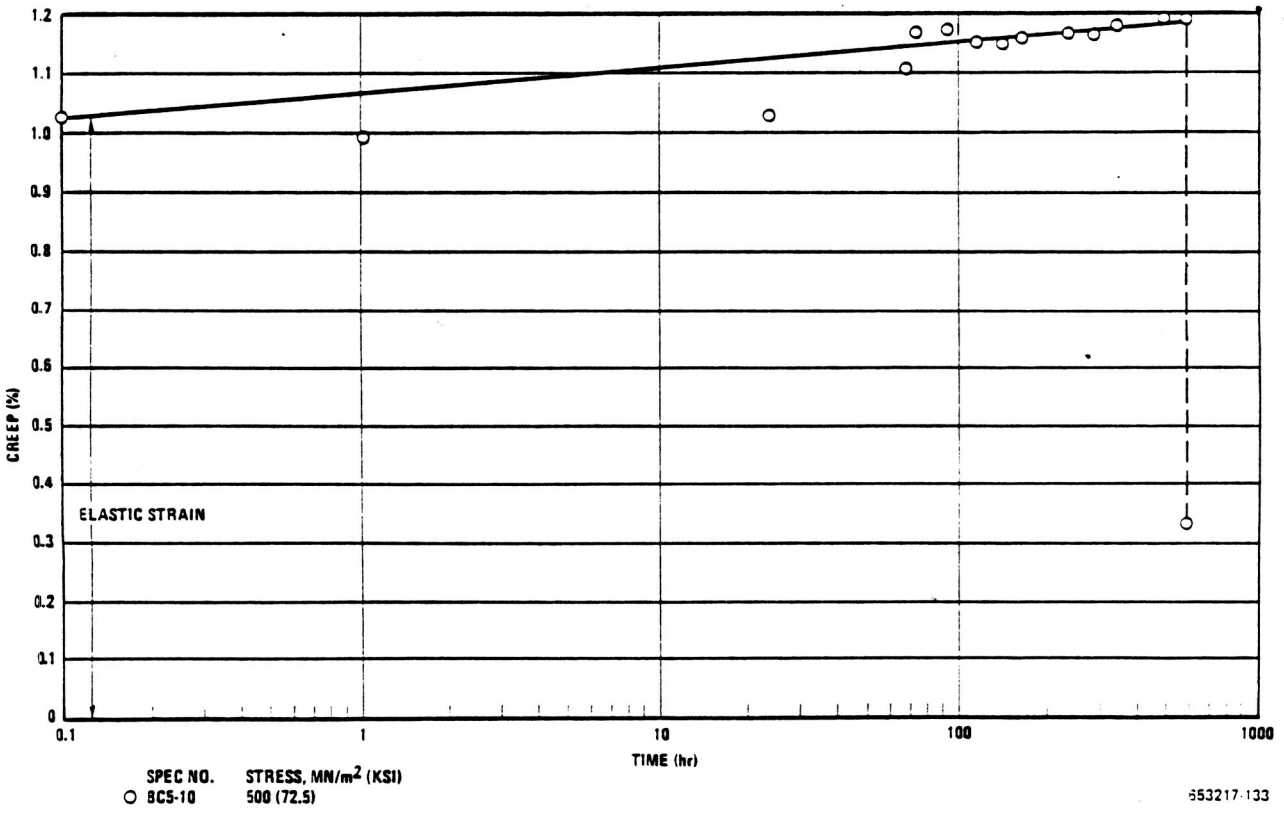



**Figure 10-18 Creep Strain for $[0° \pm 45°]_s$ G/E at 394 K (250° F)**

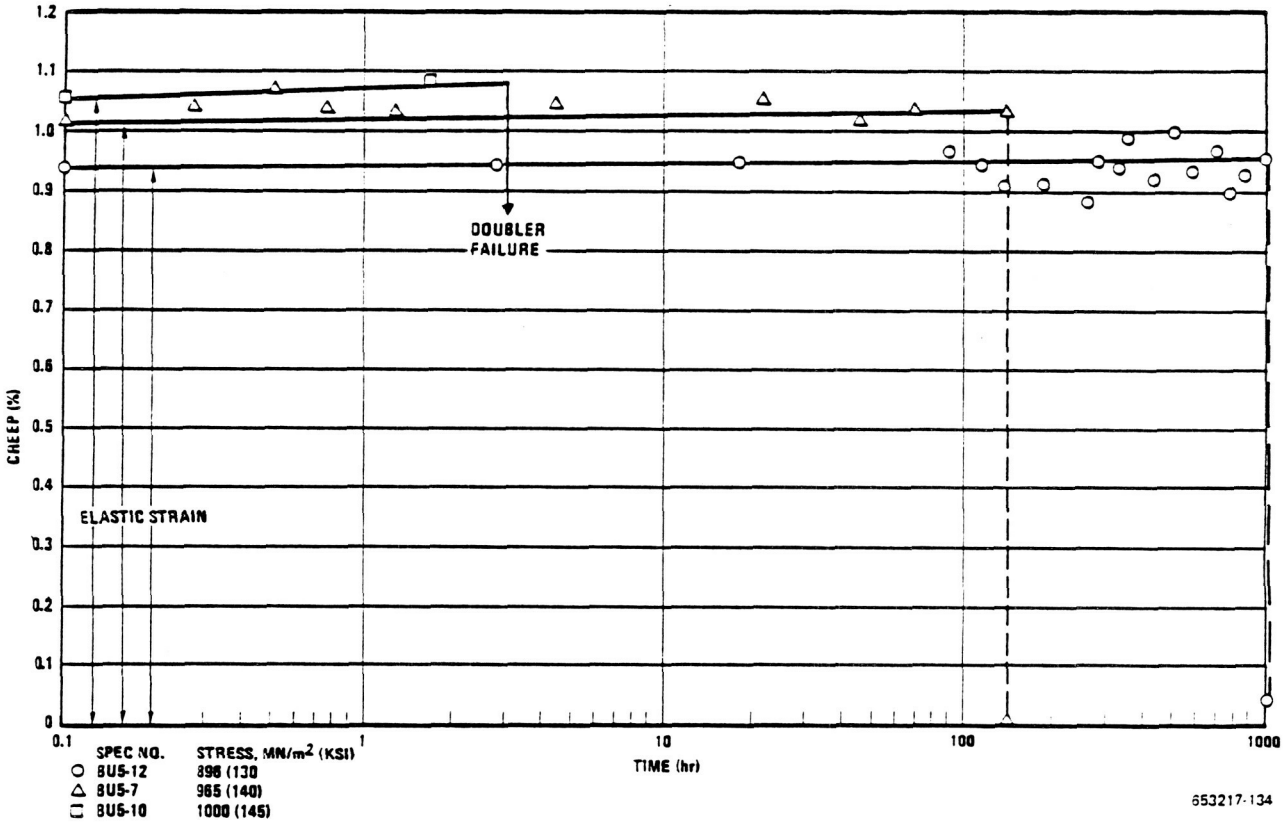



**Figure 10-19 Creep Strain for $[0°]_6$ G/E at 450 K (350° F)**

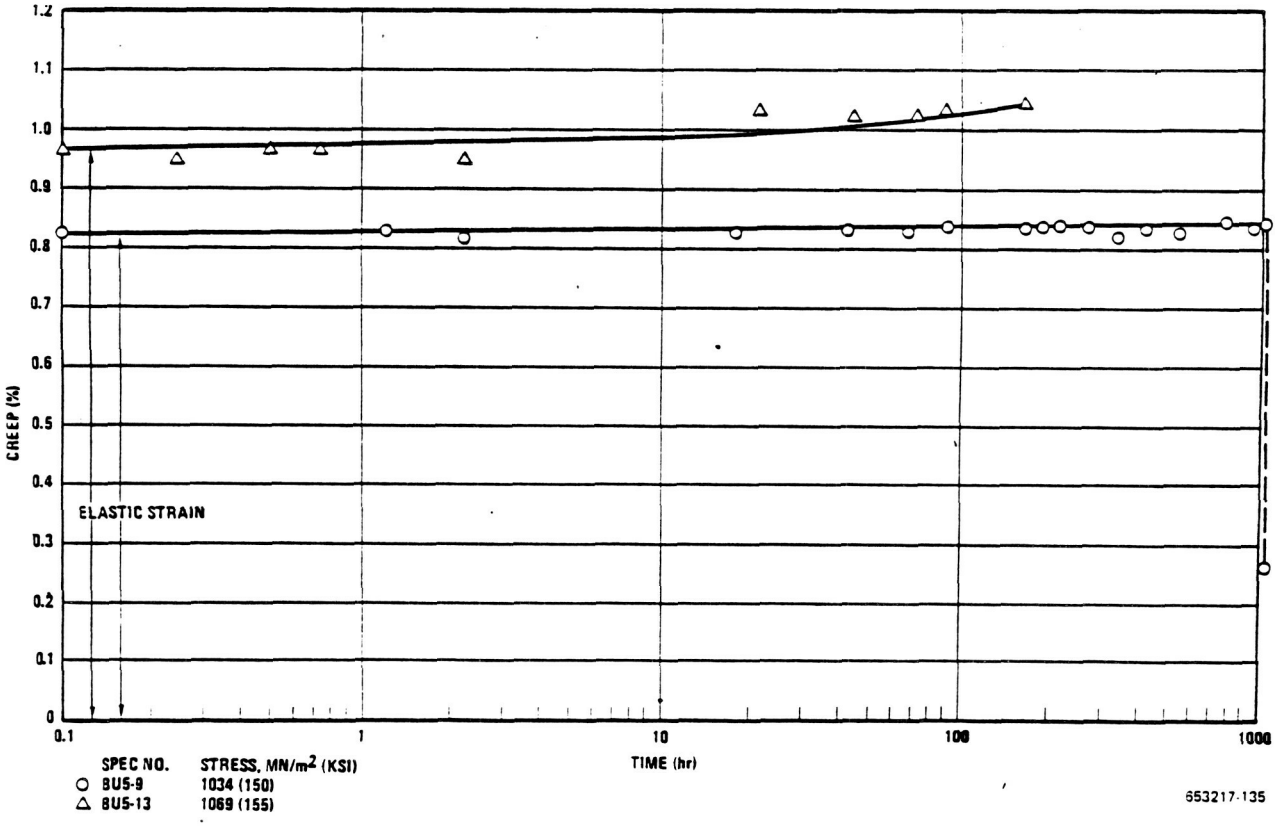



**Figure 10-20 Creep Strain for $[0°]_6$ G/E at 450 K (350° F)**

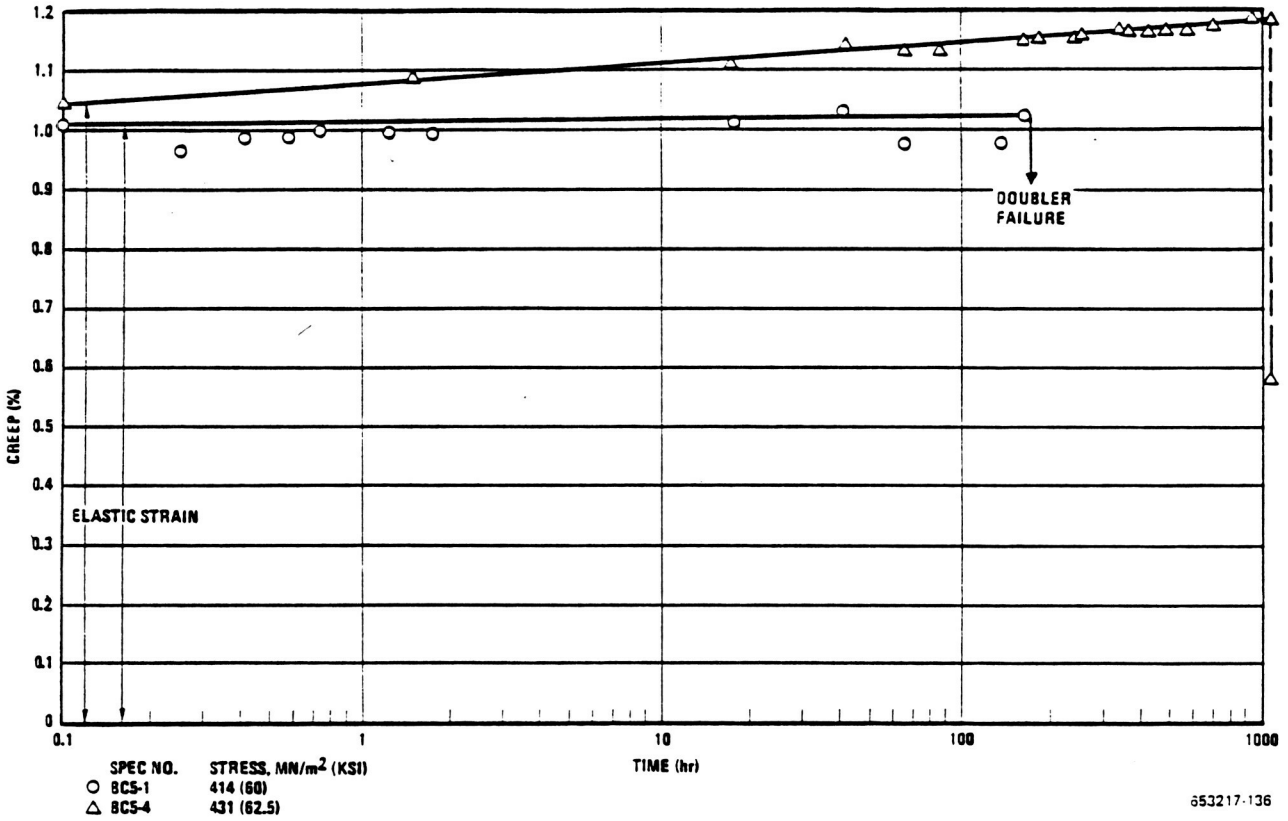



**Figure 10-21 Creep Strain for $[0° \pm 45°]_s$ G/E at 450 K (350° F)**

Creep strain versus time curves are presented in Figure 10-22 for unidirectional material at 550 K (450° F), in Figures 10-23 through 10-27 for crossplied material at 550 K (450° F), in Figures 10-28 and 10-29 for unidirectional material at 561 K (550° F), and in Figure 10-30 for crossplied material at 561 K (550° F).

Creep strain values obtained for the G/PI system at both test temperatures were also very low. For only one specimen, DC5-1 (crossplied), was a value greater than 0.1% recorded. Examples of the small creep extensions that were measured are the 0.03% creep for specimen DU5-1 (unidirectional) in 100 hours at 550 K (450° F) when loaded at 85% of the average ultimate tensile strength and the 0.07% creep for specimen DC5-8 (crossplied) in 100 hours at 561 K (550° F) when loaded at 91% of the average ultimate tensile strength.

The data obtained for the G/PI system were somewhat limited because of several doubler bond failures in the unidirectional specimens. These were caused by the combination of high shear stresses in the adhesive because of the high applied test loads and heating from the furnaces. Several specimens failures also occurred during application of the loads at the beginning of testing. In like manner to the G/E loading failures, the G/PI crossplied specimens failed at stresses within the baseline tensile data scatter band while the unidirectional specimens failed at stresses slightly below the baseline scatter band.

**10.3.4 BORON/ALUMINUM.** Results of creep testing of B/Al at 505 K (450° F) and 561 K (550° F) are listed in Table 10-5. Data are presented for 24 specimens.

Table 10-4. Summary of Creep Test Results for G/PI

| Specimen Number | Orientation | Test Temperature K | (°F) | Stress MN/m² | (ksi) | Total Creep Time (hr) | Creep Strain (%) | Comments |
|---|---|---|---|---|---|---|---|---|
| DU5-5 | $[0°]_6$ | 505 | 450 | 965 | 140 | — | — | Bond failure in 0.15 hr |
| -6 | | | | 965 | 140 | — | — | Bond failure in 0.22 hr |
| -4 | | | | 1000 | 145 | 100 | .02 | |
| -1 | | | | 1030 | 150 | 100 | .03 | |
| -3 | | | | 1070 | 155 | — | — | Failed on loading |
| -2 | | | | 1100 | 160 | — | — | Failed on loading |
| DC5-6 | $[0° \pm 45°]_s$ | 505 | 450 | 259 | 37.5 | 1000 | .08 | |
| -3 | | | | 276 | 40 | 1000 | .06 | |
| -5 | | | | 293 | 42.5 | 1000 | .05 | |
| -2 | | | | 310 | 45 | 1000 | .00 | |
| -4 | | | | 328 | 47.5 | 986 | .10 | |
| -1 | | | | 345 | 50 | [a]428 | [a].18 | Failed in 471 hours |
| DU5-11 | $[0°]_6$ | 561 | 550 | 862 | 125 | [a]46 | [a].00 | Bond failure in 58 hours |
| -8 | | | | 896 | 130 | 100 | .01 | |
| -9 | | | | 931 | 135 | 100 | .00 | |
| -12 | | | | 948 | 137.5 | — | — | Bond failure on loading |
| -7 | | | | 965 | 140 | [a]22 | [a].02 | Bond failure in 33 hours |
| -10 | | | | 1000 | 145 | — | — | Failed on loading |
| DC5-12 | $[0° \pm 45°]_s$ | 561 | 550 | 207 | 30 | 100 | .03 | |
| -11 | | | | 241 | 35 | 100 | .04 | |
| -7 | | | | 276 | 40 | 100 | .04 | |
| -8 | | | | 310 | 45 | 100 | .07 | |
| -10 | | | | 328 | 47.5 | — | — | Failed on loading |
| -9 | | | | 345 | 50 | — | — | Failed on loading |

[a]Last measurement prior to failure

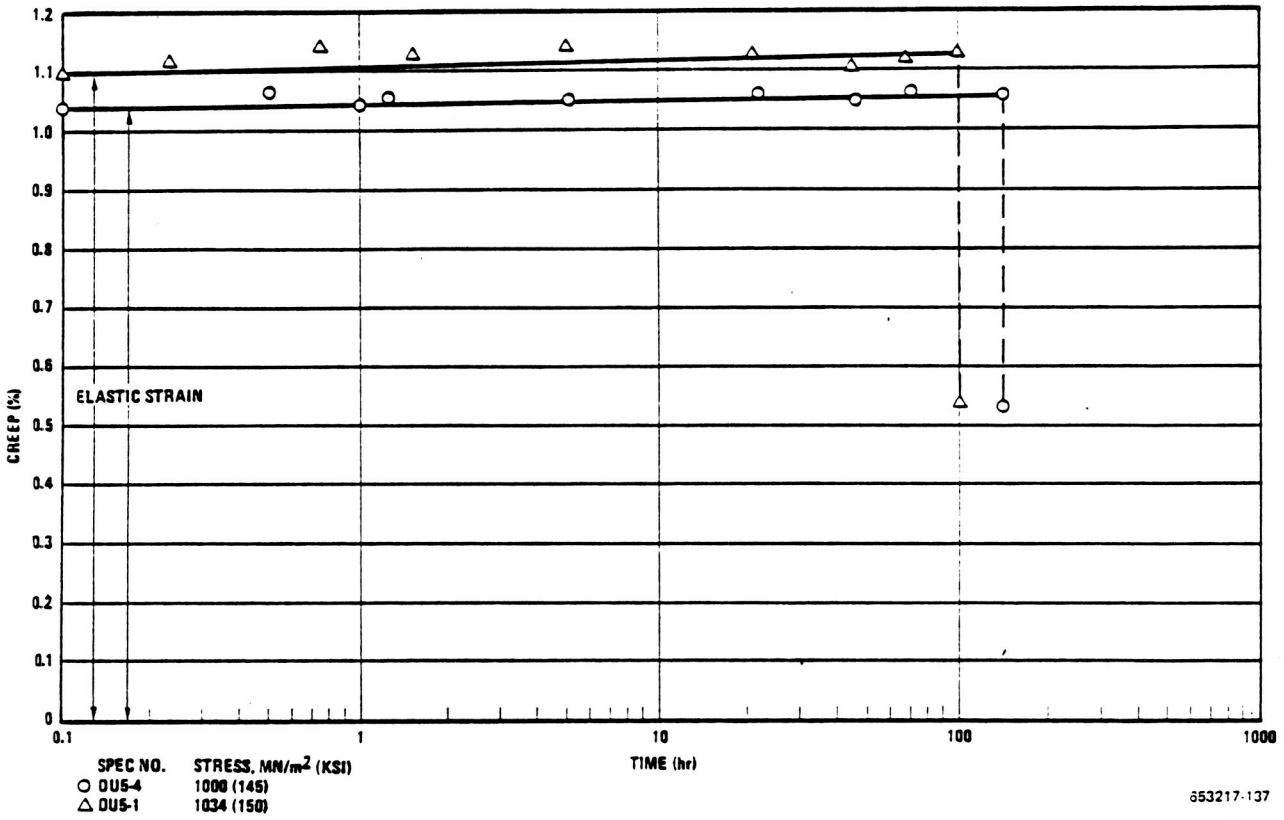



**Figure 10-22 Creep Strain for $[0°]_6$ G/PI at 505 K (450° F)**

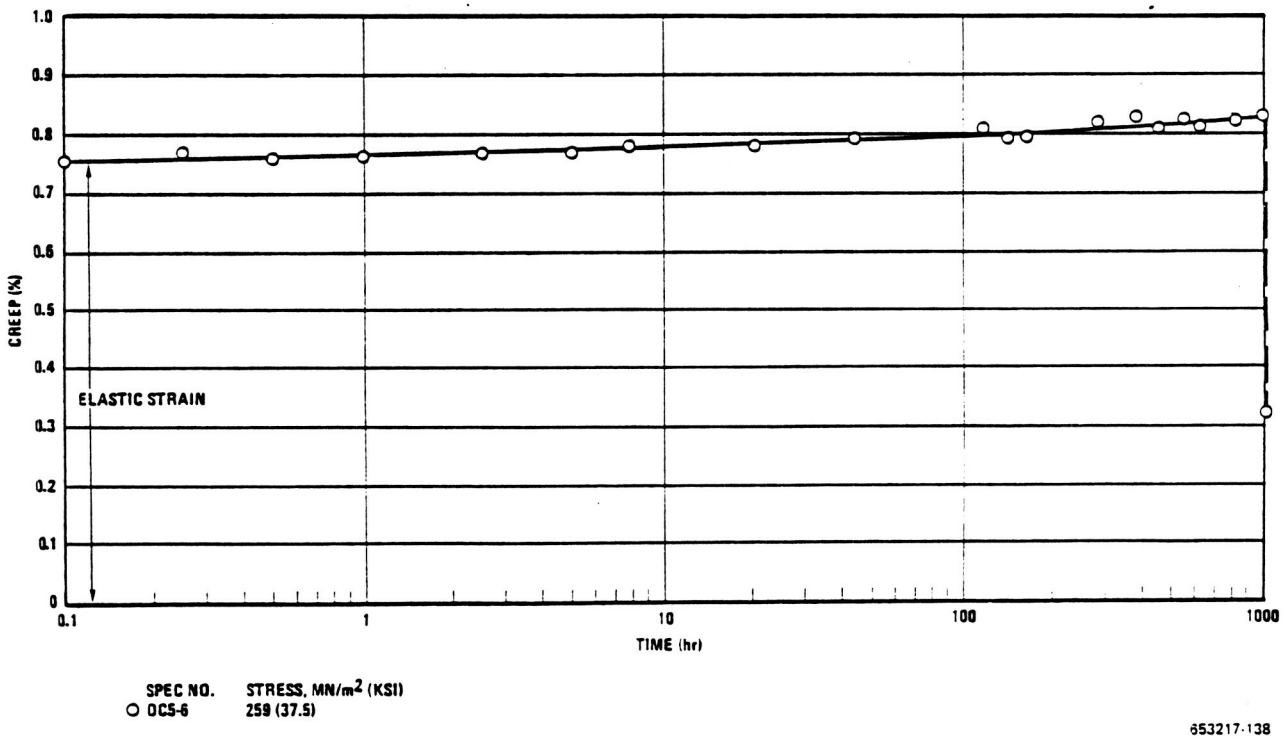



**Figure 10-23 Creep Strain for $[0° \pm 45°]_s$ G/PI at 505 K (450° F)**



ORIGINAL PAGE IS
OF POOR QUALITY

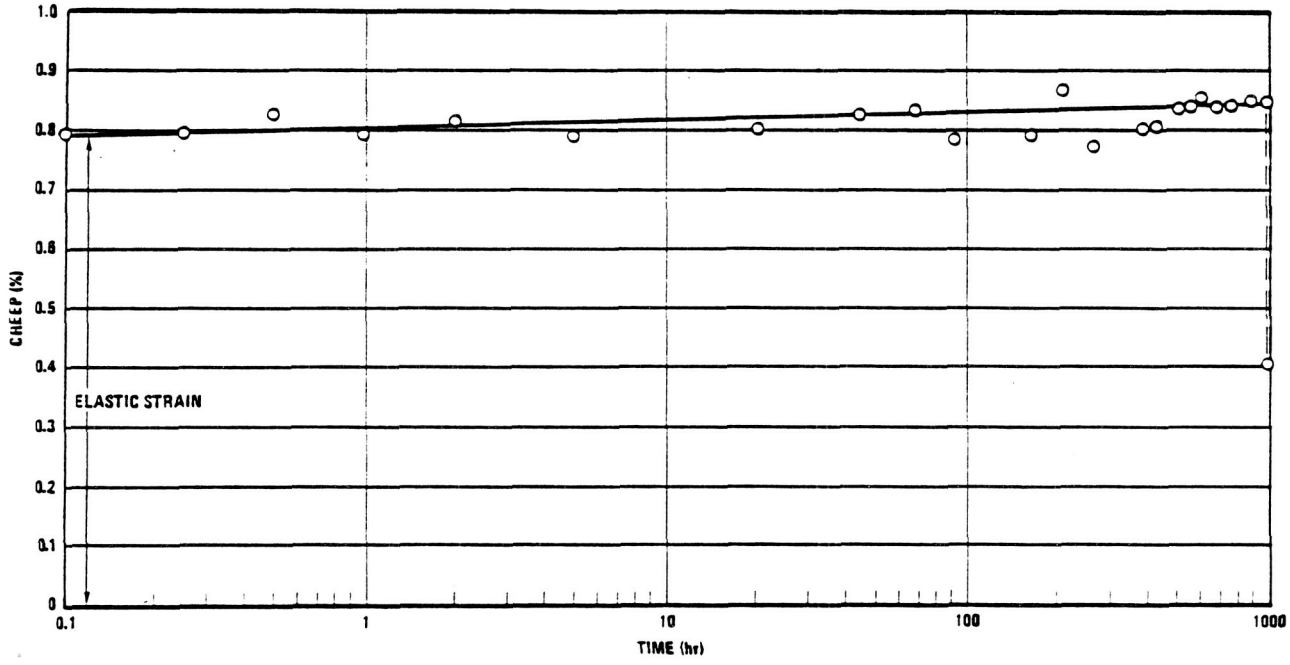



**Figure 10-24 Creep Strain for $[0° \pm 45°]_s$ G/PI at 505 K (450° F)**

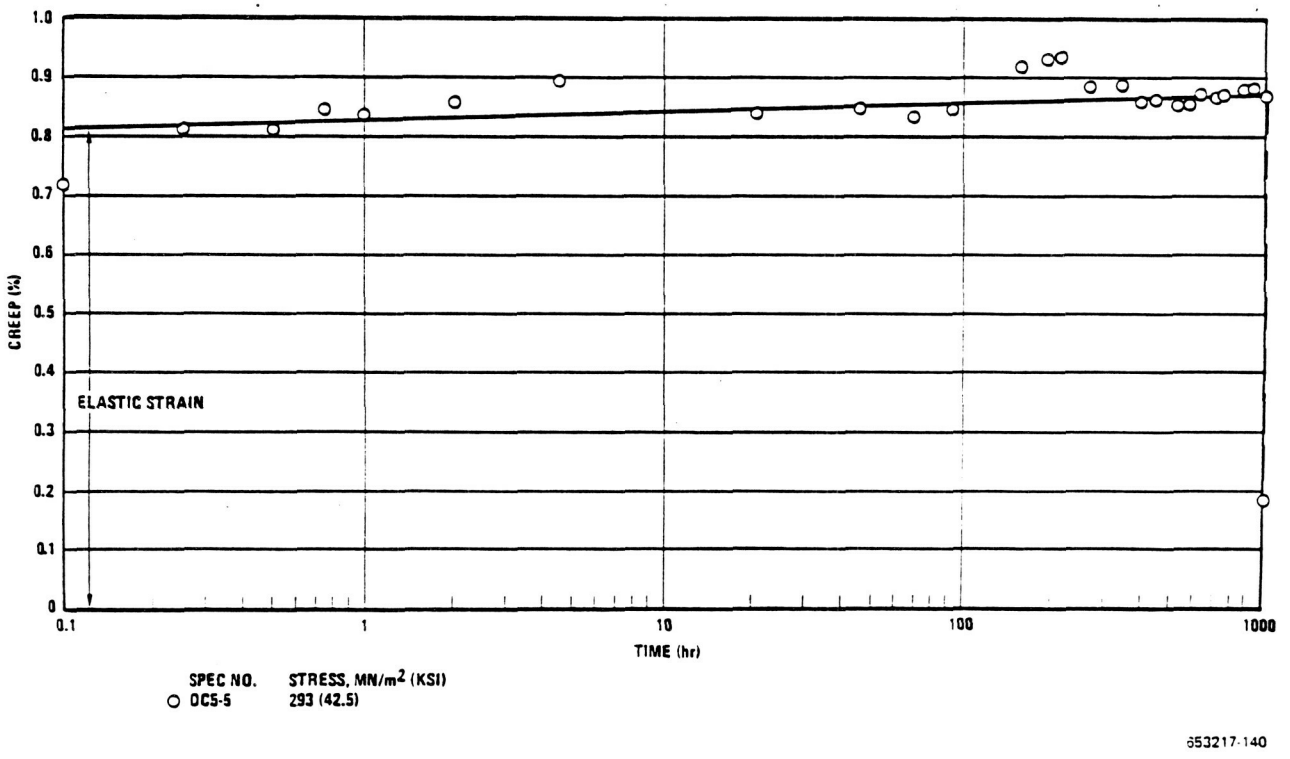



**Figure 10-25 Creep Strain for $[0° \pm 45°]_s$ G/PI at 505 K (450° F)**

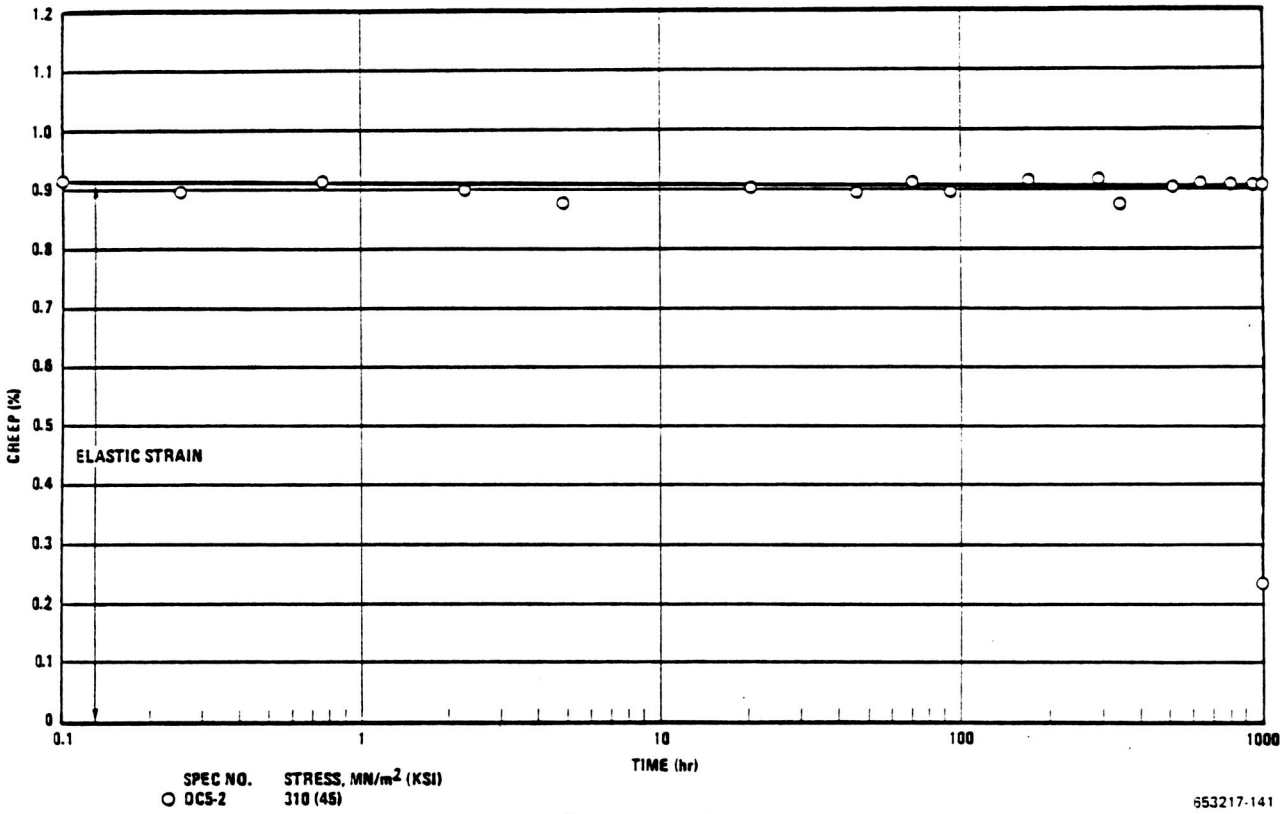



**Figure 10-26 Creep Strain for $[0° \pm 45°]_s$ G/PI at 505 K (450° F)**

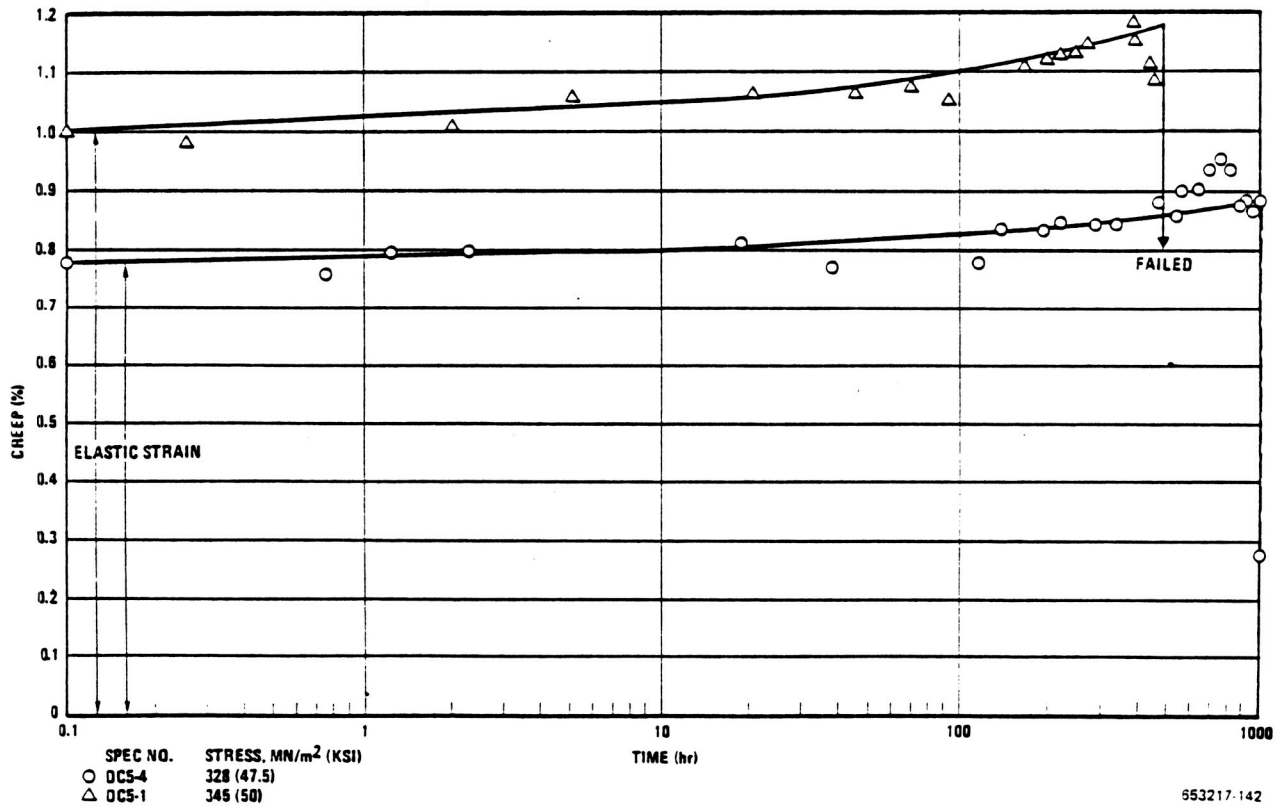



**Figure 10-27 Creep Strain for $[0° \pm 45°]_s$ G/PI at 505 K (450° F)**

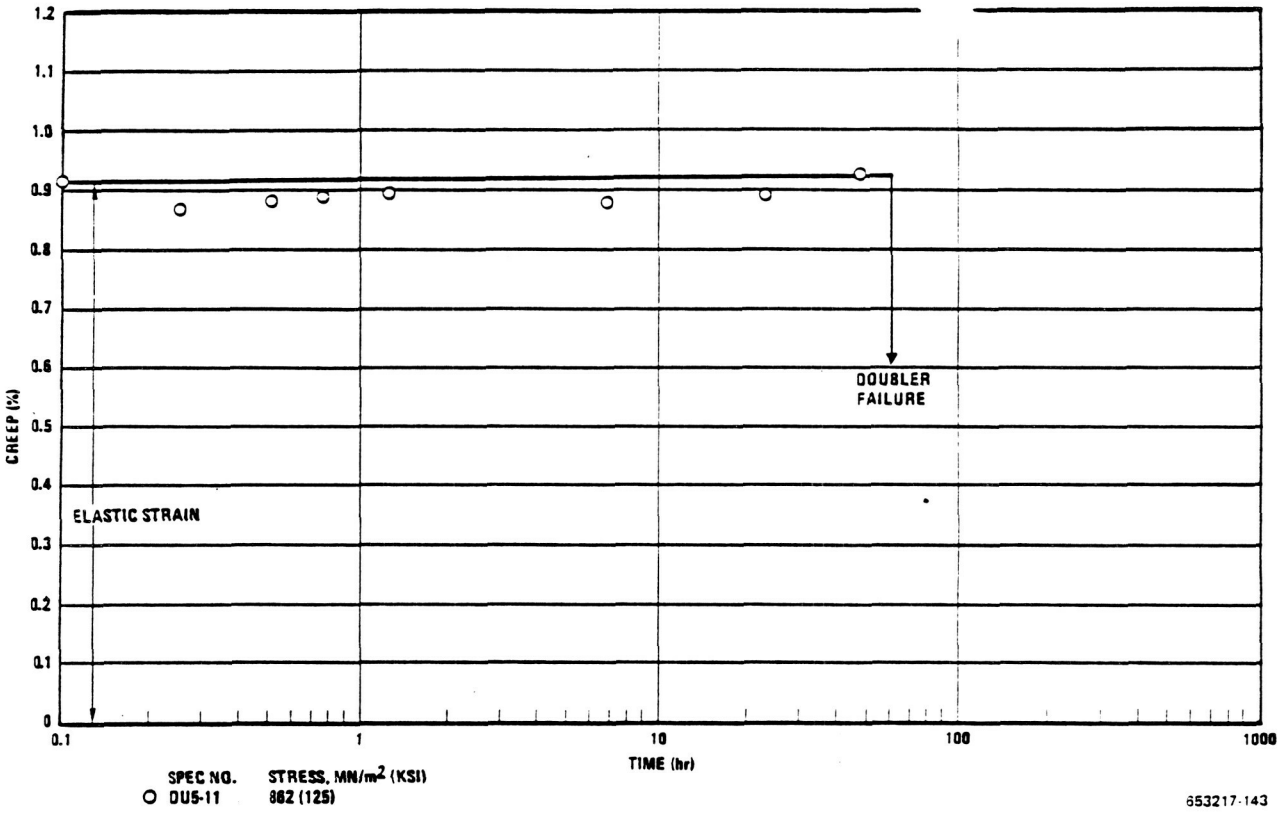



**Figure 10-28 Creep Strain for $[0°]_6$ G/PI at 561 K (550° F)**

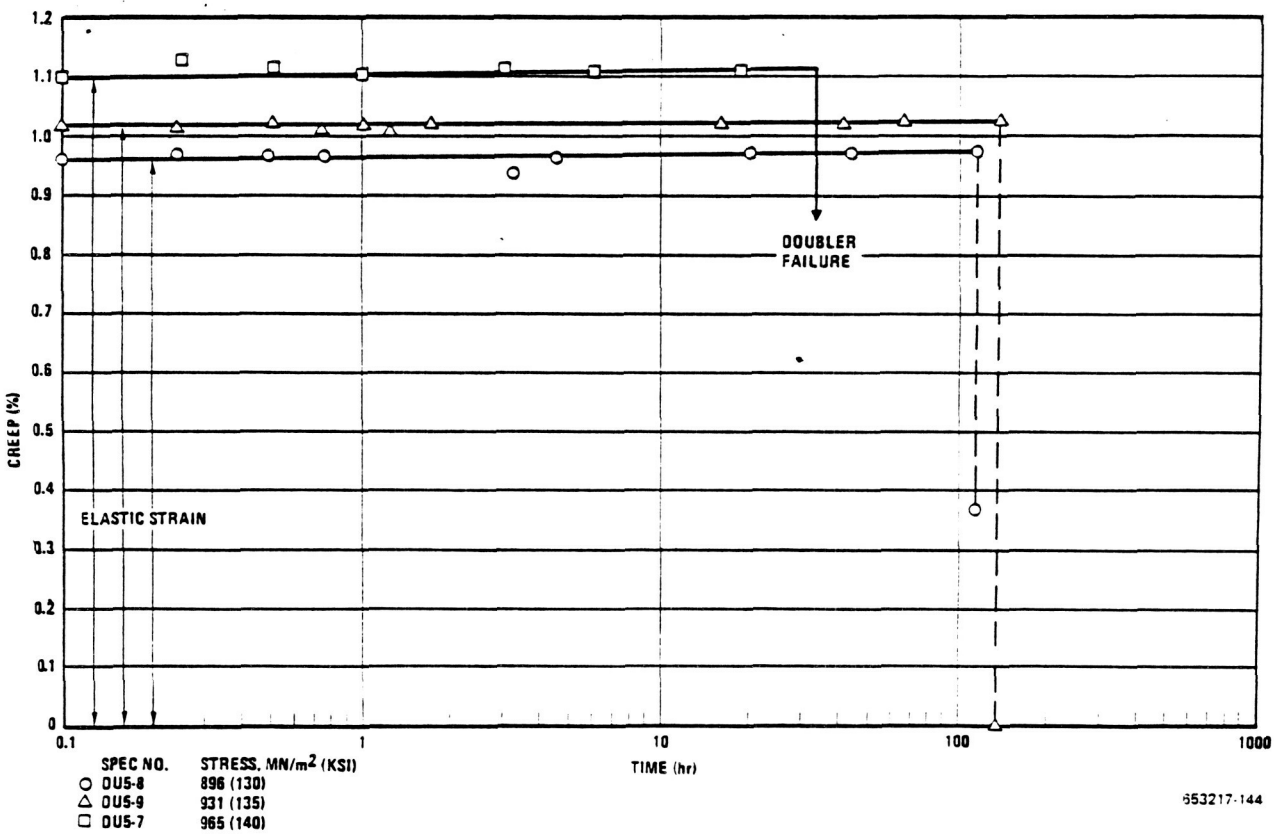



**Figure 10-29 Creep Strain for $[0°]_6$ G/PI at 561 K (550° F)**

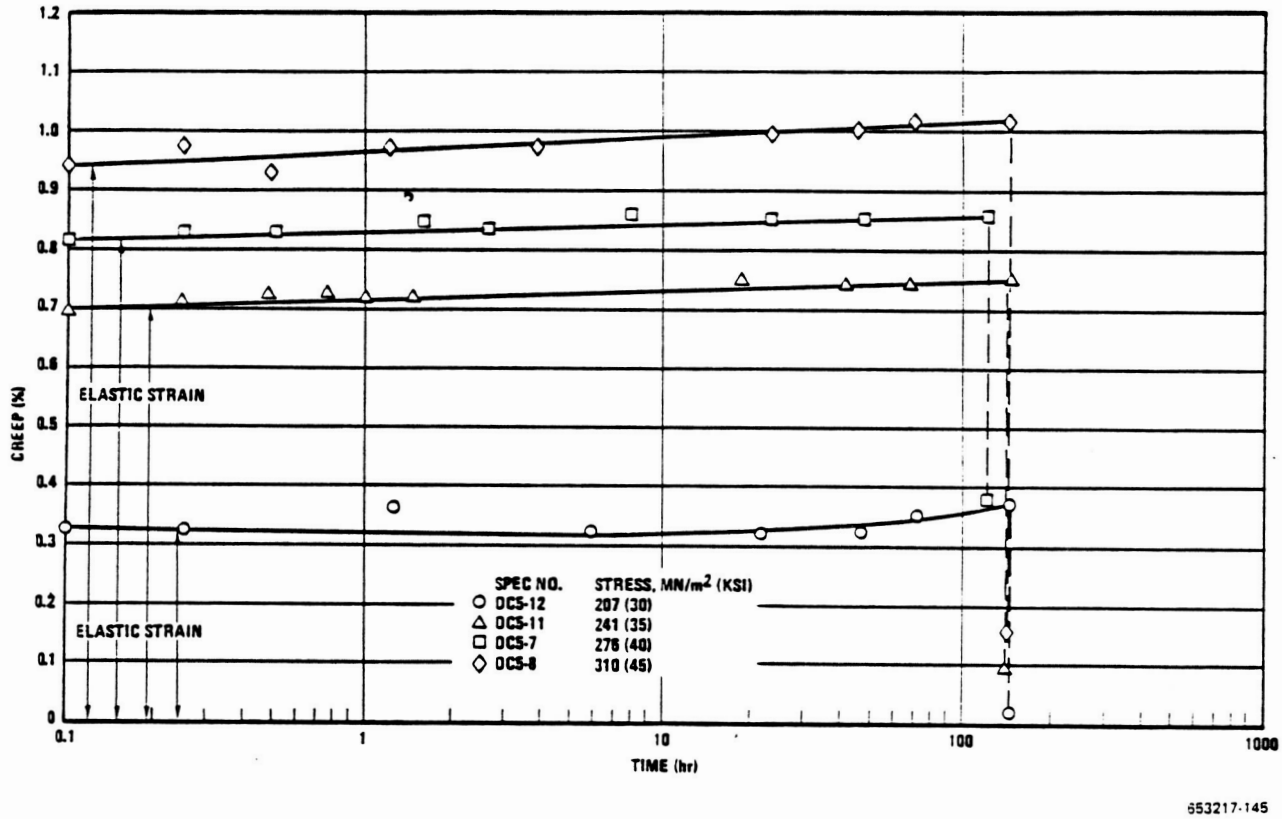



**Figure 10-30 Creep Strain for $[0° \pm 45°]_s$ G/PI at 561 K (550° F)**

Creep strain versus time curves are presented in Figures 10-31 and 10-32 for unidirectional material at 505 K (450° F), in Figures 10-33 and 10-34 for crossplied material at 505 K (450° F), in Figures 10-35 through 10-37 for unidirectional material at 561 K (550° F), and in Figures 10-38 through 10-40 for crossplied material at 561 K (550° F).

Creep strains measured for B/Al specimens were somewhat higher than for other systems but were still quite small. The unidirectional material gave values less than 0.2% with the crossplied material reaching a maximum value of only 0.31%. Several failures were recorded during test prior to completing the required 100- or 1000-hour time periods. There were also several doubler bond failures in the more highly loaded unidirectional specimens. These failures, both in the B/Al composite material at each test temperature and in the doubler bonds at 561 K (550° F), occurred at stress levels above approximately 85% of the average ultimate tensile strength for the 505 K (450° F) tests and above approximately 75% for the 561 K (550° F) tests. One specimen, EC5-12, failed during loading at a stress level, 421 $MN/m^2$ (61 ksi), slightly below the average ultimate tensile strength, 439 $MN/m^2$ (63.7 ksi), of crossplied B/Al at 561 K (550° F). The specimen had been mistakenly identified as an unidirectional specimen and was intended to have been tested at a much higher load.

The conclusion drawn from creep testing of the four composite materials is that boron or graphite filament reinforced materials with 0° plies aligned in the direction of loading undergo very little creep even at stress levels that result in fracture in short exposure times. Because of the low creep strains observed in these materials, it would appear that stress rupture tests

Table 10-5. Summary of Creep Test Results for B/Al

| Specimen Number | Orientation | Test Temperature K | Test Temperature (°F) | Stress MN/m² | Stress (ksi) | Total Creep Time (hr) | Total Creep Creep Strain (%) | Comments |
|---|---|---|---|---|---|---|---|---|
| EU5-6 | $[0°]_6$ | 505 | 450 | 1000 | 145 | 100 | 0.08 | |
| -7 | | | | 1030 | 150 | 100 | .13 | |
| -12 | | | | 1070 | 155 | — | — | Bond failure in 0.17 hr. |
| -8 | | | | 1100 | 160 | [a].5 | [a].01 | Bond failure in 1.3 hr. |
| -9 | | | | 1100 | 160 | 100 | .18 | |
| -10 | | | | 1170 | 170 | [a]21 | [a].19 | Failed in 45 hours |
| EC5-5 | $[0° \pm 45°]_s$ | 505 | 450 | 276 | 40 | 100 | .12 | |
| -11 | | | | 310 | 45 | 1000 | .24 | |
| -7 | | | | 345 | 50 | 1000 | .24 | |
| -8 | | | | 379 | 55 | 100 | .19 | |
| -10 | | | | 414 | 60 | [a]648 | [a].31 | Failed in 714 hours |
| -6 | | | | 448 | 65 | [a]1.2 | [a].09 | Failed in 2.7 hours |
| EU5-4 | $[0°]_6$ | 561 | 550 | 827 | 120 | 100 | .09 | |
| -3 | | | | 862 | 125 | 100 | .13 | |
| -5 | | | | 896 | 130 | 100 | .13 | |
| -11 | | | | 896 | 130 | 100 | .16 | |
| -2 | | | | 965 | 140 | [a]2.5 | [a].07 | Bond failure in 8 hours |
| -1 | | | | 1030 | 150 | — | — | Bond failure in 0.07 hour |
| EC5-9 | $[0° \pm 45°]_s$ | 561 | 550 | 276 | 40 | 1000 | .29 | |
| -4 | | | | 293 | 42.5 | 1000 | .18 | |
| -1 | | | | 310 | 45 | 1000 | .25 | |
| -3 | | | | 328 | 47.5 | 100 | .15 | Failed in 114 hours |
| -2 | | | | 345 | 50 | [a]18 | [a].13 | Failed in 30 hours |
| -12 | | | | 421 | 61 | — | — | Failed on loading |

[a]Last measurement prior to failure

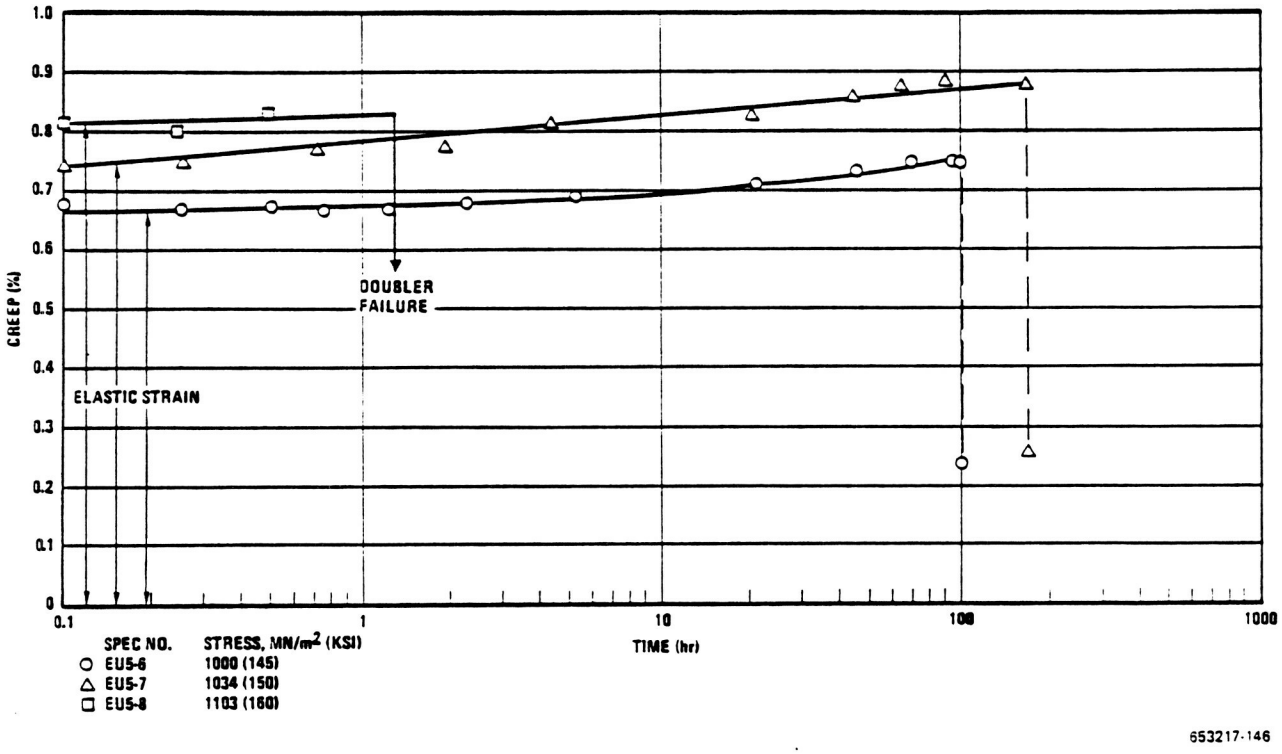



**Figure 10-31 Creep Strain for $[0°]_6$ B/Al at 505 K (450° F)**

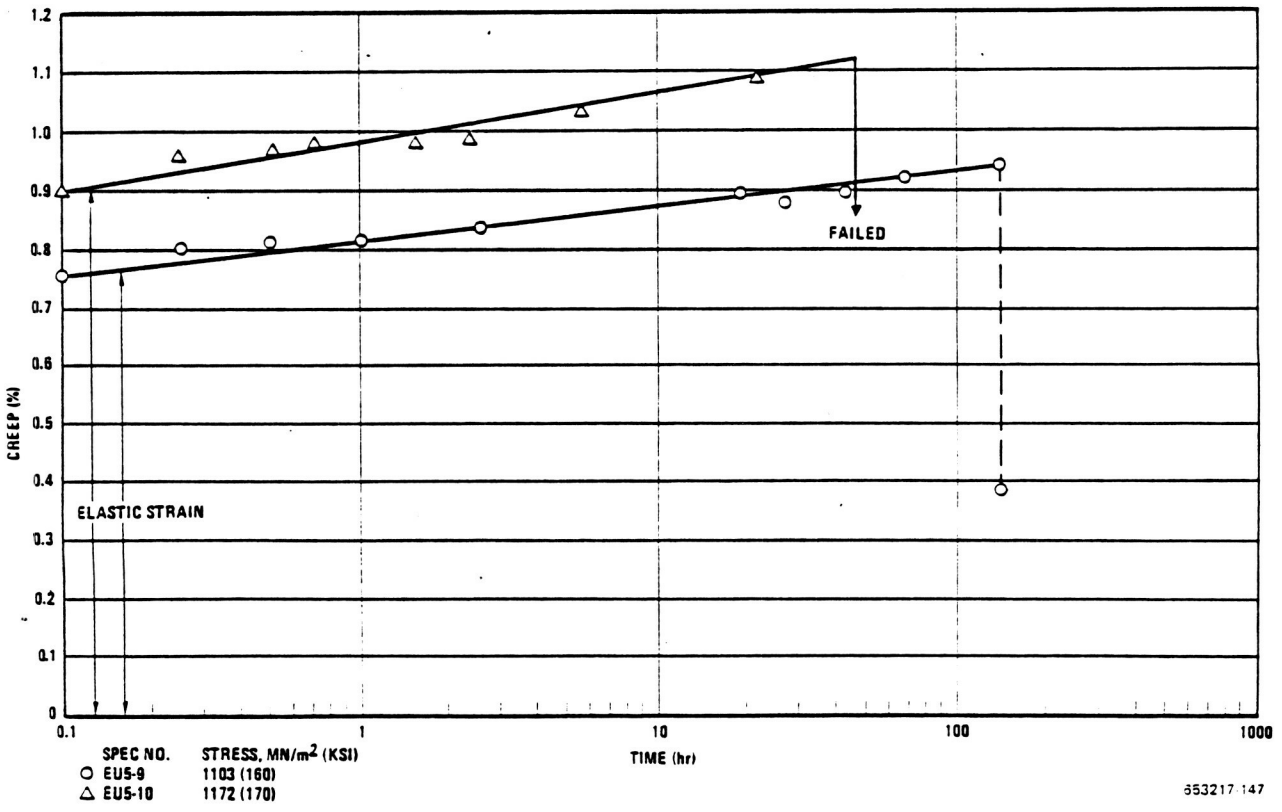



**Figure 10-32 Creep Strain for $[0°]_6$ B/Al at 505 K (450° F)**

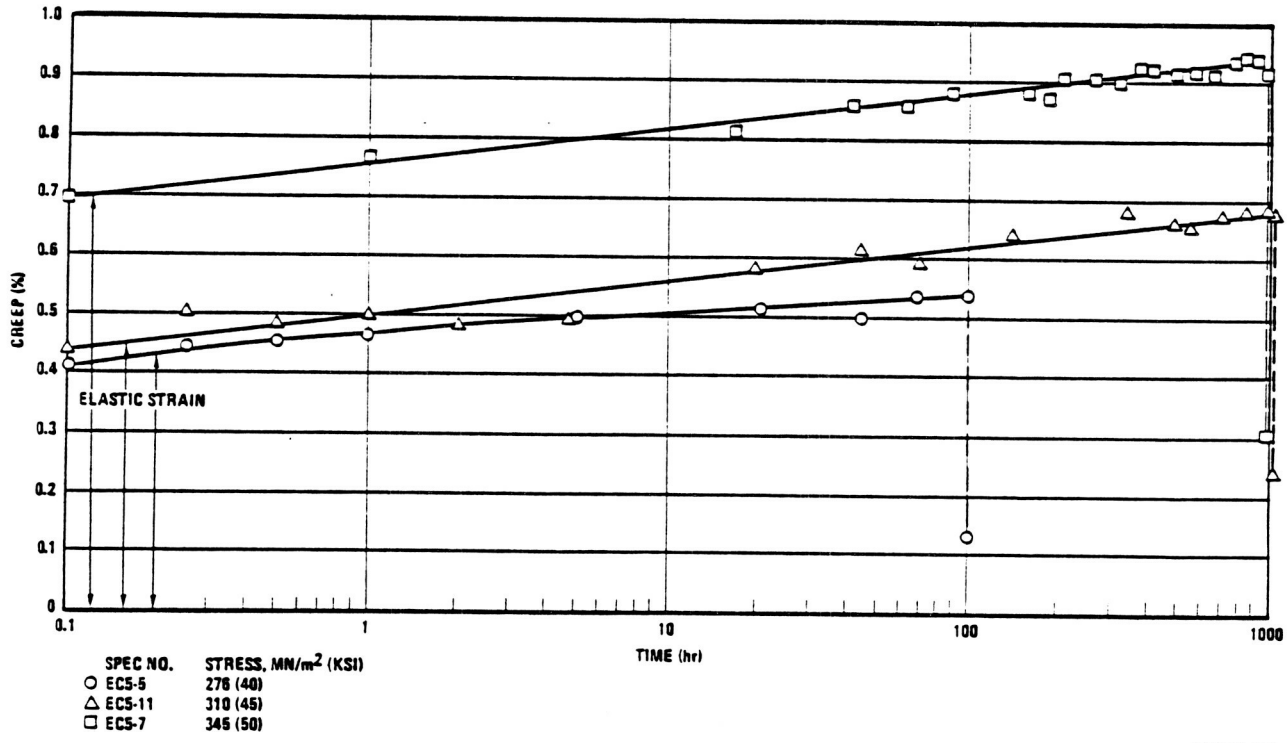



Figure 10-33 Creep Strain for $[0° \pm 45°]_s$ B/Al at 505 K (450° F)

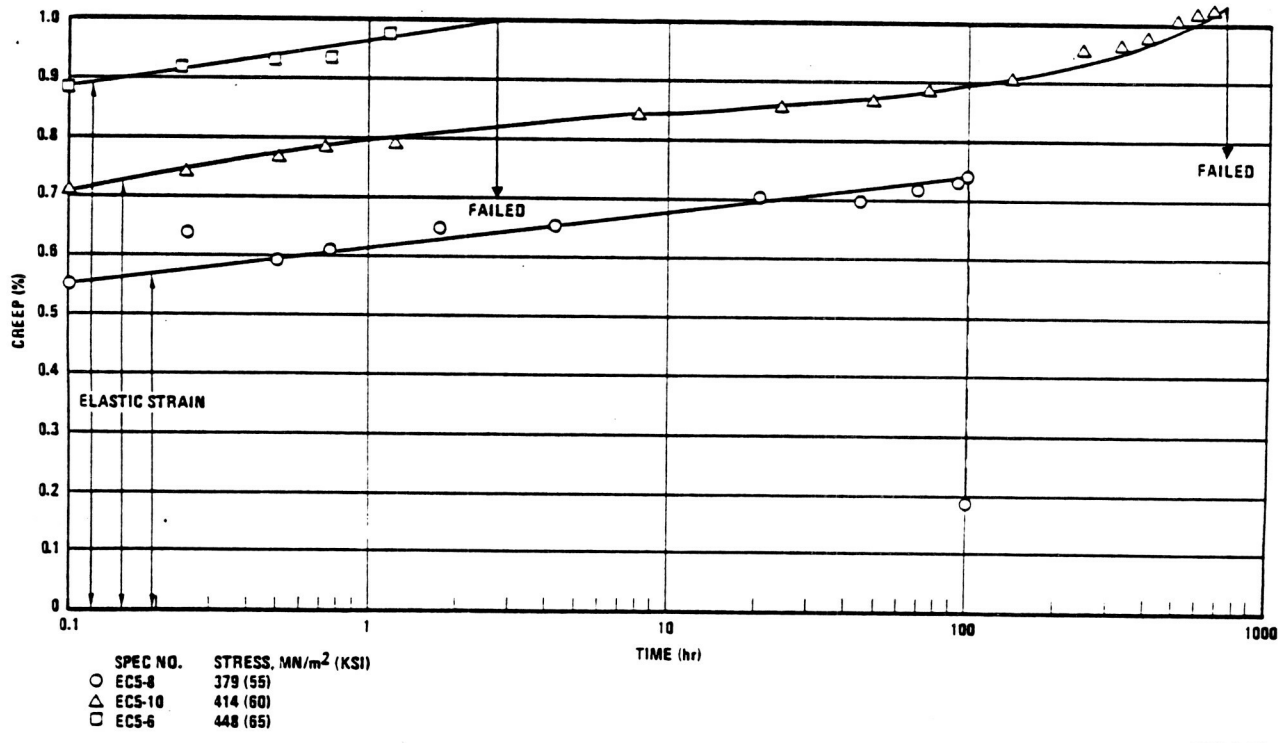



Figure 10-34 Creep Strain for $[0° \pm 45°]_s$ B/Al at 505 K (450° F)

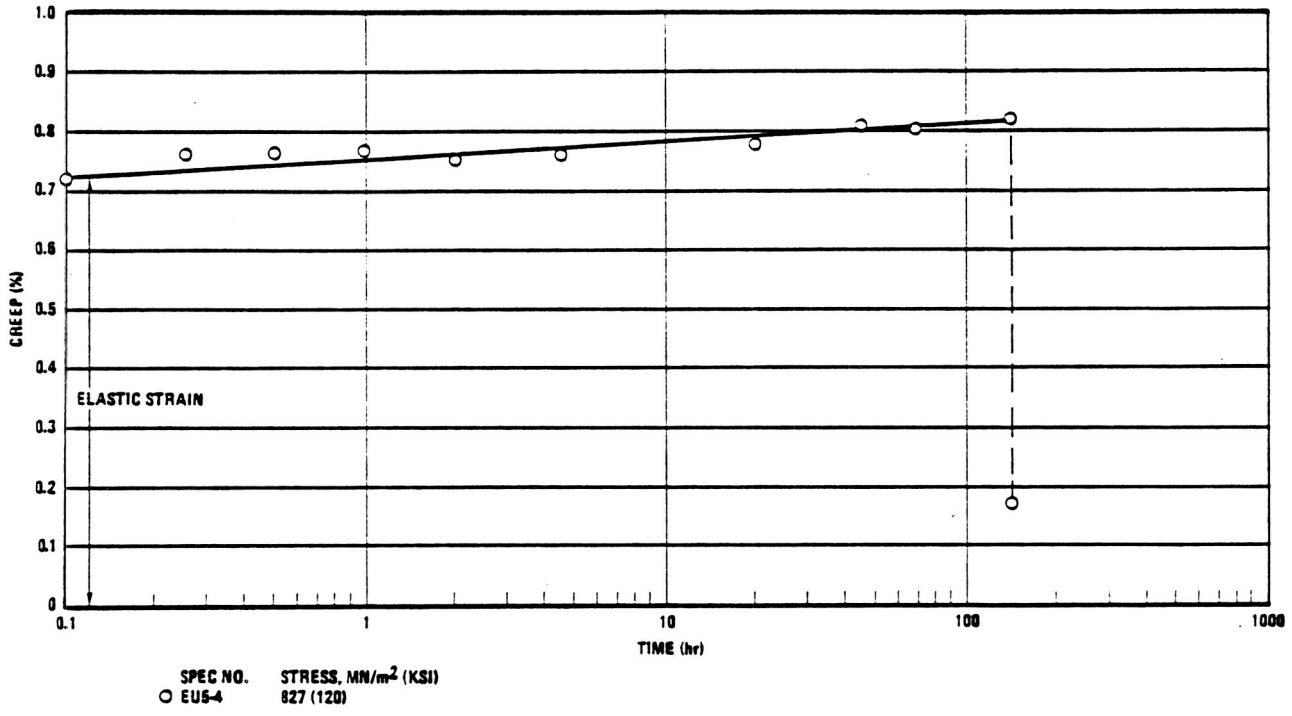



**Figure 10-35 Creep Strain for $[0°]_6$ B/Al at 561 K (550° F)**

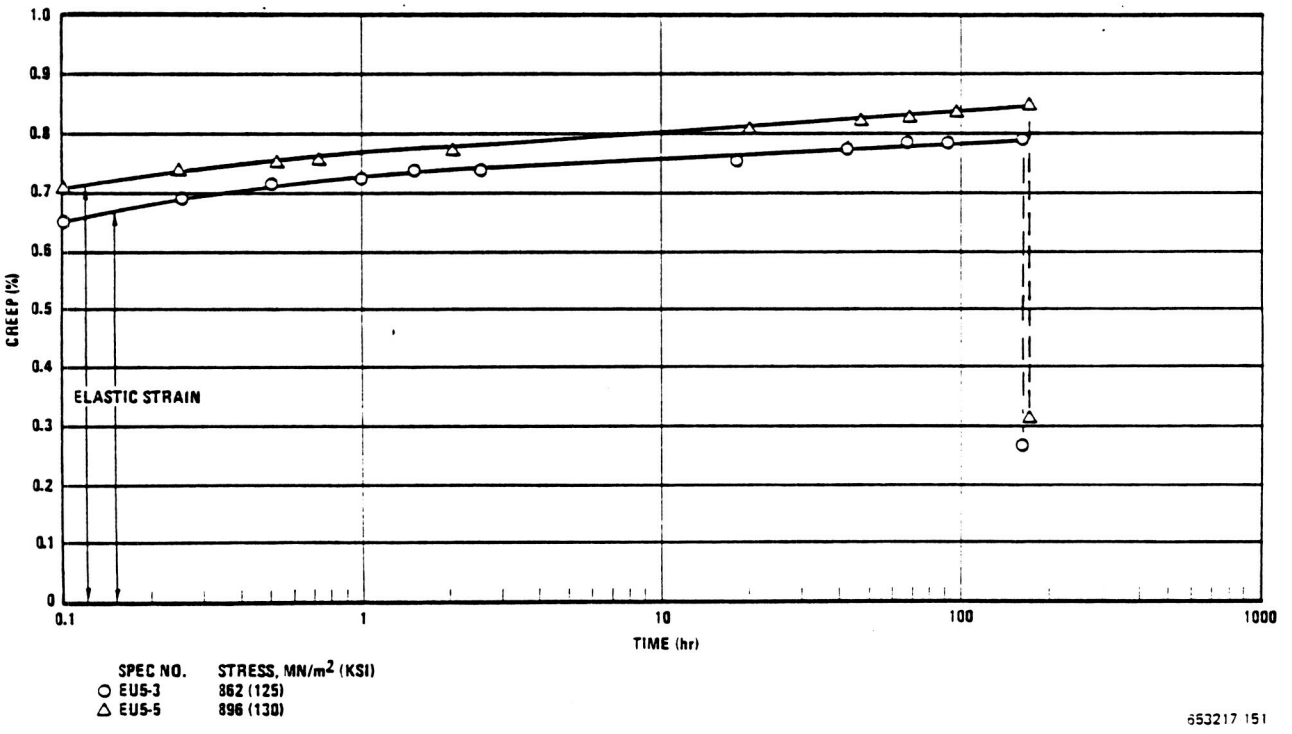



**Figure 10-36 Creep Strain for $[0°]_6$ B/Al at 561 K (550° F)**

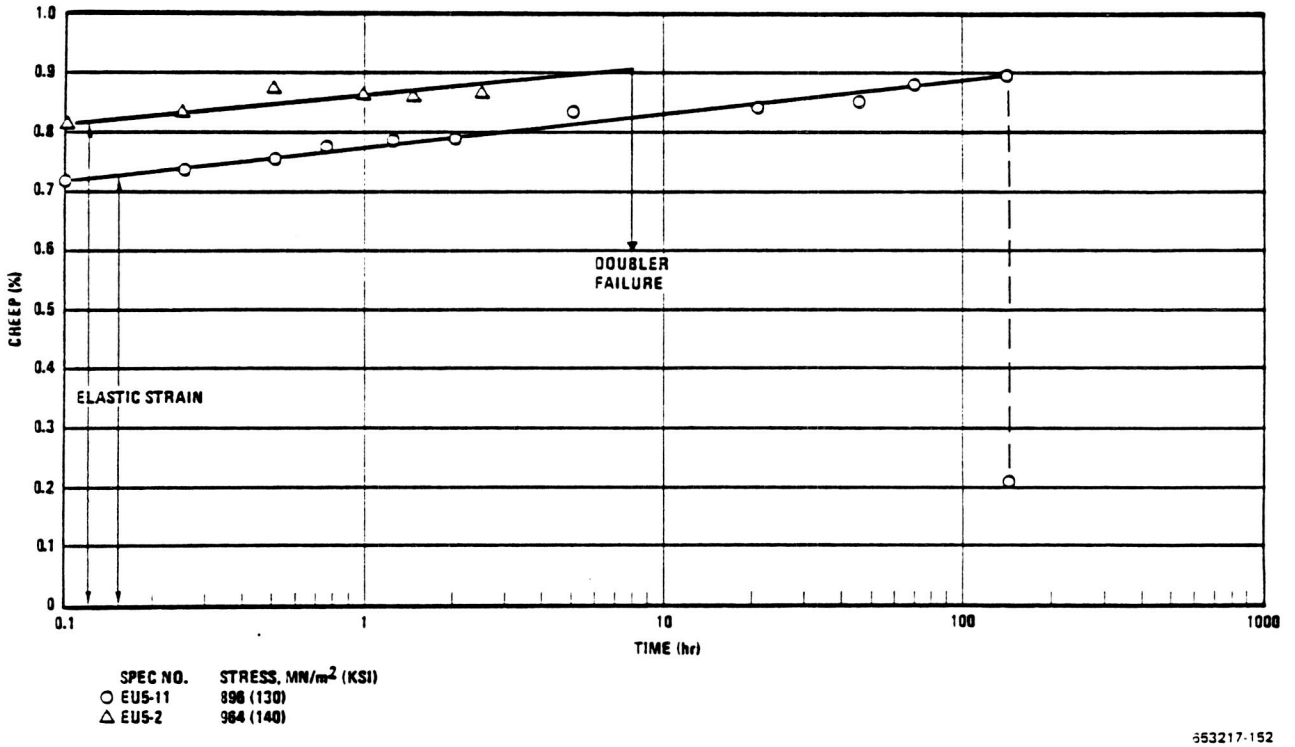



**Figure 10-37 Creep Strain for $[0°]_6$ B/Al at 561 K (550° F)**

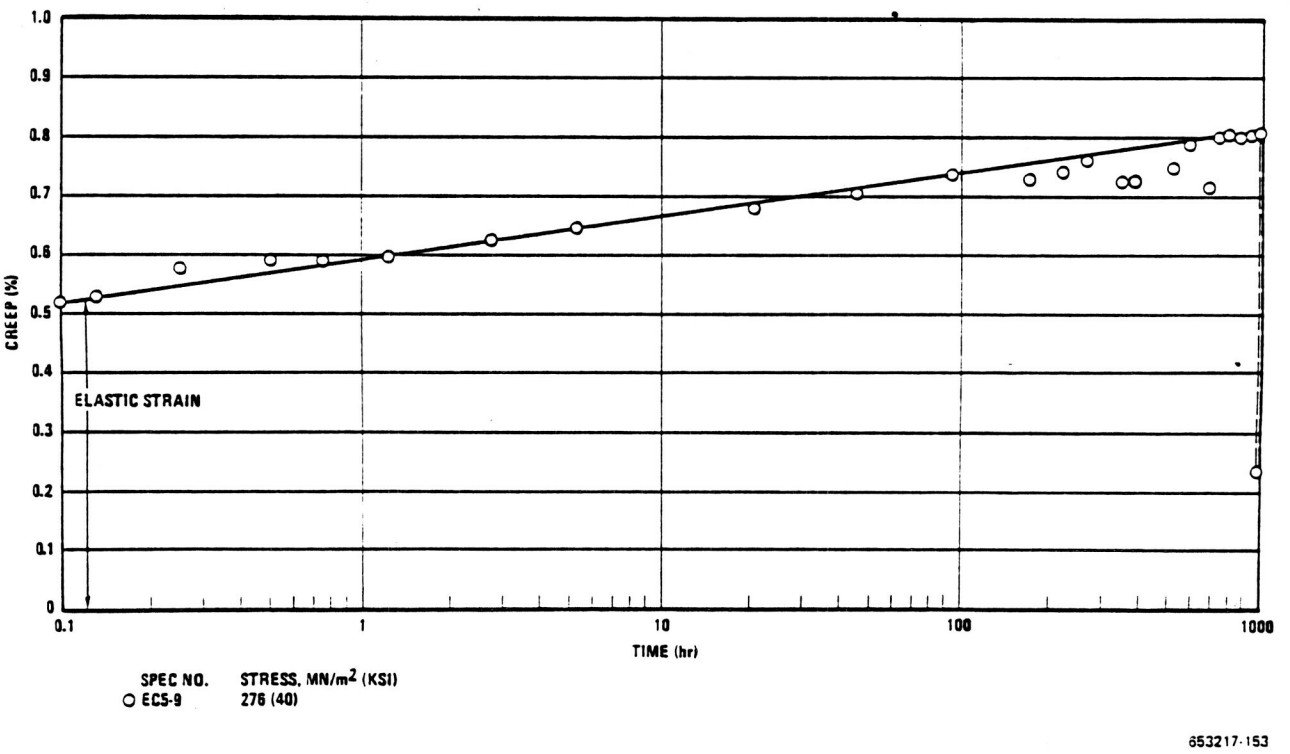



**Figure 10-38 Creep Strain for $[0° \pm 45°]_s$ B/Al at 561 K (550° F)**

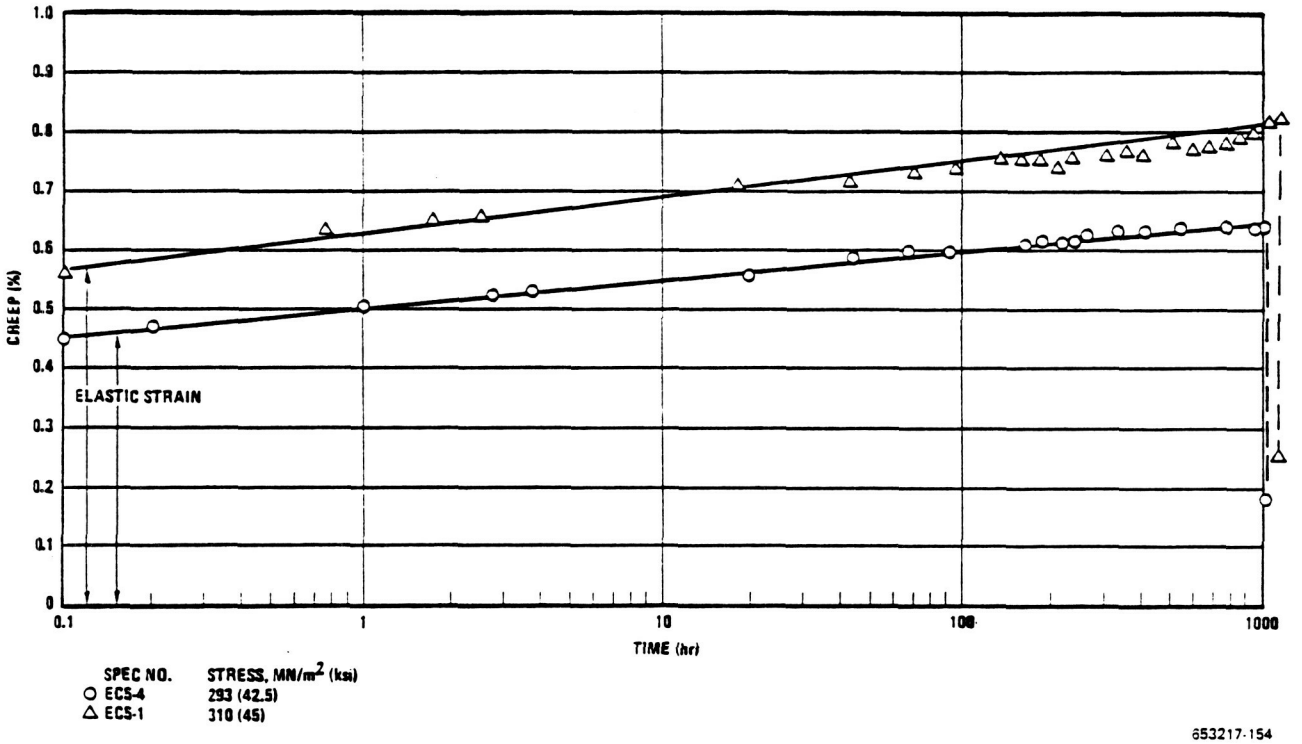



**Figure 10-39 Creep Strain for $[0° \pm 45°]_s$ B/Al at 561 K (550° F)**

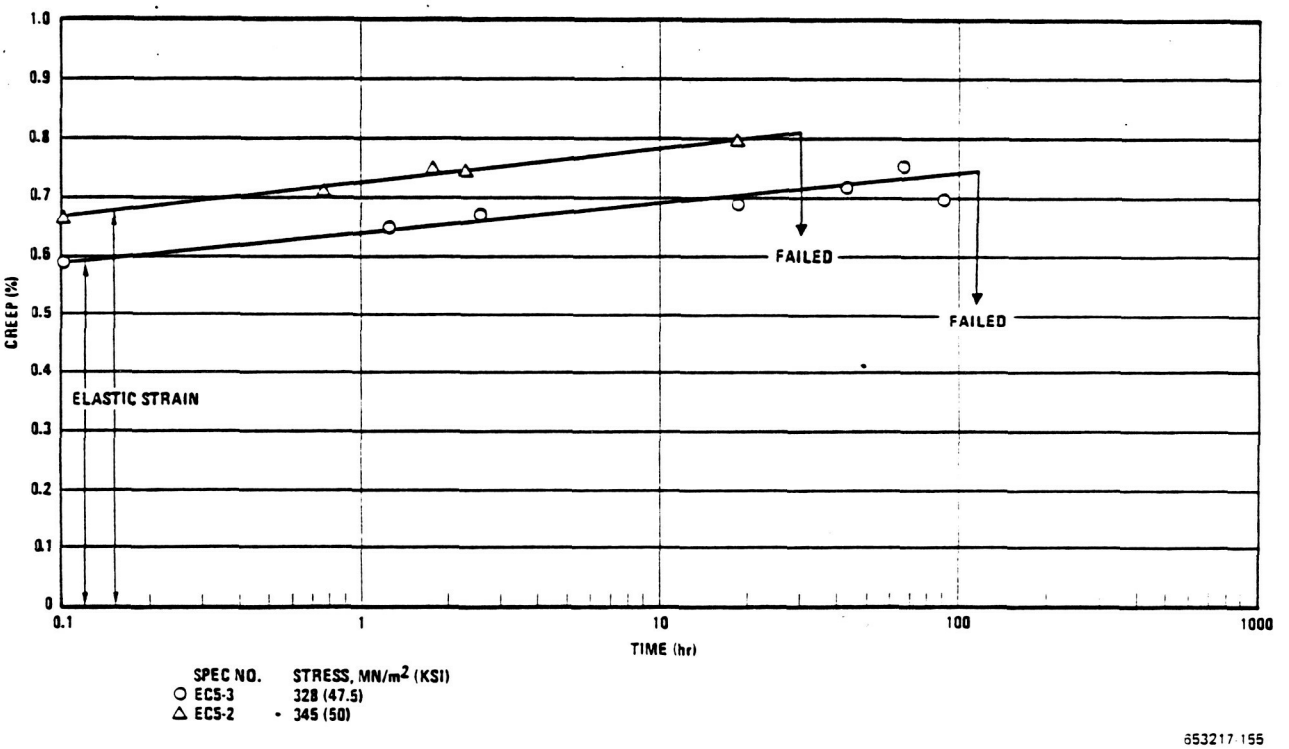



**Figure 10-40 Creep Strain for $[0° \pm 45°]_s$ B/Al at 561 K (550° F)**

could well be substituted for creep measurements. A plot of creep stress versus time for various creep strains from 0.05% to rupture would likely show a family of curves that were very closely spaced. Since the expense in obtaining creep data is far greater than that for stress rupture testing, a considerable savings could be realized.

# SECTION 11

# BASELINE FATIGUE TESTING

Fatigue testing made up a significant portion of the SCR study with four distinct parts: 1) conventional constant amplitude tests at room and elevated temperatures with flawed and unflawed test specimens; 2) constant amplitude tests on material that survived 10,000 to 36,000 hours of flight simulation exposure; 3) short-term flight simulation tests (random fatigue loads, constant elevated temperature) of 100 and 200 hours; and 4) long-term flight simulation (random fatigue loads, cyclic temperature) for up to 40,000 hours. The constant amplitude tests on unexposed material characterize the composites. Tests after flight simulation exposure provide data to compare the residual fatigue properties to original properties. The short-term flight simulation tests generate wearout analysis model data necessary to set the stress levels for the long term flight simulation tests. Finally, the long-term tests provide data on the effect of simulated supersonic flight service environments for each composite system. The bulk of these tests, those that serve as baseline for later comparisons, were performed on unexposed composite materials. It is these tests that are described in this section. In some cases, the data were available in the literature, and no additional tests were required. As a result of considerable early testing and extensive use, the B/E material fitted this category and only limited testing was necessary (ref. 40 and 41).

Test parameters that were considered in the baseline constant amplitude fatigue tests were 1) specimen layup, 2) specimen configuration, 3) test temperature, and 4) stress ratio. Specimens of both unidirectional and [0° ± 45°] crossply layups were evaluated. All test specimens were loaded in the direction of the 0° fibers. Flawed and unflawed specimens were included. The flawed specimens were fabricated with a center hole having a diameter equal to one-fourth of the specimen width. For isotropic material a specimen with this configuration would have a theoretical stress concentration factor, $K_t$, of 2.43 (ref. 28). Testing was conducted at room temperature for all systems and, in addition, at 450 K (350° F) for G/E and Celion 6000/LARC-160 G/PI and at 505 K (450° F) for HT-S/710 G/PI and B/Al. Fatigue tests were performed at stress ratios (R) of 0.1 and −1 for all systems except B/E and, in addition, at R = 10 for the Celion 6000/LARC-160 G/PI. R is defined as the algebraic ratio of the minimum stress to the maximum stress in one cycle (thus loading for the R = 0.1 tests is tension-tension, for the R = −1 test is fully reversed tension-compression, and for the R = 10 tests is compression-compression).

In addition to the baseline tests described above, three other fatigue studies are included in this section. The first was a limited program to investigate the effects of stacking sequence on fatigue strength of the [0° ± 45°] family of laminates. The second was a determination of Poisson's ratio of specimens after 10 million fatigue cycles (runout). The third was a determination of baseline fatigue strength of the thermal aging/compression study materials. These tests were done on unnotched 24 ply $[0° \pm 45°]_{s4}$ specimens at room temperature and a stress ratio, R, of −1.

## 11.1 SPECIMEN DESIGN

Specimens tested at a stress ratio, R, of 0.1 were fabricated from 6 ply $[0°]_6$ and $[0° \pm 45°]_s$ laminates. For R = −1 tests, where compressive as well as tensile loads are applied, a thicker

specimen was used. Information obtained from IITRI (private communication from K.E. Hofer, 1973) indicated that fatigue testing 6 ply composite material at R = −1 gave unreliable results. The problem was related to compressive buckling and could be overcome by the use of thicker material. For this reason the R = −1 specimens were cut from 12-ply $[0°]_{12}$ and $[0° \pm 45°]_{s2}$ laminates and the R= 10 specimens were cut from 24 ply $[0° \pm 45°]_{s4}$ laminates. Cutting, hole machining, and doubler bonding techniques were those described in Section 5. Details of the specimen geometry for the various configurations and test conditions are listed in Table 11-1. The length of the R = 0.1 specimens that were tested at elevated temperature was twice that of the room temperature specimens to allow the ends to extend well away from the furnace during testing. With this technique doubler bond failures were eliminated. Because of the compressive loads present during the R = −1 and R= 10 testing it was not feasible to extend the length of these specimens for the elevated temperature conditions. Doubler bond heating of these specimens was minimized by reducing the size of the furnace as described in Section 11.2. The widths of the various specimens were the same as those chosen for the baseline unnotched and notched tensile tests (Section 7), except that the R = −1, and R= 10 unnotched specimens were all 0.025 m (1.0 in.) in the fatigue tests rather than 0.013 m (0.5 in.).

## 11.2 TEST EQUIPMENT AND TEST PROCEDURE

Testing was performed on Baldwin-Sonntag SF1U and SF10U fatigue machines at a constant frequency of 30 Hz. Both grip ends of the specimens were placed between two L-shaped steel fixtures that were bolted to the machine loading platens. The specimens were secured to the steel plates by two .013 m (0.5 in.) diameter bolts that straddle the edges of the grip ends of the specimen. To further increase the gripping power of the fixtures, a special abrasive cloth (Bay State Gritcloth, size 320 grit) was placed at each specimen-to-fixture interface. This cloth had two beneficial features for a secure grip: 1) the open weave design, which increases the frictional holding force, and 2) the abrasive coating on both surfaces of the cloth, which becomes embedded in the contact surfaces of both the fixtures and tabs. The two bolts were torqued to a level that just secured the specimen, the alignment of the specimen was carefully checked to ensure axial loading, and final tightening was completed. Figures 11-1 through 11-3 show one of the fatigue testing machines and close-up views of the gripping fixtures with both R = 0.1 and R= −1 specimens in place.

For elevated temperature tests of the R = 0.1 specimens a 0.15 m (6 in.) long clamshell furnace was used. The length of the specimens was such as to allow the ends to extend out of the furnace far enough to prevent excessive heating of the doubler adhesive. This factor and the excellent gripping power of the end fixtures combined to eliminate doubler bond failures at elevated temperature. Figure 11-4 shows the furnace arrangement with a specimen loaded in the fatigue machine. Temperature was controlled to ± 3 K (± 5° F) with a Minneapolis Honeywell Brown Electronik controller using a chromel-alumel thermocouple atached to the specimen at the center of the gage section.

For the R = −1 and R = 10 specimens a much smaller furnace was required for the elevated temperature tests because of the limited amount of space available between the gripping fixtures. Most tests were conducted using a small ring furnace of the type shown in Figure 11-5. This could be used on all tests that were run in the smaller SF1U fatigue machine but not in the larger SF10U because of space limitations. The unidirectional B/Al specimen loads were such as to require the larger SF10U fatigue machine. For these specimens a successful technique for elevated temperature testing was developed by using a flexible heating tape, which

Table 11-1. Details of Fatigue Specimen Geometry

| Specimen Configuration | R Value | Test Temperature | Thickness (Plies) | Length m (in.) | Width m (in.) | Hole Diameter m (in.) | Test Section m (in.) |
|---|---|---|---|---|---|---|---|
| Unnotched | 0.1 | R.T. | 6 | 0.23 9 | 0.013 0.5 | — | 0.10 4 |
| | .1 | Elevated | 6 | .46 18 | .013 0.5 | — | .33 13 |
| | −1 | R.T. | 12 | .10 4 | .025 1 | — | .013 0.5 |
| | −1 | Elevated | 12 | .10 4 | .025 1 | — | .013 0.5 |
| | 10 | R.T. | 24 | .10 4 | .025 1 | — | .013 0.5 |
| | 10 | Elevated | 24 | .10 4 | .025 1 | — | .013 0.5 |
| Notched | .1 | R.T. | 6 | .23 9 | [a].025 1 | [b].0064 0.25 | .10 4 |
| | .1 | Elevated | 6 | .46 18 | [a].025 1 | [b].0064 0.25 | .33 13 |
| | −1 | R.T. | 12 | .10 4 | .025 1 | .0064 0.25 | .013 0.5 |
| | −1 | Elevated | 12 | .10 4 | .025 1 | .0064 0.25 | .013 0.5 |
| | 10 | R.T. | 24 | .10 4 | .025 1 | .0064 0.25 | .013 0.5 |
| | 10 | Elevated | 24 | .10 4 | .025 1 | .0064 0.25 | .013 0.5 |

[a]for B/Al: 0.013 (0.5)
[b]for B/Al: 0.00318 (0.125)

was wrapped around the short test section of the specimens. The heater was 0.61 m (24 in.) in length, 0.013 m (0.5 in.) wide, rated at 200 watts and had a maximum use temperature of 873 K (1112° F). Figure 11-6 shows a specimen with the heating tape in place ready for test.

Prior to testing, the resin matrix composite specimens were dried at 394 K (250° F) for 24 hours. No baking of the B/Al specimens was required. The specimen dimensions were measured, and the static and dynamic loads calculated for the particular stress level and R value desired. The notched stress values were based on net section, i.e., width minus hole diameter. After loading the specimen in the machine and carefully checking the alignment, the load levels were set, and the test initiated. The tests were continued to failure or until a maximum of 10 million cycles was obtained. The number of load cycles was measured with a counter driven by the motor rotating the dynamic load. This counter had a least count of 1000 cycles so that any failures below this value were not registered. Nine specimens were tested for each combination of: 1) material system, 2) laminate orientation, 3) specimen type (unflawed or flawed), 4) R value, and 5) test temperature. The test data were plotted on semi-logarithmic paper to obtain the characteristic S-N curves.

Initially the S-N curves were drawn to show a straight line of best fit of the data points as determined by linear regression analysis. The high degree of scatter in some of the data sets and the uncertainty of how to input the runout specimens often gave S-N curves that did not appear to be consistent with those from data sets with little scatter. For this reason the method was changed, and all curves have been drawn by hand.

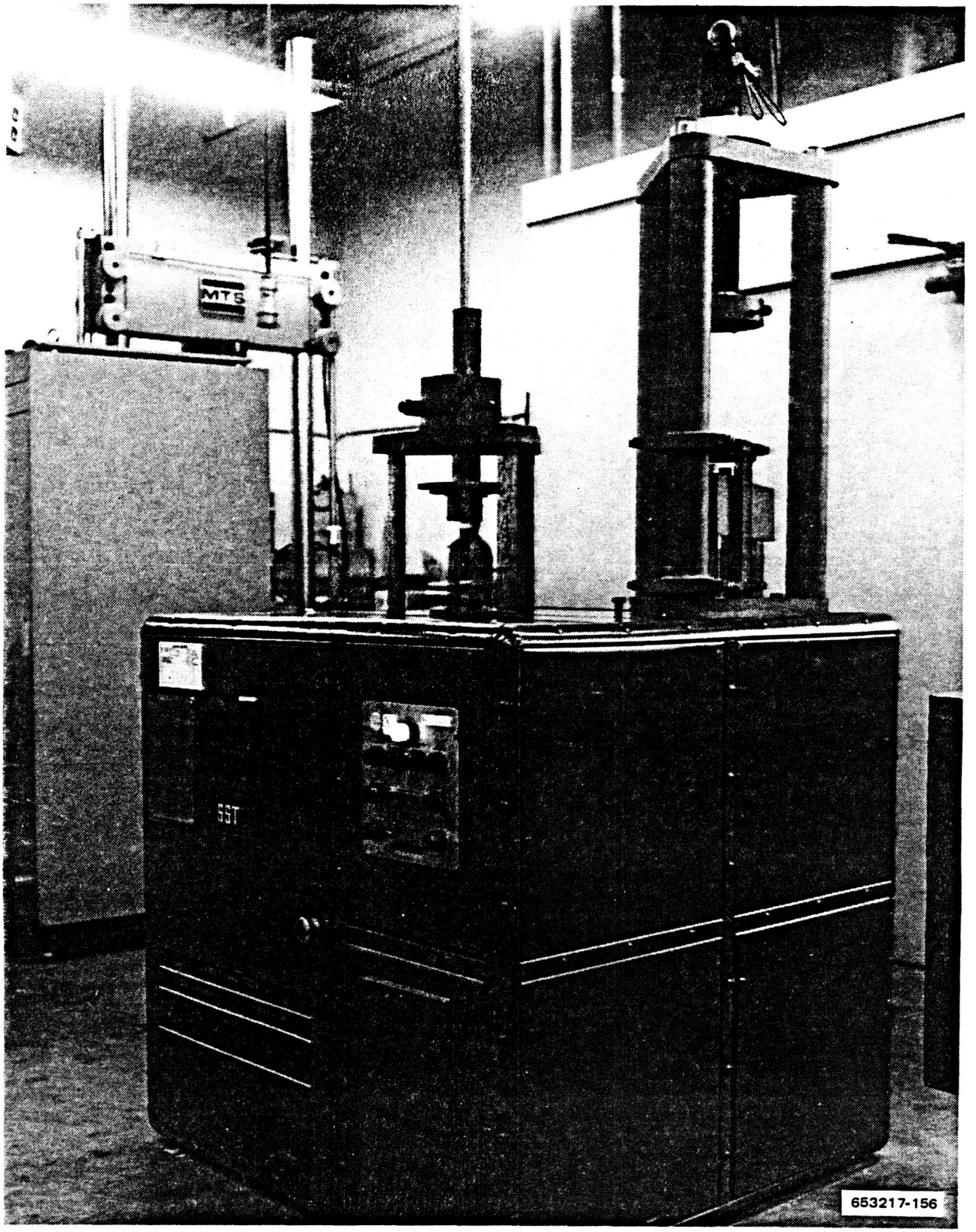



**Figure 11-1 Fatigue Testing Apparatus**



ORIGINAL PAGE IS
OF POOR QUALITY

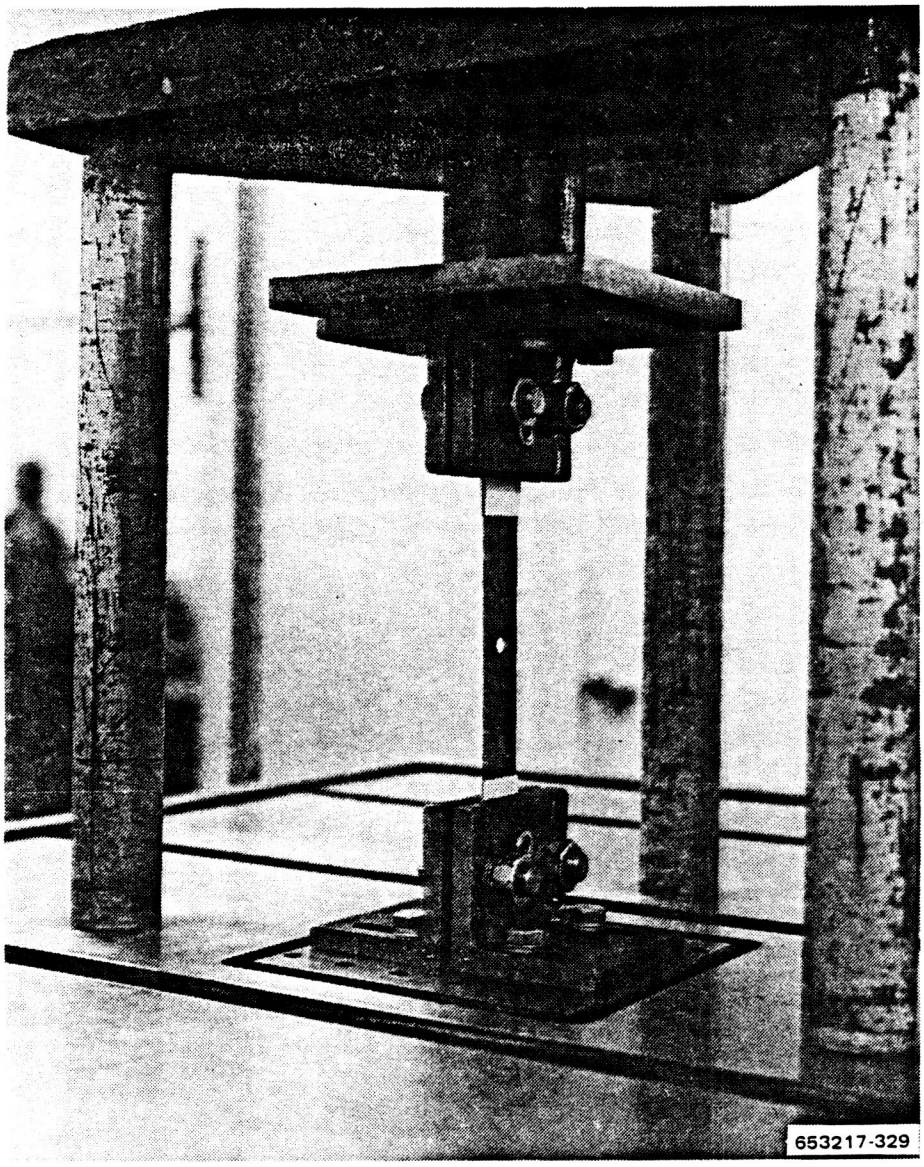



**Figure 11-2 Fatigue Specimen Mounted in Gripping Fixture for R = 0.1 Test at Room Temperature**

## 11.3 TEST RESULTS AND DISCUSSION

The overall baseline fatigue testing program is summarized in Table 11-2. This table shows the number of specimens and stress ratios that were employed at each test temperature for the five material systems. Of the total number of test specimens shown in Table 11-2, all are included in the data presented in this section although a few are not valid because of equipment malfunctions, doubler bond failures, or incorrect test loads or temperatures. These specimens are identified in the tables and figures. The data are presented in both tabular form and as S-N curves, one for each stress ratio and temperature.

**11.3.1 BORON/EPOXY AND GRAPHITE/EPOXY.** Because of the large amount of testing previously conducted by others on the B/E system, no baseline fatigue testing was required.



ORIGINAL PAGE IS
OE POOR QUALITY

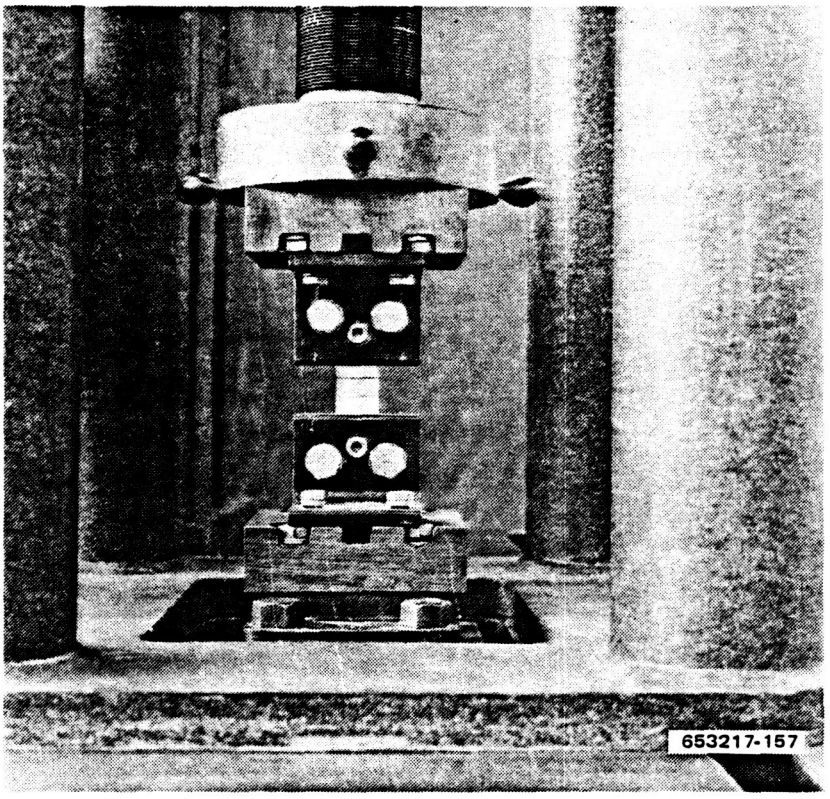



**Figure 11-3 Fatigue Specimen Mounted in Gripping Fixture for R = −1 Test at Room Temperature**

However, to determine more precisely the effects of the flight simulation exposure it was desirable to have baseline fatigue data from this same batch of material using the same specimen configuration and test technique as used during the post exposure evaluation. For this reason baseline fatigue data were determined for B/E for the same test conditions and specimen configurations as were later used in evaluating the B/E flight simulation specimens after 10,000 hours of exposure. These were room temperature tests on unnotched and notched $[0° \pm 45°]_s$ crossply material tested at an R value of 0.1. The results are listed in Table 11-3 and plotted in Figure 11-7. The slopes of the S-N curves are quite different for the two specimen configurations. The notched material has a relatively flat curve lying near 414 MN/m$^2$ (60 ksi). The S-N curve for the unnotched material is much steeper, with fatigue strengths below $10^5$ cycles greater than the notched specimens but with lower strength for lifetimes greater than $10^5$ cycles.

For G/E a complete set of fatigue tests was performed. The results are listed in Tables 11-4 through 11-11 and individual S-N curves are plotted in Figures 11-8 through 11-15. On these S-N curves the individual data points have been included. In the discussion of the fatigue data, several of the S-N curves have been combined to more clearly show the effects of the test parameters, i.e., stress ratio, temperature, or specimen configuration. On these curves the data points have been omitted for clarity.

Several points are apparent from an examination of the G/E baseline fatigue data. The test parameter that exhibited the greatest influence on the fatigue strength was the stress ratio, R. In every case the tests conducted at R = −1 gave considerably lower fatigue properties than



ORIGINAL PAGE IS
OF POOR QUALITY

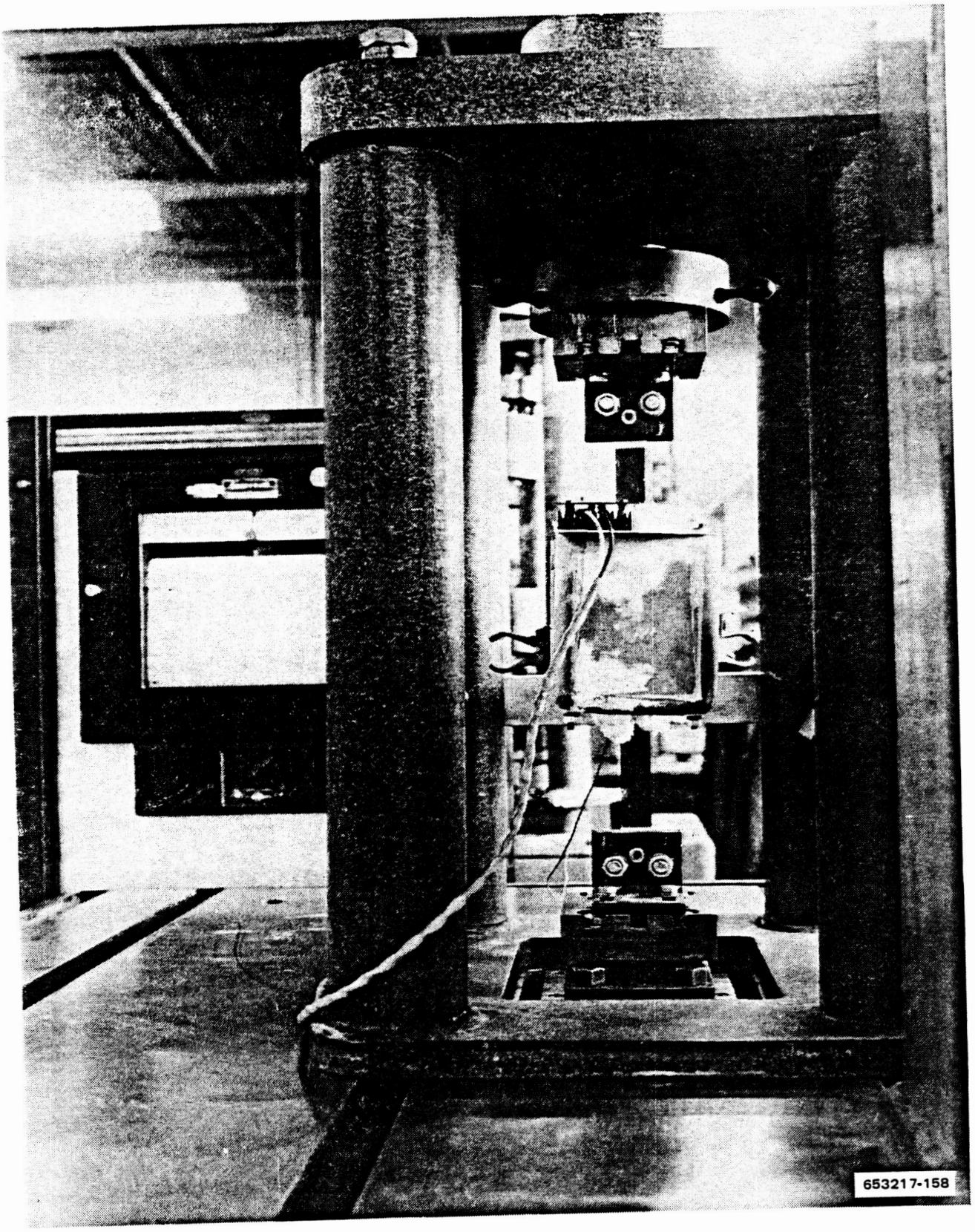



**Figure 11-4 Furnace Arrangement for R = 0.1 Fatigue Test at Elevated Temperature**



ORIGINAL PAGE IS
OF POOR QUALITY

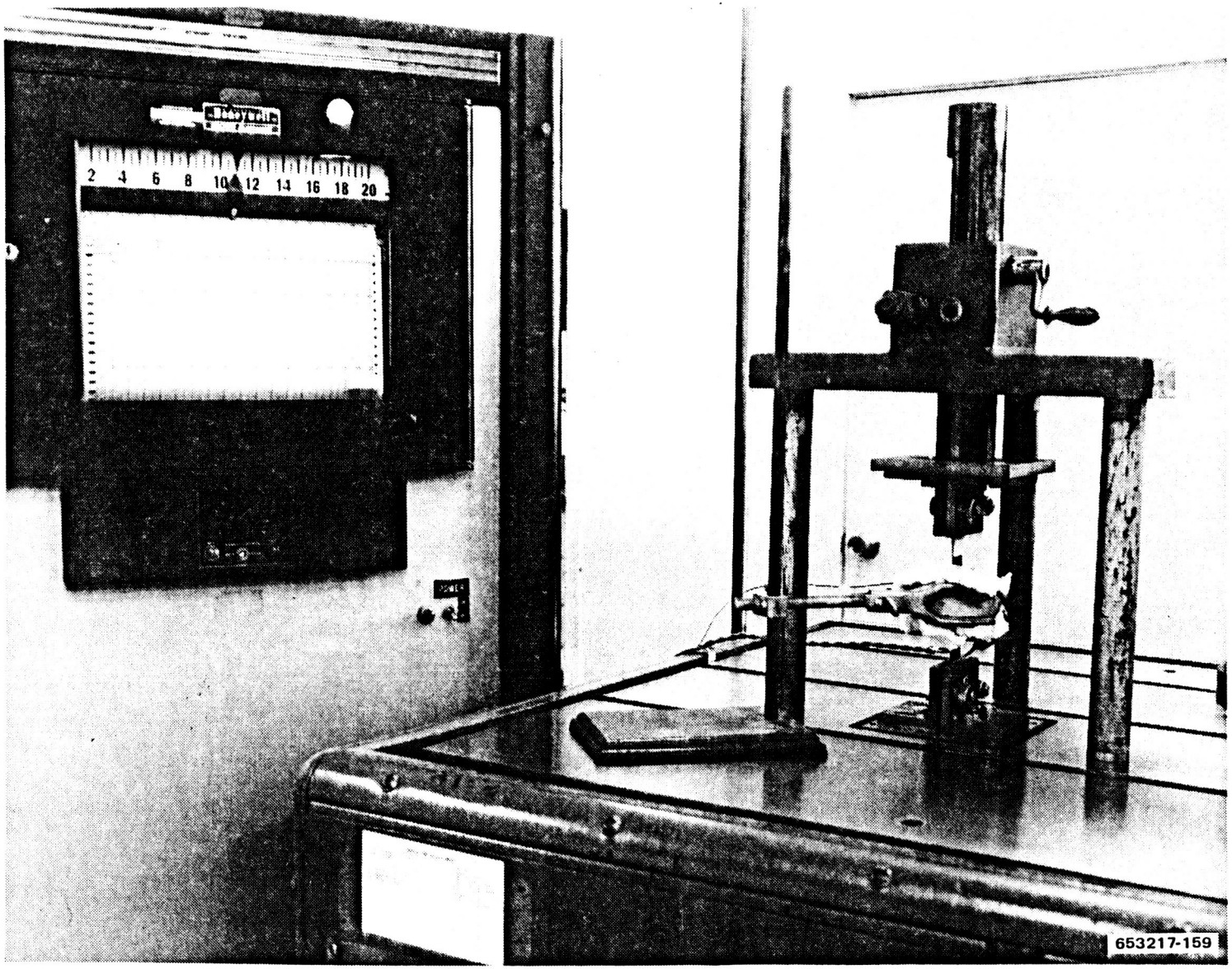



**Figure 11-5 Small Ring Furnace for Elevated Temperature Fatigue Testing**



ORIGINAL PAGE IS
OF POOR QUALITY

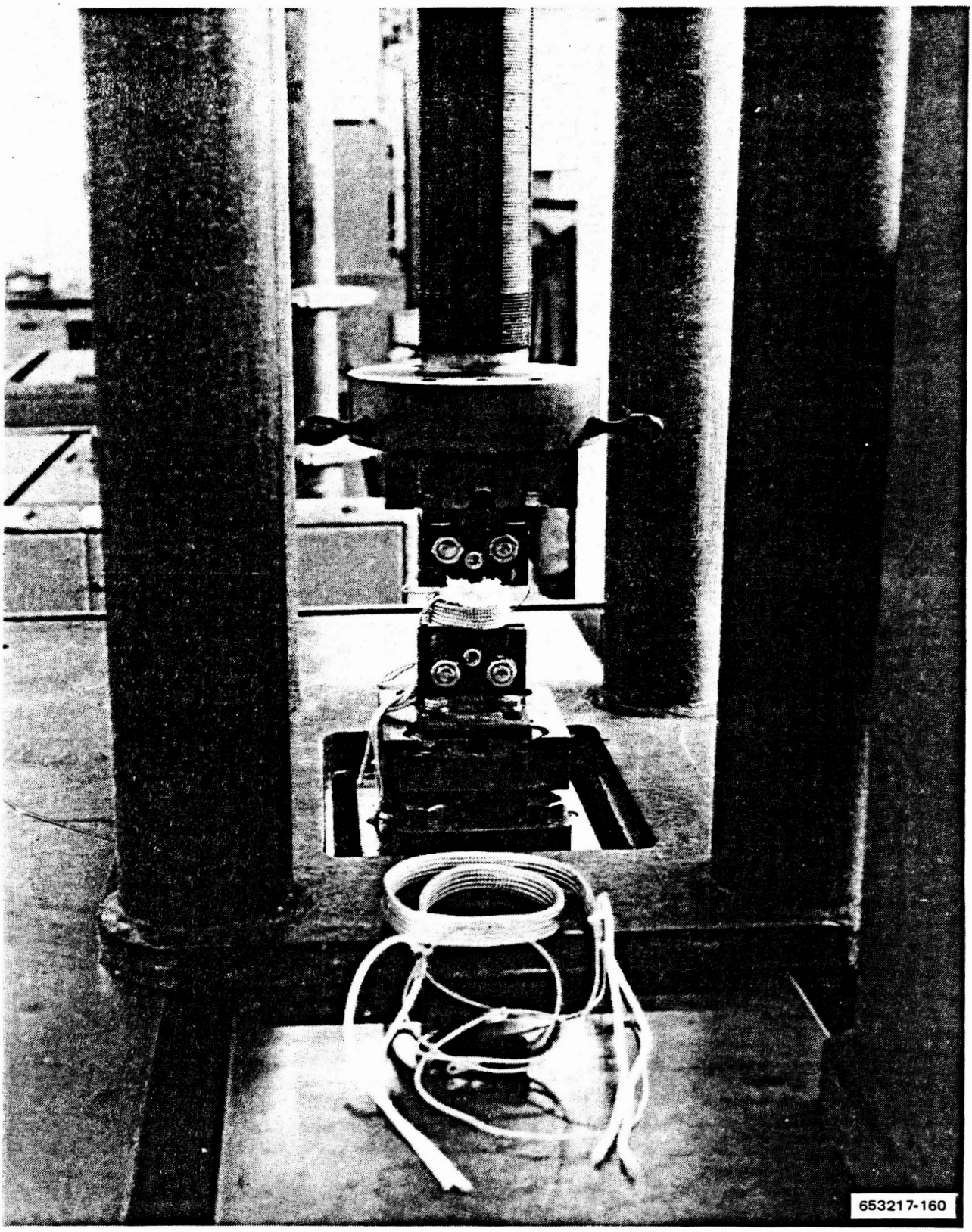



**Figure 11-6 Elevated Temperature, R = −1 Fatigue Test Setup Showing Use of Flexible Heating Tape**

ORIGINAL PAGE IS
OF POOR QUALITY

**Table 11-2. Summary of Fatigue Test Program**

| Material System | Laminate Orientation | Specimen Configuration | Number of Tests per Stress Ratio: 297 K (75° F) R = 0.1 | 10 | −1.0 | 450 K (350° F) 0.1 | 10 | −1.0 | 505 K (450° F) 0.1 | 10 | −1.0 |
|---|---|---|---|---|---|---|---|---|---|---|---|
| 5505/4 B/E | [0° ± 45°] | Unnotched | 5 | — | — | — | — | — | — | — | — |
| | | Notched | 5 | — | — | — | — | — | — | — | — |
| A-S/3501-5 G/E | [0° ± 45°] | Unnotched | 9 | — | 9 | 9 | — | 9 | — | — | — |
| | | Notched | 9 | — | 9 | 9 | — | 9 | — | — | — |
| | [0°] | Unnotched | 9 | — | 9 | 9 | — | 9 | — | — | — |
| | | Notched | 9 | — | 9 | 9 | — | 9 | — | — | — |
| HT-S/710 G/PI | [0° ± 45°] | Unnotched | 9 | — | 9 | — | — | — | 9 | — | 9 |
| | | Notched | 9 | — | 9 | — | — | — | 9 | — | 9 |
| | [0°] | Unnotched | 9 | — | 9 | — | — | — | 9 | — | 9 |
| | | Notched | 9 | — | 9 | — | — | — | 9 | — | 9 |
| Celion 6000/ LARC-160 G/PI | [0° ± 45°] | Unnotched | 9 | 9 | 9 | 9 | 9 | 9 | — | — | — |
| | | Notched | 9 | 9 | 9 | 9 | 9 | 9 | — | — | — |
| B/Al | [° ± 45°] | Unnotched | 9 | | 9 | — | | — | [a]9 | | 9 |
| | | Notched | 9 | | 9 | — | | — | [a]9 | | 9 |
| | [0°] | Unnotched | 9 | | 9 | — | | — | [a]9 | | 9 |
| | | Notched | 9 | | 9 | — | | — | [a]9 | | 9 |

[a]Test Temperature was 561 K (550°)

**Table 11-3. Axial Fatigue Data for [0° ± 45°]$_s$ B/E, R = 0.1**

| Specimen Number | Test Temperature K | (°F) | Specimen Type | Maximum MN/m$^2$ | (ksi) | Cycles | Comments |
|---|---|---|---|---|---|---|---|
| AC72-1 | 297 | 75 | Unnotched | 414 | 60 | 227,000 | |
| -2 | | | | 448 | 65 | 31,000 | |
| -3 | | | | 345 | 50 | 3,534,000 | |
| -4 | | | | 483 | 70 | 8,000 | |
| -5 | | | | 310 | 45 | 10,116,000 | Did not fail |
| AC71-4 | 297 | 75 | Notched | 345 | 50 | 10,090,000 | Did not fail |
| -5 | | | | 414 | 60 | 1,386,000 | |
| -6 | | | | 483 | 70 | <1,000 | |
| -7 | | | | 431 | 62.5 | 462,000 | |
| -8 | | | | 448 | 65 | <1,000 | |

those run at R values of 0.1. Generally, the effect of a notch (center hole) was to reduce the fatigue strength, and an increase in temperature from 297 K (75° F) to 450 K (350° F) also caused a drop in strength. Figures 11-16 and 11-17 compare the results of axial fatigue testing at room temperature and stress ratios of R = 0.1 and R = −1 for both unnotched and notched specimens. These data show the fatigue life for a stress ratio of R = −1 to be much lower than for R = 0.1. For both stress ratios, the fatigue life for notched specimens is less than for

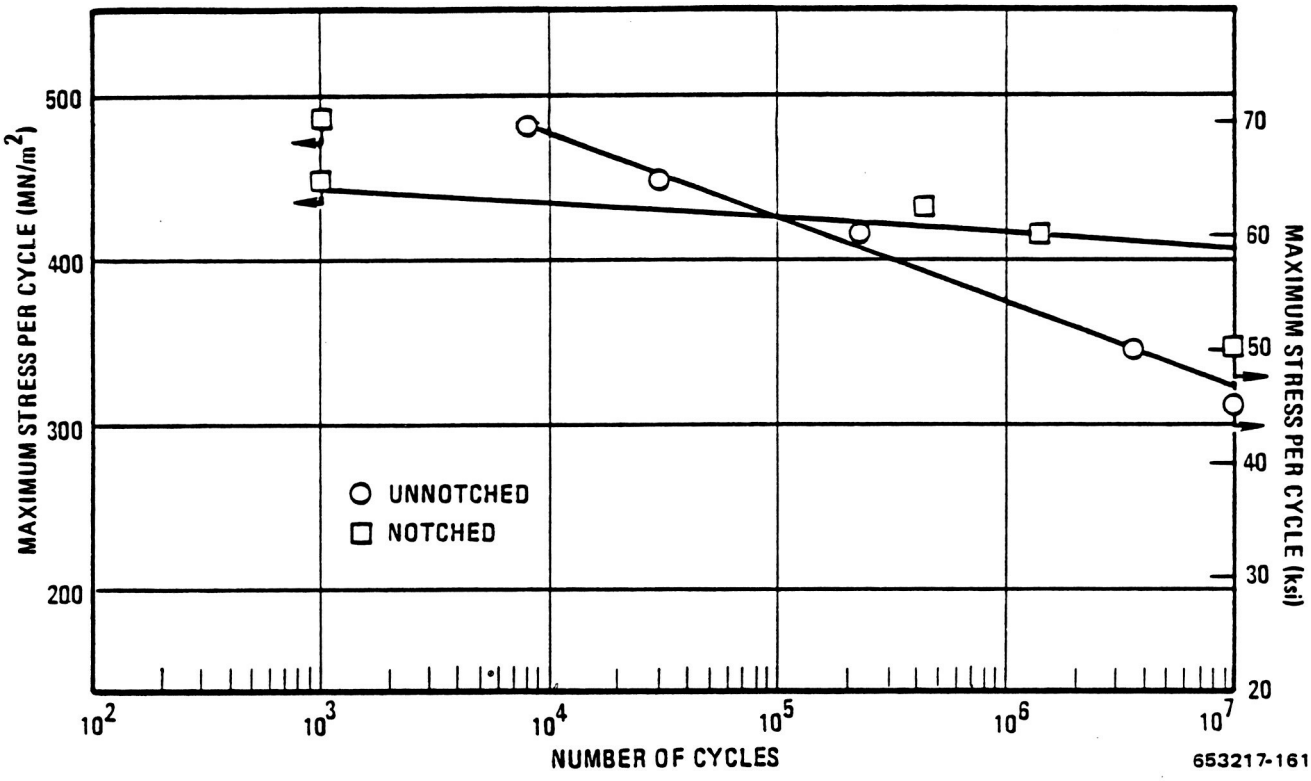



**Figure 11-7 Axial Fatigue Properties of $[0° \pm 45°]_s$ B/E at 297 K (75° F) and a Stress Ratio, R, of 0.1**

unnotched specimens except the unidirectional material tested at R = −1, where no notch effect was observed. Similar data are presented in Figures 11-18 and 11-19 for testing at 450 K (350 ° F). Again the fatigue strength is greatly reduced for the R = −1 tests compared to those conducted at a stress ratio of R = 0.1. The presence of a notch is shown to reduce the fatigue strength for the R = 0.1 tests, but not for the R = −1 tests. Further, the unidirectional notched specimens performed better than those that were unnotched. The reason for this behavior is not clearly understood at this time, but may be related to the phenomenon of crack blunting brought on by the combination of high compressive loading and a matrix softened because of elevated temperature exposure.

Two problems were experienced early in the G/E fatigue test program. The first was doubler bond failures in the room temperature, R = − 1, unnotched, crossply specimens. After the first two specimens failed, the remaining doublers were removed and rebonded using a modification of the bonding procedure and substituting a higher shear strength adhesive. These specimens gave satisfactory results. The second problem occurred with the room temperature, R = 0.1, unnotched, unidirectional specimens. Six of these nine specimens failed in the G/E but inside the doublers. These failures are thought to have been caused, in part, by nonuniform clamping pressure applied by the test machine grips because of the warped condition of the doublers. Changes in the adhesive bonding process were made to eliminate this problem in the remaining specimens.

One measure of the fatigue resistance of a material is the percent of the ultimate strength at which the fatigue limit or endurance limit (run-out) occurs. Fatigue limit is the limiting value of the stress below which a material can presumably endure an infinite number of stress cycles, i.e., the stress at which the S-N curve becomes horizontal. For certain materials and test conditions no fatigue limit occurs and some value of N (number of cycles) is chosen. Many of the S-N

Table 11-4. Axial Fatigue Data for $[0° \pm 45°]_s$ G/E, Unnotched, R = 0.1

| Specimen Number | Test Temperature K | (°F) | Maximum Stress MN/m² | (ksi) | Cycles | Comments |
|---|---|---|---|---|---|---|
| BC72-20 | 297 | 75 | 414 | 60 | 11,830,000 | |
| -21 | | | 483 | 70 | < 1,000 | |
| -22 | | | 448 | 65 | < 1,000 | |
| -23 | | | 431 | 62.5 | 12,165,000 | Did not fail |
| -24 | | | 448 | 65 | < 1,000 | |
| -25 | | | 431 | 62.5 | 340,000 | |
| -26 | | | 431 | 62.5 | < 1,000 | |
| -27 | | | 448 | 65 | 1,121,000 | |
| -28 | | | 465 | 67.5 | 10,140,000 | Did not fail |
| BC72-47 | 450 | 350 | 445 | 50 | 1,274,000 | |
| -48 | | | 276 | 40 | 10,165,000 | Did not fail |
| -49 | | | 414 | 60 | 60,000 | |
| -50 | | | 379 | 55 | 6,181,000 | |
| -51 | | | 310 | 45 | 10,000,000 | Did not fail |
| -52 | | | 396 | 57.5 | 1,000 | |
| -53 | | | 362 | 52.5 | 3,000 | |
| -54 | | | 328 | 47.5 | 10,000,000 | Did not fail |
| -55 | | | 379 | 55 | 1,000 | |

curves obtained during testing of the composites in this study were of this type. For these curves a value of $10^7$ cycles was used.

The percentages of the ultimate strengths at $10^7$ cycles have been calculated for each of the groups of G/E specimens and are listed in Table 11-12. For [0° ± 45°] crossply material tested in tension-tension fatigue, R = 0.1, the values average 86% for both room and elevated temperature and unnotched and notched configurations. Similar tests on unidirectional material averaged about 60% of the ultimate strength at $10^7$ cycles. Values for the same types of tests except for tension-compression fatigue, R = −1, were considerably lower, 34% for crossply and 28% for unidirectional. To show how these values compare to typical aircraft aluminum sheet alloys, Table 11-13 was prepared. Data were obtained (ref. 42) for 0.0023 m (0.090 in.) thick 2024-T3 and 7075-T6 aluminum alloy sheet at room temperature. For tension-tension fatigue the G/E composite is far superior to the aluminum alloys particularly for notched configurations. For tension-compression fatigue the advantage is not as great although the notched G/E is still considerably higher than either of the notched aluminum alloys. For either type of fatigue loading the G/E material is less sensitive to a notch than the aluminum alloys.

### 11.3.2 GRAPHITE/POLYIMIDE

**11.3.2.1 HT-S/710 G/PI.** A complete set of fatigue data was also obtained for the HT-S/710 G/PI system. For this material the elevated temperature selected was 505 K (450° F). The results of the numerous tests are listed in Tables 11-14 through 11-21 and individual S-N curves are plotted in Figures 11-20 through 11-27. Again, all the data points have been included in these S-N plots. These curves have been combined in Figures 11-28 through 11-31 to show the effects of the different test parameters.

Table 11-5. Axial Fatigue Data for $[0° \pm 45°]_{s2}$ G/E, Unnotched, R = −1

| Specimen Number | Test Temperature K | (°F) | Maximum Stress MN/m² | (ksi) | Cycles | Comments |
|---|---|---|---|---|---|---|
| BC72-11 | 297 | 75 | 414 | 60 | < 1,000 | |
| -12 | | | 276 | 40 | 16,000 | |
| -13 | | | 345 | 50 | 1,000 | |
| -14 | | | 310 | 45 | 3,000 | |
| -15 | | | 276 | 40 | 3,000 | |
| -16 | | | 241 | 35 | 28,000 | Bond failure |
| -17 | | | 241 | 35 | 5,000 | |
| -18 | | | 207 | 30 | 87,000 | Bond failure |
| -19 | | | 172 | 25 | 10,400,000 | |
| BC72-38 | 450 | 350 | 207 | 30 | 5,000 | |
| -39 | | | 138 | 20 | 10,159,000 | Did not fail |
| -40 | | | 172 | 25 | 15,560,000 | Did not fail |
| -41 | | | 241 | 35 | 3,000 | |
| -43 | | | 190 | 27.5 | 2,131,000 | |
| -44 | | | 207 | 30 | 38,000 | |
| -45 | | | 190 | 27.5 | 38,000 | |
| -46 | | | 172 | 25 | 10,007,000 | Did not fail |
| -47 | | | 224 | 32.5 | 9,000 | |

In like manner to the results obtained with the G/E material, the factor having the most pronounced effect on fatigue strength was the stress ratio, R. In all cases, with the other parameters identical, specimens tested in an R value of −1 gave fatigue strengths at $10^3$ cycles (determined from S-N curve) that were less than those obtained at $10^7$ cycles for specimens tested at an R value of 0.1. The effect of a notch was generally to reduce the fatigue strength but, again, there were exceptions. Notched specimen curves were higher than unnotched for both [0°] material at 297 K (75° F) and R = 0.1, Figure 11-29, and [0° ± 45°] material at 505 K (450° F) and R = 0.1, Figure 11-30. For [0°] material at 297 K (75° F) and R = −1, Figure 11-29, and at 505 K (450° F) and R = −1, Figure 11-31, the unnotched and notched curves crossed each other. The HT-S/710 G/PI fatigue data, primarily the [0°] results, showed a good deal more scatter than was found in the G/E data, and this may have contributed to the inconsistencies in the effects of a notch on HT-S/710 G/PI fatigue strength. The effect of increasing the temperature for the R = −1 tests was a slight reduction in fatigue strength. For the R = 0.1 tests both decreases and increases in fatigue properties were observed depending on the laminate orientation and the specimen configuration. Additional fatigue testing would be useful in determining the effects that a notch or an increase in test temperature contribute to the fatigue strength of HT-S/710 G/PI.

In testing one group of specimens (12 ply, unidirectional, notched, R = −1, room temperature, Table 11-21, Figure 11-27) many of the failures occurred in the composite under the bonded end doublers rather than in the test section through the center hole. This type of failure is not uncommon for unidirectional composites tested in fatigue. During fatigue cycling vertical cracks initiate at the edges of, and tangent to, the center hole, dividing the specimen into three parallel strips. Failure can then occur anywhere along the two outside load carrying strips and

Table 11-6. Axial Fatigue Data for $[0° \pm 45°]_s$ G/E, Notched, R = 0.1

| Specimen Number | Test Temperature K | (°F) | Maximum Stress MN/m² | (ksi) | Cycles | Comments |
|---|---|---|---|---|---|---|
| BC71-10 | 297 | 75 | 276 | 40 | 10,468,000 | Did not fail |
| -11 | | | 345 | 50 | <1,000 | |
| -12 | | | 310 | 45 | 12,723,000 | Did not fail |
| -13 | | | 328 | 47.5 | 10,313,000 | Did not fail |
| -14 | | | 345 | 50 | 10,116,000 | Did not fail |
| -15 | | | 379 | 55 | 15,284,000 | Did not fail |
| -16 | | | 448 | 65 | <1,000 | |
| -17 | | | 414 | 60 | <1,000 | |
| -18 | | | 396 | 57.5 | <1,000 | |
| BC71-28 | 450 | 350 | 345 | 50 | 10,006,000 | Did not fail |
| -29 | | | 362 | 52.5 | <1,000 | |
| -30 | | | 379 | 50 | <1,000 | |
| -31 | | | 310 | 45 | 13,368,000 | Did not fail |
| -32 | | | 328 | 47.5 | 10,125,000 | Did not fail |
| -33 | | | 345 | 50 | <1,000 | |
| -34 | | | 345 | 50 | 26,000 | Failed under doubler |
| -35 | | | 345 | 50 | <1,000 | |
| -36 | | | 336 | 48.75 | <1,000 | |

often is initiated at the highly stressed regions at the end doublers. The same failure mechanism was prevalent in the unidirectional B/Al specimens tested under the same conditions.

A table similar to the one presented earlier for the G/E data has been prepared to show the percentage of the HT-S/710 G/PI ultimate strengths at which the fatigue limit (or $10^7$ cycles) occurred. The results, Table 11-22, were quite similar to the G/E system except for being slightly lower in value. Tests at an R value of 0.1 give approximately 75% for the crossply material and 60% for the unidirectional material. Again, for stress ratios of −1 the values were considerably lower, 27% and 24% respectively for the crossply and unidirectional layups. In a comparison with similar data for typical aircraft aluminum sheet alloys (Table 11-13) the HT-S/710 G/PI is superior, particularly for the notched material. While the advantage is not as great as that shown by the G/E system, G/PI retains these excellent fatigue properties up to 505 K (450 ° F), well above the maximum use temperatures of either the epoxy or aluminum systems. To show the same comparison with a structural material having a higher maximum use temperature than the aluminum alloys, Table 11-23 was prepared. Data were obtained (ref. 42) for 0.0016 m (0.063 in.) thick Ti-6Al-4V titanium alloy sheet at 297 K (75 ° F) and 589 K (600 ° F). The G/PI composite is as good or better than the titanium alloy up to 505 K (450 ° F) for all comparisons except the unnotched unidirectional material tested in tension-compression fatigue. Again, data scatter in the [0 °] results may be a factor. In like manner to the G/E — aluminum alloy comparison the advantage held by the HT-S/710 G/PI over the titanium alloy is particularly evident in the notched data.

**11.3.2.2 Celion 6000/LARC-160 G/PI.** As discussed previously only [0 ° ± 45 °] crossplied specimens of the Celion 6000/LARC-160 system were evaluated in the fatigue study. However, in addition to the R = 0.1 and −1 tests a series of R = 10 tests was included. The results of the

Table 11-7. Axial Fatigue Data for $[0° \pm 45°]_{s2}$ G/E, Notched, R = −1

| Specimen Number | Test Temperature K | (°F) | Maximum Stress MN/m² | (ksi) | Cycles | Comments |
|---|---|---|---|---|---|---|
| BC71-1 | 297 | 75 | 276 | 40 | 17,000 | |
| -2 | | | 207 | 30 | 164,000 | |
| -3 | | | 138 | 20 | 282,000 | |
| -4 | | | 69 | 10 | 15,418,000 | Did not fail |
| -5 | | | 172 | 25 | 127,000 | |
| -6 | | | 241 | 35 | 24,000 | |
| -7 | | | 207 | 30 | 4,000 | |
| -8 | | | 103 | 15 | 17,308,000 | Did not fail |
| -9 | | | 121 | 17.5 | 10,500,000 | Did not fail |
| BC71-19 | 450 | 350 | 207 | 30 | 17,000 | |
| -20 | | | 172 | 25 | 1,000 | Machine malfunction |
| -21 | | | 172 | 25 | 665,000 | |
| -22 | | | 190 | 27.5 | 434,000 | |
| -23 | | | 155 | 22.5 | 12,160,000 | Did not fail |
| -24 | | | 172 | 25 | 1,689,000 | |
| -25 | | | 190 | 27.5 | 670,000 | |
| -26 | | | 207 | 30 | 89,000 | |
| -27 | | | 155 | 22.5 | 12,470,000 | Did not fail |

tests are listed in Tables 11-24 through 11-29 and S-N curves are plotted in Figures 11-32 through 11-37. Additional S-N curves have been prepared to show the effects of the various test parameters. These are shown in Figures 11-38 and 11-39. The elevated temperature selected was 450 K (350 °F), the same as that used for the flight simulation exposure testing.

The effect of stress ratio, R, is clearly shown in Figures 11-38 and 11-39. The application of compression loading during the fatigue cycle significantly lowered the fatigue properties of the Celion 6000/LARC-160 G/PI. Completely reversed, tension-compression, R = − 1, loading gave the lowest fatigue lives for each combination of specimen configuration and test temperature.

Fatigue strengths determined from the compression-compression tests, R = 10, were somewhat higher than those for R = −1 but well below those for the R = 0.1 loading. The effect of a notch was, without exception, to lower the fatigue strength of this system. The effect was moderate, ranging from 4 to 11% at room temperature and 1 to 19% at elevated temperature. Increasing the test temperature to 450 K (350 °F) generally lowered the fatigue strength. These decreases were also moderate ranging from 1 to 18% at $10^7$ cycles. Some crossover of the S-N curves for the two temperature was observed. This occurred for the R = 0.1 and −1 tests in the lower cycle regions of the S-N curves.

Some testing difficulties were experienced with two series of fatigue tests. The first was for the 6 ply, unnotched, R = 0.1, room temperature group of specimens. All failures except one occurred at the composite in the region under the bonded end doublers. Failures during tensile testing are frequently found at this location because of high gripping stresses. It is thought that the end failures did not significantly alter the S-N curve for this group of specimens. The

Table 11-8. Axial Fatigue Data for $[0°]_6$ G/E, Unnotched, R = 0.1

| Specimen Number | Test Temperature K | (°F) | Maximum Stress $MN/m^2$ | (ksi) | Cycles | Comments |
|---|---|---|---|---|---|---|
| BU72-20 | 297 | 75 | 1,030 | 150 | 42,000 | |
| -21 | | | 965 | 140 | 17,000 | Failed under doubler |
| -22 | | | 965 | 140 | 8,000 | Failed under doubler |
| -23 | | | 896 | 130 | 14,620,000 | Did not fail |
| -24 | | | 931 | 135 | 70,000 | Failed under doubler |
| -25 | | | 931 | 135 | 10,184,000 | Did not fail |
| -26 | | | 965 | 140 | 17,000 | Failed under doubler |
| -27 | | | 1,000 | 145 | 47,000 | Failed under doubler |
| -28 | | | 1,070 | 155 | 19,000 | Failed under doubler |
| BU72-47 | 450 | 350 | 965 | 140 | 1,073,000 | |
| -48 | | | 896 | 130 | 10,156,000 | Did not fail |
| -49 | | | 1,030 | 150 | 2,000 | |
| -50 | | | 1,000 | 145 | 5,000 | |
| -51 | | | 979 | 142 | 316,000 | |
| -52 | | | 948 | 137.5 | 9,482,000 | Did not fail |
| -53 | | | 983 | 142.5 | 103,000 | |
| -54 | | | 1,000 | 145 | 1,000 | |
| -55 | | | 965 | 140 | 8,548,000 | |

second problem area was for the 24 ply, unnotched, R = 10 tests at room temperature. Four of these specimens failed at the doubler bonds rather than in the composite. These bond failures were attributed to the much higher loading required because of the greater cross sectional area of the 24 ply laminates. Again, the S-N curve, Figure 11-34, is thought to be representative of this group of specimens based on the samples that failed in a conventional manner.

The fatigue data for Celion 6000/LARC-160 G/PI have been summarized in Table 11-30 by comparing the runout strength ($10^7$ cycles) with the ultimate tensile strength for the various test series. The results were very similar to those for HT-S/710 G/PI for the R = 0.1 tests and slightly better for the R = 1 tests. The same advantage over aluminum and titanium alloys held by the HT-S/710 material is also shown by Celion 6000/LARC-160 G/PI except for the somewhat lower maximum use temperature, 450 K (350 °F) versus 505 K (450 °F).

**11.3.3 BORON/ALUMINUM.** Results of the B/Al fatigue testing program are listed in Tables 11-31 through 11-38. These data have been plotted in S-N diagrams in Figures 11-40 through 11-47. The fatigue curves have also been combined in Figures 11-48 through 11-51 to show the effects of the different test parameters. The elevated temperature initially selected for testing was 561 K (550 ° F), but this was later reduced to 505 K (450 ° F) because of severe surface degradation of the aluminum. Consequently, half of the elevated temperature tests (those at R = 0.1) were conducted at 561 K (550 ° F) and the other half (R = −1) at 505 K (450 ° F).

Figures 11-48 through 11-51 again show the pronounced effect that the stress ratio, R, has on the fatigue strength. For all combinations of orientation, temperature, and specimen configuration that were evaluated, the R = −1 tests gave values well below those of R = 0.1. The

Table 11-9. Axial Fatigue Data for $[0°]_{12}$ G/E, Unnotched, R = −1

| Specimen Number | Test Temperature K | (°F) | Maximum Stress MN/m² | (ksi) | Cycles | Comments |
|---|---|---|---|---|---|---|
| BU72-11 | 297 | 75 | 620 | 90 | <1,000 | |
| -12 | | | 483 | 70 | 10,003,000 | Did not fail |
| -13 | | | 517 | 75 | 12,000 | |
| -14 | | | 448 | 65 | 3,517,000 | |
| -15 | | | 414 | 60 | 12,592,000 | Did not fail |
| -16 | | | 448 | 65 | 10,202,000 | Did not fail |
| -17 | | | 500 | 72.5 | 3,000 | |
| -18 | | | 500 | 72.5 | 19,000 | |
| -19 | | | 534 | 77.5 | 5,000 | |
| BU72-38 | 450 | 350 | 552 | 80 | <1,000 | |
| -39 | | | 379 | 55 | 75,000 | |
| -40 | | | 414 | 60 | 37,000 | |
| -43 | | | 483 | 70 | 3,000 | |
| -44 | | | 448 | 65 | 31,000 | |
| -45 | | | 345 | 50 | 307,000 | |
| -46 | | | 310 | 45 | 56,000 | |
| -1 | | | 276 | 40 | 3,215,000 | |
| -2 | | | 241 | 35 | 5,269,000 | |
| -3 | | | 207 | 30 | 10,904,000 | Did not fail |

effect of the center hole in the notched specimens, generally, was a decrease in fatigue strength. For some groups of specimens the effect was slight and for one, the unidirectional material tested at 297 K (75° F) and R = −1, the notched fatigue strength was well above the unnotched strength at the lower end of the S-N curve. The effect of raising the test temperature from 297 K (75° F) to 561 K (550° F) was to significantly reduce the fatigue strength at $10^7$ cycles. For fatigue lives of $10^5$ or less and at an R value of 0.1, the effect of temperature on fatigue life was not very great. The specimens, however, exhibited extensive surface attack in the outer aluminum layer. Because of this poor performance the R = −1 test temperature was lowered to 505 K (450° F). As shown in Figures 11-50 and 11-51 the slopes of the S-N curves for these tests were similar to those obtained at room temperature, and the fatigue strengths were only slightly lowered.

Examination of the B/Al specimens that were fatigue tested at 561 K (550° F) revealed severe degradation of the aluminum matrix material, as shown in Figures 11-52 and 11-53. The surface of the specimens showed multiple cracks and roughness caused by localized deformation. The surface appearance suggests that the degradation may have been caused by grain growth and embrittlement at the grain boundaries. A temperature gradient analysis of the hot zone of the furnace together with an examination of the degraded specimens indicated a minimum threshold temperature of 505 K (450° F) to 533 K (500° F) to cause matrix degradation. To better substantiate this, two of the specimens originally scheduled for 561 K (550° F) were fatigue tested at 505 K (450° F) under the same conditions (stress level and environment) as used on the 561 K (550° F) tests. Test data is reported in Table 11-36. Visual and metallographic

Table 11-10. Axial Fatigue Data for $[0°]_6$ G/E, Notched, R = 0.1

| Specimen Number | Test Temperature K | (°F) | Maximum Stress $MN/m^2$ | (ksi) | Cycles | Comments |
|---|---|---|---|---|---|---|
| BU71-10 | 297 | 75 | 896 | 130 | 507,000 | |
| -11 | | | 862 | 125 | 1,688,000 | |
| -12 | | | 931 | 135 | 36,000 | |
| -13 | | | 965 | 140 | 183,000 | |
| -14 | | | 879 | 127.5 | 401,000 | |
| -15 | | | 914 | 132.5 | 26,000 | |
| -16 | | | 862 | 125 | 625,000 | Failed under doubler |
| -17 | | | 845 | 122.5 | 1,116,000 | |
| -18 | | | 827 | 120 | 12,630,000 | Did not fail |
| BU71-28 | 450 | 350 | 965 | 140 | 1,000 | |
| -29 | | | 896 | 130 | 425,000 | |
| -30 | | | 827 | 120 | 55,000 | |
| -31 | | | 827 | 120 | 15,415,000 | Did not fail |
| -32 | | | 931 | 135 | 1,000 | |
| -33 | | | 862 | 125 | 1,000 | |
| -34 | | | 862 | 125 | 1,071,000 | |
| -35 | | | 879 | 127.5 | 12,143,000 | Did not fail |
| -36 | | | 914 | 132.5 | 11,050,000 | Did not fail |

examinations of the specimens revealed little or no matrix degradation at the lower temperature. The effect of environment was also briefly examined. Two fatigue tests were performed at 561 K (550° F) in an inert atmosphere (nitrogen gas for the first test and argon gas for the second one) to determine the effect, if any, on matrix degradation. The tests were run at the same temperature, stress levels, and for approximately the same number of cycles as previous tests performed in air (see Table 11-34). Visual and metallographic examinations indicated a significant decrease in matrix degradation. This implies that oxygen and/or moisture play an important role in the degradation process. One other test variable was stress level. For tests in air at 561 K (550° F) the effect was observed at all cyclic stress levels evaluated, although the number of cycles for degradation was substantially greater at the low stress levels than for the higher stress levels. A minimum threshold stress level was not determined. However, one is believed to be required since notched fatigue specimens (center hole notch) did not show matrix degradation in the unstressed areas (see Figure 11-52). Additional studies of the surface degradation problem, particularly effects of environment, should be conducted to identify the degradation mechanism and to develop solutions, e.g., protective coatings or change of matrix alloys.

A table similar to those presented earlier for both G/E and G/PI data has been prepared to show the percentage of the B/Al ultimate strengths at which the fatigue limit (or $10^7$ cycles) occurred. The results for the eight B/Al fatigue curves are presented in Table 11-39. In comparing these data with those for the organic matrix materials, several differences are apparent. For tension-compression loading the B/Al system exhibits relatively higher fatigue limits than the organic matrix systems at both room and elevated temperatures. For tension-tension

Table 11-11. Axial Fatigue Data for $[0°]_{12}$ G/E, Notched, R = −1

| Specimen Number | Test Temperature K | (°F) | Maximum Stress MN/m² | (ksi) | Cycles | Comments |
|---|---|---|---|---|---|---|
| BU71-1 | 297 | 75 | 827 | 120 | <1,000 | |
| -2 | | | 552 | 80 | 3,000 | |
| -3 | | | 483 | 70 | 10,000,000 | Did not fail |
| -4 | | | 517 | 75 | 25,000 | |
| -5 | | | 500 | 72.5 | 17,000 | |
| -6 | | | 500 | 72.5 | 35,000 | |
| -7 | | | 517 | 75 | 14,000 | |
| -8 | | | 483 | 70 | 92,000 | |
| -9 | | | 483 | 70 | 2,382,000 | |
| BU71-19 | 450 | 350 | 552 | 80 | 2,000 | |
| -20 | | | 483 | 70 | 58,000 | |
| -21 | | | 414 | 60 | 9,770,000 | |
| -22 | | | 448 | 65 | 2,000 | |
| -23 | | | 448 | 65 | 5,020,000 | |
| -24 | | | 517 | 75 | 17,000 | |
| -25 | | | 465 | 67.5 | 448,000 | |
| -26 | | | 431 | 62.5 | 10,155,000 | Did not fail |
| -27 | | | 534 | 77.5 | 12,000 | |

loading at room temperature the unidirectional B/Al data are comparable with those for G/E and G/PI while the crossply data are similar to the G/PI but lower than the G/E data. At 561 K (550° F) the B/Al was inferior to either the G/E at 450 K (350° F) or the G/PI at 505 K (450° F). In a comparison with similar data for the aluminum alloys listed in Table 11-13 the B/Al is superior. This is particularly apparent for the notched specimens. In like manner to the G/PI system, B/Al retains the excellent fatigue properties to 505 K (450° F), well above that for aluminum alloys. To show the same comparison with the Ti-6Al-4V alloy as was presented earlier for G/PI, Table 11-40 was prepared. The titanium alloy sheet data are the same as those listed in Table 11-23. With the exception of the unnotched, R = 0.1 results at 561 K (550 ° F) (surface degradation temperature) the B/Al is superior to the titanium alloy. This is particularly demonstrated by the notched fatigue data.

**11.3.4 STACKING SEQUENCE EVALUATION.** A limited program was conducted to investigate the effects of stacking sequence on the $[0° \pm 45°]_s$ family of laminates. Two systems, B/E and G/E, were evaluated. Room temperature tensile and fatigue tests (R = 0.1 were made on specimens of the following three laminate stacking sequences:

$$[0°, 45°, -45°, -45°, 45°, 0°]$$

$$[45°, 0°, -45°, -45°, 0°, 45°]$$

$$[45°, -45°, 0°, 0°, -45°, 45°]$$

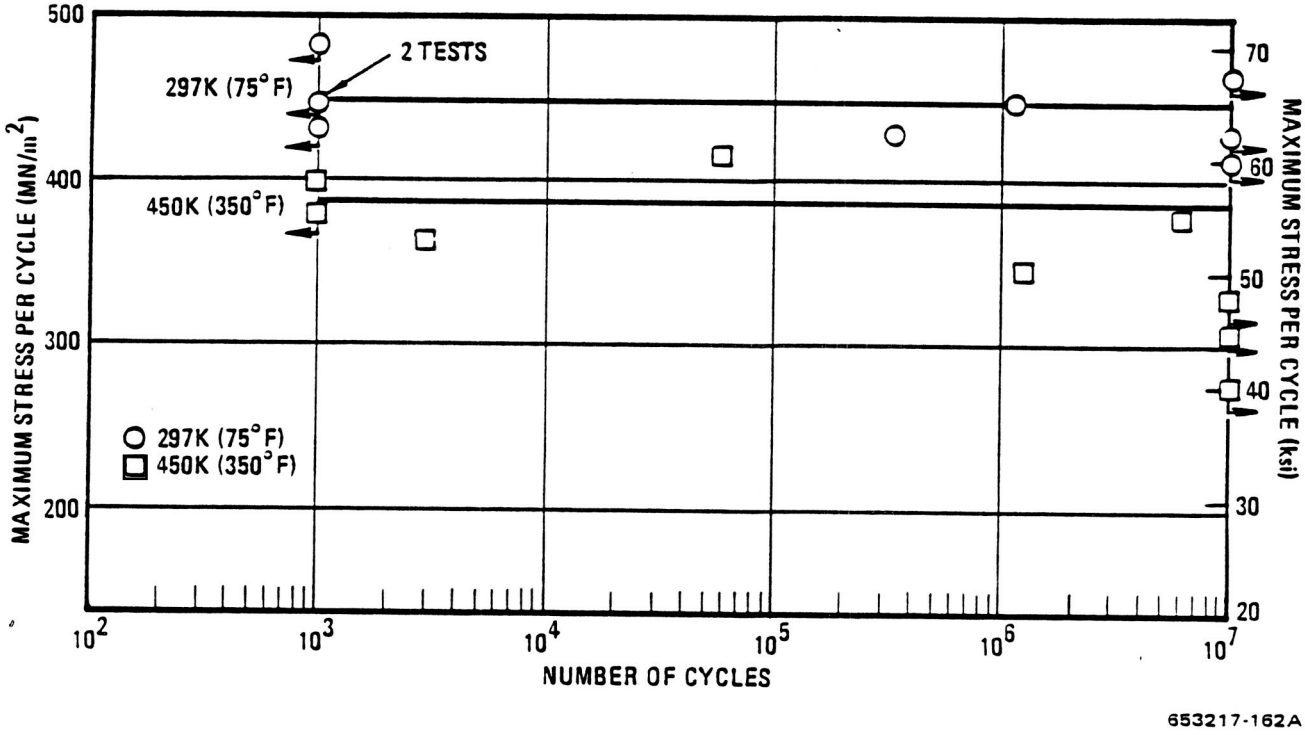



**Figure 11-8 Axial Fatigue Properties of Unnotched $[0° \pm 45°]_s$ G/E at a Stress Ratio, R, of 0.1**

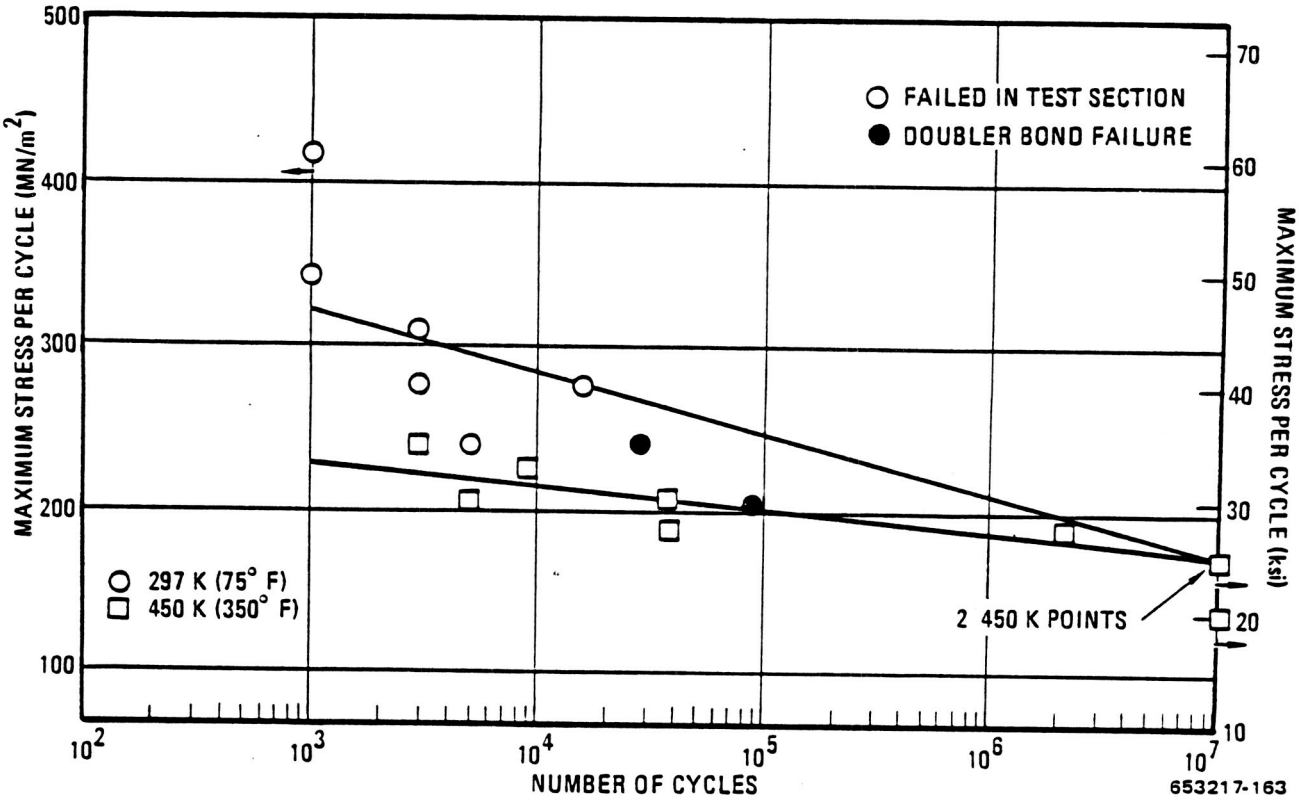



**Figure 11-9 Axial Fatigue Properties of Unnotched $[0° \pm 45°]_{s2}$ G/E at a Stress Ratio, R, of −1**

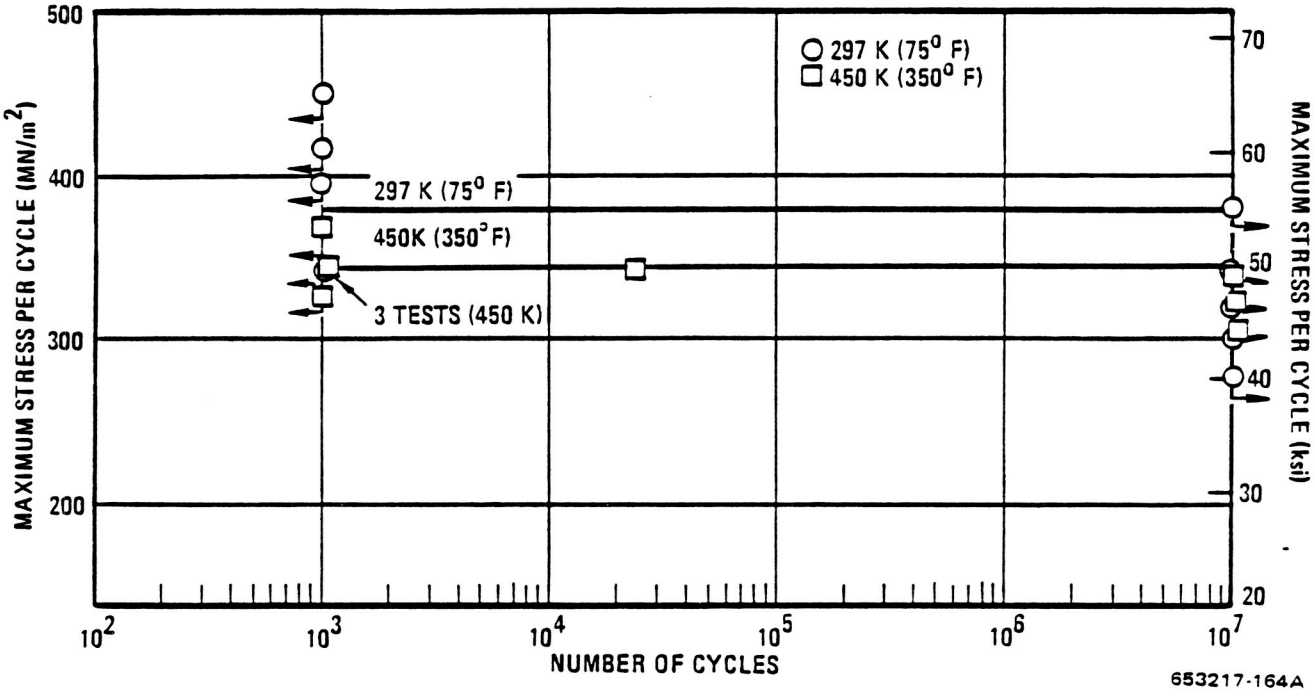



**Figure 11-10 Axial Fatigue Properties of Notched $[0° \pm 45°]_s$ G/E at a Stress Ratio, R, of 0.1**

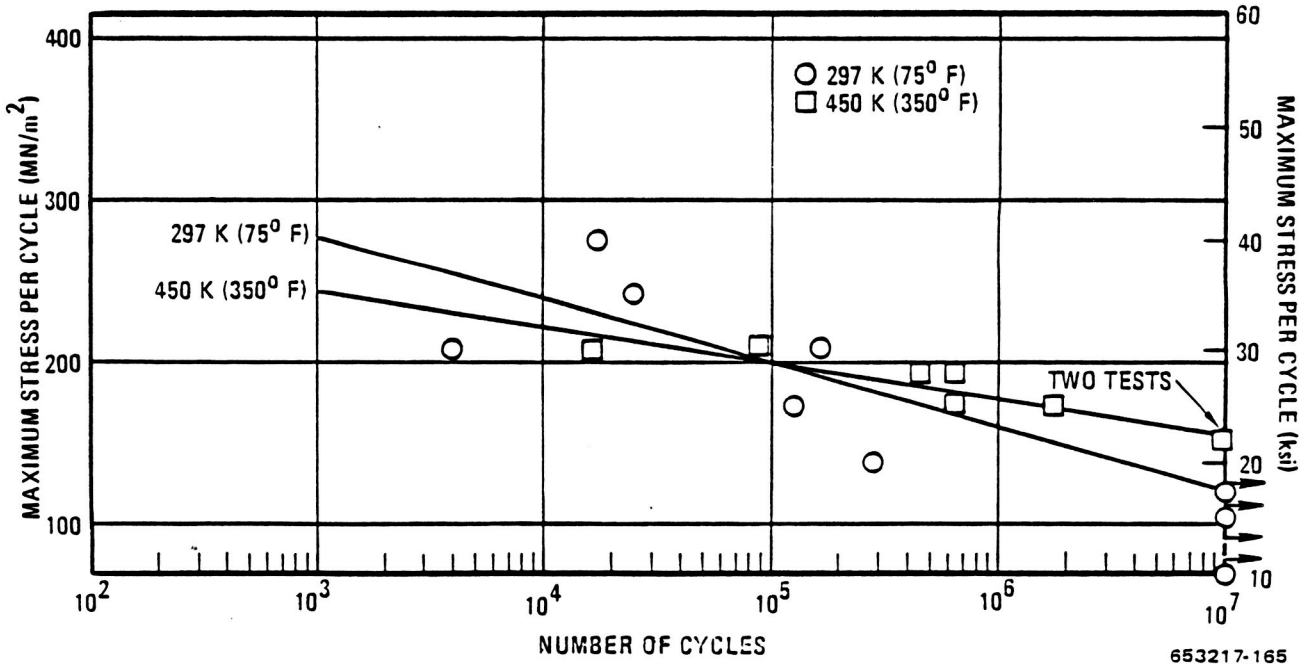



**Figure 11-11 Axial Fatigue Properties of Notched $[0° \pm 45°]_{s2}$ G/E at a Stress Ratio, R, of $-1$**

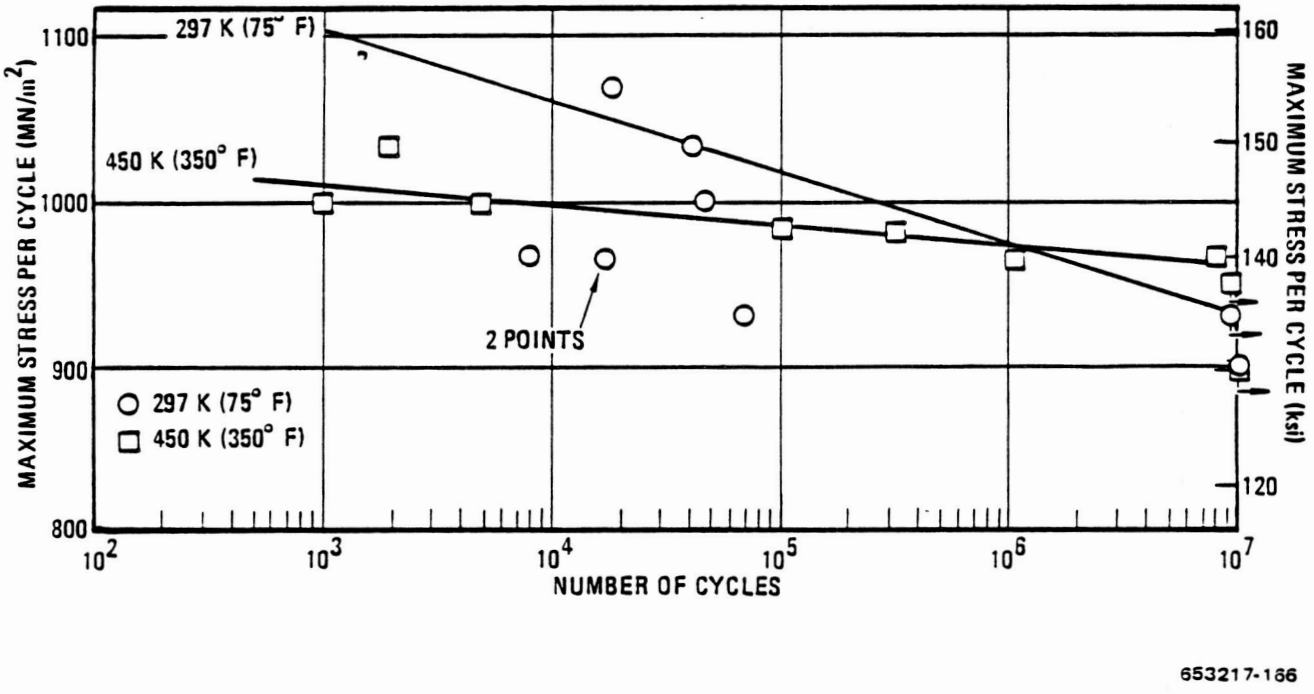



**Figure 11-12 Axial Fatigue Properties of Unnotched $[0°]_6$ G/E at a Stress Ratio, R, of 0.1**

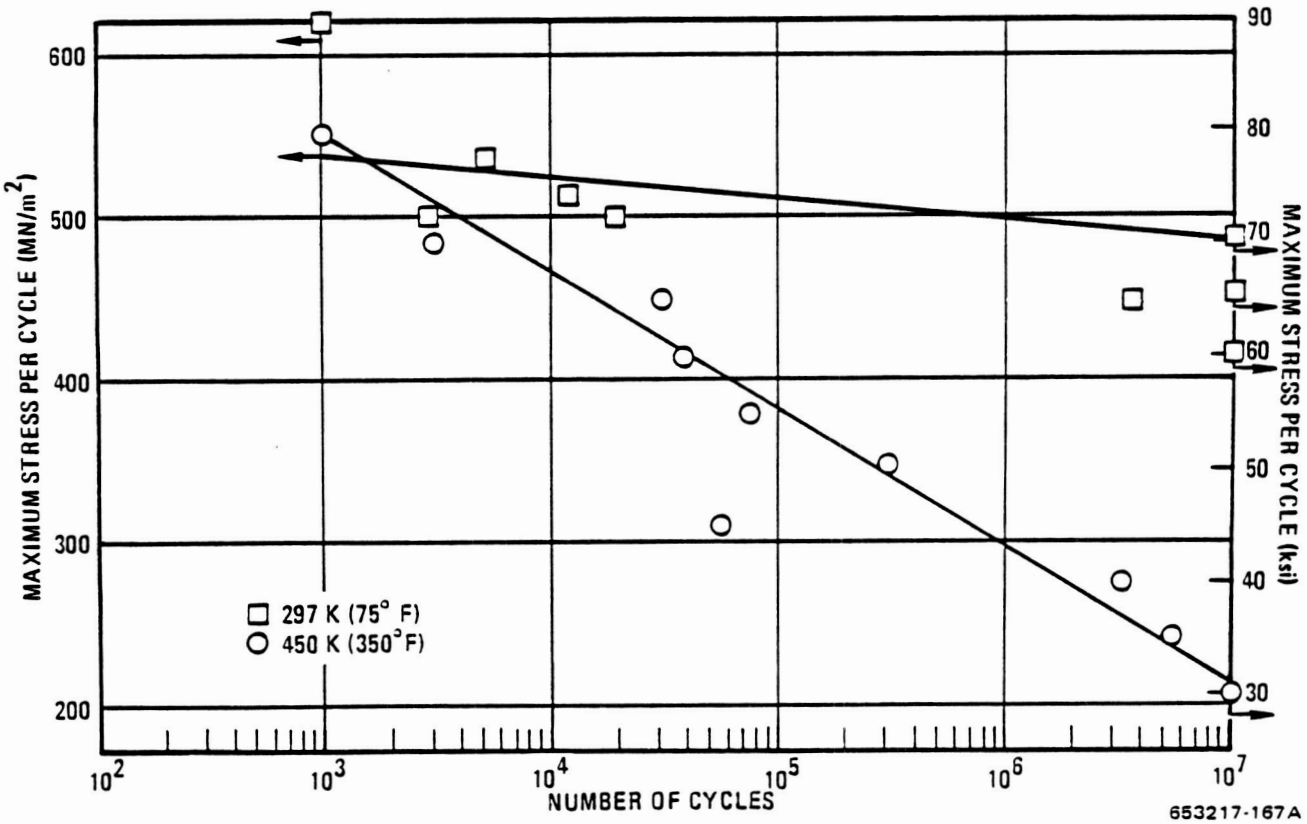



**Figure 11-13 Axial Fatigue Properties of Unnotched $[0°]_{12}$ G/E at a Stress Ratio, R, of −1**

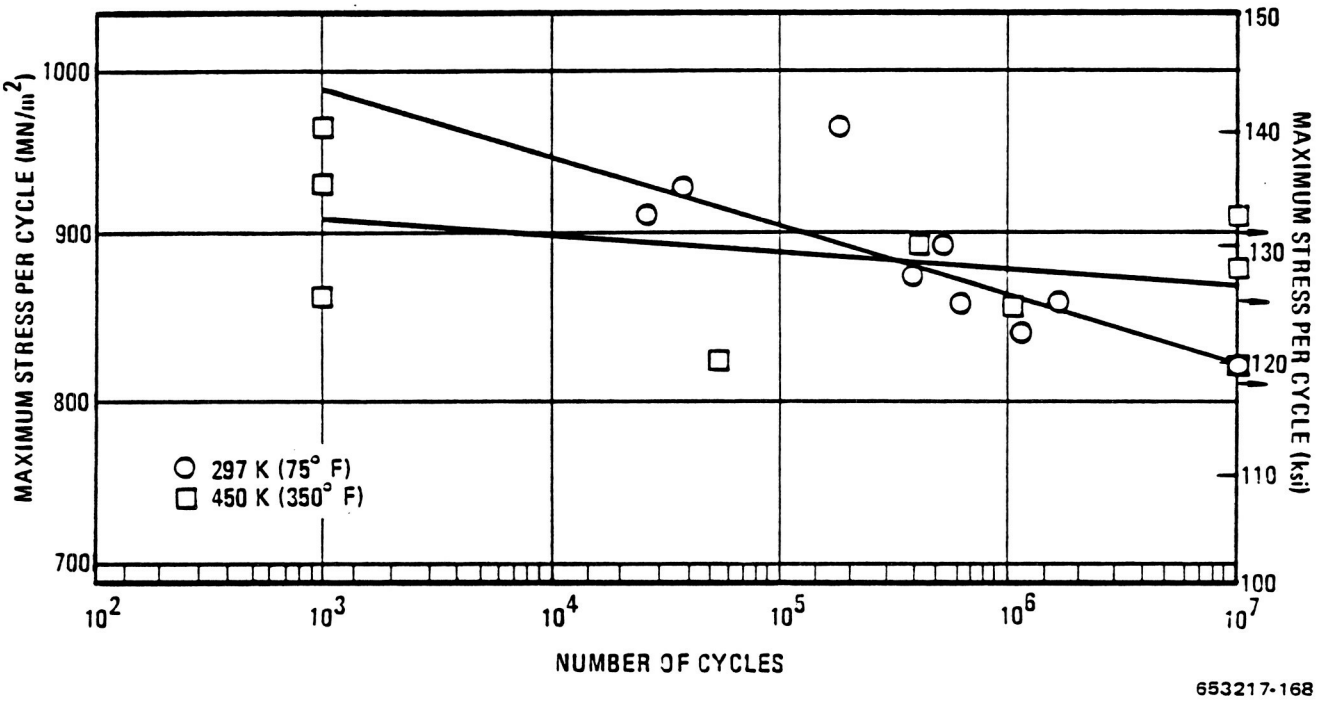



**Figure 11-14 Axial Fatigue Properties of Notched $[0°]_6$ G/E at a Stress Ratio, R, of 0.1**

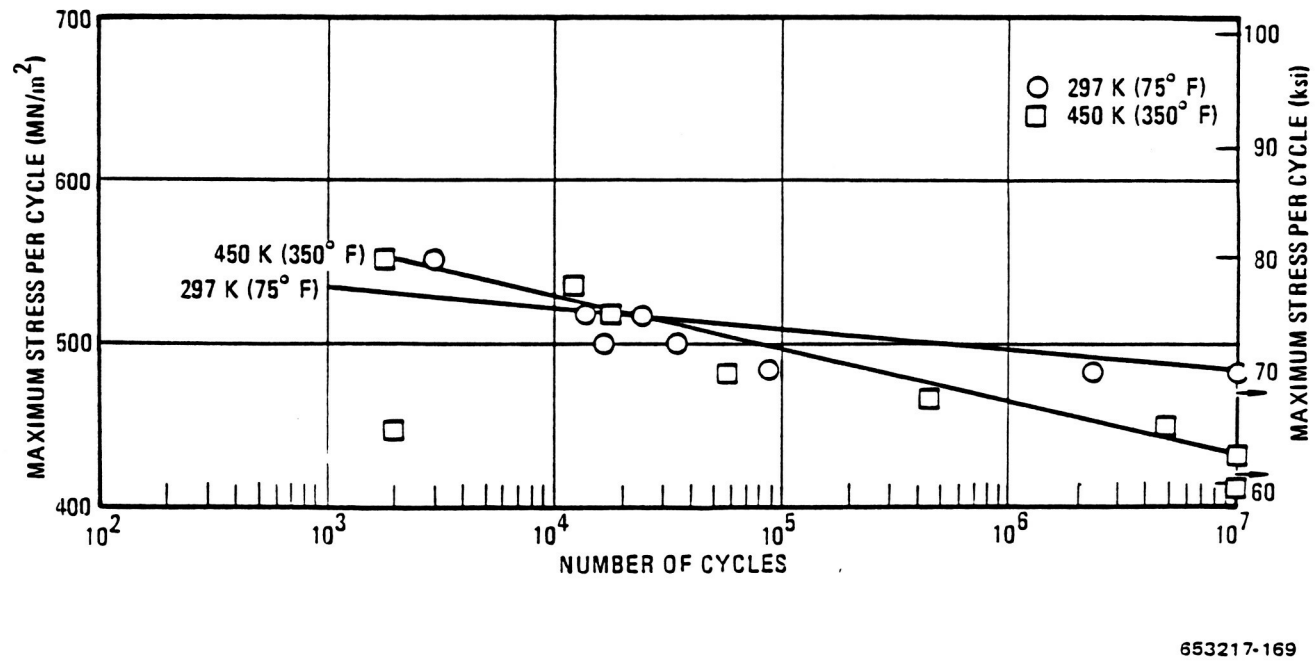



**Figure 11-15 Axial Fatigue Properties of Notched $[0°]_{12}$ G/E at a Stress Ratio, R, of −1**

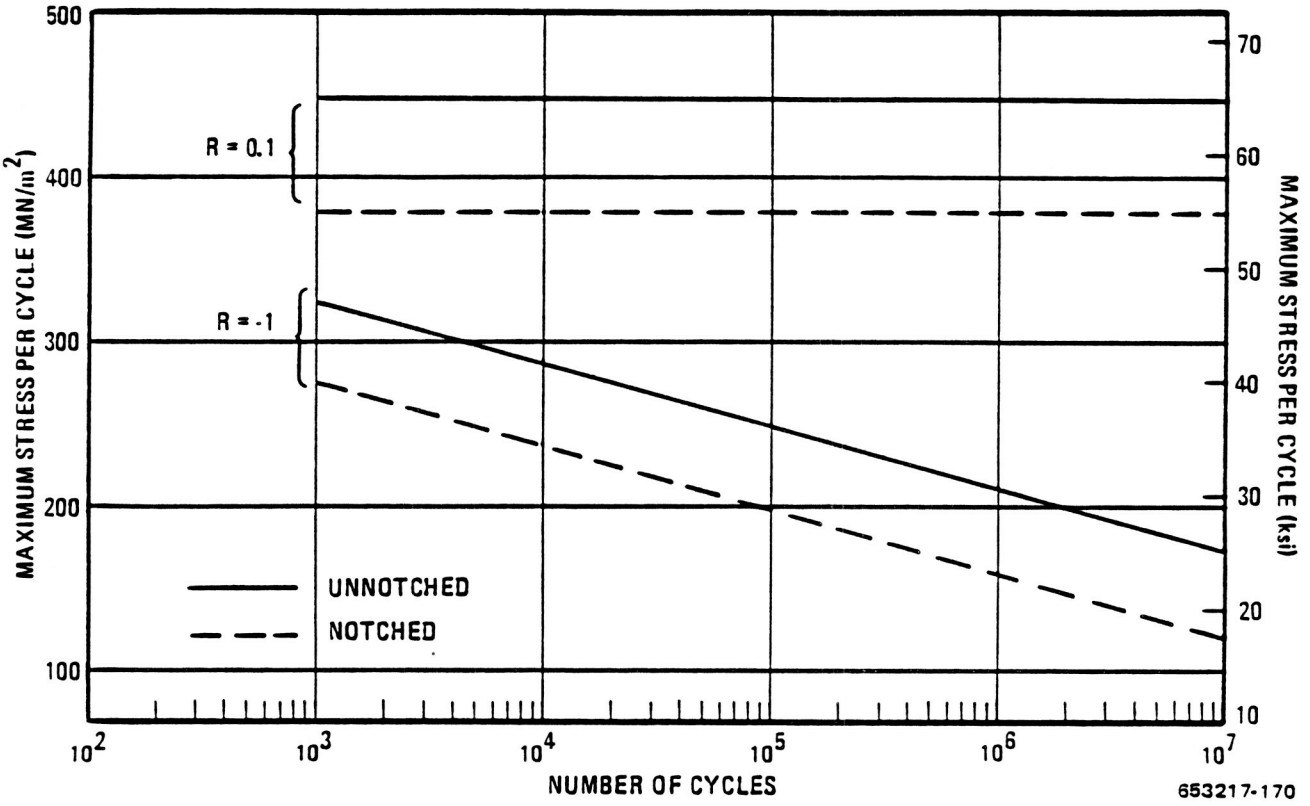



**Figure 11-16 Axial Fatigue Properties of [0° ± 45°] G/E at 297 K (75° F)**

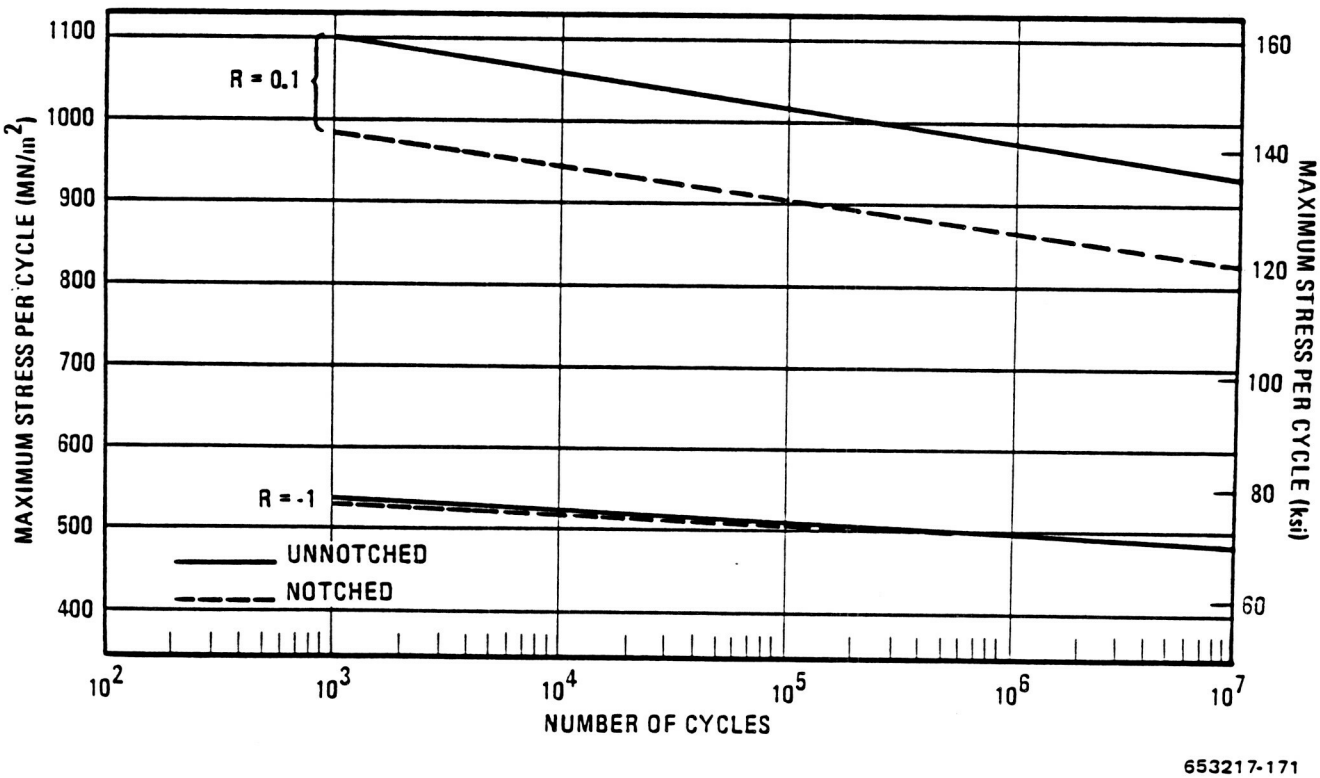



**Figure 11-17 Axial Fatigue Properties of [0°] G/E at 297 K (75° F)**

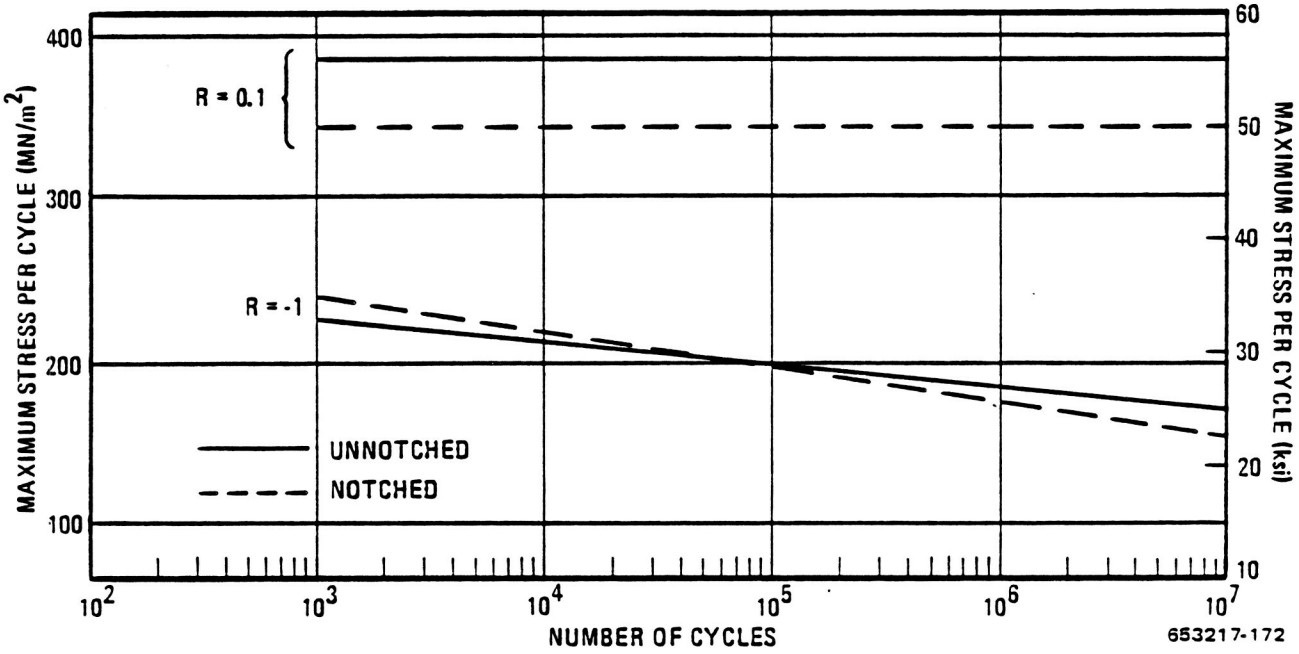



**Figure 11-18 Axial Fatigue Properties of [0° ± 45°] G/E at 450 K (350° F)**

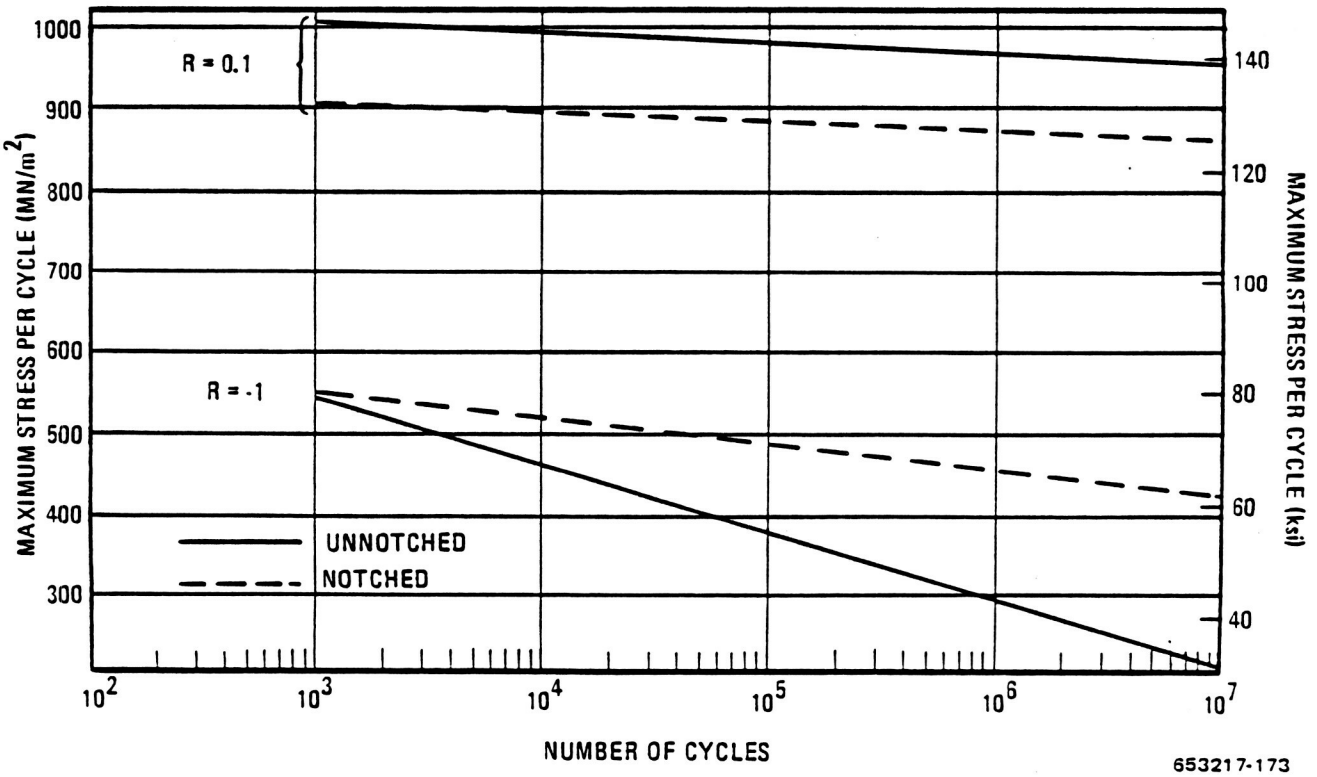



**Figure 11-19 Axial Fatigue Properties of [0°] G/E at 450 K (350° F)**

Table 11-12. Strength at Fatigue Limit or $10^7$ Cycles Expressed as Percentage of Ultimate Tensile Strength for G/E

| Orientation | Specimen Configuration | Temperature K | Temperature (°F) | R Value | Fatigue Strength at $10^7$ Cycles (%) |
|---|---|---|---|---|---|
| [0° ± 45°] | Unnotched | 297 | 75 | 0.1 | 90 |
| | Notched | 297 | 75 | .1 | 92 |
| | Unnotched | 450 | 350 | .1 | 77 |
| | Notched | 450 | 350 | .1 | 83 |
| | Unnotched | 297 | 75 | −1.0 | 35 |
| | Notched | 297 | 75 | −1.0 | 29 |
| | Unnotched | 450 | 350 | −1.0 | 34 |
| | Notched | 450 | 350 | −1.0 | 37 |
| [0°] | Unnotched | 297 | 75 | .1 | 60 |
| | Notched | 297 | 75 | .1 | 60 |
| | Unnotched | 450 | 350 | .1 | 60 |
| | Notched | 450 | 350 | .1 | 64 |
| | Unnotched | 297 | 75 | −1.0 | 31 |
| | Notched | 297 | 75 | −1.0 | 35 |
| | Unnotched | 450 | 350 | −1.0 | 13 |
| | Notched | 450 | 350 | −1.0 | 32 |

Table 11-13. Comparison of Strength at Fatigue Limit or $10^7$ Cycles Expressed as Percentage of Ultimate Tensile Strength for G/E and Two Aluminum Alloys Tested at Room Temperature

| Specimen Configuration | R Value | Fatigue Strength at $10^7$ Cycles (% of $F_{tu}$) Graphite/Epoxy [0° ± 45°] | Graphite/Epoxy [0°] | Aluminum Alloy 2024-T3 | Aluminum Alloy 7075-T6 |
|---|---|---|---|---|---|
| Unnotched | 0.1 | 90 | 60 | 49 | 47 |
| [a]Notched | .1 | 92 | 60 | 27 | 24 |
| Unnotched | −1.0 | 35 | 31 | 29 | 24 |
| [a]Notched | −1.0 | 29 | 35 | 16 | 13 |

[a]G/E, center notch, theoretical $K_t = 2.43$
Al Alloys, edge notch, $K_t = 2$

Table 11-14. Axial Fatigue Data for $[0° \pm 45°]_s$ HT-S/710 G/PI, Unnotched, R = 0.1

| Specimen Number | Test Temperature K | (°F) | Maximum Stress $MN/m^2$ | (ksi) | Cycles | Comments |
|---|---|---|---|---|---|---|
| DC72-20 | 297 | 75 | 414 | 60 | <1,000 | |
| -21 | | | 345 | 50 | 1,000 | |
| -22 | | | 276 | 40 | 5,622,000 | |
| -23 | | | 310 | 45 | 1,000 | |
| -24 | | | 293 | 42.5 | 12,045,000 | Did not fail |
| -25 | | | 310 | 45 | 10,184,000 | Did not fail |
| -26 | | | 328 | 47.5 | 3,000 | |
| -27 | | | 328 | 47.5 | 14,000 | |
| -28 | | | 328 | 47.5 | 3,000 | |
| DC72-47 | 505 | 450 | 345 | 50 | 1,000 | |
| -48 | | | 276 | 40 | 18,000 | |
| -49 | | | 207 | 30 | 10,008,000 | Did not fail |
| -50 | | | 310 | 45 | 4,000 | |
| -51 | | | 241 | 35 | 14,974,000 | |
| -52 | | | 259 | 37.5 | 10,230,000 | Did not fail |
| -53 | | | 276 | 40 | 6,764,000 | |
| -54 | | | 276 | 40 | 6,000 | Failed under doubler |
| -55 | | | 276 | 40 | 30,000 | |

Table 11-15. Axial Fatigue Data for $[0° \pm 45°]_{s2}$ HT-S/710 G/PI, Unnotched, R = −1

| Specimen Number | Test Temperature K | (°F) | Maximum Stress $MN/m^2$ | (ksi) | Cycles | Comments |
|---|---|---|---|---|---|---|
| DC72-11 | 297 | 75 | 172 | 25 | 169,000 | |
| -12 | | | 190 | 27.5 | 77,000 | |
| -13 | | | 121 | 17.5 | 10,150,000 | Did not fail |
| -14 | | | 155 | 22.5 | 15,394,000 | Did not fail |
| -15 | | | 190 | 27.5 | 20,000 | |
| -16 | | | 172 | 25 | 56,000 | |
| -17 | | | 155 | 22.5 | 4,647,000 | |
| -18 | | | 207 | 30 | 1,000 | |
| -19A | | | 138 | 20 | 1,036,000 | |
| DC72-38 | 505 | 450 | 138 | 20 | 2,908,000 | |
| -39 | | | 103 | 15 | 245,000 | |
| -40 | | | 69 | 10 | 10,004,000 | Did not fail |
| -41 | | | 172 | 25 | 58,000 | |
| -42 | | | 121 | 17.5 | 10,200,000 | Did not fail |
| -43 | | | 155 | 22.5 | 1,419,000 | |
| -44 | | | 207 | 30 | 5,000 | |
| -45 | | | 241 | 35 | <1,000 | |
| -46 | | | 190 | 27.5 | 3,000 | |

Table 11-16. Axial Fatigue Data for $[0° \pm 45°]_s$ HT-S/710 G/PI, Notched, R = 0.1

| Specimen Number | Test Temperature K | (°F) | Maximum Stress MN/m² | (ksi) | Cycles | Comments |
|---|---|---|---|---|---|---|
| DC71-10 | 297 | 75 | 310 | 45 | <1,000 | |
| -11 | | | 276 | 40 | 10,200,000 | Did not fail |
| -12 | | | 293 | 42.5 | 10,141,000 | Did not fail |
| -13 | | | 310 | 45 | <1,000 | |
| -14 | | | 302 | 43.75 | 3,000 | |
| -15 | | | 297 | 43.125 | 2,000 | |
| -16 | | | 293 | 42.5 | 10,175,000 | Did not fail |
| -17 | | | 276 | 40 | 10,288,000 | Did not fail |
| -18 | | | 297 | 43.125 | 15,370,000 | Did not fail |
| DC71-28 | 505 | 450 | 276 | 40 | 15,375,000 | Did not fail |
| -29 | | | 310 | 45 | 3,068,000 | Failed near doubler |
| -30 | | | 345 | 50 | 14,604,000 | Did not fail |
| -31 | | | 379 | 55 | <1,000 | |
| -32 | | | 362 | 52.5 | <1,000 | |
| -33 | | | 345 | 50 | 1,000 | |
| -34 | | | 345 | 50 | 117,000 | |
| -35 | | | 328 | 47.5 | 6,000 | |
| -36 | | | 310 | 45 | <1,000 | |

Table 11-17. Axial Fatigue Data for $[0° \pm 45°]_{s2}$ HT-S/710 G/PI, Notched, R = −1

| Specimen Number | Test Temperature K | (°F) | Maximum Stress MN/m² | (ksi) | Cycles | Comments |
|---|---|---|---|---|---|---|
| DC71-1 | 297 | 75 | 41 | 6 | 10,256,000 | Did not fail |
| -2 | | | 207 | 30 | <1,000 | |
| -3 | | | 138 | 20 | 462,000 | |
| -4 | | | 121 | 17.5 | 330,000 | |
| -5 | | | 103 | 15 | 3,421,000 | |
| -6 | | | 138 | 20 | 114,000 | |
| -7 | | | 172 | 25 | 1,000 | |
| -8 | | | 155 | 22.5 | 47,000 | |
| -9 | | | 86 | 12.5 | 12,532,000 | Did not fail |
| DC71-19 | 505 | 450 | 103 | 15 | 2,591,000 | |
| -20 | | | 121 | 17.5 | 1,137,000 | |
| -21 | | | 86 | 12.5 | 10,220,000 | Did not fail |
| -22 | | | 138 | 20 | 27,000 | |
| -23 | | | 155 | 22.5 | 11,000 | |
| -24 | | | 172 | 25 | 1,000 | |
| -25 | | | 129 | 18.75 | 60,000 | |
| -26 | | | 112 | 16.25 | 2,018,000 | |
| -27 | | | 95 | 13.75 | 2,569,000 | |

Table 11-18. Axial Fatigue Data for $[0°]_6$ HT-S/710 G/PI, Unnotched, R = 0.1

| Specimen Number | Test Temperature K | (°F) | Maximum Stress MN/m² | (ksi) | Cycles | Comments |
|---|---|---|---|---|---|---|
| DU72-20 | 297 | 75 | 758 | 110 | 3,000 | |
| -21 | | | 690 | 100 | 3,000 | |
| -22 | | | 620 | 90 | 17,648,000 | Did not fail |
| -23 | | | 655 | 95 | 9,000 | Bond failure |
| -24 | | | 655 | 95 | 10,290,000 | Did not fail |
| -25 | | | 672 | 97.5 | 7,000 | |
| -26 | | | 690 | 100 | 2,000 | Bond failure |
| -27 | | | 672 | 97.5 | 2,000 | |
| -28 | | | 655 | 95 | 52,000 | |
| DU72-47 | 505 | 450 | 690 | 100 | 10,180,000 | Did not fail |
| -48 | | | 758 | 110 | 12,000 | |
| -49 | | | 724 | 105 | 4,000 | |
| -50 | | | 724 | 105 | 17,256,000 | Did not fail |
| -51 | | | 741 | 107.5 | 100,000 | |
| -52 | | | 724 | 105 | 12,015,000 | |
| -53 | | | 776 | 112.5 | 3,480,000 | |
| -54 | | | 810 | 117.5 | 70,000 | |
| -55 | | | 845 | 122.5 | <1,000 | |

Table 11-19. Axial Fatigue Data for $[0°]_{12}$ HT-S/710 G/PI, Unnotched, R = −1

| Specimen Number | Test Temperature K | (°F) | Maximum Stress MN/m² | (ksi) | Cycles | Comments |
|---|---|---|---|---|---|---|
| DU72-11 | 297 | 75 | 345 | 50 | 19,000 | |
| -12 | | | 241 | 35 | 8,404,000 | Failed under doubler |
| -13 | | | 276 | 40 | 39,000 | Failed under doubler |
| -14 | | | 259 | 37.5 | 70,000 | |
| -15 | | | 207 | 30 | 10,584,000 | Did not fail |
| -16 | | | 483 | 70 | 1,000 | |
| -17 | | | 448 | 65 | <1,000 | |
| -18 | | | 379 | 55 | 22,000 | |
| -19A | | | 310 | 45 | 39,000 | Failed under doubler |
| -46 | | | 138 | 20 | 10,257,000 | Did not fail |
| DU72-38 | 505 | 450 | 276 | 40 | 1,154,000 | |
| -39 | | | 310 | 45 | 6,452,000 | |
| -40 | | | 345 | 50 | 155,000 | |
| -41 | | | 414 | 60 | <1,000 | |
| -42 | | | 379 | 55 | 7,000 | |
| -43 | | | 276 | 40 | 3,000 | |
| -44 | | | 207 | 30 | 12,232,000 | Did not fail |
| -45 | | | 293 | 42.5 | 6,000 | |

Table 11-20. Axial Fatigue Data for $[0°]_6$ HT-S/710 G/PI, Notched, R = 0.1

| Specimen Number | Test Temperature K | (°F) | Maximum Stress MN/m² | (ksi) | Cycles | Comments |
|---|---|---|---|---|---|---|
| DU71-10 | 297 | 75 | 655 | 95 | 10,160,000 | Did not fail |
| -11 | | | 724 | 105 | 10,000,000 | Did not fail |
| -12 | | | 793 | 115 | 10,175,000 | Did not fail |
| -13 | | | 862 | 125 | 685,000 | |
| -14 | | | 896 | 130 | 4,000 | |
| -15 | | | 879 | 127.5 | 1,000 | |
| -16 | | | 827 | 120 | 3,000 | |
| -17 | | | 810 | 117.5 | 634,000 | |
| -18 | | | 845 | 122.5 | 421,000 | |
| DU71-28 | 505 | 450 | 758 | 110 | 2,000 | |
| -29 | | | 620 | 90 | 58,000 | |
| -30 | | | 552 | 80 | 10,111,000 | Did not fail |
| -31 | | | 690 | 100 | 6,000 | |
| -32 | | | 586 | 85 | 9,000 | |
| -33 | | | 586 | 85 | 4,000 | |
| -34 | | | 569 | 82.5 | 3,640,000 | |
| -35 | | | 655 | 95 | 5,885,000 | |
| -36 | | | 586 | 85 | 10,,000,000 | Did not fail |

Fabrication of the test panels and preparation of the tensile and fatigue specimens were accomplished using the same procedures described in Section 5. Tensile and fatigue tests were conducted using the techniques also described earlier.

Results of the tensile tests of the three stacking sequences for each material are given in Table 11-41. The data show that the position of the 0° layers in the layup appears to influence the tensile strength of both systems. The strength is lowest with the 0° layers on the outside and increases as these layers move toward the center. The effect is small for B/E and may not be significant because of the very limited test data. Comparison of these data with the baseline data in Section 7 shows some discrepancies. The baseline B/E strengths of 619 MN/m² (89.7 ksi) for the Phase I material and 531 MN/m² (77.0 ksi) for the Phase II material fall above and below the corresponding value of 550 MN/m² (79.8 ksi) obtained for the $[0°, 45°, -45°]_s$ stacking sequence panel. While these differences are quite large for data scatter no other explanation could be found. For the G/E $[0°, 45°, -45°]_s$ stacking sequence panel the two tensile strength values fell within the wide scatter band of the baseline tensile test data for the Phase I material. The tensile modules values obtained from the stacking sequence panels showed considerable variation among the three layups of the G/E material and for both materials even more variation from the baseline values of Table 7-3 and 7-5. The baseline values were obtained from strain gage measurements, which have generally been more reliable than the extensometer method used on the stacking sequence specimens. The large variation of modulus with stacking sequence for G/E would not be expected and is thought to be the result of extensometer errors.

Table 11-21. Axial Fatigue Data for $[0°]_{12}$ HT-S/710 G/PI, Notched, R = −1

| Specimen Number | Test Temperature K | (°F) | Maximum Stress MN/m² | (ksi) | Cycles | Comments |
|---|---|---|---|---|---|---|
| DU71-1 | 297 | 75 | 83 | [a]12 | 10,268,000 | Did not fail |
| -2 | | | 110 | [a]16 | 15,377,000 | Did not fail |
| -3 | | | 414 | 60 | 2,000 | Failed under doubler |
| -4 | | | 345 | 50 | 12,000 | Failed under doubler |
| -5 | | | 310 | 45 | 1,443,000 | Failed under doubler |
| -6 | | | 328 | 47.5 | 3,000 | Failed under doubler |
| -7 | | | 379 | 55 | 25,000 | Failed near doubler |
| -8 | | | 345 | 50 | 12,000 | Failed under doubler |
| -9 | | | 414 | 60 | 1,068,000 | |
| DU71-19 | 505 | 450 | 483 | 70 | <1,000 | |
| -20 | | | 345 | 50 | 7,000 | |
| -21 | | | 414 | 60 | 2,000 | |
| -22 | | | 276 | 40 | 1,893,000 | |
| -23 | | | 310 | 45 | 6,000 | |
| -24 | | | 241 | 35 | 3,867,000 | |
| -25 | | | 207 | 30 | 10,149000 | Did not fail |
| -26 | | | 310 | 45 | 10,021,000 | Did not fail |
| -27 | | | 345 | 50 | 10,173,000 | Did not fail |

[a]Low stress levels were the result of an error in calculating the fatigue machine loads.

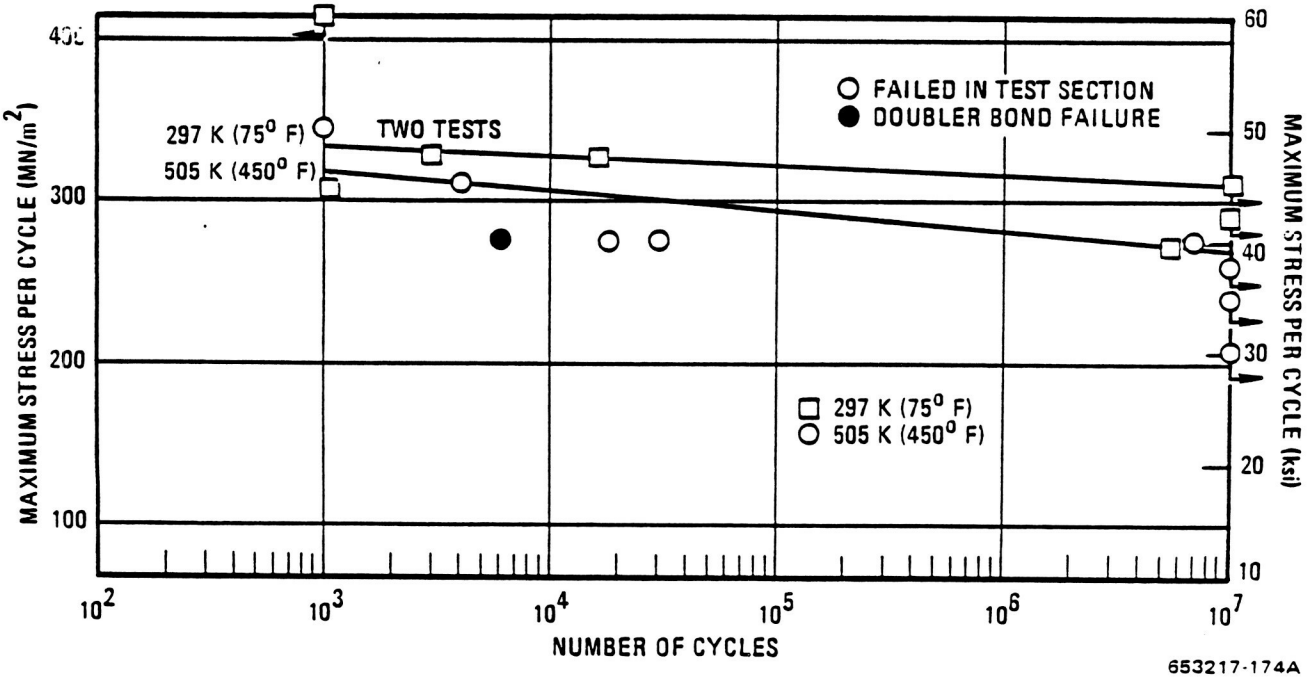



Figure 11-20 Axial Fatigue Properties of Unnotched $[0° \pm 45°]_s$ HT-S/710 G/PI at a Stress Ratio, R, of 0.1

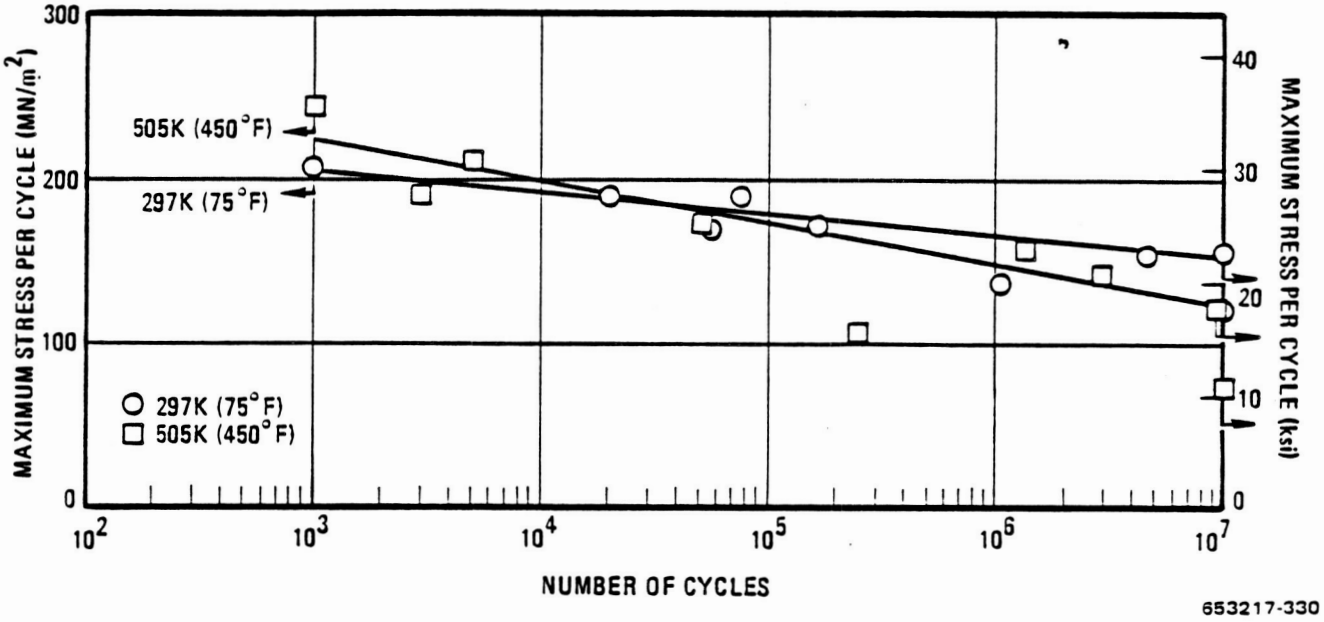



**Figure 11-21 Axial Fatigue Properties of Unnotched $[0° \pm 45°]_{s2}$ HT-S/710 G/PI at a Stress Ratio, R, of −1**

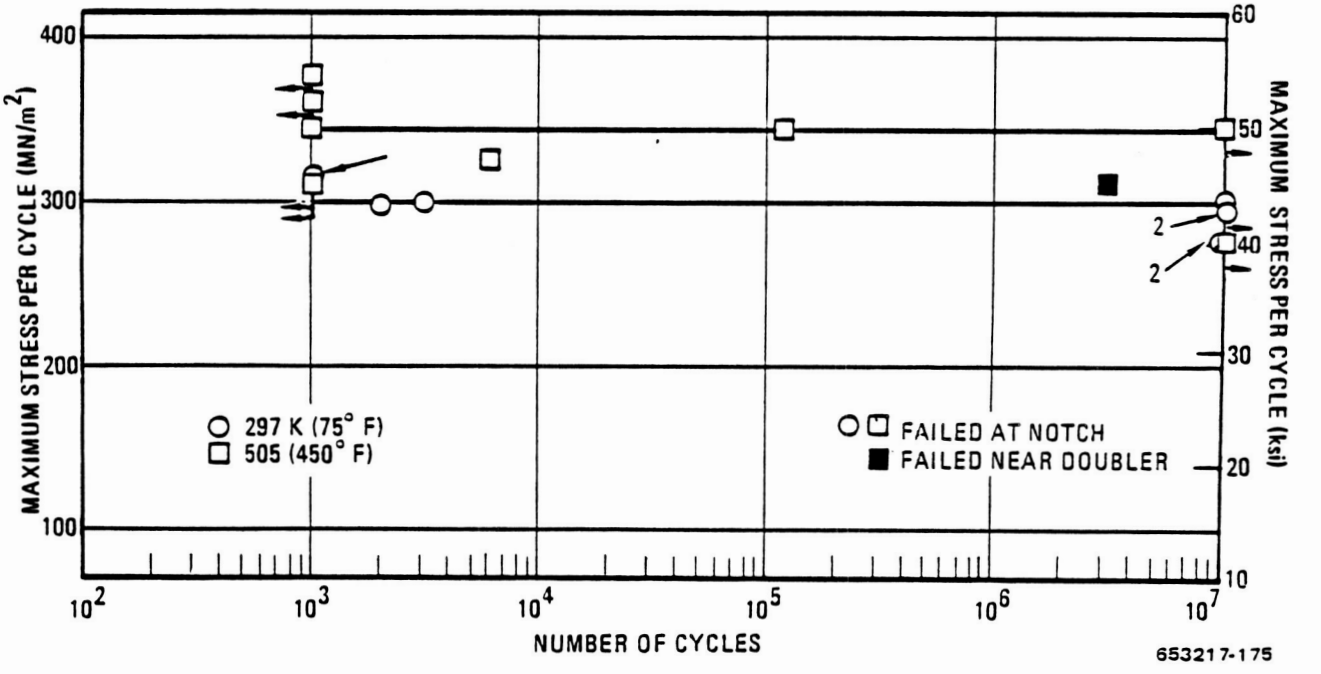



**Figure 11-22 Axial Fatigue Properties of Notched $[0° \pm 45°]_s$ HT-S/710 G/PI at a Stress Ratio, R, of 0.1**

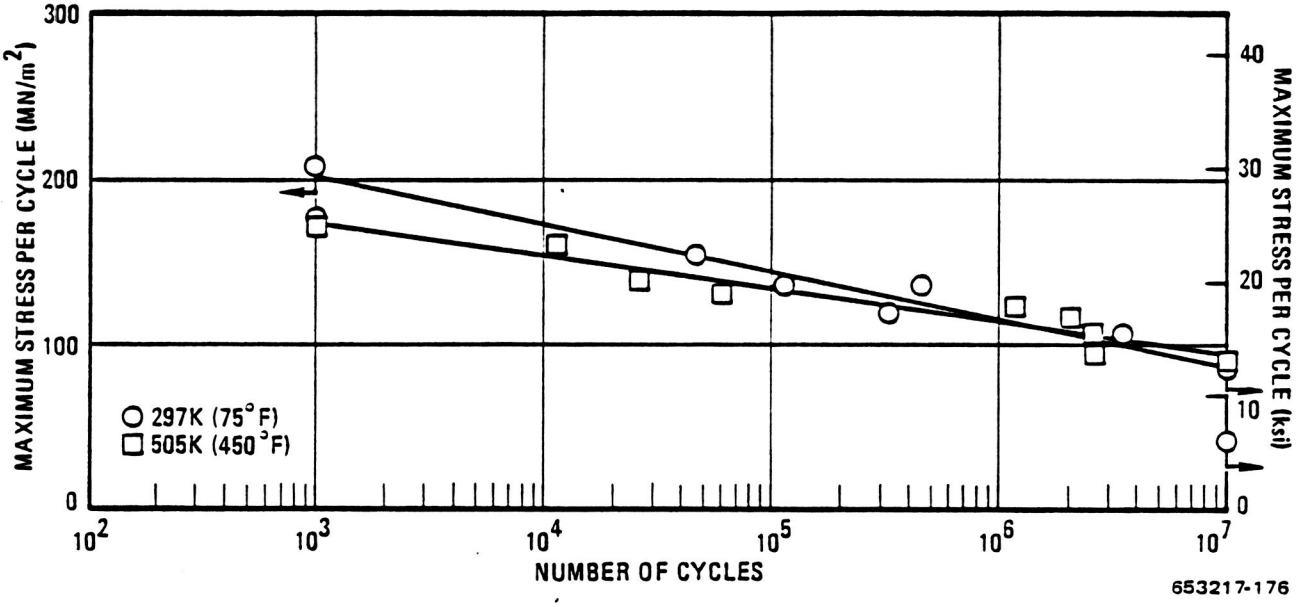



**Figure 11-23 Axial Fatigue Properties of Notched $[0° \pm 45°]_{s2}$ HT-S/710 G/PI at a Stress Ratio, R, of −1**

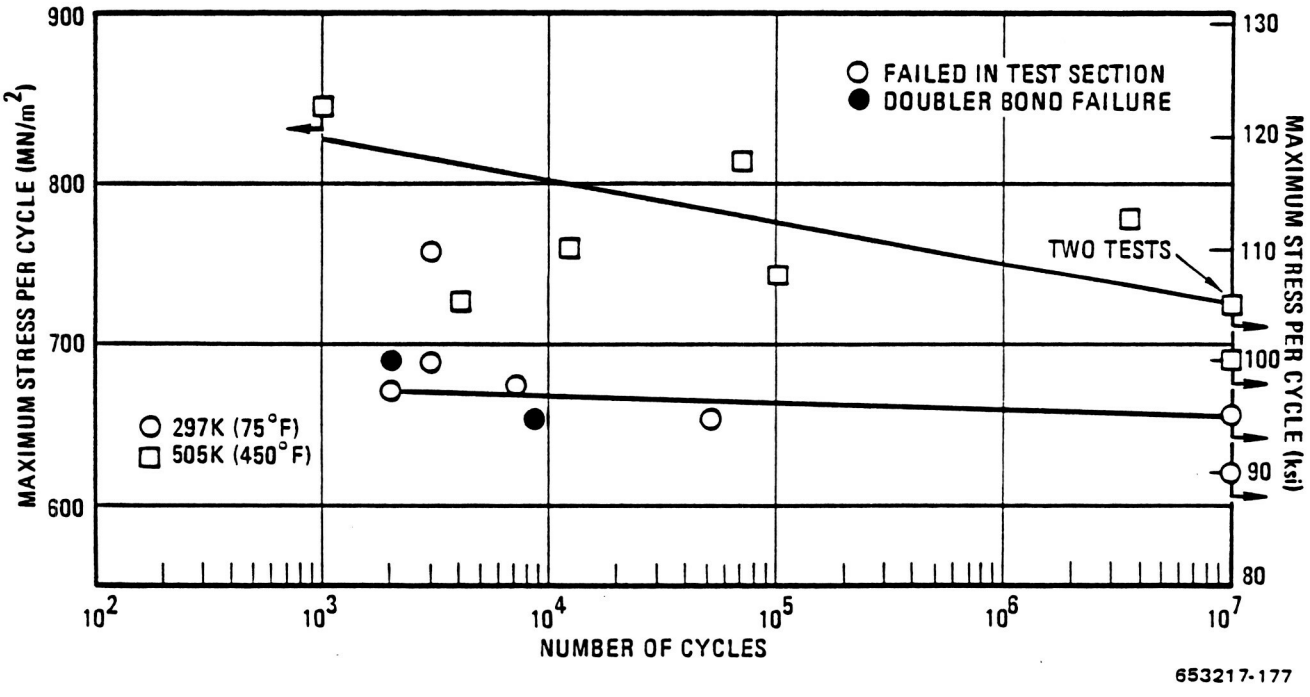



**Figure 11-24 Axial Fatigue Properties of Unnotched $[0°]_6$ HT-S/710 G/PI at a Stress Ratio, R, of 0.1**

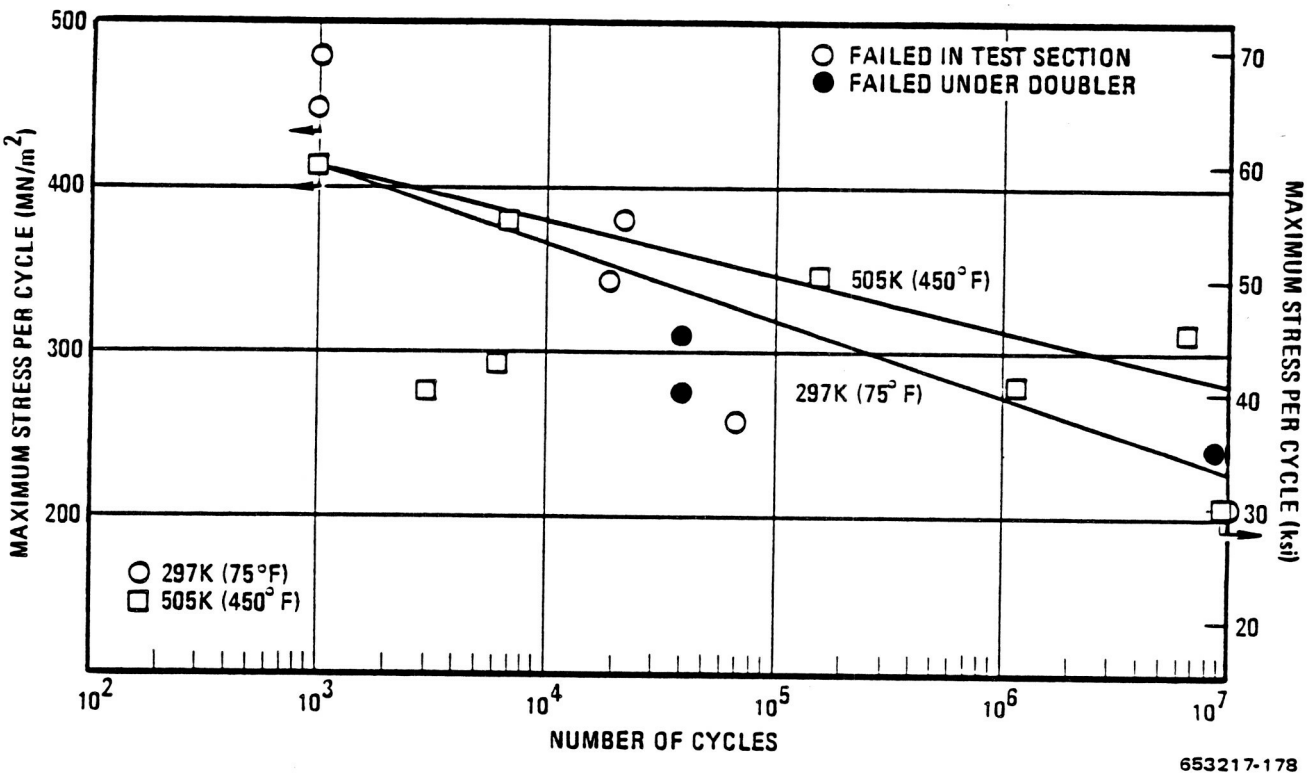



**Figure 11-25 Axial Fatigue Properties of Unnotched $[0°]_{12}$ HT-S/710 G/PI at a Stress Ratio, R, of −1**

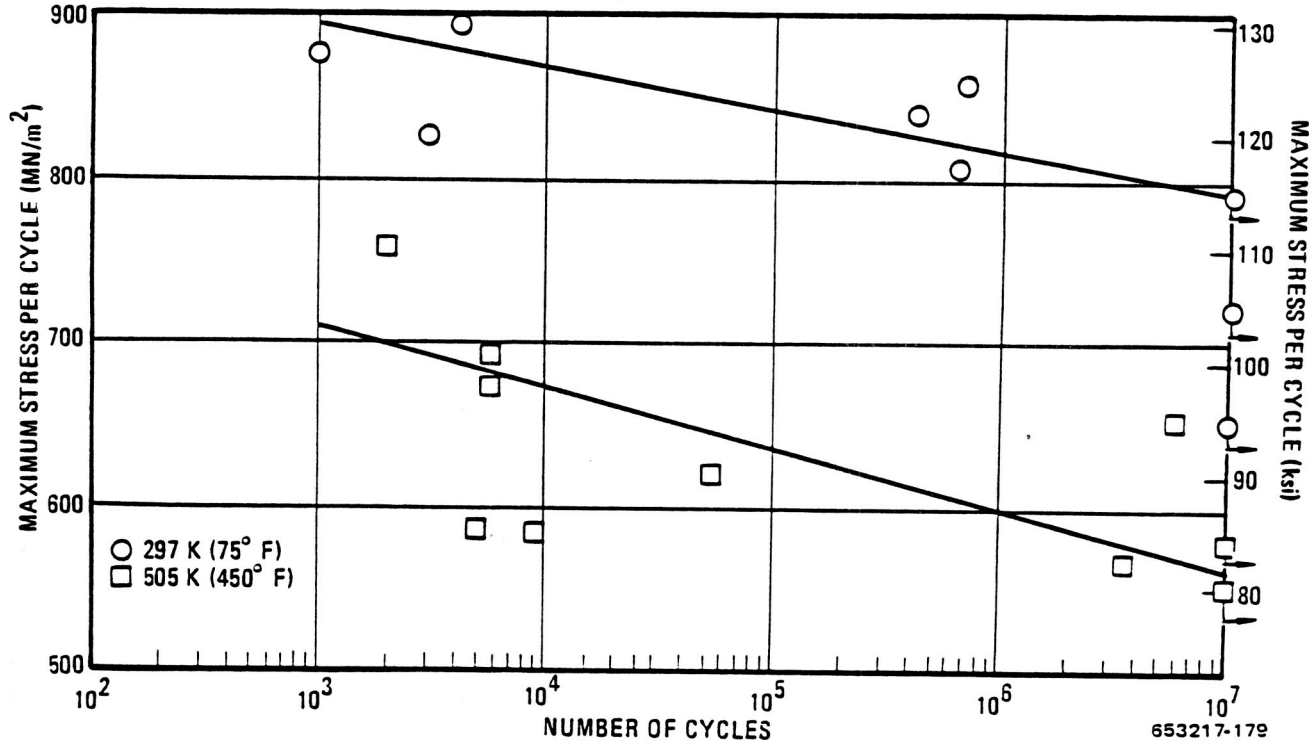



**Figure 11-26 Axial Fatigue Properties of Notched $[0°]_6$ HT-S/710 G/PI at a Stress Ratio, R, of 0.1**

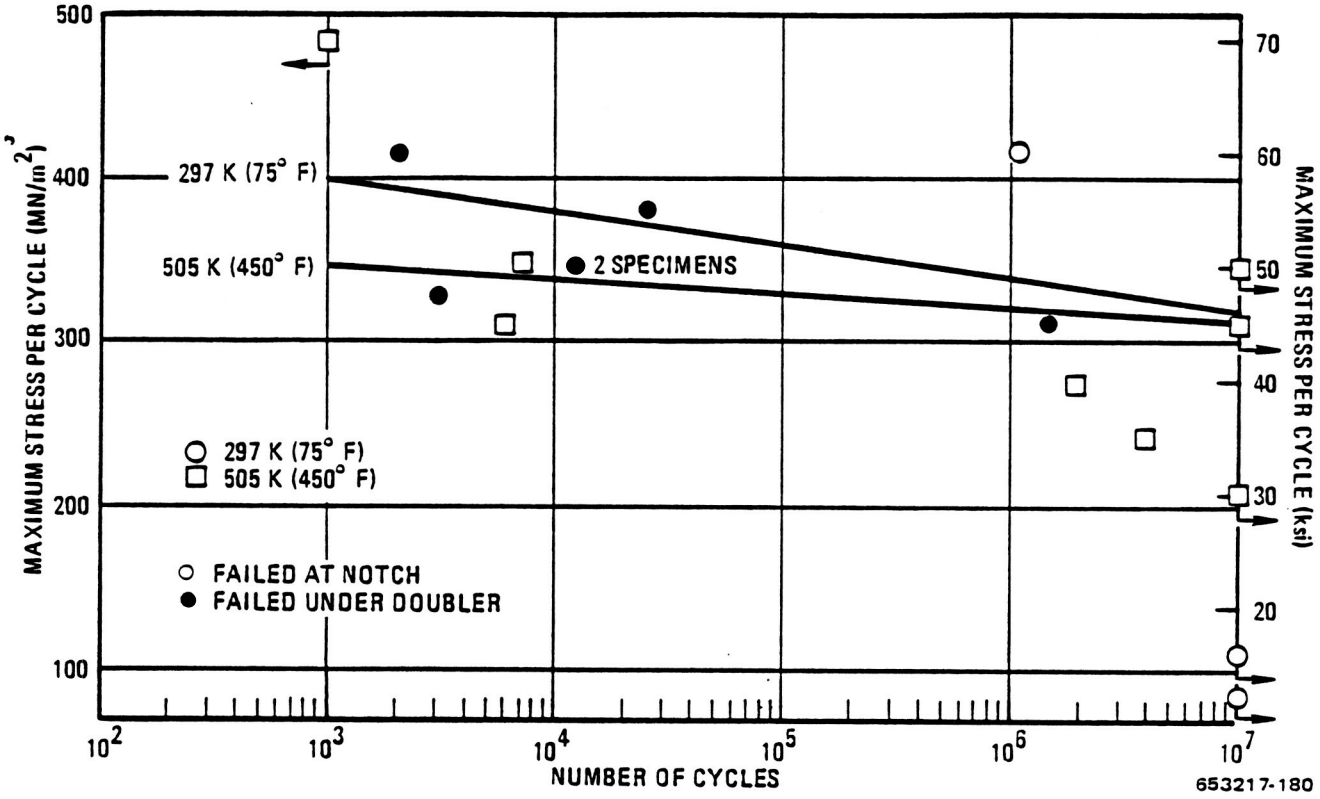



**Figure 11-27 Axial Fatigue Properties of Notched $[0°]_{12}$ HT-S/710 G/PI at a Stress Ratio, R, of −1**

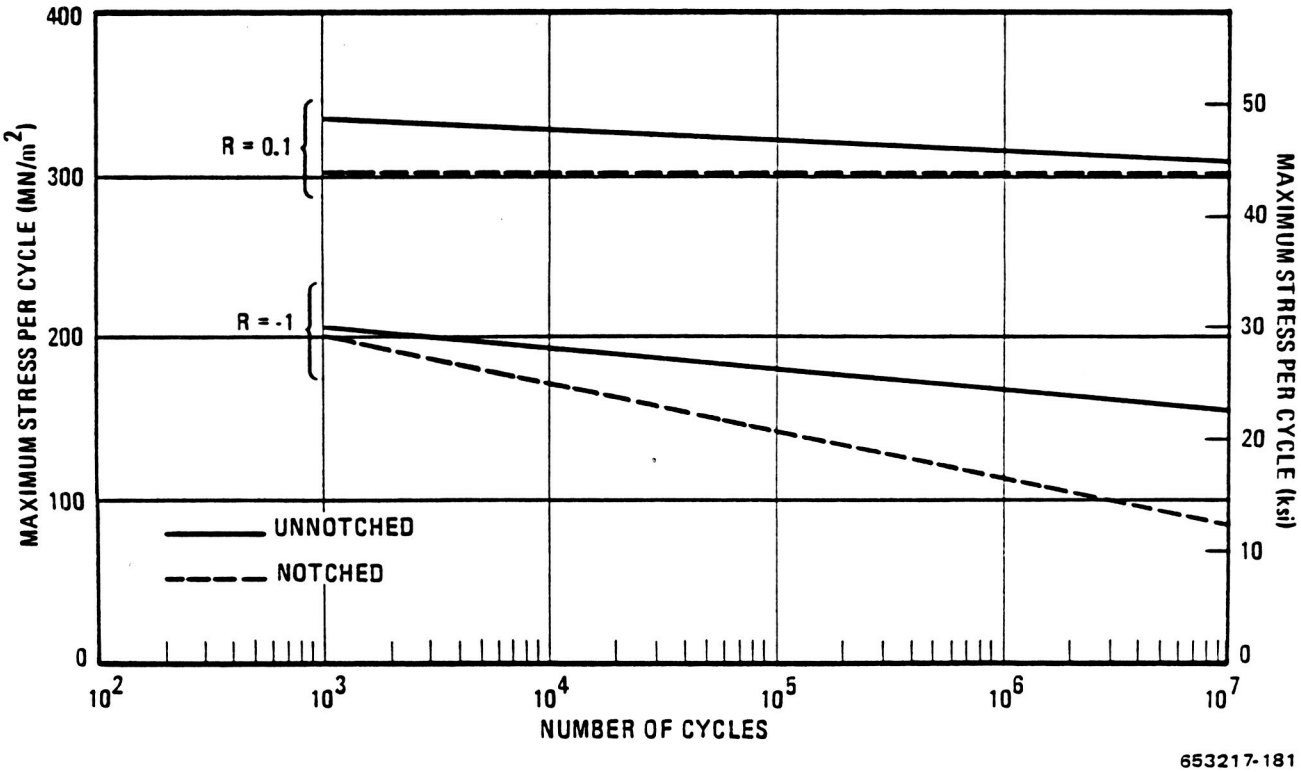



**Figure 11-28 Axial Fatigue Properties of [0° ± 45°] HT-S/710 G/PI at 297 K (75° F)**

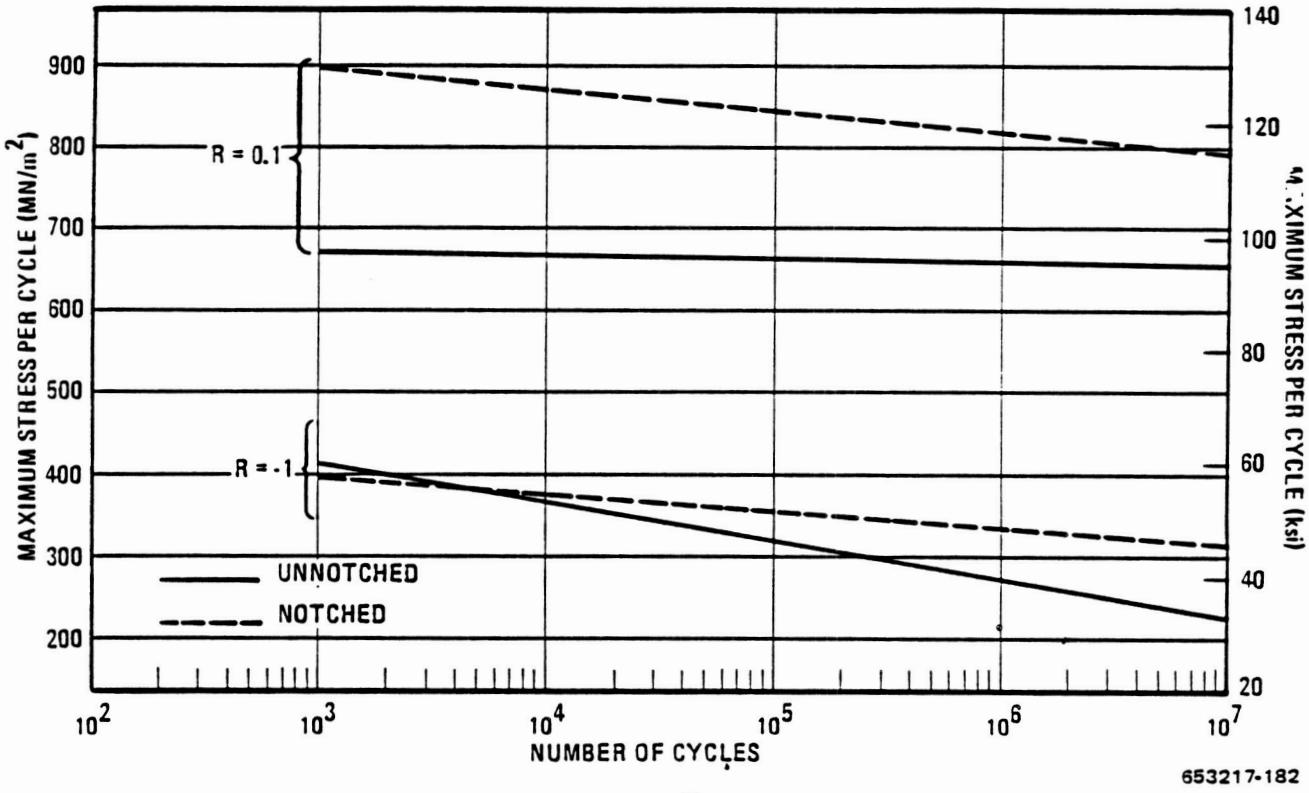



**Figure 11-29 Axial Fatigue Properties of [0°] HT-S/710 G/PI at 297 K (75° F)**

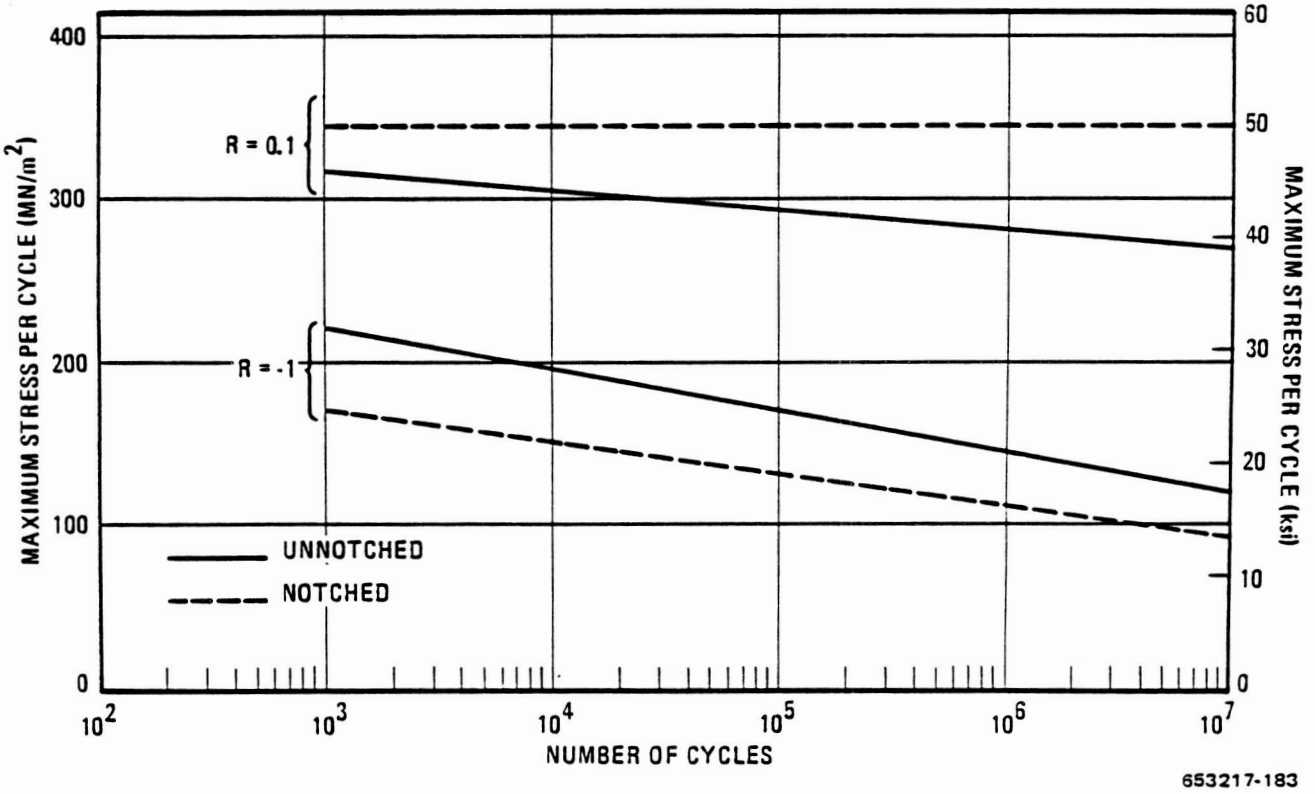



**Figure 11-30 Axial Fatigue Properties of [0° ± 45°] HT-S/710 G/PI at 505 K (450° F)**

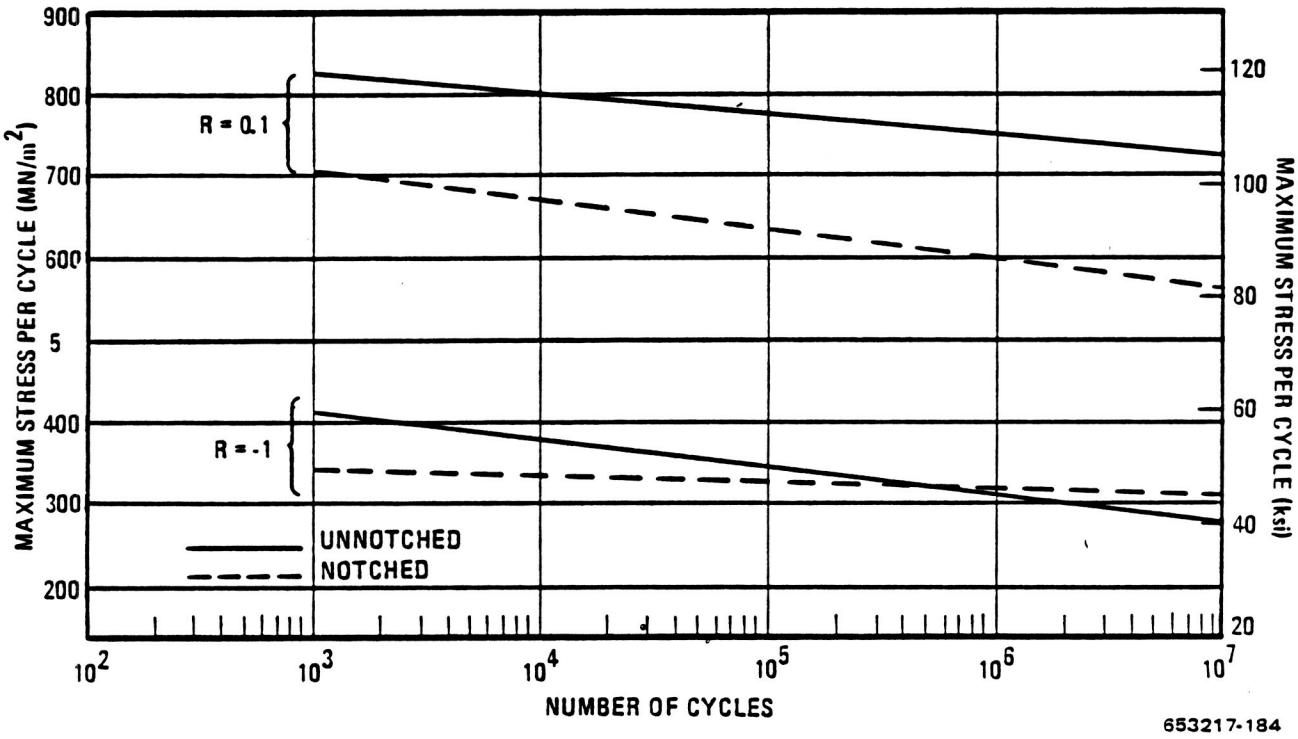



**Figure 11-31 Axial Fatigue Properties of [0°] HT-S/710 G/PI at 505 K (450° F)**

The fatigue tests were all carried out at room temperature at an R value of 0.1 using unnotched specimens. The test results are tabluated in Tables 11-42 and 11-43 and S-N curves are plotted in Figures 11-54 and 11-55. These limited data indicate that the position of the 0° layers in the composite has an effect on both tensile and fatigue strength. In like manner to the tensile results the fatigue properties are lowest with the 0° layers on the outside and highest with the 0° layers at the center. The S-N curves for the B/E system show the relationship between fatigue strength and stacking sequence quite clearly. The same effect, while apparent in the G/E curves, is not as distinct because of the increased scatter of the data.

The data presented in this section indicate that the $[45°, -45°, 0°]_s$ sequence of the $[0° \pm 45°]$ family of laminates would have the best room temperature tensile and fatigue properties. For all testing of crossplied laminates on the balance of the test program, however, the stacking sequence that was selected was the $[0°, 45°, -45°]_s$ sequence. The reason for this choice was that the joint strength to attachments, i.e., doublers, is much higher when made to an unidirectional ply than to an off-axis ply. Consequently, to minimize doubler bond failures in the various types of test specimens the $[0°, 45°, -45°]_s$ layup was used for all crossplied panels.

**11.3.5 POISSON'S RATIO EVALUATION.** One of the tasks included in the constant amplitude baseline fatigue study was a series of residual Poisson's ratio tests on specimens that survived 10 million fatigue cycles at room temperature at a stress ratio of −1. Determinations were made on unidirectional specimens of G/E, HT-S/710 G/PI, and B/Al. Strain gage installation and test procedures were the same as those described in Section 7. The condition of the specimens (stress level and number of fatigue cycles) and the results of the Poisson's ratio tests are tabulated in Table 11-44. Also included are the tensile strength and modulus values obtained during the same tests. For the organic matrix materials, G/E and G/PI, the 10 million fatigue cycles appeared to have little effect on the value of Poisson's ratio. For the metal matrix system, B/Al, however, one specimen exhibited a drastic decrease in Poisson's ratio with the

Table 11-22. Strength at Fatigue Limit or $10^7$ Cycles Expressed as Percentage of Ultimate Tensile Strength for HT-S/710 G/PI

| Orientation | Specimen Configuration | Temperature K | Temperature (°F) | R Value | Fatigue Strength at $10^7$ Cycles (%) |
|---|---|---|---|---|---|
| [0° ± 45°] | Unnotched | 297 | 75 | 0.1 | 60 |
| | Notched | 297 | 75 | .1 | 85 |
| | Unnotched | 505 | 450 | .1 | 57 |
| | Notched | 505 | 450 | .1 | 100 |
| | Unnotched | 297 | 75 | −1.0 | 30 |
| | Notched | 297 | 75 | −1.0 | 24 |
| | Unnotched | 505 | 450 | −1.0 | 26 |
| | Notched | 505 | 450 | −1.0 | 28 |
| [0°] | Unnotched | 297 | 75 | .1 | 55 |
| | Notched | 297 | 75 | .1 | 63 |
| | Unnotched | 505 | 450 | .1 | 60 |
| | Notched | 505 | 450 | .1 | 50 |
| | Unnotched | 297 | 75 | −1.0 | 19 |
| | Notched | 297 | 75 | −1.0 | 25 |
| | Unnotched | 505 | 450 | −1.0 | 23 |
| | Notched | 505 | 450 | −1.0 | 27 |

second showing a moderate loss. Modulus values were slightly lower after fatigue cycling for the G/E and G/PI systems. All of the specimens showed significant decreases in tensile strength. It should be pointed out, however, that the specimen configuration, 2.5 cm (1 in.) by 10.2 cm (4 in.) with a 1.3 cm (0.5 in.) gage section was not a good one for tensile testing and was not the one used for the baseline as received tests. Also, all but one of the specimens failed under the end doublers.

The purpose of these tests was to attempt to determine the amount of damage accumulated after 10 million stress cycles at different values of maximum stress. Based on the residual Poisson's ratio results alone, the resin matrix composite systems, G/E and G/PI, appear to have experienced only slight damage while the B/Al metal matrix system was significantly affected by the fatigue cycling. The more highly stressed B/Al specimen showed the greater decrease in Poisson's ratio. Additional testing would be required to verify these findings.

**11.3.6 BASELINE FATIGUE DATA FOR THE THERMAL AGING/COMPRESSION STUDY.** The final portion of the baseline fatigue study was determination of S-N curves for the 24 ply A-S/3501 G/E and Celion 6000/LARC-160 G/PI to be evaluated in the Thermal Aging/Compression study. All of these tests were conducted at room temperature at a stress ratio of −1. The specimen configuration was the same as the unnotched, 24 ply, R = 10 specimen described in Table 11-1. For G/E, fatigue testing was performed in the same machine (SF10U) used for the Phase I baseline test program at a constant frequency of 30 Hz. Loads for the somewhat thicker lami-

Table 11-23. Comparison of Strength at Fatigue Limit or $10^7$ Cycles Expressed as Percentage of Ultimate Tensile Strength for G/PI and Ti-6Al-4V Titanium Alloy at Room and Elevated Temperatures

| Specimen Configuration | R Value | Fatigue Strength at $10^7$ Cycles (% of $F_{tu}$) | | | | | |
|---|---|---|---|---|---|---|---|
| | | Graphite/Polyimide [0° ± 45°] | | Graphite/Polyimide [0°] | | Ti-6 Al-4V Alloy Solution-treated and aged | |
| | | 297 K (75° F) | 505 K (450° F) | 297 K (75° F) | 505 K (450° F) | 297 K (75° F) | 589 K (600° F) |
| Unnotched | 0.1 | 60 | 57 | 55 | 60 | 50 | 52 |
| [a]Notched | 0.1 | 85 | 100 | 63 | 50 | 23 | 29 |
| Unnotched | −1.0 | 30 | 26 | 19 | 23 | 32 | 25 |
| [a]Notched | −1.0 | 24 | 28 | 25 | 27 | 16 | 19 |

[a]G/PI, center notch, theoretical $K_t$, = 2.43
Ti-6Al-4V Alloy, center notch, $K_t$ = 2.82

Table 11-24. Axial Fatigue Data for $[0° \pm 45°]_s$ Celion 6000/LARC-160 G/PI, Unnotched, R = 0.1

| Specimen Number | Test Temperature K | (°F) | Maximum Stress $MN/m^2$ | (ksi) | Cycles | Comments |
|---|---|---|---|---|---|---|
| FC72-19 | 297 | 75 | 345 | 50 | 10,056,000 | Did not fail |
| -20 | | | 414 | 60 | 10,281,000 | Did not fail |
| -21 | | | 483 | 70 | 563,000 | Failed under doubler |
| -22 | | | 517 | 75 | 1,000 | Failed under doubler |
| -23 | | | 500 | 72.5 | 1,000 | Failed under doubler |
| -24 | | | 483 | 70 | 28,000 | Failed under doubler |
| -25 | | | 448 | 65 | 4,453,000 | |
| -26 | | | 465 | 67.5 | 12,849,000 | Did not fail |
| -27 | | | 483 | 70 | 3,740,000 | Failed under doubler |
| FC72-28 | 450 | 350 | 483 | 70 | 147,000 | |
| -29 | | | 517 | 75 | < 1,000 | |
| -30 | | | 448 | 65 | 82,000 | |
| -31 | | | 414 | 60 | 2,356,000 | |
| -32 | | | 379 | 55 | 7,503,000 | |
| -33 | | | 483 | 70 | 81,000 | |
| -34 | | | 500 | 72.5 | 56,000 | |
| -35 | | | 517 | 75 | 9,000 | |
| -36 | | | 552 | 80 | < 1,000 | Failed under doubler |

nates of Celion 6000/LARC-160 G/PI were higher than those for the G/E and could not be held by the conventional L-shaped steel fixtures used for the other composite materials. The slipping problem was solved by using large hydraulic grips. These large gripping fixtures, however, required a change to an MTS Closed-Loop Tension-Torsion machine. The cycling capabilities of the MTS machine with the large hydraulic grips installed limited the test frequency to 5 Hz rather than the 30 Hz used for all other constant amplitude fatigue testing. Figure 11-56 shows the test machine and grips with a specimen ready for testing.

Results of the fatigue tests are listed in Table 11-45 for the two materials. S-N curves are plotted in Figures 11-57 and 11-58. A comparison of these curves with those for the 12 ply materials presented previously (Figure 11-9 for G/E and Figure 11-33 for G/PI) shows good agreement, particularly for the G/PI. The effect of fatigue cycling the G/PI at 5 Hz rather than 30 Hz appeared to be slight. As a check, one of the specimens that was tested at the lowest load was run successfully using the 30 Hz test setup. This data point, (Specimen F3-8) fell on the best fit line for the 5 Hz data.

Table 11-25. Axial Fatigue Data for $[0° \pm 45°]_{s2}$ Celion 6000/LARC-160 G/PI, Unnotched, R = −1

| Specimen Number | Test Temperature K | (°F) | Maximum Stress MN/m² | (ksi) | Cycles | Comments |
|---|---|---|---|---|---|---|
| FC72-1 | 297 | 75 | 212 | 30.8 | 12,916,000 | Did not fail |
| -2 | | | 345 | 50 | < 1,000 | |
| -3 | | | 276 | 40 | 1,000 | |
| -4 | | | 241 | 35 | 728,000 | |
| -5 | | | 259 | 37.5 | 74,000 | |
| -6 | | | 276 | 40 | 2,000 | |
| -7 | | | 224 | 32.5 | 519,000 | |
| -8 | | | 259 | 37.5 | 39,000 | |
| -9 | | | 241 | 35 | 34,000 | |
| FC72-10 | 450 | 350 | 207 | 30 | 176,000 | |
| -11 | | | 172 | 25 | 10,192,000 | Did not fail |
| -12 | | | 190 | 27.5 | 10,030,000 | Did not fail |
| -13 | | | 224 | 32.5 | 838,000 | |
| -14 | | | 259 | 37.5 | 110,000 | |
| -15 | | | 293 | 42.5 | 19,000 | |
| -16 | | | 310 | 45 | 4,000 | |
| -17 | | | 328 | 47.5 | < 1,000 | |
| -18 | | | 207 | 30 | 4,409,000 | |

Table 11-26. Axial Fatigue Data for $[0° \pm 45°]_{s4}$ Celion 6000/LARC-160 G/PI, Unnotched, R = 10

| Specimen Number | Test Temperature K | (°F) | Maximum Stress MN/m² | (ksi) | Cycles | Comments |
|---|---|---|---|---|---|---|
| FC72-37 | 297 | 75 | 310 | 45 | 298,000 | |
| -38 | | | 345 | 50 | 49,000 | |
| -39 | | | 379 | 55 | 4,000 | Bond failure |
| -40 | | | 276 | 40 | 30,673,000 | Did not fail |
| -41 | | | 379 | 55 | 3,000 | Bond failure |
| -42 | | | 362 | 52.5 | 2,000 | Bond failure |
| -43 | | | 293 | 42.5 | 1,199,000 | |
| -44 | | | 328 | 47.5 | 455,000 | Bond failure |
| -45 | | | 310 | 45 | 10,112,000 | Did not fail |
| FC72-46 | 450 | 350 | 310 | 45 | 17,000 | |
| -47 | | | 345 | 50 | 1,000 | |
| -48 | | | 276 | 40 | 9,008,000 | |
| -49 | | | 293 | 42.5 | 10,167,000 | Did not fail |
| -50 | | | 310 | 45 | 394,000 | |
| -51 | | | 328 | 47.5 | 215,000 | |
| -52 | | | 328 | 47.5 | 275,000 | |
| -53 | | | 336 | 48.75 | 566,000 | |
| -54 | | | 336 | 48.75 | 118,000 | |

Table 11-27. Axial Fatigue Data for $[0° \pm 45°]_s$ Celion 6000/LARC-160 G/PI, Notched, R = 0.1

| Specimen Number | Test Temperature K | (°F) | Maximum Stress MN/m² | (ksi) | Cycles | Comments |
|---|---|---|---|---|---|---|
| FC71-19 | 297 | 75 | 483 | 70 | 1,080,000 | |
| -20 | | | 500 | 72.5 | 18,000 | |
| -21 | | | 517 | 75 | <1,000 | |
| -22 | | | 465 | 67.5 | <1,000 | |
| -23 | | | 465 | 67.5 | <1,000 | |
| -24 | | | 465 | 67.5 | <1,000 | |
| -25 | | | 414 | 60 | 10,000,000 | Did not fail |
| -26 | | | 448 | 65 | 10,000,000 | Did not fail |
| -27 | | | 483 | 70 | <1,000 | |
| FC71-28 | 450 | 350 | 379 | 55 | 8,058,000 | |
| -29 | | | 483 | 70 | <1,000 | |
| -30 | | | 414 | 60 | 7,859,000 | |
| -31 | | | 448 | 65 | 4,250,000 | |
| -32 | | | 465 | 67.5 | 1,567,000 | |
| -33 | | | 483 | 70 | 1,101,000 | |
| -34 | | | 517 | 75 | <1,000 | |
| -35 | | | 500 | 72.5 | 1,502,000 | |
| -36 | | | 345 | 50 | 10,030,000 | Did not fail |

Table 11-28. Axial Fatigue Data for $[0° \pm 45°]_{s2}$ Celion 6000/LARC-160 G/PI, Notched, R = −1

| Specimen Number | Test Temperature K | (°F) | Maximum Stress MN/m² | (ksi) | Cycles | Comments |
|---|---|---|---|---|---|---|
| FC71-1 | 297 | 75 | 207 | 30 | 149,000 | |
| -2 | | | 224 | 32.5 | 419,000 | |
| -3 | | | 241 | 35 | 24,000 | |
| -4 | | | 259 | 37.5 | 23,000 | |
| -5 | | | 276 | 40 | 2,000 | |
| -6 | | | 293 | 42.5 | 2,000 | |
| -7 | | | 190 | 27.5 | 10,031,000 | Did not fail |
| -8 | | | 241 | 35 | 64,000 | |
| -9 | | | 207 | 30 | 292,000 | |
| FC71-10 | 450 | 350 | 241 | 35 | 312,000 | |
| -11 | | | 276 | 40 | 3,000 | |
| -12 | | | 259 | 37.5 | 6,000 | |
| -13 | | | 224 | 32.5 | 14,000 | |
| -14 | | | 224 | 32.5 | 76,000 | |
| -15 | | | 190 | 27.5 | 1,386,000 | |
| -16 | | | 172 | 25 | 3,468,000 | |
| -17 | | | 155 | 22.5 | 10,518,000 | Did not fail |
| -18 | | | 207 | 30. | 668,000 | |

Table 11-29. Axial Fatigue Data for $[0° \pm 45°]_{s4}$ Celion 6000/LARC-160 G/PI, Notched, R = 10

| Specimen Number | Test Temperature K | (°F) | Maximum Stress $MN/m^2$ | (ksi) | Cycles | Comments |
|---|---|---|---|---|---|---|
| FC71-37 | 297 | 75 | 310 | 45 | <1,000 | |
| -38 | | | 241 | 35 | 21,455,000 | |
| -39 | | | 276 | 40 | 10,372,000 | Did not fail |
| -40 | | | 293 | 42.5 | 6,000 | |
| -41 | | | 302 | 43.75 | 1,000 | |
| -42 | | | 284 | 41.25 | 6,000 | |
| -43 | | | 284 | 41.25 | 42,000 | |
| -44 | | | 276 | 40 | 75,000 | |
| -45 | | | 276 | 40 | 4,004,000 | |
| FC71-46 | 450 | 350 | 293 | 42.5 | 4,000 | |
| -47 | | | 276 | 40 | 6,000 | |
| -48 | | | 241 | 35 | 7,390,000 | Temp. over-shoot |
| -49 | | | 259 | 37.5 | 10,060,000 | Did not fail |
| -50 | | | 276 | 40 | 10,000 | |
| -51 | | | 310 | 45 | <1,000 | |
| -52 | | | | — | — | Machine malfunction |
| -53 | | | 267 | 38.75 | 1,704,000 | |
| -54 | | | 293 | 42.5 | 3,000 | |

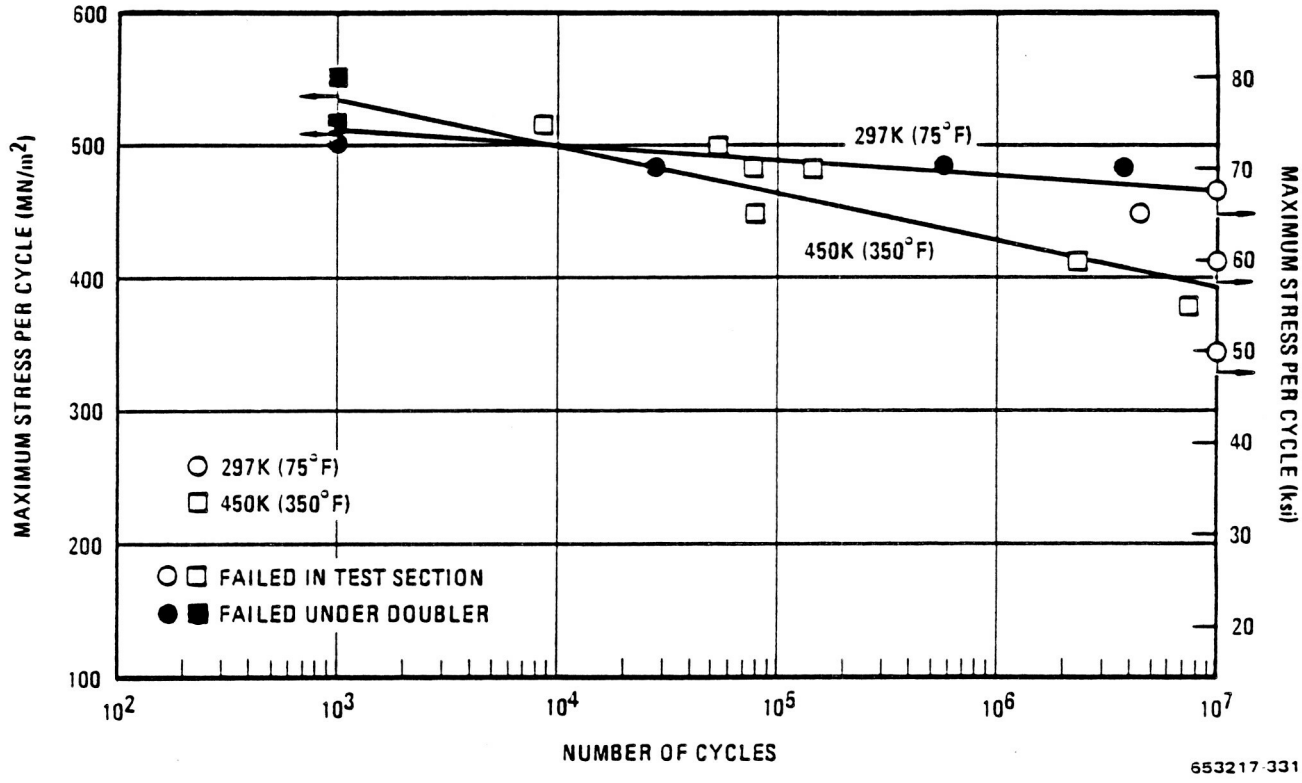



**Figure 11-32 Axial Fatigue Properties of Unnotched $[0° \pm 45°]_s$ Celion 6000/LARC-160 G/PI at a Stress Ratio, R, of 0.1**

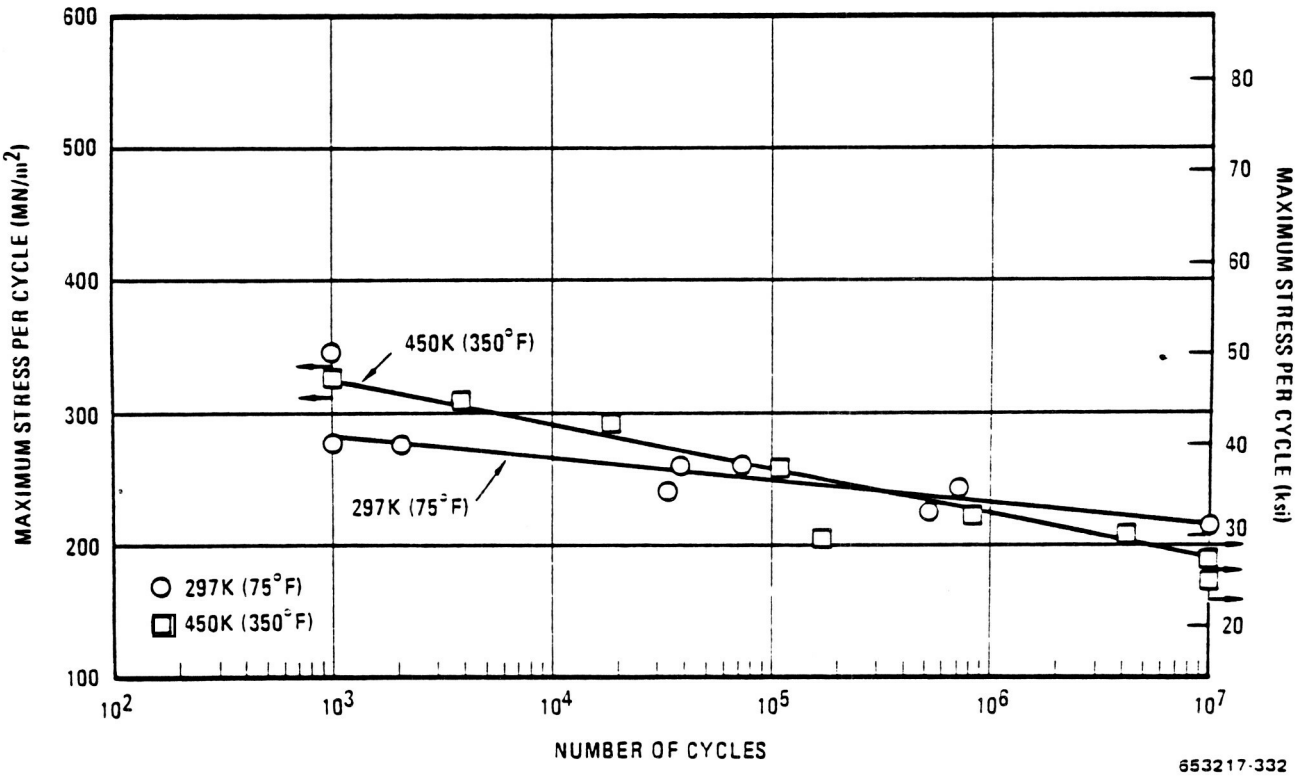



**Figure 11-33 Axial Fatigue Properties of Unnotched $[0° \pm 45°]_{s2}$ Celion 6000/LARC-160 GPI at a Stress Ratio, R, of −1**

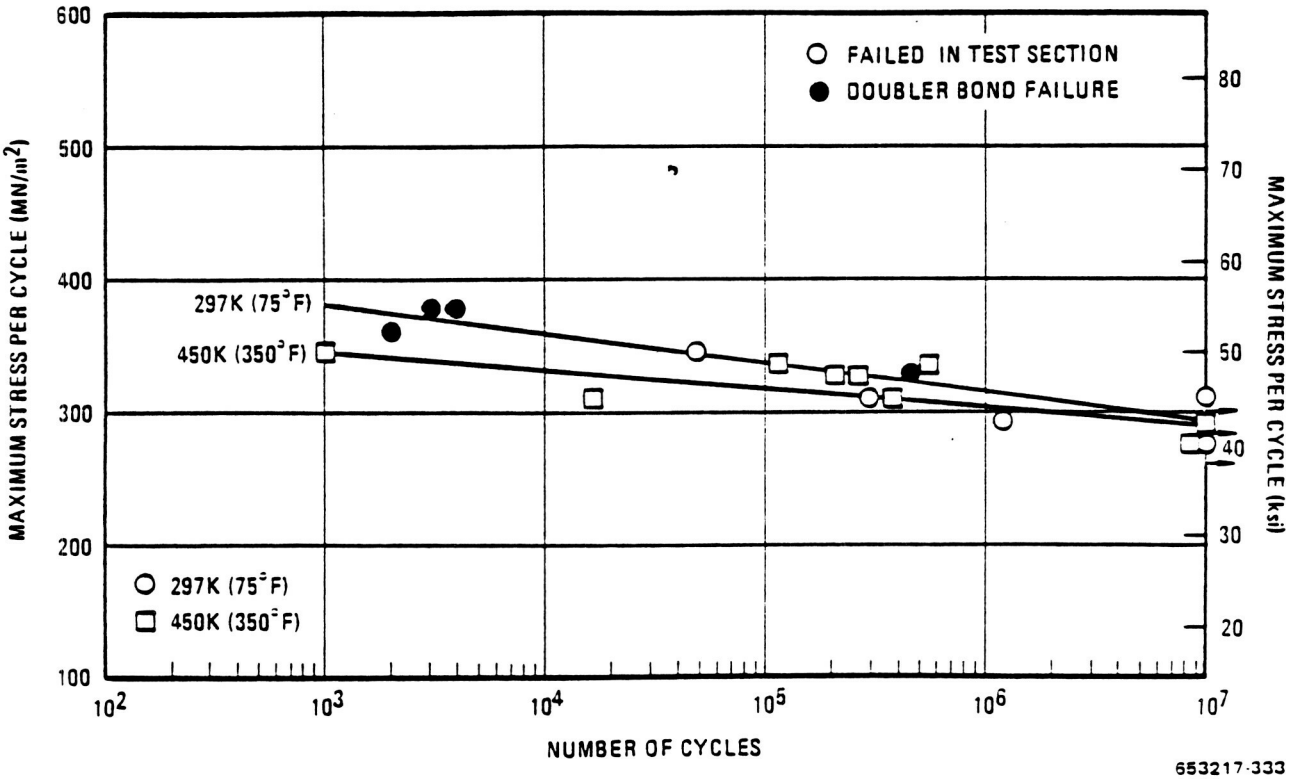



**Figure 11-34 Axial Fatigue Properties of Unnotched $[0° \pm 45°]_{s4}$ Celion 6000/LARC-160 G/PI at a Stress Ratio, R, of 10**

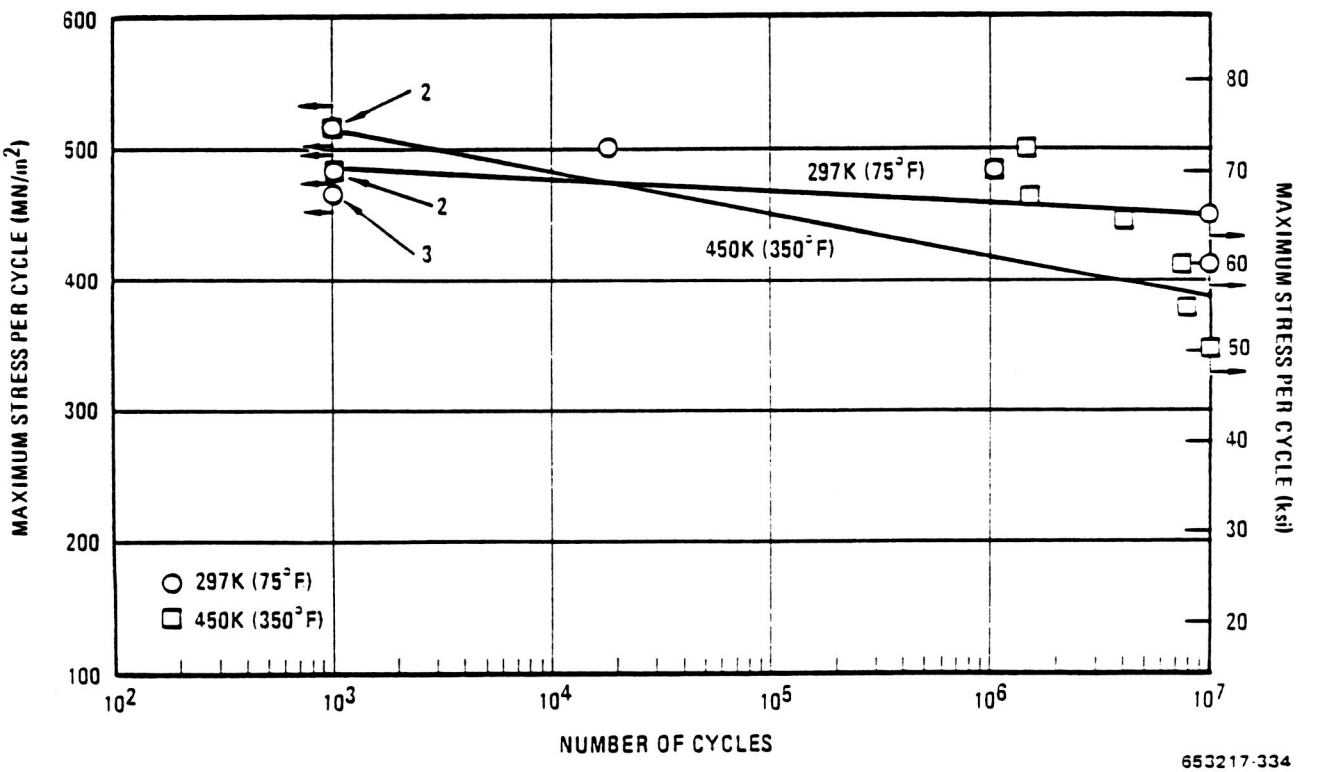



**Figure 11-35 Axial Fatigue Properties of Notched $[0° \pm 45°]_s$ Celion 6000/LARC-160 G/PI at a Stress Ratio, R, of 0.1**

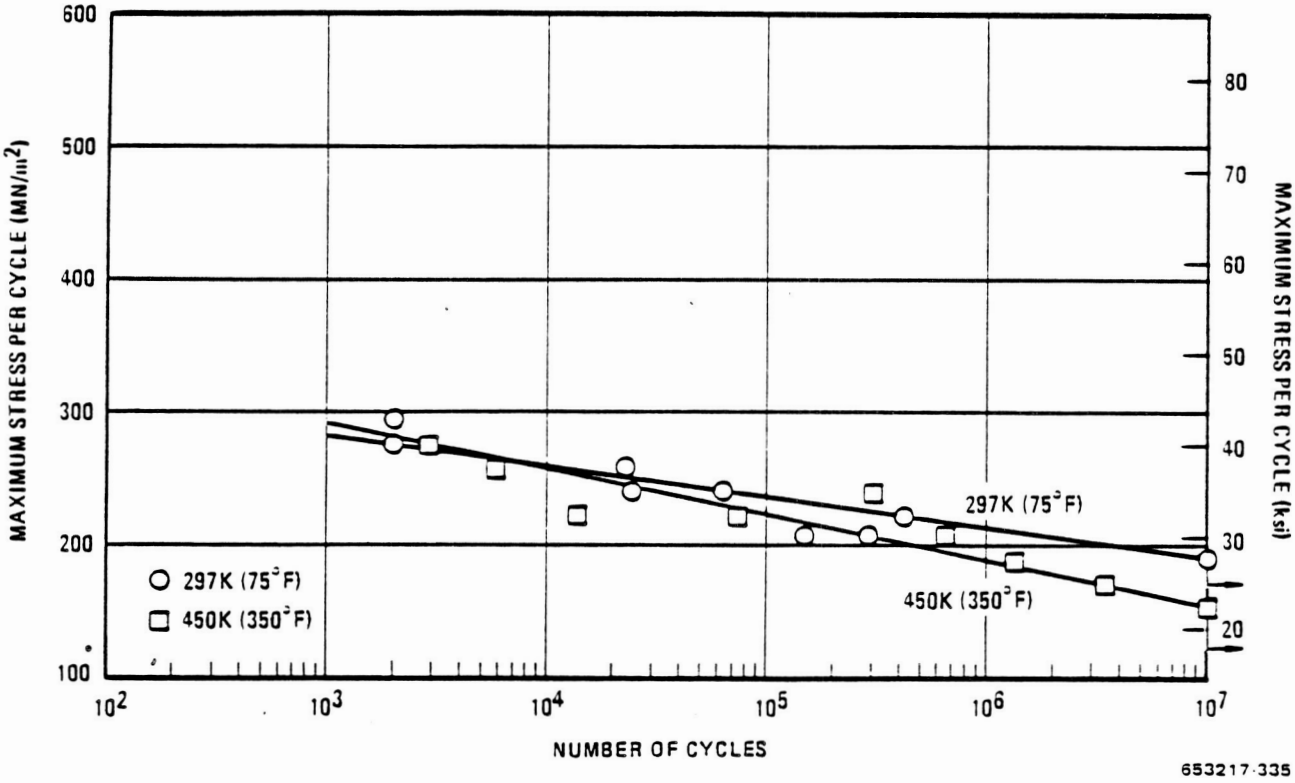



**Figure 11-36 Axial Fatigue Properties of Notched $[0° \pm 45°]_{s2}$ Celion 6000/LARC-160 G/PI at a Stress Ratio, R, of −1**

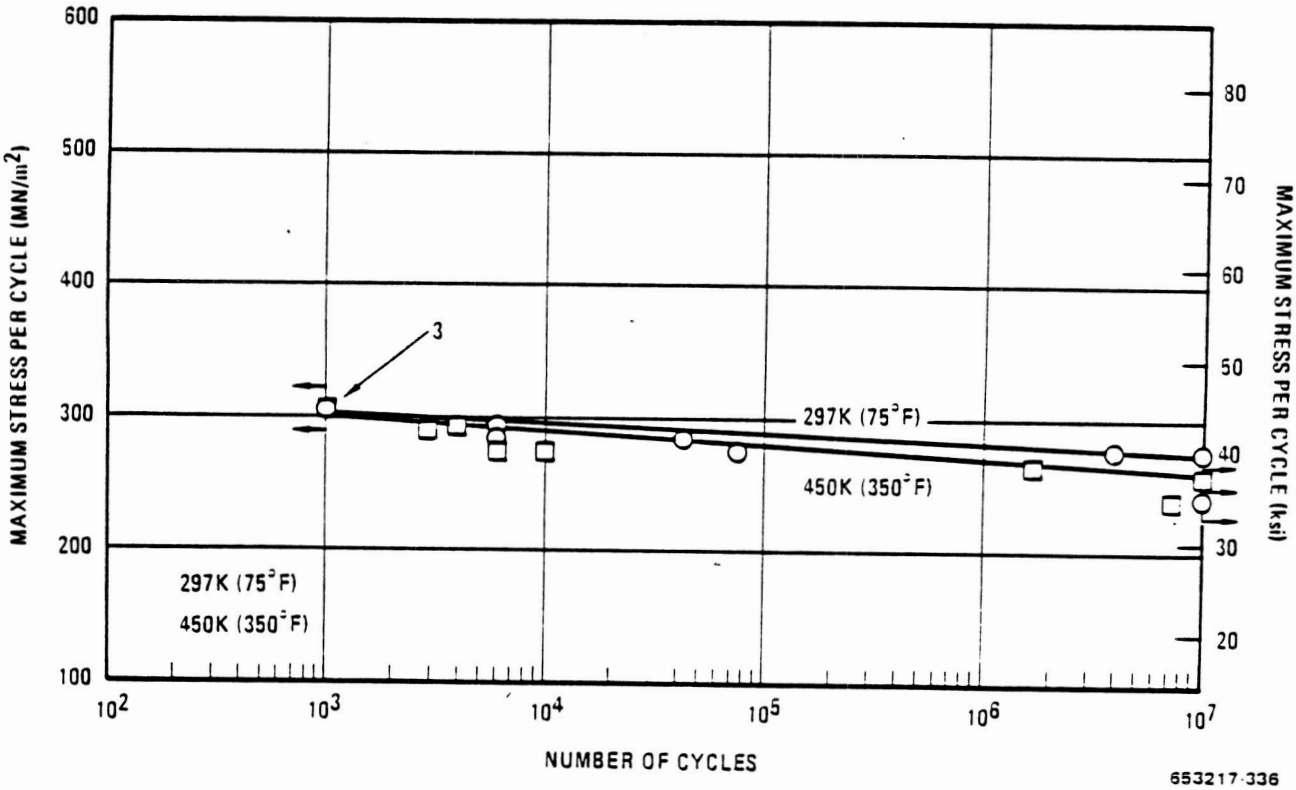



**Figure 11-37 Axial Fatigue Properties of Notched $[0° \pm 45°]_{s4}$ Celion 6000/LARC-160 G/PI at aStress Ratio, R, of 10**

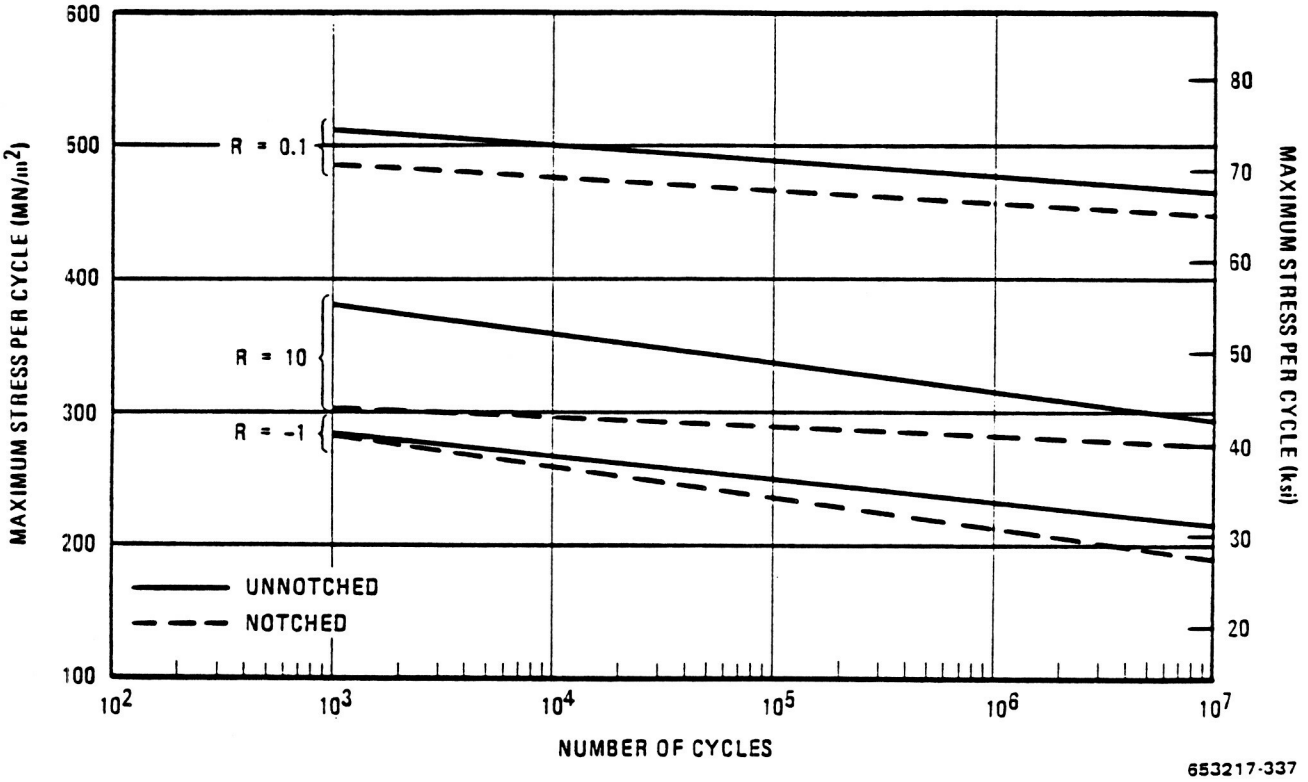



**Figure 11-38 Axial Fatigue Properties of [0° ± 45°] Celion 6000/LARC-160 G/PI at 297 K (75°F)**

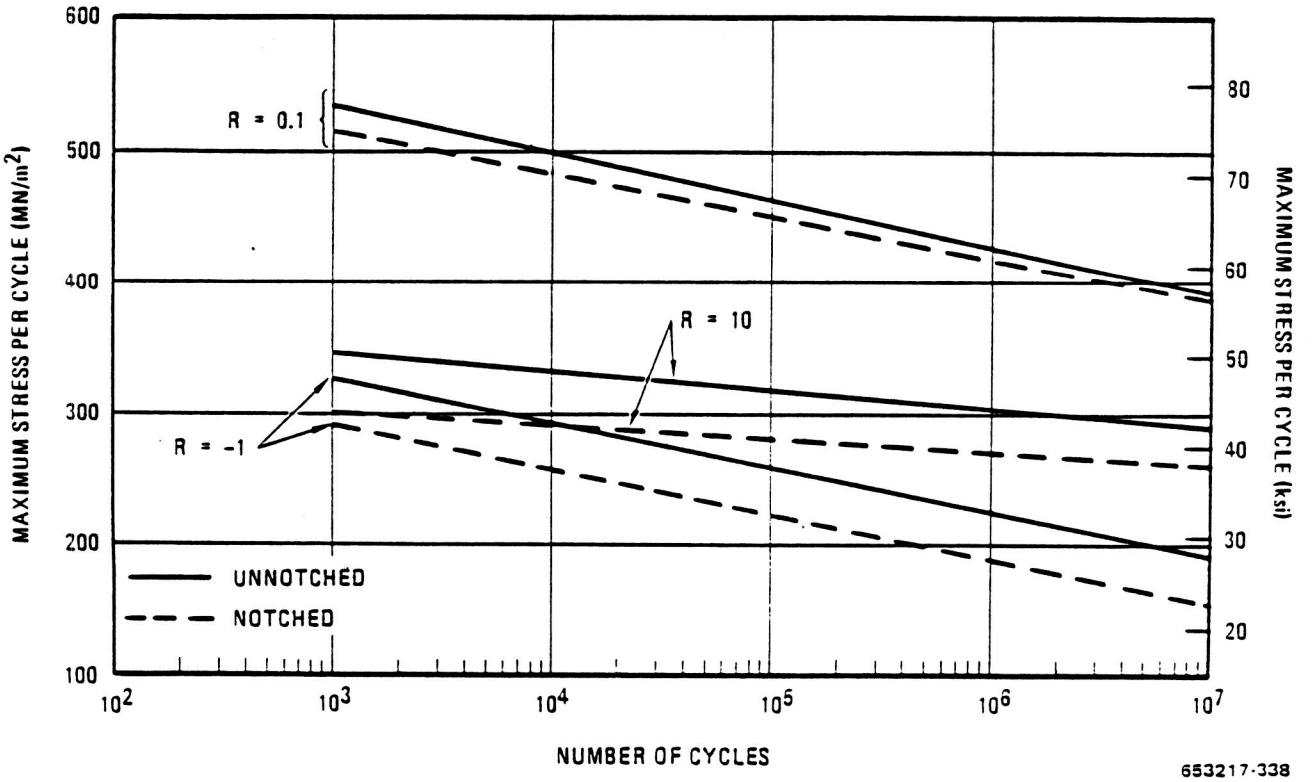



**Figure 11-39 Axial Fatigue Properties of [0° ± 45°] Celion 6000/LARC-160 G/PI at 450 K (350°F)**

Table 11-30. Strength at Fatigue Limit or $10^7$ Cycles Expressed as Percentage of Ultimate Tensile Strength for Celion 6000/LARC-160 G/PI

| Orientation | Specimen Configuration | Temperature K | Temperature (°F) | R Value | Fatigue Strength at $10^7$ Cycles (%) |
|---|---|---|---|---|---|
| [0° ± 45°] | Unnotched | 297 | 75 | 0.1 | 66 |
| | Notched | 297 | 75 | .1 | 100 |
| | Unnotched | 450 | 350 | .1 | 56 |
| | Notched | 450 | 350 | .1 | 81 |
| | Unnotched | 297 | 75 | 10 | 42 |
| | Notched | 297 | 75 | 10 | 64 |
| | Unnotched | 450 | 350 | 10 | 42 |
| | Notched | 450 | 350 | 10 | 55 |
| | Unnotched | 297 | 75 | −1.0 | 30 |
| | Notched | 297 | 75 | −1.0 | 45 |
| | Unnotched | 450 | 350 | −1.0 | 27 |
| | Notched | 450 | 350 | −1.0 | 33 |

Table 11-31. Axial Fatigue Data for $[0° \pm 45°]_s$ B/Al, Unnotched, R = 0.1

| Specimen Number | Test Temperature K | Test Temperature (°F) | Maximum Stress $MN/m^2$ | Maximum Stress (ksi) | Cycles | Comments |
|---|---|---|---|---|---|---|
| EC72-20 | 297 | 75 | 262 | 38 | 17,451,000 | Did not fail |
| -21 | | | 379 | 55 | 1,876,000 | |
| -22 | | | 414 | 60 | 72,000 | |
| -23 | | | 345 | 50 | 33,360,000 | Did not fail |
| -24 | | | 448 | 65 | 716,000 | |
| -25 | | | 483 | 70 | 1,686,000 | |
| -26 | | | 517 | 75 | 17,000 | |
| -27 | | | 465 | 67.5 | 122,000 | |
| -28 | | | 414 | 60 | 2,627,000 | |
| EC72-47 | 561 | 550 | 414 | 60 | 53,000 | |
| -48 | | | 379 | 55 | 201,000 | |
| -49 | | | 345 | 50 | 571,000 | |
| -50 | | | 310 | 45 | 1,780,000 | |
| -51 | | | 276 | 40 | 2,691,000 | |
| -52 | | | 241 | 35 | 9,385,000 | |
| -53 | | | 224 | 32.5 | 9,341,000 | |
| -54 | | | 207 | 30 | 10,551,000 | |
| -55 | | | 448 | 65 | 66,000 | |



C-5

Table 11-32. Axial Fatigue Data for $[0° \pm 45°]_{s2}$ B/Al, Unnotched, R = −1

| Specimen Number | Test Temperature K | (°F) | Maximum Stress MN/m² | (ksi) | Cycles | Comments |
|---|---|---|---|---|---|---|
| EC72-11 | 297 | 75 | 345 | 50 | 38,000 | |
| -12 | | | 379 | 55 | 8,000 | |
| -13 | | | 310 | 45 | 72,000 | |
| -14 | | | 276 | 40 | 448,000 | |
| -15 | | | 207 | 30 | 6,610,000 | |
| -16 | | | 241 | 35 | 788,000 | |
| -17 | | | 190 | 27.5 | 15,437,000 | Did not fail |
| -18 | | | 414 | 60 | 1,000 | |
| -19 | | | 362 | 52.5 | 2,000 | |
| EC72-38 | 505 | 450 | 276 | 40 | 58,000 | |
| -39 | | | 207 | 30 | 861,000 | |
| -40 | | | 345 | 50 | 4,000 | |
| -41 | | | 379 | 55 | 2,000 | |
| -42 | | | 310 | 45 | 7,000 | |
| -43 | | | 241 | 35 | 52,000 | |
| -44 | | | 138 | 20 | 10,006,000 | Did not fail |
| -45 | | | 172 | 25 | 10,111,000 | Did not fail |
| -46 | | | 259 | 37.5 | 38,000 | |

Table 11-33. Axial Fatigue Data for $[0° \pm 45°]_s$ B/Al, Notched, R = 0.1

| Specimen Number | Test Temperature K | (°F) | Maximum Stress MN/m² | (ksi) | Cycles | Comments |
|---|---|---|---|---|---|---|
| EC71-10 | 297 | 75 | 345 | 50 | 492,000 | |
| -11 | | | 276 | 40 | 10,150,000 | Did not fail |
| -12 | | | 414 | 60 | 24,000 | |
| -13 | | | 379 | 55 | 1,192,000 | |
| -14 | | | 310 | 45 | 10,130,000 | Did not fail |
| -15 | | | 448 | 65 | 5,000 | |
| -16 | | | 396 | 57.5 | 901,000 | |
| -17 | | | 362 | 52.5 | 2,913,000 | |
| -18 | | | 328 | 47.5 | 10,085,000 | Did not fail |
| EC71-28 | 561 | 550 | 345 | 50 | No data | Temp. over-shoot |
| -29 | | | 276 | 40 | 2,634,000 | |
| -30 | | | 241 | 35 | 5,490,000 | |
| -31 | | | 207 | 30 | 10,100,000 | Did not fail |
| -32 | | | 310 | 45 | 790,000 | |
| -33 | | | 345 | 50 | 477,000 | |
| -34 | | | 414 | 60 | 91,000 | |
| -35 | | | 448 | 65 | 79,000 | |
| -36 | | | 224 | 32.5 | 8,247,000 | |

Table 11-34. Axial Fatigue Data for $[0° \pm 45°]_{s2}$ B/Al, Notched, R = −1

| Specimen Number | Test Temperature K | (°F) | Maximum Stress MN/m² | (ksi) | Cycles | Comments |
|---|---|---|---|---|---|---|
| EC71-1 | 297 | 75 | 276 | 40 | 247,000 | |
| -2 | | | 310 | 45 | 60,000 | |
| -3 | | | 241 | 35 | 547,000 | |
| -4 | | | 345 | 50 | 8,000 | |
| -5 | | | 207 | 30 | 6,480,000 | |
| -6 | | | 379 | 55 | < 1,000 | Failed under doubler |
| -7 | | | 172 | 25 | 10,195,000 | Did not fail |
| -8 | | | 328 | 47.5 | 7,000 | |
| -9 | | | 224 | 32.5 | 1,227,000 | |
| EC71-19A | 505 | 450 | 207 | 30 | 739,000 | |
| -20 | | | 241 | 35 | 42,000 | |
| -21 | | | 276 | 40 | 10,000 | |
| -22 | | | 172 | 25 | 2,309,000 | |
| -23 | | | 138 | 20 | 12,710,000 | Did not fail |
| -24 | | | 310 | 45 | 4,000 | |
| -25 | | | 345 | 50 | 2,000 | |
| -26 | | | 224 | 32.5 | 26,000 | |
| -27 | | | 259 | 37.5 | 12,000 | |

Table 11-35. Axial Fatigue Data for $[0°]_6$ B/Al, Unnotched, R = 0.1

| Specimen Number | Test Temperature K | (°F) | Maximum Stress MN/m² | (ksi) | Cycles | Comments |
|---|---|---|---|---|---|---|
| EU72-20 | 297 | 75 | 758 | 110 | 12,140,000 | Did not fail |
| -21 | | | 1,000 | 145 | 302,000 | |
| -22 | | | 931 | 135 | 54,000 | |
| -23 | | | 862 | 125 | 76,000 | |
| -24 | | | 827 | 120 | 2,000 | |
| -25 | | | 827 | 120 | 798,000 | |
| -26 | | | 1,030 | 150 | 48,000 | |
| -27 | | | 896 | 130 | 30,559,000 | Did not fail |
| -28 | | | 1,100 | 160 | 181,000 | |
| EU72-47 | 561 | 550 | 862 | 125 | 2,185,000 | |
| -48 | | | 827 | 120 | 3,209,000 | |
| -49 | | | 793 | 115 | 3,104,000 | |
| -50 | | | 758 | 110 | 3,761,000 | |
| -51 | | | 724 | 105 | 4,080,000 | |
| -52 | | | 827 | 120 | 2,980,000 | Nitrogen Atmosphere |
| -53 | | | 965 | 140 | 1,564,000 | |
| -54 | | | 965 | 140 | 1,856,000 | Argon Atmosphere |
| -55 | | | 1,030 | 150 | 610,000 | |

Table 11-36. Axial Fatigue Data for $[0°]_{12}$ B/Al, Unnotched, R = −1

| Specimen Number | Test Temperature K | (°F) | Maximum Stress MN/m² | (ksi) | Cycles | Comments |
|---|---|---|---|---|---|---|
| EU72-11 | 297 | 75 | 690 | 100 | 3,000 | |
| -12 | | | 655 | 95 | 229,000 | |
| -13 | | | 638 | 92.5 | < 1,000 | |
| -14 | | | 638 | 92.5 | 8,000 | |
| -15 | | | 620 | 90 | 9,000 | |
| -16 | | | 552 | 80 | 10,000,000 | Did not fail |
| -17 | | | 586 | 85 | 646,000 | |
| -18 | | | 603 | 87.5 | 21,000 | |
| -19 | | | 569 | 82.5 | 6,000 | |
| -46 | | | 414 | 60 | 10,087,000 | Did not fail |
| EU72-38 | 505 | 450 | 425 | 61.7 | 12,000 | |
| -39 | | | 345 | 50 | 10,120,000 | Did not fail |
| -40 | | | 379 | 55 | 10,153,000 | Did not fail |
| -41 | | | 414 | 60 | 10,005,000 | Did not fail |
| -42 | | | 620 | 90 | < 1,000 | |
| -43 | | | 483 | 70 | 1,332,000 | |
| -44 | | | 552 | 80 | 51,000 | |
| -45 | | | 586 | 85 | 5,000 | |

Table 11-37. Axial Fatigue Data for $[0°]_6$ B/Al, Notched, R = 0.1

| Specimen Number | Test Temperature K | (°F) | Maximum Stress MN/m² | (ksi) | Cycles | Comments |
|---|---|---|---|---|---|---|
| EU71-10 | 297 | 75 | 1,000 | 145 | 76,000 | |
| -11 | | | 896 | 130 | 4,634,000 | |
| -12 | | | 827 | 120 | 4,546,000 | |
| -13 | | | 758 | 110 | 10,002,000 | Did not fail |
| -14 | | | 1,030 | 150 | 39,000 | |
| -15 | | | 965 | 140 | 120,000 | |
| -16 | | | 1,100 | 160 | < 1,000 | |
| -17 | | | 931 | 135 | 1,469,000 | |
| -18 | | | 793 | 115 | 1,761,000 | |
| EU71-28 | 561 | 550 | 862 | 125 | 930,000 | |
| -29 | 561 | 550 | 690 | 100 | 3,732,000 | |
| -30 | 561 | 550 | 620 | 90 | 5,482,000 | |
| -31 | 505 | 450 | 620 | 90 | 10,179,000 | Did not fail |
| -32 | 505 | 450 | 862 | 125 | 996,000 | |
| -33 | 561 | 550 | 827 | 120 | 1,057,000 | |
| -34 | 561 | 550 | 965 | 140 | 60,000 | |
| -35 | 561 | 550 | 896 | 130 | 330,000 | |
| -36 | 561 | 550 | 758 | 110 | 2,974,000 | |

Table 11-38. Axial Fatigue Data for $[0°]_{12}$ B/Al, Notched, R = −1

| Specimen Number | Test Temperature K | (°F) | Maximum Stress MN/m² | (ksi) | Cycles | Comments |
|---|---|---|---|---|---|---|
| EU71-1 | 297 | 75 | 586 | 85 | 310,000 | Failed under doubler |
| -2 | | | 620 | 90 | 560,000 | Failed under doubler |
| -3 | | | 655 | 95 | 887,000 | Failed under doubler |
| -4 | | | 724 | 105 | 34,000 | Failed under doubler |
| -5 | | | 758 | 110 | 9,000 | |
| -6 | | | 793 | 115 | 3,000 | Failed under doubler |
| -7 | | | 690 | 100 | 62,000 | Failed under doubler |
| -8 | | | 552 | 80 | 12,486,000 | Did not fail |
| -9 | | | 586 | 85 | 2,977,000 | Failed under doubler |
| EU71-19A | 505 | 450 | 552 | 80 | 6,000 | |
| -20 | | | 483 | 70 | 18,000 | |
| -21 | | | 414 | 60 | 4,253,000 | |
| -22 | | | 448 | 65 | 3,931,000 | |
| -23 | | | 566 | 82.1 | 4,000 | |
| -24 | | | 379 | 55 | 10,829,000 | |
| -25 | | | 517 | 75 | 9,000 | |
| -26 | | | 465 | 67.5 | 2,398,000 | |
| -27 | | | 431 | 62.5 | 554,000 | |

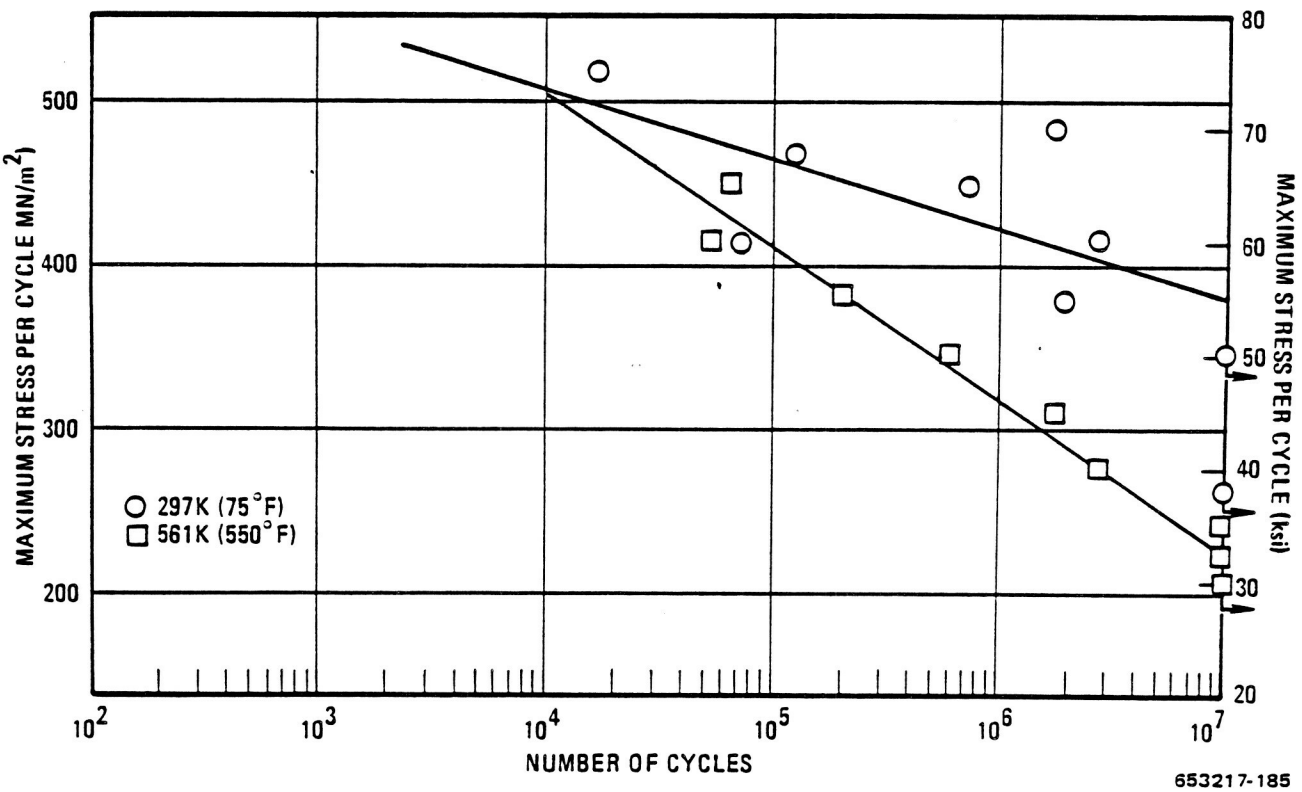



Figure 11-40 Axial Fatigue Properties of Unnotched $[0° \pm 45°]_s$ B/Al at a Stress Ratio, R, of 0.1

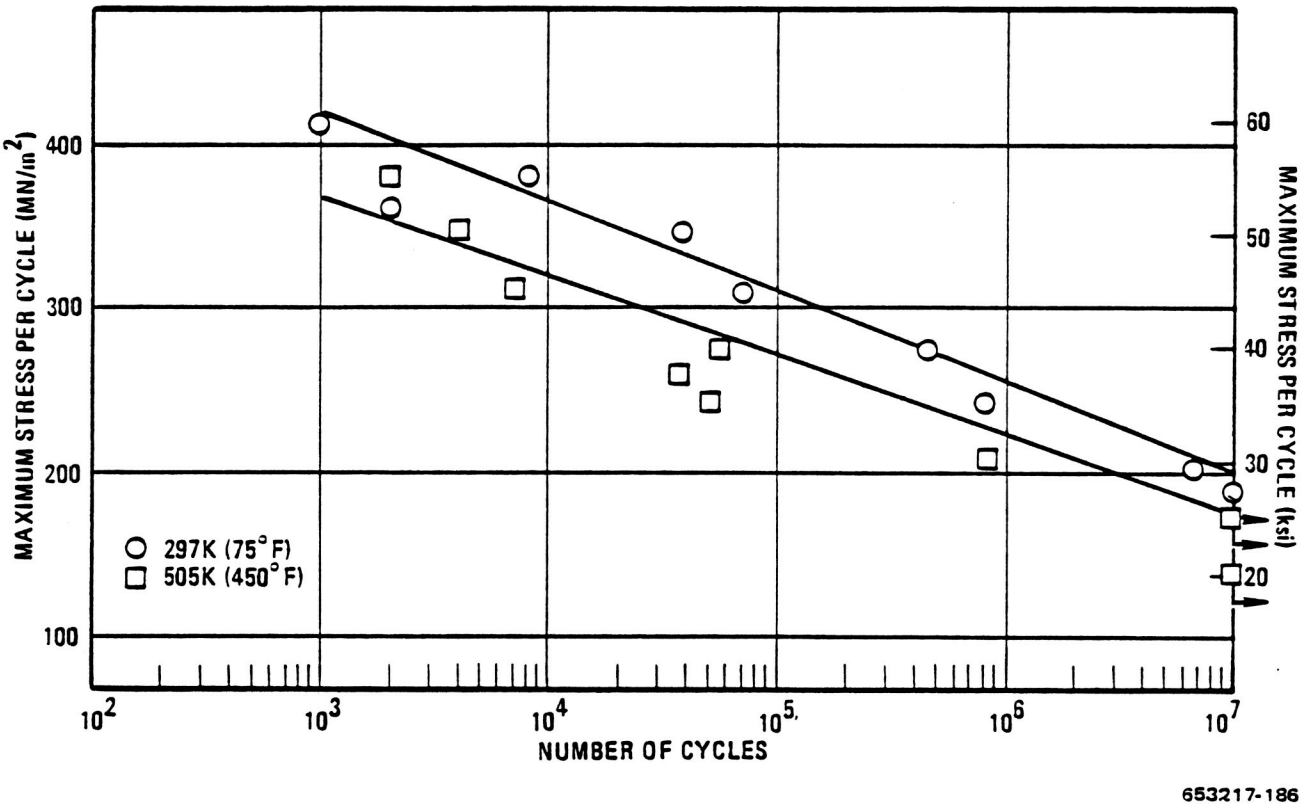



**Figure 11-41 Axial Fatigue Properties of Unnotched $[0° \pm 45°]_{s2}$ B/Al at a Stress Ratio, R, of −1**

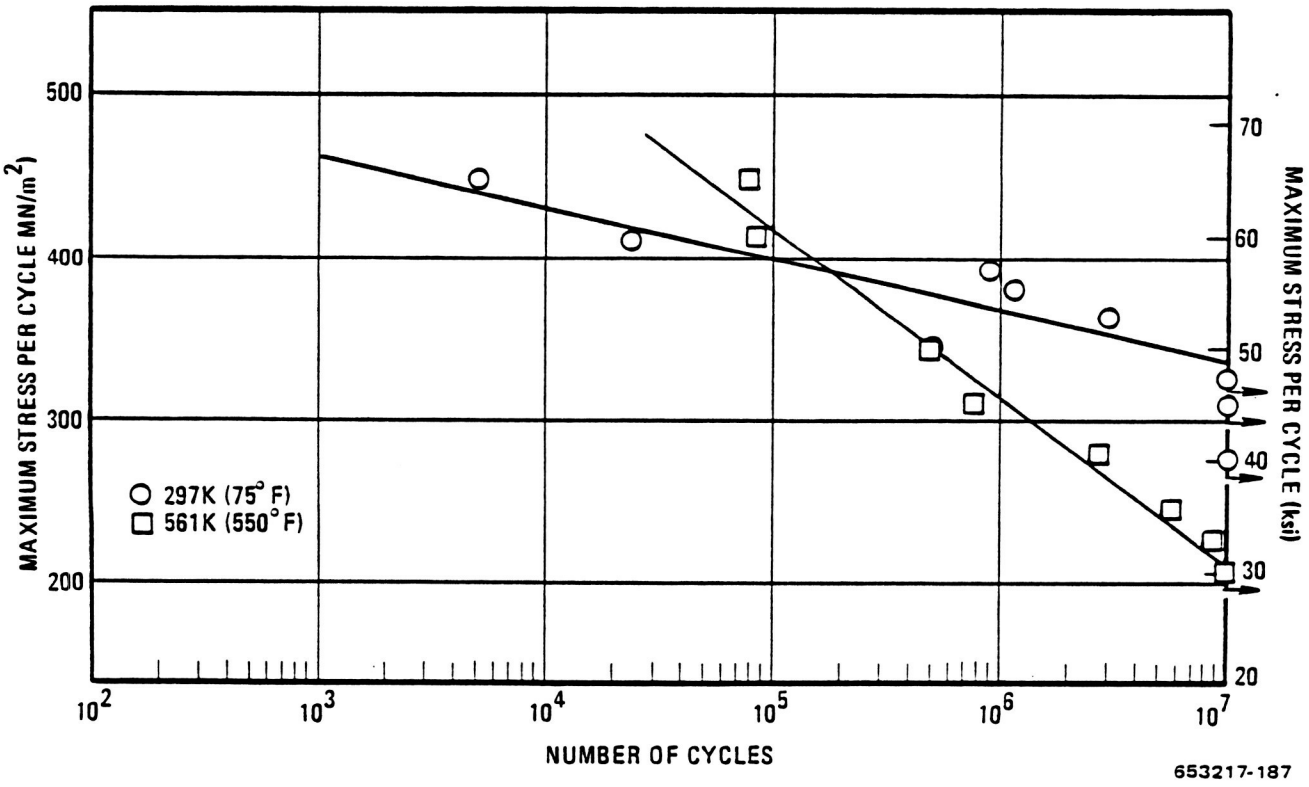



**Figure 11-42 Axial Fatigue Properties of Notched $[0° \pm 45°]_s$ B/Al at a Stress Ratio, R, of 0.1**

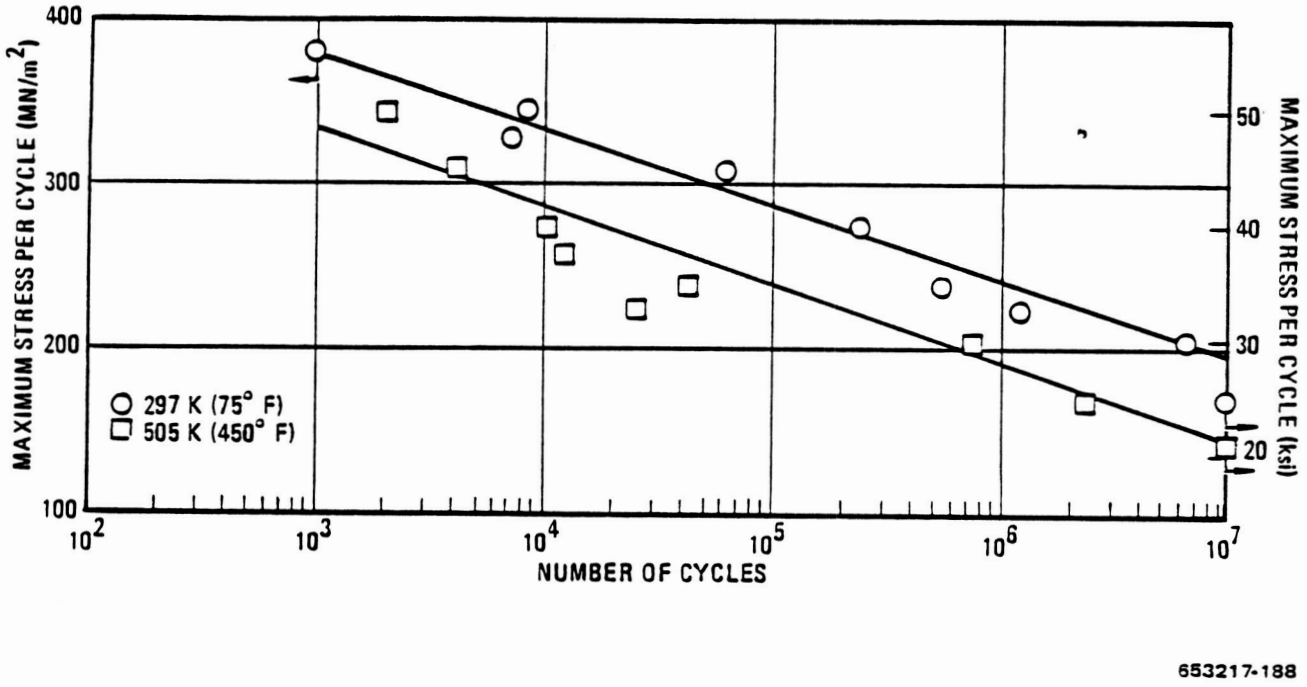



**Figure 11-43 Axial Fatigue Properties of Notched $[0° \pm 45°]_{s2}$ B/Al at a Stress Ratio, R, of −1**

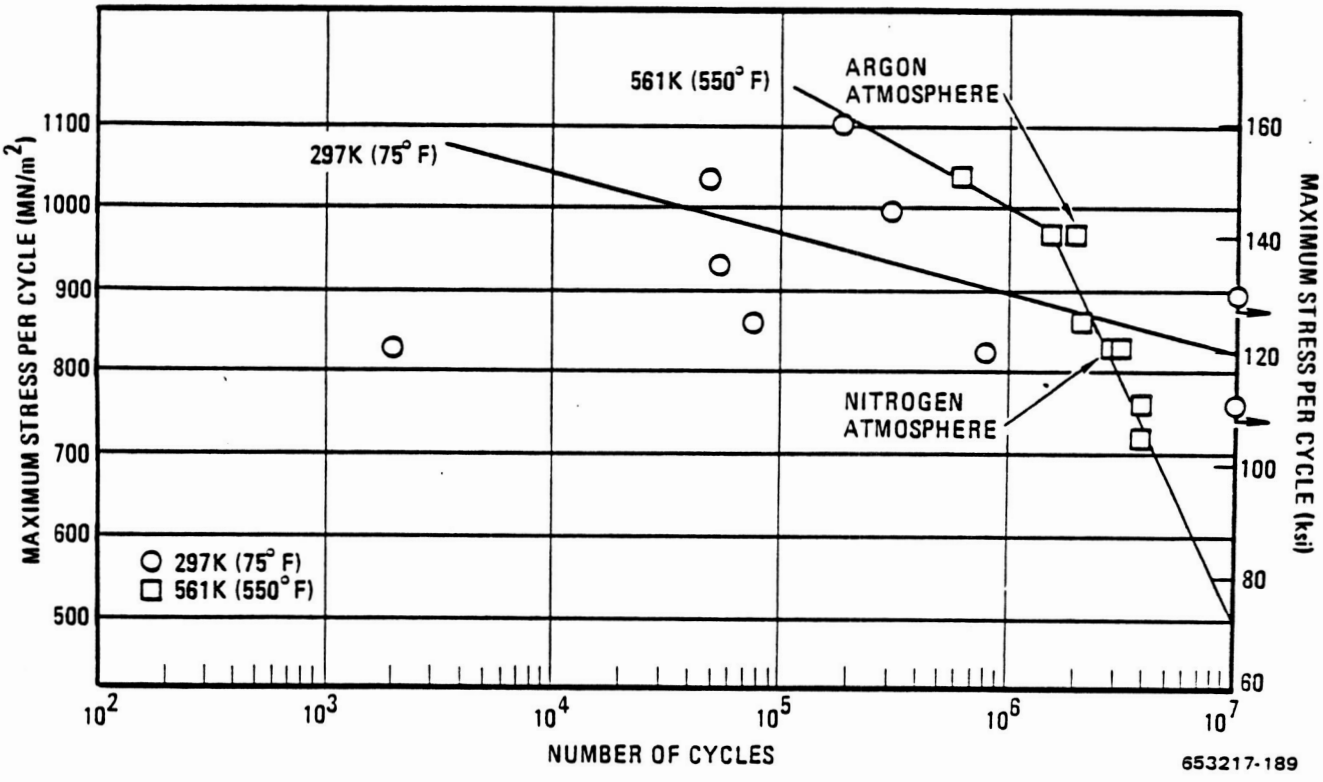



**Figure 11-44 Axial Fatigue Properties of Unnotched $[0°]_6$ B/Al at a Stress Ratio, R, of 0.1**

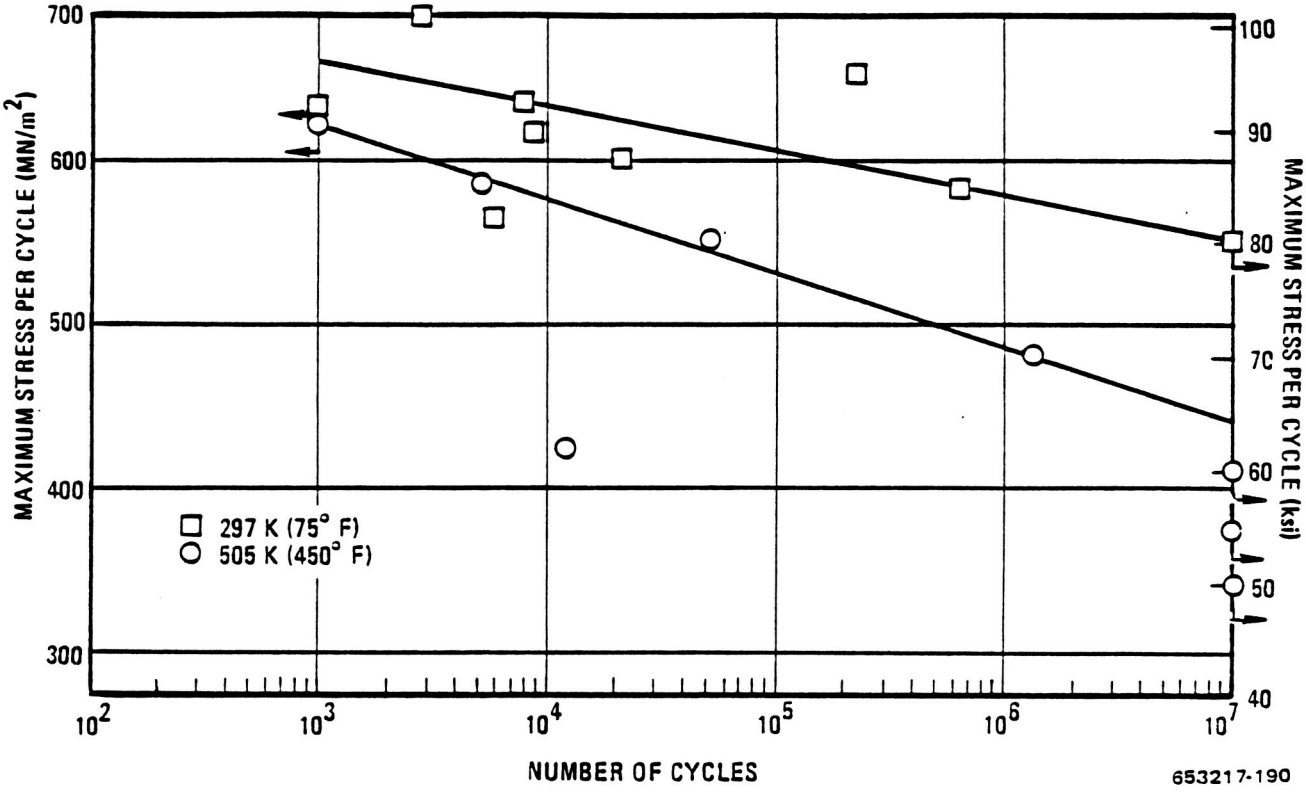



**Figure 11-45 Axial Fatigue Properties of Unnotched $[0°]_{12}$ B/Al at a Stress Ratio, R, of −1**

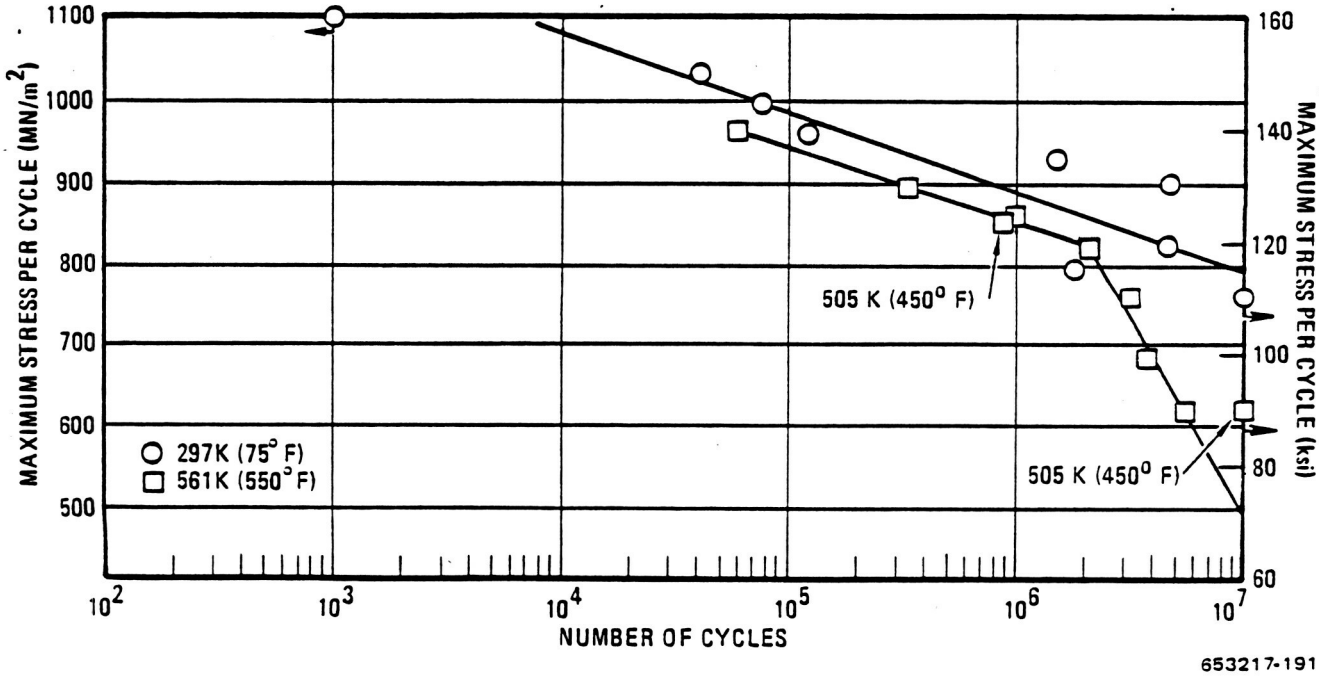



**Figure 11-46 Axial Fatigue Properties of Notched $[0°]_6$ at a Stress Ratio, R, of 0.1**

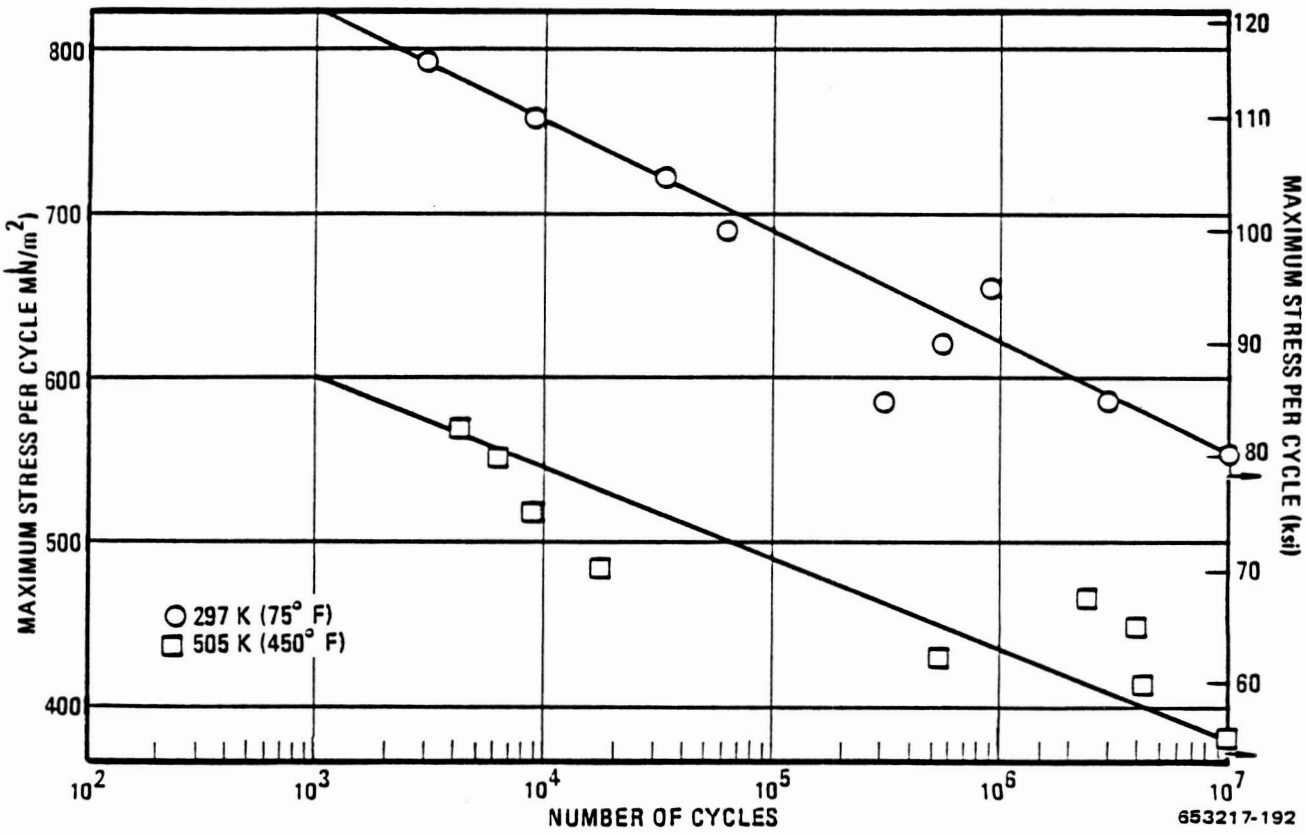



**Figure 11-47 Axial Fatigue Properties of Notched $[0°]_{12}$ B/Al at a Stress Ratio, R, of −1**

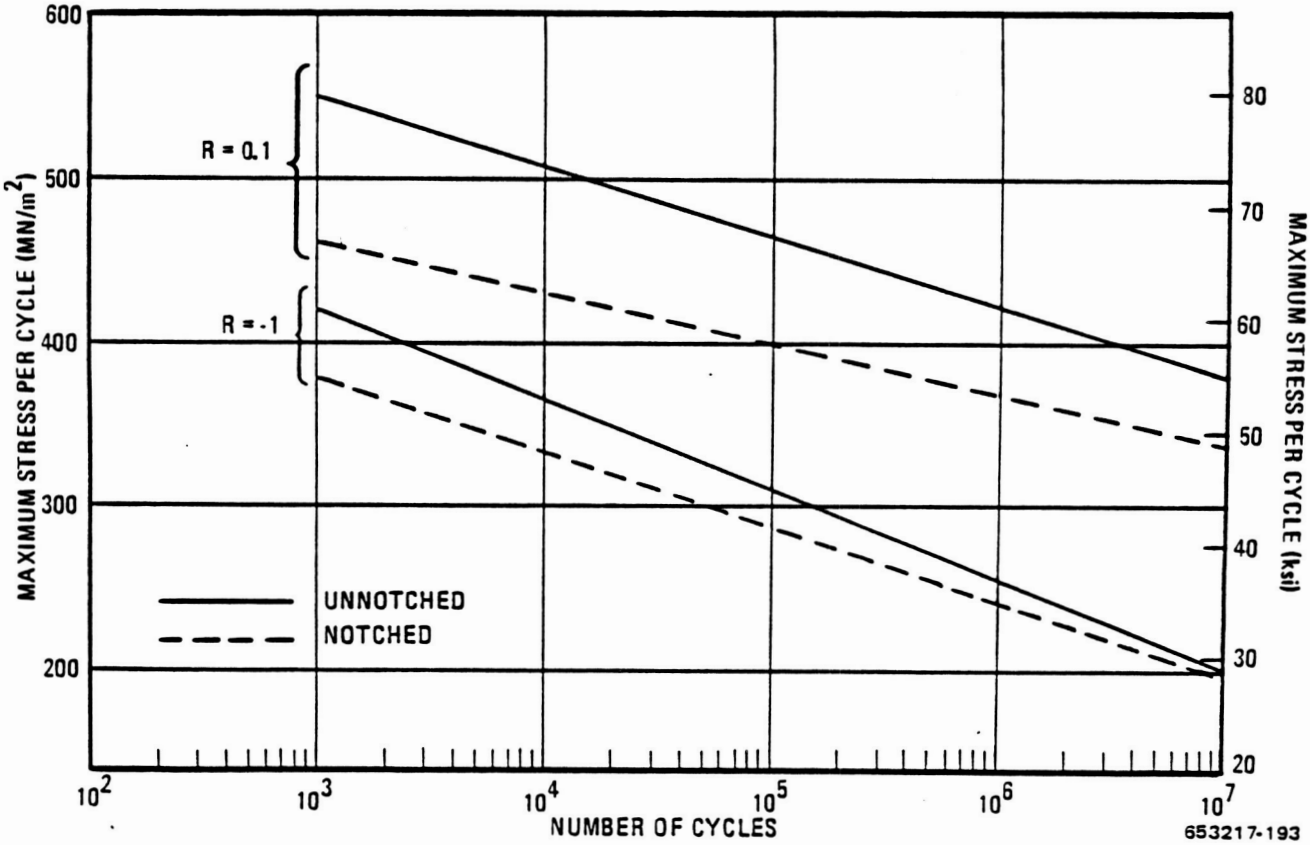



**Figure 11-48 Axial Fatigue Properties of [0° ± 45°] B/Al at 297 K (75° F)**

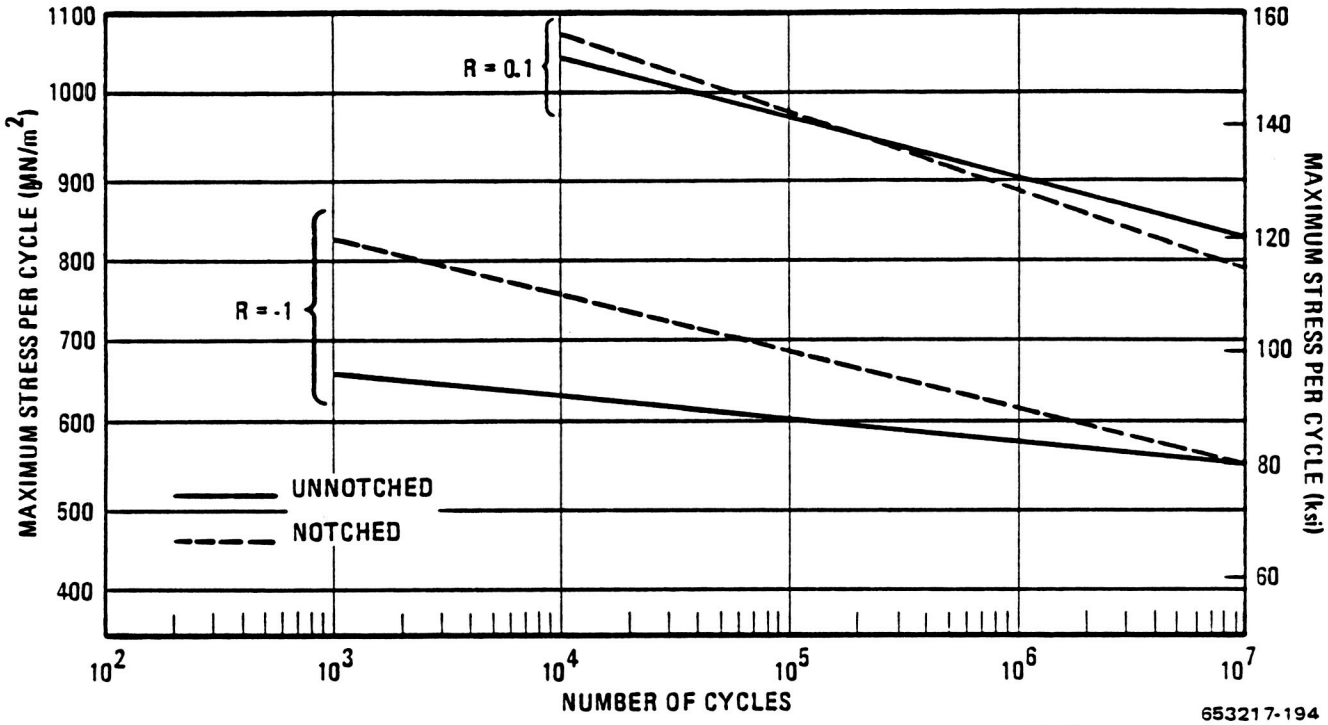



**Figure 11-49 Axial Fatigue Properties of [0°] B/Al at 297 K (75° F)**

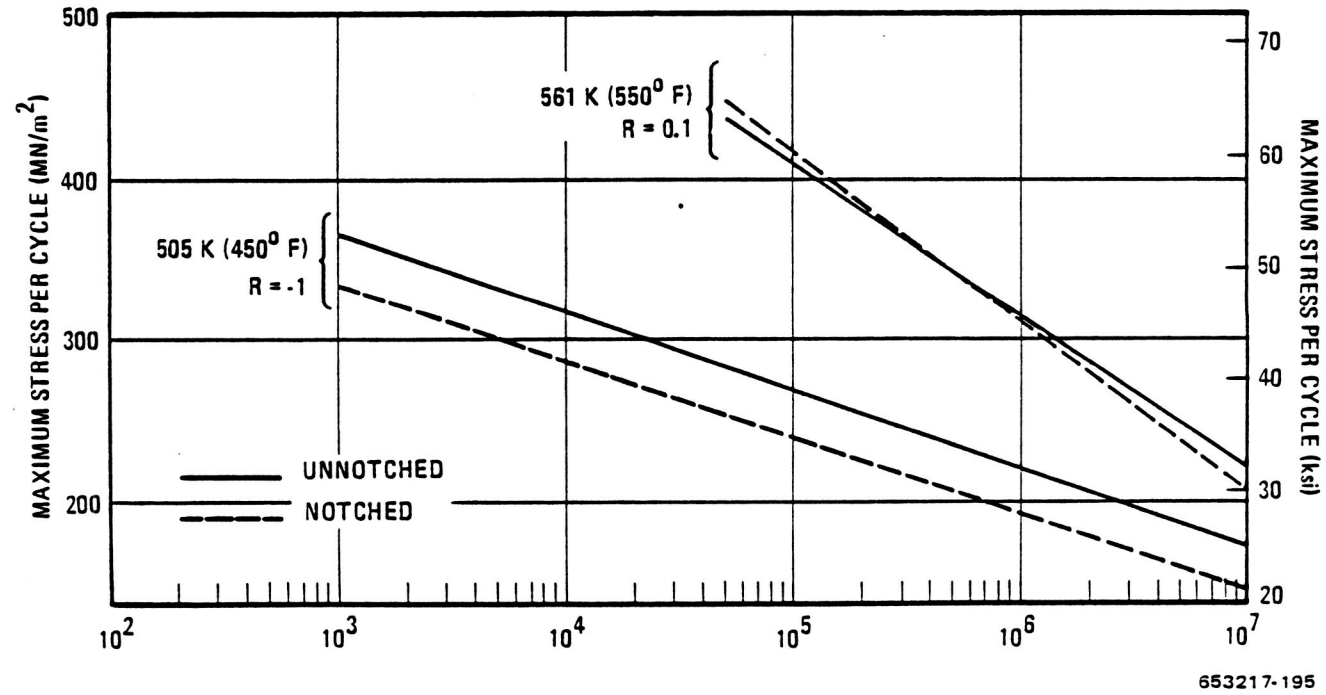



**Figure 11-50 Axial Fatigue Properties of [0° ± 45°] B/Al at Elevated Temperatures**

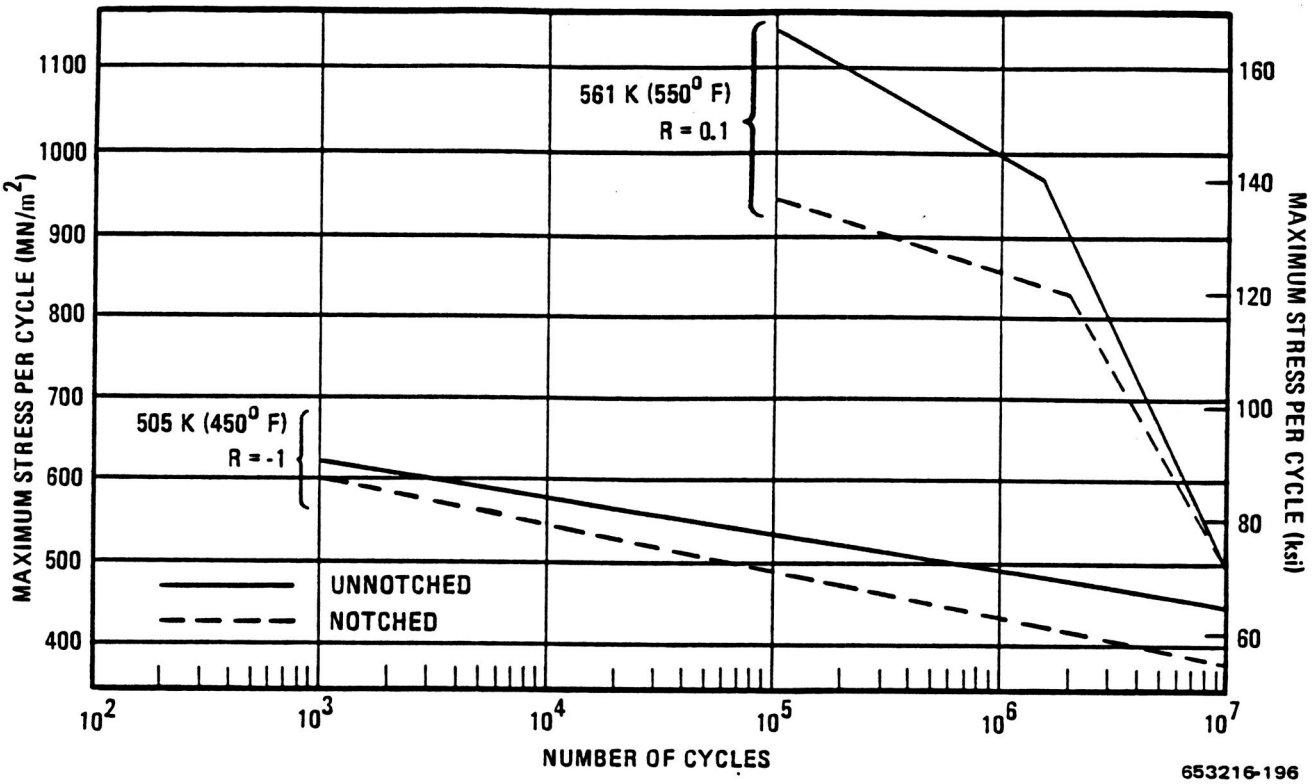



**Figure 11-51 Axial Fatigue Properties of [0°] B/Al at Elevated Temperatures**

ORIGINAL PAGE IS
OF POOR QUALITY

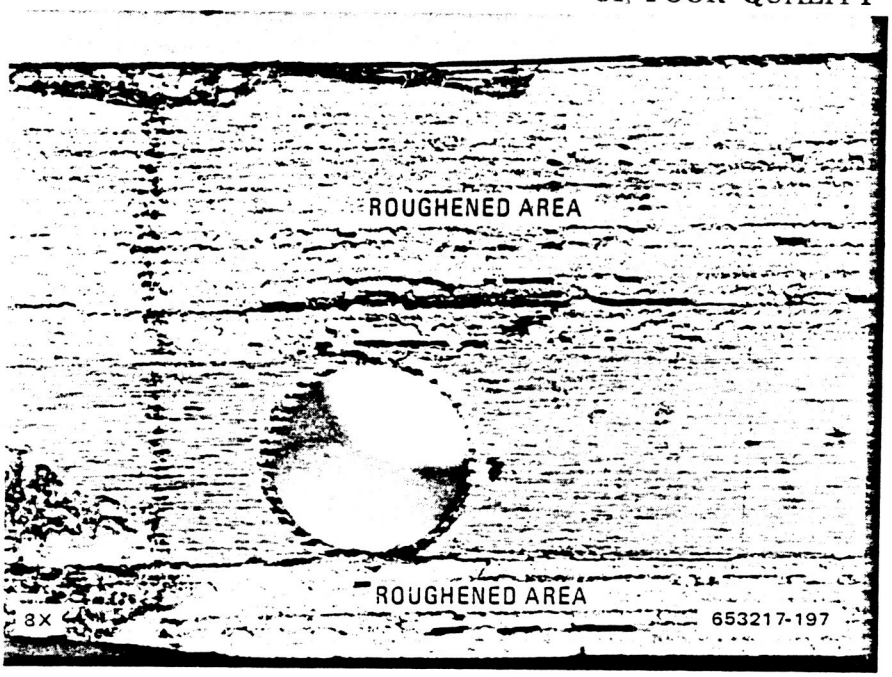



**Figure 11-52 Surface Roughening of B/Al Specimen Fatigued at 561 K (550° F) in Air. (Roughening is confined to stressed areas on either side of the hole.)**

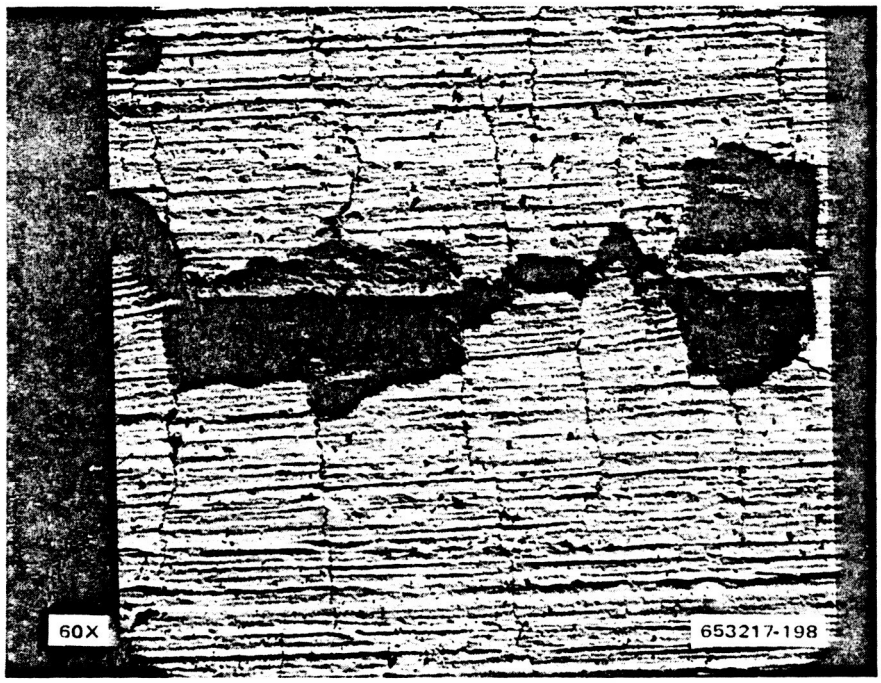



**Figure 11-53 Area of Degraded B/Al Surface Showing Reticulation and Exposed (Aluminum-Covered) Boron Fiber**

ORIGINAL PAGE IS
OF POOR QUALITY

Table 11-39. Strength at Fatigue Limit or $10^7$ Cycles Expressed as Percentage of Ultimate Tensile Strength for B/Al

| Orientation | Specimen Configuration | Temperature K | Temperature (°F) | R Value | Fatigue Strength at $10^7$ Cycles (%) |
|---|---|---|---|---|---|
| [0° ± 45°] | Unnotched | 297 | 75 | 0.1 | 74 |
| | Notched | 297 | 75 | .1 | 71 |
| | Unnotched | 561 | 550 | .1 | 50 |
| | Notched | 561 | 550 | .1 | 47 |
| | Unnotched | 297 | 75 | −1.0 | 39 |
| | Notched | 297 | 75 | −1.0 | 41 |
| | Unnotched | 505 | 450 | −1.0 | 38 |
| | Notched | 505 | 450 | −1.0 | 32 |
| [0°] | Unnotched | 297 | 75 | .1 | 57 |
| | Notched | 297 | 75 | .1 | 64 |
| | Unnotched | 561 | 550 | .1 | [a]38 |
| | Notched | 561 | 550 | .1 | [a]43 |
| | Unnotched | 297 | 75 | −1.0 | 38 |
| | Notched | 297 | 75 | −1.0 | 45 |
| | Unnotched | 505 | 450 | −1.0 | 33 |
| | Notched | 505 | 450 | −1.0 | 33 |

[a]Determined by extrapolation.

**Table 11-40. Comparison of Strength at Fatigue Limit or $10^7$ Cycles Expressed as Percentage of Ultimate Tensile Strength for B/Al and Ti-6Al-4V Titanium Alloy at Room and Elevated Temperatures**

| Specimen Configuration | R Value | Fatigue Strength at $10^7$ Cycles (% of $F_{tu}$) | | | | | |
|---|---|---|---|---|---|---|---|
| | | Boron/Aluminum | | | | Ti-6Al-4V Alloy Solution-treated and aged | |
| | | [0° ± 45°] | | [0°] | | | |
| | | 297 K (75° F) | 505 K (450° F) | 297 K (75° F) | 505 K (450° F) | 297 K (75° F) | 589 K (600° F) |
| Unnotched | 0.1 | 74 | [b]50 | 57 | [b]38 | 50 | 52 |
| [a]Notched | 0.1 | 71 | [b]47 | 64 | [b]43 | 23 | 29 |
| Unnotched | −1.0 | 39 | 38 | 38 | 33 | 32 | 25 |
| [a]Notched | −1.0 | 41 | 32 | 45 | 33 | 16 | 19 |

[a]B/Al, center notch, theoretical $K_{t,} = 2.43$
Ti-6Al-4V Alloy, center notch, $K_t = 2.82$

[b]Test Temperature was 561 K (550° F)

Table 11-41. Room Temperature Tensile Data for B/E and G/E Stacking Sequence Test Panels

| Material System | Stacking Sequence | Tensile Strength $MN/m^2$ | (ksi) | Tensile Modulus $GN/m^2$ | (Msi) |
|---|---|---|---|---|---|
| B/E | $[0°, 45°, -45°]_s$ | 525 | 76.2 | 66 | 9.6 |
| | | 576 | 83.5 | 61 | 8.8 |
| | | 550 | 79.8 | 63 | 9.2 |
| | $[45°, 0°, -45°]_s$ | 556 | 80.6 | 63 | 9.2 |
| | | 584 | 84.7 | 63 | 9.1 |
| | | 570 | 82.6 | 63 | 9.2 |
| | $[45°, -45°, 0°]_s$ | 576 | 83.5 | 61 | 8.9 |
| | | 580 | 84.1 | 61 | 8.9 |
| | | 578 | 83.8 | 61 | 8.9 |
| G/E | $[0°, 45°, -45°]_s$ | 506 | 73.4 | 48 | 6.9 |
| | | 539 | 78.2 | 47 | 6.8 |
| | | 523 | 75.8 | 47 | 6.8 |
| | $[45°, 0°, -45°]_s$ | 664 | 96.3 | 52 | 7.5 |
| | | 652 | 94.5 | 52 | 7.5 |
| | | 658 | 95.4 | 52 | 7.5 |
| | $[45°, -45°, 0°]_s$ | 699 | 101.4 | 55 | 8.0 |
| | | 675 | 97.9 | 56 | 8.1 |
| | | 687 | 99.6 | 55 | 8.0 |

**Table 11-42. Room Temperature Axial Fatigue Data for B/E Stacking Sequence Test Panels, Unnotched, R = 0.1**

| Specimen Number | Stacking Sequence | Maximum Stress $MN/m^2$ | Maximum Stress (ksi) | Cycles | Comments |
|---|---|---|---|---|---|
| A62-1 | $[0°, 45°, -45°]_s$ | 448 | 65 | 1,000 | |
| -2 | | 414 | 60 | 1,000 | |
| -3 | | 379 | 55 | 3,000 | |
| -4 | | 345 | 50 | 294,000 | |
| -5 | | 379 | 55 | 178,000 | |
| -6 | | 345 | 50 | 132,000 | |
| -7 | | 310 | 45 | 3,015,000 | |
| -8 | | 310 | 45 | 10,145,000 | Did not fail |
| -9 | | 379 | 55 | 8,000 | |
| A63-1 | $[45°, 0°, -45°]_s$ | 448 | 65 | 2,000 | |
| -2 | | 414 | 60 | 81,000 | |
| -3 | | 379 | 55 | 2,372,000 | Did not fail |
| -4 | | 448 | 65 | 1,000 | |
| -5 | | 414 | 60 | 34,000 | |
| -6 | | 448 | 65 | 9,000 | |
| -7 | | 414 | 60 | 21,000 | Failed under doubler |
| -8 | | 379 | 55 | 5,733,000 | |
| -9 | | 396 | 57.5 | 111,000 | |
| A61-1 | $[45°, -45°, 0°]_s$ | 448 | 65 | 58,000 | Failed under doubler |
| -2 | | 414 | 60 | 407,000 | |
| -3 | | 431 | 62.5 | 16,000 | |
| -4 | | 448 | 65 | 4,000 | Failed under doubler |
| -5 | | 414 | 60 | 4,950,000 | Did not fail |
| -6 | | 483 | 70 | 1,000 | |
| -7 | | 448 | 65 | 2,000 | |
| -8 | | 431 | 62.5 | 7,000 | |
| -9 | | 414 | 60 | 1,825,000 | |

Table 11-43. Room Temperature Axial Fatigue Data for G/E Stacking Sequence Test Panels, Unnotched, R = 0.1

| Specimen Number | Stacking Sequence | Maximum Stress $MN/m^2$ | (ksi) | Cycles | Comments |
|---|---|---|---|---|---|
| B62-1 | $[0°, 45°, -45°]_s$ | 379 | 55 | 13,000 | |
| -2 | | 414 | 60 | 39,000 | |
| -3 | | 448 | 65 | 36,000 | |
| -4 | | 483 | 70 | 1,000 | |
| -5 | | 448 | 65 | 10,000 | |
| -6 | | 414 | 60 | 7,220,000 | Did not fail |
| -7 | | 431 | 62.5 | 1,000 | |
| -8 | | 431 | 62.5 | 2,000 | |
| -9 | | 431 | 62.5 | 34,000 | |
| B63-1 | $[45°, 0°, -45°]_s$ | 483 | 70 | 2,000 | |
| -2 | | 448 | 65 | 34,000 | |
| -3 | | 483 | 70 | 1,000 | |
| -4 | | 517 | 75 | 1,000 | |
| -5 | | 448 | 65 | 22,000 | |
| -6 | | 414 | 60 | 114,000 | Failed under doubler |
| -7 | | 414 | 60 | 2,306,000 | Did not fail |
| -8 | | 431 | 62.5 | 33,000 | |
| -9 | | 431 | 62.5 | 21,000 | |
| B61-1 | $[45°, -45°, 0°]_s$ | 379 | 55 | 2,001,000 | Did not fail |
| -2 | | 552 | 80 | 1,000 | |
| -3 | | 517 | 75 | 1,000 | |
| -4 | | 483 | 70 | 3,000 | |
| -5 | | 448 | 65 | 2,157,000 | Did not fail |
| -6 | | 483 | 70 | 1,000 | |
| -7 | | 465 | 67.5 | 3,000 | |
| -8 | | 465 | 67.5 | 3,000 | |
| -9 | | 448 | 65 | 2,295,000 | Did not fail |

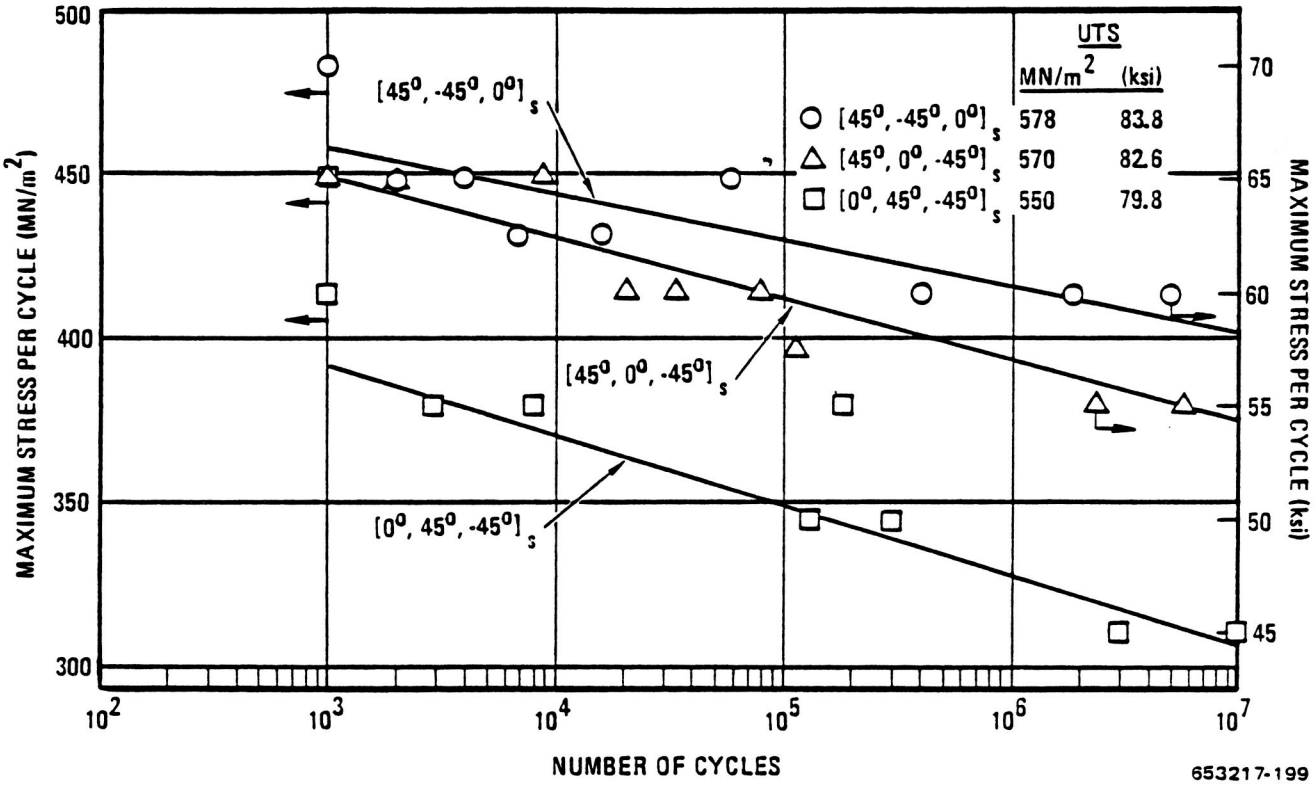



**Figure 11-54 Axial Fatigue of B/E Laminates Showing Effect of Stacking Sequence, 297 K (75° F), R = 0.1**

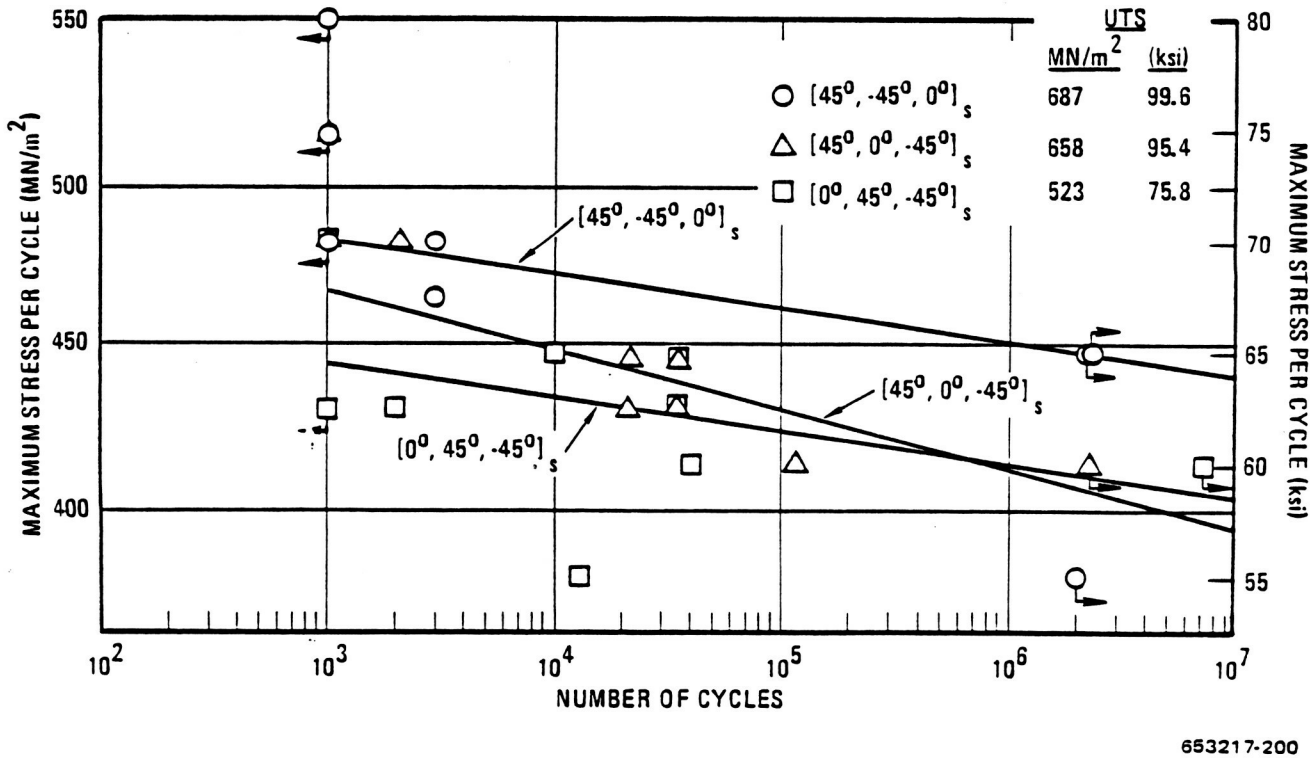


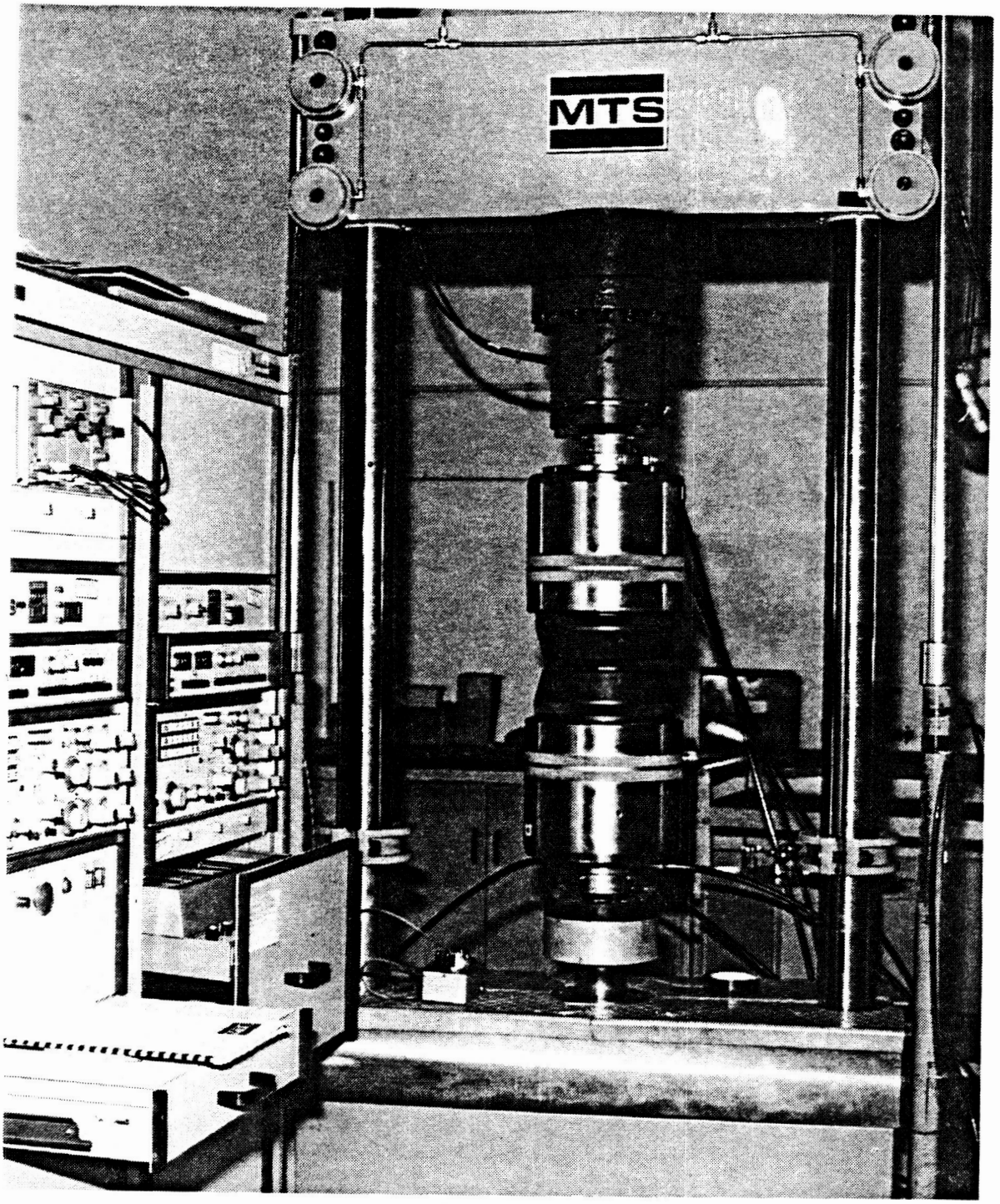

**Figure 11-55 Axial Fatigue of G/E Laminates Showing Effect of Stacking Sequence, 297 K (75° F), R = 0.1**

**Table 11-44. Results of Residual Poisson's Ratio Testing of Run-Out Fatigue Specimens at Room Temperature**

| Material System | Specimen Number | Condition: Number of Cycles | Condition: Fatigue Stress MN/m² | Condition: Fatigue Stress (ksi) | Poisson's Ratio | Tensile Strength MN/m² | Tensile Strength (ksi) | Tensile Modulus (GN/m²) | Tensile Modulus (Msi) |
|---|---|---|---|---|---|---|---|---|---|
| G/E, $[0°]_{12}$ | — | Baseline | | | 0.33 | 1540 | 224 | 141 | 20.4 |
| | BU72-12 | $10.0 \times 10^6$ | 483 | 70 | .28 | [a]1,100 | [a]159 | 130 | 18.8 |
| | BU72-15 | 12.6 | 414 | 60 | .33 | [a]1,000 | [a]145 | 123 | 17.9 |
| | BU72-16 | 10.2 | 448 | 65 | .31 | [a]1,280 | [a]186 | 129 | 18.7 |
| HT-S/710 | — | Baseline | | | [b].39 | 1,190 | 172 | 126 | 18.3 |
| G/PI, $[0°]_{12}$ | DU72-15 | 10.6 | 207 | 30 | .41 | [a]807 | [a]117 | 118 | 17.1 |
| | DU72-46 | 10.3 | 138 | 20 | .33 | [a]945 | [a]137 | 117 | 17.0 |
| B/A1, $[0°]_{12}$ | — | Baseline | | | .28 | 1,450 | 210 | 194 | 28.2 |
| | EU72-16 | 10.0 | 552 | 80 | .10 | [a]470 | [a]68 | 191 | 27.7 |
| | EU72-46 | 10.1 | 414 | 60 | .23 | 1,010 | 147 | 201 | 29.2 |

[a]Failed under doubler

[b]505 K (450° F) value




653217-339

**Figure 11-56 Fatigue Testing Machine with Hydraulic Grips Installed**



ORIGINAL PAGE IS
OF POOR QUALITY

Table 11-45. Baseline Axial Fatigue Data for $[0° \pm 45°]_{s4}$ A-S/3501 G/E and Celion 6000/LARC-160 G/PI Thermal Aging/Compression Study Materials, 297K (75°F), R = −1, Unnotched

| Material Number | Specimen Number | Maximum Stress MN/m² | (ksi) | Cycles | Comments |
|---|---|---|---|---|---|
| G/E | B3-1 | 207 | 30 | 978,000 | Failed under doubler |
| | -2 | 241 | 35 | 453,000 | |
| | -3 | 276 | 40 | 10,000 | |
| | -4 | 258 | 37.5 | 13,000 | |
| | -5 | 224 | 32.5 | 8,452,000 | |
| | -6 | 207 | 30 | 10,287,000 | Did not fail |
| | -7 | 241 | 35 | 27,000 | |
| | -8 | 241 | 35 | 9,000 | Failed under doubler |
| | -9 | 224 | 32.5 | 28,000 | |
| G/PI | F3-1 | 238 | 34.5 | 215,000 | Bond failure |
| | -2 | 276 | 40 | 61,470 | |
| | -3 | 310 | 45 | 500 | Bond failure |
| | -4 | 310 | 45 | 8,980 | |
| | -5 | 328 | 47.5 | 340 | |
| | -6 | 258 | 37.5 | 59,800 | |
| | -7 | 238 | 34.5 | 883,860 | |
| | -8 | 207 | 30 | 10,040,000 | Did not fail |
| | -9 | 293 | 42.5 | 13,820 | |

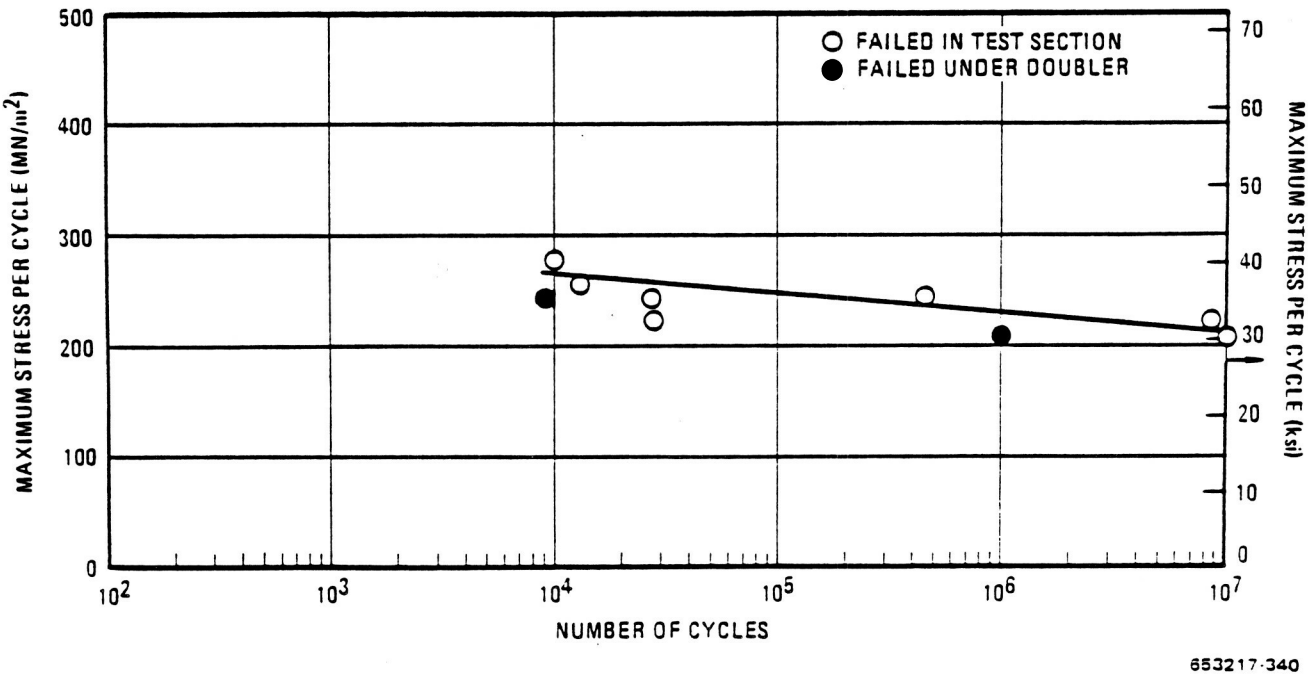



Figure 11-57 Axial Fatigue Properties of $[0° \pm 45°]_{s4}$ G/E, 297K (75°F), R = −1, Unnotched

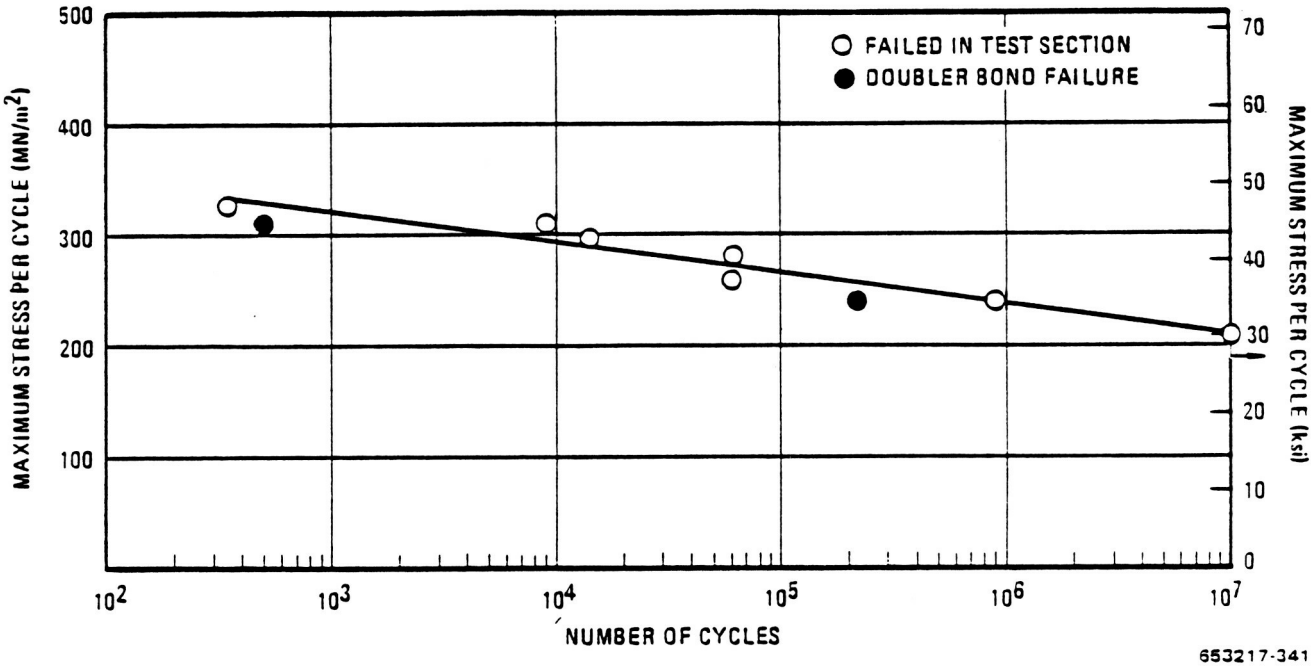



**Figure 11-58 Axial Fatigue Properties of $[0° \pm 45°)_{s4}$ Celion 6000/LARC-160 G/PI, 297 K (75°F), R = −1, Unnotched**

# SECTION 12

# FLIGHT SIMULATION TESTING

## 12.1 INTRODUCTION

The objective of this portion of the program was to subject in real time each of the composite systems to the load-temperature history that would be experienced by a supersonic transport during its 50,000-hour life. To do this a flight simulation apparatus was constructed that was capable of loading a number of large specimens of each composite system using a random loading pattern while the specimens were heated to the temperatures corresponding to those expected to be encountered during flight. As the composites had different strengths and maximum use temperatures, it was necessary that the flight simulator be capable of providing the load and temperature suited to each composite. The apparatus had to be large enough to allow the testing of a number of replicates of each system to provide adequate statistical data for proper evaluation of the endurance of the material. In addition, the simulator had to be capable of automatically testing a large number of specimens reliably for an extended period of time.

A load spectrum was generated using the exceedance curves for a supersonic cruise aircraft, and this purely random spectrum was recorded on tape in a form suitable for load generation in real time so that 25,000 two-hour flights (50,000 hours) could be simulated. Each flight contained climb, cruise, descent, and landing loads with the temperatures corresponding to each portion of the flight. A typical load and temperature profile is shown in Figure 12-1.

The original intent of the program was to use the wearout model developed by Halpin (ref. 6) to predict the life and set the peak load levels for the flight simulation tests of all the composite systems. Once a random load spectrum had been generated, the test conditions for each composite system could be set by increasing or decreasing the magnitudes of the entire spectrum. This was done by setting the magnitude of the peak load in the spectrum. To set these peak loads, accelerated tests were run by increasing the frequency of the spectrum. A quarter of a lifetime and half a lifetime of loads were applied in 100 hours and 200 hours respectively. This was done with the specimens held at a constant temperature corresponding to what was considered to be the maximum use temperature for each individual composite system. These accelerated tests, referred to as short-term tests, were conducted so that the loads normally applied during a two-hour flight were applied in about one minute. Figure 12-2 shows a flight picked at random and plotted to show the nature of load variation as the specimen is held at its maximum use temperature. These data in conjunction with the baseline properties were to be used to calculate, by means of the wearout theory, the peak load to be applied during flight simulation testing of each composite. In Phase I short term tests were conducted on the five materials originally selected for evaluation: B/E, G/E, B/PI, HT-S/710 G/PI, and B/Al. The B/PI system, however, was removed early from the short term testing because of numerous specimen failures (see Appendix A). Of the remaining systems only the B/E and G/E proved to be amenable to the wearout model for selecting long term loads. The difficulty encountered for the G/PI and B/Al materials was that for the loads applied during accelerated testing the residual strength was observed to increase between one-quarter lifetime and one-half lifetime. This was contrary to the model, which is based on strength decreasing with time. The manner in which the flight simulation loads were determined for the G/PI and B/Al specimens as well

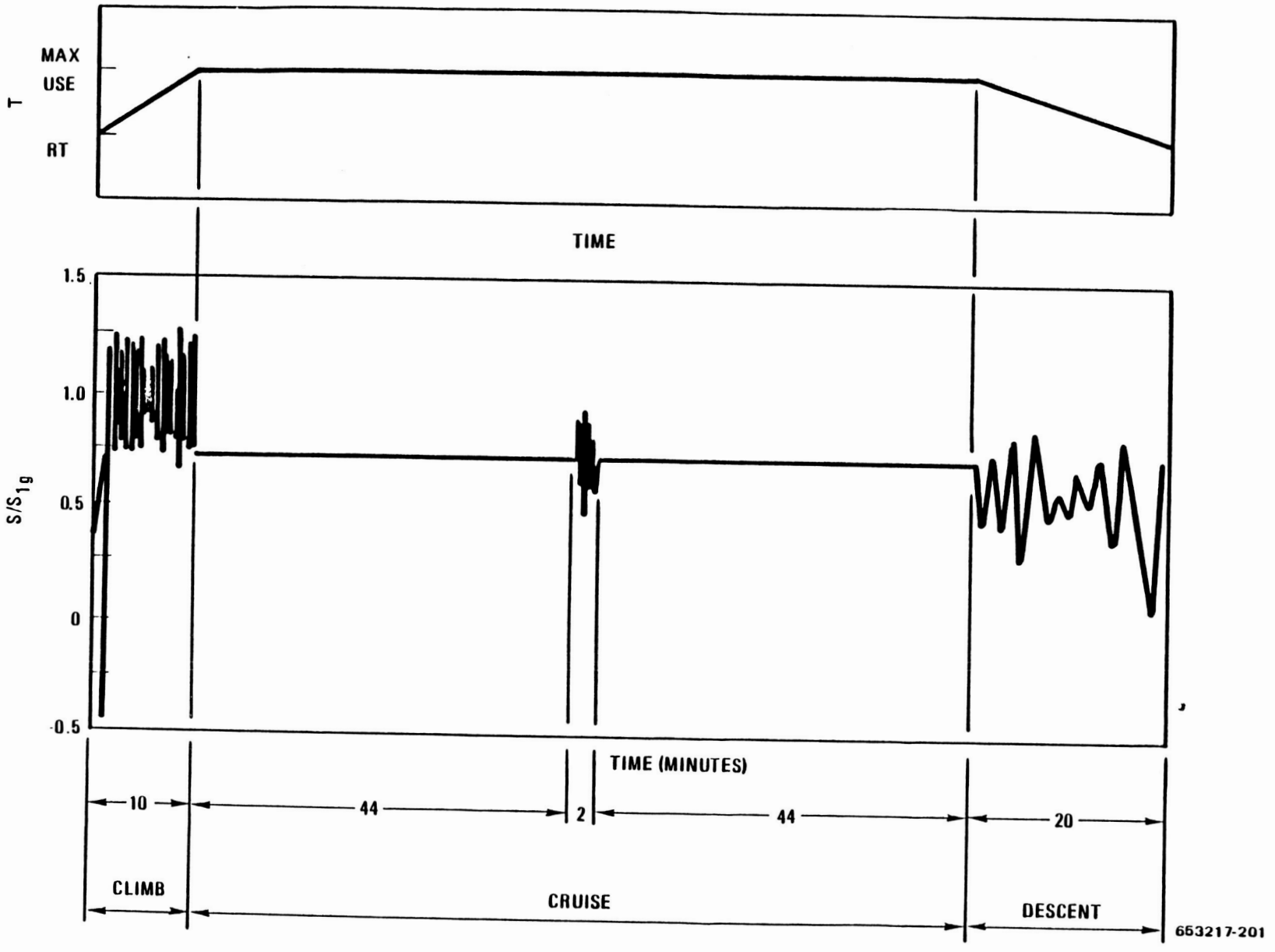



**Figure 12-1 Typical Flight Simulation Cycle Showing Load and Temperature Profile**

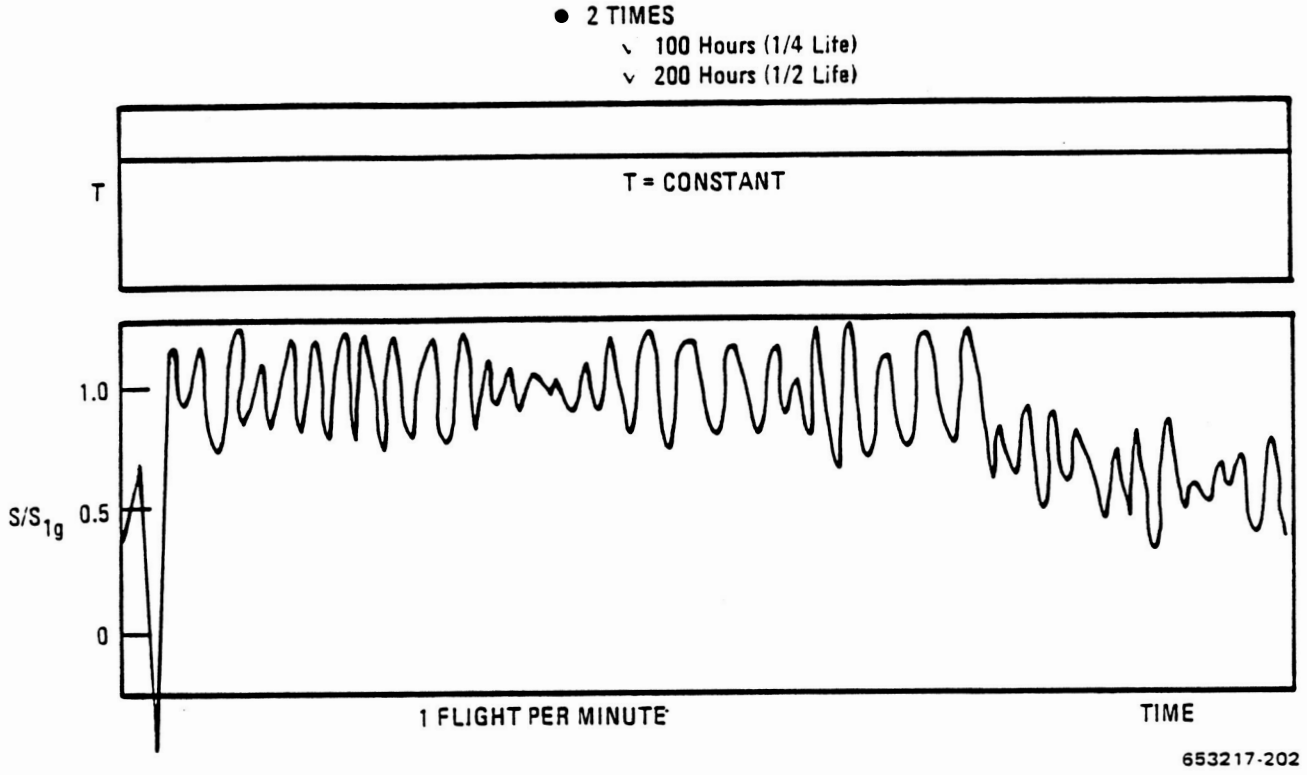



**Figure 12-2 Typical Accelerated or Short-Term Flight Simulation Cycle Showing Loads and Temperature Profile**

as the details of the wearout analysis of the B/E and G/E specimens are discussed later in the section.

Following the short-term tests the four composite systems were subjected to the Phase I 10,000 hours of flight simulation exposure. The G/E specimens experienced a high failure rate and the B/E specimens suffered from extensive visual degradation during these 10,000 hours.

Because of this greater than expected damage to the epoxy systems new specimens were prepared, and the long term tests were restarted for B/E and G/E. The maximum test temperature was reduced using thermal aging data obtained earlier in the program. For the HT-S/710 G/PI and B/Al systems a portion of the specimens with 10,000 hours of exposure were removed for residual property evaluations. Flight simulation testing of the remaining specimens continued for the 50,000 hour Phase II evaluation. Shortly after the start of the Phase II flight simulation tests the new material, Celion 6000/LARC-160 G/PI, was added to the program. Long term specimens were prepared and introduced into test for 10,000 hours of exposure. No short term testing of the Celion 6000/LARC-160 system was conducted because of the poor results obtained with the HT-S/710 G/PI and the delays that would have occurred in flight simulation testing of the other systems. Determination of the long term flight simulation loads for the Celion 6000/LARC-160 specimens is discussed later in the section.

## 12.2 DESCRIPTION OF SIMULATOR

The flight simulation apparatus was built to test five composite materials and has the capability of cycling loads and temperatures on 100 test specimens simultaneously. The apparatus is

divided into 10 independent test setups each of which contains 10 identical specimens. The flight simulation testing equipment is shown in Figure 12-3. There are 10 load frames, five of which are facing forward, and five more directly behind the front five. The small cabinet at the right of the simulator is the control console, which is shown in greater detail in Figure 12-4.

**12.2.1 TEST FIXTURES.** The test fixtures consist of 10 basic load frames, 10 whiffletree assemblies, attachment hardware for 100 specimens, 100 removable specimen stiffener assemblies, 20 heat lamp rack assemblies, and lateral support hardware.

The lateral support between a whiffletree assembly and its specimens is a beam containing five linear motion bearings. They allow motion in the load direction only. The travel of the clevis fitting, which passes through a bearing, is limited and adjustable in each direction. Specimen or doubler failures are detected by means of microswitches activated when the clevis motion exceeds the preset values in either loading direction. Activation of a microswitch immediately dumps the hydraulic pressure and reduces the load to zero.

**12.2.2 LOAD PROGRAMMER AND CONTROLLERS.** The MTS digital load programmer and associated load controllers are shown in Figure 12-5. Ten of the 60 available controllers are used for the 10 basic load frames. The load programmer and controllers program and control the fatigue loading spectrum and synchronize the heating and cooling cycles.

**12.2.3 PROGRAMMER SAFETY FEATURES.** The load programmer provides the following self-checking features that automatically stop all test operations if activated.

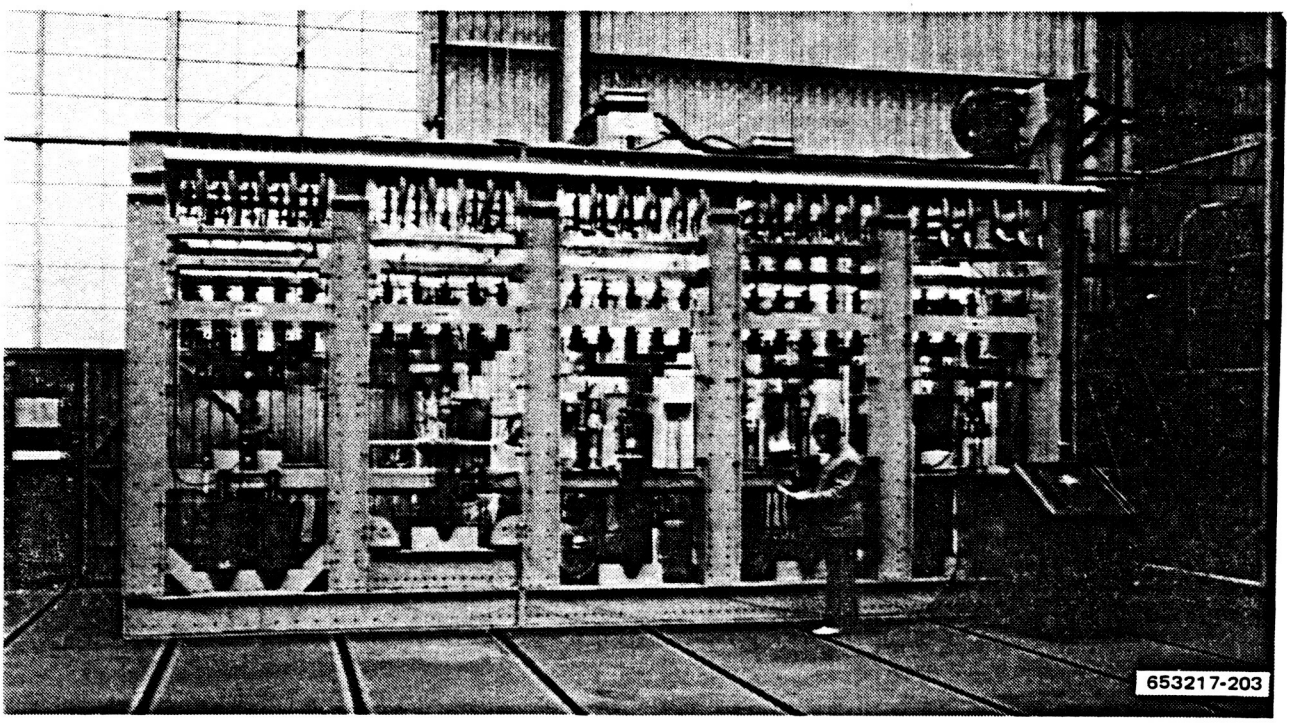



**Figure 12-3 Flight Simulation Equipment**



ORIGINAL PAGE IS
OF POOR QUALITY

ORIGINAL PAGE IS
OF POOR QUALITY

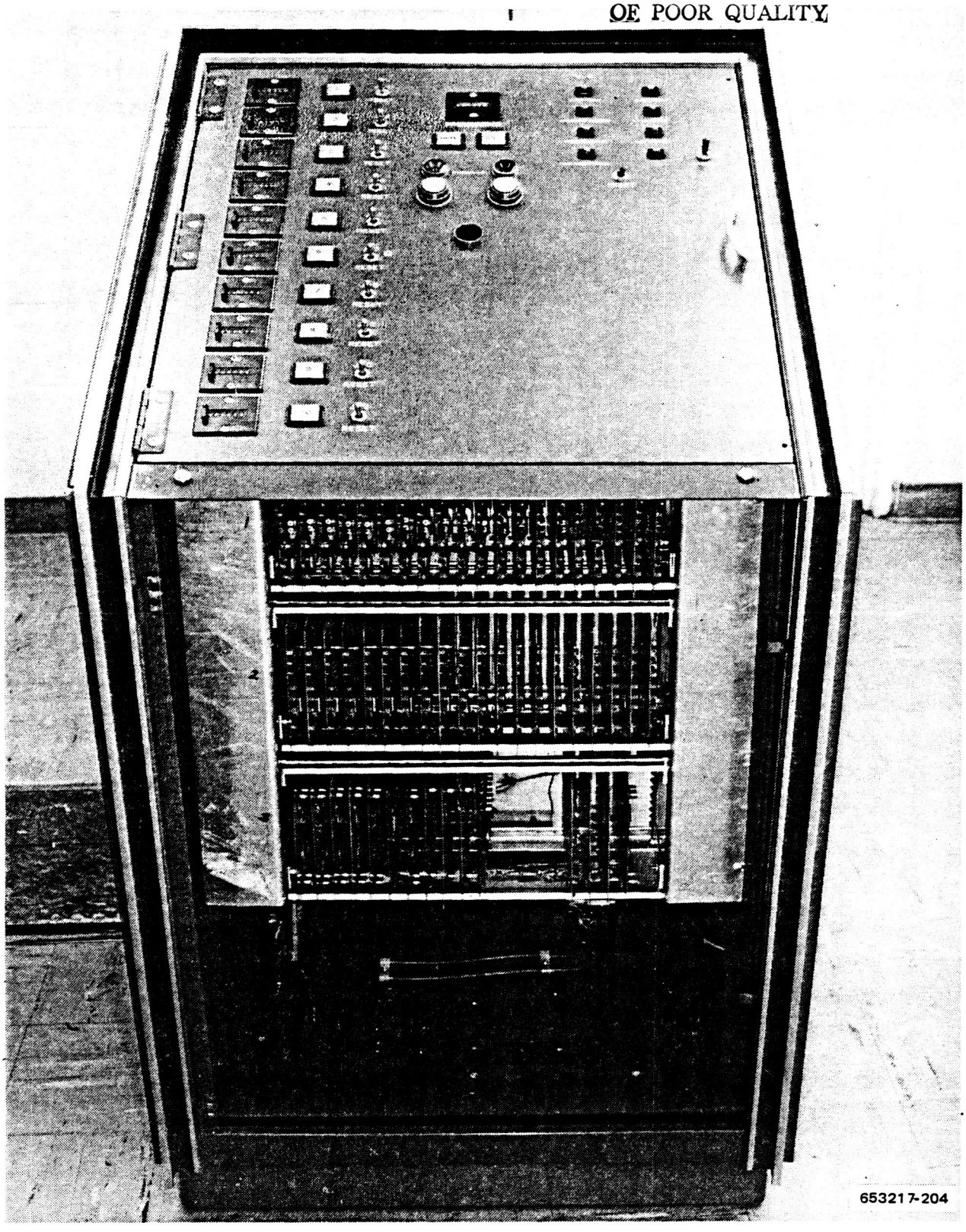



**Figure 12-4 SCR Flight Simulation Apparatus — Control Console**

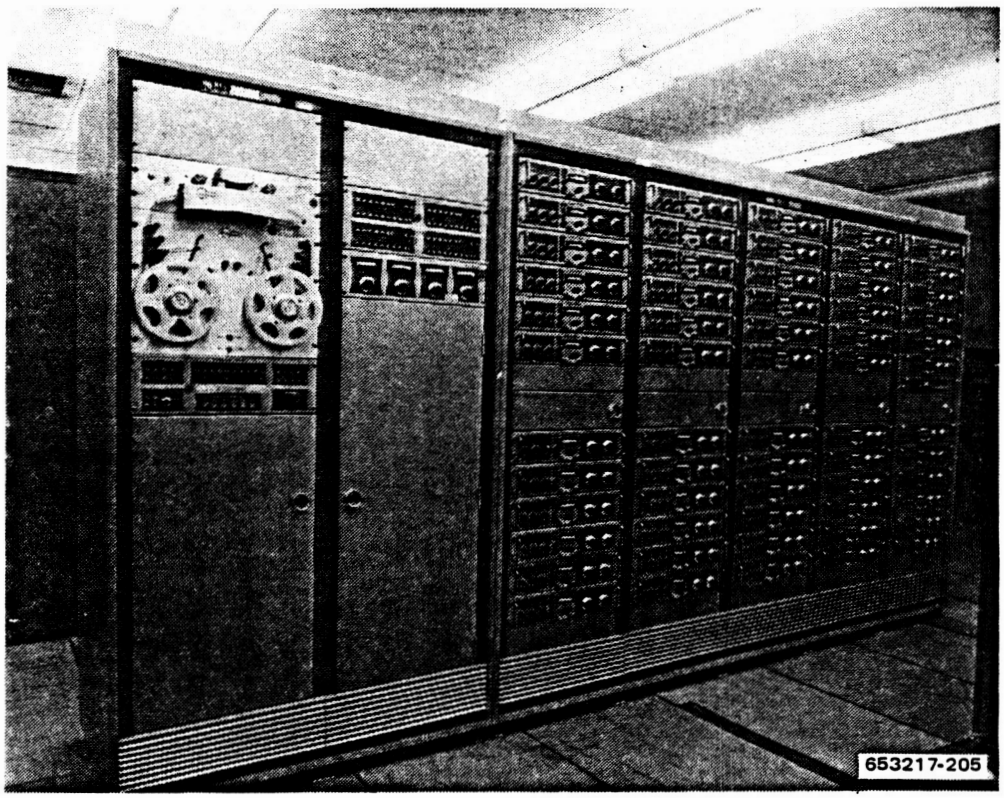



**Figure 12-5 Programmer and Load Controllers**

a. The load controller ERROR DETECTOR is activated if the error between the command and feedback system exceeds a preset value.

b. Program HOLD is activated if a malfunction occurs in timing, parity, or the power supply.

c. END OF PROGRAM code at the end of a punched tape places the program in "hold." If the test program is not manually restarted within a few minutes, all operations are deactivated.

**12.2.4 HYDRAULIC SYSTEM.** The hydraulic system consists of a hydraulic power source with oil reservoir level and oil temperature detectors, a manifold pressure dump valve, distribution manifolds and lines, and hydraulic actuating cylinders with pressure dump valves, filters, and servo valves.

Two hydraulic power sources were used during the test program. One 50 gpm pump of the 200 gpm Pump Station was used for the short-term tests. A 7 gpm portable hydraulic pump was used for the long-term tests.

**12.2.5 HEATING SYSTEM.** The test specimens are heated by 800-watt infrared quartz heat lamps. The heat is directed to the specimens by parabolic reflectors as shown in Figure 12-6. The lamps and reflectors are positioned so that they heat a 0.05 m (2 in.) strip on each half of the specimens. As discussed more fully in Section 12.3, this arrangement doubles the number of residual strength specimens that can be obtained from each long-term specimen. For each test setup, the five upper lamps and the five lower lamps are assembled in an upper rack and a lower



ORIGINAL PAGE IS
OF POOR QUALITY

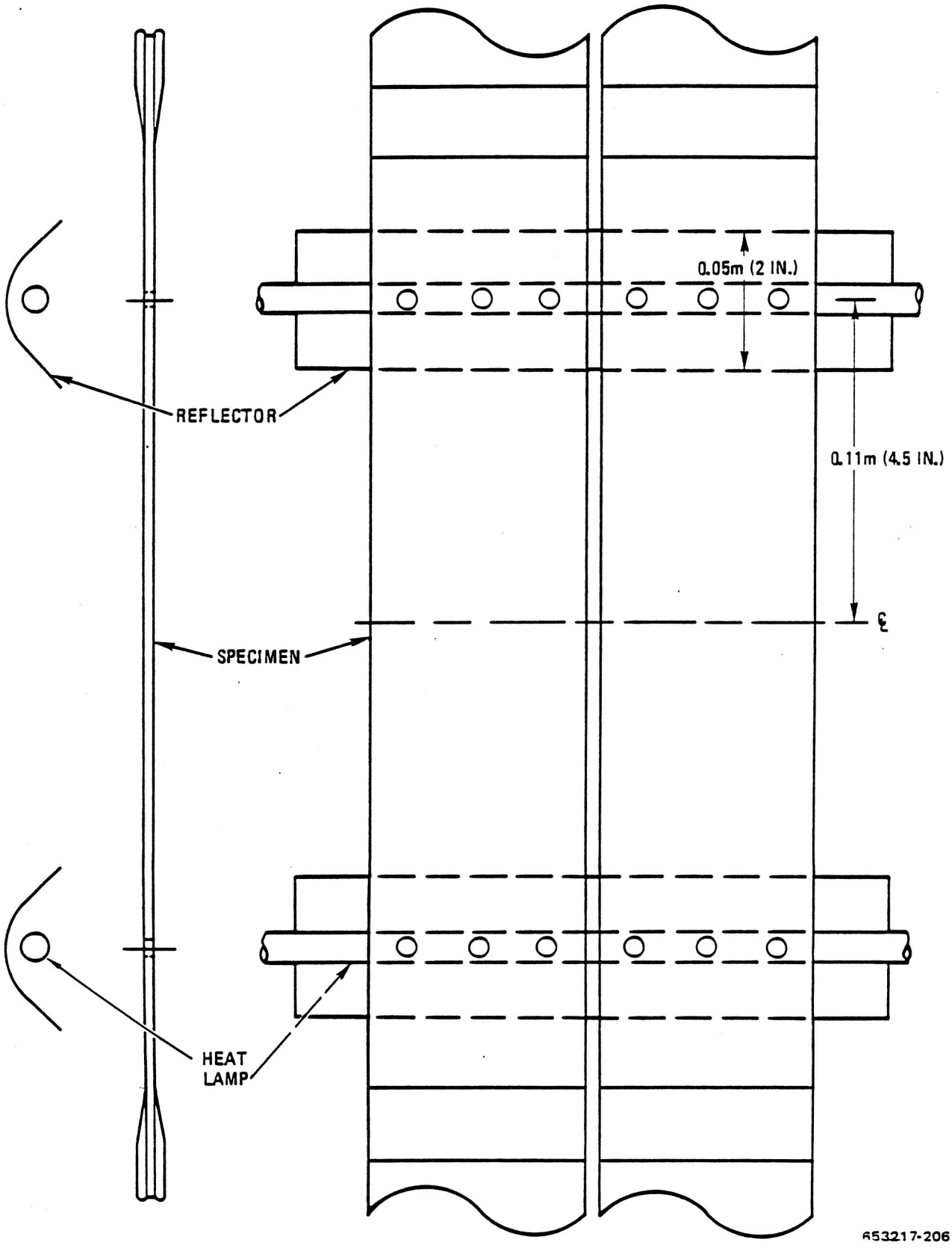



**Figure 12-6 Heating System Showing Arrangement of Specimens, Quartz Heatlamps, and Parabolic Reflectors**

rack. Each lamp rack is an independent heating system with its own temperature controller, control thermocouple, monitor thermocouple, and temperature error detection thermocouple.

The temperature cycling for the long-term test is synchronized with the loads by using the STEP code in the load programmer. STEP codes are programmed at the start and end of the heating period. The first STEP code activates the low temperature checking circuit for 10 milliseconds. If the specimen temperature is not less than 311 K (100° F), all test operations for that specific setup are deactivated. If the specimen temperature is less than 311 K (100° F), then power is applied to the heat lamps. The power is not controlled until the desired specimen temperature is obtained. The temperature controller and its control thermocouple will maintain the desired temperature within ± 6 K (10° F). The temperature error detector thermocouple makes an independent and continuous check against over-temperature occurrences. (This thermocouple is also used by the low temperature checking circuit.) In case of an over-temperature occurrence, all test operations for that specific setup are deactivated. The second STEP code removes the power to the heat lamps, and the specimens are allowed to cool.

**12.2.6 COOLING SYSTEM.** A large centrifugal blower driven by a five horsepower motor provides the cooling air for the test specimens. The cooling air is distributed to 50 locations by a duct system. At each location a nozzle directs the cooling air to a pair of test specimens. Air flow at each location can be adjusted by physically changing the nozzle outlet area. These nozzles are shown near the top in Figure 12-3. Figure 12-7 is a closeup view of the nozzles in operation during the long-term tests.

**12.2.7 CONTROL CONSOLE.** The control console, shown in Figures 12-4 and 12-8, contains the temperature control and checking circuits, malfunction/shutdown logic circuits, and system control and indicator circuits.

The control console front panel contains the following controls and indicators.

a. Ten setup counters to maintain the load programmer block count for each set up.

b. Ten dump switches/indicators to manually dump or indicate an automatic dump of any setup.

c. Ten JOG-RESET toggle switches to energize the hydraulics of each setup.

d. PROGRAMMER counter to indicate load programmer block count.

e. RUN and HOLD switches/indicators to provide remote control of load programmer.

f. LOAD and UNLOAD switches and indicators to provide remote control of the hydraulic pump pressure to all setups.

g. DUMP switch/indicator to completely shut down the hydraulic pump.

h. OVER TEMPERATURE, LOW TEMPERATURE, SPECIMEN FAILURE, LOAD ERROR, RAM OVERTRAVEL, MANUAL LOCK indicators to indicate which malfunction caused a test to stop. The numbered setup indicator will also indicate which setup is related to the malfunction.

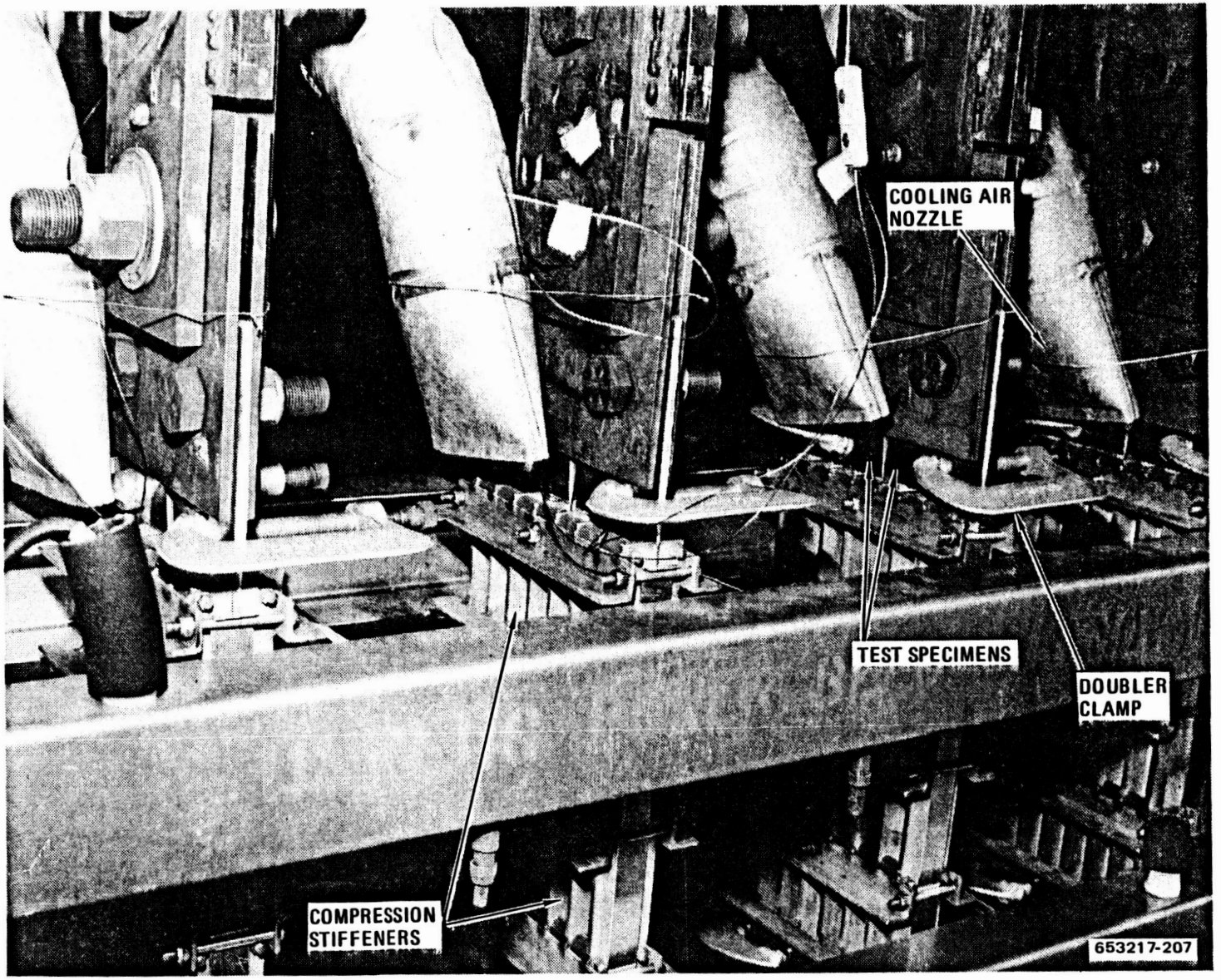



**Figure 12-7 Closeup-View of Flight Simulation Apparatus Showing Cooling Air Nozzles, B/Al Doubler Clamps, and Compression Stiffeners**



ORIGINAL PAGE IS
OF POOR QUALITY




**Figure 12-8 Control Console**

**12.2.8 DATA RECORDING SYSTEM.** All data are recorded on a high speed digital recorder. The 10 loads and 20 monitor thermocouples can be recorded on magnetic tape at a maximum sampling rate of six times per second. Data can then be printed out in engineering units.

Data are recorded periodically to confirm that loads appear to be reasonable and that the temperature cycle profile is correct. Loads cannot be confirmed exactly because the programmed loads are not known due to the random nature of the spectrum.

**12.2.9 MONITOR/SAFETY SYSTEM.** A Metrascope is used as a monitor and a limit detect safety system. Channels 1 through 10 display the tension loads up to 100% with the limits set to 105%. Channels 11 through 20 display the compression loads (1 through 10) up to 25% with



ORIGINAL PAGE IS
OF POOR QUALITY

the limits set at 30%. Channels 21 through 40 display the temperatures of each monitor thermocouple for each of the 20 lamp racks. The temperature limit is set 5% above the maximum temperature for a given setup.

If any limit is exceeded, the main electrical circuit breaker is thrown to its OFF position. All heat lamps go off, the hydraulic pressure at the manifold is dumped, the load programmer goes into HOLD, and all 10 setups are individually dumped. The channel that exceeded the limit is indicated by a flashing line on that channel.

**12.2.10 CHECKOUT.** Tests were performed to check out the loading mechanism and the distribution of loads by the whiffletree assemblies. A set of 10 strain gaged aluminum specimens was prepared and calibrated. The specimens were installed in the flight simulator and loaded to three load levels in the region of interest. Both the total applied load and the 10 individual loads were found to be within desired limits. The individual loads on each specimen were within ±3% of the desired load.

During checkout of the loading system, a dummy B/E short-term exposure specimen was intentionally loaded to failure in the simulator to determine the effects of individual specimen failures on the load levels of similar specimens within the same whiffletree arrangement. Each whiffletree contains five pairs of specimens. The specimens are loaded by a command from the programmer. This load program command signal is continuously compared to the signal from the load cell, and if the difference is more than a fixed amount, the loading mechanism shuts down. To check the response times of this arrangement in the event of specimen failure, the loads were monitored on two adjacent specimens, the specimen paired to the failed specimen, and one specimen in the adjacent pair. The strain gage and recorder arrangement used had a combined response time of well under 0.01 second. At failure, the load on the specimen paired to the failed specimen dropped to zero in 0.01 second. A compressive load of 10% of the tensile load was recorded for a duration of 0.01 second. The adjacent specimen lost about 20% of its tensile load for 0.02 second and recovered to 95% of the original load, which it maintained until the load was dumped at 0.18 second; the load then decayed linearly to zero in about 1 second.

**12.2.11 AUTOMATIC OPERATION.** To do long-term testing at the lowest cost and to be able to complete 50,000 hours testing in the shortest total time, the simulator must be automatic and be capable of operating unattended a high percentage of the time. During the Phase I 10,000 hour tests the simulator operated on the average of 125 hours per week or about 75% of the time available. The monitoring and safety features were largely responsible for the off time. They were, however, very important in order to avoid destroying or damaging specimens during flight simulation testing. There were a number of other factors that have restricted the average run time to 125 hours per week. When equipment of this type is operated year after year, periodic maintenance must be performed. Recorders, heat lamps, hydraulic cylinders, bearings and electronic components must be serviced or replaced. The equipment must be shut down to remove broken specimens. When shutdown occurs in early evening or during the weekend, additional time is lost because the resin matrix specimens must be dried before operation is resumed.

During the Phase II tests, which consisted of almost 40,000 hours of exposure, simulation operation dropped to an average of about 100 hours per week. The Phase II flight simulation required almost seven years to complete. Reasons for the decrease in operating efficiency were numerous but were generally related to the many years of almost continuous operation of the apparatus.

One of the major problems was frequent parity errors in the programming system with subsequent shutdown of the test apparatus. The problem was finally resolved with a parity error resetting meter after many months of intermittent operation. Another lengthy delay was caused by a faulty tape reader. In-house repair was not successful so that the device had to be returned to the manufacturer for refurbishing. Similar problems were experienced with the Metrascope, the primary monitor and limit detect safety system, and extensive repair and replacement of several components were required. During the latter portion of the test program the flight simulation apparatus required considerable maintenance, primarily because of numerous hydraulic leaks. Other problems that affected the operation of the flight simulation apparatus and contributed to the reduction in the weekly average run times are listed below:

Programmer problems with the tape drive, tape reader, bearings, lamps, etc.

Temperature control and faulty overtemperature indications

Load control problems

Hydraulic pump or line failures and oil leaks

System oil spills

Hydraulic pumps overhaul

Servoblock repeated failures

Power supply failure (28 Vdc)

Controller circuit failure problems

Power failures

Servo amplifier problems

Various electronic and mechanical component failures

Doubler bond failures (primarily B/Al)

Specimen failures

System calibration and specimen inspections

High priority mainline contract tests

Flood damage in programmer room during heavy rains

Cooling system motor failure

## 12.3 SPECIMEN CONFIGURATION

The unnotched specimen configuration for the long-term tests is shown in Figure 12-9. The composite portion of the specimen was 0.076 m (3 in.) by 0.46 m (18 in.). The tapered doublers bonded at each end of the specimen extended the overall length to 0.56 m (22 in.). Aluminum spacers of the same thickness as the composite were used to fill the gaps between the titanium doublers in the regions where the pin holes were located. The specimens were pin loaded to ensure uniform loading for the whiffletree arrangement used. Half of the resin matrix long-term specimens were prepared with notches consisting of 0.0064 m (0.25 in.) diameter holes. As shown in Figure 12-10, these holes were located so that they were centered in each of the six 0.025 m (1 in.) by 0.23 m (9 in.) post-test specimens to be cut from the notched long-term

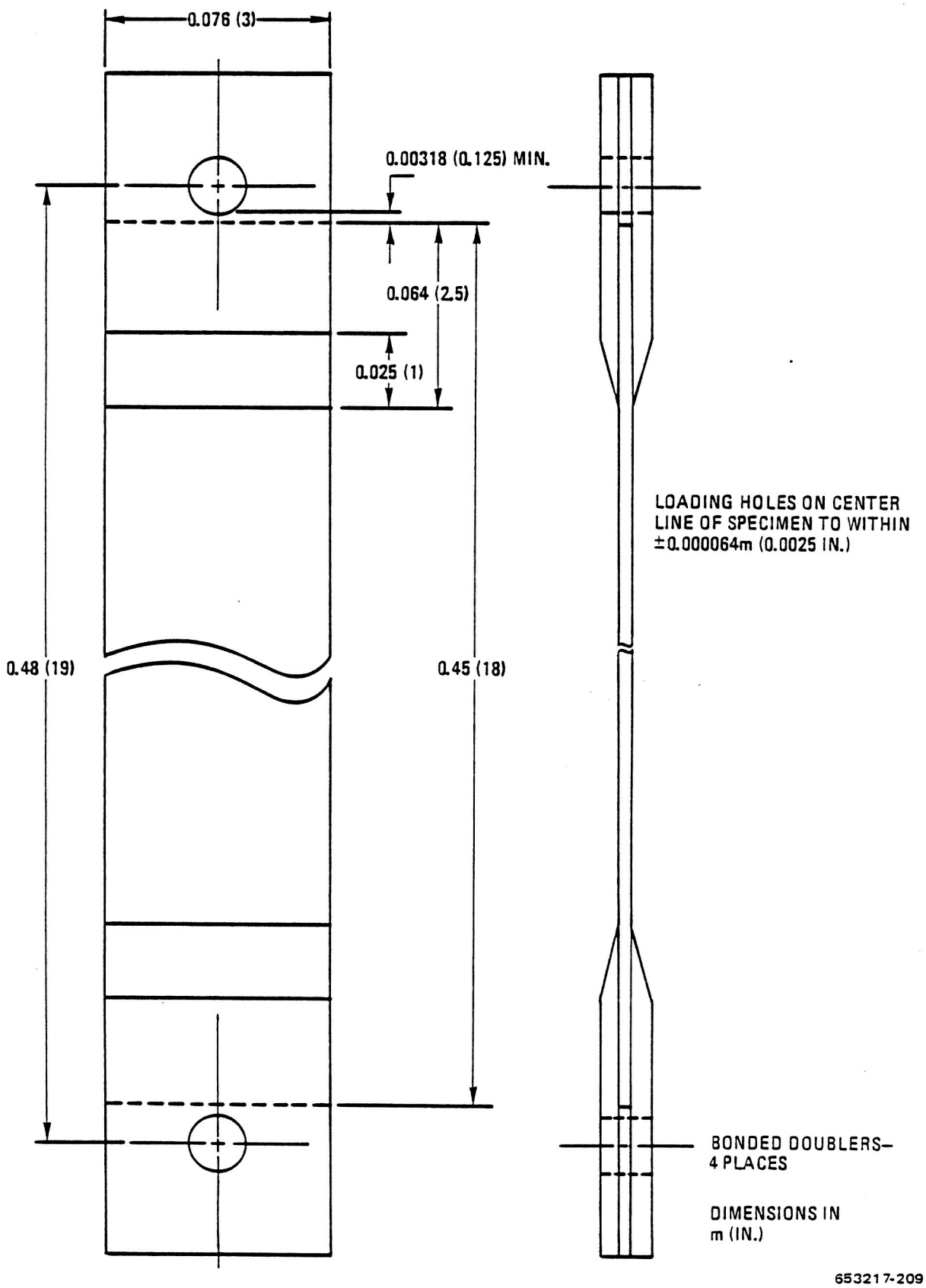



**Figure 12-9 Long-Term Flight Simulation Specimen**

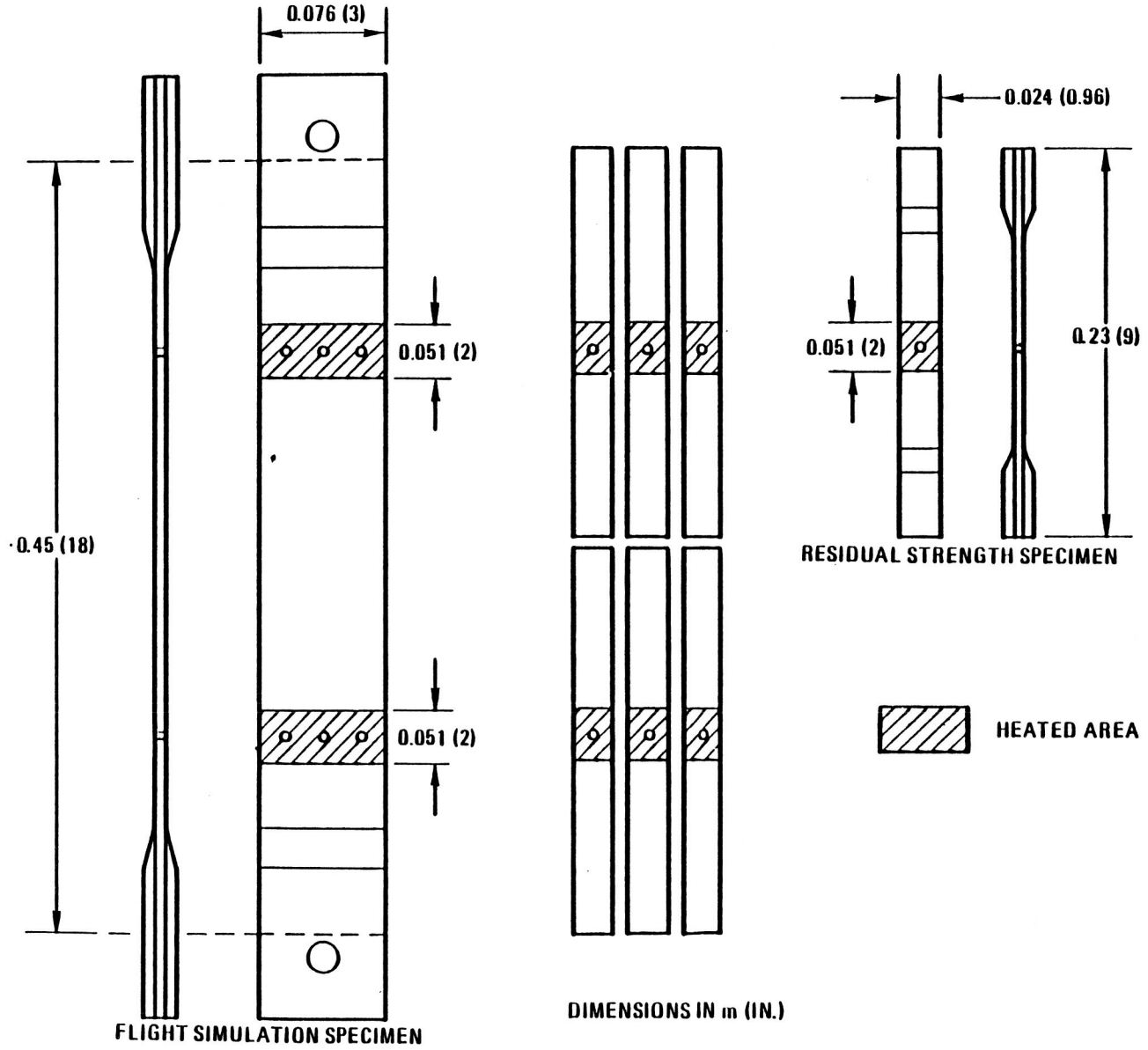



**Figure 12-10 Cutting Plan for Post-Test of Notched Long-Term Specimens**

specimens after flight simulation exposure. These specimens were used to determine the residual notched tensile or fatigue strength of the composite after flight simulation. The unnotched long-term specimens were also cut into smaller pieces for residual strength testing. The original plan was to cut each long-term specimen into twelve 0.013 m (0.5 in.) by 0.23 m (9 in.) post-test specimens. As discussed later, this plan was slightly modified as a result of the condition of the specimens at the completion of 10,000 hours of exposure. All of the post-test tensile and fatigue specimens used bonded doublers as shown at the right in Figure 12-10. Two sets of quartz heat lamps 0.23 m (9 in.) apart were positioned so that they heated a 0.05 m (2 in.) strip on each half of the long-term specimen (see Figure 12-6). This arrangement placed the 0.05 m (2 in.) heated zones at the centers of the post-test specimens. The edges of the heated zones were 0.025 m (1 in.) from the doublers so that the adhesive was not subjected to the operating temperature of the composite during simulation. Temperature measurements taken during testing showed the titanium end doublers to be approximately 69 K (125° F) cooler than the 408 K (275× F) heated zones of the epoxy specimens and approximately 117 K (210° F) cooler than the 505 K (450° F) heated zones of the G/PI and B/Al specimens. One modification was made to the B/Al specimens to increase the efficiency of heating during flight simulation exposure. The heated zones on the sides facing the quartz heat lamps were coated with flat black, heat resistant paint to reduce reflection from the aluminum surface.

The requirements for the short-term flight simulation specimens were less restrictive than for the long-term specimens because only residual tensile strength properties were to be obtained after the 100 and 200 hours of exposure. With this in mind a short-term specimen was designed that could be tensile tested after flight simulation with no further modifications, i.e., machining or doubler bonding. The specimen that was used is shown in Figure 12-11. A further advantage in using the 0.025 m (1 in.) wide specimen rather than the 0.076 m (3 in.) wide long-term configuration was a considerable savings in material. To satisfy the pin loading requirement of the flight simulation apparatus it was necessary to use the 0.05 m (2 in.) wide end doublers shown in Figure 12-11. The space between each set of doublers not occupied by the end of the composite material was filled with aluminum sheet of the same thickness as the composite. Also shown in Figure 12-11 is the notched specimen used for half of the resin matrix short-term tests. The 0.0064 m (0.25 in.) diameter holes, one in each half, are centered in the 0.05 m (2 in.) heated zones in like manner to the long-term specimens.

## 12.4 RANDOM LOAD SPECTRUM

The objective of the SCR spectrum generation task was to provide a load simulation that would be representative of flight conditions during the life of a supersonic cruise aircraft and would be acceptable and remain acceptable to all concerned parties during this long real-time flight simulation test program. Developments (ref. 43 and 44) in random flight-by-flight load simulation have produced a simple method for generating a random load sequence that matches the desired load-exceedance relationships on a mission segment basis. These studies have shown the importance of including the random character of the individual load, adhering to flight-by-flight profiles, and including the ground-air-ground load for each flight.

Several assumptions were made to define the loading spectrum. The mission profile and loads data were obtained from reference 4. These data were also used for the study described in reference 5. The life of a supersonic cruise aircraft was assumed to consist of 25,000 flights of two hours duration each. For this work, each flight was assumed to be an "operational flight" as defined by reference 4. Each flight consisted of a 10-minute climb, a 90-minute cruise, a

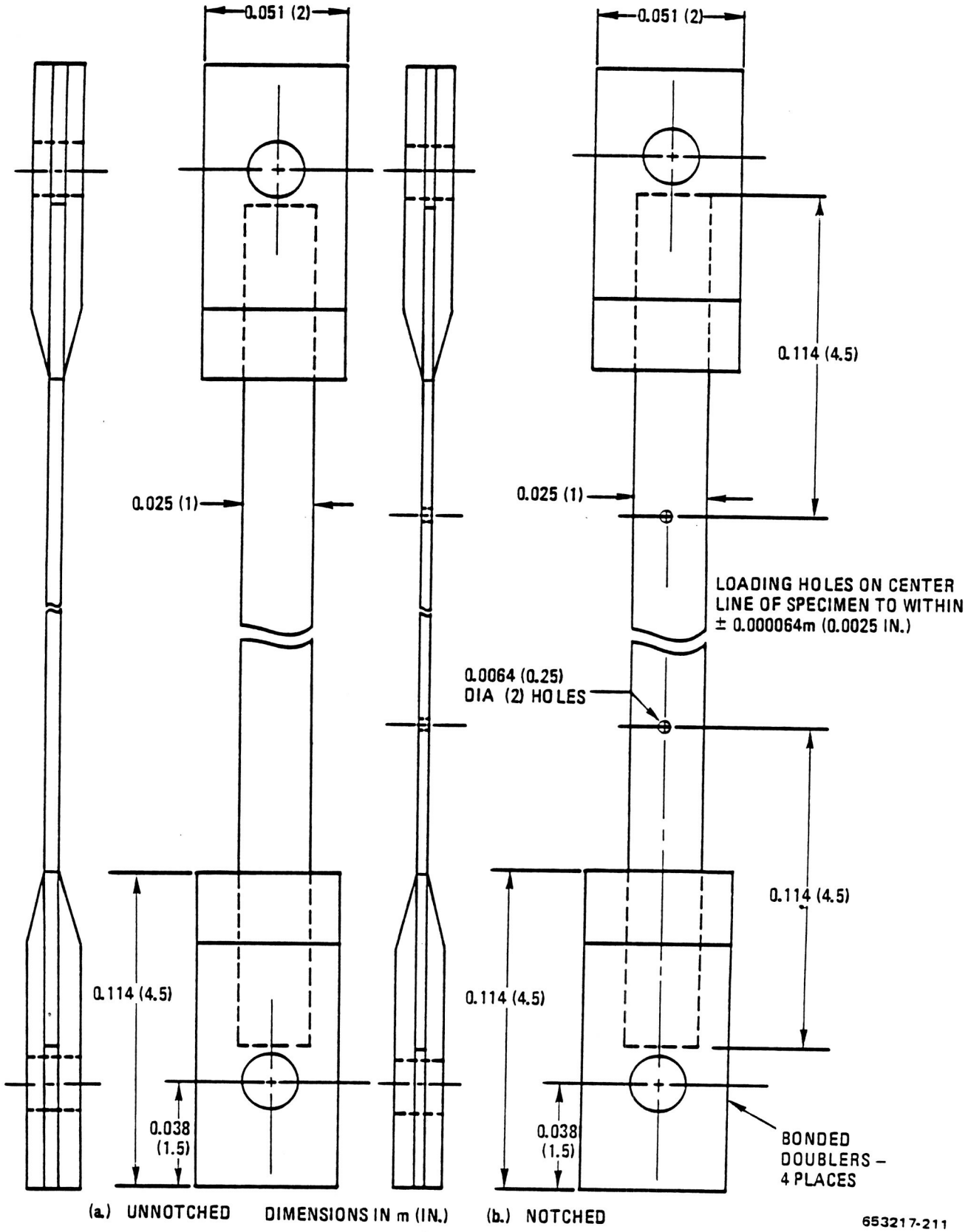



**Figure 12-11 Short-Term Flight Simulation Specimens**

20-minute descent, and a single landing load. The number of loads per flight and the number of loads in each of the segments were modeled after the reference 4 load sequence. However, the loads were randomized such that all the loads expected to occur in 10,000 flights were included. Since the 90-minute cruise was scheduled to include only about eight loads per flight, the mean load was held for 44 minutes before and after the imposition of a two-minute cruise loading period. The climb and descent loads were distributed over the entire climb and descent time.

To simulate the mission thermal profile for a Mach 3 cruise, an elevated temperature was applied to the specimens. From room temperature at the beginning of climb, the temperature was increased uniformly to the maximum use temperature for each material. Once the random load spectrum was generated, the magnitude of the loads and the maximum use temperature or cruise temperature was adjusted to suit each of the composite systems being studied. Both the load magnitudes and cruise temperatures were set using data from the baseline measurements and test data obtained by using the load spectrum at an accelerated rate. The loading rate was increased so that the loads normally occurring during a two-hour flight would occur in one minute. These accelerated tests were run at the cruise temperature and are referred to as short-term tests.

**12.4.1 SPECTRUM GENERATION FOR THE LONG-TERM TESTS.** The segment exceedance curves from reference 4 are shown in Figures 12-12, 12-13, and 12-14. The Gaussian process line needed for the random simulation is shown in each figure. The mapping function data are shown in Table 12-1.

The $N_o$ values for each segment were arrived at by the following argument. The long-term test simulation of reference 4 considered 10,000 flights. In this simulation it was desired to maintain the number of load values at 80 per flight. Since 20 dwell signals were required per flight to maintain the mean cruise load during heating and one landing load was included in each flight, there were 101 loads per flight for a total of 1.01 million loads for the 10,000 flights. For this work these 1.01 million loads are applied in 25,000 flights, thus requiring about 40 loads per flight. Since there are actually only 32 minutes of loading per two-hour flight, the overall cyclic frequency, $N_p$, of load values is calculated as:

$$N_p = 40 \text{ cycles}/32 \text{ minutes} = 1.25 \text{ cpm}$$
$$= 75{,}000 \text{ cycles}/1000 \text{ hours}$$

The average number of mean crossings per unit time, $N_o$, is defined as the product of the irregularity factor ($R = 0.9$) and $N_p$, giving:

$$N_o = (0.9)N_p = 67{,}500 \text{ cycles}/1000 \text{ hours}$$

The 10-minute climb, 90-minute cruise, and 20-minute descent segments represent 31%, 6.25%, and 62.5% of the total loading time, respectively. For this program spectrum, the climb, cruise, and descent segments contain 70%, 12%, and 18% of the total number of loads. The $N_o$ values for each segment were calculated as:

$$N_o \text{(Climb)} = N_o (0.7)/(0.31) = 152{,}000 \text{ cyc/kseg hr}$$
$$N_o \text{(Cruise)} = N_o (0.12)/(0.0625) = 129{,}600 \text{ cyc/kseg hr}$$
$$N_o \text{(Descent)} = N_o (0.18)/(0.625) = 19{,}440 \text{ cyc/kseg hr}$$

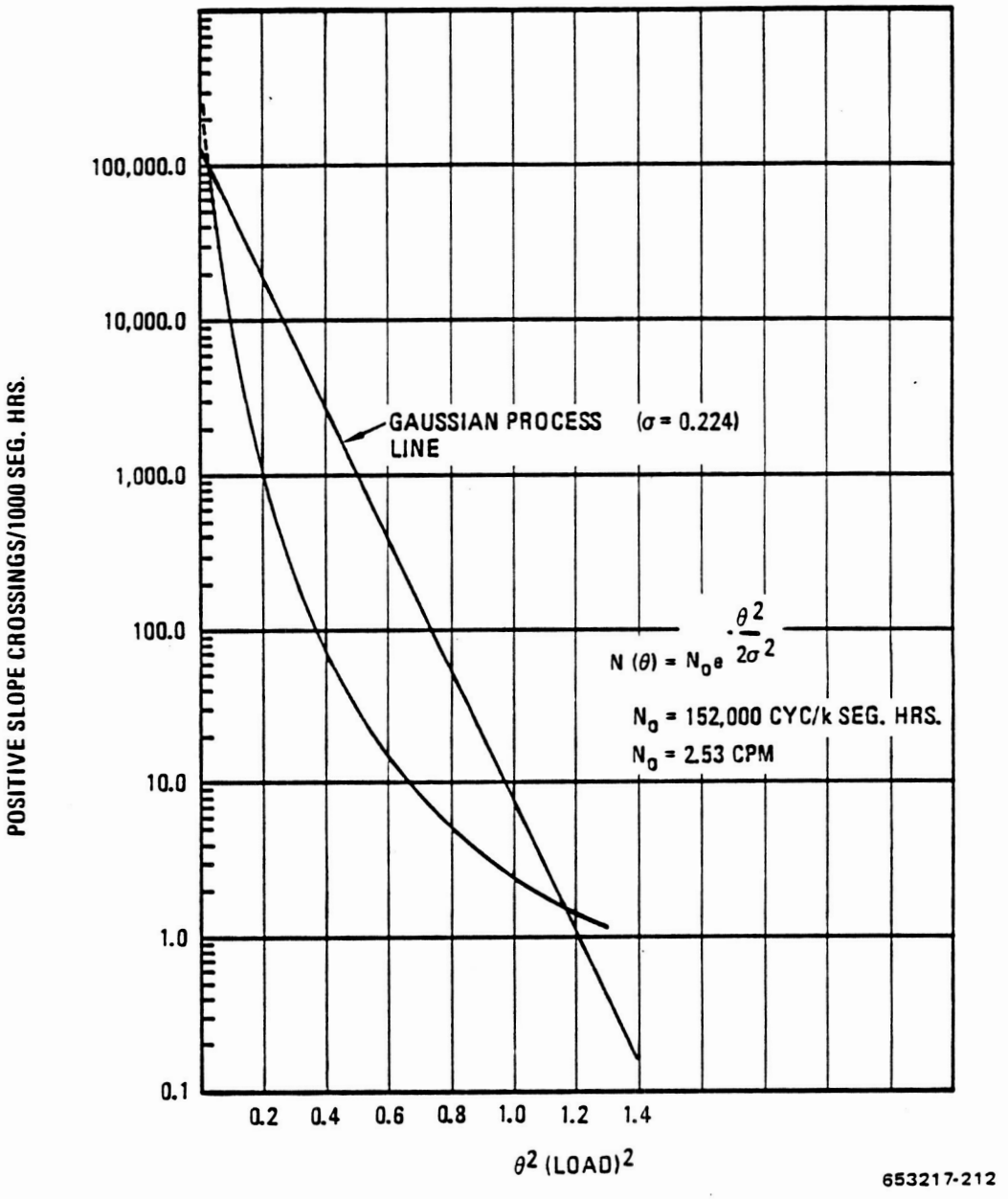



**Figure 12-12 Climb Exceedance Curve**

These values along with the other mission parameters were input to the General Dynamics Simulated History of Aircraft Missions (SHAM) computer procedure, which generated the load history (ref. 44). A typical mission is shown in Figure 12-15.

**12.4.2 SPECTRUM FOR THE SHORT-TERM TESTS.** To set the magnitudes of the long-term loads for each composite system some accelerated tests were performed. This was accomplished by increasing the frequency of loading to the point where a half of a lifetime of loads could be applied to specimens of each composite system in 200 hours. These groups of specimens were held at constant temperatures. The temperatures chosen were their maximum use temperatures. These tests, which were run for 100 hours and 200 hours, are referred to as the short-term tests. The objective of the short-term tests was to apply as many mission loads as

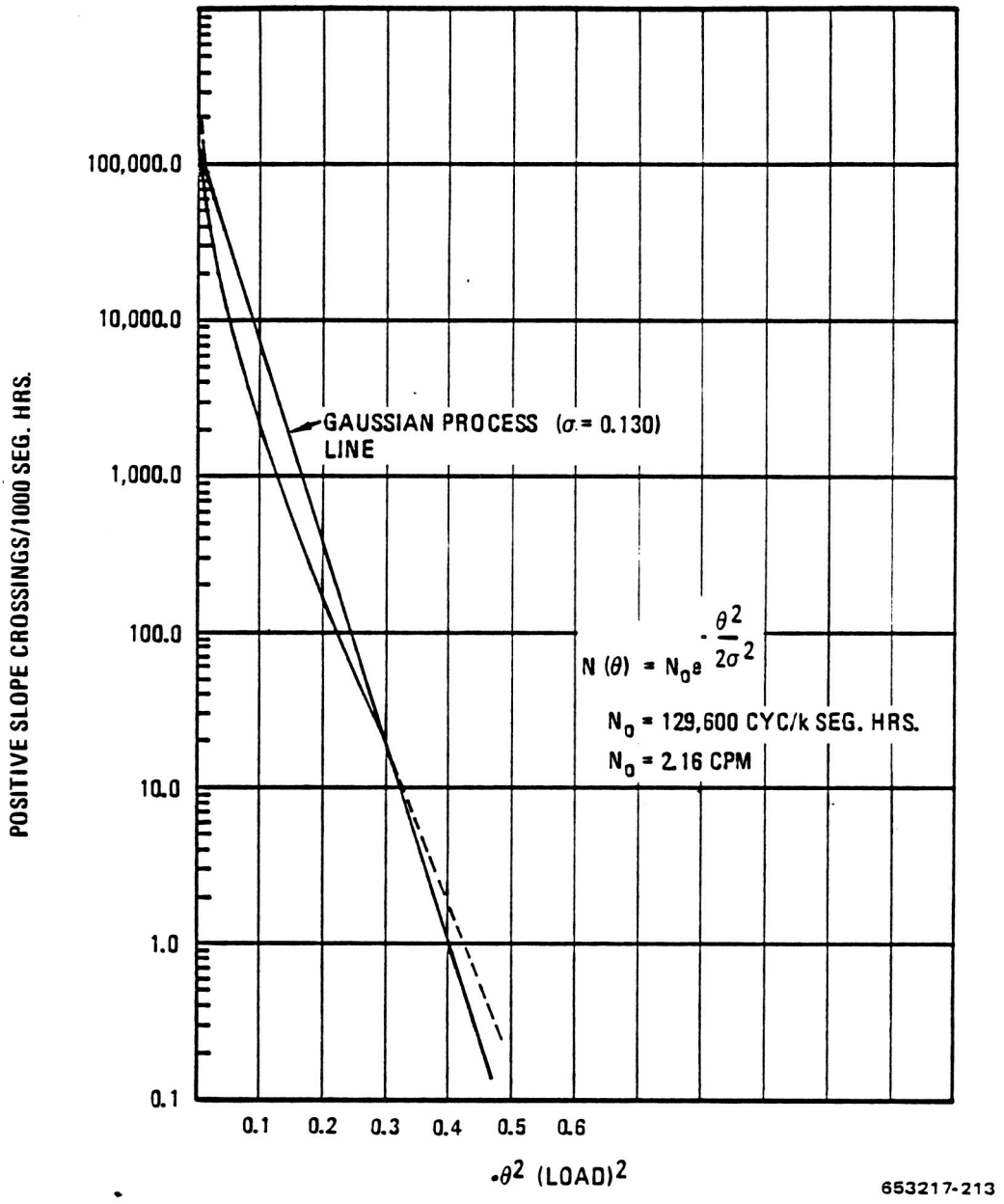



**Figure 12-13 Cruise Exceedance Curve**

possible to the specimens in a short time. The random character of the loads, the flight-by-flight sequence, and the landing load were all maintained in the accelerated spectrum.

It can be shown that the minimum periods of the long-term test climb, cruise, and descent segments are 8.5, 10, and 66.25 sec/load, respectively. To obtain a maximum cyclic rate of 50 cpm, the minimum period for each segment should be 0.6 sec/load. The acceleration factors were thus calculated as:

(AF) climb = 8.5/0.6 = 14.167

(AF) cruise = 10/0.6 = 16.67

(AF) descent = 66.25/0.6 = 110.417

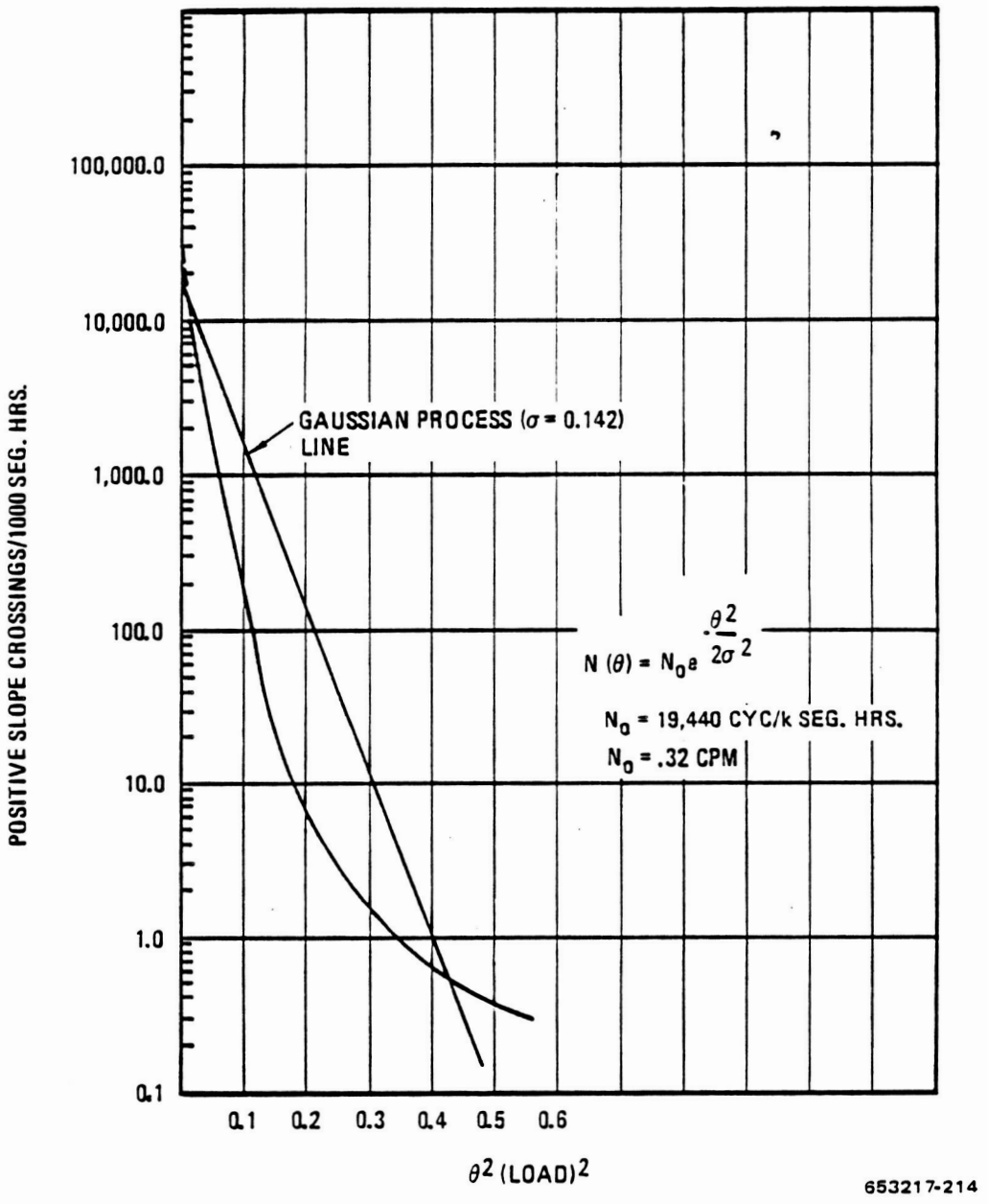



**Figure 12-14 Descent Exceedance Curve**

These acceleration factors and the long-term test mission data were input to the SHAM procedure to produce the short-term test history. A flight lasts about 60 seconds and is divided into approximately 25 climb loads in 42 seconds, six cruise loads in seven seconds, and seven descent loads and one landing load in 11 seconds. A typical load sequence is shown in Figure 12-16. The accelerated spectrum results in an overall rate of one minute per flight, so that in 100 hours of testing, about one fourth of a cruise aircraft lifetime (6000/25,000) can be imposed.

## 12.5 WEAROUT MODEL

At the time these tests were started a wearout model had been developed and used on epoxy matrix composite systems. The fatigue and residual strength data from the short-term service

Table 12-1. Mapping Function Data

| Crossing/ (k segment hr) | $\left(\text{Gaussian Load}\right)^2$ | $\left(\text{Real Load}\right)^2$ | Gaussian Load | Real Load | $\sigma$ | N (cpm) |
|---|---|---|---|---|---|---|
| | | Climb Segment | | | | |
| 152,000 | 0 | 0 | 0 | 0 | 0.224 | 2.53 |
| 100,000 | 0.04 | 0.04 | 0.2 | 0.2 | | |
| 10,000 | .27 | .095 | .520 | .308 | | |
| 1,000 | .50 | .205 | .707 | .453 | | |
| 100 | .73 | .375 | .854 | .612 | | |
| 10 | .96 | .655 | .980 | .809 | | |
| 5 | 1.03 | .79 | 1.015 | .889 | | |
| 2 | 1.13 | 1.05 | 1.063 | 1.025 | | |
| 1 | 1.2 | 1.43 | 1.095 | 1.196 | | |
| | | Cruise Segment | | | | |
| 130,000 | 0 | 0 | 0 | 0 | .130 | 2.16 |
| 100,000 | 0.01 | 0.01 | 0.1 | 0.1 | | |
| 10,000 | .09 | .045 | .3 | .212 | | |
| 1,000 | .165 | .130 | .406 | .361 | | |
| 100 | .245 | .225 | .495 | .474 | | |
| 10 | .32 | .325 | .576 | .570 | | |
| 1 | .4 | .425 | .632 | .652 | | |
| | | Descent Segment | | | | |
| 19,000 | 0 | 0 | 0 | 0 | .142 | 0.324 |
| 8,500 | .035 | .035 | .187 | .187 | | |
| 1,000 | .12 | .06 | .346 | .245 | | |
| 100 | .215 | .12 | .464 | .346 | | |
| 10 | .305 | .18 | .552 | .424 | | |
| 3 | .355 | .24 | .596 | .490 | | |
| 1 | .4 | .34 | .632 | .583 | | |
| 0.5 | .43 | .44 | .656 | .663 | | |

history tests on two of the four composite systems, i.e., G/E and B/E specimens, were analyzed using the wearout model developed in references 6 and 45 and previously used in references 46 and 47.

The wearout or fatigue model is reviewed here and examples of its use will be given for the epoxy system in the section on short-term test results. This model is based on four assumptions (three physical and one mathematical form).

a. Materials fail because of the presence of preexisting flaws.

b. Flaws grow in a deterministic manner. The manner is determined by material properties, state, and magnitude of the stresses at the flaw perimeter; history of applied stress; and the thermal and mechanical history.

c. The critical load for a structure is a function of instantaneous flaw state, and the distribution of residual strengths defines the flaw field statistics.

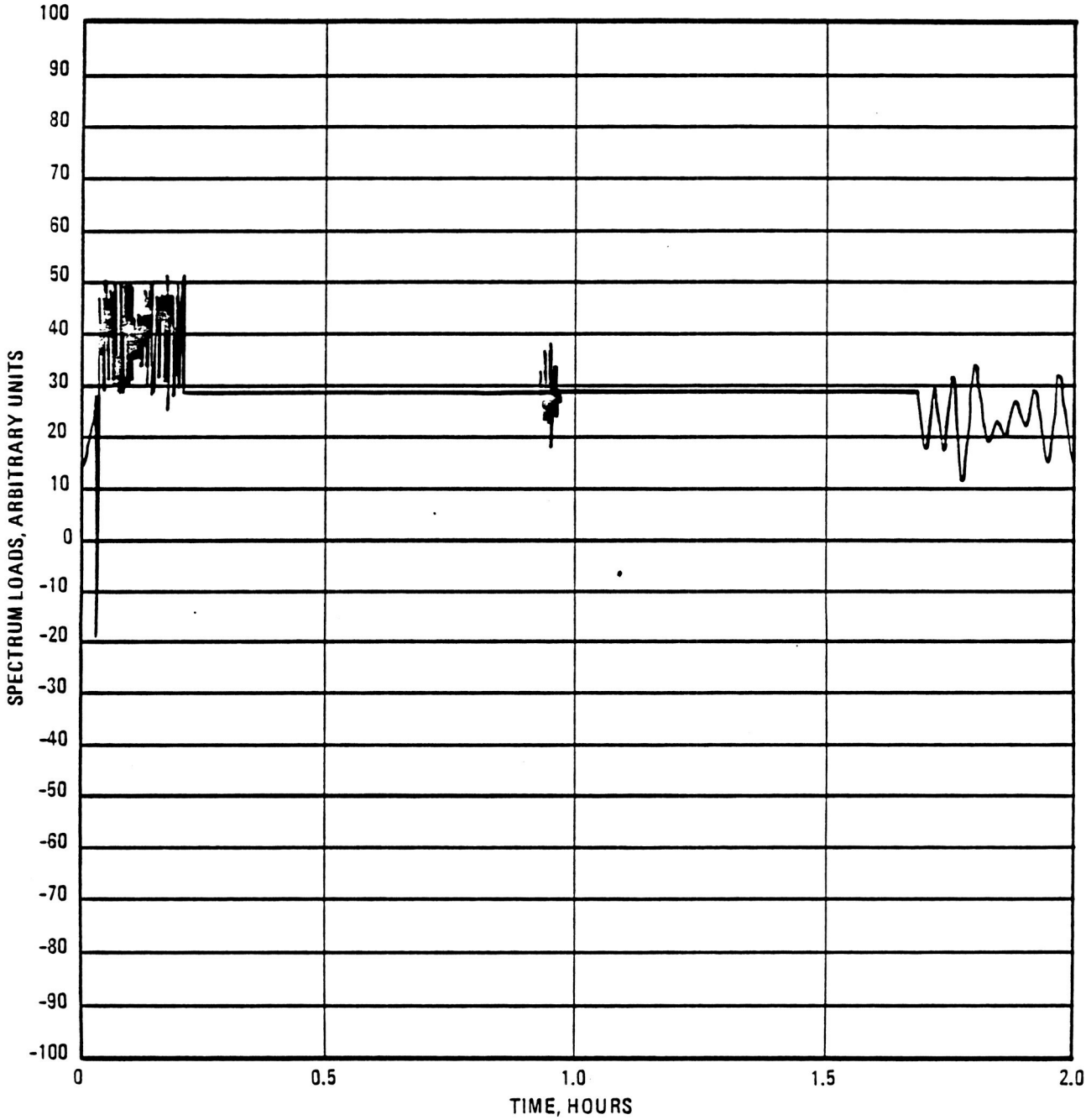



**Figure 12-15 Typical Mission for Long-Term Testing**

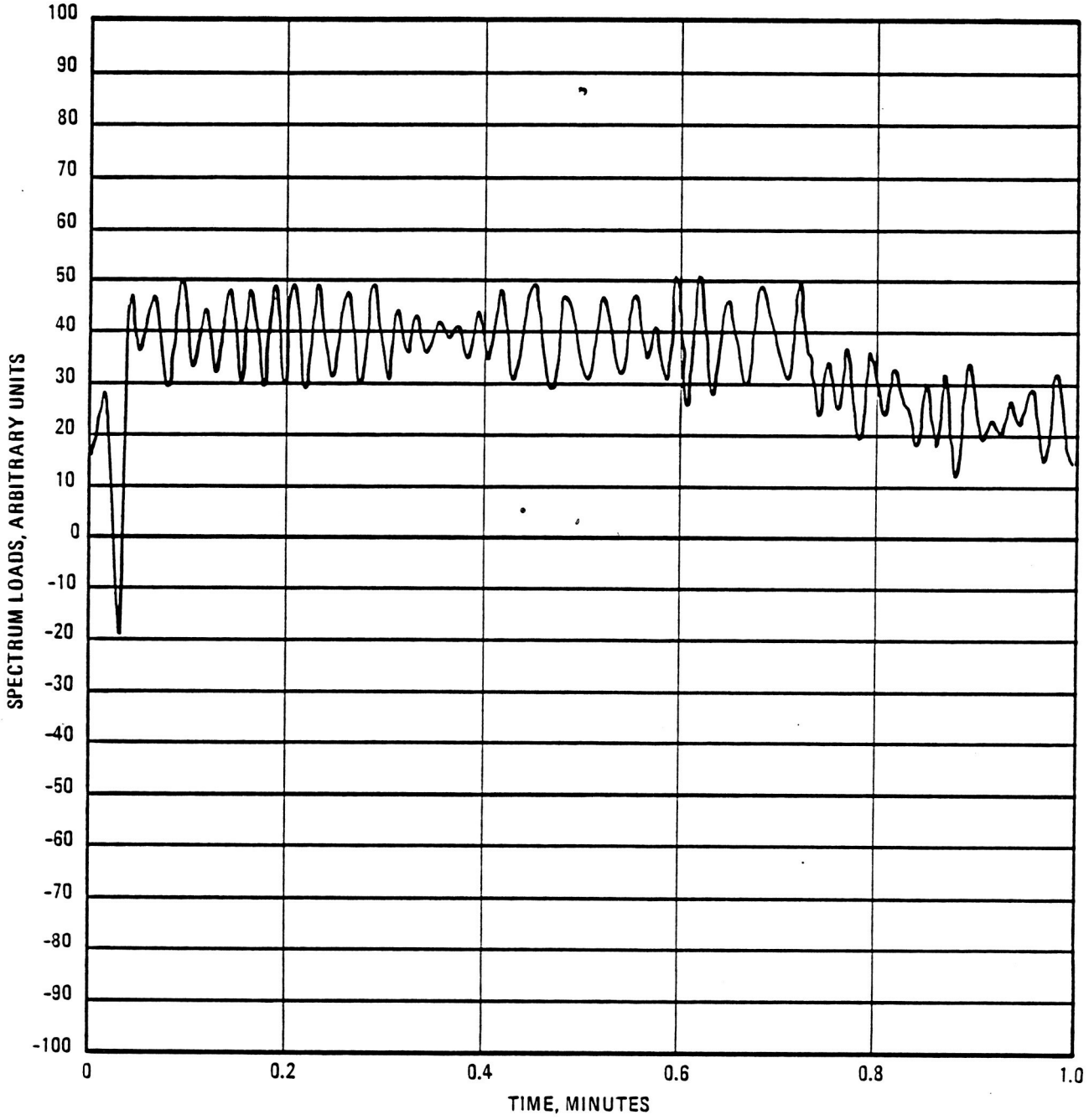



**Figure 12-16 Typical Mission for Short-Term Testing**

d. Damage rate accumulation is of the functional form:

$$\frac{\partial C}{\partial t} = M \cdot C^{r}, \tag{1}$$

where C is the flaw length and r is the flaw growth rate exponent.

The residual strength function $F_R^{(t)}$ can be shown to have the form

$$F_R^{(t)} = \left[ F_R^{(t_o)^{2(r-l)}} - A_4 (r-l) A_1^S (t-t_o) \right]^{\frac{1}{2(r-l)}} \tag{2}$$

where:

$A_1 = F_{max}/F_{ref.}$ with $F_{max}$ being the truncation load a measure of rms stress and $F_{ref}$ being a reference rms stress level.

The term $A_4$ is related to the history-dependent constant (M) in Equation (1).

The term r is the exponent of the flaw state (C) in Equation (1).

The term $-1/s$ is the slope of the ln $F_{max}$ $-$ ln t curve and is related to r.

The term t refers to time and $t_o$ is a reference time condition.

If the initial assumptions are correct, the results of varying stress history, environmental conditions, and geometry are contained in $A_4$.

Note that Equation (2) is a strictly monotonic decreasing function of time. Therefore, time t must be measured after the initial stress relaxation occurs. If this point in time is considered to be the time origin, t = o, Equation (2) may be considered applicable for all positive values of t. F (t = o) is the initial static strength of the component possessing a Weibull (extreme value) distribution:

$$P(F(t_o) > F) = \exp\left\{ -\left( \frac{F}{\beta_o} \right)^{\alpha_o} \right\} \tag{3}$$

where $\alpha_o$ and $\beta_o$ are the shape and scale parameters, respectively, for the Weibull distribution. Introducing the Weibull flaw distribution, Equation (3), into Equation (2) gives the time-varying residual strength distribution of the form:

This equation is represented functionally as

$$f(P, F_R) = A_4 t$$

Therefore, the constant $A_4$ is the slope of the linear regression equation fitted to the empirical data. The iteration sequence is begun with an assumed value of "r" and repeated until the error term, i.e., the probabilistic squared difference between the model and the observed data, becomes a minimum.

$$P\left(F_R(t) > F_R\right) = \exp - \left[ \frac{F_R^{2(r-1)} + (r\text{-}1)\, A_4 A_1^S\, t}{\beta_o^{2(r-1)}} \right]^{\frac{\alpha_o}{2(r-1)}} \tag{4}$$

for $F_R > F_{max}$

$$P(0 < F_R(t) < F_{max}) = 0$$

and

$$P\left(F_R(t) = 0\right) = 1 - P(F_R(t) > F_{max})$$

The probabilistic Equation (4) does not involve the reference time $t_o$, which appears in Equation (2), and agrees with Equation (3) when t = o. For fixed time t, it follows from Equation (4) that the transformed variable $F_R(t)^{2(r-1)}$ has a truncated three-parameter Weibull distribution.

The distribution depicted in Equation (4) has a limiting form for $(F_{max}/\beta_o)2(r-1) << 1$, which gives the lifetime distribution as:

$$P(T > t) = P\left[F_R(t) > F_{max}\right] = \exp - (t/\beta_f)^{\alpha_f} \tag{5}$$

where:

$$\alpha_f = \frac{\alpha_o}{2(r-1)} \tag{6}$$

$$\beta_f = \frac{\beta_o^{2(r-1)}}{(r-1)\, A_4\, A_1^S} \tag{7}$$

If specimen behavior is found to be consistent with the model, the following responses would be expected.

a. The lifetime shape parameter would be independent of rms stress, temperature, and humidity.

b. Both the truncation load-endurance data and initial shape parameter to fatigue shape parameter relationship will yield consistent values of r.

c. Characteristic strengths and endurances will shift log-linearly.

The program used to fit the wearout model to the experimental data sample is based on minimizing the "error" between the prediction (model) and the data. The model parameters $\alpha_o$, $\beta_o$, and $t_o$ and the experimental data are available as "known" values for input. The program uses an iteration procedure to minimize the error (variance). The iterative solution may be accomplished by determining either the value of "r" or of "$A_4$" that gives a minimum error.

When the value of r is to be used in iteration, a value of $A_4$ must first be determined. The probabilistic model may be written in the form:

$$\frac{\left\{\beta_o \left[\ln \frac{1}{P}\right]^{\frac{1}{\alpha_o}} - F_R(t)\right\}^{2(r-1)}}{A_1^{2r(r-1)}} = A_4 (t-t_o)$$

where:

$$P = P\ (F_R(t) > F_R)$$

and

$$A_1^{2r} = 1$$

The application of this model to the short-term test data is shown in Section 12.6. That section will clarify the determination of parameters $A_4$, s, and $A_1$.

$\alpha$, $\beta$ — Weibull shape and scale parameters for the distribution of the tensile data.

$\alpha_o$, $\beta_o$ — Weibull parameters at time zero.

$\alpha_f$, $\beta_f$ — $\frac{\alpha_o}{2(r-1)}$ , $\frac{\beta_o^{2(r-1)}}{(r-1)A_4A_1^S}$

$\alpha_T$, $\beta_T$ — Weibull parameters at a temperature, T.

$\beta_{RT}$ — Room temperature value.

$\beta_{MLE}$ — Calculated using pooled $\alpha$ by formula

$$\beta = \left[\frac{\sum_{i=1}^{n} X_i^{\alpha}}{n}\right]^{\frac{1}{\alpha}}$$ where n is number of specimens.

$\beta_{LT}$ — $\beta$ for long term test.

$\sigma$ — Relates to slope of Gaussian process line. Slope = $-\frac{1}{2\sigma^2}$ See Figure 12-13.

$\Theta$ — Load for exceedance curves expressed in number of g's.

$a_T$ — $\frac{\beta_T}{\beta_{RT}}$, ratio of $\beta$ at temperature to $\beta$ at room temperature.

$A_1$ — $\frac{F_{max}}{F_{ref}}$, where $F_{max}$ is the truncation load, a measure of rms stress, and $F_{ref}$ is a reference rms stress level.

$A_4$ — This term is related to the history dependent constant (M) in Equation (1).

C — Flaw length.

$f_c$ — $(3)^{-\frac{1}{\alpha_o}}$ is the penalty for least of three as a function of the shape parameter, $\alpha_o$.

$f_r$ — $(100)^{-\frac{1}{\alpha}}$ is the risk factor obtained from failure statistics by assuming a 1% static failure rate is acceptable.

$f_T$ — Strength retention factor at elevated temperature obtained from the ln $a_T$ versus T curve.

F — Static strength.

$F_R(t)$ — Residual strength function.

g — Acceleration due to gravity.

M — Proportionality constant in Equation (1).

$N_o$ — R $N_p$ is the average number of mean crossings per unit time.

$N_p$ — Overall cyclic frequency of loads.

$P(F_R(t) > F_R)$ — Probability function.

r — Flaw growth rate exponent.

R — Irregularity factor.

s — The term $-\frac{1}{s}$ is the slope of the ln $F_{max}$ versus ln t curve and is related to r.

t — Time. $t_o$ is a reference time condition.

T — Temperature.

## 12.6 SHORT-TERM FLIGHT SIMULATION

The short-term tests were intended to provide the data necessary to set reasonable load levels for the long-term tests. These load levels were extremely important to the success of the long-term tests. A selection that was too high could result in failure of all the specimens prior to completion of 50,000 hours of exposure. Conversely, a very low load level might result in neither specimen failures nor measureable changes in residual strength after 50,000 hours. The

short-term tests were accomplished by accelerating the loading rate such that half a lifetime of loads was applied in 200 hours. During loading the specimens were exposed to the maximum use temperature for each composite material system. The loads for the short-term tests were set to induce some fatigue failures. Specimens that did not fail were tested for residual strength. These fatigue life and residual strength data were then used with the static baseline data to fit the wearout model and set the loads for the long-term tests.

The short-term tests were additionally intended to check out the flight simulation apparatus and to provide the modes and statistics of failure.

**12.6.1 TEST PLAN AND PROCEDURES.** For each of the four Phase I material systems a total of 40 specimens, in groups of 10, were subjected to the short-term flight simulation exposure tests. For B/Al, both unidirectional and $[0° \pm 45°]_s$ crossplied materials were tested while only $[0° \pm 45°]_s$ crossplied material was tested for the resin matrix systems. The unidirectional B/Al was included because its significantly higher transverse strength and transverse and shear modulii, than those of the resin systems, offer a much greater potential for structural applications. The originally scheduled unidirectional resin matrix specimens were changed to a notched $[0° \pm 45°]_s$ crossply configuration. Tests were conducted for time periods of 100 and 200 hours. At the accelerated rate of loading that was used, this represented one-fourth and one-half lifetimes respectively. All tests on any one system were conducted at the same temperature and load level.

Following the 100- and 200-hour exposures, all unfailed specimens were tested for residual tensile strength at the same temperature as used for the short-term tests.

**12.6.1.1 Temperature Selection.** Selection of the short-term test temperatures was to be based on the results of the baseline tensile tests. It was planned to select a temperature in the region just below that where a distinct change in the slope of the strength versus temperature curve occurred. Generally, however, no distinct fall-off in strength was observed out to the maximum tensile test temperatures used for any of the materials. At the time that the short-term tests were ready to begin, the thermal aging exposures had not been running long enough to provide data for selection of the flight simulation temperatures. Data from the literature for use in selecting the maximum use temperatures for 50,000-hour service was also lacking. However, at the time that the long-term tests were expected to start it was thought that sufficient thermal aging data would then be available and that a rational selection of exposure temperatures could be made at that time. Therefore, the temperatures selected for the short-term tests were in the region covered by the thermal aging tests. For the epoxy systems 422 K (300° F) and for B/Al 505 K (450° F) were chosen. These temperatures were midway between those at which thermal aging exposures were currently in progress. To obtain a better comparison between the B/Al and the HT-S/710 G/PI systems, 505 K (450° F) was also chosen for G/PI even though the midway temperature of the thermal aging tests was 533 K (500° F).

**12.6.1.2 Selection of Short Term Loads.** The loads for the short-term tests were set as high as possible to produce early fatigue failure and provide a basis for subsequent stress variations. The room temperature static ultimate strength is reduced by two independent factors to arrive at the desired load. One of these factors is strength retention at elevated temperature, $f_T$. It was obtained from a retention curve as described below. The other factor is a risk factor, $f_r$, and was obtained from failure statistics by assuming that a 1% static failure rate is acceptable.

Because no baseline tests were performed on B/E, its reduction factors were obtained from existing data. The procedure for the reduction of the G/E, HT-S/710 G/PI, and B/Al data is described here.

The baseline data provides a starting point for setting the peak loads to be used during the short-term tests. The raw failure load data for a given material, notch condition, and temperature were fit with a Weibull distribution by linear regression to obtain the scale parameter, $\beta$, and the shape parameter, $\alpha$. The temperature retention curve was plotted in the form of ln $a_T$ versus temperature, where $a_T$ is the ratio of $\beta$ at a given temperature to $\beta$ at room temperature. The portion of this curve that exhibits linearity permits statistical pooling of the data over that temperature range. The pooling was accomplished by scaling each data point (load value) to its raw $\beta$ estimate and using this ratio as the random variable. The resulting $\alpha$ was the pooled $\alpha$ for that material and notch condition over the temperature range of interest. Using maximum likelihood estimation techniques, a better estimate of the $\beta$ for each temperature was obtained from the original load data and the pooled $\alpha$. These new $\beta$ estimates were used to refine the ln $a_T$ versus T curve so that the temperature factor, $f_T$, could be obtained directly from the plot. The risk factor, $f_r$, was calculated from the pooled $\alpha$ as the first failure of 100 samples, or

$$f_r = (100)^{-\frac{1}{\alpha}}$$

The permissible peak load was then the product:

$$\text{peak load} = f_r f_t \beta_{RT}$$

The procedure for load selection is demonstrated below using the baseline tensile data for unnotched $[0° \pm 45°]_s$ G/E in a typical calculation:

1. Fit a Weibull distribution to each set of raw load data (a distribution for each temperature, material, and notch condition).
2. Plot temperature retention in the form of a ln $a_T$ versus T curve, where $a_T$ is $\beta_T/\beta_{RT}$.
3. From Step 2, determine which sets of data may be pooled (based on linear part of ln $a_T$ versus T curve).
4. Pool several temperatures by using $X/\beta_T$ as the random variable. Obtain a pooled $\alpha$ for that material and notch condition.
5. Recompute $\beta_T$ based on pooled $\alpha$ and original load data (use maximum likelihood estimator). Refine $a_T$ versus T with $\beta_{MLE}$.
6. Compute risk factor based on 1% failure rate $f_r = (100)^{-\frac{1}{\alpha}}$
7. Find temperature retention factor ($f_T$) from refined $a_T$ versus T.
8. Calculate peak load equal to $f_r f_T \beta_{RT}$.

Using the 35 tensile strength values in Table 12-2, the procedure is followed to calculate the peak short-term load for G/E.

**Table 12-2. Baseline Tensile Data — Unnotched $[0° \pm 45°]_s$ G/E**

| Specimen No. | Temperature K | Temperature (°F) | Load N | Load (lb) | $\mu$ N | $\mu$ (lb) | $\beta$ N | $\beta$ (lb) | $\alpha$ | $\beta/\beta_{RT}$ | Load/$\beta$ | $\beta_{MLE}$ N | $\beta_{MLE}$ (lb) | $\beta/\beta_{RT}$ |
|---|---|---|---|---|---|---|---|---|---|---|---|---|---|---|
| BC01-1 | 218 | −67 | 3870 | 870 | 4034 | 907 | 4190 | 942 | 11.79 | 0.89 | 0.96 | 4114 | 925 | 0.88 |
| -2 | | | 3879 | 872 | | | | | | | .93 | | | |
| -3 | | | 4359 | 980 | | | | | | | 1.04 | | | |
| BC01-6 | 297 | 75 | 5031 | 1131 | 4444 | 999 | 4702 | 1057 | 7.40 | 1.0 | 1.07 | 4684 | 1053 | 1.00 |
| -7 | | | 3905 | 878 | | | | | | | .83 | | | |
| -8 | | | 4377 | 984 | | | | | | | .93 | | | |
| BC01-4 | 394 | 250 | 4257 | 957 | 4644 | 1044 | 4875 | 1096 | 9.61 | 1.04 | .87 | 4991 | 1122 | 1.07 |
| | | | 4101 | 922 | | | | | | | .84 | | | |
| -16 | | | 3914 | 880 | | | | | | | .80 | | | |
| -22 | | | 4871 | 1095 | | | | | | | 1.00 | | | |
| -23 | | | 4448 | 1000 | | | | | | | .91 | | | |
| -24 | | | 5782 | 1300 | | | | | | | 1.19 | | | |
| -25 | | | 4804 | 1080 | | | | | | | .99 | | | |
| -26 | | | 4848 | 1090 | | | | | | | .99 | | | |
| -27 | | | 4670 | 1050 | | | | | | | .96 | | | |
| -28 | | | 4724 | 1062 | | | | | | | .97 | | | |
| BC01-9 | 408 | 275 | 4492 | 1010 | 4537 | 1020 | 4750 | 1068 | 9.34 | 1.01 | .95 | 4710 | 1059 | 1.01 |
| -10 | | | 4097 | 921 | | | | | | | .86 | | | |
| -17 | | | 5026 | 1130 | | | | | | | 1.06 | | | |
| BC01-11 | 422 | 300 | 4919 | 1106 | 4635 | 1042 | 4790 | 1077 | 13.16 | 1.02 | 1.03 | 4715 | 1060 | 1.01 |
| -18 | | | 4270 | 960 | | | | | | | .89 | | | |
| -19 | | | 4715 | 1060 | | | | | | | .98 | | | |
| BC01-12 | 436 | 325 | 4657 | 1047 | 4662 | 1048 | 4786 | 1076 | 17.09 | 1.02 | .97 | 4715 | 1060 | 1.01 |
| -13 | | | 5249 | 1180 | | | | | | | 1.03 | | | |
| -20 | | | 4404 | 990 | | | | | | | .92 | | | |
| BC01-14 | 450 | 350 | 4008 | 901 | 4644 | 1044 | 4853 | 1091 | 10.49 | 1.03 | .83 | 4862 | 1093 | 1.04 |
| -15 | | | 4884 | 1098 | | | | | | | 1.01 | | | |
| -21 | | | 4670 | 1050 | | | | | | | .96 | | | |
| -29 | | | 4715 | 1060 | | | | | | | .97 | | | |
| -30 | | | 4635 | 1042 | | | | | | | .96 | | | |
| -31 | | | 3941 | 886 | | | | | | | .81 | | | |
| -32 | | | 4270 | 960 | | | | | | | .88 | | | |
| -33 | | | 5293 | 1190 | | | | | | | 1.09 | | | |
| -34 | | | 4670 | 1050 | | | | | | | .96 | | | |
| -35 | | | 5338 | 1200 | | | | | | | 1.10 | | | |

1. The $\beta$ and $\alpha$ columns of the table list the value calculated from the data at each temperature.

2. Figure 12-17 shows a plot of ln $a_T$ versus temperature using the values listed in the $a_T = \beta/\beta_{RT}$ column.

3. From Figure 12-17, it was determined to pool all the data.

4. All temperatures were used and the data shown in the Load/$\beta$ column was ordered and used to find a pooled $\alpha$. The computer makes this calculation. However, for clarity the nature of this calculation is shown in Table 12-2 and the Weibull plot in Figure 12-18. The pooled $\alpha$ for this case is 12.71.

5. Recompute $\beta_T$ based on $\alpha = 12.71$ and original load data for each temperature. The maximum likelihood estimator formula is

$$\beta = \left[\left(\sum_{i=1}^{n} X_i^{\alpha}\right) / N\right]^{1/\alpha}$$

Results of this calculation are shown in Table 12-2 in the $\beta_{MLE}$ and $\beta/\beta_{RT}$ columns. Now use this data to refine ln $a_T$ versus T plot using $\beta_{MLE}$. These points leave Figure 12-17 essentially unchanged.

6. Risk factor based on 1% failure rate was then calculated as $f_r = (100)^{-\frac{1}{12.71}} = 0.70$.

7. The temperature retention factor was considered to be 1.0 for this case.

8. The peak load is equal to:

$$0.70 \times 1.0 \times [4684 \text{ N } (1053 \text{ lb})] = 3278 \text{ N } (737 \text{ lb})$$

Because the tensile specimens were 0.013 m (0.5 in.) wide, the peak load per inch is 6557 N (1474 lb).

In a similar manner the baseline test data for the other composite systems were analyzed for both the notched and unnotched cases. The B/Al data were calculated for unidirectional and crossplied materials. The reduction factors and calculated peak loads are given in Table 12-3.

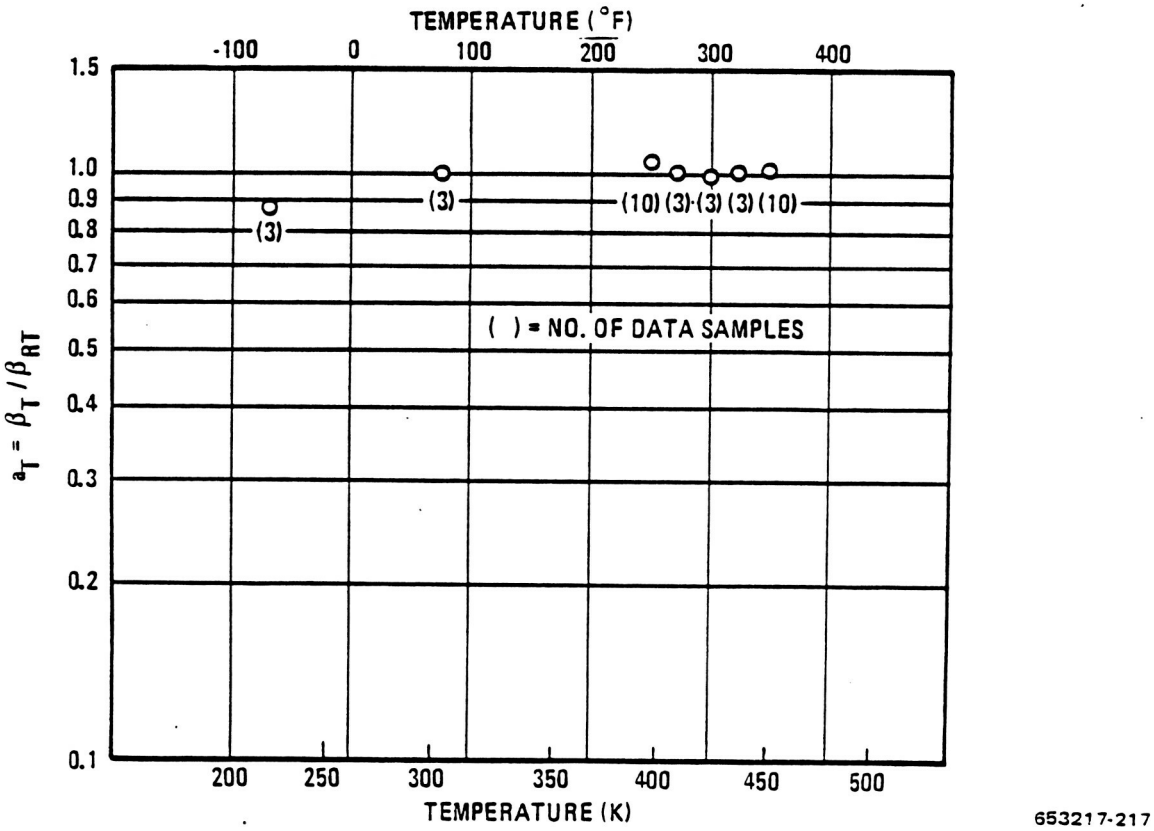



**Figure 12-17 Strength Retention of Unnotched $[0° \pm 45°]_s$ G/E at Various Temperatures**

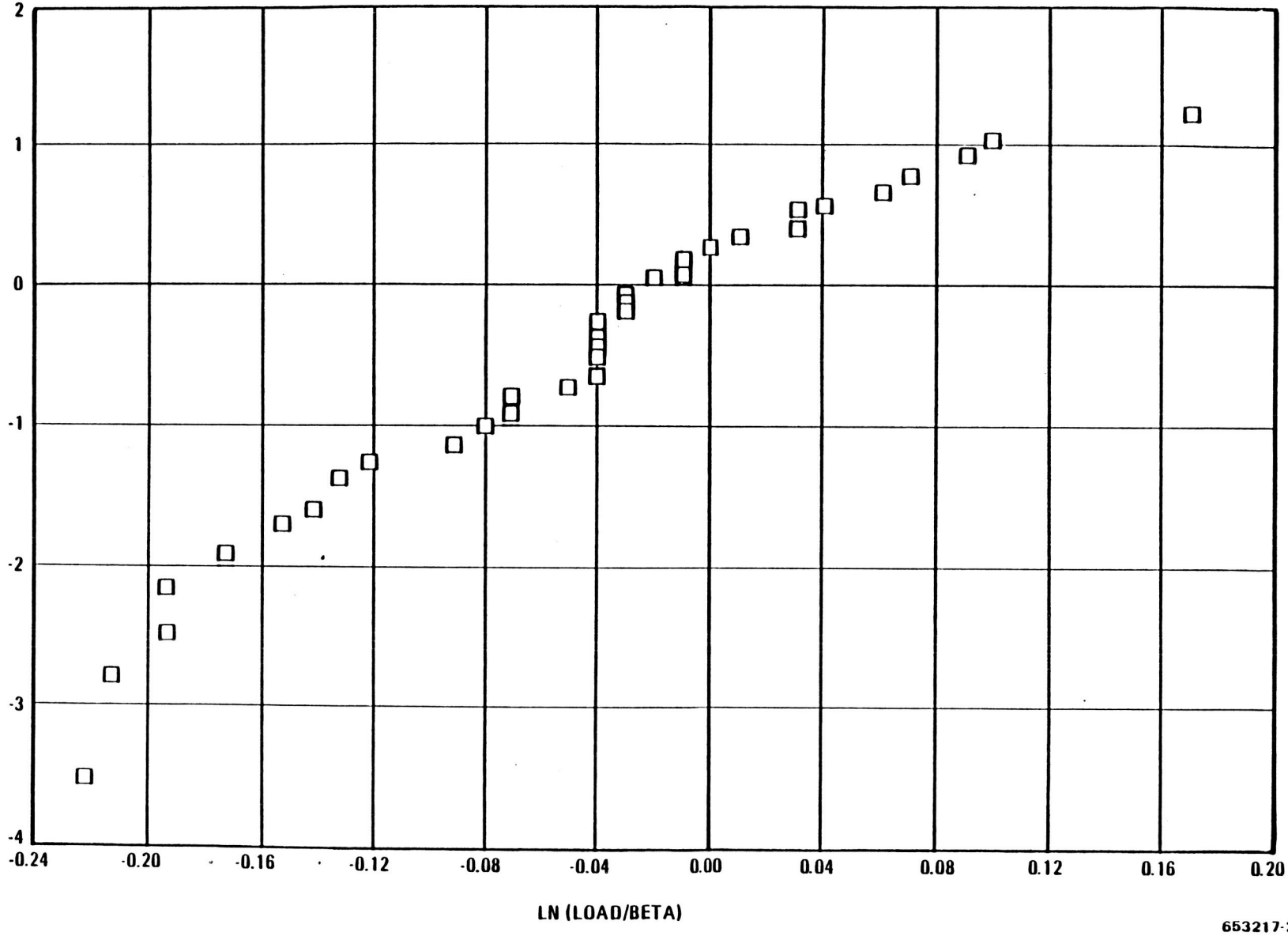



**Figure 12-18 Plot of Pooled Data to Determine $\alpha$ for G/E**

**Table 12-3. Summary of Reduction Factors, Loads, and Stresses for Short-Term Tests**

| Material | Condition | $f_r$ | $f_T$ | [a]Peak Load N | (lb) | [b]Landing Load N | (lb) | Peak Stress MN/m² | (ksi) | Landing Stress MN/m² | (ksi) | [c]One g Stress MN/m² | (ksi) |
|---|---|---|---|---|---|---|---|---|---|---|---|---|---|
| B/E | Unnotched | 0.79 | 0.80 | 6218 | 1398 | −1557 | −350 | 321 | 46.6 | − 80 | −11.7 | 161 | 23.3 |
| | Notched | .79 | .80 | 3483 | 783 | − 872 | −196 | 248 | 36.0 | − 62 | − 9.0 | 124 | 18.0 |
| G/E | Unnotched | .70 | 1.0 | 6557 | 1474 | −1637 | −368 | 338 | 49.1 | − 85 | −12.3 | 169 | 24.6 |
| | Notched | .68 | 1.0 | 3616 | 813 | − 903 | −203 | 249 | 36.1 | − 62 | − 9.0 | 125 | 18.1 |
| B/Al | $[0°]_6$ | .77 | .91 | 25,310 | 5690 | −6325 | −1422 | 956 | 138.8 | −239 | −34.7 | 478 | 69.4 |
| | $[0° \pm 45°]_s$ | .71 | .82 | 8451 | 1900 | −2117 | − 476 | 345 | 50.0 | − 86 | −12.5 | 173 | 25.0 |
| G/PI | Unnotched | .68 | 1.0 | 4946 | 1112 | −1237 | − 278 | 207 | 30.1 | − 52 | − 7.5 | 104 | 15.1 |
| | Notched | .68 | 1.0 | 2593 | 583 | − 649 | − 146 | 141 | 20.5 | − 35 | − 5.1 | 71 | 10.3 |

Note: Stresses based on the following thicknesses:

| | |
|---|---|
| B/E, Unnotched: | 0.00076 m (0.030 in.) |
| B/E, Notched: | .00074 m (.029 in.) |
| G/E, Unnotched: | .00076 m (.030 in.) |
| G/E, Notched: | .00076 m (.030 in.) |
| G/PI, Unnotched: | .00094 m (.036 in.) |
| G/PI, Notched: | .00089 m (.035 in.) |
| B/Al $[0°]_6$: | .00104 m (.041 in.) |
| B/Al $[0° \pm 45°]_s$: | .00097 m (.038 in.) |

[a] Peak load = $f_r f_T \beta_{RT}$

[b] Landing load is defined as negative 25% of peak load

[c] One g stress is defined as 50% of peak stress

**12.6.1.3 Test Procedure.** Before installing the short-term specimens in the flight simulation apparatus, width and thickness measurements were determined, and the average cross-sectional areas were calculated for each set of 10. These areas were used to obtain the flight simulation stresses and, for specimens that did not fail, to calculate the residual tensile strengths after post-exposure testing. The specimens were then installed in the test machine, thermocouples were attached, the compression stiffening grids were bolted in place, and all resin-matrix specimens were heated to 422 K (300° F) for 24 hours to remove any absorbed moisture. Before starting the tests, each set of 10 specimens was proof loaded to the maximum load value that it would experience during the 100- or 200-hour, short-term exposure.

Once started, the short-term testing of any one set continued uninterrupted until completion unless specimen failure or equipment malfunction occurred. If the test was halted for 24 hours or more, an additional moisture bakeout of four hours was performed on all except the B/Al specimens.

At the completion of the 100- or 200-hour flight simulation exposures, the specimens were removed from the simulator and visually examined with a stereo microscope to check for changes in appearance or the presence of surface flaws such as cracks or delaminations. After the visual examination, the short-term specimens were tensile tested at the same temperatures at which they had been exposed. Testing was performed in a Tinius-Olson Universal testing machine at a head rate of 0.0013 m (0.05 in.) per minute. Heating of the specimens was accomplished with two ring furnaces that encircled the specimen at the two areas that had been

heated during the simulation exposures. This technique was used rather than an environmental chamber to prevent the possibility of premature failures in the doubler adhesive. The two ring furnaces were independently controlled by manually adjusting two power supplies. Temperature was monitored with thermocouples attached to the two test sections. The specimens were heated to the desired test temperature in approximately 10 minutes and then held at temperature for an additional 10 minutes before testing. Temperature was held to ± 3 K (5 ° F) during both the hold period and while testing. Figure 12-19 shows a specimen in the testing machine with the two ring furnaces in place. If the resin matrix specimens were not tensile tested within 48 hours of completion of the flight simulation exposure, they were given a bake-out treatment at 394 K (250 ° F) for at least 24 hours to remove any absorbed moisture.

**12.6.1.4 Problem Areas.** In addition to providing the data necessary to set the load levels for the long-term tests, the short-term test program was also intended to check out the loading facility and the suitability of specimen design and fabrication. Numerous deficiencies in the flight simulation apparatus were detected and corrective measures were taken. Some of the equipment problems included: malfunctioning of solid-state power control switches, voltage transients that interfered with the temperature control circuits, lack of proper safety valves in the hydraulic system, improperly positioned lamps and thermocouples, and intermittent shutdowns of the entire system caused by both electronic and mechanical difficulties with the programming systems. Because of the complexity of the flight simulation apparatus and the extremely long run times involved in the test program, it was not unexpected that equipment malfunctions and component wearouts would occur from time to time.

One problem involving support equipment rather than the simulator was caused by movement of the compression stiffeners (steel grids bolted to the specimens to prevent buckling), see Figure 12-7, during fatigue cycling. These fixtures tended to rotate slightly and/or ride too low on the specimens, leaving an unsupported column of composite approximately 0.0025 m (0.1 in.) long at the top. During the compressive loading portion of the cycle some buckling or bending could occur. It was most noticeable for the unidirectional B/Al where the compressive loads were considerably greater than those for the other materials. Spacers were prepared that, when inserted between the lower grips and the stiffeners, supported the stiffener, assured that they were centered about the specimen, and greatly reduced the unsupported column of composite material. The spacers also reduced rotation of the stiffeners during fatigue loading. One other problem caused by the compression fixtures was abrasion of the soft B/Al specimens during fatigue cycling (a-form of fretting corrosion). The addition of the spacers reduced the relative movement between the stiffener and specimen and, thereby, eliminated much of the wearing. Further reduction in the abrasion of the aluminum surface of the B/Al specimens was accomplished by application of a stratified Teflon coating to the compression stiffeners. By the time these modifications were completed, however, considerable surface abrasion had occurred on the B/Al short-term specimens.

A problem encountered early in the testing of the B/Al short-term specimens was premature failure at the edge of the end doublers caused by undercutting of the B/Al during removal of excess adhesive when fitting the compression stiffeners. The problem was eliminated in the long-term tests by modifying the fabrication procedures. Another problem was a bond failure at the titanium doublers of the crossply specimens. A solution to this problem was found by installing a Ti-6Al-4V rivet on each end of the specimens through the titanium doublers and the B/Al material. A more difficult problem was the attachment of end doublers to the

ORIGINAL PAGE IS
OF POOR QUALITY

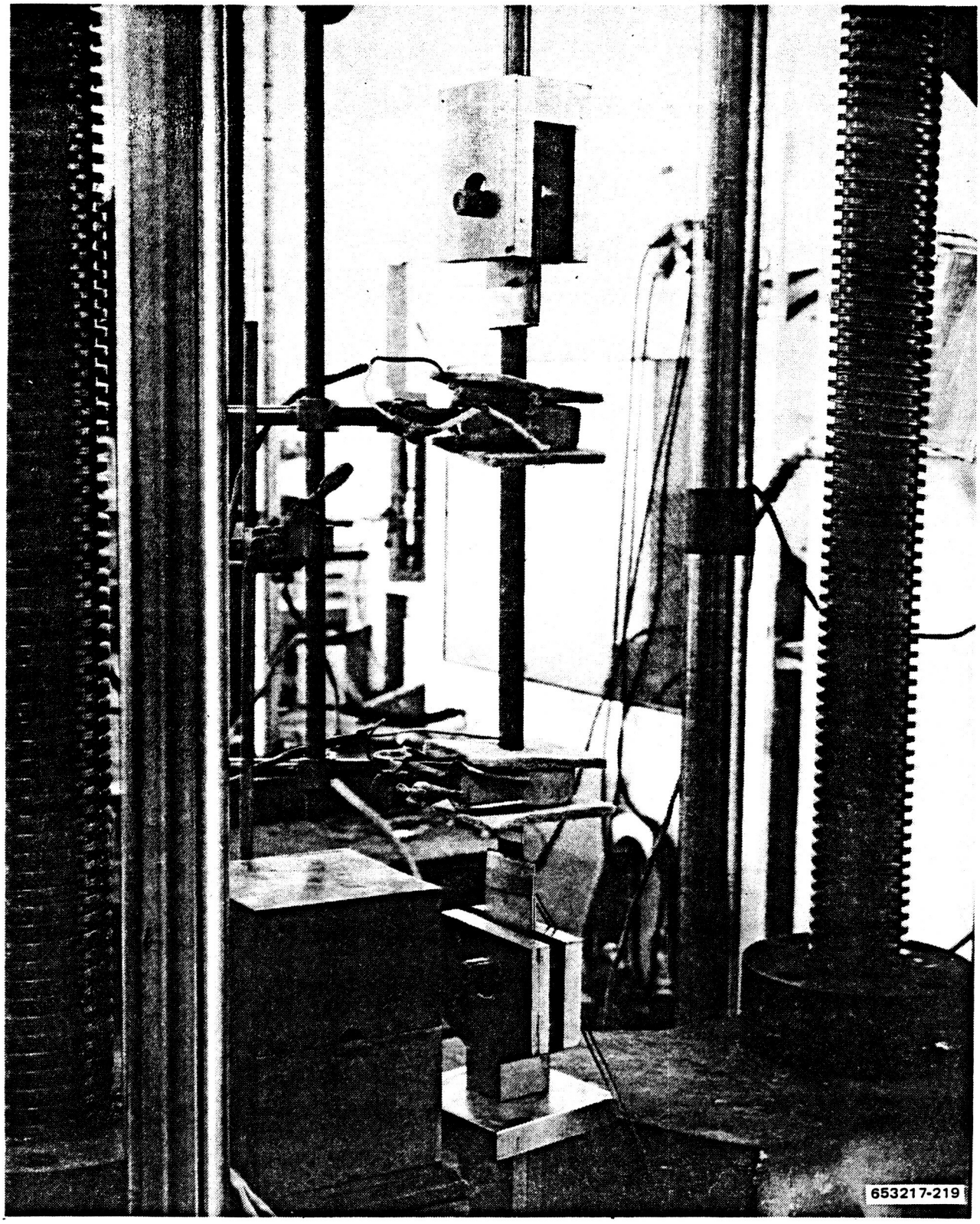



**Figure 12-19 Test Setup for Residual Strength Determinations After 100-hr and 200-hr Short-Term Simulation Exposures**

unidirectional specimens. For these specimens, the test loads were much higher than used for the crossply specimens with correspondingly higher shear stresses at the doublers. For unidirectional specimens, rivets did not solve the problem. Failures occurred in the doublers by shearout of the B/Al behind the rivets. Other techniques that were considered were brazing, diffusion bonding, diffusion braze bonding, spot welding, and mechanical clamping. The method selected was a clamping device on each end of the B/Al unidirectional short-term specimens. The clamp was placed near the tip of the doublers in the tapered portion. To assure uniform contact between the clamps and the doublers, flats were milled on each side at the contact areas. The purpose of the clamps was to increase the normal force reacting on the specimen and to decrease the tendency of the doublers to peel during flight cycle loading. An overall view of a B/Al specimen is shown in Figure 12-20 with a closeup view of the tapered section of the doubler shown in Figure 12-21. This technique proved to be successful for the short-term tests and was also used for the long-term testing of both the crossplied and unidirectional B/Al. Figure 12-7 shows the clamps in use during the long-term tests.

**12.6.2 SHORT-TERM TEST RESULTS.** Following the short-term flight simulation exposures, all specimens were removed from the test apparatus, examined visually, and then tensile tested for residual strength at the same temperature as was used for the flight simulation tests. The following sections describe the results of these examinations and tensile tests.

#### 12.6.2.1 Post Simulation Examinations

**B/E, $[0° \pm 45°]_s$, unnotched, 100 hours.** After 100 hours the major change in the specimens was a distinct discoloring in the two heated zones of each specimen. These color changes were very similar to those observed during the thermal aging tests at 450 K (350° F) and, hence, were considered normal for these exposure conditions. A slight amount of surface damage in the

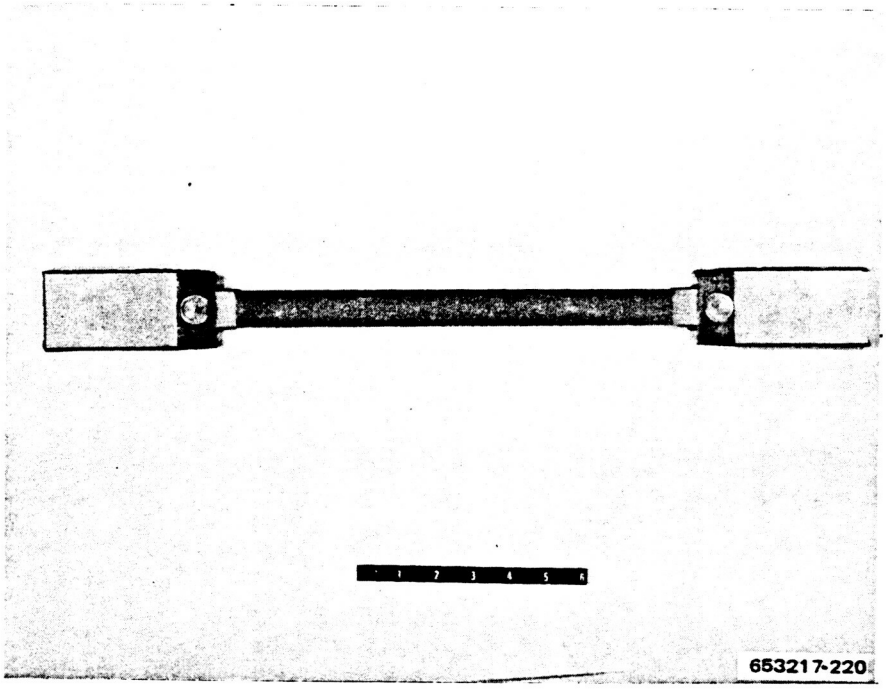



**Figure 12-20 Overall View of B/Al Short-Term Specimen with Flats Milled in Titanium Doublers for Clamps**



ORIGINAL PAGE IS
OF POOR QUALITY

ORIGINAL PAGE IS
OF POOR QUALITY

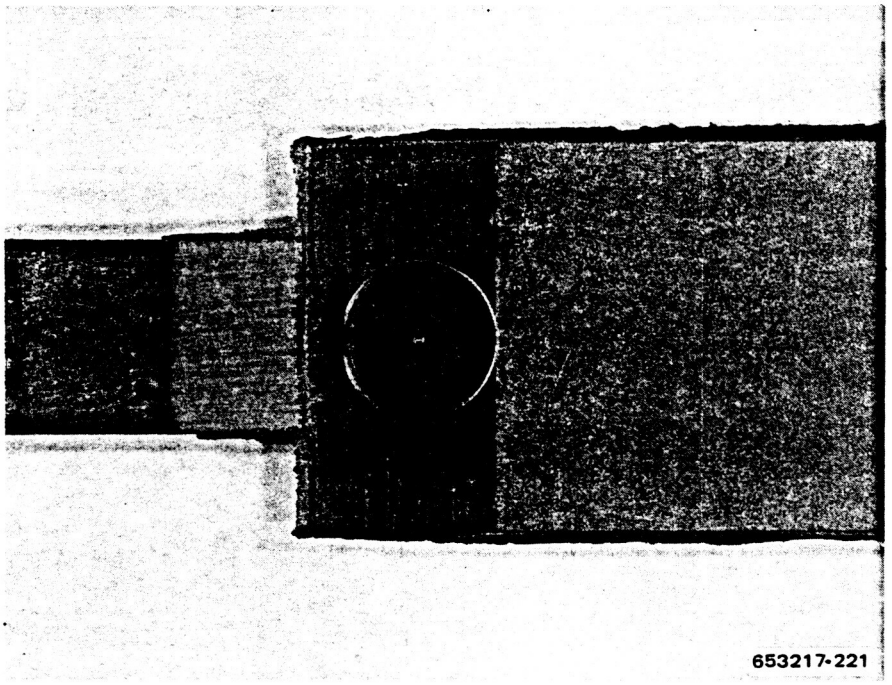



**Figure 12-21 Closeup-View of Tapered Section of Titanium Doubler Showing Flat Area for Attaching Clamp**

areas where the compression stiffeners supported the specimens was visible. No fibers were damaged, however, and the effect on the residual tensile properties was considered to be negligible.

**B/E, $[0° \pm 45°]_s$, unnotched, 200 hours.** The added 100 hours of flight simulation exposure did not change the appearance of these specimens from that described above.

**B/E $[0° \pm 45°]_s$, notched 100 hours and 200 hours.** The overall appearance of the notched specimens was identical to the unnotched samples previously discussed. In the vicinity of the notches, 0.0064 m (0.25 in.) diameter holes in the center of the heated areas, no apparent damage was visible. In machining these notches, by drilling with a diamond tool, a very small amount of chipping occurred on the back side of each hole. Small portions of some of the boron filaments were broken off, and several of the filaments were exposed where the epoxy matrix had been removed. No degradation of either the exposed filaments or the matrix was visible after the 100- or 200-hour exposures.

**G/E, $[0° \pm 45°]_s$, unnotched, 100 hours.** Seven of the 10 specimens in this group survived the 100 hours of exposure. Discoloration in the heated areas was not as noticeable as for the B/E specimens and, again, was quite similar to that found during thermal aging of G/E at 450 K (350° F). Only one of the seven specimens (BC84-7) experienced any visible damage. In this specimen, a small crack was found in the outer 0° ply in one of the heated areas. This crack and delamination of the outer ply is shown in Figure 12-22, an edge view of the specimen. Also visible in the photo is a crack that passes through the second, third, and fourth plies and extends for several mm between the fourth and fifth plies. The effect of this flaw on the residual tensile strength, however, was minor (see Section 12.6.2.2, Table 12-6).

Three of the specimens in this set failed during the flight simulation exposure, one in 10.6 hours and the other two both at 54.2 hours. The first, BC84-6, is shown in Figure 12-23. While three breaks occurred along the length of the specimen, it is thought that the failure initiated in the heated zone. Multiple fractures of this type are common to these long specimens. This is especially true when failed in a "soft" test machine with the sudden release of a large amount of stored energy.

The second specimen (BC84-2, 54.2 hours) also failed in one of the heated areas and was also a fatigue failure. This specimen was of interest in that a crack had also formed at the other heated area but did not propagate sufficiently to fail the specimen at that location. An edge view of this crack is shown in Figure 12-24. The crack, while not deep, has extended through all six plies. Some delamination of the outer layers is also evident.

The third specimen (BC84-1, 54.2 hours), which was in the same set of two as BC84-2, failed in the doubler. Although it has been established that no transfer of load from a failed specimen to an adjacent one occurs, the failure of BC84-2 is thought to have been responsible in some unknown way for the apparently simultaneous failure of BC84-1. The time of failure and location of fracture make it improbable that this was a true random fatigue failure. Hence, this specimen was discounted in the data analysis.

**G/E $[0° \pm 45°]_s$, unnotched, 200 hours.** These 10 specimens completed 200 hours with no failures. The specimens experienced color changes similar to the others of this system and minor abrasion from the compression stiffeners. No edge cracks were found except for some slight splintering of the outer plies in several of the specimens. These effects were small and were observed only at the edges.

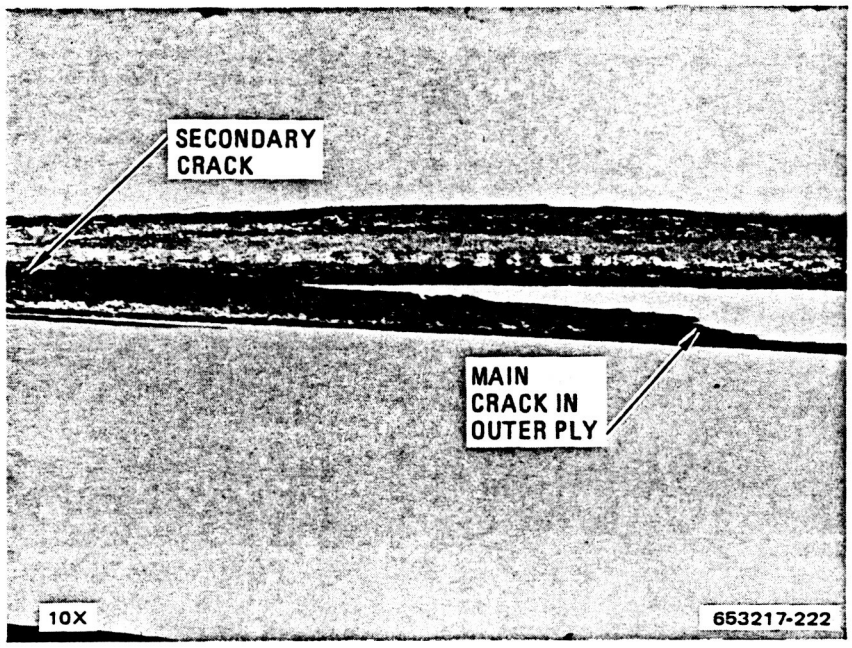


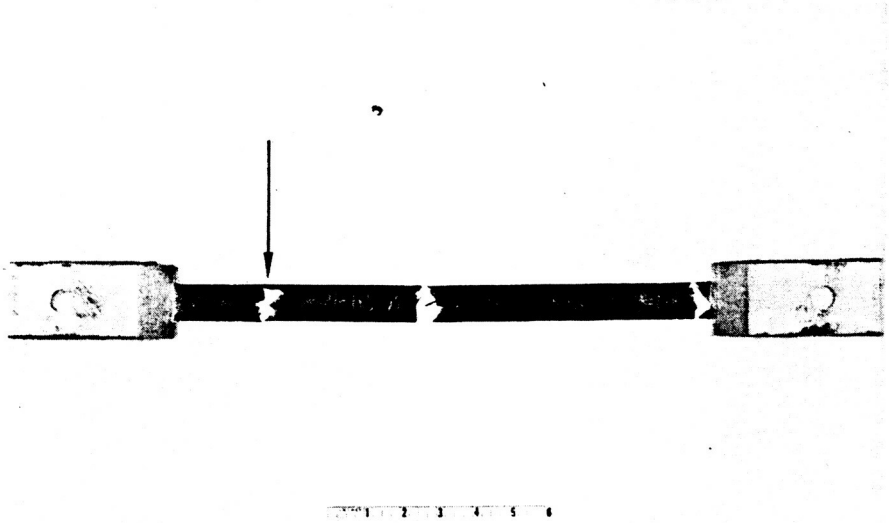

**Figure 12-22 Edge Crack and Delamination in Specimen BC84-7, G/E, Unnotched, After 100-hr Simulation Exposure at 422 K (300° F)**



ORIGINAL PAGE IS
OF POOR QUALITY

ORIGINAL PAGE IS
OF POOR QUALITY

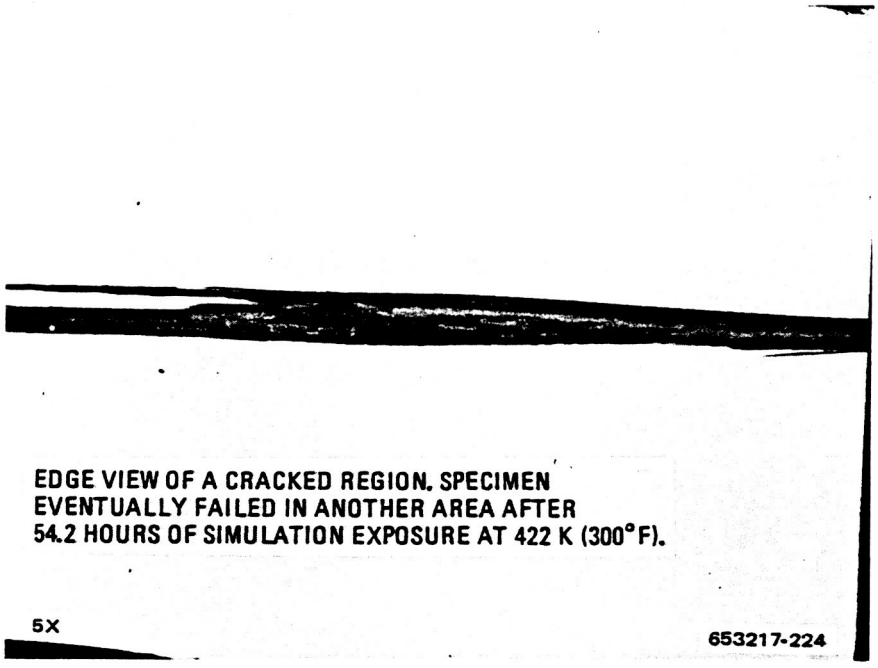
ORIGINAL PAGE IS
OF POOR QUALITY



INITIAL FAILURE BELIEVED TO HAVE INITIATED
IN THE HEATED ZONE (ARROW).

653217-223

**Figure 12-23 Specimen BC84-6, G/E, Unnotched**



EDGE VIEW OF A CRACKED REGION. SPECIMEN
EVENTUALLY FAILED IN ANOTHER AREA AFTER
54.2 HOURS OF SIMULATION EXPOSURE AT 422 K (300°F).

5X

653217-224

**Figure 12-24 Specimen BC84-2, G/E, Unnotched**

**G/E $[0° \pm 45°]_s$, notched, 100 hours.** These 10 specimens completed 100 hours with no failures. The specimens experienced color changes similar to the unnotched specimens and minor abrasion from the compression stiffeners. Minor cracking of the inner surface of several of the holes was visible. With the exception of one specimen, these cracks were very shallow and did not appear to be very significant. The exception was specimen BF84-8, which contained a crack in the outer one or two plies extending from one of the holes for approximately 0.0025 m (0.1 in.). Figure 12-25 shows the location and extent of the crack on the surface of the specimen while Figure 12-26 shows the crack extending into the inner surface of the hole. Smaller branch cracks are also visible in the two middle plies. An overall view of this specimen is shown in Figure 12-27.

**G/E, $[0° \pm 45°]_s$, notched, 200 hours.** These specimens, all of which completed 200 hours, were very similar in appearance to the previous group. The only difference was at the inner surface of the holes. After 200 hours, the number of fine cracks was increased over that observed for the 100 hour specimens. These cracks were still small and quite shallow, however. These cracks, which were found in about half of the specimens, did not seem to influence the residual tensile properties.

**B/Al, $[0° \pm 45°]_s$, unnotched, 100 hours.** Examination of these specimens with a stereo microscope revealed the presence of numerous transverse cracks in the B/Al in the regions adjacent to the end doublers. These cracks were found in seven of the 10 specimens of this group. Figure 12-28 is an enlargement of the flawed area in one of these specimens. All of the transverse cracks were located in regions that had been undercut during the process of removing excess adhesive that had flowed from under the titanium end doublers during bonding. It was necessary to remove this adhesive so that the compression fixtures would fit securely to the

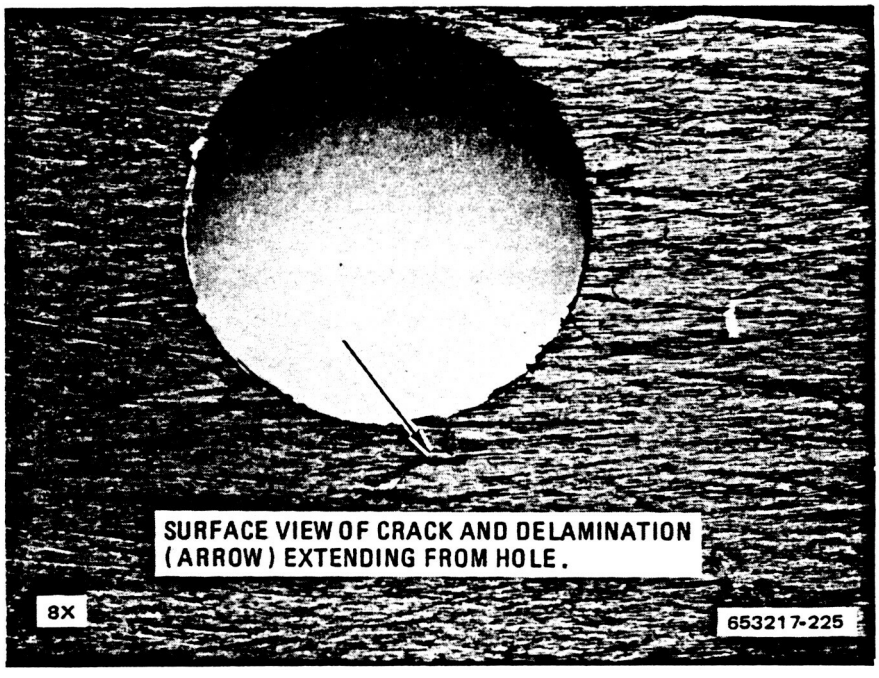
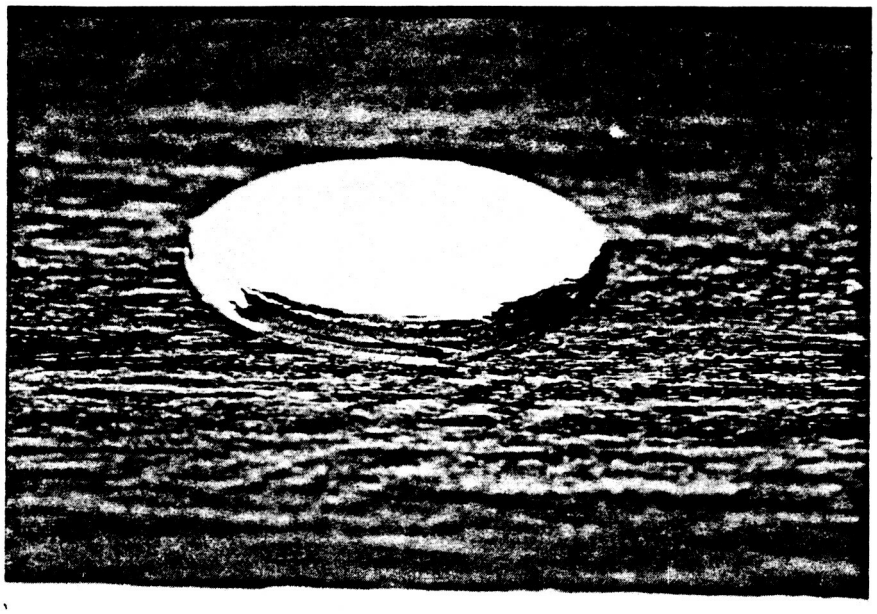



**Figure 12-25 Specimen BF84-8, G/E, Notched, After 100-hr Simulation Exposure at 422 K (300° F)**



ORIGINAL PAGE IS
OF POOR QUALITY

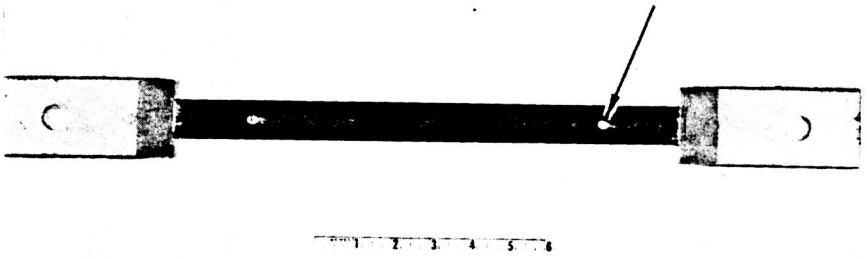
ORIGINAL PAGE IS
OF POOR QUALITY



8X

653217-226

**Figure 12-26 View of Main Crack and Several Branch Cracks at Edge of Hole in Specimen BF84-8, G/E, Notched, After 100-hr Simulation Exposure at 422 K (300° F)**



CRACK SHOWN IN FIGURES 12-25 AND 12-26
LOCATED AT ARROW.

653217-227

**Figure 12-27 Overall View of Specimen BF84-8, G/E, Notched After 100-hr Simulation Exposure at 422 K (300° F)**

test section between the doublers. The combination of a very hard adhesive and soft annealed aluminum led to the problem. Also, only about 0.00001 m (0.0004 in.) of aluminum covers the first layer of boron filaments, so that very little abrasion was required before exposing the boron filaments. The consequences of the undercutting of the specimens with the attendant transverse cracking were twofold. Examination of the specimen (EC84-9) that broke after 65.4 hours of exposure suggests that failure was premature and was caused by the growth of these transverse cracks in an abraded region. This is readily apparent from a comparison of the failed edge of specimen EC84-9 (Figure 12-29) with the transverse cracks shown in Figure 12-28. The second consequence of these transverse cracks was that residual strength testing of the exposed specimens in their present condition would probably be of little value because of the likelihood of premature failure of at least seven of the samples (those that were cracked). Therefore, rather than test the full size specimens, subsize coupons 0.013 m (0.5 in.) by 0.15 m (6 in.) were cut from an area adjacent to the end doublers, one from each short-term specimen. Figure 12-30 is a sketch showing the details of how the subsize specimens were prepared. Note that half of the heated test section is covered by one of the doublers on the subsize specimen. Cutting of the residual strength coupons in this manner had the advantage that they could be taken from undamaged areas of the short-term specimens. Several specimens showed surface damage where the compression stiffeners had been clamped. Again it was the low abrasion resistance of the soft aluminum that contributed to this surface damage.

**B/Al, $[0° \pm 45°]_s$, unnotched, 200 hours.** During the first 100 hours of exposure, doubler bond failures were experienced on five of the specimens. At the end of 100 hours, all specimens were removed from the apparatus, new doublers were attached where bond failures had occurred, and rivets were installed in the doublers of all 10 specimens. No more bond failures were observed during the remainder of the test. Four specimens did fail in the B/Al, however, before completing 200 hours of exposure. All four failed at the same time (one with 105 hours of test

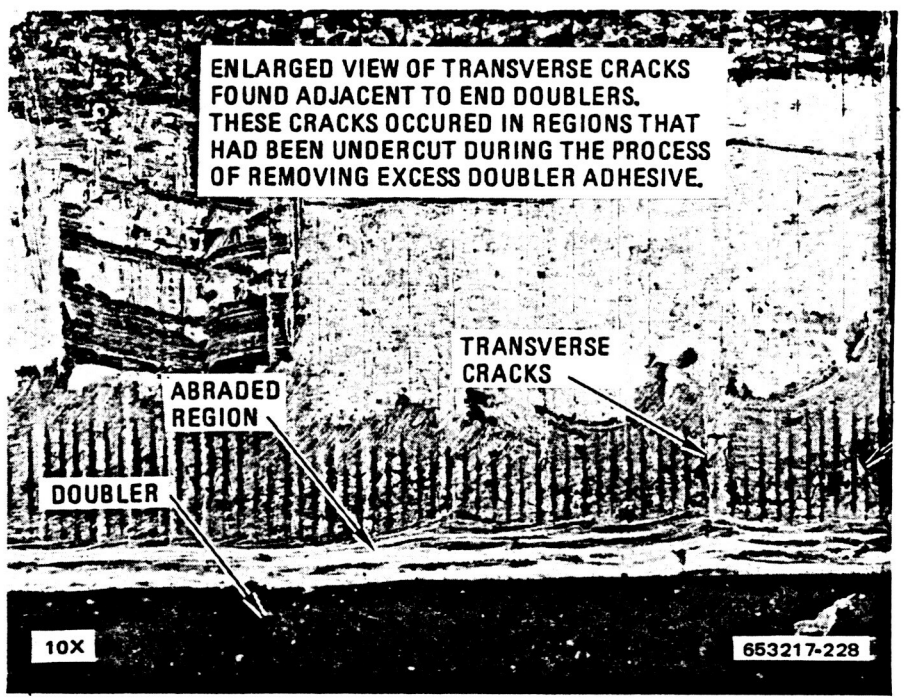



**Figure 12-28 Specimen EC84-4, B/Al, Crossply, After 100-hr Simulation Exposure at 505 K (450°F)**



ORIGINAL PAGE IS
OF POOR QUALITY

ORIGINAL PAGE IS
OF POOR QUALITY

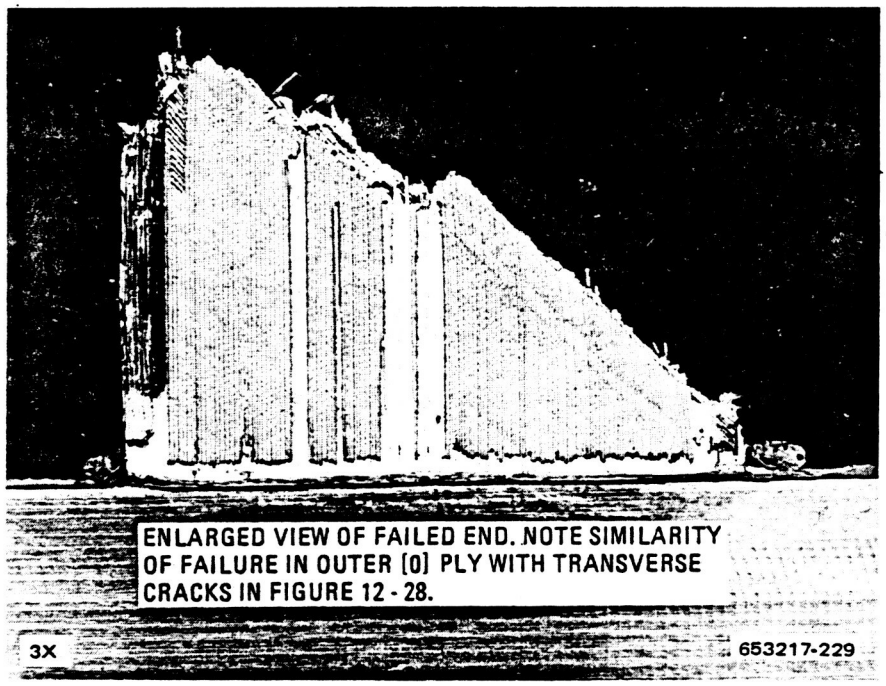
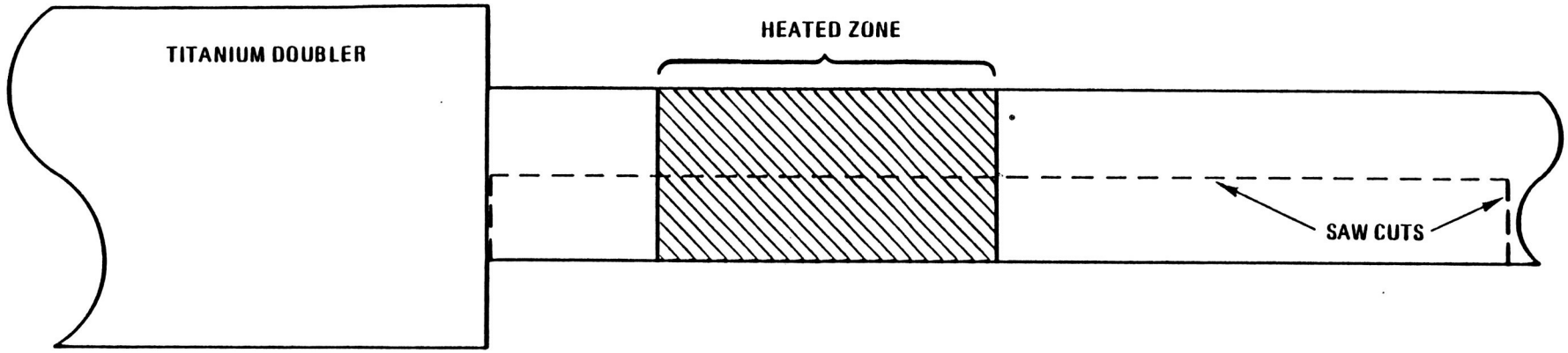


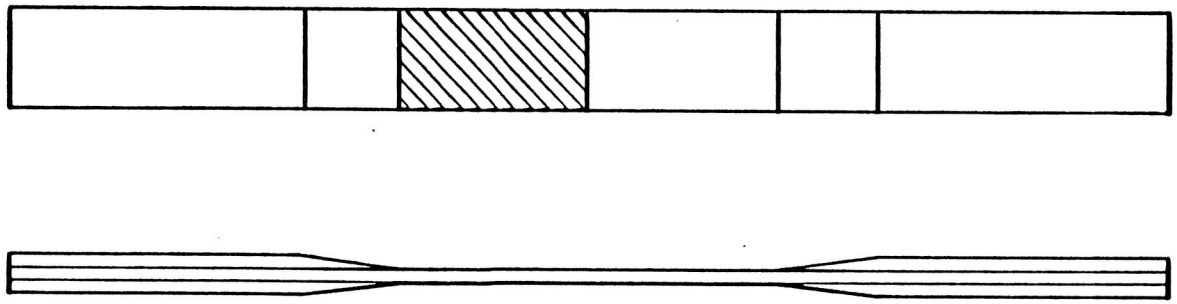

**Figure 12-29 Specimen EC84-9, B/Al, Crossply, Which Failed After 65.4 hr of Simulation Exposure at 505 K (450° F)**

time and three with 136 hours). Three failed in the heated zones, and the fourth specimen failed about 0.008 m (0.3 in) from a doubler. Failure undoubtedly occurred during a very high load portion of the random load spectrum, but the probability of four true fatigue failures occurring simultaneously is quite small. All four specimens had abraded regions at the site of the fractures. Of these, three appeared to have been severe enough to possibly have initiated the fracture. Figure 12-31 shows one of these specimens. Fracture occurred 45° to the length of the specimen except in the region of the abrasion. Test coupons were cut from the heated areas of these specimens at the ends away from the fractures.

The remaining six specimens completed 200 hours without failures. Examination of these specimens with a stereo microscope revealed the wear marks caused by the relative motion of the specimens and compression stiffeners. This is a type of fretting corrosion that in aluminum is generally accompanied by a black powdery residue of aluminum oxide. The effect is clearly visible in Figure 12-31. Also noticeable on the specimens were numerous surface cracks located in the heated zones. An example of these cracks is shown in Figure 12-32. In all cases, these longitudinal cracks extend from regions where one or more of the outer layer boron fibers have fractured. Although not observed during the original examination, a recheck of the 100-hour, short-term specimens also revealed cracks of this type. For the 10 specimens, however, only two very small cracks were found. Apparently, the approximate time period required to form these cracks was between 100 and 200 hours. Similar surface cracking was observed during constant amplitude fatigue testing of B/Al at 561 K (550° F). The surface roughness seen on the fatigue specimens was not present on the short term specimens, however. For the few constant amplitude fatigue tests performed at 505 K (450° F) (same temperature as used for short-term tests), surface roughness was also not observed.




(a) SHORT-TERM SPECIMEN

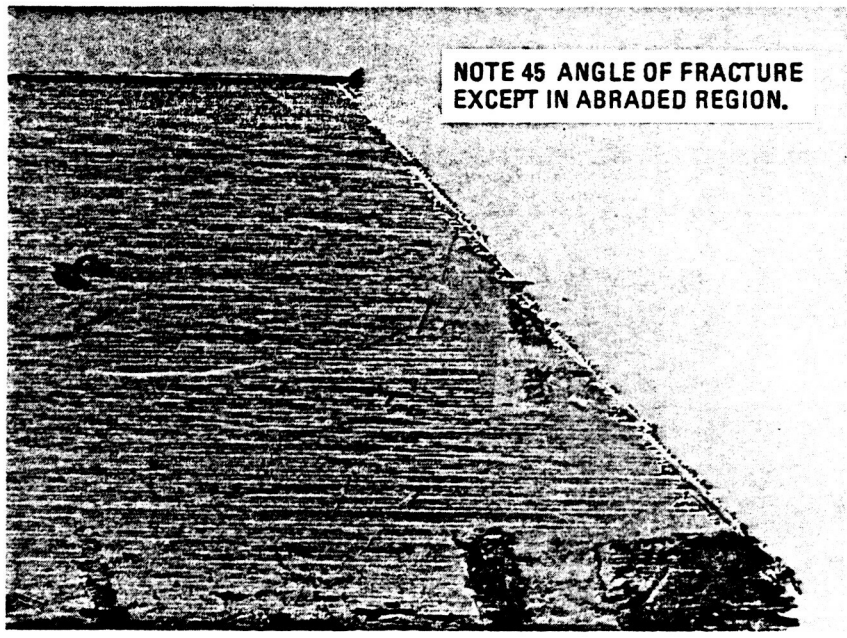


(b) SUBSIZE TENSILE SPECIMEN

653217-230

**Figure 12-30 Cutting Plan for Obtaining Subsize Residual Strength Coupons from the B/Al Short-Term Specimens**

ORIGINAL PAGE IS
OF POOR QUALITY




3X 653217-231

**Figure 12-31 Enlarged View of Failed End of Specimen EC82-7, B/Al, Crossply, Which Failed After 135.8 hr of Simulation Exposure at 505 K (450° F)**



8X 653217-232

**Figure 12-32 Enlarged View of Surface Cracks Found in Heated Zones of B/Al Crossply Specimens After 200 hr of Simulation Exposure at 505 K (450° F), Specimen EC82-3**

**B/Al, $[0°]_6$, unnotched, 100 and 200 hours.** Considerable difficulty was experienced during short-term testing of the unidirectional B/Al specimens. The major problem involved shear failures in the doubler bonds. These failures generally occurred at the upper bonds where test temperatures reached slightly higher values (406 K (270 ° F) maximum versus 372 K (210 ° F) maximum at the lower bond). The doubler bond failures were the result of the considerably higher loads required for the unidirectional material than were required for the crossplied B/Al specimens. These high loads, in combination with several other factors, also led to numerous failures in the B/Al. These included:

a. Failures in the B/Al very close to the edge of the doublers. At the bottom end, these failures were initiated by the stiffening grids gouging into the soft aluminum during the compression load. Additional failures occurred at regions that had been undercut during the process of removing excess adhesive that had flowed from under the titanium end doublers during bonding. These failures occurred during the high tensile loads.

b. The compression stiffening grids could ride too low on the specimens, leaving an unsupported column of B/Al approximately 0.0025 m (0.1 in.) long. During the compressive load, some buckling could occur. In severe cases, longitudinal splitting and/or failure occurred.

c. Specimens that were riveted to increase doubler reliability all failed in the doublers by shearout of the B/Al behind the rivets.

d. Abrasion of the soft aluminum surface of the specimens with eventual breakage of the underlying boron fibers was caused by movement of the stiffening grids during fatigue cycling. These damaged regions could ultimately initiate failure.

One of the objectives of the short-term tests was to uncover these testing problems and devise solutions prior to the start of the 50,000-hour, long-term test program. The mechanical clamping technique discussed earlier provided a very noticeable improvement in doubler bond reliability. Spacers inserted between the lower grips and compression stiffeners greatly decreased the unsupported column of B/Al and in turn reduced the incidence of compressive buckling failures. The combination of these spacers and the Teflon coating on the stiffeners significantly reduced the fretting fatigue abrasion of the soft aluminum surface of the B/Al specimens.

Because of these testing difficulties, the number of specimens that survived the 100- and 200-hour short-term exposures was less than originally planned. Nine specimens with 100 hours and six with 200 hours were available for residual strength testing. Several of the specimens were close to failure at one end as a result of small buckles. Many specimens also exhibited damage in the form of wear marks from stiffener abrasion and surface cracks and edge delaminations. It was possible, however, to cut subsize coupons, 0.013 m (0.5 in.) by 0.15 m (6 in.), from good areas of each of the short-term specimens as shown previously in Figure 12-30. The surface cracks were much less pronounced in the unidirectional specimens than observed in the 200-hour crossply specimens. Again no surface roughening similar to that found after fatigue testing at 516 K (550 ° F) was seen on the unidirectional short-term specimens.

**HT-S/710 G/PI, $[0° \pm 45°]_s$, unnotched, 100 hours.** In like manner to the unidirectional B/Al, the number of unnotched G/PI short-term specimens was somewhat less than originally planned. The reasons for this were twofold:

a. During proof loading of the G/PI system, nine of the unnotched specimens failed. These specimens, however, failed in a manner similar in appearance to the baseline tensile specimens. The reason for the premature failures was thought to be either: 1) an error in the applied load, or 2) lower than expected material strength. The first reason seemed unlikely as three independent strain measuring systems were used to monitor the loads. However, as a further check, 10 strain gaged dummy specimens of aluminum were installed in the flight simulation apparatus. Load checks in the region of interest indicated that the total applied load and the 10 individual loads were in agreement for all the measuring systems. To check the tensile properties of the panel (LRC-59) from which the short-term specimens were cut, two specimens were obtained from the small piece remaining from the panel. Several additional tensiles were also cut from the failed short-term specimens. These were then tensile tested at 505 K (450° F) using both a normal loading rate, 0.0013 m (0.05 in.) per minute, and a rate similar to that used during the proof test. The results, which were independent of load rate, showed the short-term panel to have an average tensile strength about 69 $MN/m^2$ (10 ksi) lower than the panel from which the baseline data were obtained. This same 69 $MN/m^2$ (10 ksi) lower value was found for the panel (LRC-60) that supplied the notched short-term specimens. Using the data from panels LRC-59 and 60 and that from additional specimens cut from the short-term specimens that had failed during the proof test, revised short-term loads were determined and testing was begun. However, because of the loss of the specimens during the first proof test, only seven specimens each were available for the 100-hour and 200-hour unnotched short-term exposures. No notched short-term specimens had failed so that full sets of 10 were available for the 100-hour and 200-hour time periods.

b. During the short-term testing of the G/PI specimens, almost all the 200-hour unnotched specimens were failed during a compressive overload. The accident occurred as the result of an operator error when an incorrect hydraulic valve was opened. Testing was interrupted while seven additional specimens were fabricated from spare material. Again a full set of specimens could not be prepared because of a lack of extra material. Just before completing the short-term tests, another compressive overload occurred. This incident resulted in four additional specimen failures, three unnotched and one notched. The cause of the overload was traced to the load programmer. The malfunction, which could have occurred later during long-term testing, was corrected. Again, one objective of the short-term test program was to uncover the problems and equipment deficiencies that, if not found, could be very costly during the long-term test program.

The five unnotched specimens of this group completed the 100 hours of exposure with almost no change in color or surface texture. There was a slight amount of surface damage on four of the specimens from the stiffening grids, but this was not believed to have had any effect on residual tensile properties. All of the specimens showed slight edge cracking, generally in the heated regions or near the doublers. A typical example can be seen in Figure 12-33. Again, these edge cracks probably did not affect the residual tensile strength, although in a compression or shear test they likely would have been important.

**HT-S/710 G/PI, $[0° \pm 45°]_s$, unnotched, 200 hours.** The added 100 hours of flight simulation expoposure did not change the appearance of these specimens from that described above.

**HT-S/710 G/PI, $[0° \pm 45°]_s$, notched, 100 hours and 200 hours.** The overall appearance of the notched specimens was identical to the unnotched specimens previously discussed. Slight surface damage from the stiffening grids and shallow edge cracks were visible on most of the specimens. Figure 12-34 shows an edge view of one of the edge cracked specimens. During residual strength testing, failure occurred at the hole in this notched specimen approximately 0.004 m (1.6 in.) from the edge crack. Two of the 200-hour specimens also showed slight cracks at the holes. The cracks were small and were not thought to have been a factor during residual strength testing.

**12.6.2.2 Residual Tensile Strength Data.** Following the examination of the 100-hour and 200-hour short-term flight simulation specimens, residual tensile strength tests were conducted. These tensile tests were made at the same temperatures as the simulation exposures, 422 K (300 ° F) for the B/E and G/E systems and 505 K (450 ° F) for both the HT-S/710 G/PI and B/Al materials. Full sets of residual strength data were obtained for the epoxies except for the 100-hour unnotched G/E where three simulation failures occurred. Only partial sets of data were available from the G/PI and B/Al systems because of the numerous testing and material problems previously discussed in Section 12.6.2.1. The test results, both tensile strengths and failure loads, are given in Tables 12-4 and 12-5 for B/E, Tables 12-6 and 12-7 for G/E, Tables 12-8 and 12-9 for G/PI, and Tables 12-10 and 12-11 for B/Al. The widths of the unnotched resin matrix specimens were 0.025 m (1.0 in.). The notched specimens were also 0.025 m (1.0 in.) wide but with 0.0064 m (0.25 in.) diameter holes. All the B/Al residual strength specimens were 0.013 m (0.50 in.) in width.

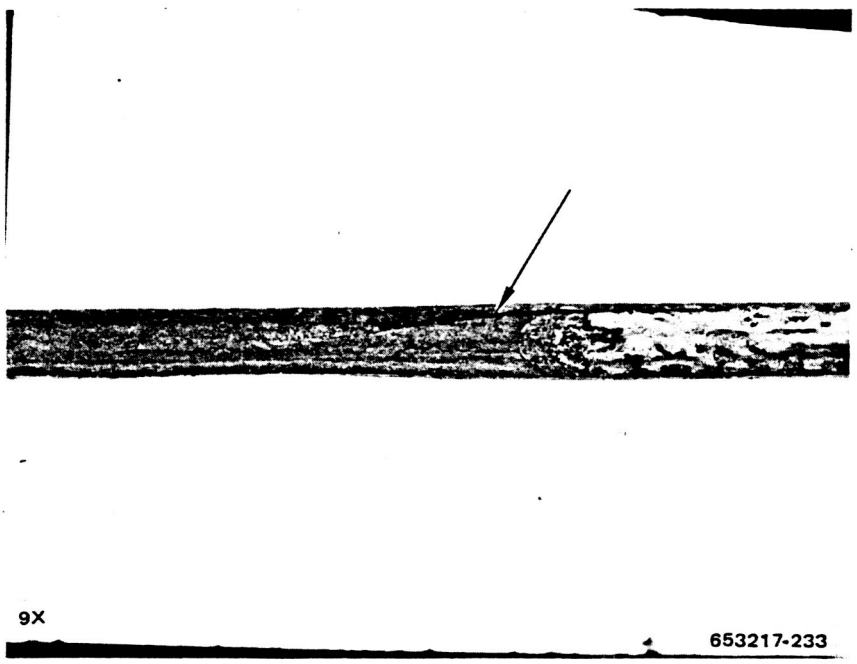



**Figure 12-33 Edge Cracking (arrow) in Specimen DC82-5, G/PI, Unnotched, After 100-hr Simulation Exposure at 505 K (450° F)**

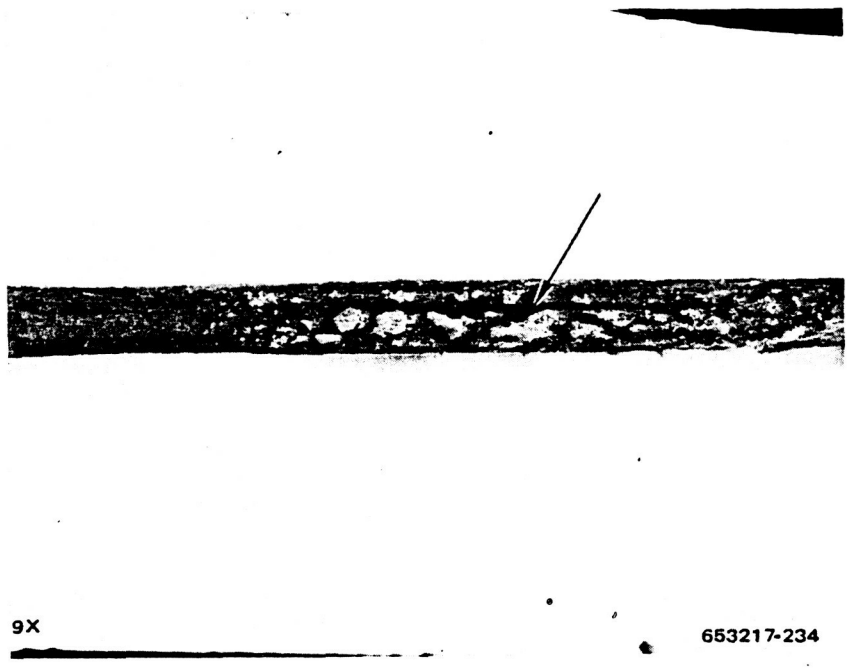



**Figure 12-34** **Edge Cracking (arrow) in Specimen DF81-5, G/PI, Notched, After 100-hr Simulation Exposure at 505 K (450° F)**

ORIGINAL PAGE IS
OF POOR QUALITY

**Table 12-4. Short-Term Residual Strength Data, $[0° \pm 45°]_s$, B/E, Unnotched, Exposed at 422 K (300° F) and Tensile Tested at 422 K (300° F)**

| Specimen Number | Exposure Time (hr) | | Load kN | Load (kip) | Tensile Strength $MN/m^2$ | Tensile Strength (ksi) |
|---|---|---|---|---|---|---|
| AC82-1 | 100 | | 10.7 | 2.415 | 541 | 78.4 |
| -2 | 100 | | 10.7 | 2.405 | 553 | 80.2 |
| -3 | 100 | | 10.7 | 2.410 | 552 | 80.1 |
| -4 | 100 | | 8.94 | 2.010 | 474 | 68.8 |
| -5 | 100 | | 9.83 | 2.210 | 523 | 75.9 |
| -6 | 100 | | 9.65 | 2.170 | 502 | 72.8 |
| -7 | 100 | | 10.2 | 2.300 | 539 | 78.2 |
| -8 | 100 | | 9.92 | 2.230 | 516 | 74.8 |
| -9 | 100 | | 9.90 | 2.225 | 518 | 75.2 |
| -10 | 100 | | 10.0 | 2.250 | 533 | 77.3 |
| | | ave | 10.1 | 2.260 | 525 | 76.2 |
| AC83-1 | 200 | | 9.54 | 2.145 | 483 | 70.1 |
| -2 | 200 | | 8.01 | 1.800 | 405 | 58.8 |
| -3 | 200 | | 8.72 | 1.960 | 456 | 66.2 |
| -4 | 200 | | 9.83 | 2.210 | 516 | 74.9 |
| -5 | 200 | | 9.65 | 2.170 | 502 | 72.8 |
| -6 | 200 | | 9.90 | 2.225 | 512 | 74.2 |
| -7 | 200 | | 9.30 | 2.090 | 487 | 70.6 |
| -8 | 200 | | 8.45 | 1.900 | 443 | 64.2 |
| -9 | 200 | | 9.59 | 2.155 | 501 | 72.6 |
| -10 | 200 | | 8.67 | 1.950 | 462 | 67.0 |
| | | ave | 9.17 | 2.060 | 477 | 69.1 |

Table 12-5. Short-Term Residual Strength Data, $[0° \pm 45°]_s$, B/E, Notched, Exposed at 422 K (300° F) and Tensile Tested at 422 K (300° F)

| Specimen Number | Exposure Time (hr) | | Load kN | Load (kip) | Notched Tensile Strength $MN/m^2$ | | Notched Tensile Strength (ksi) |
|---|---|---|---|---|---|---|---|
| AF84-1 | 100 | | 6.12 | 1.377 | 416 | (a) | 60.4 |
| -2 | 100 | | 6.41 | 1.440 | 452 | | 65.5 |
| -3 | 100 | | 6.32 | 1.420 | 445 | | 64.6 |
| -4 | 100 | | 6.23 | 1.400 | 433 | | 62.8 |
| -5 | 100 | | 6.85 | 1.540 | 485 | | 70.3 |
| -6 | 100 | | 6.04 | 1.357 | 427 | | 62.0 |
| -7 | 100 | | 6.05 | 1.360 | 423 | | 61.3 |
| -8 | 100 | | 5.38 | 1.210 | 379 | | 55.0 |
| -9 | 100 | | 6.36 | 1.430 | 446 | | 64.7 |
| -10 | 100 | | 6.61 | 1.485 | 467 | | 67.8 |
| | | ave | 6.24 | 1.400 | 437 | | 63.4 |
| AF82-1 | 200 | | 5.96 | 1.340 | 420 | | 60.9 |
| -2 | 200 | | 6.49 | 1.458 | 451 | | 65.4 |
| -3 | 200 | | 5.98 | 1.345 | 430 | | 62.3 |
| -4 | 200 | | 4.98 | 1.120 | 354 | | 51.4 |
| -5 | 200 | | 6.32 | 1.420 | 471 | | 68.3 |
| -6 | 200 | | 6.41 | 1.440 | 475 | | 68.9 |
| -7 | 200 | | 5.78 | 1.300 | 419 | | 60.7 |
| -8 | 200 | | 5.78 | 1.300 | 419 | | 60.7 |
| -9 | 200 | | 5.69 | 1.280 | 403 | | 58.4 |
| -10 | 200 | | 5.56 | 1.250 | 412 | | 59.8 |
| | | ave | 5.90 | 1.330 | 425 | | 61.7 |

[a] Net section strength, i.e., based on total width less hole diameter.

**Table 12-6. Short-Term Residual Strength Data, $[0° \pm 45°]_s$, G/E, Unnotched, Exposed at 422 K (300° F) and Tensile Tested at 422 K (300° F)**

| Specimen Number | Exposure Time (hr) | | Load kN | Load (kip) | Tensile Strength $MN/m^2$ | Tensile Strength (ksi) |
|---|---|---|---|---|---|---|
| BC84-1 | [a]54.2 | | — | — | — | — |
| -2 | [a]54.2 | | — | — | — | — |
| -3 | 100 | | 7.09 | 1.595 | 426 | 61.8 |
| -4 | 100 | | 8.09 | 1.818 | 445 | 64.5 |
| -5 | 100 | | 9.34 | 2.100 | 492 | 71.4 |
| -6 | [a]10.6 | | — | — | — | — |
| -7 | 100 | | 8.94 | 2.010 | [b]465 | [b]67.4 |
| -8 | 100 | | 11.1 | 2.499 | 565 | 81.9 |
| -9 | 100 | | 8.45 | 1.900 | 460 | 66.7 |
| -10 | 100 | | 9.96 | 2.240 | 501 | 72.7 |
| | | ave | 9.00 | 2.020 | 479 | 69.5 |
| BC81-1 | 200 | | 10.3 | 2.325 | 547 | 79.4 |
| -2 | 200 | | 8.27 | 1.860 | 405 | 58.7 |
| BC82-3 | 200 | | 10.0 | 2.250 | 552 | 80.1 |
| -4 | 200 | | 9.74 | 2.190 | 523 | 75.8 |
| -5 | 200 | | 7.34 | 1.650 | 381 | 55.2 |
| -6 | 200 | | 6.56 | 1.475 | 365 | 52.9 |
| -7 | 200 | | 9.67 | 2.175 | 484 | 70.2 |
| -8 | 200 | | 8.10 | 1.820 | 420 | 60.9 |
| -9 | 200 | | 10.1 | 2.260 | 516 | 74.8 |
| -10 | 200 | | 9.56 | 2.150 | 501 | 72.6 |
| | | ave | 8.96 | 2.020 | 469 | 68.1 |

[a] These specimens failed during flight simulation exposure testing.

[b] This specimen had a small crack in the test section after the 100-hr simulation exposure. Failure during tensile testing occurred at this location.

Table 12-7. Short-Term Residual Strength Data, $[0° \pm 45°]_s$, G/E, Notched, Exposed at 422 K (300° F) and Tensile Tested at 422 K (300° F)

| Specimen Number | Exposure Time (hr) | | Load kN | Load (kip) | Notched Tensile Strength $MN/m^2$ | Notched Tensile Strength (ksi) |
|---|---|---|---|---|---|---|
| | | | | | (a) | |
| BF84-1 | 100 | | 5.69 | 1.280 | 403 | 58.4 |
| -2 | 100 | | 5.36 | 1.205 | 405 | 58.8 |
| -3 | 100 | | 6.05 | 1.360 | 439 | 63.6 |
| -4 | 100 | | 5.60 | 1.260 | 412 | 59.7 |
| -5 | 100 | | 6.29 | 1.415 | 434 | 62.9 |
| -6 | 100 | | 6.05 | 1.360 | 424 | 61.5 |
| -7 | 100 | | 6.29 | 1.415 | 436 | 63.2 |
| -9 | 100 | | 5.78 | 1.300 | 425 | 61.6 |
| -10 | 100 | | 6.00 | 1.350 | 450 | 65.2 |
| | | ave | 5.90 | 1.330 | 425 | 61.7 |
| BF82-1 | 200 | | 5.69 | 1.280 | 392 | 56.9 |
| -2 | 200 | | 4.98 | 1.120 | 367 | 53.3 |
| -3 | 200 | | 5.20 | 1.170 | 414 | 60.0 |
| -4 | 200 | | 5.87 | 1.320 | 444 | 64.4 |
| -5 | 200 | | 6.16 | 1.385 | 452 | 65.6 |
| -6 | 200 | | 5.65 | 1.270 | 438 | 63.5 |
| -7 | 200 | | 5.43 | 1.220 | 429 | 62.2 |
| -8 | 200 | | 5.69 | 1.280 | 465 | 67.4 |
| -9 | 200 | | 5.38 | 1.210 | 394 | 57.1 |
| -10 | 200 | | 4.17 | .937 | 343 | 49.8 |
| | | ave | 5.42 | 1.220 | 414 | 60.0 |

[a] Net section strength, i.e., based on total width less hole diameter.

Table 12-8. Short-Term Residual Strength Data, $[0° \pm 45°]_s$, HT-S/710 G/PI, Unnotched, Exposed at 505 K (450° F) and Tensile Tested at 505 K (450° F)

| Specimen Number | Exposure Time (hr) | | Load kN | Load (kip) | Tensile Strength $MN/m^2$ | Tensile Strength (ksi) |
|---|---|---|---|---|---|---|
| DC81-12 | 100 | | 8.12 | 1.825 | 402 | 58.3 |
| DC82-5 | 100 | | 7.83 | 1.760 | 395 | 57.3 |
| -9 | 100 | | 7.41 | 1.665 | 425 | 61.7 |
| -10 | 100 | | 7.34 | 1.650 | 388 | 56.3 |
| -12 | 100 | | 8.32 | 1.870 | 393 | 57.0 |
| | | ave | 7.80 | 1.750 | 401 | 58.1 |
| DC85-2 | 200 | | 7.03 | 1.580 | 316 | 45.9 |
| -4 | 200 | | 7.34 | 1.650 | 339 | 49.1 |
| -5 | 200 | | 7.58 | 1.705 | 384 | 55.7 |
| -7 | 200 | | 7.03 | 1.580 | 348 | 50.5 |
| -9 | 200 | | 7.90 | 1.775 | 426 | 61.8 |
| -10 | 200 | | 7.72 | 1.735 | 368 | 53.4 |
| | | ave | 7.43 | 1.670 | 364 | 52.7 |

**Table 12-9. Short-Term Residual Strength Data, $[0° \pm 45°]_s$, HT-S/710 G/PI, Notched, Exposed at 505 K (450° F) and Tensile Tested at 505 K (450° F)**

| Specimen Number | Exposure Time (hr) | | Load kN | Load (kip) | Tensile Strength $MN/m^2$ | Tensile Strength (ksi) |
|---|---|---|---|---|---|---|
| | | | | | (a) | |
| DF81-1 | 100 | | 4.11 | 0.925 | 241 | 34.9 |
| -2 | 100 | | 4.83 | 1.085 | 301 | 43.7 |
| -3 | 100 | | 4.89 | 1.100 | 295 | 42.8 |
| -4 | 100 | | 4.07 | .915 | 240 | 34.8 |
| -5 | 100 | | 5.38 | 1.210 | 325 | 47.1 |
| -6 | 100 | | 4.71 | 1.060 | 294 | 42.6 |
| -7 | 100 | | 4.29 | .965 | 266 | 38.6 |
| -8 | 100 | | 4.56 | 1.025 | 285 | 41.3 |
| -9 | 100 | | 4.67 | 1.050 | 286 | 41.5 |
| -10 | 100 | | 3.83 | .860 | 234 | 34.0 |
| | | ave | 4.53 | 1.020 | 277 | 40.1 |
| DF82-1 | 200 | | 5.11 | 1.148 | 319 | 46.3 |
| -2 | 200 | | 3.91 | .880 | 236 | 34.2 |
| -3 | 200 | | 5.60 | 1.260 | 328 | 47.6 |
| -4 | 200 | | 4.20 | .945 | 247 | 35.8 |
| -5 | 200 | | 4.91 | 1.104 | 305 | 44.2 |
| -7 | 200 | | 4.50 | 1.012 | 265 | 38.5 |
| -8 | 200 | | 4.92 | 1.105 | 308 | 44.6 |
| -9 | 200 | | 4.78 | 1.075 | 295 | 42.8 |
| -10 | 200 | | 5.27 | 1.185 | 311 | 45.1 |
| | | ave | 4.80 | 1.080 | 290 | 42.1 |

[a] Net section strength, i.e., based on total width less hole diameter.

Table 12-10. Short-Term Residual Strength Data, $[0° \pm 45°]_s$, B/Al, Unnotched, Exposed at 505 K (450° F) and Tensile Tested at 505 K (450° F)

| Specimen Number | Exposure Time (hr) | | Load kN | Load (kip) | Tensile Strength $MN/m^2$ | Tensile Strength (ksi) |
|---|---|---|---|---|---|---|
| EC84-1 | 100 | | 7.56 | 1.700 | 604 | 87.6 |
| -2 | 100 | | 7.12 | 1.600 | 566 | 82.1 |
| -3 | 100 | | 7.34 | 1.650 | 574 | 83.3 |
| -4 | 100 | | 7.21 | 1.620 | 561 | 81.4 |
| -5 | 100 | | 5.78 | 1.300 | 457 | 66.3 |
| -6 | 100 | | 7.29 | 1.640 | 580 | 84.1 |
| -7 | 100 | | 6.56 | 1.475 | 519 | 75.3 |
| -8 | 100 | | 6.14 | 1.380 | 471 | 68.3 |
| -9 | [a]65.4 | | — | — | — | — |
| -10 | 100 | | 7.07 | 1.590 | 556 | 80.7 |
| | | ave | 6.90 | 1.550 | 543 | 78.8 |
| EC82-1 | [a]105 | | 6.20 | 1.395 | 509 | 73.8 |
| -2 | [a]136 | | 5.27 | 1.185 | 415 | 60.2 |
| -3 | 200 | | 5.12 | 1.150 | 401 | 58.1 |
| -4 | 200 | | 5.43 | 1.220 | 423 | 61.3 |
| -5 | 200 | | 5.72 | 1.285 | 434 | 63.0 |
| -6 | 200 | | 6.52 | 1.465 | 507 | 73.6 |
| -7 | [a]136 | | 4.94 | 1.110 | 383 | 55.5 |
| -8 | 200 | | 4.25 | .955 | 323 | 46.8 |
| -9 | 200 | | 4.49 | 1.010 | 348 | 50.5 |
| -10 | [a]136 | | 6.83 | 1.535 | 521 | 75.6 |
| | | ave | 5.48 | 1.230 | 426 | 61.8 |

[a] These specimens failed during flight simulation exposure testing.

Table 12-11. Short-Term Residual Strength Data, $[0°]_6$ B/Al, Unnotched, Exposed at 505 K (450° F) and Tensile Tested at 505 K (450° F)

| Specimen Number | Exposure Time (hr) | | Load kN | Load (kip) | Tensile Strength $MN/m^2$ | Tensile Strength (ksi) |
|---|---|---|---|---|---|---|
| EU85-1 | 100 | | 17.6 | 3.950 | 1460 | 211 |
| -3 | 100 | | 19.0 | 4.280 | 1610 | 233 |
| -6 | 100 | | 17.8 | 4.010 | 1490 | 216 |
| -9 | 100 | | 17.3 | 3.900 | 1410 | 205 |
| EU86-3 | 100 | | 17.3 | 3.900 | 1390 | 201 |
| -6 | 100 | | 18.0 | 4.050 | 1550 | 225 |
| EU87-11 | 100 | | 21.8 | 4.910 | 1560 | 226 |
| -12 | 100 | | 21.7 | 4.880 | 1560 | 227 |
| -14 | 100 | | 12.5 | 2.820 | 882 | 128 |
| | | ave | 18.1 | 4.080 | 1430 | 208 |
| EU87-1 | 200 | | 21.1 | 4.750 | 1460 | 211 |
| -2 | 200 | | 21.5 | 4.850 | 1520 | 221 |
| -5 | 200 | | 20.5 | 4.600 | 1450 | 210 |
| -6 | 200 | | 21.3 | 4.780 | 1520 | 221 |
| -7 | 200 | | 23.0 | 5.180 | 1630 | 236 |
| -8 | 200 | | 20.9 | 4.700 | 1480 | 214 |
| | | ave | 21.4 | 4.810 | 1510 | 219 |

**12.6.3 SHORT-TERM ANALYSIS.** Using the residual strength measurements from Section 12.6.2 and the baseline data from Section 7.1.2, the peak loads for the long-term, real-time flight simulation tests were calculated. The wearout model equations discussed previously in Section 12.5 were programmed into a desk top computer (HP9830) to calculate the parameters r, $A_4$, $\alpha_f$, and $\beta_f$ starting with $\alpha_0$, $\beta_0$, and the short-term residual strength data. The results for G/E and B/E are listed in Table 12-12. For HT-S/710 G/PI and B/Al the wearout model was not successful (to be discussed later). Since the long-term specimens were three times as wide as the short-term specimens they were expected to exhibit a reduced static strength. This expectation was based on the increase in complexity (least of three identical specimens). The strength reduction can also be thought of as a scaling effect since the long-term specimens have three times the stressed volume of the short-term specimens. The expected strength of the long-term specimen is $\beta_{LT} = f_c \beta_{ST}$ where the scaling factor, $f_c = (3)^{\frac{-1}{\alpha_o}}$ is the penalty for least of three as a function of the shape parameter, $\alpha_o$. The values of $f_c$ are listed in Table 12-12.

## Table 12-12. Long-Term Model Parameters for B/E and G/E

| Material | Condition | $\alpha_O$ | $\beta_O$ Short Term Peak Load | | | | r | $A_4$ | $\alpha_f$ | $\beta_f$ | $f_c$ | $\beta_{LT}$ | | $A_1$ | Long Term Peak Load | |
|---|---|---|---|---|---|---|---|---|---|---|---|---|---|---|---|---|
| | | | kN/m | (klp/in) | kN/m | (klp/in) | | | | | | kN/m | (klp/in) | | kN/m | (klp/in) |
| B/E | Unnotched | 19.5 | 403 | 2.300 | 245 | 1.398 | 5 | 131 | 2.44 | 1.50 | 0.95 | 383 | 2.185 | 0.94 | 230 | 1.314 |
| | Notched | 19.5 | 254 | 1.450 | 137 | .783 | 5 | 2.77 | 2.44 | 1.76 | .95 | 241 | 1.378 | .96 | 132 | .752 |
| G/E | Unnotched | 12.71 | 371 | 2.120 | 258 | 1.474 | 7 | 395 | 1.06 | 3.47 | .92 | 341 | 1.950 | .90 | 232 | 1.325 |
| | Notched | 12.03 | 226 | 1.288 | 142 | .813 | 7 | .564 | 1.00 | 6.16 | .91 | 205 | 1.172 | .93 | 132 | .756 |

A few other assumptions are necessary to predict the loads applied in the long-term tests to achieve the desired results. The problem is to apply loads high enough to produce measureable effects without failing all specimens in fatigue. A reliability of 0.80 at one lifetime was the desired goal. In other words, one out of five specimens used for the long-term tests would be expected to fail in fatigue prior to the completion of the 50,000 hours of exposure.

One remaining parameter of the wearout model, s, must also be determined. The parameter, s, is the exponent on the stress or load ratio that defines the power law time response to changing loads. This parameter is obtained by subjecting specimens to various magnifications of the random spectrum to obtain a random S-N curve. The slope of the random S-N curve is $-\frac{1}{s}$.

Since no such tests were performed for the current program, s has been estimated from data in reference 46 and 47 to be 11.0. The assumption of s is not felt to be too serious in this case because the loads required for the desired long-term response are not very different from the loads applied in the short-term tests.

To calculate the appropriate $A_1$ for the desired results, Equations (5) and (7) (Section 12.5) are combined by eliminating $\beta_f$ to arrive at:

$$A_1 = \left[ \frac{\beta_o^{2(r-1)} (-\ln R)^{1/\alpha f}}{(r-1)\, A_4\, t} \right] \frac{1}{s}$$

The results of this calculation are also listed in Table 12-12. Using the model parameters of Table 12-12 and the wearout model equations of Section 12.5 the peak long-term loads were obtained by an iteration process to give 80% survival at one lifetime (50,000 hours). These values are given in Table 12-12.

The computer was used to plot the wearout model curves shown in Figures 12-35 through 12-38 for the unnotched and notched G/E and B/E systems. The horizontal peak load lines have been set for 80% survival at one lifetime.

Wearout model curves could not be plotted for the HT-S/710 G/PI and B/Al systems because the wearout model did not work for these materials. In some cases the short-term residual strength value, $\beta$, and the shape parameter, $\alpha$, increased with time. The 200-hour or half lifetime residual strength values were actually higher than the 100-hour or quarter lifetime values, and the spread in the data was decreased. One method initially considered for determining the long-term peak loads for G/PI and B/Al was to take two-thirds of the "A" basis allowable tensile strength value for the particular composite considered. However, it was thought that this method did not place sufficient importance on the shape parameter, $\alpha$, which for B/Al was higher than for G/PI. The method that was used was to essentially reapply the risk factor, $f_r = (100)^{-\frac{1}{\alpha}}$, to the short-term peak load using the worst case $\alpha$ as determined from the baseline, 100-hour, or 200-hour strength data. This amounted to setting the long-term loads for these two systems by applying the square of the risk factor, $f_r$, times the complexity factor, $f_c$, to the baseline $\beta$ for each system at the temperature at which the long-term simulation was to be performed. The results of these calculations for HT-S/710 G/PI and B/Al are given in Table 12-13.

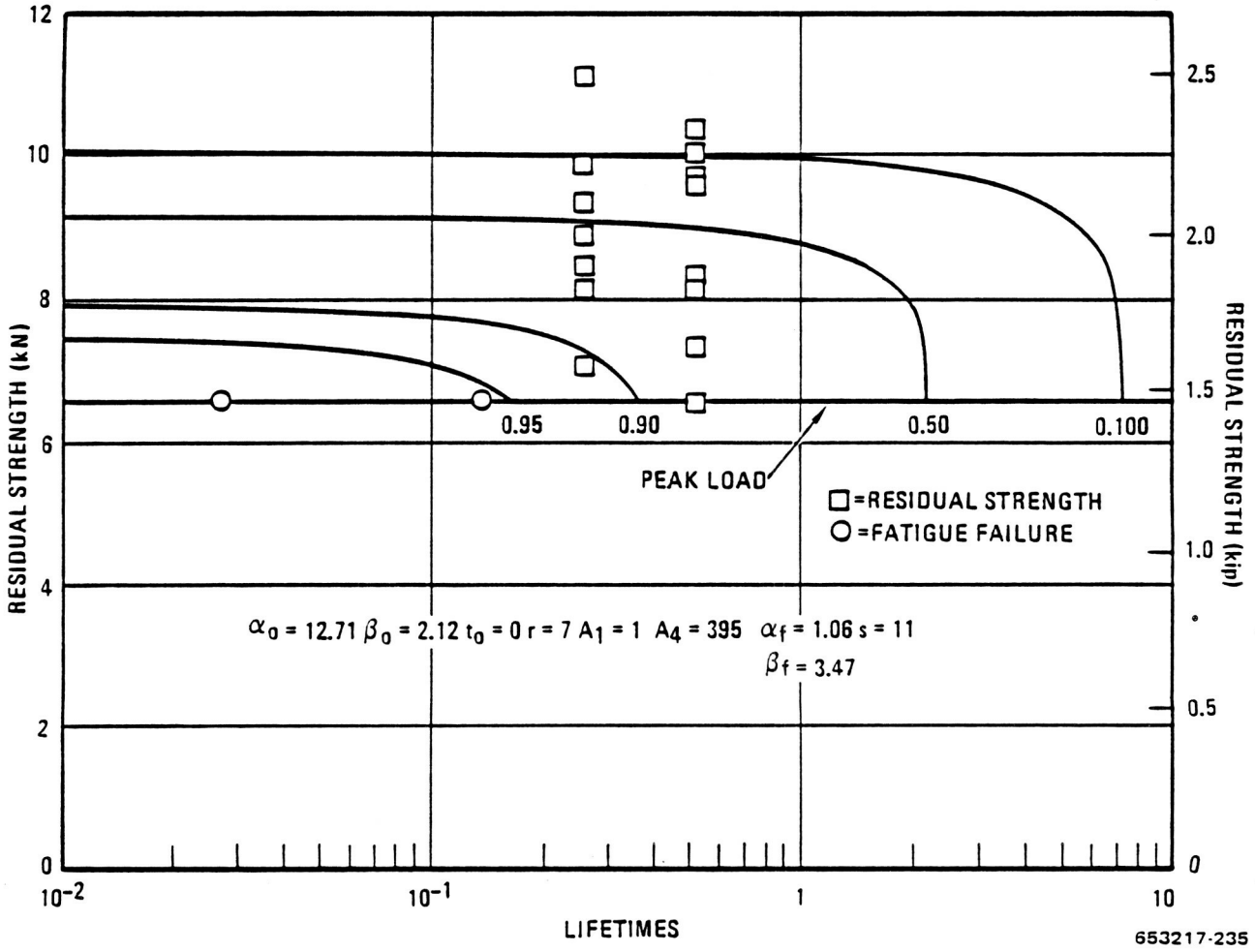



**Figure 12-35 Wearout Model for Unnotched $[0° \pm 45°]_s$ G/E**

**Table 12-13. Long-Term Peak Loads for HT-S/710 G/PI and B/Al**

| Material | Condition | [a]$\beta_T$ kN/m | [a]$\beta_T$ (kip/in) | $\alpha_T$ | $f_r$ | $f_r^2$ | $f_c$ | [b]Peak Load kN/m | [b]Peak Load (kip/in) |
|---|---|---|---|---|---|---|---|---|---|
| HT-S/710 G/PI | Unnotched | 366 | 2.09 | 10.7 | 0.65 | 0.42 | 0.90 | 140 | 0.800 |
| | Notched | 233 | 1.33 | 10.0 | .63 | .40 | .90 | 83.4 | 0.476 |
| B/Al | $[0°]_6$ | 1566 | 8.94 | 14.7 | .73 | .53 | .93 | 778 | 4.44 |
| | $[0° \pm 45°]_s$ | 427 | 2.44 | 13.6 | .71 | .51 | .92 | 200 | 1.144 |

[a] $\beta_T = f_T \beta_{RT}$ where T = 505 K (450° F)
[b] Peak Load $= f_r^2 f_c \beta_T$

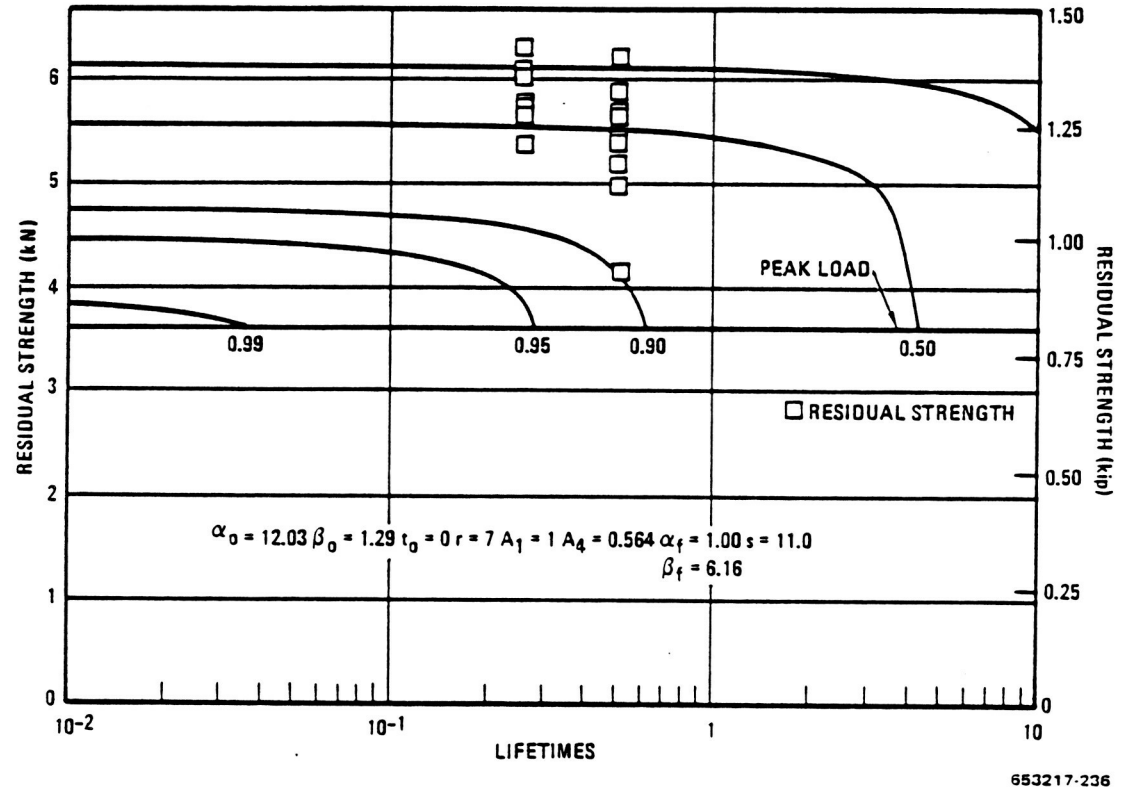



**Figure 12-36 Wearout Model for Notched $[0° \pm 45°]_s$ G/E**

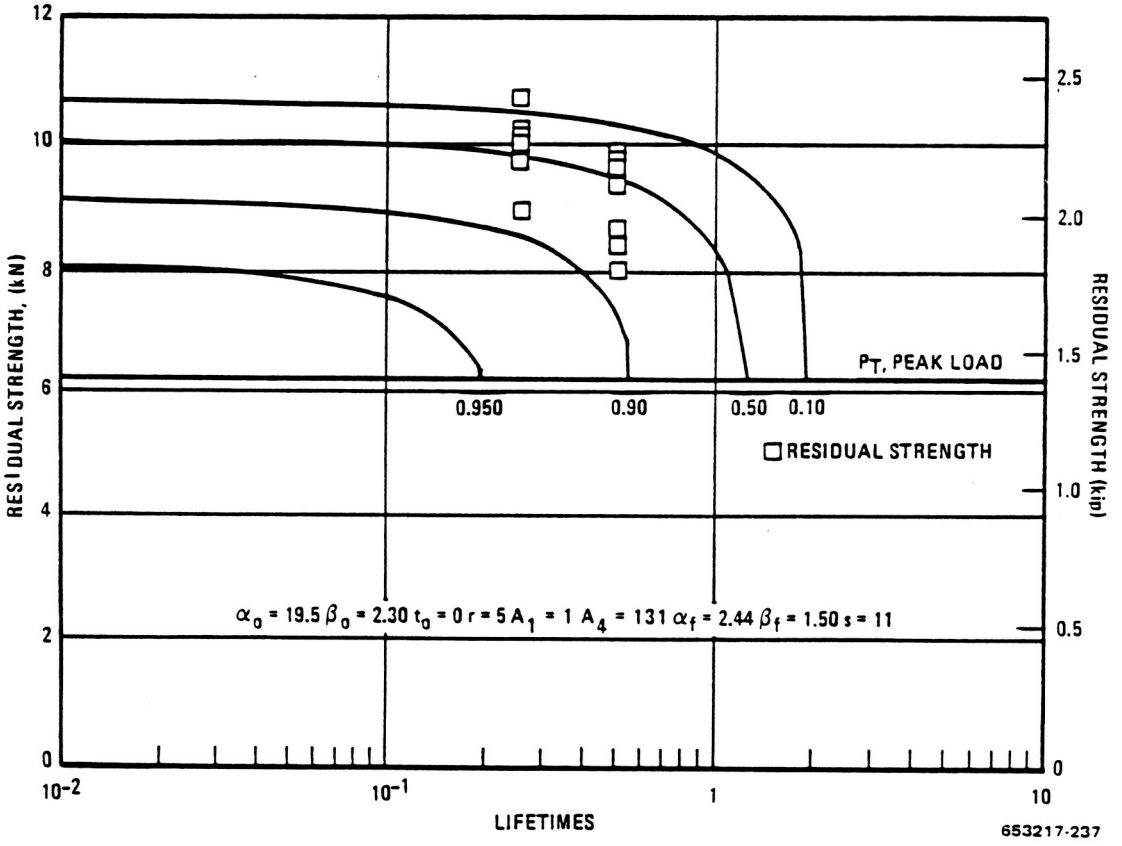



**Figure 12-37 Wearout Model for Unnotched $[0° \pm 45°]_s$ B/E**

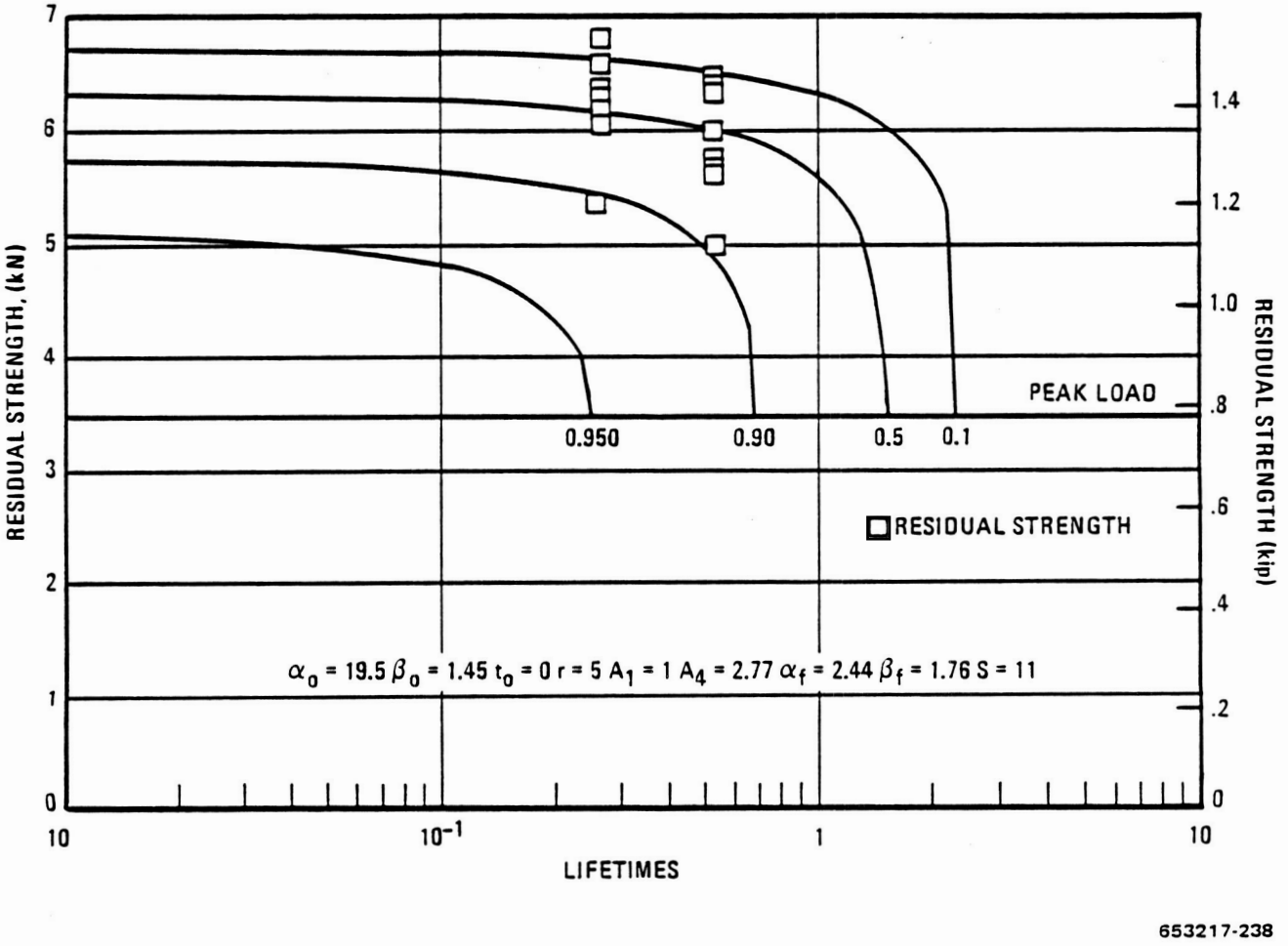



**Figure 12-38 Wearout Model for Notched $[0° \pm 45°]_s$ B/E**

The wearout model also could not be used to calculate the long term loads for Celion 6000/LARC-160 as no short term testing was performed on this system. The procedure for long term load selection, for both unnotched and notched specimens, was similar to that described earlier for the short term loads (Section 12.6.1.2). The baseline unnotched and notched tensile strength data were used to find the values of the scale parameter $\beta$ and a pooled value for $\alpha$, the Weibull shape parameter. For Celion 6000/LARC-160 the data for all temperatures (Tables 12-14 and 12-15) were suitable for pooling. The risk factor based on 1% failure was calculated as $f_n = (100)^{-1/\alpha}$. Since the pooled $\alpha$ for the unnotched samples was 28 and the $\alpha$ for the ten specimens at 450K (350 °F) was 22 (Table 12-14) the more conservative value of 22 was used. This approach was also used in earlier calculations for other systems. A temperature retention factor ($f_T$) of 1.00 was chosen for the unnotched case for 450K (350 °F) and 1.08 for the notched case for use at 450K (350 °F). The factor $f_c$ was $(6)^{-1/\alpha}$ for the unnotched specimens since the baseline specimens were 0.013 m (0.50 in.) wide and the long term specimens were 0.076 m (3.00 in.) wide. For the unnotched specimen it was (3) since the baseline specimens were 0.025 m (1.00 in.) wide. Both factors turned out to be equal because of the difference in the pooled $\alpha$ values, $f_c = 0.92$.

## Table 12-14. Baseline Tensile Data of $[0° \pm 45°]_s$ Celion 6000/LARC-160 G/PI

POOLED $\alpha = 28$

| Specimen No. | Temperature K | (°F) | Breaking Load for 0.013 m (0.50 in.) Spec. kN | (kip) | Breaking Load per Inch kN/m | (kip/in) | $\beta$ kN/m | (kip/in) | $\alpha$ | $\beta/\beta_{RT}$ | Load/$\beta$ | $\beta_{MLE}$ kN/m | (kip/in) | $\beta/\beta_{RT}$ |
|---|---|---|---|---|---|---|---|---|---|---|---|---|---|---|
| FC01-1 | 218 | −67 | 7.219 | 1.623 | 568.4 | 3.246 | 597.2 | 3.410 | 41 | 1.06 | 0.95 | 595.1 | 3.398 | 1.05 |
| -2 | | | 7.495 | 1.685 | 590.2 | 3.370 | | | | | .99 | | | |
| -3 | | | 7.740 | 1.740 | 609.4 | 3.480 | | | | | 1.02 | | | |
| -4 | 297 | 75 | 7.473 | 1.680 | 588.4 | 3.360 | 566.0 | 3.232 | 24 | 1.00 | 1.04 | 567.6 | 3.241 | 1.00 |
| -5 | | | 7.540 | 1.695 | 593.7 | 3.390 | | | | | 1.05 | | | |
| -6 | | | 6.984 | 1.570 | 549.9 | 3.140 | | | | | .97 | | | |
| -7 | | | 7.340 | 1.650 | 577.9 | 3.300 | | | | | 1.02 | | | |
| -8 | | | 7.073 | 1.590 | 556.9 | 3.180 | | | | | .98 | | | |
| -9 | | | 7.059 | 1.587 | 555.8 | 3.174 | | | | | .98 | | | |
| -10 | | | 6.695 | 1.505 | 527.1 | 3.010 | | | | | .93 | | | |
| -11 | | | 6.939 | 1.560 | 546.4 | 3.120 | | | | | .97 | | | |
| -12 | | | 6.672 | 1.500 | 525.4 | 3.000 | | | | | .93 | | | |
| -13 | | | 6.157 | 1.465 | 513.1 | 2.930 | | | | | .91 | | | |
| -14 | 394 | 250 | 7.762 | 1.745 | 611.2 | 3.490 | 604.2 | 3.450 | 24 | 1.07 | 1.01 | 605.2 | 3.456 | 107 |
| -15 | | | 6.850 | 1.540 | 539.4 | 3.080 | | | | | .89 | | | |
| -16 | | | 7.829 | 1.760 | 616.4 | 3.520 | | | | | 1.02 | | | |
| -17 | 450 | 350 | 7.428 | 1.670 | 584.7 | 3.340 | 568.4 | 3.246 | 22 | 1.00 | 1.03 | 568.1 | 3.244 | 1.00 |
| -18 | | | 7.206 | 1.620 | 567.4 | 3.240 | | | | | 1.0 | | | |
| -19 | | | 6.695 | 1.505 | 527.1 | 3.010 | | | | | .93 | | | |
| -20 | | | 6.628 | 1.490 | 521.9 | 2.980 | | | | | .92 | | | |
| -21 | | | 6.308 | 1.418 | 496.6 | 2.836 | | | | | .87 | | | |
| -22 | | | 6.628 | 1.490 | 521.9 | 2.980 | | | | | .92 | | | |
| -23 | | | 7.286 | 1.638 | 573.7 | 3.276 | | | | | 1.01 | | | |
| -24 | | | 7.397 | 1.663 | 564.9 | 3.226 | | | | | 1.02 | | | |
| -25 | | | 7.473 | 1.680 | 588.4 | 3.360 | | | | | 1.04 | | | |
| -26 | | | 7.028 | 1.580 | 553.4 | 3.160 | | | | | .97 | | | |
| -27 | 478 | 400 | 7.139 | 1.605 | 562.1 | 3.210 | 558.3 | 3.188 | 120 | 0.99 | 1.01 | 556.2 | 3.176 | 0.98 |
| -28 | | | 7.028 | 1.580 | 553.4 | 3.160 | | | | | .99 | | | |
| -29 | | | 7.006 | 1.575 | 551.6 | 3.150 | | | | | .99 | | | |
| -30 | 505 | 450 | 7.095 | 1.595 | 558.6 | 3.190 | 550.9 | 3.146 | 40 | .97 | 1.01 | 549.2 | 3.138 | .97 |
| -31 | | | 6.539 | 1.470 | 514.8 | 2.940 | | | | | .93 | | | |
| -32 | | | 7.028 | 1.580 | 553.4 | 3.160 | | | | | 1.00 | | | |
| -33 | 533 | 500 | 6.872 | 1.545 | 541.4 | 3.090 | 551.3 | 3.148 | 145 | .97 | .98 | 549.5 | 3.138 | .97 |
| -34 | | | 7.006 | 1.575 | 551.6 | 3.150 | | | | | 1.00 | | | |
| -35 | | | 7.028 | 1.580 | 553.4 | 3.160 | | | | | 1.00 | | | |

ORIGINAL PAGE IS
OE POOR QUALITY

## Table 12-15. Baseline Notched Tensile Data of $[0° \pm 45°]_s$ Celion 6000/LARC-160 G/PI

POOLED $\alpha = 14$

| Specimen No. | Temperature K | (°F) | Breaking Load for 0.013 m (0.50 in.) Spec. kN | (kip) | Breaking Load per Inch kN/m | (kip/in) | $\beta$ kN/m | (kip/in) | $\alpha$ | $\beta/\beta_{RT}$ | Load/$\beta$ | $\beta_{MLE}$ kN/m | (kip/in) | $\beta/\beta_{RT}$ |
|---|---|---|---|---|---|---|---|---|---|---|---|---|---|---|
| FC01-1 | 218 | −67 | 7.073 | 1.590 | 371.3 | 2.120 | 365.0 | 2.084 | 50 | 0.95 | 1.02 | 362.1 | 2.068 | 0.93 |
| -2 | | | 6.717 | 1.510 | 352.5 | 2.013 | | | | | 0.97 | | | |
| -3 | | | 6.850 | 1.540 | 359.5 | 2.053 | | | | | .99 | | | |
| -4 | 297 | 75 | 6.361 | 1.430 | 334.0 | 1.907 | 383.9 | 2.192 | 10 | 1.0 | .87 | 389.6 | 2.225 | 1.0 |
| -5 | | | 5.961 | 1.340 | 330.5 | 1.887 | | | | | .86 | | | |
| -6 | | | 6.539 | 1.470 | 343.2 | 1.960 | | | | | .89 | | | |
| -7 | | | 7.473 | 1.680 | 392.3 | 2.240 | | | | | 1.02 | | | |
| -8 | | | 8.140 | 1.830 | 427.3 | 2.440 | | | | | 1.11 | | | |
| -9 | | | 7.295 | 1.640 | 383.0 | 2.187 | | | | | 1.00 | | | |
| -10 | | | 8.096 | 1.820 | 425.0 | 2.427 | | | | | 1.11 | | | |
| -11 | | | 6.405 | 1.440 | 336.2 | 1.920 | | | | | .88 | | | |
| -12 | | | 6.494 | 1.460 | 341.0 | 1.947 | | | | | .89 | | | |
| -13 | | | 7.028 | 1.580 | 369.0 | 2.107 | | | | | .96 | | | |
| -14 | 394 | 250 | 7.206 | 1.620 | 378.3 | 2.160 | 371.4 | 2.121 | 16 | .97 | 1.02 | 370.6 | 2.116 | .95 |
| -15 | | | 7.295 | 1.640 | 383.0 | 2.187 | | | | | 1.03 | | | |
| -16 | | | 5.916 | 1.330 | 310.5 | 1.773 | | | | | .84 | | | |
| -17 | 450 | 350 | 6.761 | 1.520 | 355.0 | 2.027 | 415.0 | 2.370 | 22 | 1.08 | .86 | 411.9 | 2.352 | 1.06 |
| -18 | | | 7.918 | 1.780 | 415.6 | 2.373 | | | | | 1.00 | | | |
| -19 | | | 7.562 | 1.700 | 397.0 | 2.267 | | | | | .96 | | | |
| -20 | | | 7.918 | 1.780 | 415.6 | 2.373 | | | | | 1.00 | | | |
| -21 | | | 7.073 | 1.590 | 371.3 | 2.120 | | | | | .89 | | | |
| -22 | | | 8.155 | 1.840 | 429.6 | 2.453 | | | | | 1.04 | | | |
| -23 | | | 7.651 | 1.720 | 401.6 | 2.293 | | | | | .97 | | | |
| -24 | | | 8.007 | 1.800 | 420.3 | 2.400 | | | | | 1.01 | | | |
| -25 | | | 7.651 | 1.720 | 401.6 | 2.293 | | | | | .97 | | | |
| -26 | | | 8.318 | 1.870 | 436.6 | 2.493 | | | | | 1.05 | | | |
| -27 | 478 | 400 | 8.585 | 1.930 | 450.6 | 2.573 | 415.4 | 2.372 | 10 | 1.08 | 1.08 | 421.7 | 2.408 | 1.08 |
| -28 | | | 6.405 | 1.440 | 336.2 | 1.920 | | | | | .81 | | | |
| -29 | | | 7.562 | 1.700 | 397.0 | 2.267 | | | | | .96 | | | |
| -30 | 505 | 450 | 9.341 | 2.100 | 490.3 | 2.800 | 468.4 | 2.675 | 18 | 1.22 | 1.05 | 465.8 | 2.660 | 1.2 |
| -31 | | | 8.674 | 1.950 | 455.3 | 2.600 | | | | | .97 | | | |
| -32 | | | 7.962 | 1.790 | 418.0 | 2.387 | | | | | .89 | | | |
| -33 | 533 | 500 | 8.007 | 1.800 | 420.3 | 3.400 | 440.3 | 2.514 | 12 | 1.15 | .95 | 442.7 | 2.528 | 1.14 |
| -34 | | | 8.985 | 2.020 | 471.6 | 2.693 | | | | | 1.07 | | | |
| -35 | | | 7.117 | 1.600 | 373.5 | 2.133 | | | | | .85 | | | |

Table 12-16 shows the reduction factors and the calculated peak loads for the Celion 6000/ LARC-160 G/PI long term flight simulation tests. The loads used on the HT-S/710 G/PI are also listed for comparison. The peak loads for Celion 6000/LARC-160 were considerably higher than those calculated for HT-S/710. The scale parameter $\beta$ was found to be consistently higher and the shape parameter $\alpha$ was also much higher.

**Table 12-16. Long-Term Peak Loads for $[0° \pm 45°]_s$ G/PI**

| Material | Condition | [a]$\beta_T$ kN/m | [a]$\beta_T$ (kip/in) | $\alpha_T$ | $f_r$ | $f_r^2$ | $f_c$ | [b]Peak Load kN/m | [b]Peak Load (kip/in) |
|---|---|---|---|---|---|---|---|---|---|
| HT-S/710 | Unnotched | 366 | 2.09 | 10.7 | 0.65 | 0.42 | 0.90 | 140 | 0.800 |
| | Notched | 233 | 1.33 | 10.0 | .63 | .40 | .90 | 83.4 | .476 |
| Celion 6000/ LARC-160 | Unnotched | 567 | 3.24 | 22 | .81 | .53 | .92 | 338 | 1.93 |
| | Notched | 443 | 2.53 | 14 | .72 | .51 | .92 | 198 | 1.13 |

[a] $\beta_T = f_T \beta_{RT}$ where T = 505 K (450° F) for HT-S/710 and 450 K (350°F) for Celion 6000/LARC-160
[b] Peak Load = $f_r^2 f_c \beta_T$

Using the load levels specified in Table 12-16 one of the unnotched Celion 6000/LARC-160 G/PI specimens failed after only 1.3 hours of exposure. Because of this early failure another look was taken at the process of load selection. The original unnotched loads were calculated using the baseline unnotched tensile data obtained at seven different temperatures. All 35 specimens were taken from panel III-5. Because the flight simulation specimens were taken from panels III-8, III-9, and III-10, revised loads were calculated using the quality assurance (QA) tensile data for these three panels. The QA data consisted of three tests each at 297 K (75°F) and 450 K (350°F) for each panel. The Weibull scale and shape parameters calculated from these data are given in Table 12-17 along with the values used in the original load determinations. Using the QA data from panels III-8, III-9, and III-10 resulted in a reduction in the peak long term load from 338 kN/m (1.93 kip/in) to 277 kN/m (1.582 kip/in).

This load level also proved to be excessive with a second unnotched specimen failure occurring after 138 hours of exposure. As these specimens were intended to have an 80% expectation of completing 50,000 hours of exposure, a further reduction in the peak load level was necessary. To increase the data base for the Celion 6000/LARC-160 G/PI system, QA tensile data from all the 6 ply panels were used in calculating a revised peak load. The Weibull scale and shape parameters calculated from QA tensile data from seven test panels (42 specimens) are listed in Table 12-17. The recalculated peak load was 183 kN/m (1.043 kip/in). This value was now lower than the peak load that had been chosen for the notched specimens (based on notched baseline tensile data). Since the notched baseline tensile strengths were consistently lower than the unnotched baseline tensile strengths it was felt that the same relationship should be held for the flight simulation peak loads. As no notched tensile data were obtained during QA testing, the value of $\alpha_T$ (a measure of data scatter) obtained from the QA unnotched tensile data was used to recalculate $f_r$ and $f_c$. These values were then used with the $\beta_T$ obtained from the notched baseline tensile data to calculate a revised peak load of 143 kN/m (0.819 kip/in) for the notched

Table 12-17. Long-Term Peak Loads for $[0° \pm 45°]_s$ G/Pl

| Material | Condition | [a]$\beta_T$ kN/m | [a]$\beta_T$ (kip/in) | $\alpha_T$ | $f_r$ | $f_r^2$ | $f_c$ | [b]Peak Load kN/m | [b]Peak Load (kip/in) |
|---|---|---|---|---|---|---|---|---|---|
| ORIGINAL LOADS | | | | | | | | | |
| HT-S/710 | Unnotched | 366 | 2.09 | 10.7 | 0.65 | 0.42 | 0.90 | 140 | 0.800 |
| | Notched | 233 | 1.33 | 10.0 | .63 | .40 | .90 | 83.4 | 0.476 |
| Celion 6000/ LARC-160 | Unnotched | 567 | 3.24 | 22 | .81 | .53 | .92 | 338 | 1.93 |
| | Notched | 443 | 2.53 | 14 | .72 | .51 | .92 | 198 | 1.13 |
| REVISED LOADS | | | | | | | | | |
| QA Data from Panels 8,9 & 10 | Unnotched | 595 | 3.397 | 14.4 | .73 | .53 | .88 | 277 | 1.582 |
| QA Data from Panels 4,5,7, 8,9,10 & 11 | Unnotched | 562 | 3.212 | 9.8 | .625 | .39 | .83 | 183 | 1.043 |
| $\alpha_T$ from QA Data | Notched | 443 | 2.53 | 9.8 | .625 | .39 | .83 | 143 | .819 |

[a] $\beta_T = f_T\beta_{RT}$ where T = 505 K (450° F) for HT-S/710 and 450 K (350°F) for Celion 6000/LARC-160
[b] Peak Load = $f_r^2 f_c \beta_T$

flight simulation tests (see Table 12-17). With the recalculated peak loads both the unnotched and notched specimens completed 10,000 hours of flight simulation exposure without additional failures.

The peak long-term loads for the five materials, Tables 12-12, 12-13, and 12-17, were used to calculate the peak, landing, and one g stresses presented in Table 12-18.

Table 12-18. Long-Term Peak Loads and Stresses

| Material | Condition | Long-Term Peak Load kN/m | (kip/in) | Total Peak Load for 0.076 m (3.0 in) Specimen kN | (kip) | Peak Stress MN/m² | (ksi) | Landing Stress MN/m² | (ksi) | One g Stress MN/m² | (ksi) |
|---|---|---|---|---|---|---|---|---|---|---|---|
| B/E | Unnotched | 230 | 1.314 | 17.5 | 3.94 | 302 | 43.8 | −75.5 | −10.9 | 151 | 21.9 |
| | Notched | 132 | .752 | 10.1 | 2.26 | 239 | 34.6 | −60.0 | −8.7 | 120 | 17.3 |
| G/E | Unnotched | 232 | 1.325 | 17.7 | 3.98 | 305 | 44.2 | −76.5 | −11.1 | 153 | 22.1 |
| | Notched | 132 | .756 | 10.1 | 2.27 | 232 | 33.6 | −57.9 | −8.4 | 116 | 16.8 |
| HT-S/710 G/PI | Unnotched | 140 | .800 | 10.7 | 2.40 | 153 | 22.2 | −38.6 | −5.6 | 76.5 | 11.1 |
| | Notched | 83.4 | .476 | 6.36 | 1.43 | 125 | 18.2 | −31.7 | −4.6 | 63 | 9.1 |
| Celion 6000/ | Unnotched | 183 | 1.043 | 13.9 | 3.13 | 243 | 34.8 | −60.0 | −8.7 | 122 | 17.4 |
| LARC-160 G/PI | Notched | 143 | .819 | 10.9 | 2.46 | 191 | 27.3 | −47.7 | −6.8 | 95 | 13.7 |
| B/Al | $[0°]_6$ | 778 | 4.44 | 59.3 | 13.32 | 747 | 108.3 | −187 | −27.1 | 374 | 54.2 |
| | $[0° \pm 45°]_s$ | 200 | 1.144 | 15.3 | 3.43 | 208 | 30.1 | −51.7 | −7.5 | 104 | 15.1 |

## 12.7 LONG-TERM FLIGHT SIMULATION

The main emphasis of the entire program was on the long-term tests and that is why they were approached so carefully. The objective of the long-term test program was to determine the behavior of advanced composites in the operating environment of supersonic cruise aircraft. Specimens were to be exposed for real-time periods of 10,000, 25,000, and 50,000 hours. The tests would be unsuccessful if the environmental conditions (loads or temperatures) were set either too high or too low. If the conditions could be set so that a given number failed by the end of the required 50,000 hours of exposure, not only would the behavior of the composites be determined but also a predictive capability would be demonstrated.

**12.7.1 TEST PLAN AND PROCEDURES.** For each material system of Phase I, B/E, G/E, HT-S/710 G/PI, and B/Al, a total of 20 long-term specimens was installed in the flight simulation apparatus. The resin matrix specimens were all fabricated from 6 ply panels having a $[0° \pm 45°]_s$ crossplied orientation. Ten were unnotched and 10 were notched (see Figures 12-9 and 12-10 for specimen configurations). The B/Al specimens, all of which were unnotched, were fabricated, half from 6 ply unidirectional and half from 6 ply $[0° \pm 45°]_s$ crossply panels. Five specimens from each material/orientation/configuration set were to be exposed for 10,000 hours (equivalent to 5000 of the two-hour flights) for the Phase I evaluation. The other five specimens of each set were to remain in the simulation apparatus until 50,000 hours (25,000 flights) of exposure had been completed (Phase II) or until excessive specimen failures made it uneconomical to continue operation of the simulator.

Several modifications to the Phase II test plan were made at the completion of 10,000 hours of exposure. The first was the addition of three unnotched long-term specimens to each material/orientation set. These specimens were installed in the flight simulation apparatus after the 10,000-hour specimens were removed. The added specimens were to be exposed for 25,000 hours to provide additional residual strength data between the originally scheduled 10,000- and 50,000-hour time periods. The second modification was caused by a high failure rate of the G/E specimens and extensive visual degradation of the B/E specimens during the first 10,000

hours. All of the original B/E and G/E flight simulation specimens were removed, and new specimens were fabricated to replace them. These specimens, which were all unnotched, were installed in the simulator as follows:

Bay 5 5 B/E, 10,000-hr specimens
5 G/E, 10,000-hr specimens

Bay 6 3 B/E, 25,000-hr specimens
3 G/E, 25,000 hr specimens

Bay 7 5 B/E, 50,000-hr specimens
5 G/E, 50,000-hr specimens

The random load spectrum remained unchanged except that the load levels were now the average of those applied previously for the two epoxy materials. The change (shown below for the maximum tensile loads) was quite small, less than 1%.

Previous B/E load: 17.53 MN (3942 lb)

Previous G/E load: 17.68 MN (3975 lb)

Revised load: 17.60 MN (3958 lb)

An increase in testing efficiency was possible by intermixing the two systems as the flight simulation exposures could be performed in three bays rather than the four required if the systems were run separately. The maximum test temperature during flight simulation testing of B/E and G/E was reduced to 373 K (212 °F). This temperature was determined from a log time versus 1/T plot of G/E thermal aging data obtained earlier in the program. The curve represents the time/temperature combinations at which significant degradation of the epoxy matrix begins. Extrapolation of the curve to 50,000 hours gave the new test temperature.

The final modification to the Phase II test plan was the addition of the new material, Celion 6000/LARC-160 G/PI. Ten unnotched and 10 notched specimens were prepared and installed in the flight simulation apparatus for 10,000 hours of exposure testing.

The flight simulation cycle, shown earlier in Figure 12-1, is two hours in length and consists of three parts: climb, cruise, and descent. The time-temperature-load history of a typical flight is shown in Table 12-19. Each flight is concluded with one compressive load cycle. The load spectrum is applied in a random manner.

**Table 12-19. Time-Temperature-Load History for Typical Long-Term Flight Simulation Cycle**

| Item | Climb (Heating) | Cruise (Held at Constant Temperature) | | | Descent (Cooling) |
|---|---|---|---|---|---|
| Time | 10 minutes | 44 minutes | 2 minutes | 44 minutes | 20 minutes |
| [a]Load | 25 cycles | constant | 6 cycles | constant | 7 cycles |

[a]One additional compressive load per two-hour flight.

The cruise portion of the simulation cycle was conducted at a constant temperature for each material system. The intent of the program was to select the temperature that was considered to be the maximum use temperature for each composite for long-time (50,000-hour) service. For the HT-S/710 G/PI and B/Al materials, the short-term results and data from the thermal aging studies then in progress indicated that 505 K (450° F) was probably a good upper limit, and this temperature was selected. For the two epoxy systems, the short-term results obtained at 422 K (300° F) gave no reason to change the exposure temperature, and 1000-hour thermal aging data at 394 K (250° F) and 450 K (350° F), which was then available, also indicated no problem with the 422 K (300° F) temperature. Therefore, the long-term flight simulation exposures were begun using these temperatures for the cruise portions of the cycle. Shortly after starting the tests, the 5000-hour thermal aging results for the epoxy systems became available. The data indicated that severe degradation of the epoxy matrix with significant decreases in tensile strength had occurred at 450 K (350° F). No effects were observed at 394 K (250° F). Primarily because of the thermal aging data, but also as a result of discussions with various individuals who were well versed in composite usage and research and development, the maximum exposure temperature for the epoxy long-term tests was lowered to 408 K (275° F). At the time that the temperature was changed, the epoxy specimens had received only approximately 1000 hours of exposure. As discussed earlier the 408 K (275° F) cruise temperature was also found to be excessive, and, following the 10,000 hours exposure of Phase I, new epoxy specimens were prepared for Phase II and the maximum exposure temperature was again lowered, this time to 373 K (212° F). The selection of 450 K (350° F) as the maximum use temperature for the Celion 6000/LARC-160 system was based on minimal data from the then current literature. Sufficient thermal aging results from this study were not yet available.

Selection of the maximum load levels for the long-term flight simulation exposure tests has been discussed earlier in the short-term test results analysis section. A summary of the types and numbers of long-term specimens with the test conditions for each is given in Table 12-20.

Before installing the long-term specimens in the flight simulation apparatus, width and thickness measurements were made at several locations in the test sections of all specimens, and average cross-sectional areas were calculated for each set of specimens. These measurements were used to obtain the flight simulation stresses shown in Table 12-20 and could be used for the residual strength determinations for specimens that experienced surface degradation during the long-term exposure tests. The specimens were then installed in the test machine, thermocouples were attached, the compression stiffening grids were bolted in place, and all resin-matrix specimens were heated to their respective cruise temperatures and held for 24 hours to remove any absorbed moisture. Before starting the tests, each set of 10 specimens was proof loaded to the maximum value that would be experienced during the 50,000 hours of exposure to the random load spectrum.

At the completion of 10,000 hours of flight simulation testing, all unfailed Phase I specimens were removed from the simulator and visually examined with a stereo microscope to check for changes in appearance or the presence of surface flaws such as loose or bare fibers, cracks, or delaminations. Photographs were made of typical specimens and of those with significant changes in appearance as a result of the 10,000 hours of exposure. The large, 0.076 m (3 in.) by 0.46 m (18 in.), long-term specimens were then cut into smaller pieces, which were fabricated into various types of specimens and tested for determination of residual strength values.

Table 12-20. Summary of Long-Term Test Program

| Material System | Orientation | Configuration | Number of Specimens | | | Cruise Temperature | | Peak Stress | |
|---|---|---|---|---|---|---|---|---|---|
| | | | 10,000 hr | 25,000 hr | 50,000 hr | K | (°F) | MN/m² | (ksi) |
| B/E 5505/4 | $[0° \pm 45°]_s$ | Unnotched | 10 | 0 | 0 | 408 | 275 | 302 | 43.8 |
| | | Notched | 10 | 0 | 0 | 408 | 275 | 239 | 34.6 |
| B/E 5505/4 | $[0° \pm 45°]_s$ | Unnotched | 5 | 3 | 5 | 373 | 212 | 303 | 44 |
| | | Notched | 0 | 0 | 0 | — | — | — | — |
| G/E A-S/3501-5 | $[0° \pm 45°]_s$ | Unnotched | 10 | 0 | 0 | 408 | 275 | 305 | 44.2 |
| | | Notched | 10 | 0 | 0 | 408 | 275 | 232 | 33.6 |
| G/E A-S/3501-5 | $[0° \pm 45°]_s$ | Unnotched | 5 | 3 | 5 | 373 | 212 | 303 | 44 |
| | | Notched | 0 | 0 | 0 | — | — | — | — |
| G/PI HT-S/710 | $[0° \pm 45°]_s$ | Unnotched | 5 | 3 | 5 | 505 | 450 | 153 | 22.2 |
| | | Notched | 5 | 0 | 5 | 505 | 450 | 125 | 18.2 |
| G/PI Celion 6000/ LARC-160 | $[0° \pm 45°]_s$ | Unnotched | 10 | 0 | 0 | 450 | 350 | 236 | 34.2 |
| | | Notched | 10 | 0 | 0 | 450 | 350 | 184 | 26.7 |
| B/Al | $[0° \pm 45°]_s$ | Unnotched | 5 | 3 | 5 | 505 | 450 | 208 | 30.1 |
| | $[0°]_6$ | Unnotched | 5 | 3 | 5 | 505 | 450 | 747 | 108.3 |

Similar procedures were carried out for Phase II specimens that completed 25,000 hours of exposure. These included B/E, G/E, and a portion of the B/Al specimens. The three 25,000 hour HT-S/170 G/PI specimens failed to complete the required 25,000 hours of exposure.

The objective of the Phase II flight simulation test program was to subject the B/Al, HT-S/710 G/PI, B/E, and G/E specimens to 50,000 hours of exposure followed by residual strength testing. None of the B/Al or G/PI specimens survived the simulation testing to 50,000 hours so that the originally scheduled post-exposure test plan could not be accomplished. However, one-half of each failed simulation specimen was salvaged for residual strength testing, and a revised test plan with considerably fewer tests was conducted. For the B/E and G/E systems the decision was made to halt testing after about 36,000 hours in order to have sufficient material for residual strength testing. Two of the B/E specimens had already failed (near 33,000 hours) and the likelihood of additional failures was high.

**12.7.2 PHASE I LONG-TERM TEST RESULTS.** Once started, the long-term tests were intended to continue uninterrupted 24 hours a day, seven days a week except for brief shutdowns to change the program tapes, retighten the B/Al doubler clamps, remove failed specimens, and provide equipment maintenance. Some unexpected problems did occur from time to time, however, and these often required extended amounts of downtime to correct. The monitoring and safety devices were also responsible for numerous shutdowns when test conditions tended to stray slightly from the allowable ranges. Any shutdown during nonworking hours could not be corrected until the next working day and could result in losses of one to 16 hours of exposure (up to 62 hours on a weekend) depending on the time of shutdown. If the tests were halted for 24 hours or more an additional four hours were lost because of the moisture bakeout of the

resin matrix specimens. At the completion of the short-term tests and at regular intervals during the long-term tests, the flight simulation apparatus was given an overhaul, which, as a minimum consisted of changing the piston rod seals in the hydraulic cylinders and replacing the quartz heat lamps. Any worn bearings or bushings in mechanical systems and any questionable electronic components were replaced as necessary.

The short-term test program was very successful in checking out the flight simulation apparatus, the suitability of the test specimen design, and the test procedures required to ensure long-time reliable operation during the long-term exposures. Many problems were uncovered and corrected. Some additional problems were encountered, however, after the long-term tests were begun. One problem that occurred with the compression stiffening grids affected only the long-term specimens. If the grids rotated slightly during testing, the attachment screws, see Figure 12-39, could bear against the specimen edges and in time could wear away a portion of the material, forming an edge notch. This could not occur with the short-term specimens because of the much narrower widths involved. Several long-term specimens were found where the grid screws had begun to bear against the edges, but, with the exception of one G/E specimen, the effects were very slight. The G/E specimen failed prior to 10,000 hours with the failure location near one of the end doublers away from the heated zone. There was some edge damage in the vicinity of the fracture site, and this damage was believed to have been the cause of failure. The problem of the screws bearing against the specimen edges was eliminated by adding aluminum strips between the edges of the specimens and the attachment screws, Figure 12-39. During the short-term testing a problem of abrasion of the soft B/Al specimens during fatigue cycling was identified. This was caused by the relative motion of the specimens and compression stiffeners and led to a form of fretting corrosion. In an attempt to reduce this abrasion, the B/Al compression stiffeners were covered with a stratified Teflon coating, a single coat, self-lubricating finish designed for relatively low temperature heat curing. During baking, a fluorocarbon-rich surface stratum is formed that provides the low friction properties. The technique helped to reduce the wearing of the surface, but at the completion of short-term testing the Teflon coating had worn away in several locations. It was also noted that the uncoated stiffener grids used on the short-term resin matrix specimens had also caused some abrasion of these specimens. Consequently, all the grids were modified for the long-term tests. However, because of the high cost of stratified Teflon, the grids were covered with an adhesive-backed fiberglass/Teflon tape. This reduced, but did not eliminate, the surface wearing problem. One other problem occurred with the unidirectional B/Al long-term specimens. From time to time specimens exhibited failures in the adhesive bonds between the B/Al and the titanium doublers. The adhesive, HT-424, which is quite porous, slowly oxidized and eventually failed under the much larger loads used for the unidirectional B/Al. No damage was done to the specimens, but testing time was lost while the specimens were removed and new end doublers were attached. This problem continued throughout the test program. The remainder of the problems were with the equipment and involved periodic failure or erratic behavior of mechanical, electronic, or hydraulic components as a result of the rather severe service requirements of the flight simulation apparatus.

Periodically during the 10,000 hours of exposure in Phase I, the test specimens were examined in the test apparatus for changes in appearance or damage as a result of the simulation cycles. During two of these examinations all of the compression stiffening grids were removed so that the specimens could be studied more closely and, where desired, photographs could be made. It was during the first of these examinations that the problem of the grid screws bearing against the specimen edges was found. Figure 12-40 shows the most severe example of this edge damage. This specimen, BC92-4, later failed at 9669 hours but not at the edge notches. At the

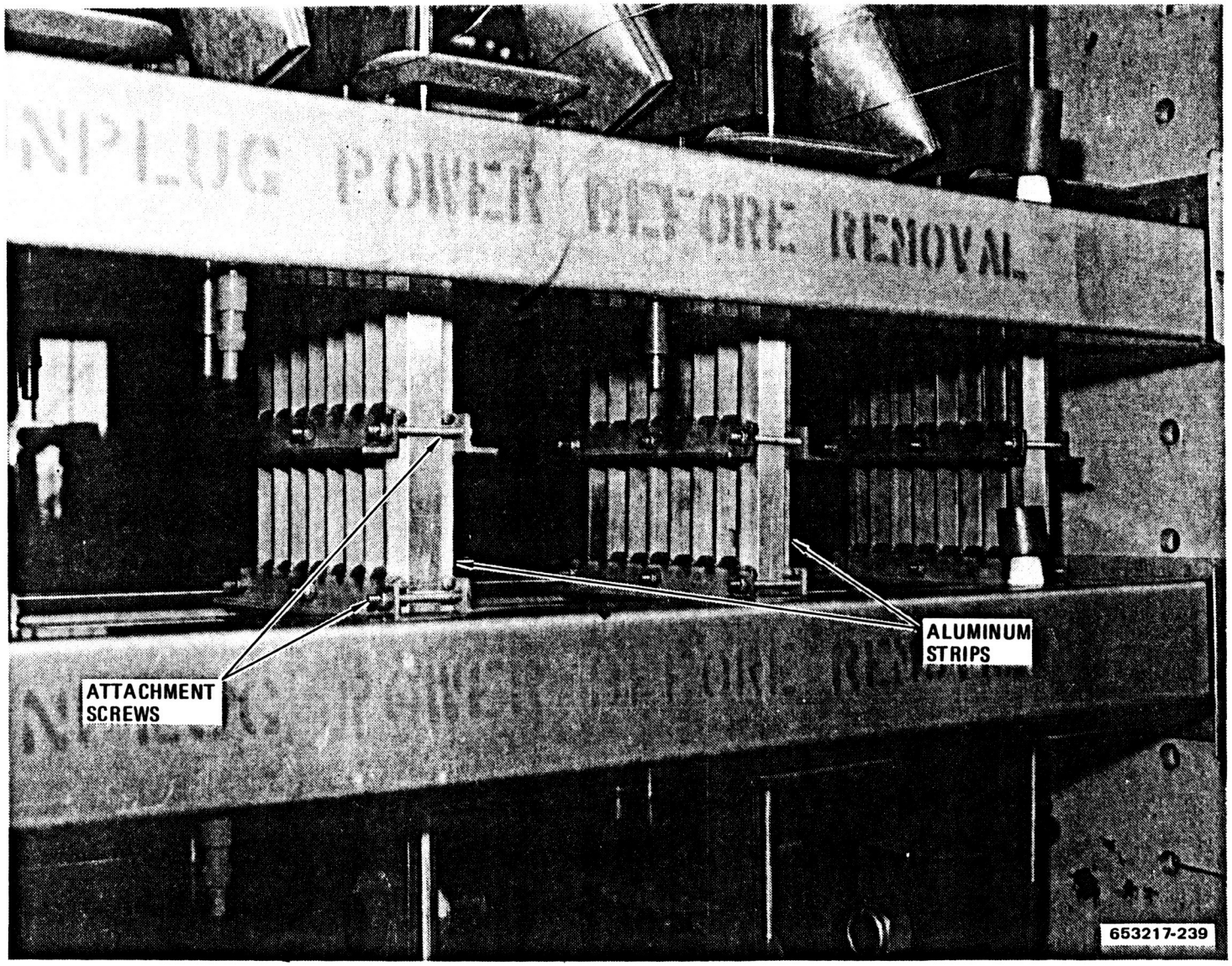



**Figure 12-39 Closeup-View of Flight Simulation Apparatus Showing Attachment Screws for Compression Stiffeners and Aluminum Protection Strips**



ORIGINAL PAGE IS
OF POOR QUALITY

ORIGINAL PAGE IS
OF POOR QUALITY

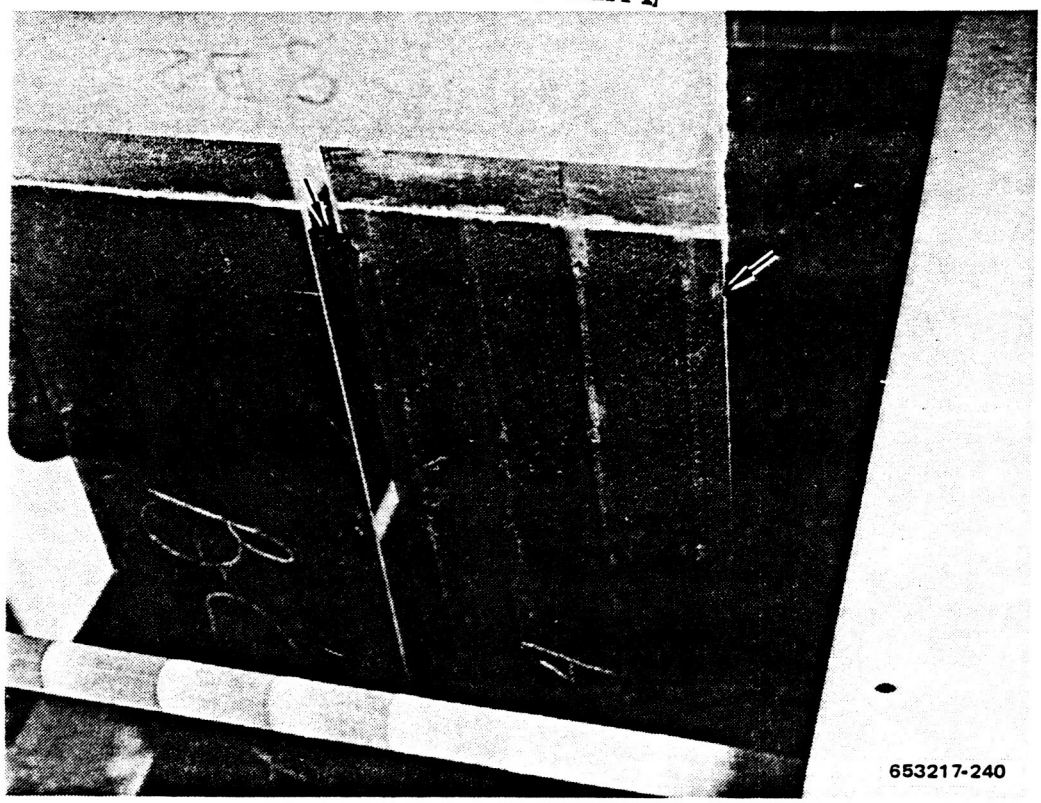



**Figure 12-40 G/E Long-Term Specimen BC92-4 Showing Edge Damage (arrows) from Compression Stiffener Screws**

time of the first examination, the two epoxy systems had accumulated approximately 4500 hours of exposure and the HT-S/170 G/PI and B/Al systems approximately 1700 hours. The results of the examination of the four composite systems were as follows:

a. B/E—The two heated zones on each specimen were discolored and on several of the unnotched specimens exposed and broken boron fibers were visible. Several specimens also had shallow edge notches from the stiffener grid screws.

b. G/E—Some slight discoloring of the heated zones was visible and several specimens were edge notched from the stiffener screws. At the time of this examination several of the unnotched specimens had already failed. The unfailed ones, however, appeared to be in good condition. None of the notched specimens had failed, but three of the 10 showed considerable damage in the form of cracks and delaminations at the edges and at the holes. Figure 12-41 shows the specimen with the most extensive damage (BF91-4). This specimen was removed because failure appeared imminent.

c. G/PI—After 1700 hours of exposure the only visible changes were very slight wear marks on the edges of one of the unnotched specimens.

d. B/Al—These specimen had also been exposed for only 1700 hours and were in good condition. Three specimens had slight edge notching from the stiffener screws and there was some surface abrasion from the stiffeners.

ORIGINAL PAGE IS
OF POOR QUALITY

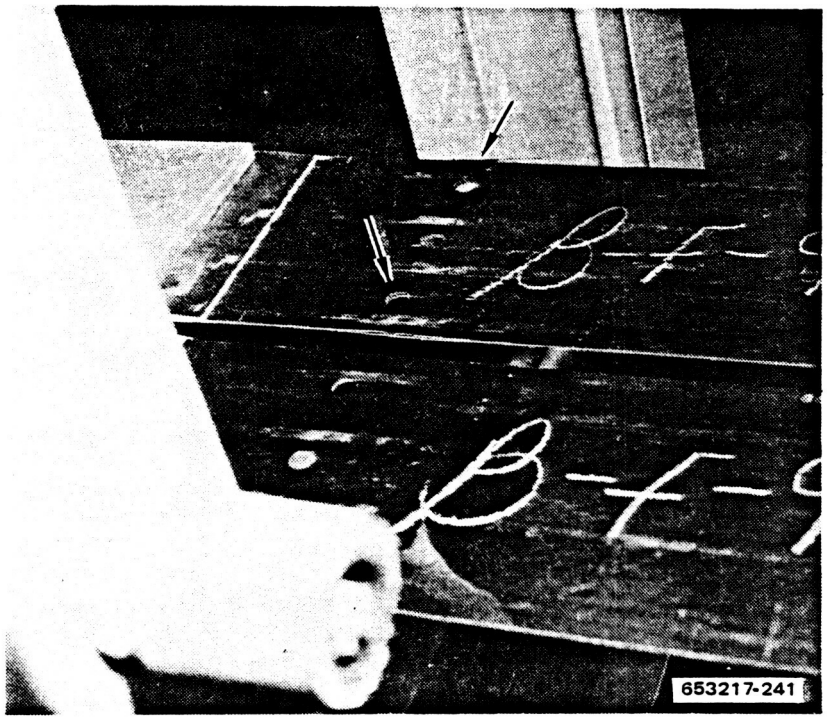



**Figure 12-41 G/E Long-Term Specimen BF91-4 Showing Cracks and Delaminations (arrows) at Edges and Holes**

The next thorough examination was made just before the completion of 10,000 hours on the epoxy specimens (approximately 9000 hours for the epoxies and 6000 for the HT-S/710 G/PI and B/Al specimens). The results of the examination of the four composite systems was as follows:

a. B/E—These specimens showed the most damage as a result of the flight simulation exposures even though, in contrast to the G/E system, none had failed. The two heated zones on each specimen were discolored and in several instances showed exposed and broken fibers where portions of the epoxy resin had fallen away. In the notched B/E specimens some longitudinal surface cracks tangent to the holes were observed.

b. G/E—At the time of this examination 11 of the 20 G/E specimens had failed or had been removed from the exposure apparatus because of showing significant damage. Of the remaining specimens the only visible effects were color changes in the heated zones at the top and bottom of each specimen and some small longitudinal cracks tangent to the holes in the notched specimens. These cracks were believed to extend only through the outer 0° ply in both the B/E and G/E specimens.

c. G/PI—These specimens appeared to be in excellent condition with only slight color changes in the heated zones.

d. B/Al—The only visible effects were longitudinal stripes on the surface where some of the Teflon tape from the stiffening grids had adhered.

Figures 12-42 through 12-45 are photographs of typical specimens of each composite material that were made during this examination with the specimens installed in the flight simulation apparatus. Only the B/E specimens, Figure 12-42, show any visible damage.

ORIGINAL PAGE IS
OF POOR QUALITY

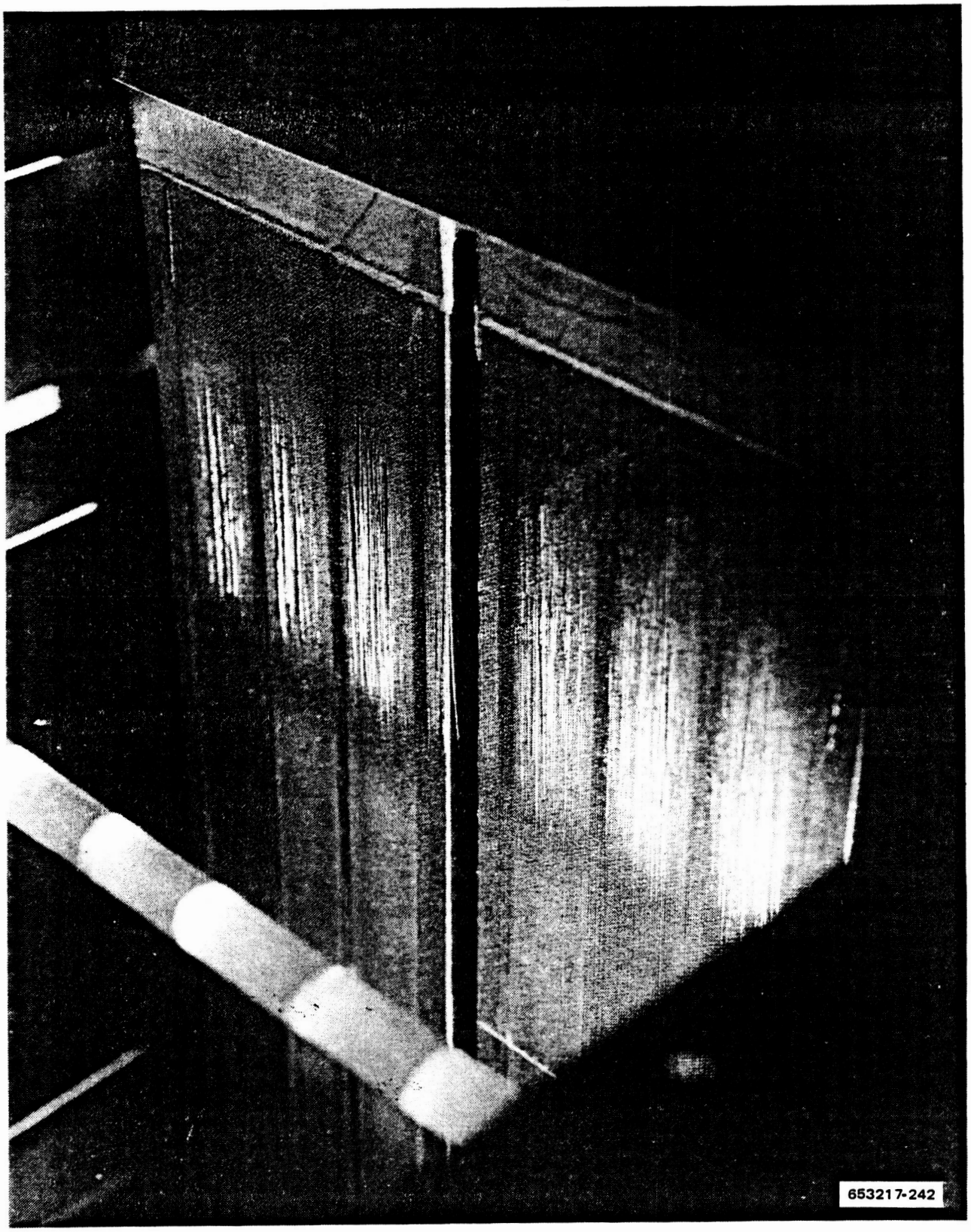



**Figure 12-42 B/E Long-Term Specimens After Approximately 9000-hr of Exposure Showing Broken and Exposed Boron Fibers**

C-6

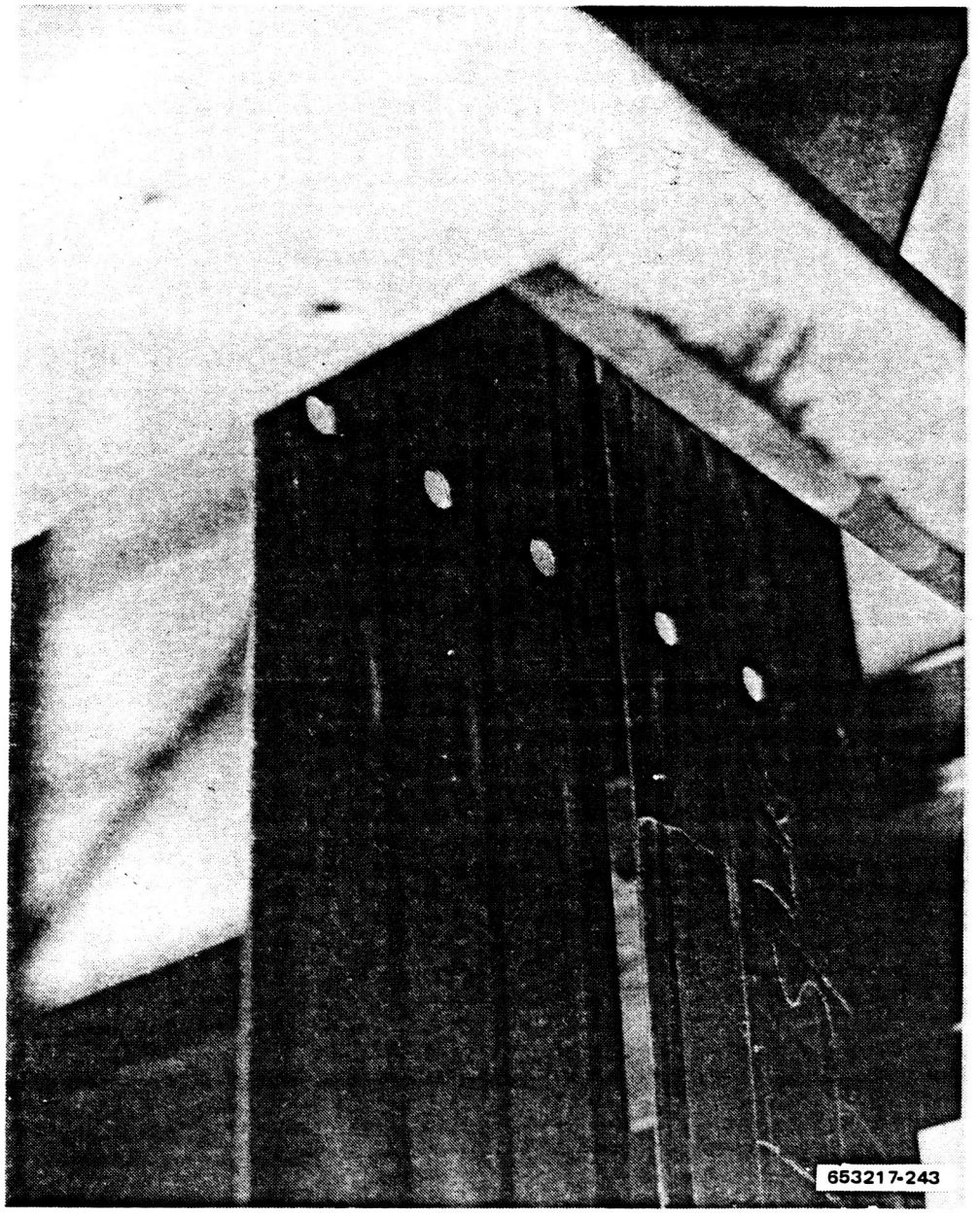



**Figure 12-43 G/E Long-Term Specimens After Approximately 9000-hr of Exposure**

ORIGINAL PAGE IS
OF POOR QUALITY

ORIGINAL PAGE IS
OF POOR QUALITY

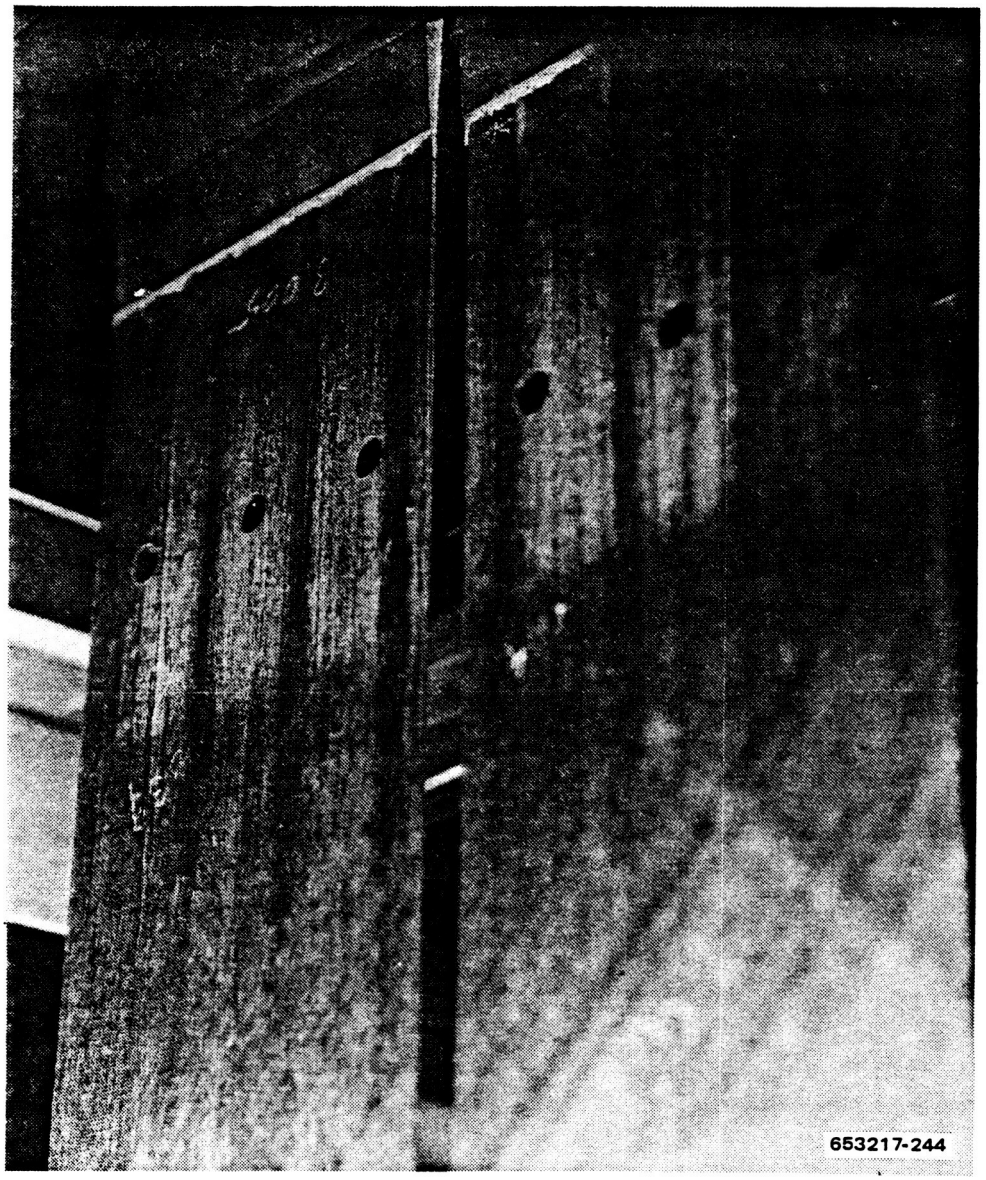



**Figure 12-44 G/PI Long-Term Specimens After Approximately 6000-hr of Exposure**

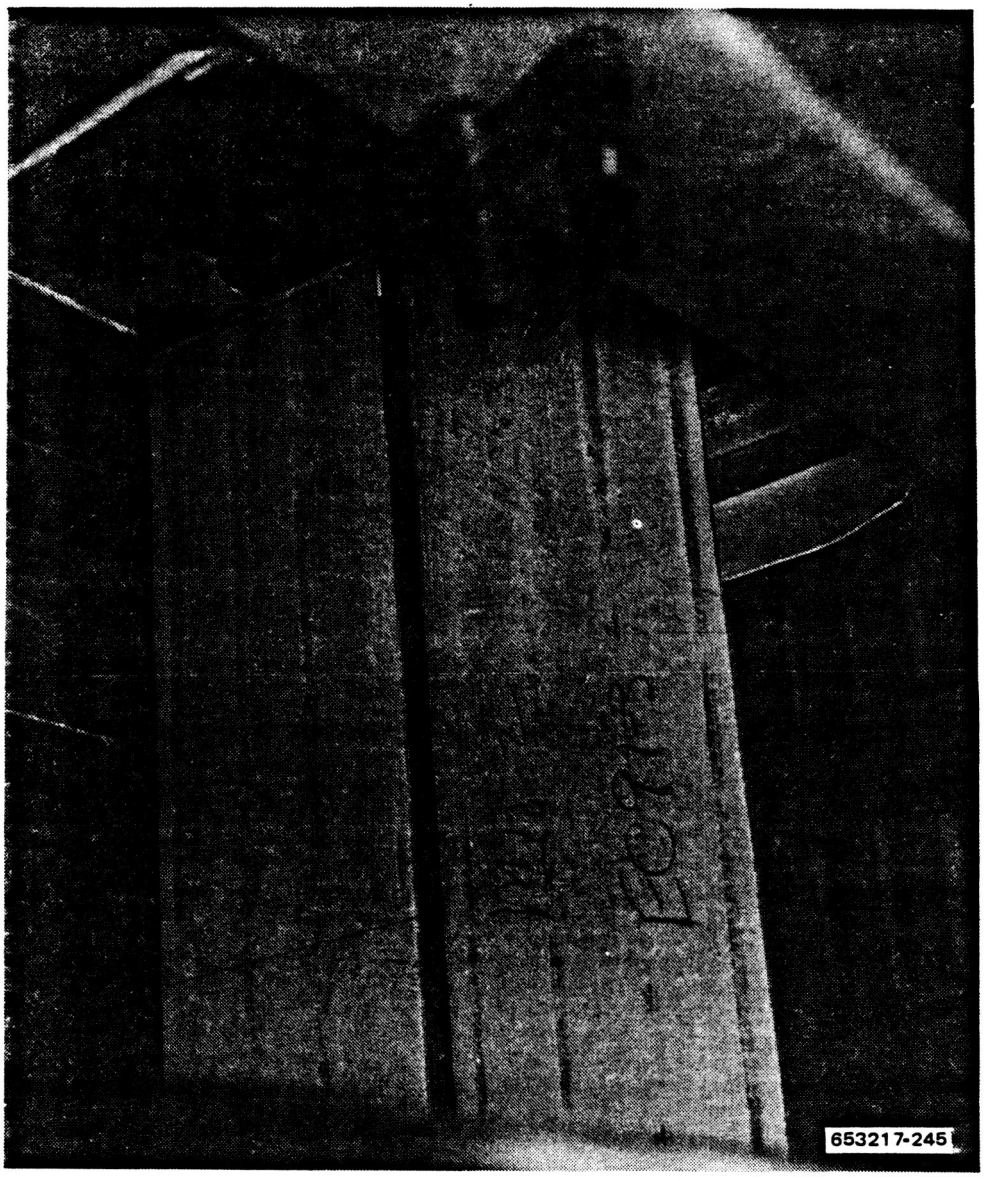



**Figure 12-45 B/Al Long-Term Specimens After Approximately 6000-hr of Exposure**

ORIGINAL PAGE IS
OF POOR QUALITY

In setting the load levels for the long-term flight simulation tests, the expectation was for 80% of the specimens of each system to complete 50,000 hours of exposure. The 20% failure rate would amount to, on average, four specimens for each composite material system. In general, these failures would be expected to occur during Phase II of the test program. For the G/E system a much higher failure rate was observed. Twelve of the 20 G/E specimens either failed outright or were removed from test because of severe damage. Some of the badly damaged specimens were removed for further inspection and because of the likelihood of imminent failure were not returned. The others were in such poor condition that when a specimen in the same setup failed the damaged one was also removed to decrease the amount of equipment downtime. Table 12-21 lists the G/E specimens that did not survive the 10,000 hours of flight simulation and also shows the amount of exposure time logged when removed because of failure or significant degradation.

**Table 12-21. G/E Long-Term Specimens Removed Because of Failure or Significant Degradation**

| Specimen No. | Type | Exposure (hr) | Failure or Damage Location |
|---|---|---|---|
| BC91-1 | Unnotched | 4515 | Heated zone; failed |
| BC91-2 | Unnotched | 6683 | Heated zone; not failed |
| BC91-3 | Unnotched | 6683 | Heated zone; failed |
| BC91-4 | Unnotched | 4524 | Heated zone; not failed |
| BC91-5 | Unnotched | 2696 | Heated zone; failed |
| BC92-3 | Unnotched | 4053 | Heated zone; failed |
| BC92-4 | Unnotched | 9669 | Heated zone; failed |
| BC92-5 | Unnotched | 4524 | Near doubler; failed |
| BF91-2 | Notched | 7520 | Heated zone; failed |
| BF91-3 | Notched | 7520 | Heated zone; not failed |
| BF91-4 | Notched | 4549 | Heated zone; not failed |
| BF91-5 | Notched | 4549 | Heated zone; not failed |

All of the specimens except one failed in either the upper or lower heated zones. The specimens, which are 0.46 m (18 in.) long, are heated in two zones that are 0.11 m (4.5 in.) on either side of the centerline. Figure 12-46 shows three of the specimens, all of which failed in one of the heated sections. The two specimens with over 4000 hours of exposure also showed considerable damage in the heated zones opposite the failures in the form of edge delaminations. This can be seen in Figure 12-47. The 2669-hour specimen, BC91-5, did not show delamination in the unfailed heated zone. Another difference between the 2669-hour specimen and the two 4000-hour specimens of Figure 12-46 is the appearance of the fracture. The 2669-hour specimen has failed in a manner similar to the unexposed baseline specimens with little loss of the epoxy resin from around the graphite tows. After 4000 hours of exposure, however, the epoxy resin

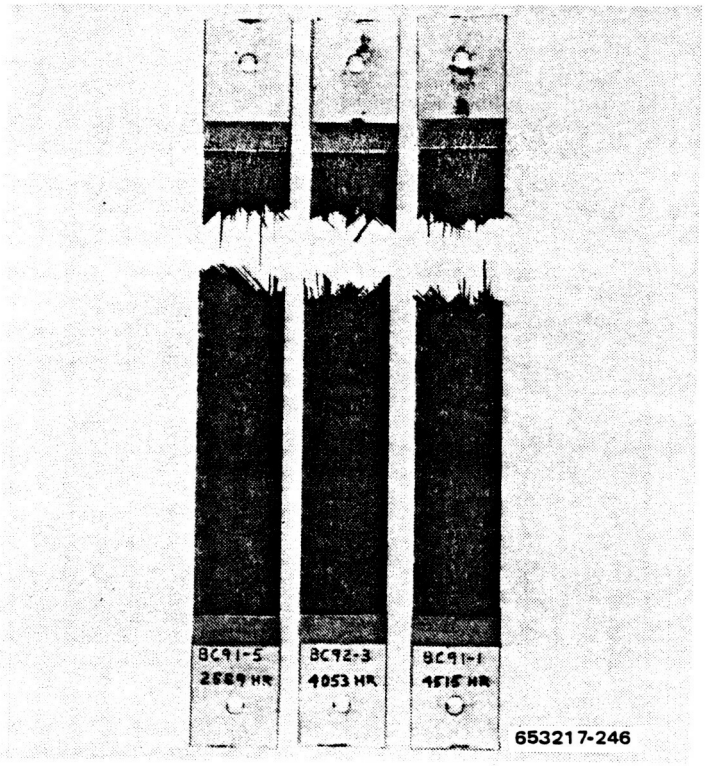



**Figure 12-46 G/E Long-Term Specimens That Failed During Flight Simulation Testing Before Completion of 10,000-hr of Exposure**

ORIGINAL PAGE IS
OF POOR QUALITY

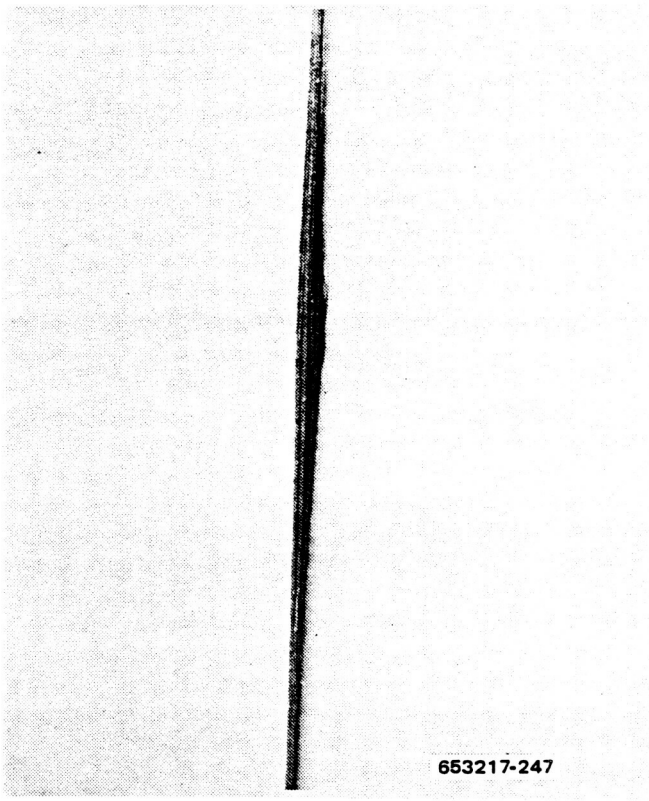



**Figure 12-47 G/E Long-Term Specimen BC92-3 Showing Edge Delaminations in Heated Zone. (Specimen had failed at opposite heated zone after 4053-hr of exposure)**

ORIGINAL PAGE IS
OF POOR QUALITY

matrix has begun to crumble during failure leaving many bare graphite tows. Similar effects were observed during tensile testing of the 450 K (350 ° F) thermal age specimens after 5000 or more hours of exposure. Closeup views of the two different fracture appearances are shown in Figure 12-48 and Figure 12-49. The failure mechanism that was responsible for these early failures of the G/E specimens appeared to be a combination of several factors. Based on earlier thermal aging data the time at temperature, 4000 hours at 408 K (275 ° F), itself, is not sufficient to explain the brittle nature of the epoxy matrix. Added to this, however, are the effects of the thermal expansion stress during the 2000 thermal cycles and the tensile and compressive loads. As the matrix becomes embrittled as a result of oxidation the thermal and mechanical stresses act to produce microcracking and eventual loss of the outer epoxy layer. This can lead to accelerated oxidation as the filaments in the outer layers fail, thereby exposing the underlying resin to the oxidizing environment. The compressive load which occurs once per flight cycle is also important because of the lowered compressive resistance of the graphite tows as the matrix is degrading. It is these compressive loads that are responsible for the numerous delaminations observed in the heated zones of many of the specimens. A good example of a specimen that was about to fail by this mechanism is shown on the right in Figure 12-50. The edge view of the same specimen, Figure 12-51, shows clearly the loss of matrix on both surfaces with the exposed and broken graphite filaments and the extensive delamination caused by the compressive loading. This specimen would undoubtedly have failed very soon if it had not been removed from test.

The specimen on the left in Figure 12-50 was the only G/E specimen that did not fail in the heated zone. A closeup view of the fracture is shown in Figure 12-52. The arrows in the figure

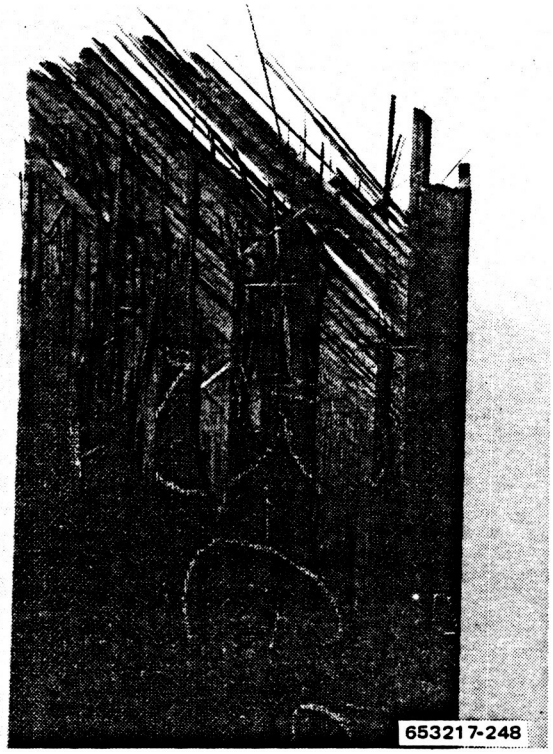
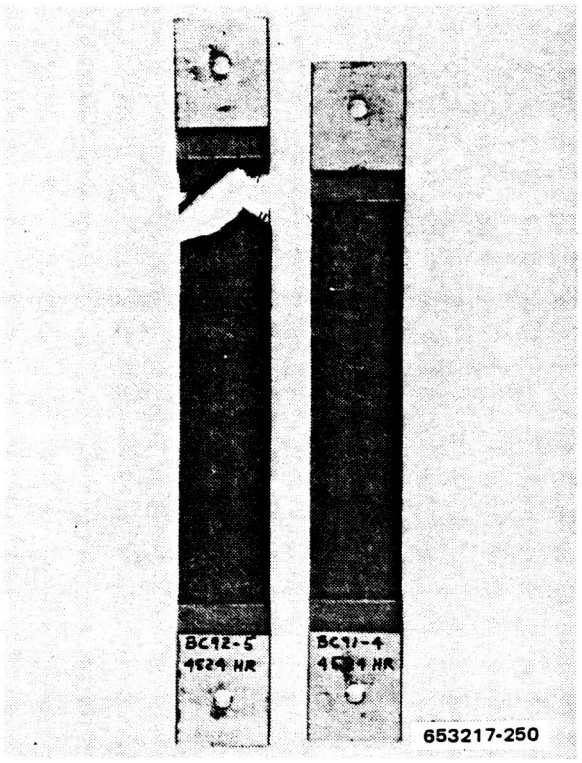



**Figure 12-48 G/E Long-Term Specimen BC91-5 Showing Fracture Appearance After Failure in 2669 hr. (No significant loss of resin from around the graphite tows has occurred)**




**Figure 12-49 G/E Long-Term Specimen BC91-1 Showing Fracture Appearance After Failure in 4515 hr. (Loss of resin from around graphite tows is readily apparent)**




ORIGINAL PAGE IS
OF POOR QUALITY

**Figure 12-50 G/E Long-Term Specimens That were Removed from Test Before Completion of 10,000 hr of Exposure**

ORIGINAL PAGE IS
OF POOR QUALITY

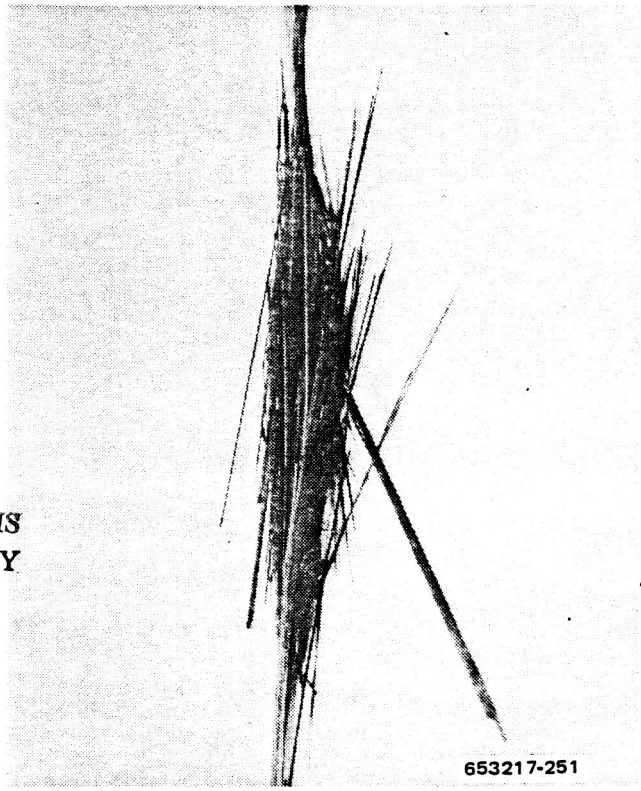



**Figure 12-51 Edge View of G/E Long-Term Specimen BC91-4 Showing Exposed and Broken Graphite Filaments and Extensive Delamination. (Specimen was removed from test after 4524-hr)**

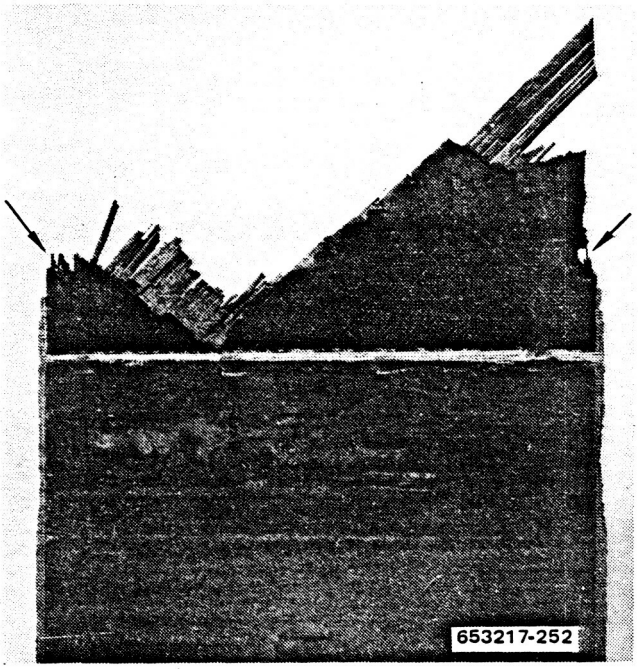



**Figure 12-52 G/E Long-Term Specimen BC92-5 Showing Fracture Appearance After Failure in 4524-hr (Failure was probably the result of edge notches (at locations shown) caused by rotation of the compression stiffener grids)**

point to locations where stiffener grid screws could bear against the specimen edges if the grids rotated slightly. It appears likely that it was edge notches of this type that caused the early failure of specimen BC92-5. The fracture location and appearance were also quite different from the other failures.

One other specimen failure occured during the long-term testing prior to completion of 10,000 hours. This was unidirectional B/Al specimen EU91-1 which failed out of the heated zone after 2454 hours. The specimen, shown in Figure 12-53, apparently failed because of a misaligned bearing in one branch of the whiffletree used to apply the fatigue loads. This caused the compressive loads to be misaligned with the axis of the specimen and resulted in the stiffening grid being pushed into the specimen at one end. Figure 12-54, a closeup of the fracture, shows where the four bearing surfaces of the stiffener were forced into the B/Al at the edge of the end doubler and initiated the failure.

None of the B/E or G/PI long-term specimens failed during the 10,000 hours of flight simulation exposure in Phase I.

At the completion of 10,000 hours of flight simulation exposure the Phase I long-term specimens were removed from the test apparatus. In addition, because of the high failure rate of the G/E and the extensive surface damage visible on the B/E, all remaining Phase II epoxy specimens were also removed. The revised flight simulation test plan for the B/E and G/E systems was described in Section 12.7.1. The specimens were examined visually with the aid of a stereo microscope and photographed. Based on the number and condition of the specimens

ORIGINAL PAGE IS
OF POOR QUALITY

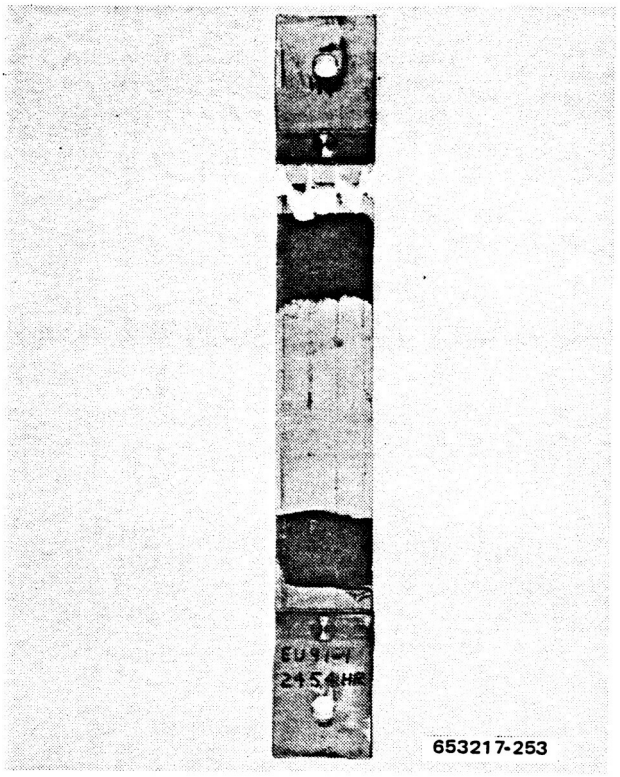



**Figure 12-53 B/Al Long-Term Specimen That Failed During Flight Simulation Testing Before Completion of 10,000 hr of Exposure**

ORIGINAL PAGE IS
OF POOR QUALITY

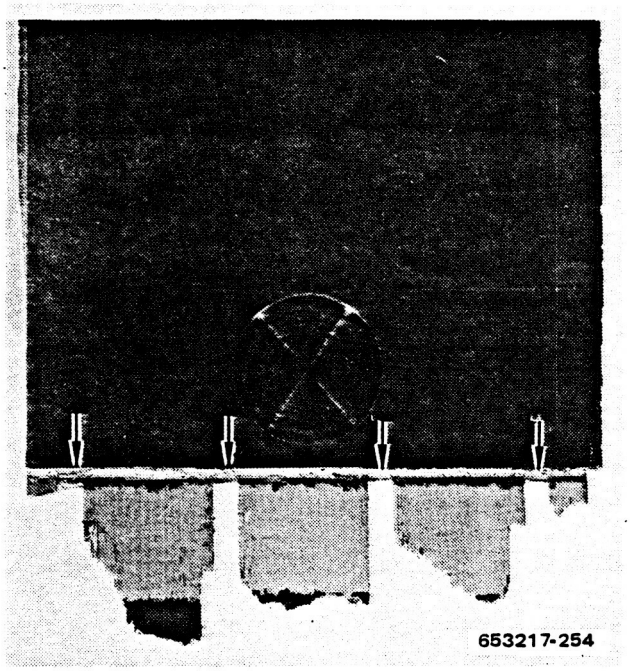



**Figure 12-54 B/Al Long-Term Specimen EU91-1 Showing Fracture Appearance After Failure in 2454 hr. (Failure was initiated at locations (arrows) where stiffener grid was forced into the B/Al)**

and information gained during the overall test program, a residual strength testing plan was prepared. As will be discussed later, the test plan was somewhat different from the one originally scheduled. Cutting plans were prepared and the long-term specimens were machined into residual strength specimens, which were then tested. The results of the specimen examinations and residual strength tests are presented in the following sections.

### 12.7.2.1 Post Simulation Examinations — Phase I

**B/E, $[0° \pm 45°]_s$, unnotched and notched.** All of the B/E specimens survived 10,000 hours of flight simulation exposure without fracture at temperatures to 408K (275 °F). The specimens did, however, experience considerable surface damage in the heated areas. The outer portions of the epoxy matrix had crumbled away in numerous places revealing the boron fibers, many of which had failed. In contrast to the G/E specimens no edge delaminations were observed at either the outside edges or at the holes in the notched specimens. Photographs showing both sides of three unnotched and three notched specimens are presented in Figures 12-55 to 12-58. The B/E laminates have a glass scrim cloth as the outer layer on one side. This side shows distinct color changes (to a light brown) in the heated zones. On the other side the epoxy resin has darkened somewhat, particularly in the heated zones. The effect of shielding of the surface by the compression stiffening grids is very evident. A few loosened and broken boron fibers are visible in Figure 12-55 and 12-57, the non scrim-cloth sides. A better view of these exposed boron fibers is shown in Figure 12-59 for an unnotched specimen and in Figure 12-60 for a notched specimen. These regions where the matrix has broken away at the surface and exposed the fibers were observed only in the heated zones in the areas not covered by the stiffening grids. Exposed fibers were also found in the heated areas on the scrim-cloth side of the B/E specimens, but these were generally hidden under the glass cloth. Figure 12-61 shows a closeup

ORIGINAL PAGE IS
OF POOR QUALITY

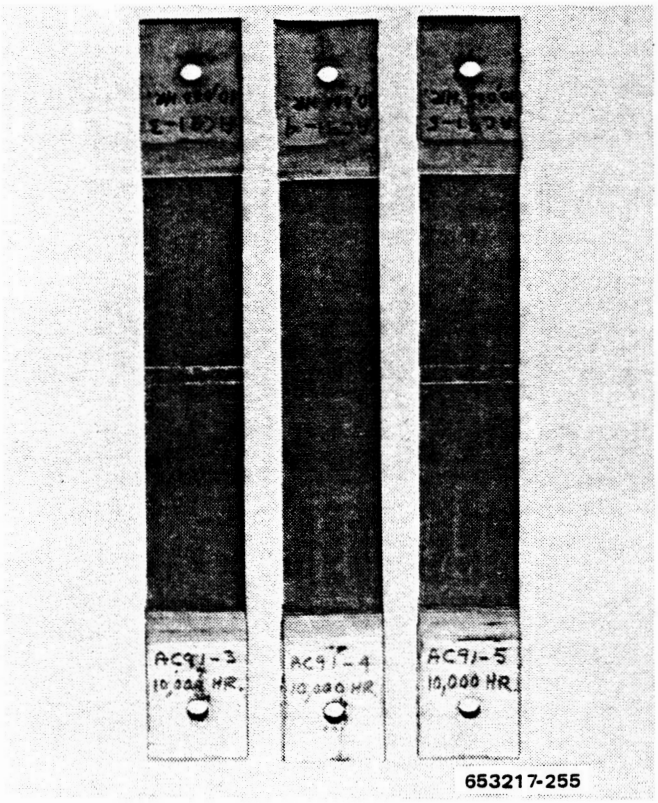



**Figure 12-55 B/E Long-Term Specimens After 10,000 hr of Flight Simulation Exposure**




**Figure 12-56 B/E Long-Term Specimens After 10,000-hr of Flight Simulation Exposure (Glass scrim cloth side)**

ORIGINAL PAGE IS
OF POOR QUALITY

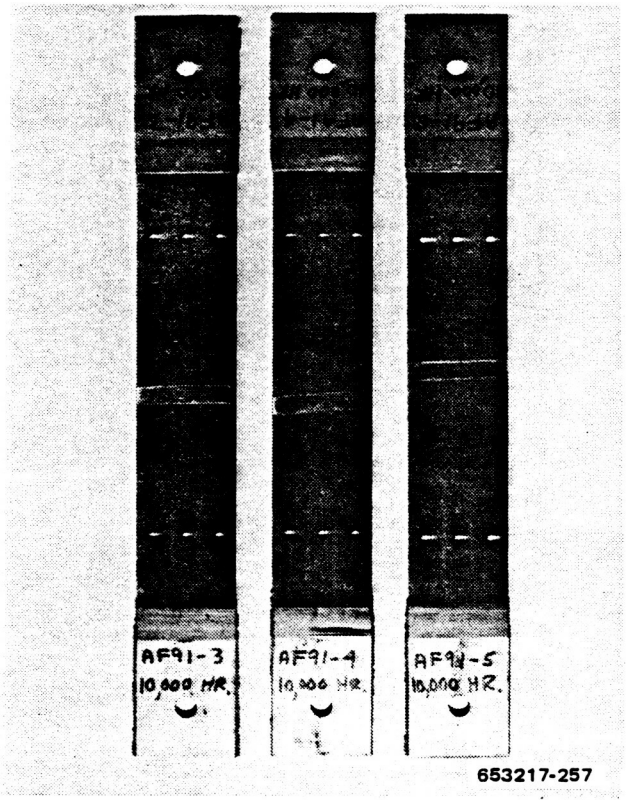



**Figure 12-57 B/E Notched Long-Term Specimens After 10,000-hr of Flight Simulation Exposure**

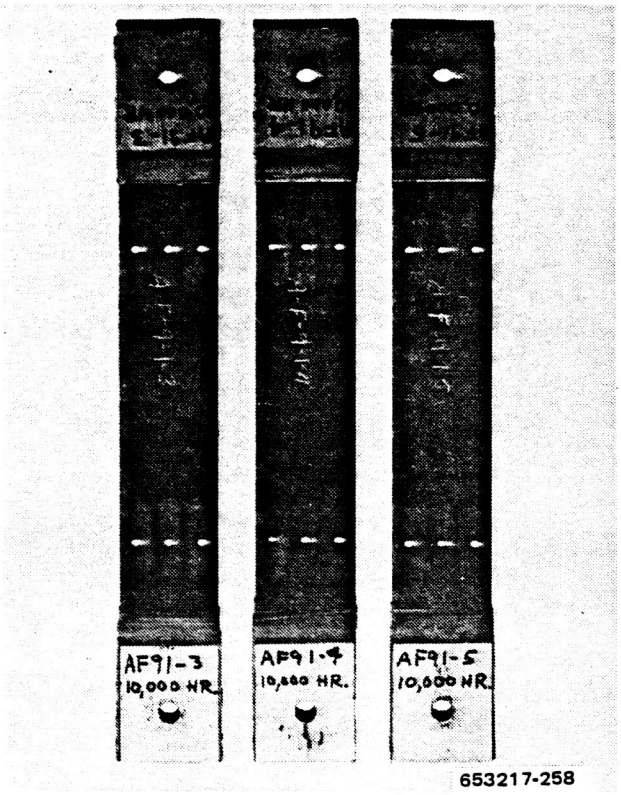



**Figure 12-58 B/E Notched Long-Term Specimens After 10,000-hr of Flight Simulation Exposure (Glass scrim cloth side)**

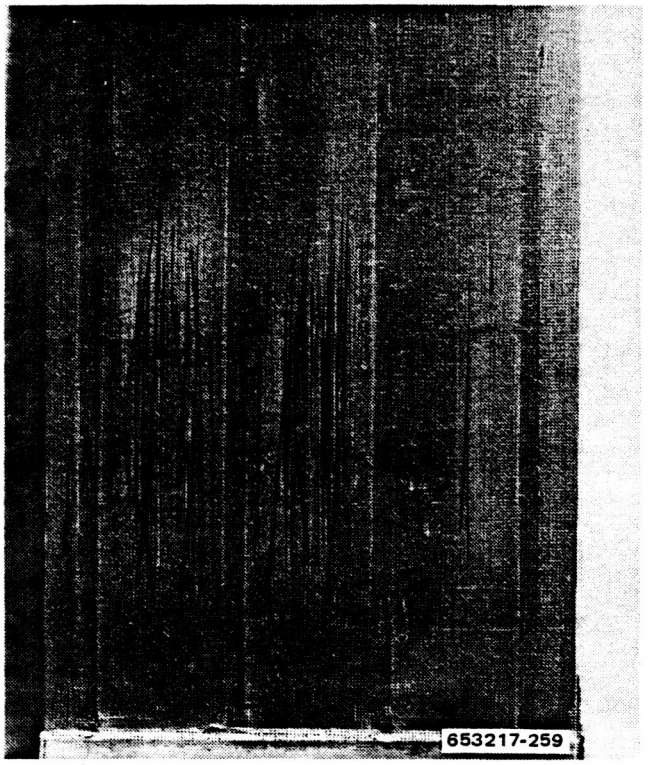



**Figure 12-59 B/E Long-Term Specimen AC91-5 After 10,000-hr of Flight Simulation Exposure Showing Loosened and Broken Boron Fibers**

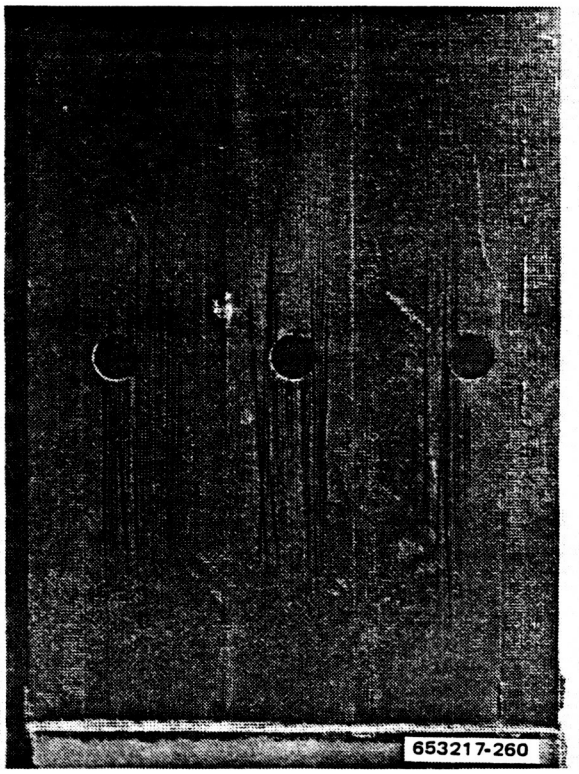


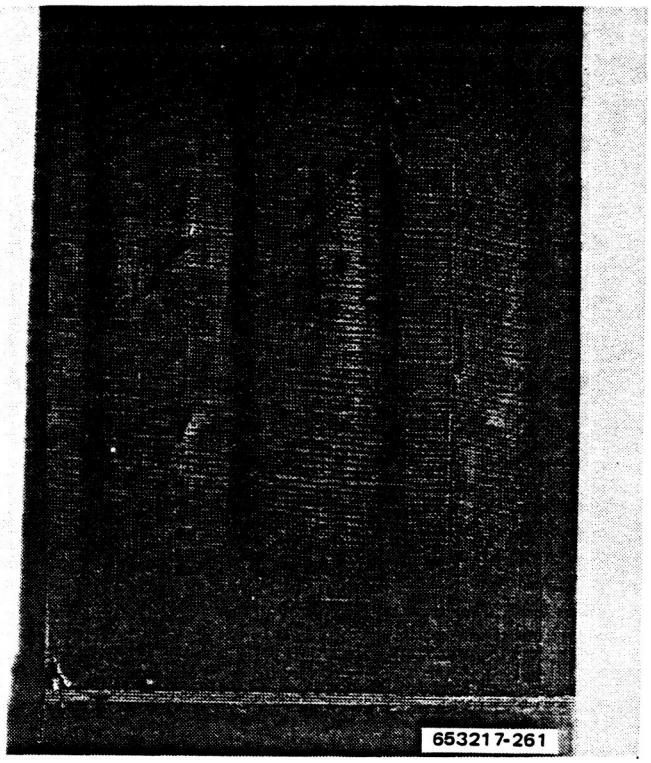

**Figure 12-60 B/E Notched Long-Term Specimen AF91-5 After 10,000 hr of Flight Simulation Exposure Showing Loosened and Broken Boron Fibers**

ORIGINAL PAGE IS
OF POOR QUALITY

view of the heated zone on the scrim-cloth side. The disturbed areas of the glass cloth are caused by loosened and broken boron fibers beneath the cloth.

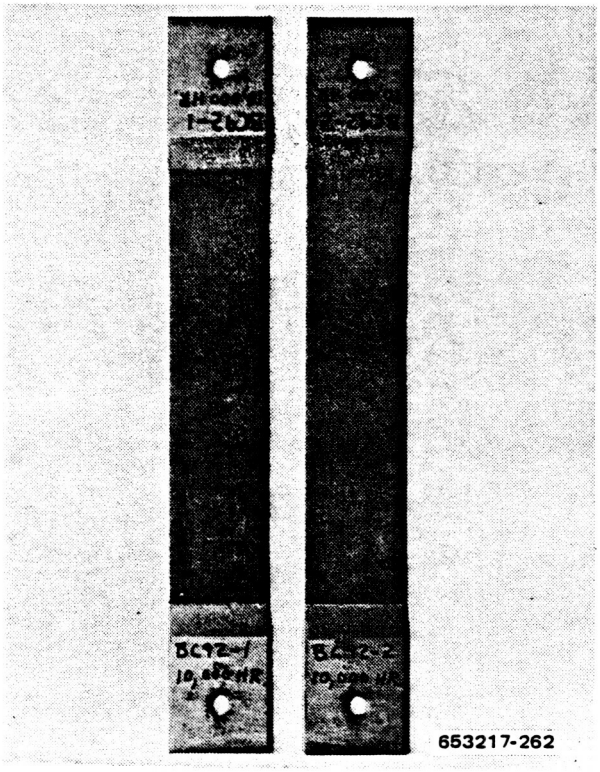
**G/E, $[0° \pm 45°]_s$, unnotched and notched.** Only two unnotched and six notched G/E specimens from the original 20 Phase I and Phase II specimens survived the 10,000 hours of exposure at maximum temperatures of 408K (275 °F). The two unnotched specimens are shown in Figure 12-62 and 12-63. Unlike the failed specimens these appeared to be in reasonably good condition. No surface or edge cracks or delaminations were found. The heated zones had undergone some color changes, particularly between the stiffening grids. These areas had a worn or eroded looking appearance and, in several places, the graphite tows were very close to being exposed as a result of the loss of the epoxy matrix on the outer surface. The notched specimens that survived the 10,000 hours of flight simulation exposure were similar in appearance to the unnotched specimens except for some damage at the holes. Four of the specimens had longitudinal cracks near the holes and some delaminations at the edges of the holes. Two of the notched specimens that completed 10,000 hours are shown in Figure 12-64 and 12-65. Specimen BF92-3 is one with cracks at the holes but they are not readily visible in this photograph. The material on the surface of the specimens at one end is residue of the adhesive used to attach the thermocouples.

One of the specimens that appeared to be in good condition during the second inspection with the grids removed (9404 hours of exposure) is shown in Figure 12-66. Compressive failure in one of the heated zones occurred soon after the inspection, 9669 hours. No evidence of the impending failure was seen during the examination after 9404 hours. A higher magnification view of this specimen and two others that were removed from test prior to 10,000 hours




ORIGINAL PAGE IS
OF POOR QUALITY

**Figure 12-61 B/E Long-Term Specimen AC91-4 After 10,000 hr of Flight Simulation Exposure. (Glass scrim cloth side. The disturbed areas of the glass cloth are caused by loosened and broken boron fibers below the cloth)**




ORIGINAL PAGE IS
OF POOR QUALITY

**Figure 12-62 G/E Long-Term Specimens After 10,000 hr of Flight Simulation Exposure**

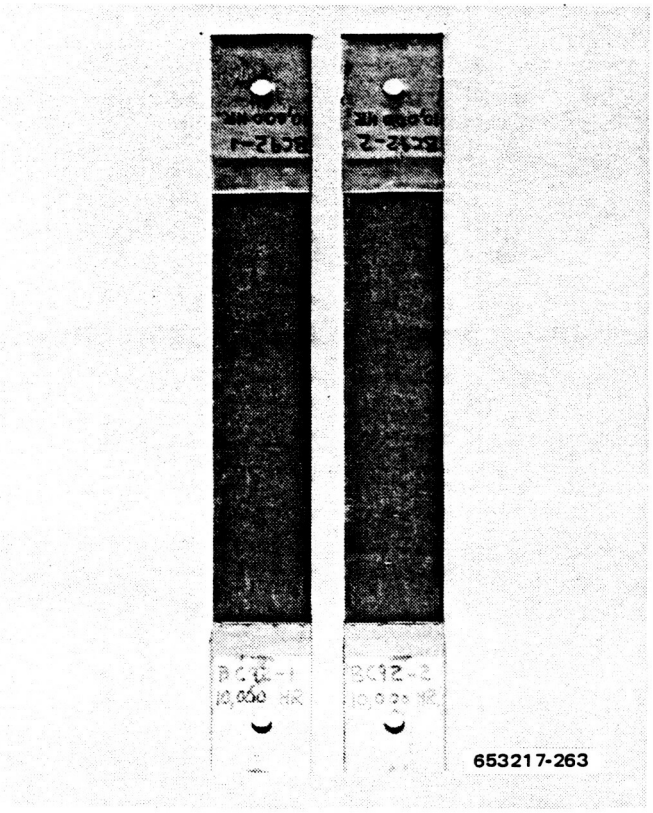



**Figure 12-63 G/E Long-Term Specimens After 10,000 hr of Flight Simulation Exposure (Opposite sides of specimens in Figure 12-62)**

ORIGINAL PAGE IS
OF POOR QUALITY

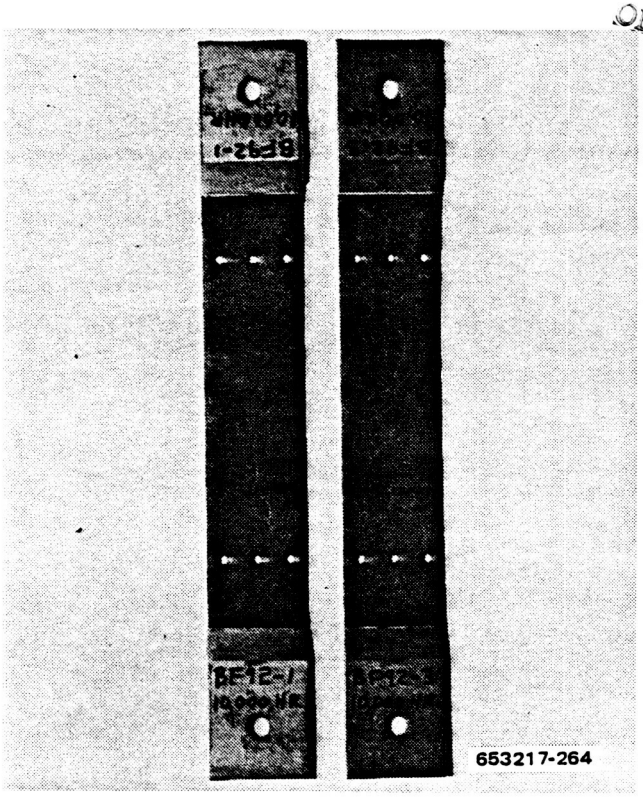



**Figure 12-64 G/E Notched Long-Term Specimens After 10,000 hr of Flight Simulation Exposure**

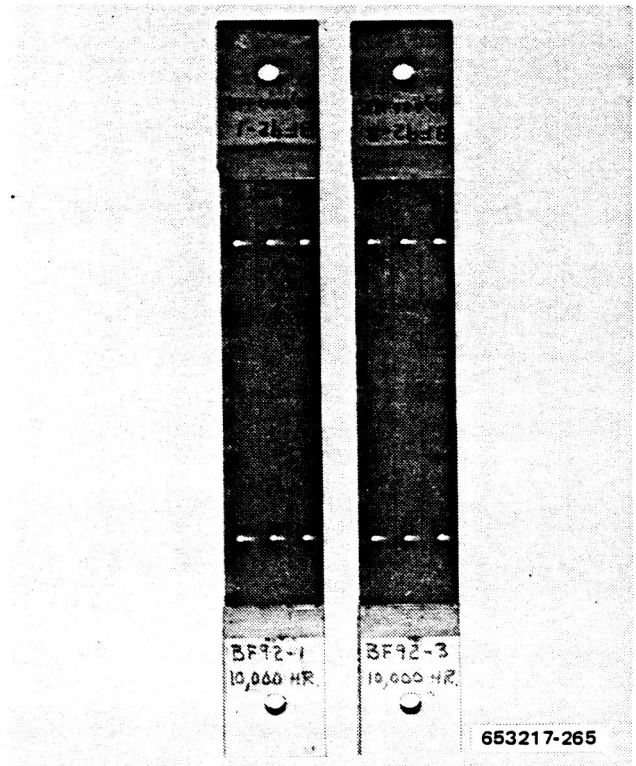



**Figure 12-65 G/E Notched Long-Term Specimens After 10,000 hr of Flight Simulation Exposure (Opposite sides of specimens in Figure 12-64)**

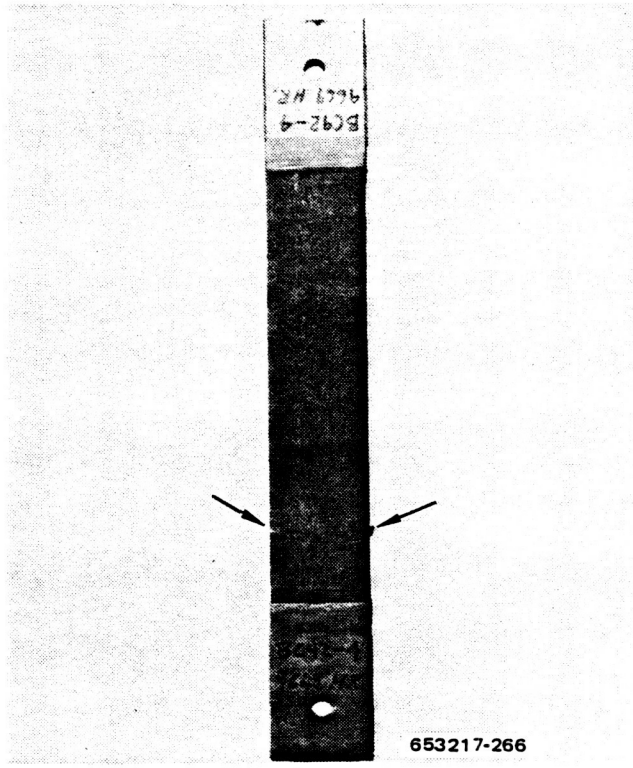



**Figure 12-66 G/E Long-Term Specimen BC92-4 After 9669 hr of Flight Simulation Exposure. (Specimen failed (arrows) in compression at heated zone)**

because of severe damage is shown in Figure 12-67. The damage level in these specimens increases from left to right in the photograph. Inspection of the specimens suggests a failure mechanism slightly different from that proposed early in the test program and described in Section 12.7.2. In these specimens and also those in Figure 12-68, initial failure is thought to occur by delamination of the outer [0°] plies in the heated zones between the stiffening grids. The combination of thermal cycling stresses and the mechanical fatigue stresses acting at the ply interface overcomes the relatively low interlaminar strength, and delamination occurs. The outer plies retain their strength during the tensile loads, but during the one compressive load per cycle all the load is carried by the low strength $\pm 45°$ plies. At this point two effects occur. The $\pm 45°$ plies begin to fail from the tensile and compressive fatigue loads, and oxidation with accompanying breaking up of the matrix of the outer plies is accelerated. The first specimen in Figure 12-67, BC91-2, was removed from test shortly after delamination of the outer plies occurred in the regions between the grids. Some damage to the inner $\pm 45°$ plies was visible but the amount was small. The specimen still maintained its rigidity. In the regions that were beneath the 0.00318 m (0.125 in.) wide grids, transverse cracks can be seen. The second specimen, BC92-4, had sustained an increased amount of damage before being removed from test. Delamination and transverse cracking of the outer plies was much more extensive and the inner $\pm 45°$ plies were badly broken. The specimen was no longer rigid and could easily be bent at the damaged heated zone. Some bare graphite fibers were also visible at the edges of the cracks and delaminations. These fibers were typical of those found in badly oxidized thermal aging test specimens, i.e., rather fuzzy appearing with no resin adhering to them. The final specimen in Figure 12-67, BC91-4, shows the greatest degree of degradation of the three. In addition to delamination of the outer plies and considerable inner ply damage, the surface has



ORIGINAL PAGE IS
OF POOR QUALITY

ORIGINAL PAGE IS
OF POOR QUALITY

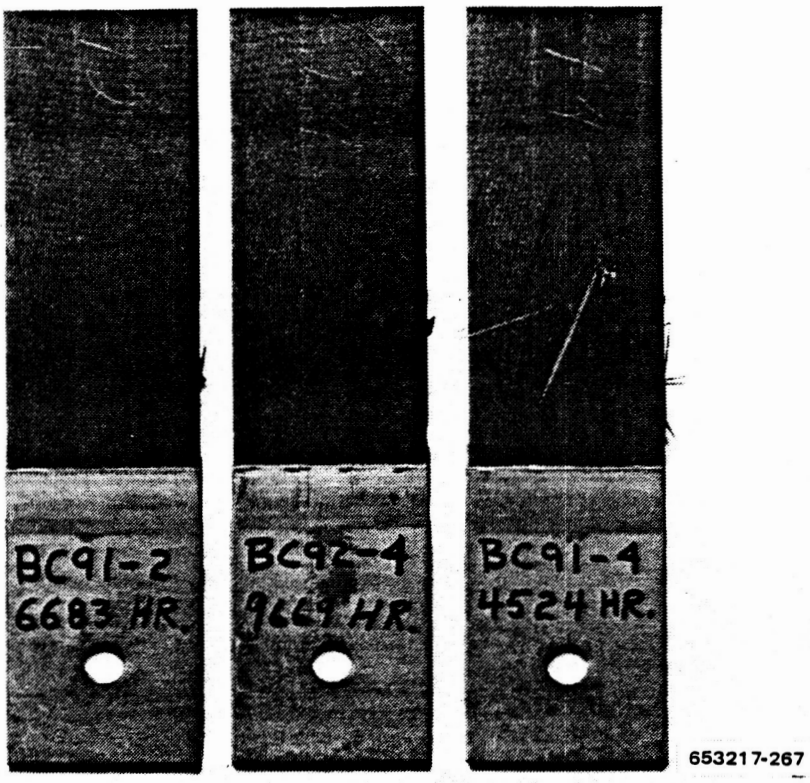



**Figure 12-67 G/E Long-Term Specimens that were Removed from Test Before Completion of 10,000 hr of Exposure. (Increasing levels of damage in the specimens are visible in moving from left to right)**

also experienced a great deal of tensile failure of the graphite fibers. Much of the epoxy resin matrix from the outer plies has oxidized and crumbled away, leaving bare graphite fibers exposed. This specimen had the least rigidity of the three. For these three specimens total time of flight simulation exposure was apparently not a factor in the onset of initial failure.

A similar set of the notched specimens showing varying degrees of damage is pictured in Figure 12-68. The first, BF91-5, shows the onset of delamination of the outer 0° plies, some longitudinal cracking near the holes, and some slight damage to the inner [±45°] plies. The degree of delamination varies from one side of the specimen to the other. This can be seen from the closeup photographs of Figure 12-69. Severe delamination has occurred at one edge, a lesser amount in the center as shown at the three holes, and none at all at the opposite edge. The second specimen, BF91-4, had delaminated throughout the heated zone and shows increased longitudinal cracking and the onset of transverse cracking in the regions under the stiffening grids. The ridigity or resistance to bending at the heated zone has decreased somewhat. The third specimen, BF91-3, is very close to fracture with severe cracking of all the plies. The epoxy surface is heavily oxidized with many graphite fibers exposed. The specimen has almost no bending resistance across the notched region. The final specimen of the set, BF91-2, has fractured with considerable damage throughout the heated zone. In like manner to the 5000-and 10,000-hour 450 K (350° F) thermal aging specimens, many of the graphite fibers are visible as a result of the loss of the brittle oxidized epoxy resin.

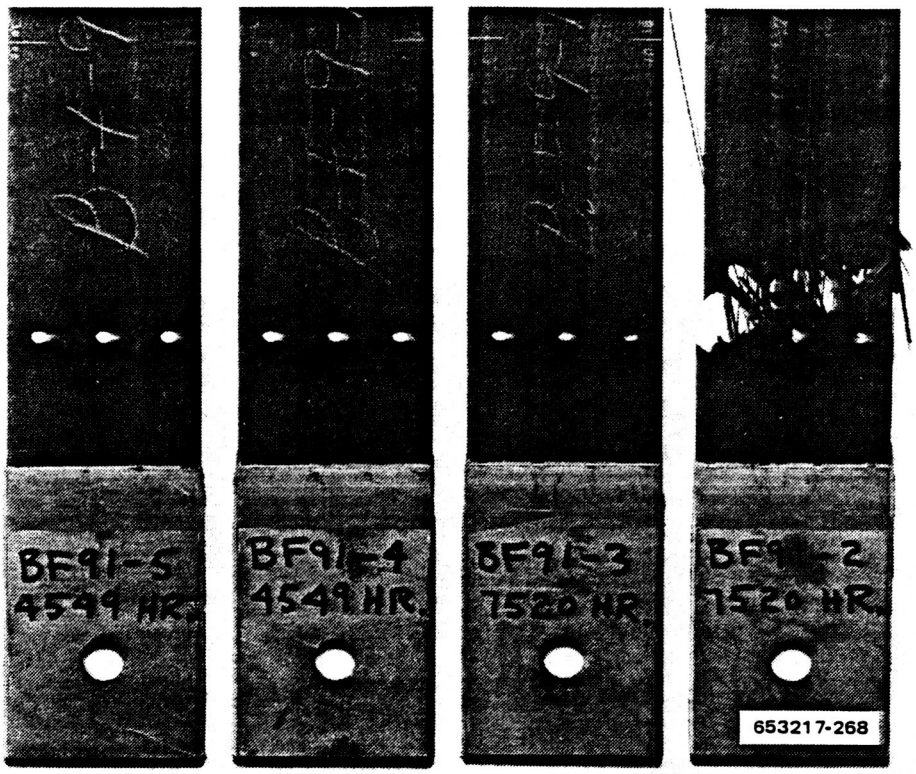



**Figure 12-68 G/E Notched Long-Term Specimens that were Removed from Test Before Completion of 10,000 hr of Exposure. (Increasing levels of damage in the specimens are visible in moving from left to right)**

Figure 12-70 shows the effect of exposure time on the fracture appearance with respect to loss of resin from the graphite fibers. In 2669 hours, oxidation has not embrittled the matrix sufficiently to cause the resin to break away from the fibers during failure. The second specimen, BC91-1, after exposure of 4515 hours begins to show the bare graphite fibers caused by the crumbling away of the oxidized matrix. The effect increases with exposure time as can be seen in the other two specimens in Figure 12-70.

**G/PI, $[0° \pm 45°]_s$, unnotched and notched.** All of the Phase I HT-S/710 G/PI long-term specimens completed 10,000 hours of flight simulation exposure at maximum temperatures of 505K (450 °F). Photographs showing both sides of typical unnotched and notched specimens are presented in Figures 12-71 to 12-74. All of the specimens were discolored in the regions between the stiffening grids in the heated zones. All of the specimens also had exposed graphite fibers in these same areas. Generally the exposed fibers were found on the side of the specimen that faced the quartz heating lamps. However, for three specimens loose surface fibers were observed on both surfaces. Typically, these regions of exposed graphite fibers were approximately 0.025 m (1 in.) in length in the center of the heated zones. Figure 12-75 shows a closeup view of these damaged areas on an unnotched specimen and Figure 12-76 the same for a notched specimen. The amount of exposed fibers on the notched specimens was less than that found on the unnotched specimens. Some slight edge cracks were found in the heated zones of a few of the specimens. An example is shown in Figure 12-77. At 10,000 hours of exposure the edge cracks did not appear to be a serious problem. The appearance of the holes in the notched



ORIGINAL PAGE IS
OF POOR QUALITY

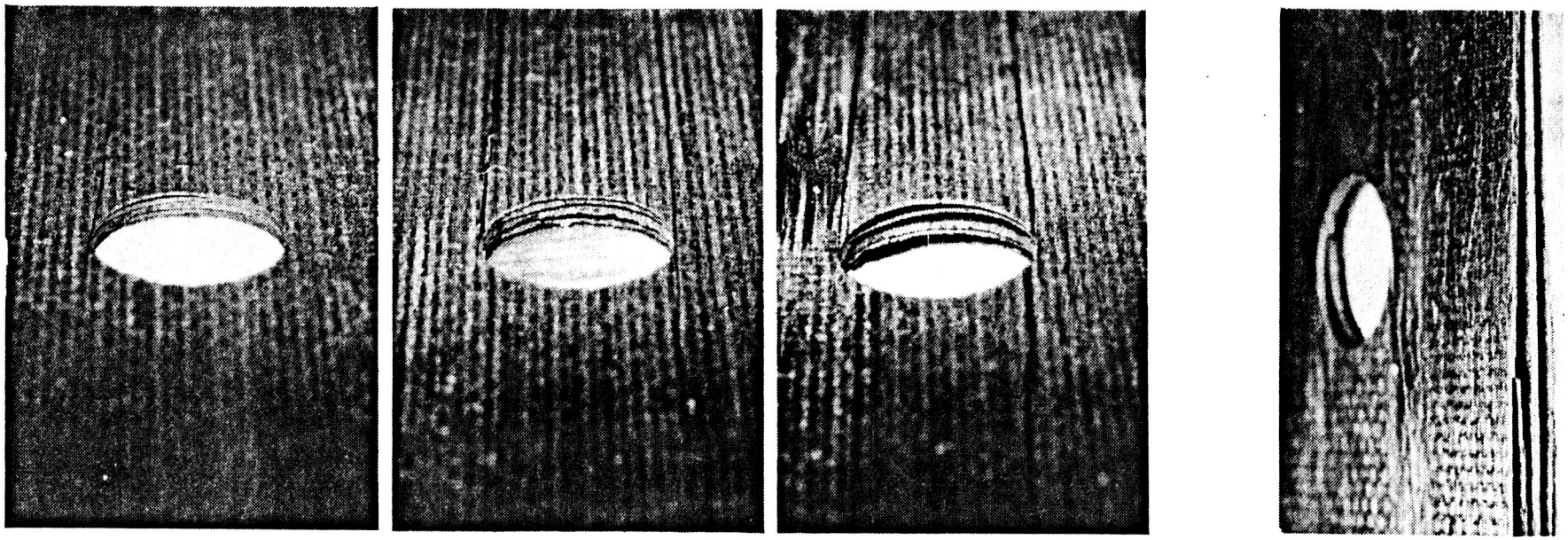



**Figure 12-69 G/E Notched Long-Term Specimen BF91-5 After 4549 hr of Flight Simulation Exposure Showing Variation in Degree of Delamination Across Width of Specimen**

ORIGINAL PAGE IS
OF POOR QUALITY

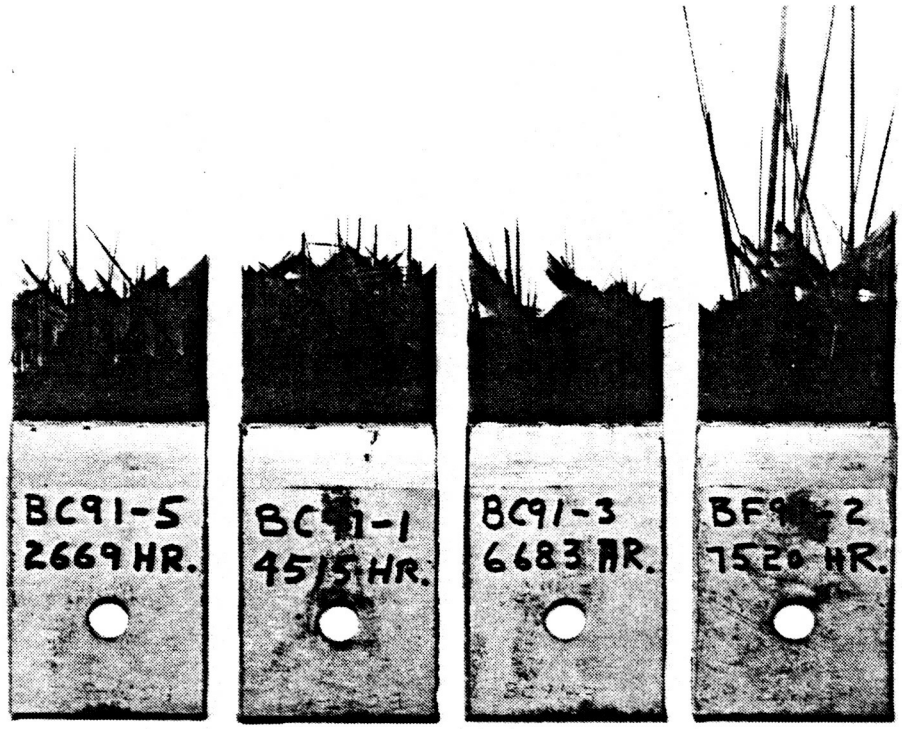
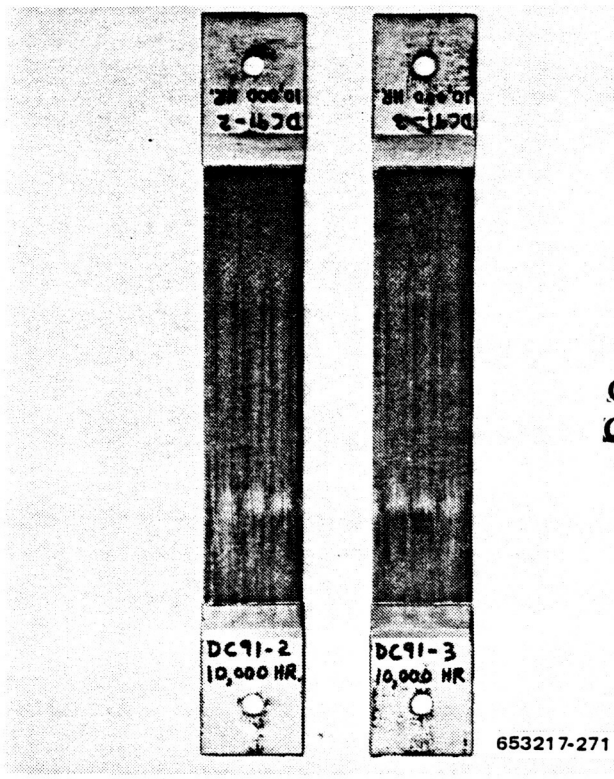



**Figure 12-70 G/E Long-Term Specimens that Failed During Flight Simulation Testing Before Completion of 10,000 hr of Exposure. (Specimens show progressive loss of resin from the graphite fibers with exposure time)**




ORIGINAL PAGE IS
OE POOR QUALITY

**Figure 12-71 G/PI Long-Term Specimens After 10,000 hr of Flight Simulation Exposure**

ORIGINAL PAGE IS
OF POOR QUALITY

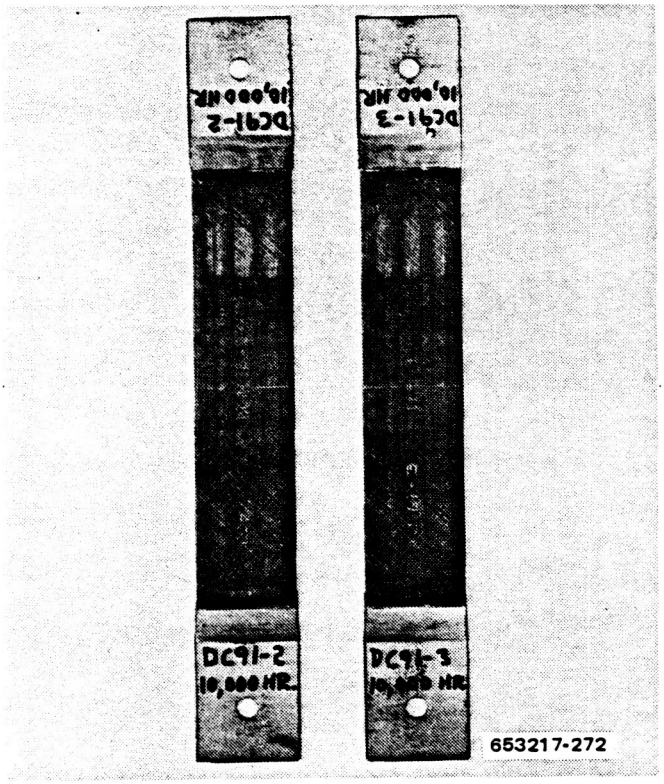



**Figure 12-72 G/PI Long-Term Specimens After 10,000 hr of Flight Simulation Exposure (Opposite sides of specimens in Figure 12-71)**

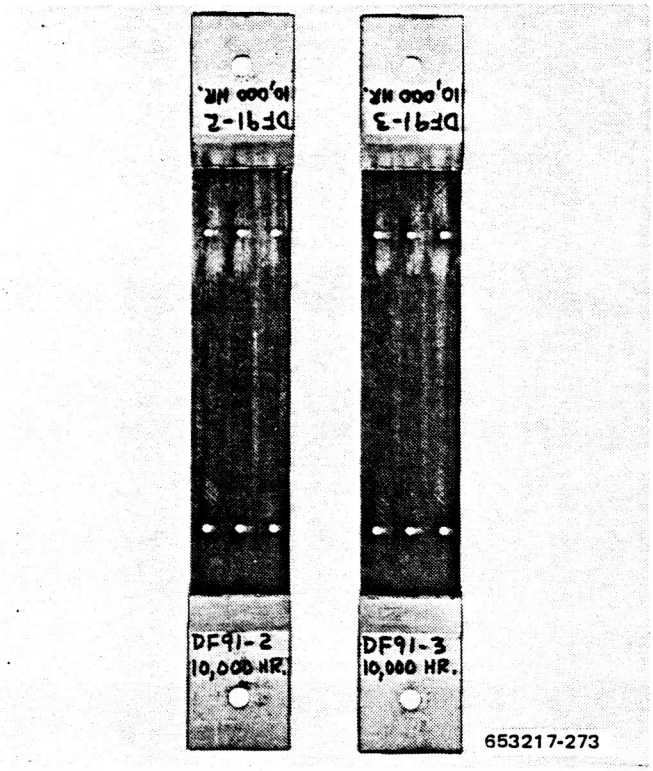



**Figure 12-73 G/PI Notched Long-Term Specimens After 10,000 hr of Flight Simulation Exposure**

ORIGINAL PAGE IS
OF POOR QUALITY

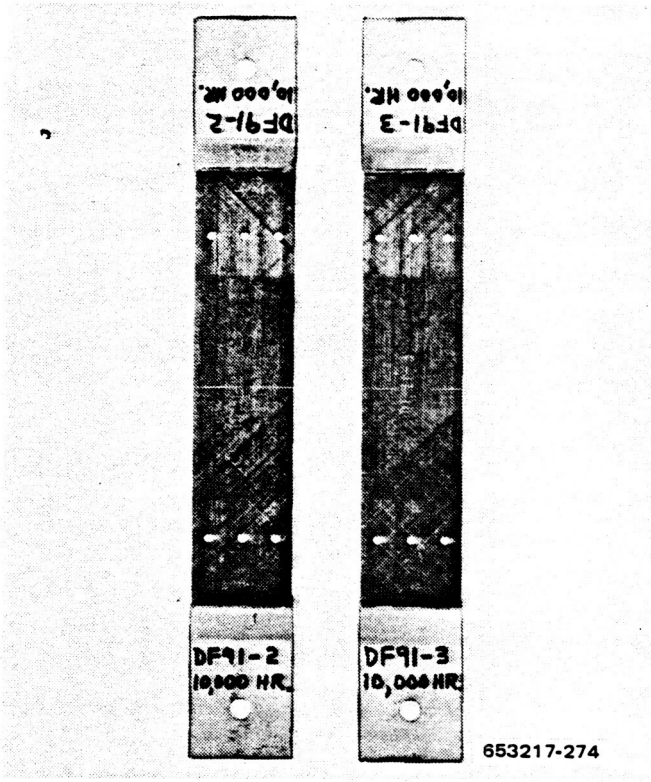



**Figure 12-74 G/PI Notched Long-Term Specimens After 10,000 hr of Flight Simulation Exposure (Opposite sides of specimens in Figure 12-73)**




**Figure 12-75 G/PI Long-Term Specimen DC91-3 After 10,000 hr of Flight Simulation Exposure Showing Exposed Graphite Fibers in Heated Zone**

ORIGINAL PAGE IS
OR QUALITY

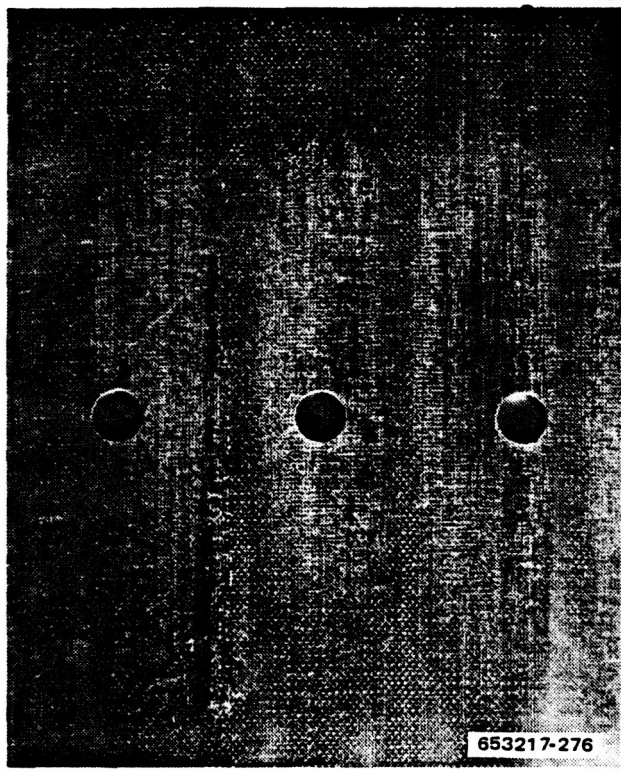



**Figure 12-76 G/PI Notched Long-Term Specimen DF91-2 After 10,000 hr of Flight Simulation Exposure Showing Exposed Graphite Fibers in Heated Zone**

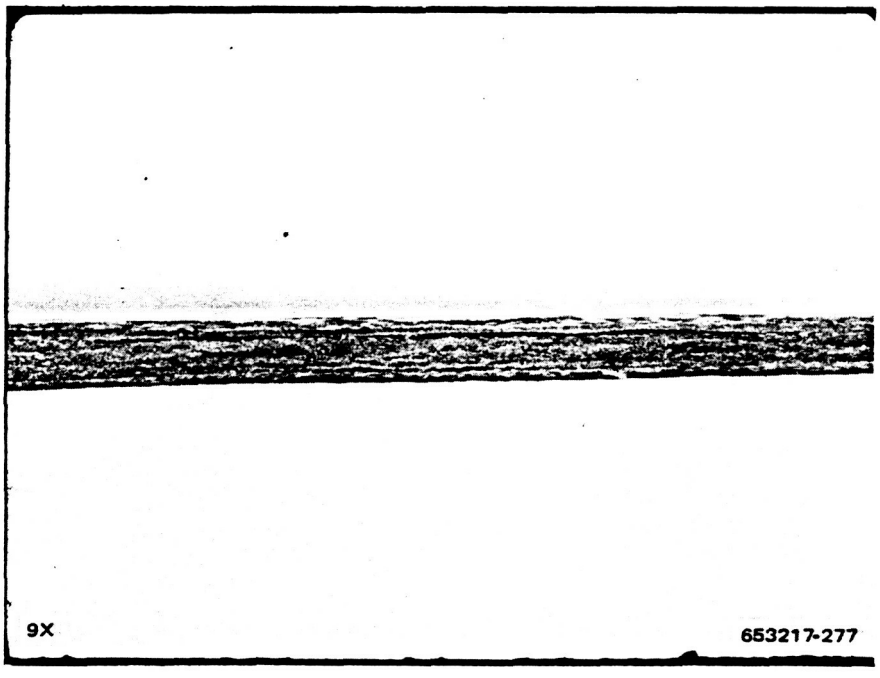



**Figure 12-77 G/PI Long-Term Specimen DC91-1 Showing Slight Edge Cracks in Heated Zone After 10,000 hr of Flight Simulation Exposure**

specimens was generally quite good. Slight horizontal cracks tangent to the holes were observed in three of the specimens. These were very short and appeared to extend only through the outer ply. Some slight delaminations or cracks were present in some of the holes, but, again, these also appeared to be very shallow and not a serious problem at this time.

**B/Al, $[0° \pm 45°]_s$ and $[0°]_6$, unnotched.** All of the $[0° \pm 45°]_s$ crossplied specimens and four of the five unidirectional B/Al long-term specimens completed 10,000 hours of exposure at maximum temperatures of 505K (450 °F). Front and back views of typical specimens are shown in Figures 12-78 and 12-79 for crossply material and in Figures 12-80 and 12-81 for unidirectional material. The heated zones on the sides facing the quartz heat lamps have been coated with flat black, heat resistant paint to reduce reflection from the aluminum surface and thereby increase the efficiency of the heaters. The only noticeable effects on these photographs are the vertical stripes where the stiffener grids were attached. These markings are residue from the Teflon coating on the grids, and in some areas, regions of wear where the soft aluminum surface has been eroded by the rubbing action of the stiffener during fatigue cycling. Careful examination of the surface in the heated zones reveals a roughened surface and some small shallow cracks. The effect is similar to, but not as extensive as, that observed in the specimens that were fatigue tested in air at 561 K (550 ° F). The surface roughening occurred on both sides but was more difficult to see on the painted side. A magnified view of the heated zone on the unpainted side of a crossplied specimen is shown in Figure 12-82. A photograph taken from the unheated center section of the same specimen is also shown in Figure 12-82 for comparison. The roughened surface was found on both the crossplied and the unidirectional specimens. One other observation was made on the unidirectional specimens. The specimens were flat except in the heated zones where the surface was very irregular (wavy) in the transverse direction. Edge cracks and delaminations were found in two of the crossplied specimens, generally in the heated zones. Figure 12-83 is an enlarged view of the worst area found on these two specimens. An ultrasonic C-scan of the same specimen is shown in Figure 12-84. The regions marked on the C-scan are the areas of the specimen where edge cracks were observed with a stereo microscope. The correlation was quite good. The C-scan indicates the cracks to extend approximately 0.006 m (0.25 in.) into the specimen.

**12.7.2.2 Residual Strength Data — Phase I.** The original test plan for residual strength determinations assumed that all five specimens of each set would complete 10,000 hours of exposure and that all of the specimen width would be available for cutting into subsize specimens. For two of the materials, G/E and unidirectional B/Al, all of the Phase I specimens did not survive 10,000 hours. Also, earlier tests on material from the unfailed end of a G/E specimen, BC92-3, that had failed in 4053 hours showed considerable variation in tensile properties across the width of the specimen. Specimens that were shielded by the stiffening grids gave tensile values of 551 $MN/m^2$ (79.9 ksi) and 545 $MN/m^2$ (79.0 ksi) while a specimen that was cut from between the grids gave 163 $MN/m^2$ (23.5 ksi). Because of these results the decision was made to cut the specimens from the unnotched long-term specimens from the material between the grids. This reduced the number of 0.013 m (0.5 in.) wide residual strength specimens that could be obtained from one long-term specimen from 10 to six. For the notched long-term specimens the entire width was used (as was originally planned) so that the number of residual strength specimens remained the same (six per specimen). During the course of the test program, particularly for the thermal aging and the flight simulation tests, it became apparent that compressive and shear properties of the composites were of considerable importance in addition to

ORIGINAL PAGE IS
OF POOR QUALITY

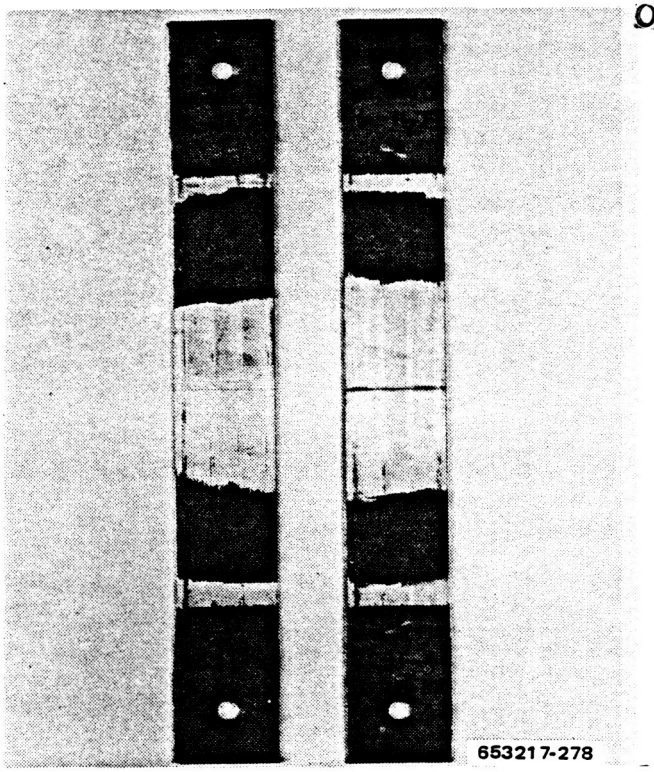



**Figure 12-78 Crossply B/Al Long-Term Specimens After 10,000 hr of Flight Simulation Exposure**

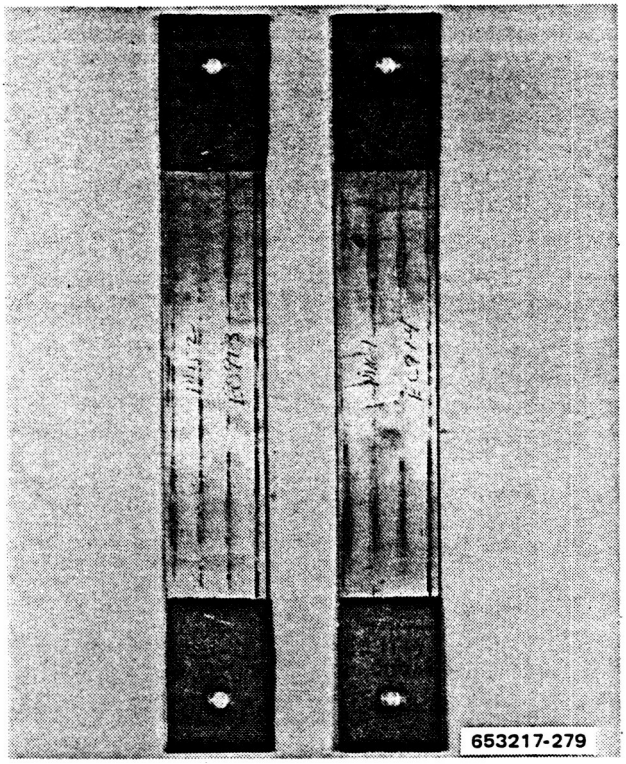



**Figure 12-79 Crossply B/Al Long-Term Specimens After 10,000 hr of Flight Simulation Exposure (Opposite sides of specimens in Figure 12-78)**

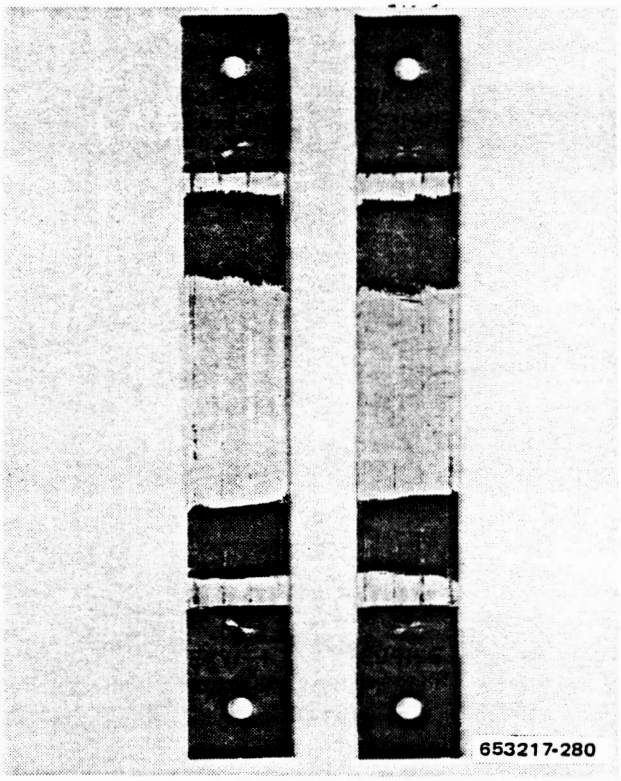
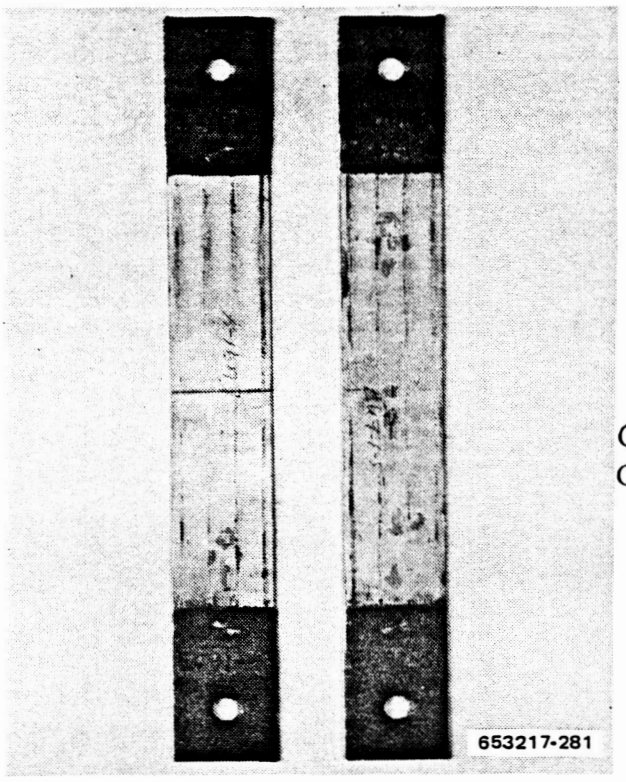
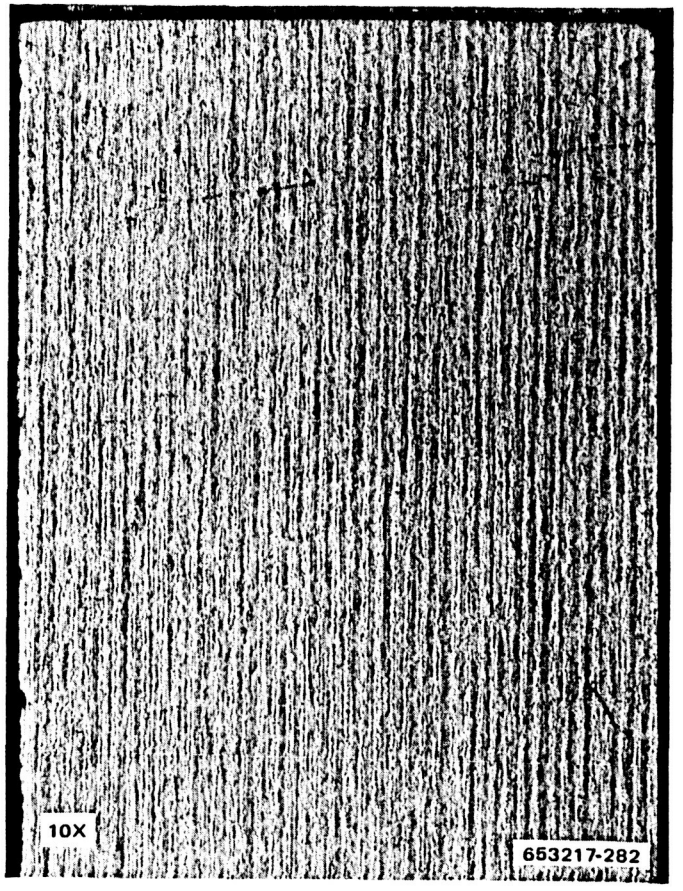



**Figure 12-80 Unidirectional B/Al Long-Term Specimens After 10,000 hr of Flight Simulation Exposure**

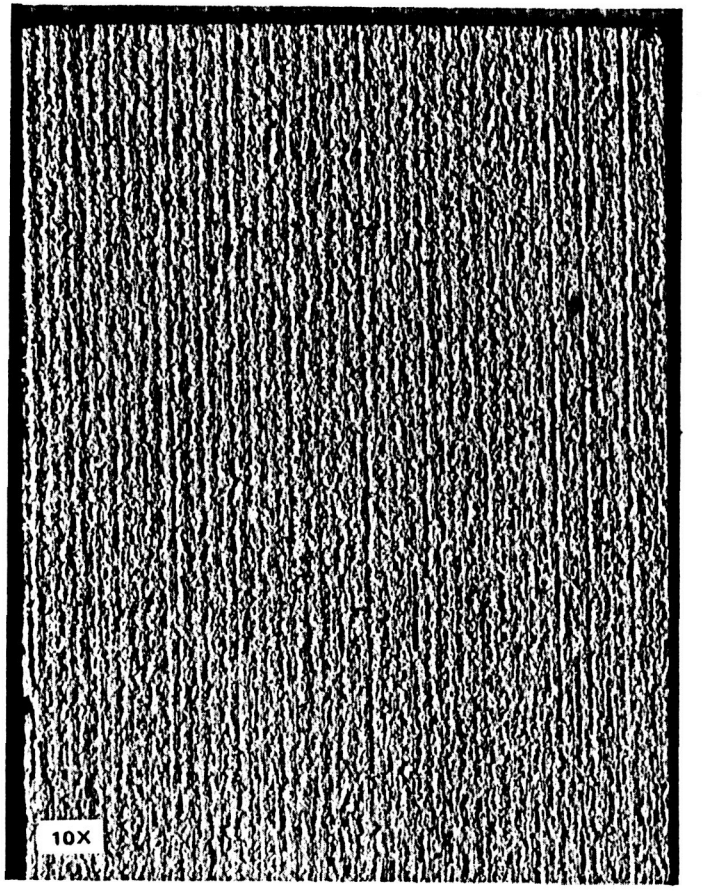



ORIGINAL PAGE IS
OF POOR QUALITY

**Figure 12-81 Unidirectional B/Al Long-Term Specimens After 10,000 hr of Flight Simulation Exposure (Opposite sides of specimens in Figure 12-80)**




HEATED ZONE




CENTER SECTION

**Figure 12-82 B/Al Long-Term Specimen EC91-1 After 10,000 hr of Flight Simulation Exposure Showing Roughened Surface Observed in Heated Zones (Photograph on right shows smooth surface of unheated center section for comparison)**



ORIGINAL PAGE IS OF POOR QUALITY

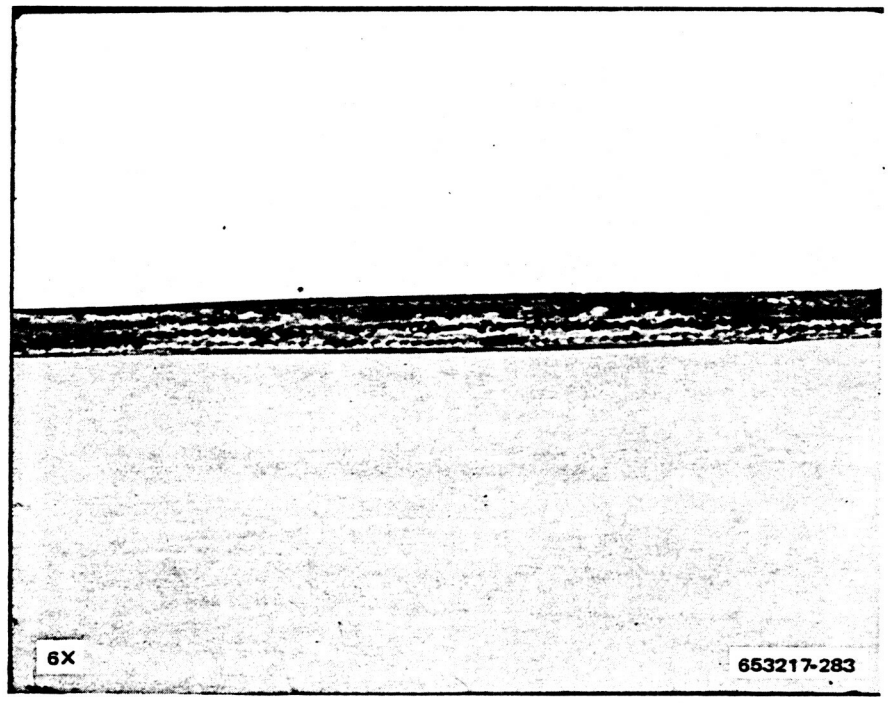


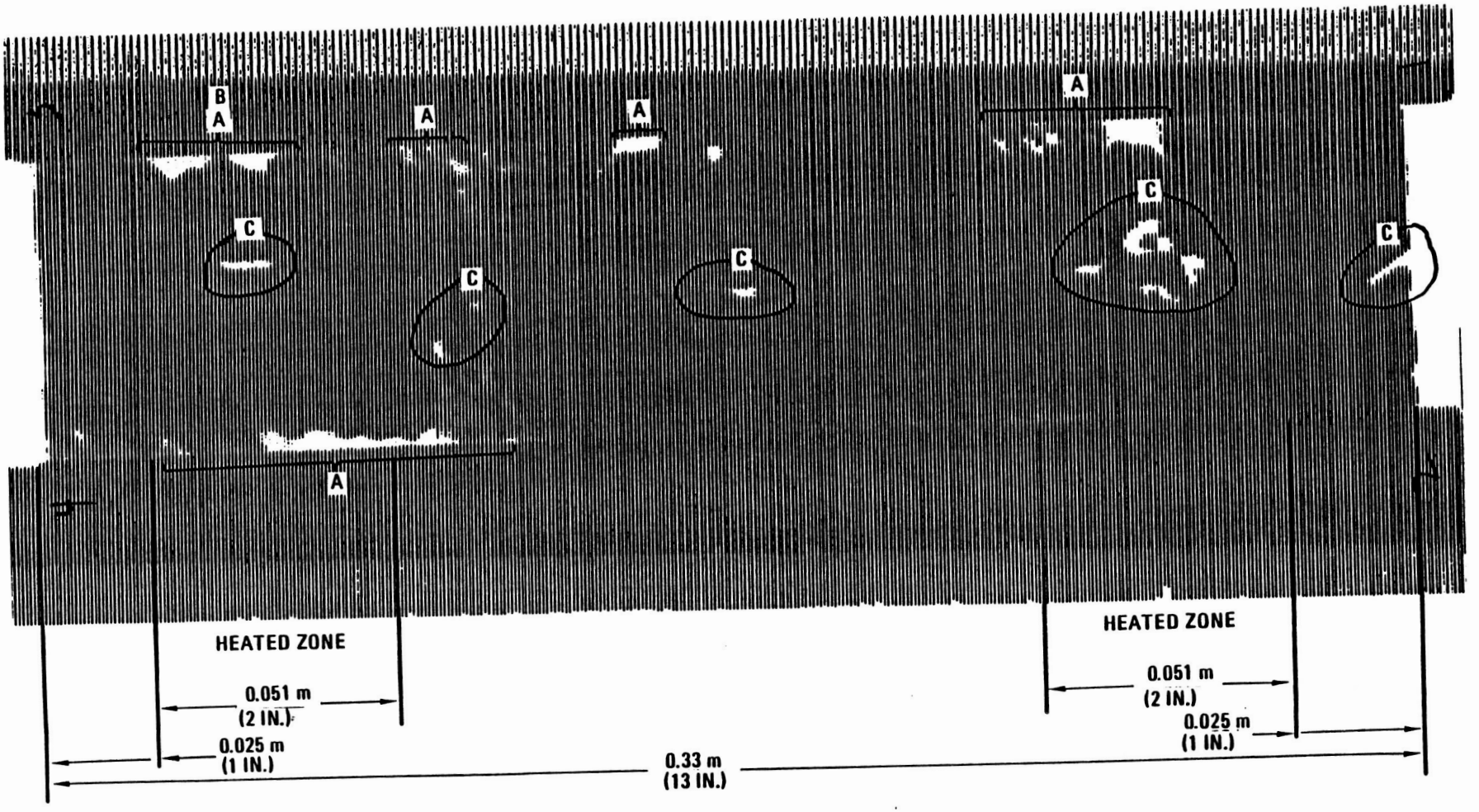

**Figure 12-83 B/Al Long-Term Specimen EC91-1 After 10,000 hr of Flight Simulation Exposure Showing Edge Cracking in Heated Zone**

the tensile characteristics toward which the study was primarily directed. The combination of these three factors 1) less than 100% survival, 2) loss of material from under grids, and 3) increased importance of residual compressive and shear properties resulted in a change in the Phase I residual strength test plan. Table 12-22 shows both the original and the revised plans for the G/E and B/E systems. Similar information for the HT-S/710 G/PI and B/Al systems is listed in Table 12-23. The number of tests from the G/E unnotched long-term specimens was limited by the amount of material available (two and one-half specimens). Two specimens survived 10,000 hours and the unfailed end of BC92-4, which failed in 9669 hours, was undamaged and considered usable. The number of tests from the G/E notched, B/E unnotched, and B/E notched long-term specimens was intentionally kept small because the poor condition of the specimens did not appear to warrant a full scale residual strength test program. The 10,000 hour flight simulation exposure of the epoxy systems was repeated using less severe test conditions as described in Section 12.7.1. The revised test plans for the HT-S/710 G/PI and B/Al systems were developed to derive as much useful data as possible from a limited amount of test material, all of which was used.

All of the 0.013 m (0.5 in.) wide unnotched tensile and fatigue and B/Al notched tensile and shear specimens were cut from the 0.01 m (0.7 in.) wide portions of the flight simulation specimens between the stiffening grids. The approximate locations of these specimens (six per long-term specimen) can be seen in Figure 12-81 where the residue of the Teflon tape has outlined the location occupied by the grid during flight simulation testing. Bonding of doublers was required on only one end of each of the residual tensile and fatigue specimens as the titanium doubler from the flight simulation specimen was still attached to the other end.



ORIGINAL PAGE IS
OF POOR QUALITY




A. EDGE CRACKS VISIBLE WITH STEROGRAPHIC MICROSCOPE AT THESE LOCATIONS.

B. PHOTOGRAPH IN FIGURE 12-83 SHOWS THIS REGION.

C. THESE SPOTS CAUSED BY THERMOCOUPLE ADHESIVE THAT REMAINED ON SURFACE.

653217-284

**Figure 12-84 Ultrasonic C-Scan of B/Al Long-Term Exposure Specimen EC91-1 After 10,000 hr of Flight Simulation Exposure (Size reduced by approximately 25%)**



ORIGINAL PAGE IS
OF POOR QUALITY

**Table 12-22. Residual Strength Test Plan for Phase I B/E and G/E After 10,000 hr of Flight Simulation Testing**

| Material System | Flight Simulation Specimen Type | | Test Type | Temperature K | Temperature (°F) | Number of Specimens Original Plan | Number of Specimens Revised Plan |
|---|---|---|---|---|---|---|---|
| B/E | $[0° \pm 45°]_s$ | Unnotched | Tensile | 297 | 75 | 10 | 6 |
| | | | Notched Tensile | 297 | 75 | 10 | 0 |
| | | | Fatigue | 297 | 75 | 10 | 9 |
| | | | Compressive | 297 | 75 | 0 | 7 |
| | | | Tensile | 450 | 350 | 5 | 0 |
| | | | Notched Tensile | 450 | 350 | 5 | 0 |
| | $[0° \pm 45°]_s$ | Notched | Notched Tensile | 297 | 75 | 10 | 6 |
| | | | Notched Fatigue | 297 | 75 | 10 | 9 |
| | | | Notched Tensile | 450 | 350 | 5 | 0 |
| G/E | $[0° \pm 45°]_s$ | Unnotched | Tensile | 297 | 75 | 10 | 4 |
| | | | Notched Tensile | 297 | 75 | 10 | 0 |
| | | | Fatigue | 297 | 75 | 10 | 7 |
| | | | Compressive | 297 | 75 | 0 | 2 |
| | | | Tensile | 450 | 350 | 5 | 0 |
| | | | Notched Tensile | 450 | 350 | 5 | 0 |
| | $[0° \pm 45°]_s$ | Notched | Notched Tensile | 297 | 75 | 10 | 6 |
| | | | Notched Fatigue | 297 | 75 | 10 | 9 |
| | | | Notched Tensile | 450 | 350 | 5 | 0 |

The notched resin matrix flight simulation specimens were 0.073 m (3 in.) wide with three equally spaced 0.0064 m (0.25 in.) diameter holes across the width. Shearing of the specimens would produce three identical 0.025 m (1 in.) wide residual strength specimens with a centrally located hole. For composite material, however, the specimens must be cut with a saw having a finite blade width, approximately 0.0015 m (0.06 in.). Consequently, the notched tensile and fatigue specimens could be cut from the flight simulation specimen in at least three different ways: equal widths with offset holes; unequal widths with centered holes; and equal widths with centered holes. A check of reference 28 showed that the various configurations had very little difference in $K_t$ factors. The one selected was specimens of equal widths with offset holes in the two outer specimens. The difference in $\frac{\sigma_{max}}{\sigma}$ values for the specimen with a centered hole and one with an offset hole was negligible (3.28 versus 3.30). Again, bonding of doublers was required on only one end.

The residual compressive tests were performed using the specimen and test procedures described in Section 7. To get a sufficiently thick specimen for compressive testing from the 6 ply flight simulation specimens it was necessary to bond three or four layers together. From these 18 or 24 ply panels the 0.0064 m (0.25 in.) wide compressive specimens could be cut. Two

**Table 12-23. Residual Strength Test Plan for Phase I HT-S/710 G/PI and B/Al After 10,000 hr of Flight Simulation Testing**

| Material System | Flight Simulation Specimen Type | | Test Type | Temperature K | Temperature (°F) | Number of Specimens Original Plan | Number of Specimens Revised Plan |
|---|---|---|---|---|---|---|---|
| HT-S/170 G/PI | $[0° \pm 45°]_s$ | Unnotched | Tensile | 297 | 75 | 10 | 5 |
| | | | Notched Tensile | 297 | 75 | 10 | 5 |
| | | | Fatigue | 297 | 75 | 10 | 9 |
| | | | Compressive | 297 | 75 | 0 | 4 |
| | | | Tensile | 505 | 450 | 5 | 5 |
| | | | Notched Tensile | 505 | 450 | 5 | 0 |
| | $[0° \pm 45°]_s$ | Notched | Notched Tensile | 297 | 75 | 10 | 10 |
| | | | Notched Fatigue | 297 | 75 | 10 | 10 |
| | | | Shear | 297 | 75 | 0 | 4 |
| | | | Notched Tensile | 505 | 450 | 5 | 5 |
| B/Al | $[0° \pm 45°]_s$ | Unnotched | Tensile | 297 | 75 | 10 | 4 |
| | | | Notched Tensile | 297 | 75 | 10 | 4 |
| | | | Fatigue | 297 | 75 | 10 | 8 |
| | | | Compressive | 297 | 75 | 0 | 4 |
| | | | Tensile | 505 | 450 | 5 | 4 |
| | | | Notched Tensile | 505 | 450 | 5 | 4 |
| | $[0°]_6$ | Unnotched | Tensile | 297 | 75 | 10 | 4 |
| | | | Notched Tensile | 297 | 75 | 10 | 4 |
| | | | Fatigue | 297 | 75 | 10 | 7 |
| | | | Shear | 297 | 75 | 5 | 3 |
| | | | Compressive | 297 | 75 | 0 | 4 |
| | | | Tensile | 505 | 450 | 5 | 0 |
| | | | Notched Tensile | 505 | 450 | 5 | 0 |
| | | | Shear | 505 | 450 | 5 | 0 |

specimens, made by laminating three or four 0.01 m (0.75 in.) wide pieces together, used the entire width of one end of a flight simulation specimen. Four compressive specimens, using one entire flight simulation specimen, were made for the crossplied B/E, G/PI, B/Al, and the unidirectional B/Al materials. The limited amount of G/E available allowed only two compressive specimens of this material. Since there were no failures of the B/E flight simulation specimens and the number of residual strength specimens was already reduced, sufficient material was available for another type of laminated compressive specimen. These were made by bonding four pieces together that were cut from the areas between the grids. Two flight simulation specimens provided enough material for three of the 0.0064 m (0.25 in.) wide compressive specimens. These two types of B/E compressive specimens were intended to show the effect of the stiffening grids on shielding the composite material during flight simulation exposure.

Residual interfiber shear strength tests were performed on the unidirectional B/Al material. No unidirectional resin matrix specimens were included in the flight simulation test program,

however, and, therefore, no residual shear strength tests were originally scheduled. Examination of the failed G/E flight simulation specimens indicated that interlaminar shear strength played an important role in the premature failures and obtaining residual shear properties would be very useful. There was one half of a 10,000-hour notched HT-S/170 G/PI simulation specimen that was not used for residual strength testing, and a method was devised to use this material to fabricate four short beam shear specimens. As shown in Figure 12-85 three strips were cut from between the grid marks in the heated zone and bonded together to make an 18 ply laminate. The four short beam shear specimens, 0.015 m (0.60 in.) by 0.0064 m (0.25 in.), were cut from material just above and below the holes. As the heated zone in the simulation specimen was 0.05 m (2 in.) long and the holes 0.0064 m (0.25 in.) in diameter, there was sufficient room for cutting the specimens above and below the holes. The layout of the specimens was as shown in Figure 12-85.

**B/E, $[0° \pm 45°]_s$, unnotched and notched.** Residual tensile, notched tensile, and compressive data for B/E after 10,000 hours of flight simulation exposure are listed in Table 12-24. Elastic modulus values are included for all unnotched tensile and compressive tests. Compressive data are shown for the two methods of test specimen fabrication described earlier. Baseline tensile, notched tensile, and compressive values are also included in Table 12-24. Residual axial fatigue data at room temperature and a stress ratio, R, of 0.1 for unnotched and notched specimens are presented in Table 12-25, and S-N curves are plotted in Figures 12-86 and 12-87. Also included on the graphs are S-N curves (no data points) for unexposed material tested under the same conditions (presented earlier in Section 11, Baseline Fatigue Testing).

The unnotched tensile strength was considerably lowered as a result of the 10,000 hours of flight simulation exposure while the notched strength was lowered only 10%. The notched properties of the resin matrix systems have generally shown smaller decreases than the unnotched after exposure. This may, in part, result from the method of specimen cutting where portions of the notched specimens had been shielded by the stiffening grids, whereas the unnotched specimens were cut from material between the grids. Compressive strength was degraded slightly more than the unnotched tensile strength. The residual compressive data also show the effect of the stiffening grid in protecting the underlying material. Specimens cut from the entire width had a compressive strength approximately one-third greater than specimens cut from between the grids. As shown in Figures 12-86 and 12-87, the fatigue properties were considerably lowered by the long-term exposure cycling.

**G/E, $[0° \pm 45°]_s$, unnotched and notched.** Residual tensile, notched tensile, compressive, and elastic modulus values for G/E after 10,000 hours of flight simulation exposure are listed in Table 12-26. Data for unexposed material are also included in the table. Residual axial fatigue data at room temperature and a stress ratio, R, of 0.1 for unnotched and notched specimens are presented in Table 12-27, and S-N curves are plotted in Figures 12-88 and 12-89. S-N curves for unexposed material are shown on the fatigue plots for comparison.

Eight unnotched and four notched long-term specimens of G/E did not complete 10,000 hours of exposure, either because of complete failure or significant damage in the heated zones. In spite of this the residual tensile properties, particularly for the unnotched specimens, were not severely degraded. The compressive strength was, however, greatly affected. After 10,000 hours of flight simulation the compressive strength was reduced by approximately one-half. This decrease would be anticipated if the failure mechanism proposed for the specimens that

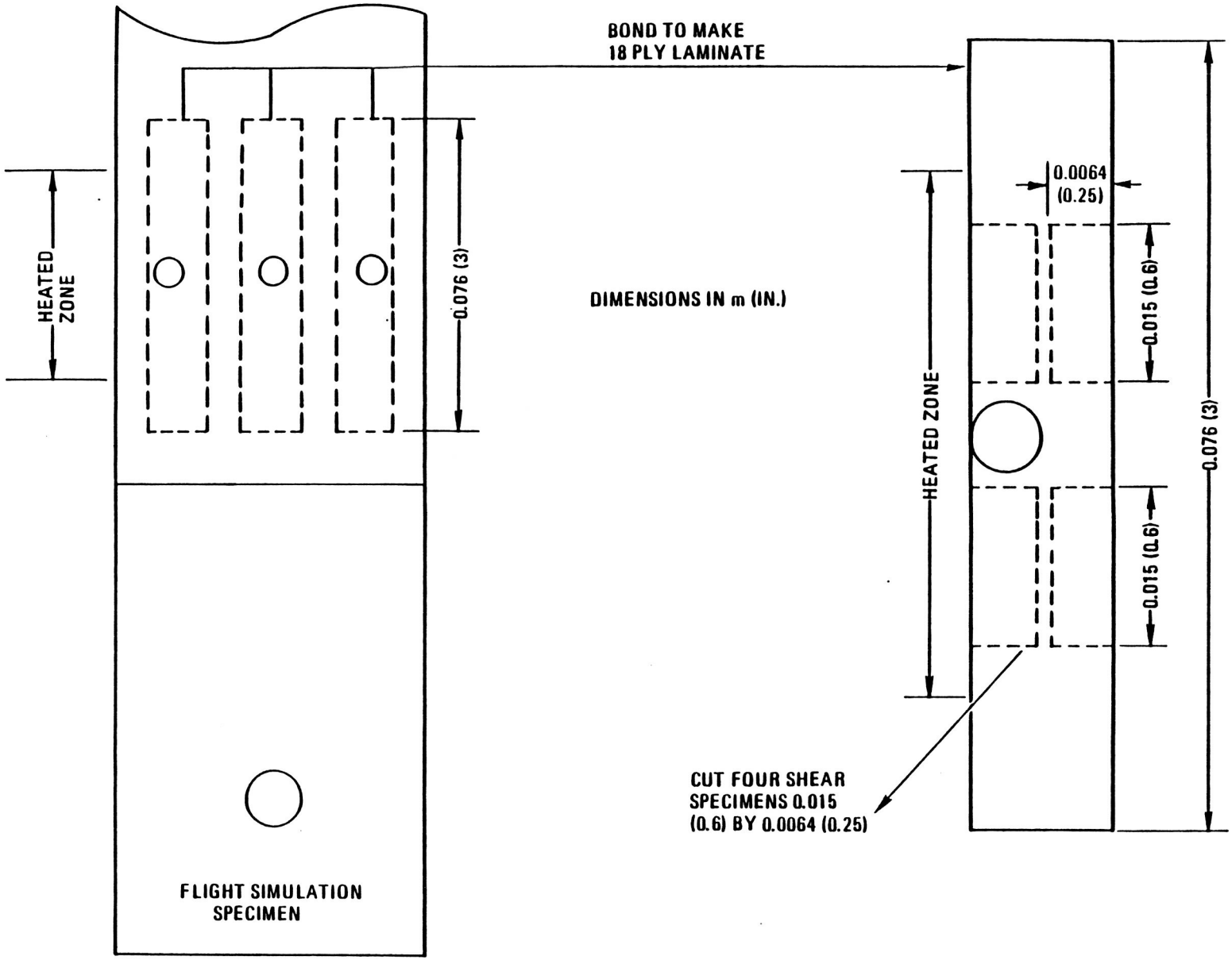



Figure 12-85 Plan for Cutting Short Beam Shear Specimen from G/PI Flight Simulation Specimen

**Table 12-24. Strength and Modulus Properties of $[0° \pm 45°]_s$ B/E at 297 K (75° F) Before and After 10,000 hr of Flight Simulation Exposure**

| Specimen Number | Flight Simulation Specimen Number | | Strength MN/m² | Strength (ksi) | Modulus GN/m² | Modulus (Msi) |
|---|---|---|---|---|---|---|
| Unnotched Tensile: 10,000 hr | | | | | | |
| A912-1 | AC91-2 | | 392 | 56.8 | 68.9 | 10.0 |
| -2 | -2 | | 373 | 54.1 | 73.8 | 10.7 |
| A913-1 | -3 | | 498 | 72.2 | 86.2 | 12.5 |
| -2 | -3 | | 400 | 58.0 | 76.5 | 11.1 |
| A914-1 | -4 | | 362 | 52.5 | 71.7 | 10.4 |
| -2 | -4 | | 337 | 48.9 | 60.0 | 8.7 |
| | | av | 394 | 57.1 | 72.8 | 10.6 |
| Baseline | | av | 618 | 89.7 | 94.5 | 13.7 |
| Notched Tensile: 10,000 hr | | | | | | |
| AF913-1 | AF91-3 | | 452 | 65.6 | | |
| -2 | -3 | | 411 | 59.6 | | |
| -3 | -3 | | 412 | 59.7 | | |
| AF915-1 | -5 | | 315 | 45.7 | | |
| -2 | -5 | | 366 | 53.1 | | |
| -3 | -5 | | 424 | 61.5 | | |
| | | av | 397 | 57.5 | | |
| Baseline | | av | 461 | 64.2 | | |
| Compressive: 10,000 hr (entire specimen width used) | | | | | | |
| A9C-1 | AC91-1 | | 834 | 120.9 | 84.1 | 12.2 |
| -2 | -1 | | 934 | 135.4 | 82.0 | 11.9 |
| -3 | -1 | | 834 | 120.9 | 86.2 | 12.5 |
| -4 | -1 | | 1086 | 154.9 | 82.7 | 12.0 |
| | | av | 918 | 133.0 | 83.8 | 12.2 |
| Compressive: 10,000 hr (cut from between grids) | | | | | | |
| A9C-5 | AC91-5 | | 741 | 107.5 | 79.3 | 11.5 |
| -6 | -5 & AC92-5 | | 709 | 102.9 | 72.4 | 10.5 |
| -7 | AC92-5 | | 754 | 109.3 | 82.0 | 11.9 |
| | | av | 735 | 106.6 | 77.9 | 11.3 |
| Baseline | | av | 1540 | 223.4 | 102 | 14.8 |

**Table 12-25. Residual Axial Fatigue Data for $[0° \pm 45°]_s$ B/E at 297 K (75° F) After 10,000 hr of Flight Simulation Exposure, R = 0.1**

| Specimen Number | Flight Simulation Specimen Number | Specimen Type | Maximum Stress MN/m² | Maximum Stress (ksi) | Cycles | Comments |
|---|---|---|---|---|---|---|
| A912-3 | AC91-2 | Unnotched | 310 | 45 | <1,000 | |
| A913-3 | -3 | | 276 | 40 | 7,975,000 | |
| -4 | -3 | | 293 | 42.5 | 47,000 | |
| -5 | -3 | | 276 | 40 | 5,872,000 | |
| -6 | -3 | | 310 | 45 | <1,000 | |
| A914-3 | -4 | | 293 | 42.5 | 600,000 | |
| -4 | -4 | | 241 | 35 | 15,234,000 | Did not fail |
| -5 | -4 | | 259 | 37.5 | 10,245,000 | Did not fail |
| -6 | -4 | | 293 | 42.5 | 1,000 | |
| AF913-4 | AF91-3 | Notched | 345 | 50 | 10,000,000 | Did not fail |
| -5 | -3 | | 414 | 60 | 1,000 | |
| -6 | -3 | | 379 | 55 | <1,000 | |
| AF914-1 | -4 | | 362 | 52.5 | <1,000 | |
| -2 | -4 | | 345 | 50 | <1,000 | |
| -3 | -4 | | 328 | 47.5 | <1,000 | |
| AF915-4 | -5 | | 310 | 45 | 149,000 | |
| -5 | -5 | | 293 | 42.5 | 1,213,000 | |
| -6 | -5 | | 276 | 40 | 12,729,000 | Did not fail |

did not survive the flight simulation exposures was correct. The residual fatigue properties were significantly lowered with the unnotched material again experiencing a greater decrease than the notched.

**G/PI, $[0° \pm 45°]_s$, unnotched and notched.** Results of the 297 K (75° F) and 505 K (450° F) tensile tests on unnotched and notched HT-S/710 G/PI after 10,000 hours of flight simulation exposure are presented in Tables 12-28 and 12-29. Also included are the baseline data for comparison purposes. Two types of notched tensile specimens were tested. The first, Table 12-28, was cut from unnotched flight simulation specimens and was notched after exposure. The second, Table 12-29, was cut from the notched flight simulation specimens after being exposed in the notched condition. Table 12-30 gives the compressive and short beam shear data for G/PI before and after flight simulation exposure of 10,000 hours. Results of the residual fatigue tests on the unnotched and notched G/PI material at 297 K (75° F) and a stress ratio, R, of 0.1 are listed in Table 12-31 and plotted as S-N curves in Figures 12-90 and 12-91. Data for unexposed G/PI tested under the same conditions are shown on the fatigue plots for comparison.

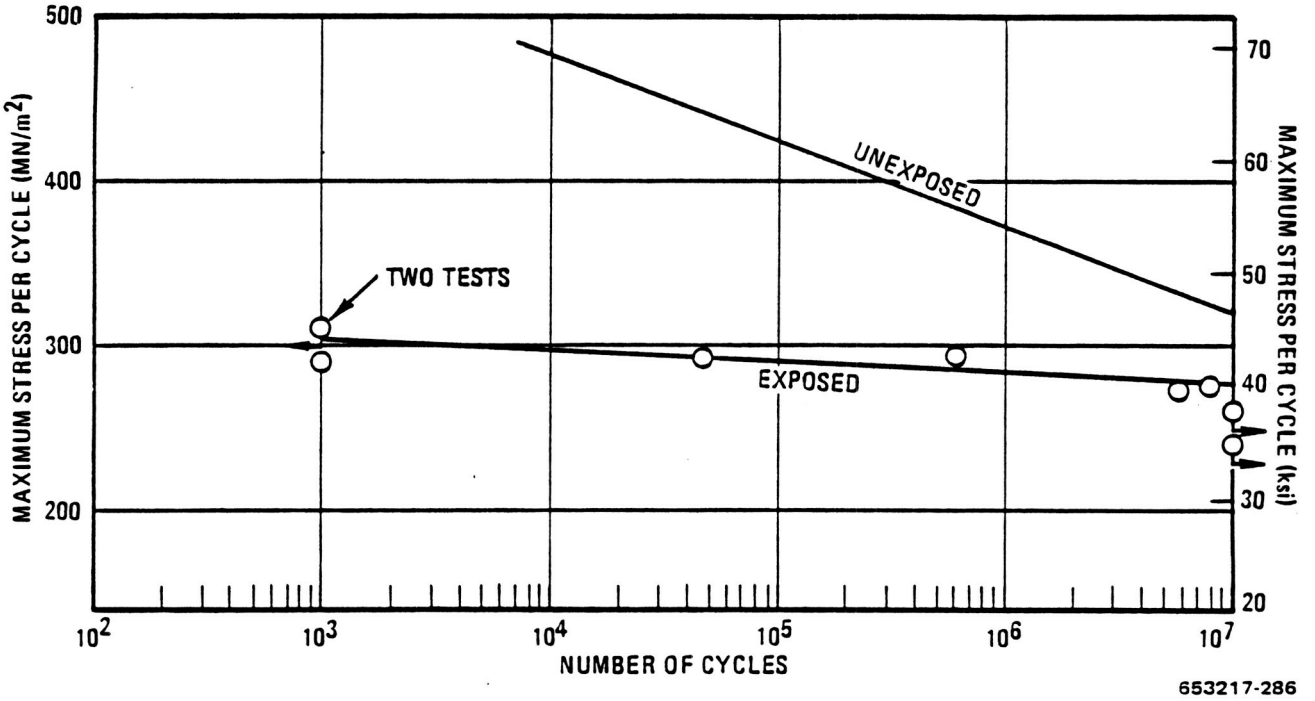



**Figure 12-86 Axial Fatigue Properties of $[0° \pm 45°]_s$ B/E Before and After 10,000 hr Flight Simulation Exposure, 297 K (75°F), R = 0.1, Unnotched**

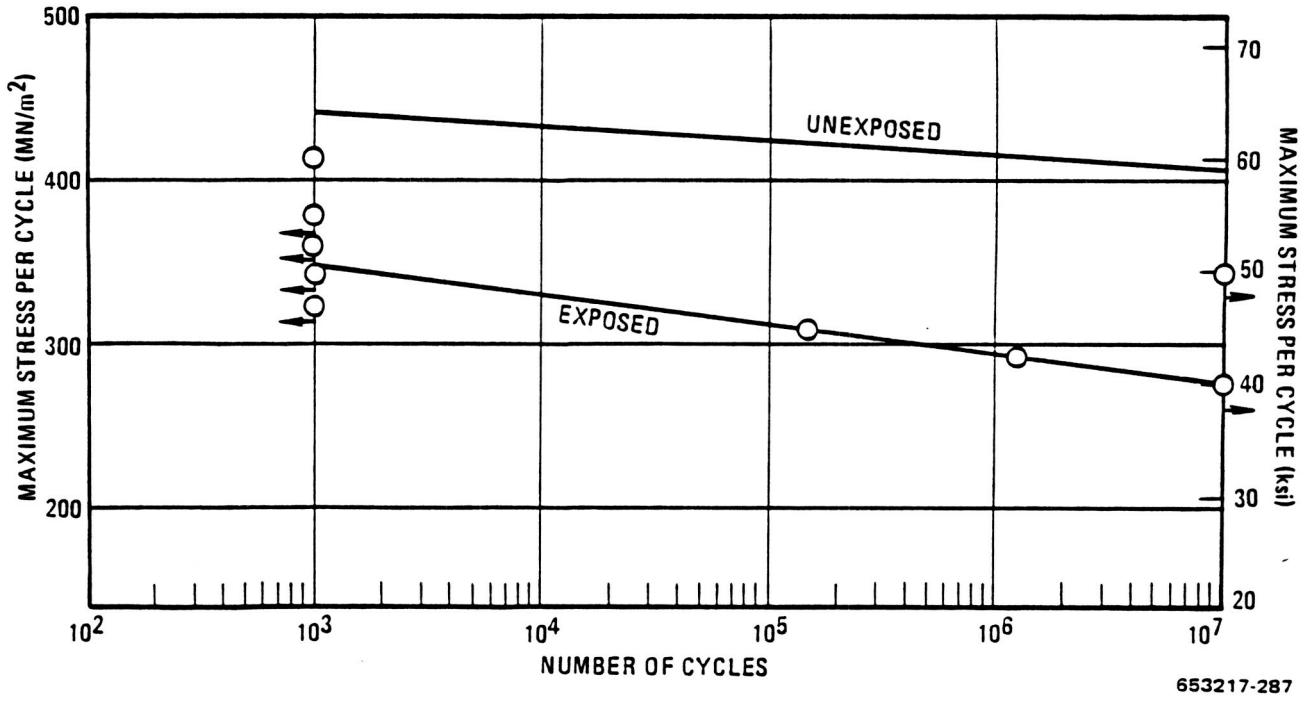



**Figure 12-87 Axial Fatigue Properties of $[0° \pm 45°]_s$ B/E Before and After 10,000 hr of Flight Simulation Exposure, 297 K (75°F), R = 0.1, Notched**

**Table 12-26. Strength and Modulus Properties of $[0° \pm 45°]_s$ G/E at 297 K (75° F) Before and After 10,000 hr of Flight Simulation Exposure**

| Specimen Number | Flight Simulation Specimen Number | | Strength MN/m² | Strength (ksi) | Modulus GN/m² | Modulus (Msi) |
|---|---|---|---|---|---|---|
| Unnotched Tensile: 10,000 hr | | | | | | |
| B921-1 | BC92-1 | | 429 | 62.2 | 39 | 5.7 |
| -2 | -1 | | 427 | 62.0 | 46 | 6.7 |
| B922-1 | -2 | | 410 | 59.5 | 46 | 6.6 |
| -2 | -2 | | 411 | 59.6 | 50 | 7.2 |
| | | av | 419 | 60.8 | 45 | 6.6 |
| Baseline | | av | 496 | 71.9 | 57 | 8.3 |
| Notched Tensile: 10,000 hr | | | | | | |
| BF911-1 | BF91-1 | | 413 | 59.9 | | |
| -2 | -1 | | 445 | 64.6 | | |
| -3 | -1 | | 377 | 54.7 | | |
| BF923-1 | BF92-3 | | 388 | 56.3 | | |
| -2 | -3 | | 470 | 68.2 | | |
| -3 | -3 | | 362 | 52.5 | | |
| | | av | 409 | 59.4 | | |
| Baseline | | av | 412 | 59.7 | | |
| Compressive: 10,000 hr (entire specimen width used) | | | | | | |
| B9C-1 | BC92-1 | | 316 | 45.8 | 46 | 6.6 |
| -2 | -1 | | 293 | 42.5 | 47 | 6.8 |
| | | av | 304 | 44.2 | 46 | 6.7 |
| Baseline | | av | 570 | 82.7 | 46 | 6.6 |

Table 12-27. Residual Axial Fatigue Data for $[0° \pm 45°]_s$ G/E at 297 K (75° F) After 10,000 hr of Flight Simulation Exposure, R = 0.1

| Specimen Number | Flight Simulation Specimen Number | Specimen Type | Maximum Stress MN/m² | Maximum Stress (ksi) | Cycles | Comments |
|---|---|---|---|---|---|---|
| B922-3 | BC92-2 | Unnotched | 379 | 55 | <1,000 | |
| -4 | -2 | | 345 | 50 | 6,968,000 | |
| -5 | -2 | | 362 | 52.5 | 3,000 | |
| -6 | -2 | | 328 | 47.5 | 1,000 | |
| B924-1 | BC92-4 | | 310 | 45 | 4,000 | |
| -2 | -4 | | 276 | 40 | 18,000 | |
| -3 | -4 | | 224 | 32.5 | 10,466,000 | Did not fail |
| BF925-1 | BF92-5 | Notched | 276 | 40 | 1,829,000 | |
| -2 | -5 | | 310 | 45 | 1,143,000 | |
| -3 | -5 | | 345 | 50 | 2,000 | |
| -4 | -5 | | 328 | 47.5 | 2,571,000 | Bond failure |
| -5 | -5 | | 362 | 52.5 | 112,000 | Bond failure |
| -6 | -5 | | 379 | 55 | 1,000 | |
| BF923-4 | -3 | | 328 | 47.5 | 630,000 | |
| -5 | -3 | | 362 | 52.5 | 1,662,000 | |
| -6 | -3 | | 241 | 35 | 5,778,000 | |

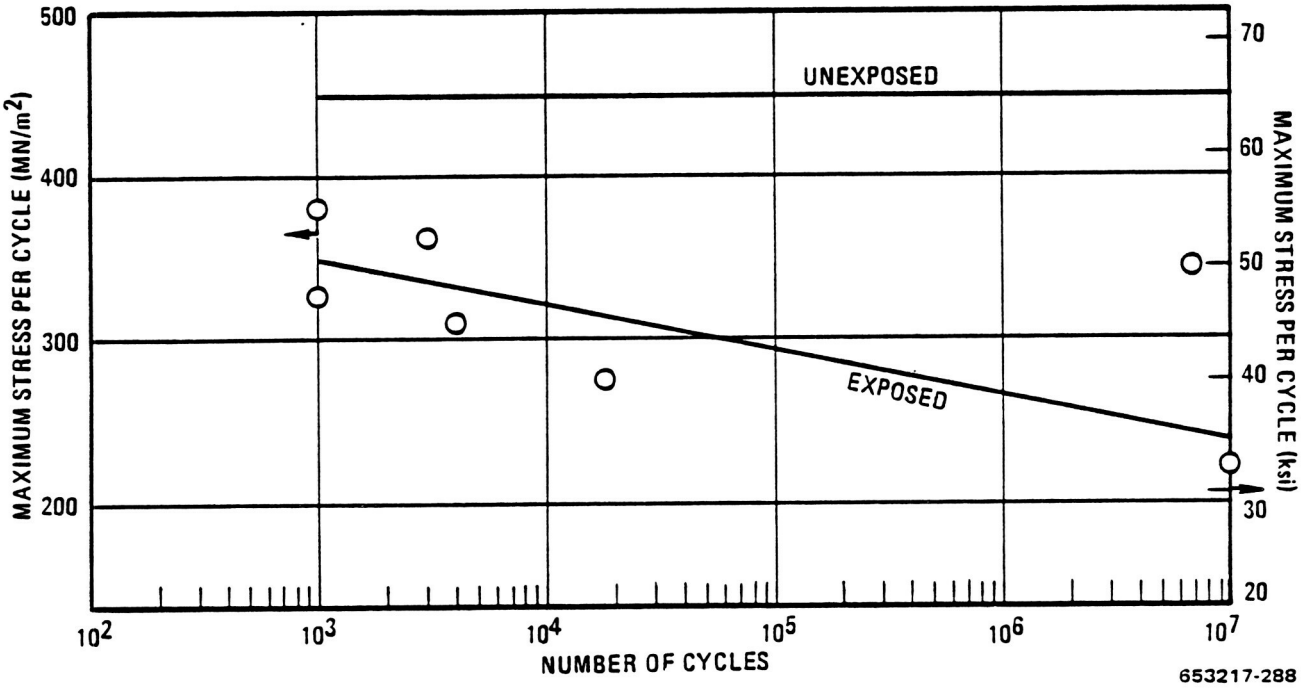



**Figure 12-88 Axial Fatigue Properties of $[0° \pm 45°]_s$ G/E Before and After 10,000 hr of Flight Simulation Exposure, 297 K (75° F), R = 0.1, Unnotched**

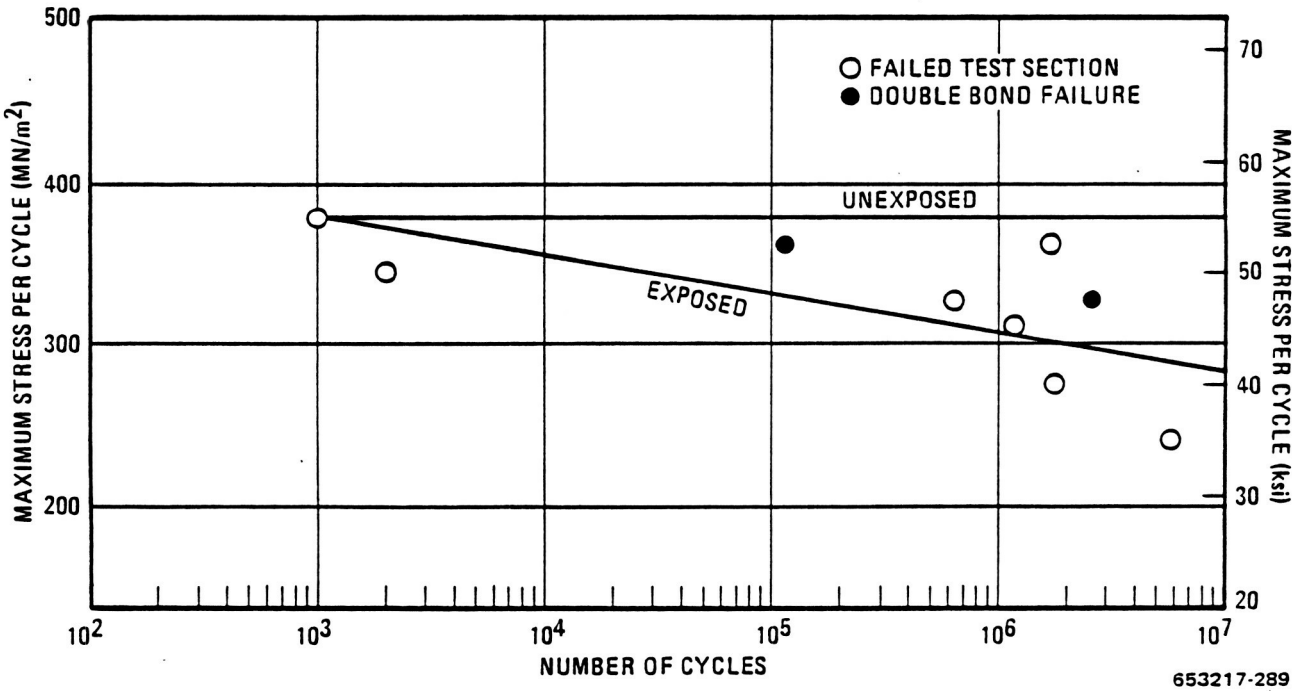



**Figure 12-89 Axial Fatigue Properties of $[0° \pm 45°]_s$ G/E Before and After 10,000 hr of Flight Simulation Exposure, 297 K (75° F), R = 0.1, Notched**

**Table 12-28. Strength and Modulus Properties of $[0° \pm 45°]_s$ HT-S/710 G/PI Before and After 10,000 hr of Flight Simulation Exposure. (Unnotched flight simulation specimen)**

| Specimen Number | Flight Simulation Specimen Number | Temperature K | Temperature (°F) | | Strength MN/m² | Strength (ksi) | Modulus GN/m² | Modulus (Msi) |
|---|---|---|---|---|---|---|---|---|
| Unnotched Tensile: 10,000 hr | | | | | | | | |
| D912-1 | DC91-2 | 297 | 75 | | 405 | 58.8 | 47 | 6.8 |
| -2 | -2 | | | | 331 | 48.0 | 46 | 6.6 |
| -3 | -2 | | | | 225 | 32.7 | 41 | 5.9 |
| -4 | -2 | | | | 323 | 46.8 | 46 | 6.7 |
| -5 | -2 | | | | 510 | 74.0 | — | — |
| D914-6 | -4 | | | | 423 | 61.4 | 48 | 6.9 |
| D915-1 | -5 | | | | 372 | 54.0 | 46 | 6.7 |
| | | | | av | 370 | 53.7 | 46 | 6.6 |
| Baseline | | | | av | 519 | 75.3 | 53 | 7.7 |
| D912-6 | DC91-2 | 505 | 450 | | 334 | 48.5 | 36 | 5.2 |
| -1 | -3 | | | | 411 | 59.6 | 54 | 7.8 |
| -2 | -3 | | | | 303 | 43.9 | 42 | 6.1 |
| | -3 | | | | 225 | 32.7 | 37 | 5.4 |
| -4 | -3 | | | | 296 | 43.0 | 41 | 6.0 |
| | | | | av | 314 | 45.5 | 42 | 6.1 |
| Baseline | | | | av | 470 | 68.2 | 47 | 6.8 |
| Notched Tensile: 10,000 hr | | | | | | | | |
| D915-2 | DC91-5 | 297 | 75 | | 385 | 55.8 | | |
| -3 | -5 | | | | 198 | 28.7 | | |
| -4 | -5 | | | | 336 | 48.8 | | |
| -5 | -5 | | | | 346 | 50.2 | | |
| -6 | -5 | | | | 199 | 28.8 | | |
| | | | | av | 293 | 42.5 | | |
| Baseline | | | | av | 357 | 51.8 | | |

**Table 12-29. Notched Tensile Strength of $[0° \pm 45°]_s$ HT-S/710 G/PI Before and After 10,000 hr of Flight Simulation Exposure. (Notched flight simulation specimen)**

| Specimen Number | Flight Simulation Specimen Number | Temperature K | Temperature (°F) | | Strength MN/m² | Strength (ksi) |
|---|---|---|---|---|---|---|
| Notched Tensile: 10,000 hr | | | | | | |
| DF911-1 | DF91-1 | 297 | 75 | | 348 | 50.5 |
| -2 | -1 | | | | 427 | 61.9 |
| -3 | -1 | | | | 342 | 49.6 |
| -4 | -1 | | | | 315 | 45.7 |
| -5 | -1 | | | | 355 | 51.5 |
| -6 | -1 | | | | 247 | 35.8 |
| DF912-1 | -2 | | | | 261 | 37.8 |
| -2 | -2 | | | | 323 | 46.9 |
| -3 | -2 | | | | 376 | 54.5 |
| DF914-1 | -4 | | | | 271 | 39.3 |
| | | | | av | 326 | 47.4 |
| Baseline | | | | av | 357 | 51.8 |
| DF914-3 | DF91-4 | 505 | 450 | | 256 | 37.2 |
| -4 | -4 | | | | 294 | 42.7 |
| -5 | -4 | | | | 377 | 54.7 |
| -6 | -4 | | | | 397 | 57.6 |
| DF915-1 | -5 | | | | 336 | 48.7 |
| | | | | av | 332 | 48.2 |
| Baseline | | | | av | 336 | 48.8 |

While no HT-S/710 G/PI specimens failed during the 10,000 hours of flight simulation exposure, the unnotched tensile strength at both room and elevated temperatures decreased by about one-third. The residual notched tensile data appear to indicate a difference in the average amount of degradation depending on whether the notch was machined in the specimen before or after exposure. Those specimens that were notched after exposure showed a greater average decrease in strength. Further analysis of the data, however, indicates that the location from which the residual notched tensile specimen was cut from the flight simulation specimen may be more important. Six notched tensile specimens are cut from a flight simulation specimen, two from the center and four from the outer edges (see Figure 12-10 for cutting plan). The center specimens are shielded during exposure by two metal strips of the compressive stiffening grids while the outer specimens are each shielded by only one. The locations of these strips with respect to where the six residual strength specimens are cut can be seen in Figure 12-65. In addition to having two, presumably, higher strength portions, the center specimens are symmetric with respect to these shielded portions. The outer specimens have a shielded portion on only one side of the center hole, and consequently, may experience uneven loading,

**Table 12-30. Compressive and Short Beam Shear Strength Properties of $[0° \pm 45°]_s$ HT-S/710 G/PI at 297 K (75° F) Before and After 10,000 hr of Flight Simulation Exposure**

| Specimen Number | Flight Simulation Specimen Number | | Strength MN/m² | Strength (ksi) | Modulus GN/m² | Modulus (Msi) |
|---|---|---|---|---|---|---|
| Compressive: 10,000 hr | | | | | | |
| D9C-1 | DC91-1 | | 326 | 47.3 | 41 | 5.9 |
| -2 | -1 | | 299 | 43.3 | 41 | 6.0 |
| -3 | -1 | | 264 | 38.3 | 39 | 5.6 |
| -4 | -1 | | 274 | 39.7 | 41 | 5.9 |
| | | av | 291 | 42.2 | 40 | 5.8 |
| Baseline | | av | 377 | 54.7 | 46 | 6.7 |
| Short Beam Shear: 10,000 hr | | | | | | |
| D9S-1 | DF91-5 | | 18 | 2.6 | | |
| -2 | -5 | | 18 | 2.6 | | |
| -3 | -5 | | 16 | 2.3 | | |
| -4 | -5 | | 17 | 2.4 | | |
| | | av | 17 | 2.5 | | |
| Baseline | | av | 37 | 5.4 | | |

**Table 12-31. Residual Axial Fatigue Data for $[0° \pm 45°]_s$ HT-S/710 G/PI at 297 K (75° F) After 10,000 hr of Flight Simulation Exposure, R = 0.1**

| Specimen Number | Flight Simulation Specimen Number | Specimen Type | Maximum Stress MN/m² | Maximum Stress (ksi) | Cycles | Comments |
|---|---|---|---|---|---|---|
| D913-5 | DC91-3 | Unnotched | 293 | 42.5 | <1,000 | |
| -6 | -3 | | 241 | 35 | <1,000 | |
| D914-1 | -4 | | 207 | 30 | <1,000 | |
| -2 | -4 | | 172 | 25 | 12,262,000 | Did not fail |
| -3 | -4 | | 190 | 27.5 | 10,256,000 | Did not fail |
| -4 | -4 | | 198 | 28.75 | <1,000 | |
| -5 | -4 | | 190 | 27.5 | 10,269,000 | Did not fail |
| DF912-4 | DF91-2 | Notched | 276 | 40 | 1,099,000 | |
| -5 | -2 | | 270 | 39.1 | 15,405,000 | Did not fail |
| -6 | -2 | | 283 | 41.1 | 10,219,000 | Did not fail |
| DF913-1 | -3 | | 345 | 50 | <1,000 | |
| -2 | -3 | | 310 | 45 | 4,000 | |
| -3 | -3 | | 310 | 45 | 1,000 | |
| -4 | -3 | | 293 | 42.5 | 53,000 | |
| -5 | -3 | | 293 | 42.5 | 2,424,000 | |
| -6 | -3 | | 293 | 42.5 | <1,000 | |
| DF914-2 | -4 | | 293 | 42.5 | 6,000 | |

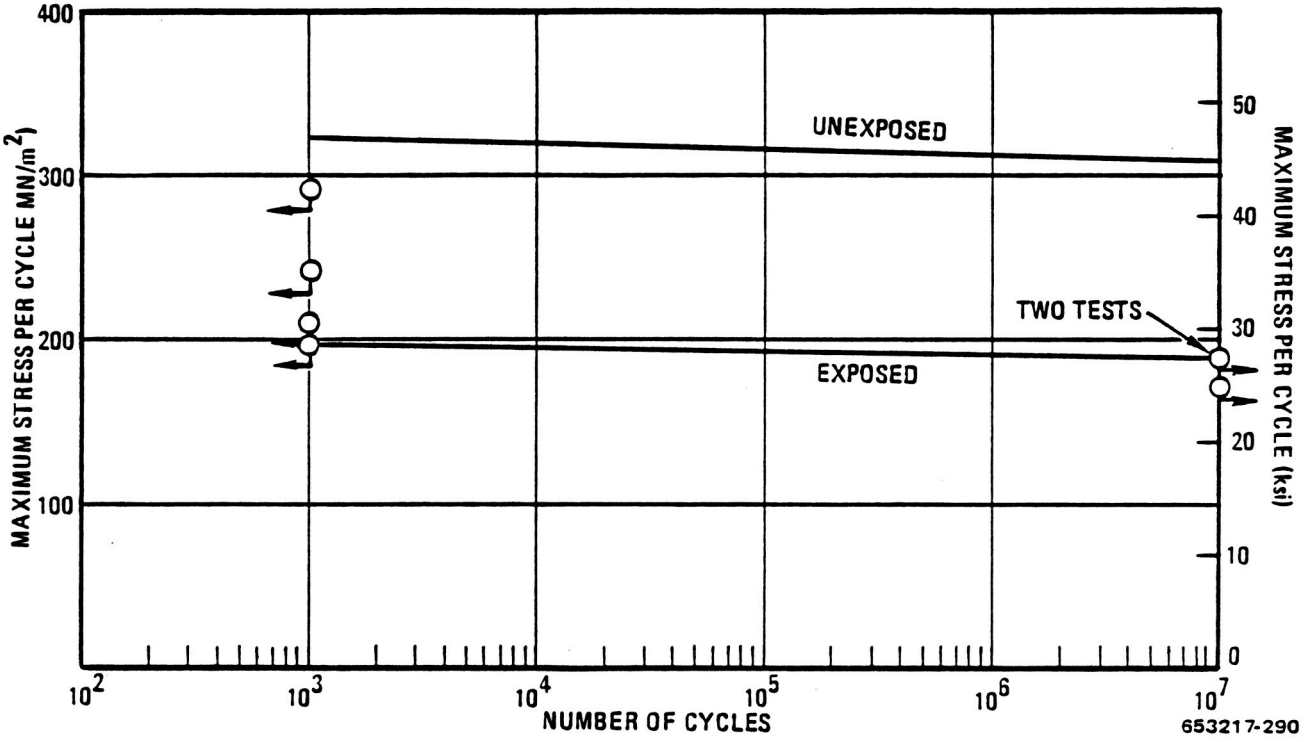



**Figure 12-90 Axial Fatigue Properties of $[0° \pm 45°]_s$ HT-S/710 G/PI Before and After 10,000 hr of Flight Simulation Exposure, 297 K (75°F), R = 0.1, Unnotched**

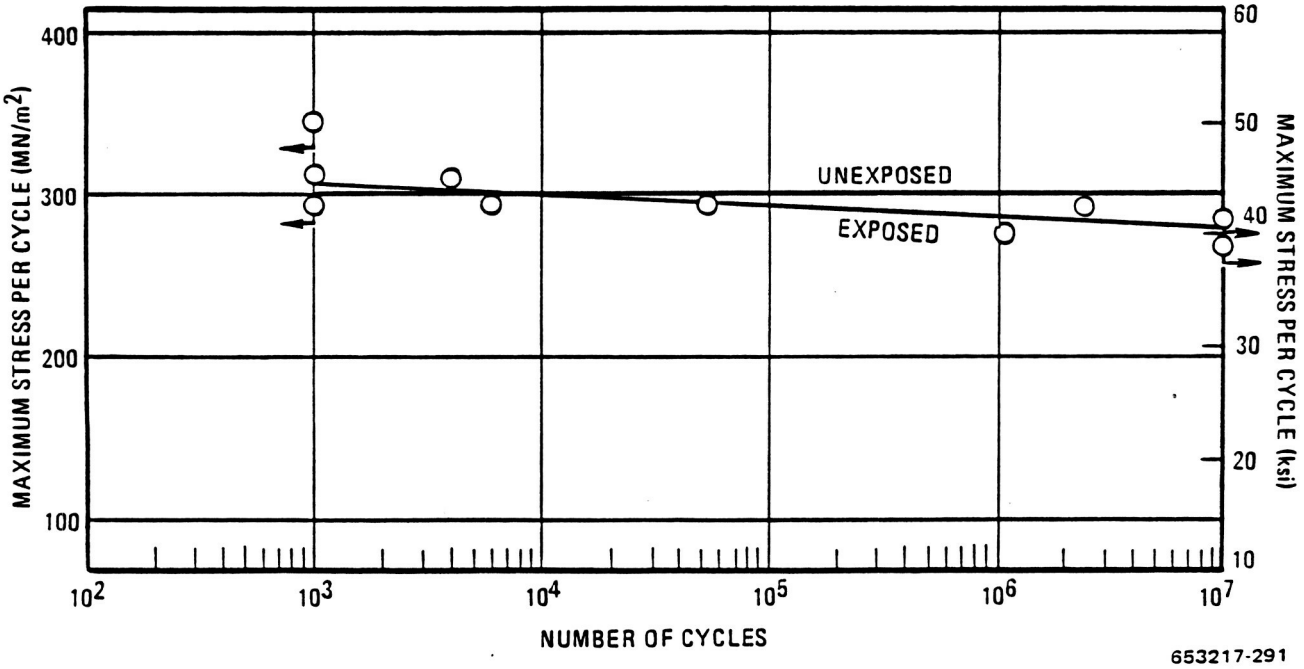



**Figure 12-91 Axial Fatigue Properties of $[0° \pm 45°]_s$ HT-S/710 G/PI Before and After 10,000 hr of Flight Simulation Exposure, 297 K (75°F), R = 0.1, Notched**

which could initiate premature failure. To check out these effects the outer specimen (dash numbers 1, 3, 4, and 6) and center specimen (dash numbers 2 and 5) notched tensile strengths are compared in Table 12-32. The data are listed by temperature, without regard to whether the notches were introduced before or after flight simulation. For the room temperature tests, where sufficient data are available there is a distinct difference in the two types of specimens. The more heavily shielded center specimens were approximately 25% higher in notched tensile strength. In like manner to the G/E material, the G/PI experienced a significant reduction in compressive strength after 10,000 hours of exposure. The decrease was not as great as that for G/E, however, approximately 25% as compared to 50%. It is interesting to note that the loss in tensile strength was greater than that for compressive strength. Again, however, specimen location may be playing a role as the compressive specimens were prepared from the entire width of the specimens while the tensile specimens were cut from the unshielded areas. The residual short beam shear data indicate an apparent major reduction in interlaminar shear strength has occurred as a result of the 10,000 hours of flight simulation exposure. This degradation, if real, correlates well with the failure mechanism proposed earlier for the G/E specimens. The data, however, are limited, and the effect of bonding 6 ply laminates together to form 18 ply short beam shear specimens requires additional study to determine the usefulness of the results. The unnotched fatigue properties were greatly affected with a lowering of the S-N curve of approximately 40% over the entire range from $10^3$ to $10^7$ cycles. The notched fatigue strength, on the other hand, was just slightly lowered by the 10,000 hours of exposure.

**B/Al, $[0° \pm 45°]_s$ and $[0°]_6$, unnotched.** Results of the room and elevated temperature tensile tests on unnotched and notched B/Al before and after 10,000 hours of flight simulation expo-

**Table 12-32. Effect of Specimen Location on Residual Notched Tensile Strength of $[0° \pm 45°]_s$ HT-S/710 G/PI After 10,000 hr of Flight Simulation Exposure**

| Flight Simulation Specimen Number | Temperature K | Temperature (°F) | | Outer Specimen Strength MN/m² | Outer Specimen Strength (ksi) | Center Specimen Strength MN/m² | Center Specimen Strength (ksi) |
|---|---|---|---|---|---|---|---|
| DC91-5 | 297 | 75 | | 198 | 28.7 | 385 | 55.8 |
| -5 | | | | 336 | 48.8 | 346 | 50.2 |
| -5 | | | | 199 | 28.8 | | |
| DF91-1 | | | | 348 | 50.5 | 427 | 61.9 |
| -1 | | | | 342 | 49.6 | 355 | 51.5 |
| -1 | | | | 315 | 45.7 | | |
| -1 | | | | 247 | 35.8 | | |
| -2 | | | | 261 | 37.8 | 323 | 46.9 |
| -2 | | | | 376 | 54.5 | | |
| -4 | | | | 271 | 39.3 | | |
| | | | av | 289 | 41.9 | 367 | 53.2 |
| DF91-4 | 505 | 450 | | 256 | 37.2 | 377 | 54.7 |
| -4 | | | | 294 | 42.7 | | |
| -4 | | | | 397 | 57.6 | | |
| -5 | | | | 336 | 48.7 | | |
| | | | av | 321 | 46.6 | 377 | 54.7 |

sure are presented in Tables 12-33 and 12-34. Residual compressive data for both crossply and unidirectional B/Al are presented in Table 12-35. No baseline compressive tests were conducted on either of the B/Al layups. Also included in Table 12-35 are interfiber shear strength data from unidirectional B/Al before and after flight simulation exposure. Results of the residual fatigue tests on the unnotched crossply and unidirectional B/Al material at 297 K (75 ° F) and a stress ratio, R, of 0.1 are listed in Table 12-36 and plotted as S-N curves in Figures 12-92 and 12-93. Fatigue curves for unexposed B/Al tested under the same conditions are also included in Figures 12-92 and 12-93 for comparison.

**Table 12-33. Unnotched and Notched Tensile Properties of $[0° \pm 45°]_s$ B/Al Before and After 10,000 hr of Flight Simulation Exposure**

| Specimen Number | Flight Simulation Specimen Number | Temperature K | Temperature (°F) | | Strength MN/m² | Strength (ksi) | Modulus GN/m² | Modulus (Msi) |
|---|---|---|---|---|---|---|---|---|
| Unnotched Tensile: 10,000 hr | | | | | | | | |
| EC911-1 | EC91-1 | 297 | 75 | | 409 | 59.3 | 103 | 15.0 |
| -2 | -1 | | | | 399 | 57.9 | 134 | 19.4 |
| -3 | -1 | | | | 406 | 58.9 | 160 | 23.2 |
| -4 | -1 | | | | 301 | 43.7 | 159 | 23.1 |
| | | | | av | 379 | 55.0 | 139 | 20.2 |
| Baseline | | | | av | 516 | 74.8 | 154 | 22.4 |
| EC911-5 | EC91-1 | 505 | 450 | | 264 | 38.3 | — | — |
| -6 | -1 | | | | 415 | 60.2 | 143 | 20.7 |
| EC912-1 | -2 | | | | 404 | 58.6 | — | — |
| -2 | -2 | | | | 359 | 52.1 | — | — |
| | | | | av | 360 | 52.3 | | |
| Baseline | | | | av | 452 | 65.6 | 121 | 17.6 |
| Notched Tensile: 10,000 hr | | | | | | | | |
| EC912-3 | EC91-2 | 297 | 75 | | 303 | 44.0 | | |
| -4 | -2 | | | | 478 | 69.4 | | |
| -5 | -2 | | | | 478 | 69.3 | | |
| -6 | -2 | | | | 364 | 52.8 | | |
| | | | | av | 406 | 58.9 | | |
| Baseline | | | | av | 479 | 69.5 | | |
| EC913-1 | EC91-3 | 505 | 450 | | 283 | 41.4 | | |
| -2 | -3 | | | | 303 | 44.0 | | |
| -3 | -3 | | | | 381 | 55.3 | | |
| -4 | -3 | | | | 354 | 51.3 | | |
| | | | | av | 330 | 47.9 | | |
| Baseline | | | | av | 443 | 64.3 | | |

**Table 12-34. Unnotched and Notched Tensile Properties of $[0°]_6$ B/Al at 297 K (75° F) Before and After 10,000 hr of Flight Simulation Exposure**

| Specimen Number | Flight Simulation Specimen Number | | Strength MN/m² | (ksi) | Modulus GN/m² | (Msi) |
|---|---|---|---|---|---|---|
| Unnotched Tensile: 10,000 hr | | | | | | |
| EU913-1 | EU91-3 | | 1070 | 155 | 231 | 33.5 |
| -2 | -3 | | 972 | 141 | 240 | 34.8 |
| -3 | -3 | | 1000 | 145 | 170 | 24.6 |
| -4 | -3 | | 1290 | 187 | 172 | 25.0 |
| | | av | 1080 | 157 | 203 | 29.5 |
| Baseline | | av | 1450 | 210 | 198 | 28.7 |
| Notched Tensile: 10,000 hr | | | | | | |
| EU913-5 | EU91-3 | | 869 | 126 | | |
| -6 | -3 | | 1080 | 157 | | |
| EU914-1 | -4 | | 896 | 130 | | |
| -2 | -4 | | 924 | 134 | | |
| | | av | 942 | 137 | | |
| [a]Baseline | | av | 1220 | 177 | | |

[a]Estimated from notched tensile strength versus temperature curve for $[0°]_6$ B/Al, Figure 7-23.

**Table 12-35. Compressive and Interfiber Shear Strength Properties of B/Al at 297 K (75° F) Before and After 10,000 hr of Flight Simulation Exposure**

| Specimen Number | Flight Simulation Specimen Number | Orientation | | Strength MN/m² | Strength (ksi) | Modulus GN/m² | Modulus (Msi) |
|---|---|---|---|---|---|---|---|
| Compressive: 10,000 hr | | | | | | | |
| EC9C-1 | EC91-5 | $[0° \pm 45°]_s$ | | [a] >910 | [a]>132 | 143 | 20.8 |
| -2 | -5 | | | [a]>1250 | [a]>182 | 147 | 21.3 |
| -3 | -5 | | | [a]>1420 | [a]>206 | 117 | 17.0 |
| -4 | -5 | | | [a]>1020 | [a]>148 | 112 | 16.3 |
| | | | av | | | 130 | 18.8 |
| EU9C-1 | EU92-4 | $[0°]_6$ | | | | 212 | 30.7 |
| -2 | -4 | | | 1550 | 225 | 197 | 28.5 |
| -3 | -4 | | | (a) | (a) | 207 | 30.0 |
| -4 | -4 | | | 1870 | 271 | 207 | 30.0 |
| | | | av | 1570 | 227 | 206 | 29.8 |
| Interfiber shear: 10,000 hr | | | | | | | |
| EU915-4 | EU91-5 | $[0°]_6$ | | 69.6 | 10.1 | | |
| -5 | -5 | | | 72.4 | 10.5 | | |
| -6 | -5 | | | 70.3 | 10.2 | | |
| | | | av | 70.8 | 10.3 | | |
| Baseline | | | av | 93.1 | 13.5 | | |

[a]Doubler bond shear failure.

**Table 12-36. Residual Unnotched Axial Fatigue Data for B/Al at 297 K (75° F) After 10,000 hr of Flight Simulation Exposure, R = 0.1**

| Specimen Number | Flight Simulation Specimen Number | Orientation | Maximum Stress MN/m² | Maximum Stress (ksi) | Cycles | Comments |
|---|---|---|---|---|---|---|
| EC913-5 | EC91-3 | $[0° \pm 45°]_s$ | 345 | 50 | 824,000 | |
| -6 | -3 | | 379 | 55 | 130,000 | |
| EC914-1 | -4 | | 310 | 45 | 1,789,000 | |
| -2 | -4 | | 396 | 57.5 | 7,000 | |
| -3 | -4 | | 276 | 40 | 13,704,000 | Did not fail |
| -4 | -4 | | 362 | 52.5 | 190,000 | |
| -5 | -4 | | 414 | 60 | 38,000 | |
| -6 | -4 | | 293 | 42.5 | 2,986,000 | |
| EU914-3 | EU91-4 | $[0°]_6$ | 827 | 120 | — | Equipment Malfunction |
| -4 | -4 | | 689 | 100 | 16,022,000 | Did not fail |
| -5 | -4 | | 827 | 120 | 2,953,000 | |
| -6 | -4 | | 862 | 125 | 2,377,000 | |
| EU915-1 | -5 | | 965 | 140 | 27,000 | |
| -2 | -5 | | 1000 | 145 | 133,000 | |
| -3 | -5 | | 1070 | 155 | 28,000 | |

The B/Al system exhibited a loss in mechanical properties of approximately one-fourth after 10,000 hours of flight simulation exposure. This loss was generally observed for both unnotched and notched tensile strength of both crossplied and unidirectional layups and for interfiber shear strength of the unidirectional material. Tests conducted at both room and elevated temperatures gave similar results. Doubler bond shear failures were a problem with the B/Al compressive specimens. The crossply specimens were particularly bad with all failing prematurely in the doubler bonds. The failure loads were quite high, however, equal to a compressive stress in one of the crossply specimens of 1420 MN/m² (206 ksi). The residual fatigue results for the crossplied material showed a decrease of, again, approximately one-fourth in the runout stress ($10^7$ cycles) after 10,000 hours of exposure. The unidirectional B/Al, on the other hand, showed very little change from the baseline fatigue data.

#### PHASE I SUMMARY

Table 12-37 summarizes the 10,000-hour, long-term flight simulation residual strength data obtained from the four composite systems. The percentage decrease in the various mechanical properties is listed for each material. The fatigue data are summarized in Table 12-38. In this table the fatigue strength at $10^7$ cycles, expressed as a percentage of the unexposed tensile strength, is compared for unexposed material and for that which has survived 10,000 hours of flight simulation exposure.

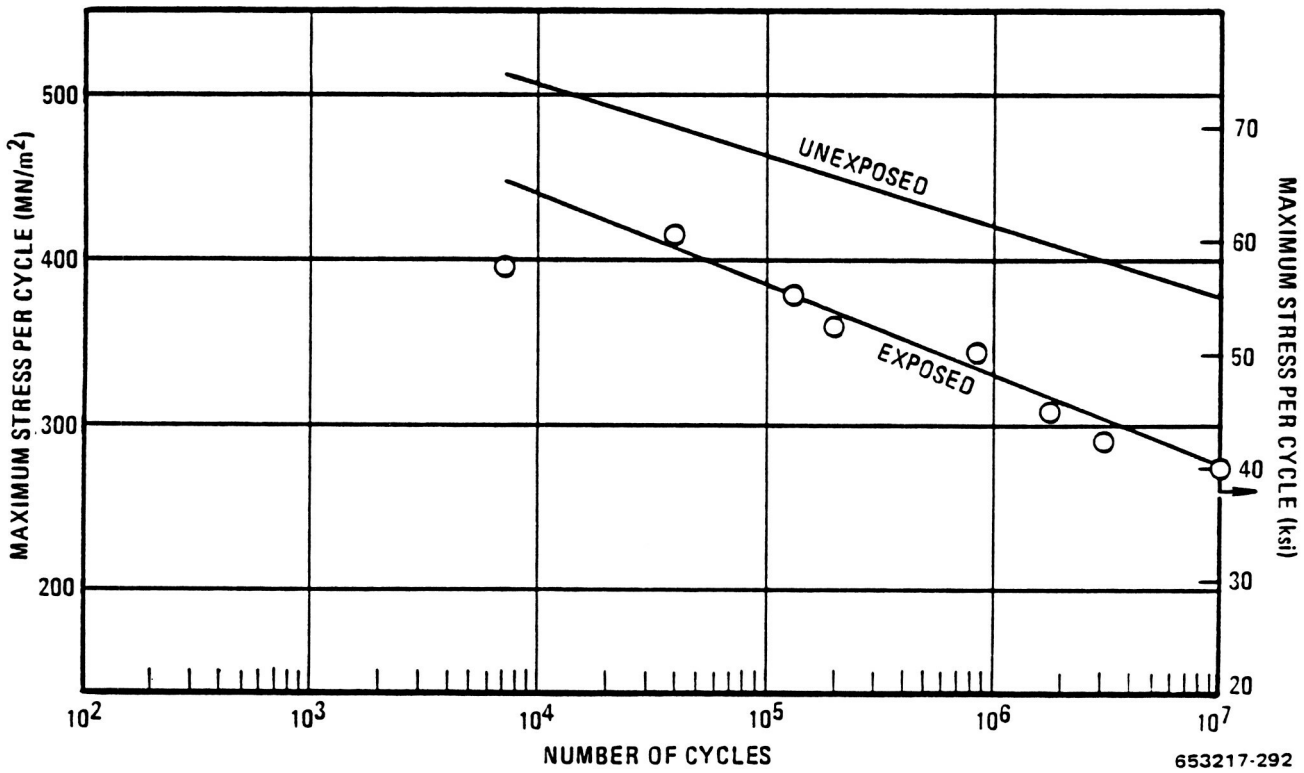



**Figure 12-92 Axial Fatigue Properties of $[0° \pm 45°]_s$ B/Al Before and After 10,000 hr of Flight Simulation Exposure, 297 K (75°F), R = 0.1, Unnotched**

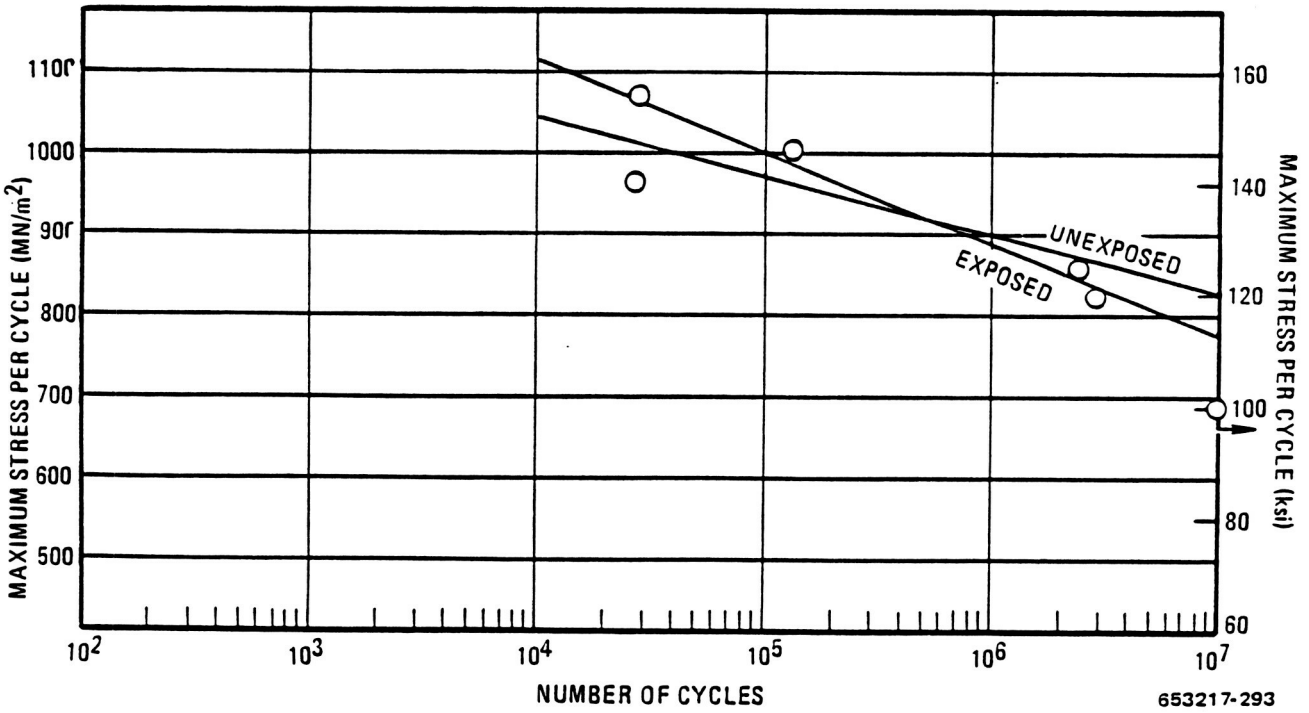



**Figure 12-93 Axial Fatigue Properties of $[0°]_6$ B/Al Before and After 10,000 hr of Flight Simulation Exposure, 297 K (75°F), R = 0.1, Unnotched**

Table 12-37. Summary of 10,000-hr Flight Simulation Residual Strength Data

| Material System | Property | Temperature K | Temperature (°F) | Property Loss (%) |
|---|---|---|---|---|
| 5505/4 B/E $[0° \pm 45°]_s$ | $F_{tu}$ | 297 | 75 | 36 |
| | $E_t$ | 297 | 75 | 23 |
| | [a]Notched $F_{tu}$ | 297 | 75 | 10 |
| | $F_{cu}$ | 297 | 75 | [b]40-52 |
| | $E_c$ | 297 | 75 | [b]18-24 |
| A-S/3501-5 G/E $[0° \pm 45°]_s$ | $F_{tu}$ | 297 | 75 | 15 |
| | $E_t$ | 297 | 75 | 20 |
| | [a]Notched $F_{tu}$ | 297 | 75 | 1 |
| | $F_{cu}$ | 297 | 75 | 47 |
| | $E_c$ | 297 | 75 | 0 |
| HT-S/710 G/PI $[0° \pm 45°]_s$ | $F_{tu}$ | 297 | 75 | 29 |
| | $E_t$ | 297 | 75 | 14 |
| | $F_{tu}$ | 505 | 450 | 33 |
| | $E_t$ | 505 | 450 | 10 |
| | [c]Notched $F_{tu}$ | 297 | 75 | 18 |
| | [a]Notched $F_{tu}$ | 297 | 75 | 8 |
| | [a]Notched $F_{tu}$ | 505 | 450 | 1 |
| | $F_{cu}$ | 297 | 75 | 23 |
| | $E_c$ | 297 | 75 | 13 |
| | $F_{su}$ | 297 | 75 | 54 |
| B/Al $[0° \pm 45°]_s$ | $F_{tu}$ | 297 | 75 | 26 |
| | $E_t$ | 297 | 75 | 10 |
| | $F_{tu}$ | 505 | 450 | 20 |
| | [c]Notched $F_{tu}$ | 297 | 75 | 15 |
| | [c]Notched $F_{tu}$ | 505 | 450 | 26 |
| B/Al $[0°]_6$ | $F_{tu}$ | 297 | 75 | 25 |
| | $E_t$ | 297 | 75 | 0 |
| | [c]Notched $F_{tu}$ | 297 | 75 | 23 |
| | $F_{su}$ | 297 | 75 | 24 |

[a]Notched flight simulation specimens
[b]Loss greater for material cut from between grids
[c]Unnotched flight simulation specimens

Table 12-37. Summary of 10,000-hr Flight Simulation Residual Strength Data — Concluded

| Material System | Property | Temperature K | Temperature (°F) | Property Loss (%) |
|---|---|---|---|---|
| | [c]Notched $F_{tu}$ | 297 | 75 | 23 |
| | $F_{su}$ | 297 | 75 | 24 |

[a]Notched flight simulation specimens
[b]Loss greater for material cut from between grids
[c]Unnotched flight simulation specimens

Table 12-38. Strength at Fatigue Limit or $10^7$ Cycles Expressed as Percentage of Ultimate Tensile Strength Before and After 10,000 hr of Flight Simulation Exposure, R = 0.1, 297 K (75° F)

| Material System | Specimen Configuration | Condition | Fatigue Strength at $10^7$ Cycles (% of Unexposed $F_{tu}$) |
|---|---|---|---|
| 5505/4 B/E $[0° \pm 45°]_s$ | Unnotched | Unexposed | 52 |
| | | Exposed | 45 |
| | Notched | Unexposed | 92 |
| | | Exposed | 62 |
| A-S/3501-5 G/E $[0° \pm 45°]_s$ | Unnotched | Unexposed | 90 |
| | | Exposed | 49 |
| | Notched | Unexposed | 92 |
| | | Exposed | 69 |
| HT-S/710 G/PI $[0° \pm 45°]_s$ | Unnotched | Unexposed | 60 |
| | | Exposed | 37 |
| | Notched | Unexposed | 84 |
| | | Exposed | 78 |
| B/Al $[0° \pm 45°]_s$ | Unnotched | Unexposed | 74 |
| | | Exposed | 54 |
| B/Al $[0°]_6$ | Unnotched | Unexposed | 57 |
| | | Exposed | 53 |

**12.7.3 PHASE II LONG TERM TEST RESULTS.** The Phase II flight simulation test program consisted of the following:

**B/E and G/E.** New specimens were prepared and flight simulation testing of the epoxy systems was restarted with the maximum test temperature reduced to 373K (212°F). All specimens were unnotched. Specimens successfully completed 10,000 hours and 25,000 hours of exposure without failure and were tested for residual strength properties. Two of the B/E specimens failed after about 33,000 hours. The three remaining B/E specimens and the five G/E specimens were removed after about 36,000 hours for residual strength testing.

**HT-S/710 G/PI.** Exposure testing was continued on the unnotched and notched specimens in the flight simulation apparatus that had completed 10,000 hours of exposure. In addition, three unnotched specimens were prepared from the second batch of prepreg (same material as used on the G/PI new material screening evaluation) for 25,000 hours of exposure. Two of these 25,000 hour specimens were damaged while being installed in the simulator. The third failed prematurely after only 5760 hours. The screening evaluation had shown this batch of material to have very poor thermo-oxidative resistance so that the early failure was not unexpected. However, at the same time as this failure two of the 50,000 hour unnotched specimens in the same bay of the simulator also failed (15,896 hours). The reason for these failures could not be determined but did not appear to be normal wearout from the thermal and fatigue environment.

One other premature failure occurred to a notched specimen as a result of a tensile overload at 20,398 hours. This failure was traced to operator error. The remainder of the HT-S/710 G/PI specimens failed at times ranging from 15,021 hours to 39,856 hours for the unnotched and 17,852 hours to 27,890 hours for the notched. These failures were believed to have been the result of wearout from the thermal and fatigue environment.

**B/Al.** Flight simulation testing was continued on the unidirectional and crossplied specimens that had completed 10,000 hours in Phase I. In addition, three unidirectional and three crossplied specimens were prepared for evaluation after 25,000 hours of exposure cycling. One major incident occurred where six crossplied specimens failed during an accidental compressive overload at 20,957 hours. The accident was the result of the combination of equipment complexity and operator error. The specimen failures were located at one end about 0.013m (0.5 in.) from the titanium doubler. Three tensile specimens, 0.013m (0.5 in.) by 0.15m (6 in.), were prepared from the failed end of one of the specimens (see Figure 12-94) and tested at room temperature. The results along with the baseline and 10,000 hour residual strength data are given in Table 12-39. As the long-term specimens still retained over 50% of their tensile strength it was decided to continue flight simulation testing with the revised specimen configuration show in Figure 12-94. This configuration proved to be satisfactory with the three 25,000 hour specimens completing testing and the other three lasting about 30,000 hours before failure.

With the exception of the 25,000 hour B/Al specimens, four of which survived the 25,000 hours, all of the remaining specimens failed to complete 50,000 hours. Failure times varied from 17,709 hours to 31,447 hours for the crossply material and 12,605 hours to 31,584 hours for the unidirectional material. With the exception of the 12,605 hour specimen, all of the other failures were believed to have been the result of wearout from the thermal/fatigue cycling.

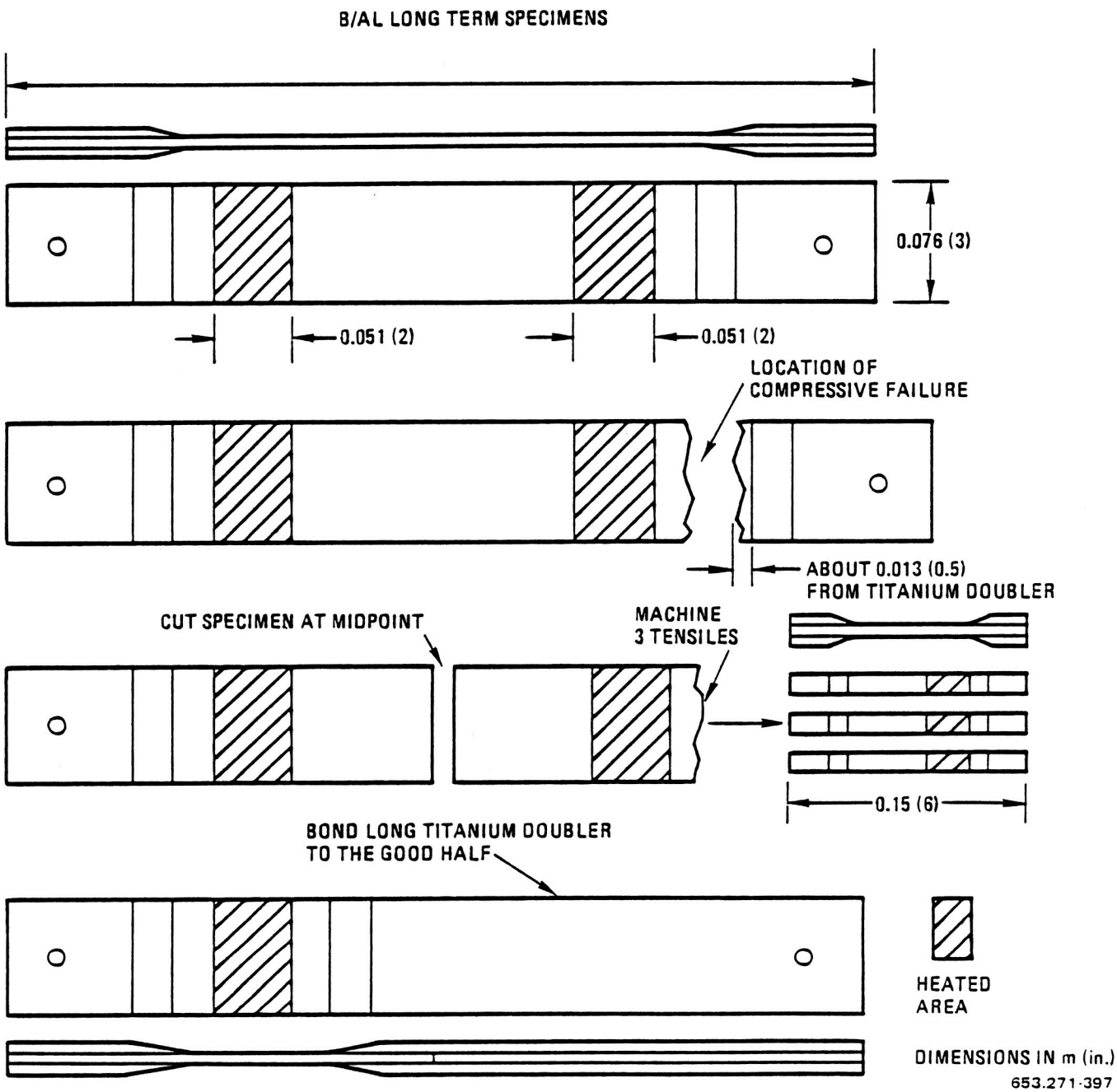



**Figure 12-94 Plan for Salvaging Crossplied B/Al Simulation Specimens Damaged by Compressive Overload**

**Celion 6000/LARC-160 G/PI.** Ten specimens each of unnotched and notched configuration were prepared from crossplied material.

Two problems occurred at the start of exposure testing of this system. The first, premature failure of two specimens, as discussed earlier in Section 12.6.3 was corrected by recalculating the peak loads. The second was a series of doubler bond failures after 0.5 hour, 13 hours, and 24 hours.

Table 12-39. Unnotched Tensile Strength of $[0° \pm 45°]_s$ B/Al Before and After Flight Simulation Exposure

| Exposure Time (hr) | Strength $MN/m^2$ | (ksi) |
|---|---|---|
| Baseline | 516 | 74.8 |
| 10,000 | 379 | 55.0 |
| 20,957 | 268 | 38.8 |

In an attempt to solve the second problem all of the specimens were removed from the flight simulation apparatus and new sets of titanium doublers were bonded to their ends. Removal of the original doublers was quite difficult, and some surface damage occurred on 80% of the specimens. The location, type, and extent of damage was noted and recorded for each specimen. Surface preparation techniques were the same as those used successfully during Phases I, but a new batch of the HT-424 adhesive was used. One change was the addition of a clamping device near the tip of the doublers in the tapered portion. This technique was used successfully on the B/Al specimens where the high flight simulation loads had caused numerous doubler failures during the short-term test program. After installation of the clamps no further doubler bond failures occurred.

With the exception of the two early failures, all of the Celion 6000/LARC-160 specimens completed 10,000 hours of exposure and were tested for residual strength properties.

As the Phase II specimens of the five composite systems were removed from simulation testing (as a result of completing 10,000 hours or 25,000 hours, because of failure or extensive damage, or, as for the epoxy specimens, after 36,374 hours to ensure sufficient material for residual strength testing), they were examined visually with the aid of a stereo microscope and photographed. Residual strength testing plans were formulated including the use of the unfailed ends of failed specimens. Cutting plans were prepared and the long-term specimens were machined into residual strength specimens, which were then tested. The results of the specimen examinations and residual strength tests are presented in the following sections.

#### 12.7.3.1 Post-Simulation Examinations — Phase II.

**B/E, $[0° \pm 45°]_s$, unnotched.** The replacement specimens of B/E completed 10,000 hours of flight simulation exposure at 373K (212°F). All of the specimens survived the 10,000 hours without fracture. The condition of the specimens was excellent. There were no loose surface fibers and no edge cracks or delaminations as had been observed on the Phase I specimens exposed at 408K (275°F). Distinct color changes were visible on the B/E specimens at the heated zones on both sides. Photographs showing both sides of three of the 10,000 hour specimens are presented in Figures 12-95 and 12-96. Examination of the surface of the specimens at 20 to 100× magnification revealed a network of fine cracks in the heated zones but none in the areas that were not heated. Similar microcracking was found on the heated zones of the Phase I long-term specimens of B/E and G/E after 10,000 hours but not on the HT-S/710 G/PI specimens exposed at 505K (450°F) for 10,000 hours. Neither the 10,000 hour thermal aging specimens or the 100 and 200 hour short-term specimens of either B/E or G/E experienced microcracking.

ORIGINAL PAGE IS
OF POOR QUALITY

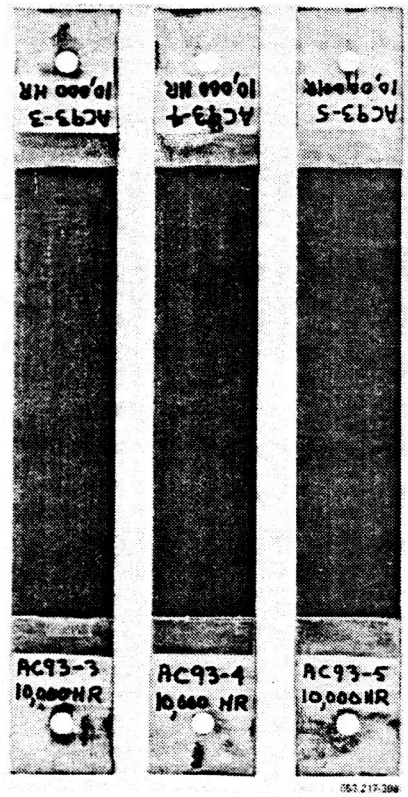



**Figure 12-95 B/E Long-Term Specimens After 10,000 hr of Flight Simlation Exposure — 373K (212°F)**

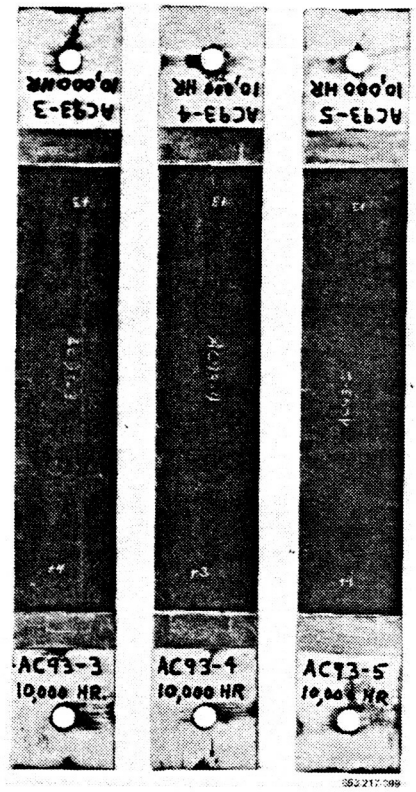



**Figure 12-96 B/E Long-Term Specimens After 10,000 hr of Flight Simulation Exposure — 373K (212°F) (Opposite sides of specimens in Figure 12-95)**

These observations indicate that some combination of extended thermal exposure, thermal cycling and fatigue loading are necessary for the initiation of surface microcracks in the epoxy matrix.

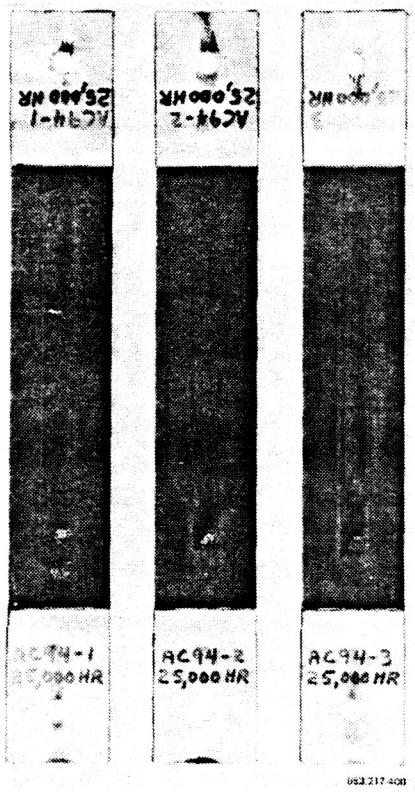
The replacement specimens of B/E also completed 25,000 hours of flight simulation exposure at 373K (212°F) without fracture. The condition of the specimens, as shown in Figures 12-97 and 12-98, was excellent. There were no loose surface fibers and no edge cracks or delaminations as had been observed on the Phase I specimens exposed at 408K (275°F) for much shorter periods of time. The only readily noticeable effects were distinct color changes at the heated zones on both sides. Again, examination of the surface of the specimens at 20× magnification revealed a network of fine cracks in the heated zones similar to those seen after 10,000 hours. In general, the 25,000 hour specimens were very similar in appearance to the specimens that had been removed after 10,000 hours of exposure.

Two of the B/E specimens failed during flight simulation exposure after passing the 33,000 hour mark. As shown in Figure 12-99, failure occurred in the heated zone for both specimens and appeared to have been the result of wearout from the thermal and fatigue environment. Figure 12-100 shows a closeup view of one of the fractures with numerous bare longitudinal boron fibers visible.

The failure mechanism for the two B/E long-term specimens, in like manner to that previously described for the Phase I G/E long-term failures, was a combination of several effects. Matrix degradation, in the form of microcracking in the heated zones, occurred through a combination of oxidation and fatigue loading. Both were necessary, i.e., microcracking was not observed on thermal aging specimens (no applied stresses) nor was it found to any extent in the center portion of the flight simulation specimens (no heating). As the microcracking progressed with exposure time, small portions of resin became loosened and the outer boron fibers (longitudinal) were no longer supported. During the one compressive load in each 2 hour cycle the outer [0°] fibers that were free could no longer carry the compressive load, which was dumped into the weaker [45°] fibers. The microcracking and loss of resin also opened additional paths for oxidation into the inner plies, further destroying the load-bearing capabilities of the composite. Delamination of the outer [0°] plies as a result of thermal cycling stresses and fatigue loading may also have contributed to failure. This effect was not as evident in the B/E failures as it was in the Phase I G/E failures, however. Examination of the lower heated zones (unfailed ends) of these two specimens revealed some loosened and broken boron fibers similar to those observed on the Phase I B/E specimens after 10,000 hours. Lowering the maximum flight simulation temperature from 408K (275°F) to 373K (212°F) greatly delayed the onset of surface microcracking sufficient to expose the outer layer of boron fibers.

After 36,374 hours of exposure some loose surface fibers were observed on the remaining three specimens. To ensure sufficient material for residual strength testing, the flight simulation tests were halted for both epoxy systems. The likelihood of completing 50,000 hours appeared to be small with the two earlier failures after 33,000 hours. The three specimens are shown in Figures 12-101 and 12-102. In general, the specimens were in good condition. Examination at 25× showed some microcracking in the heated zones with occasional loose boron fibers. There were distinct color changes but no edge cracking.

Metallographic and SEM examinations were conducted on B/E long-term specimens exposed for 10,000, 25,000, and 36,374 hours. In like manner to the thermal aging specimens, no time-dependent oxidation similar to that for G/E specimens was observed. This can be seen in the




ORIGINAL PAGE IS
OF POOR QUALITY

**Figure 12-97 B/E Long-Term Specimens After 25,000 hr of Flight Simulation Exposure — 373K (212°F)**

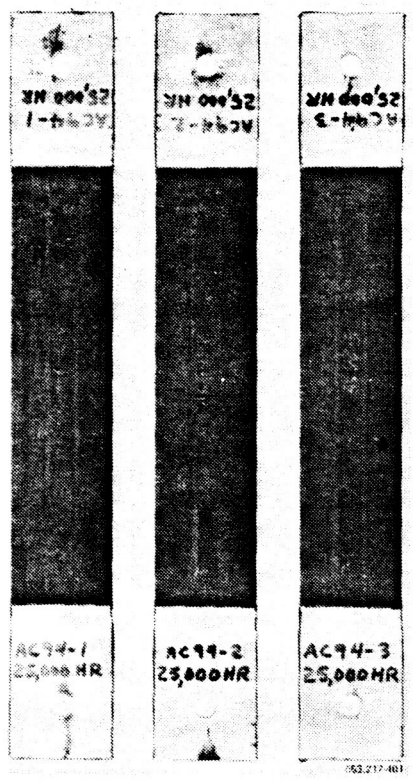



**Figure 12-98 B/E Long-Term Specimens After 25,000 hr of Flight Simulation Exposure — 373K (212°F) (Opposite sides of specimens in Figure 12-97)**

ORIGINAL PAGE IS
OF POOR QUALITY

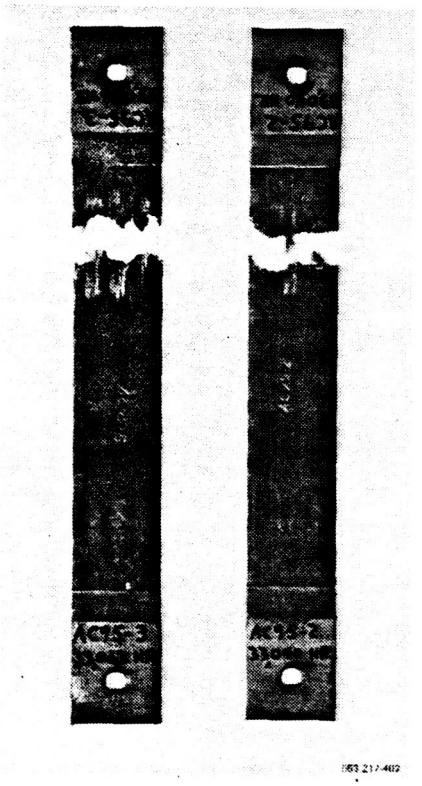


**Figure 12-99 B/E Long-Term Specimens That Failed During Flight Simulation Testing Before Completion of 50,000 hr of Exposure**

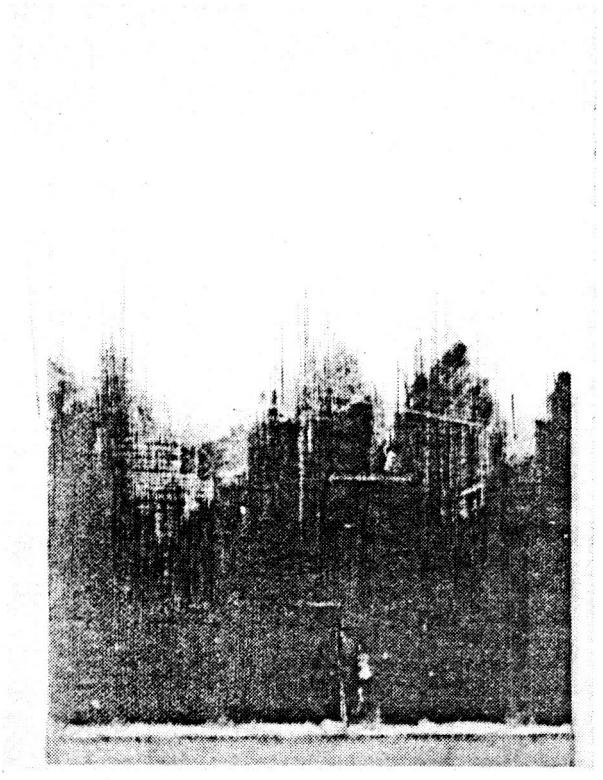


**Figure 12-100 B/E Long-Term Specimen AC95-3 Showing Fracture Appearance After Failure in 33,063 hr (Loss of resin from around boron fibers is readily apparent)**

ORIGINAL PAGE IS
OF POOR QUALITY

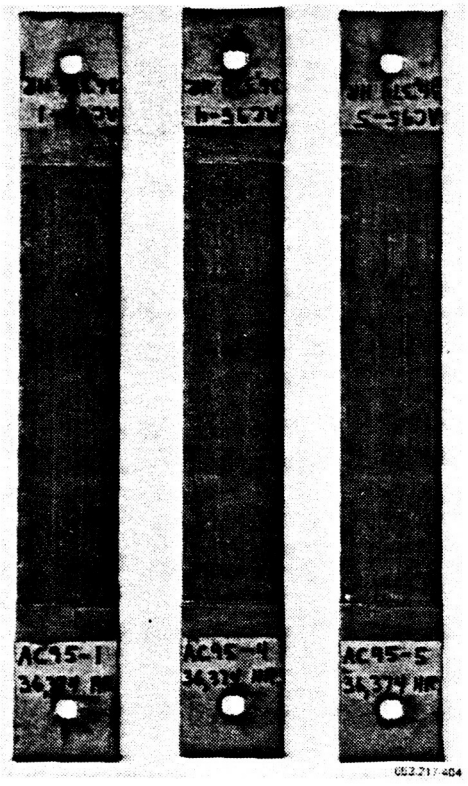



Figure 12-101 B/E Long-Term Specimens After 36,374 hr of Flight Simulation Exposure — 373K (212°F)

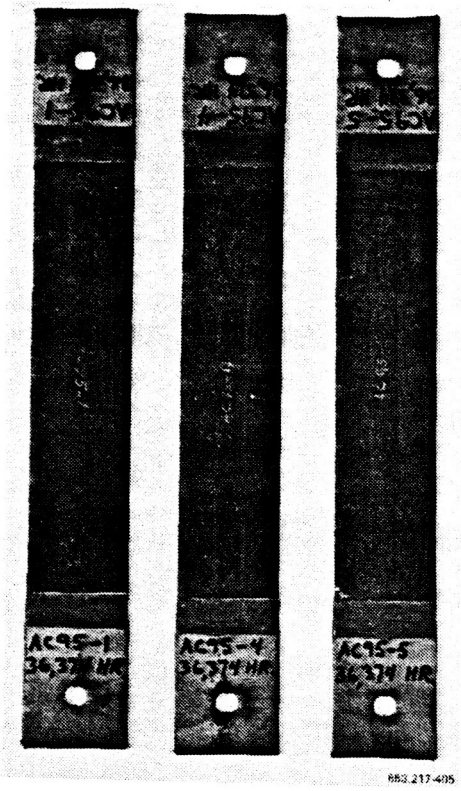



Figure 12-102 B/E Long-Term Specimens After 36,374 hr of Flight Simulation Exposure — 373K (212°F)
(Opposite sides of specimens in Figure 12-101)

SEM photomicrographs in Figure 12-103. The effect of relief polishing around the individual fibers that increases with the degree of oxidation of the epoxy resin, as found for the G/E system, is not present in this series of photos. What can be seen, however, is an increase in matrix cracking with flight simulation exposure. The effect is first visible in the 25,000 hour specimen with the loss of small pieces of resin at many of the fiber-matrix interfaces. After 36,374 hours resin loss has increased, and considerable matrix cracking is present between the fibers. Based on the thermal aging results for B/E thermal exposure alone is not sufficient to cause either surface microcracking or matrix microcracking. The flight simulation results show that the combination of fatigue loading and thermal exposure are responsible for the microcracking observed in the B/E system. Thermal cycling may also contribute to the effect.

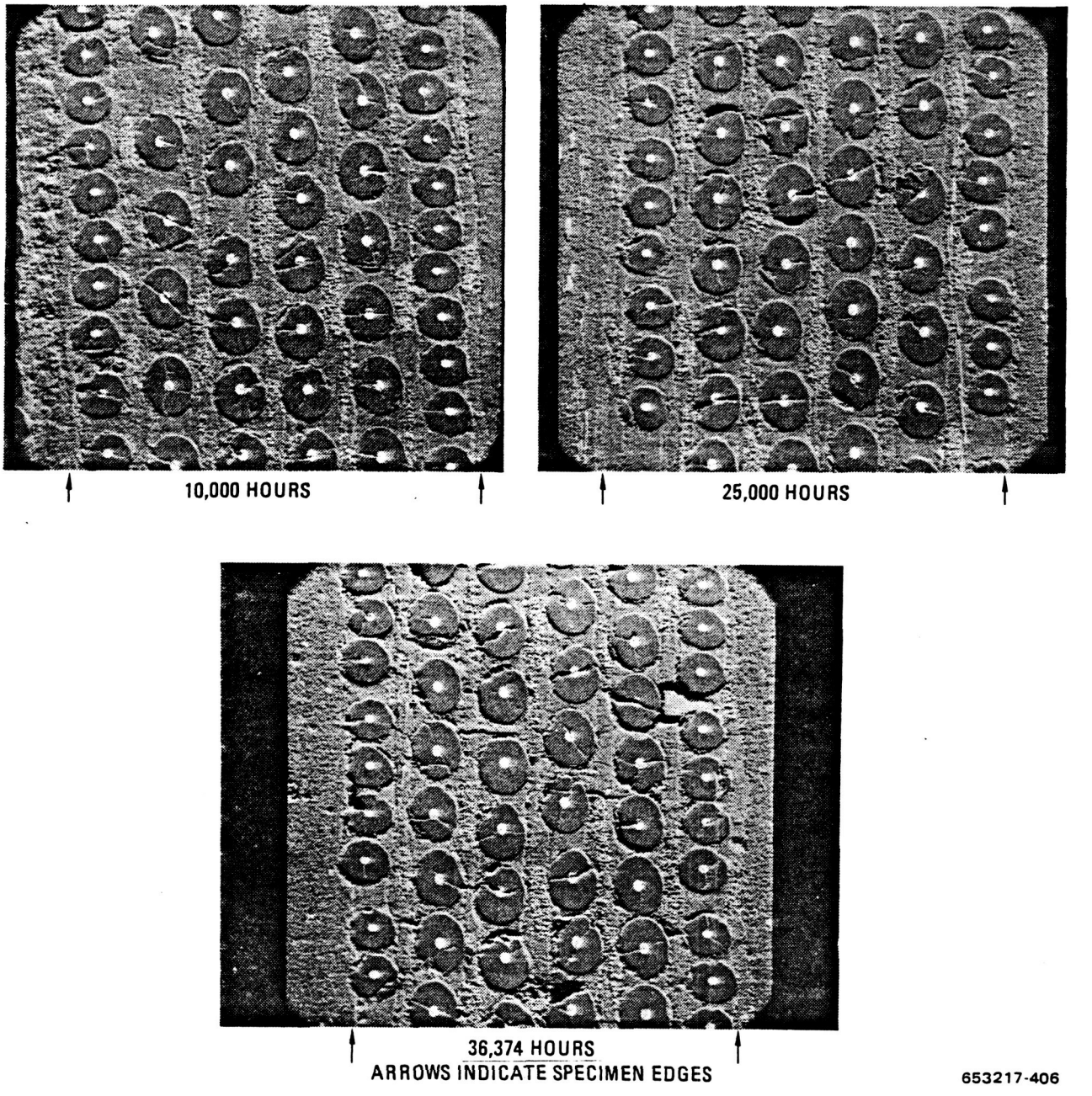



**Figure 12-103 Photomicrographs (SEM) of B/E After Flight Simulation Exposure — 373K (212°F), 100X**



ORIGINAL PAGE IS
OF POOR QUALITY

ORIGINAL PAGE IS
OF POOR QUALITY

**G/E, $[0° \pm 45°]_s$, unnotched.** The replacement specimens of G/E performed even better than the B/E during flight simulation exposure at 373 K (212 °F). All 13 specimens completed exposure cycling (36,374 hours) without failure. Comparing this with the Phase I G/E results (eight of 10 failures at 408K (275 °F) in 10,000 hours) shows the great influence that the maximum test temperature had on exposure life. Both the 10,000 hour and the 25,000 hour specimens were in excellent condition at the completion of exposure. There were no loose surface fibers, edge cracks, or delaminations. Inspection with a stereo microscope revealed a network of fine cracks in the heated zones of both the 10,000 hour and 25,000 hour sets of specimens. After 36,374 hours of flight simulation the specimens showed increased effects of the exposure. In the heated zones numerous graphite fibers were visible where the outer layer of epoxy resin appeared to have eroded away. Figure 12-104 shows a magnified view of one of these regions of exposed fibers. Increased microcracking and color changes were also present in these specimens. Even so, the condition of the specimens as shown in Figures 12-105 and 12-106 was quite good for 36,374 hours of testing.

As discussed in the thermal aging section, the extent of oxidation of the G/E could be readily detected by metallographic techniques, especially with the SEM. To study the degree of oxidation, as well as the amount of microcracking of the matrix as a result of flight simulation exposure, specimens were examined after 10,000, 25,000, and 36,374 hours. Figures 12-107 and 12-108 are metallographic and SEM results showing the entire cross section for the three exposure periods. The metallographic photomicrographs, Figure 12-107, while not showing the effects of oxidation as clearly as the SEM, do show the increase in microcracking with exposure time. These cracks appear to initiate at the surface and have penetrated the outside ply after 25,000 hours of exposure.

After 36,374 hours, cracks are also observed in the second plies although not always lined up with outside ply cracks. Very little microcracking of this type was observed in the G/E thermal

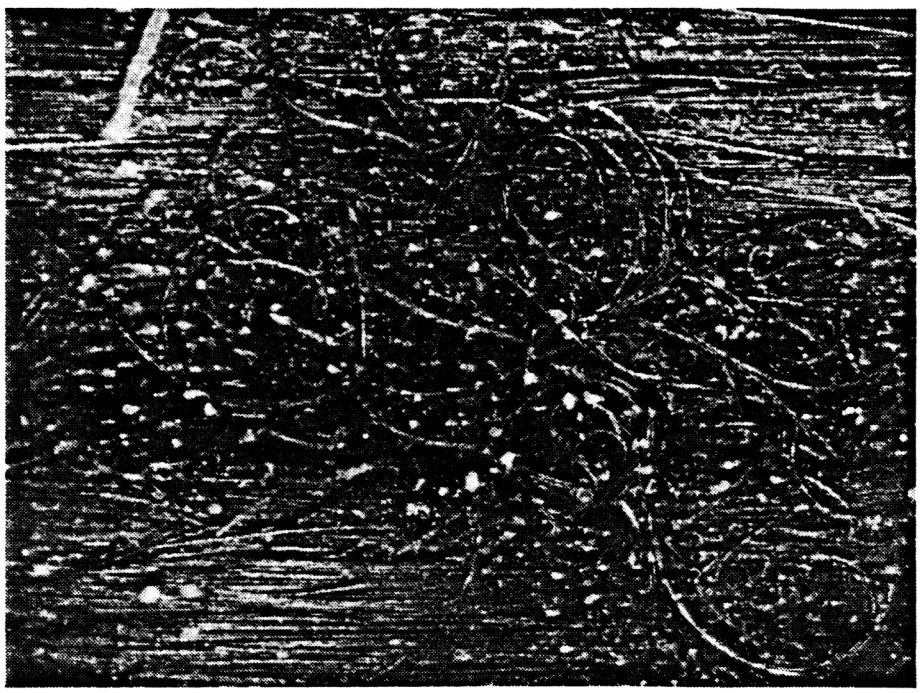


**Figure 12-104 Magnified View of Surface of G/E Specimen BC95-3 After 36,374 hr of Flight Simulation Showing Loose Graphite Fibers**

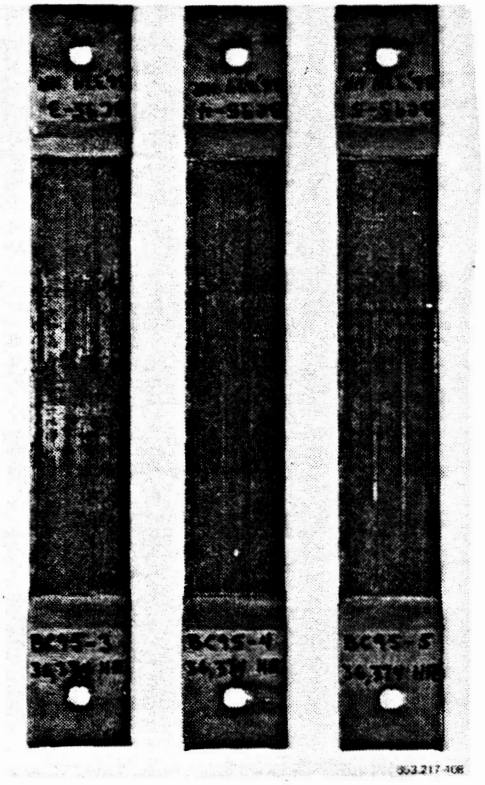
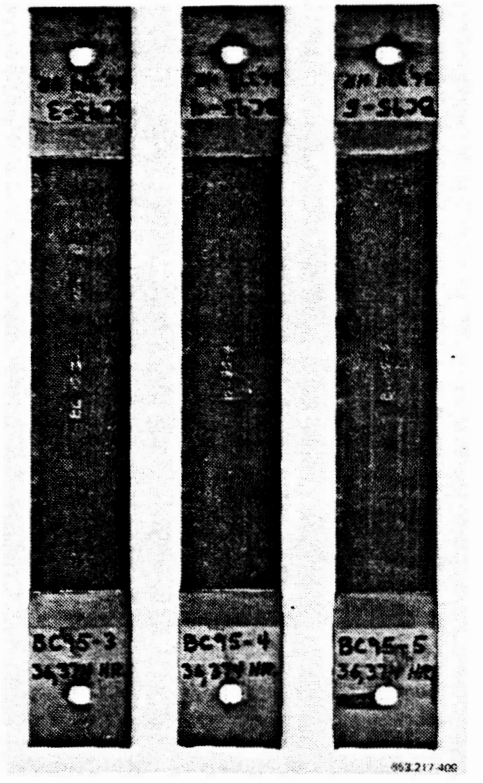


Figure 12-105 G/E Long-Term Specimens After 36,374 hr of Flight Simulation Exposure — 373K (212°F)



ORIGINAL PAGE IS
OF POOR QUALITY

Figure 12-106 G/E Long-Term Specimens After 36,374 hr of Flight Simulation Exposure — 373K (212°F)
(Opposite sides of specimens in Figure 12-105)

ORIGINAL PAGE IS
OF POOR QUALITY

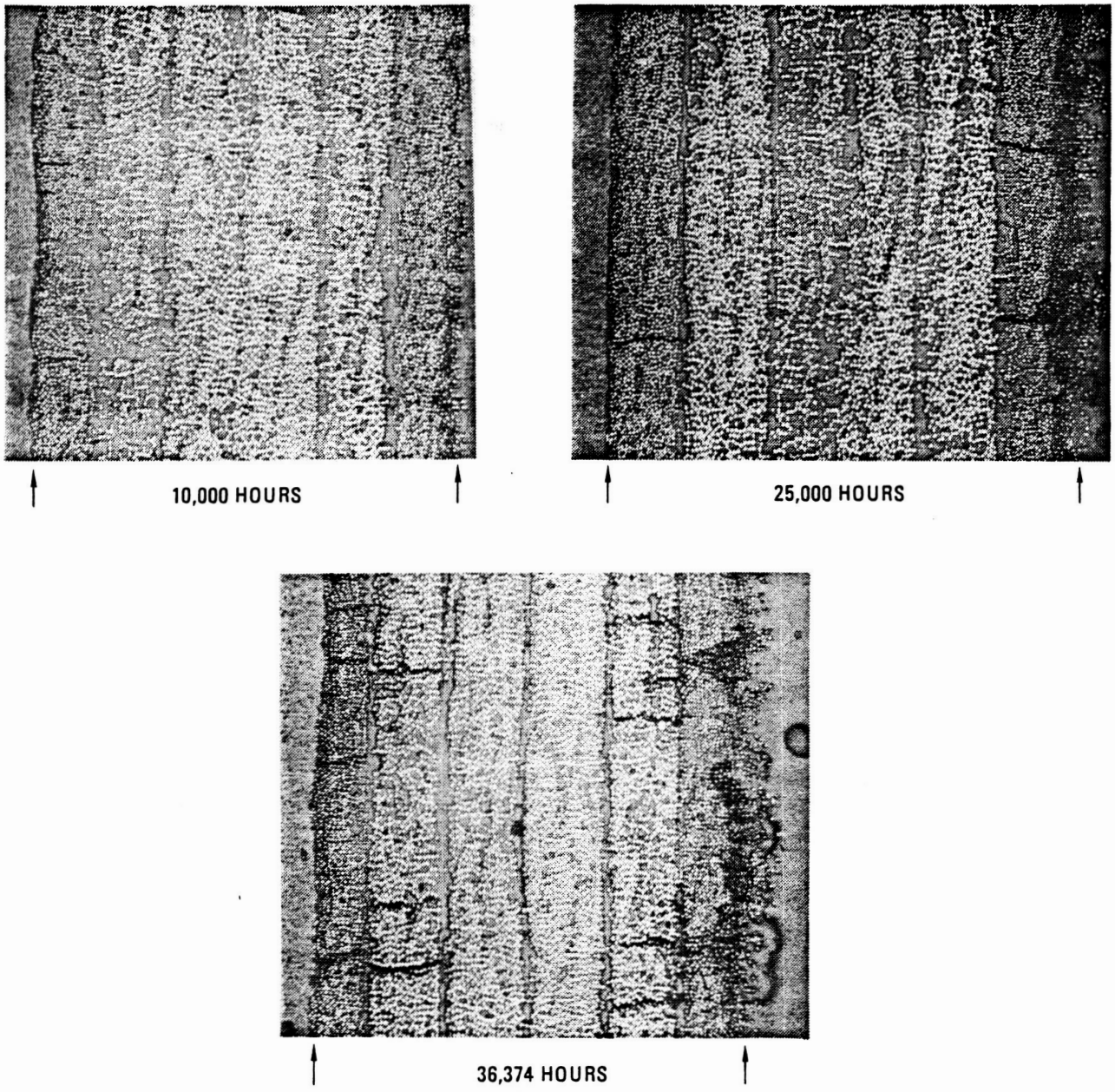
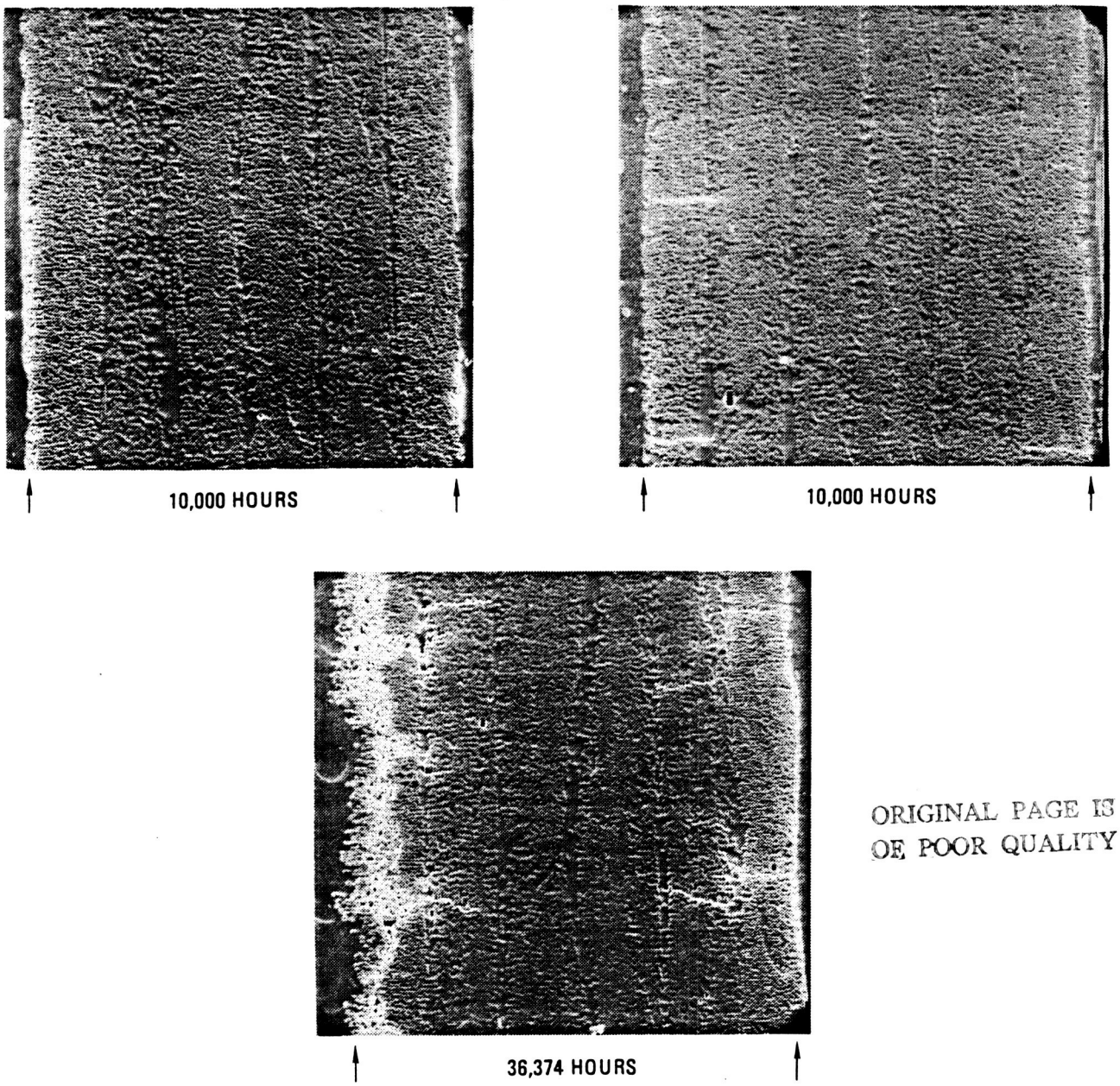



**Figure 12-107 Photomicrographs (Metallograph) of G/E After Flight Simulation Exposure — 373K (212°F), 100X**

aging specimens. The SEM photomicrographs, Figure 12-108, in addition to showing the extent of microcracking, also clearly show the increase in oxidation with exposure time. The lighter cast, beginning at the specimen edges and spreading inward with exposure time, was shown in the thermal aging study to be related to oxidation of the epoxy resin.

The changes from dark to light are caused by the amount of relief polishing around the individual fibers that increases with the degree of oxidation. When the epoxy resin oxidizes, it is more




ORIGINAL PAGE IS
OE POOR QUALITY

**Figure 12-108 Photomicrographs (SEM) of G/E After Flight Simulation Exposure — 373K (212°F), 100X**

prone to crumble, and differences in the amount of oxidation in the polished mounts can easily be detected using the SEM. As would be expected, oxidation proceeds inwardly along the cracks at a faster rate than through the matrix. This effect is clearly shown in Figure 12-108.

Slight oxidation at the outer edges is visible after 10,000 hours, increases somewhat after 25,000 hours, and is considerable after 36,374 hours. Higher magnification views of the outer plies of specimens aged for these three time periods are shown in the SEM photomicrographs of Figure 12-109. The effect of oxidation on the amount of relief polishing around the graphite

fibers shows the slight increase in oxidation from 10,000 hours to 25,000 hours and the considerable increase after 36,374 hours.

In comparison with thermal aging results, the flight simulation exposures at 373K (212°F) produced less oxidation than either the 394K (250°F) ambient or 450K (350°F) reduced pressure exposures after comparable time periods. The effect of the fatigue loading and the thermal cycling during flight simulation testing produced matrix microcracking but did not appear to increase the rate of oxidation normally experienced during thermal aging.

**HT-S/710 G/PI $[0° \pm 45°]_s$, unnotched and notched.** In contrast to the excellent performance of the G/E material, all of the HT-S/710 G/PI specimens failed during flight simulation exposure at maximum temperatures of 505K (450°F) or were removed from test because of such poor condition that failure was imminent. Table 12-40 lists the G/PI long term flight simulation specimens with their respective failure times. Three of the specimens in Table 12-40 failed at the same time, one after less than 6000 hours and the other two just prior to 16,000 hours. An investigation of the specimens and the circumstances of the incident indicated that the initial

**Table 12-40. Summary of HT-S/710 G/PI Flight Simulation Exposure Specimen Failures**

| Specimen Number | Specimen Type | Exposure Hours at Failure | Test Series (Hours) | Comments |
|---|---|---|---|---|
| DC92-1 | Unnotched | 15,896 | 50,000 | (a) |
| DC92-2 | Unnotched | 15,896 | 50,000 | (a) |
| DC92-3 | Unnotched | 39,856 | 50,000 | Wearout failure in heated zone |
| DC92-4 | Unnotched | 39,856 | 50,000 | Wearout failure in heated zone |
| DC92-5 | Unnotched | 19,400 | 50,000 | Wearout failure in heated zone |
| DC93-1 | Unnotched | 0 | 25,000 | Damaged during installation |
| DC93-2 | Unnotched | 0 | 25,000 | Damaged during installation |
| DC93-3 | Unnotched | 5,760 | 25,000 | (a) |
| DC91-S | Unnotched | 15,021 | Spare | Wearout failure in heated zone |
| DF92-1 | Notched | 18,302 | 50,000 | (b) |
| DF92-2 | Notched | 18,302 | 50,000 | Wearout failure in heated zone |
| DF92-3 | Notched | 27,890 | 50,000 | (b) |
| DF92-4 | Notched | 20,398 | 50,000 | Failure in tensile overload |
| DF92-5 | Notched | 27,890 | 50,000 | Wearout failure in heated zone |
| DF92-S | Notched | 17,852 | Spare | Wearout failure in heated zone |

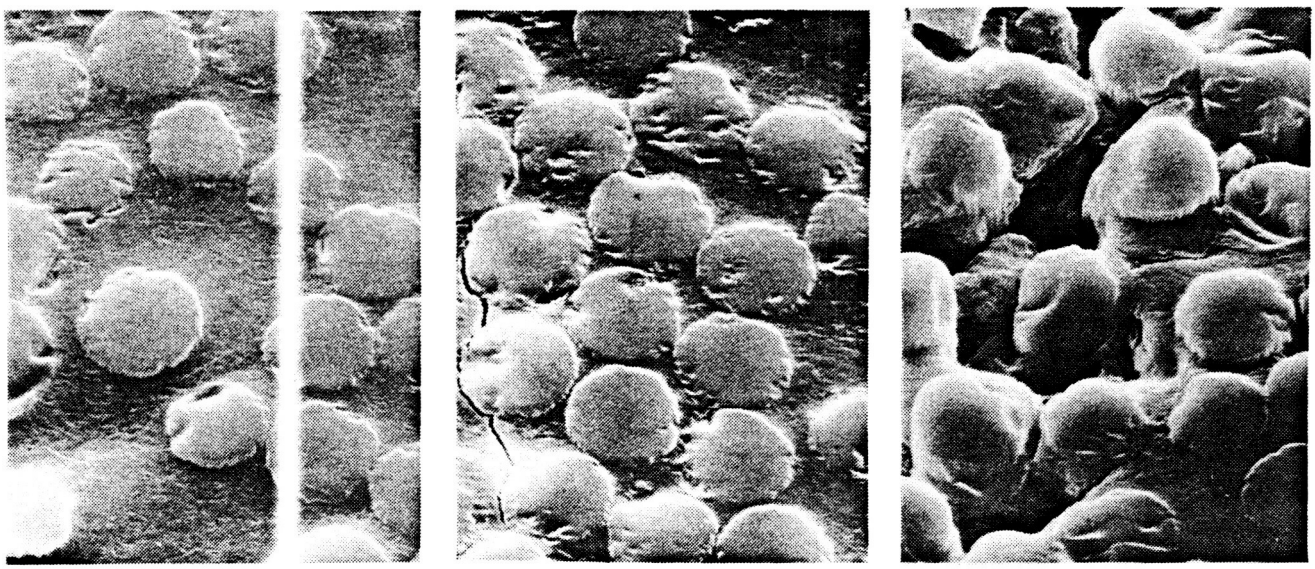
(a) All failed at the same time, see text.
(b) Did not fail but removed from test because of poor condition

ORIGINAL PAGE IS
OF POOR QUALITY

failure was to the 6000 hour specimen. This specimen had been fabricated from the screening test material that had previously shown poor thermo-oxidative properties. Failure of the other two specimens could not be explained but did not appear to have been the result of normal wearout from the thermal and fatigue cycling. One other specimen, DF92-4, also failed prematurely after 20,398 hours. Failure was traced to a tensile overload caused by operator error. The bulk of the HT-S/710 G/PI flight simulation failures appeared to be wearout failures from the thermal and fatigue exposure cycling.

Figure 12-110 shows three of the failed specimens. The failures were generally of two types. The earlier failures, e.g., DC92-5 in Figure 12-110, showed more shear transfer between plies than the later failures, DC92-3 and DC92-4 in the same figure. The failure mode for the longer time specimens was more of a flat fracture that was straight across the width, transverse to the loading direction. Somewhat similar fracture behavior was also shown by the notched specimens as shown in Figure 12-111. Here, however, the fracture paths were considerably influenced by the three holes in the center of the heated zones.

Examination of the HT-S/710 G/PI specimens with a stereo microscope showed that the surface microcracking found in the heated zones of the epoxy specimens was not present. Some edge cracking was visible, increasing with exposure time. The major effect of the flight simulation was shown by the loss of polyimide resin at the surface of the heated zones with exposure of the underlying graphite fibers. The amount of loose fibers increased with exposure time as shown in Figures 12-112 and 12-113 for specimens cycled 19,400 hours and 39,856 hours respectively. The specimen failures, usually at the upper heated zones, were characterized by considerable loose fibers and a yellow-orange color at the fracture. In like manner to the thermal aging specimens, these fracture areas also did not show the fuzzy graphite fiber appearance caused by embrittlement of the resin matrix.



10,000 HOURS 25,000 HOURS 36,374 HOURS

653217-412

**Figure 12-109 Photomicrographs (SEM) of G/E After Flight Simulation Exposure — Outside Plies — 373K (212°F), 2500X**



ORIGINAL PAGE IS
OF POOR QUALITY

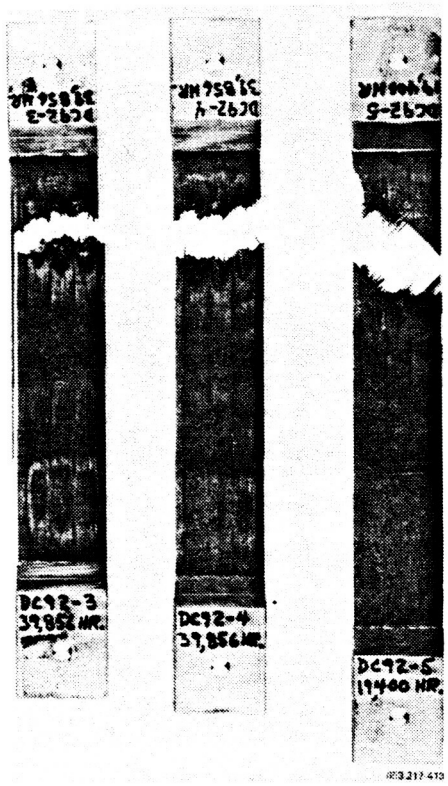
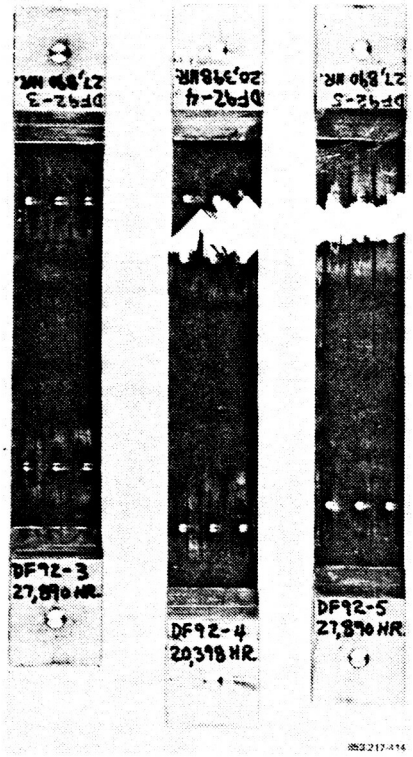



**Figure 12-110 HT-S/710 G/Pl Long-Term Specimens That Failed During Flight Simulation Testing Before Completion of 50,00 hr of Exposure**




ORIGINAL PAGE IS
OF POOR QUALITY

**Figure 12-111 HT-S/710 G/Pl Notched Long-Term Specimens That Failed During Flight Simulation Testing Before Completion of 50,000 hr of Exposure**

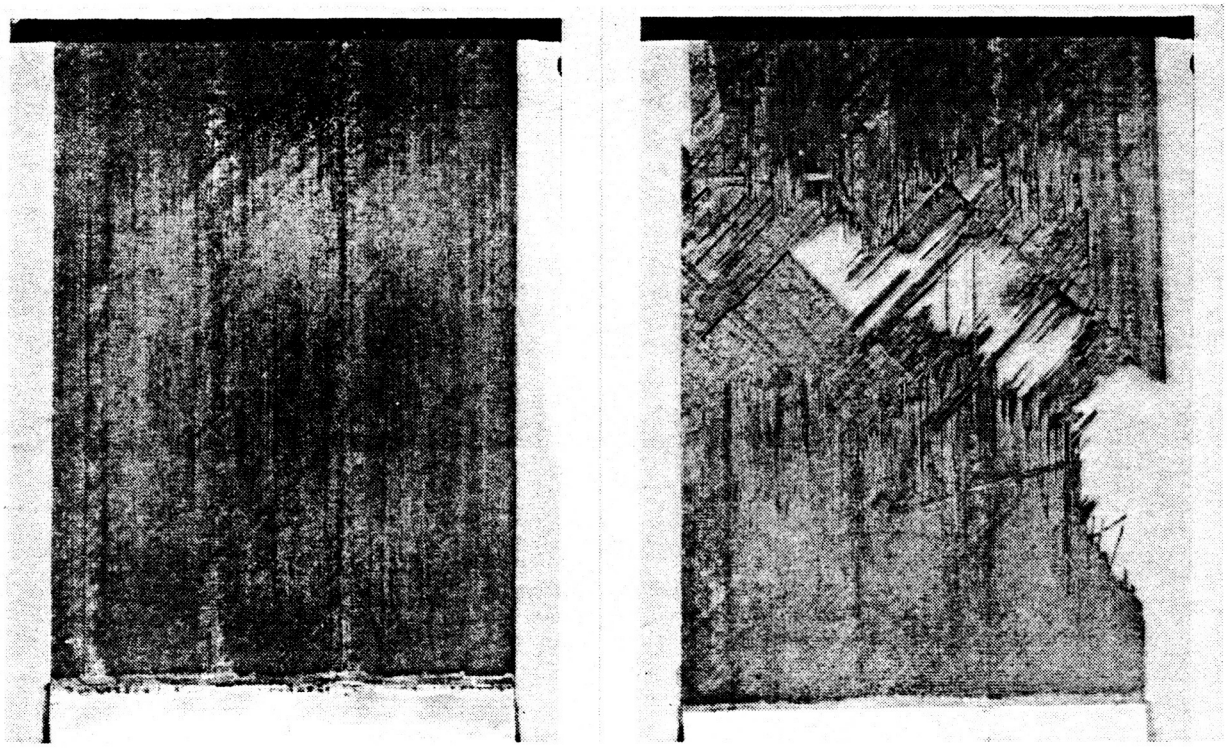


**Figure 12-112 HT-S/710 G/Pl Specimen DC92-5 After 19,400 hr of Flight Simulation Exposure Showing Exposed Graphite Fibers in Heated Zones of Unfailed and Failed Ends**

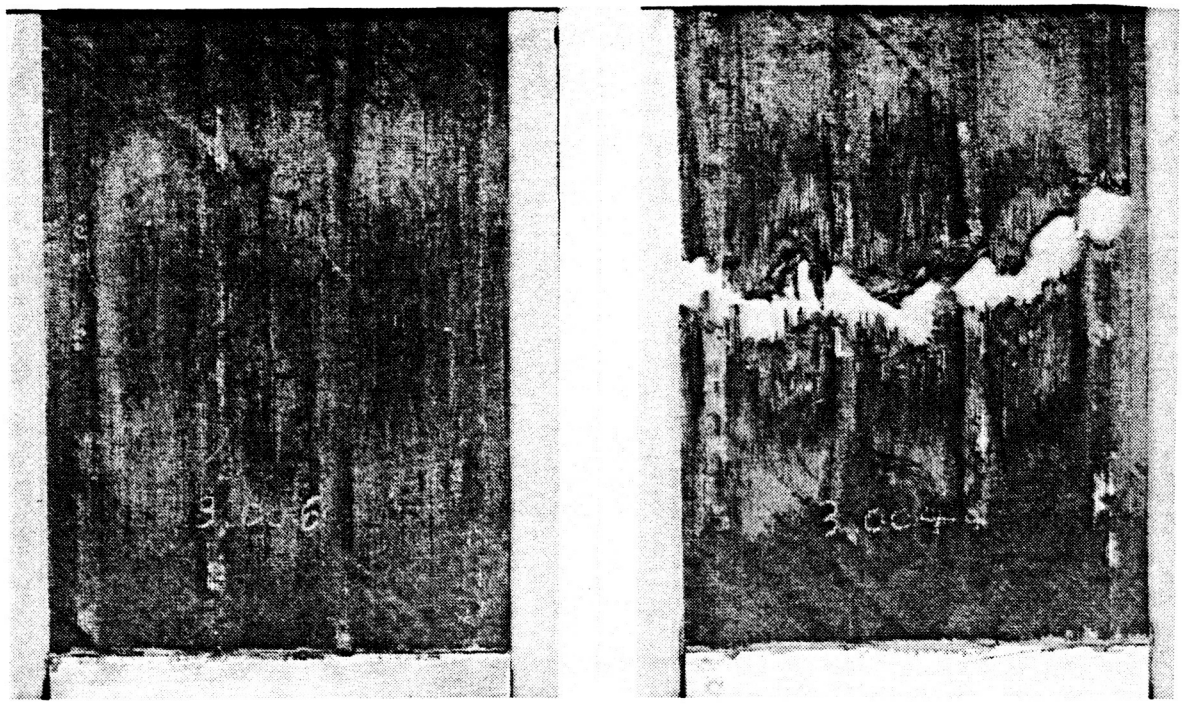


**Figure 12-113 HT-S/710 G/Pl Specimen DC92-3 After 39,856 hr of Flight Simulation Exposure Showing Exposed Graphite Fibers in Heated Zones of Unfailed and Failed Ends**



ORIGINAL PAGE IS
OF POOR QUALITY

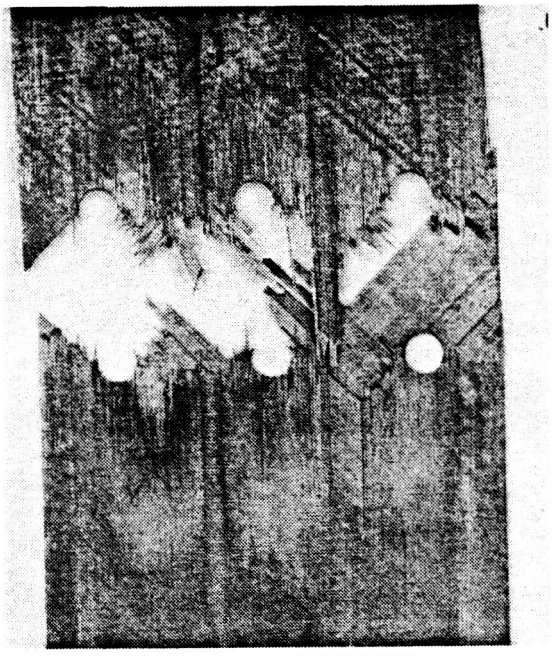
The notched specimens were similar in appearance to the unnotched as to the degree of loose surface fibers, edge cracking, and color changes. Close-up views of the fracture regions of two specimens are shown in Figure 12-114. The nature of the failure for the specimen on the right of the figure, DF92-5, is characteristic of the flat fractures seen for the longer exposure times. The other specimen, DF92-4, failed accidently from a tensile overload. Two of the notched specimens did not fail but were removed from test because of being in very poor condition. Close-up views of the heated zones where considerable damage had occurred are shown in Figure 12-115. An almost continuous series of cracks across the width of each specimen can be seen in the photographs. These specimens offered almost no resistance to bending in these regions.

In addition to edge cracking near the heated zones, the notched specimens also contained numerous cracks or delaminations at the edges of the 0.0064m (0.25 in.) holes. Again, the degree of cracking at the holes increased with exposure time. Figure 12-116 shows close-up views of the three holes at the unfailed end of one of the last notched specimens to be removed from test. This specimen exhibited the most cracks in the regions of the holes of any of the notched specimens.

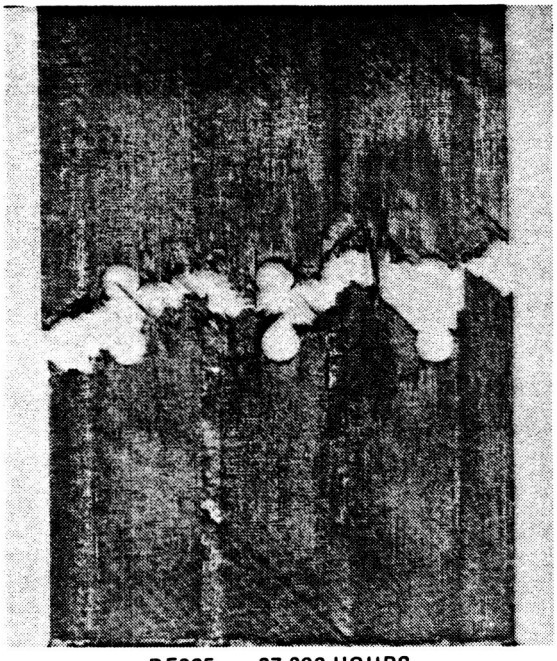
Metallographic and SEM examinations were conducted on HT-S/710 G/PI specimens after 10,000, 19,400, 27,890, and 39,856 hours of flight simulation exposure. The results were similar to those found for the same material after thermal aging at 505K (450 °F) where no metallographic changes were observed until after 50,000 hours. The flight simulation specimens showed neither the matrix cracking or surface oxidation effects typical of those previously described for the G/E flight simulation specimens.

Figure 12-117 contains SEM photomicrographs of cross sections of HT-S/710 G/PI flight simulation specimens after various exposure times. The unexposed as-received material is shown in Figure 8-35. Because of the length of the program, the photomicrographs were prepared at different times by different SEM operators. The as-received and 10,000 hour photomicrographs were shot in the secondary electron mode, the others in the backscattered mode. No changes in the microstructure could be found in the course of the 39,856 hours of exposure.

**Celion 6000/LARC-160 G/PI, $[0° \pm 45°]_s$, unnotched and notched.** All of the Celion 6000/LARC-160 G/PI specimens completed 10,000 hours of flight simulation exposure at maximum temperatures of 450K (350 °F) without failure. At the completion of 10,000 hours, all the specimens were removed from the simulation apparatus for examination prior to residual strength testing. Visually, the specimens were in very good condition as shown in Figures 12-118 and 12-119 for the unnotched configuration and Figures 12-120 and 12-121 for the notched. There were some color changes but generally less than those observed for the epoxy samples after similar exposure times. No loose surface fibers were present in the heated zones of any of the specimens. There were a few edge cracks and some cracking or delamination at some of the holes in the notched specimens. Generally these cracks were not severe. Also found were some surface cracks in the heated zones of both the unnotched and notched specimens. None of these cracks were present in the unexposed material or in the center section of the specimens that were not directly exposed to the quartz lamp heaters. Figure 12-122 shows 25× magnification views of unexposed material, unheated center section material, and material in the heated zones. The longitudinal surface cracks are readily visible in the heated zone. Similar surface cracks were also found on thermal aging samples after 10,000 hours of exposure at both 450K (350 °F) and 505K (450 °F). Examples of these are shown in Figure 12-123.



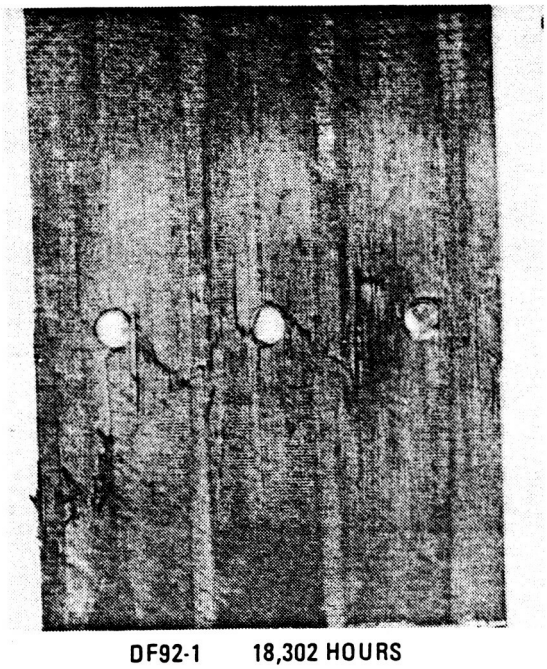
DF924 20,398 HOURS



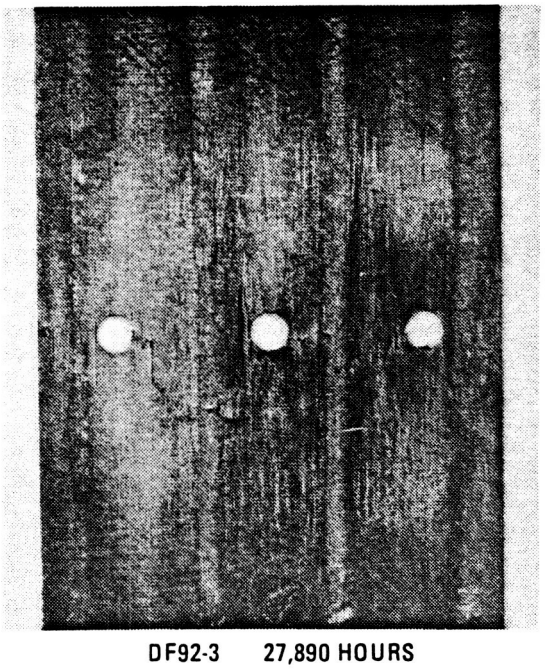
DF925 27,890 HOURS

653217-417

**Figure 12-114 HT-S/710 G/Pl Notched Long-Term Specimens That Failed During Flight Simulation**



DF92-1 18,302 HOURS



DF92-3 27,890 HOURS

653217-418

**Figure 12-115 HT-S/710 G/Pl Notched Long-Term Specimens That Were Removed From Flight Simulation Testing Before Completion of 50,000 hr of Exposure Because of Imminent Failure**



ORIGINAL PAGE IS
OE POOR QUALITY

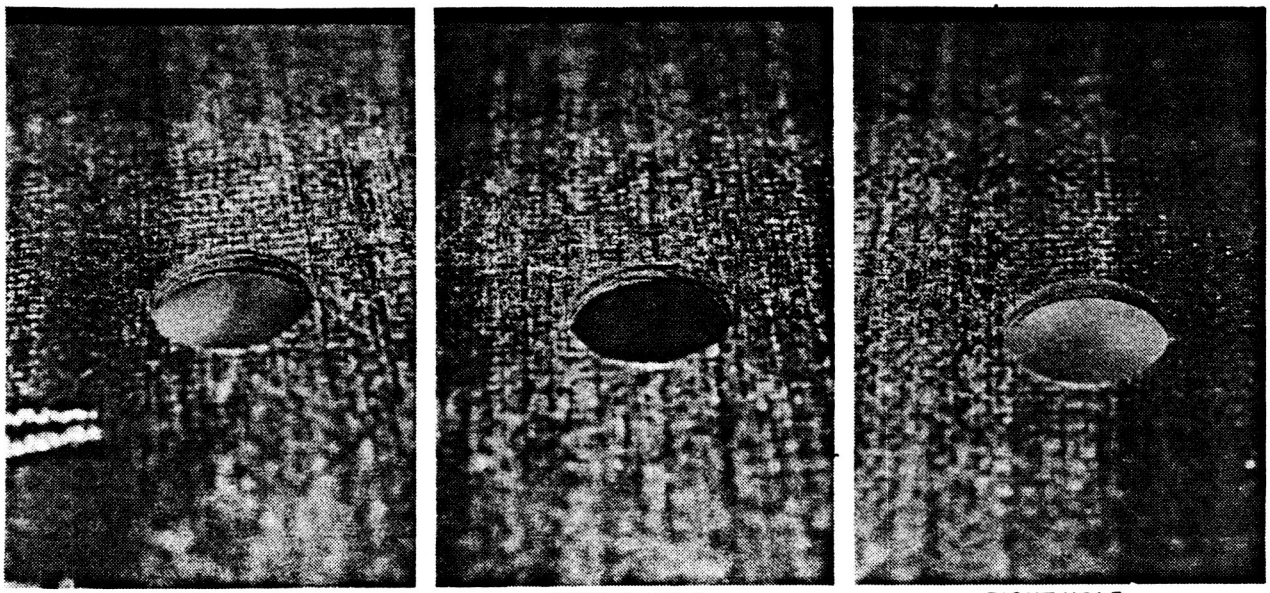



**Figure 12-116 HT-S/710 G/PI Notched Long-Term Specimen DF92-3 After 27,890 hr of Flight Simulation Exposure Showing Variation in Degree of Cracking in Holes Across Width of Specimen**

ORIGINAL PAGE IS
OF POOR QUALITY

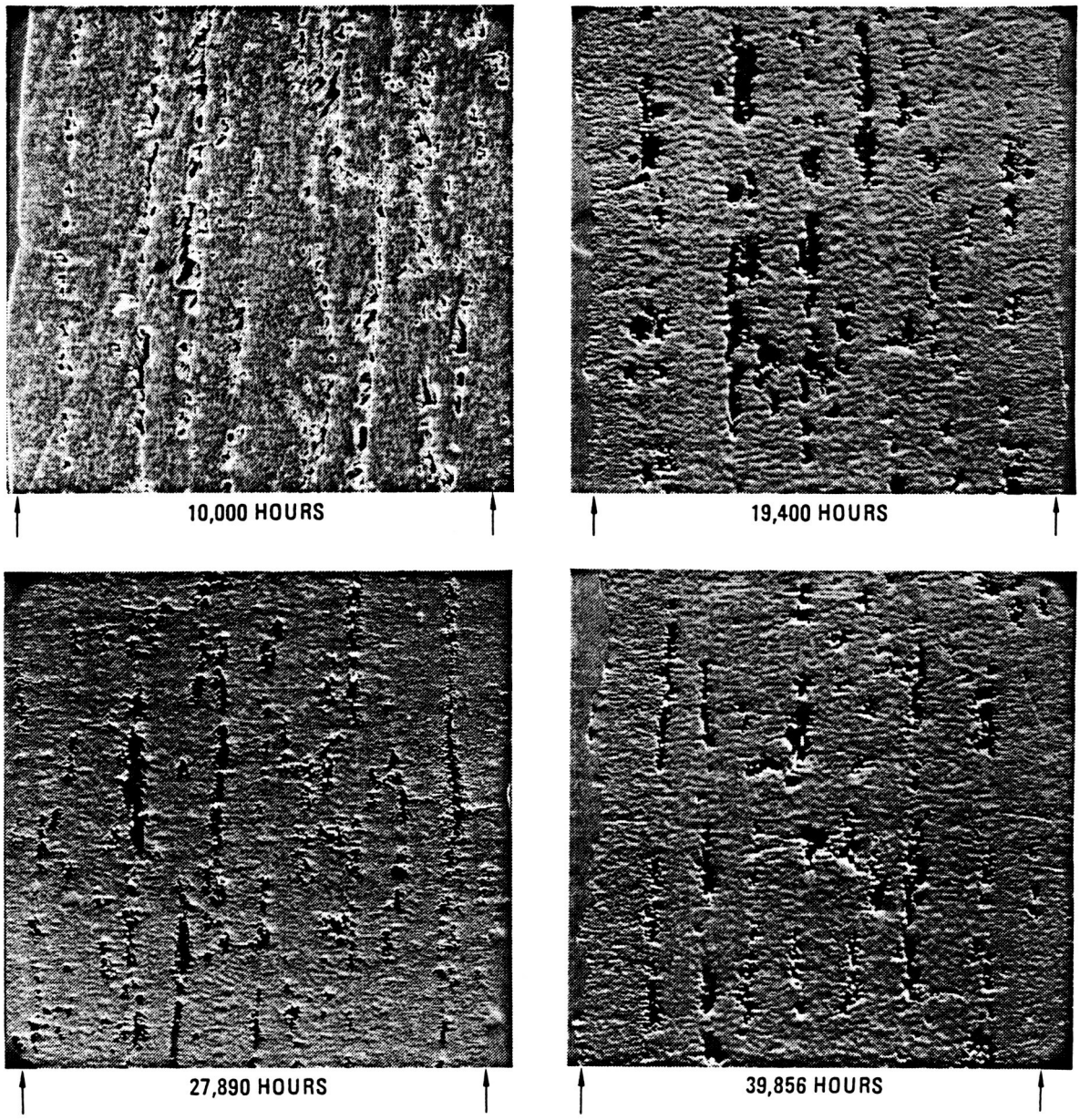



**Figure 12-117 Photomicrographs (SEM) of HT-S/710 G/PI After Flight Simulation Exposure — 505K (450°F), 100X**

It is interesting to note the circumstances under which surface microcracking occurs for the different resin matrix composites. For the epoxies, both thermal exposure and fatigue cycling were required. No surface microcracking was observed for HT-S/710 G/PI on either thermal aging or flight simulation specimens. Finally, for Celion 6000/LARC-160 G/PI, thermal exposure alone was sufficient to cause microcracking while fatigue cycling alone was not.



ORIGINAL PAGE IS
OF POOR QUALITY

ORIGINAL PAGE IS
OF POOR QUALITY

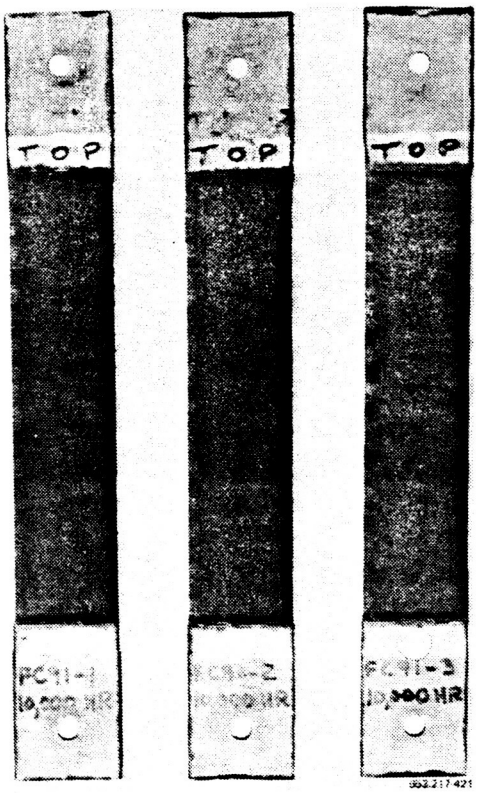



**Figure 12-118 Celion 6000/LARC-160 G/PI Long-Term Specimens After 10,000 hr of Flight Simulation Exposure**

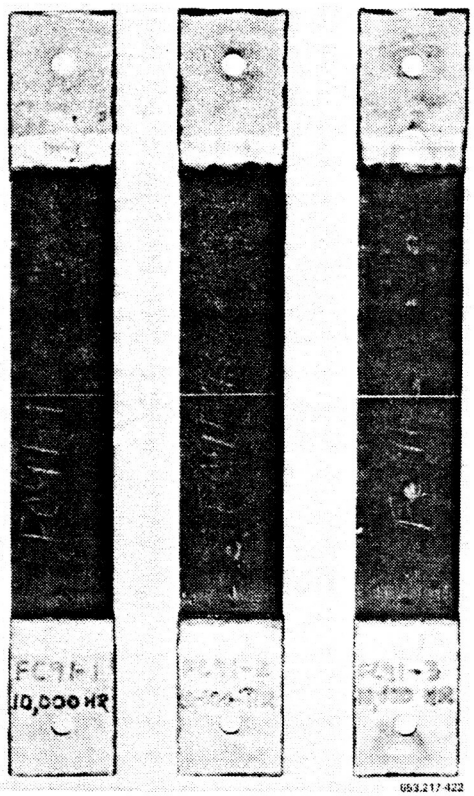



**Figure 12-119 Celion 6000/LARC-160 G/PI Long-term Specimens After 10,000 hr of Flight Simulation Exposure (Opposite sides of specimens in Figure 12-118)**

ORIGINAL PAGE IS
OF POOR QUALITY

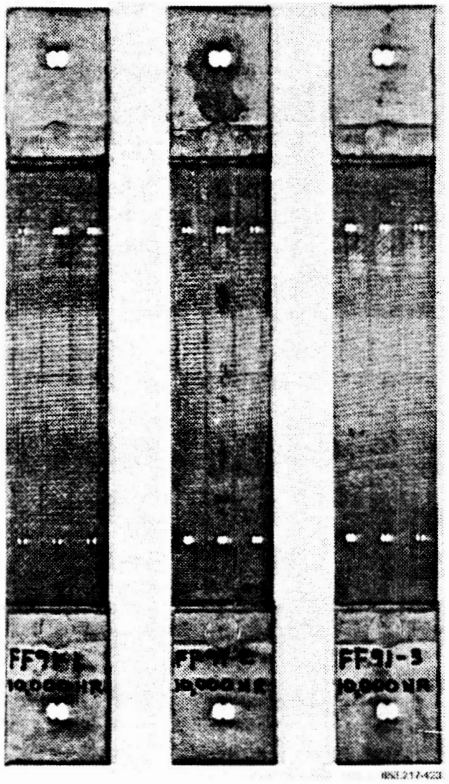



**Figure 12-120 Celion 6000/LARC-160 G/PI Notched Long-Term Specimens After 10,000 hr of Flight Simulation Exposure**

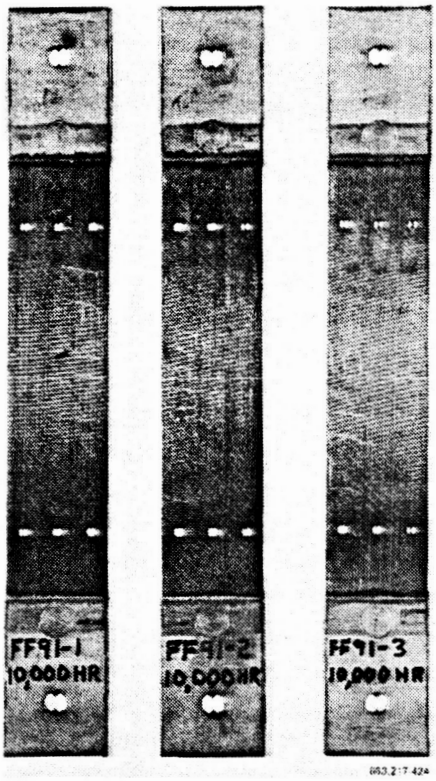
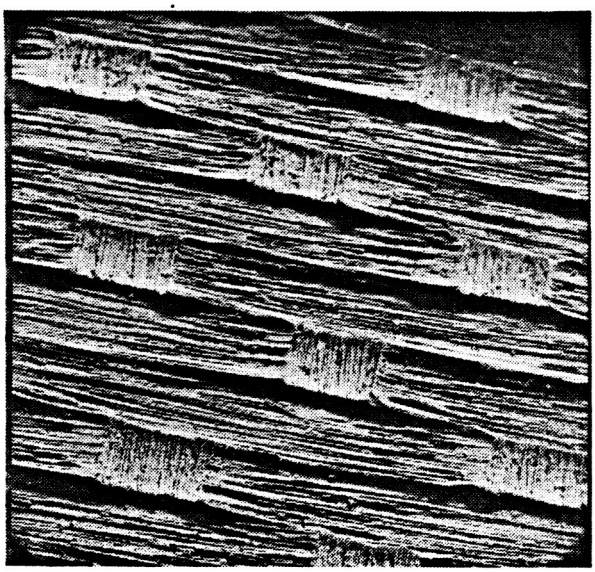
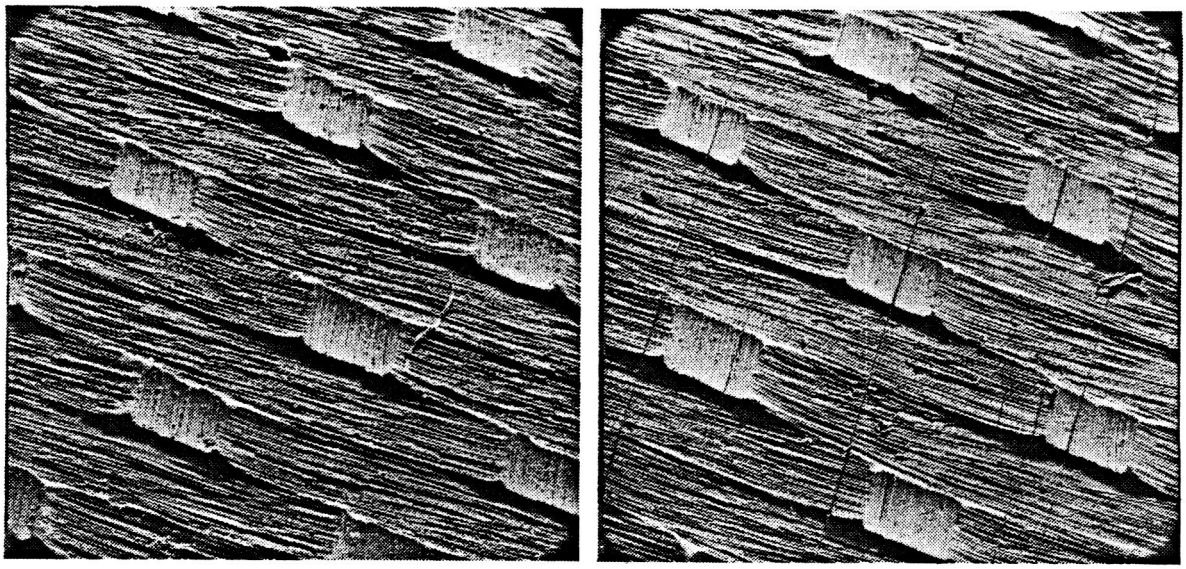



**Figure 12-121 Celion 6000/LARC-160 G/PI Notched Long-Term Specimens After 10,000 hr of Flight Simulation Exposure (Opposite sides of specmens in Figure 12-120)**

ORIGINAL PAGE IS
OF POOR QUALITY



UNEXPOSED



EXPOSED
UNHEATED CENTER SECTION

EXPOSED
HEATED ZONE

653217-425

**Figure 12-122 Photomicrographs (SEM) of Celion 6000/LARC-160 G/PI Before (upper) and After (lower) 10,000 hr of Flight Simulation Exposure, 25X**

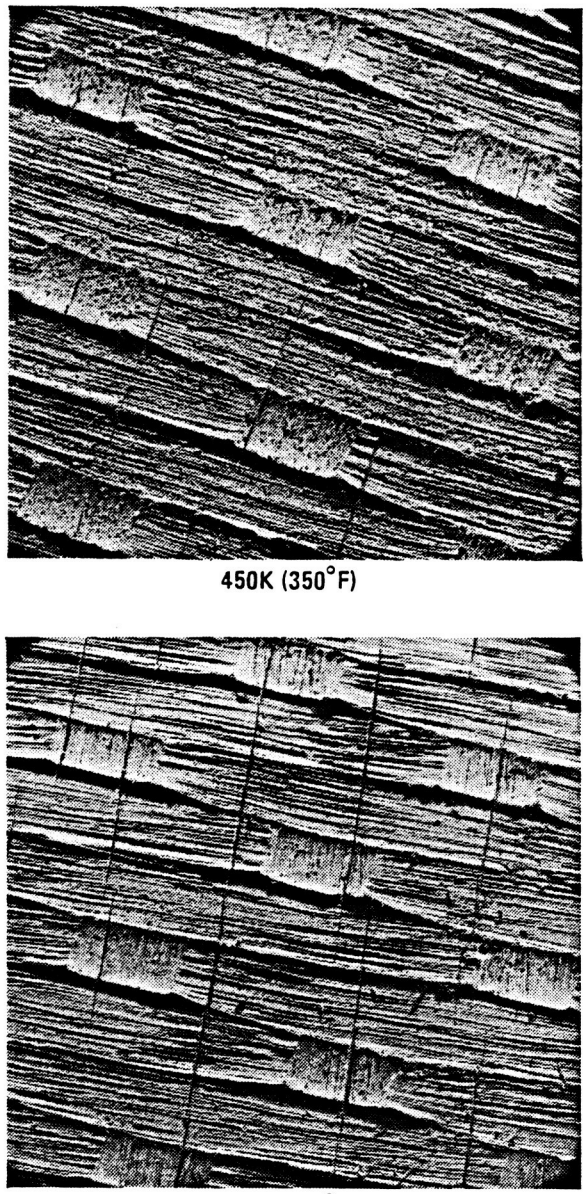



**Figure 12-123 Photomicrographs (SEM) of Celion 6000/LARC-160 G/PI After10,000 hr of Thermal Aging in One Atmosphere Air at Indicated Temperature Showing Surface Microcracks, 25X**

Metallographic and SEM examinations showed the effects of 10,000 hours of flight simulation to be quite similar to 10,000 hours of thermal aging except for an increase in matrix microcracking or void formation. This was not unexpected with the fatigue loading present in the flight simulation exposure cycles. Figure 12-124 shows these differences in the microstructure for the two test conditions after 10,000 hours at 450K (350 °F). At higher magnifications the SEM revealed evidence of oxidation similar to that shown in Figure 8-40 for thermal aging at 450K (350 °F); i.e., considerable oxidation in the outer plies but almost none in the center plies.



ORIGINAL PAGE IS
OF POOR QUALITY

ORIGINAL PAGE IS
OF POOR QUALITY

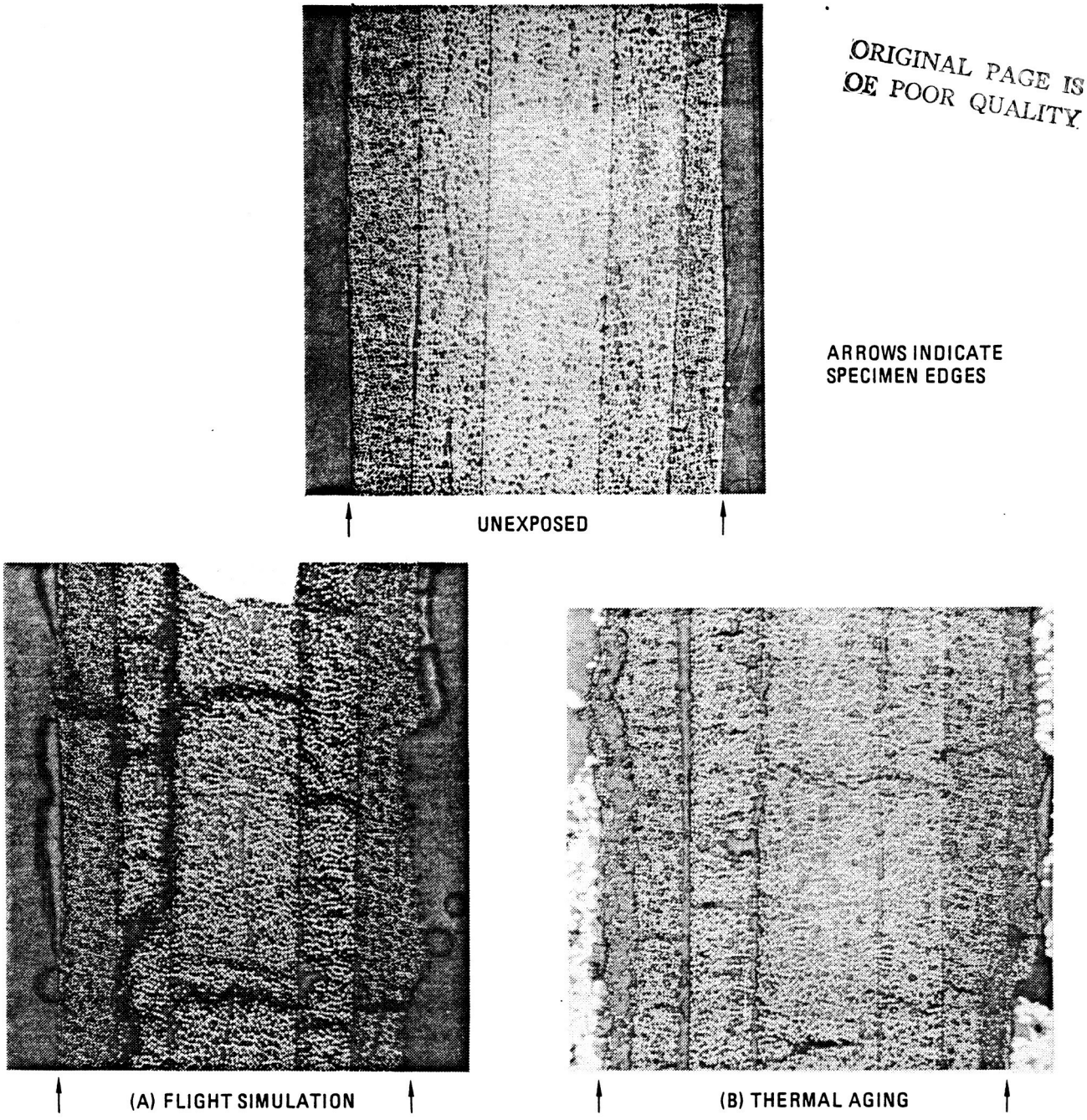



**Figure 12-124 Photomicrographs (Metallograph) of Celion 6000/LARC-160 G/PI Before (upper) and After (lower) 10,000 hr of (a) Flight Simulation Exposure and (b)Thermal Aging in Air at 450K (350°F), 100X**

**B/Al, $[0° \pm 45°]_s$ and $[0°]_6$, unnotched.** Table 12-41 lists the 15 Phase II B/Al flight simulation specimens and the number of hours of exposure that each completed. For the 25,000 hour group, four of the six survived. None of the 50,000 hour specimens reached their goals. Failure times ranged from just under 8000 hours to almost 32,000 hours. The following is a description of the four groups of specimens: 25,000 hours, $[0° \pm 45°]_s$; 50,000 hours, $[0° \pm 45°]_s$; 25,000 hours, $[0°]_6$; 50,000 hours, $[0°]_6$.

Table 12-41. Summary of B/Al Phase II Flight Simulation Exposures

| Specimen Number | Orientation | Exposure Hours Completed | Test Series (Hours) | Comments |
|---|---|---|---|---|
| EC92-1 | $[0° \pm 45°]_s$ | 29,327 | 50,000 | (a), Wearout failure in heated zone |
| EC92-2 | $[0° \pm 45°]_s$ | 31,447 | 50,000 | (a), Wearout failure in heated zone |
| EC92-3 | $[0° \pm 45°]_s$ | 17,707 | 50,000 | Wearout failure in heated zone |
| EC92-4 | $[0° \pm 45°]_s$ | 19,519 | 50,000 | Wearout failure in heated zone |
| EC92-5 | $[0° \pm 45°]_s$ | 30,447 | 50,000 | (a), Wearout failure in heated zone |
| EC93-1 | $[0° \pm 45°]_s$ | 27,402 | 25,000 | (a), (b), Did not fail |
| EC93-2 | $[0° \pm 45°]_s$ | 27,402 | 25,000 | (a), (b), Did not fail |
| EC93-3 | $[0° \pm 45°]_s$ | 27,402 | 25,000 | (a), (b), Did not fail |
| EU91-2 | $[0°]_6$ | 17,519 | 50,000 | Failed in unheated center section |
| EU92-1 | $[0°]_6$ | 17,702 | 50,000 | Failed near doubler at edge of heated zone |
| EU92-2 | $[0°]_6$ | 31,584 | 50,000 | Wearout failure in heated zone |
| EU92-3 | $[0°]_6$ | 12,605 | 50,000 | Failed at edge of heated zone |
| EU93-1 | $[0°]_6$ | 7,692 | 25,000 | Failed near doubler |
| EU93-2 | $[0°]_6$ | 23,588 | 25,000 | Wearout failure in heated zone |
| EU93-3 | $[0°]_6$ | 25,000 | 25,000 | Did not fail |

(a) Specimen failed in the simulation apparatus during compressive overload at 20,957 hours. Specimen was modified and returned to test. See Figure 12-94.
(b) Because of operator error the 25,000 hour specimens were not removed from test until 27,402 hours.

The three 25,000 hour crossplied specimens were among those that were modified to the configuration shown in Figure 12-94 after failing during the compressive overload at 20,957 hours. These revised specimens successfully completed 27,402 hours of exposure, after which they were removed from the simulator for examination and residual strength testing. A bookkeeping error was responsible for not halting the exposure cycling after 25,000 hours as originally intended.

Figures 12-125 and 12-126 show the two sides of the three crossplied specimens after removal at 27,402 hours. While the three specimens completed cycling without failure, there was considerable surface damage and edge cracking. Some surface wrinkling was also present. Magnified views of the surface of one of the specimens are shown in Figure 12-127. The surface roughening, first noted on the 10,000 hour specimens (Figure 12-82), is quite severe after 27,494 hours. Extensive longitudinal cracking of the aluminum and fracture of the outer ply boron filaments can also be seen in the photographs. These surface cracks and broken filaments were found on both sides of two of the three specimens. The third, EC93-3, had only the roughened surface and edge cracking.

ORIGINAL PAGE IS
OF POOR QUALITY

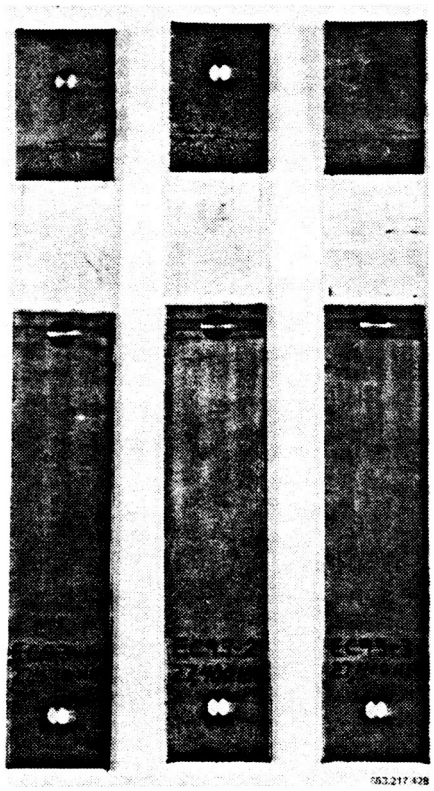


Figure 12-125 Crossply B/Al Long-Term Specimens After 27,402 hr of Flight Simulation Exposure (Specimens were redoublered after compression overload failure)




Figure 12-126 Crossply B/Al Long-Term Specimens After 27,402 hr of Flight Simulation Exposure (Opposite sides of specimens in Figure 12-125)

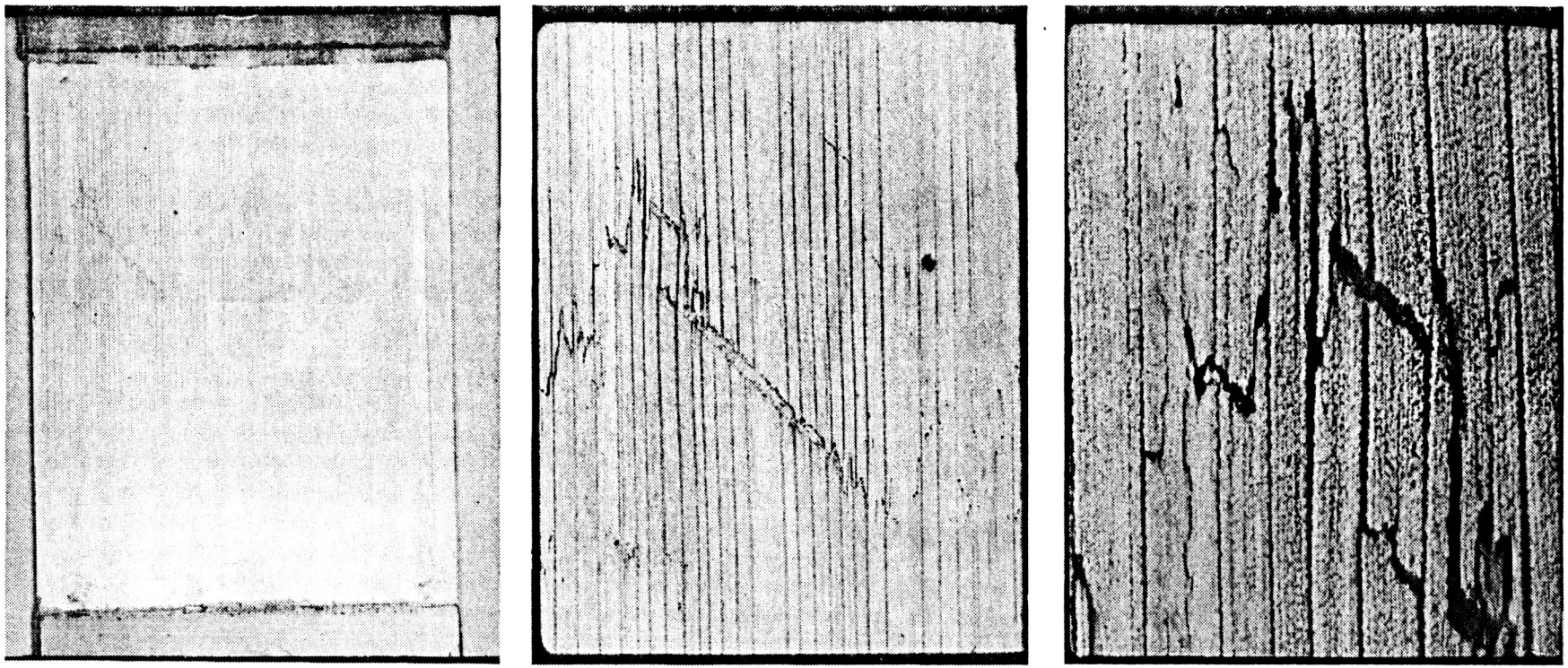



**Figure 12-127 B/Al Long-Term Specimen EC93-1 After 27,494 hr of Flight Simulation Exposure Showing Roughened Surface, Surface Cracking in the Aluminum and Fractured Outer-Ply Baron Filaments**

ORIGINAL PAGE IS
OF POOR QUALITY

ORIGINAL PAGE IS
OF POOR QUALITY

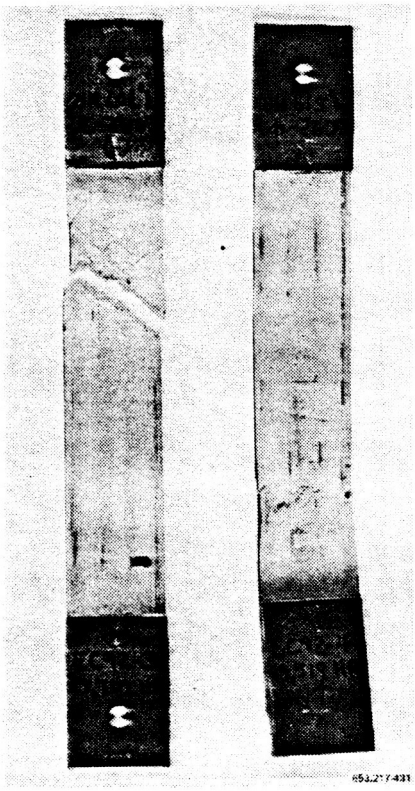


Figure 12-128 Crossply B/Al Long-Term Specimens That Failed During Flight Simulation Testing Before Completion of 50,000 hr of Exposure

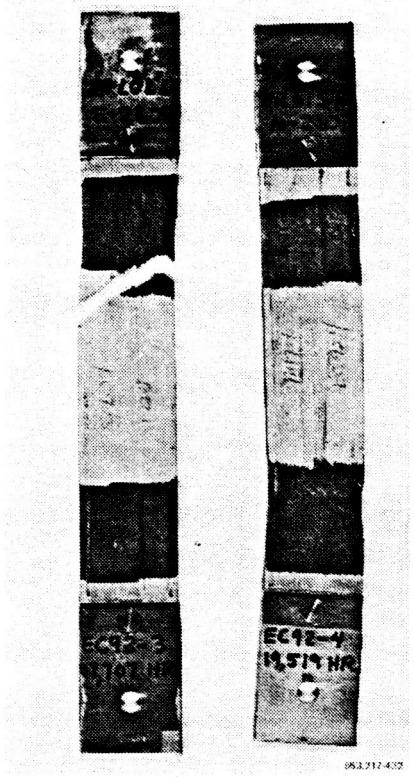
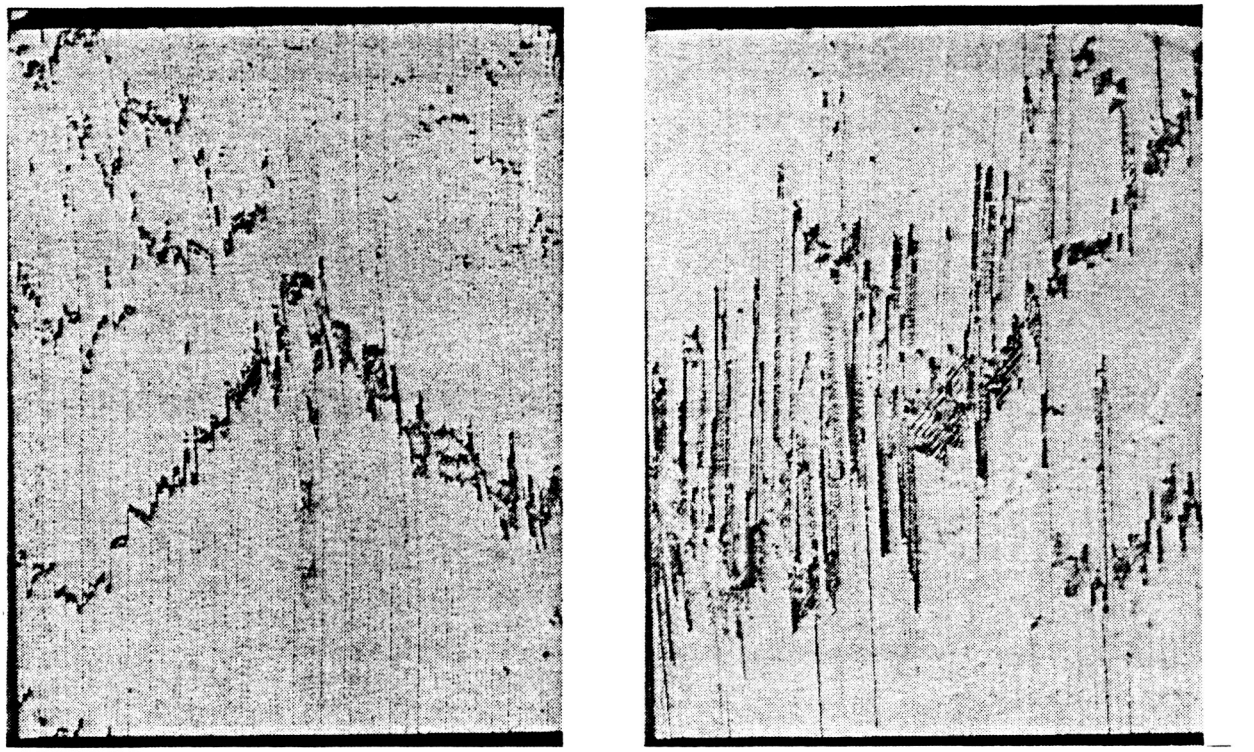



Figure 12-129 Crossply B/Al Long-Term Specimens That Failed During Flight Simulation Testing Before Completion of 50,000 hr of Exposure (Opposite sides of specimens in Figure 12-128)

ORIGINAL PAGE IS
OF POOR QUALITY



5X EC92-3 5X EC92-4 653217-433

**Figure 12-130 B/Al Long-Term Specimens EC92-3 (17,707 hr) and EC92-4 (19,519 hr) Showing Roughened Surfaces, Surface Cracking in the Aluminum, and Fractured Outer-Ply Boron Filaments**

For the 50,000 hour, $[0° \pm 45°]_s$ group of specimens, two failed prior to completing 20,000 hours. The remaining three failed during the compressive overload at 20,957 hours, were modified to the configuration shown in Figure 12-94, and were reintroduced to test. The three modified specimens completed approximately 30,000 hours of exposure before final failure.

Figures 12-128 and 12-129 are front and back views of the first two specimens. The fracture areas showed some necking down and numerous surface wrinkles. The wrinkles or bulges were quite severe for specimen EC92-4. Surface cracking, both in the Al and the boron filaments in the outer ply was extensive in the region of the failures. This can be seen in the magnified views of Figure 12-130 taken from near the failures. As was observed for the 10,000 hour specimens the degree of surface roughening varied considerably between the heated areas and the unheated center sections of these specimens. Figure 12-131 shows the difference after 19,519 hours of exposure. Also shown in Figure 12-131 are a series of connected openings or holes in the surface of the Al. These openings are aligned in the longitudinal direction of the specimens parallel to the boron filaments in the outer ply.

The remaining three specimens of this group are shown in Figures 12-132 and 12-133. All three failed near the 30,000 hour mark. The failure appearances were quite different among these specimens. Fracture occurred along a direction 45 degrees to the load in one of the specimens,

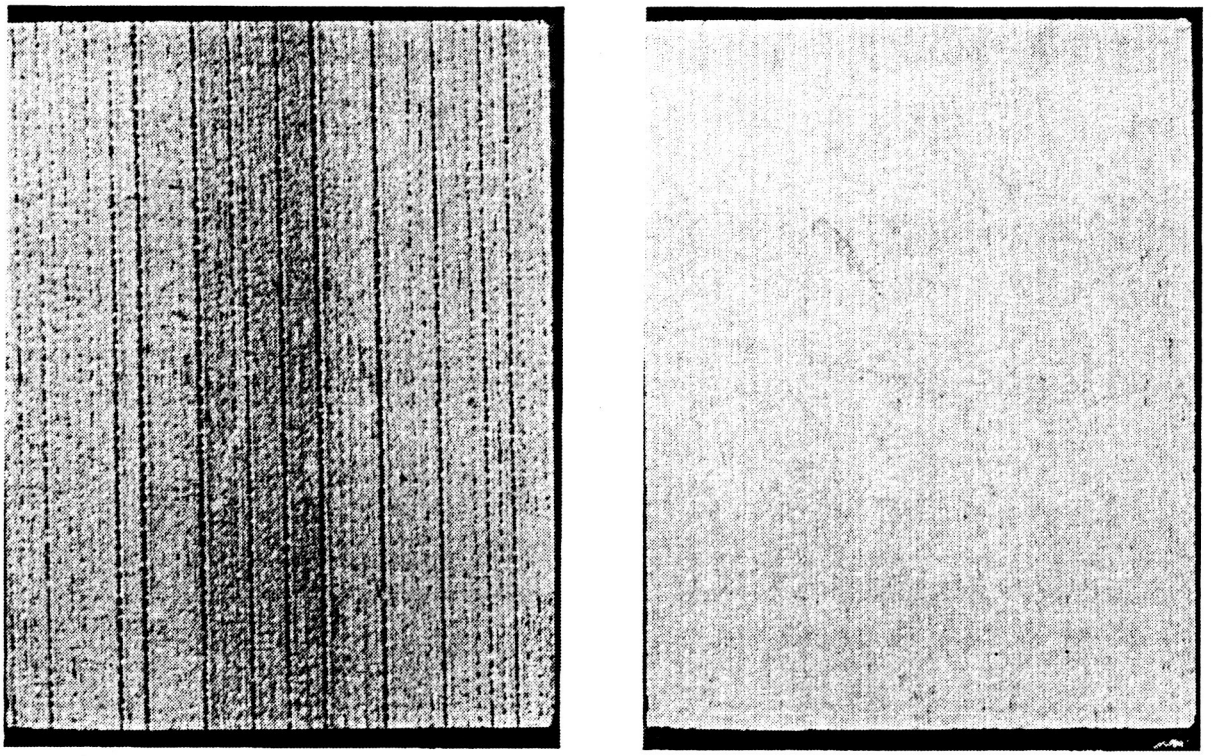



**Figure 12-131 B/Al Long-Term Specimen EC92-4 After 19,519 hr of Flight Simulation Exposure Showing Roughened Surface Observed in Heated Zones (Photograph on right shows considerably smoother surface of unheated center section for comparison)**

EC92-1. Damage to the surface was also considerably less than for the other two specimens. Specimen EC92-5 showed extensive necking in contrast to the other two. Failure for this specimen was along two intersecting 45 degree directions. For the third specimen, EC92-2, fracture occurred almost perpendicular to the loading direction for two thirds of the width and at 45 degrees for the remainder. Higher magnification views of these failures and the surface away from the failures are shown in Figures 12-134, 12-135, and 12-136.

The three 25,000 hour unidirectional specimens are shown in Figures 12-137 and 12-138. Only one specimen survived the 25,000 hours of exposure. The first failure, specimen EU93-1, occurred in less than 8000 hours. The failure was similar to that described earlier for specimen EU91-1 in Section 12.7.2 where the stiffening grid was forced into the B/Al at the edge of an end doubler during a compressive load. Figure 12-139 shows where the four bearing surfaces of the stiffening grid were forced into the B/Al. Figure 12-140 is a SEM photomicrograph of one of these areas. The effect of the grid bearing on the soft Al matrix was a smearing over of the Al, which is readily visible in the photomicrograph. The second specimen failure, EU93-2, occurred in the heated zone at 23,588 hours and appeared to be a wearout failure. The overall condition of these specimens was somewhat better than the crossply specimens after similar exposure periods. Fewer surface and edge cracks and a lesser degree of surface roughening were observed for the unidirectional specimens. Figure 12-141 shows the specimen surface after 25,000 hours of exposure for areas in the heated zone and the unheated center section.



ORIGINAL PAGE IS
OE POOR QUALITY

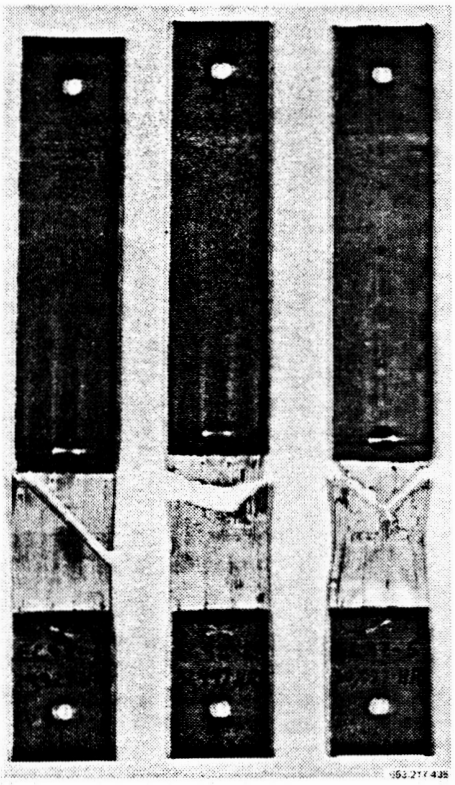


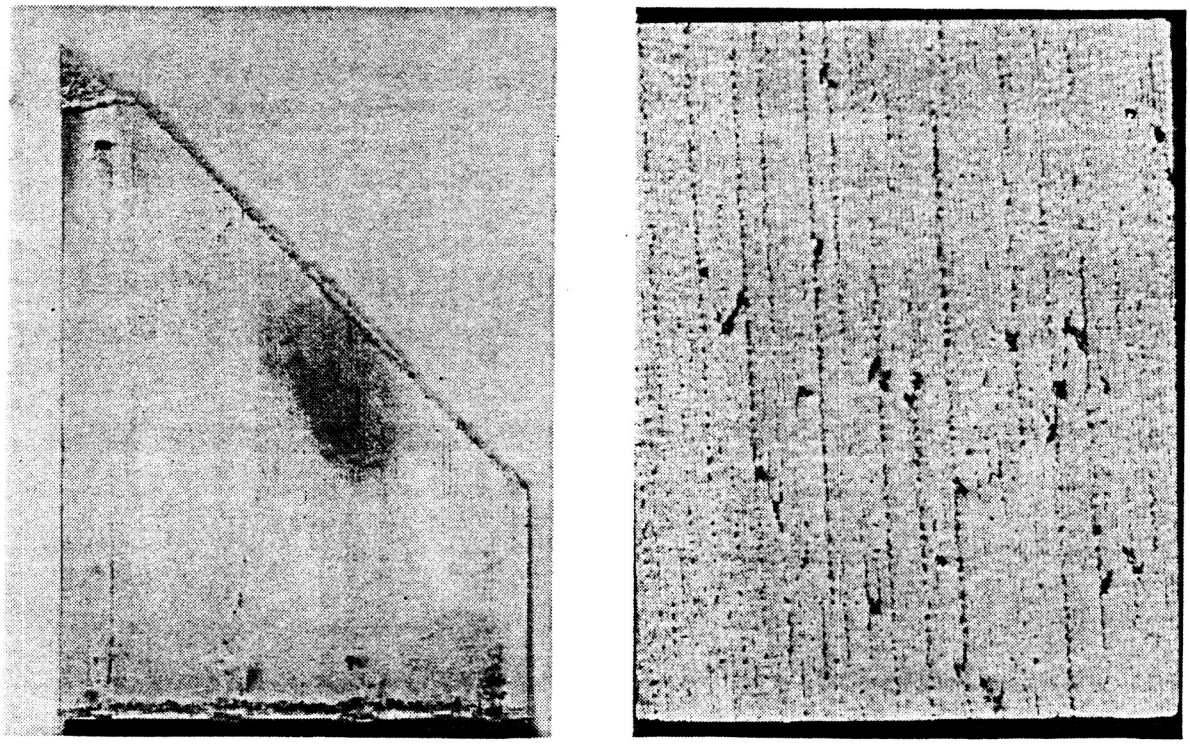
Figure 12-132 Crossply B/Al Long-Term Specimens That Failed During Flight Simulation Testing Before Completion of 50,000 hr of Exposure (Specimens were redoublered after compression overload failure)



ORIGINAL PAGE IS
OE POOR QUALITY

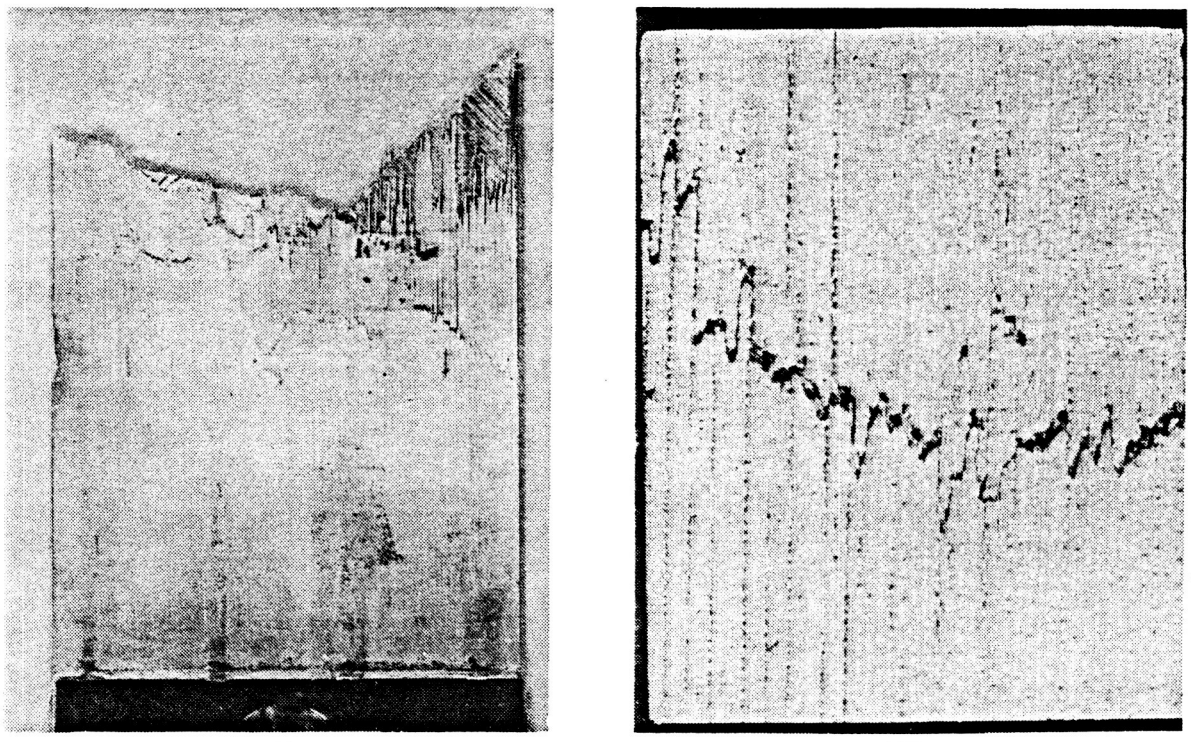
Figure 12-133 Crossply B/Al Long-Term Specimens That Failed During Flight Simulation Testing Before Completion of 50,000 hr of Exposure (Opposite sides of specimens in Figure 12-132)

ORIGINAL PAGE IS
OF POOR QUALITY



1X 10X 653217-437

**Figure 12-134 B/Al Long-Term Specimen EC92-1 After 29,327 hr of Flight Simulation Exposure Showing Fracture and Surface Away from Failure**



1X 10X 653217-438

**Figure 12-135 B/Al Long-Term Specimen EC92-2 After 31,447 hr of Flight Simulation Exposure Showing Fracture and Surface Away from Failure**

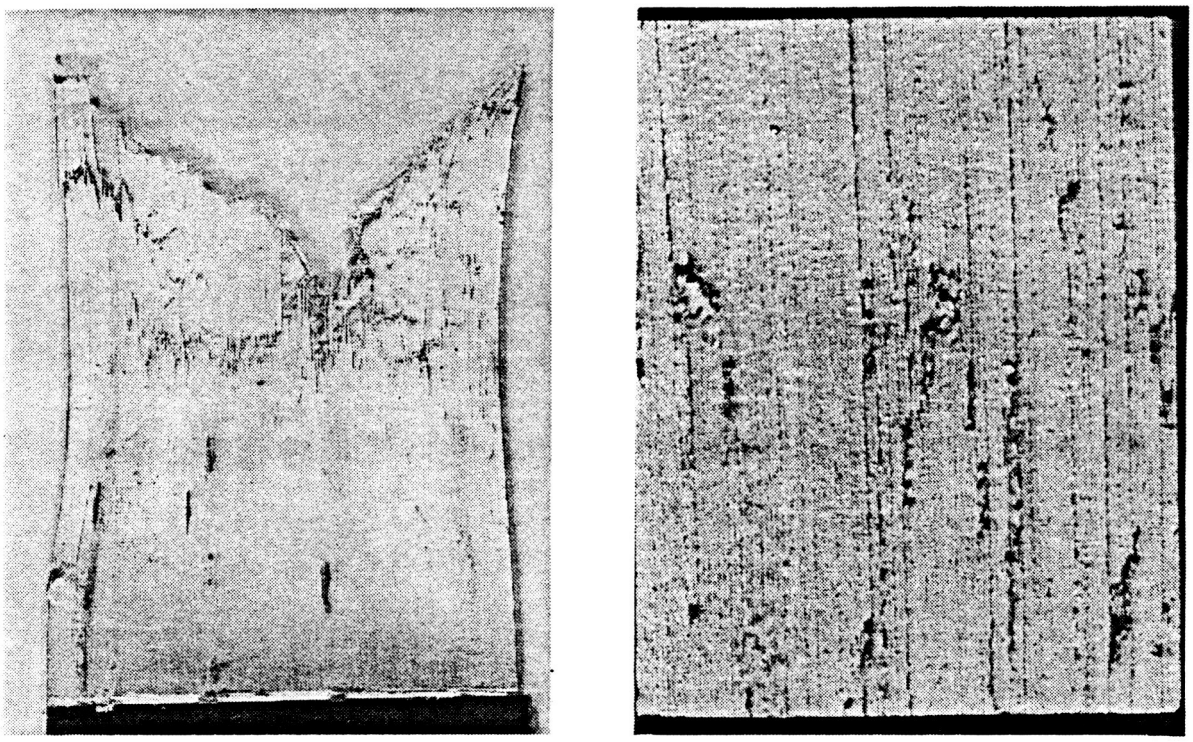



**Figure 12-136 B/Al Long-Term Specimen EC92-5 After 30,477 hr of Flight Simulation Exposure Showing Fracture and Surface Away from Failure**

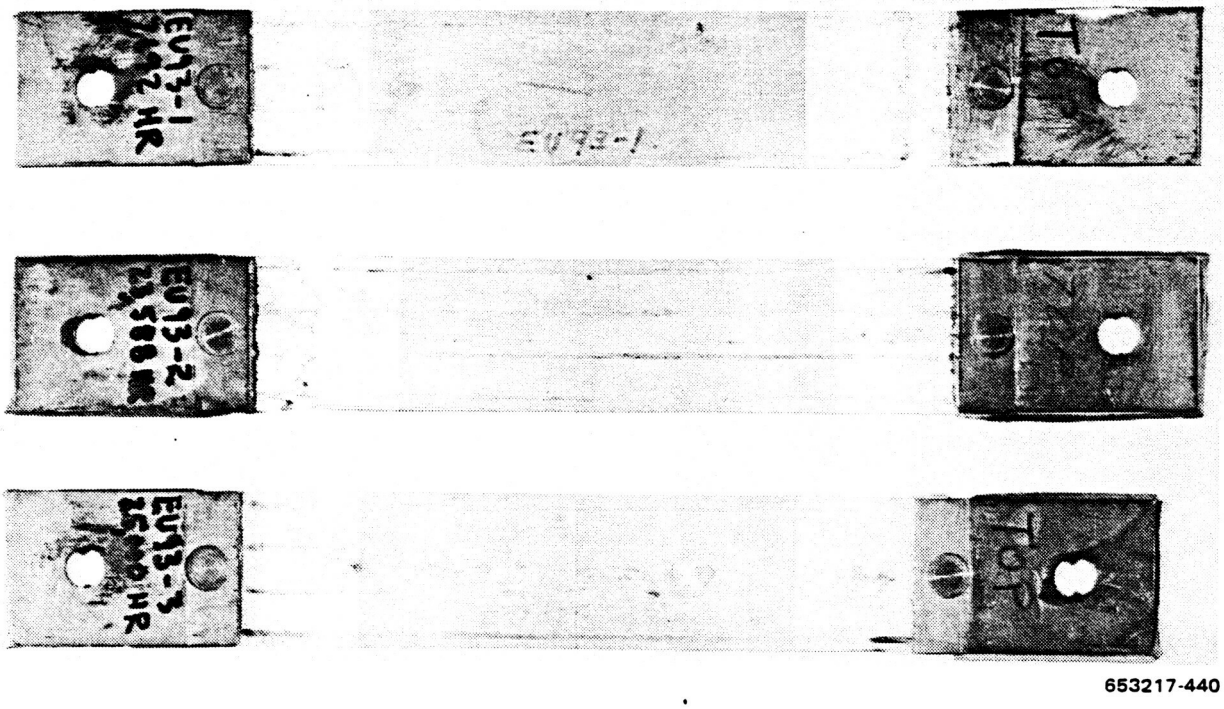



**Figure 12-137 25,000 hr Unidirectional B/Al Long-Term Specimens After Flight Simulation Exposure. Two Specimens Failed Prior to 25,000 hr**



ORIGINAL PAGE IS
OF POOR QUALITY

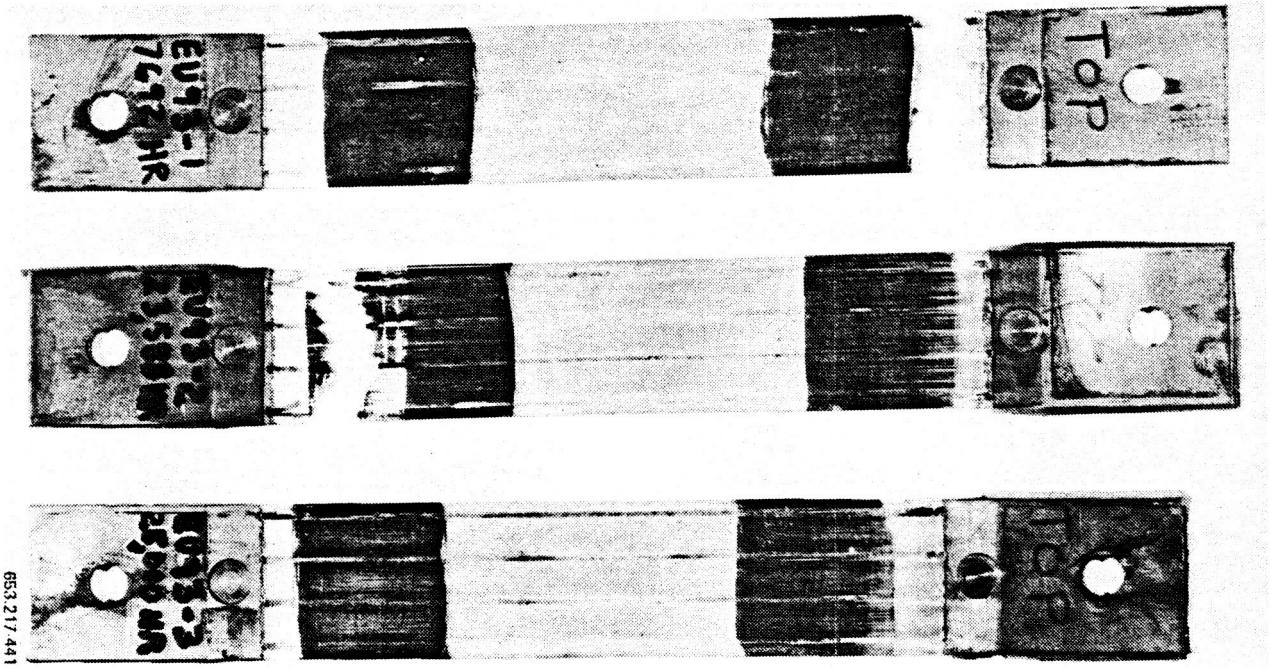



**Figure 12-138 25,000 hr Unidirectional B/Al Long-Term Specimens After Flight Simulation Exposure (Opposite sides of specimens in Figure 12-137)**

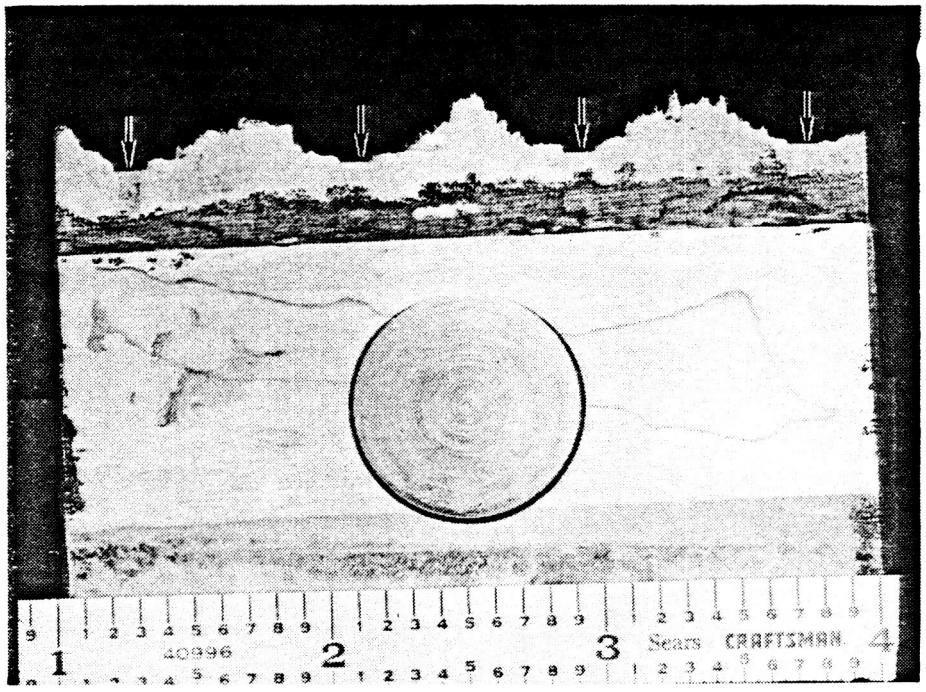
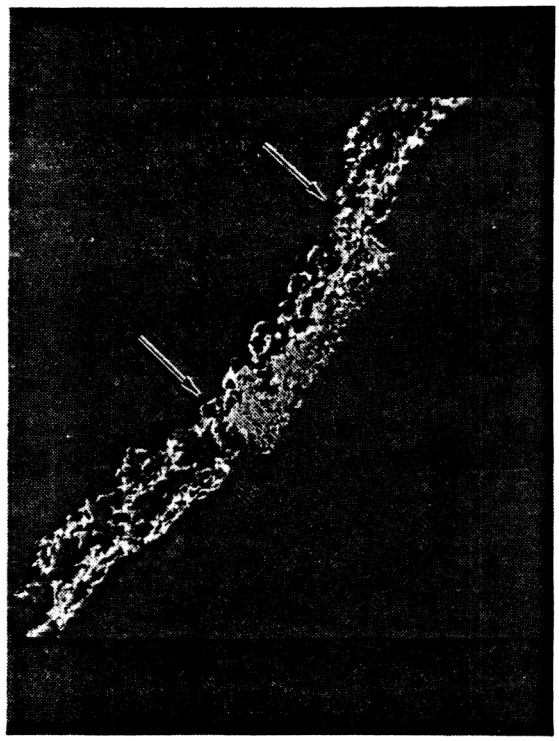



**Figure 12-139 B/Al Long-Term Specimen EU93-1 Showing Fracture Appearance After Failure in 7692 hr (Failure was initiated at locations (arrows) where stiffener grid was forced into the B/Al)**



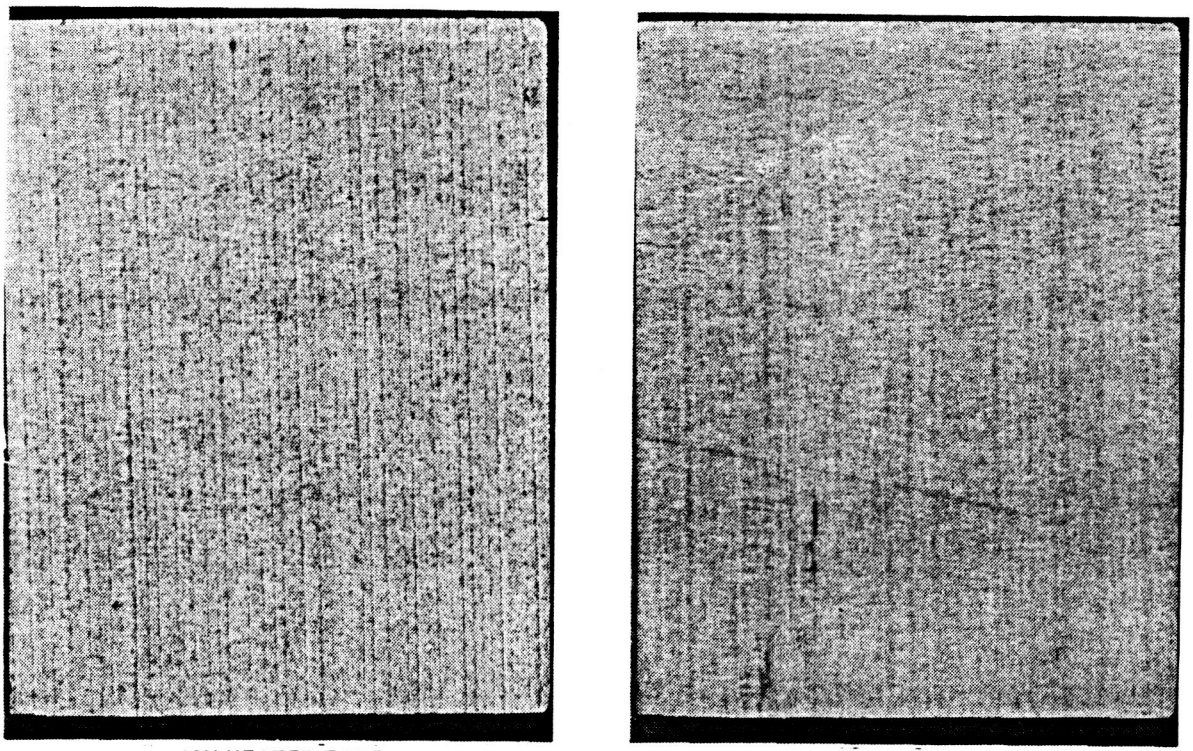
ORIGINAL PAGE IS
OF POOR QUALITY

ORIGINAL PAGE IS
OF POOR QUALITY



13X 653217-443

**Figure 12-140 SEM Photomicrograph of Region Where Stiffener Grid was Forced into Aluminum Matrix Near End Doubler of Specimen EU93-1 After 7692 hr of Flight Simulation Exposure (Contact area located between arrows)**



10X HEATED ZONE 10X CENTER SECTION 653217-444

**Figure 12-141 B/Al Long-Term Specimen EU93-3 After 25,000 hr of Flight Simulation Exposure Showing Roughened Surface Observed in Heated Zones (Photograph on right shows considerably smoother surface of unheated center section of comparison)**

ORIGINAL PAGE IS
OF POOR QUALITY

The degree of surface roughening is less than that shown in Figure 12-131 for a crossplied specimen after 19,519 hours of exposure.

The 50,000 hour unidirectional B/Al specimens did not fare any better than the crossply specimens with all failing to reach the 50,000 hour goal. Failure times ranged from 12,605 hours to 31,584 hours. Front and back views of these specimens are shown in Figures 12-142 and 12-143. The first failure, EU92-3, occurred after 12,605 hours at the edge of the heated zone. Other than the fracture the specimen condition was very good. Whether this early failure was the result of wearout could not be determined.

The next two failures, both after slightly less than 18,000 hours, occurred away from the heated zones. One was near the specimen center and the other near one of the end doublers. Neither specimen appeared to have failed as a result of wearout. The condition of these specimens was better than crossply specimens after similar exposure times. Some surface rippling and roughening were visible in the heated zones, but very few surface cracks were present. For specimen EU92-1 there was some evidence that the compression stiffeners may have lead to the failure in a manner similar to that described earlier for specimen EU93-1.

The last specimen of this group, EU92-2, failed after 31,584 hours in the heated zone in what is thought to have been the result of wearout. Again, the degree of surface cracking in the region of the failure was considerably less than observed previously for the crossply specimens. There was considerable surface roughening in the heated zones, however, as shown in Figure 12-144. The degree of surface roughening has increased substantially over that present after 25,000 hours as can be seen by comparison with the unidirectional specimen shown in Figure 12-141.

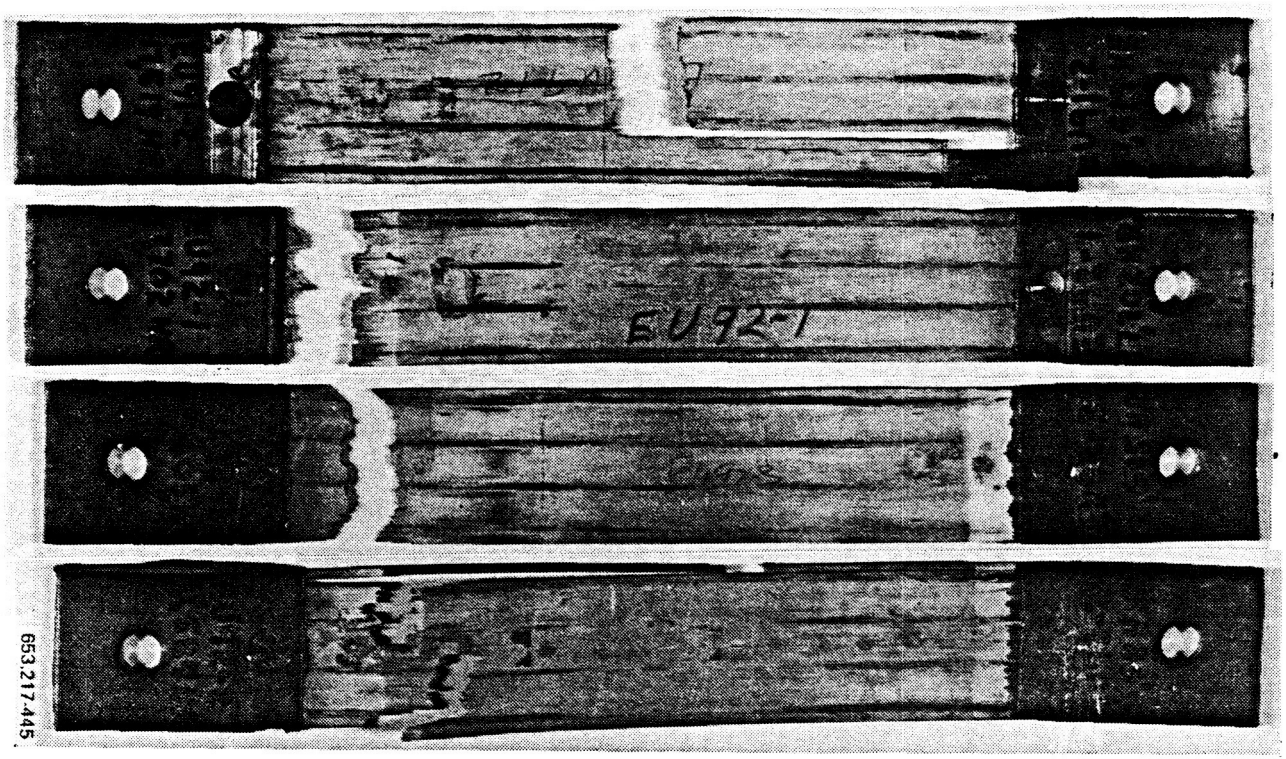
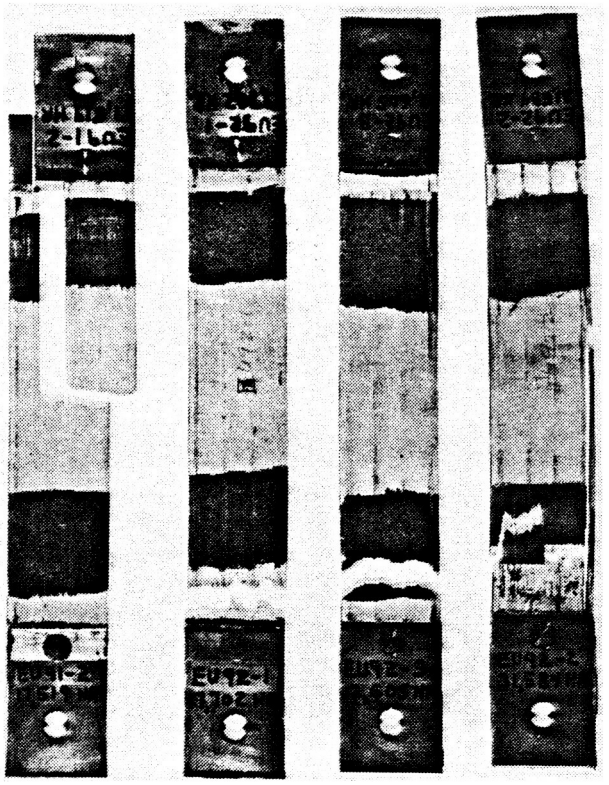


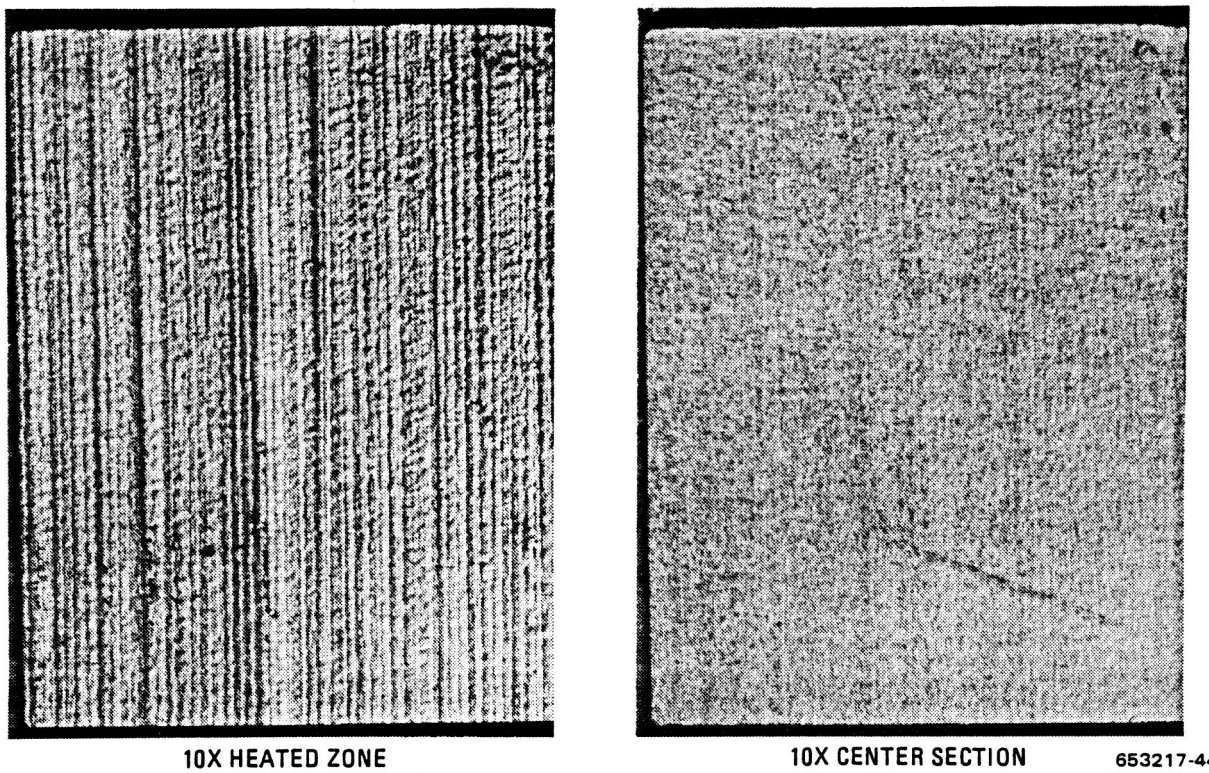

**Figure 12-142 Unidirectional B/Al Long-Term Specimens That Failed During Flight Simulation Testing Before Completion of 50,000 hr of Exposure**

ORIGINAL PAGE IS
OF POOR QUALITY



653217-446

**Figure 12-143 Unidirectional B/Al Long-Term Specimens That Failed During Flight Simulation Testing Before Completion of 50,000 hr of Exposure (Opposite sides of specimens in Figure 12-142)**



10X HEATED ZONE

10X CENTER SECTION

653217-447

**Figure 12-144 B/Al Long-Term Specimen EU92-2 After 31,584 hr of Flight Simulation Exposure Showing Roughened Surface Observed in Heated Zones (Photograph on right shows considerably smoother surface of unheated center section for comparison)**

**12.7.3.2 Residual Strength Data — Phase II.** Residual strength test plans were formulated for the Phase II materials prior to the start of exposure. These plans stressed tensile and fatigue tests of both unnotched and notched configurations at ambient and elevated temperatures. It was necessary to modify these plans, however, for several reasons. Of prime importance was the failure of any of the specimens to survive 50,000 hours of exposure. Specimens either failed, or, in the case of the epoxies, were removed from test prior to reaching 50,000 hours. For the specimens that failed to complete the required number of exposure hours, their unfailed ends could generally be salvaged for residual strength testing. Other factors affecting the change in test plans were the increased importance of residual compressive and shear properties and loss of test material from under the compressive grids.

In keeping with the rationale of Phase I, unnotched tensile and fatigue and short beam shear specimens were machined from material that was not shielded by the compression stiffening grids. For the notched tensile, notched fatigue, and compressive specimens the entire width of the flight simulation specimens was used. To get sufficiently thick specimens for compressive and short beam shear testing it was necessary to bond several layers together. All required three layers (18 ply) except the epoxy compressive specimens, which required four layers (24 ply). No compressive specimens were made from the B/Al material because of the testing difficulties encountered with the 10,000 hour compressive tests of Phase I. Specimen preparation techniques, configurations, and test procedures were generally identical to those used during Phase I. In Phase I, bonding of doublers was required on only one end of each of the residual tensile and fatigue specimens as the titanium doubler from the flight simulation specimen was still attached to the other end. In Phase II, it was often necessary to bond doublers to both ends of the specimens because of the poor condition of the adhesive holding the original titanium doublers on the long term specimens. This was particularly true for the longer exposure times.

**B/E, $[0° \pm 45°]_s$ and G/E, $[0° \pm 45°]_s$, unnotched.** Because of the high failure rate of the G/E specimens and the extensive visual degradation of the B/E specimens during Phase I, all of the original B/E and G/E flight simulation specimens were removed at the end of 10,000 hours. New specimens were fabricated to replace them, and flight simulation testing was restarted with the maximum test temperature reduced from 408K (275°F) to 373K (212°F). All of the replacement specimens were unnotched.

The specimens of both B/E and G/E completed 10,000 hours and 25,000 hours without failure. Two B/E specimens failed near 33,000 hours. Because of the likelihood of additional failures and in order to obtain the maximum amount of residual strength data, flight simulation testing of the remaining specimens was halted after 36,374 hours.

The test plan for residual strength testing of the epoxy specimens is given in Table 12-42. Material was available for test with accumulative exposure periods of 10,000 hours, 25,000 hours, and 36,374 hours. The number of tensile and fatigue tests of the 36,374 hour B/E material had to be reduced because of the two flight simulation specimen failures near 33,000 hours.

Table 12.42. Residual Strength Test Plan for Phase II B/E and G/E After Flight Simulation Testing

| Material System | Flight Simulation Specimen Type | Test Type | Temperature K | Temperature (°F) | Number of Specimens 10,000 hr | 25,000 hr | 36,374 hr |
|---|---|---|---|---|---|---|---|
| B/E | $[0° \pm 45°]_s$ Unnotched | Tensile | 297 | 75 | 8 | 3 | 6 |
| | | Notched Tensile | 297 | 75 | 4 | 0 | 3 |
| | | Fatigue | 297 | 76 | 9 | 6 | 6 |
| | | Compressive | 297 | 75 | 4 | 4 | 4 |
| | | Shear | 297 | 75 | 4 | 4 | 4 |
| G/E | $[0° \pm 45°]_s$ Unnotched | Tensile | 297 | 75 | 8 | 3 | 8 |
| | | Notched Tensile | 297 | 75 | 4 | 0 | 4 |
| | | Fatigue | 297 | 75 | 9 | 6 | 9 |
| | | Compressive | 297 | 75 | 4 | 4 | 4 |
| | | Shear | 297 | 75 | 4 | 4 | 4 |

Residual tensile and notched tensile data before and after 10,000 hours, 25,000 hours, and 36,374 hours of flight simulation exposure are listed in Tables 12-43 and 12-44 for B/E and Tables 12-45 and 12-46 for G/E. Elastic modulus values are included for the unnotched tensile tests. The tensile strength values have been plotted as a function of exposure time in Figures 12-145 and 12-146. Residual compressive and short beam shear data before and after the same exposure periods are listed in Tables 12-47 and 12-48 for B/E and Tables 12-49 and 12-50 for G/E. Elastic modulus values are given for the compressive tests. The compressive and shear strength values have also been plotted as a function of exposure time and are shown in Figures 12-147 and 12-148. Residual axial fatigue data at room temperature and a stress ratio, R, of 0.1 for unnotched specimens are presented in Tables 12-51 and 12-52, and S-N curves are plotted in Figures 12-149 and 12-150. Also included on the graphs are S-N curves (no data points) for unexposed material tested under the same conditons (presented earlier in Section 11, Baseline Fatigue Testing).

**Table 12-43. Strength and Modulus Properties of $[0° \pm 45°]_s$ B/E at 297K (75°F) Before and After Flight Simulation Exposure**

| Specimen Number | Flight Simulation Specimen Number | | Strength MN/m² | Strength (ksi) | Modulus GN/m² | Modulus (Msi) |
|---|---|---|---|---|---|---|
| Unnotched Tensile: 10,000 hr | | | | | | |
| A931-1 | AC93-1 | | 492 | 71.3 | 79.3 | 11.5 |
| -2 | -1 | | 457 | 66.3 | 66.9 | 9.7 |
| -3 | -1 | | 551 | 79.9 | 69.6 | 10.1 |
| -4 | -1 | | 468 | 67.9 | 70.3 | 10.2 |
| -5 | -1 | | 487 | 70.6 | 68.3 | 9.9 |
| -6 | -1 | | 527 | 76.4 | 71.7 | 10.4 |
| A935-4 | -5 | | 533 | 77.3 | 71.7 | 10.4 |
| -6 | -5 | | 474 | 68.7 | 63.4 | 9.2 |
| | | av | 498 | 72.3 | 70.3 | 10.2 |
| Unnotched Tensile: 25,000 hr | | | | | | |
| A941-1 | AC94-1 | | 447 | 64.9 | 61 | 8.8 |
| -2 | -1 | | 482 | 69.9 | 59 | 8.6 |
| -3 | -1 | | 483 | 70.1 | 61 | 8.9 |
| | | av | 471 | 68.3 | 60 | 8.8 |
| Unnotched Tensile: 36,374 hr | | | | | | |
| A951-1 | AC95-1 | | 450 | 65.3 | 69 | 10.0 |
| -2 | -1 | | 336 | 48.7 | 69 | 10.0 |
| -3 | -1 | | 419 | 60.8 | — | — |
| -4 | -1 | | 450 | 65.2 | 70 | 10.1 |
| -5 | -1 | | 414 | 60.1 | 90 | 13.1 |
| -6 | -1 | | 410 | 59.4 | 85 | 12.4 |
| | | av | 413 | 59.9 | 77 | 11.1 |
| Baseline (Phase II Material) | | av | 531 | 77.0 | 70.3 | 10.2 |

**Table 12-44. Notched Tensile Strength of $[0° \pm 45°]_s$ B/E at 297K (75°F) Before and After Flight Simulation Exposure (Unnotched Flight Simulation Specimen)**

| Specimen Number | Flight Simulation Specimen Number | | Strength $MN/m^2$ | Strength (ksi) |
|---|---|---|---|---|
| Notched Tensile: 10,000 hr | | | | |
| A934-1 | AC93-4 | | 396 | 57.4 |
| -2 | -4 | | 441 | 63.9 |
| -3 | -4 | | 380 | 55.1 |
| A935-5 | -5 | | 423 | 61.3 |
| | | av | 410 | 59.4 |
| Notched Tensile: 36,374 hr | | | | |
| A954-4 | AC95-4 | | 385 | 55.8 |
| -5 | -4 | | 403 | 58.4 |
| -6 | -4 | | 361 | 52.4 |
| | | av | 383 | 55.5 |
| Baseline (Phase I Material) | | av | 443 | 64.2 |

**Table 12-45. Strength and Modulus Properties of $[0° \pm 45°]_s$ G/E at 297K (75°F) Before and After Flight Simulation Exposure**

| Specimen Number | Flight Simulation Specimen Number | | Strength $MN/m^2$ | Strength (ksi) | Modulus $GN/m^2$ | Modulus (Msi) |
|---|---|---|---|---|---|---|
| Unnotched Tensile: 10,000 hr | | | | | | |
| B931-1 | BC93-1 | | 747 | 108.3 | 61 | 8.8 |
| -2 | -1 | | 661 | 95.9 | 61 | 8.9 |
| -3 | -1 | | 686 | 99.5 | 59 | 8.6 |
| -4 | -1 | | 587 | 85.1 | 61 | 8.9 |
| -5 | -1 | | 705 | 102.3 | 59 | 8.5 |
| -6 | -1 | | 554 | 80.4 | 56 | 8.1 |
| B935-4 | -5 | | 492 | 71.4 | 52 | 7.5 |
| -6 | -5 | | 609 | 88.3 | 52 | 7.6 |
| | | av | 630 | 91.4 | 58 | 8.4 |
| Unnotched Tensile: 25,000 hr | | | | | | |
| B941-1 | BC94-1 | | 632 | 91.7 | 46 | 6.6 |
| -2 | -1 | | 647 | 93.8 | 48 | 7.0 |
| -3 | -1 | | 583 | 84.6 | 48 | 7.0 |
| | | av | 621 | 90.0 | 47 | 6.9 |
| Unnotched Tensile: 36,374 hr | | | | | | |
| B953-1 | BC95-3 | | 623 | 90.3 | 59 | 8.5 |
| -2 | -3 | | 574 | 83.3 | 53 | 7.7 |
| -3 | -3 | | 652 | 94.5 | 54 | 7.9 |
| -4 | -3 | | 609 | 88.3 | 64 | 9.3 |
| -5 | -3 | | 487 | 70.7 | 62 | 9.0 |
| -6 | -3 | | 598 | 86.8 | 74 | 10.7 |
| B955-4 | -5 | | 520 | 75.4 | 79 | 11.4 |
| -6 | -5 | | 487 | 70.6 | 57 | 8.2 |
| | | av | 540 | 82.5 | 67 | 9.1 |
| Baseline (Phase II Material) | | av | 550 | 79.7 | 53 | 7.7 |

**Table 12-46. Notched Tensile Strength of $[0° \pm 45°]_s$ G/E at 297K (75°F) Before and After Flight Simulation Exposure (Unnotched Flight Simulation Specimen)**

| Specimen Number | Flight Simulation Specimen Number | | Strength $MN/m^2$ | Strength (ksi) |
|---|---|---|---|---|
| Notched Tensile: 10,000 hr | | | | |
| B934-1 | BC93-4 | | 478 | 69.4 |
| -2 | -4 | | 385 | 55.9 |
| -3 | -4 | | 459 | 66.5 |
| B935-5 | -5 | | 456 | 66.1 |
| | | av | 445 | 64.5 |
| Notched Tensile: 36,374 hr | | | | |
| B952-4 | BC95-2 | | 476 | 69.0 |
| -5 | -2 | | 488 | 70.9 |
| -6 | -2 | | 426 | 61.8 |
| | | av | 463 | 67.2 |
| Baseline (Phase I Material) | | av | 412 | 59.7 |



C-7

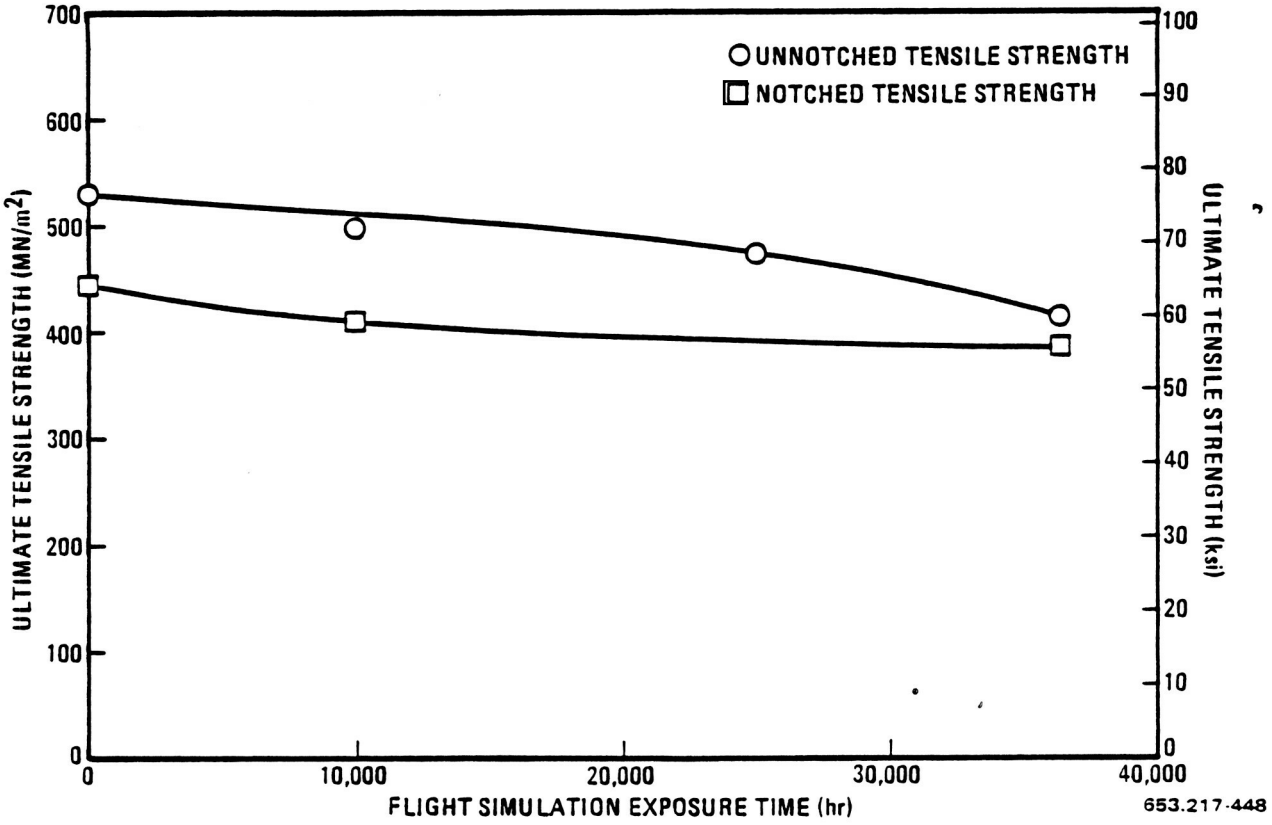



**Figure 12-145 Residual Tensile Strength of $[0° \pm 45°]_s$ B/E at 297K (75°F) After Flight Simulation Exposure at a Maximum Temperature of 373K (212°F)**

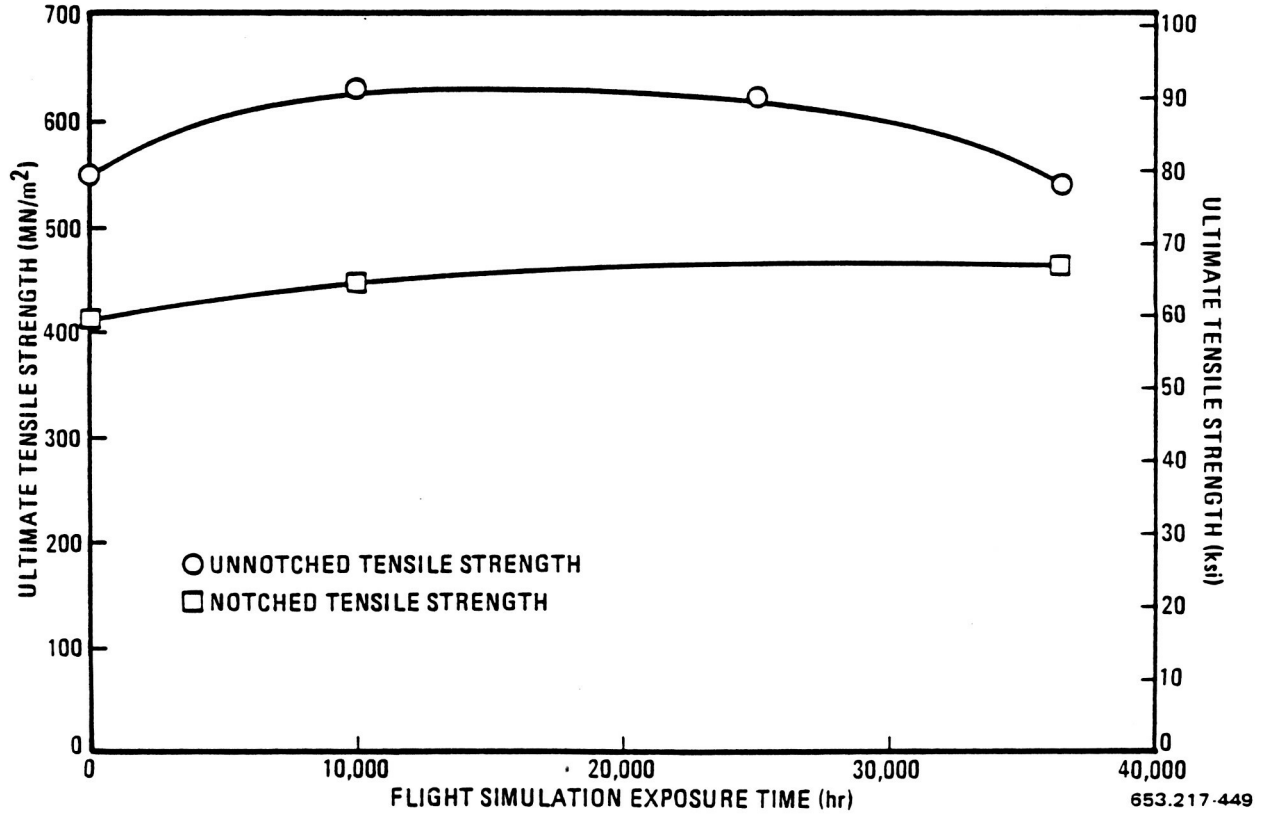



**Figure 12-146 Residual Tensile Strength of $[0° \pm 45°]_s$ G/E at 297K (75°F) After Flight Simulation Exposure at a Maximum Temperature of 373K (212°F)**

**Table 12-47. Compressive Strength of $[0° \pm 45°]_s$ B/E at 297K (75°F) Before and After Flight Simulation Exposure**

| Specimen Number | Flight Simulation Specimen Number | | Strength MN/m² | Strength (ksi) | Modulus GN/m² | Modulus (Msi) |
|---|---|---|---|---|---|---|
| Compressive: 10,000 hr | | | | | | |
| A9C-8 | AC93-3 | | 1,160 | 169 | 69.0 | 10.0 |
| -9 | -3 | | 1,230 | 179 | 70.3 | 10.2 |
| -10 | -3 | | 1,170 | 170 | 71.0 | 10.3 |
| -11 | -3 | | 1,170 | 170 | 69.6 | 10.1 |
| | | av | 1,190 | 172 | 70.3 | 10.2 |
| Compressive: 25,000 hr | | | | | | |
| A9C-12 | AC94-3 | | 1,040 | 151 | 68 | 9.9 |
| -13 | -3 | | 924 | 134 | 66 | 9.5 |
| -14 | -3 | | 1,090 | 158 | 67 | 9.7 |
| -15 | -3 | | 1,090 | 158 | 68 | 9.9 |
| | | av | 1,030 | 150 | 67 | 9.8 |
| Compressive: 36,374 hr | | | | | | |
| A9C-16 | AC95-5 | | 492 | 71.4 | 74 | 10.8 |
| -17 | -5 | | 430 | 62.4 | 58 | 8.4 |
| -18 | -5 | | 826 | 119.9 | 65 | 9.4 |
| -19 | -5 | | 687 | 99.7 | 60 | 8.7 |
| | | av | 609 | 88.4 | 64 | 9.3 |
| Baseline (Phase II Material) | | av | 1,540 | 223 | 102 | 14.8 |

**Table 12-48. Short Beam Shear Strength of $[0° \pm 45°]_s$ B/E at 297K (75°F) Before and After Flight Simulation Exposure**

| Specimen Number | Flight Simulation Specimen Number | | Strength MN/m² | (ksi) |
|---|---|---|---|---|
| Short Beam Shear: 10,000 hr | | | | |
| A9S-1 | AC93-5 | | 66 | 9.5 |
| -2 | -5 | | 65 | 9.4 |
| -3 | -5 | | 65 | 9.4 |
| -4 | -5 | | 68 | 9.9 |
| | | av | 66 | 9.6 |
| Short Beam Shear: 25,000 hr | | | | |
| A9S-5 | AC94-2 | | 45 | 6.5 |
| -6 | -2 | | 48 | 7.0 |
| -7 | -2 | | 45 | 6.5 |
| -8 | -2 | | 41 | 5.9 |
| | | av | 45 | 6.5 |
| Short Beam Shear: 36,374 hr | | | | |
| A9S-13 | AC95-4 | | 30 | 4.3 |
| -14 | -4 | | 30 | 4.4 |
| -15 | -4 | | 25 | 3.6 |
| -16 | -4 | | 29 | 4.2 |
| | | av | 29 | 4.1 |
| Baseline (Phase I Material) | | av | 66 | 9.5 |

Table 12-49. Compressive Strength of $[0° \pm 45°]_s$ G/E at 297K (75°F) Before and After Flight Simulation Exposure

| Specimen Number | Flight Simulation Specimen Number | | Strength MN/m² | Strength (ksi) | Modulus GN/m² | Modulus (Msi) |
|---|---|---|---|---|---|---|
| Compressive: 10,000 hr | | | | | | |
| B9C-3 | BC93-3 | | 551 | 79.9 | 46 | 6.7 |
| -4 | -3 | | 527 | 76.5 | 43 | 6.3 |
| -5 | -3 | | 576 | 83.6 | 46 | 6.6 |
| -6 | -3 | | 576 | 83.5 | 43 | 6.3 |
| | | av | 558 | 80.9 | 45 | 6.5 |
| Compressive: 25,000 hr | | | | | | |
| B9C-7 | BC94-3 | | 620 | 89.9 | 51 | 7.4 |
| -8 | -3 | | 622 | 90.2 | 50 | 7.3 |
| -9 | -3 | | 574 | 83.2 | 50 | 7.2 |
| -10 | -3 | | 618 | 89.6 | 50 | 7.2 |
| | | av | 608 | 88.2 | 50 | 7.3 |
| Compressive: 36,374 hr | | | | | | |
| B9C-11 | BC95-1 | | 470 | 68.2 | 48 | 7.0 |
| -12 | -1 | | 497 | 72.2 | 50 | 7.2 |
| -13 | -1 | | 564 | 81.9 | 50 | 7.3 |
| -14 | -1 | | 592 | 85.8 | 54 | 7.8 |
| | | av | 531 | 77.0 | 51 | 7.3 |
| Baseline (Phase I Material) | | av | 570 | 82.7 | 46 | 6.6 |

**Table 12-50. Short Beam Shear Strength of $[0° \pm 45°]_s$ G/E at 297K (75°F) Before and After Flight Simulation Exposure**

| Specimen Number | Flight Simulation Specimen Number | | Strength MN/m² | Strength (ksi) |
|---|---|---|---|---|
| Short Beam Shear: 10,000 hr | | | | |
| B9S-1 | BC93-5 | | 66 | 9.5 |
| -2 | -5 | | 61 | 8.9 |
| -3 | -5 | | 63 | 9.2 |
| -4 | -5 | | 62 | 9.0 |
| | | av | 63 | 9.2 |
| Short Beam Shear: 25,000 hr | | | | |
| B9S-5 | BC94-2 | | 68 | 9.8 |
| -6 | -2 | | 68 | 9.8 |
| -7 | -2 | | 68 | 9.9 |
| -8 | -2 | | 70 | 10.2 |
| | | av | 68 | 9.9 |
| Short Beam Shear: 36,374 hr | | | | |
| B9S-9 | BC95-2 | | 53 | 7.7 |
| -10 | -2 | | 59 | 8.6 |
| -11 | -2 | | 45 | 6.5 |
| -12 | -2 | | 55 | 8.0 |
| | | av | 53 | 7.7 |
| Baseline (Phase I Material) | | av | 74 | 10.7 |

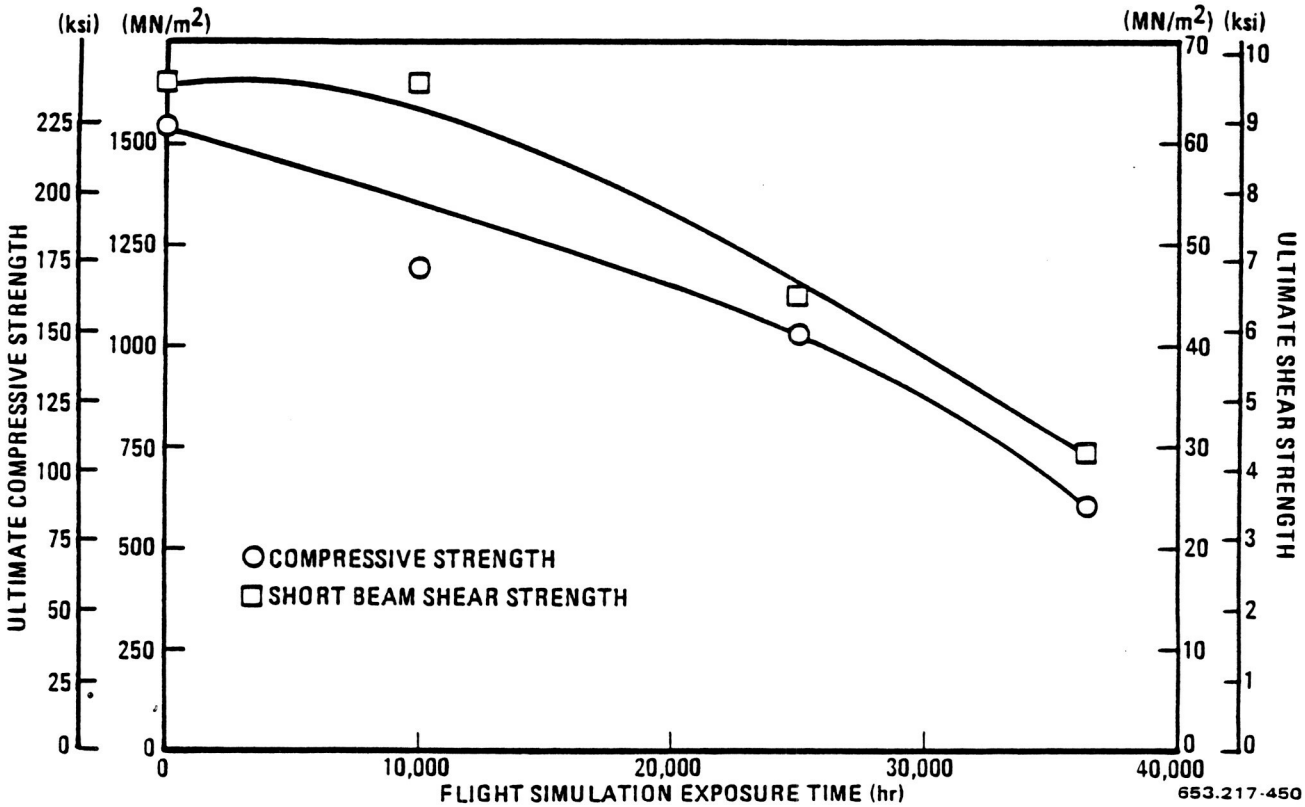



**Figure 12-147 Residual Compressive and Short Beam Shear Strength of $[0° \pm 45°]_s$ B/E at 297K (75°F) After Flight Simulation Exposure at a Maximum Temperature of 373K (212°F)**

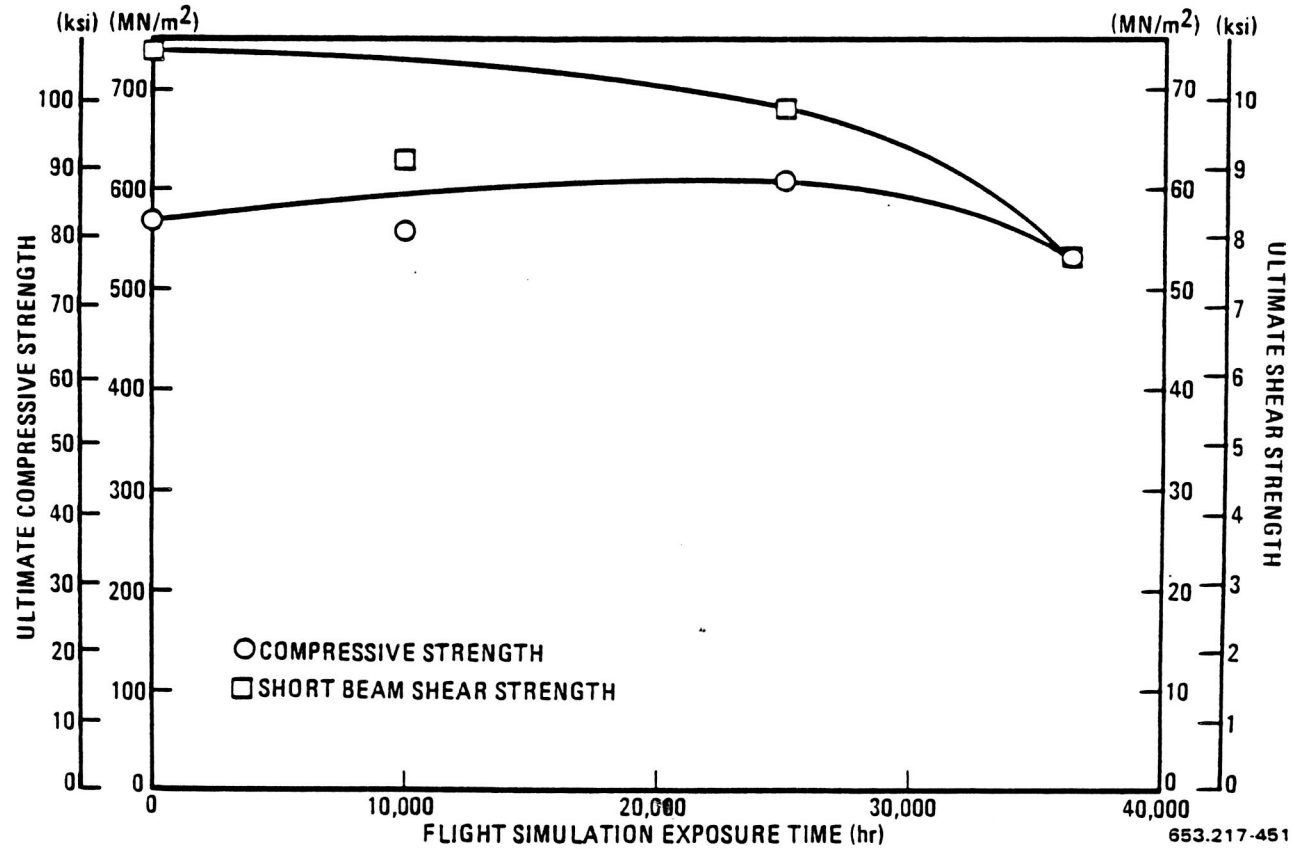



**Figure 12-148 Residual Compressive and Short Beam Shear Strength of $[0° \pm 45°]_s$ G/E at 297K (75°F) After Flight Simulation Exposure at a Maximum Temperature of 373K (212°F)**

Table 12-51. Residual Axial Fatigue Data for $[0° \pm 45°]_s$ B/E at 297K (75°) After Flight Simulation Exposure, R = 0.1, Unnotched

| Specimen Number | Flight Simulation Specimen Number | Maximum Stress $MN/m^2$ | Maximum Stress (ksi) | Cycles | Comments |
|---|---|---|---|---|---|
| 10,000 hr | | | | | |
| A932-1 | AC93-2 | 345 | 50 | 639,000 | |
| -2 | -2 | 414 | 60 | 1,000 | |
| -3 | -2 | 276 | 40 | 10,223,000 | Did not fail |
| -4 | -2 | 310 | 45 | 3,162,000 | |
| -5 | -2 | 379 | 55 | 441,000 | |
| -6 | -2 | 396 | 57.5 | 304,000 | |
| A934-4 | -4 | 328 | 47.5 | 2,493,000 | |
| -5 | -4 | 293 | 42.5 | 15,440,000 | Did not fail |
| -6 | -4 | 362 | 52.5 | 484,000 | |
| 25,000 hr | | | | | |
| A941-4 | AC94-1 | 362 | 52.5 | 200,000 | |
| -5 | -1 | 310 | 45 | 199,000 | Failed under doubler |
| -6 | -1 | 310 | 45 | 12,000,000 | Did not fail |
| A942-4 | -2 | 345 | 50 | 145,000 | |
| -5 | -2 | 379 | 55 | 6,000 | |
| -6 | -2 | 328 | 47.5 | 349,000 | |
| 36,374 hr | | | | | |
| A952-1 | AC95-2 | 310 | 45 | 6,000 | |
| -2 | -2 | 276 | 40 | 9,462,000 | |
| -3 | -2 | 293 | 42.5 | 347,000 | Failed under doubler |
| A953-1 | -3 | 328 | 47.5 | 4,500 | |
| -2 | -3 | 284 | 41.25 | 1,771,000 | |
| -3 | -3 | 302 | 43.75 | 10,000 | |

**Table 12-52. Residual Axial Fatigue Data for $[0° \pm 45°]_s$ G/E at 297K (75°) After Flight Simulation Exposure, R = 0.1, Unnotched**

| Specimen Number | Flight Simulation Specimen Number | Maximum Stress $MN/m^2$ | Maximum Stress (ksi) | Cycles | Comments |
|---|---|---|---|---|---|
| 10,000 hr | | | | | |
| B932-1 | BC93-2 | 414 | 60 | 10,286,000 | Did not fail |
| -2 | -2 | 483 | 70 | 2,034,000 | |
| -3 | -2 | 552 | 80 | 1,238,000 | |
| -4 | -2 | 586 | 85 | < 1,000 | |
| -5 | -2 | 517 | 75 | 11,000 | |
| -6 | -2 | 448 | 65 | 10,332,000 | Did not fail |
| B934-4 | -4 | 500 | 72.5 | 60,000 | |
| -5 | -4 | 534 | 77.5 | < 1,000 | |
| -6 | -4 | 552 | 80 | 355,000 | |
| 25,000 hr | | | | | |
| B941-4 | BC94-1 | 552 | 80 | 5,000 | Failed under doubler |
| -5 | -1 | 483 | 70 | 594,000 | Failed under doubler |
| -6 | -1 | 414 | 60 | 1,069,000 | |
| B942-4 | -2 | 379 | 55 | 10,000,000 | Did not fail |
| -5 | -2 | 517 | 75 | 740,000 | |
| -6 | -2 | 492 | 71.3 | 118,000 | Failed under doubler |
| 36,374 hr | | | | | |
| B954-1 | BC95-4 | 586 | 85 | 11,000 | |
| -2 | -4 | 448 | 65 | 2,850,000 | |
| -3 | -4 | 483 | 70 | 645,000 | |
| -4 | -4 | 517 | 75 | 117,000 | |
| -5 | -4 | 552 | 80 | 29,000 | |
| -6 | -4 | 414 | 60 | 2,080,000 | |
| B955-1 | -5 | 603 | 87.5 | 2,000 | |
| -2 | -5 | 379 | 55 | 8,039,000 | |
| -3 | -5 | 414 | 60 | 895,000 | |

Lowering the maximum test temperature for flight simulation exposure of the epoxies from 408K (275°F) to 373K (212°F) resulted in a significant improvement in the performance of these materials. The G/E system was particularly impressive with only the shear strength exhibiting a major decrease in value after 36,374 hours of exposure. For the B/E system the losses in tensile and compressive strengths after 36,374 hours were comparable to those in Phase I in only 10,000 hours of exposure.

The unnotched and notched tensile strengths of the B/E material were slightly lowered (less than 10%) by 10,000 hours of flight simulation exposure. The modulus was unchanged. For the G/E system the unnotched and notched tensile strengths and the modulus were higher for the

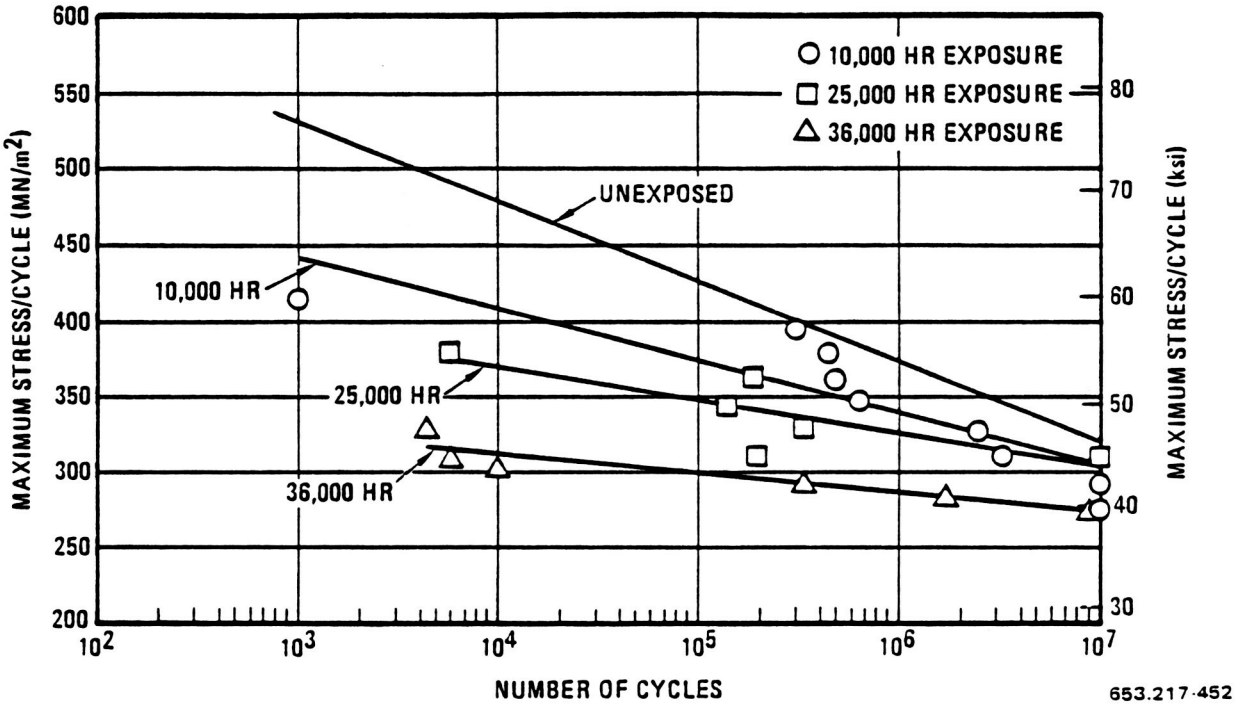



**Figure 12-149 Axial Fatigue Properties of $[0° \pm 45°]_s$ B/E Before and After Flight Simulation Exposure, 297K (75°F), R = 0.1, Unnotched**

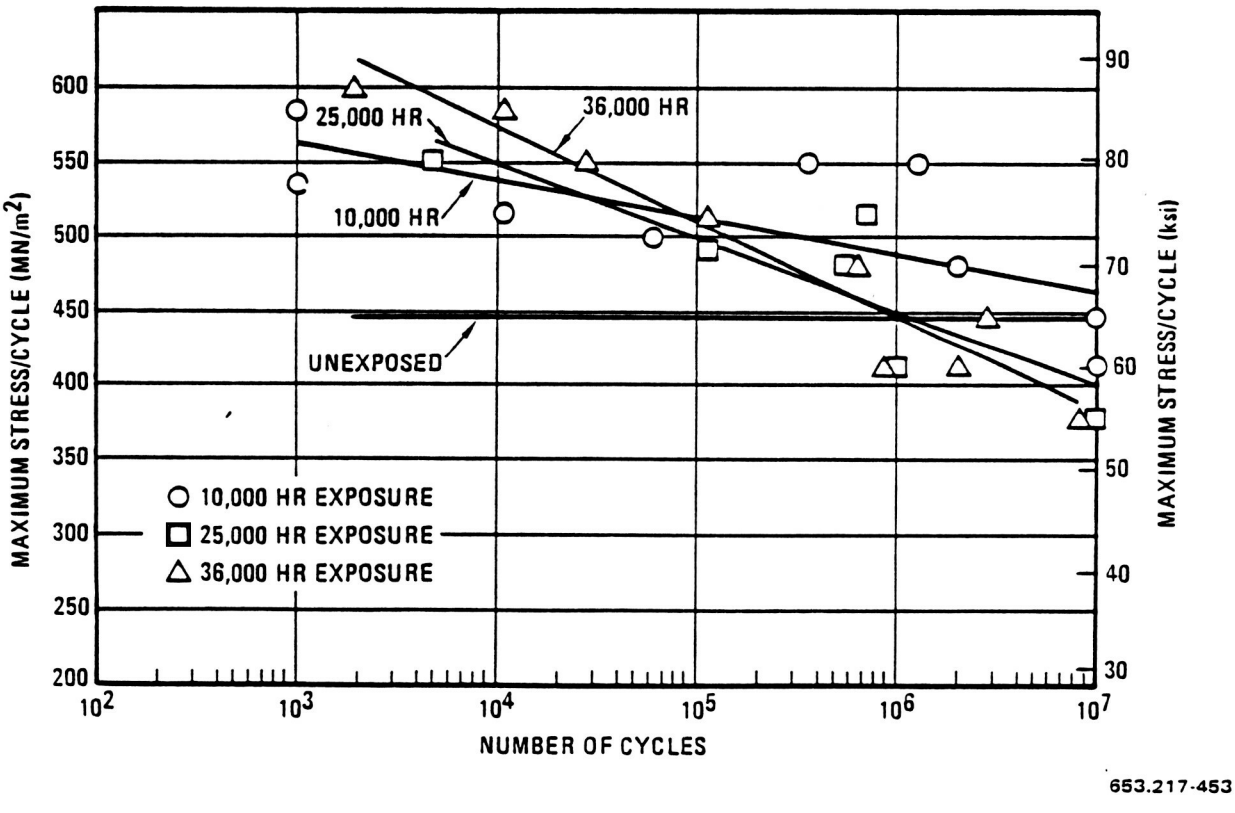



**Figure 12-150 Axial Fatigue Properties of $[0° \pm 45°]_s$ G/E Before and After Flight Simulation Exposure, 297K (75°F), R = 0.1, Unnotched**

exposed material than for the baseline specimens. The effect of 10,000 hours of flight simulation exposure on the matrix properties, compressive and shear strengths, was not very large except for the B/E compressive strength, which showed a decrease of approximately 25%. The results were much improved over those of Phase I for both epoxy systems. As shown in Figures 12-149 and 12-150 the fatigue properties of B/E were somewhat lowered by the 10,000 hours of long-term exposure cycling while the G/E fatigue strengths after cycling were higher than those obtained during the baseline fatigue tests.

As shown in Table 12-43, the tensile strength of the B/E material was lowered approximately 10% by 25,000 hours of flight simulation exposure. The G/E material behaved even better with essentially no change in the tensile strength as a result of the exposure. Modulus values were decreased for both systems by about 10%. The effect of 25,000 hours of flight simulation exposure on the matrix properties, compressive and shear, was slight for the G/E but substantial for the B/E system. Compressive and shear strength of the B/E decreased by about one-third after 25,000 hours of cycling. The G/E showed no change in compressive strength and a 7% loss in shear strength. A further decrease in the fatigue strength of the B/E was observed, but, again the amount was small. For G/E the 25,000 hours of exposure produced a decrease in fatigue strength only for fatigue lifetimes of $10^6$ or greater.

The 36,374 hours of exposure had a significant effect on the B/E system. Residual strength losses ranged from about 20% for tensile to near 60% for both compressive and shear. The two flight simulation failures after approximately 33,000 hours of exposure were undoubtedly the result of these very low residual compressive and shear strength properties. The G/E system, on the other hand, survived the 36,374 hours of flight simulation exposure with little loss in tensile or compressive strength. The major effect was a decrease in shear strength of 28%. The B/E showed a further decrease in fatigue strength while the G/E S-N curve was very similar to that obtained after 25,000 hours of exposure. The data are plotted in Figures 12-149 and 12-150.

In summary of these data, the B/E and G/E systems survived 25,000 hours of flight simulation exposure at a cruise temperature of 373K (212°F) with little visual damage. Some microcracking of the surface was observed in the heated zones but was not thought to be serious. Mechanical property degradation was minimal for the G/E material. For the B/E system, however, a 30% decrease in compressive and shear strengths and a 10% decrease in tensile strength were observed. After 36,374 hours of exposure the condition of the specimens was also quite good, although a few loose fibers were now visible in the heated zones of both the B/E and G/E specimens. Some increase in surface microcracking was also present. Mechanical property degradation of the G/E system was limited to a slight change in compressive strength but a significant loss in shear strength. The B/E system was severely degraded by the 36,374 hours of exposure, particularly for the matrix properties, compressive and shear strengths.

**HT-S/710 G/PI, $[0° \pm 45°]_s$, unnotched and notched.** The amount of residual strength data obtained for the HT-S/710 G/PI system was less than that originally planned because of two factors. First, the three 25,000 hour specimens were fabricated from the second batch of HT-S/710 prepreg ordered later in the program. This batch of material was found to have very poor thermooxidative properties during the new material screening tests. While two of the three 25,000 hour specimens were damaged during installation and were unusable, the third

failed to complete 6,000 hours of flight simulation exposure. It is believed that had the two other specimens not been damaged they also would not have survived much more than 6,000 hours of test. The second factor that reduced the number of residual strength specimens was the failure of all the unnotched and notched 50,000 hour specimens prior to completion of 50,000 hours. The test parameters of temperature and fatigue loading were selected such that 80% of the specimens were expected to survive 50,000 hours. This did not occur, and in fact, all of the specimens failed prior to reaching 40,000 hours.

It was possible, however, to salvage a half of each failed flight simulation specimen for fabrication of residual strength specimens. The residual strength test plan was selected to emphasize tensile strength as well as the matrix dominated properties, compressive strength and shear strength. The limited material available for specimens did not allow any residual fatigue testing or testing at other than room temperature. Table 12-53 shows the number of specimens of each type and the approximate number of hours of exposure each received. The exact exposure times can be found in the data tables that follow.

**Table 12-53. Residual Strength Test Plan for HT-S/710 G/PI After Flight Simulation Testing**

| | Number of Specimens Per Exposure Time | | | | |
|---|---|---|---|---|---|
| Test Type | 16,000 hr | 18,000 hr | 20,000 hr | 28,000 hr | 40,000 hr |
| [a]Unnotched Tensile | 6 | | | | 3 |
| [b]Notched Tensile | | 6 | 3 | 3 | |
| [a]Compressive | 2 | | 2 | | 2 |
| [b]Shear | | 4 | | 4 | |

[a]Cut from unfailed ends of unnotched flight simulation specimens
[b]Cut from unfailed ends of notched flight simulation specimens

Residual tensile and notched tensile data before and after flight simulation exposure are listed in Tables 12-54 and 12-55. Elastic modulus values are included for the unnotched tensile tests. The tensile strength values have been plotted as a function of exposure time in Figure 12-151. Also included in Figure 12-151 are data obtained in Phase I for 10,000 hours of exposure. Residual compressive and short beam shear data before and after flight simulation exposure are listed in Tables 12-56 and 12-57 and plotted as a function of time in Figure 12-152. The residual strength data for 10,000 hours obtained in Phase I are also shown on the curves. In Figure 12-153 the residual tensile and compressive modulii are plotted for the various exposure times.

Table 12-54. Strength and Modulus Properties of $[0° \pm 45°]_s$ HT-S/710 G/PI at 297K (75°F) Before and After Flight Simulation Exposure

| Specimen Number | Flight Simulation Specimen Number | | Strength MN/m² | Strength (ksi) | Modulus GN/m² | Modulus (Msi) |
|---|---|---|---|---|---|---|
| Unnotched Tensile: 15,458 hr | | | | | | |
| D91S-1 | DC91-S | | 188 | 27.3 | 39 | 5.7 |
| -2 | -S | | 189 | 27.4 | 54 | 7.9 |
| -3 | -S | | 287 | 41.6 | 41 | 5.9 |
| D921-1 | DC92-1 | | 310 | 45.0 | 44 | 6.4 |
| -2 | -1 | | 430 | 62.3 | 56 | 8.1 |
| -3 | -1 | | 375 | 54.4 | 44 | 6.4 |
| | | av | 296 | 43.0 | 46 | 6.7 |
| Unnotched Tensile: 39,856 hr | | | | | | |
| D924-1 | DC92-4 | | 46 | 6.7 | 32 | 4.7 |
| -2 | -4 | | 56 | 8.1 | 54 | 7.9 |
| -3 | -4 | | 179 | 25.9 | 31 | 4.5 |
| | | av | 94 | 13.6 | 39 | 5.7 |
| Baseline | | av | 519 | 75.3 | 53 | 7.7 |

At the completion of the Phase I 10,000 hours of flight simuation exposure the HT-S/710 G/PI material had experienced significant losses in shear strength (54%), tensile strenth (29%), and compressive strength (23%). With the additional exposure during Phase II out to 40,000 hours, the residual tensile and compressive strengths continued to decrease. The tensile strength, in particular, was severely affected with a loss of over 80% of the unexposed baseline value. Both the compressive and shear strengths decreased almost 60%, but the major portion of these changes occurred in the first 10,000 hours for shear and 20,000 hours for compressive strength. In like manner to the epoxy systems, the notched tensile strength was least affected by flight simulation exposure with a loss in value of approximately 25% in 28,000 hours. No notched tensile strength data were obtained for 40,000 hours as none of the notched flight simulation specimens completed more than 28,000 hours of exposure.

It should be kept in mind that comparisons of the various properties may not be entirely valid because of the role of specimen location on strength levels. The tensile and shear specimens were cut from the unshielded areas of the flight simulation specimens while the compressive and notched tensile specimens were prepared from the entire width. Also, the effect of bonding 6 ply laminates together to form 18 ply compressive and short beam shear specimens requires additional study to determine the validity of the results.

In summary of these data none of the HT-S/710 G/PI specimens survived 50,000 hours of flight simulation exposure. Specimens experienced wearout failures from the thermal and fatigue exposure cycling at time periods ranging from 15,000 hours to 40,000 hours. Unlike the

epoxy systems, no surface microcracking was observed. However, loss of polyimide resin from the surface in the heated zones occurred, thereby exposing the underlying graphite fibers. Cracking and delamination at the edges and at the holes was also found. Both surface resin loss and edge cracking increased with exposure time. Residual strength properties obtained from the undamaged ends of failed specimens were generally poor. Tensile, compressive, and shear strengths had all decreased by 50% or more in the first 20,000 hours of exposure. The effect of the cyclic fatigue loading and perhaps the thermal cycling can be seen by comparing these results with those from the thermal aging tests at the same temperature. After 25,000 hours of thermal aging at 505K (450°F) in one atmosphere air, almost no loss in tensile strength was measured.

**Table 12-55. Notched Tensile Strength of $[0° \pm 45°]_s$ HT-S/710 G/PI at 297K (75°F) Before and After Flight Simulation Exposure. (Notched flight simulation specimen)**

| Specimen Number | Flight Simulation Specimen Number | | Strength $MN/m^2$ | Strength (ksi) |
|---|---|---|---|---|
| Notched Tensile: 18,077 hr | | | | |
| DF92S-1 | DF92-S | | 257 | 37.3 |
| -2 | -S | | 304 | 44.1 |
| -3 | -S | | 134 | 19.4 |
| DF922-1 | -2 | | 324 | 47.0 |
| -2 | -2 | | 326 | 47.3 |
| -3 | -2 | | 277 | 40.2 |
| | | av | 270 | 39.2 |
| Notched Tensile: 20,398 hr | | | | |
| DF924-1 | DF92-4 | | 319 | 46.2 |
| -2 | -4 | | 221 | 32.1 |
| -3 | -4 | | 244 | 35.4 |
| | | av | 261 | 37.9 |
| Notched Tensile: 27,890 hr | | | | |
| DF923-1 | DF92-3 | | 245 | 35.5 |
| -2 | -3 | | 316 | 45.8 |
| -3 | -3 | | 242 | 35.1 |
| | | av | 268 | 38.8 |
| Baseline | | av | 357 | 51.8 |

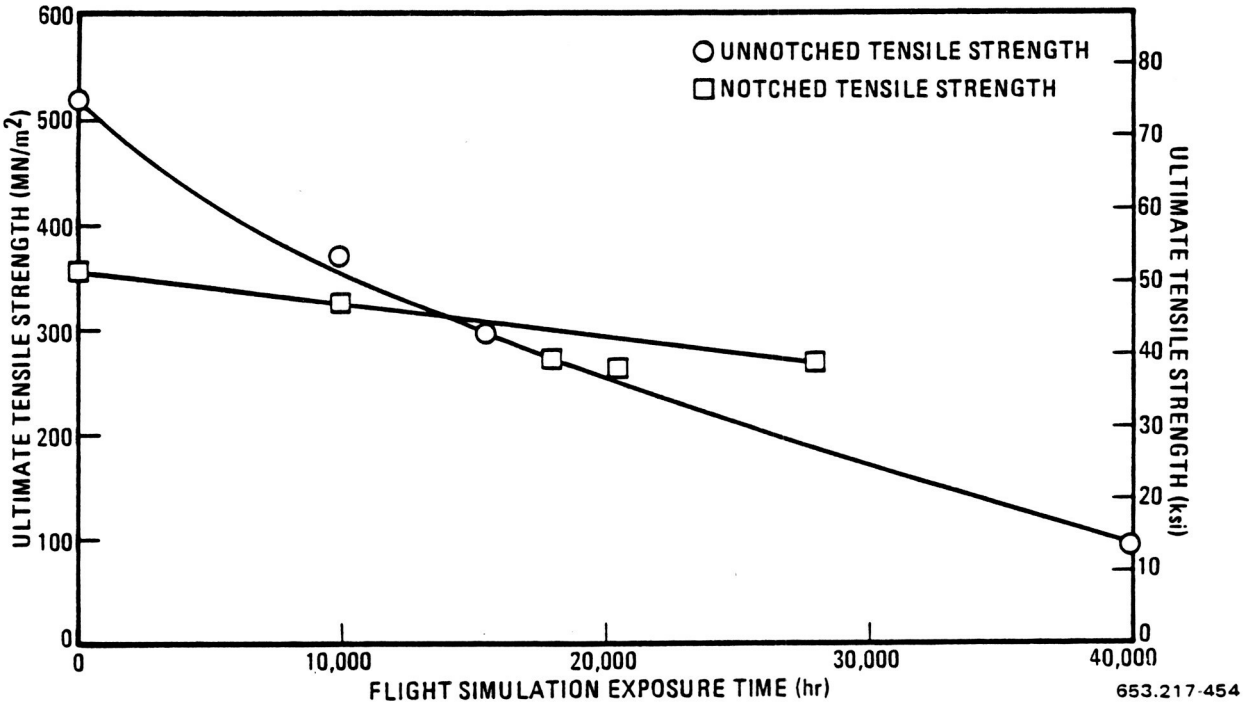



**Figure 12-151 Residual Tensile Strength of $[0° \pm 45°]_s$ HT-S/710 G/PI at 297K (75°F) After Flight Simulation Exposure at a Maximum Temperature of 505K (450°F)**

**Table 12-56. Compressive Strength Properties of $[0° \pm 45°]_s$ HT-S/710 G/PI at 297K (75°F) Before and After Flight Simulation Exposure**

| Specimen Number | Flight Simulation Specimen Number | | Strength $MN/m^2$ | Strength (ksi) | Modulus $GN/m^2$ | Modulus (Msi) |
|---|---|---|---|---|---|---|
| Compressive: 15,896 hr | | | | | | |
| D9C-5 | DC92-2 | | 248 | 36.0 | 37 | 5.4 |
| -6 | -2 | | 232 | 33.7 | 37 | 5.3 |
| | | av | 240 | 34.8 | 37 | 5.4 |
| Compressive: 19,400 hr | | | | | | |
| D9C-7 | DC92-5 | | 193 | 28.0 | 29 | 4.2 |
| -8 | -5 | | 188 | 27.3 | 30 | 4.4 |
| | | av | 191 | 27.6 | 30 | 4.3 |
| Compressive: 39,856 hr | | | | | | |
| D9C-9 | DC92-3 | | 135 | 19.6 | 30 | 4.3 |
| -10 | -3 | | 180 | 26.1 | 29 | 4.2 |
| | | av | 158 | 22.8 | 29 | 4.2 |
| Baseline | | av | 377 | 54.7 | 46 | 6.7 |

**Table 12-57. Short Beam Shear Strength Properties of $[0° \pm 45°]_s$ HT-S/710 G/PI at 297K (75°F) Before and After Flight Simulation Exposure**

| Specimen Number | Flight Simulation Specimen Number | | Strength MN/m² | Strength (ksi) |
|---|---|---|---|---|
| Short Beam Shear: 18,302 hr | | | | |
| D9S-5 | DF92-1 | | 21 | 3.0 |
| -6 | -1 | | 20 | 2.9 |
| -7 | -1 | | 17 | 2.4 |
| -8 | -1 | | 20 | 2.8 |
| | | av | 20 | 2.7 |
| Short Beam Shear: 27,890 hr | | | | |
| D9S-9 | DF92-5 | | 14 | 2.0 |
| -10 | -5 | | 19 | 2.8 |
| -11 | -5 | | 15 | 2.2 |
| -12 | -5 | | 18 | 2.6 |
| | | av | 17 | 2.4 |
| Baseline | | av | 37 | 5.4 |

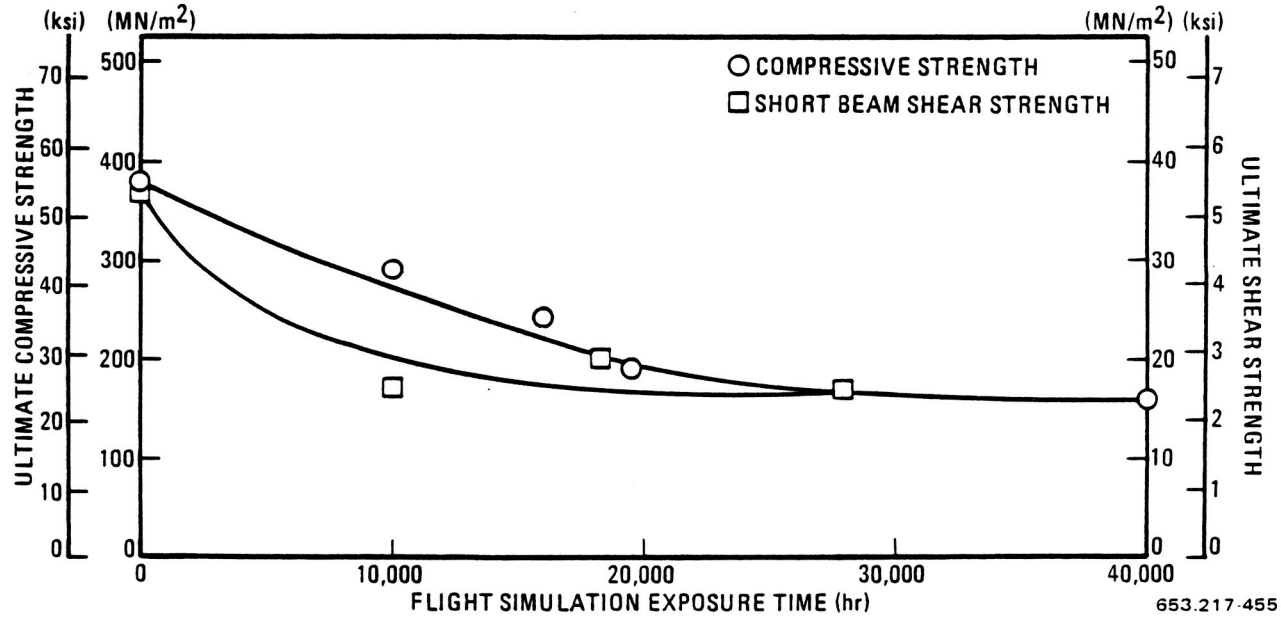



**Figure 12-152 Residual Compressive and Short Beam Shear Strength of $[0° \pm 45°]_s$ HT-S/710 G/PI at 297K (75°F) After Flight Simulation Exposure at a Maximum Temperature of 505K (450°F)**

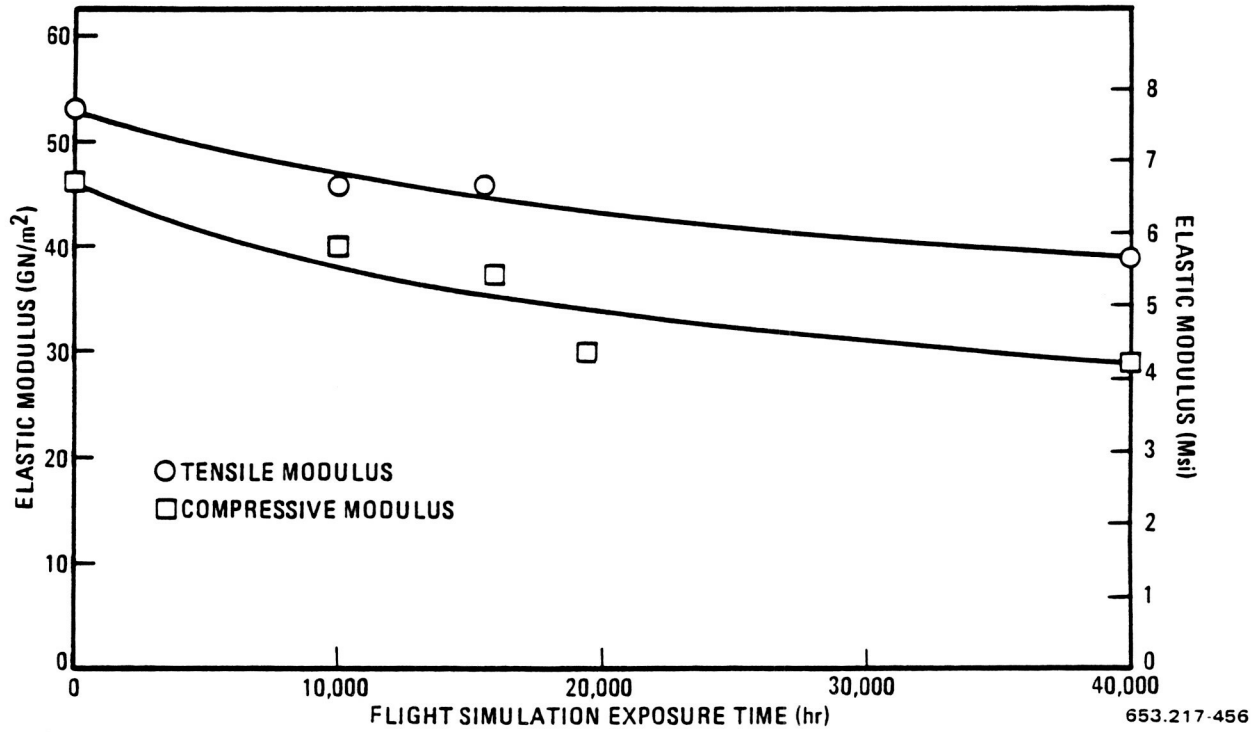



**Figure 12-153 Residual Tensile and Compressive Modulus of $[0° \pm 45°]_s$ HT-S/710 G/PI at 297K (75°F) After Flight Simulation Exposure at a Maximum Temperature of 505K (450°F)**

**Celion 6000/LARC-160 G/PI, $[0° \pm 45°]_s$, unnotched and notched.** The original plan for flight simulation testing of this system included exposure times of 10,000 hours and 25,000 hours at a maximum temperature of 450K (350°F). Because of time and financial restrictions, the 25,000 hour exposures were not funded. Consequently, at the completion of 10,000 hours there was an extra set of both unnotched and notched specimens available for residual strength testing. This excess material was used for compressive and shear tests and for some additional tensile, notched tensile, and notched fatigue tests. The original and revised test plans for Celion 6000/LARC-160 G/PI are shown in Table 12-58. Results of the 297K (75°F) and 450K (350°K) tensile tests on unnotched and notched G/PI after 10,000 hours of flight simulation exposure are presented in Tables 12-59 through 12-61. Also included are the baseline data for comparison purposes. Two types of notched tensile specimens were tested. The first, Table 12-60, was cut from unnotched flight simulation specimens and was notched after exposure. The second, Table 12-61, was cut from the notched flight simulation specimens after being exposed in the notched condition. Table 12-62 gives the compressive and short beam shear data for G/PI before and after flight simulation exposure of 10,000 hours. Results of the residual fatigue tests are listed in Tables 12-63 and 12-64. The data in Table 12-63 were obtained from specimens cut from unnotched flight simulation specimens and tested at 297K (75°F) and a stress ratio, R, of 0.1 in both unnotched and notched configurations. The data in Table 12-64 were obtained from notched specimens cut from notched flight simulation specimens and tested at 297K (75°F) and 450K (350°F) and a stress ratio, R, of 0.1. The fatigue results are plotted as S-N curves in Figures 12-154 through 12-157. Curves for unexposed Celion 6000/LARC-160 G/PI tested under the same conditions are shown on the fatigue plots for comparison.

**Table 12-58. Residual Strength Test Plan for Celion 6000/LARC-160 G/PI After 10,000 hr of Flight Simulation Testing**

| Flight Simulation Specimen Type | Test Type | Temperature | | Number of Specimens | |
|---|---|---|---|---|---|
| | | K | (°F) | Original Plan | Revised Plan |
| $[0° \pm 45°]_s$ Unnotched | Tensile | 297 | 75 | 10 | 10 |
| | Notched Tensile | 297 | 75 | 10 | 10 |
| | Fatigue | 297 | 75 | 10 | 10 |
| | Compressive | 297 | 75 | 0 | 4 |
| | Notched Fatigue | 297 | 75 | 0 | 9 |
| | Tensile | 450 | 350 | 5 | 10 |
| | Notched Tensile | 450 | 350 | 5 | 5 |
| $[0° \pm 45°]_s$ Notched | Notched Tensile | 297 | 75 | 10 | 10 |
| | Notched Fatigue | 297 | 75 | 10 | 10 |
| | Shear | 297 | 75 | 0 | 8 |
| | Notched Tensile | 450 | 350 | 5 | 10 |
| | Notched Fatigue | 450 | 350 | 0 | 12 |

**Table 12-59. Strength and Modules Properties of $[0° \pm 45°]_s$ Celion 6000/LARC-160 G/PI Before and After 10,000 hr of Flight Simulation Exposure. (Unnotched flight simulation specimen)**

| Specimen Number | Flight Simulation Specimen Number | Temperature K | Temperature (°F) | | Strength $MN/m^2$ | Strength (ksi) | Modulus $GN/m^2$ | Modulus (Msi) |
|---|---|---|---|---|---|---|---|---|
| Unnotched Tensile: 10,000 hr | | | | | | | | |
| F911-1 | FC91-1 | 297 | 75 | | 510 | 73.9 | 57 | [a] 8.3 |
| -2 | -1 | | | | 482 | 69.9 | 63 | [a] 9.1 |
| -3 | -1 | | | | 647 | 93.9 | 63 | [a] 9.2 |
| -4 | -1 | | | | 674 | 97.7 | 74 | 10.7 |
| -5 | -1 | | | | 645 | 93.5 | 63 | 9.2 |
| -6 | -1 | | | | 703 | 102 | 61 | 8.9 |
| F913-1 | -3 | | | | 581 | 84.2 | 104 | 15.1 |
| -2 | -3 | | | | 631 | 91.5 | 66 | 9.6 |
| -3 | -3 | | | | 598 | 86.8 | 57 | 8.3 |
| F914-1 | -4 | | | | 678 | 98.3 | 83 | 12.1 |
| | | | | av | 614 | 89.1 | 69 | 10.0 |
| Baseline | | | | av | 703 | 102 | 59 | 8.6 |
| F912-1 | FC91-2 | 450 | 350 | | 540 | 78.3 | 57 | [a] 8.3 |
| -2 | -2 | | | | 510 | 73.9 | 74 | [a]10.7 |
| -3 | -2 | | | | 542 | 78.6 | 71 | [a]10.3 |
| -4 | -2 | | | | 649 | 94.2 | 70 | 10.1 |
| -5 | -2 | | | | 574 | 83.2 | 57 | 8.3 |
| -6 | -2 | | | | 587 | 85.1 | 53 | 7.7 |
| F913-4 | -3 | | | | 630 | 91.4 | 51 | 7.4 |
| -5 | -3 | | | | 596 | 86.5 | 51 | 7.4 |
| -6 | -3 | | | | 584 | 84.7 | 45 | 6.5 |
| F914-4 | -4 | | | | 731 | 106 | 74 | 10.7 |
| | | | | av | 594 | 86.2 | 60 | 8.7 |
| Baseline | | | | av | 696 | 101 | 58 | 8.4 |

[a]Stain gage measurement

**Table 12-60. Notched Tensile Strength of $[0° \pm 45°]_s$ Celion 6000/LARC-160 G/PI Before and After 10,000 hr of Flight Simulation Exposure. (Unnotched flight simulation specimen)**

| Specimen Number | Flight Simulation Specimen Number | Temperature K | Temperature (°F) | | Strength $MN/m^2$ | Strength (ksi) |
|---|---|---|---|---|---|---|
| Notched Tensile: 10,000 hr | | | | | | |
| F923-1 | FC92-3 | 297 | 75 | | 618 | 89.7 |
| -2 | -3 | | | | 548 | 79.5 |
| -3 | -3 | | | | 589 | 85.4 |
| -4 | -3 | | | | 491 | 71.2 |
| -5 | -3 | | | | 592 | 85.8 |
| -6 | -3 | | | | 552 | 80.1 |
| F924-1 | -4 | | | | a | a |
| -2 | -4 | | | | 603 | 87.4 |
| -3 | -4 | | | | a | a |
| F922-1 | -2 | | | | 547 | 79.4 |
| | | | | av | 567 | 82.3 |
| Baseline | | | | av | 427 | 62.0 |
| F922-2 | FC92-2 | 450 | 350 | | 568 | 82.4 |
| -3 | -2 | | | | 587 | 85.1 |
| -4 | -2 | | | | 591 | 85.7 |
| -5 | -2 | | | | 607 | 88.0 |
| -6 | -2 | | | | 583 | 84.6 |
| | | | | av | 587 | 85.2 |
| Baseline | | | | av | 475 | 68.9 |

[a]Failed under doubler

**Table 12-61. Notched Tensile Strength of $[0° \pm 45°]_s$ Celion 6000/LARC-160 G/PIBefore and After 10,000 hr of Flight Simulation Exposure. (Notched flight simulation specimen)**

| Specimen Number | Flight Simulation Specimen Number | Temperature K | Temperature (°F) | | Strength $MN/m^2$ | Strength (ksi) |
|---|---|---|---|---|---|---|
| Notched Tensile: 10,000 hr | | | | | | |
| FF911-1 | FF91-1 | 297 | 75 | | 443 | 64.3 |
| -2 | -1 | | | | 643 | 93.4 |
| -3 | -1 | | | | a | a |
| -4 | -1 | | | | 419 | 60.8 |
| -5 | -1 | | | | 510 | 74.0 |
| -6 | -1 | | | | 389 | 56.4 |
| FF913-1 | -3 | | | | a | a |
| -2 | -3 | | | | 623 | 90.4 |
| -3 | -3 | | | | 663 | 96.2 |
| FF914-1 | -4 | | | | 528 | 76.7 |
| | | | | av | 527 | 76.5 |
| Baseline | | | | av | 427 | 62.0 |
| FF912-1 | FF91-2 | 450 | 350 | | a | a |
| -2 | -2 | | | | a | a |
| -3 | -2 | | | | 592 | 85.9 |
| -4 | -2 | | | | 361 | 52.4 |
| -5 | -2 | | | | 441 | 64.0 |
| -6 | -2 | | | | 431 | 62.5 |
| FF913-4 | -3 | | | | 456 | 66.1 |
| -5 | -3 | | | | 432 | 62.7 |
| -6 | -3 | | | | 532 | 77.2 |
| FF914-4 | -4 | | | | 332 | 48.2 |
| | | | | av | 447 | 64.9 |
| Baseline | | | | av | 475 | 68.9 |

[a]Failed under doubler

**Table 12-62. Compressive and Short Beam Shear Strength Properties of $[0° \pm 45°]_s$ Celion 6000/LARC-160 G/PI at 297K (75°F) Before and After 10,000 hr of Flight Simulation Exposure**

| Specimen Number | Flight Simulation Specimen Number | | Strength MN/m² | Strength (ksi) | Modulus GN/m² | Modulus (Msi) |
|---|---|---|---|---|---|---|
| Compressive: 10,000 hr | | | | | | |
| F9C-1 | FC91-5 | | 565 | 81.9 | 41 | 5.9 |
| -2 | -5 | | 544 | 78.9 | 47 | 6.9 |
| -3 | -5 | | 596 | 86.5 | 48 | 7.0 |
| -4 | -5 | | 492 | 71.5 | 56 | 8.2 |
| | | av | 549 | 79.7 | 48 | 7.0 |
| Baseline | | av | 584 | 84.7 | 52 | 7.5 |
| Short Beam Shear: 10,000 hr | | | | | | |
| F9S-1 | FF92-3 | | 21 | 3.1 | | |
| -2 | -3 | | 24 | 3.5 | | |
| -3 | -3 | | 21 | 3.0 | | |
| -4 | -3 | | 21 | 3.1 | | |
| -5 | -3 | | 35 | 5.1 | | |
| -6 | -3 | | 35 | 5.1 | | |
| -7 | -3 | | 30 | 4.4 | | |
| -8 | -3 | | 35 | 5.1 | | |
| | | av | 28 | 4.0 | | |
| Baseline | | av | 51 | 7.4 | | |

Table 12.63. Residual Axial Fatigue Data for $[0° \pm 45°]_s$ Celion 6000/LARC-160 G/PI at 297K (75°F) After 10,000 hr of Flight Simulation Exposure, R = 0.1. (Unnotched flight simulation specimen)

| Specimen Number | Flight Simulation Specimen Number | Specimen Type | Maximum Stress $MN/m^2$ | Maximum Stress (ksi) | Cycles | Comments |
|---|---|---|---|---|---|---|
| F914-2 | FC91-4 | Unnotched | 448 | 65 | 191,000 | |
| -3 | -4 | | 483 | 70 | 2,000 | |
| -5 | -4 | | 465 | 67.5 | 97,000 | |
| -6 | -4 | | 500 | 72.5 | 459,000 | |
| F921-1 | FC92-1 | | 414 | 60 | 2,503,000 | |
| -2 | -1 | | 517 | 75 | <1,000 | |
| -3 | -1 | | 431 | 62.5 | 1,005,000 | |
| -4 | -1 | | 379 | 55 | 10,077,000 | Did not fail |
| -5 | -1 | | 500 | 72.5 | 3,000 | |
| -6 | -1 | | 396 | 57.5 | 12,423,000 | Did not fail |
| F924-4 | FC92-4 | Notched | 607 | 88.1 | <1,000 | |
| -5 | -4 | | 559 | 81.1 | 2,000 | |
| -6 | -4 | | 538 | 78.0 | 51,000 | |
| F925-1 | -5 | | 512 | 74.3 | 1,480,000 | |
| -2 | -5 | | 488 | 70.8 | 451,000 | |
| -3 | -5 | | 467 | 67.7 | 9,000 | |
| -4 | -5 | | 443 | 64.2 | 82,000 | |
| -5 | -5 | | 419 | 60.7 | 194,000 | |
| -6 | -5 | | 373 | 54.1 | 13,067,000 | Did not fail |

**Table 12-64. Residual Axial Notched Fatigue Data for $[0° \pm 45°]_s$ Celion 6000/LARC-160 G/PI After 10,000 hr of Flight Simulation Exposure, R = 0.1. (Notched flight simulation specimen)**

| Specimen Number | Flight Simulation Specimen Number | Temperature K | Temperature (°F) | Maximum Stress $MN/m^2$ | Maximum Stress (ksi) | Cycles | Comments |
|---|---|---|---|---|---|---|---|
| FF914-2 | FF91-4 | 297 | 75 | 516 | 74.8 | 5,000 | |
| -3 | -4 | | | 493 | 71.5 | 8,000 | |
| -5 | -4 | | | 423 | 61.3 | 2,000 | |
| -6 | -4 | | | 374 | 54.2 | 175,000 | |
| FF915-1 | -5 | | | 353 | 51.2 | 10,057,000 | Did not fail |
| -2 | -5 | | | 562 | 81.5 | 2,000 | |
| -3 | -5 | | | 400 | 58.0 | 258,000 | |
| -4 | -5 | | | 445 | 64.5 | 19,000 | |
| -5 | -5 | | | 377 | 54.7 | 53,000 | |
| -6 | -5 | | | 423 | 61.4 | 7,000 | |
| FF921-1 | FF92-1 | 450 | 350 | 483 | 70 | 123,000 | |
| -2 | -1 | | | 448 | 65 | — | Machine malfunction |
| -3 | -1 | | | 500 | 72.5 | 11,000 | |
| -4 | -1 | | | 448 | 65 | 72,000 | |
| -5 | -1 | | | 414 | 60 | 359,000 | |
| -6 | -1 | | | 396 | 57.5 | 297,000 | |
| FF922-1 | -2 | | | 379 | 55 | 1,156,000 | |
| -2 | -2 | | | 552 | 80 | 2,000 | |
| -3 | -2 | | | 276 | 40 | 11,395,000 | |
| -4 | -2 | | | 345 | 50 | 170,000 | |
| -5 | -2 | | | 310 | 45 | 1,541,000 | |
| -6 | -2 | | | 483 | 70 | 3,000 | |

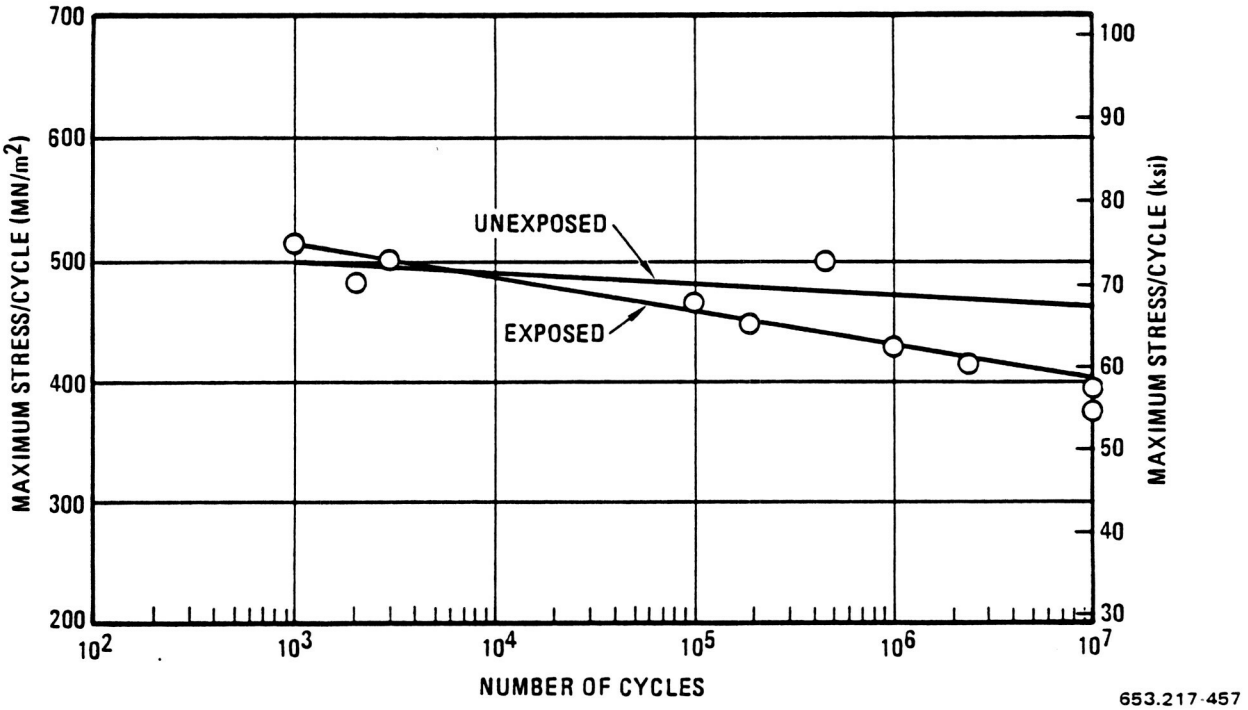



**Figure 12-154 Axial Fatigue Properties of $[0° \pm 45°]_s$ Celion 6000/LARC-160 G/PI Before and After 10,000 hr of Flight Simulation Exposure, 297K (75°F), R = 0.1, Unnotched. (Unnotched flight simulation specimen)**

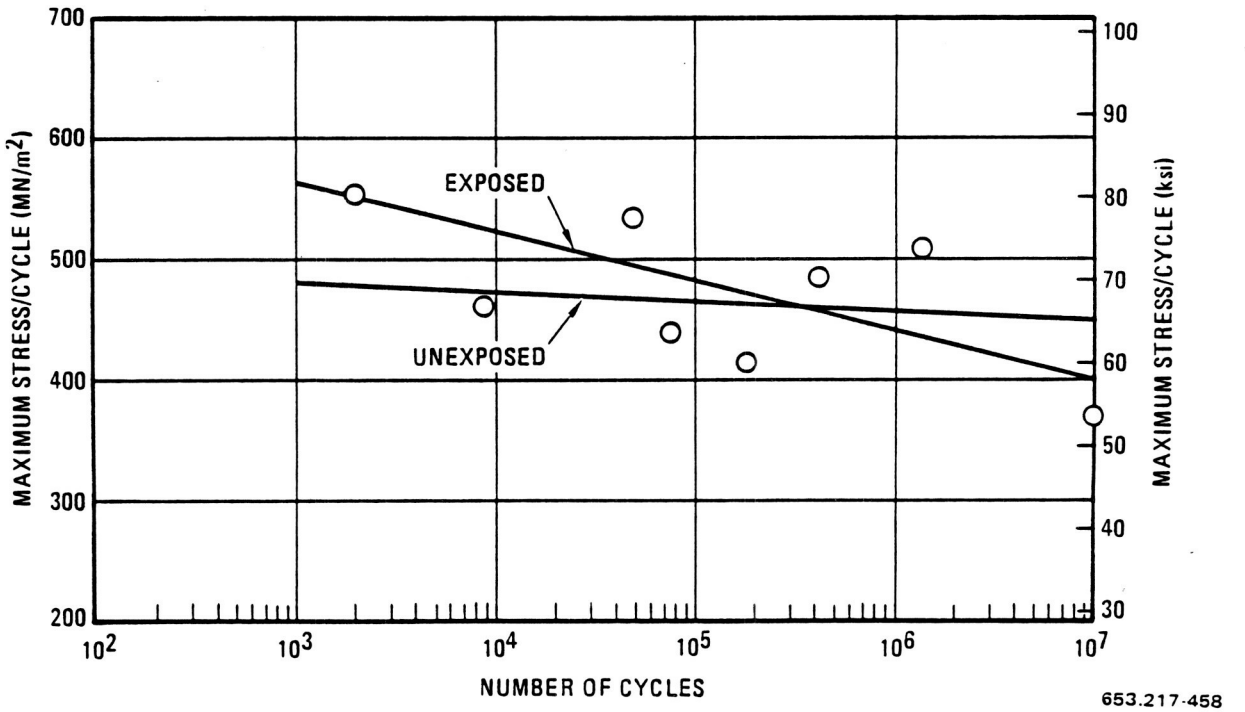



**Figure 12-155 Axial Fatigue Properties of $[0° \pm 45°]_s$ Celion 6000/LARC-160 G/PI Before and After 10,000 hr of Flight Simulation Exposure, 297K (75°F), R = 0.1, Notched. (Unnotched flight simulation specimen)**

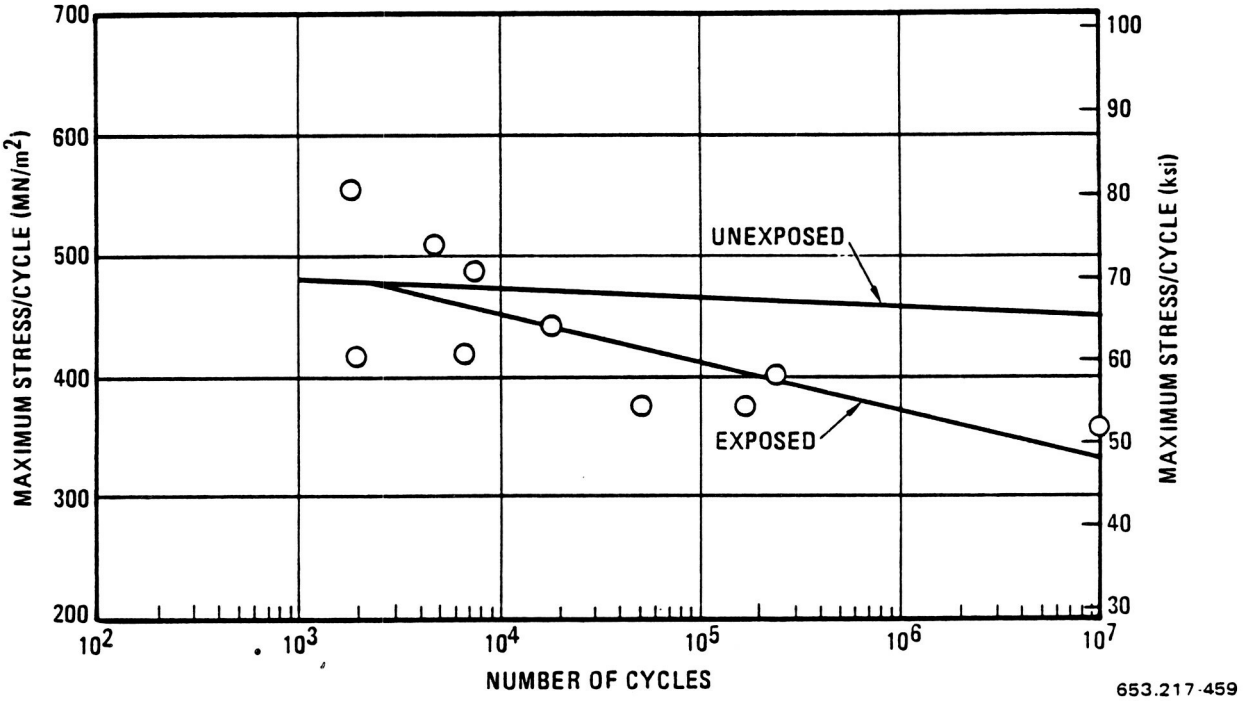



**Figure 12-156 Axial Fatigue Properties of $[0° \pm 45°]_s$ Celion 6000/LARC-160 G/PI Before and After 10,000 hr of Flight Simulation Exposure, 297K (75°F), R = 0.1, Notched. (Notched flight simulation specimen)**

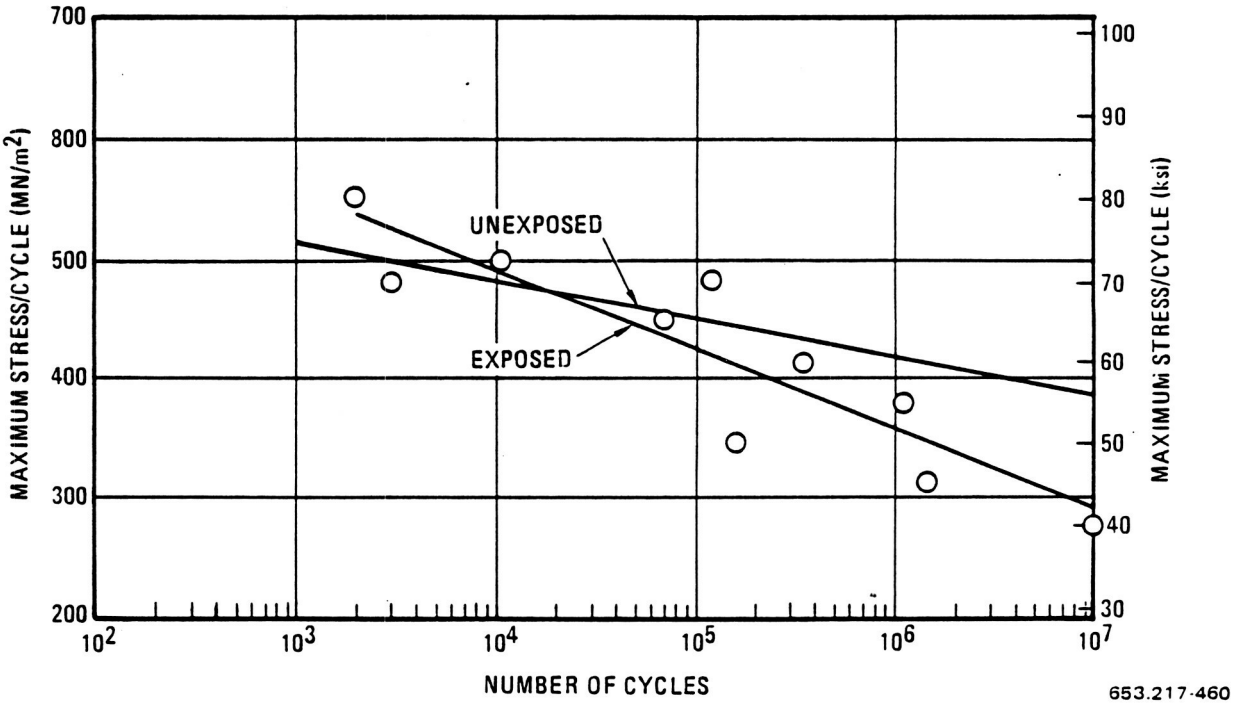



**Figure 12-157 Axial Fatigue Properties of $[0° \pm 45°]_s$ Celion 6000/LARC-160 G/PI Before and After 10,000 hr of Flight Simulation Exposure, 450K (350°F), R = 0.1, Notched. (Notched flight simulation specimen)**

After 10,000 hours of flight simulation exposure at a maximum test temperature of 450K (350°F) the Celion 6000/LARC-160 material exhibited slight losses in unnotched tensile strength and compressive strength, almost no loss in notched tensile strength, but a severe reduction in shear strength. The results for the Celion 6000/LARC-160 were considerably better than those for the HT-S/710 G/PI after 10,000 hours. In both cases, however, shear strength was drastically reduced by the flight simulation exposure. Surprisingly, the flight simulation residual properties of Celion 6000/LARC-160 were higher than those obtained after 10,000 hours of thermal aging at the same temperature. Here again the property most degraded was the shear strength.

Two groups of notched tensile specimens were tested. One group was notched after flight simulation exposure, and the other was notched before exposure and exposed in the notched condition. While both groups of specimens retained their strength after flight simulation, the specimens that were exposed in the unnotched condition possessed significantly higher values after exposure, particularly at the elevated test temperature.

With the extra flight simulation specimens of Celion 6000/LARC-160 G/PI that were available it was possible to increase the amount of residual fatigue testing over that originally scheduled. Both unnotched and notched residual fatigue curves, Figures 12-154 and 12-155, of specimens cut from unnotched flight simulation specimens showed slight decreases from the baseline curves. These decreases were more pronounced at the high cycle portions of the curves. For flight simulation specimens that were in the notched condition during exposure the residual fatigue properties (only notched residual strength specimens were tested) showed a greater decrease from the baseline. Again the decrease was greater for higher cycles. The S-N curves for specimens cut from notched flight simulation specimens are shown in Figures 12-156 and 12-157. Also apparent from these curves is that the effect of test temperature on both baseline and residual fatigue strength was small. In like manner to residual notched tensile strength, the major effect on residual fatigue strength is the configuration of the flight simulation specimen. That is, material exposed in the notched condition shows a greater decrease in residual notched properties than does material exposed in the unnotched condition.

**B/Al, $[0° \pm 45°]_s$ and $[0°]_6$, unnotched.** The amount of residual strength data for B/Al, like that for the HT-S/710 G/PI system, was considerably less than originally planned because of numerous specimen failures during flight simulation exposure at maximum temperatures of 505K (450°F). Some of the 25,000 hour specimens survived, but all of the 50,000 hour specimens failed before reaching that goal. Table 12-65 shows the test plan for the material that could be salvaged from the few specimens that survived and the unfailed ends of those that did not.

Table 12-65. Residual Strength Test Plan for B/Al After Flight Simulation Testing — 297K (75°K) Unnotched Tensile Strength

| Exposure Time (hr) | Number of Residual Strength Specimens | | |
|---|---|---|---|
| | $[0° \pm 45°]_s$ | $(0°]_6$ | $[90°]_6$ |
| 13,000 | | 3 | 3 |
| 18,000 | 3 | 11 | |
| 20,000 | 3 | | |
| 21,000 | 3 | | |
| 24,000 | | | 6 |
| 25,000 | | 6 | |
| 27,000 | 9 | | |
| 32,000 | | 3 | |

Because of the small amount of material available for specimens and the widely ranging failure times, only room temperature tensile testing was performed. In addition to the $[0° \pm 45°]_s$ and $[0°]_6$ specimens, a small number of 0.076m (3 in.) by 0.013 m (0.5 in.) transverse tensile specimens were cut from the heated zones of specimens that had failed in such a manner so to preserve enough heated zone material for testing. These [90°] specimens were cut from the failed ends of the flight simulation specimens.

Results of the unnotched tensile tests on B/Al before and after flight simulation exposure are presented in Tables 12-66 through 12-68. Elastic modulus values are included for the longitudinal $[0° \pm 45°]_s$ and $[0°]_6$ tests. The longitudinal tensile strength data have also been plotted as a function of exposure time in Figures 12-158 and 12-159. Data obtained in Phase I for 10,000 hours of exposure are also plotted on the graphs.

In Phase I the B/Al system showed losses in mechanical properties of approximately one-fourth after 10,000 hours of flight simulation exposure. For the $[0° \pm 45°]_s$ crossplied material the tensile strength continued to decrease with exposure time although not at as great a rate. After 27,000 hours the tensile strength was slightly less than one-half of the unexposed value. Modulus values for the exposed $[0° \pm 45°]_s$ B/Al showed considerable scatter. The data appear to indicate little change in modulus for the first 20,000 hours of simulation testing but a severe decrease after 27,000 hours.

**Table 12-66. Strength and Modulus Properties of $[0° \pm 45°]_s$ B/Al at 297K (75°F) Before and After Flight Simulation Exposure**

| Specimen Number | Flight Simulation Specimen Number | | Strength MN/m² | Strength (ksi) | Modulus GN/m² | Modulus (Msi) |
|---|---|---|---|---|---|---|
| Unnotched Tensile: 17,707 hr | | | | | | |
| EC923-1 | EC92-3 | | 257 | 37.3 | 79 | 11.5 |
| -2 | -3 | | 276 | 40.0 | 193 | 28.0 |
| -3 | -3 | | 338 | 49.0 | 97 | 14.1 |
| | | av | 290 | 42.1 | 123 | 17.9 |
| Unnotched Tensile: 19,519 hr | | | | | | |
| EC924-1 | EC92-4 | | 303 | 43.9 | 179 | 25.9 |
| -2 | -4 | | 301 | 43.7 | 125 | 18.2 |
| -3 | -4 | | 255 | 37.0 | 150 | 21.8 |
| | | av | 286 | 41.5 | 151 | 22.0 |
| Unnotched Tensile: 20,957 hr | | | | | | |
| EC925-1 | EC92-5 | | 278 | 40.3 | | |
| -2 | -5 | | 268 | 38.8 | | |
| -3 | -5 | | 257 | 37.3 | | |
| | | av | 268 | 38.8 | | |
| Unnotched Tensile: 27,402 hr | | | | | | |
| EC931-1 | EC93-1 | | 299 | 43.4 | 120 | 17.4 |
| -2 | -1 | | 225 | 32.6 | 80 | 11.6 |
| -3 | -1 | | 49 | 7.1 | — | — |
| EC932-1 | -2 | | 207 | 30.0 | 44 | 6.4 |
| -2 | -2 | | 228 | 33.0 | 42 | 6.1 |
| -3 | -2 | | 217 | 31.4 | 74 | 10.8 |
| EC933-1 | -3 | | 271 | 39.3 | 105 | 15.2 |
| -2 | -3 | | 288 | 41.7 | 115 | 16.7 |
| -3 | -3 | | 217 | 31.5 | 84 | 12.2 |
| | | av | 222 | 32.2 | 83 | 12.1 |
| Baseline | | av | 516 | 74.8 | 154 | 22.4 |

For the unidirectional B/Al tested in the fiber direction the tensile strength decreased by 25% after the first 10,000 hours of exposure but very little thereafter, out to almost 32,000 hours. An exception to this was the data from the specimen that failed at 12,605 hours. However, two of these three specimens failed at locations that were not in the heated zone of the flight simulation specimen from which they were cut. For the $[0°]_6$ material no decrease in elastic modulus was observed for the 32,000 hours of flight simulation.

**Table 12-67. Strength and Modulus Properties of $[0°]_6$ B/Al at 297K (75°F) Before and After Flight Simulation Exposure**

| Specimen Number | Flight Simulation Specimen Number | | Strength MN/m² | Strength (ksi) | Modulus GN/m² | Modulus (Msi) |
|---|---|---|---|---|---|---|
| Unnotched Tensile: 12,605 hr | | | | | | |
| [a]EU923-4 | EU92-3 | | 660 | 96.5 | 190 | 27.6 |
| [a] -5 | -3 | | 448 | 65.0 | 213 | 30.9 |
| -6 | -3 | | 1240 | 180.0 | 207 | 30.0 |
| | | av | 786 | 114 | 203 | 29.5 |
| Unnotched Tensile: 17,519 hr | | | | | | |
| EU912-1 | EU91-2 | | 1250 | 181 | 200 | 29.0 |
| -2 | -2 | | 1150 | 167 | 183 | 26.5 |
| -3 | -2 | | 1000 | 145 | 158 | 22.9 |
| -4 | -2 | | 1050 | 152 | 191 | 27.7 |
| -5 | -2 | | 979 | 142 | 218 | 31.6 |
| | | av | 1080 | 157 | 190 | 27.5 |
| Unnotched Tensile: 17,702 hr | | | | | | |
| EU921-1 | EU92-1 | | 1360 | 197 | 209 | 30.3 |
| -2 | -1 | | 1370 | 199 | 221 | 32.0 |
| -3 | -1 | | 1310 | 190 | 205 | 29.7 |
| 4 | -1 | | 952 | 138 | 299 | 43.3 |
| -5 | -1 | | 1050 | 152 | 165 | 23.9 |
| -6 | -1 | | 1160 | 169 | 197 | 28.6 |
| | | av | 1200 | 174 | 216 | 31.3 |
| Unnotched Tensile: 25,000 hr | | | | | | |
| EU933-1 | EU93-3 | | 1030 | 150 | 206 | 29.9 |
| -2 | -3 | | 1450 | 210 | 223 | 32.3 |
| -3 | -3 | | 1250 | 182 | 197 | 28.5 |
| -4 | -3 | | 848 | 123 | 222 | 32.2 |
| -5 | -3 | | 1030 | 150 | 231 | 33.5 |
| -6 | -3 | | 1180 | 171 | 218 | 31.6 |
| | | av | 1130 | 164 | 216 | 31.3 |
| Unnotched Tensile: 31,584 hr | | | | | | |
| EU922-1 | EU92-2 | | 1050 | 152 | 223 | 32.3 |
| -2 | -2 | | 1100 | 159 | 210 | 30.5 |
| -3 | -2 | | 896 | 130 | 213 | 30.9 |
| | | av | 1020 | 147 | 215 | 31.2 |
| Baseline | | av | 1450 | 210 | 198 | 28.7 |

[a]Specimen failed outside of heated zone

**Table 12-68. Transverse Tensile Properties of $[0°]_6$ B/Al at 297K (75°F) Before and After Flight Simulation Exposure**

| Specimen Number | Flight Simulation Specimen Number | | Strength MN/m² | Strength (ksi) |
|---|---|---|---|---|
| Transverse Tensile: 12,605 hr | | | | |
| EU923-1 | EU92-3 | | 59 | 8.6 |
| -2 | -3 | | 66 | 9.5 |
| -3 | -3 | | 62 | 9.0 |
| | | av | 62 | 9.0 |
| Transverse Tensile: 23,588 hr | | | | |
| EU932-1 | EU93-2 | | 72 | 10.4 |
| -2 | -2 | | 65 | 9.4 |
| -3 | -2 | | 65 | 9.5 |
| -7 | -2 | | 64 | 9.3 |
| -8 | -2 | | 61 | 8.8 |
| -9 | -2 | | 61 | 8.8 |
| | | av | 65 | 9.4 |
| Baseline | | av | 79 | 11.5 |

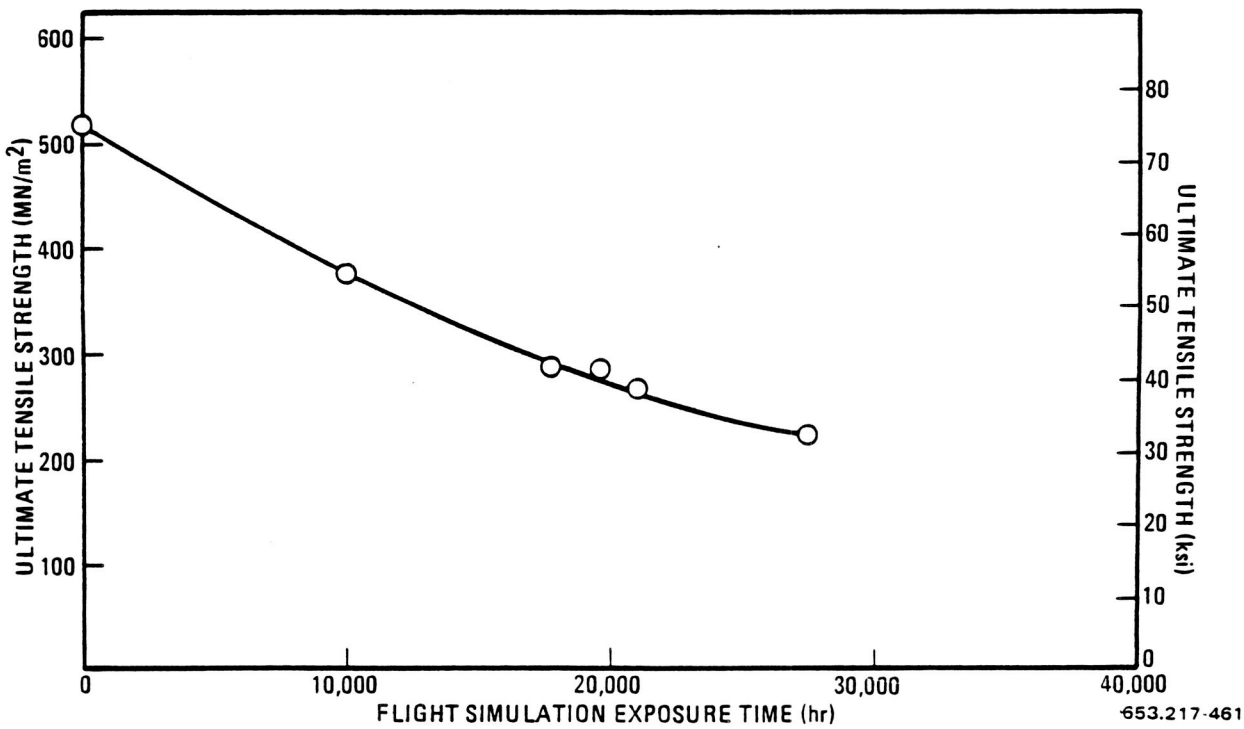



**Figure 12-158 Residual Tensile Strength of $[0° \pm 45°]_s$ B/Al at 297K (75°F) After Flight Simulation Exposure at a Maximum Temperature of 505K (450°F)**

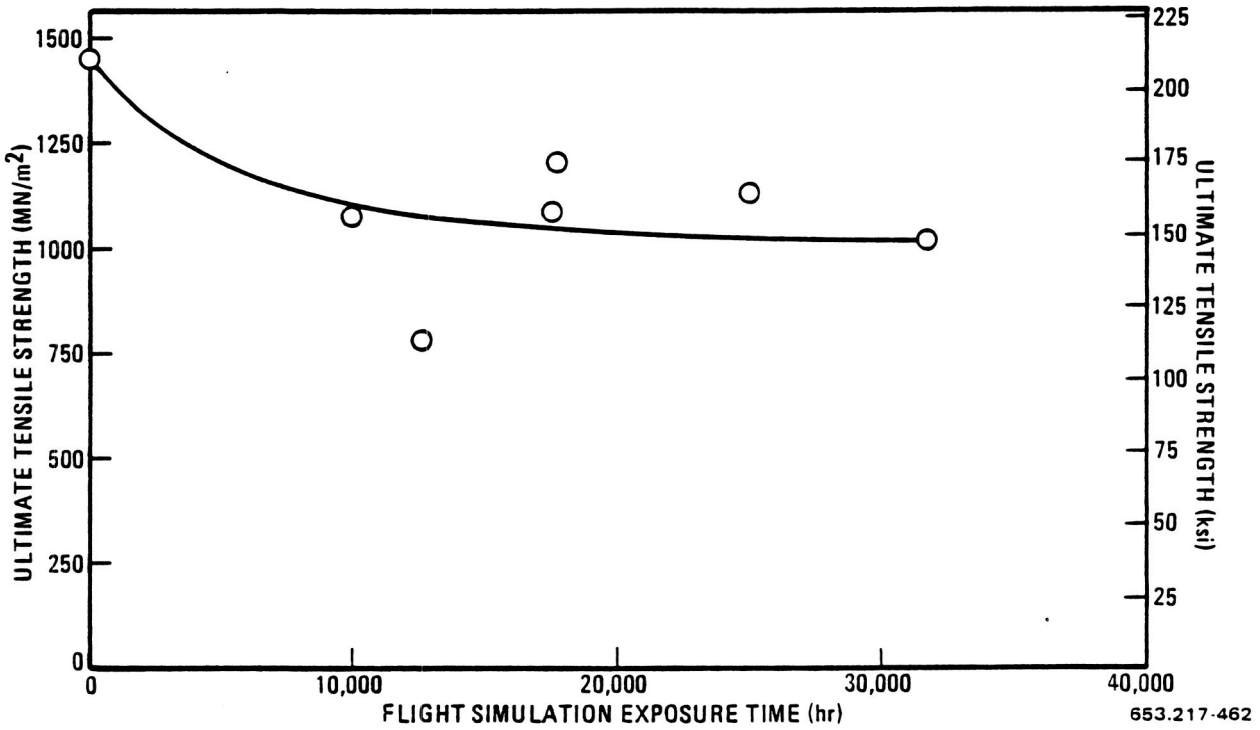



**Figure 12-159 Residual Tensile Strength of $[0° \pm 45°]_s$ B/Al at 297K (75°F) After Flight Simulation Exposure at a Maximum Temperature of 505K (450°F)**

The limited data for transverse tensile strength show a loss of about 20% after 24,000 hours of exposure.

Examination of the flight simulation specimens after exposure both with a low power, stereo microscope and using metallographic techniques revealed damage only at the surface and specimen edges. The damage consisted of surface roughening, longitudinal cracking of the aluminum, and fracture of the outer ply boron filaments. This surface damage is believed to have been responsible for the decrease in tensile properties observed during residual strength testing. The loss in tensile strength for the crossplied material was greater than that for the unidirectional material for two reasons. First, the surface damage was more severe, as noted in Section 12.7.3.1 for the crossplied specimens. Second, the $[0° \pm 45°]_s$ crossplied material obtains a large percentage of its strength from the two [0°] plies. As these are located on the outsides, any surface damage will be concentrated in the high strength portion of the specimens.

#### PHASE II SUMMARY

Table 12-69 summarizes the Phase II, long term flight simulation residual strength data obtained from the five composite systems. The percentage change in the various mechanical properties is listed for each material. For several entries in the table data was not available at exactly 25,000 hours or 36,000 hours. These values were obtained from the property versus exposure time curves. The fatigue data from the two epoxy systems and Celion 6000/LARC-160 G/PI are summarized in Table 12-70. In this table the fatigue strength at $10^7$ cycles, expressed as a percentage of the unexposed tensile strength is compared for unexposed material and for that which has survived various periods of flight simulation exposure.

**Table 12-69. Summary of Phase II Flight Simulation Residual Strength Data**

| Material System | Property | Temperature K | Temperature (°F) | % Property Loss In 10,000 hr | % Property Loss In 25,000 hr | % Property Loss In 36,000 hr |
|---|---|---|---|---|---|---|
| 5505/4 B/E $[0° \pm 45°]_s$ | $F_{tu}$ | 297 | 75 | 6 | 11 | 22 |
| | $E_t$ | 297 | 75 | 0 | 14 | 0 |
| | [a]Notched $F_{tu}$ | 297 | 75 | 7 | — | 14 |
| | $F_{cu}$ | 297 | 75 | 23 | 33 | 60 |
| | $E_c$ | 297 | 75 | 31 | 34 | 37 |
| | $F_{su}$ | 297 | 75 | 0 | 32 | 57 |
| A-S/3501-5 G/E $[0° \pm 45°]_s$ | $F_{tu}$ | 297 | 75 | 0 | 0 | 0 |
| | $E_t$ | 297 | 75 | 0 | 10 | 0 |
| | [a]Notched $F_{tu}$ | 297 | 75 | 0 | — | 0 |
| | $F_{cu}$ | 297 | 75 | 2 | 0 | 7 |
| | $E_c$ | 297 | 75 | 2 | 0 | 0 |
| | $F_{su}$ | 297 | 75 | 14 | 7 | 28 |
| HT-S/710 G/PI $[0° \pm 45°]_s$ | $F_{tu}$ | 297 | 75 | 29 | 59 | 76 |
| | $E_t$ | 297 | 75 | 10 | 21 | 25 |
| | [b]Notched $F_{tu}$ | 297 | 75 | 8 | 23 | — |
| | $F_{cu}$ | 297 | 75 | 23 | 54 | 58 |
| | $E_c$ | 297 | 75 | 13 | 30 | 35 |
| | $F_{su}$ | 297 | 75 | 54 | 55 | — |

**Table 12-69. Summary of Phase II Flight Simulation Residual Strength Data — Concluded**

| Material System | Property | Temperature K | Temperature (°F) | % Property Loss In 10,000 hr | % Property Loss In 25,000 hr | % Property Loss In 36,000 hr |
|---|---|---|---|---|---|---|
| Celion 6000/ LARC-160 G/PI $[0° \pm 45°]_s$ | $F_{tu}$ | 297 | 75 | 13 | — | — |
| | $E_t$ | 297 | 75 | 0 | — | — |
| | $F_{tu}$ | 450 | 350 | 15 | — | — |
| | $E_t$ | 450 | 350 | 0 | — | — |
| | [a]Notched $F_{tu}$ | 297 | 75 | 0 | — | — |
| | [a]Notched $F_{tu}$ | 450 | 350 | 0 | — | — |
| | [b]Notched $F_{tu}$ | 297 | 75 | 0 | — | — |
| | [b]Notched $F_{tu}$ | 450 | 350 | 6 | — | — |
| | $F_{cu}$ | 297 | 75 | 6 | — | — |
| | $E_c$ | 297 | 75 | 7 | — | — |
| | $F_{su}$ | 297 | 75 | 46 | — | — |
| B/Al $[0° \pm 45°]_s$ | $F_{tu}$ | 297 | 75 | 26 | 55 | — |
| | $E_t$ | 297 | 75 | 10 | 37 | — |
| B/Al $[0°]_6$ | $F_{tu}$ | 297 | 75 | 25 | 29 | [c]30 |
| | $E_t$ | 297 | 75 | 0 | 0 | [c]0 |
| B/Al $[90°]_6$ | $F_{tu}$ | 297 | 75 | 17 | 21 | — |

[a]Unnotched flight simulation specimens
[b]Notched flight simulation specimens
[c]31,584 hr

**Table 12-70. Strength at Fatigue Limit or $10^7$ Cycles Expressed as Percentage of Ultimate Tensile Strength Before and After Flight Simulation Exposure, R = 0.1**

| Material System | Specimen Configuration | Condition | Fatigue Test Temperature K | Fatigue Test Temperature (°F) | Fatigue Strength at $10^7$ Cycles (% of Unexposed $F_{tu}$) |
|---|---|---|---|---|---|
| 5505/4 B/E $[0° \pm 45°]_s$ | Unnotched | Unexposed | 297 | 75 | 60 |
| | | Exposed 10,000 hr | 297 | 75 | 57 |
| | | Exposed 25,000 hr | 297 | 75 | 57 |
| | | Exposed 36,374 hr | 297 | 75 | 52 |
| A-S/3501-5 G/E $[0° \pm 45°]_s$ | Unnotched | Unexposed | 297 | 75 | 81 |
| | | Exposed 10,000 hr | 297 | 75 | 85 |
| | | Exposed 25,000 hr | 297 | 75 | 73 |
| | | Exposed 36,374 hr | 297 | 75 | 70 |
| Celion 6000/ LARC-160 G/PI $[0° \pm 45°]_s$ | Unnotched | Unexposed | 297 | 75 | 67 |
| | | Exposed 10,000 hr | 297 | 75 | 58 |
| | Notched | Unexposed | 297 | 75 | 100 |
| | | Exposed 10,000 hr | 297 | 75 | 93 |
| | | Exposed 10,000 hr | 297 | 75 | 77 |
| | | Unexposed | 450 | 350 | 81 |
| | | Exposed 10,000 hr | 450 | 350 | 61 |

[a]Unnotched flight simulation specimens

[b]Notched flight simulation specimens

# SECTION 13

# THERMAL EXPOSURE TEST PROGRAM SUMMARY

This section presents an overview of the thermal exposure test programs with emphasis on trends observed for each of the materials. Specific tests included in the summary are the baseline tensile, compressive, and shear tests; the thermal aging tests; the short-term tests; the long-term tests; and the baseline and post-flight simulation constant amplitude fatigue tests. The thermal aging tests are included in the summary even though they generally showed that significant aging effects occur at temperatures higher than the selected maximum use temperature. In the combined load/environment tests, some of the thermal aging effects were triggered at lower temperatures by the combination of load cycles, thermal cycles, and time at temperature.

Test data are presented in two ways. To aid the observation of trends, strength (stress) has been plotted as a function of the various tests performed, where the tests are ordered either in increasing test time or test sequence. Selected individual data have been plotted to observe data scatter. For the constant amplitude fatigue tests, the cyclic stress at $10^7$ cycles ($\sigma_{10^7}$) has been plotted to indicate the relative severity of the effect of fatigue cycling. Ten million cycles were chosen in keeping with summary charts presented previously in both Sections 11 and 12. When fatigue effects are indicated by this simplified plotting method, the actual S-N curves should be referred to for more insight into the relative effects. In addition, to show the effects of the thermal exposures on specific properties, residual strengths have been compared to baseline strengths by means of bar charts. The bar charts have been prepared for crossply B/E, G/E, G/PI, and B/Al and unidirectional B/Al as these were the layups and materials for which flight simulation data were available. For the resin matrix composites, the residual notched tensile and notched fatigue values were obtained from notched flight simulation specimens. The residual notched tensile data for B/Al were obtained from material that was notched after flight simulation. The fatigue strengths shown on the bar charts were also for $10^7$ cycles in keeping with summary charts presented previously in both Sections 11 and 12.

For the B/E and G/E systems, two sets of flight simulation exposure and residual strength results are presented. The first, obtained in Phase I, is for 10,000 hours of exposure at a maximum temperature of 408 K (275 °F). The second set of results, obtained during Phase II, is for exposure out to 36,374 hours at a maximum temperature of 373 K (212 °F). In Phase I both unnotched and notched flight simulation specimens of B/E and G/E were exposed. Only unnotched specimens were evaluated in Phase II. The materials from which the specimens were fabricated were obtained at different times, and, particularly for the G/E system, comparisons between the Phase I results and those of Phase II were not always possible.

The new material addition in Phase II, Celion 6000/LARC-160, was flight simulation tested in both the unnotched and notched condition but only for 10,000 hours.

Also added to the test program during Phase II was an evaluation of thermal aging/compression effects for two of the resin matrix systems, A-S/3501 G/E and Celion 6000/LARC-160 G/PI. Some of these data are included in the bar charts for the Celion 6000/LARC-160 G/PI. The thermal aging/compression specimens of G/E were from a different batch of prepreg than either the

thermal aging/tensile specimens or the flight simulation specimens, and, for that reason, those data are not included.

## B/E — PHASE I

**B/E, $[0° \pm 45°]_s$, unnotched.** Figures 13-1 and 13-2 summarize the available tests for the unnotched B/E. As no baseline tensile testing was performed (except for three tests at room temperature), the mean strength at 422 K (300 °F) was estimated to be 545 MN/m$^2$ (79 ksi) and the Weibull shape parameter, $\alpha$, was obtained from reference 40 as 19.5. This value of $\alpha$ translates to a coefficient of variation of about 5%, and indicates that B/5505 B/E is a well-controlled repeatable composite system.

The short-term tests with a peak stress of 321 MN/m$^2$ (46.6 ksi), at a constant 422 K (300 °F), showed the typical reduction in mean strength and increase in scatter with time. No fatigue failures occurred, and the residual strength failure mode was the same as that for the room temperature baseline tests.

Wearout analysis was performed to select the peak stress of 302 MN/m$^2$ (43.8 ksi) for the long-term tests.

After the first 1000 hours, the cruise temperature was lowered from 422 K (300 °F) to 408 K (275 °F). No fatigue failures occurred in the 10,000 hours of Phase I. Residual tensile strength tests showed more scatter than expected, with five specimens between 338 MN/m$^2$ (49 ksi) and 400 MN/m$^2$ (58 ksi) and one at 496 MN/m$^2$ (72 ksi). The average decrease at room temperature was approximately 35%. The residual compressive tests showed even greater reductions in properties with a decrease of slightly more than 50%. Although the residual strength failure mode was the same as the baseline, the specimens were severely oxidized in the heated zones. Recall that the wearout analysis had assumed that no thermal aging effects would be experienced below the apparent maximum use temperature. This assumption was violated by the long-term chemical and physical changes experienced by the epoxy resin. In the Phase II tests the cruise temperature was changed to 373 K (212 °F) for the epoxy systems. The thermal aging results (Figure 13-2) have shown that with no applied loads or temperature cycling no degradation of tensile properties, and probably none for compressive properties as well, occurs during 10,000 hours exposure at 394 K (250 °F). However, at 450 K (350 °F) significant tensile and severe compressive property degradation was observed. No thermal aging data were obtained at the flight simulation temperature of 422 K (300 °F) or 408 K (275 °F). The post long-term fatigue tests at R = 0.1 and 297 K (75 °F) indicated a $\sigma_{10^7}$ value of 276 MN/m$^2$ (40 ksi) compared to the baseline value of 324 MN/m$^2$ (47 ksi).

The combination of load, temperature, and thermal cycling has severly degraded the unnotched B/E specimens at a temperature at which thermal aging alone would probably not cause extensive damage.

**B/E, $[0° \pm 45°]_s$, notched.** Figure 13-3 summarizes the trend data for the notched B/E. The residual properties after flight simulation exposure are summarized in Figure 13-2.

The 422 K (300 °F) baseline mean strength was calculated to be about 462 MN/m$^2$ (67 ksi) net stress and the same $\alpha$ value of 19.5 was assumed. The short-term specimens were cycled to a peak stress of 248 MN/m$^2$ (36 ksi) at 422 K (300 °F) and exhibited the typical wearout effects of reduced mean and increased scatter. Failure modes were net tension.

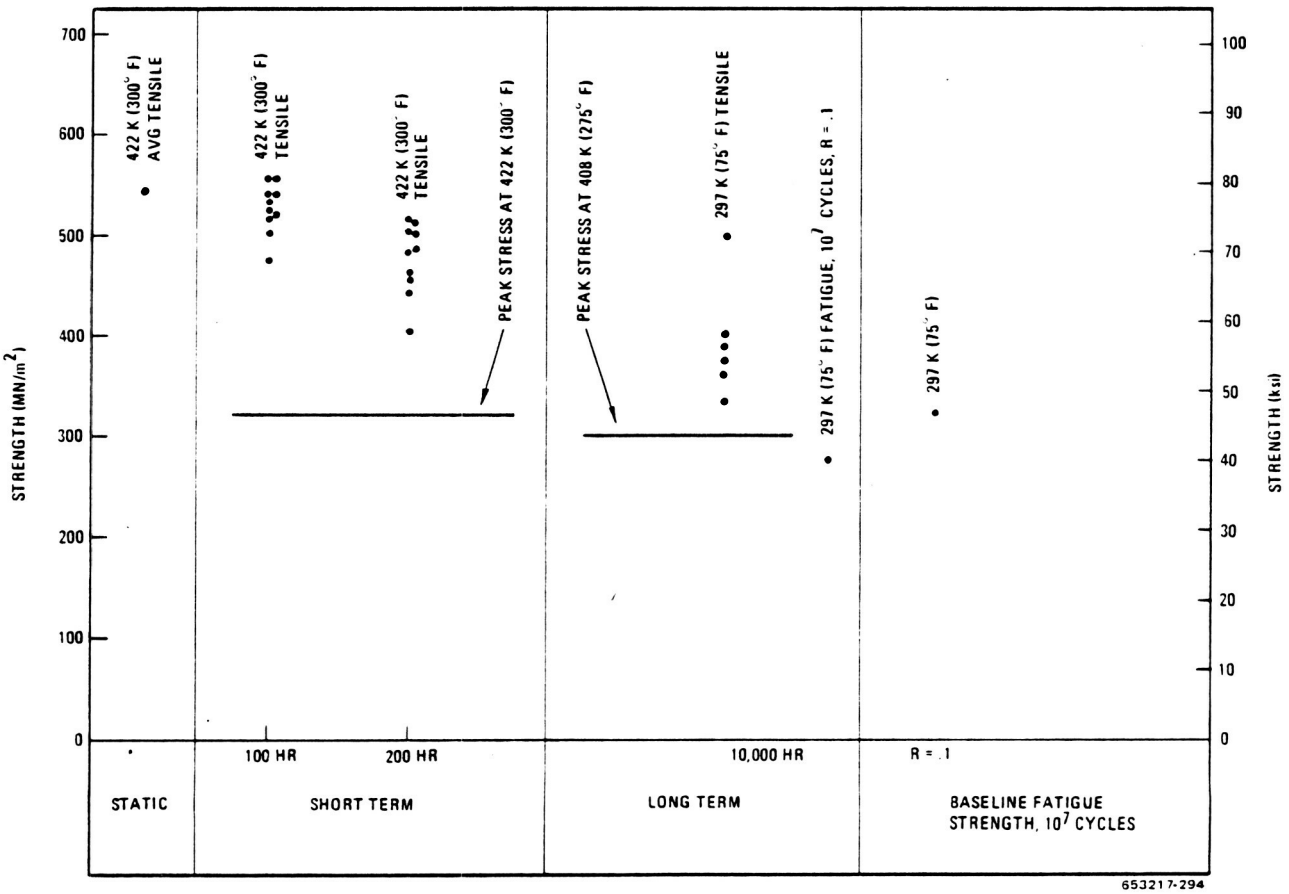



**Figure 13-1 Phase I Unnotched $[0° \pm 45°]_s$ B/E**

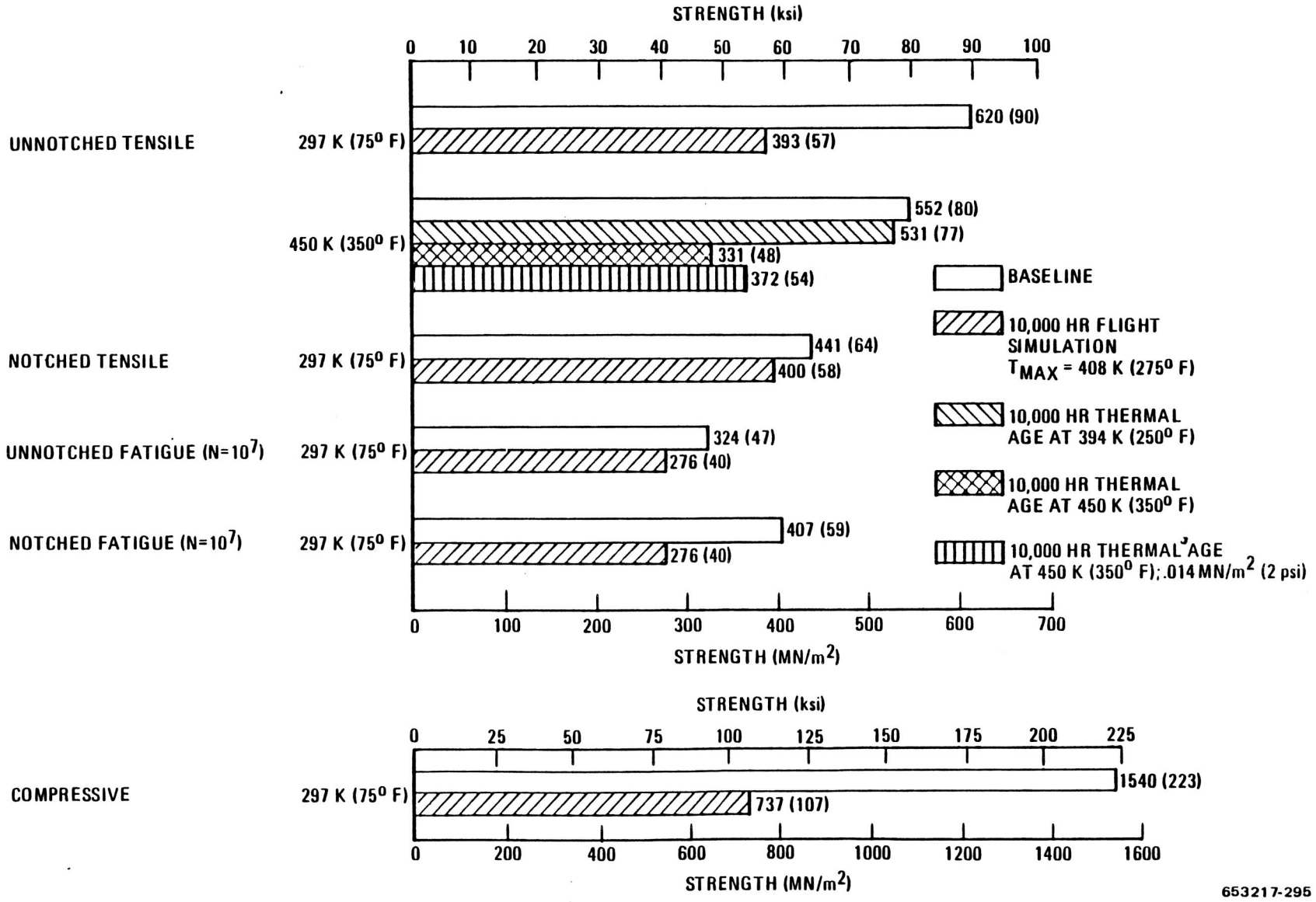



**Figure 13-2 Summary of Residual Properties of $[0° \pm 45°]_s$ B/E After Thermal Exposure — Phase I**

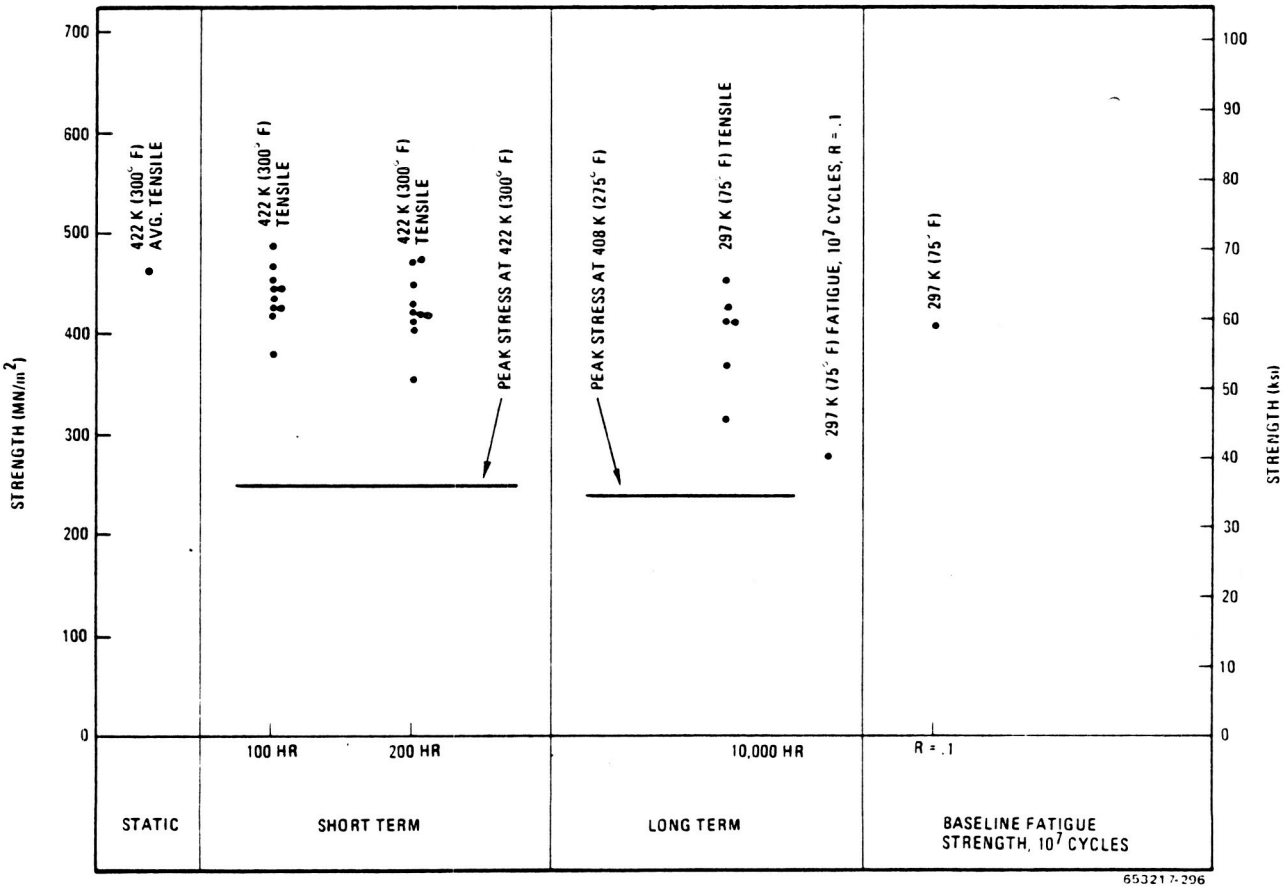



**Figure 13-3 Phase I Notched $[0° \pm 45°]_s$ B/E**

Wearout analysis was used to select the long-term peak stress of 239 $MN/m^2$ (34.6 ksi). The temperature of the cruise leg was reduced from 422 K (300 °F) to 408 K (275 °F) after about 1000 hours. No fatigue failures occurred in 10,000 hours. The residual strength specimens also failed in net tension with the values scattered between 317 $MN/m^2$ (46 ksi) and 455 $MN/m^2$ (66 ksi) and having an average value of 400 $MN/m^2$ (58 ksi). Again the epoxy resin sustained severe chemical and physical damage in the heated zones from the combination of load, temperature, and oxidation.

The R = 0.1 fatigue strengths for $10^7$ cycles at 297 K (75 °F) before and after the long-term tests were 407 $MN/m^2$ (59 ksi) and 276 $MN/m^2$ (40 ksi), substantiating the degrading effects of flight simulation exposure.

## B/E — PHASE II

**B/E, $[0° \pm 45°]_s$, unnotched.** Because of the severe degradation that occurred during Phase I, new flight simulation specimens (all were unnotched) were fabricated for Phase II, and testing was restarted using a maximum exposure temperature of 373 K (212 °F). Three batches of specimens were included for evaluation: after 10,000 hours, 25,000 hours, and 50,000 hours of exposure. Two of the 50,000 hour specimens failed after just over 33,000 hours. Because additional failures appeared imminent, and, to preserve sufficient material for residual strength testing, exposure was halted near 36,000 hours.

Figures 13-4 and 13-5 summarize the results of the Phase II testing of the unnotched B/E. Included in the bar charts of Figure 13-5 are results of the 50,000 hour thermal aging studies for comparison with the 10,000 hour and 36,000 hour flight simulation residual strength data.

No fatigue failures occurred during the first 10,000 hours or 25,000 hours of Phase II. Residual tensile strength of the B/E had decreased slightly but was still 90% of the baseline value after 25,000 hours. Almost no loss in R = 0.1, 297 K (75 °F) fatigue strength was found after 10,000 hours or 25,000 hours. For the specimens removed from test after 36,000 hours, a tensile strength loss of 22% was measured. The post long-term fatigue test gave a $\sigma_{10^7}$ value after 36,000 hours at 373 K (212 °F) the same as that after 10,000 hours at 408 K (275 °F). While the fiber dominated properties, tensile strength and tensile-tensile fatigue strength, were not greatly affected by the 36,000 hours of exposure, the same was not true of the matrix dominated properties. Both the compressive and shear strengths exhibited losses of about 60%. Unlike the Phase I specimens cycled to a maximum temperature of 408 K (275 °F), the Phase II specimens showed almost no surface damage up through 25,000 hours. After 36,000 hours a few loose boron fibers were visible in the heated zones of the flight simulation specimens. Thermal aging results for 50,000 hours of exposure are shown in Figure 13-5. The data indicate that 50,000 hours with no applied loads or temperature cycling at 394 K (250 °F) degrades the tensile strength to the same degree as 36,374 hours of flight simulation exposure at 373 K (212 °F), i.e., a loss of slightly over 20%.

For the B/E system, lowering the maximum temperature to 373 K (212 °F) resulted in 25,000 hours of flight simulation exposure with negligible surface damage and good retention of tensile and fatigue properties. However, a loss of compressive and shear strength properties of about one-third is a major concern. After 36,000 hours of exposure, surface erosion sufficient to expose boron filaments, combined with significant tensile strength losses and severe compressive and shear strength degradation, rules out the likelihood of use for 50,000 hours of service at even the low temperature of 373 K (212 °F).

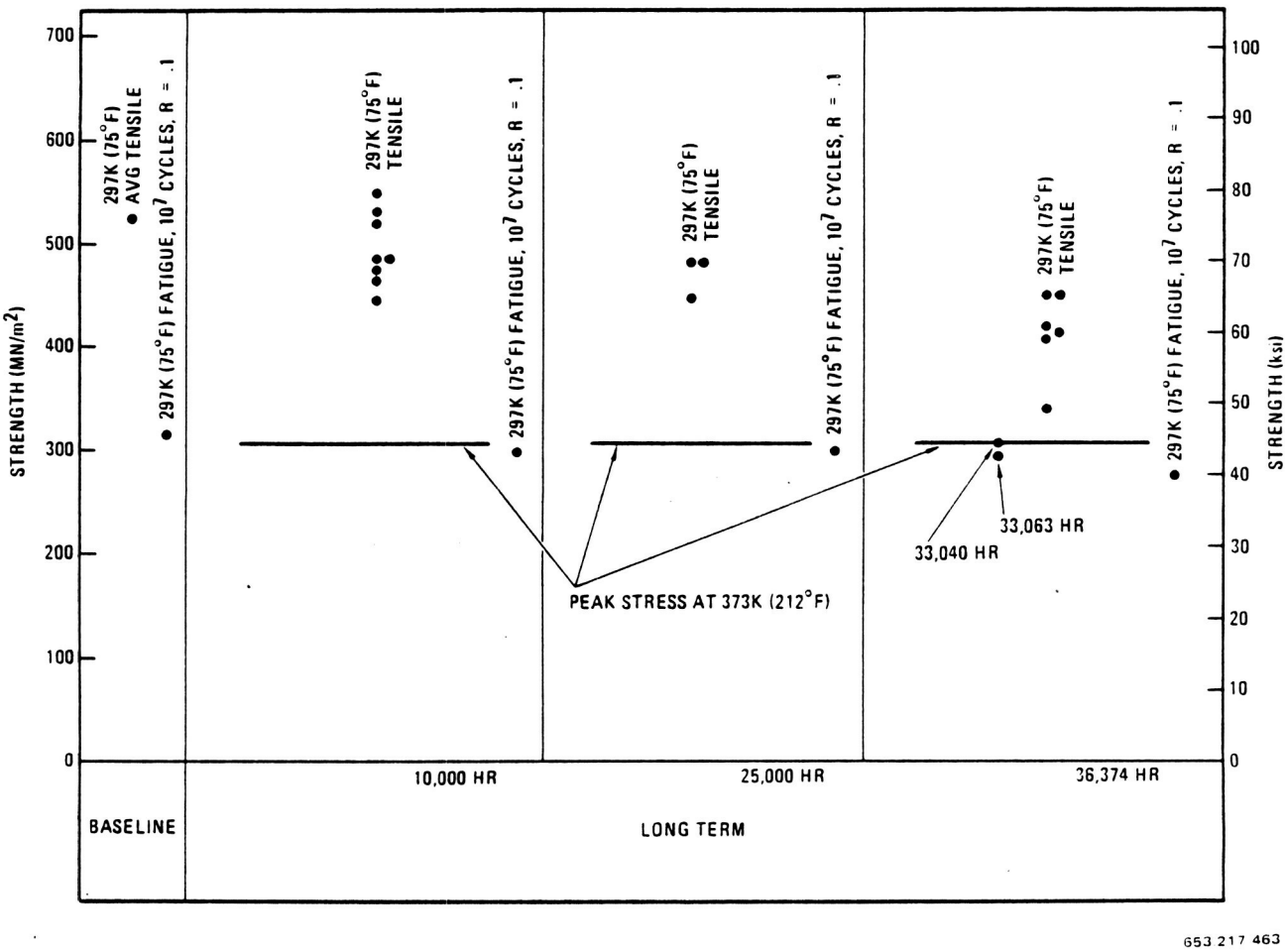



**Figure 13-4 Phase II Unnotched $[0° \pm 45°]_s$ B/E**

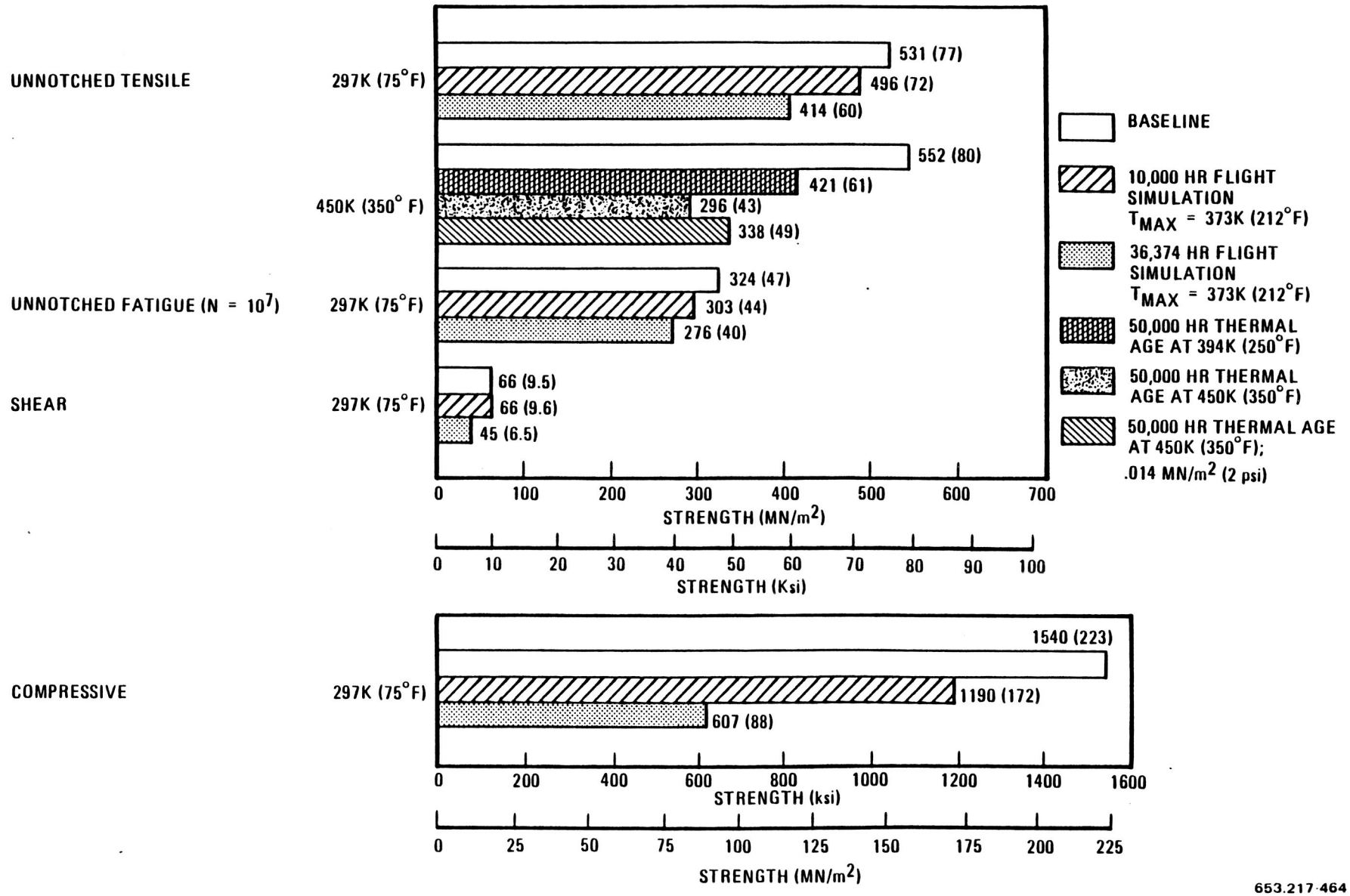



**Figure 13-5 Summary of Residual Properties of $[0° \pm 45°]_s$ B/E After Thermal Exposure — Phase II**

## G/E — PHASE I

**G/E, $[0° \pm 45°]_s$, unnotched.** The baseline mean strength of the G/E unnotched specimens at 408 K (275 °F) to 436 K (325 ° F) (Figure 13-6) was about 496 MN/m$^2$ (72 ksi) with a calculated Weibull $\alpha$ of 12.7. This low value of shape parameter indicates poor reproducibility that impedes the clear interpretation of test trends.

The short-term specimens were cycled to a peak stress of 338 MN/m$^2$ (49.1 ksi) at 422 K (300 °F), and typical wearout was observed, including two early fatigue failures. Failure mode was net tension, the same as the baseline tests.

The wearout analysis was used to select the peak long-term stress of 305 MN/m$^2$ (44.2 ksi), and after 1000 hours, the cruise temperature was reduced to 408 K (275 °F). Multiple fatigue failures occurred, principally by progressive delamination. The few residual strength results (Figures 13-6 and 13-7) showed only a slight reduction in the mean tensile strength but a drastic reduction in the mean compressive strength. The combination of severe oxidation and delamination growth during flight simulation exposure was a major impact to the program.

In like manner to the B/E system, thermal exposure without load at 450 K (350 °F) produced severe degradation of the matrix and a very large decrease in tensile strength. No compressive tests were performed, but the appearance of the failed specimens indicated that compressive properties would also be poor. Thermal aging at 394 K (250 °F) and at 450 K (350 °F) at reduced pressure, however, gave no degradation in properties after at least 10,000 hours of exposure.

The post long-term test value of $\sigma_{10^7}$ after R = 0.1 fatigue at room temperature was down to 241 MN/m$^2$ (35 ksi) from the 448 MN/m$^2$ (65 ksi) baseline. The low value of the baseline $\sigma_{10^7}$, 386 MN/m$^2$ (56 ksi), after R = 0.1 fatigue at 450 K (350 °F) is probably attributable mostly to material variability. Constant amplitude fatigue at R = −1 during baseline testing was shown to produce severe reductions in strength. Compressive failures are suspected for these tests that produced $\sigma_{10^7}$ values of 172 MN/m$^2$ (25 ksi) at 297 K (75 °F) and 172 MN/m$^2$ (25 ksi) at 450 K (350 °F). In hindsight, the test program, expecially for the graphite systems, should have emphasized compressive effects.

**G/E, $[0° \pm 45°]_s$, notched.** Broad scatter was again evident in the baseline notched G/E with an $\alpha$ value of 12.0 and a mean strength of about 414 MN/m$^2$ (60 ksi) (Figures 13-7 and 13-8).

The short-term tests, cycled to a peak stress of 249 MN/m$^2$ (36.1 ksi) at 422 K (300 °F), produced no fatigue failures, but showed decreasing strength and increasing scatter. The residual strength failure mode was net tension.

After wearout analysis, the long-term specimens were cycled to a peak stress of 232 MN/m$^2$ (33.6 ksi). The temperature was again reduced from 422 K (300 °F) to 408 K (275 °F) after about 1000 hours. The badly oxidized residual tensile strength specimens retained a surprising amount of their original notched strength, exhibiting values from 358 MN/m$^2$ (52 ksi) to 469 MN/m$^2$ (68 ksi).

Again tensile fatigue testing did not discriminate the effects too well, with the post long-term testing $\sigma_{10^7}$ value (R = 0.1) at 297 K (75 °F) being 283 MN/m$^2$ (41 ksi), compared to the baseline values of 379 MN/m$^2$ (55 ksi) and 345 MN/m$^2$ (50 ksi) at 297 K (75 °F) and 450 K (350 °F).

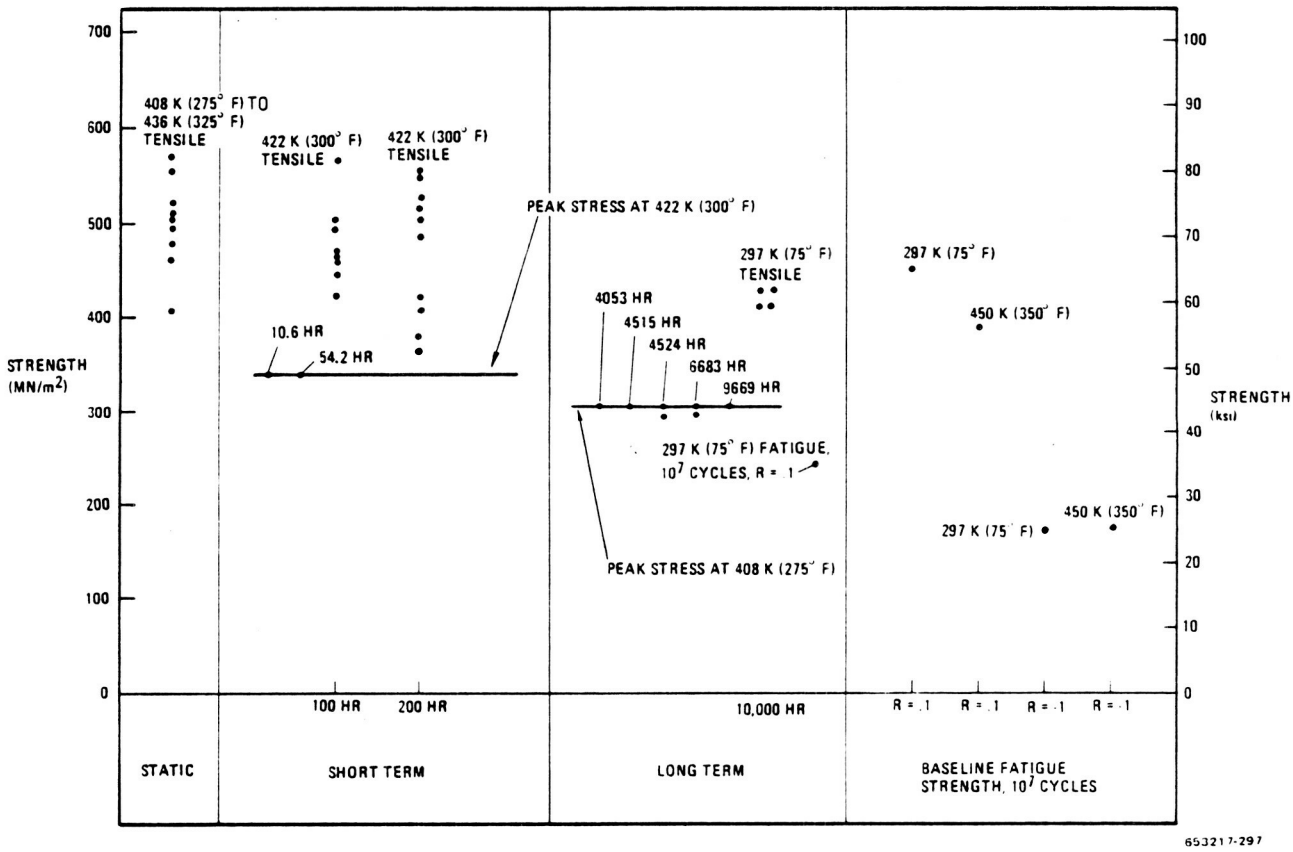



**Figure 13-6 Phase I Unnotched $[0° \pm 45°]_s$ G/E**

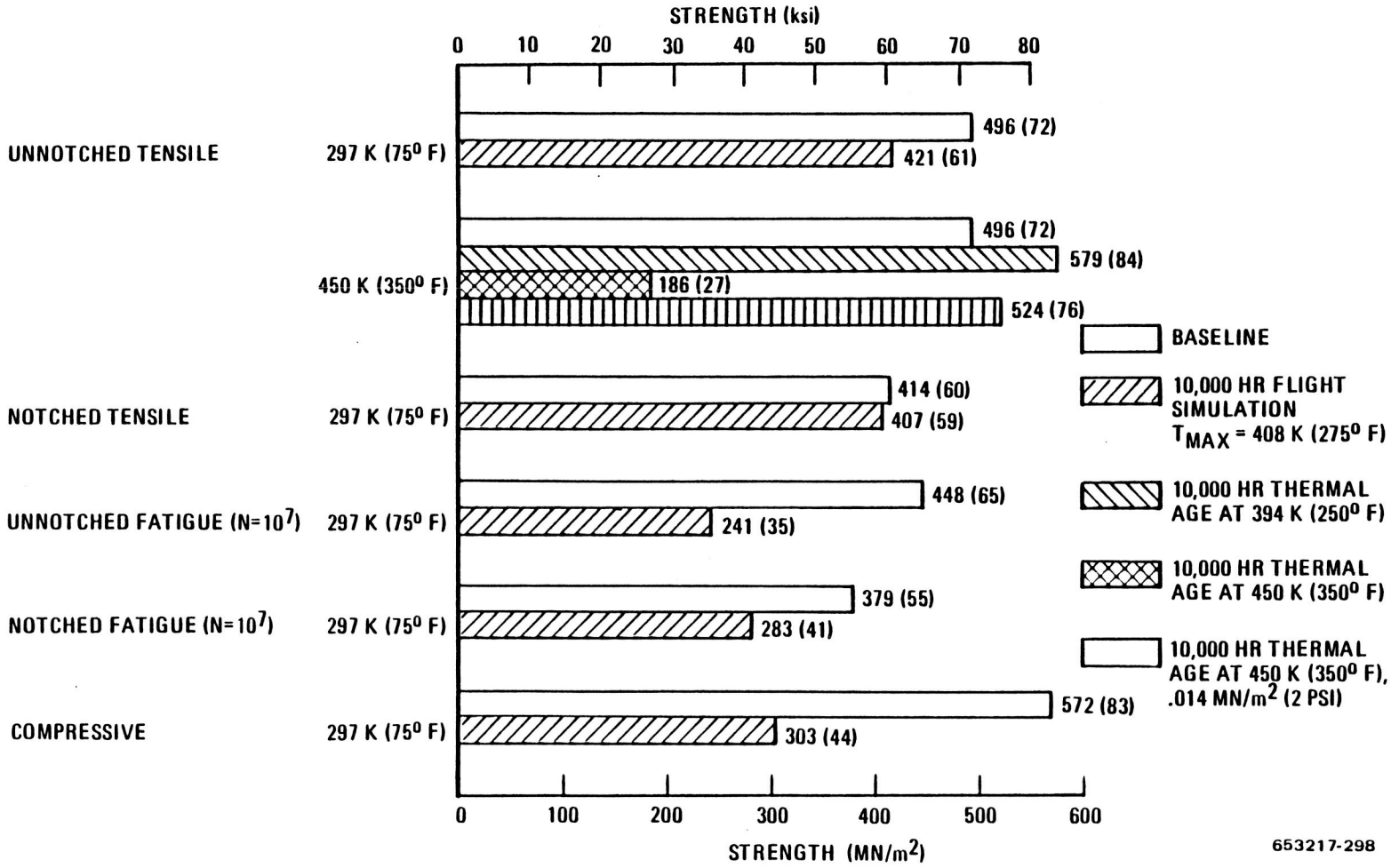



**Figure 13-7 Summary of Residual Properties of $[0° \pm 45°]_s$ G/E After Thermal Exposure — Phase I**

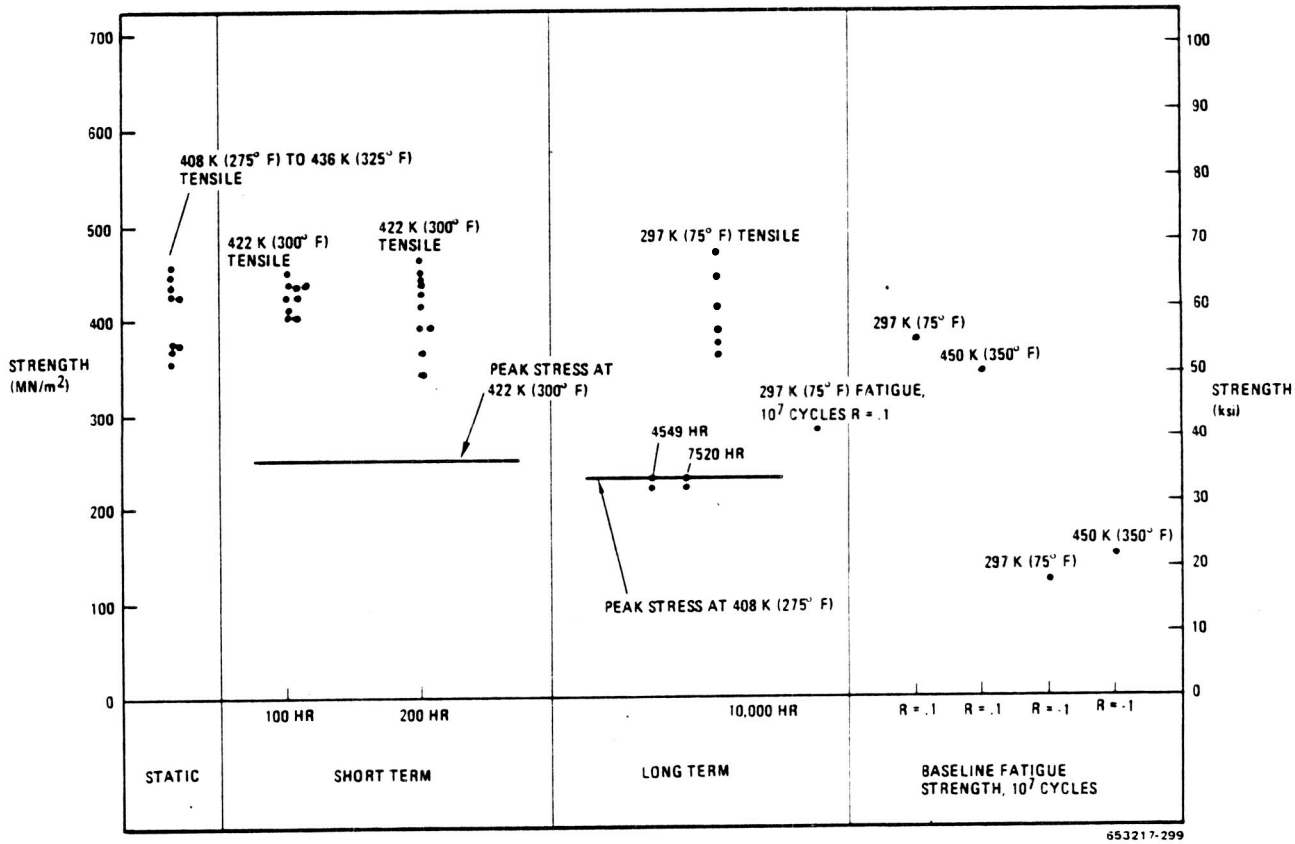



**Figure 13-8 Phase I Notched $[0° \pm 45°]_s$ G/E**

The stress ratio of R = −1 showed the much more severe effects of compression with $\sigma_{10^7}$ values of 124 MN/m$^2$ (18 ksi) and 152 MN/m$^2$ (22 ksi) at 297 K (76 °F) and 450 K (350 °F) respectively, for the baseline tests.

## G/E — PHASE II

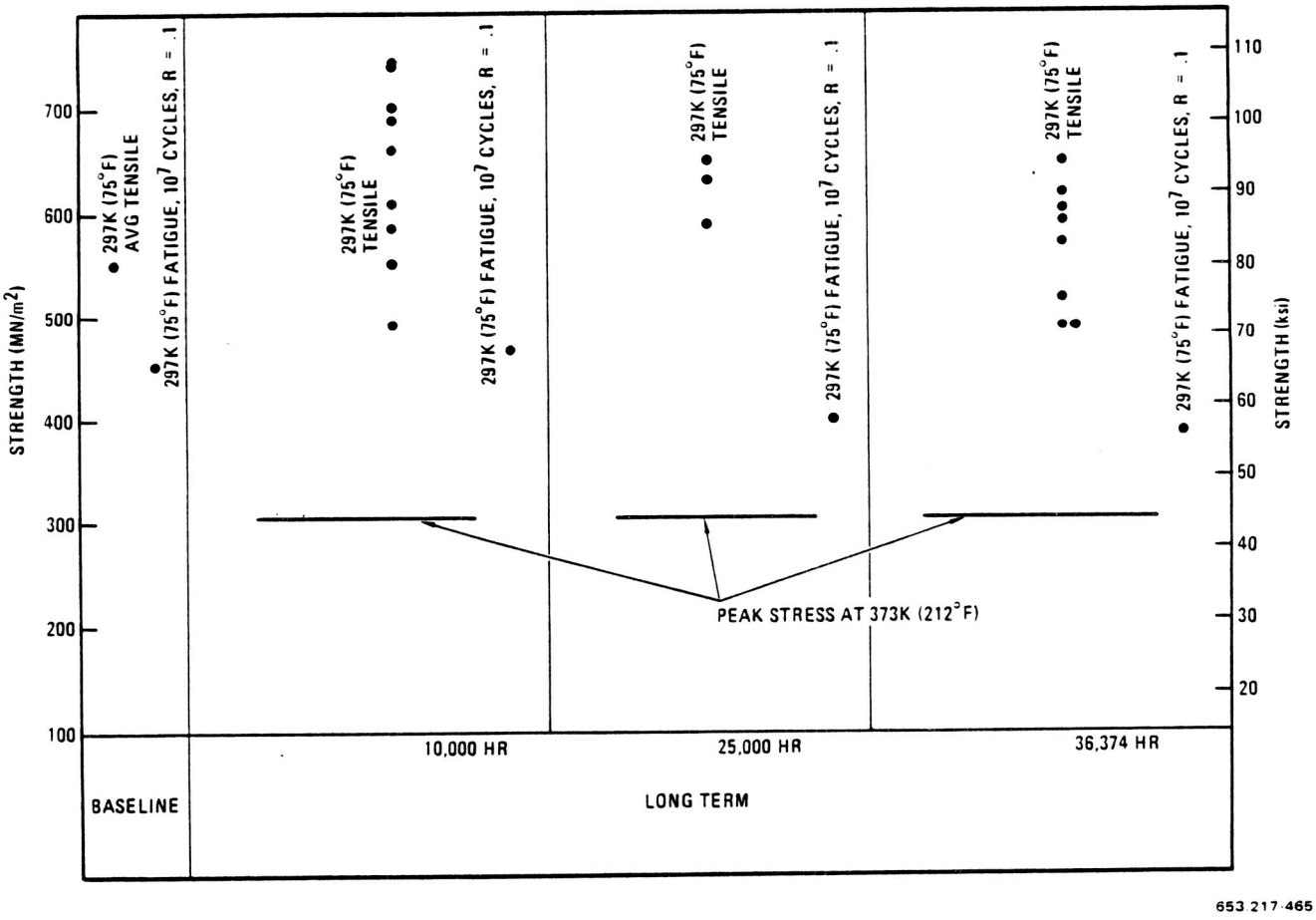
**G/E, $[0° \pm 45°]_s$, unnotched.** A second set of unnotched flight simulation specimens was also fabricated for the G/E system following the poor behavior of the material when exposed at a maximum cruise temperature of 408 K (275 °F). The same lower temperature of 373 K (212 °F) as used for the B/E system was selected, and testing was halted near 36,000 hours to ensure sufficient material for residual strength evaluations.

Data for the Phase II thermal exposures are summarized in Figures 13-9 and 13-10. These data are for specimens fabricated from two different batches of G/E prepreg. All the data in Figure 13-9 are for the second batch of material (Phase II). The tensile strength values were higher for the Phase II material while the R = 0.1 fatigue properties were the same as those of the Phase I material. In Figure 13-10 the thermal aging data are from Phase I material, and the flight simulation data are from Phase II material.

The G/E specimens performed exceptionally well at the reduced flight simulation temperature. No fatigue failures occurred during the 36,000 hours of exposure. Residual tensile strength, both unnotched and notched, was not reduced after 36,000 hours. Losses in R = 0.1 fatigue strength were not seen until after 25,000 hours. The value of $\sigma_{10^7}$ decreased from the 448 MN/m$^2$ (65 ksi) baseline to 402 MN/m$^2$ (58 ksi) at 25,000 hours and only slightly lower to 386 MN/m$^2$ (56 ksi) after 36,000 hours. The matrix dominated properties also held up quite well with only negligible losses after 25,000 hours. There was, however, a significant decrease in residual shear strength after 36,000 hours from a baseline value of 74 MN/m$^2$ (10.7 ksi) to 53 MN/m$^2$ (7.7 ksi). In like manner to the B/E specimens, surface damage to the G/E was not observed until 36,000 hours of exposure and then was limited to slight loss of resin and some exposed fibers in the heated zones.

The data in Figure 13-10 appear to indicate that thermal aging at temperatures as low as 394 K (250 °F) can seriously degrade the tensile strength of G/E, while flight simulation exposure at a slightly lower temperature and slightly shorter time has no effect. However, the two data sets are from specimens fabricated from different batches of prepreg obtained several years apart. The Phase II batch (flight simulation) in addition to showing superior strength retention over the Phase I batch (thermal aging) also exhibited considerably better thermooxidative resistance. Much less loss of resin and consequently fewer exposed graphite fibers were found at the fracture areas of failed residual strength specimens after 36,000 hours of flight simulation exposure than for similar test specimens after 25,000 hours of thermal aging at 394 K (250 °F). The unfortunate necessity of using different batches of G/E prepreg makes comparison of the thermal aging and flight simulation data sets impossible.

Again, as with the B/E system, lowering the maximum temperature to 373 K (212 °F) greatly improved the performance of the G/E material. Excellent results were obtained after 25,000 hours of flight simulation, and, with the exception of some surface oxidation and erosion and a 28% loss in shear strength, the material remained in good condition after 36,000 hours of exposure. The possibility of 50,000 hours of usage at a maximum temperature of 373 K (212 °F) for the A-S/3501 G/E system cannot be ruled out.




653.217-465

**Figure 13-9 Phase II Unnotched $[0° \pm 45°]_s$ G/E**

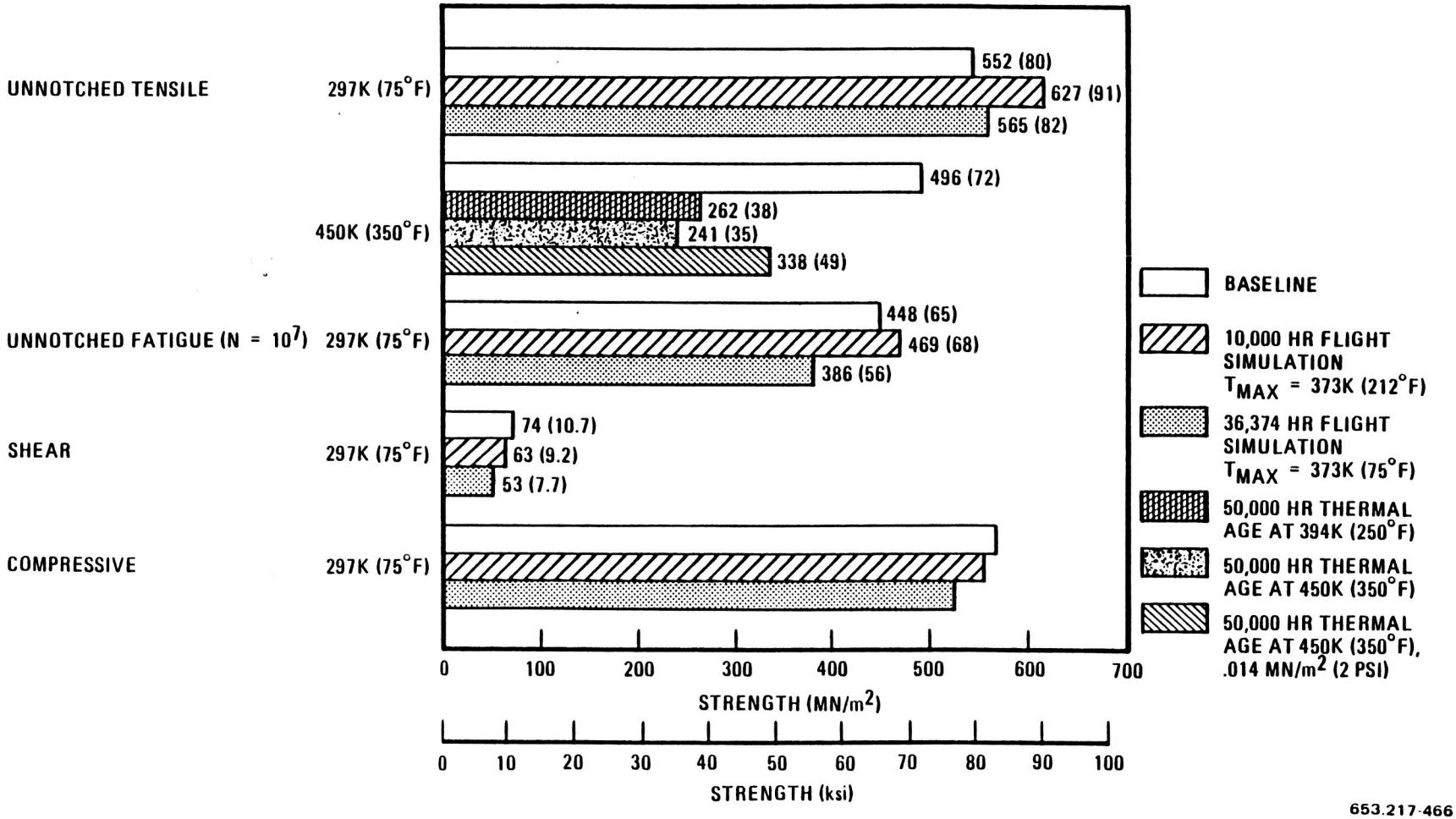



**Figure 13-10 Summary of Residual Properties of $[0° \pm 45°]_s$ G/E After Thermal Exposure — Phase II**

**HT-S/710 G/PI, $[0° \pm 45°]_s$, unnotched.** The HT-S/710 G/PI data are summarized in Figures 13-11 through 13-13. Baseline testing showed poor reproducibility, as exhibited by a mean strength at 505 K (450 °F) of 469 MN/m$^2$ (68 ksi) and an $\alpha$ value of 12.15. Notice that one of the baseline specimens reached only 296 MN/m$^2$ (43 ksi). These panels had measured void contents up to 13%, so that defect sensitive failures modes could be greatly influenced by individual specimen quality.

The 505 K (450 °F) short-term peak stress was originally selected to be 331 MN/m$^2$ (48 ksi) but nine out of ten specimens failed the proof load at 283 MN/m$^2$ (41 ksi); consequently the stresses were reduced to a peak 207 MN/m$^2$ (30.1 ksi). Tests of the short-term panels showed that they were about 69 MN/m$^2$ (10 ksi) weaker than the baseline panel. Eventually, the short-term specimens exhibited typical wearout indications of decreasing strength and increasing scatter with test time.

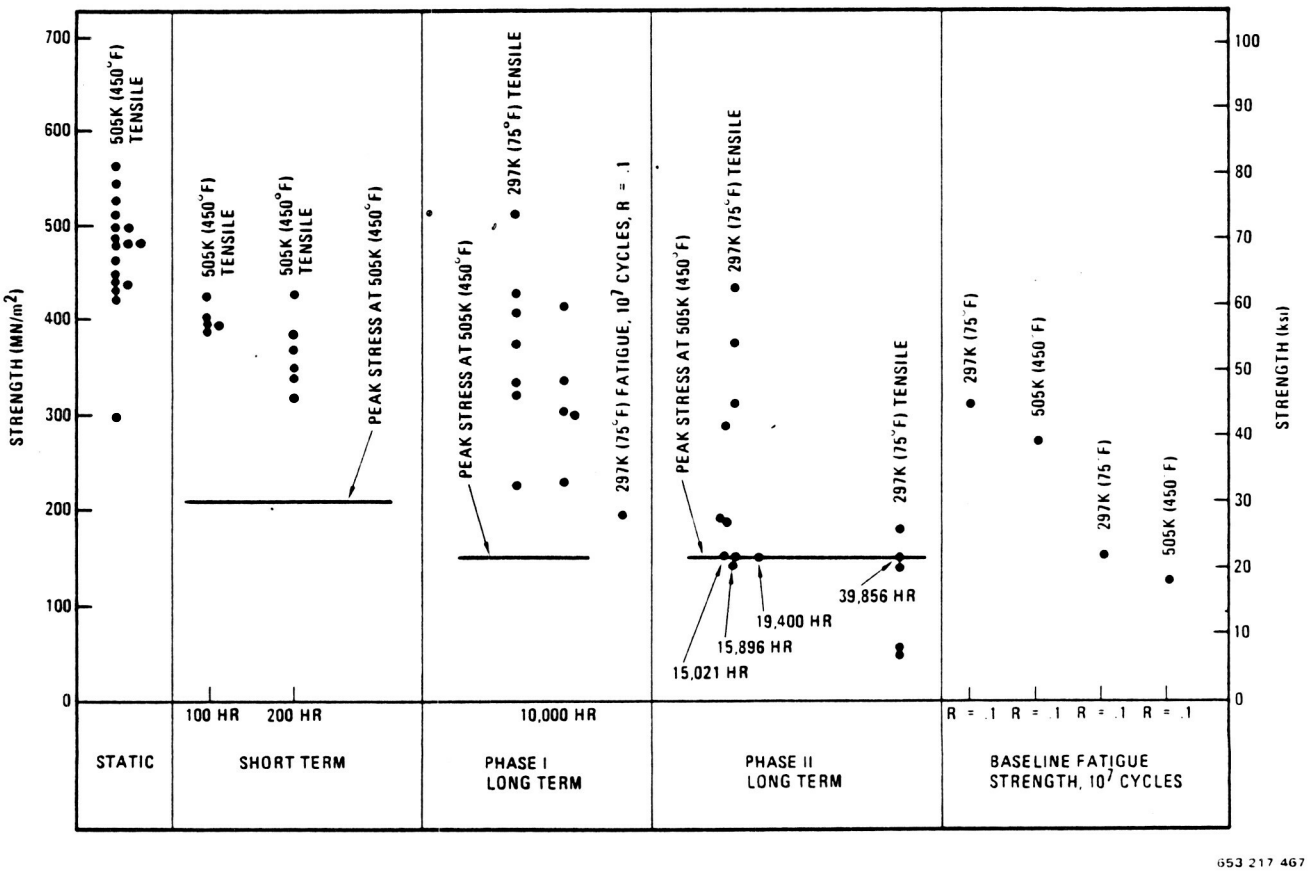
The long-term test peak stress was reduced to 153 MN/m$^2$ (22.2 ksi), and at 505 K (450 °F) maximum cruise temperature all Phase I specimens achieved 10,000 hours. Residual tensile strengths at 505 K (450 °F) ranged from 228 MN/m$^2$ (33 ksi) to 414 MN/m$^2$ (60 ksi) and at 297 K (75 °F) ranged from 228 MN/m$^2$ (33 ksi) to 510 MN/m$^2$ (74 ksi). Reproducibility was quite poor, even though the failure mode remained tensile, and no aging or delamination affects were observed. Residual compressive strength was reduced by approximately the same degree as the tensile strength. This was in contrast to the epoxy systems where compressive strength was considerably more affected by flight simulation exposure than the tensile strength. The shear strength exhibited the greatest decrease with a loss of more than 50% after 10,000 hours of flight cycling. This was an indication that G/PI flight simulation failures could be expected early in the Phase II test program if the failure mechanism proposed for the epoxy systems was operative for the polymide system as well.

The results of the 10,000-hour thermal aging exposures, Figure 13-12, clearly show the effect of aging temperature, with very little decrease in tensile strength when aged at 505 K (450 °F) and almost a 50% reduction at 561 K (550 °F).

The post long-term fatigue tests at R = 0.1 and 297 K (75 °F) produced a $\sigma_{10^7}$ value after 10,000 hours of flight cycling of only 193 MN/m$^2$ (28 ksi) as compared to the baseline values of 310 MN/m$^2$ (45 ksi) at 297 K (75 °F) and 269 MN/m$^2$ (39 ksi) at 505 K (450 °F). Panel-to-panel scatter may have influenced these results.

Again the effect of compressive stresses was demonstrated by the baseline fatigue tests at R = −1. Values of $\sigma_{10^7}$ were 152 MN/m$^2$ (22 ksi) at 297 K (75 °F) and 124 MN/m$^2$ (18 ksi) at 505 K (450 °F).

As expected, long term failures began to occur early in Phase II with all specimens eventually failing prior to 40,000 hours. The combined effect of fatigue loading, surface oxidation, and thermal cycling stresses contributed to these wearout failures. Residual tensile strength of the Phase II specimens showed a continuing decrease with exposure time, as well as wide scatter about the mean. The failure mode was tensile but with a contribution through delamination by the combined action of 1) exposed outer ply fibers from surface oxidation, 2) degraded shear and compressive strengths with time, and 3) application of stresses from thermal cycling and compressive loading.




653 217 467

**Figure 13-11 Phase I and Phase II Unnotched $[0° \pm 45°]_s$ HT-S/710 G/PI**

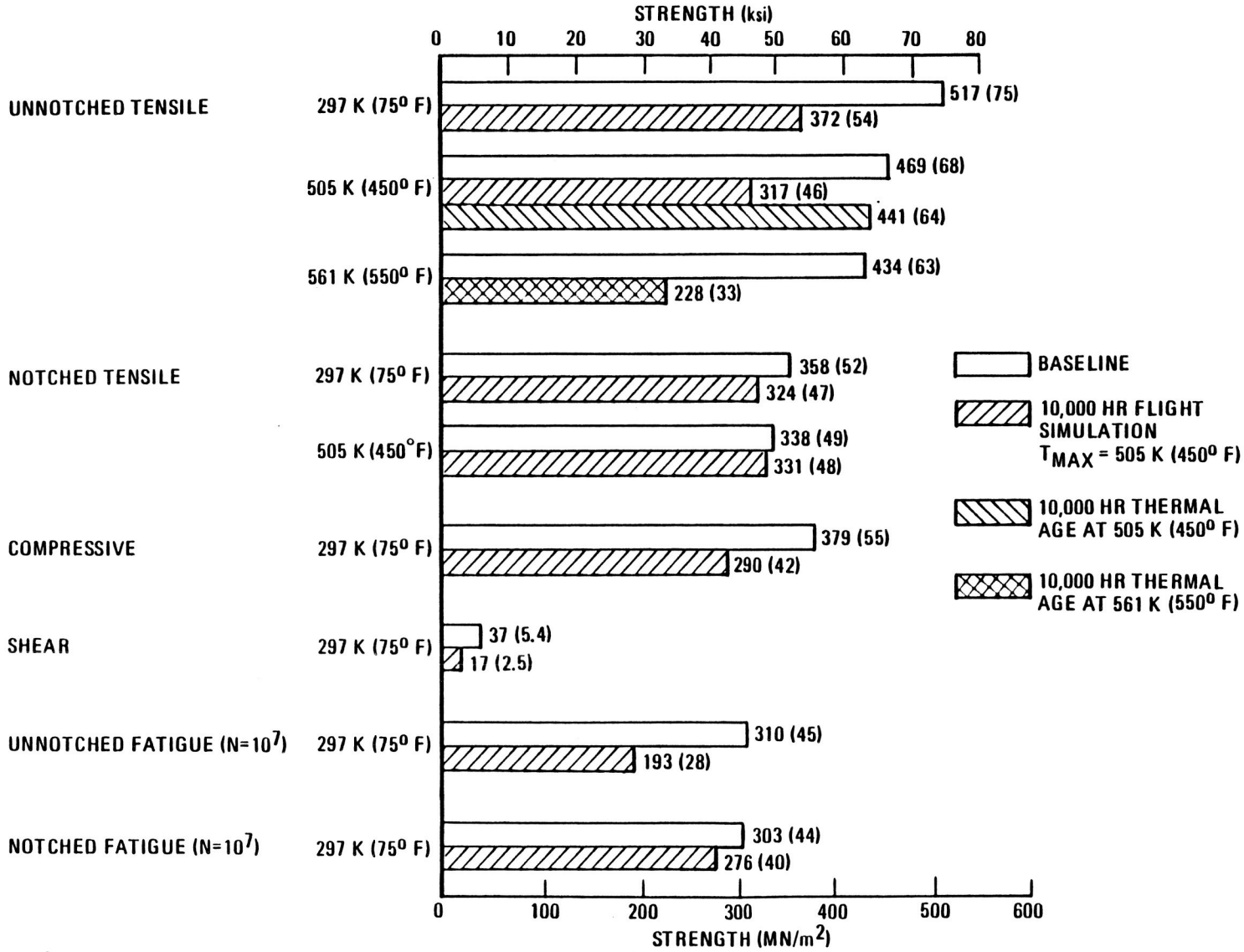



**Figure 13-12 Summary of Residual Properties of $[0° \pm 45°]_s$ HT-S/710 G/PI After Thermal Exposure — Phase I**

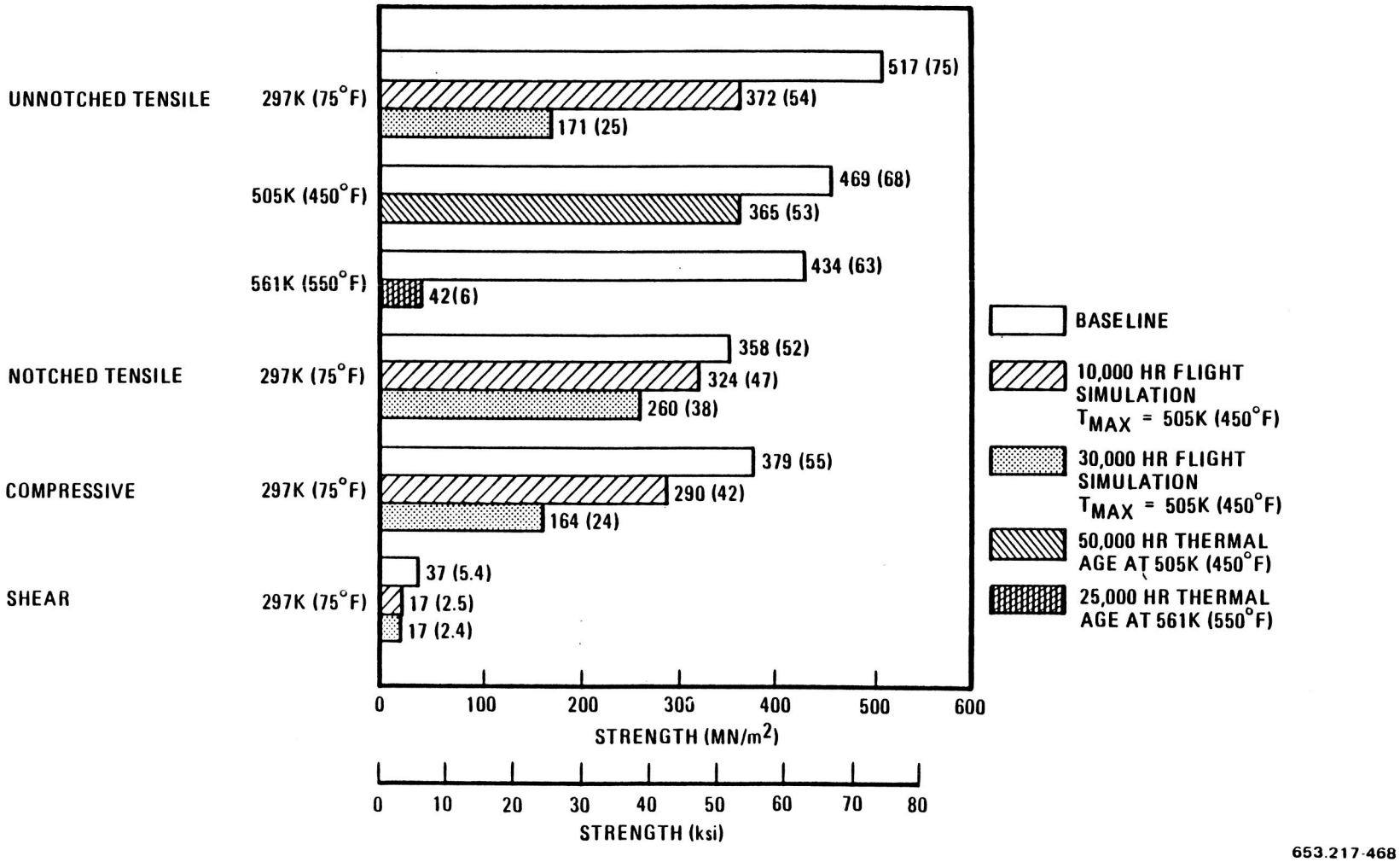



**Figure 13-13 Summary of Residual Properties of $[0° \pm 45°]_s$ HT-S/710 G/PI After Thermal Exposure — Phase II**

As shown in Figure 13-13 the 30,000 hour residual compressive and shear strengths were also reduced to less than half of the baseline values. It should be noted that the reduction in shear strength had already been observed after only 10,000 hours of exposure. Also shown in Figure 13-13 are the Phase II thermal aging results for 50,000 hours at 505 K (450 °F) and 25,000 hours at 561 K (550 °F). Again, the effect of aging temperature is clearly shown with a 90% reduction in strength in only 25,000 hours at the higher temperature versus a 20% loss in 50,000 hours at the lower temperature. Comparison of the 30,000 hour flight simulation residual strength with the 50,000 hour thermal aging residual strength, both at the same maximum temperature, shows the importance that fatigue loading and, perhaps, thermal cycling have on property degradation — a loss of two-thirds compared to only 20%.

**HT-S/710 G/PI, $[0° \pm 45°]_s$, notched.** Even these notched specimens suffered from voids, porosity, and panel-to-panel variability. As shown in Figure 13-14, their mean strength at 505 K (450 °F) was about 338 MN/m$^2$ (49 ksi). The Weibull $\alpha$ was 12.15.

The short-term peak stress was 141 MN/m$^2$ (20.5 ksi) at 505 K (450 °F), and all specimens had about the same strength after 100 and 200 hours. Net tension failures were obtained from all specimens. The long-term peak stress was 125 MN/m$^2$ (18.2 ksi). All specimens survived 10,000 hours at this relatively low stress level. Residual notched tensile strengths at 505 K (450 °F) ranged from 255 MN/m$^2$ (37 ksi) to 400 MN/m$^2$ (58 ksi), and at 297 K (75 °F) they ranged from 248 MN/m$^2$ (36 ksi) to 428 MN/m$^2$ (62 ksi). No particular strength shift was seen, but the scatter was clearly increased. The decrease in the average notched tensile strength after 10,000 hours of flight simulation exposure was quite small compared with that observed for unnotched specimens (Figure 13-12). Similar differences in properties of notched and unnotched specimens of both B/E and G/E were also observed after 10,000 hours of flight simulation.

The post long-term notched fatigue test at R = 0.1 and 297 K (75 °F) produced a $\sigma_{10^7}$ of 276 MN/m$^2$ (40 ksi) as compared to a baseline value of 303 MN/m$^2$ (44 ksi) at 297 K (75 °F) and 345 MN/m$^2$ (50 ksi) at 505 K (450 °F). Panel variability is evidently operating here to confuse the trends.

The baseline reversed loading tests at R = −1 produced much lower $\sigma_{10^7}$ values of 83 MN/m$^2$ (12 ksi) at 297 K (75 °F) and 90 MN/m$^2$ (13 ksi) at 505 K (450 °F), indicating the severe effect of compressive loading.

In like manner to the unnotched long term HT-S/710 Phase II specimens, all of the notched specimens also failed prior to reaching 50,000 hours. These wearout failures began as early as 18,000 hours and by the 28,000 hour point all had failed or had been removed from test because of their poor condition. The residual tensile properties, Figure 13-13, of the notched specimens were not as severely degraded as those of the unnotched specimens but did decrease with increasing flight cycling time and also exhibited considerable scatter.

**Celion 6000/LARC-160 G/PI, $[0° \pm 45°]_s$, unnotched.** The Celion 6000/LARC-160 G/PI data are summarized in Figures 13-15 and 13-16. The average baseline tensile strength at the flight simulation maximum exposure temperature, 450 K (350 °F), was 696 MN/m$^2$ (101 ksi). The $\alpha$ of 22 is an indication of the excellent reproducibility of these tests. For the combined 35 baseline tensile tests at seven temperatures a pooled $\alpha$ of 28 was calculated.

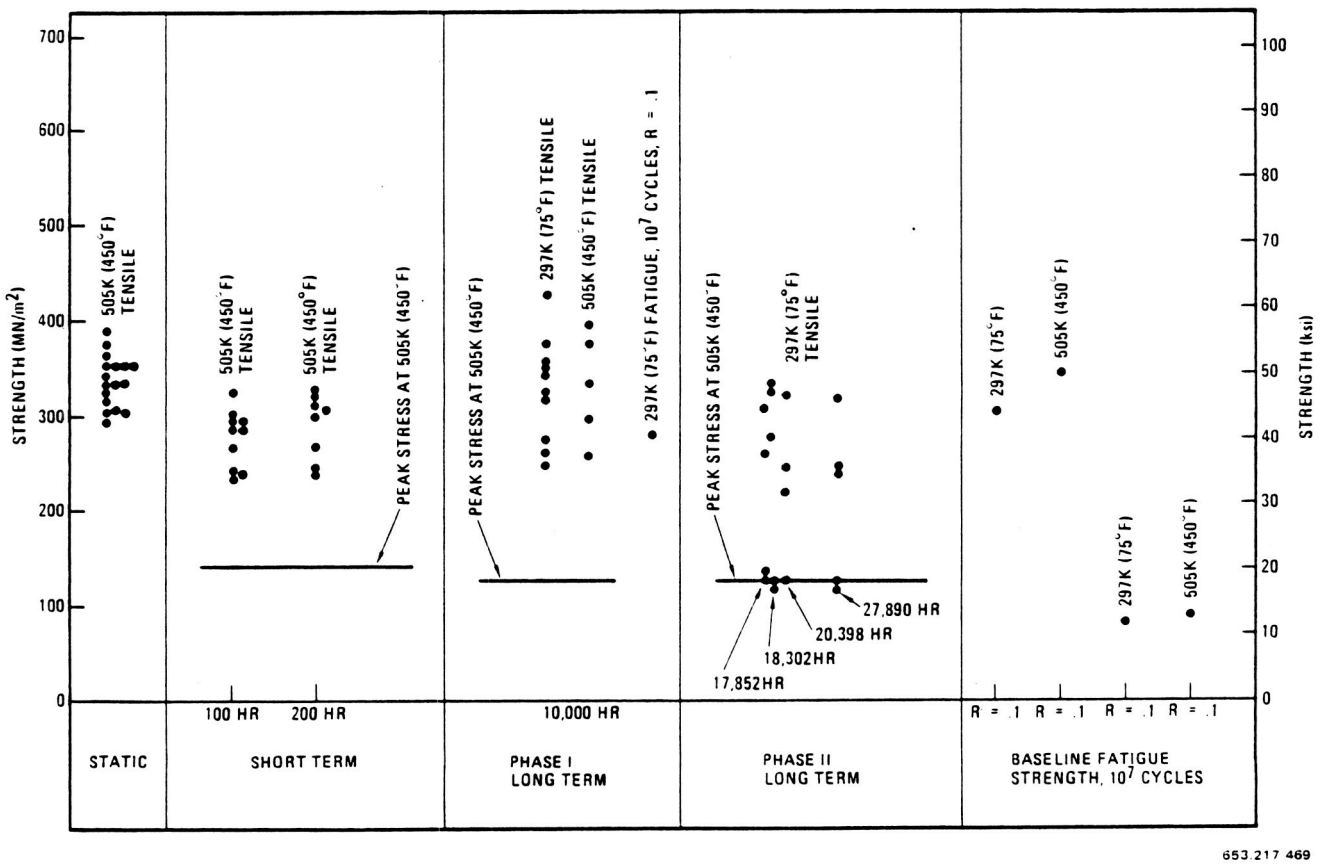
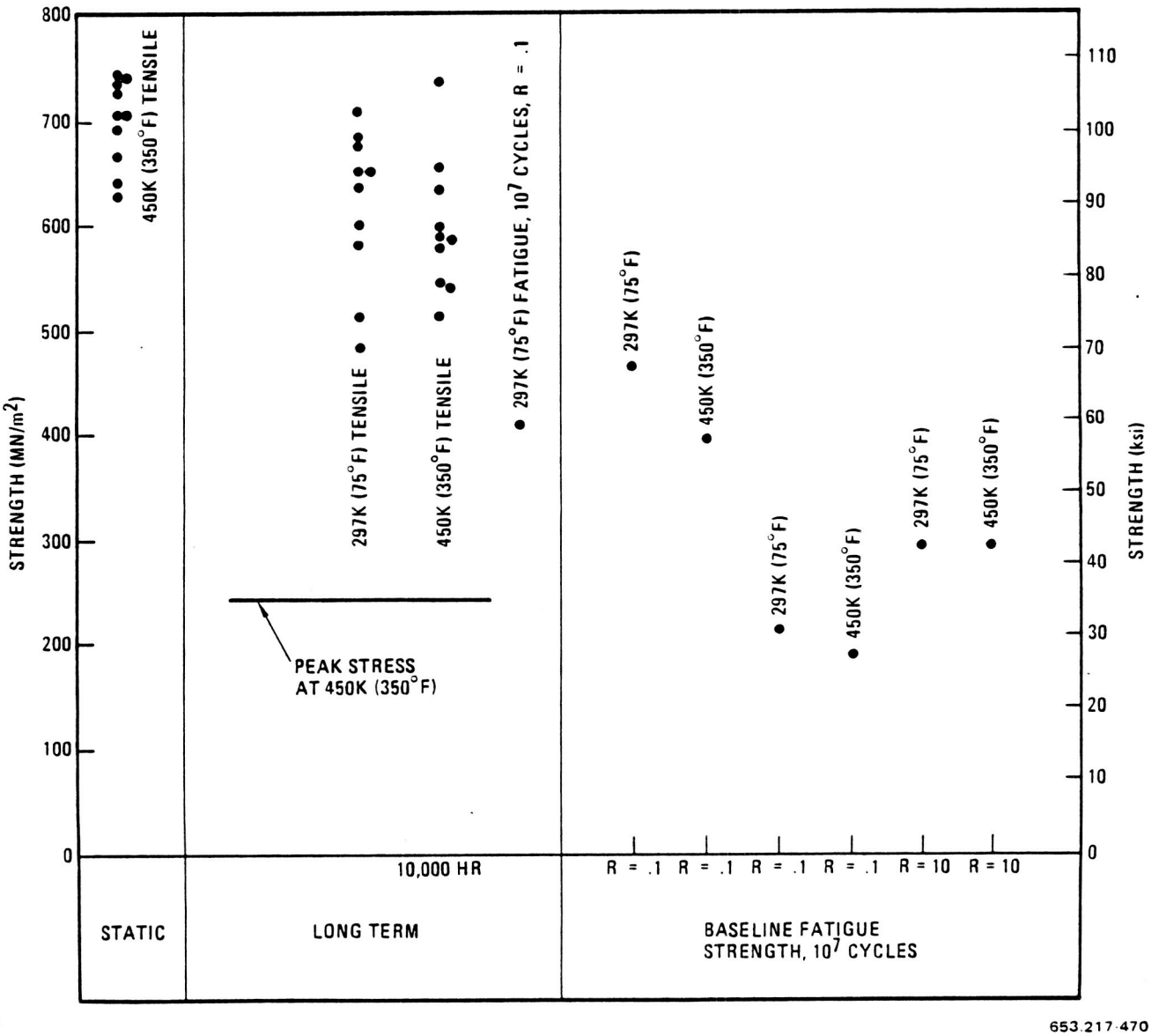



**Figure 13-14 Phase I and Phase II Notched $[0° \pm 45°]_s$ HT-S/710 GPI**




653.217-470

**Figure 13-15 Unnotched $[0° \pm 45°]_s$ Celion 6000/LARC-160 G/PI**

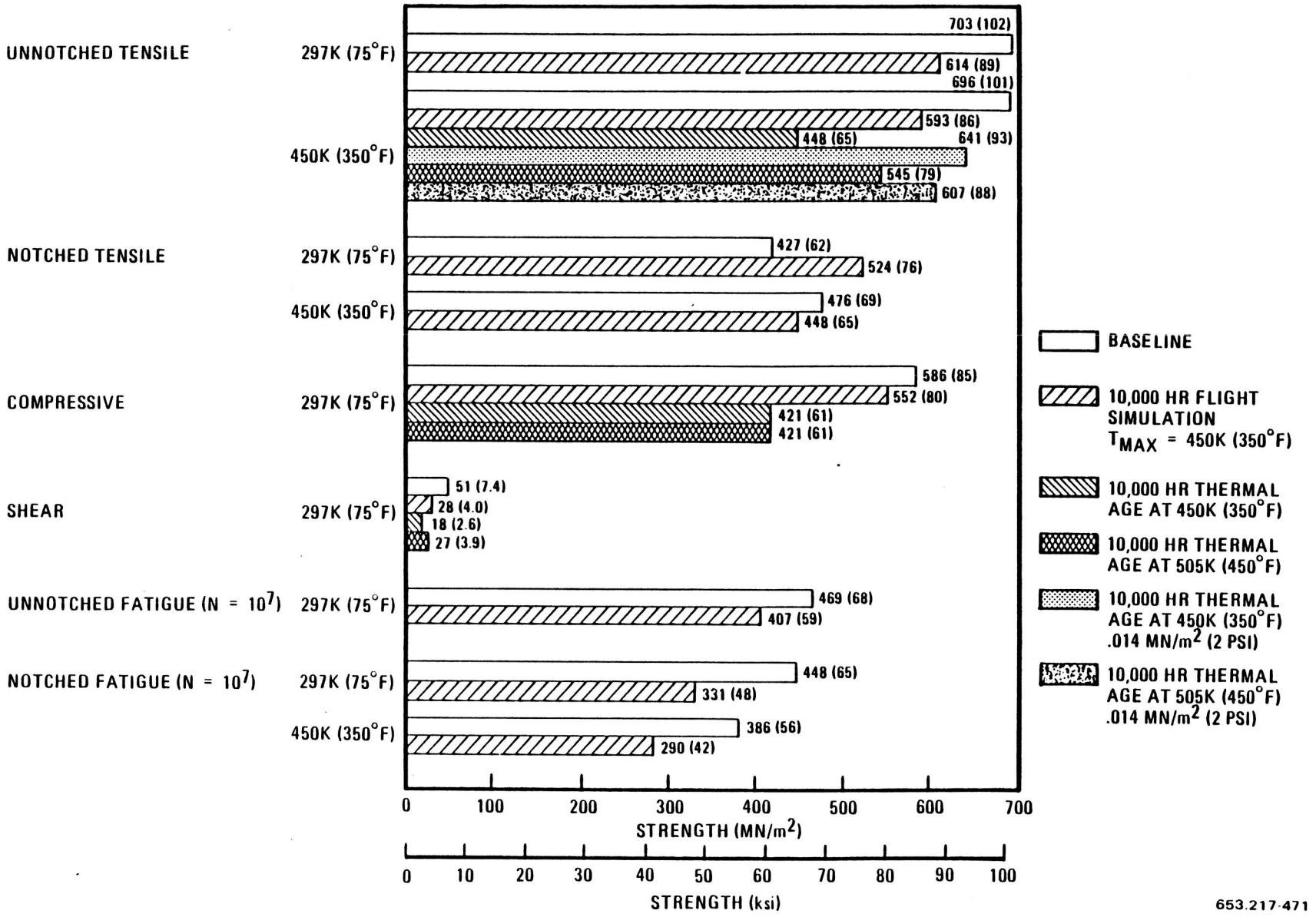



**Figure 13-16 Summary of Residual Properties of $[0° \pm 45°]_s$ Celion 600/LARC-160 G/PI After 10,000 hr of Exposure**

No short term testing of this system was conducted because of the poor results obtained with the HT-S/710 G/PI and because of the delays that would have occurred in flight simulation testing of the other systems. The procedure for selecting the long term loads was similar to that used for selecting short term loads for the other systems. An initial value of 444 $MN/m^2$ (64.4 ksi) resulted in an early failure. With a recalculated peak stress of 243 $MN/m^2$ (34.8 ksi) all the specimens completed 10,000 hours. The condition of the specimens was excellent with almost no visible surface erosion or attack except for minor surface microcracking. Tensile properties were reduced 10 to 15% with increased scatter. The failure mode remained tensile, and no aging or delamination effects were found. Again, as with the HT-S/710 G/PI system, the compressive strength was not greatly affected, but the residual shear strength was reduced by almost 50% after 10,000 hours.

Results of residual fatigue tests showed losses in $\sigma_{10^7}$ for tests at R = 0.1 and 297 K (75 °F) of about the same magnitude as the residual tensile tests, i.e., 10 to 15%. Baseline values of $\sigma_{10^7}$ for R = −1 were again considerably below those of the R = 0.1 tests. Baseline tests at an R value of 10 gave results intermediate to the R = 0.1 and R = −1 values.

The thermal aging data, Figure 13-16, are not in agreement with the flight simulation data. Again, panel to panel variability may be playing a role with these results. In general, the residual flight simulation data, tensile, compression, and shear, are superior to the post thermal aging data at equal and higher aging temperatures and for equivalent times. Additionally, the material aged at the higher temperature has shown better strength retention than that aged at the lower temperature after 10,000 hours. A post-cure effect at the higher aging temperature may be contributing to these results.

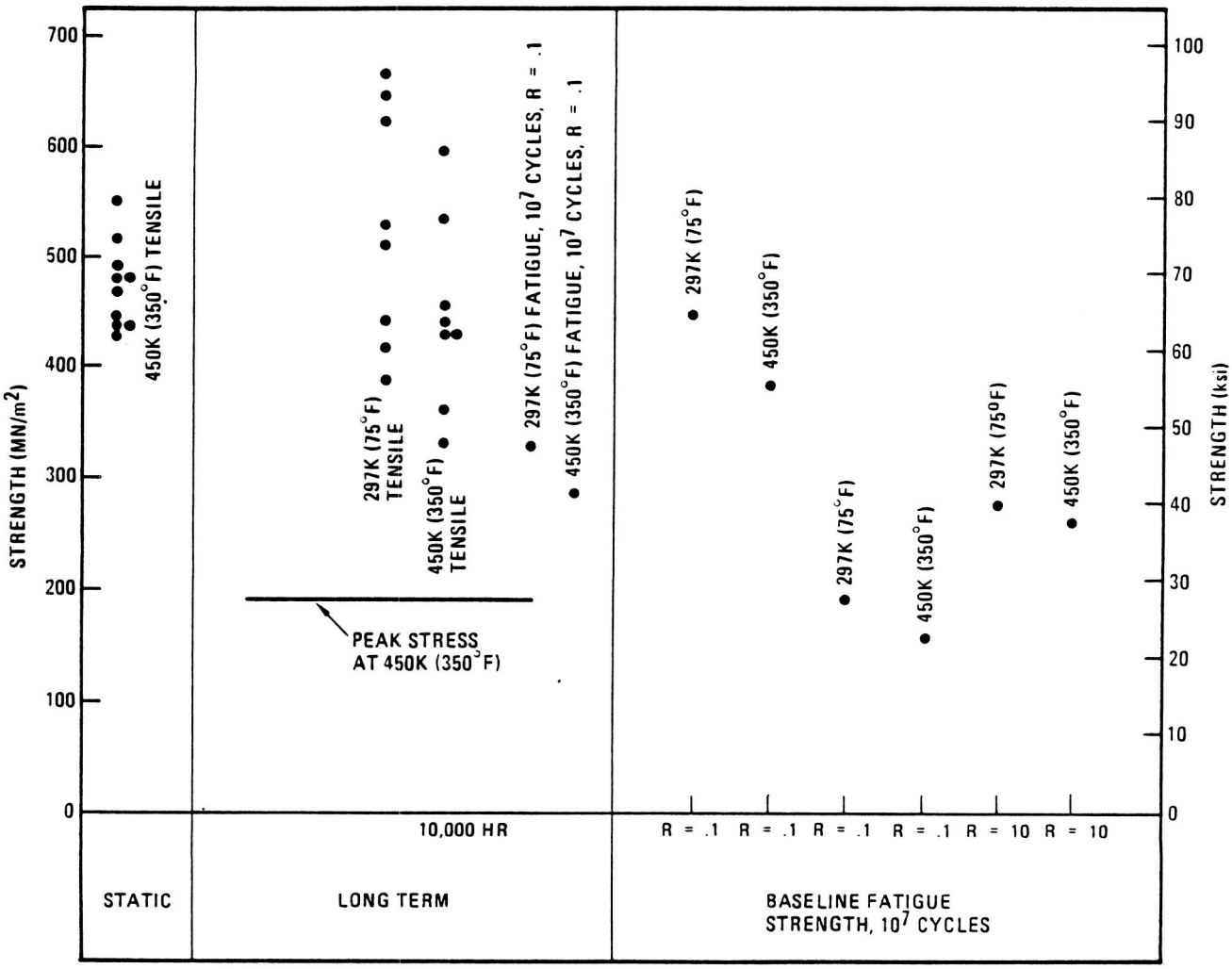
**Celion 6000/LARC-160 G/PI, $[0° \pm 45°]_s$, notched.** As shown in Figure 13-17 the mean strength of the notched Celion 6000/LARC-160 G/PI at 450 K (350 °F) was 475 $MN/m^2$ (68.9 ksi). The Weibull $\alpha$ was the same as that for the unnotched specimens, 22.

The long term peak stress of 191 $MN/m^2$ (27.3 ksi) was calculated using a procedure similar to that used for the unnotched specimens. All specimens survived the 10,000 hours in excellent condition. Residual notched tensile strengths at 297 K (75 °F) ranged from 663 $MN/m^2$ (96.2 ksi) to 389 $MN/m^2$ (56.4 ksi), and at 450 K (350 °F) they ranged from 592 $MN/m^2$ (85.9 ksi) to 332 $MN/m^2$ (48.2 ksi). The data scatter was significantly increased over that of the baseline tests, but the mean values were almost unchanged. This type of behavior after 10,000 hours of flight simulation, i.e., larger effects for unnotched specimens than for notched, was also observed for both epoxy systems and the other polymide system.

Residual fatigue testing at R = 0.1 at both 297 K (75 °F) and 450 K (350 °F) gave values of $\sigma_{10^7}$ approximately 25% lower than the baseline values.

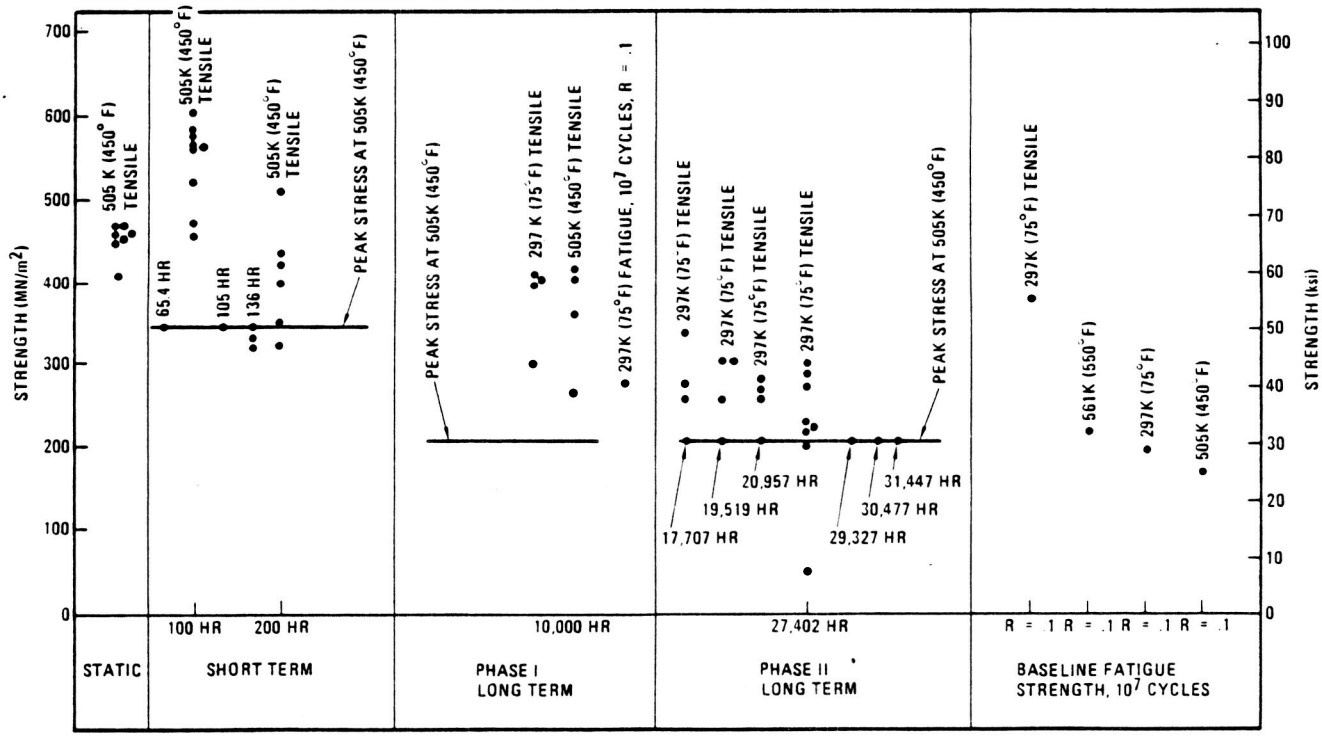
The significant effect of compressive loading on fatigue strength was again demonstrated with $\sigma_{10^7}$ values for R = −1 tests well below those for R = 0.1 tests of the baseline material.

**B/Al, $[0° \pm 45°]_s$.** Trend conclusions for B/Al were somewhat hampered by panel variability and, in Phase II, by batch variability. Recall that the Phase II, 25,000 hour and 40,000 hour thermal aging exposures were conducted on a different batch of material than that used for the Phase I thermal aging and flight simulation tests. Because the second batch of B/Al was far superior to the first batch during thermal aging, comparisons of these data with the flight simulation results are of little value and the data are not included in this summary.



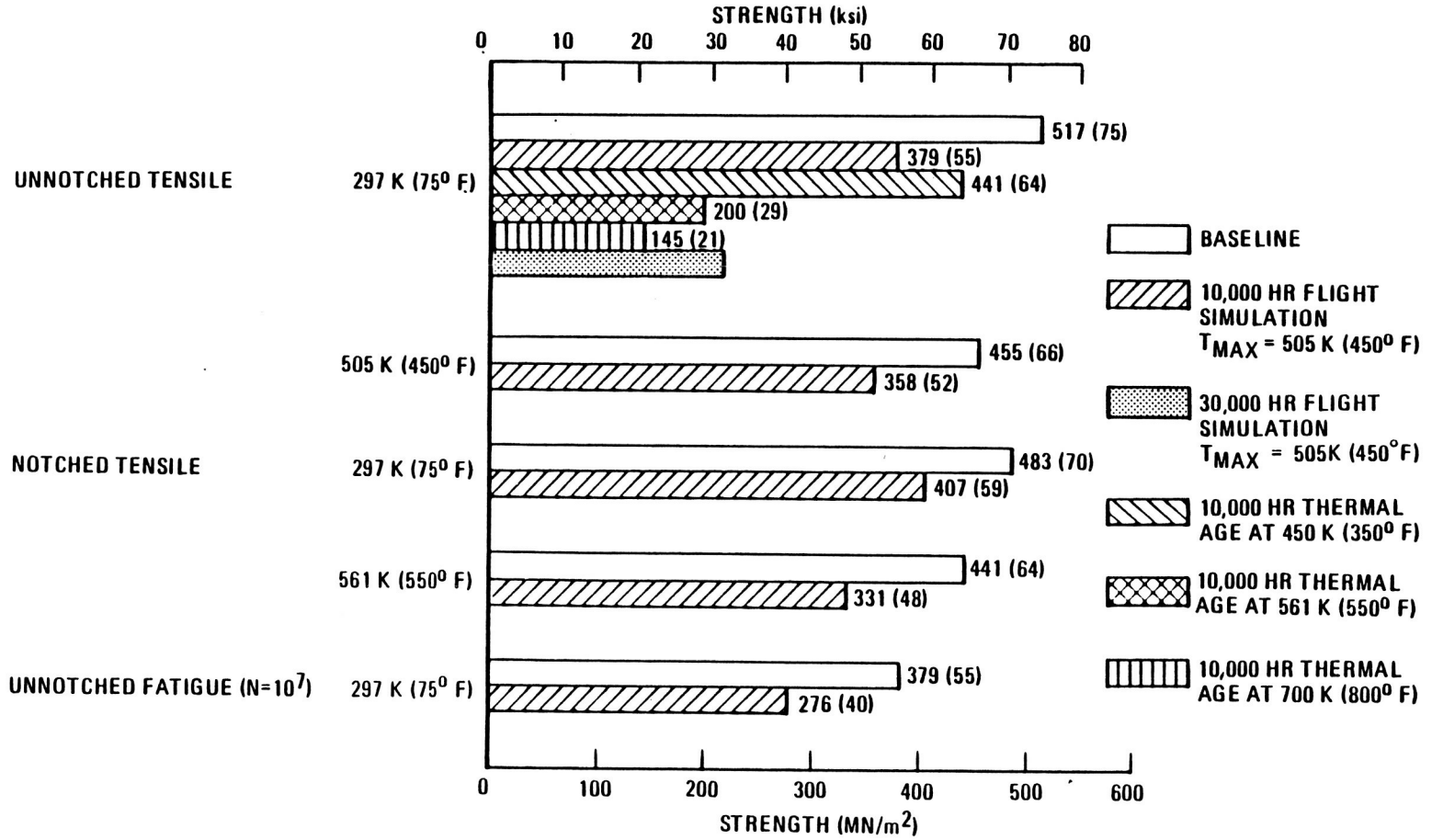

653.217 472

**Figure 13-17 Notched $[0° \pm 45°]_s$ Celion 6000/LARC-160 G/PI**




653 217 473

**Figure 13-18 Phase I and Phase II Unnotched $[0° \pm 45°]_s$ B/Al**




653.217-474

**Figure 13-19 Summary of Residual Properties of $[0° \pm 45°]_s$ B/Al After Thermal Exposure**

Figures 13-18 and 13-19 summarize the data for the crossply layup. Static strength at 505 K (450 °F) was about 455 MN/m$^2$ (66 ksi) with an $\alpha$ of 13.7.

The short-term specimens were cycled to a peak stress of 345 MN/m$^2$ (50 ksi) at 505 K (450 °F). Fatigue failures occurred in both sets of specimens, and the two had quite different mean strengths. Note the one residual strength value of 323 MN/m$^2$ (46.8 ksi), which was below the peak cyclic stress.

The long-term specimens were cycled to only 208 MN/m$^2$ (30.1 ksi), and no fatigue failures were observed during the first 10,000 hours. The 505 K (450 °F) residual tensile strengths were scattered from 262 MN/m$^2$ (38 ksi) to 414 MN/m$^2$ (60 ksi), and the 297 K (75 °F) residuals scattered from 303 MN/m$^2$ (44 ksi) to 407 MN/m$^2$ (59 ksi). The aluminum surface appeared rough, and the fibers had been degraded by the 10,000 hours at 505 K (450 °F). Residual compressive tests were not successful because of premature shear failures in the doubler bonds. However, the specimens did sustain quite high compressive stresses (well in excess of the tensile strength) before the doubler bond failure.

A significant portion of the degradation experienced by the B/Al during flight simulation exposure appears to be directly related to thermal aging effects and probably not a consequence of the fatigue loading and thermal cycling. While no 505 K (450 °F) thermal aging data were available for the first batch of material, interpolation of the 450 K (350 °F) and 561 K (550 °F) data, Figure 13-19, indicates that tensile strength losses equivalent to those determined after 10,000 hours of flight simulation could also have occurred during thermal aging at 505 K (450 °F) for 10,000 hours. Similar effects were not observed for the resin matrix systems.

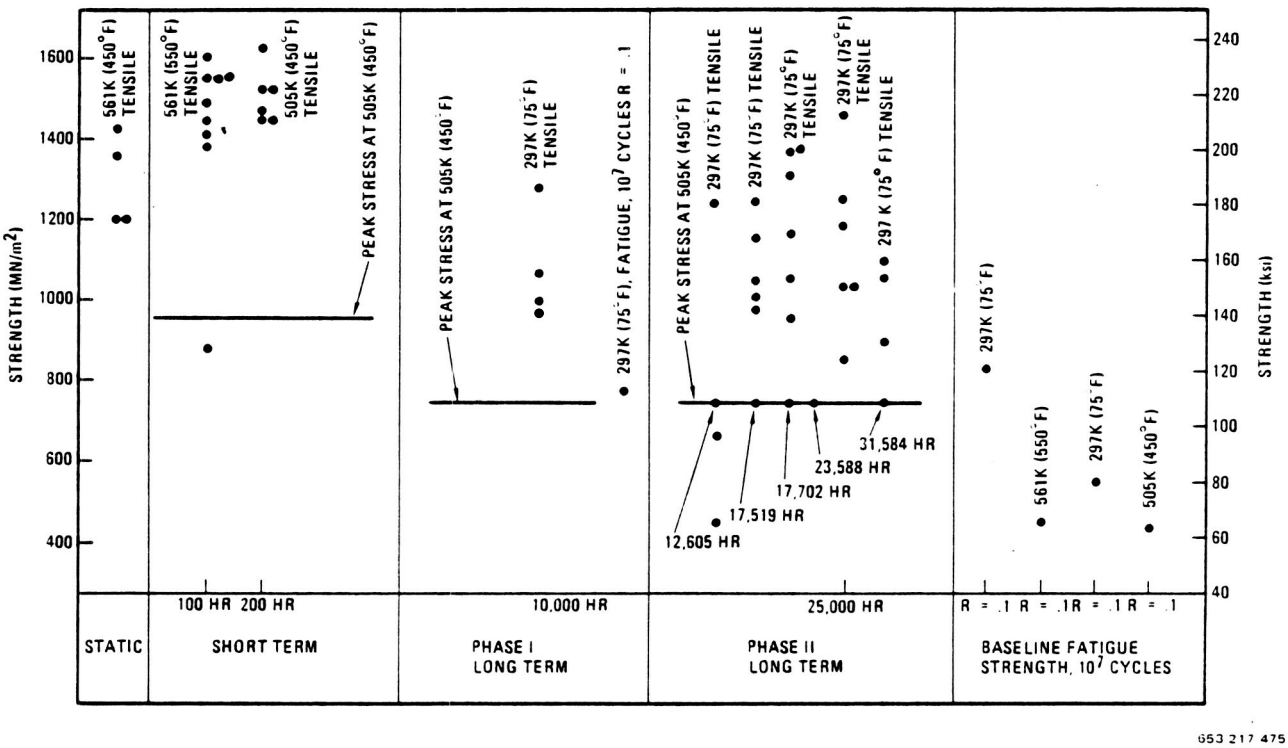
The post long-term fatigue at R = 0.1 and 297 K (75 °F) produced a $\sigma_{10^7}$ value of 276 MN/m$^2$ (40 ksi) after 10,000 hours as compared to the baseline values of 379 MN/m$^2$ (55 ksi) and 221 MN/m$^2$ (32 ksi) at 297 K (75 °F) and 561 K (550 °F) respectively. Again, the baseline reversed loading fatigue tests at R = $-1$ produced reductions in performance. The $\sigma_{10^7}$ values were 200 MN/m$^2$ (29 ksi) and 173 MN/m$^2$ (25 ksi) at 297 K (75 °F) and 505 K (450 °F) respectively.

Wearout fatigue failures began during Phase II after 17,000 hours of flight simulation cycling, and by 32,000 hours all but the three 25,000 hour specimens had failed. Surface roughening was severe and extensive longitudinal cracking of the aluminum accompanied by fracture of the outer ply boron filaments was visible on all specimens.

Residual tensile strength decreased with time from a mean of 290 MN/m$^2$ (42.1 ksi) at 17,707 hours to 222 MN/m$^2$ (32.2 ksi) after 27,402 hours. The limited material available did not allow residual strength testing other than tensile.

Early fatigue failures and a greater than 50% loss in residual tensile strength accompanied by severe surface damage after 25,000 hours does not make B/Al an attractive material for 50,000 hour use in a 505 K (450 °F) flight cycle environment.

**B/Al, $[0°]_6$.** Figure 13-20 summarizes the trend data for the unidirectional B/Al. The residual properties after flight simulation and thermal aging exposures are summarized in Figure 13-21.




653 217 475

**Figure 13-20 Phase I and II Unnotched $[0°]_6$ B/Al**

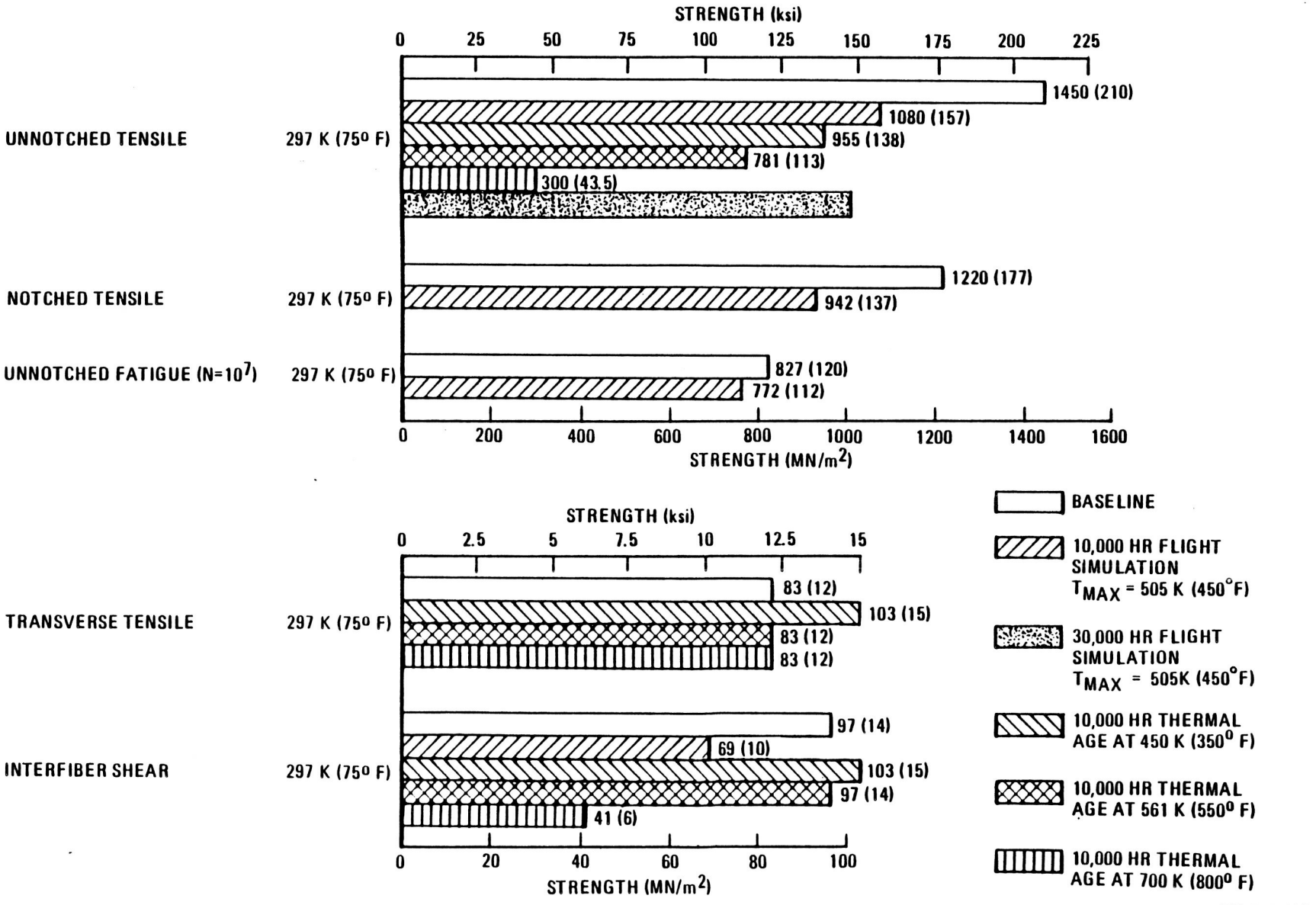



**Figure 13-21 Summary of Residual Properties of $[0°]_6$ B/Al After Thermal Exposure**

As no baseline tensile tests were conducted at 505 K (450 °F), the 561 K (550 °F) baseline data, shown in Figure 13-20, were used for selection of the short-term loads. A mean strength of 1300 $MN/m^2$ (188 ksi) was accompanied by a Weibull $\alpha$ of 17.55. Panel variability was again observed. The short-term specimens, cycled to a peak stress of 956 $MN/m^2$ (138.8 ksi) at 505 K (450 °F), seemed to get stronger with time. One exception was an individual specimen reaching only 882 $MN/m^2$ (128 ksi) after 100 hours.

The long-term specimens were cycled to a peak stress of 747 $MN/m^2$ (108.3 ksi). The residual tensile, notched tensile, and shear strengths were degraded approximately 25% by the 10,000 hours at 505 K (450 °F). Again surface roughness and fiber damage were apparent.

Again, as observed for the crossply B/Al, the decrease in unnotched tensile strength during 10,000 hours of flight simulation could be accounted for by thermal aging effects. In fact, this loss in strength was somewhat less than would be predicted for a 10,000 hour age at 505 K (450 °F). The effect of thermal aging on matrix dominated properties, transverse tensile and interfiber shear, was nil except at 700 K (800 °F) where oxidation of the boron fibers resulted in a 60% reduction of the interfiber shear strength.

Post long-term fatigue at R = 0.1 and 297 K (75 °F) achieved a $\sigma_{10^7}$ value of 772 $MN/m^2$ (112 ksi) after 10,000 hours compared with the 827 $MN/m^2$ (120 ksi) baseline value at 297 K (75 °F) and the 455 $MN/m^2$ (66 ksi) baseline at 561 K (550 °F). Scatter is again operating. The R = −1 baseline fatigue data again demonstrated compression degradation effects. The $\sigma_{10^7}$ values were 552 $MN/m^2$ (80 ksi) at 297 K (75 °F) and 441 $MN/m^2$ (64 ksi) at 505 K (450 °F).

The Phase II unidirectional B/Al flight simulation exposures were concluded with a wearout failure of the last surviving specimen just short of 32,000 hours. As with the Phase II crossplied specimens, only residual tensile strength testing could be performed because of the limited material available. The loss in tensile strength after 10,000 hours was 25%, whereas a loss in tensile strength of only 30% is indicated for the specimen that failed near 32,000 hours. However, surface degradation, including roughening, splitting, and filament fracture, as well as edge cracking were greatly increased over that observed after 10,000 hours.

Again, the B/Al system, either crossplied or unidirectional material, has not shown promise for extended usage in a thermal/fatigue environment with a maximum service temperature of 505 K (450 °F).

# SECTION 14

# CONCLUSIONS

This report describes a program to characterize the properties of several types of advanced filamentary reinforced composite material systems before and after exposure to simulated supersonic cruise environments for real times of up to 50,000 hours. Because usage of the composites was intended for the lower wing surface of a supersonic aircraft, exposure loads and subsequent residual property measurements were largely tensile. However, during the latter portion of the program a study was added to specifically examine the effect of thermal exposures on compressive and shear properties. Moisture effects were generally avoided by utilizing careful bakeout and storage procedures. Material behavior during these exposures and post exposure residual property tests provide exposure effects and reveal material failure modes and degradation mechanisms. In addition to the flight simulation exposures, the program provides extensive thermal and ambient aging data for times out to 50,000 hours. This report has also presented considerable baseline fatigue, creep, fracture, and tensile data for all the systems. In several instances, however, analysis of the test data has been partially hampered by panel-to-panel variability of each of the composite systems. Additionally, in two cases, G/E and B/Al, where material was purchased at widely spaced intervals, batch-to-batch variability prevented direct comparisons of results. The observations and conclusions relating to these baseline measurements and the environmental exposure tests are summarized briefly below.

B/5505 B/E and A-S/3501 G/E should be limited to a temperature of 373K (212°F) for cumulative exposures of 25,000 hours for B/E and 36,000 hours for G/E because of:

1. Early flight simulation test failures (caused by compressive loading and thermal cycling combined with oxidation induced matrix degradation).

2. Loss of residual strength during flight simulation and thermal aging exposures (caused by oxidation induced matrix degradation).

3. Moisture effects on elevated temperature strength (caused by matrix degradation).

HT-S/710 G/PI should be limited to 505K (450°F) for exposures of 15,000 hours because of:

1. Loss of residual tensile strength during thermal aging (caused by oxidation induced matrix degradation).

2. Loss of residual strength, primarily matrix dominated, during flight simulation exposure (caused by combined compressive and thermal stressing in conjunction with oxidation induced matrix degradation).

Celion 6000/LARC-160 G/PI should be limited to 450K (350°F) for exposures of 10,000 hours because of:

1. Loss of residual tensile, compressive, compressive fatigue, and shear strengths during thermal aging (caused by oxidation induced matrix degradation).

2. Loss of residual strength, primarily matrix dominated, during flight simulation exposure (caused by combined compressive and thermal stressing in conjunction with oxidation induced matrix degradation).

B/6061 B/Al should be limited to 505K (450 °F) for exposures of 15,000 hours because of:

1. Loss of residual tensile strength during thermal aging (caused by interface diffusion induced fiber degradation). Some loss in strength can occur at temperatures as low as 450K (350 °F).

2. High temperature fatigue effects (matrix surface cracking and fracture of outer ply boron filaments).

3. Loss of residual strength during flight simulation exposure (caused by interface diffusion induced fiber degradation, matrix surface cracking, and fracture of outer ply boron filaments).

B/P 105 AC B/PI is not suitable for this application because of severe matrix degradation during thermal aging and short-term flight simulation exposures at 505K (450 °F).

For the two epoxy systems the baseline and short-term flight simulation results were used in a wearout model to establish the long-term loading conditions. For the G/PI and B/Al materials, however, the wearout theory could not be applied because of inconsistent short-term data. The wearout model was based on a tensile failure mode and made no consideration for thermal effects. Phase I results for the epoxy systems indicated that a more comprehensive model was needed. This new model would be required to account for failure mechanism changes and thermal degradation during the course of the flight simulation exposures in order to more accurately predict complex real-time exposure effects. An alternate approach was found during the Phase II long term tests of the epoxy systems by simply reducing the maximum temperature to a level that precluded any significant thermal effects during the long exposure periods. This temperature was determined from a log time versus 1/T plot of thermal aging time-temperature combinations at which significant epoxy matrix degradation began. Extrapolation of the curve to 50,000 hours gave the revised test temperature.

The parameters necessary for surface microcracking of the resin matrix composites during thermal aging or flight simulation exposure varied for the different systems. For both epoxies the combination of thermal exposure and fatigue cycling was required. No surface microcracking was observed for HT-S/710 G/PI on either thermal aging or flight simulation specimens. Finally, for Celion 6000/LARC-160 G/PI thermal exposure alone was sufficient to cause microcracking while fatigue cycling alone was not. Surface cracking of the metal matrix composite, B/Al, was observed on specimens subjected to the combination of fatigue loading and thermal exposure.

For the epoxy systems, thermal aging at 394K (250 °F) and one atmosphere pressure produced no effects for the first 10,000 hours. Matrix degradation began between 10,000 and 25,000 hours and was severe after 50,000 hours. The fiber-controlled tensile properties, however, showed almost no change. Aging at 450K (350 °F) and one atmosphere pressure was more damaging, with matrix degradation beginning between 1000 and 5000 hours. After 5000 hours, the matrix was severely embrittled and crumbled away during tensile testing, leaving

many bare fibers. Tensile properties were considerably reduced for aging times of 5000 hours or longer. Reduced pressure exposures at 450K (350°F) delayed the effects but did not eliminate them.

The HT-S/710 G/PI system survived 25,000 hours of thermal aging at 505K (450°F) with no effects. Some decrease in tensile strength was measured after 50,000 hours, but matrix degradation was not observed. Raising the aging temperature to 561K (550°F) reduced the time at which tensile strength decreases were observed to 10,000 hours. In like manner to the 505K (450°F) exposures, this initial fall-off in tensile strength was not accompanied by matrix embrittlement. After 25,000 hours the material was partially delaminated and showed high weight loss. The tensile strength was greatly reduced and severe matrix embrittlement had occurred. Degradation after 50,000 hours was such that the specimens could not be tested. Again, aging effects were less severe for exposures conducted in a reduced pressure environment.

The effects of 10,000 hours of thermal aging at 450K (350°F) and 505K (450°F) in one atmosphere air on Celion 6000/LARC-160 G/PI were significant losses in tensile strength, beginning as early as 500 hours, and some matrix degradation. Tensile strength losses were higher for the 450K (350°F) exposures, 35%, than for those at 505K (450°F), about 20%, and were accompanied by greater matrix degradation. Weight loss during aging, however, was higher at the higher temperature. For the reduced pressure exposures no matrix degradation was observed, and strength losses were only of the order of 10% after 10,000 hours. The 10,000 hour performance of the Celion 6000/LARC-160 G/PI in one atmosphere air at 450K (350°F) was no better than that of G/E and at 505K (450°F) was considerably worse than that of HT-S/710 G/PI.

The B/6061 boron/aluminum used in the Phase II portion of the thermal aging evaluation (batch 2) was much superior to that used during Phase I (batch 1). The Phase I data indicated a maximum use temperature of only 450K (350°F) for exposures longer than 10,000 hours. The Phase II data, on the other hand, indicate that a maximum use temperature of 505K (450°F) for 40,000 hours of exposure is possible. Some precautions may be required, however, to protect the material edges to prevent oxidation of the boron fibers.

Results of the thermal aging/compression study showed that 10,000 hours of thermal aging in one atmosphere air at 373K (212°F) and 394K (250°F) produced no significant reduction in compressive strength or compressive fatigue strength of G/E. The major effect of the thermal exposure was a considerable decrease in shear strength of 6 ply material. These reductions were observed as early as 1000 hours and increased to 40% or more by 10,000 hours. In contrast to the G/E system, thermal aging of Celion 6000/LARC-160 G/PI at 450K (350°F) and 505K (450°F) produced significant reductions in compressive, shear, and fatigue strengths after 10,000 hours of exposure. In like manner to the thermal aging/tension results for this material, the compressive and 6 ply shear strength losses were higher for the 450K (350°F) age. The other properties, however, showed greater decreases at the higher aging temperature. Weight loss was also greater at the higher temperature. For the 6 ply specimens these losses were quite large, greater than 8%. Again, as with the G/E system, the property most affected was the shear strength of the 6 ply material. Losses of 65% were found after 10,000 hours at 450K (350°F). Extensive edge cracking, particularly in the 24 ply specimens, was found as early as 1000 hours into the exposure. After 10,000 hours these cracks extended throughout the matrix. One set of 6 ply specimens was coated with a solution of a polyphenylquinoxaline (PPQ) in an effort to improve the thermooxidative stability of the G/PI material. Preliminary

results were promising, with slight improvements over the uncoated specimens in almost every case.

For the resin matrix systems, matrix degradation by oxidation was shown to be a major contributor to mechanical property losses during thermal aging. For G/E and Celion 6000/LARC-160 G/PI the extent of oxidation could readily be detected by metallographic techniques, especially with the SEM. No evidence of time dependent oxidation similar to that for the G/E and Celion 6000/LARC-160 G/PI systems was observed for either the B/E or HT-S/710 G/PI thermal aging specimens. Examination of the B/E samples gave almost no information, while studies of HT-S/710 G/PI revealed increased porosity and fiber-matrix separation accompanied by numerous fine cracks at the fiber-matrix interface as thermal exposure time increased.

For the B/Al metal matrix system, thermal aging strength decreases were primarily fiber related rather than caused by degradation of the aluminum matrix by oxidation. Reactions at the boron filament/aluminum matrix interface during high temperature exposure led to changes in the transverse tensile and shear failure modes from primarily matrix to increased contributions from interfacial fracture and, for the Phase I batch, filament splitting. It was this observation that indicated that the boron fibers in the Phase II B/Al had a considerably improved thermal stability over that of the Phase I fibers.

Fatigue strength was found to be very dependent on the stress ratio used in testing. Results for tension-compressive loading (R=-1) and compressive-compressive loading (R=10) were considerably lower than those obtained for tension-tension loading (R=0.1). The R=10 S-N curves were just slightly higher than those at R=-1 for Celion 6000/LARC-160 G/PI, the only system tested at all three R values. The effect of a notch was generally to reduce the fatigue strength. However, some exceptions were observed at elevated temperature. Severe degradation of the aluminum matrix was found after fatigue testing at 561K (550 °F). Testing in an argon or nitrogen atmosphere or lowering the temperature to 505K (450 °F) significantly decreased the matrix degradation.

Absorption of moisture by the epoxy systems caused a significant decrease in short time elevated temperature strength. Moisture effects were considerably less damaging for the G/PI systems, particularly for the Celion 6000/LARC-160. Loss of resin from the surface sufficient to expose a large number of graphite fibers was experienced by both epoxy and polyimide matrix composites when exposed for 50,000 hours to weather and atmospheric contaminants. Significant losses in elevated temperature flexural strength, probably as a result of absorbed moisture, were also found.

Uncoated B/Al is subject to pitting and subsequent intergranular corrosion cracking when exposed for long periods in an industrial-seacoast environment. These corrosion cracks, many extending to a depth of 0.00018m (0.007 in.) after 50,000 hours of exposure, can seriously degrade the matrix controlled properties by acting as crack starters. An aluminized polyimide coating developed for high temperature corrosion protection was found to prevent this pitting and intergranular corrosion cracking during the 50,000 hours of outdoor exposure.

Boron or graphite reinforced composite materials with 0° plies aligned in the direction of loading undergo very little creep even at stress levels, which result in facture in short exposure times. Because of the low creep strains observed in these materials it is suggested that stress rupture tests be substituted for creep measurements.

A major goal of this program was to develop a predictive capability such that by properly setting the experimental conditions (loads and temperatures) a number of advanced composite materials could complete 50,000 hours of real-time exposure to a supersonic cruise environment with an 80% survival rate. This goal was not accomplished. Two factors were largely responsible:

1. The inadequacy of the wearout theory because no consideration had been given to thermal effects and the attendant failure mechanism changes during the course of the exposures.

2. Data scatter of the composite systems, including in-panel variability, panel-to-panel variability, and batch-to-batch variability.

One material, however, did show a potential for successfully surviving 50,000 hours of flight simulation. The G/E system completed 36,000 hours at a maximum flight simulation temperature of 373K (212°F) with the only significant effect being a 28% loss in shear strength. As the tests were halted prematurely (to prevent further B/E failures) the possibility exists that the G/E specimens may have lasted the full 50,000 hours of exposure.

# SECTION 15

# REFERENCES


1. Hoffman, S.: Bibliography of Supersonic Cruise Aircraft Research (SCAR) Program From 1972 to Mid-1977, NASA RP 1003, 1977.

2. Hoffman, S.: Bibliography of Supersonic Cruise Research (SCR) Program From 1977 to Mid-1980, NASA RP 1063, 1980.

3. Hoffman, S.: Bibliography of Supersonic Cruise Research (SCR) Program From 1980 to 1983, NASA RP 1117, 1984.

4. Imig, L. A.; and Illg, W.: Fatigue of Notched Ti-8Al-1Mo-1V Titanium Alloy at Room Temperature and 550 °F (560 °K) With Flight-by-Flight Loading Representative of a Supersonic Transport, NASA TND-5294, 1969.

5. Imig, L. A.: and Garrett, L. E.: Fatigue-Test Acceleration With Flight-by-Flight Loading and Heating to Simulate Supersonic-Transport Operation, NASA TND-7380, 1973.

6. Halpin, J. C.; Jerina, K. L.; and Johnson, T. A.: Analysis of the Test Methods for High Modulus Fibers and Composites, ASTM STP 521, American Society for Testing and Materials, 1973, pp. 5-64.

7. Structural Design Guide for Advanced Composite Applications, Second Edition, Advanced Composites Division, AFML, 1971.

8. Hertz, J.; Christian, J. L.; and Varlas, M.: Advanced Composite Applications for Spacecraft and Missiles, AFML-TR-71-186, 1972.

9. Christian, J. L.: Development and Evaluation of Advanced Metal-Matrix Composite Materials, Rep. GDC-ERR-1571, General Dynamics/Convair, 1970.

10. Forest, J. D.; and Christian, J. L.: Development and Application of Aluminum/Boron Composite Material, AIAA Paper No. 68-975, October 1968.

11. Christian, J. L.; and Jones, R. C.: Development and Evaluation of Improved Boron/Aluminum Composite Material, Rep. GDC-ERR-1450, General Dynamics/Convair, 1970.

12. Forest, J. D.; and Christian, J. L.: Development and Application of High Matrix Strength Aluminum/Boron, presented at ASM Metals Engineering Congress, October 1969.

13. Christian, J. L.: Material and Fabrication Development and Application Studies of Aluminum/Boron-Stainless Steel Composites, presented at ASME 15th Annual International Gas Turbine Conference, Brussels, Belgium, May 1970.

14. Miller, M. F.: Schaefer, W. H.: Weisinger, M. D.; et al: Development of Improved Metal-Matrix Fabrication Techniques for Aircraft Structures, AFML-TR-71-181, 1971.

15. Shockey, P. D.; Hofer, K. E.; Kaminski, B. E.; Lemon, G. H.; and McKague, E. L.: Development of Engineering Data for Advanced Composite Materials, Vol. I-Static and Thermophysical Properties, Vol. II-Fatigue and Load Rate Characteristics, AFML-TR-70-108, 1972.

16. Shockey, P. D.; Hofer, K. E.; and Wright, W. D.: Structural Airframe Application of Advanced Composite Materials, Vol. IV-Mechanical Properties-Static, AFML-TR-69-101, 1969.

17. Development of Engineering Data on the Mechanical and Physical Properties of Advanced Composites Materials, AMFL-TR-72-205 - Part I, 1972.

18. Advanced Composites Data for Aircraft Structural Design, Report No. NA-71-679-9, North American Rockwell, 1972.

19. Beeler, D. R.; and Chase, V. A.: Advanced Polyimide Composites, SAE Conference, Oct. 1968.

20. Vaughan, R. W.: Glass Reinforced P13N Polyimide Laminates Having Improved Processing Characteristics, 15th National SAMPE Conference, April 1969.

21. Vaughan, R. W.; Jones, R. J.; Sheppard, C. H.; and Burns, E. A.: Development of Low Void Polyimide Resin for Autoclave Processing of Glass and Graphite Reinforced Composites, National SAMPE Conference, Oct. 1971.

22. Petker, I.; et al: High-Strength, High-Modulus Filament-Reinforced Composites, AFML-TR-67-395, 1968.

23. Birchfield, E. B.; and Kollmansberger, R.: Develop Fabrication/Processing Techniques for High Temperature Advanced Composites for Use in Aircraft Structures, AFML-TR-72-91, 1972.

24. Scheck, W. G.: Development of Design Data for Graphite Reinforced Epoxy and Polyimide Composites, Rep. GDC-DBG70-005, General Dynamics/Convair, 1974.

25. Stuckey, J.; and Scheck, W. G.: Development and Evaluation of Graphite and Boron Polyimide Composites, National SAMPE Technical Conference, Oct. 1972, Palo Alto, California.

26. Prunty, J.: Design, Fabrication, and Test of a Graphite/Epoxy Metering Shell (GEMS), Rep. CASD-NAS75-015, General Dynamics/Convair, 1975.

27. Chase, V. A.; and Harrison, E. S.: Develop and Demonstrate Manufacturing Processes for Fabricating Graphite Filament Reinforced Polyimide (Gr/Pl) Composite Structural Elements, NASA CR-172497, February 1985.

28. Peterson, R. E.: Stress Concentration Design Factors. John Wiley and Sons, Inc., 1953.

29. Waddoups, M. E.; Eisenmann, J. R.; and Kaminski, B. E.: Macroscopic Fracture Mechanics of Advanced Composite Materials. J. Composite Materials, 5, 1971, p. 446.

30. Konish, H. J., Jr.: A Study of Fracture Phenomena in Fiber Composite Laminates, AFML-TR-73-145, Vol. III, 1973.

31. Adsit, N. R.; and Waszczak, J. P.: Fracture Mechanics Correlation of Boron/Aluminum Coupons Containing Stress Risers, ASTM Symposium on Fracture Mechanics of Composites, 1974.

32. Paris, P. C.; and Sih, G. C.: Stress Analysis of Cracks. Fracture Toughness Testing and its Applications, ASTM STP 381, American Society for Testing and Materials, 1970, pp. 30-83.

33. Chase, V.; and Beeler, D.: Manufacturing Methods for Large High-Temperature Sandwich Structures, AFML-TR-70-211, 1970.

34. Jones, R. L.: Evaluation of Electron Scanning Microscopes, Rep. ERR-FW-1188, General Dynamics/Convair, 1972.

35. Metcalfe, A. G., ed.: Interfaces in Metal Matrix Composites, Academic Press, 1974.

36. Hertz, J.: Investigation Into the High Temperature Strength Degradation of Fiber-Reinforced Resin Composites During Ambient Aging, NASA CR-124290, 1973.

37. Shirrell, C. D.: Halpin, J. C.; and Browning, C. E.: Moisture — An Assessment of Its Impact on the Design of Resin Based Advanced Composites, Third Conf. on Fibrous Composites in Flight Vehicle Design, November 4-6, 1975, NASA TMX-3377, April 1976.

38. Schaefer, W. H.; and Christian, J. L.; et al.: Evaluation of the Structural Behavior of Filament Reinforced Metal Matrix Composites, AFML-TR-69-36, 1969.

39. Treadway, D. G.; Sutherland, W. M.; and Keller, E. E.: Aerospace Corrosion Prevention Studies, Rep. GDCA-ERR-1612, General Dynamics/Convair, 1971.

40. Shockey, P. D.; Anderson, J. D.; and Hofer, K. E.: Structural Airframe Application of Advanced Composite Materials - Vol. V, Mechanical Properties-Fatigue, AFML-TR-69-101, 1970.

41. Shockey, P. D.; and Hofer, K. E.: Development of Engineering Data for Advanced Composite Materials, Vol. II, Fatigue and Load Rate Characteristics, AFML-TR-70-108, 1972.

42. Military Standardization Handbook, Metallic Materials and Elements for Aerospace Vehicle Structures, MIL-HDBK-5B, Department of Defense, Washington, D. C., 1975.

43. Wolff, R. V.; and Lemon, G. H.: Reliability Prediction for Adhesive Bonds, AFML-TR-72-121, 1972.

44. Waddoups, M. E.; Wolff, R. V.; and Wilkins, D. J.: Reliability of Complex Large Scale Composite Structure-Proof of Concept, AFML-TR-73-160, 1973.

45. Halpin, J. C.; Johnson, T. A.; and Waddoups, M. E.: Kinetic Fracture Models and Structural Reliability, International Journal of Fracture Mechanics, Vol. 8, 1972.

46. Wolff, R. V.; and Lemon, G. H.: Reliability Prediction for Composite Joints-Bonded and Bolted, AFML-TR-74-197, 1974.

47. Wolff, R. V.; Wilkins, D. J.; Lemon, G. H.; Orringer, O. R.; and Shinozuka, M.: Life Assurance of Composite Structures, Vol. II - Technology, Vol. III -Element Characterization, AFFDL-TR-77-50, 1977.

# APPENDIX A

## AN ANALYSIS OF THE B/P105AC BORON POLYIMIDE SYSTEM

Approximately midway through Phase I of the program the decision was made to cancel all testing of the B/P105AC boron/polyimide system. The removal of the B/PI was based on very low tensile properties found for the majority of the panels and extensive thermal degradation observed during thermal aging and short-term flight simulation testing. The following is a brief description of the problems experienced with this material system, and what are believed to have been the reasons for the poor results.

In mid 1973, 28 kg (62 lb) of B/P105AC prepreg was ordered from AVCO Corporation with delivery expected in one to two months. Because of difficulties encountered by AVCO in obtaining the polyimide resin from the manufacturer, Ciba-Geigy, delivery was delayed until the end of 1973. Upon receipt of the prepreg, quality assurance testing was performed. The material was found to be acceptable. Two quality assurance panels were then fabricated. Before quality assurance testing could be completed, however, Ciba-Geigy informed us that they would no longer produce the P105AC resin (see letter on Page A-2), and as they were the only source of this material, testing was put on hold.

After a four-month delay, permission was received from NASA to resume fabrication and testing as it was thought that AVCO Corporation would obtain a license to produce the resin. The quality assurance panels were ultrasonically C-scanned, specific gravity and resin, fiber, and void contents were determined, and quality assurance mechanical property data were obtained. The results (see Tables 6-8 and 6-9) indicated the materials to be acceptable. Only the room temperature shear strength of the unidirectional material was on the low side, 55 $MN/m^2$ (8 ksi), compared to an expected value of about 69 to 83 $MN/m^2$ (10 to 12 ksi). Based on the quality assurance tests, the required number of full size panels were fabricated.

At about this time in the program, mid 1974, the start of short-term testing of B/PI had fallen well behind schedule. Since only crossplied specimens were to be used in the short-term tests, the main effort in baseline testing was, therefore, on the crossplied material. Baseline tensile and notched tensile tests were performed. Results are given in Tables A-1 and A-2. The data were typical of good material; consequently short-term specimens were prepared and installed in the flight simulation apparatus.

Baseline testing of the unidirectional material, which previously had been given low priority, was now started. Also during this time period, the end of 1974, results from the thermal aging tests were becoming available, and proof testing of the short-term specimens was begun. All three of these tests gave indications of a potential problem with the B/PI material system.

Unidirectional tensile strengths, Table A-3, were only half of what was considered normal. The notched unidirectional tensile strength, Table A-4, were somewhat higher but still unacceptable. The three notched specimens tested at room temperature gave particularly low values. These specimens and all of the unnotched specimens were cut from panel LRC-32. The remaining notched specimens were cut from panel LRC-34.

**Plastics Operations**
CIBA-GEIGY Corporation
Ardsley, New York 10502
914 478 3131

CIBA–GEIGY

November 15, 1973

Dear Customer,

It is necessary for us to discontinue one of our polyimide products, P105AC, when present stocks are exhausted. This is occasioned by the unanticipated withdrawal from commerce of one of the monomers required, thiodianiline. P105A, an earlier version, was replaced by P105AC early in 1973. The former product also was based on this monomer and cannot be re-introduced. Adhesive composition, LSU-1106, also containing thiodianiline is similarly affected.

Our P13N polyimide family contains no thiodianiline and is not affected. We encourage use of P13N in your applications. If changes in processing are required due to different flow characteristics, our Development & Applications Laboratory stands ready to render necessary assistance.

We are sorry for any inconvenience that this reluctant but unavoidable decision may have caused. CIBA-GEIGY appreciates your valued business and looks forward to providing continuing requirements for high quality engineering resins.

Very truly yours,

Stephen S. Hirsch
Manager, Business Development

SSH:jk

Table A-1. Baseline Tensile Properties $[0° \pm 45°]_s$ B/Pl

| Specimen Number | Temperature K | Temperature (°F) | | Tensile Strength MN/m² | Tensile Strength (ksi) | Tensile Modulus GN/m² | Tensile Modulus (Msi) |
|---|---|---|---|---|---|---|---|
| CC01-1 | 218 | -67 | | 450 | 65.3 | 88 | 12.7 |
| -2 | | | | 478 | 69.4 | 79 | 11.5 |
| -3 | | | | 513 | 74.4 | 84 | 12.2 |
| | | | av | 480 | 69.7 | 84 | 12.1 |
| CC01-4 | 297 | 75 | | 510 | 74.0 | [a]105 | [a]15.3 |
| -5 | | | | 505 | 73.2 | [a]110 | [a]16.0 |
| -6 | | | | 565 | 81.9 | [a] 91 | [a]13.2 |
| | | | av | 527 | 76.4 | 102 | 14.8 |
| CC01-7 | 505 | 450 | | 490 | 71.1 | [a] 66 | [a] 9.5 |
| -8 | | | | 484 | 70.2 | [a] 66 | [a] 9.5 |
| -9 | | | | 547 | 79.4 | [a] 62 | [a] 9.0 |
| -22 | | | | 539 | 78.2 | — | — |
| -23 | | | | 518 | 75.2 | — | — |
| -24 | | | | 478 | 69.4 | — | — |
| -25 | | | | 538 | 78.1 | — | — |
| -26 | | | | 565 | 81.9 | — | — |
| -27 | | | | 549 | 79.6 | — | — |
| -28 | | | | 494 | 71.6 | — | — |
| -29 | | | | 443 | 64.2 | — | — |
| -30 | | | | 544 | 78.9 | — | — |
| -31 | | | | 525 | 76.2 | — | — |
| -32 | | | | 555 | 80.5 | — | — |
| -33 | | | | 562 | 81.5 | — | — |
| -34 | | | | 522 | 75.7 | — | — |
| -35 | | | | 494 | 71.7 | — | — |
| | | | av | 520 | 75.5 | 65 | 9.3 |
| CC01-10 | 533 | 500 | | 501 | 72.6 | — | — |
| -11 | | | | 465 | 67.5 | — | — |
| -12 | | | | 483 | 70.1 | — | — |
| | | | av | 483 | 70.1 | | |
| CC01-13 | 561 | 550 | | 446 | 64.7 | [a] 58 | [a] 8.4 |
| -14 | | | | 437 | 63.4 | [a] 55 | [a] 8.0 |
| -15 | | | | 447 | 64.8 | [a] 56 | [a] 8.1 |
| | | | av | 443 | 64.3 | 56 | 8.2 |
| CC01-16 | 589 | 600 | | 415 | 60.2 | — | — |
| -17 | | | | 452 | 65.6 | — | — |
| -18 | | | | 463 | 67.1 | — | — |
| | | | av | 443 | 64.3 | | |
| CC01-19 | 616 | 650 | | 444 | 64.4 | — | — |
| -20 | | | | 468 | 67.9 | — | — |
| -21 | | | | 482 | 69.9 | — | — |
| | | | av | 465 | 67.4 | | |

[a] Strain gage measurement

Table A-2. Baseline Notched Tensile Properties of $[0° \pm 45°]_s$ B/Pl

| Specimen Number | Temperature K | Temperature (°F) | | Notched Tensile Strength MN/m² | Notched Tensile Strength (ksi) |
|---|---|---|---|---|---|
| CC02-1 | 218 | -67 | | 444 [a] | 64.4 |
| -2 | | | | 432 | 62.7 |
| -3 | | | | 458 | 66.4 |
| | | | av | 445 | 64.5 |
| CC02-4 | 297 | 75 | | 503 | 73.0 |
| -5 | | | | 424 | 61.5 |
| -6 | | | | 404 | 58.6 |
| | | | av | 444 | 64.4 |
| CC02-7 | 505 | 450 | | 396 | 57.5 |
| -8 | | | | 379 | 54.9 |
| -9 | | | | 377 | 54.7 |
| -22 | | | | 383 | 55.5 |
| -23 | | | | 380 | 55.1 |
| -24 | | | | 342 | 49.6 |
| -25 | | | | 381 | 55.2 |
| -26 | | | | 379 | 54.9 |
| -27 | | | | 399 | 57.8 |
| -28 | | | | 372 | 54.0 |
| -29 | | | | 367 | 53.3 |
| -30 | | | | 372 | 54.0 |
| -31 | | | | 358 | 52.0 |
| -32 | | | | 369 | 53.5 |
| -33 | | | | 361 | 52.4 |
| -34 | | | | 356 | 51.6 |
| -35 | | | | 372 | 54.0 |
| | | | av | 373 | 54.1 |
| CC02-10 | 533 | 500 | | 416 | 60.4 |
| -11 | | | | 395 | 57.3 |
| -12 | | | | 423 | 61.3 |
| | | | av | 411 | 59.7 |
| CC02-13 | 561 | 550 | | 392 | 56.9 |
| -14 | | | | 398 | 57.7 |
| -15 | | | | 381 | 55.3 |
| | | | av | 390 | 56.6 |
| CC02-16 | 589 | 600 | | 396 | 57.5 |
| -17 | | | | 388 | 56.3 |
| -18 | | | | 388 | 56.3 |
| | | | av | 391 | 56.7 |
| CC02-19 | 616 | 650 | | 437 | 63.4 |
| -20 | | | | 425 | 61.7 |
| -21 | | | | 459 | 66.5 |
| | | | av | 440 | 63.9 |

[a] Net section strength, i.e., based on total width less hole diameter.

Table A-3. Baseline Tensile Properties $[0°]_6$ B/PI

| Specimen Number | Temperature K | Temperature (°F) | | Tensile Strength MN/m² | Tensile Strength (ksi) |
|---|---|---|---|---|---|
| CU01-22 | 505 | 450 | | 848 | 123 |
| -23 | | | | 765 | 111 |
| -24 | | | | 717 | 104 |
| -25 | | | | 800 | 116 |
| -26 | | | | 772 | 112 |
| -27 | | | | 779 | 113 |
| -28 | | | | 945 | 137 |
| -29 | | | | 572 | 82.9 |
| -30 | | | | 657 | 95.3 |
| | | | av | 761 | 110 |
| CU01-10 | 533 | 500 | | 630 | 91.4 |
| -11 | | | | 627 | 91.0 |
| -12 | | | | 910 | 132 |
| | | | av | 722 | 105 |
| CU01-16 | 561 | 550 | | 510 | 74.0 |
| -17 | | | | 606 | 87.9 |
| -18 | | | | 331 | 48.0 |
| | | | av | 482 | 70.0 |
| CU01-19 | 589 | 600 | | 421 | 61.0 |
| -20 | | | | 690 | 100 |
| -21 | | | | 745 | 108 |
| | | | av | 619 | 89.7 |

Results of thermal aging exposures at 505 K (450° F) and 561 K (550° F) for times to 1000 hours were also very poor. Tensile testing of specimens aged for 500 hours gave low strength values with the specimens literally falling apart during the tests. Specimens aged 1000 hours failed by delamination during the doubler bonding operation and could not even be tested.

The third indication of unsatisfactory material came during the short-term tests. At 75% of the proof load used for the short-term exposures, four of the specimens failed. The stress levels were approximately 350 MN/m² (50 ksi), well below the average $F_{tu}$ of 520 MN/m² (76 ksi) obtained from the baseline tests. The appearance of the failed specimens, which prior to proof loading had been baked out for 72 hours at 478 K (400° F) to remove any absorbed moisture, was similar to those from the thermal aging tests. The resin had crumbled away in the region of the failures leaving bare boron filaments.

At the beginning of the short-term testing of the G/PI system, a few of the B/PI specimens that had survived the proof test were included in with the G/PI specimens. One of these failed after only seven hours, while the remaining ones were badly damaged and about to fail. The appearance was similar to those described above with the resin breaking away from the boron filaments. Figure A-1 shows the heated area of one of the unfailed specimens. It is held together by the boron filaments with only a small amount of resin remaining.

Table A-4. Baseline Notched Tensile Properties of $[0°]_6$ B/Pl

| Specimen Number | Temperature K | Temperature (°F) | | Notched Tensile Strength MN/m² | Notched Tensile Strength (ksi) |
|---|---|---|---|---|---|
| CU02-4 | 297 | 75 | | 717 [a] | 104 |
| -5 | | | | 557 | 80.8 |
| -6 | | | | 469 | 68.0 |
| | | | av | 581 | 84.3 |
| CU02-7 | 505 | 450 | | 669 | 97.1 |
| -8 | | | | 896 | 130 |
| -9 | | | | 862 | 125 |
| -22 | | | | 1250 | 181 |
| -23 | | | | 1320 | 191 |
| -24 | | | | 1190 | 173 |
| -25 | | | | 703 | 102 |
| -26 | | | | 1230 | 179 |
| -27 | | | | 1080 | 156 |
| -28 | | | | 1100 | 159 |
| -29 | | | | 1110 | 161 |
| -30 | | | | 1120 | 162 |
| -31 | | | | 903 | 131 |
| -32 | | | | 910 | 132 |
| -33 | | | | 882 | 128 |
| -34 | | | | 827 | 120 |
| -35 | | | | 862 | 125 |
| | | | av | 995 | 144 |
| CU02-10 | 533 | 500 | | 1240 | 180 |
| -11 | | | | 1200 | 174 |
| -12 | | | | 1070 | 155 |
| | | | av | 1170 | 170 |
| CU02-13 | 561 | 550 | | 1190 | 173 |
| -14 | | | | 1130 | 164 |
| -15 | | | | 952 | 138 |
| | | | av | 1090 | 158 |
| CU02-16 | 589 | 600 | | 979 | 142 |
| -17 | | | | 1110 | 161 |
| -18 | | | | 1040 | 151 |
| | | | av | 1040 | 151 |
| CU02-19 | 616 | 650 | | 910 | 132 |
| -20 | | | | 1010 | 146 |
| -21 | | | | 979 | 142 |
| | | | av | 966 | 140 |

[a] Net section strength, i.e., based on total width less hole diameter.

ORIGINAL PAGE IS
OF POOR QUALITY

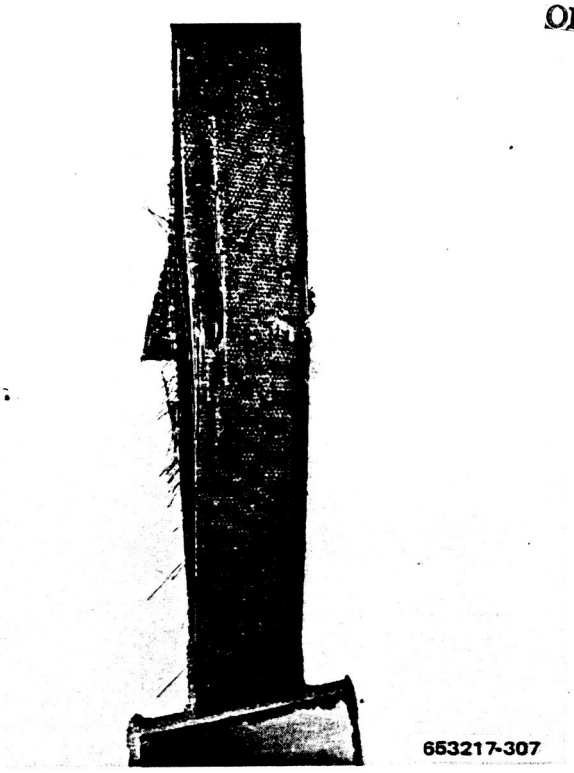



**Figure A-1 Heated Area of B/PI Short-Term Specimen After Only 7 hr of Flight Simulation Exposure at 505 K (450° F)**

To check the extent of the material problem and determine the cause, the following tasks were performed:

a. Measured tensile properties of the remaining panels.

b. Measured specific gravity, resin content, and fiber content of all tested panels.

c. Conducted metallographic and SEM evaluations.

The results of the tensile tests are listed in Table A-5. Only two panels had acceptable tensile properties. LRC-33 and LRC-35. It was from LRC-33 that the crossplied baseline tensile specimens were cut.

Values of specific gravity, resin content, fiber content, and percent voids are listed in Table A-6. There appears to be no correlation between these values and the tensile data of Table A-6.

Two specimens were submitted for metallographic examination, one that had been thermal aged at 561 K (550° F) for 1000 hours, and a baseline tensile specimen. The aged specimen could not be sectioned or mounted as the resin matrix crumbled away during preparation. The tensile specimen, shown at 100X magnification in Figure A-2, revealed several points of interest and offered possible explanations for the poor behavior of the material. First, the spacing of the filaments within the plies was very nonuniform with many of the filaments touching each

Table A-5. Tensile Data for B/PI Panels Tested at 297 K (75° F)

| Panel Number | Orientation | | Tensile Strength MN/m$^2$ | Tensile Strength (ksi) | Intended Use (a) |
|---|---|---|---|---|---|
| LRC-32 | $[0°]_6$ | | 1100 | 159 | 0, 7 |
| | | | 965 | 140 | |
| | | | 896 | 130 | |
| | | av | 987 | 143 | |
| LRC-33 | $[0° \pm 45°]_s$ | | 510 | 74.0 | 0 |
| | | | 505 | 73.2 | |
| | | | 565 | 81.9 | |
| | | av | 527 | 76.4 | |
| LRC-34 | $[0°]_6$ | | 1360 | 198 | 0, 7 |
| | | | 1190 | 172 | |
| | | | 1160 | 169 | |
| | | av | 1240 | 180 | |
| LRC-35 | $[0° \pm 45°]_s$ | | 530 | 76.8 | 0, 7 |
| | | | 512 | 74.2 | |
| | | | 512 | 74.2 | |
| | | av | 518 | 75.1 | |
| LRC-36 | $[0° \pm 45°]_s$ | | 415 | 60.2 | 8 |
| | | | 410 | 59.4 | |
| | | av | 412 | 59.8 | |
| LRC-37 | $[0° \pm 45°]_s$ | | 461 | 66.8 | 8 |
| | | | 486 | 70.5 | |
| | | av | 474 | 68.6 | |
| LRC-38 | $[0° \pm 45°]_s$ | | 387 | 56.2 | 8 |
| | | | 389 | 56.4 | |
| | | av | 388 | 56.3 | |
| LRC-39 | $[0°]_6$ | | 917 | 133 | 1, 5 |
| | | | 917 | 133 | |
| | | | 876 | 127 | |
| | | av | 906 | 131 | |
| LRC-40 | $[0° \pm 45°]_s$ | | 412 | 59.7 | 0, 5 |
| | | | 415 | 60.2 | |
| | | | 432 | 62.6 | |
| | | av | 420 | 60.8 | |
| LRC-41 | $[0° \pm 45°]_s$ | | 360 | 52.2 | 1 |
| | | | 395 | 57.3 | |
| | | av | 378 | 54.7 | |

Table A-5. Tensile Data for B/PI Panels Tested at 297 K (75° F) — Concluded

| Panel Number | Orientation | | Tensile Strength MN/m² | Tensile Strength (ksi) | Intended Use (a) |
|---|---|---|---|---|---|
| LRC-42 | $[0° \pm 45°]_s$ | | 436 | 63.2 | 9 |
| | | | 437 | 63.4 | |
| | | av | 436 | 63.3 | |
| LRC-43 | $[0° \pm 45°]_s$ | | 398 | 57.7 | 9 |
| | | | 412 | 59.7 | |
| | | av | 405 | 58.7 | |

[a] 0 Baseline
1 Thermal Aging
2 Ambient Aging
5 Creep
7 Fatigue
8 Short-term Exposure
9 Long-term Exposure

Table A-6. Specific Gravities and Resin, Fiber, and Void Contents of B/PI Panels

| Panel Number | Orientation | Specific Gravity | Resin Content (wt %) | Fiber Content (wt %) (a) | Void Content (vol. %) |
|---|---|---|---|---|---|
| LRC-32 | $[0°]_6$ | 1.98 | 28.4 | 71.6 | 3.6 |
| LRC-33 | $[0° \pm 45°]_s$ | 1.97 | 32.5 | 67.5 | 0.8 |
| LRC-34 | $[0°]_6$ | 1.93 | 26.9 | 73.1 | 7.0 |
| LRC-35 | $[0° \pm 45°]_s$ | 1.94 | 30.6 | 69.4 | 3.8 |
| LRC-37 | $[0° \pm 45°]_s$ | 1.91 | 33.5 | 66.5 | 3.4 |
| LRC-38 | $[0° \pm 45°]_s$ | 1.98 | 26.3 | 73.7 | 4.7 |
| LRC-39 | $[0°]_6$ | 1.98 | 27.0 | 73.0 | 4.2 |
| LRC-40 | $[0° \pm 45°]_s$ | 1.90 | 37.2 | 62.8 | 1.0 |
| LRC-41 | $[0° \pm 45°]_s$ | 1.91 | 31.0 | 69.0 | 4.9 |

[a] Includes approximately 9% glass fiber from scrim cloth.

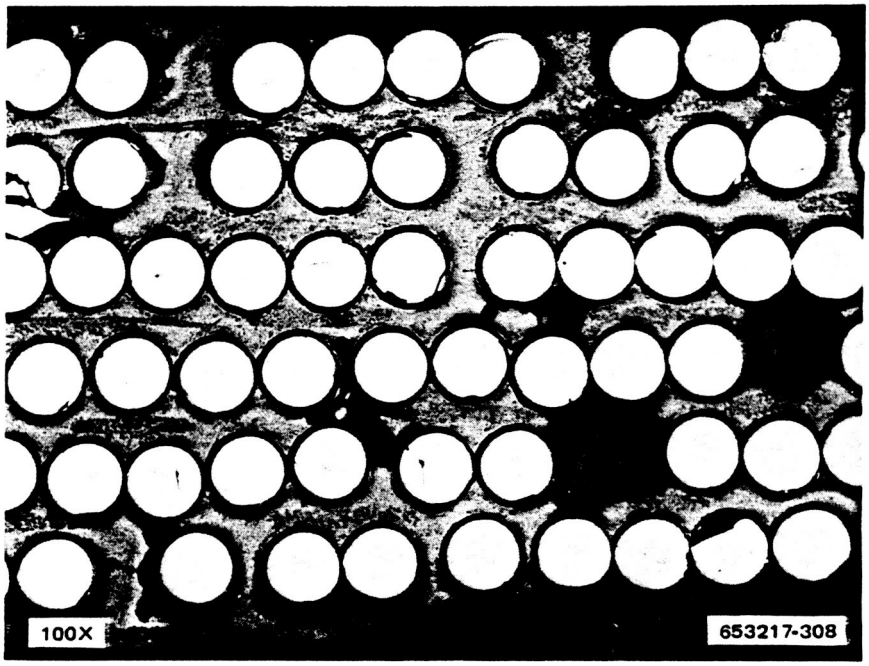



**Figure A-2 Photomicrograph of a Transverse Section of $[0°]_6$ B/PI Showing Nonuniform Filament Spacing and an Indication of Poor Bonding of the Resin to the Boron Filaments**

other. For example, in this photomicrograph, as many as six touching filaments in a row can be seen. Efficient distribution of stresses within a composite and, hence, high strength, particularly in the transverse directions, requires good bonding of the matrix to the filaments with a minimum of filament-to-filament contact. The second, and more important feature of the photomicrograph, was the apparent lack of contact or bonding between the fibers and the resin matrix. This is difficult to show conclusively with a light microscope with its poor depth of field. Because of the significance of this apparent lack of bonding, additional examinations were made using a scanning electron microscope (SEM), an instrument with excellent depth of field.

The photomicrographs in Figures A-3 and A-4 clearly show examples of the separation between filaments and the matrix in both unidirectional and crossplied specimens. Further evidence of poor bonding of the resin to the boron is shown in Figures A-5 and A-6 by the pullout of the filaments from the matrix and the fact that the filaments are smooth with almost no resin adhering to the surface.

It is this lack of bonding of the resin to the filaments that is believed to have been responsible for the poor tensile behavior of the B/P105AC system. Whether the problem was caused by the filaments (dirty or contaminated surface, for example) or by the resin is not known. There had been reported during this time period, however, instances of the P105AC resin going bad in storage, and this may well have been the case for the batch of material evaluated on this program.

The reason for the unsatisfactory performance of the specimens during thermal aging and short-term flight simulation was apparently a combination of two effects. These were the poor bonding of the matrix to the filaments discussed above combined with a resin matrix material that was not capable of extended service at 505 K (450° F).



ORIGINAL PAGE IS
OF POOR QUALITY

ORIGINAL PAGE IS
OF POOR QUALITY

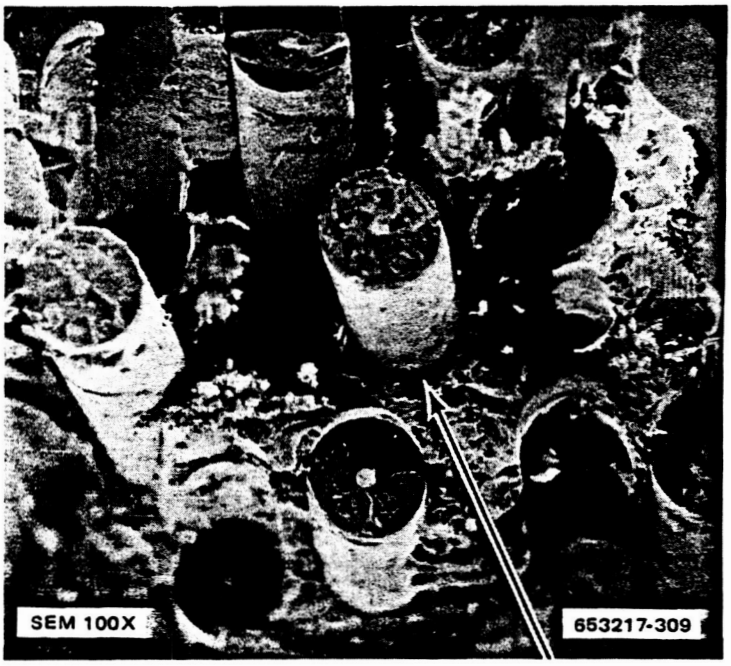



**Figure A-3 Fracture Surface of $[0°]_6$ B/PI Tensile Specimen Showing (arrow) Poor Bonding Between Boron Filament and Resin Matrix**

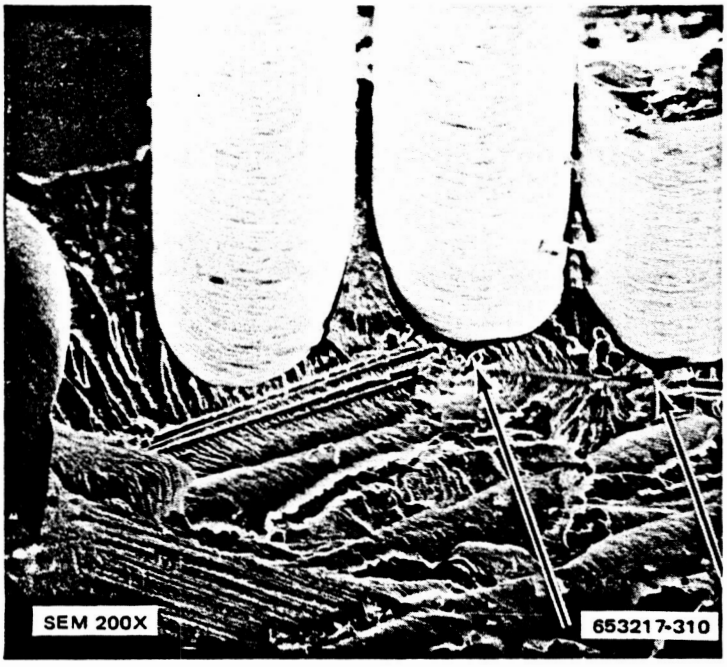



**Figure A-4 Fracture Surface of $[0° \pm 45°]_s$ B/PI Tensile Specimen Showing (arrows) Poor Bonding Between Filaments and Resin Matrix**

ORIGINAL PAGE IS
OE POOR QUALITY

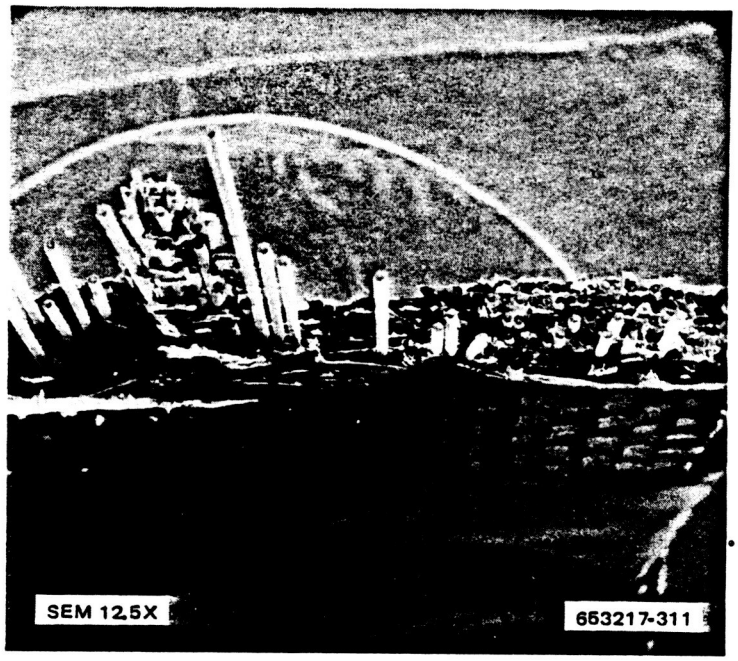



**Figure A-5 Fracture Surface of $[0°]_6$ B/PI Tensile Specimen Showing Pullout of the Boron Filaments from the Matrix (an indication of poor matrix-to-filament bond)**

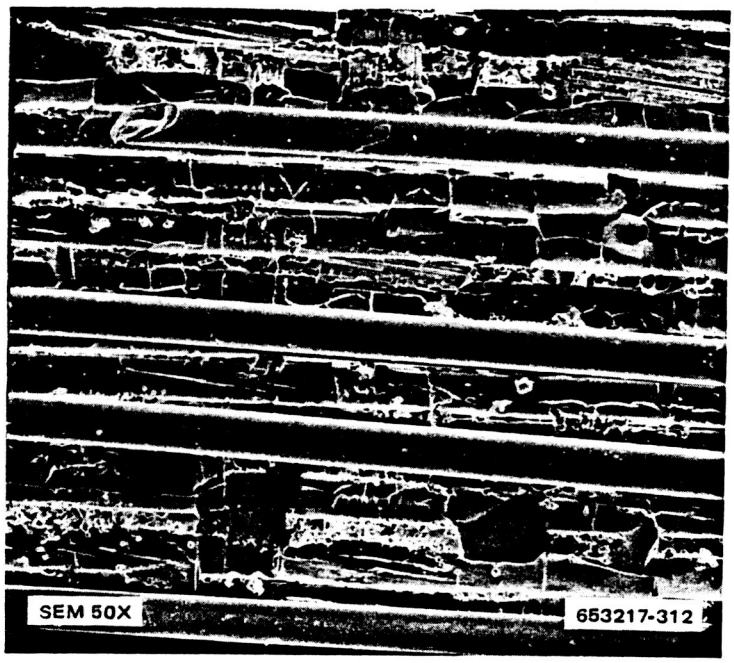



**Figure A-6 B/PI $[0°]_6$ Specimen Tensile Tested at 505 K (450° F) After a 500-hr Thermal Age at 505 K (450° F). (Most of the resin has broken away, leaving bare boron filaments and scrim cloth)**

# APPENDIX B

# QUALITY ASSURANCE TEST PROCEDURES

## B.1 PREPREG VOLATILE CONTENT

Cut three specimens of the material, each approximately 0.051 by 0.051 m (2.0 by 2.0 in.), from an area of the sample away from the edges. The specimen may be any shape that will fit into a preweighed and fired crucible or disposable aluminum dish but may not be rolled up or more than one ply. Weigh each crucible on an analytical balance to the nearest 0.1 mg ($W_2$). Place the test specimen in the crucible and record the total weight to the nearest 0.1 mg ($W_1$). Place the crucible containing the specimen in a preheated air circulating oven (for epoxy resin use 436 K (325 ° F) for $15^{+1}_{-0}$ minutes and for polyimide resin use 450 K (350 ° F) for $20^{+1}_{-0}$ minutes), cool to room temperature, and weigh to the nearest 0.1 mg ($W_3$). The mean value of the three volatile determinations calculated as follows was reported:

$$\text{Volatile Content, weight percent} = \frac{W_1 - W_3}{W_1 - W_2} \times 100$$

where:

$W_1$ = Weight of crucible plus specimen before volatile removal

$W_2$ = Weight of crucible

$W_3$ = Weight of crucible plus specimen after volatile removal

## B.2 PREPREG RESIN SOLIDS AND FIBER CONTENT

Cut three specimens of the material, each approximately 0.051 by 0.051 m (2.0 by 2.0 in.), from an area of the sample away from the edges. Weigh a specimen to the nearest 0.1 mg ($W_1$), place in a 300 ml tall-form beaker, and add 25 ml of dimethyl formamide (DMF) technical grade. Place the beaker on a hot plate and heat to boiling for 10 to 15 minutes. Remove the beaker from the hot plate and allow to cool to room temperature. Pour off the DMF, being careful not to lose any fibers. Rinse the fiber residue two or three times in acetone. After removing most of the acetone, place the fibers in a tared aluminum cup (throwaway type) and dry for 30 minutes minimum in an oven at 436 K (325 ° F). Determine the weight of fibers ($W_2$) to the nearest 0.1 mg and record. The mean value of three fiber and resin solids content determinations calculated as follows was reported:

$$\text{Fiber Content, weight percent} = \frac{W_2}{W_1} \times 100$$

$$\text{Resin plus volatiles, weight percent} = 100 - \frac{W_2}{W_1} \times 100$$

$$\text{Resin Solids Content, weight percent} = 100 - \frac{W_2}{W_1} \times 100 - \text{Volatile Content}$$

where:

$W_1$ = weight of specimen

$W_2$ = weight of fibers

Volatile Content = See Section B.1

### B.3 PREPREG RESIN FLOW

Cut six pieces of style 181 glass fabric, 0.10 by 0.10 m (4.0 by 4.0 in.) square, for bleeder and two squares of Teflon coated glass fabric of the same size, for separator. Weigh to the nearest 0.1 mg ($W_1$) on an analytical balance. Cut two pieces of the material to be tested 0.051 by 0.051 m (2.0 by 2.0 in.) and weigh with the separator and bleeder to the nearest 0.1 mg ($W_2$). Cross ply the two specimens and sandwich them between the separator and the bleeder with the bleeder on the outside. Place in a preheated press and cure for $15^{+1}_{-0}$ minutes under 0.69 $MN/m^2$ (100 psig) at 436 K (325° F) for the epoxy system and at 450 K (350° F) for the polyimide system. Remove the crossply test specimen from the separator and bleeder. Weigh the separator plus bleeder to the nearest 0.1 mg ($W_3$). The mean value of three flow determinations calculated as follows was reported:

$$\text{Percent Flow} = \frac{W_3 - W_1}{W_2 - W_1} \times 100$$

where:

$W_1$ = Weight of glass fabric plus Teflon coated glass fabric

$W_2$ = Weight of glass fabric, Teflon coated glass fabric, and specimens

$W_3$ = Weight of glass fabric plus Teflon coated glass fabric after cure

### B.4 LAMINATE SPECIFIC GRAVITY

The method used for determining the specific gravity of the laminates was by displacement of water. The test procedure was in accordance with Federal Test Method Standard No. 406, Method 5011. Cut three pieces of the laminate to be tested 0.013 by 0.013 m (0.5 by 0.5 in.). Using an analytical balance and a specific gravity bridge, weigh the specimen in air ($W_1$) and in distilled water ($W_2$) at 296 ± 1.1 K (73.5 ± 2° F). The mean value of three specific gravity determinations calculated as follows was reported:

$$\text{Specific Gravity} = \frac{W_1}{W_1 - W_2}$$

where:

$W_1$ = weight of specimen in air

$W_2$ = weight of specimen in water

## B.5 LAMINATE RESIN AND FIBER CONTENT

The test specimen was approximately 0.013 by 0.013 m (0.5 by 0.5 in.) by laminate thickness. The cured resin and fiber content was determined by acid/peroxide digestion as follows:

1. Weigh the test specimen to the nearest 0.1 mg ($W_1$), place in a 300 ml tall-form beaker, and add 20 ml of concentrated sulfuric acid. Place the beaker on a hot plate and heat the acid until vigorous fuming occurs.

2. When the composite is visibly disintegrated and resin particles and fibers are dispersed throughout the sulfuric solution, carefully add the hydrogen peroxide (50% strength) dropwise down the side of the beaker. Rubber gloves and a fume hood with appropriate safety glass shield shall be used throughout the addition, and precautions shall be taken as recommended by the applicable safety regulations and procedures for handling hydrogen peroxide.

3. The reaction is considered complete when the hot sulfuric acid solution below the fibers becomes clear and colorless. At this point add two more ml of hydrogen peroxide to the solution, and heat the solution to fumes for another 10 minutes to ensure complete decomposition of the polymer. Remove the beaker from the hot plate, and allow to cool to 294 to 300 K (70° to 80° F) and then place in an ice bath.

4. Collect fibers by vacuum filtration through a medium-porosity, sintered-glass crucible that has been weighed to nearest 0.1 mg ($W_2$). After the sulfuric acid has been filtered off, wash the fibers in the crucible thoroughly with 600 ml of distilled water, adding a few milliliters at a time. Verify removal of sulfuric acid traces by checking pH of the filtrate drops.

5. Remove the crucible from the filtering system and place in an open beaker in an oven at 422 K (300° F) for 45 minutes. After drying, cool the crucible in a desiccator and weigh to the nearest 0.1 mg ($W_3$).

The resin and fiber content were calculated according to the following equations:

$$\text{Resin Content, weight percent} = \frac{W_1-(W_3-W_2)}{W_1} \times 100$$

$$\text{Fiber Content, weight percent} = \frac{W_3-W_2}{W_1} \times 100$$

where:

$W_1$ = Weight of test specimen

$W_2$ = Weight of crucible

$W_3$ = Weight of crucible plus fibers after acid/peroxide digestion

## B.6 B/Al LAMINATE FIBER VOLUME

The test specimen was approximately 0.013 by 0.013 m (0.5 by 0.5 in.) by laminate thickness. The fiber volume was determined as follows:

1. Wash, dry, and weigh the test specimen to the nearest 0.1 mg ($W_1$).
2. Leach the fibers from the samples in a 50% solution of sodium hydroxide at approximately 339 K (150° F).
3. Wash, dry, and weigh the collected fibers to the nearest 0.1 mg ($W_2$).

Assuming a density of 2700 kg/m$^3$ for the aluminum and a density of 2510 kg/m$^3$ for the 5.6 mil boron, the volume percentages of fibers were calculated according to the following equation:

$$\text{Fiber Volume, volume percent} = \frac{\dfrac{W_2}{\varrho_F}}{\dfrac{W_1 - W_2}{\varrho_A} + \dfrac{W_2}{\varrho_F}} \times 100$$

where:

$W_1$ = Weight of test specimen

$W_2$ = Weight of fibers

$\varrho_F$ = Density of fibers

$\varrho_A$ = Density of aluminum

## B.7 LONGITUDINAL FLEXURAL STRENGTH

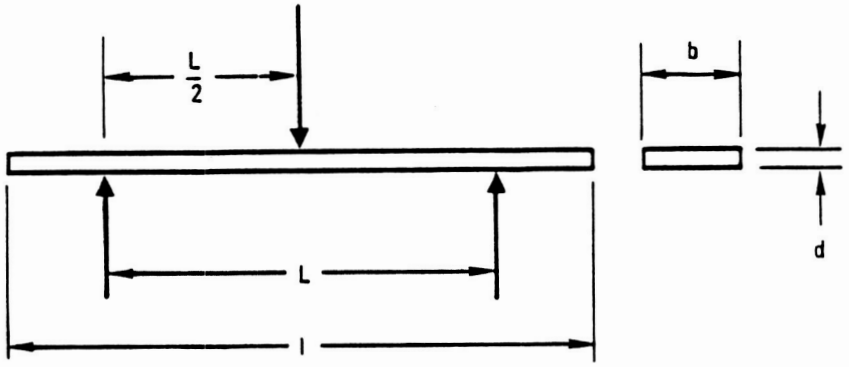
The test method used for determining logitudinal flexural strength was generally in accordance with ANSI/ASTM D 790-71 and Federal Test Method Standard No. 406, Method 1031. Specimens were cut with the fibers aligned parallel to the longitudinal axis. The specimen configuration with the loading geometry is shown in Figure B-1. Testing was done with three point loading using a span to thickness ratio of 32 to 1. The specimens, with the smooth side up, were loaded to failure at 0.0025 m (0.10 in.) per minute crosshead speed in standard test machines (Instron, Tinius-Olsen, or Baldwin). The longitudinal flexural strengths were calculated according to the following formula:

$$F_L = \frac{3PL}{2\,bd^2}$$

where:

$F_L$ = Ultimate longitudinal flexural strength

P = Maximum load carried by the specimen




Specimen Dimensions

Length (l) = 0.076 m (3.0 in.)

Width (b) = 0.01270 m (0.500 in.)

Thickness (d) = Approximately 0.0015 m (0.060 in.)

Span/Thickness Ratio $(\frac{L}{d})$ = 32 to 1

Loading head and reaction supports are 0.00635 m (0.250 in.) diameter steel rod

Overhang must be the same over each end

653217-313

Figure B-1. Longitudinal Flexural Specimen

L = Support span

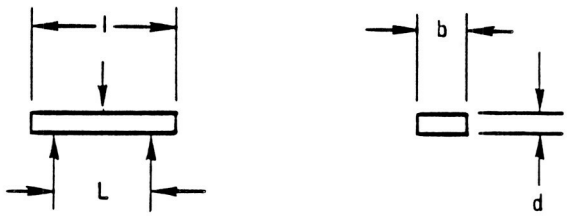
b = Specimen width

d = Specimen thickness

## B.8 SHORT BEAM SHEAR STRENGTH

The test method used for determining short beam shear strength was generally in accordance with ANSI/ASTM D2344-76. Specimens were cut with the fibers aligned parallel to the longitudinal axis. The specimen configuration with the loading geometry is shown in Figure B-2. Testing was done with three point loading using a span to thickness ratio of 4 to 1. The specimens, with the smooth side up, were loaded to failure at 0.0025 m (0.10 in.) per minute crosshead speed in standard test machines (Instron, Tinius-Olsen, or Baldwin). The short beam shear strengths were calculated according to the following formula:

$$\tau = \frac{3P}{4bd}$$




Specimen Dimensions

Length (l) = 0.0152 m (0.60 in.)

Width (b) = 0.00635 m (0.250 in.)

Thickness (d) = Approximately 0.0015 m (0.060 in.)

Span/Thickness Ratio $(\frac{L}{d})$ = 4 to 1

Loading head and reaction supports are 0.00318 m (0.125 in.) diameter steel rod

Overhang must be the same over each end

653217-314

Figure B-2. Short Beam Shear Specimen

where:

$\tau$ = Ultimate short beam shear strength

P = Maximum load carried by the specimen

b = Specimen width

d = Specimen thickness

| 1. Report No. NASA CR-178272 | 2. Government Accession No. | 3. Recipient's Catalog No. |
|---|---|---|
| 4. Title and Subtitle<br>Time-Temperature-Stress Capabilities of Composite Materials for Advanced Supersonic Technology Application | | 5. Report Date<br>MAY 1987<br>6. Performing Organization Code |
| 7. Author(s)<br>J. R. Kerr and J. F. Haskins | | 8. Performing Organization Report No.<br>GDC-CRAD-85-005 |
| 9. Performing Organization Name and Address<br>Convair Division of General Dynamics Corporation<br>5001 Kearny Villa Road<br>San Diego, California 92123 | | 10. Work Unit No.<br>11. Contract or Grant No.<br>NAS 1-12308 |
| 12. Sponsoring Agency Name and Address<br>National Aeronautics and Space Administration<br>Washington, DC 20546 | | 13. Type of Report and Period Covered<br>Contractor Report<br>14. Sponsoring Agency Code<br>505-63-01-06 |

15. Supplementary Notes

Langley Contract Monitors: B. A. Stein and D. R. Rummler

16. Abstract

Advanced composites will play a key role in the development of the technology required for the design and fabrication of future supersonic vehicles. However, implementation of the material into vehicle usage is contingent upon accelerating the demonstration of service capacity and design technology. Because of the added material complexity and lack of extensive service data, laboratory replication of the flight service will provide the most rapid method of documenting the airworthiness of advanced composite systems. Consequently, a laboratory program was conducted to determine the time-temperature-stress capabilities of several high temperature composite materials. Tests included in this study were thermal aging, environmental aging, fatigue, creep, fracture, tensile, and real-time flight simulation exposure. The program had two phases. The first included all the material property determinations and aging and simulation exposures up through 10,000 hours. The second continued these tests up to 50,000 cumulative hours. This report presents the results of the Phase I baseline and 10,000 hour aging and flight simulation studies, the Phase II 50,000 hour aging studies, and the Phase II flight simulation tests, some of which extended to almost 40,000 hours.

| 17. Key Words (Suggested by Author(s)) | 18. Distribution Statement |
|---|---|
| Composite Materials, Thermal Aging, Environmental Aging, Fatigue, Creep, Tensile, Shear, Fracture, Flight Simulation Exposure, Boron, Graphite, Epoxy Resins, Polyimide Resins, Aluminum, Supersonic Vehicles, SCR | Unclassified - Unlimited<br>Subject Category 24 |

| 19. Security Classif. (of this report) | 20. Security Classif. (of this page) | 21. No. of Pages | 22. Price |
|---|---|---|---|
| Unclassified | Unclassified | 672 | |

*For sale by the National Technical Information Service, Springfield, Virginia 22151